सत्यमेव जयते

INDIAN AGRICULTURAL
RESEARCH INSTITUTE, NEW DELHI

7635

I.A.R.I.6.
GIP NLK—H-3 I.A.R.I.—10-5-55—15,000

THE
PROCEEDINGS
OF
THE PHYSICAL SOCIETY

FROM JANUARY 1937 TO NOVEMBER 1937

VOLUME 49

Published by
THE PHYSICAL SOCIETY
1 Lowther Gardens, Exhibition Road
London, S.W. 7

Printed at
THE UNIVERSITY PRESS, CAMBRIDGE

PRINTED IN GREAT BRITAIN

OFFICERS AND COUNCIL, 1937–1938

President:

T. SMITH, M.A., F.Inst.P., F.R.S.

Vice-Presidents:

Who have filled the Office of President.

Sir OLIVER J. LODGE, D.Sc., LL.D., F.Inst.P., F.R.S.
Sir J. J. THOMSON, O.M., Sc.D., F.Inst.P., F.R.S.
Prof. Sir CHARLES VERNON BOYS, LL.D., F.Inst.P., F.R.S.
Prof. C. H. LEES, D.Sc., F.Inst.P., F.R.S.
Prof. Sir W. H. BRAGG, K.B.E., M.A., F.Inst.P., F.R.S.
ALEXANDER RUSSELL, M.A., D.Sc., F.Inst.P., F.R.S.
Sir FRANK E. SMITH, K.C.B., C.B.E., D.Sc., F.Inst.P., Sec. R.S.
Prof. O. W. RICHARDSON, M.A., D.Sc., F.R.S.
W. H. ECCLES, D.Sc., F.Inst.P., F.R.S.
Prof. Sir A. S. EDDINGTON, M.A., D.Sc., F.R.S.
Prof. A. O. RANKINE, O.B.E., D.Sc., F.Inst.P., F.R.S.
The Right Hon. Lord RAYLEIGH, M.A., Sc.D., LL.D., F.Inst.P., F.R.S.

Vice-Presidents:

R. S. WHIPPLE, M.I.E.E., F.Inst.P.
EZER GRIFFITHS, D.Sc., F.Inst.P., F.R.S.
D. OWEN, B.A., D.Sc., F.Inst.P.
J. H. AWBERY, B.Sc., F.Inst.P.

Hon. Secretaries:

W. JEVONS, D.Sc., Ph.D., F.Inst.P.
ALLAN FERGUSON, M.A., D.Sc., F.Inst.P.

Hon. Foreign Secretary:

Prof. O. W. RICHARDSON, M.A., D.Sc., F.R.S.

Hon. Treasurer:

R. W. PAUL, M.I.E.E., F.Inst.P.

Hon. Librarian:

J. H. BRINKWORTH, D.Sc., A.R.C.S., F.Inst.P.

Ordinary Members of Council:

Prof. W. WILSON, D.Sc., Ph.D., F.R.S.
T. Y. BAKER, B.A., F.Inst.P.
Prof. C. D. ELLIS, B.A., Ph.D., F.R.S.
Prof. G. I. FINCH, M.B.E., F.Inst.P.
H. SHAW, D.Sc., A.R.C.S., F.Inst.P.
Prof. H. R. ROBINSON, D.Sc., Ph.D., F.Inst.P., F.R.S.
H. T. FLINT, D.Sc., Ph.D.
L. F. BATES, D.Sc., Ph.D., F.Inst.P.
L. HARTSHORN, D.Sc., A.R.C.S.
Prof. F. L. HOPWOOD, D.Sc., F.Inst.P.
A. B. WOOD, D.Sc., F.Inst.P.
C. V. DRYSDALE, C.B., O.B.E., D.Sc., M.I.E.E., F.Inst.P.

Editor of the Proceedings:

Capt. C. W. HUME, M.C., B.Sc.

Assistant Secretary:

Miss J. I. DENNIS

CONTENTS

Extra part. 31 *August* 1937

Report of a conference on the conduction of electricity in solids

PAGE
N. F. Mott. Introduction v
R. W. Pohl. Electron conductivity and photochemical processes in alkali-halide crystals 3
R. W. Gurney and N. F. Mott. Trapped electrons in polar crystals . . 32
Discussion 36
R. Hilsch. Alkali-halide phosphors containing heavy metals 40
J. T. Randall. The effects of temperature on the intensity of fluorescence of some impurity solids 46
Discussion 57
J. H. de Boer and E. J. W. Verwey. Semi-conductors with partially and with completely filled 3*d*-lattice bands 59
Discussion 72
G. Borelius. Resistance of alloys with disordered and ordered arrangement of atoms 77
W. L. Bragg, C. Sykes and A. J. Bradley. A study of the order-disorder transformation 96
C. H. Desch. Age-hardening alloys 103
Discussion 108
G. I. Finch. The structure of thin metallic films 113
E. T. S. Appleyard. Some factors influencing the resistance of thin metal films 118
A. Féry. A study of the electrical properties of thin films of platinum obtained by cathode sputtering in air and other gases (He, N_2, O_2 and H_2) 136
J. Bernamont. Fluctuations in the resistance of thin films 138
J. E. Lennard-Jones. The migration and aggregation of metal atoms on solid surfaces 140
Discussion 151

Part 1. 1 *January* 1937

J. S. Rogers. Further experiments on the photographic action of gamma rays and on their absorption coefficients 1
N. R. Campbell and R. S. Rivlin. The effect of hydrogen on the time-lag of argon-filled photoelectric cells 12
William Band. Thermomagnetic properties of nickel wire. Part 3 14
E. A. Owen and E. L. Yates. X-ray investigation of pure iron-nickel alloys. Part 1: Thermal expansion of alloys rich in nickel 17
J. G. G. Conybeare. The resistance of palladium and palladium-gold alloys . 29
R. Cockburn. A determination of the fundamental types of electron oscillations in a triode valve 38

PAGE

J. C. M. **Brentano**. An X-ray goniometer using beams of large aperture for photographically recording crystal-powder reflections 61

Reviews of books 78

Part 2. 1 *March* 1937

J. H. E. **Griffiths**. A circuit for counting impulses at high speeds of counting . 85

A. C. B. **Lovell**. The electrical conductivity of thin films of the alkali metals spontaneously deposited on glass surfaces 89

R. C. **Parker**. The smoke method of measuring supersonic velocities . . 95

A. K. **Taylor**. Photometric test plates 105

John S. **Anderson**. The measurement of distortion in a gauge protection lens . 112

V. E. **Cosslett**. The structure and electrical conductivity of thin films of indium 121

H. L. **Cox** and D. G. **Sopwith**. The effect of orientation on stresses in single crystals and of random orientation on strength of polycrystalline aggregates . 134

E. N. **da C. Andrade** and R. **Roscoe**. Glide in metal single crystals . . . 152

E. A. **Owen** and E. L. **Yates**. X-ray investigation of pure iron-nickel alloys. Part 2. Thermal expansion of some further alloys 178

J. S. **Preston** and F. W. **Cuckow**. A photoelectric spectrophotometer of high accuracy 189

C. S. **Hallpike**, H. **Hartridge** and A. F. **Rawdon-Smith**. The response of the mammalian cochlea to phase-reversal in a continuous musical tone . . 190

Demonstration of the portable photoelectric daylight-factor meter . . . 194

Demonstration of the audible effect of a sudden change of phase in the current supplied to a telephone receiver 194

Reviews of books 198

Part 3. 1 *May* 1937

W. N. **Bond**. The viscosity of air 205

R. **Naismith**. Ionospheric conditions during the solar eclipse of 19 June 1936 . 214

H. **Buckley**. Note on the radiation between two coaxial radiating cylinders . 225

L. F. **Bates** and L. C. **Tai**. The magnetic properties of manganese amalgams . 230

Wilfred W. **Barkas**. Wood-water relationships, Part 3: Molecular sorption of water by Sitka spruce wood 237

H. **Jones**. The phase boundaries in binary alloys, Part 1: The equilibrium between liquid and solid phases 243

H. **Jones**. The phase boundaries in binary alloys, Part 2: The theory of the α, β phase boundaries 250

N. F. **Mott**. The energy of the superlattice in β brass 258

D. M. **Myers**. The division of primary electron current between grid and anode of a triode 264

A. G. **Quarrell**. Structural changes during the growth of metal films . . 279

Ralph H. V. M. **Dawton**. Intensities of X-ray reflections from single crystals of sodium between 120 and 370° K. 294

PAGE

E. A. OWEN and E. L. YATES. An X-ray investigation of pure iron-nickel alloys. Part 3: The thermal expansion of alloys rich in iron 307

E. A. OWEN, E. L. YATES and A. H. SULLY. An X-ray investigation of pure iron-nickel alloys. Part 4: The variation of lattice-parameter with composition . 315

E. A. OWEN, E. L. YATES and A. H. SULLY. An X-ray investigation of pure iron-nickel alloys. Part 5: The variation of thermal expansion with composition . 323

Reviews of books 326

Part 4. 1 *July* 1937

W. D. WRIGHT and F. H. G. PITT. The saturation-discrimination of two trichromats 329

J. H. NELSON. The colour-vision characteristics of a trichromat, Part 2 . . 332

C. W. WILSON. The effect of secondary beta radiation on gamma-ray measurements made in air 338

H. LOWERY, H. WILKINSON and D. L. SMARE. On the optical constants of alloys of the copper-zinc system 345

N. F. MOTT. The theoretical interpretation of the optical constants of copper-zinc alloys 354

WM. H. GEORGE. Sensitivity variation of X-ray photographic films . . . 357

HARALD NORINDER. Rapid variations in the magnetic field produced by lightning discharges 364

R. KINGSLAKE. The knife-edge test for spherical aberration 376

E. N. DA C. ANDRADE and L. C. TSIEN. The velocity-distribution in a liquid-into-liquid jet 381

L. R. G. TRELOAR. Secondary-electron emission from complex surfaces . . 392

M. C. JOHNSON and F. A. VICK. Thermionic approximations to the gas-covered fraction of an adsorbing surface, applied to the temperature dependence of oxygenation and oxidation of a tungsten filament 409

R. W. POWELL. The thermal and electrical conductivity of a sample of Acheson graphite from 0° C. to 800° C. 419

Demonstration of a microscope for use with ultraviolet light, employing a reflecting optical system of aplanatic properties 427

Reviews of books 429

Part 5. 1 *September* 1937

W. H. S. CHANCE. The optical glassworks at Benediktbeuern 433

ALLAN H. BRIGGS. The estimation of ametropia by the coincidence optometer . 444

E. F. FINCHAM. The coincidence optometer 456

R. E. REASON. The development of the Fincham coincidence optometer . . 469

E. G. RICHARDSON. An experimental study of turbulence diffusion . . . 479

G. BURNISTON BROWN. The vortex motion causing edge tones 493

G. BURNISTON BROWN. The mechanism of edge-tone production 508

MARY D. WALLER. The production of Chladni figures by means of solid carbon dioxide: Part 1, bars and other metal bodies 522

PAGE

W. JEVONS, L. A. BASHFORD and H. V. A. BRISCOE. Ultraviolet band-systems of GeCl and GeBr 532

W. JEVONS, L. A. BASHFORD and H. V. A. BRISCOE. The ultraviolet band-system of germanium monoxide 543

W. JEVONS and L. A. BASHFORD. Ultra-violet band systems of SnBr and SiBr . 554

Y. P. PARTI and R. SAMUEL. Absorption spectra of some carbon and tin halides in the vapour state 568

E. A. OWEN and JOHN IDWAL JONES. The effect of pressure and temperature on the occlusion of hydrogen by palladium 587

E. A. OWEN and JOHN IDWAL JONES. The palladium-hydrogen system . . 603

L. F. BATES and P. F. ILLSLEY. The magnetic properties of iron amalgams . 611

F. E. HOARE and G. W. BRINDLEY. The diamagnetic susceptibilities of dissolved and hydrated salts 619

Reviews of books 629

Part 6. 1 *November* 1937

L. F. BATES and P. G. DAY. The electrical resistance of manganese amalgams . 635

L. F. BATES and A. W. IRELAND. The magnetic properties of silver amalgams . 642

WALTER G. CADY. The longitudinal piezoelectric effect in Rochelle-salt crystals . 646

H. C. WEBSTER. An aperiodic amplifier for investigating the wave-form of atmospherics 654

H. C. WEBSTER. Applications of the modulating electrode of television cathode-ray tubes in investigations of the wave-form of atmospherics 658

H. DENNIS TAYLOR. On the use of rotating parallel-plane glass blocks for cinematography and for projection with continuously moving films . . . 663

H. H. POTTER. The electrical resistance of ferromagnetics 671

S. L. HUSSAIN and R. SAMUEL. Absorption spectra and photodissociation of halides and oxyhalides of sulphur, selenium and tellurium 679

Presentation of the fourteenth Duddell Medal to PROFESSOR WALTER G. CADY, 9 July 1937 693

Obituary Notices 694

Reviews of books 711

Index to volume 49 718

PROCEEDINGS AT THE MEETINGS OF THE PHYSICAL SOCIETY

SESSION 1936–37

Except where the contrary is stated the meetings were held at the Imperial College of Science and Technology, South Kensington, the President being in the Chair.

9 *October* 1936

John Silvey Preston and John Martin Sleeman Speirs were elected Fellows of the Society.

The President announced that the Council had elected Richard Arthur Buckingham to Student Membership.

The following papers were read:

"The constancy of the velocity of sound at sonic frequencies", by F. A. WALCH, Ph.D.

"Vibration of a building partition at audio frequencies", by J. E. R. CONSTABLE, M.A., Ph.D., B.Sc., F.Inst.P.

"Vibration pattern of a wall transmitting sound", by J. E. R. CONSTABLE, M.A., Ph.D., B.Sc., F.Inst.P. and G. H. ASTON, M.A., Ph.D., B.Sc.

The following papers were read in title:

"Secondary emission from copper due to slow positive ions of argon", by F. LLEWELLYN JONES, M.A., D.Phil. and W. H. WILLOTT, Ph.D., B.Sc., A.Inst.P.

"X-ray investigation of pure iron-nickel alloys, Part I. Thermal expansion of alloys rich in nickel", by E. A. OWEN, M.A., Sc.D., D.Sc., F.Inst.P. and E. L. YATES, M.Sc., Ph.D.

Dr P. B. MOON showed some experiments in illustration of his paper on "The passage of neutrons through paraffin wax".

— —

23 *October* 1936

The following were elected Fellows of the Society: Julius Hartmann, Stanley Hill, Otto Paul Theodor Kantorowicz, John Walter Kolbert, Harald Ernst Norinder, John Keith Roberts, Francis Arthur Vick.

The President announced that the Council had elected W. E. Trevelyan to Student Membership.

The following papers were read:

"A photoelectric spectrophotometer of high accuracy", by J. S. PRESTON, M.A., A.M.I.E.E., F.Inst.P. and F. W. CUCKOW, B.Sc.

"The resistance of palladium and palladium-gold alloys", by J. C. C. CONYBEARE.

The following papers were read in title:

"The ignition of explosive gases", by G. MOLE.

"Wireless waves reflected from the ionosphere at oblique incidence", by F. T. FARMER, B.Sc. and J. A. RATCLIFFE, M.A.

"A self-synchronizing time base for the distant observation of wireless pulse transmissions", by S. H. W. H. FALLOON, B.A. and F. T. FARMER, B.Sc.

"The electrical conductivity of barium chloride and its variation with temperature", by V. J. JEHU, B.Sc.

Prof. F. L. HOPWOOD, D.Sc., F.Inst.P., gave a demonstration of some experiments with singing tubes and coupled acoustic systems.

13 *November* 1936

Nevill Francis Mott and Kenneth John Proud were elected Fellows of the Society.

The President announced that the Council had elected John Anthony Chaldecott to Student Membership.

The following papers were read:

"The determination of the possible wave-lengths of electron oscillations in a triode valve", by R. COCKBURN, M.Sc., A.Inst.P.

"The viscosity of air", by W. N. BOND, M.A., D.Sc., F.Inst.P.

The following paper was read in title:

"Further experiments on the photographic action of γ rays and on their absorption coefficients", by J. S. ROGERS, B.A., M.Sc., F.Inst.P.

The following demonstrations were given by members of the staff of the Research Laboratories of the General Electric Company, Ltd.:

(i) A demonstration of phosphorescence.
(ii) A demonstration of a property of a hot spiral wire.
(iii) An experiment demonstrating the high electrical resistance of certain glasses.

27 *November* 1936

The following were elected Fellows of the Society: Emil Samuel Conradi, Robert Crispin Evans, R. Satyanarayan, William Hodge Taylor.

The President announced that the Council had elected Gordon Edward Erskine to Student Membership.

The following papers were read:

"The effect of hydrogen on the time lag of argon-filled photoelectric cells", by N. R. CAMPBELL, Sc.D., F.Inst.P. and R. S. RIVLIN.

"The smoke method of measuring supersonic velocities", by R. C. PARKER, B.Sc., Ph.D.

"An X-ray goniometer for photographically recording crystal-powder reflections by means of beams of large aperture", by J. C. M. Brentano, D.Sc., F.Inst.P.

"Thermomagnetic properties of nickel wire, Part III", by William Band, M.Sc.

A demonstration entitled "The response of the ear to the phase reversal of a continuous musical tone" was given by Professor H. Hartridge, Dr C. S. Hallpike and Mr A. F. Rawdon-Smith.

3 *December* 1936

The Meeting was held in the rooms of the Royal Society, Burlington House, London, W. 1, by kind permission of the President and Council.

Mr W. H. S. Chance delivered an address on "The optical glass works at Benediktbeuern".

The following papers were read:

"The measurement of distortion in a gauge projection lens", by J. S. Anderson, M.A., D.Sc., F.Inst.P.

"Photometric test plates", by A. K. Taylor, A.C.G.I., M.I.E.E.

11 *December* 1936

Cyril Dean Butler was elected a Fellow of the Society.

The following papers were read:

"A circuit for counting impulses at high counting speeds", by J. H. E. Griffiths.

"The structure and electrical conductivity of thin films of indium", by V. E. Cosslett, B.Sc., Ph.D.

The following papers were read in title:

"The effect of orientation on the stresses developed on the slip planes of single crystal specimens. With a note on the effect of random orientation on the strength of polycrystalline specimens", by H. L. Cox, B.A. and D. G. Sopwith, B.Sc.Tech., A.M.I.Mech.E.

"X-ray investigation of pure iron-nickel alloys, Part II. Thermal expansion of alloys containing between 41 and 24 per cent nickel", by E. A. Owen, M.A., Sc.D., D.Sc., F.Inst.P. and E. L. Yates, M.Sc., Ph.D., A.Inst.P.

A demonstration entitled "The photoelectric daylight factor meter" was given by Mr G. P. Barnard, A.Inst.P.

5, 6, 7 *January* 1937

The Twenty-seventh Annual Exhibition of Scientific Instruments and Apparatus was held at the Imperial College of Science and Technology.

The following discourses were delivered:

"Electrical measurements in the 'eighties, particularly those associated with Ayrton and Perry", by Sir JAMES SWINBURNE, M.I.E.E., F.R.S., on January 5th.

"The influence of industrial research on the development of scientific instruments", by HARRY MOORE, D.Sc., A.R.C.S., F.Inst.P., on January 6th.

22 *January* 1937

Cecil Baker and Norman Wright Robinson were elected Fellows of the Society.

The President announced that the Council had elected the following to Student Membership: Ethel Eva Widdowson, Arthur Charlesby, Ewart Harold Parfrey.

The prizes and certificates awarded for the eighth competition in craftsmanship and draughtsmanship were presented.

The following paper was read:

"Glide in metal single crystals", by E. N. da C. ANDRADE, F.R.S. and R. ROSCOE, Ph.D.

The following paper was read in title:

"The electrical conductivity of thin films of the alkali metals spontaneously deposited on glass surfaces", by A. C. B. LOVELL.

A demonstration of an experiment illustrating the Kutta-Joukowski effect was given by Professor E. N. da C. ANDRADE, F.R.S.

12 *February* 1937

The following were elected Fellows of the Society: Hugh Colin Webster, Donald Arthur Wright, Grenville Dennis Yarnold.

The President announced that the Council had elected Frank Scowen to Student Membership.

The following paper was read:

"Ionospheric conditions during the solar eclipse of June 19th, 1936", by R. NAISMITH, A.M.I.E.E.

The following papers were read in title:

"The radiation between two coaxial radiating cylinders", by H. BUCKLEY, M.Sc., F.Inst.P.

"The magnetic properties of manganese amalgams", by L. C. BATES, D.Sc., Ph.D., F.Inst.P. and L. C. TAI, B.Sc.

"X-ray investigation of pure iron-nickel alloys. Part III: Thermal expansion of alloys rich in iron. Part IV: Variation of lattice parameter and thermal expansion coefficient with composition", by E. A. OWEN, M.A., Sc.D., D.Sc., F.Inst.P., E. L. YATES, M.Sc., Ph.D., A.Inst.P. and A. H. SULLY, M.Sc.

A demonstration of a ripple tank was given by Mr J. W. COTTINGHAM.

26 *February* 1937

The following were elected Fellows of the Society: A. A. Dee, Percy K. Boulnois, Ronald W. Douglas (transfer from Student Membership), Alexander Jenkins (transfer from Student Membership).

The following papers were read:

"Intensities of X-ray reflections from single crystals of sodium between 120 and 370° K.", by RALPH H. V. M. DAWTON.

"Structural changes during the growth of metal films", by A. G. QUARRELL, B.Sc., Ph.D., A.R.C.S.

The following papers were read in title:

"Wood water relationships, III. Further study of molecular sorption of water by Sitka spruce wood", by W. W. BARKAS, M.Sc.

"The division of primary electron current between grid and anode of a triode", by D. M. MYERS.

A demonstration of directly moulded optical systems and lenses was given by members of the staff of Combined Optical Industries, Ltd. (By arrangement with Major F. A. Freeth, O.B.E., F.R.S.)

12 *March* 1937

Annual General Meeting

The Minutes of the previous Annual General Meeting were read and accepted as correct.

The Reports of the Council and Hon. Treasurer were adopted.

The Officers and the Council for 1937–8 and the Auditors were elected.

Votes of thanks were accorded to the retiring Officers and Council and to the Governors of the Imperial College of Science and Technology.

Ordinary Meeting

The following were elected Fellows of the Society: William Henry Rann, Harry Wilman, K. Mendelssohn, L. J. Comrie, William Cochrane.

The following papers were read:

"The effect of secondary beta radiation on gamma-ray measurements made in air", by C. W. WILSON, M.Sc.

"The energy of the superlattice in β brass", by N. F. MOTT, M.A., F.R.S.

"A discussion of the factors which determine the phase boundaries in binary alloys. Part I: The equilibrium between liquid and solid phases. Part II: The theory of the α, β phase boundaries", by H. Jones.

A demonstration of a transmission photoelectric densitometer with semi-automatic plotting mechanism and improved voltage stabiliser was given by L. V. Chilton and R. J. Hercock. (By arrangement with Mr Olaf Bloch.)

9 *April* 1937

The following were elected Fellows of the Society: James Howard Eagle Griffiths, Douglas Roaf.

The following papers were read:

"On the optical constants of alloys of the copper-zinc system", by H. Lowery, D.Sc., Ph.D., F.Inst.P., H. Wilkinson, M.Sc.Tech. and D. L. Smare, M.Sc.Tech.

"The theoretical interpretation of the optical constants of copper-zinc alloys", by N. F. Mott, M.A., F.R.S.

The following papers were read in title:

"Sensitivity variation of X-ray photographic films", by W. H. George, M.Sc., Ph.D., F.Inst.P.

"Rapid variations in the magnetic field produced by lightning discharges", by Harald Norinder, Ph.D.

A demonstration of a special form of double pendulum was given by Dr R. S. Clay.

23 *April* 1937

The following were elected Fellows of the Society: Alan Ewart Walter Austen (transfer from Student Membership), Frederick David Edwards, Albert John Philpot.

A demonstration of band systems of diatomic oxides in the uncondensed discharge in air was given by W. Jevons, D.Sc., Ph.D.

The following papers were read:

"Thermionic approximations to the gas-covered fraction of an adsorbing surface, applied to the temperature-dependence of oxygenation and oxidation of a tungsten filament", by M. C. Johnson, M.A., D.Sc., A.Inst.P. and F. A. Vick, B.Sc., Ph.D., A.Inst.P.

"The thermal and electrical conductivities of a sample of Acheson graphite from 0° c. to 800° c.", by R. W. Powell, B.Sc.

7 *May* 1937

A demonstration of Professor Carl Seashore's tests on certain psycho-physical functions, viz. discrimination of pitch, rhythm, intensity, time and consonance, was given by H. Lowery, D.Sc., Ph.D., F.Inst.P.

A demonstration of a new irradiation monochromator was given by J. W. PERRY. (By the courtesy of Messrs Adam Hilger, Ltd.)

The following papers were read:

"The velocity distribution in a liquid-into-liquid jet", by E. N. DA C. ANDRADE, F.R.S. and L. C. TSIEN, B.Sc.

"Secondary-electron emission from complex surfaces", by L. R. G. TRELOAR, B.Sc.

28 *May* 1937

Douglas Stuart Spens Steuart was elected a Fellow of the Society.

The President announced that the Council had elected John Gilbert Daunt to Student Membership.

Mr B. K. JOHNSON gave a demonstration of a microscope, employing a reflecting optical system of aplanatic properties, for use with infra-red visible or ultra-violet radiation.

The following papers were read:

"The colour-vision characteristics of a trichromat, Part II", by J. H. NELSON, A.R.C.S., B.Sc.

"The saturation-discrimination of two trichromats", by W. D. WRIGHT, D.Sc., A.R.C.S. and F. H. G. PITT, Ph.D., A.R.C.S.

"The knife-edge test for spherical aberration", by R. KINGSLAKE, M.Sc., A.R.C.S.

3 *June* 1937

The Meeting was held in the rooms of the Royal Society, Burlington House, London, W. 1, by kind permission of the President and Council.

The following papers were read:

"The coincidence optometer", by E. F. FINCHAM, F.Inst.P.

"The development of the Fincham coincidence optometer", by R. E. REASON, A.R.C.S.

"The estimation of ametropia by the coincidence optometer", by ALLAN H. BRIGGS, M.Sc., M.B., Ch.B., D.O.M.S.

11 *June* 1937

George Allan Whipple was elected a Fellow of the Society.

A lecture demonstration dealing with calculating machines and their use in physical problems was given by Dr L. J. COMRIE.

The following paper was read:

"The production of Chladni figures by means of solid carbon dioxide: I. Bars and other metal bodies", by Miss MARY D. WALLER, B.Sc., F.Inst.P.

The following papers were read in title:

"The effect of pressure and temperature on the occlusion of hydrogen by palladium", by E. A. OWEN, M.A., D.Sc., F.Inst.P. and J. I. JONES, Ph.D.

"Ultra-violet band-systems of GeCl and GeBr", by W. JEVONS, L. A. BASHFORD and H. V. A. BRISCOE.

"The ultra-violet band system of germanium monoxide", by W. JEVONS, L. A. BASHFORD and H. V. A. BRISCOE.

25 *June* 1937

The following were elected Fellows of the Society: Philip M. Morse, Walter John Charles Chapple (transfer from Student Membership).

A demonstration of a model of a vibrating molecule was given by Dr W. H. J. CHILDS, of the Royal Institution.

The following paper was read:

"The vortex motion causing edge tones and the mechanism of its production", by G. B. BROWN, M.Sc., Ph.D.

The following papers were read in title:

"An experimental study of turbulence diffusion", by E. G. RICHARDSON, B.A., Ph.D., D.Sc.

"The diamagnetic susceptibilities of dissolved and hydrated salts", by F. E. HOARE, Ph.D. and G. W. BRINDLEY, Ph.D.

"The magnetic properties of iron amalgams", by L. F. BATES, D.Sc., Ph.D. and P. F. ILLSLEY.

---

26 *June* 1937

A visit was arranged to the Fuel Research Station at East Greenwich and the National Maritime Museum.

9 *July* 1937

The Fourteenth Duddell Medal was presented to Professor W. G. CADY, of the Wesleyan University, Middletown, Connecticut, U.S.A.

The following paper was read:

"The longitudinal effect in Rochelle salt crystals", by W. G. CADY.

The following papers were read in title:

"An aperiodic amplifier for investigating the wave form of atmospherics", by H. C. WEBSTER.

"Applications of the modulating electrode of television cathode ray tubes in investigations of the wave form of atmospherics", by H. C. WEBSTER.

A demonstration of piezo-electric apparatus was given by members of the staff of the National Physical Laboratory.

13, 14, 15, 16 *July* 1937

An informal conference on the conduction of electricity in solids was held at the H. H. Wills Physical Laboratory, University of Bristol, under the joint auspices of the Physical Society and the University of Bristol.

The following papers were read:

"Electron conductivity and photochemical processes in alkali-halide crystals", by R. W. Pohl.

"Trapped electrons in polar crystals", by R. W. Gurney and N. F. Mott.

"Alkali-halide phosphors containing heavy metals", by R. Hilsch.

"The effects of temperature on the intensity of fluorescence of some impurity solids", by J. T. Randall.

"Semi-conductors with partially and with completely filled 3*d*-lattice bands", by J. H. de Boer and E. J. W. Verwey.

"Resistance of alloys with disordered and ordered arrangement of atoms", by G. Borelius.

"A study of the order-disorder transformation", by W. L. Bragg, C. Sykes and A. J. Bradley.

"Age-hardening alloys", by C. H. Desch.

"The structure of thin metallic films", by G. I. Finch.

"Some factors influencing the resistance of thin metal films", by E. T. S. Appleyard.

"A study of the electrical properties of thin films of platinum obtained by cathode spluttering in air and other gases (He, N_2, O_2 and H_2)", by A Fery.

"Fluctuations in the resistance of thin films", by J Bernamont.

"The migration and aggregation of metal atoms on solid surfaces", by J. E. Lennard-Jones.

REPORT OF COUNCIL FOR THE YEAR ENDING FEBRUARY 28, 1937

MEETINGS

DURING the period under review 14 Ordinary Science Meetings were held at the Imperial College of Science and Technology. At these meetings 56 papers were presented, of which 33 were read in title. Fourteen demonstrations were given.

A Science Meeting was held on June 5, 1936, at Bedford College by the kind invitation of Professor W. Wilson, F.R S. Before the meeting the Physics Department was open to members of the Society and their guests, who were also entertained to tea by Professor Wilson.

A Special Optical Meeting was held on the evening of December 3, 1936, in the rooms of the Royal Society, by kind permission of the President and Council. Mr W. H. S. Chance delivered an address on "The Optical Glass Works at Benediktbeuern", and two papers on optical subjects were also read and discussed.

SUMMER MEETING AT THE RESEARCH LABORATORIES OF THE GENERAL ELECTRIC COMPANY

A visit was paid on June 19, 1936, to the Research Laboratories of the General Electric Company, Ltd., Wembley, by the kind invitation of the Director, Mr C. C. Paterson. During the tour of the laboratories many interesting demonstrations were shown by members of the staff. About 220 members and friends were present.

THE GUTHRIE LECTURE

The Twenty-first Guthrie Lecture was delivered on May 15, 1936, by Professor F. A. Lindemann, F.R.S., who took as his subject "Physical Ultimates".

THE DUDDELL MEDAL

The Council has awarded the Fourteenth Duddell Medal to Professor W. G. Cady of the Wesleyan University, Middletown, Connecticut, U.S.A., for his work on quartz resonators.

ANNUAL EXHIBITION

The Twenty-seventh Annual Exhibition was held on January 5, 6 and 7, 1937, at the Imperial College of Science and Technology, by the courtesy of the Governing Body.

Seventy-eight firms exhibited their products in the Trade Section and four firms displayed technical literature. In addition to the Trade Section there were nineteen exhibits in the Research and Educational Section contributed by Research Associations, Government and Industrial Laboratories and private individuals. As in previous years, the exhibits entered for the Apprentices and Learners Competition held in conjunction with the Exhibition were on view. The attendance during the three days was over 7000.

The following discourses were given:

"Electrical Measurements in the 'Eighties, particularly those associated with Ayrton and Perry", by Sir James Swinburne, M.I.E.E., F.R.S.

"The Influence of Industrial Research on the Development of Scientific Instruments", by Harry Moore, D.Sc., A.R.C.S., F.Inst.P.

PROGRESS REPORTS

The sales of Volume II have been very satisfactory and the stock is now almost exhausted.

Volume III was published recently and will be found to be as comprehensive in scope as the two preceding volumes.

SPECIAL OPTICAL MEETINGS

A new series of meetings to be devoted to the discussion of optical subjects has been inaugurated. These meetings are additional to the ordinary science meetings held on Fridays, and take place as frequently as the offer of suitable papers, demonstrations, lectures or discussions permits. The time and place of meeting is chosen to suit the convenience of members engaged in the optical industry. The first meeting of this series was held on December 3, 1936, and details are given in another section of the report.

APPOINTMENT OF ASSISTANT SECRETARY

The Council has appointed Miss J. I. Dennis Assistant Secretary.

HERBERT SPENCER LEGACY

A legacy of £1241 was bequeathed to the Society during the year by the late Herbert Spencer. It has been decided that part of this legacy may be used for grants to Fellows of the Society who are undertaking research in some branch of physical science which involves the construction of special apparatus, the cost of which cannot be otherwise provided for. Another part of this legacy has been allocated to the Joint Library Committee for the purpose of repairing books of historic interest.

CONFERENCE AT BRISTOL

An Informal Conference on the Conduction of Electricity in Solids and allied subjects has been arranged under the joint auspices of the Physical Society and the University of Bristol at the H. H. Wills Physical Laboratory, University of Bristol, from Tuesday, July 13, to Friday, July 16, 1937.

REPRESENTATION ON OTHER BODIES

The Physical Society has been represented on other bodies as follows:

British National Committee for Physics: Mr T. Smith, Dr E. Griffiths, Mr J. H. Awbery, Professor A. M. Tyndall.

British National Committee for Scientific Radio: Professor E. V. Appleton, Dr A. B. Wood, Professor L. S. Palmer.

Committee of Management of Science Abstracts: Professor A. Ferguson, Dr D. Owen, Mr J. H. Awbery, Dr W. Jevons.

Board of the Institute of Physics: Dr D. Owen, Dr A. B. Wood.

Joint Committee on Symbols for Thermodynamics: Professor A. Ferguson, Mr J. H. Awbery, Professor A. C. Egerton, Professor G. I. Finch.

British Standards Institution Committee on Optical Projection Apparatus: Professor A. F. C. Pollard, Dr R. S. Clay.

British Standards Institution Committee on Radio Interference Suppression: Professor G. I. Finch.

Organizing Committee for a Discussion on Lubrication and Lubricants (Institution of Mechanical Engineers): Professor G. I. Finch.

OBITUARY

The Council records with deep regret the deaths of the following Fellows: Professor A. Anderson, Mr D. J. Blaikley, Sir Henry H. Cunynghame, Mr W. W. Drury, Professor G. Forbes, Mr C. E. Haselfoot, Mr C. E. Holland, Dr C. V. Jackson, Sir Herbert Jackson, Mr A. C. Jolley, Mr J. A. Morrow, Sir Joseph E. Petavel, Professor J. Rice, Mr J. Rose-Innes, Dr J. H. Vincent, Dr R. S. Willows.

MEMBERSHIP ROLL AT DECEMBER 31, 1936

	Total Dec. 31, 1935	Changes during 1936				Total Dec. 31, 1936
Honorary Fellows	11				–	11
Honorary Fellows (Optical Society)	7				–	7
Ex-officio Fellows	4				–	4
Ordinary Fellows	940	Elected		36		
		Student transfers ...		5		
				41		
		Deceased	14			
		Resigned or lapsed ...	22			
				36		
		Net change			5	945
Students	84	Elected		15		
		Transferred to Fellows	5			
		Resigned or lapsed ...	8			
				13		
		Net increase			2	86
Total Membership	1046	Net increase			7	1053

REPORT OF THE HONORARY TREASURER

The accounts reveal a satisfactory financial position. The anticipated saving in the cost of the "Proceedings" mentioned in last year's report has been realized.

The Society desires to thank the Council of the Royal Society for a grant of £100 towards the cost of publications.

The Society's investments have been valued at market prices on December 31st, 1936 through the courtesy of the Manager of the Charing Cross Branch of the Westminster Bank.

(Signed) ROBERT W. PAUL
Honorary Treasurer

February 18*th*, 1937

INCOME AND EXPENDITURE ACCOUNT FOR THE YEAR ENDED 31ST DECEMBER, 1936

1935 £	s.	d.	EXPENDITURE	£	s.	d.	£	s.	d.
			To						
583	*0*	*0*	"Science Abstracts"				501	0	0
			Normal Publications:						
2299	*17*	*0*	"Proceedings" and Exhibition Catalogue	1790	2	6			
39	*19*	*11*	Notices	39	8	6			
204	*5*	*11*	Editorial and General Expenses .	201	2	10			
							2030	13	10
			Special Publications:						
514	*2*	*7*	"Reports on Progress in Physics" (Vol. II)				714	15	1
634	*11*	*5*	"*Reports of International Conference*"						
350	*15*	*2*	Postage on Normal Publications and General Correspondence . . .				310	9	5
32	*19*	*0*	Expenses at Meetings . . .				34	16	8
8	*18*	*11*	Periodicals and Library . . .				6	15	11
			Institute of Physics:						
528	*16*	*0*	Clerical Assistance and Office Expenses	625	3	0			
272	*13*	*4*	Electricity, Labour and Sundries in connexion with Exhibition . . .	295	5	0			
							920	8	0
92	*3*	*9*	Sundry Expenses				97	6	5
40	*0*	*0*	Honoraria to Lecturers . . .				20	0	0
49	*7*	*1*	*Printing and despatching List of Members*						
			Balance, being excess of Income over Expenditure, carried forward to Accumulated Fund				616	5	11
£5651	*10*	*1*					£5252	11	3

1935 £	s.	d.	INCOME	£	s.	d.	£	s.	d.
			By						
			Subscriptions:						
56	*14*	*0*	Entrance Fees	35	14	0			
1654	*18*	*10*	Fellows*	1687	6	2			
4	*4*	*0*	Voluntary†	4	4	0			
39	*13*	*6*	Students	44	2	0			
109	*0*	*9*	For "Science Abstracts" and Advance Proofs	114	3	7			
							1885	9	9
30	*0*	*0*	Transfer from Life Composition Fund of amounts paid by Fellows now deceased				70	0	0
			Sales:						
955	*11*	*2*	Normal Publications . . .	927	6	10			
569	*11*	*11*	International Conference Reports .	112	1	9			
514	*11*	*10*	"Progress Reports" (Vol. II) . .	749	17	9			
							1789	6	4
396	*2*	*3*	Advertisements in Publications . .				409	9	8
			Dividends from Investments . .	270	9	2			
			Less Transfer to Duddell Memorial Fund	14	0	0			
258	*11*	*2*					256	9	2
			Royal Society Grant for Publications				100	0	0
774	*2*	*7*	Exhibitors' and other Payments on account of Exhibition				741	16	4
288	*8*	*1*	*Balance, being excess of Expenditure over Income, carried forward to Accumulated Fund*						
£5651	*10*	*1*					£5252	11	8

---

* Eighty-eight Fellows paid reduced subscriptions by the arrangement with the Institute of Physics, the total rebate being £34. 10*s.* 2*d.*

† Voluntary subscriptions are subscriptions paid by Fellows who compounded for the low sum of £10.

BALANCE SHEET AS ON 31ST DECEMBER, 1936

LIABILITIES	£	s.	d.	£	s.	d.	£	s.	d.
Sundry Creditors				1264	14	3			
Life Compositions:									
As on December 31, 1935 . .	1562	10	0						
Add Payment during year . .	31	10	0						
	1594	0	0						
Less Transfer to Income and Expenditure Account of amounts paid by Fellows now deceased .	70	0	0	1524	0	0			
Subscriptions paid in advance:									
Members	61	3	9						
Publications	154	4	11	215	8	8	3004	2	11
SPECIAL FUNDS									
W. F. Stanley Trust Fund . . .				397	0	0			
Duddell Memorial Trust Fund . .				430	0	9			
Optical Convention 1926, Trust Account				49	1	8			
Special Reports on Physics Account .				83	1	0			
Herbert Spencer Legacy . . .				1241	0	0	2200	3	5
GENERAL FUND									
Accumulated Fund:									
As on December 31, 1935 . .				3546	0	9			
Add Increase in value of Investments				15	18	0			
Add Balance of Income and Expenditure Account . . .				616	5	11			
				4178	4	8			
A. W. Scott Bequest . . .				174	15	3	4352	19	11
							£9557	6	3

ASSETS	£	s.	d.	£	s.	d.
Investments at Market Value on December 31*st*, 1936:						
£2100 Consolidated Stock 2½%	1768	0	0			
£1000 War Loan 3½% Inscribed "A" Account .	1052	0	0			
£750 War Loan 3½% Registered	788	0	0			
£650 Funding Loan 4%	752	0	0			
£500 India 3½% Stock	490	0	0			
£400 Lancaster Corporation 3%	388	0	0			
£399 London Midland and Scottish Railway 4% Debenture Stock	426	0	0			
£1000 London Midland and Scottish Railway 4% Preference Stock	905	0	0			
£500 London and North Eastern Railway 4% Debenture Stock	530	0	0			
£150 Southern Railway 5% Debenture Stock .	201	0	0			
£300 Southern Railway Preferred Ordinary Stock .	285	0	0			
£442 Southern Railway Deferred Ordinary Stock .	112	0	0			
£400 War Loan 3½% Inscribed "B" Account .	421	0	0	8118	0	0
Dividends due from Investments				38	12	10
Inland Revenue—Income Tax claimed for 1936 . .				18	12	9
Subscriptions due				16	5	6
Sundry Debtors				158	14	1
Cash at Bank: Current	694	19	10			
Cash on Deposit	500	0	0			
Cash in hand	12	1	3	1207	1	1
				£9557	6	3

NOTE: These accounts do not include the usual liabilities incurred in 1936 in respect of publications to be issued in 1937, amounting to approximately £953.

Stock of publications on December 31st, 1936. At Honorary Treasurer's valuation . . . £1410. 3*s*. 0*d*.

ROBERT W. PAUL, *Honorary Treasurer.*

We have audited the above Balance Sheet and have obtained all the information and explanations we have required. We have verified the bank balances and the Investments. In our opinion such Balance Sheet is properly drawn up so as to exhibit a true and correct view of the state of the Society's affairs according to the best of our information and the explanations given to us and as shown by the books of the Society.

SPENCER HOUSE, SOUTH PLACE, E.C. 2
February 18*th*, 1937.

KNOX, CROPPER & CO.,
Chartered Accountants.

LIFE COMPOSITION FUND ON DECEMBER 31ST, 1936

	£	s.	d.
45 Fellows paid £10	450	0	0
1 Fellow paid £15	15	0	0
16 Fellows paid £21	336	0	0
1 Fellow paid £30	30	0	0
22 Fellows paid £31. 10s.	693	0	0
	£1524	0	0

SPECIAL FUNDS

W. F. STANLEY TRUST FUND

	£	s.	d.		£	s.	d.
Carried to Balance Sheet	397	0	0	£300 Southern Railway Preferred Ordinary Stock	285	0	0
				£442 Southern Railway Deferred Ordinary Stock	112	0	0
	£397	0	0		£397	0	0

DUDDELL MEMORIAL TRUST FUND

CAPITAL

	£	s.	d.		£	s.	d.
Carried to Balance Sheet	421	0	0	£400 War Loan 3½% Inscribed "B" Account	421	0	0

REVENUE

	£	s.	d.		£	s.	d.
Engraving medals	12	12	0	Balance on December 31st, 1935	22	12	9
Honorarium to Medallist	15	0	0	Interest	14	0	0
Balance carried to Balance Sheet	9	0	9				
	£36	12	9		£36	12	9

OPTICAL CONVENTION, 1926, TRUST ACCOUNT

	£	s.	d.		£	s.	d.
Balance carried to Balance Sheet	49	1	8	Balance on December 31st, 1935	39	11	9
				Sales of Publications	9	9	11
	£49	1	8		£49	1	8

A. W. SCOTT BEQUEST

	£	s.	d.		£	s.	d.
Expenses in connexion with Library	11	4	3	Balance on December 31st, 1935	185	19	6
Balance carried to Balance Sheet	174	15	3				
	£185	19	6		£185	19	6

"SPECIAL REPORTS ON PHYSICS" ACCOUNT

	£	s.	d.		£	s.	d.
Balance carried to Balance Sheet	83	1	0	Balance on December 31st, 1935	83	1	0

HERBERT SPENCER LEGACY

	£	s.	d.		£	s.	d.
Balance carried to Balance Sheet	1241	0	0	Cash received during year	1241	0	0

REPORT

OF A

JOINT COMMITTEE

OF

THE CHEMICAL SOCIETY,
THE FARADAY SOCIETY,
AND THE PHYSICAL SOCIETY

ON

SYMBOLS

FOR

THERMODYNAMICAL AND PHYSICO-CHEMICAL QUANTITIES

AND

CONVENTIONS

RELATING TO THEIR USE

ADOPTED AS RECOMMENDED PRACTICE
in
The Proceedings of the Physical Society,
The Transactions of the Faraday Society,
The Journal of the Chemical Society,
and
British Chemical Abstracts

Members of any of the three Societies may obtain extra copies of this Report at 4*d*. per copy or 5*s*. per 25 copies, post free, on application to the Secretary of the appropriate Society.

Non-members may purchase copies of the Report at 6*d*. per copy or 7*s*. 6*d*. per 25 copies, post free, from the Assistant Secretary, The Chemical Society, Burlington House, Piccadilly, London, W.1.

PART I.

INTRODUCTION.

The objects of the Joint Committee have been :

(i) **To correlate the views of chemists and physicists with regard to the use of symbols for quantities employed in thermodynamics, and to eliminate as far as possible the confusion that has arisen through the considerable diversity of usage in this field** (see Part II below).

(ii) **To deal similarly with symbols for other quantities which are of interest to both chemists and physicists** (see Part III below).

The Joint Committee has examined the recommendations contained in the published reports of other bodies which have been concerned with symbols in recent years. In regard to symbols for thermodynamical quantities, particular attention was given to the "Report on Symbols, Units, and Nomenclature" of the International Conference on Physics (1934); and in regard to symbols for physico-chemical quantities, to the old "List of Physico-Chemical Symbols" which the Chemical Society had decided to revise, and to a provisional draft of "Standard Chemical Symbols and Abbreviations", drawn up recently by the British Standards Institution (largely on the basis of the old Chemical Society list).

Through the good offices of Mr. Sanford A. Moss, of the American Standards Association, an interim report of the Joint Committee was communicated informally to an "Informal International Conference on Letter Symbols for Heat and Thermodynamics" held in New York in September 1936; and the Joint Committee has had access to an advance copy of a preliminary report of this Conference. Consideration has also been given to a "Preliminary List of Abbreviations" recently circulated by the Royal Society.

The Joint Committee has given due consideration to usages adopted by authors of well-known text-books on relevant subjects; and to special lists of symbols in current use by workers in various fields, drawn up by individual members of the Committee.

In submitting this Report the Joint Committee wishes to draw attention to the fact that although recommendations regarding the use of physico-chemical symbols have been put forward in the past by a number of committees, these bodies have nearly always been representative of *either* physicists *or* chemists, and not as in the present instance of both.

In carrying out its work the Joint Committee has been guided by the following principles :

(i) **Symbols and conventions regarding their use should be chosen from among those already widely adopted, unless there are definite objections to all current usages.**

In choosing between possible alternative symbols and conventions preference should be given, in general, to the **practice and needs of chemists and physicists,** and to practice in English-speaking countries.

It is fully recognised that it would be highly advantageous to secure complete agreement with workers in fields other than chemistry and physics—especially with engineers in regard to thermodynamical symbols. It has to be realised, however, that this involves special difficulties, due not only to the strong feelings which workers in particular fields hold in favour of their accustomed symbols, but also to the *limited number of alphabets and founts* available for the representation of the large number of quantities to be referred to in the various branches of science and technology. Nevertheless, care has been taken to avoid as far as possible any direct conflict with established usage in related fields, and thus to leave open the way to a wider range of agreement in the future.

Where general agreement on preference for a particular symbol or convention is not reached, **alternatives** should be given; but one of such alternatives may be indicated as the **first preference.**

(ii) **Symbols for quantities constituting a well-defined class should, if possible, belong to the same alphabet, fount, and case, which should be such as to permit of modification in accordance with a uniform scheme for the representation of any important series of corresponding derived quantities.**

Methods of modifying symbols by means of **subscripts, superscripts, etc.** should be systematised as far as possible.

(iii) **There should bo no departure from the standard practice of mathematicians regarding the use of signs, operator symbols, etc.**

It is recognised that the detailed recommendations contained in Parts II and III of the Report will not cover all the requirements of workers in any particular field, but it is hoped that they will afford a common basis for practice in a wide range of specialised branches of science.

An important advance towards uniformity of usage will have been achieved if the quantities which appear in the lists below are represented whenever possible by the symbol recommended, or, when this is not possible, by an alternative symbol chosen in accordance with the principles set forth above. It is realised that owing to the limited number of available alphabets many of the symbols appearing in the following lists will have to be used in certain branches of science for quantities which are not referred to in this Report. There can be no objection to this provided that there is no danger of confusion with the quantities which the symbol represents in the lists below.

PART II.

SYMBOLS FOR QUANTITIES EMPLOYED IN GENERAL THERMODYNAMICS, WITH CONVENTIONS RELATING TO THEIR USE.

(Where two or more symbols separated by commas are given for a quantity, these symbols are to be regarded as alternatives for which no preference is expressed. On the other hand, where two symbols are separated by a dotted line, the former is the first preference.)

1. Quantities of energy entering or leaving a system: general symbols:

Heat	q
*Work	w . . . W

For **heat** entering the system q is positive; for heat leaving the system it is negative. The symbol q should never be used with the opposite convention as to sign.

For **work** the question of sign is left open, for, although there is much support on historical grounds and from the standpoint of convenience in certain relations for treating work done *by* the system as positive, there is also support for the reverse convention which would result in all forms of energy entering the system being treated as positive.

Subscripts p, v, T, etc., may be added to either of the above symbols to indicate conditions of constant pressure, volume, temperature, etc. The subscript q may be added to w or W to indicate adiabatic conditions, and the subscript w to q to show that no work is done in a process.

2. General properties of the System itself.

Temperature, on absolute scale, (°K)	T
Pressure	p, P
Volume	v, V
General thermodynamic functions	
intrinsic energy	U . . . E
enthalpy, total heat, or heat content	H ($= U + pv$) †
entropy	S
*free energy (Helmholtz)	A . . . F ($= U - TS$)
thermodynamic potential, Gibbs function, or free energy (Lewis and Randall)	G ($= H - TS$)

---

* In an endeavour to attain international uniformity, the suggestion that A should be used as the preferred symbol for Helmholtz free energy has been adopted. It is important, therefore, that this symbol shall *not* be used to denote the work done by or on a system.

† May also be defined in terms of generalised forces and co-ordinates as $U + \Sigma Xx$, where X corresponds to p and x to v.

Heat capacity per gram (specific heat)	
at constant volume	c_v
at constant pressure	c_p
per mol (molecular heat)	
at constant volume	C_v
at constant pressure	C_p
Ratio of specific heats	γ
Latent heat per gram	l
per mol	L
Heat of reaction	see note below
Vapour pressure constant	i
Chemical potential	μ
Activity	a

The above symbols represent the magnitudes of the properties specified and should not be used, either by themselves or with the addition of suffixes or bars, to denote changes in these magnitudes. An *increase* in a property X should be denoted by ΔX, and a *decrease* by $-\Delta X$, or, if the change is *very small*, by δX and $-\delta X$ respectively. The forms dX and ∂X should be used only for the respective *differential* and *partial differential.*

The value of a property X for a particular system or for a system in a particular state may be indicated by means of a numeral subscript, e.g. X_{I}, X_{II}, X_1, X_2, etc. An increase in the value of X when the system changes from state 1 to state 2, may be represented by $(\Delta X)_{1,2}$ or $(\Delta X)_{1\rightarrow 2}$ $(= X_2 - X_1)$.

Subscripts A, B, C, etc. may be used for reference to the molecular species A, B, C, etc.

Note on Heat of Reaction:

It is recommended that all thermochemical data be expressed by quoting the equation of the chemical reaction followed by the value of ΔH or ΔU: e.g. for the heat of reaction at a constant pressure of 1 atmosphere—

$CH_3OH(liq.) + 1\frac{1}{2}O_2(gas) = CO_2(gas) + 2H_2O(liq.)$; $\Delta H_{298} = -173{,}630$ cal.

and for the heat of reaction at constant volume: $\Delta U_{298} = -173{,}330$ cal.

The use of a special symbol, such as Q, to denote the heat *evolved* in a chemical reaction—as was formerly customary in thermochemistry—is not recommended. The most important point is, however, that in using ΔU, ΔH, (or the general symbol q) to denote heat of reaction they must have a positive value for an endothermic reaction and a negative value for an exothermic reaction.

PART III.

SYMBOLS FOR PHYSICO-CHEMICAL QUANTITIES, WITH CONVENTIONS RELATING TO THEIR USE.

(including symbols for thermodynamic quantities given in Part II.)

A. GENERAL RECOMMENDATIONS REGARDING ALPHABETS AND FOUNTS.

In order to make the best use of the limited number of alphabets and founts commonly available and thus minimise the number of uses to which each letter in a given fount and case is put, the following recommendations are made :

(a) **Symbols for quantities** (except purely mathematical constants—see (b) below) should be printed in *italic* (*not* roman) type when they are not greek. See list below, B (2).

It is recommended that **symbols for certain important physical constants in common use**—see list below, B (1)—should be printed in ***black italic*** type. This will relieve the pressure on certain overworked letters and have the advantage that symbols for these quantities having known constant values will stand out against symbols for variables in equations. It is understood that all reputable printers can supply black italic in addition to Clarendon and other black types, so that there should be no risk of confusion with the broad-faced black roman type commonly employed for representing vector quantities. In writing, as distinct from printing, it is suggested that where possible the symbols for these physical constants be represented by cursive letters, e.g. $\mathscr{F}$ as distinct from F, or, especially in blackboard writing, by means of a different colour. In typescript these symbols may be underlined in red, to distinguish them from those to be printed in ordinary italic (underlined in black).

(b) **Symbols for purely mathematical constants and symbols denoting mathematical operations**—see list below, B (3a)—should be printed in roman (*not* italic) type when they are not greek.

(c) **Symbols for the chemical elements** should always be printed in roman type.

(d) **Abbreviations for words**—as distinct from symbols for quantities—should be printed in roman type and followed by a full stop. Examples of single-letter abbreviations are given below, B (3b).

Single capital letters used as abbreviations should be printed in SMALL ROMAN TYPE so that they stand out in the text and are readily distinguished from symbols for the chemical elements.

B. LISTS OF RECOMMENDED SYMBOLS AND CONVENTIONS,

including single-letter abbreviations.

(*Where two or more symbols separated by commas or semicolons are given for a quantity, these symbols are to be regarded as alternatives for which no preference is expressed. On the other hand, where two symbols are separated by a dotted line, the former is the first preference.*)

1. To be Printed in Black Italic.

(*Certain important physical constants.*)

$\boldsymbol{F}$	Faraday's constant.
$\boldsymbol{J}$	Mechanical equivalent of heat.
$\boldsymbol{N}$	Avogadro's number.
$\boldsymbol{R}$	Gas constant per mol. Rydberg's constant.
$\boldsymbol{c}$	Velocity of light in vacuo.
$\boldsymbol{e}$	Electronic charge (charge equal and opposite in sign to that of an electron).
$\boldsymbol{g}$	Acceleration due to gravity (standard value, if variation from standard is significant).
$\boldsymbol{h}$	Planck's constant.
$\boldsymbol{k}$	Boltzmann's constant.
$\boldsymbol{m}$	Rest mass of an electron.

2. To be Printed in Ordinary Italic, when not Greek.

General Physics and Chemistry.

Length	l
mean free path of molecules	
height	h
diameter, distance	d
diameter of molecules	σ
radius	r
Mass	m
molecular weight	M
atomic weight	A
atomic number	Z
gram-equivalent weight	Z, J
Time	t
time interval, especially half- or mean-life	τ
frequency	ν
Velocity	v; c, (u, v, w)
of ions	u (with subscript)
angular	ω
Acceleration	f . . . a
due to gravity (as variable)	g

Force	F, (X, Y, Z)
Moment of inertia	I
Pressure	p, P
especially osmotic	Π
Volume	v, V
Density	$\rho \ldots d$
Compressibility	$\kappa \ldots K$
Viscosity	η
Fluidity	ϕ
Surface area	$A \ldots s$
Angle of contact	θ
Surface tension	$\gamma \ldots \sigma$
Parachor	$[P]$
Surface concentration excess	Γ
Number of mols	n
Concentration, mol fraction	N, x
in other terms	c, C
Solubility	s
Diffusion coefficient	D
Chemical equilibrium constant (products/reactants)	K
solubility product	$K_s \ldots L$
Velocity constant of chemical reaction	k
Number of molecular collisions per second	Z
Partition function	f
Efficiency, of any process	η
Wave function	ψ

Heat and Thermodynamics.

Temperature, on absolute scale, (°K)	T
on other scales	$\theta \ldots t$
Thermal conductivity	k
Energy (general symbol)	E
Work done by or on a system	$w \ldots W$
Heat entering a system	q
Specific heat	c_p and c_v
molecular heat	C_p and C_v
Ratio of specific heats	γ
Latent heat, per g.	l
per mol	L
Intrinsic energy	$U \ldots E$
Enthalpy, total heat, or heat content	H
Entropy	S
Free energy (Helmholtz)	$A \ldots F$
Thermodynamic potential, Gibbs function, free energy (G. N. Lewis)	G

Vapour pressure constant	i
Chemical potential	μ
Activity	a
coefficient (for molar concentration)	f
Osmotic coefficient	g
Van 't Hoff's factor	i

Electricity.

Quantity of electricity	Q
especially electrostatic charge	e
Potential (difference)	V
Volta potential	
electrokinetic potential	ζ
especially electromotive force of voltaic cells	E
Potential gradient, in electric field	X
Electronic exit work function	ϕ
Current	I
Resistance	R
specific resistance	ρ . . . r
specific conductance	κ . . . σ
Inductance, self	L
mutual	M
Electrostatic capacity	C
Dielectric constant	ϵ
Dipole moment	μ

Electrochemistry.

Degree of electrolytic dissociation	α
Valency of an ion	z
Ionic strength	I
Equivalent conductance	Λ
equivalent ionic conductance, "mobility"	l (with subscript)
Transport number	T (with subscript) . . . n (with subscript)
Single electrode potential	e (with subscript), E (with subscript)
Electrolytic polarisation, overvoltage	η . . . π

Magnetism.

Magnetic field strength	H
flux	ϕ
permeability	μ
susceptibility—volume	κ
mass	χ
moment	M
induction	B

Optics.

Wave length	λ
Wave number	ν
Intensity of light	I
Refractive index	n (with subscript) . . . μ (with subscript)
specific refraction	r (with subscript)
molecular refraction	$[R]$ (with subscript)
Molar extinction coefficient	ϵ
Angle of (optical) rotation	α
specific rotation	$[\alpha]$
Specific magnetic rotation	ω

3. To be Printed in Roman, when not Greek.

(a) *Examples of Mathematical Constants and Operators.*

Base of natural logarithms	e
Ratio of circumference to diameter	π
Differential	d
partial	∂
Increment	Δ
very small increment	δ
Sum	Σ
Product	Π
Function	f, φ

(b) *Examples of single-letter abbreviations.*

*Ampère (in sub-units)	a.
Volt	v.
Ohm	Ω.
Watt	w.
Farad	F.
Henry	H.
Centigrade	C.
Fahrenheit	F.
Kelvin	K.
Ångstrom unit	A.
micron	μ.
metre	m.
gram	g.
litre	l.
Röntgen unit	r.
†Normal (concentration)	N.
†Molar (concentration)	M.

---

* *E.g.* " ma." for " milliampère "; but " amp." is preferred for " ampère."

† Separated by a hyphen (and no full stop) from a chemical formula which follows it.

The following prefixes to abbreviations for the names of units should be used to indicate the specified multiples or sub-multiples of these units:

M	mega-	$10^{6} \times$
k	kilo-	$10^{3} \times$
d	deci-	$10^{-1} \times$
c	centi-	$10^{-2} \times$
m	milli-	$10^{-3} \times$
μ	micro-	$10^{-6} \times$

e.g., MΩ. denotes megohm; kw., kilowatt; and μg., microgram. The use of μμ. instead of mμ. to denote 10^{-7} cm., or of γ to denote microgram is deprecated.

4. Subscripts and other Modifying Signs.

(a) *Subscripts to symbols for quantities.*

I, II . . . 1, 2 .	*especially with symbols for thermodynamic functions*, referring to different systems or different states of a system.
A, B .	referring to molecular species A, B, etc.
i	referring to a typical ionic species i.
u	referring to an undissociated molecule.
+, −	referring to a positive or negative ion, or to a positive or negative electrode.
p, *v*, *T*	indicating constant pressure, volume, and temperature respectively.
q	indicating adiabatic conditions.
w	indicating that no work is performed.
p, *c*, *a*	*with symbol for an equilibrium constant*, indicating that it is expressed in terms of pressure, concentration, or activity.
G, V, L X	referring to gas, vapour, liquid, and crystalline states, respectively.
f, e, s, t, d	referring to fusion, evaporation (vaporisation of liquid), sublimation, transition, and dissolution or dilution respectively.
c	referring to the critical state or indicating a critical value.
0	referring to a standard state, or indicating limiting value at infinite dilution.
C, D, F	*with symbols for optical properties*, referring to a particular wavelength.

Where a subscript has to be added to a symbol which already carries a subscript, the two subscripts may be separated by a comma or the symbol with the first subscript may be enclosed in parentheses with the second subscript outside.

(b) *Other modifying signs.*

o	*as right-hand superscript to symbol*, referring to a standard state.
[ ]	*enclosing formula of chemical substance*, indicating its molar concentration.
{ }	*enclosing formula of chemical substance*, indicating its molar activity.

In crystallography it is recommended that:

Millerian indices be enclosed in parentheses, ( );
Laue indices be unenclosed;
Indices of a plane family be enclosed in braces, { };
Indices of a zone axis or line be enclosed in brackets, [ ].

Numerals attached to a symbol for a chemical element in various positions have the following meanings:

upper left	mass number of atom.
lower left	nuclear charge of atom.
lower right	number of atoms in molecule.

e.g., $^{7}_{3}\mathrm{Li}$; $^{2}_{1}\mathrm{H}_2$ (= D_2).

C. ALPHABETICAL INDEX OF RECOMMENDED SYMBOLS, and single-letter abbreviations.

including all those given in the above lists (Section B) except prefixes, subscripts and other modifying signs.

The name of any quantity for which a given symbol is a second preference is printed in parentheses.

A	free energy—Helmholtz; atomic weight; surface area.
A.	Ångstrom unit.
a	activity; (acceleration).
a.	ampère, in sub-units—see footnote, p. 11.
B	magnetic induction.
C	concentration; electrostatic capacity.
	with subscript: molecular heat capacity.
C.	Centigrade.
$\mathbf{c}$	velocity of light in vacuo.
c	velocity; concentration.
	with subscript: specific heat.
D	diffusion coefficient.
d	diameter; distance; (density).
d	differential.
∂	partial differential.
E	energy; (intrinsic energy); potential difference, especially electromotive force of voltaic cells.
	with subscript: single electrode potential.
$\boldsymbol{e}$	electronic charge—charge equal and opposite in sign to that of an electron.
e	quantity of electricity, especially electrostatic charge.
	with subscript: single electrode potential.
e	base of natural logarithms.
$\boldsymbol{F}$	Faraday's constant.
F	force; (free energy—Helmholtz).
F.	farad, Fahrenheit.
f	acceleration; activity coefficient, for molar concentration; partition function.

f	function.
G	thermodynamic potential, Gibbs function, free energy—G. N. Lewis.
$\boldsymbol{g}$	acceleration due to gravity, standard value.
g	acceleration due to gravity, as a variable; osmotic coefficient.
g.	gram.
H	enthalpy, total heat, heat content; magnetic field strength.
H.	henry.
$\boldsymbol{h}$	Planck's constant.
h	height.
I	moment of inertia; ionic strength; electric current; intensity of light.
i	vapour pressure constant; van 't Hoff's factor.
$\boldsymbol{J}$	mechanical equivalent of heat.
J	gram-equivalent weight.
K	chemical equilibrium constant; (compressibility).
	K_s solubility product.
K.	Kelvin.
$\boldsymbol{k}$	Boltzmann's constant.
k	thermal conductivity; velocity constant of chemical reaction.
L	latent heat per mol; self inductance; (solubility product).
l	latent heat per g.; length; mean free path of molecules.
	with subscript: equivalent ionic conductance, " mobility ".
l.	litre.
M	molecular weight; mutual inductance; magnetic moment.
M.	molar concentration.
$\boldsymbol{m}$	rest mass of an electron.
m	mass.
m.	metre.
$\boldsymbol{N}$	Avogadro's number.
N	mol fraction.
N.	normal concentration.
n	number of mols.
	with subscript: (transport number).
	with subscript: refractive index.
P	pressure.
$[P]$	parachor.
p	pressure.
Q	quantity of electricity.
q	heat entering a system.
$\boldsymbol{R}$	gas constant per mol; Rydberg's constant.
R	electrical resistance.
$[R]$	*with subscript:* molecular refraction.
r	radius; (specific resistance).
	with subscript: specific refraction.
r.	Röntgen unit.
S	entropy.
s	solubility; (surface area).
T	temperature, on absolute Kelvin scale.
	with subscript: transport number.
t	time; (temperature—not on absolute scale).

U	intrinsic energy.
u	velocity component. *with subscript:* velocity of ions.
V	volume; potential, potential difference, including Volta potential.
v.	volt.
v	volume; velocity; velocity component.
W	(work done by or on a system).
w.	watt.
w	work done by or on a system; velocity component.
X	force component; potential gradient in electric field.
x	mol fraction.
Y	force component.
Z	force component; g.-equivalent weight; number of molecular collisions per second; atomic number.
z	valency of an ion.
α	degree of electrolytic dissociation; angle of optical rotation.
$[\alpha]$	specific optical rotation.
$\mathit{\Gamma}$	surface concentration excess.
γ	ratio of specific heats; surface tension.
Δ	increment.
δ	very small increment.
ϵ	dielectric constant; molar extinction coefficient.
ζ	electrokinetic potential.
η	efficiency of any process; viscosity; electrolytic polarisation, overvoltage.
θ	angle of contact; temperature—not on absolute scale.
κ	compressibility; specific conductance; magnetic susceptibility—volume.
$\mathit{\Lambda}$	equivalent conductance.
λ	wave length.
μ	chemical potential; dipole moment; magnetic permeability. *with subscript:* (refractive index).
μ.	micron.
ν	frequency; wave number.
$\mathit{\Pi}$	pressure, especially osmotic pressure.
Π	product.
π	(electrolytic polarisation, overvoltage).
π	ratio of circumference to diameter.
ρ	density; specific resistance.
Σ	sum.
σ	diameter of molecules; (surface tension); (specific conductance).
τ	time interval, especially half or mean life.
ϕ	fluidity; electronic exit work function; magnetic flux.
φ	function.
χ	magnetic susceptibility—mass.
ψ	wave function.
Ω.	ohm.
ω	angular velocity; specific magnetic rotation.

Note.—The following distinctive letters have not been used in the above lists:

Italic capitals: O.
Lower case italic: b, j, o, y.
Greek capitals: Θ, Ξ, Υ, Φ, Ψ.
Lower case greek: β, ξ.

J. H. AWBERY.
F. G. DONNAN.
A. C. G. EGERTON.
H. J. T. ELLINGHAM.
A. FERGUSON.
G. I. FINCH.
C. F. GOODEVE.
J. R. PARTINGTON.
E. K. RIDEAL (*Chairman*).

9*th June*, 1937.

PRINTED IN GREAT BRITAIN BY RICHARD CLAY & SONS, LIMITED,
BUNGAY, SUFFOLK.

THE PROCEEDINGS OF
THE PHYSICAL SOCIETY

VOL. 49, PART 1 *January* 1, 1937 No. 270

FURTHER EXPERIMENTS ON THE PHOTOGRAPHIC ACTION OF GAMMA RAYS AND ON THEIR ABSORPTION COEFFICIENTS

BY J. S. ROGERS, B.A., M.SC., F.INST.P., University of Melbourne

Received 12 *June* 1936. *Read in title* 13 *November* 1936

ABSTRACT. The photographic action of γ rays is intensified by using technical X-ray intensifying screens more than by using lead foil. These intensifying screens, however, intensify the longer wave-lengths more than the shorter. It has been found that the heterochromatic γ-ray spectrum from radium (B + C) can be analysed into two apparently homogeneous components. Both components, however, appear to have an effective wave-length which is shorter the higher the atomic number of the absorbing material. These results can be explained, at least approximately, by a consideration of the absorption of the main lines in the γ-ray spectrum of radium (B + C). This explanation suggests the presence in this spectrum of lines of moderate intensity of wave-length less than 5·6 X.

§ 1. INTENSIFYING-SCREENS FOR γ RAYS

IN two earlier papers(1, 2) an account has been given of the use of the photographic action of γ rays in the determination of the absorption coefficients of the γ rays from radium (B + C) in a number of elements. In these experiments the photographic action was intensified by using thin lead foil on either side of the Agfa duplitized X-ray film, the lead foil increasing the photographic action approximately 1·7 times.

Frilley(3) has mentioned, without giving quantitative results, that the best intensifying screens for γ-ray photography were those used for X-ray diagnosis. It was decided to investigate these. The type of screen used was the Patterson Speed Intensifying Screen of the thin type, which has a highly glossy surface. It was found that such screens used in conjunction with either Agfa or Ilford X-ray duplitized film produced a fairly uniform photographic blackening but not as uniform as that produced when lead intensifying screens were employed.

In these tests an aluminium film holder was made so that the film could be placed (1) between two pieces of aluminium or (2) between two pieces of lead foil or (3) between two pieces of the Patterson Screen. The film was placed, for each intensifier, at the same distance from the source, and distance pieces of aluminium sheet were used on the side of the film distant from the source to ensure that the film should be tightly packed in the film holder. The intensifying action was examined for γ rays from radium (B + C) under two conditions of filtering. In the first a single glass tube containing 100 mg. of radium was employed so that the rays were lightly filtered, partly in the glass wall of the tube and partly by the aluminium of the film holder between source and film. The total filtering amounted approximately to 6 mm. of aluminium. In the second 400 mg. of radium in 4 glass tubes in line was filtered by 1·42 cm. of lead so that the total filtering amounted to the equivalent of 1·6 cm. of lead. With this filtering it has been already shown$^{(3)}$ that the γ rays from radium (B + C) are exponentially absorbed.

The time of exposure was chosen for each method of intensification so that the photographic density was less than 0·8, i.e., in the range of densities for which the density is proportional to the time of exposure. In order that all the films, which were to form one set in a comparison, should be developed under identical conditions they are all developed together and fixed together. The measured photographic actions are set out in table 1 below, in which the photographic action produced with aluminium on both sides of the film is taken as unity.

Table 1.* Relative intensifying action for γ rays. Agfa film

Intensifier	Relative photographic action	
	Filter 6 mm. aluminium	Filter 1·6 cm. lead
Aluminium	1	1
Lead foil	1·70 ± 0·04	1·80 ± 0·06
Patterson screen	5·88 ± 0·02	3·65 ± 0·02
	Ilford film	
Aluminium	1	1
Lead foil	1·66 ± 0·04	1·54 ± 0·02
Patterson screen	6·1	3·9

One interesting point about the results is that there is very little variation in the ratio of the intensifying action of lead to aluminium with the change of filtering, in other words, with the change in effective wave-length of the γ rays. This holds for both types of films examined. On the other hand, when Patterson screens are used, the intensifying action is much greater for lightly filtered radiations, having the longer effective wave-lengths, than for the more heavily filtered radiation.

Thus if a mixed beam of γ rays consisting, say, of a hard and a soft component is to be photographically analysed by absorption in such a way that the relative intensities of the two components are to be measured, it is necessary to use lead intensifying screens. On the other hand, if it is a question of determining an absorption coefficient, then there is no objection to using the X-ray screens provided it can be assumed that the effective wave-length of the beam remains constant as soon as the absorption becomes exponential. When it was decided to measure absorption coefficients under different filterings, in the manner described below under § 4, Patterson X-ray screens were used, as these considerably reduced the time of exposure. It was, however, first necessary to show that the variation of photographic density with time of exposure, for constant intensity of source, was linear over a range of densities. For both Agfa and Ilford films this law was found to hold over the range of densities 0·3 to 0·8. It was necessary also to investigate the variation of density with intensity, and although this was not done directly, it was done by finding, with the films intensified by X-ray screens, the absorption coefficients in lead of the γ rays from radium (B + C) filtered by 1·6 cm. of lead. The results are set out in table 2, in which it will be seen that the same values of the absorption coefficient are obtained, within the limits of experimental error, whether aluminium, lead or Patterson screens are used to intensify the photographic action.

---

* A comparison was also made of the photographic action produced in Agfa and Ilford films exposed under the same conditions. It was found for a filter of 6 mm. of aluminium that the photographic density produced in Ilford was twice that produced in Agfa film, and with a filter of 1·6 cm. of lead the ratio of densities Ilford : Agfa = 1·6.

Table 2. Values of the absorption coefficient in lead

(Filter 1·6 cm. of lead)

Intensifying screen and film	Value of (cm.$^{-1}$)
Aluminium or lead with Agfa	0·532 ± 0·004
Patterson screen with Agfa	0·539 ± 0·008
Patterson screen with Ilford	0·523 ± 0·005

§ 2. THE DEVELOPMENT OF FILMS

In the previous experiments with Agfa film a metol-hydroquinone developer was used, the development taking 5 minutes at 18° C. In any experiment in which different films had to be compared they were developed together under constant agitation to ensure that they should receive the same conditions of development. When, owing to the greater photographic action produced in Ilford film, its use was decided upon, the variation in density produced by varying conditions of development was investigated. A number of pieces of film were exposed under identical conditions to γ rays and these were developed in pairs, together with a piece of unexposed film. From the last-named the density of the chemical fog was measured. The variation of density with time of development (3 to 6 minutes) at 18° C. is shown by curve *A*, figure 1. The variation of density with temperature of developer, for 5 minutes' development, is shown by curves *B* and *C* in the same figure. Curve *B* was obtained with a freshly mixed sample of developer and *C* with the same developer after it had been stored in a dark bottle for 3 days. It will be seen from the curves that if the chemical fog is to be kept below a reasonable amount the temperature of development must not exceed 20° C. for 5 minutes' development. In the experiments described below the temperature of the developer was maintained at 18° C.

§ 3. THE ABSORPTION OF γ RAYS FROM RADIUM (B+C) IN THIN LAYERS OF ALUMINIUM, COPPER, TIN AND LEAD

The absorption in the above four metals was measured before the rays were finally exponentially absorbed. The source was a single glass tube containing about 100 mg. of radium and was supported in front of a wooden block. The filtering of the rays was equivalent to that effected by 6 mm. of aluminium. With one exception the film used was Agfa. Lead intensifying foils were used throughout.

For each thickness of absorber two films were used, and the time of exposure was chosen to produce a density of approximately 0·6. The time to produce a density of 0·6 could then be calculated, and the reciprocal of this time could be used to give a measure of the intensity of the radiations falling on the film. If the logarithm of the intensity was plotted against the thickness of absorber, the curve became straight when the absorption was exponential. From the earlier part of the curve, together with the exponential curve extrapolated back to zero thickness, the intensity of the softer component could be obtained. This softer component was found to be exponentially absorbed, except that the first point on this curve, that corresponding to zero thickness, was above the exponential curve and thus indicated the presence of a still softer component. Figure 2 shows such a curve for tin.

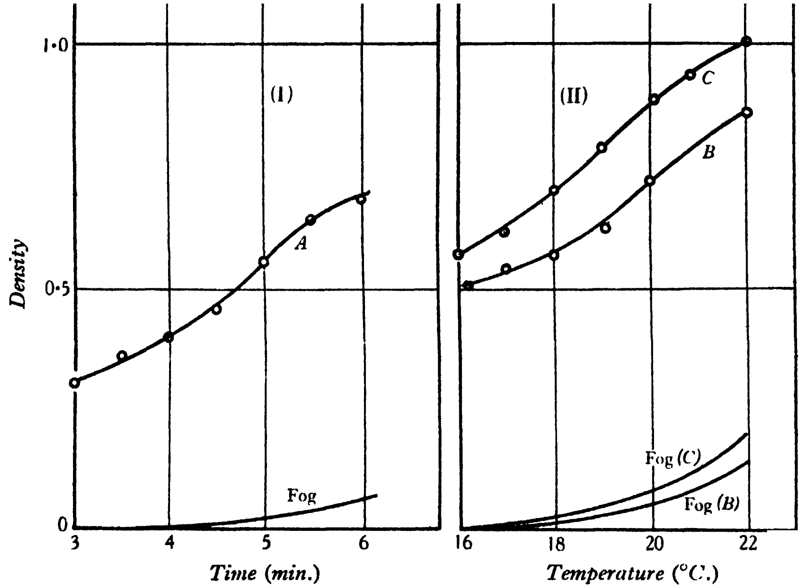

Figure 1. Variation of density with (I) time of development at 18° C.; (II) temperature of developer for time 5 min.

One of the first points that arose from this investigation was that, although the absorption coefficient in aluminium for the harder radiations was the same whether they were filtered in lead or aluminium until the absorption became exponential, the same rule did not hold for copper or tin. Thus the absorption coefficient in copper for γ rays filtered by 1·6 cm. of lead is 0·381 cm.$^{-1}$, but the absorption in copper for rays filtered by copper until the absorption becomes exponential is 0·419 cm.$^{-1}$ For further illustrations of this point see table 5 below.

A summary of the results obtained for the softer radiations is given in table 3. The absorption coefficients μ are given in the second column, the mass absorption coefficients in the third, the ratio of the intensities of the harder to the softer components in the fourth, and the thickness of absorber before the absorption becomes exponential in the fifth. As these absorption coefficients are determined from the

Table 3. Absorption coefficients in aluminium, copper, tin and lead of the softer γ radiations from radium (B + C)

Element	μ (cm.$^{-1}$)	μ/ρ (cm.^{2}g.$^{-1}$)	Intensity ratio harder/softer	d (cm.)	ρd (g. cm.$^{-2}$)
Aluminium	0·48	0·18	2·6	7·4	20
Copper	$2{\cdot}1_1$	0·24	1·9	2·6	23
Tin	$1{\cdot}1_7$	0·16	1·5	3·3	24
Lead	$2{\cdot}5_8$	0·23	1·7	1·6	18

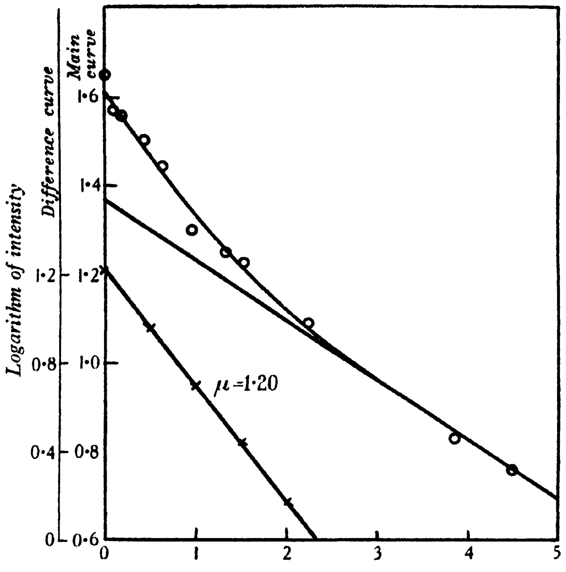

Figure 2. Absorption of γ rays from radium (B + C) in tin.

difference between two curves, the accuracy of determination is not so great as for the harder components. The accuracy of determination in table 3 is about 7 per cent, judging by the departure of individual determinations from the mean. The accuracy of the intensity ratio is limited by the same cause. This ratio is given for zero thickness of absorber, that is to say for a filtering of 6 mm. of aluminium. It will be seen that under these conditions the harder component is approximately twice as intense as the softer. However, if this ratio is to be correct then true intensities, irrespective of wave-length, must be recorded on the film. As mentioned above the photographic action of softer γ rays is intensified approximately equally with that of the harder rays by lead foil when the intensifying action is referred to that of aluminium. This does not, however, establish that the true intensities of all radiations are correctly recorded, for the intensities on the film must be due to the absorption of energy from the beam in the film itself, either directly or through the intensifiers. As the absorption of γ rays decreases with wave-length, the intensity of the shorter wave-lengths will not be fully recorded, and hence the intensity of the harder

I. A. R. I.

component may be greater than twice that of the softer. Kohlrausch(4) has reported a soft component of which the intensity is one-eighth of the hard component. His results were, however, difficult to obtain, as he had a medium component of intensity nearly equal to that of the hard component which arose, as has already been pointed out(1, 2), from rays softened in the channel wall used to produce a parallel beam of γ rays.

The values of the absorption coefficients in lead and aluminium can be compared with the results obtained by others. Thus for aluminium Kohlrausch(4) found 0·57 cm.$^{-1}$ for the softer component and Rutherford and Richardson(5) 0·51, compared with the value above of 0·48. The variations are not much greater than the experimental error. For lead the agreement found between the result of Kohlrausch 4·8 and that above 2·6 is not so good.

It is interesting to note the thickness of each absorbing material necessary before the radiations are finally exponentially absorbed. It had been previously pointed out that 1·6 cm. of lead filter produced exponential absorption, whereas others, e.g., Kohlrausch, had found that the thickness of filter required was nearly 4 cm. Clark(6) about the same time as the author had found that the γ rays from radium (B + C) were exponentially absorbed after being filtered by 1·8 cm. of lead. The filter thicknesses d necessary for exponential absorption are given in table 3, and in the last column the product of d and the filter density ρ is seen to be nearly constant. It is, however, difficult to decide the exact point at which the curve becomes exponential, so that there is some uncertainty as to the exact value of ρd. Its approximate constancy indicates that the exponential absorption of the rays is merely a question of the amount of matter to be traversed.

It was pointed out by Kohlrausch and substantiated by the author that μ ρ for the harder rays, of wave-length 7 X., is approximately constant, μ/ρ being equal to 0·044. Although the experimental values of μ/ρ for the softer component are not nearly so constant, much of the variation may be due to the rather large experimental error in the determination of the absorption coefficients.

Wave-lengths of softer radiations. Some of the effective wave-lengths of the softer radiations can be obtained from an examination of the mass absorption coefficients of X rays of short wave-length. This is done in table 4 below in which the values of μ experimentally determined are given, together with the wave-lengths of the X rays which have the same values of absorption coefficient(7). The value of the wave-length for tin is somewhat less than 50 X. The effective wave-length for softer radiations in lead is taken from a table prepared by Gentner(8).

Table 4. Effective wave-lengths of softer radiations

Element	Experimental value of μ/ρ	Effective wave-length (X.)	μ/ρ for wave-length
Aluminium	0·18	125	0·178
Copper	0·24	72	0·23
Tin	0·16	< 50	0·32
Lead	0·23	31	

It will be seen that the effective wave-length of the softer component decreases with the atomic number of the absorbing material.

§4. THE VALUES OF THE ABSORPTION COEFFICIENTS FOR THE HARDER γ RADIATIONS FROM RADIUM (B+C) WITH DIFFERENT FILTERINGS

When it was found for tin or copper that the value of the absorption coefficient depended on whether the γ rays were filtered by lead or by the element in question until the absorption became exponential, a series of experiments was carried out in which the absorption coefficients in aluminium, copper, tin and lead were obtained with γ rays filtered by aluminium, copper, tin and lead. The source was 400 mg. of radium in four tubes arranged in line. The values of the absorption coefficients are set out in table 5 and the results for lead are shown in figure 3. The thicknesses of the filters are as set out in column 5 of table 3, and the absorbing thicknesses were aluminium 10 cm., copper 3 cm., tin 4 cm., lead 1·4 cm. At least three points were used on each curve to determine the slope.

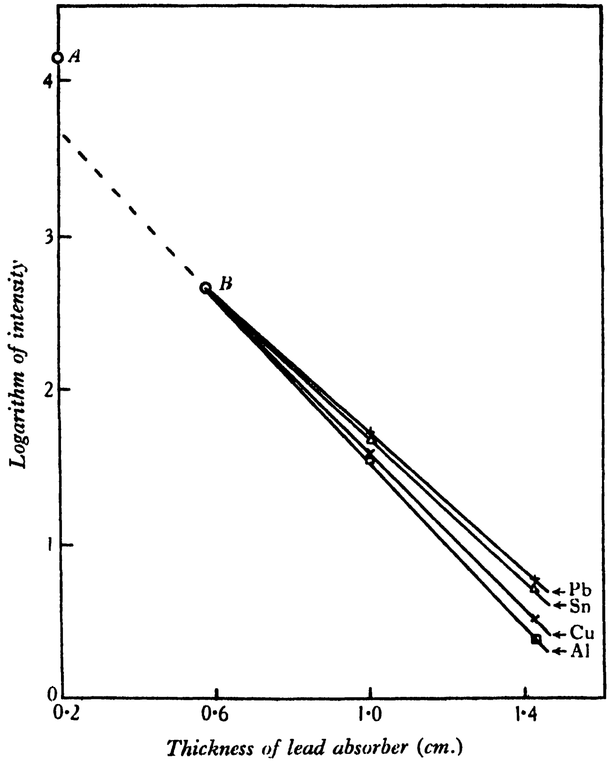

Figure 3. Absorption in lead of γ rays from radium (B+C), previously made exponential in various filters. All curves have been adjusted to pass through point *B*. Point *A* is for aluminium-filtered rays.

In these experiments the photographic action was intensified by Patterson screens, except for the determinations with lead-filtered rays which had been obtained previously with lead-foil intensifying-screens. The accuracy of the determinations is given as the mean departure from the mean result and varies between 2 and 4 per cent.

Table 5. Absorption coefficients with different filterings

Absorber / Filter	Aluminium	Copper	Tin	Lead
Aluminium	0·124 ± 0·004	0·399 ± 0·010	0·341 ± 0·013	0·606 ± 0·023
Copper	0·123 ± 0·002	0·419 ± 0·016	0·320 ± 0·002	0·581 ± 0·016
Tin	0·119 ± 0·002	0·387 ± 0·018	0·316 ± 0·010	0·554 ± 0·02
Lead	0·123	0 381	0·293	0·533

As can be seen from the table, the absorption coefficients determined in aluminium do not depend on the nature of the filter, but for tin and lead the nature of the filter has a marked influence on the absorption coefficient, in that the lower the atomic number of the filter the greater is the absorption coefficient, i.e., the longer is the effective wave-length. It was found for rays filtered with aluminium, copper and tin that the points for zero thickness of lead used as absorber did not fall on the exponential straight line, and the curve becomes exponential only after a thickness of 5 mm. of lead. (The point for 2 mm. of lead is shown for aluminium-filtered rays in figure 3.) This applies also for the absorption in tin of γ rays filtered with aluminium, while for the remainder the point of zero thickness of absorber falls on the exponential curve.

Somewhat similar filtering effects were found by Ahmad$^{(9)}$ for the γ rays from radium (B + C) in filters of iron, lead and mercury, the thicknesses of the filters being 6·5 cm. of iron, 1 cm. of lead and 3·41 cm. of mercury. The results here obtained for copper and lead can be compared with Ahmad's results for iron and mercury, since the product ρd for these are 51 (iron) and 46 (mercury). As the atomic number of iron is 26 and that of copper 29, the results of iron-filtering should be comparable with those of copper-filtering, as should those of mercury (80) with lead (82). The comparison of Ahmad's results with the author's are set out in table 6.

Table 6. Variation in value of absorption coefficient with filtering

Absorber	$\frac{\mu \text{ with iron filter}}{\mu \text{ with mercury filter}}$ (Ahmad)	$\frac{\mu \text{ with copper filter}}{\mu \text{ with lead filter}}$ (Rogers)
Aluminium	1·05	1·00
Copper	1·06	1·10
Tin	1·09	1·09
Lead	1·12	1·09

An examination of the results indicates a general agreement in that the filter with the lower atomic number produces a greater absorption coefficient. The numerical agreement is moderately good except that Ahmad finds a variation in aluminium whereas none is found here.

§ 5. DISCUSSION OF RESULTS

In spite of the heterogeneous nature of the γ rays from radium (B + C) the experiments indicate that these rays can be analysed into two apparently homogeneous components in that each appears to be exponentially absorbed. If, however, the mixed beam is passed through increasing thicknesses of an element until it becomes exponentially absorbed in further thicknesses of the element, the effective wave-length of the filtered beam is shorter the higher the atomic number of the filtering element. Thus if aluminium-filtered and lead-filtered rays are separately absorbed in lead, the absorption coefficients are respectively 0·606 and 0·533 cm.$^{-1}$ Further, the effective wave-length of the softer component of the γ rays, as determined from their absorption coefficients, is shorter the higher the atomic number of the absorbing material.

These results can be explained at least approximately by considering the reduction in intensity of the main γ-ray lines in the spectrum of radium (B + C) as the rays pass through matter.* The present discussion will be limited to a consideration of the absorption in aluminium and lead, the elements of least and greatest atomic number that have been investigated.

The absorption of γ rays takes place by three main processes, namely (i) Compton scattering, which is taken into consideration by the Klein-Nishina formula; (ii) the photoelectric effect, which for shorter-wave-length γ rays can be calculated from the results of Hulme and others(10), and (iii) pair-production. The last-named process is inoperative for wave-lengths greater than 12 X. For wave-lengths shorter than this in the known γ-ray spectrum of radium (B + C) it assumes importance only for elements of high atomic number. Thus in the absorption by lead of γ rays of wave-length 7 X., pair-production accounts for 5 per cent only of the total absorption.

The more intense lines in the γ-ray spectrum of radium (B + C) are given in table 7. The intensities of most of the lines are those determined by Ellis and Aston(11). The intensities for the first two lines of the table are obtained from unpublished work on the γ-ray spectrum. The line 160 X. (really two lines 160 and 165 X.) is photographically the most intense line of the spectrum and has been allotted intensity 1, while the intense lines near 140 X. have been allotted intensity 0·45.

If the absorption coefficients for these different wave-lengths are known, the effective absorption coefficient μ for a thickness d cm. of absorber can be calculated from the equation

$$\mu = \frac{1}{d} \log \frac{\Sigma I'_0}{\Sigma I'_0 e^{-\mu' d}},$$

where the I'_0 terms are the incident intensities and the μ's are the corresponding absorption coefficients.

The absorption coefficients for both aluminium and lead can be obtained for wave-lengths greater than 50 X. from Allen's determination with X rays. For lead the absorption coefficients for wave-lengths less than this have recently been summarized by Gentner.$^{(8)}$* For aluminium the Klein-Nishina formula gives, for wave-lengths less than 50 X. the absorption coefficients with sufficient accuracy for the present purpose; thus for 36·3 X. the photoelectric part of the absorption in aluminium is approximately ½ per cent of that due to Compton scattering. The absorption coefficients used in the calculation are set out in table 7.

---

* As the spectrum is heterogeneous it would, however, be anticipated that there would be no exponential absorption for the beam as a whole, for with increasing thickness of absorber the absorption coefficient should steadily decrease.

Table 7. The more intense lines of the γ-ray spectrum of radium (B + C) and their absorption coefficients in aluminium and lead

Wave-length (X.)	Intensity	μ in aluminium (cm.^{1})	μ in lead (cm.$^{-1}$)
(160)	(1)	0·577	—
(140)	(0·45)	0·527	—
50·8	0·115	0·311	11·5
41·6	0·258	0·279	4·56
34·9	0·450	0·255	3·16
20·2	0·658	0·213	1·31
10·9	0·206	0·154	0·72
6·94	0·258	0·123	0·53
5·57	0·074	0·107	0·49

It will be seen that, for wave-lengths greater than 50 X., the absorption coefficients are so great, owing to the great importance of the photoelectric absorption, that radiation of these wave-lengths will be reduced to negligible intensity in very small thicknesses of lead.

The calculated effective absorption coefficients for the γ-ray lines given in table 7 are set out in table 8.

Table 8. Effective absorption coefficients (cm.$^{-1}$)

Filter	Absorber	
	1·4 cm. lead	6·0 cm. aluminium
1·6 cm. lead	0·65	0·149
7·4 cm. aluminium	0·91	0·178

It will be seen that in lead there is an excess of 40 per cent in the absorption coefficient for aluminium-filtered rays over lead-filtered rays. In aluminium the two absorption coefficients are more nearly equal, the excess being 19 per cent; experimentally no excess is found. It will be noted, however, that all the absorption coefficients are considerably higher than those found experimentally; see table 5 above. This would be accounted for if there are γ-ray lines of moderate intensity of shorter wave-length than those given in table 7. There is some experimental evidence for the presence of such lines, for Skobeltzyn$^{(12)}$ has found from tracks of recoil electrons that these are γ rays with energies of 3×10^6 electron-volts, whereas the rays of highest energy in the table are $2{\cdot}2 \times 10^6$ eV. Steadman$^{(13)}$ has also found evidence of γ rays of shorter wave-length than those given in the table. Not only will the presence of such short-wave-length lines reduce the values of the absorption coefficients, but also it will make the absorption coefficients in aluminium of differently filtered rays more nearly equal. Thus if the presence of a line of 4·65 X.[*] of intensity 0·4 in the scale of intensities of table 7 is assumed, the values of the absorption coefficients of lead-filtered rays are 0·58 cm.$^{-1}$ in lead and 0·126 in aluminium, and the coefficients for aluminium-filtered rays are 0·72 in lead and 0·147 in aluminium. For all the values here are much nearer the experimental values than those in table 8 so that there must be γ-ray lines of considerable intensity having wave-lengths shorter than 5·6 X.

---

* There is, however, a discrepancy between the values for lead for shortest wave-lengths found by Allen and the longest wave-lengths summarized by Gentner.

Finally from the calculated values in table 8 for the absorption coefficients of the more penetrating radiations those of the softer radiations also can be calculated. It is necessary, in carrying out this calculation for aluminium, to take into consideration the lines of 160 and 140 X. The calculated absorption coefficient is then 0·57 cm.$^{-1}$, which is somewhat higher than the experimental value of 0·48. The lines of 160 and 140 X. need not be considered for lead, for they are reduced to negligible intensity in considerably less than 1 mm. of lead; moreover in determining the experimental values of the absorption coefficient the point for zero thickness of lead was not included. The calculated absorption coefficient for the softer radiations in lead is found to be 2·6 cm.$^{-1}$, which is very close to the experimental value.

§6. ACKNOWLEDGMENTS

These experiments were carried out in the Commonwealth Radium Laboratory, University of Melbourne, and the author wishes to express his thanks to Mr A. H. Turner, M.Sc. of that laboratory for making available its facilities. He also is grateful to Dr L. H. Martin, with whom certain points in this paper have been discussed.

REFERENCES

(1) Rogers, J. S. *Proc. phys. Soc.* **43**, 59 (1931).
(2) Rogers, J. S. *Proc. phys. Soc.* **44**, 349 (1932).
(3) Frilley, M. *Ann. Phys.*, Paris, **11**, 483 (1929).
(4) Kohlrausch, K. W. F. *S.B. Akad. Wiss. Wien*, **126**, 441 (1917).
(5) Rutherford, E. and Richardson. *Phil. Mag.* **25**, 722 (1913).
(6) Clark, L. H. *Phil. Mag.* **12**, 913 (1931).
(7) Allen's results. See Compton and Allison, *X-Rays in Theory and Experiment.*
(8) Gentner, W. *J. Phys. Radium*, **6**, 9, 278 (1935).
(9) Ahmad. *Proc. roy. Soc.* **109**, 206 (1925).
(10) Hulme, H. R. and others. *Proc. roy. Soc.* **149**, 131 (1935).
(11) Ellis, C. D. and Aston, G. H. *Proc. roy. Soc.* **129**, 180 (1930).
(12) Skobeltzyn, D. *Z. Phys.* **58**, 598 (1929).
(13) Steadman, L. T. *Phys. Rev.* **36**, 460 (1930).

---

[*] This particular wave-length was assumed to illustrate the point as its absorption coefficients are accurately known.

THE EFFECT OF HYDROGEN ON THE TIME-LAG OF ARGON-FILLED PHOTOELECTRIC CELLS

By N. R. CAMPBELL and R. S. RIVLIN
A communication from the Staff of the Research Laboratories of
The General Electric Company Limited, Wembley, England

Received 19 *October* 1936. *Read* 27 *November* 1936

ABSTRACT. In a previous paper of this series⁽¹⁾ it was stated that the addition of small quantities of hydrogen to the argon filling of a photoelectric cell with unsensitized potassium cathode reduced the time-lag greatly. The amount of hydrogen necessary for this effect has now been determined roughly. A Pirani gauge has been found very suitable for determining a small proportion of hydrogen in argon.

§ 1. APPARATUS

The previous paper of this series⁽¹⁾ left undetermined the proportion of hydrogen required to produce the decrease in time-lag described in § 5; it was thought that somewhat elaborate apparatus would be required to determine the proportion of hydrogen present in argon at low pressure.

It has been found that the problem can be solved very simply and with sufficient accuracy by the use of a Pirani gauge. The gauge was of the simple type in which a constant p.d. is maintained across the bridge, and the out-of-balance current is read. Figure 1 shows typical calibration curves obtained against a McLeod gauge. The thick line refers to pure argon; the thin lines terminating on it refer to mixtures of argon and hydrogen in which the argon pressure is constant. It will be seen that the various thin lines are all very similar, so that it is easy to interpolate between them.

Accordingly all that is necessary is to attach such a gauge to the cell, fill it with argon to a suitable pressure, and draw the thin line in figure 1 terminating on the thick line at this pressure. When the reading of the gauge is varied by adding hydrogen (through a palladium tube) or withdrawing it (through a palladium tube or by absorption at the potassium surface), the corresponding pressure, and therefore the proportion of hydrogen, is read off on this thin line. Of course it is assumed that there is no absorption, or other change, affecting the quantity of free argon; everything pointed to the truth of this assumption.

§ 2. RESULTS

The results obtained by this method can be stated thus, the pressure of argon in the cell being about 0·2 mm. The effect of introducing a small proportion of hydrogen into argon is (1) to decrease the magnification at a given voltage, (2) to decrease the time-lag at a given magnification and therefore, a fortiori, at a given voltage. Both these effects increase rapidly as the amount of hydrogen is increased up to (say) 2 per cent by volume; the rate of increase then falls off and becomes negligible at about 6 per cent. Accordingly the statement made previously that the effect is produced by *small* proportions of hydrogen is correct. The exact variation of the effects with amount of hydrogen is complicated and depends on the nature of the cell; it is useless to describe the experiments in detail until some coordinating theory can be suggested.

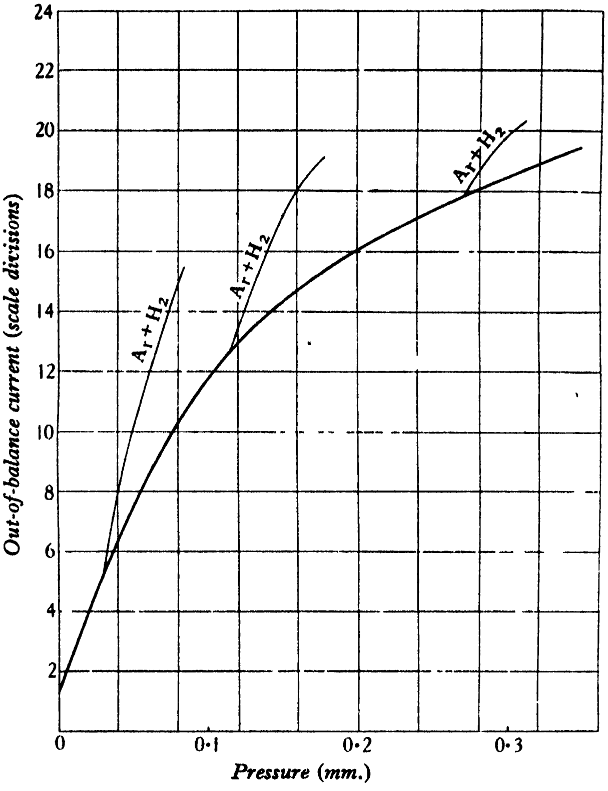

Figure 1. Calibration of Pirani gauge.

Effect (1) is already known$^{(2)}$. Effect (2) is that described in the previous paper. A third effect described in that paper, namely a decrease in the emission from the potassium, was not obtained again; it doubtless depends on the extent to which the potassium has already adsorbed or absorbed hydrogen.

It is to be observed that effects (1) and (2) were correlated with hydrogen free in the cell. It is conceivable that the direct cause was hydrogen absorbed on the cathode in an amount which is in equilibrium with the amount free in the cell. But nothing was observed that confirms that suggestion.

REFERENCES

(1) CAMPBELL, N. R., NOBLE, H. R. and STOODLEY, L. G. *Proc. phys. Soc.* **48**, 589 (1936).
(2) DEIMEL, C. *Phys. Z.* **37**, 610 (1936).

THERMOMAGNETIC PROPERTIES OF NICKEL WIRE, PART 3

By WILLIAM BAND, Professor of Physics, Yenching
University, Peiping, China

Received 21 *October* 1936. *Read in title* 27 *November* 1936

ABSTRACT. The paper constitutes a brief report of results of a complete and careful analysis of observations previously published on the e.m.fs. found in nickel wires.

RESULTS published previously in parts 1 and 2(1) have been subjected to a careful and detailed analysis of all corrections, the homogeneous e.m.fs. measured in part 2 being employed in the corrections to the results in part 1. The results of this analysis, details of which have to be omitted owing to lack of space, are best exhibited graphically. The figures given are self-explanatory.

The most important points brought out by these curves are: (*a*) There is a constant potential gradient susceptibility remaining in the material at temperatures well above the Curie point; (*b*) there is a Villari reversal phenomenon of the potential-gradient susceptibility under different tensional strains; (*c*) the magnetic change of the Thomson specific heat is found to vanish, under all tensions, at a definite Curie point which coincides with the temperature at which the potential-gradient susceptibility becomes independent of temperature.

The first two points are interpreted as showing that the magnetic change in potential-gradient is not entirely ferromagnetic in origin: the ferromagnetism of nickel is known not to show any Villari reversal, and to vanish at the Curie point. They can also be interpreted in terms of Bridgman's theory of thermoelectricity.

According to Bridgman's theory the e.m.f. E_{ab} in the circuit is not, as is usually assumed, due to a combination of contact and internal e.m.fs., the Peltier heat being in fact accompanied by no driving e.m.f. The total driving e.m.f. in the circuit has to be derived from the formula(2)

$$\delta E = -\delta T\left[\int_0^T (\sigma/T)\,dT + f(T)\right] \qquad \text{......(1)},$$

where $f(T)$ is some function identical for all metals and contributing nothing to the total e.m.f. in any circuit, which works out as

$$E_{ab} = \int_{T_1}^{T_2} \Delta\gamma \, . \, dT \qquad \text{......(2)},$$

where

$$\Delta\gamma = -\int_0^T \{(\sigma_a - \sigma_b)/T\} \, . \, dT \qquad \text{......(3)}.$$

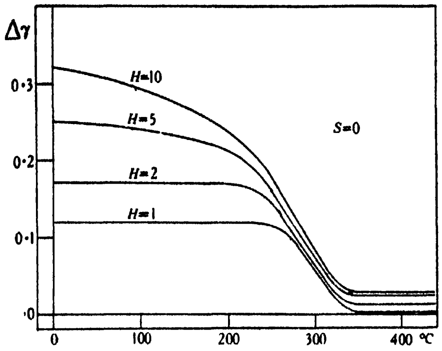

Figure 1. Thomson potential-gradient susceptibility. Changes in Thomson potential-gradient due to fields under 1, 2, 5, 10 amperes current at zero tension as functions of temperature. (10 amperes gave 303 G.)

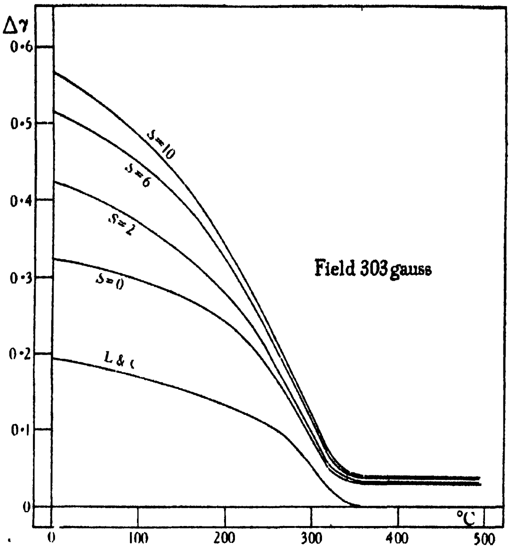

Figure 2. Thomson potential-gradient susceptibility. Changes in Thomson potential-gradient due to a field of 303 G., under tensions of 0, 2, 6, 10 kg., as function of temperature. (1 kg. gave 127·3 kg./cm².)

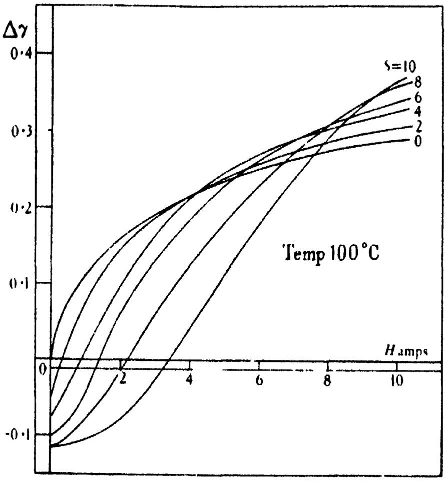

Figure 3. Relationship between Thomson potential-gradient, magnetization and strain. At a mean temperature of 100° C. the change produced in the Thomson potential-gradient as a function of magnetic field for tensions of 0, 2, 4, 6, 8, 10 kg.

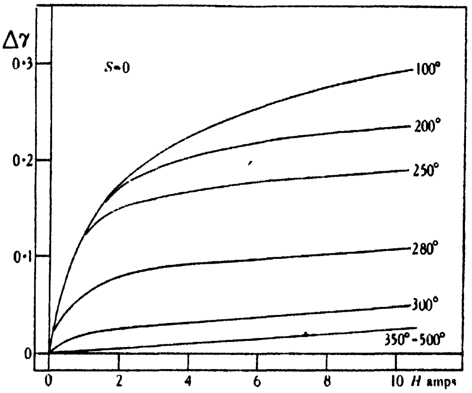

Figure 4. Relationship between Thomson potential-gradient, magnetization and temperature. At zero tension the change in Thomson potential-gradient as function of magnetic field for temperatures of 100, 200, 250, 280, 300 and between 350–500° C.

The coefficient γ is evidently what is generally known as the Thomson potential-gradient.

The constant values of $\Delta\gamma$ found at temperatures above the Curie point are the

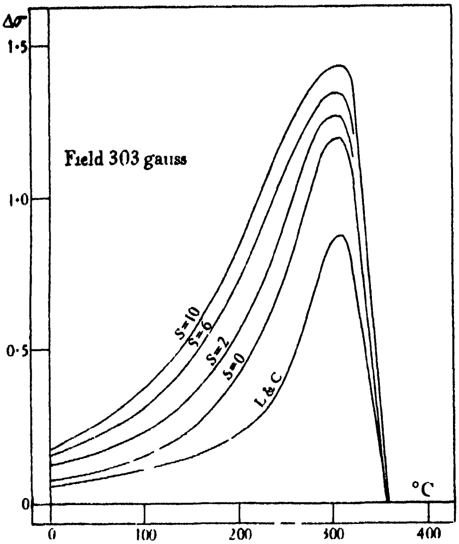

Figure 5. Thomson heat susceptibility. The change in Thomson specific heat, calculated by the Kelvin formula from the gradients of our curves, and due to a field of 303 G. under tensions 0, 2, 6, 10 kg. as a function of temperature. The curve marked "L. & C." has been drawn from data published by Lowance and Constant(3).

values of the integral in equation (3) when T is put equal to the Curie-point temperature. There is no mathematical reason why these should be zero.

No explanation has been found for the antisymmetrical part of the e.m.fs. examined in part II.

REFERENCES

(1) Hsü and Band. *Proc. phys. Soc.* **47**, 910 (1935); **48**, 168 (1936).
(2) Bridgman. *The Thermodynamics of Electrical Phenomena in Metals*, p. 63, equation II. 14. The MacMillan Co. (1934).
(3) Lowance and Constant. *Phys. Rev.* **48**, 257 (1935).

X-RAY INVESTIGATION OF PURE IRON-NICKEL ALLOYS. PART 1: THERMAL EXPANSION OF ALLOYS RICH IN NICKEL

By Professor E. A. OWEN, M.A., D.Sc., F.Inst.P.

and

E. L. YATES, M.Sc., Ph.D., A.Inst.P.
University College of North Wales, Bangor

Received 24 *June* 1936. *Read in title* 9 *October* 1936

ABSTRACT. The thermal expansion of pure iron-nickel alloys having compositions ranging between 97 and 73 atoms of nickel per cent was measured by the X-ray method. Close agreement was found between the expansion of the crystal lattices and the expansion of specimens of material consisting of composite masses of crystals, such as were used by previous workers who employed the ordinary methods of measurement. For the alloys examined, which were all rich in nickel, the addition of iron to the nickel lattice was found to have two effects: (*a*) the nickel lattice expanded approximately in proportion to the amount of iron added, and (*b*) the temperature of the discontinuity in the thermal-expansion curve was raised with the addition of iron, but not in proportion to the amount of iron added. No change in structure took place at the temperature of magnetic transformation; the face-centred structure persisted from room-temperature through the transformation temperature up to 600° C., the highest temperature reached in the investigation. No ageing effect was observed with an alloy containing 94 atoms of nickel per cent, the lattice parameter showing no consistent change over a period of 15 months.

§ 1. INTRODUCTION

Owing to their importance in industry, the iron-nickel alloys have been extensively investigated. They have been found to possess many interesting and unusual properties. The presence of small quantities of impurities considerably alters their properties and gives rise to phenomena which are difficult to follow, especially as the quantities of impurities involved may be very small. To avoid complications of this nature it was decided in the first instance to investigate alloys made from the pure elements in the hope that the results thus obtained would form the basis for further work on alloys containing small amounts of a third constituent.

Previous investigators have found that all the alloys solidify as solid solutions which upon cooling suffer both phase and magnetic transformations. It is upon these transformations that many of the peculiar properties of the alloys depend.

In the present investigation, an account of which will be given in this and subsequent papers, a detailed examination was made of the lattice dimensions and structures at different temperatures with the object of throwing more light if possible on the transformations that occur and of studying the thermal expansion of the alloys in its relation to these transformations.

This paper deals with the thermal expansion of five alloys rich in nickel.

§ 2. HEAT TREATMENT AND PREPARATION OF THE ALLOYS

The alloys were kindly provided by the Mond Nickel Company, Ltd.; their compositions are given in table 1.

Table 1. Composition of alloys

Alloy	Nickel-content	
	Weight per cent	Atoms per cent
97	96·75	96·6
94	93·95	93·7
91	91·04	90·7
83	82·86	82·2
74	74·00	73·0

Although the alloys had been lump-annealed at 1150° C. for 20 hours in a nitrogen atmosphere before they were received, they were submitted to further heat treatment before powders were prepared from them. For this purpose a small lump of each alloy was enclosed in a pyrex glass tube which was evacuated and sealed. Each tube, wrapped in asbestos cloth, was placed in a furnace maintained at 800° C. and was allowed to remain at that temperature for a number of days before being cooled slowly to the temperature of the room. Measurements made on alloy 74 showed that this further heat treatment was not necessary because no appreciable difference in the lattice parameter was observed between specimens which had received no lump annealing and others which had received respectively 3, 6 or 12 days' annealing at 800° C. The initial heating which the ingots had received was therefore adequate to produce uniformity of composition.

Filings taken from the ingots were annealed to remove distortion due to filing. Care was taken in the filing operation not to apply too great a pressure, in order to minimize contamination with particles torn from the file. The filings were passed through a 100-mesh sieve before being sealed in evacuated pyrex glass tubes. These tubes after sealing were placed in deep holes in an iron block which fitted into the furnace; the temperature was recorded by a calibrated thermocouple placed in close contact with the middle of the block. The annealing was then carried out according to plan.

Difficulty was experienced with some of the alloys in obtaining spectral lines suitable for accurate measurement. When filings of alloy 74, for example, were annealed at 300° C. for 10½ hours and cooled moderately fast in air, the lattice was still too distorted to yield spectral lines. The distortion might be due to the cold work done in filing, or to the rapid cooling to room-temperature. On the assumption that both effects were present, the filings were annealed at a higher temperature of 800° C. for 2 hours and were allowed 90 hours to cool to room temperature. After this treatment good lines were obtained, but they showed that the material was now over-annealed. In an attempt to find the conditions necessary to produce the best reflection lines, some more powder was annealed at 500° C. for 12 hours and cooled over a further period of 33 hours. A marked improvement in the definition of the lines was observed. These observations showed that the annealing at 800° C. was too severe, while that at 300° C. was insufficient to remove the effects of cold work.

It was found during the course of the work on alloy 74 that not only the temperature of annealing is important, but also the rate of cooling from this temperature to room-temperature. A powder heated at 600° C. may yield good lines at that temperature, but no lines at room-temperature if it is cooled in too short a time. The necessity for a slow rate of cooling after annealing becomes less as the nickel-content of the alloy increases, as good lines being obtained for quenched as for slowly cooled specimens of pure nickel.

The annealing treatment given to the alloys described in this paper is recorded in detail in table 2.

Table 2

Alloy no.	Lump annealing			Powder annealing		
	Temperature (°C.)	Time (days)	Period of cooling (days)	Temperature (°C.)	Time (hours)	Period of cooling (hours)
97 (1)	800	6	—	690	12	27
(2)	800	6	—	500	14	24
94 (1)	800	6	—	690	12	27
(2)	800	6	—	500	14	24
(3)	800	6	—	600	15	225
91 (1)	800	6	—	690	12	27
(2)	800	6	—	500	14	24
(3)	800	6	—	600	15	144
(4)	800	6	—	600	7	108
(5)	800	6	—	700	12	29
83 (1)	800	6	—	690	12	27
(2)	800	6	—	500	14	24
74 (0)	—	—	—	300	10½	—
(1)	—	—	—	800	2	90
(2*a*)	860	3	—	800	2	90
(2*b*)	860	3	—	500	12	33
(3*a*)	860	6¼	—	800	2	90
(3*b*)	860	6¼	—	500	12	33
(4)	800	12	4½	600	14	48

§ 3. PROCEDURE

The high-temperature precision camera employed in this work was made to fit inside a strong airtight box and all exposures at temperatures above that of the room were made *in vacuo*. The vacuum was maintained by keeping a rotary oil pump connected to the sealed chamber, an oil-trap immersed in freezing mixture being inserted between the two.

The powder to be studied was cemented to a specially prepared copper sheet about 2 mm. thick, to the face of which one junction of a calibrated thermocouple was attached with silver solder. This sheet was held firmly in position on the camera by means of thin copper foil and springs; it was separated from the camera by a thin sheet of mica. Before proceeding it was important to investigate whether the adhesive used to mount the specimen on the thermo-sheet had any effect on the lattice parameter of the alloy. The adhesive, which was a dilute solution of seccotine, charred at about 300° C. and there was risk that the residue might combine with the alloy at the higher temperatures reached.

An attempt was made to eliminate the adhesive by pressing the powder into V-shaped grooves cut in the face of the thermo-sheet in such a way that the powder could be made to lie evenly in them when the thermo-sheet was placed vertically in the chamber. With this arrangement it was found that the temperature of the powder was lower than that recorded by the thermocouple.

The next attempt to eliminate the adhesive necessitated the rearrangement of the whole apparatus so that the X-rays fell vertically from above on the thermo-sheet, which was now horizontal, with its concave surface upwards. In this position, the powder could be sprinkled evenly on the sheet without any adhesive having to be used. The temperature of the powder was again lower than that indicated by the thermocouple. Exposures made with silver powder showed that the temperatures were in error by as much as 10 per cent. To take one example, when the silver powder was at a temperature of 321° C., deduced from the value of its parameter, the thermo-sheet upon which it lay was at a temperature of 350° C. On cementing the powder to the thermo-sheet, the discrepancy disappeared. The results of some of the experiments made in this direction are recorded in table 3.

Table 3

Film no.	Temperature as given by thermo-sheet (°C.)	Lattice parameter of silver (A.)	Temperature as given by the lattice parameter	
B 3	350	$4{\cdot}1023_2$	321	No adhesive
B 4	353	$4{\cdot}1015_5$	313	,,
B 5	351	$4{\cdot}1046_2$	348	With adhesive
B 6	350	$4{\cdot}1036_2$	336	No adhesive
B 7	352	$4{\cdot}1054_7$	356	With adhesive
B 8	506	$4{\cdot}1192_2$	508	,,

The temperatures given in the fourth column were obtained from the {lattice-parameter, temperature} curve of silver, which had been determined previously. It is evident from these results that the adhesive serves the double purpose of holding the powder in position and of ensuring good thermal contact between the powder and the thermo-sheet.

It was found, when a specimen was used to obtain a series of photographs at high temperatures, and exposures at room temperature were interspersed among these, that the parameter at room temperature remained constant if the powder retained its metallic lustre. This was evidence that the charred adhesive did not combine with the alloy to any measurable extent at the temperatures reached.

It was noticed in the preliminary stages of the work that some of the alloys lost their metallic lustre on being heated in the evacuated chamber, but the adhesive was not responsible for this. A thorough investigation into the cause of the tarnish was essential before proceeding further. As a first step a polished sheet of copper was left for three days in the evacuated chamber, and at the end of this period the sheet was found to be tarnished although it had remained at room-temperature all the time. The tarnish was of a sulphurous nature, and steps were therefore taken to rid all parts of the apparatus of sulphur and water vapour. The walls of the enclosure were carefully cleaned with ammonia, and the rubber washers and pressure-tubing connexions were boiled in caustic soda. Finally two small dishes, one containing potassium hydroxide and the other phosphorous pentoxide, were inserted in the enclosure, which as has already been stated was separated from the oil-pump by an oil-trap immersed in ice. With these precautions the discoloration of the powder did not occur, but it was found necessary to maintain a pressure in the chamber not exceeding 0·001 mm. of mercury.

All the photographs taken after this were obtained with powder held in position on the thermo-sheet by a thin layer of adhesive, and the above precautions were taken to remove from the chamber any gases and vapours that might be likely to affect the specimen.

The length of time during which the powder when mounted on the camera was kept at the temperature of exposure before the actual exposure was made varied between wide limits. It was found with the alloys now under investigation that heating for half an hour before the exposure gave the same result as heating for much longer periods. The powders before being exposed at high temperature to X-rays were subjected to three different heat treatments. (1) The powder was maintained at the required temperature for half an hour or more; unless the contrary is stated, this method was the one usually adopted. (2) The powder was heated rapidly to a temperature 100° C. lower than that at which the exposure was to be made and gradually brought up to the temperature of exposure over a period of at least half an hour; (*h*) in the tables that follow indicates the use of this method. (3) The material was heated to a temperature 100° C. higher than that at which the exposure was required and was allowed to cool slowly to the temperature of exposure over a period of at least half an hour; (*c*) indicates the use of this method. The temperature during the exposure was always kept steady.

The satisfactory agreement between the values of the lattice parameter of a given specimen obtained by these three methods shows that the temperature could be accurately controlled and determined. The high-temperature exposures were not made in order of increasing or decreasing temperature; a random sequence was adopted in order to eliminate progressive temperature errors. It was always arranged, when high-temperature photographs were taken with a given specimen, that a few photographs at ordinary temperature should be taken to ascertain whether the lattice returned to its normal dimensions. This precaution served as a useful check on the state of the material after heating; if by any chance the vacuum chamber became contaminated with vapours which at the higher temperatures reacted vigorously with the alloy, this reading taken at room temperature would at once demonstrate the fact and the material would have to be discarded.

§4. SOURCES OF ERROR

There is no need to discuss in detail the sources of error in the determination of lattice parameters with the precision camera, as these have been considered in previous papers. It may however be pointed out that when the same camera, radiation, and film-measuring instrument are used throughout a series of lattice-parameter determinations of the same alloy, and when precautions are taken to keep the conditions of exposure constant, an accuracy of about 0·004 per cent is attainable in an individual result relative to others in the same series of lattice-parameter determinations. An accuracy greater than 0·007 per cent cannot be claimed for the absolute value of any single lattice-parameter determination.

By frequently checking the thermocouple calibration, and by measuring the lattice parameters of silver at definite temperatures, the error in the temperature-determination was reduced to less than 1 per cent. The thermal expansion of silver had been the subject of previous investigation and it was then pointed out that the lattice-parameter values of this metal can be conveniently employed as a check on the temperature-determinations.

Owing to the limits set by the accuracy of the lattice-parameter measurements, the coefficient of thermal expansion cannot be determined to an accuracy greater than about 4 per cent. If several determinations are made, the accuracy of the mean will of course be higher than this. In addition the method yields a {lattice-parameter, temperature} curve which serves a useful purpose in that by its means any irregularities are immediately detected.

One point in connexion with the determination of coefficients of thermal expansion of materials by the X-ray method should be emphasized. With the precision camera employed it would be impossible to obtain well-defined lines and resolved doublets if any distortion existed in the material examined. In consequence the specimen has to be carefully heat-treated until it yields well-defined lines even at the largest glancing angles (about 85°) possible with the camera. In these circumstances the values of the thermal coefficients apply to material which is entirely free from internal stresses.

The K characteristic radiations of copper and manganese were employed. Copper radiation was reflected in the (331) and (420) planes and was used with alloys 74 and 83; manganese radiation was reflected in the (311) planes and was used with alloys 91, 94 and 97. This latter radiation was obtained by the electro-deposition of manganese on a copper target by immersion in a weakly acid solution of manganous chloride. The wave-lengths employed in the calculations were: CuKα_1, 1·537395 A.; CuKα_2, 1·541232 A.; MnKα_1, 2·09751 A. and MnKα_2, 2·10149 A.

§5. RESULTS

Alloys 97, 94 *and* 91. The use of manganese radiation in the investigation of the thermal expansion of these three alloys made it possible to obtain lines in favourable positions on the films for accurate determination of the parameters. The results obtained are collected in table 4.

Table 4

Alloy ... 97			94			91		
Nickel-content (per cent by weight) 96·75			93·95			91·04		
Film no.	Temperature (°C.)	Lattice parameter (A.)	Film no.	Temperature (°C.)	Lattice parameter (A.)	Film no.	Temperature (°C.)	Lattice parameter (A.)
E 536	11	3·5204$_1$	E 515	16	3·5242$_1$	V 1	12	3·5275$_7$
E 531	13	3·5208$_2$	V 37, E 510	17	3·5241$_8$	E 489, E 494	16	3·5277$_8$
E 537, E 538	14	3·5206$_2$	V 34	18	3·5243$_4$	E 493	17	3·5277$_9$
E 523	16	3·5207$_9$	E 495	19	3·5240$_7$	V 22, V 27	21	3·5279$_4$
E 519	17	3·5209$_2$	E 496, E 504	20	3·5243$_9$	V 24	22	3·5281$_3$
E 530	20	3·5206$_4$	E 513	101 (*h*)	3·5280$_6$	V 20	102 (*c*)	3·5318$_1$
E 524	101 (*h*)	3·5246$_7$	E 514	200 (*c*)	3·5331$_2$	V 18	201 (*c*)	3·5366$_8$
E 532	154 (*h*)	3·5274$_6$	V 35	297 (*h*)	3·5379$_6$	V 29	249 (*c*)	3·5388$_5$
E 525	198 (*c*)	3·5293$_5$	E 512	338 (*c*)	3·5400$_4$	V 21	301 (*h*)	3·5419$_1$
E 529	248 (*c*)	3·5317$_0$	E 501	363 (*c*)	3·5420$_0$	V 30	328 (*h*)	3·5423$_4$
E 534	294 (*h*)	3·5346$_1$	E 497	404 (*h*)	3 5446$_5$	V 17	360	3·5454$_9$
E 520	304 (*h*)	3·5351$_5$	E 518	432 (*h*)	3·5462$_2$	V 5	396 (*h*)	3·5474$_1$
E 527	351 (*c*)	3·5376$_5$	E 511	437 (*h*)	3·5467$_7$	V 19	403 (*h*)	3·5481$_6$
E 522	404 (*h*)	3·5411$_6$	E 499	451 (*c*)	3·5477$_5$	V 31	422 (*c*)	3·5491$_7$
E 533	455 (*h*)	3·5441$_4$	E 502	486 (*c*)	3·5498$_2$	V 25	454 (*h*)	3·5515$_2$
E 521	509 (*c*)	3·5476$_2$	V 36	508 (*h*)	3·5507$_3$	V 28	501 (*h*)	3·5544$_5$
E 535	552 (*c*)	3·5500$_0$	E 517	516 (*c*)	3·5510$_3$	V 26	546 (*c*)	3·5573$_4$
E 526	606 (*h*)	3·5529$_3$	E 516	519 (*c*)	3·5514$_0$	V 6	591 (*h*)	3·5589$_4$
			E 500	554 (*h*)	3·5535$_4$	V 23	605	3·5605$_1$
			E 503	598 (*h*)	3·5559$_7$			

The film numbers included in this table give an indication of the order in which the exposures were made. It is impossible without the aid of a graph to detect the changes that take place at certain temperatures in the three alloys. The figure includes the curves for these three alloys together with the curve for pure nickel(1), which is included for comparison with the other data. In each case a change in slope is noticed, but it occurs at a different temperature with each alloy. For pure nickel it occurs at about 370° C., but it increases to 390° C. for alloy 97, 430° C. for alloy 94 and 490° C. for alloy 91. The discontinuities are accentuated if the slope is plotted against the temperature.

There is a similarity between the thermal expansion of these three iron-nickel alloys and that of pure nickel. The addition of iron to nickel causes the nickel lattice to expand approximately in proportion to the amount of iron added, and it also raises the temperature of the discontinuity observed in the {parameter, temperature} curve. The discontinuity occurs with nickel at the temperature of magnetic transformation. The discontinuities in the other alloys are also closely associated with the magnetic transformation. For instance, Hanson and Hanson(2) found that the thermal arrest temperatures of a 90·71-per-cent alloy were 487° C. during heating and 457° C. during cooling. The discontinuity now found with alloy 91 which contains 91·04-per-cent nickel occurs at about 490° C. The same sort of agreement is obtained with the other alloys.

The coefficient of thermal expansion of each alloy increases as the temperature is raised, and reaches a maximum value at the temperature of discontinuity, i.e. at the transformation temperature. Approximate values of the coefficients of expansion at various temperatures for the three alloys 97, 94 and 91 are collected in table 5.

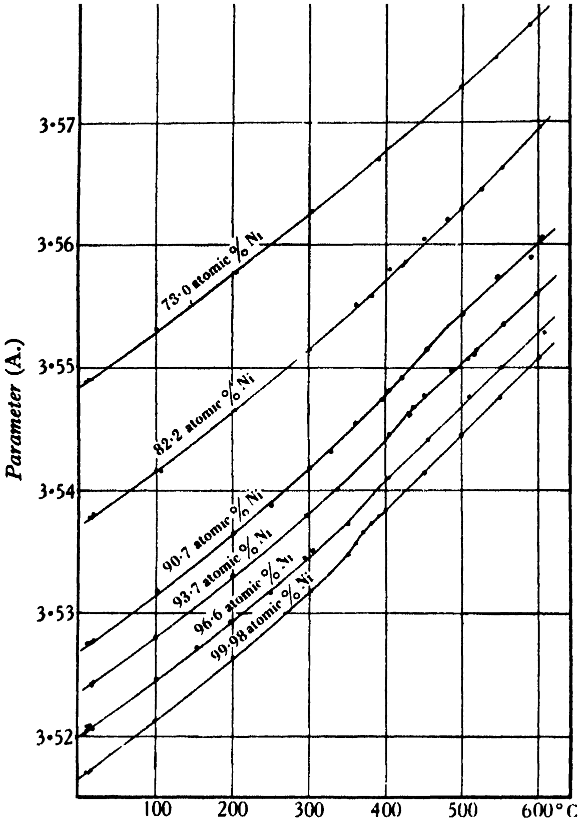

Ageing test on alloy 94. In order to make sure that the lattice parameters of the alloys at this end of the equilibrium diagram remained constant over long periods of time, an ageing test was made on alloy 94. The investigation was carried out over a period extending from January 1934 to March 1935. The results of the measurements are summarized in table 6.

These results show that there is no consistent change in the lattice parameter over a total period of 15 months and that in the case of this particular alloy there is no ageing effect.

Alloys 83 *and* 74. Difficulty was experienced with the alloys in obtaining X-ray diffraction lines but this was overcome by cooling the annealed filings slowly instead of rapidly. Even after the right heat treatment for the alloys had been found the lines obtained were always faint. This effect was noticed also with alloys of higher iron-content.

Table 5

Temperature (°C.)	True coefficient of thermal expansion × 10^6		
	Alloy 97	Alloy 94	Alloy 91
0	12·8	12·8	12·7
100	13·2	13·3	13·4
200	14·0	14·2	14·3
300	16·1	15·9	15·7
380	19·2	—	—
390	19·6	—	—
400	16·7	18·8	17·7
420	—	19·4	—
430	—	19·7	—
440	—	16·5	—
480	—	—	19·7
490	—	—	20·0
500	16·7	16·5	16·4
600	16·7	16·5	16·4

Table 6. Ageing test on alloy 94

Film no.	Specimen	Temperature (°C.)	Lattice parameter (A.)	Date of measurement
E 313	1	14	$3{\cdot}5241_9$	January 5 1934
E 314	2	14	$3{\cdot}5242_2$	
V 34	1	18	$3{\cdot}5243_4$	23 June 1934
E 496	2	20	$3{\cdot}5245_1$	24 July 1934
E 510	3	17	$3{\cdot}5242_8$	9 October 1934
E 509	2	15	$3{\cdot}5243_3$	29 March 1935
E 518	3	14	$3{\cdot}5240_0$	

The investigation of these two alloys was carried out with copper radiation which yielded two doublets; the presence of the two doublets compensated in some measure for the adverse positions of the lines and their poor intensity. In the early stages of the work it was observed that the lattice did not always return to its normal dimensions at room-temperature after being heated to high temperatures. This effect, as in the case of the other alloys, was directly connected with the discoloration of the powder which sometimes occurred at the higher temperatures. Even when every precaution was taken to remove the cause of this discoloration the powders still showed on occasions a tendency to lose their metallic lustre. To minimize the effect the powders were used only once for a high-temperature exposure. In addition a careful examination of the heated powder was made after each exposure and if it showed signs of deterioration the film was discarded.

With both the alloys difficulty was found in obtaining lines between 550 and 600° C. The magnetic transformations for these alloys occur between these two temperatures(2). The results obtained with the alloys are collected in table 7.

With the exception of the points 606° C. for alloy 74 and those at 553 and 601° C. for alloy 83, the points connecting lattice parameter with temperature lie

Table 7

Alloy ...	83		74		
Nickel-content (per cent by weight)	82·86		74·00		
Film no.	Temperature (°C.)	Lattice parameter (A.)	Film no.	Temperature (°C.)	Lattice parameter (A.)
E 354, E 369	13	$3{\cdot}5378_5$	E 292	8	$3{\cdot}5488_2$
E 367	14	$3{\cdot}5377_9$	E 284, E 285, E 286, E 287, E 301, E 302	12	$3{\cdot}5490_0$
E 358	15	$3{\cdot}5377_1$	E 312	15	$3{\cdot}5493_0$
E 364	18	$3{\cdot}5381_9$	E 282, E 296	16	$3{\cdot}5491_8$
E 365	100	$3{\cdot}5416_7$	E 294	101	$3{\cdot}5531_6$
E 361	107 (*c*)	$3{\cdot}5415_7$	E 303	205	$3{\cdot}5577_8$
E 356	203 (*h*)	$3{\cdot}5466_2$	E 293	303	$3{\cdot}5627_7$
E 359	302	$3{\cdot}5515_8$	E 297	390	$3{\cdot}5670_8$
E 363	361	$3{\cdot}5551_3$	E 295	498	$3{\cdot}5728_9$
E 379	382 (*h*)	$3{\cdot}5557_9$	E 306	543	$3{\cdot}5753_1$
E 374	383 (*h*)	$3{\cdot}5557_9$	E 310	587	$3{\cdot}5780_0$
E 355	404 (*h*)	$3{\cdot}5580_1$	E 283	606	$3{\cdot}5803_2$
E 376	422 (*h*)	$3{\cdot}5583_0$			
E 381	425 (*h*)	$3{\cdot}5586_4$			
E 366	450 (*h*)	$3{\cdot}5605_2$			
E 384	481 (*h*)	$3{\cdot}5621_1$			
E 360	500	$3{\cdot}5629_2$			
E 372	524	$3{\cdot}5645_1$			
E 368	553 (*h*)	$3{\cdot}5665_9$			
E 357	601 (*h*)	$3{\cdot}5695_8$			

satisfactorily on smooth curves. The deviations from these curves at the highest temperatures are due probably to the proximity of the magnetic transformation of these alloys. The difficulties encountered at these elevated temperatures restricted the number of observations that could be taken without unduly prolonging the investigation. It is to be noted also that about 600° C. is the working limit of temperature for the camera.

The curves showing the relation between parameter and temperature are included in the figure. The values of the coefficient of thermal expansion at different temperatures calculated from these curves are recorded in table 8.

Table 8

Temperature (°C.)	Coefficient of thermal expansion $\times 10^6$	
	Alloy 83	Alloy 74
0	12·4	12·2
100	13·3	12·9
200	14·2	13·5
300	15·1	14·2
400	16·0	14·9
500	16·9	15·6
600	17·8	16·4

The variation of the true coefficient of thermal expansion with temperature is linear within experimental error between room-temperature and 500° C.

§ 6. CONCLUSIONS

There is a close agreement between the results of the X-ray crystal method of determining the coefficients of thermal expansion and those obtained with methods employed by other workers, notably Guillaume(3) and Chevenard(4), who used larger masses of material. This fact demonstrates again that the metal as a whole, consisting of a composite mass of crystals, expands at the same rate as the lattice of a single crystal of the material.

In preparing the alloys for this investigation special care was given to the purity of the two constituent metals. Freedom from impurities is important with these alloys, as the presence of very small quantities of carbon is known to produce a marked effect upon the properties of nickel and iron and of their alloys. For this reason special attention was paid in the course of the work to the effect of the adhesive employed for mounting the powder on the thermo-sheet. In all the cases examined no effect could be detected, probably because the alloys were not raised to temperatures high enough to enable them to combine with the carbon. The point had however to be thoroughly investigated before it could be stated with any degree of certainty that the adhesive produced no effect.

The X-ray method of measuring the coefficients of thermal expansion of materials has been discussed in a previous paper. The accuracy of which the method is capable depends in great measure on the expansibility of the material under investigation. As a rule a fair accuracy can be attained, but what is important in the method is that only a small quantity of the material is required, and that the measurement is always made when the material is in thermal equilibrium and free from internal stresses.

In the present instance the method was found to be amply sensitive enough to establish beyond doubt the somewhat sudden changes in parameter which occur in the alloys at the temperatures of magnetic transformation. Owing to the proximity of the atomic numbers of iron and nickel, it would be impossible from the measurement of the relative intensities of the spectral lines to state whether a re-distribution of the atoms amongst the lattice points in the alloy crystals takes place in passing through the transformation temperature. Pure nickel however exhibits the same phenomenon, and it is unlikely that in this case a redistribution of atoms amongst the lattice points occurs. But there may take place, as the element or alloy passes through the transformation temperature, a reorientation of the atoms which would cause the observed abnormal increase in the expansion of the lattice followed by a sudden decrease. It would appear that at a certain temperature the thermal agitation of the atoms is sufficient to release the nickel atom from the binding forces which keep it in position, and that above this temperature it may take up any random orientation, the lattice then expanding in a uniform and normal manner.

No change in structure takes place as the alloy is taken through the temperature of magnetic transformation. The face-centred structure persists from room-temperature through the temperature of transformation up to 606° C., the highest temperature reached in the present work. Solution of iron in nickel takes place by the substitution of an iron atom for an atom in the nickel lattice.

The results recorded in this paper show that for the alloys considered, which are rich in nickel, the addition of iron to the nickel lattice has two effects: (1) the nickel lattice is expanded approximately in proportion to the amount of iron added, and (2) the temperature of the discontinuity in the thermal-expansion curve is raised with the addition of iron, but not proportionately to the amount of iron added.

§ 7. ACKNOWLEDGMENT

The authors wish to record their indebtedness to Dr L. B. Pfeil of the Mond Nickel Company for his advice and for kindly preparing the alloys and supplying their compositions.

REFERENCES

(1) OWEN and YATES. *Phil. Mag.* **21**, 809 (1936).
(2) HANSON and HANSON. *J. Iron Steel Inst.* **102**, 39 (1920).
(3) GUILLAUME. *Proc. phys. Soc.* **32**, 374 (1920).
(4) CHEVENARD. *Rev. de Mét.* **11**, 841 (1914); **14**, 618 (1917); *Comptes Rendus*, **159**, 53 (1914).

THE RESISTANCE OF PALLADIUM AND PALLADIUM-GOLD ALLOYS

By J. G. G. CONYBEARE, H. H. Wills Physical Laboratory,
The University, Bristol

Communicated by Prof. A. M. Tyndall, F.R.S. 27 July 1936. Read 23 October 1936

ABSTRACT. Measurements of the electrical resistances of palladium and four alloys of palladium and gold have been made from liquid oxygen temperature to about 1000° C. It is found that the variation of resistance with temperature for these alloys resembles that of constantan for compositions up to about 60 atoms per cent of gold, where there is a change over to the normal type of resistance curve. This, and the results for pure palladium, are shown to be in agreement with the quantum-mechanical theory of conductivity as applied by Mott to the transition metals.

§ 1. INTRODUCTION

In two recent papers Mott$^{(1, 2)}$ has shown that it is possible on the basis of the quantum theory developed by Bloch to explain certain anomalies in the electrical and magnetic properties of the transition metals. It is found that the energies of the electrons in a crystalline metal are confined to bands of energy levels, each band corresponding to a single stationary state of the isolated atom. The number of levels or states in each band is equal to the product of the statistical weight of the atomic state and the number of atoms in the crystal. Thus the d bands contain five states per atom and the s band one. The distribution of electrons in each band is governed by the Pauli principle; i.e. there cannot be more than two electrons in each state.

Now it is essential that if a substance is to be a conductor the bands occupied by electrons should not be completely full, for then it would be impossible for an electron to acquire energy in an applied electric field since all the states to which it might pass would be occupied. But in palladium the number of electrons per atom is just sufficient to fill all the bands up to the $4d$. Hence the metal would be an insulator unless the $5s$ and $4d$ bands overlap, in which case the ten electrons which would otherwise fill the $4d$ band will be shared between the $5s$ and $4d$ bands and there will be vacant states in each band to which electrons may make transitions. Similarly the $4s$ and $3d$ bands of nickel and the $6s$ and $5d$ bands of platinum must overlap, and both s and d electrons make contributions to the conductivity of these metals; see figure 1.

In the classical theory of conduction the conductivity is given by $\sigma = \frac{1}{2}ne^2/mv$, where n is the number of electrons per unit volume, e the electronic charge, m the mass of the electron and ν the frequency with which the electron collides with and is scattered by the atoms of the metal. In the quantum theory this formula still holds but ν must be calculated by the usual quantum-mechanical method, being proportional to the probability of scattering. Further, since we are dealing with s and d electrons in the transition metals, we must write

$$\sigma=\frac{1}{2}\frac{n_s e^2}{m_s\nu_s}+\frac{1}{2}\frac{n_d e^2}{m_d\nu_d}.$$

Calculations by Fuchs(1) show that the s electrons in copper and silver behave approximately as free electrons and the same would be expected for the s electrons of nickel and palladium which have similar atomic fields. Thus m_s is approximately the actual mass m_0 of a free electron. But the motion of the d electrons from atom to atom under the influence of an external field is much slower owing to the small overlap between one d wave function and that of a neighbouring atom. This is equivalent to taking $m_d \gg m_0$ so that the s electrons are mainly responsible for the conductivity. The conductivity thus depends on n_s and ν_s.

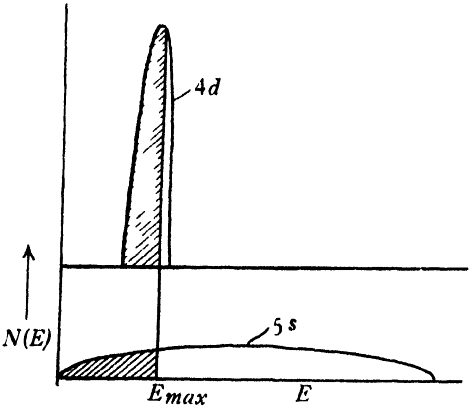

Figure 1. Density of electronic states $N(E)$ in the 5s and 4d bands of palladium plotted against their energy E. The shaded portions represent occupied states.

In a perfect lattice with no atomic vibrations the conductivity would be infinite. The scattering probability is found to be proportional to the mean-square displacement of the vibrating atoms, which is proportional to $T/M\Theta^2_D$ (where T is the absolute temperature, M is the mass of the atom, and Θ_D is the Debye characteristic temperature), and to the density of states $N(E)_{\text{max.}}$ in the neighbourhood of the final state, i.e. at the surface of the Fermi distribution, the energy loss on scattering being small. In the normal metals copper, silver, gold, tungsten, etc., only the s electrons are conduction electrons and since they behave approximately as free electrons $N(E)$ will hardly vary with the energy of states at the surface of the Fermi distribution and the resistance is quite accurately proportional to $T/M\Theta^2_D$. Since Θ_D depends on the volume it is not constant but decreases as the metal expands. Hence the resistance actually increases more rapidly than a linear law would imply. But in the transition metals there is also the possibility of the s electrons making transitions to the d band and of d electrons making transitions to the s band as well as of $s \rightarrow s$ and $d \rightarrow d$ transitions. Since the s electrons make the chief contribution to the conductivity we need only consider the $s \rightarrow d$ transitions.

It is essential to the theory that the d band should be narrow. This is probable owing to the small overlap between the wave functions and consequently the small interaction between the d shells of neighbouring atoms. We see, therefore, that the density of states at the surface of the Fermi distribution will be larger in the d band than in the s band. $s \rightarrow d$ transitions are therefore more probable than $s \rightarrow s$ transitions, which is the reason for the relatively large resistance of the transition metals. Moreover, a consideration of the susceptibilities of silver-palladium alloys shows that the d band is nearly full, having 9·4 electrons per atom (see below). The density of vacant states in the d band will therefore decrease rapidly with increasing energy. Hence when the metal is heated and more electrons are raised to higher states by acquisition of thermal energy, the density $N_d(E)$ of d states to which the s electrons with most energy can make transitions will have decreased and the probability of such transitions will be less. Hence as the temperature rises the electrons will remain longer in the s state before being scattered to a d state, and the resistance will increase less rapidly than that of a normal metal. For s electrons with energies greater than the upper limit of the d band this scattering-probability will be small and will decrease much less rapidly. Hence a temperature will be reached where the resistance is again approximately proportional to T, i.e. we expect a flex in the {resistance, temperature} curve. The temperature at which the flex occurs will depend on the value of $E_{\text{max.}}$, being lower as $E_{\text{max.}}$ increases. In addition of course the decrease of Θ_D will ultimately make the resistance increase more rapidly than the linear law as in a normal metal.

Calculation based on these considerations gives the expression for the resistance

$$\rho \propto \frac{T}{M\Theta^2_D}\left[1 - \frac{\pi^2}{6}\left(\frac{T}{T_0}\right)^2\right],$$

where T_0 is a constant called the degeneracy temperature for the d shell and T is small compared with T_0. From the observed resistances, $T_0 = 2100^\circ$ K. for palladium and 3100° K. for platinum.

Owing to the uncertainty in computing the variation of Θ_D with temperature it is simpler to express the result as

$$\left(\frac{\rho}{\rho_0}\right) = \left(\frac{\rho}{\rho_0}\right)_N (1 - \text{constant } T^2),$$

where $\left(\frac{\rho}{\rho_0}\right)_N$ is the ratio for a normal metal;

or
$$\left(\frac{\rho}{\rho_0}\right)_N - \left(\frac{\rho}{\rho_0}\right) = AT^3,$$

where A is approximately constant but increases slightly with T.

By taking copper as the normal metal it is found that a formula of this type fits the experimental values for platinum quite well though the value of A actually decreases slightly with rise of temperature. It is therefore of interest to determine whether this formula also applies to palladium.

We now consider the effects of alloying palladium with metals containing one *s* electron per atom. The susceptibility of palladium-silver$^{(4)}$ and palladium in which hydrogen is occluded$^{(5, 6)}$, referred to above, decreases with increasing concentration of silver or hydrogen until, at about 60 atoms per cent, it has fallen to zero and afterwards becomes negative (diamagnetic). This is explained as follows: It is concluded that the high paramagnetism of palladium and platinum is proportional to the density of states in the *d* band, i.e. to $N_d(E)_{\text{max.}}$. Now it is evident from figure 1 that since the density of vacant *d* states is much greater than the density of *s* states, most of the extra *s* electrons of silver or hydrogen will go into the *d* band until it is full, thus reducing the value of $N_d(E)_{\text{max.}}$. The experiments show that about 0·6 additional electrons per atom are sufficient to fill the *d* band completely, i.e. in pure palladium there are 9·4 electrons per atom in the *d* band, the remaining 0·6 being in the *s* band.

Further evidence is obtained from the measurements of Giebel$^{(7)}$ on the resistance and temperature coefficient of palladium-gold alloys. The resistance of a disordered alloy is R_0+r_t at $t°$ C., where R_0 is the resistance due to disorder (*Restwiderstand*) and r_t the resistance due to thermal motion of the atoms (scattering). As gold is added to palladium we expect that the vacant *d* states will be gradually filled and consequently, owing to reduction in $N_d(E)_{\text{max.}}$, that r_t will decrease rapidly up to about 60 atoms per cent of gold. For greater quantities of gold the increasing number of *s* electrons will cause a further decrease of resistance except that this will be counterbalanced by the greater scattering-power of the heavier gold atoms. Hence for concentrations of between 60 per cent and 100 per cent of gold, r_t will be approximately constant. The results obtained by Giebel bear out these conclusions$^{(7)}$.*

It has been shown above for pure palladium that as the temperature is raised and the density of *d* states to which the *s* electrons can be scattered decreases, the resistance increases less rapidly than that of a normal metal. But by the addition of gold to palladium the density of vacant *d* states is, as it were, artificially decreased. The rate of decrease of $N(E)$ with increasing E thus becomes greater and we should expect the rate of increase of r_t to be even less rapid than for palladium, except in so far as the resistance is increased by the decrease of Θ_D as gold atoms replace palladium. We should also expect that for each alloy the increase of resistance due to decrease of Θ_D with rising temperature would ultimately become predominant and that there would be a flex in the {resistance, temperature} curve as there is (theoretically) in pure palladium, and that a change over to the normal type of resistance curve would occur at about 60 per cent of gold. Experiments have therefore been made to carry the resistance-measurements for palladium to higher temperatures than heretofore and to test the above conclusions for the palladium-gold alloys.

---

* Cf. Rosenhall$^{(8)}$ for similar measurements on palladium, silver, and hydrogen. The resistance of certain palladium-silver alloys actually decreases with the addition of hydrogen owing to the rapid decrease in r_t. See figure 5 of the cited paper.

§ 2. EXPERIMENTAL METHOD

The palladium and the alloys were obtained from Messrs Johnson Matthey and Co. in the form of rods 2 mm. in diameter, the rods being 18 cm. long in the case of the palladium and 12 cm. long in the case of the alloys. The palladium was 99·98-per-cent pure and the alloys, which were specially prepared, contained respectively 25, 40, 55 and 65 atoms per cent of gold. The method used was to measure the p.d. between two points on the rod when a constant current was passed through it. The current was set to a constant value (about 2 A.) by means of a Weston substandard mirror-scale ammeter and the p.d. was measured on a Tinsley potentiometer reading in steps of 10μV. up to 19 mV. The current-setting could be repeated to an accuracy greater than $\frac{1}{40}$ per cent.

The temperature was measured with a calibrated platinum, platinum-rhodium thermocouple. For the temperatures about 0° C. the specimen was mounted in a vacuum furnace consisting of a Vitreosil tube 34 in. long by $1\frac{1}{4}$ in. internal diameter wound over 15 in. of its length near the lower end with nichrome wire and containing a mild steel liner to give greater uniformity of temperature. Each rod was cut in half and the two halves R were spot-welded to nickel rods N of the same diameter and $\frac{1}{4}$ in. apart, which served as current leads, figure 2. The reason for this symmetrical arrangement is explained later. The potential leads were nickel wires attached by spot welding at P and the thermocouple was similarly attached midway between them at S. Spot welding did not seem to affect the value of ρ/ρ_0 though it usually produced an increase in ρ_0 of about 1 per cent. The whole was suspended from a glass cap C and held axially in the furnace by a quartz spacer at the lower end of the rods. The leads passed through fine tubes T in the cap; a side tube and ground joint G enabled the furnace to be connected to a diffusion pump. Sealing-wax was used for the seals, one of these near the windings having to be water-cooled. The pressure was less than 10^{-6} mm. except at the highest temperatures, where owing to the evolution of gas it sometimes rose to about 10^{-4} mm. The temperature variation along the specimen was always less than $\frac{1}{2}$° C., and thermoelectric e.m.fs. due to the temperature-gradient were eliminated in the usual way by reversing the current and potential leads. For temperatures below 0° C. the specimen was immersed in a vacuum flask containing liquid oxygen, solid carbon dioxide and acetone or liquid ethylene.

In the measurements on the 55 per cent alloy and to a less extent with the 40 per cent alloy it was observed that the p.d. increased slowly to a maximum each time the current was reversed. Tests showed that the mean value of the p.d. read immediately after reversing the current was the same as that obtained by allowing the p.d. to come to a steady value and subtracting from this the residual e.m.f. measured immediately after switching off the current. The residual e.m.f. decreased slowly after the current had been cut off. The true p.d. was therefore taken as the mean of the values immediately after reversal of the current. The effect was explained as due to Peltier heating and cooling at the junctions of the specimen and nickel rods, which in these alloys would be expected to be abnormally large. This heat was conducted along the specimen and slowly altered the temperature at the points of contact of the potential leads. Since the effect reverses with the current, the reversal of the connections to the potential leads would make the drift in the p.d. appear in the same direction in each case. This also explains why the effect dies away when the current is cut off.

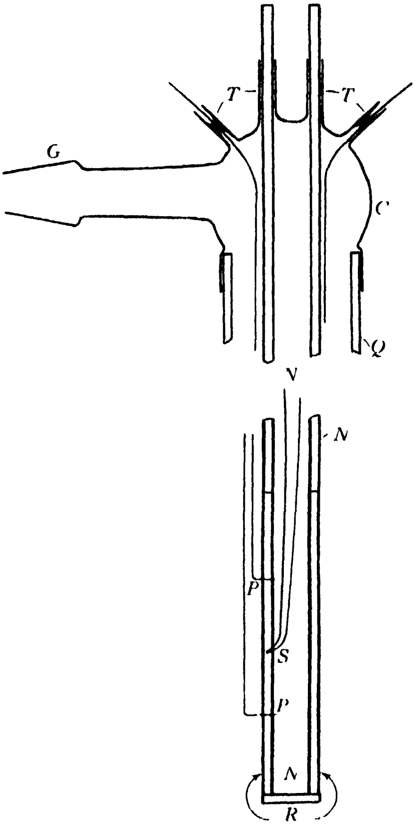

Figure 2. Symmetrical arrangement of rods R to allow for free expansion of the specimen on heating. Q is the top of the furnace tube. (Not drawn to scale.)

§ 3. RESULTS

The experimental values for palladium and the alloys are shown in table 1 as the ratio of the resistance ρ at T° K. to the resistance ρ_0 at 0° C. The values for palladium agree well with those given by Holborn$^{(9)}$. σ_0 is the specific resistance at 0° C.

It was observed that although the values of ρ/ρ_0 for palladium hardly changed during annealing there was a considerable increase in the specific resistance σ_0. The value of σ_0 at 0° C. after a preliminary heating to 650° C. was $10{\cdot}63 \times 10^{6}$ ohm-cm., and after annealing at 970 to 1000° C. for three days (when the resistance appeared to have become constant) was $12{\cdot}38 \times 10^{-6}$. It was for this reason that the symmetrical arrangement, in which the specimen was allowed to expand freely

Table 1

Metal or alloy	Palladium before annealing	Palladium after annealing	65 % gold	55 % gold	40 % gold	25 % gold
σ_0 / Temp. (° K.)	$10{\cdot}63\times10^{-6}$	$12{\cdot}38\times10^{-6}$	$14{\cdot}31\times10^{-6}$	$20{\cdot}67\times10^{-6}$	$29{\cdot}46\times10^{-6}$	$28{\cdot}68\times10^{-6}$
90·2	0·2283	0·2327	0·8850	0·8901	0·9037	0·8170
169·3	0·5788	—	—	—	—	—
194·6	0·6840	—	—	—	—	—
273·2	1·000	1·000	1·000	1·000	1·000	1·000
373	1·372	1·370	1·063	1·057	1·042	1·086
473	1·730	1·708	1·128	1·116	1·080	1·166
573	2·078	2·039	1·200	1·172	1·114	1·237
673	2·395	2·357	1·271	1·221	1·145	1·299
773	2·704	2·645	1·335	1·267	1·175	1·358
873	2·972	2·907	1·403	1·314	1·204	1·416
973	3·220	3·152	1·482	1·368	1·240	1·472
1073	3·449	3·382	1·566	1·430	1·283	1·527
1173	—	3·597	1·655	1·493	1·325	1·585
1250	—	—	1·740	1·548	1·363	1·633
1273	—	3·803	—	—	—	—

during heating, was adopted. As first set up the specimen was bent slightly after being heated and it was thought that this might have produced fine cracks along the crystal boundaries. However a second specimen of palladium set up as in figure 2 also showed the same behaviour. This could not be due to the absorption of impurities given off by the iron tube, as the latter was well baked out beforehand at about 1200° C. in an induction furnace, and the palladium had not developed a *Restwiderstand*. The diameter of the specimen was measured before and after heating and the evaporation reported by Holborn(9) could not be detected. It seems possible to explain this increase by the growth of crystals in the metal and the development of small fissures between them. A similar increase was observed in the alloys and in each case examination of the specimen under the microscope after annealing revealed the presence of fairly large crystals.

The agreement between these results for palladium and the expression obtained by Mott is shown in table 2 by the constancy of the figures in the third column. Gold is chosen for the comparison, since of the normal metals its compressibility and thermal expansion are nearest to those of palladium. The values of $(\rho/\rho_0)_{\mathrm{Au}}$ are the means of those obtained by Holborn(9) and Northrup(10).

Table 2

$(\rho/\rho_0)_{\mathrm{Au}}-(\rho/\rho_0)_{\mathrm{Pd}}$	T (° K.)	$\frac{\text{Column 1}}{T^3}\times10^9$
0·181	573	9·62
0·325	673	10·66
0·469	773	10·15
1·24	1073	10·04
2·63	1273	9·84

At the highest temperatures the $\{\rho/\rho_0, T\}$ curve appears to be straightening out prior to turning upwards as was expected by the theory, that is to say the flex is outside the range of the measurements.

The values of ρ/ρ_0 for each alloy are those obtained after annealing until the resistance had become constant. In all cases the final values repeated to within 0·1 per cent.

§ 4. DISCUSSION OF RESULTS

If the resistance of each alloy is plotted against the absolute temperature, the resulting curve produced back to cut the resistance axis will give an intercept R_0 which will not differ greatly from the true *Restwiderstand*. The resistance at any other temperature $t°$ C. can then be expressed as $R_0 + r_t$. Since we are only interested in the thermal part of the resistance, the ratio r_t/r_0 is plotted against T in figure 3 for the various alloys together with the curve for pure palladium deduced in the same way.* These curves clearly show that as gold is added to palladium the resistance ratio at first increases less rapidly with increasing temperature but that a change-over occurs between 55 and 65 per cent of gold. The fact that the decrease

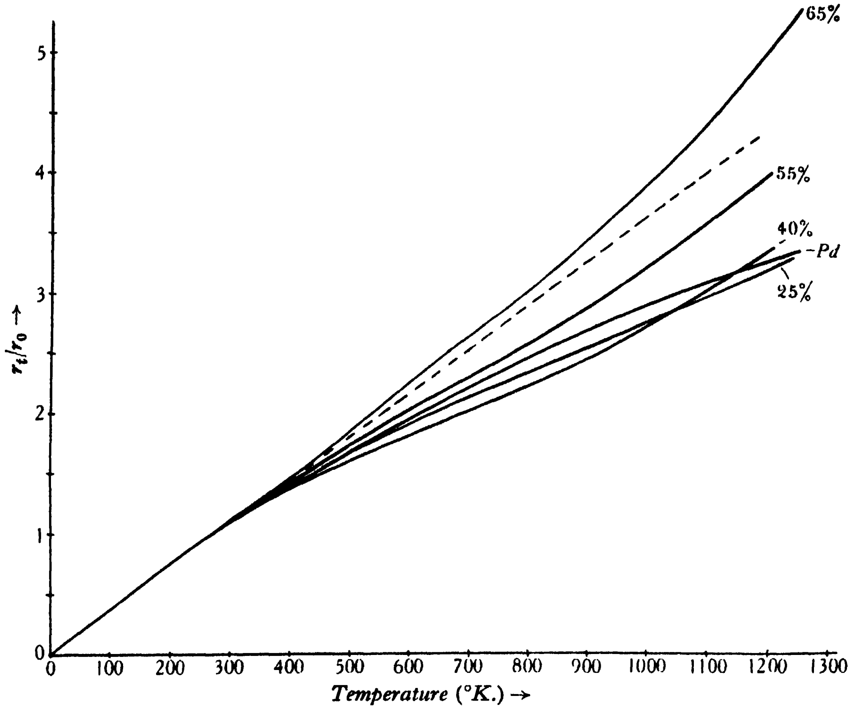

Figure 3. Relation between r_t/r_0 and the absolute temperature for pure palladium and alloys containing 25, 40, 55 and 65 atoms per cent of gold.

---

* Owing to the form of the {resistance, temperature} curve of palladium, which in the neighbourhood of absolute zero behaves like a normal metal, this treatment is equivalent to considering the value of R_0 for palladium to be negative.

in r_t does not continue up to 60 per cent of gold is presumably due to a decrease in Θ_D as gold is added.

It was at first expected that the position of the flex in the curve would move down to lower temperatures as the concentration of gold was increased. However, it is found that the flex temperature for the 55-per-cent alloy is intermediate between the corresponding temperatures for the 25- and 40-per-cent alloys. But the point at which the turn-up begins depends not only on the position of $E_{\max.}$ but also on the variation of Θ_D with T, and the addition of gold will probably cause changes in this variation which might account for the above expectation not being realized. It will be noticed that the variation of the resistance for the 55-per-cent gold alloy resembles that of the copper-nickel alloys containing about the same proportion of copper (constantan). The two alloys are in fact similar from a theoretical point of view though the latter is complicated by the ferromagnetism of nickel. It will be further noticed that the curve for the 65-per-cent alloy has not strictly the same shape as that for a normal metal but has a small hump at about 600° K. It seems unlikely that at this temperature there is a change in the distribution of electrons between the *s* and *d* bands and the re-appearance of some vacant states in the *d* band. It is more likely that the alloy, like Invar, has an anomalous coefficient of expansion. Thus if it contracted with rise of temperature in the region of 600° K. the consequent increase in Θ_D would cause a decrease in the resistance. There is little doubt however that in the main the results are in agreement with the theory.

§ 5. ACKNOWLEDGMENTS

The writer wishes to express his best thanks to Prof. N. F. Mott and Dr H. H. Potter for suggesting this problem, and for much helpful advice and criticism, both theoretical and experimental, throughout. He is also indebted to the Department of Scientific and Industrial Research for a personal grant and to the Colston Research Society of the University of Bristol for the provision of the alloys.

REFERENCES

(1) MOTT. *Proc. phys. Soc.* **47**, 571 (1935).
(2) —— *Proc. roy. Soc.* **153**, 699 (1936); **156**, 368 (1936).
(3) FUCHS. *Proc. roy. Soc.* **151**, 585 (1935).
(4) SVENSSON. *Ann. Phys.*, Lpz., **14**, 699 (1932).
(5) AHARONI and SIMON. *Z. phys. Chem.* **4**, 175 (1929).
(6) SVENSSON. *Ann. Phys.*, Lpz., **18**, 302 (1933).
(7) GIEBEL. *Z. anorg. Chem.* **70**, 240 (1911).
(8) ROSENHALL. *Ann. Phys.*, Lpz., **24**, 297 (1935).
(9) HOLBORN, L. *Ann. Phys.*, Lpz., **59**, 145 (1919).
(10) NORTHRUP, E. F. *J. Franklin Inst.* **177**, 287 (1914).

A DETERMINATION OF THE FUNDAMENTAL TYPES OF ELECTRON OSCILLATIONS IN A TRIODE VALVE

By R. COCKBURN, M.Sc., A.Inst.P.

Received 27 *November* 1935. *Read* 13 *November* 1936.

ABSTRACT. It is confirmed experimentally that with a retarding-field triode, electron oscillations can be maintained whose wave-lengths are determined completely by the external circuit (Gill-Morell oscillations); and that, in addition, oscillations can be obtained with wave-lengths completely independent of the external circuit, provided the latter does not approach resonance with them (Barkhausen-Kurz oscillations).

The dependence of the Barkhausen-Kurz oscillations on the valve-dimensions and operating conditions is examined in detail. It is found that for any given set of conditions there are not one, but two possible fundamental wave-lengths: type A, of shorter wave-length, and type B, of longer wave-length, both of which may give harmonics.

For any valve of grid radius r_g, and at constant anode voltage, characteristic curves

$$\frac{\lambda_A \sqrt{V_g}}{r_g} = F_A\left(\frac{i_g}{i_0}\right) \quad \text{and} \quad \frac{\lambda_B \sqrt{V_g}}{r_g} = F_B\left(\frac{i_g}{i_0}\right)$$

may be obtained, where λ_A and λ_B are the wave-lengths of the A- and B-type oscillations, V_g is the grid voltage, and i_g/i_0 is the degree of saturation of the grid-cathode space. Except for certain limiting conditions, the dependence of F_A and F_B on valve-dimensions and operating conditions is small, a slight decrease being obtained with decrease of the ratio (grid spacing)/(grid radius), or with decrease of grid voltage.

By application of the theory developed in an earlier paper, the shape of the characteristic A curve establishes that the A-type oscillations are due to the periodic transit of electrons between the cathode and virtual cathode. The shape of the characteristic B curve, on the other hand, shows that the B-type oscillations are not due to any such transit of electrons, and leads to the conclusion that they are determined by the resonant circuit formed by the grid-plate capacity in parallel with the equivalent inductance of the electron cloud between these electrodes.

§ 1. INTRODUCTION

Electron oscillations may be produced either by the retarding-field triode or by the magnetron. The latter has been examined in detail by Megaw(1). In the present paper, only the retarding-field method is considered. Summaries of the numerous investigations employing this method have been given by Pierret(2), Wenstrom(3), Megaw(4), and Wagner and Hollmann(5).

Although electron oscillations were first discovered fifteen years ago and have since been subject to continuous investigation, there is thus far no generally accepted theory of their maintenance, and furthermore there has been considerable divergence in the experimental results recorded. In particular, in regard to the nature of the oscillations, some workers have concluded that the wave-lengths maintained are determined completely by the external circuit (Gill-Morell oscillations), while others have found them to be determined only by the valve operating conditions and dimensions (Barkhausen-Kurz oscillations). Many other workers have found the wave-lengths to depend to some degree on all the variables.

Although the existence of Barkhausen-Kurz oscillations, as defined above, has been fairly generally accepted, a complete investigation into their dependence on conditions within the valve has not previously been attempted, most workers confining their attention to the Gill-Morell oscillations. This is probably due to the fact that, whereas the amplitude of the Gill-Morell oscillations is of the order of some milliamperes, the Barkhausen-Kurz oscillations are invariably of very small amplitude, of the order of 1 microampere. For certain critical adjustments their amplitude may increase to perhaps 10 microamperes, and such direct observations on Barkhausen-Kurz oscillations as are available have usually been confined to these optima.

With such limited results it is not possible to choose definitely between the many theories put forward to account for the Barkhausen-Kurz oscillations. These fall roughly into two classes. On the one hand are the theories which assume the oscillations to be due to some periodic transit of electrons within the valve. Various transits have been suggested, but the original theory of Barkhausen and Kurz(6), that the periodic time of the oscillations is equal to the transit time of electrons oscillating between cathode and plate, is probably most generally accepted. On the other hand are the theories which assume the oscillations to be due to a resonant circuit formed by some part of the electrode system, modified in various ways by the presence of space charge. A theory of this nature has been put forward recently by Rostagni(7).

In the present paper it is shown that in general the retarding-field triode can maintain both Gill-Morell and Barkhausen-Kurz oscillations. Particular attention has been paid to the Barkhausen-Kurz oscillations, and it has been found that there exist two distinct types: one due to the periodic to-and-fro motion of the electrons about the grid of the valve, and the other to a resonant circuit formed by the grid-plate capacity in parallel with the equivalent inductance of the electron cloud between these electrodes. The existence of two types of Barkhausen-Kurz oscillations, associated with such different mechanisms, has not hitherto been realized.

The cause of the maintenance of the oscillations is not dealt with in the present paper.

§ 2. PROCEDURE

The circuit, figure 1, used by the author is essentially the same as that used by Barkhausen and Kurz and most subsequent workers, the Lecher wires which form the tunable external circuit being connected to the grid and plate of the valve. The effective length of this circuit is altered by varying the position of the shorting condenser C_1. The grid and plate leads are connected to the terminals of this condenser, where there are potential nodes. The plate lead includes a suspended-coil galvanometer, of sensitivity $5 \cdot 10^{-9}$ A./mm. at 1 m., with a variable shunt, and with provision for applying a balancing current.

The onset of oscillations is detected by the accompanying increase of plate current. It is known⁽⁸⁾ that when the plate potential is only slightly different from that of the cathode the increase in plate current is roughly proportional to the amplitude of the oscillatory current. This method of measurement was adopted in the present experiments because of its great sensitivity. Although with all conditions adjusted for optimum maintenance oscillatory currents of the order of 5 mA. were obtained, the usual amplitudes, of less than 1 microampere, are quite impossible to measure directly. Furthermore, for accurate measurements of wave-length very slight changes in the oscillatory current must be detected.

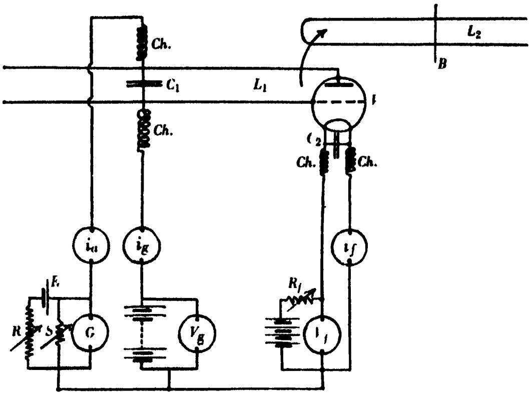

Figure 1. Circuit for the examination of electron oscillations. V, valve; L_1, external circuit; L_2, Lecher tuning circuit; B, shorting bridge; C_1, bridging condenser; C_2, filament blocking condenser; $Ch.$, chokes; S, variable shunt; E, backing e.m.f.; R, regulating resistance for E; R_f, filament current regulating resistance.

The wave-lengths of the oscillations were measured by means of the usual second Lecher-wire circuit L_2, magnetically coupled at one end to the external circuit L_1 of the valve. As their length is varied by means of the short-circuiting bridge B, the absorption of energy from the valve circuit, which occurs when the effective length of the Lechers is a multiple of half a wave-length, is indicated by a decrease of plate current.

§ 3. EFFECT OF THE EXTERNAL CIRCUIT: BARKHAUSEN-KURZ AND GILL-MORELL OSCILLATIONS

Preliminary experiments on the effect of varying the length of the external circuit showed that, for nearly all the valves examined, Barkhausen-Kurz oscillations of small amplitude could be maintained, in addition to the larger amplitude Gill-Morell oscillations. The length l of the external circuit is measured from the valve legs and does not include the portion formed by the leads inside the valve. At constant grid voltage V_g the variations of the maintained wave-length λ and of the plate current i_a with variation of l were determined for various fixed values of grid current i_g. A typical set of results for one valve, no. 6, at $V_g = 50$ V. is shown in figure 2, which shows that between $l = 5$ cm. and $l = 20$ cm., and between $l = 80$ cm. and $l = 120$ cm., Gill-Morell oscillations are obtained whose wave-lengths are determined by the natural wave-length of the external circuit. These oscillations are maintained for any value of i_g, from 2 to 8 mA. approximately. The slight decrease in wave-length obtained with increase of i_g is due to the fact that the external circuit includes the grid-plate capacity; it has been established$^{(9)}$ that the dielectric constant of space-charge is less than unity, so that any increase in the grid current will decrease the grid-plate capacity, and hence also the natural wave-length of the external circuit.

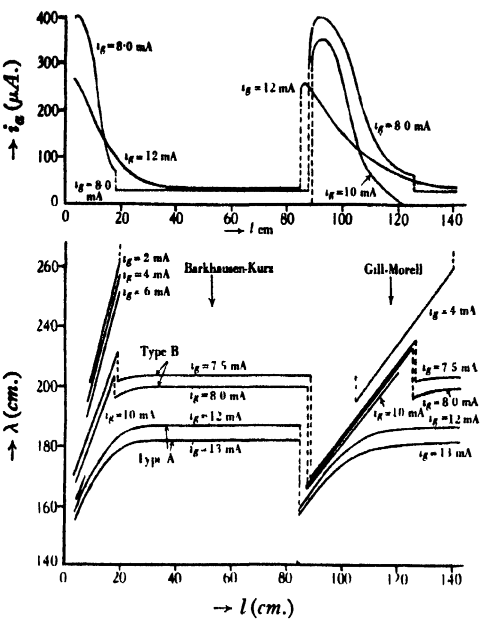

Figure 2. Variation of plate current i_a and wave-length λ with circuit-length l, for various grid currents i_g. Valve 6. $V_g = 50$ V.

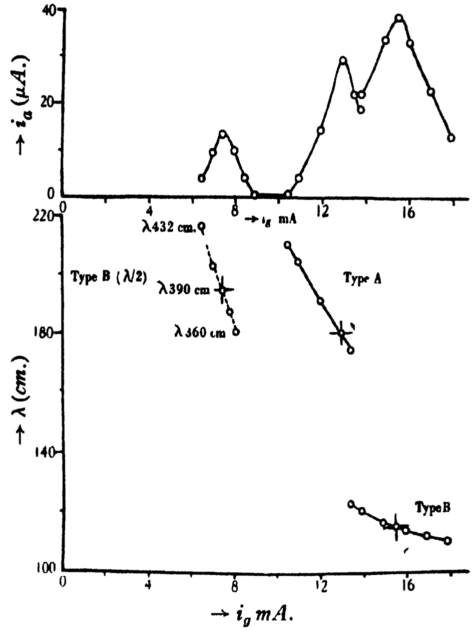

Figure 3. Barkhausen-Kurz oscillations. Variation of plate current and wave-length with grid current i_g at constant grid voltage. Valve 6. $V_g = 50$ V. $l = 30$ cm. → 70 cm.

Between $l = 30$ cm. and $l = 80$ cm. the figure shows that Barkhausen-Kurz oscillations, with wave-lengths independent of the external circuit, are maintained for values of i_g in the region of 7·5 mA. and 12 mA. respectively. No oscillations could be obtained between $i_g = 9$ mA. and $i_g = 11$ mA. It is shown later that the Barkhausen-Kurz oscillations maintained at the two values of i_g are of different types, distinguished throughout the paper as types A and B.

§ 4. THE BARKHAUSEN-KURZ OSCILLATIONS

It is clear that the wave-lengths of the Gill-Morell oscillations are determined by the characteristics of the external circuit. The following experiments are mainly concerned with the identification of the Barkhausen-Kurz oscillations.

With the external circuit maintained within such limits that only Barkhausen-Kurz oscillations were obtained, the dependence of their wave-lengths on the valve operating conditions and dimensions was examined. For this purpose a series of specially constructed valves was used in which the various dimensions were varied in turn. All the valves except one were of the AT 40 type, having concentric cylindrical electrodes, and a tungsten filament rated at 6 V., 2·5 A. The grid was a helix of wire with the turns short-circuited by the supporting bar. The pressure in these valves was of the order of 10^{-6} mm. of mercury, and was certainly not more than 10^{-5} mm. The relevant data of the valves are given in table 1.

Table 1. Data of valve-dimensions

Experiment	Valve reference	Grid radius r_g (cm.)	Anode radius / Grid radius r_p/r_g	Turns/cm. grid helix p
4·2·1	5 AT 40	0·21	5·0	6
	6	0·22	3·7	6
	7	0·21	6·0	6
	8	0·21	2·95	6
4·2·2	6 AT 40	0·22	3·7	6
	10	0·22	3·7	4
	11	0·22	3·7	8·5
	12	0·22	3·7	11
4·2·3	6 AT 40	0·22	3·7	6
	17	0·15	3·5	6·4
	18	0·25	4·1	6·4
	19	0·35	3·5	6·4
5	20 Dario	0·15	4·1	13

AT 40 type. Tungsten filament, length 2·7 cm., radius 0·005 cm., length of grid 2·0 cm. Diameter of grid wire 0·018 cm., length of plate 1·82 cm.

Dario type. Oxide-coated filament, length 2·2 cm., radius 0·0005 cm., length of grid 1·82 cm., diameter of wires 0·018 cm., length of anode 1·5 cm.

4·1. *The dependence of the Barkhausen-Kurz oscillations on valve operating conditions.* In the first instance the valve-dimensions were maintained constant, and the dependence of the Barkhausen-Kurz oscillations on the valve operating conditions was determined. For a given valve the variation of wave-length with emission current was found for different values of grid voltage. Since in all these experiments the plate is maintained at zero potential, the plate current is extremely small, and the total emission current differs only slightly from the measured grid current.

A typical {wave-length, grid current} curve obtained with valve 6 at $V_g = 50$ V., together with the corresponding {plate current, grid current} curve, is shown in figure 3. The curves are found to be practically independent of the length l of the external circuit between $l=30$ cm. and $l=70$ cm. It will be noted that oscillations are obtained over a wide range of grid-current values, maxima of amplitude occurring for three definite currents. It is found that with variation of grid voltage, the ratios (optimum value of grid current)/(saturation value of grid current) were practically constant. The saturation value of grid current i_0 is here defined as the value which just reduces the cathode field to zero. Actually, owing to the initial velocities of emission of the electrons, a somewhat greater current can be obtained by further increasing the cathode temperature. The experimental method adopted for measuring i_0 has been described in an earlier paper(10). Throughout the present paper the ratio i_g/i_0 is called the "degree of saturation" and will refer to the grid-cathode space.

If for a given valve the {wave-length, grid current} curves at various grid voltages are plotted in the form $\lambda\sqrt{V_g}=f\,(i_g/i_0)$, they are found to correspond closely. The results for valve 6 are shown in figure 4. It is shown in § 5 that the small divergence from complete correspondence is due mainly to the slight dependence of the effective grid structure on grid voltage, and that if allowance were made for this effect the curves would correspond almost completely. The curves $\lambda\sqrt{V_g}=f\,(i_g/i_0)$, which are drawn for all the valves examined, will be referred to as the "characteristic curves".

From figure 4 it will be seen that there are two possible modes of oscillation, giving rise respectively to the shorter and longer Barkhausen-Kurz wave-lengths. The existence of such shorter and longer wave-lengths has been noted by Schiebe(11) and by Hollmann(12) but the matter has not been further investigated. Hollmann considered that the two modes were due primarily to the same cause, a periodic transit of electrons within the valve. The experiments described later show, on the contrary, that they are due to the oscillations of entirely different systems within the valve. They constitute two types, which are found to be of general occurrence in all the valves examined, and will be referred to as "types A and B", the shorter wave-length corresponding to type A and the longer to type B. Both types of oscillation readily give first harmonics, particularly when the wave-length of the external circuit approaches half the fundamental value. The characteristic curves are not otherwise distorted in these circumstances, and no higher harmonics have been observed. The harmonic curves have been omitted from figure 4 for the sake of clearness.

4·2. *The dependence of the Barkhausen-Kurz oscillations on valve-dimensions.* The characteristic curves provide a convenient method of showing the effect of the valve operating conditions on the wave-lengths of the Barkhausen-Kurz oscillations, and their dependence on the valve-dimensions will now be examined. Since these curves are not quite independent of grid voltage the effect of variation of valve-dimensions is shown for one voltage only, although the results in general apply at all voltages.

4·2·1. *Variation of plate radius.* Four valves, nos. 5, 6, 7, 8, were examined which differed only in their respective plate radii, the ratio of plate radius r_p to grid radius r_g varying from $r_p/r_g = 6{\cdot}0$ to $r_p/r_g = 2{\cdot}95$. A typical set of characteristic curves obtained at $V_g = 50$ V. is shown in figure 5. It will be seen that with the exception of valve 8, which had the smallest plate radius, the characteristic curves are unaffected by variation of plate radius. A detailed discussion of the curves of valve 8 is deferred until § 5. Figure 5 also shows that for all the valves oscillations are obtainable for $i_g/i_0 > 0{\cdot}4$. This result is of some interest in view of Gill's(13) theory of maintenance, which requires that the extent of the oscillation region shall depend on plate radius.

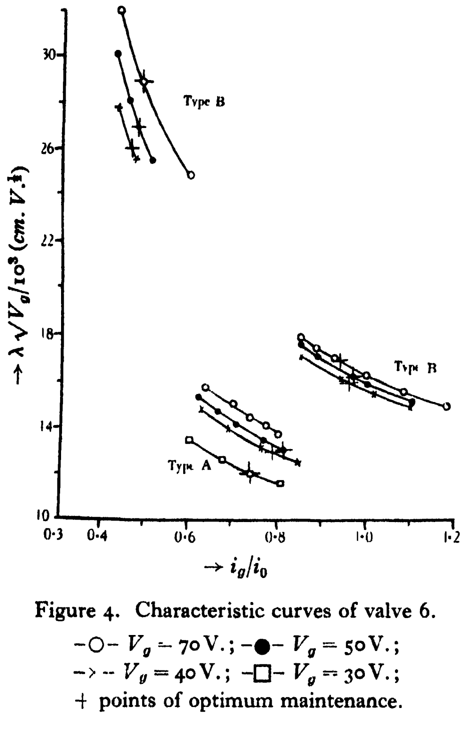

Figure 4. Characteristic curves of valve 6.
−○− $V_g = 70$V.; −●− $V_g = 50$V.;
−×− $V_g = 40$V.; −□− $V_g = 30$V.;
+ points of optimum maintenance.

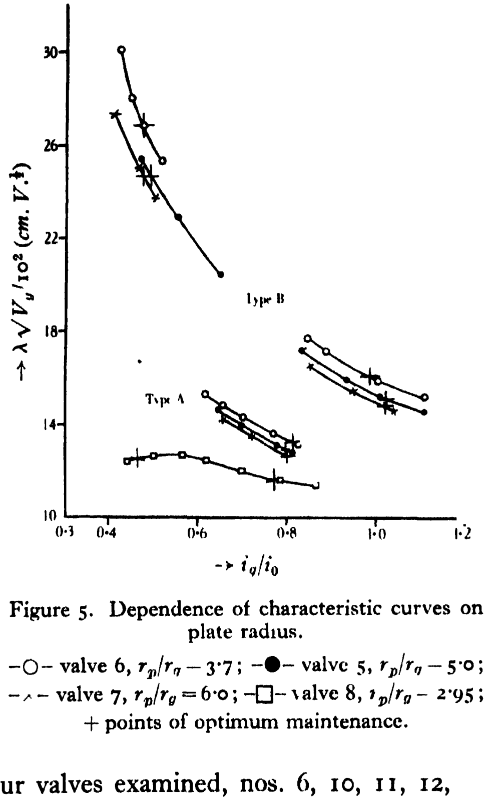

Figure 5. Dependence of characteristic curves on plate radius.
−○− valve 6, $r_p/r_g = 3{\cdot}7$; −●− valve 5, $r_p/r_g = 5{\cdot}0$;
−×− valve 7, $r_p/r_g = 6{\cdot}0$; −□− valve 8, $r_p/r_g = 2{\cdot}95$;
+ points of optimum maintenance.

4·2·2. *Variation of grid pitch.* The four valves examined, nos. 6, 10, 11, 12, differed only in the number of turns p per cm. of the grid helix, which varied from $p = 11$ to $p = 4$. Valve 10, which had a very open grid ($p = 4$), gave no detectable Barkhausen-Kurz oscillations. This is in accordance with the observations of other workers. The characteristic curves of the remaining three valves at $V_g = 50$ V. are shown in figure 6. It will be seen that the variation of grid pitch has little effect on the curves, an increase in p of 100 per cent causing a diminution of only about 10 per cent in the wave-lengths.

An interesting point arises with valve 12, which had a close-mesh grid ($p = 11$). Experiments so far have shown that the A-type oscillations are always obtained for degrees of saturation from 0·6 to 0·8, with an optimum value at about 0·8. With valve 12 this only held for $V_g < 50$ V.; for $V_g > 50$ V. the A-type oscillations are replaced by the B type. The part of the characteristic curve obtained in this region at $V_g=60$ V. is shown dotted in figure 6. A similar result is noted in the next section.

4·2·3. *Variation of grid radius.* In the four valves examined, nos. 6, 17, 18, 19, the grid and anode radii were varied, the ratio r_p/r_g, and all other dimensions, being maintained constant. The grid radius varied from $r_g=0{\cdot}15$ to $r_g=0{\cdot}35$ cm. It was found that valve 17 ($r_g=0{\cdot}15$) gave no detectable oscillations. Taking into account the result obtained above with valve 10, it would appear that the Barkhausen-Kurz oscillations are not maintained if the ratio (grid spacing)/(grid radius) exceeds a certain value approximating to unity.

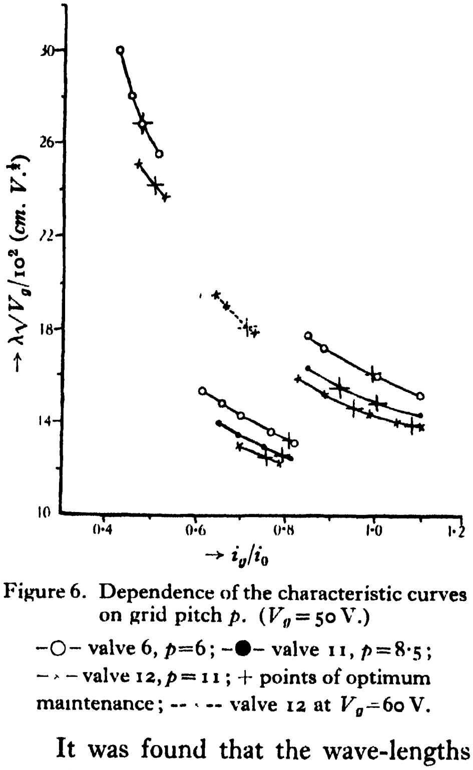

Figure 6. Dependence of the characteristic curves on grid pitch p. ($V_g=50$ V.)

–O– valve 6, $p=6$; –●– valve 11, $p=8{\cdot}5$; –×– valve 12, $p=11$; + points of optimum maintenance; --×-- valve 12 at $V_g=60$ V.

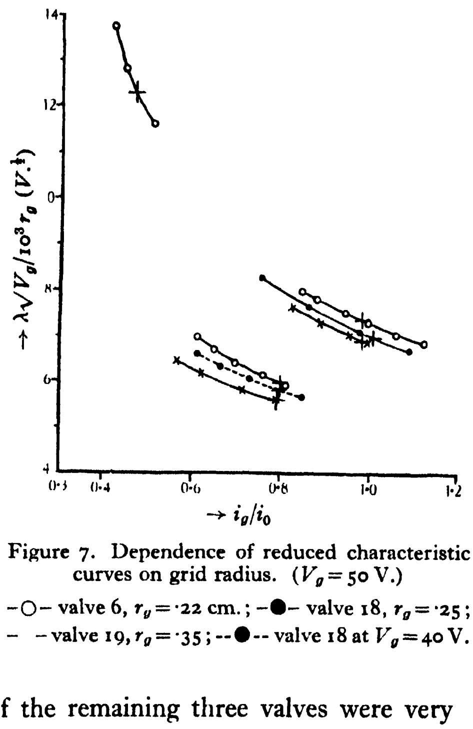

Figure 7. Dependence of reduced characteristic curves on grid radius. ($V_g=50$ V.)

–O– valve 6, $r_g=\cdot22$ cm.; –●– valve 18, $r_g=\cdot25$; – –valve 19, $r_g=\cdot35$; --●-- valve 18 at $V_g=40$ V.

It was found that the wave-lengths of the remaining three valves were very nearly proportional to the grid radii. Reduced characteristic curves $\lambda\sqrt{V_g}/r_g=f(i_g/i_0)$ were therefore drawn for these valves. The curves obtained at $V_g=50$ V. are shown in figure 7. It will be seen that these curves correspond closely, an increase of 50 per cent in r_g causing a diminution of 10 per cent in the values of $\lambda\sqrt{V_g}/r_g$. The cause of this variation, and of the slight variation with grid pitch and grid voltage, will be further discussed in § 5.

For valve 18, B-type oscillations replaced the A type for $V_g>40$ V. This confirms the result obtained earlier with valve 12, that in certain cases, most probably with valves in which the ratio (grid spacing)/(grid radius) is small, increase of grid voltage tends to cause the A-type oscillations to be replaced by the B type.

4·2·4. *Summary of the results of paragraphs* 4·2. The main results with regard to the dependence of the Barkhausen-Kurz oscillations on the valve-dimensions may be briefly summarized as follows. For nearly all the valves examined Barkhausen-Kurz oscillations are obtained for any value of $i_g/i_0 > 0{\cdot}4$, provided the ratio (grid spacing)/(grid radius) < 1 approximately. These oscillations are of two types: type B, of longer wave-length, are usually most strongly maintained at $i_g/i_0 = 0{\cdot}5$ and $i_g/i_0 = 1{\cdot}0$; and type A, of shorter wave-length, at $i_g/i_0 = 0{\cdot}8$, although with increase of grid voltage type A are liable to be replaced by type B.

The reduced characteristic curves $\lambda_A \sqrt{V_g}/r_g = F_A(i_g/i_0)$ and $\lambda_B \sqrt{V_g}/r_g = F_B(i_g/i_0)$ are, to a first approximation, independent of valve-dimensions, if $r_p/r_g > 3$. These curves afford, therefore, a most convenient way of representing the results obtained with any valve. Since they do depend to some extent, however, on the grid voltage and on the grid structure, it will be necessary, until the cause of this dependence has been examined more thoroughly, to specify these conditions when giving the characteristic curves.

When $r_p/r_g < 3$, F_A is subject to modification; this effect is fully discussed in the next section.

§ 5. THE NATURE OF THE BARKHAUSEN-KURZ OSCILLATIONS: TYPE A

The nature of the Barkhausen-Kurz oscillations will now be considered. The existence of reduced characteristic curves which are practically independent of valve-dimensions is consistent with most of the theories which have been put forward to account for these oscillations. Fortunately definite evidence of the nature of the A-type oscillations can be obtained from the characteristic curves of two of the valves examined, nos. 8 and 20, which are shown in figures 8 and 9. For both these valves the A-type oscillations extend over a much greater range than is usual, the B type only occurring for $i_g/i_0 > 1$, and in the case of valve 8 only when $V_g > 70$ V.

The particular interest in the curves lies in their unusual shape. Referring to figure 8, it will be seen that as i_g/i_0 is increased, the characteristic A curves show an increase in wave-length preceding the usual decrease which has been observed in all the other valves. It will now be shown that this effect can only be explained on the view that the periodic time of the A-type oscillations is determined by the time of transit of electrons within the valve, and that part of this transit occurs in the grid-plate space.

It is first necessary to examine the conditions obtaining between the grid and plate. Of the electrons leaving the cathode, only a certain proportion strike the grid immediately, the remainder penetrating into the grid-plate space. Here they experience a retarding field which brings them to rest at or near the plate. They then accelerate back towards the grid where again a certain proportion pass through, to be brought to rest at the cathode, when the process is repeated. The current passing between the grid and plate is thus a definite fraction of the total emission current, depending on the proportion captured by the grid at each transit. For some value of emission current, the current passing between the grid and plate will be sufficient to reduce the field at the plate to zero, just as in a normal diode, and the space is then saturated. Of course this can only happen if the grid-cathode space does not itself become saturated first.

Gill(13) has shown that the onset of grid-plate saturation, when the plate is a few volts positive to the cathode, may be detected by measuring the dependence of the plate current on emission current. By extrapolating the results obtained at various plate potentials an approximate result for plate at zero potential is obtained. In the case of valve 8 it was found that at any given grid voltage the onset of grid-plate saturation corresponded with the maxima in wave-length shown in figure 8. For all the other valves, owing to their larger plate radii, grid-plate saturation set in at much lower values of i_g/i_0. Since oscillations have not been obtained for such low values, the maxima in wave-length are not observed with these valves.

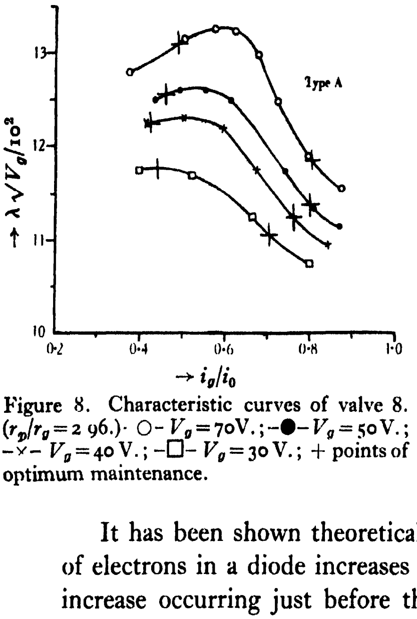

Figure 8. Characteristic curves of valve 8. ($r_p/r_g = 2\ 96$.)· ○- $V_g = 70$V.; -●- $V_g = 50$V.; -×- $V_g = 40$ V.; -□- $V_g = 30$ V.; + points of optimum maintenance.

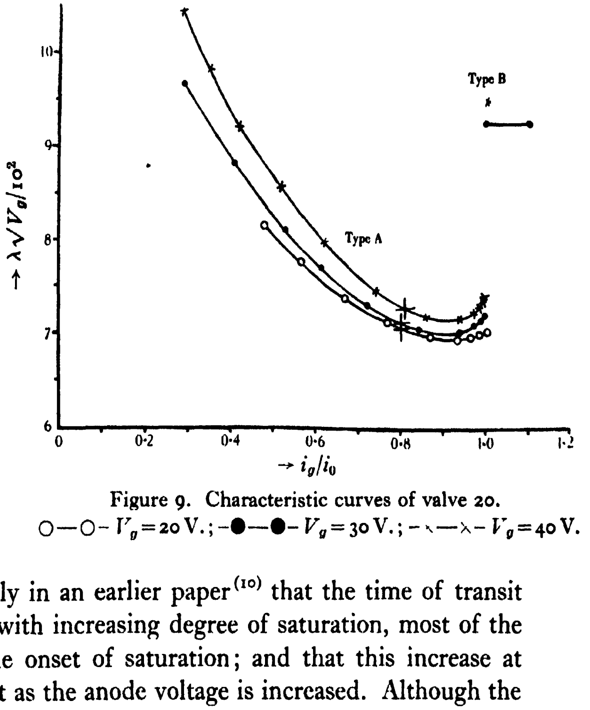

Figure 9. Characteristic curves of valve 20.
○—○- $V_g = 20$ V.; -●—●- $V_g = 30$ V.; -×—×- $V_g = 40$ V.

It has been shown theoretically in an earlier paper(10) that the time of transit of electrons in a diode increases with increasing degree of saturation, most of the increase occurring just before the onset of saturation; and that this increase at saturation becomes more apparent as the anode voltage is increased. Although the theory was developed for plane electrodes it will hold qualitatively for cylindrical electrodes. Applying these results to the grid-plate space of the valve, where the grid forms the anode with a virtual cathode at the plate, it will be seen that the increase in wave-length, and hence of periodic time of the oscillations, corresponds with the increase of electron transit time between grid and plate at the onset of saturation of the space; and, further, that the increase in wave-length becomes more apparent as the grid voltage is increased. Since such an increase is deducible on no other theory, the effect must be regarded as establishing definitely that the periodic time of the A-type oscillations is determined by the time of transit of electrons within the valve, and that part of the transit occurs between grid and plate.

With regard to the subsequent decrease in wave-length observed with increase of i_g/i_0, it has been pointed out by Gill(13) and by Tonks(14) that with any further increase in current the virtual cathode must move away from the plate towards the grid. This causes the electron transit time between grid and virtual cathode to decrease, producing the decrease in wave-length normally observed with increase of emission current.

Referring again to figure 8, it may be noted that the onset of grid-plate saturation, indicated by the maximum in wave-length, occurs at greater values of i_g/i_0 as V_g is increased. Experiments in which the plate was used as collecting electrode for those electrons which escaped capture by the grid showed that this variation with grid voltage was due partly to the variation of the grid-capture fraction, and partly to the variation of the effective length of the grid-plate space. If the effective grid structure were independent of the grid voltage, the maxima would occur at a constant value of i_g/i_0, and if the abscissae of the curves in figure 8 were adjusted in the correct proportion for this condition to be simulated, the curves would correspond closely except in the region of the maxima. Here a variation with grid voltage is to be expected, since the increase of transit time, and hence of wave-length, becomes less with increase of grid voltage; and, further, the velocity distribution of the electrons will tend to round off the cusp that would otherwise be expected. If the same adjustments were made to the curves of the other valves, nos. 5, 6, and 7, having the same grid structure as valve 8, a similar correspondence would be obtained. Thus the dependence of the characteristic curves on grid voltage is due mainly to the variation of the effective grid structure. As is shown in the Appendix, a further slight variation in the curves is also to be expected on account of the finite velocities of emission of the electrons from the cathode.

Further observations on the onset of grid-plate saturation showed that the value of i_g/i_0 at which this occurs decreases slightly with increase of grid radius, or of the number of turns per cm. of the grid helix. This explains the slight decrease in wave-length observed in these circumstances (paragraphs 4·2·2 and 4·2·3).

The main conclusions drawn from the curves of valve 8 with regard to the nature of the A-type oscillations are corroborated and extended by the curves of valve 20. This valve is of similar type to the others which have been examined, but differs in an important particular. Whereas all the other valves had high-temperature tungsten cathodes, valve 20 had a low-temperature oxide-coated cathode. Referring to figure 9 it will be seen that at $i_g/i_0 = 1$, the characteristic curves show a small but quite definite rise, which becomes more apparent as the grid voltage is increased. It is clear that this increase in wave-length is attributable to the increase in the time of transit of the electrons between cathode and grid. The effect is small, since the cathode-grid transit time is normally only a small part of the total transit time which determines the periodic time of the A-type oscillations. It is not observed with any of the other valves, since they have high-temperature cathodes, and the electrons have a consequent large average emission velocity. It has been shown theoretically[(10)] that this will have the effect of making the increase of transit time at saturation less apparent.

The qualitative results obtained with valves 8 and 20 thus establish that the A-type oscillations consist of a periodic transit of electrons which is affected by the conditions of both cathode-grid and grid-plate spaces. The most probable and only feasible electron path is from the cathode through the grid to the position of zero potential in front of the plate, and back to the cathode. This is indeed the original hypothesis put forward by Barkhausen and Kurz to explain the oscillations first observed by them. Assuming that the periodic time of the A-type oscillations is equal to twice the time of transit of an electron from cathode to virtual cathode, it is possible to calculate exactly the part of the characteristic curve obtained after grid-plate saturation has set in, provided certain data regarding the effective grid structure are known. In the case of valves 5, 6, 7, 8, these data may be obtained from the curves of valve 8. The calculation is given in Appendix (1); and in figure 10 the theoretical curve thus obtained for $V_g = 50$ V. is shown in comparison with the corresponding practical curves of valves 5, 6, 7, 8.

The quantitative agreement of the curves of valves 5, 6, and 7 with the theoretical curve is good. In the case of valve 8 it will be seen that as i_g/i_0 tends to unity the wave-lengths predicted by the theory are too small; this is due to neglecting in the calculations the increase in cathode-grid transit time which occurs at this stage. For the lower values of i_g/i_0, in the region of the maximum, there is considerable discrepancy between the theoretical curve and that of valve 8. This is due to the distribution of electron velocities, which although always obtained in practice was not considered in the calculations. As has been pointed out earlier, the distribution of velocities rounds off the cusp which would otherwise be expected at the maximum, and it is evident that the effect is large and extends considerably on either side of this point. In this connexion it is interesting to note that if the plate radius of valve 8 were still further reduced, the part of the curve where the wave-length decreases with increasing current would diminish in extent. Eventually, when $r_p/r_g = 2{\cdot}5$ approximately, saturation of the grid-plate and cathode-grid spaces would occur together, and the wave-length would then be practically independent of i_g/i_0. This has been confirmed experimentally in the case of an MT 5 valve in which $r_p/r_g = 2{\cdot}5$.

§ 6. THE NATURE OF THE BARKHAUSEN-KURZ OSCILLATIONS: TYPE B

Now that the mechanism of the A-type oscillations is established, it becomes clear that the nature of the B-type oscillations is entirely different. In the first place, if the A-type oscillations are determined by the transit of electrons from cathode to virtual cathode and back, it is difficult to visualize a longer periodic transit which would give rise to the longer B-type. Again, the effect of the external circuit is markedly different. Referring to figure 2 it will be seen that as the external circuit is shortened and approaches resonance with the A-type oscillations maintained at

$i_g = 12$ mA., their wave-length is gradually pulled into tune with that of the external circuit, this being accompanied by a large increase in amplitude. This pulling-into-tune effect was examined by Hollmann(12), who showed that it was due to the shortening of the electron transit time by the increasing amplitude of the oscillatory voltage on the grid. If the B-type oscillations were also determined by an electron transit, a similar pulling-into-tune effect would be expected in their case also. It is significant that this is not observed; the B-type oscillations are simply replaced by the true external circuit oscillations.

Careful observation of any of the characteristic B curves fails to reveal any increase in wave-length at the onset of cathode-grid saturation, such as was observed in the A curve of valve 20 (figure 9). As regards the more obvious effect, the maximum in wave-length occurring at the onset of grid-plate saturation, direct observation has not been possible, since no valve has yet been found to give B-type oscillations at this point. With several valves oscillations were observed to commence at degrees of saturation only slightly greater. Thus, in the case of valve 6, it may be calculated from the dimensions and the observations on valve 8, that grid-plate saturation occurs at $i_g/i_0 = 0{\cdot}3$ approximately, for $V_g = 50$ V. The B-type oscillations commence at $i_g/i_0 = 0{\cdot}4$, but there is no sign of any limitation of wave-length.

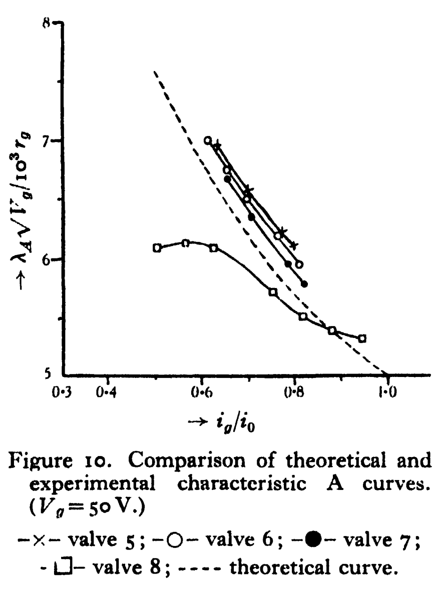

Figure 10. Comparison of theoretical and experimental characteristic A curves. ($V_g = 50$ V.)
–×– valve 5; –○– valve 6; –●– valve 7; -□– valve 8; ---- theoretical curve.

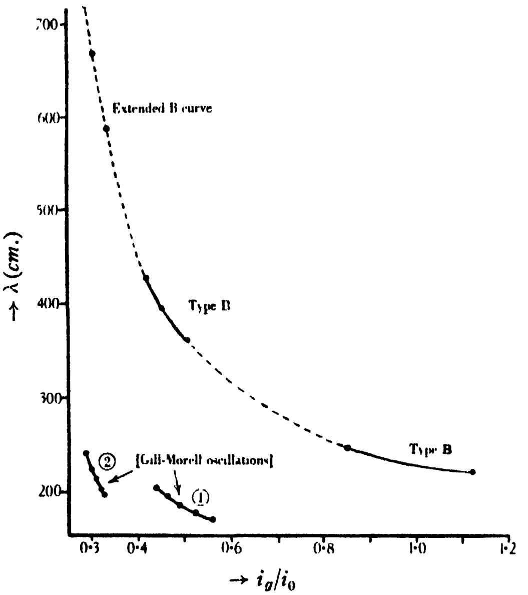

Figure 11. Extension of the characteristic B curve from observations on Gill-Morell oscillations. (Valve 6, $V_g = 50$ V.)

However, from observations on the true external circuit (Gill-Morell) oscillations, the B curve can be extended to lower values of i_g/i_0, and, as is shown below, this extension makes it quite clear that the B-type oscillations are not determined by transit time.

Extension of the characteristic B curve by means of observations on the Gill-Morell oscillations. An examination of the Gill-Morell oscillations obtained with any given valve showed that there was, for each wave-length maintained, a definite value of i_g/i_0, nearly independent of grid voltage, at which maximum amplitude of oscillations was obtained. In figure 11 are shown the results obtained with valve 6 at $V_g = 50$ V., the wave-length being shown as a function of the corresponding optimum degree of saturation. For comparison the corresponding B curve is shown. It will be seen that the results obtained with the Gill-Morell oscillations give two distinct curves marked (1) and (2); and that for curve (1) the wave-lengths are exactly half the corresponding B wave-lengths. It is clear, therefore, that in this region the value of i_g/i_0 at which the Gill-Morell oscillations are most strongly maintained occurs when the first harmonic of the B oscillations is in resonance with them. It is reasonable to assume that in the region of curve (2) optimum maintenance of the Gill-Morell oscillations occurs when their wave-length corresponds with the second harmonic of the B-type oscillations. The corresponding portion of the B curve obtained on this assumption is shown by the broken line in figure 11. It will be seen that the parts of the B curve obtained directly, and the extension deduced from the Gill-Morell observations, form a smooth curve, thus confirming the deduction.

The characteristic B curve of valve 6, figure 12, has now been extended down to $i_g/i_0 = 0{\cdot}3$ at which point saturation of the grid-plate space is just occurring. It is clear that there is no limitation of wave-length, and that as $i_g/i_0 \to 0$ the wave-length tends to infinity. There is thus, for the B-type oscillations, a complete absence of any of the effects observed with those of the A type, and it may be taken as established beyond doubt that they are not determined by a periodic transit of electrons.

The only theory that appears capable of explaining the observed results is that of Rostagni(7), who from observations on the Gill-Morell oscillations infers the existence within the valve of a resonant circuit formed by the electron cloud between the grid and plate. He has shown that a system of electrons in statistical equilibrium between a pair of electrodes will, owing to its inertia, behave like an inductance when an a.c. potential is applied to the electrodes; this inductance in parallel with the electrode capacity forming a resonant circuit. Rostagni shows that for a uniform distribution of electrons between plane parallel electrodes, the natural pulsatance ω of this circuit is given by

$$\omega = \sqrt{\frac{4\pi N e^2}{m}},$$

where N is the number of electrons per cm.^{3} and m and e have their usual meanings. According to this formula the wave-length of the system varies inversely as the square root of the electron-density, and the theory will therefore yield a characteristic curve similar to that obtained experimentally.

A possible criticism of the application of the theory is the apparent non-uniformity of the electron-density within the valve, since it is difficult to visualize how a non-uniform system can have one definite frequency. There are, however, two main causes of non-uniformity. In a normal diode the electron-density will be greatest at the cathode and least at the anode; on the other hand, with a current passing between cylindrical electrodes, the electron-density will tend to be greater at the smaller electrode. Thus in the grid-plate space of the retarding field triode, where a virtual cathode is formed at or near the larger electrode, we may reasonably expect the electron-density to be fairly constant.

In appendix (2), Rostagni's theory is applied to the calculation of the characteristic B curve, but as might be anticipated the result is very approximate. The theoretical curve obtained for valve 6 at $V_g = 50$ V. is shown in figure 12. It will be seen that the observed wave-lengths are longer than those predicted by the theory.

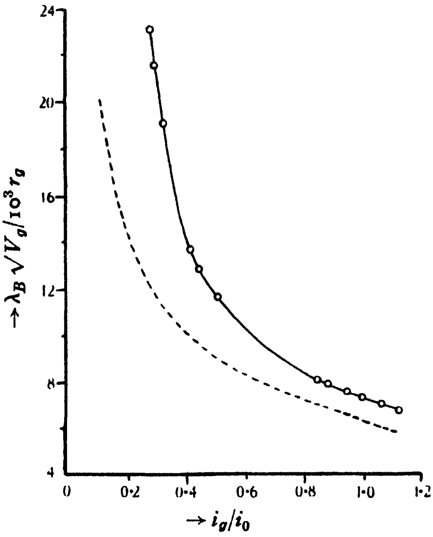

Figure 12. Comparison between theoretical and practical characteristic B curves. (Valve 6, $V_g = 50$ V.) --- theoretical curve; — practical curve.

This may reasonably be ascribed, in part, to the increase of the electrode capacity due to their supports, an effect which was not allowed for in the calculations. There is a further cause for the considerable divergence which occurs as i_g/i_0 is reduced below 0·4. As is clear from the curve of valve 8, figure 10, a shortening in the transit time from the calculated value may occur considerably before the grid-plate space becomes unsaturated. This will produce a decrease in the electron-density, and so cause the B wave-lengths to be longer than the calculated value.

§7. CONCLUSION

It has been shown that a cylindrical triode with positive grid, and with plate at a potential near that of the cathode, will maintain oscillations whose periodic time is comparable with the time of transit of electrons within the valve, provided that the ratio (grid spacing)/(grid radius) is not greater than a certain value which approximates to unity. If the external circuit presents a wave-length suitable for maintenance, oscillations will be maintained in the external circuit (Gill-Morell oscillations); otherwise oscillations of much smaller amplitude are maintained within the valve, their wave-length being determined by the valve-operating conditions and dimensions (Barkhausen-Kurz oscillations).

The Barkhausen-Kurz oscillations are of two types: a shorter type A due to the periodic transit of electrons from the cathode to the virtual cathode and back, and a longer type B due to a resonant circuit formed by the grid-plate capacity in parallel with the equivalent inductance of the electron cloud between these electrodes. The type actually obtained depends mainly on the degree of saturation of the grid-cathode space. The reason for this is not so far apparent.

For every valve, characteristic curves

$$\frac{\lambda_A\sqrt{V_g}}{r_g}=F_A\left(\frac{i_g}{i_0}\right) \quad \text{and} \quad \frac{\lambda_B\sqrt{V_g}}{r_g}=F_B\left(\frac{i_g}{i_0}\right)$$

may be obtained, and over a wide range of values of i_g/i_0, F_A and F_B are nearly independent of valve-dimensions. They decrease slightly with decrease of grid voltage, or with decrease of the ratio (grid spacing)/(grid radius). Variation of plate radius has no effect on the extent of the curves, but when $r_p/r_g < 3$, F_A is subject to modification, and with further reduction of r_p/r_g, $F_A\ (i_g/i_0)$ becomes practically constant.

Some of the data obtained in the course of this investigation bear closely on the cause of maintenance of the oscillations. It is hoped to deal with this aspect of the problem in a future communication.

§ 8. ACKNOWLEDGMENT

I should like to thank Dr D. Owen for his very helpful criticism and interest during the preparation of this paper.

APPENDIX

§ 1. CALCULATION OF THE CHARACTERISTIC A CURVE AFTER GRID-PLATE SATURATION HAS OCCURRED

Considering a valve with concentric cylindrical electrodes, let r_c, r_g, and r_p be the radii of the cathode grid and plate respectively; let the grid be maintained at a positive potential V_g, and the plate at zero potential relative to the cathode. Referring to figure 13, let i_g be any current in the grid-cathode space and i_u be the corresponding current in the grid-plate space, such that a virtual cathode is formed of radius $r_u < r_p$. It is assumed in the first instance that electrons are emitted from the cathode with negligible initial velocities.

Owing to grid capture, i_u will not be equal to i_g but to some fraction ψ of it. It is assumed that ψ is constant with variation of current. Thus

$$i_u = \psi i_g.$$

Then using Langmuir's$^{(15)}$ equation for the saturation current between cylindrical electrodes,

$$i_u = \psi i_g = \frac{2\sqrt{2}}{9}\sqrt{\left(\frac{e}{m}\right)}\,\kappa\,\frac{L_1}{\beta_u^2}\frac{V_g^{\frac{3}{2}}}{r_g} \qquad \ldots\ldots(1)$$

$$= 14{\cdot}65\,.\,10^{-6}\frac{L_1 V_g^{\frac{3}{2}}}{\beta_u^2 r_g}\text{ ampères} \qquad \ldots\ldots(1a),$$

where e and m have their usual meanings, κ is the dielectric constant of the medium, L_1 the effective length of the electrodes in the grid-plate space, and $\beta_u^2 = f(r_u/r_g)$. The variation of β_u^2 with r_u/r_g is shown in figure 14.

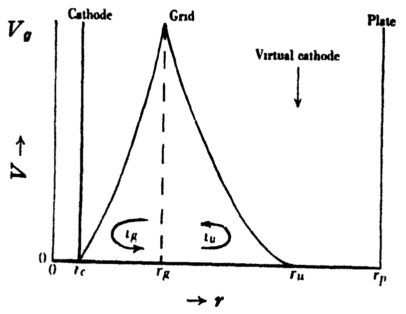

Figure 13. Voltage distribution after saturation of the grid-plate space has set in.

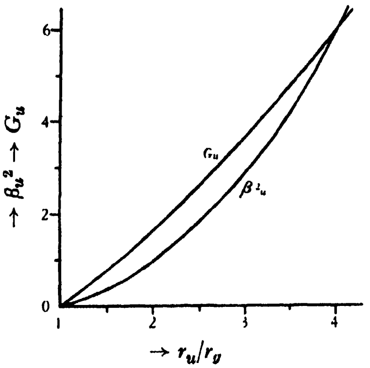

Figure 14. Variation of G_u and β_u^2 with r_u/r_g.

Similarly the grid-cathode saturation current i_0 is given by the equation

$$i_0 = 14{\cdot}65\,.\,10^{-6}\frac{L_2 V_g^{\frac{3}{2}}}{\beta_c^2 r_g}\text{ ampères} \qquad \ldots\ldots(2),$$

where L_2 is the effective length of the electrodes in the grid-cathode space, and $\beta_c^2 = f(r_c/r_g) = 1{\cdot}1$ for the values of r_c/r_g such as occurred in the experiments.

Then from equations (1 *a*) and (2),

$$\beta_u^2 = 1{\cdot}1\,\frac{L_1}{\psi L_2}\frac{1}{i_g/i_0} \qquad \ldots\ldots(3).$$

Now since for the valves used in the experiments the lengths of the cathode and plate were maintained constant, the ratio L_1/L_2 depends only on the grid structure; and equation (3) shows that β_u^2, and hence r_u, is determined by this structure, and by the degree of saturation of the grid-cathode space. The position of the virtual cathode is thus independent of the plate radius. The function $L_1/\psi L_2$ cannot as yet be calculated directly from the dimensions of the grid. However, for one particular value of $i_g/i_0 = i_p/i_0$ the virtual cathode will be formed at the plate, when $r_u = r_p$, and the corresponding value of $\beta_u^2 = \beta_p^2$ is then known. In the case of valve 8 the value of i_p/i_0 is indicated definitely by the maximum in wave-length, and since

$$1\cdot1\,\frac{L_1}{\psi L_2} = \beta_p^2\,\frac{i_p}{i_0} \qquad \text{......(3}a\text{)},$$

the function $1\cdot1\ L_1/\psi L_2$ may be calculated. The value obtained will, of course, apply also to the valves 5, 6, and 7, which have the same grid structure as valve 8; and for these valves the position of the virtual cathode can be calculated from equation (3) for any value of i_g/i_0.

The electron transit time T_{GU} between grid and virtual cathode is given by McPetrie's(16) equation

$$T_{GU} = G_u\,\frac{2r_g}{\sqrt{(2V_g\,e/m)}} \qquad \text{......(4)},$$

where $G_u = f\,(r_u/r_g)$ and is obtained from figure 14.*

The cathode-grid transit time T_{CG}, when a negligible current is passing, is calculated from Schiebe's(11) equation

$$T_{CG} = f\left(\frac{r_c}{r_g}\right)\frac{2r_g}{\sqrt{(2V_g\,e/m)}} \qquad \text{......(5)},$$

where $f\,(r_c/r_g)$ approximates to 0·6 for the usual values of r_c/r_g such as obtained in the experiments. In order to simplify the ensuing calculations, it is assumed that the cathode-grid transit time remains constant, the increase with current being neglected; this will affect the final result only slightly since T_{CG} is normally small compared with T_{GU}.

So far the effect of the initial velocities of emission has not been considered. The main effect is to reduce the transit time from the value for zero initial velocities, and this effect is normally too large to be neglected. It has been shown(10), in the case of plane electrodes carrying their saturation current, that the transit time when the electrons are emitted with an average initial velocity of V_0 volts is approximately $\{1 - 2\,(V_0/V_g)^{\frac{1}{2}}\}$ times the transit time when $V_0 = 0$. Assuming this correction to apply in the present case, the periodic time T_A of the oscillations is given by

$$T_A = 2\,(T_{GU} + T_{CG})\,\delta \qquad \text{......(6)},$$

where

$$\delta = 1 - 2\,(V_0/V_g)^{\frac{1}{2}} \qquad \text{......(7)};$$

and from equations (4) and (5)

$$\lambda_A = cT_A = \frac{2cr_g}{\sqrt{(2V_g\,e/m)}}\,\{2G_u + 1\cdot2\}\,\delta,$$

where c is the velocity of the electromagnetic waves. Substituting numerical values for e, m, c, and with λ_A and r_g in cm. and V_g in volts,

$$\frac{\lambda_A\sqrt{V_g}}{r_g\,10^3} = F\,(i_g/i_0)\,\delta \qquad \text{......(8)},$$

where

$$F\,(i_g/i_0) = 2G_u + 1\cdot2 \qquad \text{......(9)}.$$

It will be seen that owing to the finite velocities of emission the characteristic curve given by equations (8) and (9) will not be completely independent of V_g. In the following table, $F(i_g/i_0)\,\delta$ is calculated for valves 5, 6, 7, 8, for a range of values of i_g/i_0 at $V_g=50$ V.

---

* A direct method of calculating T_{GU} has been given recently by Fortescue(17).

For valve 8 in which $r_p/r_g=2{\cdot}95$, $\beta_p{}^2=2{\cdot}8$; and by experiment (figure 8), $i_p/i_0=0{\cdot}54$ at $V_g=50$ V.; thus from equation (3 *a*)

$$1{\cdot}1\,\frac{L_1}{\psi L_2}=1{\cdot}52,$$

and equation (3) becomes

$$\beta_u{}^2=\frac{1{\cdot}52}{i_g/i_0}.$$

For the cylindrical tungsten cathodes such as were used in the experiments $V_0=0{\cdot}2$ V. approximately, and

$$\delta=1-2\,(0{\cdot}2/50)^{\frac{1}{2}}=0{\cdot}87.$$

i_g/i_0	$\beta_u{}^2$	r_u/r_g	G_u	$F(i_g/i_0)$	$F(i_g/i_0)\,\delta$
0·5	3·02	3·05	3·75	8·7	7·55
0·6	2·52	2·83	3·30	7·8	6·8
0·7	2·15	2·66	2·95	7·1	6·2
0·8	1·89	2·55	2·70	6·6	5·7
0·9	1·68	2·42	2·45	6·1	5·3
1·0	1·52	2·32	2·27	5·74	5·0

The curve $\lambda_A\sqrt{V_g}/10^3\,r_g=F(i_g/i_0)\,\delta$ is shown in figure 10.

§ 2. CALCULATION OF THE CHARACTERISTIC B CURVE

2·1. *Derivation of Rostagni's equation.* Rostagni's equation may be derived most simply in the following manner. For a fuller treatment the original paper(7) should be consulted.

Consider a pair of plane parallel electrodes of area A, separated a distance d, with a cloud of electrons of uniform density N in statistical equilibrium between them. Let a small a.c. potential $\overline{V}=V_0\,\epsilon^{j\omega t}$ be applied between the electrodes.

Then if we neglect collisional friction

$$m\,\frac{d^2x}{dt^2}=-e\,\frac{V_0}{d}\,\epsilon^{j\omega t} \qquad \text{......(10)},$$

whence integrating

$$\frac{dx}{dt}=\frac{j}{\omega}\,\frac{e}{m}\,\frac{V_0}{d}\,\epsilon^{j\omega t} \qquad \text{......(11)},$$

the constant of integration being zero, since the electrons are in statistical equilibrium

The a.c. current $\overline{\imath}$ between the electrodes is given by

$$\overline{\imath}=-AeN\,\frac{dx}{dt}=-\frac{j}{\omega}\,\frac{Ne^2A}{m\ \ d}\,V_0\,\epsilon^{j\omega t} \qquad \text{......(12)},$$

$$=\overline{V}/j\omega L,$$

where
$$L=\frac{m}{Ne^2}\frac{d}{A} \qquad \text{......(13)},$$
the cloud of electrons thus corresponding to an inductance.

The capacity C of the electrodes is given by
$$C=\frac{A\kappa}{4\pi d} \qquad \text{......(14)}.$$
Thus the system has a natural pulsatance
$$\omega=\frac{1}{\sqrt{CL}}=\sqrt{\frac{4\pi Ne^2}{\kappa m}} \qquad \text{......(15)},$$
and if λ_B be the corresponding wave-length
$$\lambda_B=\frac{c}{e}\cdot\sqrt{\frac{\pi m\kappa}{N}},$$
or substituting numerical values
$$\lambda_B=\frac{3{\cdot}35\cdot 10^6}{\sqrt{N}}\text{ cm.} \qquad \text{......(16)}.$$

2·2. *Calculation of the average value of N.* Referring to figure 13, if n be the total number of electrons present in the grid-plate space
$$ne=i_u T_{GU};$$
but the volume of the space containing the electrons is given by
$$v=\pi\,(r_u{}^2-r_g{}^2)\,L_1,$$
whence
$$N=\frac{n}{v}=\frac{i_u}{\pi e}\frac{T_{GU}}{(r_u{}^2-r_g{}^2)\,L_1} \qquad \text{......(17)}.$$

Substituting for i_u, $\beta_u{}^2$, and T_{GU} from equations (1), (3) and (4),
$$N=\frac{4\kappa}{9\pi e}\frac{G_u\,(i_g/i_0)\,\delta}{\{r_u{}^2/r_g{}^2-1\}\,\{1{\cdot}1\,L_1/\psi L_2\}}\frac{V_g}{r_g{}^2} \qquad \text{......(18)},$$
the correction δ (equation 7) having been inserted since $V_0\neq 0$.

With V_g in volts and r_g in cm., $4\kappa/9\pi e=10^6$; hence substituting for N in equation (16) and rearranging
$$\frac{\lambda_B\sqrt{V_g}}{10^3 r_g}=F_B\left(\frac{i_g}{i_0}\right)\frac{1}{\sqrt{\delta}} \qquad \text{......(19)},$$
where
$$F_B\left(\frac{i_g}{i_0}\right)=3{\cdot}35\sqrt{\frac{1{\cdot}1\,L_1/\psi L_2\,\{r_u{}^2/r_g{}^2-1\}}{(i_g/i_0)\,G_u}} \qquad \text{......(19}a\text{)}.$$
Substituting the results obtained earlier for valves 5, 6, 7 and 8,
$$1{\cdot}1\,L_1/\psi L_2=1{\cdot}52, \quad \delta=0{\cdot}87,$$
we obtain
$$\frac{\lambda_B\sqrt{V_g}}{10^3 r_g}=4{\cdot}45\sqrt{\frac{\{r_u{}^2/r_g{}^2-1\}}{(i_g/i_0)\,G_u}} \qquad \text{......(20)}.$$
In practice it will be found that $\{r_u{}^2/r_g{}^2-1\}/G_u=2$ approximately for all values of i_g/i_0; whence
$$\frac{\lambda_B\sqrt{V_g}}{10^3 r_g}=\frac{6{\cdot}30}{\sqrt{i_g/i_0}}\text{ approximately} \qquad \text{......(20}a\text{)}.$$

When the grid-plate space becomes unsaturated r_u remains constant and equal to r_p, but the transit time, represented by G_u, will decrease. Thus as i_g/i_0 is reduced below the value 0·3 for valve 6, at which grid-plate saturation occurs, the wavelengths obtained in practice will be longer than given by equations (20) and (20*a*).

The theoretical curve calculated from equation (20*a*) is shown in figure 12, together with the experimental curve of valve 6.

REFERENCES

(1) Megaw, E. C. S. *J. Instn elect. Engrs*, **72**, 326 (1933).
(2) Pierret, E. *Onde élect.* **8**, 373 (1929).
(3) Wenstrom, W. H. *Proc. Inst. Radio Engrs*, N.Y., **20**, 95 (1932).
(4) Megaw, E. C. S. *J. Instn elect. Engrs*, **72**, 313 (1933).
(5) Wagner, K. W. and Hollmann, H. E. *Elekt. Nachr.-Tech.* **11**, 418 (1934).
(6) Barkhausen, H. and Kurz, K. *Phys. Z.* **21**, 1 (1920).
(7) Rostagni, A. *Atti Accad. Torino*, **66**, 123, 217, 383 (1931).
(8) Potapenko, G. *Phys. Rev.* **39**, 625 (1932).
(9) Benham, W. E. *Phil. Mag.* **11**, 457 (1931).
(10) Cockburn, R. *Proc. phys. Soc.* **47**, 810 (1935).
(11) Schiebe, A. *Ann. Phys.*, Lpz., **73**, 54 (1924).
(12) Hollmann, H. E. *Proc. Instn Radio Engrs*, N.Y., **17**, 229 (1929).
(13) Gill, E. W. B. *Phil Mag.* **49**, 993 (1929); **12**, 843 (1931).
(14) Tonks, L. *Phys. Rev.* **30**, 501 (1927).
(15) Langmuir, I. *Phys. Rev.* **2**, 450 (1913).
Langmuir, I. and Blodgett, K. *Phys. Rev.* **22**, 347 (1923).
(16) McPetrie, J. S. *Phil. Mag.* **16**, 284 (1933).
(17) Fortescue, C. L. *Wireless Engr*, **12**, 310 (1935).

DISCUSSION

Dr D. Owen: The author has introduced order into the apparently complex data regarding electronic oscillations in a triode valve. These oscillations appear to be divisible into two fundamental types. When Barkhausen and Kurz announced their discovery of electronic oscillations, they proposed a transit hypothesis for the mechanism of the oscillations. Much later Rostagni suggested the electron-plasma or electron-cloud hypothesis. It appears that the author's A type of oscillations accords with Barkhausen's mechanism, and the B type with Rostagni's. The Gill-Morell oscillations appear to be oscillations of great amplitude which occur when the external circuit is in resonance with the A type. It is not very clear, however, why a similar enhancement of amplitude should not occur in connexion with the B type, or what is the real significance of the connexion (as shown in figure 11) between Gill-Morell oscillations and the oscillations of type B. It would be useful if the author could make these points clearer.

L. Hartshorn: It struck me as very curious that in order to account for oscillations of type A we are asked to think of the time of transit of electrons between two equipotentials, while to account for those of type B we are referred to an equivalent inductance of the electrons and the capacitance between two equipotentials. Why is one method of approach applicable to oscillations A and not to B, and vice versa? I cannot help feeling that both oscillations A and B should be explicable in terms of a mass factor (electron inertia) and a spring factor (distortion of the electric field produced by their motion), and that an arbitrary difference of mental picture should not be necessary in the approach to the two modes of oscillation. What is the difference between them? Possibly A corresponds to the oscillations of the individual electrons, while B corresponds to oscillations of the distribution pattern of the electron stream. Even when we have accounted for the existence of various natural frequencies of the valve in some such way, we still have to account for the maintenance of the oscillations, probably in terms of a so-called negative resistance.

E. C. S. MEGAW: The outstanding results of the author's work seem to me to be (1) confirmation of the view that coherent oscillations can in some circumstances be maintained by an electron discharge without any electrical resonant circuit other than the electrons themselves; and (2) the indication that in a positive-grid triode there are at least two possible modes or degrees of freedom for such oscillations. As regards (1), although I disputed this point with the author some years ago, subsequent experiments seem to have established the correctness of his view beyond question. The mechanism of maintenance of coherent, or synchronized, oscillations of this kind is far from clear. A periodic variation of potential somewhere in the system would seem to be essential, and if the impedance of the external circuit is negligible in comparison with that of the discharge path, it is difficult to imagine how such a variation could arise unless space-charge limitation occurs in either the filament-grid or the grid-anode space. The author's results are apparently consistent with the supposition that these oscillations are dependent on the existence of space-charge limitation. The mechanism of these oscillations may well be similar to that of Tonks and Langmuir's plasma-electron oscillations.

As to point (2), while the author has certainly shown that there are two possible modes of oscillation, his argument to the effect that there are two different mechanisms seems less secure; and the extrapolation carried out in figure 11 is based on what may, after all, be only a coincidence. At all events it does not convince me of the validity of Rostagni's theory, which I believe is fundamentally in error in applying equations derived for statistical equilibrium to current-flow in the grid-anode space. It can also be shown by direct measurement that the effect of electron-inertia in this case is not represented by the addition of a pure inductance to the circuit.

AUTHOR's reply: With regard to the points raised by Dr Owen, it is necessary to consider the conditions for maintenance of electron oscillations. It has been shown theoretically by Mr Benham that a stream of electrons passing between two electrodes exhibits the property of negative resistance for certain narrow ranges of frequency, with a maximum value for a definite wave-length in each range. For the Gill-Morell oscillations maxima in amplitude will be obtained when their wave-length corresponds with maximum negative resistance: but maxima are also to be expected when the external circuit resonates with the equivalent circuits of the type-A and type-B oscillations to which it is coupled. The optima considered in figure 11 are due to resonance with the type-B circuit. Then enhancement of amplitude of the Gill-Morell oscillations, shown in figure 2, which appears to occur for resonance with the type-A circuit, is most probably due to correspondence with the maximum negative resistance.

In reply to Dr Hartshorn: The experimental evidence necessitating the different explanations for the two types of Barkhausen-Kurz oscillations is summarized in § 6. Provided that the space between two electrodes remains saturated, the electron-density varies inversely as the square of the transit time, and the two explanations might then be regarded as equivalent, at least qualitatively; but when, with reduction of emission current, the space becomes unsaturated, the relation no longer holds. The transit time decreases only slightly, whereas the electron-density decreases to zero, and it is then possible to distinguish between the two explanations.

The reason for the existence of wave-lengths determined by such different mechanisms appears to be closely linked with the conditions of maintenance, and I hope to deal with the question of oscillation-maintenance more fully in a further paper. While I agree with Mr Megaw that space charge appears to be the ultimate cause of maintenance, I do not consider that space-charge limitation of current is essential. The results shown in figure 8, and the fact that the range of values of i_g/i_0 for which Barkhausen-Kurz oscillations are obtained does not appear to depend on plate-radius, support this view.

As regards Mr Megaw's second point, I must admit that I am not entirely satisfied with the details of Rostagni's theory, but I am of the opinion that for oscillations of small amplitude the assumption of statistical equilibrium is sufficiently close to the truth, and gives an explanation which is at any rate qualitatively correct.

AN X-RAY GONIOMETER USING BEAMS OF LARGE APERTURE FOR PHOTOGRAPHICALLY RECORDING CRYSTAL-POWDER REFLECTIONS

By J. C. M. BRENTANO

Received March 5, 1936. *Read in title November* 27, 1936

ABSTRACT. The factors which determine the various aberrations of X-ray reflections from microcrystalline powders are considered in relation to the design of a goniometer using beams of large aperture. Expressions are derived for the aberrations from a flat layer and from a toroidal powder surface in relation to the angular setting. An instrument using wide beams is described in detail and indications are given regarding its operation. According to the procedure adopted such aberrations as lead to asymmetrical diffusion effects are reduced, and in this way sharp lines with correctly located peaks are obtained. Powder layers with spherical and toroidal surfaces are discussed in detail and data are given for their use; as compared with flat layers they make it possible to employ considerably wider beams with correspondingly shorter exposures, particularly in the range of medium and large angles.

§ 1. INTRODUCTION

The essential requirement which any X-ray goniometer must satisfy is that it must give distinct separation of X-ray beams according to the angles through which they are deflected by a crystal lattice. Any such angle is determined by the relation

$$\sin\theta = \frac{n\lambda}{2d} \qquad \ldots\ldots(1),$$

where θ is the glancing angle of incidence and of reflection with respect to the lattice planes, d their spacing, λ the wave-length and n an integer. For a given wave-length different angles of deflection 2θ are then associated with the different spacings. For any spacing or reflection which for a given wave-length is represented by a definite value of θ, a parallel monochromatic pencil will be deflected from a microcrystalline powder along the surface of a cone of aperture 4θ.

In a powder camera of the Debye type generally used a narrow X-ray pencil falls on a powder rod and the reflections are recorded as lines with an angular width of the same order as the width of the incident beam. Good definition of the reflections can then be obtained only by the use of very narrow beams.

Attention has been drawn by the writer(1, 2) to the possibility of using beams of greater angular width with correspondingly shorter exposures, by disposing the powder on such a surface that all elements of it can contribute to deflect radiation through a fixed angle 2θ to one point.

A method developed from these considerations has been used in a number of determinations and was shown to present certain advantages not only in reducing the times of exposure required for the evaluation of angles, but also in establishing particularly simple conditions for quantitative measurements. In these *Proceedings*⁽³⁾ an account has been given of the technique developed for the measurement of intensities of reflection; attention was then drawn to the importance of being able to satisfy the conditions for good angular definition in quantitative measurements, a point which will be discussed further in a forthcoming publication by Baxter and the writer. The method for obtaining well-defined deflections as required *inter alia* for accurate angular measurements and the instrument in its present form have not yet been described. This method consists essentially in distinguishing between various aberrations according to whether the diffusion they produce is symmetrically or asymmetrically distributed and using the instrument so as to reduce asymmetric effects to a negligible amount. In this way reflection lines with remarkably correct peaks are obtained.

In order to give an account of the procedure adopted we first discuss the various aberrations or diffusion effects encountered in crystal reflections from powders, with a view to collecting those expressions which are used in the operation of the instrument.

§ 2. THE ABERRATIONS ASSOCIATED WITH X-RAY REFLECTIONS FROM POWDER SURFACES

The surface on which we consider the powder particles to be placed is not a reflecting surface in the sense of an optical mirror, i.e. it does in general not represent the orientation of the lattice planes at which reflection takes place, but has the property, which meets the particular case, that lines drawn from two points A and B to any point C on it, figure 1, make an angle in C corresponding to a constant deflection at the surface. It is obtained by rotating an arc with the peripheral angle $2(\pi-\theta)$ about its chord; the points A and B are then the intersections of the arc with the axis of rotation. This surface is here called a *toroidal surface.*

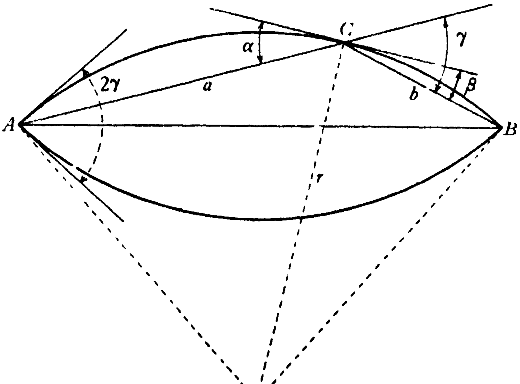

Figure 1.

This toroidal surface constitutes the geometrical locus of the points from which X rays emerging from A are deflected to B, through an angle of deflection $\gamma = 2\theta$. The aperture of the beam which can be so deflected is determined by a cone of aperture $2\gamma = 4\theta$, and this represents the maximum angular aperture through which radiation emerging from one point can be deflected by any arrangement to another point with a fixed angle of deflection 2θ.

From equation (1) a different θ and a different toroid is associated with each value λ/d, so that with a given spacing d any particular toroid will act as a monochromator for one wave-length only. A pattern corresponding to the various reflections of one wave-length according to the different spacings of the crystal particles which is of more general interest cannot be obtained by a single extended surface of this type. It is however useful to refer to the toroidal surface in comparing the efficiency of various arrangements and in determining their limits of definition.

An annular zone of the toroid and a zonal band have been used by the writer⁽⁴⁾ and by Bohlin⁽⁵⁾ respectively. Applied to photographic recording, these arrangements are unfavourable because the scattered X rays do not fall normally on the photographic film and the reflections are produced by pencils involving different magnifications between source and image.

In the present instrument which corresponds to an arrangement outlined in a previous paper⁽²⁾ an X-ray beam diverging from A falls on a powder area in C, figure 2, which can be rotated about a vertical axis; the scattered radiation is recorded on a cylindrical film disposed on a circle with C as centre. In this way we obtain normal incidence of the reflected X rays upon the photographic film and constant magnification between the source and its reflections on the film; and at the same time we can approximate to the toroid corresponding to any value of θ by setting the centre of the powder surface in C tangential to it; this is satisfied when

$$\left.\begin{aligned} \frac{\sin\alpha}{\sin\beta} &= \frac{a}{b} \\ \text{with} \qquad \alpha+\beta &= 2\theta \end{aligned}\right\} \qquad \ldots\ldots(2),$$

where α and β are the glancing angles of the incident and reflected beam and a and b the distances of the source and film from the layer. For an extended range of θ's corresponding to a certain range ζ on the film the powder is rotated and a diaphragm D, figure 2, moves with the powder surface, so as to uncover in succession only a small area of the film for which equation (2) is satisfied.

The sharpness of the reflections depends then on certain geometrical conditions. (i) With a powder layer correctly set for a reflection angle θ_1, and a point B_1 on the film, any other reflection with an angle θ_2 corresponding to a point B_2 will show a certain diffusion, which increases with the distance of B_2 from B_1 since the setting of the powder layer corresponds to the orientation of the toroid associated with θ_1 and B_1 and not to the one association with θ_2 and B_2. With a rotating diaphragm this diffusion is produced to the extent to which the layer is permitted to rotate outside its correct setting before the radiation is intercepted by the diaphragm. (ii) With a point source at A and the centre of the powder layer tangential to the toroid corresponding to a certain angle θ_1, and to the point B_1, the elements of the layer outside the centre will reflect the radiation deflected through $2\theta_1$, to points slightly away from B_1 in so far as the particular elements of the layer do not coincide with the toroid, but are at a small distance from it. (iii) For points on the film above or below the plane *ACB* radiation deflected from the centre of the layer through any particular fixed angle 2θ will trace a line corresponding to the intersection of a cone of aperture 4θ with the film. For values of 2θ either small or near 2π these lines approximate to circles, which show in general increasing diffusion for points farther away from the plane *ACB*, owing to the greater discrepancy between the orientation of the powder surface and the orientation of the toroids associated with the particular points of the film outside its centre line. (iv) If the point source in *A* is replaced by a slit normal to the plane *ACB*, the reflection with which 2θ is associated is scattered from the central part of the layer not as one cone, but as a range of cones with axes corresponding to the directions of the incident beam. Instead of one ring we have thus a system of rings, figure 3, with centres displaced along a line *EF* normal to plane *ACB*. This produces a certain diffusion and introduces a serious error into the quantitative evaluation of intensities at small angles and at angles approximating to 2π, since the microphotometric evaluation of a line involves an error depending on the extent to which the line is crossed obliquely. This effect and the effect under (iii) above apply to all powder arrangements and are not peculiar to our method. They are well known and can easily be calculated. We take account of them by avoiding elongated slit systems and by reducing the angular height of the beam for small angles. They do therefore not need to be considered here further.

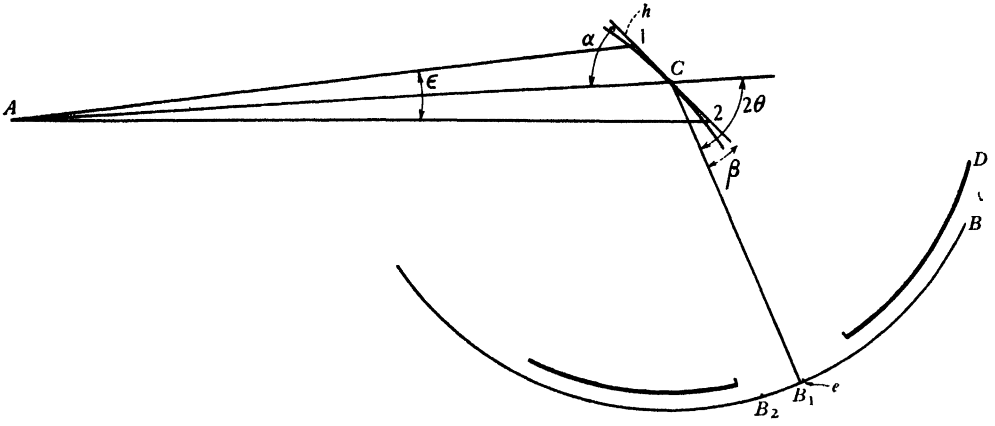

Figure 2.

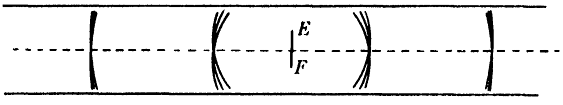

Figure 3.

§ 3. EXPRESSIONS FOR THE ABERRATION DUE TO ANGULAR DISPLACEMENT OF THE TOROIDAL SURFACE

The magnitude of the effects discussed under (i) and (ii) in § 2 depends on the surface occupied by the powder, on the angles, and on the aperture of the incident beam.

The linear displacement e of the reflection on the film, which occurs when the reflecting point is situated outside of the toroidal surface of correct definition at a distance h, is given by the projection of h on the surface of the photographic film (see the case illustrated by figure 2) and thus by

$$e = h \sin 2\theta / \sin \alpha \qquad \text{......(3)},$$

or in angular measure

$$\omega = h \sin 2\theta / b \sin \alpha \qquad \text{......(4)}.$$

Applied to the diffusion effect discussed in § 2 under (i), owing to the scattering surface being turned by an angle δ out of the position for which it represents the correct toroid, we find that a scattering point at the distance l from the axis of rotation is displaced by $h = \delta l$ and considering an incident beam of semiaperture $\epsilon/2$ the greatest distance becomes

$$l = \tfrac{1}{2}\epsilon a / \sin \alpha$$

and the greatest displacement

$$h = \tfrac{1}{2}\delta\epsilon a / \sin \alpha;$$

on introducing this into equation (3) and multiplying by a factor 2 to obtain the added effect of the two sides (1 and 2 in figure 2) of the layer, we obtain

$$e_1 = \delta\epsilon a \frac{\sin 2\theta}{\sin^2 \alpha}$$

and, to the degree of accuracy with which we can substitute for a from equation (2),

$$e_1 = \delta\epsilon b \frac{\sin 2\theta}{\sin \alpha \sin \beta} \qquad \text{......(5)},$$

or in angular measure

$$\omega_1 = \delta\epsilon \frac{\sin 2\theta}{\sin \alpha \sin \beta} \qquad \text{......(6)},$$

where α and β represent the correct angles satisfying equation (2). Equations (5) and (6) measure the extreme limits of diffusion associated with an angular displacement δ of the layer out of the orientation of correct focusing about an axis normal to ACB. We see that for a given reflection 2θ the latitude allowed in the setting of the powder so as to comply with a certain permissible diffusion is greatest when $\alpha = \beta$ or $a = b$, but varies little with the ratio $a : b$ as long as this is not far from unity. These relations also show how the latitude in setting varies with θ. For $a = b$ we have from equations (2) and (6)

$$\omega_1 = 2\delta\epsilon \cot \beta = 2\delta\epsilon \cot \theta \qquad \text{......(7)},$$

which indicates that the latitude in setting increases with increasing angle as $\cot \theta$ becomes smaller.

If instead of an angular displacement δ of the layer we consider a corresponding displacement ζ on the film, we obtain the diffusion for a point distant by the angle ζ from the point for which the layer is correctly set. Corresponding rotations of the powder and displacements of the point of correct definition on the film are interlinked by equation (2); from this by differentiation, since for any angle of deflection $\gamma=\alpha+\beta$, we have

$$\zeta=\left(1+\frac{b}{a}\frac{\cos\alpha}{\cos\beta}\right)\delta,$$

and using equation (2)

$$\zeta=(1+\cot\alpha\tan\beta)\,\delta;$$

and thus for the angular width of the diffusion

$$\omega_1=\epsilon\zeta\frac{\tan\alpha}{\tan\alpha+\tan\beta}\cdot\frac{\sin 2\theta}{\sin\alpha\sin\beta}\qquad\text{......(8).}$$

For small angles, when $\cos\alpha$ and $\cos\beta$ are both nearly unity, and the sines can be substituted for the tangents, we can write

$$\zeta=\frac{a+b}{a}\delta$$

and thus

$$\omega_1=\epsilon\zeta\frac{a}{a+b}\cdot\frac{\sin 2\theta}{\sin\alpha\sin\beta}\qquad\text{......(9),}$$

while for $a=b$

$$\omega_1=\epsilon\zeta\cot\theta\qquad\text{......(10).}$$

If a rotating diaphragm be used and moved so that the centre of the opening of aperture η satisfies equation (2) for all angles, then the extreme displacement of the powder out of its correct setting before the radiation is intercepted by the screen corresponds to $\zeta=\eta/2$, the limit of diffusion is thus

$$\omega_1=\tfrac{1}{2}\epsilon\eta\frac{1}{1+\cot\alpha\tan\beta}\cdot\frac{\sin 2\theta}{\sin\alpha\sin\beta}\qquad\text{......(11),}$$

which for $a=b$ becomes

$$\omega_1=\tfrac{1}{2}\epsilon\eta\cot\beta=\tfrac{1}{2}\epsilon\eta\cot\theta\qquad\text{......(12).}$$

§ 4. EXPRESSIONS FOR THE ABERRATION DUE TO THE REFLECTING SURFACE NOT CONFORMING WITH THE TOROID

The diffusion effect considered in § 2 (ii) and due to the scattering surface not conforming with the toroid can be rendered by simple expressions for the special case of a flat surface, which is of particular interest with regard to 'powders' consisting of a coherent microcrystalline aggregate, on which by grinding and cutting flat surfaces are most easily obtained. For a point of the flat surface in the plane *ACB* the distance h from the toroidal surface is

$$h=l^2/2r\qquad\text{......(13),}$$

where l is the distance of the point from C and r is the radius of curvature of the toroid in the plane *ACB*. Introducing the value of $r=a/2\sin\alpha$, see figure 1, in equation (3), and remembering that $l=\tfrac{1}{2}\epsilon a/\sin\alpha$, we have

$$h=\left(\frac{\epsilon}{2}\right)^2\frac{a}{\sin\alpha}$$

and for the angular diffusion

$$\omega_2 = \left(\frac{\epsilon}{2}\right)^2 \frac{a \sin 2\theta}{b \sin^2 \alpha},$$

and when equation (2) is satisfied

$$\omega_2 = \left(\frac{\epsilon}{2}\right)^2 \frac{\sin 2\theta}{\sin \alpha \sin \beta} \qquad \text{......(14)},$$

which measures the extreme diffusion to one side of the point of correct definition. Similarly with regard to the divergence ϵ' in a plane normal to *ACB* we consider that for points of the layer above or below plane *ACB* the radius of curvature of the toroid in a plane normal to *ACB* is given by $r' = a \sin \alpha = b \sin \beta$ (approximately when a is not very different from b). Substituting this in the equation corresponding to (13) and in equation (4), we have

$$\omega_2' = \tfrac{1}{2} \left(\frac{\epsilon'}{2}\right)^2 \frac{\sin 2\theta}{\sin \alpha \sin \beta} \qquad \text{......(15)}.$$

In these expressions $\epsilon/2$ and $\epsilon'/2$ are assumed to be small compared with α. More general expressions covering the case of α and ϵ respectively, ϵ' being of the same magnitude, are without interest, because for the reasons discussed in § 2 (iv) only narrow beams can be used for small angles. For small angles the beams incident at points nearer to and farther from the source (points 1 and 2 in figure 2) give different diffusions. Asymmetric beams can then be used to give the optimum condition so that the general discussion based on beams symmetrical with respect to the axis *AC* is of limited interest.*

The diffusion discussed in § 2 (i) and in § 3 and associated with an angular displacement of the powder out of its correct orientation, is expressed by essentially the same relations whether the surface is the actual toroid or a surface approximating to it; in the latter case other diffusion effects and in particular the diffusion considered in § 2 (ii) and in the present paragraph are superposed. There is a considerable advantage in reducing the latter, which is due to lack of conformity between the powder surface and the toroid, since it is in general very unequally distributed with respect to the true position of the line. In the case of the flat layer, for instance, it is all extended towards one side except in extreme cases, when a and b are unequal. This diffusion therefore affects the location of the lines very adversely, whereas the diffusion discussed in § 2 (i), due to the angular displacement of the layer out of its correct setting, is found to be very nearly symmetrically distributed for practically the whole of the angular range when the incident beam conforms with the conditions here assumed.

With curved powder layers the toroidal surface can be approximated to very closely and the asymmetric diffusion discussed in § 2 (ii) can be reduced. The rotational displacement is then the main aberration to be considered.

From the expressions (5) to (12) where ϵ appears to the first power we see that with circular apertures of the incident beam the falling off in intensity from the centre of the line is slow at first and then more rapid. In conjunction with the width of the slit in A actually a more uniform decrease of intensity results. When the slit-width is approximately equal to the linear diffusion as expressed by equation (5), lines with a well-marked narrow peak, which are most suitable for determining angles, are obtained. When $a=b$ a concave spherical surface with radius $b/\sqrt{2}$ can be used as a first general approximation to the toroid. Much better approximations are obtained over definite angular ranges with surfaces of double curvature.

---

* In the earlier brief discussion (2) of these relations we considered a and b to be approximately equal; for $a = b$ and $\alpha = \beta$ when $\sin 2\theta / \sin \alpha \sin \beta = 2 \cot \beta$ we obtain $\omega_2 = (\epsilon^2/2) \cot \beta$, while in the earlier paper we gave $\omega_2 - (\epsilon^2/4) \cot \beta$, a factor 2 having erroneously been omitted. Similarly from expression $d = b\, \delta\epsilon \cot \beta$ of the early paper we derived $\omega_1 = \delta\epsilon \cot \beta$, which measures the width of the diffusion from the centre to one edge, while the total width according to our present expression (7) is $\omega_1 = 2\delta\epsilon \cot \beta$.

The expressions (6) to (12) and (14), (15) can be used to give directly the numerical values of the diffusion in radians if the quantities ϵ, δ, ζ and η entering into them are expressed in radians. If these are given in degrees they have to be divided by the unit of angular measure, namely 57·3°. The expression (5) for the linear width gives this in the units in which b is measured, when numerical values of δ and ϵ in radians are again introduced.

§ 5. THE MAGNIFICATION EFFECT

The intensity of reflections has been discussed in another paper(3). *Ceteris paribus* it depends on the volume of the powder from which X rays are scattered, and this leads to a term $1/\mu$ as regards the absorption coefficient μ and for a flat or quasi-flat layer to a term

$$i=\sin\beta/\cos\tfrac{1}{2}(\beta-\alpha) \qquad \text{......(16)},$$

as regards its orientation. The intensity depends then further on the angle of reflection and on the scattering properties of the particular crystallites. These relations have been discussed elsewhere. Mention should be made, however, of a geometrical-optical magnification effect between the collimator slit or source and the reflections on the film, which is of particular significance in the operation of the present method. As long as the aberrations are sufficiently small the width of the reflection lines is controlled by this magnification factor and varies with the ratio b/a with a gain of specific intensity when the ratio is decreased. This gain is partly compensated by the decrease of i, equation (16), owing to the decrease of β which follows an increase of a/b for any fixed angle 2θ. We have thus from these relations

$$\epsilon\epsilon' i a/b^2 \qquad \text{......(17)},$$

as an intensity expression indicating how the specific intensity of the reflections, which determines the photographic density of the lines, depends on the quantities entering in the setting of the instrument. Term $\epsilon\epsilon'$ assumes an elliptical incident beam, for which the solid angle subtended is $\pi\epsilon\epsilon'$. Term a/b^2 is adapted to approximate to the particular conditions of recording the reflections, where the lines are projected on a circle of radius $b\sin 2\theta$ which introduces a factor $1/b$, while the geometrical-optical magnification effect owing to superpositions introduces a factor a/b and not $(a/b)^2$. With an incident X-ray beam of intensity X per unit solid angle and a slit in A of cross-section σ, the specific intensity of the reflections will be proportional to X or to $X\sqrt{\sigma}$ according to whether the width of the lines can be considered as proportional to the area σ of the slit or, in the case of geometrically

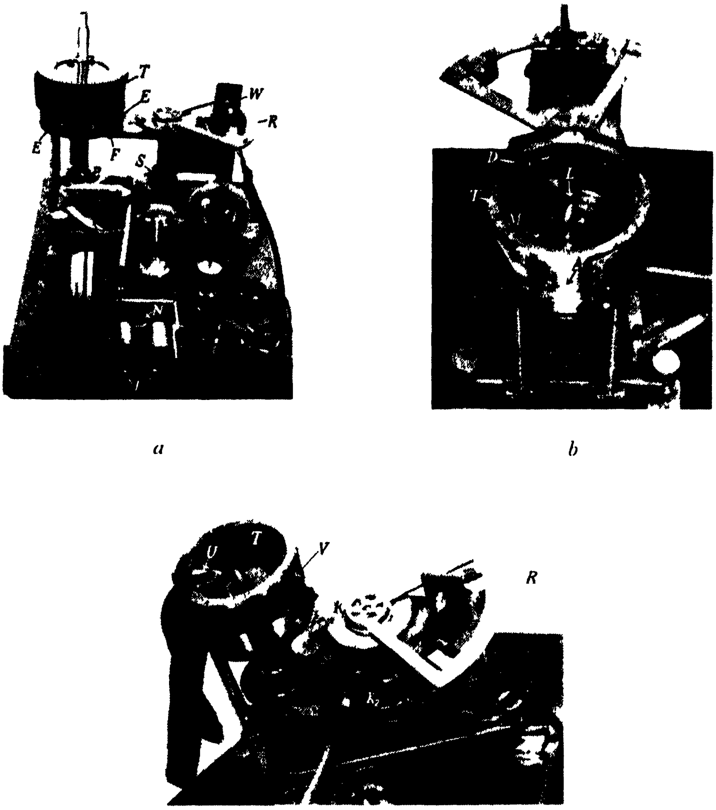

a *b*

c

Figure 4

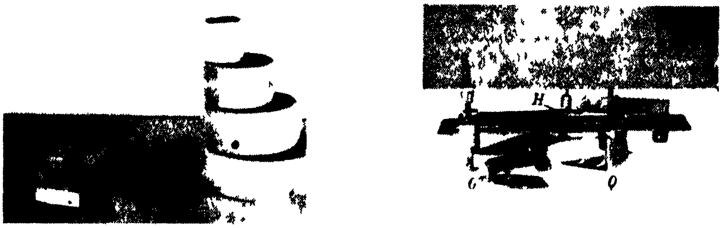

a *b*

Figure 5.

To face page 69

similar slits, to one of its linear dimensions and thus to $\sqrt{\sigma}$ only. When, however, the width of the lines is essentially determined by the limited resolving-power of the crystallites or by the aberrations and not by the entrance slit, then the specific intensity is proportional to $X\sigma$. The conditions will be chosen so as to meet each particular case. For routine crystallographic work it is convenient to arrange for the aperture of the entrance slit and the aberrations both to contribute to the width of the lines. When on the other hand the size distribution of the crystallites constituting a powder is under investigation, both the aperture of the slit and the aberrations are reduced to such an extent that the resolving-power of the crystallites becomes the essential factor in determining the width of the lines.

§ 6. DESCRIPTION OF THE GONIOMETER

The instrument comprises essentially two parallel shafts mounted in ball bearings to a platform. One of these shafts *P* supports on its upper end the holder for the powder layer *L*. Concentric with it are the rotating diaphragm *D* and the camera ring *T*, which supports the film and the collimating slit system. Diaphragm *D* is supported on an annular turntable, also mounted in ball bearings. The camera ring fits on a support *E* on which it is definitely located. The support *E* can be rotated and clamped in any position by clamping screws *F*. The axis of rotation of the camera ring with its support coincides very exactly with the axis of the shaft *P*. In the actual making of these parts, shaft *P* was used as a mandril to ensure that the various rotating parts should be truly concentric. Flat pulleys of equal diameter are fixed to the lower part of *P* and to the support of diaphragm *D*, and steel wires run from these to the driving shaft *S*. The latter carries at its upper part a pulley K_1 corresponding to the pulley at the rotating diaphragm and of the same diameter, so that both move at the same angular speed. The driving shaft carries a pulley or a cam K_2 corresponding to the lower pulley fixed to shaft *P*. When the distances *a* from slit to powder and *b* from powder to film are equal, so that the angular velocity of the powder layer should be half that of the diaphragm, the pulley K_2 on *S* has half the diameter of the corresponding pulley on *P*. For different ratios $a:b$ this pulley is replaced by a cam, so as to satisfy the correct rate of rotation of powder and diaphragm in accordance with relation (2). In many cases a sufficient approximation is obtained from a circular pulley excentrically mounted on *S*. The steel wires are held in tension by spring loaded jockey pulleys as shown in figure 4*c*.

The motion of the driving shaft *S* is obtained through a worm drive engaging in a wheel at its lower end, and the range of rotation and reversal of motion is controlled by a large sector *R* clamped at the upper end. Two movable cams on this sector, which can be adjusted to the desired range of rocking, operate a mercury switch *W* and reverse the direction of rotation of the worm. Figure 4*a* indicates the arrangement of the gears. The reversal is produced by the shift of a dog clutch operated by electromagnets which engages with one or the other of two cog wheels placed on opposite sides of the crownwheel *N*. The mercury switch controls the electromagnets *J* which are in shunt with a carbon filament lamp and a metal filament lamp is placed in series. This combination provides a large current and strong pull by the reversing magnets for the reversal after the current has been momentarily broken by the swinging over of the switch and afterwards provides a weak current, sufficient to keep the wheels engaged. This system of drive with steel wires was not only found convenient for readily obtaining the varying ratios of motion demanded for different values of *a* and *b*, but in conjunction with ball bearings for all moving parts was found to give steady motion which is most essential for quantitative measurements with a minimum of back-lash. The mechanically operated switch with an electromagnetic gear-change was found reliable and never gave a failure during two years of use.

The camera ring *T* is turned from a heavy casting. The film is pressed by a soft packing against a cylindrical surface of radius 5·73 cm., so that 1 mm. on the film surface corresponds to 1°. It is covered on the outside with lead rubber. The X rays reach the film through slots with characteristic fiducial marks at intervals of 12°. The collimating and slit system consists of tube *U*, which screws into the camera ring and is kept central very exactly by a large flange. Lead diaphragms mounted in brass, which define the aperture of the beam, can be inserted in both ends of this tube. For $a=b$ the entrance slit in *A* consists of two lead jaws mounted in brass pieces, which fit into the circular recess receiving the film. The height of the slit is determined by a circular diaphragm inserted in *U*, immediately behind the slit, while a larger circular or elliptical diaphragm at the end near the powder defines the divergence of the rays. When $a>b$, tube *U* can be reversed and fitted on a bridge piece, not shown in the figures, on the outside of the camera ring so that the film in its recess can be inserted all round it. In this position tube *U* supports the entrance slit at its outer end, while the end turned towards the camera ring receives the wider diaphragm. The interior of the camera is then entirely free from any obstruction. Opposite tube *U* a circular aperture *V* is made in the camera ring and is plugged with a celluloid disk holding a small lead ball at its centre, which serves for accurate collimating.

The fixing of the collimating diaphragms to the camera ring in conjunction with the definite location of the powder layer ensures in the simplest way that in a series of exposures taken under varying conditions, the same lines shall always take the same position with respect to the fiducial marks even when the various parts are reset. In fact it is possible to interrupt an exposure and to continue it after resetting the powder or the camera ring and collimator. The fixing of the camera ring on a support, which can be rotated, facilitates the setting of the instrument with regard to the X-ray source. This is done by first removing the camera ring and setting the instrument so that the centre of the X-ray beam falls on the position taken by the powder layer. Then the camera ring is inserted and its support unclamped. It can now be rotated until the beam passing through the collimating tube *U* appears brightest. Exact setting is obtained by observing on a fluorescent screen the beam at the back of the camera with the powder layer removed. The setting is correct when, with a small circular diaphragm in *U*, the lead ball appears as a dark centre surrounded by a narrow fluorescent ring. This setting is obtained by means of two independent operations: rotation of the camera ring about a vertical axis and tilting of the camera by the motion of the back set-screw. This adjustment is quicker and utilizes the best part of the beam with greater certainty than does the positioning of a camera with a slit system fixed to the instrument, when lateral displacements and rotations of the instrument have to be combined.

The rotating diaphragm D, figure 4*b*, consists essentially of a shield with an opening for the passage of X rays mounted on a ring with a graduated scale, which fits on the rotating platform. The opening of the diaphragm can be adjusted to the desired value of η. On the side near the collimating tube a flexible extension is provided allowing the diaphragm to be used for large angles of deflection and providing shielding for the film, when the diaphragm is moved away to smaller angles.

The support of the powder layer consists of two parts M and L. The clamping block M in figure 5*a* fits on shaft P and carries a graduated scale. Its top surface is at right angles to the axis of P and the powder holder is correctly located on M by means of two screws, which mark the line passing through the axis of rotation. The holder L consists essentially of a piece of metal of L form, the outside surfaces of which are accurately machined at right angles, and with an opening on one side for the powder. A number of these holders of simple form with openings to fit the various surfaces are shown in figure 5*a* together with surfaces of double curvature used as moulds. To prepare the powder layer the holder is placed with its opening against a mould of the desired curvature and the powder, mixed with some binding material, is introduced in a crumbly or pasty state from the back. It is essential, at least for quantitative work, not to scrape or polish the front surface of the powder as this produces preferential orientation similar to that found with layers prepared from the front side, which are useless for quantitative measurements. In the case of concave surfaces the lower edge which fits against the locating screws is recessed, so as to bring the centre of the layer over the axis of rotation.

Graduated scales on the support of the powder layer and on the rotating diaphragm are used to establish the correct angular setting with respect to the collimating tube. They are read off against reference marks on the camera ring. In the particular instrument illustrated, this is done by means of a small telescope with cross wires, fixed on the lid of the camera, which can be set in definite positions with respect to the collimating tube U. It can be made to view both scales, which are nearly at the same level and are illuminated by a small internal electric lamp. In this way the setting of the powder and of the diaphragm and their relative motion can easily be controlled.

Single crystals are set on the support M, optically adjusted and then inserted on shaft P for the exposure.

§ 7. THE MEASUREMENT OF ANGLES OF DEFLECTION

When a group of lines comprised within a comparatively narrow angular range is to be recorded no rotating diaphragm need be used. The powder layer is set so as to conform with equation (2) for some intermediate angle and the aperture of the beam then adjusted to give the required definition over the extent of ζ on either side of the focused angle determined by equations (8), (9) and (10). Owing to the diffusion effect considered in § 2 (i) the lines are then not equally sharp, those near the angle for which the layer is correctly set being sharper and narrower. When reflections of unequal intensities are being recorded it is often possible to take advantage of this by choosing the angular setting so as to make the weak lines narrower and thus enhance their specific intensities and their peak values, as was discussed in relation to quantitative intensity-measurements in a previous paper⁽³⁾. With a flat layer we have also to consider the limits of aperture imposed by the effect of § 2 (ii), equations (14) and (15). With a curved layer it is generally possible to approximate to the toroidal surface, for the particular angular range, so closely that this effect does not need to be considered in determining the aperture of the beam. Table 1 gives values for the principal radii of curvature of the toroidal surface for $a=b=5{\cdot}73$ cm. and for $a:b=1{\cdot}5$ with $a=8{\cdot}60$ cm. and $b=5{\cdot}73$ cm. for various values of 2θ; r is the radius of curvature in the plane ACB, and r' that in the plane normal to it.

Table 1

2θ (degrees)	$a:b=1$		$a:b=1{\cdot}5$	
	r (cm.)	r' (cm.)	r (cm.)	r' (cm.)
20	16·3	1·0	20·6	3·5
30	11·0	1·5	13·8	3·4
45	7·5	2·2	9·8	3·4
60	5·7	3·0	7·2	3·5
90	4·0	4·0	5·1	5·1
120	3·3	5·0	4·4	7·1
150	3·0	5·5	4·6	18·7

For practical purposes it is found that with the limits of aperture required to give good definition within a certain angular range having regard to other aberrations, the set of surfaces indicated by the table is adequate and in fact allows a sufficient overlap to meet the requirements of any angle of deflection without imposing any additional restriction on the permissible width of the beam. For very small and very large values of 2θ one or the other radius of curvature changes rapidly; this will then narrow down the angular range in which any particular surface can be used when the radius of curvature is small. This applies to r' with a equal to b in the region of small angles, but in this case the permissible vertical aperture ϵ' of the beam is reduced by the conical divergence effects considered in § 2 (iii) and (iv), so that any departure of the surface from the correct shape is less important. In exposures of this type a rocking motion is given to the powder layer through a range of about half a degree, in order to avoid spotted lines and to get better averages. An additional pulley is then inserted between shaft S and shaft P to reduce the angular velocity.

When it is desired to record reflections over a large angular range it is preferable to use the rotating diaphragm, with which all the lines are recorded under similar conditions. The apertures of the beam and of the diaphragm are then determined by the expression (11) or (12). A spherical surface will meet the more general case better than a flat layer, while for particular sections a surface of double curvature

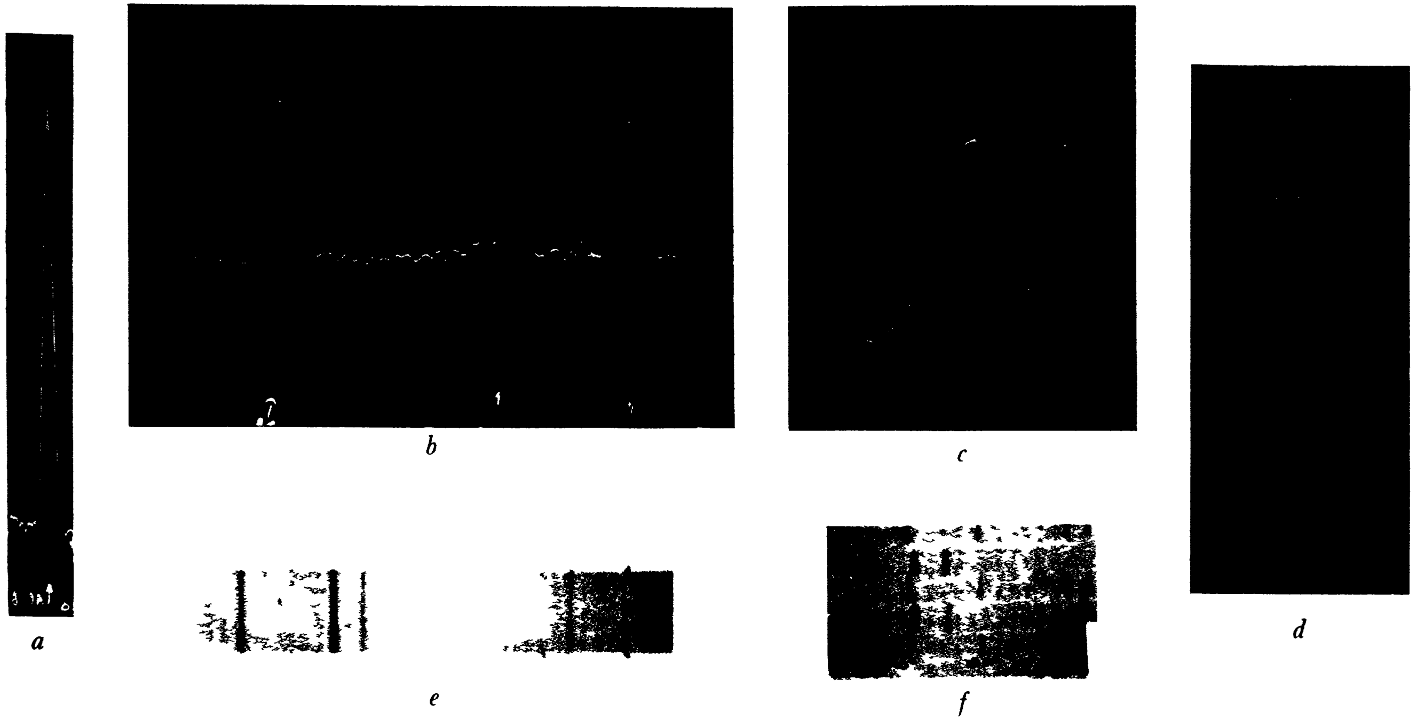

Figure 6. (*a*–*d*) microphotometric records of lines. (*a*) (220) reflection from aluminium, set at focusing angle, $\epsilon = \epsilon = 1{\cdot}5$. Photometer magnification 26 times. (*b*) reflections from aluminium and cadmium oxide recorded with rotating diaphragm. The cadmium-oxide line (middle), from a preparation generally considered to give sharp lines, is distinctly broadened. Record taken with flat layer. Indication of asymmetry. (*c*) lines of cadmium oxide and platinum (broader line). The platinum powder is constituted of crystallites of varying size, so that the base of the line is broadened. A case of vanishing size-distribution. (*d*) K_a doublet of tungsten, fine powder with crystallites giving limited resolving-power, but little vanishing-size effect. Three records, slightly displaced, taken at different points of the line with very fine microphotometer slit, to bring out the correct shape of the line. (*e*) photograph of aluminium lines obtained from a spherical layer with a beam of large aperture, $\epsilon = \epsilon = 10$. (*f*) comparative patterns of aluminium and cadmium oxide lines photographed separately on the same film. The photometric records (*a*–*d*) were taken with a valve-bridge microphotometer, *Z. phys.* **70**, 74 (1931); *Phil. Mag.* **17**, 370 (1934).

can be used. Owing to the decrease of expressions (11) and (12) with larger angles of deflection it is preferable to approximate to the toroidal surface corresponding to an angle nearer to the smaller limit of the range used. The total time of exposure then increases with the range ν covered by the record, and can be given as $t\,(\nu/\eta+2)$, where t is the exposure received by any individual section. The additive term 2 comes from the side portions, which receive only a reduced exposure and are not used for quantitative measurements. For measurements of angles part of this side range can be utilized, so that the exposure is rendered rather by $t\,(\nu/\eta+1)$. The additive terms 2 and 1 thus involve an increase of exposure, which is particularly felt for small ν's, when it is useful to make η small as well and to combine it with a larger value of ϵ.

Considering more in detail the evaluation of angles, the method can be used to obtain sharp well-defined lines with comparatively short exposures. An example of such a line is given in figure 6*a*. A record covering an extended angular range obtained by the use of a rotating diaphragm and actually taken with an early instrument was reproduced in a previous paper(2); we may refer to this reproduction to avoid repetition.

It should be noted that accurate determinations of spacings do not always require accurate angular measurements. Where it is practicable to use reflections for which, with the particular wave-length used, 2θ approaches 2π, then large changes of θ involve small changes of $\sin\theta$ and an approximate measure of θ is adequate. For this very reason, however, the angular range of θ to which this applies comprises only a very small latitude in the values of $\sin\theta$ and of the spacings d. It is for cases where a larger range of spacings has to be evaluated, which necessarily cannot all be comprised in the range of very large angles, that accurate angular measurements are required. Examples of the use of the method to meet such conditions are afforded by the determinations of the parameters of carbonates by Dawson and Adamson and by the writer(6, 7). Again, a high definition is essential when information as to the sizes of the crystallites constituting the powder particles is sought from the intensity-distribution of the individual lines, when it is essential to free the record of any other diffusion effect introduced by the goniometer. Figures 6*b* and 6*c* illustrate such examples.

The actual angles 2θ of the lines can be found in relation to the fiducial marks, subject to the satisfaction of definite geometrical relations between the slit system, the support of the film, and the powder surface. The present arrangement helps to secure these conditions and any deviations can be eliminated by calibration. The location of lines by reference to the edges of fiducial marks is however affected by the Ross effect and by other systematic errors and is not recommended when high accuracy is required; we prefer then to use a reference substance mixed with the powder and giving a pattern of lines for which the angles are well known as we have done in our measurements on carbonates(6). This procedure also eliminates any line-displacement due to the penetration of the X rays into the layer.

§ 8. MEASUREMENTS WITH BEAMS OF LARGE ANGULAR APERTURE

In the commonest uses of the instrument an extreme increase in accuracy is not of as much interest as is a shortening of exposure, retaining a definition corresponding to the usual requirements of crystal-structure investigation. This can be satisfied with beams of considerable width, obtained by placing the point of divergence A of the rays on the anticathode itself. The distance a is then larger than b and this reduces the width of the image of the anticathode spot on the film and enhances the intensities in the manner discussed in § 5. The anticathode is set at a very small glancing angle and a screen with a cross slit attached to it cuts out radiation from points outside the anticathode spot. For such exposures the goniometer is firmly connected with the X-ray tube. Figure 6*e* shows a typical record taken with a spherical layer of aluminium when $a = 8{\cdot}5$ cm. $b = 5{\cdot}73$ cm. The recorded range extended from 60° to 110° while $\epsilon = \epsilon' = 10°$ and $\eta = 20°$. The total exposure was 1·5 mA.-hr., giving the actual exposure for any part of the film as 0·43 mA.-hr.

§ 9. THE QUANTITATIVE MEASUREMENT OF INTENSITIES

The technique of quantitative intensity-measurement by this method has been discussed in other papers(3, 8, 9). It presents the advantage that by the use of powder surfaces of well-defined orientation with respect to the incident and reflected beams, conditions are established which lead to a simple quantitative evaluation of the observed reflections. With regard to the instrumental technique it is essential that the incident beam should be used at a constant aperture for the whole angular range exposed and further that for small angles of deflection the error due to the displaced ring patterns, to which we have referred in § 2 (iv), be avoided. These conditions have to be considered in choosing ϵ and ϵ'; generally ϵ' is then made smaller than ϵ. By satisfying closely the focusing condition and using a comparatively wide entrance slit in A, lines with a flattened peak and a sharp drop on both sides are obtained, and these are most suitable for quantitative measurements. When high accuracy is required conditions of extended diffusion due to defective focusing should be avoided, not only because diffused lines are unsuitable for accurate photometry, but also because the discontinuities of the background, to which attention has been drawn by Baxter and the writer, become correspondingly diffused so that overlapping results; accurate evaluation is then impossible.

§ 10. MODIFICATIONS OF THE INSTRUMENT FOR PARTICULAR REQUIREMENTS. REFLECTIONS FROM SINGLE CRYSTALS

In certain instances it is useful to increase the separation of the lines. This is done by increasing the distance b; the film is then held by an extension arm, which can be clamped to the camera ring. This is useful for small angles at which the intensity factor (16) increases with β and gives an advantage in satisfying equation

(2) when $b > a$. It partly compensates for the increase of exposure in projecting on a larger circle.

Figure 6 shows a device fitting in the camera ring by which reflections from two powder layers can be recorded on adjacent strips of a photographic film. Apart from applications in intensity-measurements to which we have referred in another paper(9), this device can be used in comparing corresponding lines of two powder specimens recorded under similar conditions. A grid Q can be displaced in front of the film by an amount equal to its spacing and according to its position uncovers alternate strips of the film. A swinging support holding two powder layers is displaced jointly with the grid by means of stem H, so that the reflections are recorded on separate strips. Figure 6*f* shows a record taken in this way. Brindley and Spiers(10) have described a similar device, in which however the reflections from two powder layers are superposed on the same strip.

The goniometer can be used to record the reflections from a single crystal and the rotating screen is then helpful in reducing the background by limiting the exposure of any particular part of the film to the time when the crystal is set so as to reflect radiation upon it. The conditions for reflection from the single crystal differ from those for a powder and the reflection from the particular set of lattice planes represented by the crystal face does not take place simultaneously from the whole of the surface, but for different points in succession as the crystal is turned. The width of the rotating diaphragm must be chosen accordingly.

§ 11. CAMERA DIMENSIONS AND ANGULAR DEFINITION

Apart from the geometrical-optical conditions here discussed, a certain diffusion is produced by the penetration of the X rays into the powder layer and by the scattering of the X rays in the photographic emulsion. These effects are well known and do not need further discussion. The former, which produces asymmetric lines, can be reduced where it is noticeable by adding to the powder an admixture of great absorbing power. Both these effects involve a certain linear broadening which affects angular measurements to a lesser extent when the camera-size is increased.

In this connexion it is of interest to consider the relation between the dimensions of the camera and the times of exposure. The angular accuracy depends upon factors controlling the angular diffusion of the beam, which for any given value 2θ do not contain the linear dimensions of the camera but only the apertures and the angles determining the setting of the powder. The intensity of the reflections is determined by the relations set out in § 5. Apart from the cases there considered we can say in a general way that with similar cameras, for a given total of scattered radiation, the specific intensity on the film is inversely proportional to the square of the dimensions. On the other hand, when a fixed value of definition is maintained, both linear dimensions of the entrance slit can be increased in proportion to the camera-size, which gives again a factor proportional to the square of the camera dimensions. We thus see that by complying with definite geometrical and optical relations, the times of exposure required for any given value of definition become independent of the linear dimensions of the camera and no gain is obtained by making the camera small. This holds good as long as the full width of the entrance slit corresponding to a certain definition can be illuminated with X rays throughout the solid angle that can be utilized in the collimator. When the anticathode itself acts as slit, its width is fixed and then it is of advantage to reduce the size of the camera when high intensities with limited definition are required.

§ 12. RANGE OF APPLICATIONS OF THE METHOD

The method described in this paper has two distinct applications. One is the quantitative evaluation of the intensities of reflections and this has been discussed previously(3). It had to be considered in the present account only in as far as the design and operation of the instrument must comply with the conditions set out in the more detailed discussion. The other application is the evaluation of the angles of reflection, and it has been shown that by a definite control of the aberrations as indicated in § 4, lines with correctly located peaks and a gradual falling off of intensity towards both sides are obtained, and these can be located with great accuracy. Where it is desired to push the accuracy very far, as in the instances referred to in § 7, incident beams with an aperture of 2° or 3° can be used; with curved powder layers an accuracy sufficient for the usual demands of structure-analysis can be attained in the medium range of deflections with beams of an aperture of 10° with correspondingly short exposures. In the region of very small angles, limits are set to the use of wide beams and this applies again to angles of deflection approximating to 2π, where the aberration considered in § 2 (iv) becomes important. For large angles the limitations introduced by this effect are not felt, since the evaluation of spacings is in that case but little affected by the limited accuracy of the angular measurement. Actually for angles of deflection approaching 180° the accuracy of the method becomes irrelevant for, in view of the smallness of the change in value of the sin function with angle for values near $\pi/2$, accurate determinations of spacings can be derived from comparatively coarse angular measurements. The particular field for the method in regard to determinations of spacings lies thus in the increase of accuracy with short exposures which can be attained in the medium angular range, extending from about 30° to 150°. The advantage of using this medium range of angles is that it accommodates a wide range of spacings; the ratio of the values of $\sin\theta$ associated with the angles of deflection 30° and 150° being 3·73, which implies that the largest spacing recorded in this range is over three and a half times larger than the smallest, while the range of spacings which can be recorded between 150° and 180° allows only a latitude of 3·5 per cent. It is for instances where lattice spacings of different length have to be evaluated and related, which cannot be accommodated on the narrow range offered at large angles, that the method has been developed.

§ 13. ACKNOWLEDGMENTS

In conclusion I wish to express my thanks to Prof. W. H. Bragg, F.R.S., for his interest in this paper, to Mr H. Bell, M.A., for reading through the manuscript and the proofs, and to the Leembruggen trust for means placed at my disposal for the construction of the instrument.

REFERENCES

(1) Brentano, J. C. M. *Arch. Sci. phys. Nat.* (4) **44**, 66 (1917).
(2) Brentano, J. C. M. *Proc. phys. Soc.* **37**, 184 (1925).
(3) Brentano, J. C. M. *Proc. phys. Soc.* **47**, 932 (1935).
(4) Brentano, J. C. M. *Arch. Sci. phys. Nat.* (5) **1**, 550 (1919).
(5) Bohlin, H. *Ann. Phys.*, Lpz., **61**, 421 (1920).
(6) Brentano, J. C. M. and Dawson, W. E. *Phil. Mag.* **3**, 411 (1927).
(7) Adamson, J. and Brentano, J. C. M. *Phil. Mag.* **7**, 507 (1929).
(8) Brentano, J. C. M. and Baxter, A. *Z. Phys.* **89**, 720 (1934).
(9) Brentano, J. C. M. *Z. Phys.* **99**, 65 (1936).
(10) Brindley, G. W. and Spiers, F. W. *Proc. Leeds phil. lit. Soc.* **3**, 73 (1935).

REVIEWS OF BOOKS

Die Interferenzen von Röntgen- und Elektronenstrahlen, by M. v. LAUE. Pp. vi+46. (Berlin: Julius Springer.) Price RM. 3.60.

Professor von Laue has collected in this pamphlet the chief results of the theories of the diffraction of X rays and electrons. As might be expected from anything written by him, the exposition is extremely clear, and the logical sequence of the rather complicated theories involved is explained without great mathematical detail.

In the last two chapters an account is given of the recent work on interferences in a single crystal produced when the X rays are excited in the crystal itself; and these results are compared with the corresponding effects in electron-diffraction which have been known for some time as Kikuchi's lines. Professor von Laue gives strong reasons for supposing that the latter are due to electrons which have made inelastic collisions in the crystal.

G. P. T.

The New Chemistry, by Prof. E. N. da C. ANDRADE, D.Sc., Ph.D., F.R.S. Pp. 58. (London: G. Bell and Sons Ltd., 1936.) 3*s*. 6*d*.

This little book which is dedicated to Professor C. D. Ellis, "who knows all about these things without believing that nothing else matters", is based on a post-graduate lecture delivered at St Mary's Hospital, London. In it the author, in his characteristically clear style, surveys recent work on the transmutation of matter which he calls "the new chemistry". The book is printed in large clear type which makes for pleasant reading, and several beautiful plates are included. The last two sentences of the book are significant and surely reflect the feelings of many physicists: "It may be that we shall never be able to utilise atomic energy, that is, mass energy, but even if this is so we may take comfort from the fact that it is certain that the atomic heat engine would be speedily followed by the atomic bomb. The pursuit of the new chemistry is none the less desirable if it does not seem possible so far to turn it to destructive ends."

H. R. L.

The Thermochemistry of the Chemical Substances, by F. R. BICHOWSKY and F. D. ROSSINI. Pp. 460, including title-page and preliminary matter. (New York: Reinhold Publishing Corporation; London: Chapman and Hall; 1936.) 35*s*. net.

Thermochemical data are based largely on the classical researches of Berthelot and Julius Thomsen, and newer researches carried out with an improved technique. The latter are dispersed throughout the literature and if a value of a thermochemical constant is required it is very difficult to find the best one. In the present monograph the authors have attempted a survey of the whole field and have given a critical set of data, in all cases explaining the reasons for their choice. The tables are very complete and include all compounds except organic substances with more than two atoms of carbon. The physical states of the substances are adequately described, and all values are recalculated in terms of moles on the basis of the 1934 international atomic weights and the calorie of 4·1850 international joules. The energy values of atoms, ions and certain molecules are given, so that the tables should also be valuable to the spectroscopist. The volume is authoritative and is a most welcome addition to the not very extensive literature on thermochemistry. It will save a great amount of time and trouble.

J. R. PARTINGTON.

Hand- und Jahrbuch der chemischen Physik, Band 9. Abschnitt III, *Anregung der Spektren*, by W. HANLE; Abschnitt IV, *Molekülspektren von Lösungen und Flüssigkeiten*, by G. SCHEIBE and W. FRÖMEL. Pp. 184+16. (Leipzig: Akademische Verlagsgesellschaft m. b. H., 1936.) M. 18.

Many of the monographs in this series, edited by A. Eucken and K. L. Wolf, have deservedly become well known to physical chemists and spectroscopists in this country. If the two now before us do not also become widely used here, the rather high price will probably be the cause. Hanle, whose monograph on the excitation of spectra occupies about three-quarters of this book, is well known for his contributions to *Ergebnisse der exakten Naturwissenschaften*, *Handbuch der Radiologie* and other collective works, as well as for his own investigations in the subject. In his present monograph, the first, and much the largest, section deals with fluorescence; the next largest with excitation by collision with electrons, atoms and ions; and the remaining shorter sections with collisions of the second kind, temperature excitation, excitation of continua, and applications to spectrographic analysis of materials and to technical light sources. The discussion includes spectra of atoms, diatomic molecules and polyatomic molecules of both inorganic and organic substances. The shorter monograph, by Scheibe and Frömel, deals in an attractive manner with the observation and interpretation of the band spectra of polyatomic molecules in liquids and solutions particularly in the visible and near ultra-violet regions. The two monographs contain, respectively, 74 and 15 figures in the text, and 17 and 9 tables of numerical data. Both are well indexed; both include numerous references to original papers, and Hanle gives also a bibliography at the end of each section.

W. J.

Klänge und Geräusche, by Dr F. TRENDELENBURG. Pp. viii+235. (Berlin: Julius Springer.) Price RM. 24.

In this exceptionally well-illustrated book the author deals with a number of aspects of sound and noise which do not find a place in other books on this subject. His connexion with the research laboratory of Siemens has given him a strong interest in the acoustics of telephony, and the book betrays this in many places. The book, in fact, is not a textbook of acoustics but forms a very interesting and readable supplementary textbook dealing with applied acoustics.

The illustrations call for praise; particularly the photographs of the structure of the ear and the X-ray photographs showing the conformation of the mouth and throat when sounding various vowel sounds.

As regards the text, one of the most important things the book teaches is the power and availability of objective acoustical measurements. As an example may be mentioned the oscillograms and analyses with which the book abounds, and which deal with a wide variety of sounds, for instance the exhaust noise of a motor cycle, speech, common musical instruments and even noise due to muscular movement. Instrumental methods are fully described in a long chapter which includes a particularly valuable account of the methods available for analysis.

An interesting account is given of the use of microphones in medicine, and oscillograms illustrating various diseases of the heart and lungs are shown. A full account is given of the effect upon music and speech of various modifications such as non-linear distortion, phase distortion and loss of certain frequency bands. The author's interest in musical matters is shown by the long chapter devoted to musical instruments, which is well supported by analyses and oscillograms. Very full attention is given to the violin, such out-of-the-way information as the form of vibration of the violin body, oscillograms of the well-known wolf tone, and even a polar diagram of the intensity-distribution round a violin being given.

Features which exemplify the up-to-date character of the book are the sections on synthetic and recorded sounds. It is surprising to discover how many systems are in use for synthesizing musical sounds and more surprising still to be told that some of them are practicable!

It is a little surprising to find that in a book which deals so fully with noise and with the acoustics of auditoria no mention is made of methods of keeping such noises from travelling into and about buildings. The omission is not a blemish, but the interest in building acoustics which the author has betrayed implies that he has information available regarding noise in buildings which could have made the book still more valuable than it is.

The above sketch of the contents of *Klänge und Geräusche* is not by any means exhaustive. Dr Trendelenburg has also dealt with the other aspects of applied acoustics which one would naturally expect to find in such a book, for instance the use of microphones and loudspeakers. The subjects which have had special mention above are those which one might not have expected to find dealt with so fully, and it is these which make the book valuable either to the advanced student who spreads his net wide or to the research worker engaged with acoustical matters.

J. E. R. C.

The Physics of Solids and Fluids, by P. P. EWALD, TH. PÖSCHL and L. PRANDTL. Translated by J. DOUGALL and W. M. DEANS. (Second Edition, 1936. Blackie.) 17*s.* 6*d.*

This excellent book, translated from matter prepared for the new edition of *Müller-Pouillet*, is distinguished by the way in which stress is laid on the behaviour of real substances—crystalline solids and viscous fluids—as against the isotopic solids and ideal liquids to which the books of, say, thirty and more years ago were almost exclusively devoted. It is, no doubt, owing to the lucid manner in which recent developments are exposed that a new edition has been demanded already.

There has been a substantial revision in the part of the book due to Professor Prandtl, *The Flow of Liquids and Gases*. The main novelty is the addition of a final chapter on flow with appreciable volume changes, which includes certain sections taken from earlier chapters in the former edition, but contains notable new matter on such points as flow round aerofoils when the velocity exceeds that of sound, the resistance of projectiles and cavitation. There are small changes elsewhere, such as the addition of a short treatment of two-dimensional flow. The book is an invaluable supplement to older treatises on the "properties of matter".

E. N. DA C. A.

A Text-Book of Physics, by CHARLES A. CULVER. Pp. x+816. (New York: The Macmillan Company.) 17*s.* o*d.* net.

Professor Culver has written a textbook very suitable for students working for examinations of Intermediate Science standard. It has been his ambition to present, and he has succeeded in presenting, the material in such a way that students of the humanities will find that science has a real cultural value. The introduction of some historical material and thumb-nail biographies of eminent physicists, and the references to original papers and to textbooks giving fuller details of the various branches of the subject, are welcome innovations in a book of this standard. The author invites constructive criticism. I suggest that in the discussion of heat units, the standard thermal unit as defined in the *S.U.N. Report* 1934 (published by The Physical Society) should be stated and that specific heat should be expressed in the appropriate units and not as a ratio. Figure 116 must be redrawn. Continuous-flow electrical calorimetric methods merit more than the passing reference that one finds. Some mention should be made of a characteristic gas equation, e.g. that of van der Waals. Refraction at a single spherical surface should be considered, if only to emphasize that most of the dioptric power of the eye is of static origin and that the eye does *not* "function as a pin-hole camera after removal of the lens". J. H. B.

Elementary Physics, by G. STEAD. Pp. xv+560. (London: J. & A. Churchill.) (5th Edition.) 12*s*. 6*d*.

It must be most gratifying for an author to find that the demand for his work is such that edition after edition is necessary. It certainly shows that the book is fulfilling a useful purpose. But this fifth edition is especially welcomed because Mr Stead has not only revised the old text, excellent in its clarity, but has introduced some hundred pages of additional matter. In doing so he has made this text-book a much more adequate guide for first-year science and medical students, to all of whom it can be confidently and warmly commended. The author adopts a sign convention for optical problems which gives the same standard formula for mirrors and lenses, but the Committee of the Physical Society on the teaching of Geometrical Optics would surely have taken exception to the sentence, "To find the power of a lens in dioptres, express its focal length in metres and turn the result upside down."

In the discussion of the laws of viscous flow the example of the delivery of water through 10 in. and 12 in. mains is unfortunate because, in general, such flows will be turbulent.

J. H. B.

Text-book of Physics, by E. GRIMSEHL, vol. V. *Physics of the Atom*, edited by R. TOMASCHEK (7th edition). Translated by L. A. WOODWARD. (London: Blackie & Son, Ltd.) Pp. xiii+474. 17*s*. 6*d*. net.

In reviewing this translation of a volume of the well-known German textbook it is advisable to begin by stating the scope of the volume, as this differs in some respects from what would be expected in an English treatise of similar title. On the side of omissions, there is no account of the fundamental work on the electron or of the gaseous discharge in any form, and while a short account is given of ionization by electrons and a fuller one of that by α particles, no mention is made of ionization by other positively charged particles or of secondary electrons released by them. For some of these the reader is referred to other volumes. On the other hand the book includes, besides the usual topics, a short account of the structure and vibrations of solids, of phosphorescence and of the internal photoelectric effect. The electrodynamics of moving media are dealt with at some length and there is a short statement of some of the problems of stellar physics. Temperature radiation is discussed, but without proofs of some of the main theorems.

The book is well produced, and the treatment is in general clear and satisfactory. A number of interesting points are mentioned which do not generally figure in a book of this character, but on the other hand the explanations are sometimes so condensed as to be difficult to follow and occasionally are even misleading, as in the case, for instance, of the account of the focusing action of the Aston mass spectrograph. In view of the admitted unreliability of his work it is unfortunate that so many of Rupp's results are mentioned, including some that are almost certainly false. In dealing with the properties of moving media Dr Tomaschek favours an ether carried by the earth, but the special theory of relativity is stated briefly. The translator has done his work well, and there are only a few clumsy sentences.

G. P. T.

Principles of Electric and Magnetic Measurements, by P. VIGOUREUX and C. E. WEBB. Pp. 392. (Blackie & Son Ltd., London and Glasgow.) 20*s*. net.

This is a textbook on experimental electricity and magnetism intended for the use of students. It differs from most previous works of a similar character in that obsolete methods of measurement are almost completely excluded, and attention is concentrated on those employed in modern research and testing laboratories, and especially methods with industrial applications. Thus part I, Electricity, includes direct and alternating current bridge methods, potentiometers, methods for radio-frequencies, thermionic valves, measurements on electrolytes, dielectrics, X rays, etc., while part II includes measurements of magnetic materials.

The proportion of the book devoted to magnetic measurements is surprisingly large. There are, for example, about 80 pages dealing with measurements of magnetic permeability and related quantities, while only 6 pages are devoted to dielectrics and 14 to electrolytes. Similarly much more space is devoted to magnetostriction than to piezoelectricity, which is surely far more important. The general student will probably find the magnetic section too detailed, though it will be very welcome to the specialist. It is to be hoped that there will be an opportunity of adjusting the balance at some time or other, for there is certainly room for a book such as this, which presents the subject from a point of view different from that of the academic writer. It will be found a useful supplement to the more orthodox works.

L. H.

Manual of Meteorology, vol. II. *Comparative Meteorology*, by Sir NAPIER SHAW, with the assistance of ELAINE AUSTIN. Pp. xlviii + 472. (Cambridge University Press.) 36*s*. net.

This is a revised edition of the second of the four volumes of the *Manual of Meteorology*. It may be described as a gazetteer of the meteorology of the globe, and is, in the main, an account of the ascertained facts relating to the atmosphere over different parts of the earth. Its outstanding feature is a series of monthly and annual charts of temperature, cloud-amount, rainfall, and pressure at sea level. In each case a separate chart is given for each hemisphere, the projection used showing the pole at the centre of the chart, with equally spaced parallels. These charts are extremely useful for purposes of reference, and are so well reproduced that it is easy to extract from them any material fact. It is also a novelty in meteorological textbooks to have each month of the year shown, instead of just the extreme months January and July. The intermediate months are in many ways even more interesting than the extreme ones, and the reader can here see the intermediate stages of such a transformation as that which occurs over Asia when the Siberian anticyclone of January is replaced eventually by the depression to the North-West of India in the summer. Many other facts are shown in charts, diagrams, or tables, and most of the known facts of the diurnal and annual variation of the meteorological elements and of their variation in the vertical appear in the book in one form or another.

A whole chapter is devoted to the vexed question of cycles in weather, though the author refrains from giving an opinion as to the value or reality of these.

The volume is a valuable work of reference, for it gives a mass of information not to be found elsewhere without much labour. The extent to which it is up-to-date may be gathered from the fact that on p. 421 are given diagrams of the vertical distribution of the mean winds during the month of December 1935 at three stations in the British Isles.

D. B.

Proceedings of the Plenary Meeting of the Comité Consultatif International pour les Communications Téléphoniques à Grande Distance at Budapest 1934. Vols. I–V. Pp. 660. English translation. (International Standard Electric Corporation.) 25*s*. 0*d*. net.

Although telegraphy and telephony were among the earliest applications of electricity and attracted the study of some of the most eminent physicists of the last century, interest in more modern times has moved from what is often regarded as the elaboration of classical conceptions. But the science thus handed to the communication engineer was a living study, and a consideration of present technique shows it to be based on a large body of scientific work of a high order. The present volume, the proceedings of the Comité Consultatif International pour les Communications Téléphoniques à Grande Distance (C.C.I.F.), forms the best medium for such a consideration, since it is an authoritative and comprehensive handbook of the science and practice of telephonic transmission, representing the consensus of international expert opinion. Nor is the scope limited by the title. Nearly any circuit may now serve as a link in an international or long-distance conversation, and the principles of the C.C.I. are accepted as the standard of the best telephone practice.

The interest of the physicist will, however, mainly be drawn to the possibility of his making new contributions to this branch of engineering, particularly in view of the recrudescence of interest in some of the less fundamental or less atomic or philosophic branches of physics. There are many such possibilities. The sections relating to definitions and measurements of desired sounds (speech and music), unwanted sounds (noise) and their equivalents show a lack of agreement and a measure of incoherence as to some of the basic concepts. Much essential statistical work of a general nature has been carried out on the nature of transmission and its impairment by continuous electrical disturbances, but the evaluation of discontinuous disturbance, which involves the physical nature of sound and the integration-time reaction of the ear, has received only a cursory consideration. On the other hand it can be argued that the telephone engineers have defined and largely determined means of measuring the acoustical quantities essential to the exercise of their profession; but it is very desirable that common absolute bases should be arrived at, so that results obtained in different fields of acoustical work may be readily comparable. It is believed that this question received attention at the recent C.C.I. meetings this year (1936) in London and Copenhagen. As regards Corrosion also the volume shows that work is well forward on such aspects as the distribution of the stray currents and potentials causing electrolytic damage, but not so much attention has been paid to the chemical and physical details of the electrochemical actions involved.

The main work of the C.C.I.F. and the greater part of the present volume relate to transmission, and this is studied in detail. Not only are the general types of circuits specified but also the components to be employed. In the text will be found the characteristics of equipment at present available and detailed descriptions of alternative methods of measurement and testing, while desirable directions of progress are indicated. Information on the most recent developments has its place in the volume, and it is interesting to note the extent of the study which the C.C.I.F. had already given in 1934 to the problems of the different types of transmission along lines by means of high frequency currents, and the uses to which they could be put

Accordingly the physicist in search of new fields of practical endeavour will be well repaid for a study of the proceedings of the C.C.I.F. He will also derive much benefit from observing how basic difficulties and uncertainties can be overcome by means of limited concepts based on a careful statistical analysis, and how the complicated problems offered by elaborate circuits and equipment can be ingeniously simplified by the use of standard forms. Grateful acknowledgment should be made to the International Standard Electric Corporation for making an English translation available. No doubt the C.C.I are wise in having an official text in one language only (diplomatic experience rather suggests that this is so) but the excellence of the present translation indicates that the difficulties, at least as regards English, might well have been overcome.

Numerical Data on Rotatory Power, by E. DARMOIS; *Numerical Data on the Raman Effect*, by M. MAGAT; *Numerical Data on Radioactivity*, by I. JOLIOT-CURIE, B. GRINBERG and R. J. WALEN. Pp. 68, 112, 57. (Paris: Gauthier-Villars.) 8*s*., 12*s*., 8*s*.

The problem of keeping in touch with the literature of physics is one which troubles most of us. It has a sub-problem, that of finding published numerical values when they are needed. The difficulty seems to have been first seen and met in Germany, where "Landolt" has ever been a help in time of trouble, but the rapid rate of growth of scientific literature, and the general upset of currencies have made so many supplementary volumes necessary, each of them at so high a price, that only the better endowed libraries can buy them without serious thought.

In France, through the International Union of Pure and Applied Chemistry, the method has been to publish volumes of data from time to time. Originally, the intention was to publish each year a single volume which would contain the data from the preceding year's literature. Unavoidable difficulties held up the work at times, and later volumes were issued containing the data for three or four years together.

The parts listed in the heading above all belong to volume XI, and it is understood that in future all volumes will be divided into a number of parts which can be purchased separately.

Two at least of the sections now under notice can fairly be classed as of topical interest, and may well expect to command a wide sale. The nuclear physics section in particular forms a very valuable compendium of the results of recent, and moderately recent, work. The section on Raman spectra differs slightly from most of the "Données Numériques" in that critical values are given, instead of the observed values. Lines observed by different authors, if agreeing within 10 cm.$^{-1}$, are assumed to be identical, and only the mean is then given.

The main difficulty in such a series of annual or quasi-annual volumes is to know in which one an isolated piece of information is to be found; to assist the user from this point of view, it is proposed to issue during the present year a substance-index covering Vols. 6–10. Such an index for Vols. 1–5 appeared some twelve years ago, and a third index volume is promised next year, to deal with Vols. 11 and 12, which will themselves contain all data up to the end of 1936.

For the sake of those who are not familiar with the series, it may be added that the main language is French, but that most explanations are given in English as well. The headings are given in addition in German and Italian. If we may venture a suggestion, it is that the size and cost of the parts might be appreciably reduced if French alone were used. A heading which prints the word "Raman" four times, accompanied in turn by Effekt, Effect, Effet and Effetto seems to be over-indulgent to the reader.

Similarly, an index of chemical names in either English or French is quite intelligible, even to a reader who has no knowledge of the language selected, provided that he knows the other. (If he knows neither, he will not be helped by having both inserted.) It may be added that full information as to past and future parts, as well as those now under review, may be obtained from the Institut de Chimie, 11 Rue Pierre Curie, Paris, V^{e}.

J. H. A.

THE PROCEEDINGS OF
THE PHYSICAL SOCIETY

VOL. 49, PART 2 *March* 1, 1937 NO. 271

LIBRARY

A CIRCUIT FOR COUNTING IMPULSES AT HIGH SPEEDS OF COUNTING

BY J. H. E. GRIFFITHS,
The Clarendon Laboratory, Oxford

Communicated by Prof. F. A. Lindemann, 1 *July* 1936. *Read* 11 *December* 1936

ABSTRACT. A simple circuit is described which gives one impulse to a recording meter for, say, 10 pulses from a Geiger-Müller counter or similar instrument. The limitations and conditions of operation are discussed, and it is shown that a correction of 10 per cent has to be applied at a counting speed of 3000 per minute.

---

§ 1. INTRODUCTION

It is often of great advantage to be able to use a high rate of counting when recording the impulses from a Geiger-Muller counter or similar instrument. The scale-of-two counter designed by Wynn-Williams(1) is excellent for this purpose, but it is rather costly to build.

This paper describes a simple method of integrating the effect of, say, 10 pulses to give one count on the recording meter. Although the resolving time is about 10 times that of the scale-of-two counter, it is sufficient for most work with Geiger-Muller counters, since a counting speed of up to 3000 per minute can be used, and it has the advantage of great simplicity and low cost. The error, which in principle might be as great as 10 because digits are not recorded, is negligible compared with the statistical error for reasonably large numbers, and can be avoided by measuring the time needed to count a fixed number instead of the number of impulses in a fixed time.

§ 2. CIRCUIT

The circuit is shown in figure 1. At each pulse delivered by the amplifier the thyratron discharges the condenser C_1 which is then recharged through R. The voltage V_2 across the large condenser C_2 rises until it becomes sufficient to discharge the neon tube T. V_2 then drops to the extinguishing potential of the neon tube and if this change of potential is v, the quantity of charge is equal to C_2v.

Let V_1 be the difference between the original potential across C_1 and the final potential at which the thyratron extinguishes. Then C_1V_1 is the quantity passed through the thyratron at each pulse and n pulses will discharge the neon tube once if

$$nC_1V_1 = C_2v.$$

This may more properly be written

$$nC_1V_1 > C_2v > (n-1)\,C_1V_1 \qquad \ldots\ldots(1),$$

an equation* which shows that considerable latitude is allowed in the operation of the circuit.

It is very important that the insulation of the condensers C_1, C_2 and C_3 should be as good as possible; for if there is a leak from the anode circuit of the thyratron to earth, charge will be lost from C_2. This will be equivalent to one pulse per minute if $C_1V_1 = 60\,V_1/R'$, where R' is the resistance to earth. This gives R' about $= 10^{10}\omega$. This order of insulation can be obtained with commercial condensers; the smaller condensers C_1 and C_3 should have mica insulation.

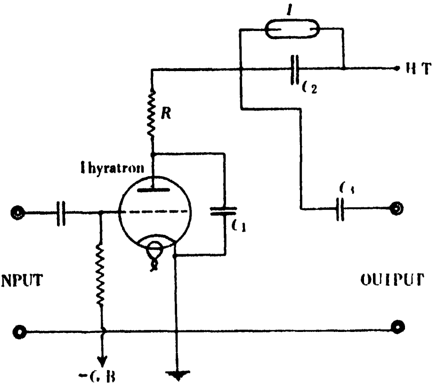

Figure 1.

However, it is only when the loss of charge during the time between two discharges of the neon tube is equivalent to one pulse that any error is caused. Thus with the resistance given above if 10 pulses occur in 30 sec., which is a very low rate of counting, the loss of charge due to leak is equivalent to half a pulse and is not recorded and, moreover, is not carried on to the next 10 pulses. Thus at higher speeds of counting a considerably higher leak can be allowed without any error being caused, and at low speeds single counting should be used.

Since the thyratron T is biased about 40 V., negative, the current to the anode is negligible.

3. THE RESOLVING TIME

There are two factors which give the resolving time, or rather the correction to be applied for pulses missed, and determine the value of R.

(1) During the time t_1 in which the grid of the thyratron is positive only a negligible amount of charge should pass through the resistance R. "Negligible"

---

* V_1 varies by the potential-difference between the sparking and extinguishing potentials of the neon tube, and this equation should be written

$$\sum_1^n C_1V_1 > C_2v > \sum_1^{n-1} C_1V_1.$$

The difference is small and the simpler equation is sufficiently accurate.

here may be taken to mean "less than V_1C_1/n". Assuming C_1 to discharge instantaneously the amount of charge is

$$t_1 \frac{V_1}{R}.$$

Hence $$t_1 \frac{V_1}{R} < \frac{V_1C_1}{n},$$

or $$nt_1 < RC_1 \qquad \text{......(2).}$$

This factor is only of importance if t_1 is not the same for every pulse.

(2) The time t between two pulses must be sufficient to allow the condenser C_1 to be completely recharged. If there are N_0 pulses per second the average time τ between pulses is $1/N_0$ and the probability that after the arrival of one pulse the next pulse will arrive in the interval between t and $t+dt$ is

$$e^{-t/\tau}.dt.$$

If V_3 is the extinguishing potential of the thyratron, the charge in C_1 after a time t is

$$V_3C_1 + V_1C_1 (1 - e^{-t/RC_1}),$$

and the deficiency of charge, i.e. the amount by which the charge on C_1 differs from the maximum value $(V_1 + V_3)\, C_1$ is

$$V_1C_1 . e^{-t/RC_1}.$$

The average deficiency of charge is given by

$$\frac{V_1C_1 \int_0^\infty e^{-t/RC_1}.e^{-t/\tau}\,dt}{\int_0^\infty e^{-t/\tau}\,dt} = V_1C_1 \frac{1}{\tau/RC_1 + 1}.$$

The operating conditions should be such that C_2v is only just greater than $(n-1)\,C_1V_1$ (see equation (1)) for in that case an amount of charge almost equal to C_1V_1 can be lost through partially unresolved pulses without any error occurring. The correction will therefore be 10 per cent when

$$n\,V_1C_1 . \frac{1}{\tau/RC_1 + 1} = V_1C_1$$

or $$\tau = (n-1)\,RC_1 > n\,(n-1)\,t_1.$$

and will decrease rapidly at lower counting speeds owing to the smoothing effect of taking ten impulses at a time. Thus the effective resolving time is considerably longer than the duration of the pulse and is determined by it.

For this reason an amplifier giving equal pulses of short duration, such as that designed by Barasch(2), should be used. The Barasch amplifier gives a pulse-duration of about 10^{-4} sec., which allows a resistance of $2{\cdot}10^5\,\Omega$. to be used if $C_1 = 0{\cdot}008\,\mu$F. τ is then $1{\cdot}4 . 10^{-2}$ sec. for a 10 per cent correction, and N_0 about 50 per second or 3000 per minute. This compares with a correction of 10 per cent at 300 per minute when using a mechanical counter with a maximum speed of 1500 per minute.

The complete unit for recording either singly or in multiples of 10 is shown in figure 2.

The switch S connected the input with either V_1 for multiple counting, or V_2 for single counting. The neon tube used is a Phillips neon indicator of the type with leads at opposite ends. The caps and resistance were removed.

To adjust the circuit for a given value of n (say 10) a change of C_1 gives a coarse adjustment, and the potentiometer P a fine adjustment. The potentiometer controls the potential across C_1, since the potential across C_2 is only controlled by the neon tube. Adjustment is best carried out by counting aurally the number of pulses for each discharge of the neon tube at a low rate of counting. The potentiometer is then set so that this number is 10, while for a slight increase of voltage it is 9.

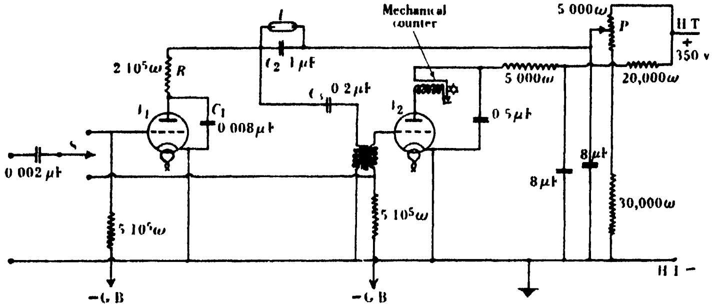

Figure 2.

Two 8-μF. electrolytic condensers are used to prevent the large pulse given by the thyratron T_2 from disturbing the first circuit. The circuit could probably be improved by using in place of R a valve or photocell or some device to ensure that current only flows into C_1 after the thyratron has extinguished itself. A larger multiplication than 10 might then be used with profit.

§ 4. ACKNOWLEDGEMENT

In conclusion I should like to thank Prof. Lindemann for his helpful advice and encouragement.

REFERENCES

(1) Wynn-Williams, C. E. *Proc. roy. Soc.* A, **136**, 312 (1932).
(2) Barasch, H. P. *Proc. phys. Soc.* **47**, 824 (1935).

THE ELECTRICAL CONDUCTIVITY OF THIN FILMS OF THE ALKALI METALS SPONTANEOUSLY DEPOSITED ON GLASS SURFACES

By A. C. B. LOVELL,
H. H. Wills Physical Laboratory, University of Bristol

Communicated by Prof. A. M. Tyndall, 5 *November* 1936. *Read in title* 22 *January* 1937

ABSTRACT. A description is given of an investigation of the electrical conductivity of the invisible thin films of the alkali metals which are deposited spontaneously on the walls of an enclosure in which they are sealed *in vacuo*. The resistivity of the films decreases in the order potassium, rubidium, caesium. The resistivity of the rubidium film is in reasonable agreement with a previous measurement given by Ives and Johnsrud. Some evidence is adduced in support of the view reached by the above workers that the thicknesses of these spontaneous deposits are of the order of those of monatomic layers.

§ 1. INTRODUCTION

This paper describes a detailed investigation of the electrical conductivity of the invisible thin films of the alkali metals which are deposited spontaneously on the walls of a vessel containing the metal *in vacuo*. The term *spontaneous deposition* will be confined to the case when the surface is either at the same temperature as the vapour to which it is exposed or at a somewhat higher temperature. A full account of another investigation by the writer on the conductivity of films of known thickness deposited under controlled conditions on cooled surfaces is in course of publication elsewhere(6, 7).

The first description of this phenomenon of spontaneous deposition occurs in the work of Elster and Geitel(1, 2), who observed that in photocells containing the alkali metals the anode showed photoelectric activity although previously cleaned of any deposit by heating.

The photoelectric properties of the films spontaneously deposited on metal surfaces were investigated by Ives(3), and Ives and Johnsrud(4) studied films of rubidium deposited on glass surfaces. It was observed that the films of rubidium on glass were electrically conducting and in darkness gave a pure ohmic resistance of $1{\cdot}3 . 10^8$ ohms on a plate measuring $1{\cdot}9 \times 4{\cdot}0$ cm. This resistance decreased under illumination as a result of the liberation of photoelectrons forming an added current along the tube under the potential gradient (the photoresistance effect).

Ives and Johnsrud(5) attempted to determine the thickness of these spontaneous deposits by measuring the shift in the phase and azimuth of polarized light reflected from the surface as a result of the presence of the film. This indicated a thickness of the order of 6 A., although the authors point out that the accuracy of the experiment was not sufficient to determine the thickness within a factor of 10. A thickness of this order would give a resistivity of the order of 10 ohm-cm., as compared with $11{\cdot}3 \times 10^{-6}$ ohm-cm. for rubidium in bulk at 0° C.

§ 2 THE EXPERIMENTAL TUBE

The spontaneous deposition occurs on the tube *A* (of soda or pyrex glass), which fits closely over the pyrex inlet *B* from the main body of the tube, figure 1. The temperature of the surface *A* can then conveniently be controlled by insertion of a heater into *B*. The deposition normally occurs over all the tube walls, and the resistance measured would be that of the tube *A* together with the parallel resistance across the outgoing leads. This is prevented by placing heaters over the outlet pinches *CC* and using an earthed guard ring *G*. The presence of thermocouples on the surface *A* gives rise to similar difficulties, and for this reason the temperature of *A* was calibrated against heater current in dummy experiments and the thermocouples were then removed.

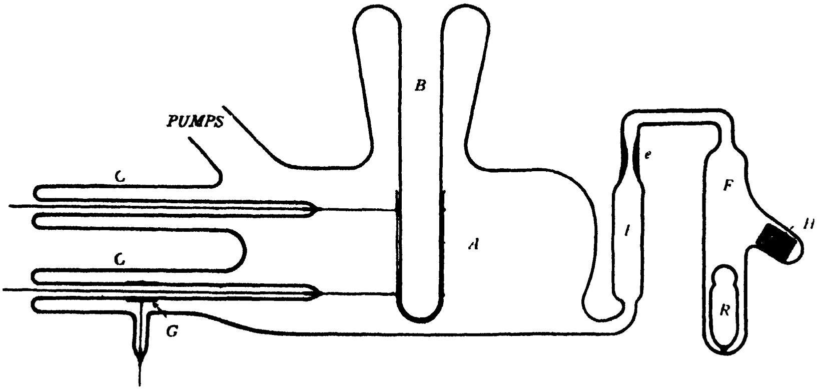

Figure 1

Contacts with the film were made by hoops of platinum wire partially embedded in the tube *A* for soda glass; and for pyrex glass by baking on small rings of colloidal graphite and wrapping platinum wire around. The whole tube was immersed in a thermostatically controlled oil bath; in this way the temperature of the alkali metal on the tube walls was maintained constant to within $\frac{1}{10}$° C. whatever the temperature of the surface *A* which, as was stated above, is independently controllable.

§ 3. INITIAL OBSERVATIONS

The initial experiments were concerned with attempts to reproduce the observations of Ives and Johnsrud(4) for rubidium on glass. The rubidium was prepared by reducing the chloride with calcium in a side tube, distilled into the experimental tube and the reaction bulb sealed off. With this arrangement it proved difficult to reproduce the results obtained by Ives and Johnsrud; on one or two occasions the films formed capriciously, but for a considerable time the causes of failure remained obscure. Eventually the failure to obtain conducting films was traced to an effect of the gas evolved during the reaction of the calcium with the rubidium chloride. It appears that foreign gas layers were put down on the surface at *A* and these inhibited the formation of conducting films. When the rubidium was separately prepared and thoroughly outgassed before being put into the experimental tube, the films were readily obtained.

§ 4. PREPARATION OF THE ALKALI METALS

Metallic rubidium and caesium have been prepared by the reduction of the respective chlorides with calcium metal *in vacuo*, the reaction being carried out in a separate vacuum apparatus. After the apparatus had been thoroughly baked out the metals were distilled successively through a train of bulbs into a group of glass ampoules, which could be sealed off at a constriction and stored for use. In the case of potassium the metal itself was distilled in a similar manner. When the alkali was to be introduced into the experimental tube one of these ampoules *R* was inserted into the tube *F*, figure 1, and broken by means of the magnetic slug *H*, and the metal was distilled into *E*. A constriction *e* then enabled the tube *F* to be sealed off. In this way the dangers referred to in § 3 were avoided. The alkali was then distilled over to cover the walls of the tube.

Prior to the breaking of the ampoule the whole tube was baked out at 500° C. for about 6 hours, the pumping tubes being thoroughly torched at the same time. The tube was continuously evacuated by a mercury diffusion pump working through a liquid-air trap. The first stages of the bake-out were carried out without liquid air over this trap in order to avoid condensation of excessive amounts of impurity. Once the bake-out had been accomplished the very greatest care had to be exercised to prevent the entry of mercury vapour into the tube.

§ 5. MEASUREMENT OF RESISTANCE

The resistance of the tube *A* was measured by means of a potentiometer and galvanometer. The current through the unwanted parallel resistance forming around the tube walls was short-circuited to earth by the guard ring *G* used in a standard manner. With 100 V. across the film it was possible to detect a resistance of 10^{13} ohms.

§ 6. RESULTS

In the initial distillation of the alkali from *E* into the experimental tube, condensation naturally occurs over the tube walls and over the surface of *A*, giving a resistance corresponding to that of the bulk metal. The alkali is cleared from *A* by placing the heater in *B* at about 150° C., and the resistance of *A* is then infinite. When *A* returns to the temperature of the oil bath the spontaneous film begins to form. A curve exhibiting the relation between resistance and time* can thus be plotted. Such a curve for caesium with the oil bath at 20° C. is shown in figure 2. It will be seen that the final resistance approaches a steady value. The formation of the film is complete in about 4 hours for caesium, and in 10 hours for rubidium. The curves of formation can be repeated by clearing the film from *A* by the heater in *B*. If, however, when the alkali is cleared from *A* the temperature of this surface is then lowered but adjusted to a value somewhat higher than that of the oil bath, then the spontaneous film comes to equilibrium more quickly but the final resistance is higher. The complete curves showing the logarithm of the resistance against temperature for a given vapour pressure of the alkali are shown in figure 3 for caesium and rubidium.

---

* The dimensions of the tube on which these measurements were made were as follows: diameter 16·8 mm., length 29·0 mm., giving the resistivity ρ as equal to $R \times 1{\cdot}82 \times$ the thickness of the film.

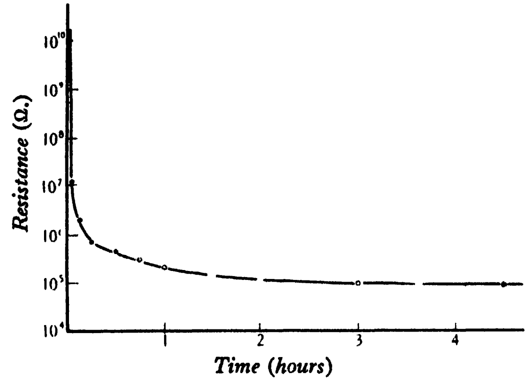

Figure 2. Formation of spontaneously deposited caesium film on soda glass.

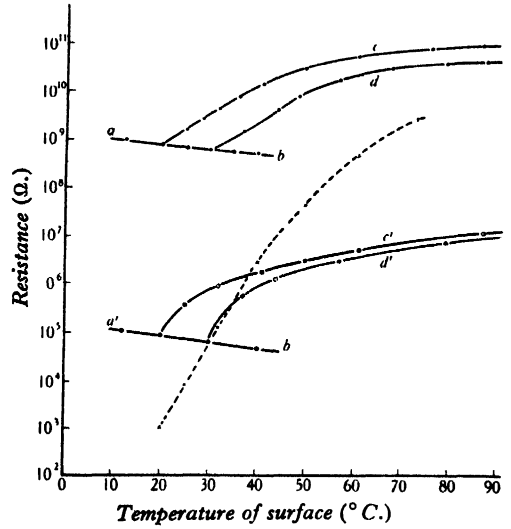

Figure 3. Curves for spontaneously deposited films. •—• Rubidium on soda glass; ×—× caesium on pyrex glass; ⊙—⊙ caesium on soda glass.

The lines *ab*, *a′b′* represent the uniform-temperature equilibrium points for these films, since they occur when the whole tube is at a uniform temperature, i.e. when the surface on which condensation occurs is at the temperature of the surroundings. It must be emphasized that the temperature conditions involved in these equilibrium points are critical, since if the temperature of the surface *A* falls slightly below that of its surroundings then normal condensation of the alkali occurs, giving a very low resistance.

The remaining curves *c*, *c′*, *d*, *d′* represent deposition on a surface at a higher temperature than its surroundings. (The oil bath keeps the alkali on the tube walls at a constant temperature, independent of the temperature of *A*, thus giving a constant vapour pressure.) Two series have been taken, *c* and *c′* with the oil bath at 20° C., and *d* and *d′* with it at 30° C.

It has been mentioned above that equilibrium is reached much more quickly when the surface *A* is at a higher temperature. For example, with caesium at 20° C. in the tube the formation of the film is completed in $\frac{3}{4}$ hour when the surface *A* is at 90° C. In the case of rubidium the time is 2 hours, and these times may be compared with 4 and 10 hours respectively for the uniform-temperature equilibrium points. Throughout the range of temperatures investigated, namely 20–90° C., the time for attaining equilibrium diminished steadily as the temperature of *A* increased, though the equilibrium resistance rose steadily of course, as is shown in figure 3. In view of its high uniform-temperature equilibrium resistance (5×10^9 ohms) potassium has not been fully investigated.

The above instances relate to deposition on soda glass surfaces. In the case of pyrex surfaces the curves are much steeper. An example for caesium with the vapour pressure at 20° C. is shown by a broken line in figure 3. In all cases the measurements have been carried out in darkness to obviate the photoresistance effect.

§ 7. DISCUSSION

These spontaneously deposited films of the alkalis are quite invisible, and the only evidence as to their thickness is that found by Ives and Johnsrud(5). From the following considerations the present investigation gives some evidence in support of their view that the films are monatomic layers.

The uniform-temperature equilibrium resistance for rubidium on soda glass at 20° C. was found in § 6 to be 8×10^8 ohms, on the tube whose measurements are given in that section. Taking Ives and Johnsrud's estimate of the thickness as 6 A. this gives the resistivity ρ as 90 ohm-cm.* For caesium on soda the resistivity is about 10^{-2} ohm-cm. and on pyrex 10^{-4} ohm-cm., the same estimate of the thickness being again used.

Now an investigation has been made by the writer of the resistivity of alkali metal films of known thickness deposited on a cooled surface under controlled conditions(6, 7). Stable or unstable films could be obtained according to the conditions, instability being characterized by a higher resistivity which increased with the time during which the films were kept *in vacuo* after deposition. Although the conditions obtaining in the course of that work were quite different from those described in the present paper, it may be pointed out that for films deposited under the worst conditions of instability resistivities of the order given above were only obtained in rubidium films having a thickness of less than 10 A. The resistivities for caesium similarly correspond to those of the films of about 3 and 10 A. respectively.

---

* In view of the uncertainties involved this shows good agreement with the resistivity of the order of 10 ohm-cm. given by Ives and Johnsrud(4) for these films, if similar assumptions are made as to their thickness.

Thus the evidence drawn from a comparison of resistivities tends to indicate that the thickness given by Ives and Johnsrud is certainly not in error by as much as a factor of 10; it thus seems reasonable to suppose that these spontaneous deposits are approximately monatomic layers.

Although there is as yet no evidence to enable speculations to be made as to the nature and structure of these spontaneously deposited films, it is of interest to point out that the present work has fitted in with the hypothesis developed in reference(7), concerning the relative instability of a given film of the three alkalis. It was found that as one passed down the series potassium, rubidium, caesium the stability of a film of given thickness steadily increased, and it was suggested that this might be accounted for by the atoms of alkali adhering more and more closely to the glass in this order. In the present work on spontaneous deposits it has been seen that the resistivities of the three alkalis decrease in the order potassium, rubidium, caesium, which would correspond to increasing coherency of the films.

§ 8. ACKNOWLEDGEMENTS

The author wishes to express his indebtedness to Dr E. T. S. Appleyard for suggesting the problem and for his continued interest. Also to the Department for Scientific and Industrial Research for a maintenance grant.

REFERENCES

(1) Elster and Geitel. *Phys. Z.* **21**, 361 (1920).
(2) Elster and Geitel. *Ann. Phys.*, Lpz., **67**, 420 (1922).
(3) Ives. *Astr. J.* **60**, 209 (1924).
(4) Ives and Johnsrud. *Astr. J.* **62**, 309 (1925).
(5) Ives and Johnsrud. *J. opt. Soc. Amer.* **15**, 374 (1927).
(6) Lovell. *Proc. roy. Soc.* A, **157**, 311 (1936).
(7) Appleyard and Lovell. *Proc. roy. Soc.* (in the Press).

Figure 1 Magnification, × 2

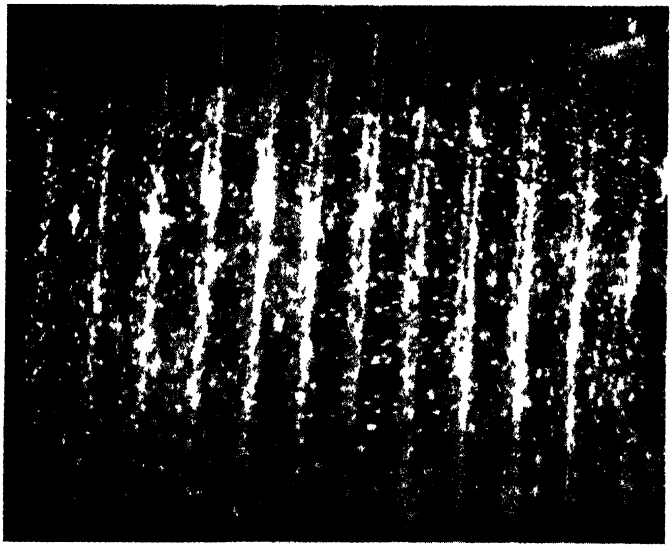

Figure 2 Magnification, × 100

THE SMOKE METHOD OF MEASURING SUPERSONIC VELOCITIES

By R. C. PARKER, B.Sc., Ph.D., University College, London

Received 31 *October* 1936. *Read in title* 27 *November* 1936

ABSTRACT. In view of certain criticisms brought against it, the smoke method used by Pearson has been further investigated. Various possible sources of error have been eliminated, and measurements of the velocity of sound have been made in air, oxygen and nitrogen in the frequency range 92·2 to 801·7 kc./sec. The results are believed to be correct to within 1 part in 3000, and no evidence of dispersion in this range has been found. An explanation is given for Pearson's results.

---

§ 1. INTRODUCTION

A new method for determining the velocity of sound at supersonic frequencies has recently been developed by Pearson(1). Results were obtained for frequencies in a range from 92·2 to 801·7 kc./sec. and showed definite evidence of dispersion. Certain criticisms have been brought against this method, and the purpose of these investigations has therefore been to repeat certain of the measurements under more precise conditions, with special attention to the points that have been called into doubt. The method has been extended and measurements on the velocity have been made in oxygen and nitrogen.

§ 2 PRINCIPLES OF THE METHOD

The method is essentially that of the familiar Kundt's tube. The length of an enclosed air column, energized by a piezo-electric quartz crystal oscillator, is adjusted for resonance conditions, and the position of the nodes in the standing wave system are marked by rings of coagulated smoke particles. The frequency n at which the quartz crystal vibrates is accurately known, and this with a measured value of the wave-length λ_t at a temperature t° C. (T° K.) enables the velocity V_t to be deduced. The velocity V_0 at 0° C. is obtained from the relation

$$V_0 = V_t \sqrt{\frac{T_0}{T}},$$

where, of course,

$$V_t = n\lambda_t.$$

The importance of this method ultimately depends upon the accuracy with which λ_t can be measured. By the introduction of certain modifications the smoke figures have been eventually obtained in a particularly clear manner. Figures 1 and 2 show rings formed at a frequency of 219 kc./sec. Their double structure is clearly visible and so confirms the theory that, at these frequencies, the particles act as obstacles to produce phenomena similar to those observed by Andrade(2) using cork dust at audio frequencies.

§ 3. MEASUREMENT OF λ

The values of V_0 given by Pearson, for each particular frequency, represents the mean of eight determinations. At a frequency of 310 kc./sec. the individual measurements of the velocity differed by 1·4 m./sec.; at other frequencies this difference was presumably greater. Such a scatter not only necessitates a large number of readings, but it suggests that there may be additional factors for which allowance has not been made. Pearson does not say what caused this scatter, though from the data supplied one can only attribute it to some error in λ_t. A preliminary set of readings made with the original apparatus confirmed this view. From eight determinations made at a frequency of 220 kc./sec. a maximum difference of 1·3 m./sec. was obtained. The wave-length was obtained by noting the position of forty nodal rings and treating the observations in the usual way, i.e. the readings were divided into two groups to give a series of values for $10\lambda_t$. The rings were so distorted and ill-formed that difficulty was experienced in setting the cross wire of the microscope accurately at their centre. The neighbouring values of λ_t often differed by 10 per cent, while the final mean had a probable error of $\frac{1}{4}$ per cent. From these readings no systematic variation in the ring-spacing was detected.

Rings of clearer definition were eventually obtained by establishing more stable conditions of oscillation, and by making sure that the plane of the crystal and piston-face were perpendicular to the axis of the tube. By means of a travelling microscope, which enabled settings to be made to within 0·002 mm., 40 rings were measured near the crystal. The readings of the nodal positions were again divided into two equal groups to give 20 values for $10\lambda_t$. The maximum divergence shown by these readings was only 0·3 per cent and a repetition of the experiment at the same temperature gave values of V_0 agreeing to within 0·1 per cent, the measurements being made, each time, along the same section of the tube.

The uniformity of the tube. The conditions which exist at supersonic frequencies make it difficult to assess, theoretically, the influence which any non-uniformity of the tube may have upon the nodal positions. It being now possible to measure the wave-length to a high degree of accuracy, an experimental investigation was made by extending the measurements along the length of the tube (35 cm.). The wave-length was seen to vary according to the portion of the tube over which measurements were made. From a minimum, which occurred near the centre of the tube, the value rose as either end was approached. The extreme values differed by 1 per cent. An explanation of this irregularity was sought by examining the tube for lack of uniformity. It was removed from the apparatus and its internal diameter measured at various points along its length. The uniformity of the tube was found to be poor; not only did it flare out at either end, but the diameter of the open end was 3 per cent in excess of that at the closed end. The cross-section was not circular, and four typical values for diameters inclined at $\pi/4$ through one section were 1·936, 1·942, 1·969 and 1·964 cm.

This tube was replaced by a German glass tube, of diameter 2 cm., specified as being of great uniformity. Measurements showed a cross-section which was circular to 0·02 mm. and a diameter constant along the tube to 0·01 mm. Rings formed in this tube were much more uniform in spacing. Groups of 40 rings measured at different sections along the tube gave values of λ_t constant to 0·4 per cent, while four independent determinations of the velocity made at a frequency of 127·5 kc./sec. showed a maximum difference of only 0·4 m./sec. For these latter values, groups of 20 rings were measured at about $200\lambda_t$ apart, the complete number of half wave-lengths separating these groups being found by obtaining an approximate value of λ_t from the sets of 20 rings.

Effect of amplitude. It had been suggested(3) that as certain crystals used by Pearson had broken on excitation, their amplitude must have been abnormally large. The appearance of the crystals did not lend support to this suggestion but invariably indicated a weakness at the groove cut for the supporting screws. This point was of importance, since change of velocity with amplitude furnished a possible explanation of any velocity increase: if the amplitude associated with any crystal was sufficiently large, the wave-front would become distorted to give an increase in the wave-velocity. Such an increase would naturally depend upon the condensation, as the velocity of a large amplitude wave is given by(4)

$$V = V_0 (1 + S)^{(1+\gamma)/2}$$

where V_0 is the velocity of the small amplitude wave, S the condensation and γ the ratio of the specific heats.

With the 219-kc./sec. crystal two measurements of the velocity were made for two different values of the amplitude, a quantity assumed to be proportional to the excitation voltage on the crystal face. The first measurements were made under the conditions formerly used, while for the second set the excitation voltage was reduced to one fifth. Now if, in the latter case, S was still large enough to cause an increase in the wave-velocity of 1/10 per cent, say, then for the case in which S was five times as great the increase in the wave-velocity would be 1 per cent. Values of V_0 for the two sets of measurements came out to be 331·7 and 331·9 m./sec., which values are substantially in agreement. Throughout the subsequent measurements the lower excitation voltages were employed, and thus there was no likelihood of any error greater than 1 in 1000 being introduced as a result of large velocity-amplitudes.

Concentration of smoke particles. Two objections may be raised against the use of smoke particles obtained from burning tobacco. In the first place the particles consist of minute drops of liquid formed on dust nuclei and so, on sedimentation, might appreciably increase the moisture-content of the air. Secondly, the particle concentration is relatively high and so might influence the wave-propagation by a loading effect. Such possibilities were obviated by using, instead of tobacco smoke, magnesium-oxide smoke at a very low concentration.

A known weight of magnesium ribbon (80 mg.) was burnt in a tank, and the smoke-laden air, after passing through a long calcium-chloride tube, was introduced into the apparatus. The volume of the tank was 5.10^5 cm.^{3} and thus the ratio of the aggregate mass of smoke particles per cm.^{3} to the mass of 1 cm.^{3} of air was 2.10^{-4}. This represents an upper limit, because the contents of the tank were stirred for

15 minutes, when the concentration decreased as a result of sedimentation and diffusion to the walls. Data on coagulation, published by Whytlaw-Grey and Patterson (5), allow this decrease to be calculated, and show that after the 15 minutes stirring the ratio mass of smoke particles to mass of air becomes 10^{-6}. A still further reduction of smoke concentration occurs when the air passes through the calcium chloride tube. It would seem safe to conclude that an added mass of the above magnitude could not influence the propagation of sound in the tube to a measurable extent.

It is interesting to obtain an estimate of the number of particles per cm.^{3} Taking for the density of the magnesium oxide smoke particles a value of 0·35 g./cm.^{3} and taking a measured value for their radii of $3 . 10^{-5}$ cm. (see a forthcoming paper by Andrade and Parker) the concentration works out at 10^5 particles per cm.^{3} At these low concentrations and at the lower frequencies the sound vibrations had to be continued for times up to two hours to obtain satisfactory rings. At the higher frequencies, however, well defined rings were formed much sooner, so that at a frequency of 801·7 kc./sec. the process was complete in about five minutes.

§ 4. VELOCITY OF SOUND IN GASES

The preliminary experiments already described were all made in air at two frequencies, namely 127·5 and 219 kc./sec. It remained to cover the rest of the frequency range. It was also decided to measure the velocity of sound in oxygen and nitrogen, for this would serve the additional purpose of verifying any evidence of dispersion. The apparatus was redesigned, since leaks are only negligible when air is the gas under consideration. The same method was used throughout, except that, in the case of nitrogen, magnesium-oxide smoke was not used. It was replaced by magnesium-nitride smoke, which was obtained by heating magnesium ribbon electrically in an atmosphere of pure nitrogen. The smoke proved satisfactory, and its adoption eliminated the question of the removal of oxygen which would have been necessary with magnesium-oxide smoke.

§ 5. APPARATUS

A cross-sectional view of the apparatus is shown in figure 3. The glass tube *A* was supported by short sleeves centrally disposed within the end faces of an outer tank *G*. The outer tank, which served as a water bath to eliminate convection, was 48 cm. long and had a square cross-section of 6 cm. The sides of the tank were covered with plate-glass windows to facilitate viewing of the glass tube. Through one end plate passed a brass tube *H* carrying a plunger which was made to fit the inside of the glass tube. The end plate *M* was detachable and a collar *P* enabled the tube and plunger to be rigidly locked in any desired position. The smoke-laden gas entered the apparatus through the tubes *L* and *H* and finally passed into the resonance space through two holes suitably drilled through a piston, which in turn was contained in the brass plunger. By means of an end cap *K* the piston could be withdrawn into the plunger to present a plane reflecting face to the on-coming sound waves.

The protruding end of the glass tube was enclosed in a rectangular brass chamber of dimensions 6 × 6 × 8 cm. Its two side faces were fitted with glass windows, and two brass stop cocks, not shown, enabled it to be separately supplied with gas.

The method of mounting the crystal is shown in figure 4. The brass ring *B*, 2·7 cm. in internal diameter and 4 cm. in external diameter, carried three pointed screws which gripped the crystal around its central groove. The two lower screws were secured into position by locking-nuts, and a third, *D*, enabled the clamping pressure to be adjusted. The holder *B* was fixed to a short brass tube *Q*; this fitted loosely over the glass tube so that the crystals were held centrally in its open end. Openings were made in both the glass and the brass tubes to give entry to the small electrode, while two further openings in *Q* enabled the electrode to be viewed. The crystals varied in length from 2 mm. to 24 mm., and hence the position of the crystal-holder had to be adjustable. The screw *D*, figure 3, passed through a slot, 1 cm. long, cut in the upper face of the chamber, and then through a hole drilled in a lower plate *R*. The second plate *R* was arranged to slide flush with the inner surface of the top face, and so, the interface surface having been smeared with vacuum grease, the screw *D* could be used to move the crystal holder without leak. The sliding plate was secured to *C* by four corner flange screws moving similarly along slots cut in the upper face.

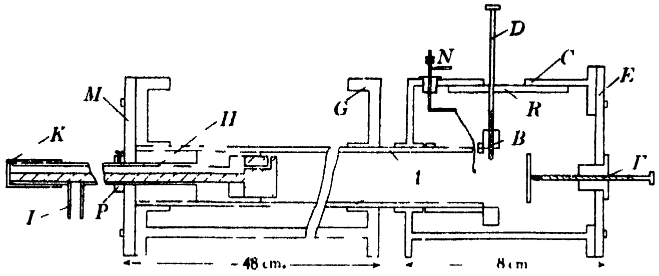

Figure 3.

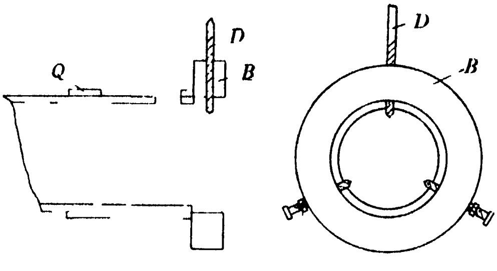

Figure 4

The two electrode-supports entered by two ebonite bushes. The large electrode was a flat copper disc 2 cm. in diameter and was attached to the screw *F*, figure 3, by a small light copper spring. Its approach to the near coppered face of the crystal could be finely adjusted. For the smaller electrode a small piece of copper foil was soldered on to a light springy wire; this was attached to a rod N. The position of this small electrode was critical, and to obtain a comprehensive adjustment the rod was mounted to move vertically and to rotate.

With this modified apparatus it was found much easier to make the necessary adjustments that were required before the crystals would oscillate. In fact, difficulty was experienced with the crystal of highest frequency only; this was an important advantage, because formerly the crystals would occasionally stop oscillating, and in the process of getting them to start again the rings would become slightly distorted owing to uncertain circulations or through momentary oscillation at some neighbouring frequency. When the crystal which had a natural frequency of 801 kc./sec. was used, the effective tube length had to be reduced to 15 cm., otherwise no rings were formed on account of the high attenuation.

A diagrammatic sketch of the complete arrangement is shown in figure 5.

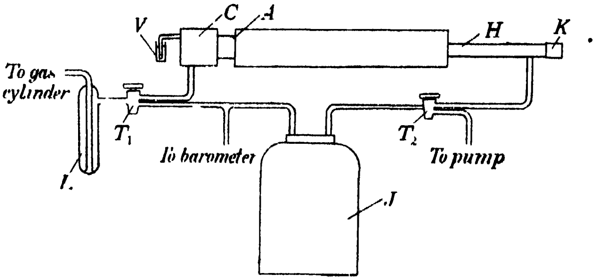

Figure 5.

The gas was admitted into the glass resonance tube A from a cylinder. Between the cylinder and A was inserted a liquid-air trap L and a stone jar J, closed by a metal cap cemented with sealing wax. The liquid-air trap served to remove any volatile gases present as impurities. In the stone jar was a length of magnesium ribbon which could be electrically heated to produce magnesium-oxide or magnesium-nitride smoke, according to which gas was used⁽⁶⁾.

In carrying out a measurement, any residual gas from the previous experiment was first removed from L and J by means of a hyvac pump, and, when the pressure had fallen to a few millimetres of mercury, gas was admitted from the cylinder and allowed to stream through the glass resonance tube A for 30 minutes, after which time the air or gas initially present was judged to be completely replaced. The magnesium ribbon in J was then fired and the resulting smoke passed with the gas into the apparatus. When sufficient had entered, the gas stream was deviated by the tap T_1 and passed directly into the chamber C, where a slight excess pressure was maintained to prevent leaks round the electrode screws. A bubble indicator V gave a check on the rate at which the gas was flowing.

To measure the rings the subsidiary chamber C and the piston arrangement H were removed. Light from a 5-ampere arc was then passed axially down the tube, and the rings were thus viewed by scattered light against a dark background.

§ 6. RESULTS

The velocity of sound was determined in air, oxygen and nitrogen. These gases were contained in 100-ft.^{3} cylinders. The impurity in the nitrogen, supplied as oxygen-free, was 0·2 per cent and that in the oxygen 0·8 per cent. These impurities were due to the presence of the rare gases. The air supplied was atmospheric, carbon dioxide and water vapour being removed by the liquid-air trap and the drying-tube.

The velocity of sound was first determined in air. The value of V_0 was taken as the mean of four determinations. A representative example of such a set is given in table 1.

Table 1. (Frequency $n = 219{\cdot}28$ kc./sec.)

Temperature (° C.)	Wave-length (mm.)	V_0 (m./sec.)
17·2	1·5600	331·8
18·0	1·5611	331·6
15·2	1·5540	331·6
15·2	1·5551	331·9

Mean value of $V_0 = 331{\cdot}7$ m./sec.

The mean values of V_0 obtained at each of the other frequencies are given in table 2.

Table 2

n (kc./sec.)	Air	Oxygen	Nitrogen
	V_0 (m./sec.)	V_0 (m./sec.)	V_0 (m./sec.)
127·53	331·9	315·3	337·1
219·28	331·7	—	337·0
297·66	331·8	315·2	336·9
485·34	331·6	315·3	336·9
801·67	331·8	315·4	337·2

In table 2 are given the values of V_0 obtained in nitrogen and oxygen respectively. As there was no indication of any dispersion, the range of frequencies was, in the case of oxygen, covered by four crystals; while in view of the preceding agreement in the velocity-measurements only two determinations were made for each V_0.

In none of the gases did the velocity show any systematic variation, and hence final values of V_0, taken as the mean of the values obtained at all frequencies, are appended in table 3. The probable error in these mean values is 3 in 10,000.

Table 3. Mean values of V_0 (m./sec.)

Air	$331{\cdot}7_6$
Oxygen	$315{\cdot}3_0$
Nitrogen	$337{\cdot}0_2$

The Kirchhoff correction, which must be applied at sonic frequencies in order to get the value of the velocity in free space, was neglected. For the correction is never greater than 1 in 3000, and this, in view of the small trace of impurity in the gases, must represent the order of accuracy of the results.

The excess of V_0 above the normal value obtained by Pearson, particularly at the lower frequencies, would seem to be due to a confusion in the ring spacing mainly caused by some bad lack of uniformity of the tube near the piston. The writer made further measurements with the original tube and obtained values in good agreement with those of Pearson. Over this particular section of the tube the ring-formation was such that, in obtaining an estimate of λ_t, the rings were liable to be miscounted. A particularly clear, though distorted, set of rings was obtained and revealed a formation as shown in figure 6. Thus, for measurement made with the microscope along the bottom of the tube (i.e. within the region *AA*) a miscount would be made. An allowance for this miscount brought the values into line with those formerly given. For measurements made above a frequency 310·2 kc./sec. the tube-length was shortened, so that the above-mentioned section of the tube was not used; the values for V_0, with the original tube, were then found to be between 331·8 and 332·2 m./sec.

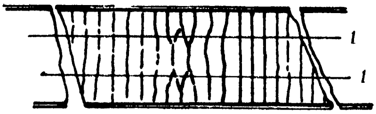

Figure 6

§7 DISCUSSION OF RESULTS

Measurements on the velocity of sound at supersonic frequencies have, in recent years, been the subject of much interest. Since the first important measurements of the velocity in air by G. W. Pierce$^{(7)}$, the acoustical interferometer has been employed by many experimenters. The irregularities in the proximity of the source and the phenomena of multiple peaks and interferometer satellites have been studied in some detail, with the result that the method is now one of precision.

J. C. Hubbard$^{(8)}$ made a detailed examination of the method and concluded that for the frequencies he used, namely 218 to 476 kc./sec., there was no change in the velocity. W. H. Pielemeier$^{(9)}$, extending the frequency range to 1216 kc./sec., obtained values of V_0 lying between 331·6 and 331·7 m./sec., which values were also constant at all frequencies. Further evidence of independence of frequency was added by C. D. Reid$^{(10)}$, who worked between frequencies of 42 and 140 kc./sec.; his final value for V_0 was 331·6$_3$ m./sec. A slightly higher value of 331·8$_5$ m./sec. was obtained by Pan Tcheng Kao$^{(11)}$, whose frequency range extended from 20 to 70 kc./sec. W. D. Hershberger$^{(12)}$ made use of the interferometer to investigate the multiple-peak phenomena noticed by Pielemeier, Kao and others; he varied the amplitude of the exciting e.m.f. within wide limits and found several attributable causes for the previously observed phenomena. He made measurements on the velocity between 20 and 70 kc./sec. and showed V_0 to be independent of the frequency. Recent work by M. Grabau(13) and G. A. Norton(14), though similarly restricted to frequencies between 20 and 70 kc./sec., show values for V_0 in excellent agreement, their respective values being 331·68 and 331·76 m./sec.

In the region of sonic frequencies W. G. Shilling and J. R. Partington(15), using the resonance-tube method, obtained the lower value of 331·4 m./sec. The measurements were made at a frequency of 3 kc./sec. Their method of applying the Helmholtz-Kirchhoff correction, particularly at high temperatures, was criticized by R. E. Cornish and E. D. Eastman(16) who, employing a similar method, deduced a value of V_0 equal to 331·5 m./sec. C. B. Vance(17) used a resonance-tube method in which lycopodium powder was used to indicate the nodal positions; he made measurements between 30 and 200 kc./sec., and to investigate various tube corrections he chose for the free velocity in air a value of 331·77 m./sec. G. W. C. Kaye and G. G. Sherratt(18), used the resonance-tube method and made measurements from 500 c./sec. to 27 kc./sec., the velocity remained constant and equal to 331·6 m./sec. Unpublished experiments of E. N. da C. Andrade, D. H. Smith and S. H. Wheeler give a value of 331·74 m./sec. for frequencies between 800 and 1400 c./sec.

The only definite evidence of dispersion existing at normal temperatures seems to be afforded by C. Ishii(19) who used frequencies up to 3000 kc./sec. From 300 to 2000 kc./sec. a normal value of 331·6 m./sec. was obtained, but at 2892 kc./sec. it had risen to 332·6 m./sec. No other worker seems to have extended the range so far.

From the theoretical work of Kneser(20), no dispersion would be anticipated in the case of air, or its constituent gases, up to frequencies here employed, viz. 800 kc./sec. Experimental evidence with regard to these gases would have to be sought at higher temperatures or at higher frequencies. The work of Kneser has received much experimental and theoretical support from Henry(21), E. Grossman(22), and, less directly, from G. G. Sherratt and E. Griffiths(23). The present author gives additional data and confirms the results obtained by the various workers with an acoustical interferometer by a method which is more direct in that λ is obtained free from many of the causes of multiple peaks and associated complexities. Thus, in the above experiment the tube was always adjusted for resonance and so did not induce in the crystal a parasitic frequency of oscillation such as that observed by Hershberger, when the moving reflector altered the acoustical load on the crystal. In the present experiments it was found that such parasitic oscillations could be induced in certain crystals by throwing the tube out of resonance, i.e. the 219·3-kc./sec. crystal would oscillate at a frequency of 201 kc./sec.

Comparatively few experiments seem to have been made on the velocity of sound in nitrogen at supersonic frequencies. Using their resonance-tube method at sonic frequencies Shilling and Partington gave a value which at 0° C. becomes 337·4 m./sec., while J. A. Van Lammeren and W. H. Keesom(24), also using a resonance-tube method, obtained values of 337·1 and 337·5 m./sec. It may be noted that the latter author's value for air obtained with the same method is 332·1 m./sec.

Shilling and Partington made observations on oxygen at some frequencies and obtained a value of the velocity equal to 314·4 m./sec. Keesom, Itterbeck and Lammeren(25), also using a resonance-tube method, gave 315·4, while Pielemeier, using incomplete satellite values from his interferometer, gave a value in close agreement with that predicted by theory, namely 314·8 m./sec. This latter value is also in very good agreement with that obtained by E. G. Richardson(26), for the average of his results between frequencies of 42 and 1800 kc./sec. is 314·9 m./sec.

§ 8. ACKNOWLEDGEMENT

In conclusion I wish to express my sincere thanks to Prof. E. N. da C. Andrade, F.R.S., who not only formulated the problem but continued to show great interest in the progress of the work and offered many valuable suggestions during the course of it.

REFERENCES

(1) Pearson. *Proc. phys. Soc.* **47**, 136 (1935).
(2) Andrade. *Philos. Trans.* A, **230**, 413 (1932).
(3) Wood, A. B. *Proc. phys. Soc.* **47**, 145 (1935), Discussion.
(4) Wood, A. B. *Sound*, p. 264. (London, 1930.)
(5) Whytlaw-Grey and Patterson. *Smoke* (1932).
(6) Parker, R. C. *Trans. Faraday Soc.* **32**, 1115 (1936).
(7) Pierce. *Proc. Amer. Acad. Arts Sci.* **60**, 284 (1925).
(8) Hubbard. *Phys. Rev.* **36**, 1668 (1930).
(9) Pielemeier. *Phys. Rev.* **36**, 1005 (1930); **38**, 1236 (1931).
(10) Reid. *Phys. Rev.* **35**, 814 (1930); **37**, 1147 (1931).
(11) Kao. *Ann. Phys.*, Paris, **17**, 315 (1932).
(12) Hershberger. *Physics*, **2**, 269 (1932).
(13) Grabau. *J. acoust. Soc. Amer.* **5**, 1 (1933).
(14) Norton. *J. acoust. Soc. Amer.* **7**, 16 (1935).
(15) Shilling and Partington. *Phil. Mag.* **6**, 920 (1928).
(16) Cornish and Eastman. *Phys. Rev.* **33**, 90, 258 (1929).
(17) Vance. *Phys. Rev.* **39**, 737 (1932).
(18) Kaye and Sherratt. *Proc. roy. Soc.* **141**, 123 (1933).
(19) Ishii. *Sci. Pap. Inst. phys. chem. Res.*, Tokyo, **560**, 201 (1935).
(20) Kneser. *Ann. Phys.*, Lpz., **11**, 777 (1931).
(21) Henry. *Proc. Camb. phil. Soc.* **28**, 249 (1932).
(22) Grossman. *Ann. Phys.*, Lpz., **13**, 681 (1932).
(23) Sherratt and Griffiths. *Proc. roy. Soc.* A, **147**, 292 (1934); **156**, 504 (1936).
(24) Lammeren and Keesom. *Proc. K. Akad. Wet. Amst.* **35**, 6, 727 (1932).
(25) Keesom, Itterbeck and Lammeren. *Proc. K. Akad. Wet. Amst.* **34**, 7, 996 (1931).
(26) Richardson. *Proc. roy. Soc.* **146**, 56 (1934).

PHOTOMETRIC TEST PLATES

By A. K. TAYLOR, A.C.G.I., M.I.E E.

Received 19 *October* 1936. *Read* 3 *December* 1936

ABSTRACT. Characteristic curves showing the variation of reflection factor with the angles of incidence and view are given for flat plates of seven materials. Suggestions are then made as to the use of these either as substandards of reflection factor or for the measurement of illumination.

§ 1. INTRODUCTION

PHOTOMETRIC test plates are required for use (*a*) with illuminometers in the measurement of brightness or illumination, and (*b*) as substandards of reflection factor. For the former purpose the test plate should have a plane matt surface with a constant apparent reflection factor* at some definite angle of view for all angles of incidence. The surface should be easy to clean without affecting its reflection characteristics, or else easy to reproduce. For the second purpose the test plate should have a plane matt surface giving a definite apparent reflection factor for certain specified angles of view and incidence. The surface must be such that its reflection factor for the conditions specified can be readily reproduced with a variation not exceeding 0·5 per cent; and this reflection factor must remain constant for a reasonable period.

Test plates made of the following materials were examined (1) white pot opal glass (ground), (2) magnesium oxide, (3) white filter paper, (4) white matt celluloid, (5) magnesium oxychloride, (6) white blotting paper, and (7) plaster of Paris.

§ 2. METHOD OF MEASUREMENT

The relative values of the apparent reflection factors were obtained by taking, with an illuminometer, readings of the brightness of the test surfaces at various angles of incidence when illuminated by the source at a constant distance. These readings, when divided by the cosines of the respective angles of incidence, were then proportional to the brightnesses of the test surfaces at those angles for an illumination numerically equal to that produced by the source at normal incidence.

The source used was an ordinary electric photometric substandard lamp of the grid type, the horizontal candle power being about 40 and the length of the grid 7 cm. The distance from the source to the test surface was in every case at least 10 times the length of the filament.

---

* The apparent reflection factor of a surface is the ratio of the brightness of the surface to that of a perfect diffuser of unit total reflection factor under equal illumination. The total reflection factor is the ratio of the total reflected light flux to the incident flux.

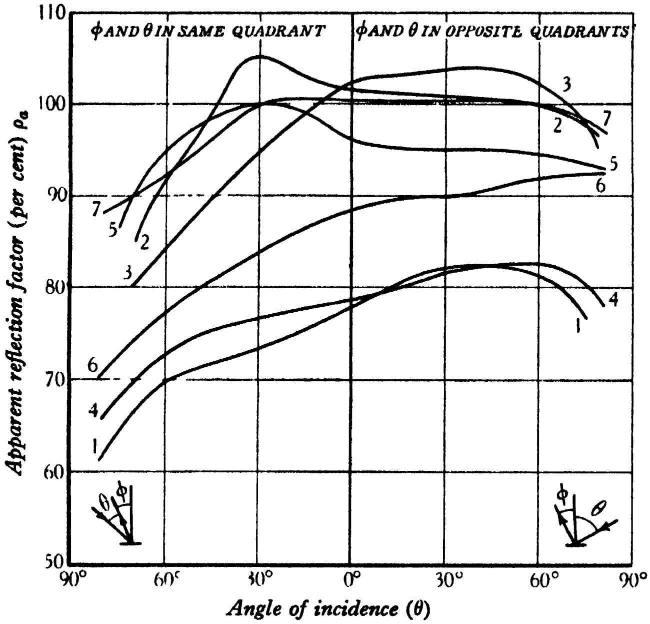

Figure 1. Variation of apparent reflection factor with angle of incidence at most favourable angle of view (see table 1). (Angle of view in plane of incidence.)

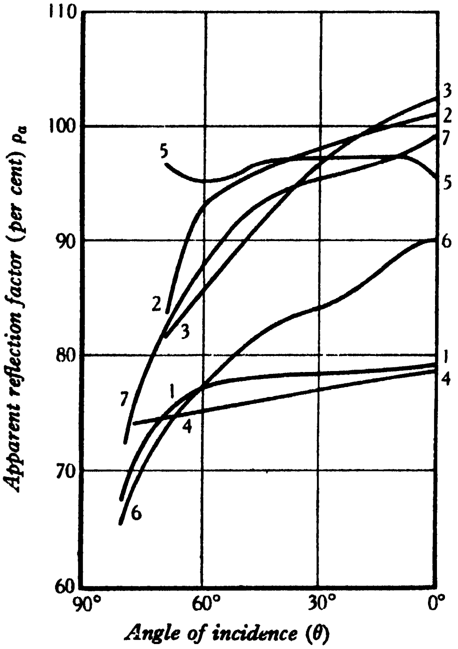

Figure 2. Variation of apparent reflection factor with angle of incidence at most favourable angle of view (see table 1). (Plane containing angle of view normal to plane of incidence.)

§ 3. RESULTS

Figures 1–4 show, for the seven materials examined, the variation in the apparent reflection factor ρ_a with the angle of incidence θ for a definite angle of view ϕ, the angles of view and incidence being in the same plane (figure 1) or in planes normal to each other (figure 2). The curves in figures 3 and 4 show the variation in the apparent reflection factor with the angle of view for normal incidence and for 45° incidence respectively.

The angles of view selected for the curves shown in figures 1 and 2 are those for which the changes in ρ_a corresponding with the changes in the angle of incidence were found to be a minimum for the material under consideration, where the angles of incidence and view were in the same plane but in opposite quadrants. It was found generally that large changes in the angle of view had very little effect on the value of ρ_a where the angles of incidence and view were in planes normal to each other.

The values of the total reflection factor ρ for a parallel beam at normal incidence, obtained by graphical integration* of the curves in figure 3, are given in table 1, which also shows for each material the amount by which ρ_a changes, expressed as a percentage of the mean value of ρ over the range of θ covered.

Table 1. Reflection factors and their variation

Material	ρ (per cent)	θ and ϕ in ...	Change in ρ_a with direction of incidence (%)					
			same plane				perpendicular planes	
		$\phi \diagdown \theta$	0–80		10–70°		10–70°	
			Max.	Mean	Max.	Mean	Max.	Mean
Pot opal glass	76	30°	4	2½	3	2	2¾	2
Magnesium oxide	98	40°	6	1¼	1½	¾	6½	4¾
White filter paper	96	20°	7	2	3	1½	12	6
White matt celluloid	—	30°	2½	1½	2	1¼	2½	1¾
Magnesium oxychloride	94	40°	2	1	1	¾	2	1
White blotting paper	93	20°	2¼	1½	2	1½	10	5
Plaster of Paris	97	30°	2	1	1½	¾	10	4½

---

* These total reflection factors have been deduced graphically from the curves for normally incident light, on the assumption that under these circumstances the brightness of the surface depends only on the angle of view. If F is the total flux incident on the surface, that leaving the surface in a direction at an angle ϕ with the normal is $F\pi^{-1}\rho_\phi \cos\phi$, and since the corresponding element of solid angle is $2\pi \sin\phi\, d\phi$ the total reflected flux is $F\int_0^{\pi/2} \rho_\phi \sin 2\phi\, d\phi$. The reflection factor is obtained by giving F the value unity, and is thus $\int_0^{\pi/2} \rho_\phi \sin 2\phi\, d\phi$. From the curves of $\rho\phi$ in figure 3 curves representing $\rho_\phi \sin 2\phi$ were plotted, and the integrals found by measuring the areas enclosed between curve and base.

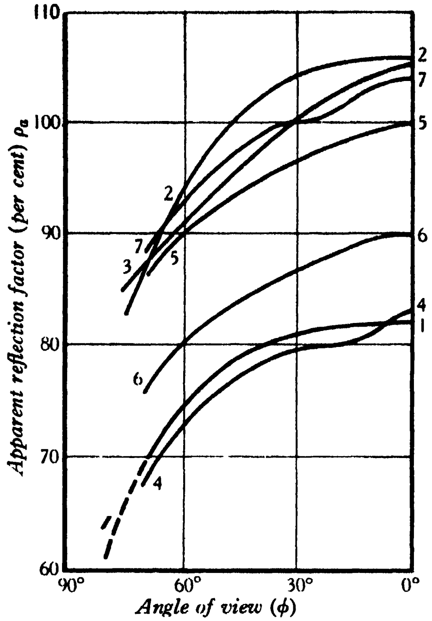

Figure 3. Variation of apparent reflection factor with angle of view for normal incidence.

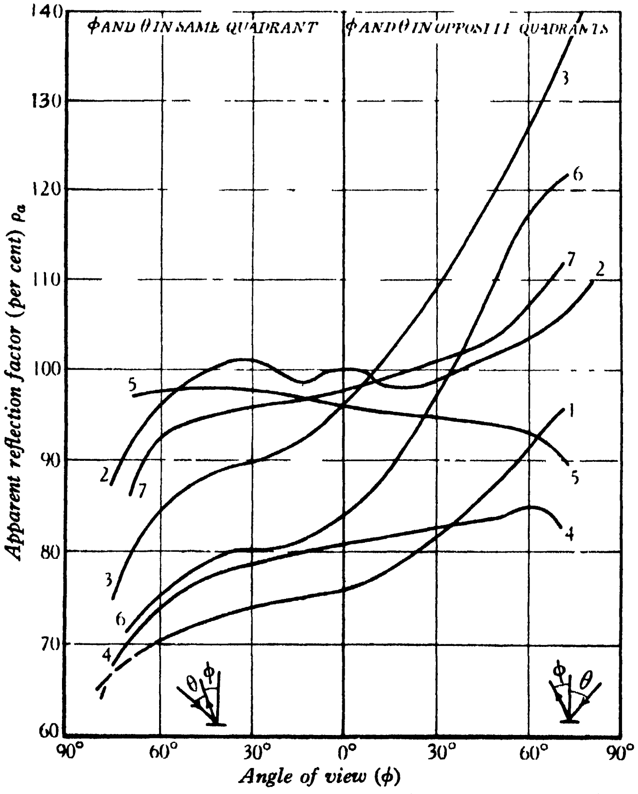

Figure 4. Variation of apparent reflection factor with angle of view with light incident at 45° in plane containing angle of view.

§4. EXPERIMENTAL DETAILS

Pot opal glass. A sample of good colourless commercial pot opal glass, about $2\frac{1}{2}$ mm. thick, ground to a medium matt surface, was mounted in a frame with a piece of black velvet in contact with the back of the sample. This surface is suitable for use when making measurements of illumination provided the angle of incidence be limited to 70°, ϕ and θ being in the same plane but in opposite quadrants, or in planes normal to each other. This surface is also suitable as a substandard of reflection factor. It is suggested that the disk should be calibrated at such an angle of incidence that the mean value of ρ_a is obtained.

Magnesium oxide. A considerable amount of work has been carried out on magnesium oxide$^{(1)}$. It was tested in the form of a flat surface upon which the oxide from burning magnesium ribbon had been smoked. It was found that unless this oxide covering was thick the original polished copper surface absorbed an appreciable amount of light. To prevent this, the surface was silver-plated before depositing the oxide; then, provided that the oxide coating was thicker than about $\frac{1}{3}$ mm., the absorption by the backing was inappreciable. Under these conditions the value of the total reflection factor ρ for diffuse incidence was found to be reproducible within 0·5 per cent for successive fresh coatings of the oxide using the same stock of ribbon.

This surface is hardly suitable for use in the measurement of illumination on account of its fragility. With regard to its use as a substandard of reflection factor, it has been found that if it is protected from dust the total diffuse reflection factor ρ for diffuse incidence will remain constant for 3 weeks within 0·15 per cent. If left for a longer period there may be a change due to the formation of magnesium carbonate. This matter has not been fully investigated, though exposure of the surface to damp CO_2 for several periods of 12 hours produced no definite change. An analysis of old coatings of MgO gave 5 per cent of carbonate.

Filter paper. Samples of best white filter paper (Muncktell's No. 0) were used, ten pieces in one pack being used to form a suitable disk 9 cm. in diameter. For the measurement of illumination this material may be used where great precision is not required, as it is usually obtainable without difficulty. As regards its use as a substandard of reflection factor, it seems likely that with clean samples the value of ρ or ρ_a would not vary by as much as $\frac{1}{2}$ per cent, provided that at least nine sheets were used in the disk. It has also been found that prolonged exposure to ultra-violet radiation does not affect the value of the reflection factor.

Matt celluloid. Samples of matt celluloid, specially sand-blasted and flattened, were obtained from one of the manufacturers of illumination photometers. When this material is used in the measurement of illumination there is a difficulty in keeping the surface flat. Moreover, it tends to become discoloured with exposure to light, and it cannot be cleaned easily without its reflection characteristics being affected.

Magnesium oxychloride. Plates of magnesium oxychloride were prepared by Mr J. S. Preston of the National Physical Laboratory by mixing magnesium oxide with a strong solution of magnesium chloride and allowing the resultant paste to set between glass plates covered with a thin film of grease to prevent sticking.* The plates used were about 2–3 mm. thick and were mechanically strong. A matt surface could be produced by grinding with carborundum powder, though care had to be taken to soak the disks thoroughly in water beforehand to prevent them from sticking to the grinding plate. Two samples were made, sample A comprising MgO 10 g., $MgCl_2.6H_2O$ 10 g., while sample B comprised MgO 10 g. and $MgCl_2.6H_2O$ 7 g.

The values of the total diffuse reflection factor for diffuse incidence were for A 0·955 and for B 0·960.

This material seems to be suitable for use in the measurement of illumination, especially for street lighting when it is necessary to measure the illumination between two lamps due to both sources. There is, however, some difficulty in cleaning the disks, so that if they are used for outdoor work care must be taken to prevent dust and moisture from reaching them. As a substandard of reflection factor this material may be useful if it can be shown that there is no appreciable change in composition with time.

Blotting paper. Samples of good white blotting paper (Ford 428) 0·6 mm. thick were flattened and mounted. The use of this material in the measurement of illumination or as a substandard of reflection factor is inadvisable owing to probable variation from sample to sample. Further it was found that a distinct discoloration was produced by one week's exposure to ultra-violet radiation from a carbon arc.

Plaster of Paris. Samples of plaster of Paris were made up with as flat a surface as possible. This material is not suitable for illumination measurements or as a substandard of reflection factor on account of the difficulties encountered in cleaning.

Selectivity. Samples of magnesium oxide, magnesium oxychloride and of plaster of Paris were tested at three regions of the spectrum corresponding approximately to 6500, 5400 and 4700 A.

The values obtained are given below:

Total diffuse reflection factor

	White light	6500 A.	5400 A.	4700 A.
Magnesium oxide				
Before exposure to air	0·973	0·973	0·973	0·972
After exposure to air	0·972	0·973	0·971	0·966
Magnesium oxychloride	0·960	0·972	0·956	0·934
Plaster of Paris	0·953	0·972	0·952	0·964

REFERENCES

(1) Preston, J. S. *Trans. opt. Soc.* **31**, 15 (1929–30).
(2) Preston, J. S. *J. sci. Instrum.* **12**, 197 (1935).

DISCUSSION

J. S. Preston. This paper is particularly interesting to those concerned with photometry in that it gives extensive information about the properties of a number of materials of possible use as test plates, whose brightness by reflected light is commonly measured with some such visual photometer as the Macbeth illuminometer. It should be interesting and instructive to compare these properties with those of translucent diffusing materials such as may be used in front of a photocell in a photoelectric illumination-meter. An examination of such translucent materials and their brightness by transmitted light would seem to offer a useful field of research.

Two points have interested me in particular in the author's results. The first arises in consideration of figure 1, in which it is seen that curves 2 and 5 are alike in showing a high value of reflection factor for angles of view in the neighbourhood of the direction of incidence, rather than at the specular angle. It is curious that in both the test plates concerned magnesium oxide is present, and perhaps the author could say whether there may be anything inherent in the fine structure of the oxide which may account for the shape of the curves and for their similarity.

Secondly, on reference to table 1 it is seen that while the behaviour of magnesium oxychloride is similar to that of plaster of Paris for observations made in the plane of incidence, it is not so for observations in the plane at right angles, in which case the brightness variations are much greater for the plaster of Paris. It would be interesting to know whether the better behaviour of the oxychloride might be due to deeper penetration of the light into the body of the diffuser, in view of the general similarity of the two materials in other respects.

Author's reply. Mr Preston's remarks certainly suggest a partial explanation of the behaviour of plates 2 and 5. As he has himself had considerable experience in making up samples containing magnesium oxide it seems probable that he is right.

I also agree that the smaller variations in the apparent reflection factor of the magnesium oxychloride plate might be explained in the way he suggests.

THE MEASUREMENT OF DISTORTION IN A GAUGE PROJECTION LENS

By JOHN S. ANDERSON, M.A., D.Sc., F.Inst.P.,
Optics Division, The National Physical Laboratory

Received 24 *June* 1936. *Read* 3 *December* 1936

ABSTRACT. The distortion of a lens working at finite magnification is deduced from measurements of the variation of magnification of an object as the latter is traversed across the object field or the image field. It is found that as regards attainable accuracy there is little to choose between the alternative methods of measuring an enlarged image of an object in the object field or a reduced image of an object in the image field. The technique of the method as applied to a new gauge projection lens is described.

§ 1. INTRODUCTION

The measurement of distortion in a lens designed for use with parallel incident light is, comparatively speaking, a simple matter. The usual method is to employ a nodal slide bench and to measure the displacements of the image of a distant object as the lens is rotated about an axis, perpendicular to the lens axis, passing through the back nodal point. With lenses designed for use at other magnifications than zero the problem is simple in theory, but the experimental procedure is more complicated. If the object and image fields are both reasonably small the normal method is first to determine the conjugate planes corresponding to the magnification required, and then to move a suitable object, such as cross-lines, to definite positions in the object plane and measure the co-ordinates of the image positions in the image plane. The distortion at any point of the field is then the displacement of the image from the position it would occupy if the magnification given by the lens were constant over the whole of these conjugate planes. If, however, either the object or the image field is comparatively large, this direct method may be difficult to carry out, for a high degree of accuracy is usually required. In these circumstances it is simpler to deduce the magnitude of the distortion from measurements of the variation of the enlargement or reduction of an object of appreciable length placed at different positions in one of the conjugate planes. The length of the object can be chosen so that the size of the image comes within the range of the most accurate instruments available for the measurements.

It often happens that when this method is used there is no marked disparity in the size of object and image. For instance, measurements at magnifications of unity and one half are not uncommon, and one quarter occurs occasionally. For these ratios it is mainly a matter of convenience whether the object of constant length is placed in the plane where the size is the larger or the smaller of the two related values. When the magnification is large, some doubt may arise whether it is better to measure variations in size on an enlarged image, where they may be expected to be measurable without refined apparatus, or on the other hand to use a large object and make fine measurements over short lengths with apparatus of high accuracy. No evidence on this point, which is both of practical importance and of theoretical interest, appears to have been published. There also appears to be a lack of a description of the experimental procedure suitable for application in such circumstances. It is therefore thought that an account based on tests recently carried out at the National Physical Laboratory on a new gauge projection lens may be of some general interest. Incidentally the results obtained indicate the order of magnitude of the residual distortion to be expected in an optical system where the removal of distortion has received special consideration.

The lens submitted was a Taylor-Hobson profile projection lens (focal length 10 in.) designed to project accurate images of objects up to 4 in. in diameter at a linear magnification of 25. As the lens gave satisfactory definition over the whole field, the main object of the test was to measure the distortion. The question of enlargement or reduction arose immediately. This was decided in the first place by a special property of the lens. In most optical systems the central ray of the effective beam of light proceeding from a point at a distance from the axis is about equally inclined to the axis on both sides of the lens. In a system intended for projecting profiles, however, it is important to have the central rays on the side where the object is placed very approximately parallel to the axis over the whole effective field. This implies that in a test of this kind of system a travelling microscope can be used very conveniently for examining and measuring a reduced image, for the displacements do not exceed the range over which accurate measurements can be made on the screw of the instrument, and the microscope itself will be correctly disposed to receive the light from the lens under test symmetrically when it is held in its normal position perpendicular to the axis of the screw. These factors led to a calibration of the lens based on measurements of an image approximately one twenty-fifth the size of the object used. It was subsequently suggested that it would be of interest to compare the results obtained on reduction with those derived on enlargement, the way in which the lens is normally used. Two series of measurements were made under these conditions, and one of these is given here to show how the two methods of calibration compare with one another.

§ 2. EXPERIMENTAL PROCEDURE

The set-up adopted for the first test is shown diagrammatically in figure 1, where *AB* represents the plane in which the gauge or other object is placed, *CD* the plane of the screen on which the image is projected, and *OP* represents the optical axis of the lens. A scale *EF*, consisting of vertical black lines on a clear background, was mounted so that it could be traversed along a horizontal 6-ft. steel optical bench, the length of the scale being parallel to the bench. The end-lines of the scale were illuminated by two lamps *L*, *L* placed behind the plane *CD*. A travelling microscope *M* was mounted so that in all positions of its run it was focussed on the plane *AB*. Adjustments of height and level were made to ensure that the plane traversed by the axis of the microscope was the same as that traversed by a line on the object scale perpendicular to the scale divisions. Both the bench and the travelling microscope were adjusted so that the optical axis of the projection lens was normal to the directions of motion of the scale and the microscope. This was done in the following way. A small illuminated pinhole was placed at *O* and a plane mirror was held against the lens mount on the side remote from *O*. The pinhole was then adjusted until its reflected image, formed by light which had passed twice through the lens, coincided with it. The pinhole was then on the optical axis of the lens, assuming that the optical and mechanical axes were coincident. This assumption was verified by noting that, on removing the plane mirror and looking along the lens axis, the images of the pinhole formed by reflection in the surfaces of the component lenses were collinear. This series of images thus defined the optical axis of the lens. The mirror was then mounted parallel to the optical bench and the mirror and bench were moved together until the series of images reflected by the mirror was collinear with the original series. The bench and scale were therefore then normal to the optical axis of the lens. The process was repeated with the illuminated pinhole on the optical axis at the other side of the lens and the mirror mounted parallel to the slide of the travelling microscope. This ensured that the focal plane of the microscope, that is the object plane *AB*, was normal to the optical axis.

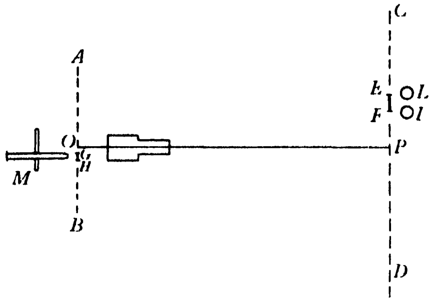

Figure 1.

A length of 100 mm. on the scale was used as the object *EF*, and the dimensions of its images *GH* in the plane *AB* were measured on the travelling microscope for different positions of the scale *EF* in the plane *CD*. Distances were measured from the points *O* and *P* where these planes were intersected by the optical axis of the lens.

The second test was effectively the first one reversed. Instead of measuring the reduced image of an object in the plane *CD*, the enlarged image of an object in the plane *AB* was measured for different positions of the object. A scale, consisting of transparent vertical lines on a dark background, was mounted so that it could be traversed in the object plane *AB*, and the base and carriage of the travelling microscope were set up behind the plane *CD*. As the object was magnified 25 times by the projection lens, it was found desirable to replace the microscope by a low-power magnifying lens focussed on a suitable scale. This change allowed measurements to be made even at the corners of the field without any alteration in the direction of the magnifier.

Adjustments similar to those of the first test were made to ensure that the optical axis of the projection lens was normal to the plane of motion of the object scale and to the plane traversed by the scale of the magnifier. A length of 4·064 mm. on the object scale was used and the dimensions of its images were measured on the screw of the travelling microscope for different positions of the scale in the object plane.

§ 3. OBSERVATIONS

The measurements made in the first test are given in table 1. The first column gives the distance of the centre of the scale from the axis of the system, the second column the length of the image, and the third column the difference between the length of the image and that of the image at the centre of the field.

Table 1. (Length of object 100·00 mm.)

Distance of centre of scale from axis (m.)	Length of image (mm.)	Difference (mm.)
−0·85	3·9850	−0·0035
−0·75	3·9855	−0·003
−0·65	3·9835	−0·005
−0·55	3·9845	−0·004
−0·45	3·9840	−0·0045
−0·35	3·9865	−0·002
−0·25	3·9875	−0·001
−0·15	3·9885	0
−0·05	3·9885	0
0	3·9885	0
+0·05	3·9880	−0·0005
+0·15	3·9880	−0·0005
+0·25	3·9875	−0·001
+0·35	3·9860	−0·0025
+0·45	3·9860	−0·0025
+0·55	3·9850	−0·0035
+0·65	3·9845	−0·004
+0·75	3·9860	−0·0025
+0·85	3·9895	+0·001

The measurements made in the second test are given in table 2. The first column gives the distance of the centre of the image of the scale in the image plane from the axis, the second column the length of the image, the third column the length of the object which would give at each part of the field an image equal in length to the image at the centre of the field, and the fourth column the difference between the length of the object and that of the object at the centre of the field. The results are thus put in the same form as those obtained in the first test.

Table 2. (Length of object 4·064 mm.)

Distance of centre of image of scale from axis (m.)	Length of image (mm.)	Length of object giving image of length 103·595 mm. (mm.)	Difference (mm.)
−0·845	103·595	4·064	0
−0·80	103·639	4·062	−0·002
−0·60	103·725	4·059	−0·005
−0·40	103·655	4·062	−0·002
−0·20	103·626	4·063	−0·001
0	103·595	4·064	0
+0·20	103·625	4·063	−0·001
+0·40	103·650	4·062	−0·002
+0·60	103·683	4·060	−0·004
+0·773	103·675	4·061	−0·003

§4. ANALYSIS OF OBSERVATIONS

To determine the reliability and consistency of the observations, a formula was fitted to the observations given in the first two columns of table 1 by the method of least squares. Preliminary examination of the figures indicated that there was no distinct evidence that more than the first two orders of distortional aberration were present, together with a uniform change of scale on proceeding from one end of the image to the other. This change of scale may be ascribed to a very slight inclination of the image plane to the position it should ideally occupy. The curve corresponding to the formula is plotted in figure 2, where the small circles ndicate the observations recorded in the second column of table 1. It will be seen that the fit is satisfactory. From this formula an expression was derived (as shown later) giving the distance of a point of the gauge or other object from the axis in terms of the corresponding distance (approximately twenty-five times greater) of the image point. If x denotes the distance of the object point from the axis in millimetres, and X the distance of the corresponding image point from the axis in metres, the equation obtained is

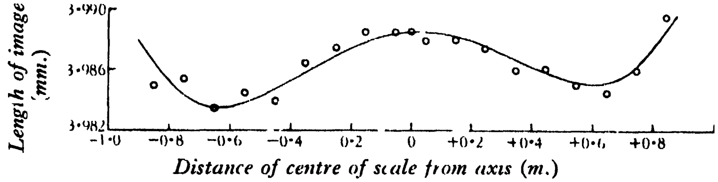

Figure 2.

$$x = 39{\cdot}88528X + 0{\cdot}05934X^2 - 0{\cdot}07187X^3 + 0{\cdot}05526X^5.$$

This formula was also used with the omission of the term involving X^2 (which corresponds to the error in normality of the object and image planes in the first test) to construct figure 3, on which are shown the observations given in table 2. It will be seen that these observations fit quite as well as those from which the formula was derived. The diagram (also other observations which are not recorded here) shows that we may regard this theoretical curve as a correct representation of the properties of the instrument. Particulars of the calibration computed from the formula just given are recorded in table 3.

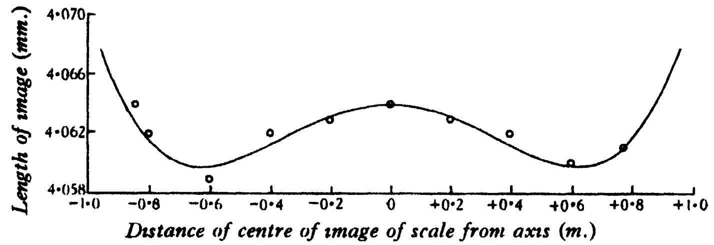

Figure 3.

Table 3

Object distance in image plane (m.)	Image distance in object plane (mm.)	Displacements towards axis represented by third and fifth order terms (mm.)	Magnification	Compensated* displacements (mm.)
0	0	0	0·0398853	0
0·05	1·99426	0·00001	0·0398851	−0·00093
0·10	3·98846	0·00007	0·0398846	−0·00180
0·15	5·98255	0·00024	0·0398837	−0·00257
0·20	7·97650	0·00056	0·0398825	−0·00318
0·25	9·97025	0·00107	0·0398810	−0·00360
0·30	11·96378	0·00181	0·0398793	−0·00380
0·35	13·95706	0·00279	0·0398773	−0·00375
0·40	15·95008	0·00403	0·0398752	−0·00344
0·45	17·94285	0·00553	0·0398730	−0·00288
0·50	19·93538	0·00726	0·0398708	−0·00209
0·55	21·92773	0·00918	0·0398686	−0·00110
0·60	23·91994	0·01123	0·0398666	+0·00001
0·65	25·91211	0·01333	0·0398648	+0·00118
0·70	27·90433	0·01536	0·0398633	+0·00228
0·75	29·89675	0·01721	0·0398623	+0·00319
0·80	31·88953	0·01869	0·0398619	+0·00374
0·85	33·88287	0·01962	0·0398622	+0·00373
0·90	35·87699	0·01976	0·0398633	+0·00294
0·95	37·87216	0·01886	0·0398654	+0·00110
1·00	39·86867	0·01661	0·0398687	−0·00208

* A positive sign indicates a displacement towards the axis of the system

The first column gives the distance of an object point on either side of the axis in metres, the second gives the corresponding image distance in millimetres, the third gives the displacements represented by the third and fifth order terms in the expression for x, and the fourth shows the variations in the magnification. From the third column it will be seen that the maximum displacement corresponding to the aberrational terms is almost 1/50 mm., that is 8 ten-thousandths of an inch.

Analysis of the distortion in this manner, though agreeing with that followed in theoretical discussions, does not correspond most closely to what is required in practice. It attaches very great importance to a quantity which in application is not by itself significant—the limit to which the magnification tends as the object considered shrinks to an infinitesimal length centered on the lens axis. Instead of this representation we require to know how far an image point may be displaced from its ideal position when we take for the magnification a mean value for the size of field considered. To determine this we write the equation between x and X in the alternative form

$$x = 39{\cdot}86659X + 0{\cdot}003345375\ [16X^5 - 20X^3 \times 1{\cdot}04046 + 5X \times (1{\cdot}04046)^2].$$

As X varies between the limits $\pm 1{\cdot}02003$ the quantity within the square brackets does not exceed the limits $\pm(1{\cdot}02003)^5$. If then we take as a reference standard the magnification 0·03986659 instead of the axial value 0·03988528, we find that the displacement of a point of the image from its computed position lies within the limits ±0·004 mm. or ±1·6 ten-thousandths of an inch. The calculated displacements corresponding to this magnification are given in the fifth column of table 3. The points for which the displacement is zero are

$$X = 0, \quad X = \pm 0{\cdot}59956, \quad X = \pm 0{\cdot}97011.$$

This suggests that the magnification could advantageously be determined by setting a symmetrically placed object 48 mm. in length to project as 1·2 m. on the screen.

The relation between the two methods of presenting the results of the calibration is shown in figure 4. The curved line shows the relation between the third and fifth order terms in the expression for x as ordinates and X as abscissae. By introducing a suitable first order term also, and thus changing the nominal magnification by a small amount, we change the axis from which ordinates are to be measured from the horizontal line, which is tangential to the curve at its centre, to the inclined straight line which cuts the curve in five points. These ordinates have the values described as compensated displacements in the fifth column of table 3.

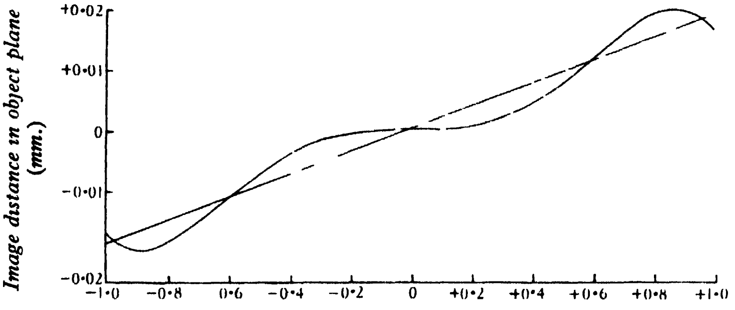

Figure 4.

§ 5. THEORY

It may be helpful to include a word on the way in which the equation for x is to be found. Suppose that an object of length $2L$ is measured, and its image is found to be of length $2l$ when the centre of the object has the co-ordinate X. If l is ascertained for several values of X, we can in a variety of ways, e.g. least squares, derive a formula

$$l=\sum_{r=0}^{m} a_r \frac{X^r}{r!},$$

which represents the observations satisfactorily. The formula we wish to construct is

$$x=f(X),$$

which is connected with the observations by the relation

$$2l=f(X+L)-f(X-L).$$

Evidently f is of order $m+1$ in X. If $f_n(X)$ denotes $\frac{d^n f(X)}{dX^n}$, and F_n stands for $f_n(0)$, we have

$$2l=\sum_{r=0}^{m} \frac{X^r}{r!} [f_r(L)-f_r(-L)],$$

so that

$$a_r=\sum_{n=0} \frac{L^{2n+1}}{(2n+1)!} F_{2n+r+1}.$$

The solution of these equations is

$$LF_{2n}=a_{2n-1}+\sum_{r=0} \frac{(-)^r (2^{2r}-2) L^{2r} B_r}{(2r)!} a_{2n+2r-1},$$

$$LF_{2n+1}=a_{2n}+\sum_{r=0} \frac{(-)^r (2^{2r}-2) L^{2r} B_r}{(2r)!} a_{2n+2r},$$

where B_r denotes the rth Bernoullian number. The first seven of these numbers are

$$B_1=\tfrac{1}{6}, \quad B_2=\tfrac{1}{30}, \quad B_3=\tfrac{1}{42}, \quad B_4=\tfrac{1}{30}, \quad B_5=\tfrac{5}{66}, \quad B_6=\tfrac{691}{2730}, \quad B_7=\tfrac{7}{6}.$$

It will be noted that F_0 is not determinable from this theory. It is an arbitrary constant of integration, and in this particular problem is given the value zero so that x and X vanish together.

§ 6. CONCLUSIONS

From the analysis of the observations it may be concluded that the projection lens will enable measurements to be made with an error not exceeding ± 0·004 mm., or ± 1·6 ten-thousandths of an inch as measured in the object plane. It also appears that, under the special conditions of this particular test at all events, there is little to choose, as regards attainable accuracy, between the two alternative methods of carrying out the test. The second set-up, in which an enlarged image of the object is formed and examined, should be the better one to employ, as the error in measuring the longer image is, with a given instrument, relatively less. It suffers, however, from the disadvantage that, as the travelling microscope has to be moved from point to point in the image field, it is more difficult to attain the requisite degree of rigidity than in the alternative method. A further disadvantage is that the test takes longer to carry out as longer distances have to be traversed by the travelling microscope. This difficulty could, of course, be overcome by using two magnifying lenses for setting on the end marks of the scale, one being fixed to the stationary portion of the travelling microscope and the other to the movable portion.

§ 7. ACKNOWLEDGEMENTS

I am indebted to Messrs Taylor, Taylor and Hobson, Ltd., of Leicester, the makers of the projection lens, for permission to publish these results, and to Mr T. Smith, M.A., F.R.S., for the analysis of the observations.

DISCUSSION

A. Warmisham. On behalf of Taylor, Taylor & Hobson, Ltd., I must acknowledge, with thanks, the excellent co-operation of the National Physical Laboratory in these measurements. Our practice is to measure distortion in the screen plane: we use a recently constructed projector in which the difficulties of this method, including those alluded to by the author, appear to have been overcome. The original design of the lens referred to in the paper is by Mr H. W. Lee.

J. W. Perry. In considering the term in X^2 in § 4 one should, I think, carefully distinguish what is primarily being tested—whether it is the formula of which the lens is a realization or the particular lens as an example of a symmetrical optical instrument. The term in X^2 is of course justifiably rejected when attention is confined to the lens formula; but when testing the lens, agreement of the nature indicated in figure 3 only establishes a presumption, strong in this instance, in favour of such rejection. Assuming the first cause for such a term to be removed by perfect *mechanical* adjustment of the testing-apparatus, two further cases may arise to cause such a term, namely (*a*) disagreement of direction of mechanical and optical axes, and (*b*) a constructional defect of asymmetry in the lens. The author has taken account of case (*a*) and I do not suggest that case (*b*) applies in this instance, but in considering the test as such the full interpretation of the X^2 term needs, I think, to be borne in mind when lenses of such a high degree of correction are being tested.

R. Kingslake. In connexion with the measurement of distortion in photographic lenses, I should like to ask the author how he would define distortion when coma is present. Is it to be regarded as a transverse displacement of the principal ray, or a displacement of some kind of centroid of the comatic light patch? The first is the usual theoretical conception of distortion, yet the second would appear more reasonable.

Author's reply. I agree with Mr Perry's remarks. In the lens under discussion there was, however, no indication of the presence of a defect of either type (*a*) or type (*b*).

With regard to Prof. Kingslake's remarks I think that Mr Smith is more qualified to supply an answer.

Mr T. Smith. As the author has appealed for my opinion on Prof. Kingslake's question, I may say that I think it important to recognize that what we do in experimental work may not correspond with any particularly simple theoretical case. If it were important to determine the theoretical setting with appreciable coma present, the best course would be to make a careful analysis of observations on an instrument of very accurately known construction.

THE STRUCTURE AND ELECTRICAL CONDUCTIVITY OF THIN FILMS OF INDIUM

By V. E. COSSLETT,
H. H. Wills Laboratory, University of Bristol

Received 1 *November* 1936. *Read* 11 *December* 1936

ABSTRACT. The high electrical resistance and negative temperature coefficient that thin films of indium, in common with other metals, exhibit when prepared under moderate vacuum conditions (10^{-4} to 10^{-5} mm.) and without exhaustive cleaning of the substrate, are shown by electron-diffraction methods to be in no way connected with the existence of any amorphous form of the metal. The lattice of freshly deposited films is found to correspond in form with that of the bulk metal but to have a spacing 0·7 per cent greater than that given by recent X-ray work, gold films here being taken as standards. With slowly deposited films the spacing increases and the axial ratio decreases with rise in temperature up to room conditions, and exposure to air carries this process further until a film showing a cubic indium lattice with spacing 3·4 per cent greater than the bulk metal is obtained. This change is accompanied by slow oxidation, the oxide lattice being 0·6 per cent larger than X-ray values indicate. It is suggested that the high resistance of these films is due to sorption of residual gas, and that the negative temperature coefficient is the result of desorption and resorption processes; changes in crystal-size with temperature are also noted and discussed. The change in lattice constants is ascribed to the action of gas within the lattice, possibly amounting to the production of intermediate stages in oxide-formation.

§ 1. INTRODUCTION

A NUMBER of experimenters have found during the past forty years that very thin films of metals, whether chemically deposited⁽¹⁾ or sputtered⁽²⁾ or produced by evaporation⁽³⁾, have a very high electrical resistivity. Whatever the metal, this resistivity is greater by many orders than that of the metal in bulk and consequently a number of workers concluded that the properties of metals are essentially modified when they are formed into thin films. This conclusion has been upset by the recent work of Lovell⁽⁴⁾ who has shown that the high resistivity is not a property of all states of the metal in thin films, but must be ascribed to disturbing factors not hitherto eliminated in their preparation. He succeeded in preparing stable films of rubidium, only a few atomic layers thick, that showed conductivities that departed from that of the bulk metal only by amounts to be expected on theoretical grounds. At the same time he was able to repeat some of the results obtained by previous investigators by particular treatment of the surface on which the films were formed.

Before the completion of his work a parallel investigation had been made by the writer on the structure of films of indium laid down by evaporation, the opportunity being taken to study their resistivity at the same time. It is unfortunate that the requirements of the determination of structure by electron-diffraction did not permit of the use of Lovell's high refinement. Nevertheless the nature of the structure of metallic films as normally obtained by evaporation in vacuo still remains a matter of interest and the following is a record of the results that have been obtained.

It is known(3, 5) that the degree of vacuum and cooling of the receiving surface have an important effect on the formation of the film, and that sputtered films may contain up to their own volume of gas(6). Care was taken, therefore, to control the rate of deposition of the film, the temperature of the surface, and the degree of vacuum. The best vacuum consistent with the structural determinations was 10^{-4} to 10^{-5} mm., and the evaporated metal was deposited on a surface cooled by liquid air. Indium was chosen as it lent itself to an accurate method of determining the density of the evaporated beam of metal atoms prior to condensation; uncertainty as to the thickness of the films formed has been one of the disadvantages in earlier work.

Some earlier investigators using X rays have claimed that thin metallic films are amorphous(7), others that they are of normal structure(8). Corresponding to these results, theories have been elaborated which ascribe the observed high resistances on the one hand to a special amorphous form of the metal(9), and on the other hand to lack of continuity in a normal crystalline structure, that is, to the formation of fissures or of isolated granules(10). The very much shorter wave-lengths employed in the electron beam, as compared with X rays, permit good spectra to be obtained with films less than 100 A. in thickness. Indeed, since Kirchner's work on evaporated films(11), several workers have obtained diffraction patterns from such films in the course of various investigations. Except in the case of antimony(12) these patterns have always corresponded to a normal structure.

No investigation had been made, however, of the structure of very thin films prepared under controlled conditions, nor of the possible correlation of structural change with electrical resistance. The results of the present work show that films of indium, from 10 to 100 atomic layers in thickness, have a crystal structure that differs only slightly from that of the pure bulk metal, and that slight structural changes can be observed to accompany changes in resistance under varying conditions. The relationship of these structural changes to the resistance-changes is not, however, in all respects clear.

§ 2. EXPERIMENTAL DETAILS

Preparation of the films. The indium was evaporated from a gun, *G*, of stainless steel supported on a quartz finger within which was the heating-coil and which was mounted eccentrically on a ground joint. The gun could thus be rotated to face either the cooled receiving surface or the filament of a collector which recorded the intensity of the evaporated beam. The collector *C* consisted of a tungsten strip, 1 mm. in width, facing a slit of length 1 cm. and width 1 cm. cut in a metal cylinder, 4 cm. long and 1 cm. in diameter, which surrounded it. The strip of tungsten, maintained at red heat, acted as collector filament at a positive potential of 240 V. with respect to the cylinder.

The action of this collector has been described fully elsewhere(13). Briefly, the metal atoms which strike the filament are positively ionized (the ionizing potential of indium being lower than the work function of tungsten oxide) and are then collected by the cylinder. The resultant current between filament and collector is a measure of the rate at which atoms are reaching the filament. When the beam-intensity has been determined in this way, the gun may be rotated to face the cooled receiving surface. For instance, a current of 3·6 A. in the heating-coil produced a beam-intensity of $6{\cdot}8 \, . \, 10^{13}$ atoms per cm² per second at the receiving surface, corresponding to a current of 1·0 μA. in the collector circuit. Assuming the metal to be uniformly distributed with normal structure in the film and every incident atom to stick when the surface is cooled with liquid air, this beam would deposit four atomic layers per minute. In order to test these assumptions, the optical density of a typical film was determined and the thickness was evaluated from the formula of Goldschmidt(14). The agreement between the two methods was satisfactory, but as the formulae for optical density are themselves only approximate, the values given in this work must be read as indicating an upper limit of film-thickness, liable to reduction if any considerable proportion of the atoms are reflected from the receiving surface.

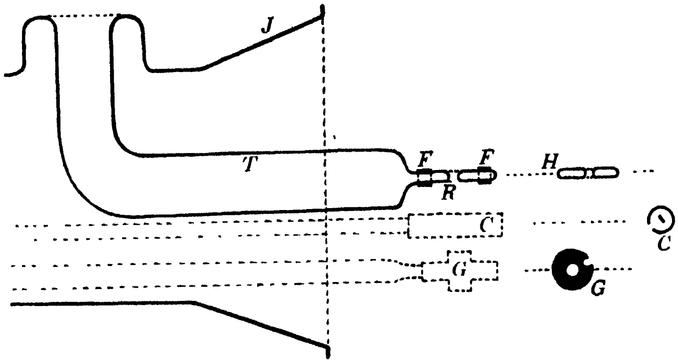

Figure 1. The evaporating system, showing the disposition of gun, collector and receiving surface *R*.

The end of a glass tube *T* was drawn out to a flat hollow tongue *H*, 1 × 2 cm., to which the receiving surface was secured by two clips of copper strip with screw fastenings, *F*, *F*. Liquid air within the tube served to cool the surface, the temperature of which was measured with a thermocouple. A small hole was drawn in the centre of the glass tongue to allow the electron beam free passage. When the receiving surface was easy to handle, for instance in glass or bakelite strips, silver was deposited at each end of it to make good contact with the copper strips. With cellulose film as substrate, two pieces of copper gauze were secured by the clips and the film was stretched between the gauzes. The cellulose film was from 100 to 300 A. thick, so that the deposited metal should overlap on to the gauze without discontinuity. The resistance of the metal film was measured directly, leads running from the copper clips to an external circuit.

The liquid-air vessel and the ground joints for the rotation of the gun and collector were all mounted on a large ground-glass joint *J* which rotated about a horizontal axis at the side of the electron-diffraction apparatus. This allowed the position of the receiving surface to be varied: during deposition it was at an angle of 45° to the horizontal, and during diffraction it was horizontal so that the electron beam could pass normally through the film.

Electron-diffraction apparatus. The apparatus used for producing the electron beam and registering the diffraction patterns was a modified form of that previously described (15), the main difference being the introduction of a focusing coil. The apparatus could be evacuated by fast pumps down to 10^{-5} mm., the electron beam entering it through a limiting diaphragm of diameter 0·1 mm.; a separate pumping system was used for the discharge tube which functioned with a cold cathode.

By using a camera box it was possible to take five photographs in succession without disturbing the vacuum. Gold films were used for calibrating purposes, the voltages employed being between 40 and 50 kV.

§ 3. RESULTS

Determination of structure. Some seventy diffraction patterns were obtained from films of indium deposited on cellulose under different conditions; in each case the diameters of the rings were measured and the lattice constants evaluated in the usual way. Significant changes in ring-breadth and intensity, as well as in lattice constant, were observed in patterns obtained from films subjected to varying treatments.

Photographs taken immediately after deposition of a film at liquid-air temperatures showed a ring pattern agreeing in relative intensities with X-ray work on bulk indium, but giving a larger lattice spacing. The structure proved to be face-centred tetragonal for which $a = 4{\cdot}61 \pm 0{\cdot}005$ A. and the axial ratio $c/a = 1{\cdot}07 \pm 0{\cdot}005$. The early X-ray work of Hull & Davey (16) gave values of 4·58 A. and 1·06, and three recent determinations (17) agree in giving 4·583 A. and 1·077 for bulk indium at room temperature. During the preparation of this paper Riedmiller (18) has published results for nickel, gold and silver films, which also show a slightly increased lattice spacing of the same order of magnitude.

On allowing the indium films to rise to room temperature a slight change, outside the experimental error, occurred in the pattern, without alteration in the relative intensities of the rings; the constants now found were 4·62 A. and 1·06. Typical photographs taken at liquid-air and room temperatures are reproduced in the plate at A and B, and the spacings calculated from individual rings are given in the table.

Accompanying this change in lattice, a change in crystal-size was indicated by the broadening of the individual rings. The ring-breadth at half intensity was 0·16 mm. at liquid-air and increased to 0·25 mm. at room temperature. Brill (19) has derived the following expression relating crystal-size with ring-breadth in electron-diffraction patterns:

$$t = \frac{\lambda}{B' \cos \frac{1}{2}\theta},$$

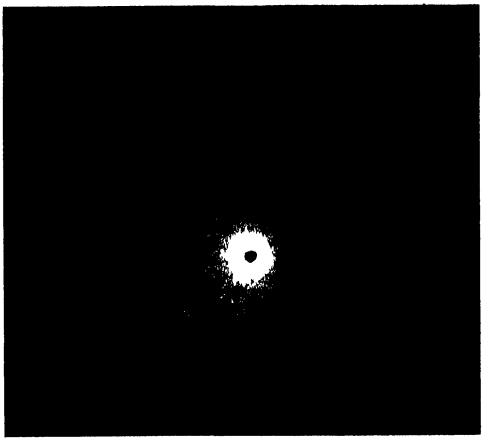

A. Indium film (20 layers) at liquid-air temperature

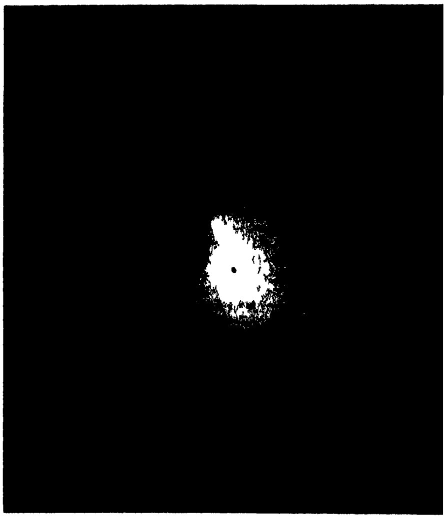

B Indium film (20 layers) at room temperature.

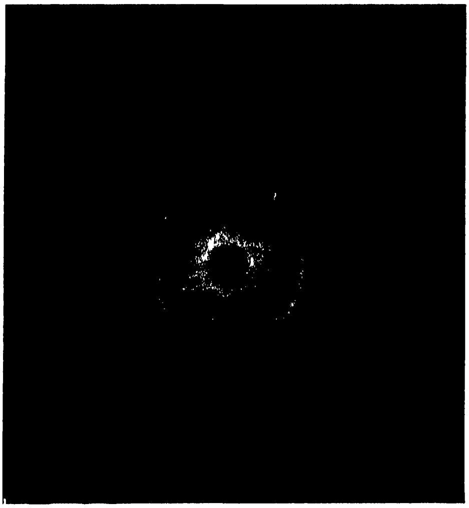

C Indium film (30 layers) partially oxidized

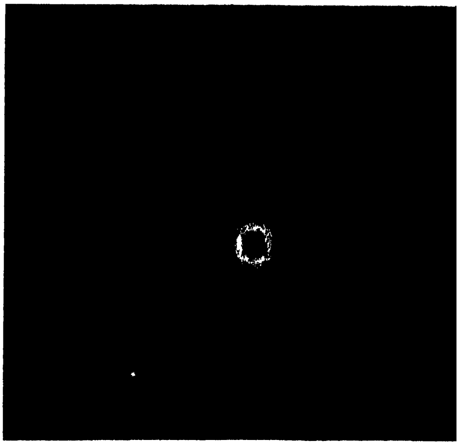

D Indium film (44 layers) almost completely

Table

Indices of ring	At liquid-air temperature		At room temperature	
	a (A.) ($c/a = 1{\cdot}06$)	*a* (A.) ($c/a = 1{\cdot}07$)	*a* (A.) ($c/a = 1{\cdot}06$)	*a* (A.) ($c/a = 1{\cdot}07$)
111	$4{\cdot}60_5$	4·59	4·61	$4{\cdot}59_5$
002	4·65	$4{\cdot}60_5$	4·63	$4{\cdot}58_5$
200	4·61	4·61	4·62	4·62
202	4·63	4·61	4·62	4·60
220	4·61	4·61	4·62	4·62
300	4·62	4·62	—	—
113	4·65	$4{\cdot}61_5$	4·62	$4{\cdot}58_5$
311	4·62	$4{\cdot}61_5$	4·62	$4{\cdot}61_5$
222	$4{\cdot}62_5$	4·61	$4{\cdot}62_5$	4·61
313 330	$4{\cdot}62_5$	$4{\cdot}60_5$	4·61	4·59
331	$4{\cdot}61_5$	4·61	—	—
402 420	$4{\cdot}61_5$	$4{\cdot}61_5$	$4{\cdot}62_5$	4·62
224	$4{\cdot}63_5$	4·61	—	—
422	4·62	$4{\cdot}61_5$	4·62	$4{\cdot}61_5$

where B' is the ideal angular breadth of a ring, λ is the wave-length, $\theta/2$ is the angle of incidence of the electron beam, and t is the mean thickness of the individual crystallites diffracting the beam The formula is derived for substances crystallizing in the cubic system, so that the crystallites are regarded as cubes of mean edge t. As indium has an axial ratio (1·077) very near to unity, this formula can be applied to the present case without serious error. The ideal breadth B' is related to the measured ring-breadth at half intensity B by

$$B = B' + b,$$

where b is the angular width of the diffracted beam itself.

In this way it is possible to calculate the mean size of the individual particles comprising the indium film. From this calculation an interesting result emerged. Taking a film which, assuming a uniform distribution of atoms, had a thickness of 104 A. (40 layers of indium atoms) the mean particle-size immediately after deposition at liquid-air temperature was found to be 210 A. In other words, considerable aggregation must have occurred during the formation of the film, so that the electron beam encounters a field covered with isolated crystallites. At this temperature it was only possible to get good diffraction patterns through certain parts of the film; the remainder of it must have been covered either with crystallites too small (less than 10 A.) to give a pattern that could be distinguished from the diffuse scattering due to the cellulose substrate, or with non-crystalline arrangements of atoms. On raising the film to room temperature the particle-size dropped to 90 A. and this was accompanied by a great increase in the area over which a good diffraction pattern could be obtained. The rise in temperature must have caused a spreading of the larger particles or the formation of new crystallites of medium size from previously amorphous atoms or very small aggregates. The increased mobility of the atoms in the surface would facilitate this process. It should be remarked that these changes in crystal-size are irreversible: cooling from room temperature back to liquid-air temperature caused no appreciable change in the ring pattern.

Similar results were obtained from indium films of various thicknesses between 10 and 40 layers; the film-thickness had no appreciable effect upon either the lattice constants or the relative intensities of the rings. In no case was any preferred orientation of atomic planes in the film evident at any temperature.

Rather different results were obtained, however, from films formed by very slow deposition. At liquid-air temperatures these give ring patterns with the same constants as rapidly deposited films: $a=4{\cdot}61$ A. and $c/a=1{\cdot}07$. On raising them to room temperature the pattern changed and approximated to a face-centred cubic structure, the constants being $a=4{\cdot}69$ A. and $c/a=1{\cdot}02$. On admitting a small amount of air, leaving it in contact with the film for some hours and then evacuating again, the structure proved to be $a=4{\cdot}72$ A. and $c/a=1{\cdot}01$, and oxide rings appeared faintly. A film exposed to air for a week showed a cubic structure with $a=4{\cdot}74$ A., and oxide rings of medium strength.

This change towards a cubic structure would appear, therefore, to be connected with oxide-formation, and it is significant that In_2O_3 has a cubic structure in which the indium atoms occupy positions corresponding to a face-centred cubic lattice with an edge of 5·06 A., as compared with the face-centred tetragonal structure, for which $a=4{\cdot}58$ A., of the pure bulk metal. When the films are deposited rapidly this marked change is not observed, nor are the films so readily oxidized. But the slight change, from 4·61 A. and 1·07 to 4·62 A. and 1·06, in raising such films from liquid-air to room temperatures is in the same direction as that in slowly deposited films. On exposure to air the former undergo a further change to 4·67 A. and 1·03. These facts suggest that residual gas interferes with film-formation when it takes place slowly, but not appreciably with rapid formation.

When the oxidation of rapidly deposited films is allowed to proceed to an observable extent, it is found to have little or no effect on the structure of the still unoxidized metal remaining in the film. C in the Plate shows a pattern obtained in this way in which the metal and oxide rings are of similar intensity; the metal constants are here 4·63 A. and 1·06, and the oxide cube edge is 10·16 A., as compared with the value of 10·12 A. given by Wyckoff(20). In such cases, the oxide must be formed as a surface layer on the large indium crystals that are formed by rapid deposition. Continued oxidation of indium films produced sharp patterns (D in the plate) giving a slightly larger value for the oxide structure, 10·18 A.

Resistivity-measurements. In view of Lovell's results it is not possible to deduce much from the resistivity-measurements made in the present work under conditions which, though definitely under better control than those of many previous experiments, were still far from ideal owing mainly to the incomplete elimination of gas. At the same time no previous experiments have been recorded for indium, and moreover the number of atoms laid down in each film was accurately known in the experiments described.

Results have been obtained which are in several respects similar to those of earlier workers with other metals. (1) According to the conditions of deposition and thickness the resistivity of the films varies from 10^4 to 10^{-1}, whereas indium in bulk gives the value $8{\cdot}4\times10^{-6}$. (2) The films show a fall in resistance when raised in temperature, part of the fall being irreversible. Thus figure 2, curve 1, gives the change in resistance of a fresh film deposited at liquid-air temperature and then raised to room temperature in situ. On cooling the film again to the same temperature, curve 2 is followed. (3) There is however another effect superposed and opposite in sign. At any temperature the films age slowly with time, with a gradual rise in resistance; thus on reheating of the film, curve 3 results. In form curve 3 does not depart very seriously from curve 2, and this suggests a slow ageing of the film which otherwise changes its resistance more or less reversibly with temperature. Lovell associates a similar but more rapid change that occurs in thinner films with the existence of gas films on the substrate; when these films were reduced to a minimum, he was able to produce films stable with time. In the present conditions, the slow oxidation of the film, which the diffraction results have demonstrated, must play an important part also in increasing the resistance. (4) These films, then, can be considered as having a negative temperature coefficient. Using films of different thickness it was found that the mean temperature coefficient decreased with decreasing resistance of the film, as shown in figure 3. In this graph have been plotted the results for all films investigated, prepared under whatever conditions, in order to show the general relationship between coefficient and resistance$^{(21)}$; in given conditions, the resistance will be proportional to the thickness of the film. (5) The higher the working vacuum the lower was the resistivity of the film formed. When the residual pressure was 10^{-3} mm. the first measurable conductivity appeared at a thickness of 160 layers, whereas at 10^{-5} mm. a film of 30 layers already conducted. It must be remembered that at a pressure

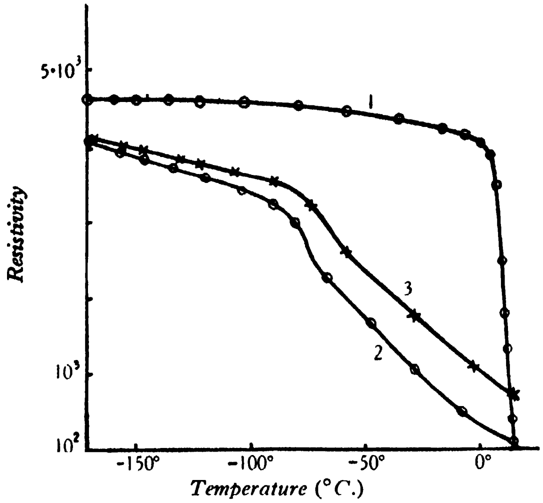

Figure 2. Change in resistivity of film (600 A. thick) with temperature.

even of 10^{-5} mm. the number of gas atoms bombarding the surface considerably exceeds the number of metal atoms which arrive there during deposition. If after deposition the pressure was changed from 10^{-5} mm. to atmospheric, the resistance rose by as much as tenfold in some cases. This was probably mostly due to oxidation, because the effect was greater in oxygen than in air. Moreover evidence of oxide-formation has been given above in the determinations of structure. But the fact that there is still some residual effect in nitrogen suggests that sorption of additional gas does also play some part in the phenomenon. (6) When the indium was deposited in turn on substrates of varying expansibilities, no significant changes were observed in the value of the temperature coefficient. The substrates used and their coefficients of expansion were: glass ($8{\cdot}5 \times 10^{-6}$), bakelite ($2{\cdot}8 \times 10^{-5}$), ice ($2{\cdot}7 \times 10^{-5}$), cellulose ($1{\cdot}4 \times 10^{-4}$) and paraffin ($1{\cdot}1 \times 10^{-4}$), as compared with that of indium in bulk ($2{\cdot}5 \times 10^{-5}$). It appeared, therefore, that the difference in expansibility between film and substrate had no appreciable effect on the change in resistance of the film with temperature.

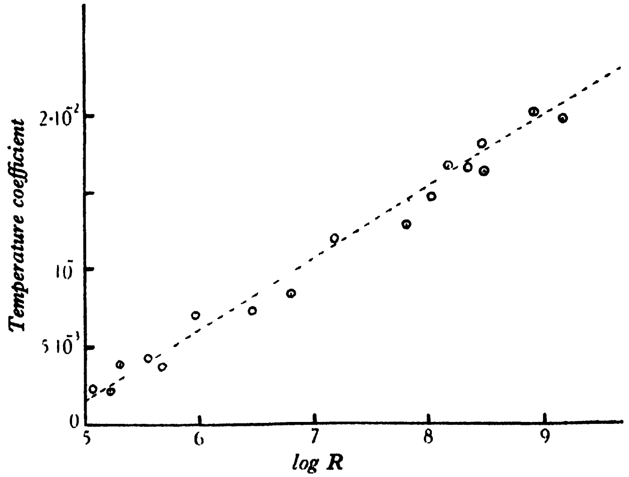

Figure 3. Change in temperature coefficient of films with resistance, independent of conditions of deposition.

§ 4. DISCUSSION

The behaviour of thin metallic films with temperature change has given rise to much discussion in the literature on their resistance. The negative temperature coefficient appears to be a property of such films prepared in the presence of appreciable residual gas, as is also their high resistivity. These characteristics are evidence that the films cannot be continuous. They differ, therefore, from the films which Lovell obtained that are quite stable, although only a few atomic layers in thickness, having the positive coefficient to be expected of a coherent uniform metallic surface.

At the same time, the structure determinations show that the crystallites which compose the film have a lattice which is only slightly different from that of the bulk metal. We must conclude therefore that a freshly deposited film is made up of a number of isolated crystalline particles, and that this island formation is responsible for the high resistivity. With rise in temperature it has been shown that a decrease in mean particle-size takes place, not at the expense of the large crystallites first formed, but by the formation of particles of medium size from those which were previously too small to give a sharp diffraction pattern. A similar process of aggregation has been observed by Andrade(22) in gold and silver films at a much higher temperature. It seems reasonable to associate this recrystallization with the irreversible part of the resistance decrease which occurs when a film is raised initially from liquid-air to room temperature.

With regard to the negative temperature coefficient, it is difficult to explain it as some have attempted to do(3, 10) by simple and regular making and breaking of bridges between crystalline island formations. Such a process could not occur to any large extent unless assisted by differing expansibilities of film and substrate. Bartlett(10), indeed, suggested that such a process gave rise to the negative temperature effect. But the present work has shown that substrates of very different expansibilities produce no appreciable variation in the coefficient. The making and breaking of contacts between different parts of the film that may take place in this way must therefore make little difference to the total resistance.

The influence of residual gas upon the film resistance has been demonstrated and suggests that this may be responsible also for the anomalous temperature coefficient. In particular, the fact that nitrogen as well as oxygen affects the film points to sorption as well as oxidation occurring. It has been shown(6) that sputtered films may contain occluded gas equal in volume to the metal itself. In the present work, the vacuum was much higher, but the deposition temperature much lower than in sputtering experiments. It is possible, therefore, that gas is absorbed in the film during formation and consequently increases the resistance, even if direct oxidation is negligible. As the temperature rises, desorption of the gas would result in a fall in the resistance. On again decreasing the temperature, resorption would occur and give rise to the reversible effect observed.

This explanation receives support from the results of the present electron-diffraction work and from a similar investigation recently made by Riedmiller(18) with films of nickel, silver and gold. He found that evaporated nickel films had a density lower by 18 per cent than that of the bulk metal and a lattice constant 1·6 per cent greater. This increase he ascribed to absorption of gas in the lattice itself; the major part of the density-change he supposed to be due to sorption of gas in a loose agglomerate of crystallites. These films were deposited at room temperature; at the very much lower deposition temperature of the present work more extensive absorption is to be expected. The determination of the structure of freshly deposited indium films (above) showed that the lattice constant is about 0·7 per cent greater than that of the bulk metal. There must, therefore, be less gas in the lattice itself than in Riedmiller's experiments, which may be bound up with the fact that the indium crystallites were ten times larger than his nickel ones. He found also that the gold films showed a 0·8-per-cent and the silver a 1-per-cent increase in size over the normal lattice. Exposure of the nickel films to air increased the discrepancy from 1·2 to 1·4 per cent, and to hydrogen up to 1·8 per cent; the nickel oxide formed had a lattice constant 2·4 per cent greater than normal. No observations of change in lattice with temperature are reported.

In the present work, the increases in spacing are of the same order; 0·7 per cent for indium and 0·6 per cent for indium oxide in rapidly deposited films, which show little variation with temperature. Films that are slowly deposited show a rapid increase in size of lattice with temperature-rise: at room temperature it is 2·4 per cent greater than normal and this increases to 3·1 per cent on short exposure to air, faint oxide rings appearing. Rapidly deposited films show a total increase of 2·0 per cent after exposure to air. In both cases the axial ratio changes also towards a more nearly cubic structure; the longest oxidation allowed produced a film of cubic structure, within the 1-per-cent error of estimation, with an indium lattice 3·4 per cent greater than normal. The drift towards the cubic structure of indium oxide, and the ready appearance of oxide rings, leave no doubt that these changes in lattice constant arise from interference of gas in the crystal lattice, as distinct from sorption into a porous film. It may be that sorption of gas or oxide-formation in the surface layers of small crystallites causes distortion of the inner metal lattice. On the other hand, it may be that intermediate stages in the formation of the oxide are being observed, oxygen first entering the lattice and modifying the metallic structure before actual formation of indium oxide crystals takes place. The largest indium spacing observed in a partially oxidized film was 4·74 A., whereas the separation of the indium atoms in the normal oxide is 5·06 A.

Whatever the process occurring, it has been established that the metal lattice becomes more nearly cubic as oxidation proceeds. A small change in this direction was observed on raising rapidly deposited films to room temperature, even when the vacuum was maintained at 10^{-5} mm. and no sign of oxide rings appeared. Hence residual gas is affecting the film structure, even at this low pressure, and this process must play a part in the slow ageing of the films—the drift towards high resistance that continues even in high vacua. In order to investigate adequately the suggested influence of gas in this way and on the negative temperature coefficient, it would be necessary to work with a very much higher vacuum than that obtainable in an electron-diffraction apparatus of the type here employed. In such conditions it would be possible to obtain films of normal resistivity and temperature coefficient, as Lovell has done with rubidium and caesium, and to investigate their structure.

5. ACKNOWLEDGEMENTS

The author wishes to express his indebtedness to Prof. A. M. Tyndall for affording the facilities that made this work possible and for his help and interest in it; and to Dr E. T. S. Appleyard for valuable advice and discussion.

REFERENCES

(1) Stone, *Phys. Rev.* **6**, 1 (1898); Oberbeck, *Ann. Phys.*, Lpz., **47**, 353 (1892); and others.

(2) Longden, *Phys. Rev.* **9**, 40 (1900); Patterson, *Phil. Mag.* (6), **4**, 652 (1902).

(3) Reinders and Hamburger, *Ann. Phys.*, Lpz., **10**, 649, 790, 905 (1931); **11**, 40 (1931); Suhrmann and Barth, *Phys. Z.* **36**, 843 (1935). Summaries of earlier work: Riede, *Z. Phys.* **28**, 177 (1924); Bartlett, *Phil. Mag.* (7), **5**, 848 (1928).

(4) Lovell, *Nature*, Lond., **137**, 493 (1936); *Proc. roy. Soc.* (in the Press).

(5) Cockcroft, *Proc. Roy. Soc.* A, **119**, 293 (1928).

(6) Büssem and Gross, *Z. Phys.* **86**, 135 (1933); **87**, 778 (1934).

(7) Ingersoll and Devinney, *Phys. Rev.* **26**, 86 (1925); Kahler, *Phys. Rev.* **18**, 210 (1921); and Kramers, ref. (9) (below).

(8) Steinberg, *Phys. Rev.* **21**, 22 (1923); Dembinska, *Z. Phys.* **54**, 46 (1929).

(9) Féry, J. *Phys. Radium*, **9**, 38 (1928); Kramers, *Ann. Phys.*, Lpz., **19**, 37 (1934); and Perucca, *Ann. Phys.*, Lpz., **4**, 252 (1930); *Z. Phys.* **91**, 660 (1934).

(10) Cf. Bartlett (ref. 3), Reinders and Hamburger (ref. 3), and Swann, *Phil. Mag.* (6), **28**, 467 (1914).

(11) Kirchner, *Z. Phys.* **76**, 576 (1932).

(12) Prins, *Z. Krystallogr.* **86**, 301 (1933); *Nature*, Lond., **131**, 760 (1933).

(13) Powell and Brata, *Proc. roy. Soc.* A, **141**, 463 (1933).

(14) Goldschmidt, *Ann. Phys.*, Lpz., **82**, 947 (1927).

(15) Cosslett, *Trans. Faraday Soc.* **30**, 981 (1934).

(16) Hull and Davey, *Phys. Rev.* **17**, 549, 571 (1921).

(17) Wyckoff, *Structure of Crystals* (Supplement 1930–4), p. 10.

(18) Riedmiller, *Z. Phys.* **102**, 408 (1936).

(19) Brill, *Kolloidzschr.* **69**, 301 (1934); *Z. Krystallogr.* **87**, 275 (1934).

(20) Wyckoff, *Structure of Crystals* (2nd ed.), p. 254.

(21) Cf. Deaglio, *Z. Phys.* **91**, 657 (1934).

(22) Andrade, *Trans. Faraday Soc.* **31**, 1137 (1935); Andrade and Martindale, *Philos. Trans.* **235**, 69 (1935).

DISCUSSION

Dr L. Hartshorn. I am particularly interested in the mechanism of electrical conductivity in these thin films. It seems clear from the author's experiments that the low conductivity and abnormal temperature coefficients are associated in some way with discontinuities in the film and the inclusion of gas molecules. It is however by no means obvious why the adsorption of gas molecules should cause a decrease of conductance, and why subsequent desorption should cause an increase. Can the author give us any idea of the mechanism of these changes? Is the electrical conductivity of an adsorbed layer of gas molecules greater or less than that of the space left when it is desorbed? Again, why should an increase of particle-size be associated with an increase of conductance? Is the change of particle-size limited to two dimensions?

I am puzzled by the statement that sputtered films may contain up to their own volume of gas. How is this volume of gas supposed to be measured? Does it mean that the number of gas molecules is of the same order as the number of atoms of the metal?

It is very curious that the theory of island-formation, the first and most obvious of the explanations advanced to explain the low electrical conductance of thin metal films, should be substantiated after the publication of so much apparent evidence to the contrary. The resistance of a discontinuous film should be different for alternating and direct currents, and we should certainly not expect to find a low electrical conductance at very high frequencies if the constituent particles possess normal properties. Again it has been claimed that the abnormal resistance vanishes at a temperature characteristic of the metal and not of the method of preparation of the film. Must we dismiss the evidence of this character as inadequate, or is it possible that the films of platinum, antimony, silver, etc. used by previous workers behave quite differently from those of indium, which does not appear to have been used previously for such work?

Mr L. R. G. TRELOAR. In connexion with the measurement of the beam-intensity by the ionization of the indium atoms by hot tungsten oxide, I should like to know whether the author is aware of any published data on the work function of the latter material. It also occurred to me that, at the filament-temperatures indicated in the paper, there might be some tendency for an appreciable proportion of the indium atoms to remain adsorbed on the oxide surface. Such an effect, if it occurred, might very well reduce the work function to an extent sufficient to cause the proportion of indium atoms ionized to fall below 100 per cent, thus giving an incorrect value of beam-intensity. It would be interesting to know whether the author has had any difficulties of this kind.

Mr D. A. WRIGHT. Although the author has been concerned primarily with the behaviour of films deposited on a cellulose substrate, I note that some study has been made of other substrates. I am particularly interested in the behaviour of thin metallic films on glass, and should like to know of the author's experience with this material, with respect to both the structure and the conductivity of the films. Has he observed crystal aggregates, and if so are their dimensions under corresponding conditions similar to those of the aggregates on cellulose? I note that the temperature coefficient of conductivity has been found to be independent of the substrate. Is this true of the actual value of the conductivity, and more particularly of the details of the irreversible ageing process? If any modification has been noticed in the case of glass, has any study been made of the variations produced by different methods of preparing the glass surfaces, e.g. by different methods of washing or by different heat treatments? I think the state of the surface will be very important, since it will certainly modify the sorption of gas upon it. It may also influence the possible production of gas from the body of the substrate, while the possibility of chemical action between the substrate and metal must not be overlooked. The state of the surface must I think be added to the other factors discussed, in seeking to explain the large variations among the results obtained by different workers.

AUTHOR'S reply. Referring to Dr Hartshorn's remarks on the mechanism of conductivity in these thin films, I must make it clear that I do not advance any single, simple explanation of this mechanism; island-formation alone cannot account for the properties of the films. The absorption of gas and the influence of surface conditions (as shown by Lovell) must enter into any complete explanation. So that these disturbing factors would not allow of a simple deduction from a.-c. measurements of resistance, although it would be interesting to have such results. The irreversible increase in particle size must be associated with improved means of communication across the film, especially if it occurs at the expense of small semi-crystalline or colloidal aggregates, as Kirchner's work suggests. In any case, it is a fact that increase in temperature immediately after film-formation results in a large irreversible increase in conductivity and in crystal size; it seems probable, *a priori*, that this latter change would be mainly two-dimensional.

The transition temperature, reported by Kramers, was not observed in this work or by Lovell, and the recent work of Suhrmann and Barth with other metals at lower temperatures and under better vacuum conditions failed to find any such effect; it seems probable that it was due to some adventitious factor in Kramers's experimental conditions. In reference to the results of Büssem and Gross, the statement that "sputtered films may contain up to their own volume of gas" means that the number of gas atoms in the films may be equal to the number of metal atoms.

With reference to Mr Treloar's remarks: the collector system was found to function perfectly and there was no evidence of accumulation of indium atoms on the surface at rates of deposition up to ten atomic layers per minute. The system has been in use in this laboratory for some time, and is fully described by Powell and Mercer, who give the electronic work function of the tungsten oxide surface as 6·13 volts, compared with an ionization potential of 5·76 volts for indium.

All the electron-diffraction results in this work were obtained from indium films deposited on collodion films, so that I am unable to give Mr Wright any information as to the structure of films deposited on glass. It was not possible to obtain other substrates sufficiently thin to transmit electrons at the voltage used, and no attempt was made to get reflection patterns from metal films on thick substrates. So far as the conductivity is concerned, no significant difference was found between films deposited on collodion, glass, or other substrates; this would suggest that there are no important structural differences on substrates not carefully cleaned. On specially cleaned surfaces other results might be expected. As reported, Lovell has shown that extraordinarily careful cleaning of a glass substrate is necessary in order to get films of nearly normal conductivity; it would be very interesting to investigate the structure of such films, by reflection methods in a high vacuum apparatus. I agree that the surface state may be all important in determining the structure of the deposited film.

THE EFFECT OF ORIENTATION ON STRESSES IN SINGLE CRYSTALS AND OF RANDOM ORIENTATION ON STRENGTH OF POLYCRYSTALLINE AGGREGATES

By H. L. COX, B.A., and
D. G. SOPWITH, B.Sc.Tech., A.M.I.Mech.E.,
The Engineering Department, National Physical Laboratory

Received 21 *October* 1936. *Read in title* 11 *December* 1936

ABSTRACT. A method of tabulating resolved shear stresses for any type of slip system has been devised. Diagrams of maximum resolved shear stress for torsion and tension as functions of orientation have been drawn both for the case of aluminium, with slip plane of type (111) and slip direction of type (110), and for the case of iron with slip direction of type (111) and any slip plane. Similar diagrams of harmonic mean stress in torsion also have been drawn. The effect of different criteria of failure in indicating the failure of polycrystalline specimens has been investigated. If elastic failure of polycrystalline specimens is determined entirely by the maximum resolved shear stress developed locally, the ratio of the yield in torsion to the yield in tension should be 0·500; whereas if elastic failure is determined by the complete yield of all the crystals of the specimen, the value of this ratio should be about 0·577.

§ 1. INTRODUCTION

The results of numerous experiments on single crystals of several different metals have shown that plastic deformation under stress often occurs entirely by slip along certain crystallographic planes in certain crystallographic directions$^{(1, 2)}$. For instance, in aluminium and other metals conforming to the face-centred cubic lattice, the possible slip planes are the four octahedral planes, and in each slip plane the intersections with the other three octahedral planes are possible slip directions. Any one of the possible combinations of slip plane and slip direction will for convenience be termed a *slip-plane-direction.*

Now, in the majority of metals, all the slip-plane-directions are crystallographically identical, so that if slip under stress occurs upon any one of them in preference to the others, the reason for this preference must be sought in the stress conditions imposed. By measurement of the deformation of single crystals of aluminium produced by static tensile stresses, Prof. G. I. Taylor$^{(2)}$ was able to show that in general slip occurred entirely in one slip-plane-direction and that the particular slip-plane-direction concerned was that for which the shear stress resolved on the slip plane and along the slip direction was a maximum. The shear stress thus associated with each slip-plane-direction will for convenience be termed a ***resolved shear stress***. Other experiments on single crystals of aluminium(3) and other metals(4) under many different types(5, 6) of stress system have shown, practically without exception, that deformation always occurs by slip in the slip-plane-direction subjected to the greatest resolved shear stress. Moreover, recent tests under fatigue stresses on specimens of aluminium consisting of more than one crystal(7) have indicated both that the effect of the intercrystalline boundaries on the stress-distribution is extremely slight and that the deformation of the individual crystals is again determined by the values of the resolved shear stresses. The determination of the values of the resolved shear stresses is therefore an essential part of any investigation of the strength of metals in relation to their crystalline structure. It is the purpose of this paper to discuss the methods by which these stresses may be determined and to state certain general conclusions that may be drawn.

§ 2. DETERMINATION OF THE PRINCIPAL STRESSES

The distribution of stress set up in any specimen by the application to its boundaries of known forces and displacements may be calculated by the theory of elasticity, by means of the relations between stress and strain appropriate to the elastic symmetry of the material of which the specimen is composed, but if the boundary conditions imposed relate to stresses alone the constant or linear stress-distribution set up is independent of the type of elastic symmetry(8). The stress-distribution set up in a circularly (or elliptically) cylindrical specimen of aeolotropic material by the application of equal and opposite torsional couples is therefore the same as the stress-distribution that would be set up by the same couples applied to a similar cylinder of isotropic material(8). The same conclusion applies also to bending by pure couples and to combined bending and torsion. The stress-distribution set up in single-crystal specimens of circularly cylindrical form by tension, torsion, flexure or any combination of these types of stress, may therefore be regarded as known, and the determination of the values of the resolved shear stresses reduces merely to the resolution of the known principal stresses along the slip-plane-directions.

§ 3. DETERMINATION OF RESOLVED SHEAR STRESSES

In order to facilitate the presentation of the theoretical analysis, attention will be confined mainly to the face-centred cubic lattice. Many of the results are, however, applicable with little or no alteration to other lattices; the necessary alterations in the case of the body-centred lattice will be indicated. In the face-centred cubic lattice, the possible slip planes are the four octahedral planes of which the Millerian indices are (111), $(\bar{1}11)$, $(1\bar{1}1)$ and $(11\bar{1})$; *these planes will be termed* 0, 1, 2 *and* 3 *respectively*:* the possible slip directions are the six intersections of the slip planes in pairs (the normals to the planes of the type 110); these directions will be termed 01, 02 etc.,

---

* Note that the numeral corresponds with the position of the bar above the Millerian indices.

01 being the intersection of the planes 0 and 1, i.e. the normal to the plane $01\bar{1}$. Since all the slip planes are indistinguishable, the numbers 0, 1, 2, 3 (and the corresponding Millerian indices) can be assigned in 24 ways; in order to avoid this ambiguity, the axis of the specimen will be taken as lying within the solid angle bounded by the three planes through the normal to the cube face 001, the normal to the slip plane 0 (111) and the slip direction 13 (101) in pairs. This convention is shown in the stereographic diagram, figure 1. The position of the axis of the specimen within the triangle shaded in figure 1 defines two of the three parameters necessary to determine completely the orientation of the crystal with respect to the principal axes of stress. The third parameter may be represented by a rotation about the specimen-axis; but for tension, torsion, and simple flexure such a rotation does not alter the stress-distribution,* so that the position of the axis defines the resolved shear stresses completely. For combined bending and torsion all three parameters must be specified.

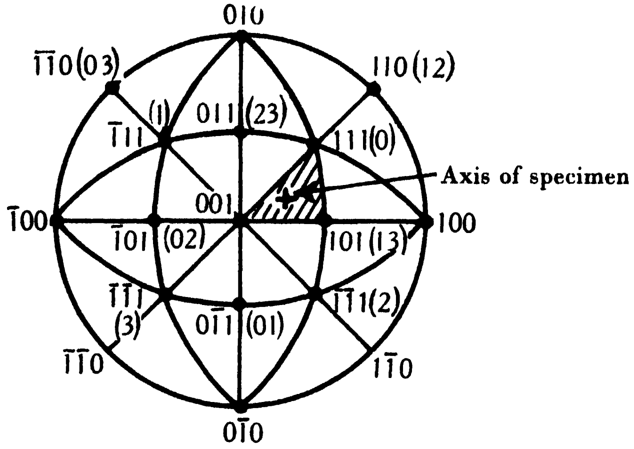

Figure 1

The orientations of the various crystallographic directions are most conveniently specified by spherical co-ordinates referred to the axis of the specimen and to a reference plane, arbitrarily chosen, through that axis; the spherical co-ordinates of the normal to the plane 0 will be written (θ_0, ψ_0), of the direction 01 (θ_{01}, ψ_{01}), and so on. The position of any point on the surface of the specimen will be specified by the angle λ between the diametral plane through the point and the reference plane. General tensile stresses will be denoted by p, general shear stresses by s; the maximum tensile stress parallel to the axis of the specimen will be denoted by P, the actual maximum shear stress due to a torque T by S (which is equal to $2T/\pi r^3$ where r is the radius of the specimen). The resolved shear stress in the slip-plane-direction 01 will be denoted by S_{01}, etc. (N.B. S_{01} is *not* in general equal to S_{10}.)

In the case of simple tension

$$S_{01} = P\cos\theta_0\cos\theta_{01}, \text{ etc.} \qquad \ldots\ldots(1).$$

---

* In the case of flexure, a rotation about the specimen-axis alters the position of the stress system but not its magnitude.

In the case of simple bending $S_{01} = P\cos\lambda\cos\theta_0\cos\theta_{01}$, the plane of bending being taken as reference plane; but the factor $\cos\lambda$ affects all the resolved shear stresses equally, so that the case of simple bending is effectively the same as that of simple tension. The greatest resolved shear stress is defined by the greatest of the products $\cos\theta_0\cos\theta_{01}$, etc. With the convention adopted in figure 1 this is $\cos\theta_2\cos\theta_{23}$; the manner in which the ratio S_{23}/P varies with the orientation will be discussed later.

In the case of simple torsion S_{01}, etc. can be expressed in the form

$$S_{01}=SA\cos(\lambda-\alpha) \qquad \ldots\ldots(2)^{(5)},$$

where $$A=\sqrt{\{-\tfrac{1}{2}(\cos 2\theta_0+\cos 2\theta_{01}+2\cos 2\theta_0\cos 2\theta_{01})\}}$$

and $$\alpha-\psi_0=\tan^{-1}[(\tan^2\theta-1)\cot(\psi_{01}-\psi_0)].^*$$

Calculation of the values of the ratios S_{01}/S, etc. by determination of the values of A and α from the equations (2) is a fairly simple process; but the values have to be determined afresh for each different orientation, and if many crystals are concerned the work becomes laborious. If the ratios S_{01}/S can be determined as functions of the position of the axis (within the triangle shaded in figure 1), the necessity for the intermediate calculation of the values of $(\theta_0\psi_0)$, $(\theta_{01}\psi_{01})$, etc. is avoided and moreover it becomes feasible to tabulate values of S_{01}/S, etc. for all possible orientations.

Let (θ, ϕ) be the spherical co-ordinates of the axis of the specimen referred to the normal to the cube face 001 as axis and the plane 010 as reference plane. As reference plane associated with the axis of the specimen as axis take the plane through the normal to the cube face 001. Let the axes $(Oxyz)$ be Ox perpendicular to the plane 100, Oy perpendicular to 010, and Oz perpendicular to 001; and let the axes $(Ox'y'z')$ be Oy' perpendicular to the reference plane through the axis of the specimen and the axis Oz, Oz' the axis of the specimen, and Ox' the perpendicular to Oy' and Oz'. Then transformation from the axes $(Oxyz)$ to the axes $(Ox'y'z')$ is effected by means of the table

$$\begin{array}{cccc} & x' & y' & z' \\ x & \cos\theta\cos\phi & -\sin\phi & \sin\theta\cos\phi \\ y & \cos\theta\sin\phi & \cos\phi & \sin\theta\sin\phi \\ z & -\sin\theta & 0 & \cos\theta \end{array}\Bigg\} \qquad \ldots\ldots(3).$$

Now, if the surface of the specimen is free from traction, at any point on the surface, one principal stress is normal to this surface and is zero. The stress system may therefore be specified by the values of the principal stresses p_1 and p_2 (p_1 being greater than p_2) and the angle β which the direction of p_1 makes with the axis of the specimen. If λ is the angle which the plane through the point considered and the axis of the specimen makes with the reference plane $y'=0$, the direction cosines with respect to $(Ox'y'z')$ of the directions of the stresses p_1 and p_2 are:

$$p_1\,(-\sin\beta\sin\lambda,\ \sin\beta\cos\lambda,\ \cos\beta),$$
$$p_2\,(\cos\beta\sin\lambda,\ -\cos\beta\cos\lambda,\ \sin\beta).$$

---

* Change of the reference plane has the effect of adding a constant angle to λ and to the values of ψ. α is therefore increased by the same constant angle, so that $\lambda-\alpha$ remains invariant.

From the table, (3), the direction cosines p_1 $(l_1 m_1 n_1)$ and p_2 $(l_2 m_2 n_2)$ with respect to the axes $(Oxyz)$ are found to be

$$l_1 = -\sin\beta \sin\lambda \cos\theta \cos\phi - \sin\beta \cos\lambda \sin\phi + \cos\beta \sin\theta \cos\phi,$$
$$m_1 = -\sin\beta \sin\lambda \cos\theta \sin\phi + \sin\beta \cos\lambda \cos\phi + \cos\beta \sin\theta \sin\phi,$$
$$n_1 = \sin\beta \sin\lambda \sin\theta + \cos\beta \cos\theta.$$

Similar relations hold for (l_2, m_2, n_2).

By equation (1), the resolved shear stress

$$S_{01} = p_1 \cos\theta'_0 \cos\theta'_{01} + p_2 \cos\theta''_0 \cos\theta''_{01},$$

where θ_0' is the angle between the normal to the plane 0 and the direction of the stress p_1, etc.; but the direction cosines of the normal to the plane 0 referred to the axes $(Oxyz)$ are $(1/\sqrt{3}, 1/\sqrt{3}, 1/\sqrt{3})$ and of the direction 01 $(0, 1/\sqrt{2}, -1/\sqrt{2})$, therefore:

$$\cos\theta'_0 = (l_1 + m_1 + n_1)/\sqrt{3}$$

and

$$\cos\theta'_{01} = (m_1 - n_1)/\sqrt{2},$$

with similar formulae for $\cos\theta''_0$, $\cos\theta'_1$, etc. etc.[*] Therefore

$$\sqrt{6}\,.\,S_{01} = p_1 (l_1 + m_1 + n_1)(m_1 - n_1) + p_2 (l_2 + m_2 + n_2)(m_2 - n_2).$$

Now, (l_1, m_1, n_1) (l_2, m_2, n_2) are of the form

$$l_1 = \sin\beta (A \sin\lambda + B \cos\lambda) + C \cos\beta, \quad l_2 = -\cos\beta (A \sin\lambda + B \cos\lambda) + C \sin\beta;$$
$$m_1 = \sin\beta (P \sin\lambda + Q \cos\lambda) + R \cos\beta, \quad m_2 = -\cos\beta (P \sin\lambda + Q \cos\lambda) + R \sin\beta;$$
$$n_1 = \sin\beta . L \sin\lambda + M \cos\beta, \quad n_2 = -\cos\beta . L \sin\lambda + M \sin\beta.$$

Any expression of the form

$$p_1 (l_1 + m_1 + n_1)(m_1 - n_1) + p_2 (l_2 + m_2 + n_2)(m_2 - n_2)\text{[†]}$$

may therefore be written in the form:

$$(p_1 \sin^2\beta + p_2 \cos^2\beta)\{(A+P+L)\sin\lambda + (B+Q)\cos\lambda\}\{(P-L)\sin\lambda + Q\cos\lambda\} \quad \ldots\ldots(4a),$$
$$+ (p_1 - p_2)\sin\beta\cos\beta\,[\{(A+P+L)\sin\lambda + (B+Q)\cos\lambda\}(R-M) + \{(P-L)\sin\lambda + Q\cos\lambda\}(C+R+M)] \ldots\ldots(4b),$$
$$+ (p_1 \cos^2\beta + p_2 \sin^2\beta)(C+R+M)(R-M) \quad \ldots\ldots(4c).$$

Now $p_1 \sin^2\beta + p_2 \cos^2\beta$ is the circumferential tension, Q,

$(p_1 - p_2)\sin\beta\cos\beta$ is the shear due to torsion, S,

and $p_1 \cos^2\beta + p_2 \sin^2\beta$ is the axial tension, P.

Uniform circumferential tension (produced, say, by internal pressure) gives a distribution of resolved shear stress that is a sinusoidal function of 2λ, torsion gives a distribution that is a sinusoidal function of λ, the mean value of any resolved shear stress being in this case zero. If P is due to simple tension, the resolved shear stress is independent of λ; but if P is itself multiplied by $\cos(\lambda-\gamma)$ the distribution is again simple-harmonic. It should be noticed that the value of γ, the angle between the plane of bending and the reference plane $y'=0$, affects the stress-distribution in combined bending and torsion but not in simple bending.

---

[*] The alterations necessary for any other type of crystal symmetry are obvious.

[†] In any lattice system the expression for resolved shear stress will be of this form, viz. $p_1 \times$ (homogeneous function of the 2nd degree in $l_1 m_1 n_1$) $+ p_2 \times$ (homogeneous function of the 2nd degree in $l_2 m_2 n_2$).

The expression in square brackets in (4*b*) above is the ratio S_{01}/S. Similar expressions for the other ratios may be obtained. Inserting the values of A, B, C, etc. the values of S_{01}, etc. may be expressed in the form

$$S_{01}/S=\frac{1}{\sqrt{6}}\{(E\cos 2\theta+F\sin 2\theta)\sin\lambda+(G\cos\theta+H\sin\theta)\cos\lambda\} \quad \ldots\ldots(5),$$

where E, F, G and H are functions of ϕ only. The expressions for E, F, G and H are given in table 1 below.

Table 1. General stress coefficients for torsion

	E	F	G	H
S_{01}	$-\cos\phi$	$\frac{1}{2}(-\cos 2\phi+\sin 2\phi+3)$	$-\sin\phi$	$-\cos 2\phi-\sin 2\phi$
S_{02}	$-\sin\phi$	$\frac{1}{2}(\cos 2\phi+\sin 2\phi+3)$	$\cos\phi$	$-\cos 2\phi+\sin 2\phi$
S_{03}	$\cos\phi-\sin\phi$	$\cos 2\phi$	$\cos\phi+\sin\phi$	$2\sin 2\phi$
S_{12}	$-\cos\phi-\sin\phi$	$\cos 2\phi$	$\cos\phi-\sin\phi$	$2\sin 2\phi$
S_{13}	$-\sin\phi$	$\frac{1}{2}(\cos 2\phi-\sin 2\phi+3)$	$\cos\phi$	$\cos 2\phi+\sin 2\phi$
S_{10}	$\cos\phi$	$\frac{1}{2}(-\cos 2\phi-\sin 2\phi+3)$	$\sin\phi$	$\cos 2\phi-\sin 2\phi$
S_{23}	$-\cos\phi$	$\frac{1}{2}(-\cos 2\phi-\sin 2\phi+3)$	$-\sin\phi$	$\cos 2\phi-\sin 2\phi$
S_{20}	$\sin\phi$	$\frac{1}{2}(\cos 2\phi-\sin 2\phi+3)$	$-\cos\phi$	$\cos 2\phi+\sin 2\phi$
S_{21}	$-\cos\phi-\sin\phi$	$-\cos 2\phi$	$\cos\phi-\sin\phi$	$-2\sin 2\phi$
S_{30}	$\cos\phi-\sin\phi$	$-\cos 2\phi$	$\cos\phi+\sin\phi$	$-2\sin 2\phi$
S_{31}	$\sin\phi$	$\frac{1}{2}(\cos 2\phi+\sin 2\phi+3)$	$-\cos\phi$	$-\cos 2\phi+\sin 2\phi$
S_{32}	$\cos\phi$	$\frac{1}{2}(-\cos 2\phi+\sin 2\phi+3)$	$\sin\phi$	$-\cos 2\phi-\sin 2\phi$

Equation (5) is of course identical with equation (2); $E\cos 2\theta+F\sin 2\theta$ corresponds to $A\sin\alpha$ and $G\cos\theta+H\sin\theta$ to $A\cos\alpha$, the angle α being measured from the plane through the axis of the specimen and the normal to the cube face 001.* But A and α are now functions of two variables only.

§4. ACTUAL MAXIMUM RESOLVED SHEAR STRESSES DUE TO TENSION AND TORSION

With the convention adopted (figure 1), the greatest resolved shear stress in the face-centred lattice due to tension is always the stress S_{23}.† It is proposed to prove that the greatest resolved shear stress in this lattice due to torsion may be either S_{01}, S_{03} or S_{31} and to examine how the value of the actual maximum resolved shear stress due to tension or torsion varies with orientation.

For this purpose it is convenient to use a method of projection different from the stereographic method normally employed. If a line representing any crystallographic direction is drawn from the centre of a sphere, of which the upward-drawn vertical diameter represents the axis of reference (e.g. the positive direction of the specimen-axis), the colatitude of the point in which this line meets the sphere is the spherical co-ordinate θ and its longitude (with reference to the arbitrary reference plane) is ψ. To obtain the stereographic diagram, these points on the surface of the sphere are projected on to the equatorial plane, where $\theta=\pi/2$, from the lowest point of the sphere, where $\theta=\pi$. All directions for which $\theta<\pi/2$ are then represented by points on a plane within a circle of radius equal to the radius of the sphere; the polar co-ordinates (r, α) in this diagram of any direction (θ, ψ) are given by $r=\tan\frac{1}{2}\theta$ and $\alpha=\psi$. In the stereographic diagram, figure 1, the axis of reference used is the normal to the cube face nearest to the axis of the specimen, the axis of the specimen being shown as a point within the triangle bounded by the three planes through the normals to the planes 001, 101, 111 in pairs. In the symmetrical stereographic diagram, this elementary triangle is bounded by two straight lines and an arc of a circle; but for the present purpose it is very much more convenient to use a method of projection that makes all three sides straight. This is achieved by projecting not from the south pole but from the centre of the sphere on to the tangential plane at the north pole $(\theta=0)$. The polar co-ordinates (r', α') of a point in this diagram representing the direction (θ, ψ) are given by $r'=\tan\theta$, $\alpha'=\psi$. Points for which $\theta \to \pi/2$ are thus projected into points that lie at a great distance from the pole of the diagram; but if attention is confined to the triangle 100, 101, 111, this disadvantage does not make itself apparent. It should be noted that the diagram obtained by this central projection consists merely in the intersections of the directions, etc. with the tangent plane to the sphere at the north pole Planes project therefore into straight lines, whereas in the stereographic projection all planes, except those through the axis, project into circular arcs.

---

* In determining the effect of combined bending and torsion, it is necessary to ascertain the sense of the shear stresses due to torsion. If the normals to the slip planes marked 0, 1, 2, 3 and the directions marked 01, 02, etc. (note particularly 03 and 12) in figure 1 are taken as positive, the values of E, F, G, H tabulated give the resolved shear stresses due to a right-handed torque. Note that α and λ are measured in the opposite sense, viz. anti-clockwise in figure 1.

† This may be proved very simply by comparison of the expressions of the type (4*c*).

The position of the axis within the elementary triangle may be specified by its direction cosines a, b and c $(c>a>b)$; or, if in the central projection, the normal to the plane 001 is taken as origin and the lines $\psi=0$ and $\psi=\pi/2$ as axes of x and y, the position of the axis may be defined by $x=a/c$ and $y=b/c$. The values of θ_0 and θ_{01} are then given by:

$$\left.\begin{aligned}\cos\theta_0&=\frac{1}{\sqrt{3}}(a+b+c)=\frac{1+x+y}{\sqrt{\{3(1+x^2+y^2)\}}}\\ \cos\theta_{01}&=\frac{1}{\sqrt{2}}(b-c)=\frac{y-1}{\sqrt{\{2(1+x^2+y^2)\}}}\end{aligned}\right\}\qquad\ldots\ldots(6).$$

Similar expressions for all the other θ values may be written down. From equations (2) above

$$\begin{aligned}A^2_{01}&=-\tfrac{1}{2}(\cos 2\theta_0+\cos 2\theta_{01}+2\cos 2\theta_0\cos 2\theta_{01})\\ &=(\cos 2\theta_0+\cos^2\theta_{01}-4\cos^2\theta_0\cos^2\theta_{01}).\end{aligned}$$

Using the relations of the type (6), we find

$$\left.\begin{aligned}6A^2_{01}&=2(a+b+c)^2+3(b-c)^2-4(b-c)^2(a+b+c)^2\\ 6A^2_{02}&=2(a+b+c)^2+3(c-a)^2-4(c-a)^2(a+b+c)^2\end{aligned}\right\}\qquad\ldots\ldots(7),$$

and similar expressions for $6A^2_{03}$, etc.

Taking differences and remembering that $c > a > b > 0$ and that $a^2+b^2+c^2=1$, we have

$$6\,(A^2_{01}-A^2_{02}) = \{(b-c)^2-(c-a)^2\}\,\{3-4\,(a+b+c)^2\}$$
$$= (b-a)\,(a+b-2c)\,(-1-8\Sigma bc) < 0.$$

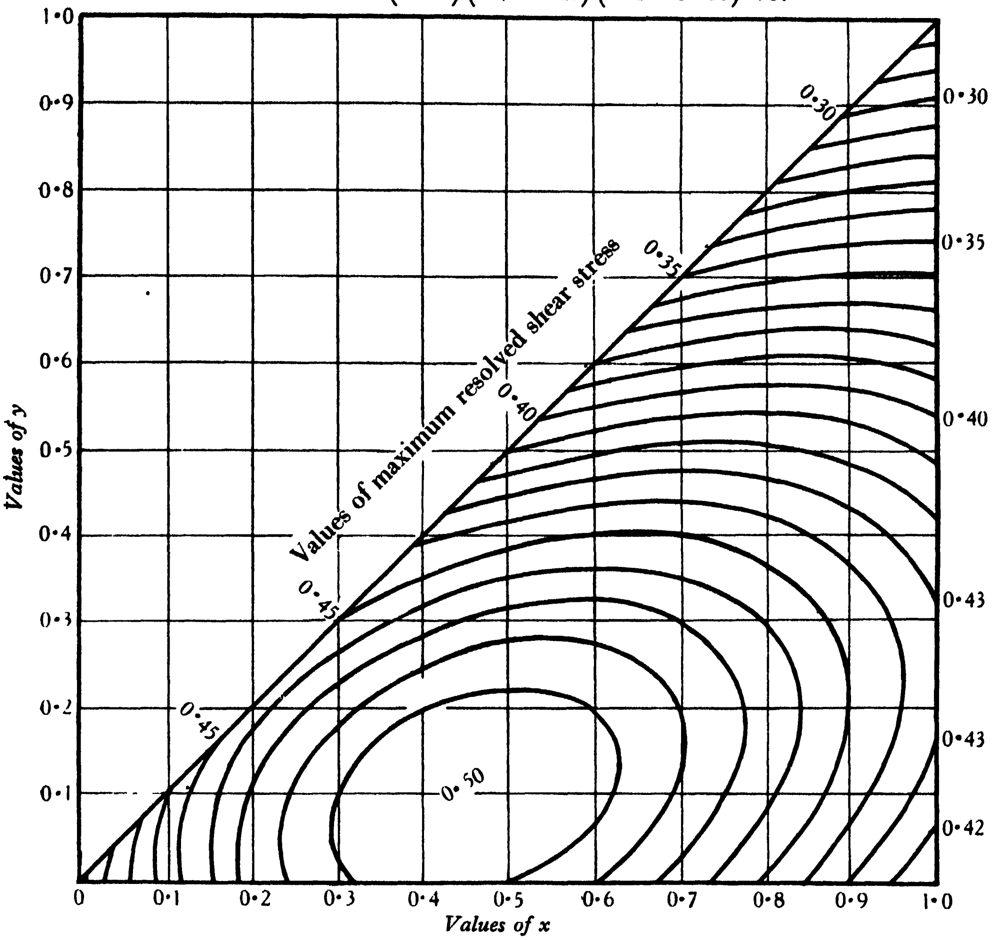

Figure 2

Similarly it may be shown that

$$A^2_{10} < A^2_{03} \qquad\qquad A^2_{13} < A^2_{31}$$
$$A^2_{20} < A^2_{02} \text{ or } A^2_{03} \qquad\qquad A^2_{21} < A^2_{03} \text{ or } A^2_{12}$$
$$A^2_{30} < A^2_{03} \qquad\qquad A^2_{12} < A^2_{03} \text{ or } A^2_{31}$$
$$A^2_{23} < A^2_{32} \qquad\qquad A^2_{32} < A^2_{31} \text{ or } A^2_{30}$$

The three coefficients remaining are A_{02}, A_{03} and A_{31}

$$6\,(A^2_{02}-A^2_{03}) = (c-b)\,(b+c-2a)\,(-1-8\Sigma bc) > 0 \text{ if } 2a > b+c, \; < 0 \text{ if } 2a < b+c.$$
$$6\,(A^2_{02}-A^2_{31}) = 4c\,\{4b\,(2a^2+ab+b^2)-a-2b\}.$$
$$6\,(A^2_{03}-A^2_{31}) = 8ac\,(a+b)\,(2b-2c-a)+(b+c)\,(2a-b+c)\,(1+8ab).$$

The three equations $A^2_{02}-A^2_{03}=0$, $A^2_{02}-A^2_{31}=0$ and $A^2_{03}-A^2_{31}=0$ define three lines within the elementary triangle that intersect in a common point

$$x\,(=a/c)=\frac{1+\sqrt{51}}{2\sqrt{51}-3},\quad y\,(=b/c)=\frac{5}{2\sqrt{51}-3},$$

and these lines divide the elementary triangle into three regions, in each of which one of the coefficients A_{02}, A_{03} and A_{31} exceeds the other two. The three regions are shown in figure 3, and in this diagram contours of constant A are also shown.

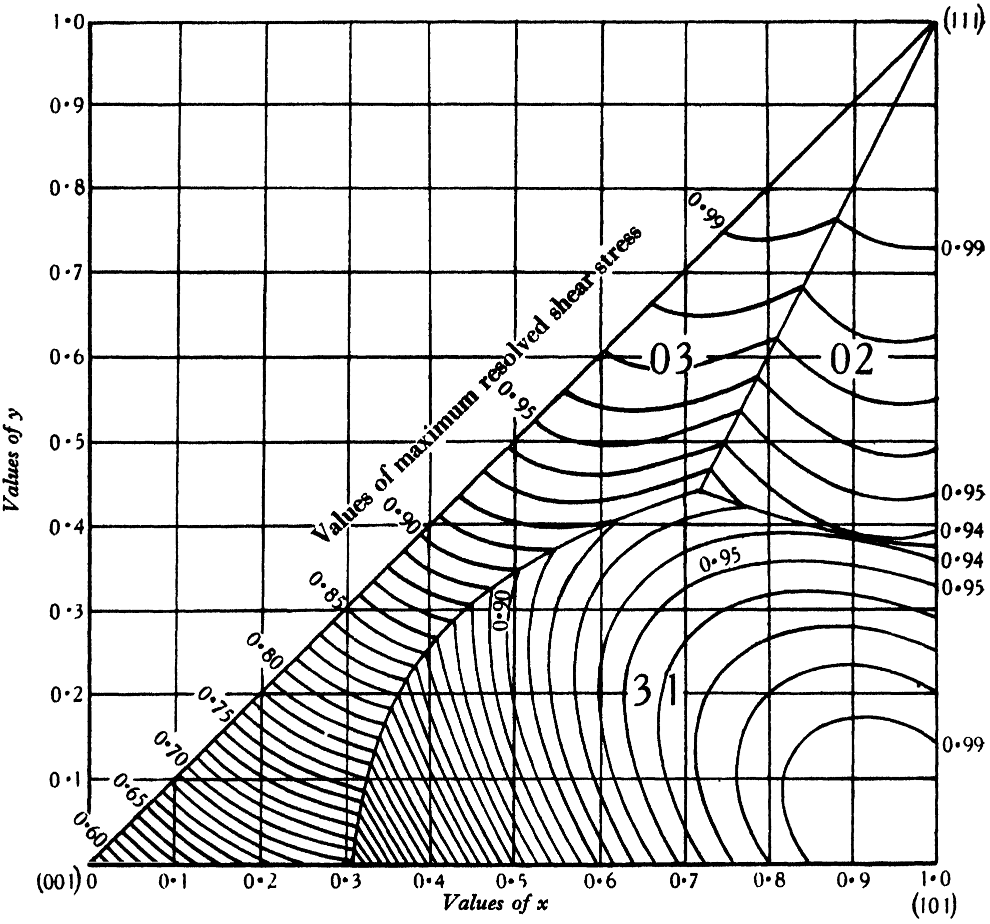

Figure 3

The preparation of a diagram similar to figure 3 for the case of tension is a much simpler matter; for the maximum stress is S_{23} and it is necessary only to calculate contours for this one stress-value. From equation (6) we have

$$S_{23}=T\cos\theta_2\cos\theta_{23}=T\,(a-b+c)\,(b+c)/\sqrt{6}$$

$$=T\,\frac{(1+x-y)\,(1+y)}{\sqrt{6}\,(1+x^2+y^2)} \qquad \text{......(8)},$$

where $x=a/c$, $y=b/c$ as before.

Contours of constant maximum stress are therefore ellipses with parallel axes, the major axis of each ellipse making an angle $\pi/8$ with the line $y=0$. The actual contour map for this case is shown in figure 2.

§ 5. MAXIMUM STRESSES WHEN THE SLIP PLANE MAY BE ANY PLANE THROUGH ANY ONE OF A NUMBER OF CRYSTALLOGRAPHIC DIRECTIONS

The necessary modifications to the analysis given in §§ 3 and 4 to provide for other systems of slip planes and slip directions may be made without difficulty; but in view of the behaviour of single crystals of iron$^{(9, 10, 11)}$, the case in which the slip plane may be any plane through the slip direction is worth special attention. In this case general analysis on the lines of § 3 is scarcely feasible, for the direction cosines of the slip plane are not known. A variable parameter representing rotation of the slip plane about the slip direction must be included, and this parameter will appear in the expression (4), whence its value must be determined to render the value of the whole expression a maximum. The slip plane thus varies not only with λ but also with the relative values of the three stress components Q, S and P, so that expressions similar to (4*a*), (4*b*) and (4*c*) would be of little use. The two more important cases of tension (or bending) and torsion may however be investigated separately.

Again to facilitate the presentation of the analysis, attention will be confined to the case of iron. In this case the slip directions are the normals to the octahedral planes; these directions will be designated 0, 1, 2 and 3 with the same convention as to the position of the specimen-axis as in the case of the face-centred lattice, figure 1. In the case of tension, the maximum resolved shear stress in the direction 0 is given by $S_0 = T\cos\theta_0\cos\theta$ with the condition

$$\sin\theta_0\sin\theta\cos(\psi_0-\psi)+\cos\theta_0\cos\theta=0,$$

where θ, ψ are the co-ordinates of the slip plane. It may easily be shown that

$$S_0=\frac{T\cos\theta_0\sin\theta_0}{\sqrt{\{\cos^2\theta_0\sec^2(\psi_0-\psi)+\sin^2\theta_0\}}} \qquad \ldots\ldots(9).$$

There is no restriction on the value of ψ, so that the maximum value of S_0 is merely $\frac{1}{2}T\sin 2\theta_0$. In this case there is no advantage in expressing the stress coefficients in terms of the co-ordinates (θ, ϕ) of the axis of the specimen (see figure 1); for the lines along which $S_0=S_1$, etc. can be found very easily from the equation

$$\sin 2\theta_0 = \sin 2\theta_1$$

and the side on which $S_0>S_1$ may be determined by inspection. It may easily be shown that the maximum stress is either S_0 or S_2. The line (within the elementary triangle) along which $S_0=S_2$ is given by $2\theta_0=\pi-2\theta_2$, whence $\cos^2\theta_0+\cos^2\theta_2=1$ and, from equation (6), $(1+x+y)^2+(1+x-y)^2=3\,(1+x^2+y^2)$ or $(x-2)^2+y^2=3$. This is a circle with centre at $x=2$, $y=0$ and radius $\sqrt{3}$. The contours of constant maximum resolved shear stress for the case of tension are shown in figure 4. The contours of constant S_0 are ellipses and hyperbolas and those of constant S_2 are hyperbolas.

In the case of torsion, the stress factors may be expressed in the form

$$S^2_0 = \cos^2\theta_0 \cos^2(\lambda-\psi_0) + \cos^2 2\theta_0 \sin^2(\lambda-\psi_0)^{(11)};$$

but here again there is no advantage in conversion to the co-ordinates (θ, ϕ) of the axis of the specimen. The maximum value of S_0 is either $\cos\theta_0$ or $\cos 2\theta_0$

$$\cos 2\theta_0\,| > |\cos\theta_0|, \text{ if } \theta_0 > \frac{\pi}{3}\Big].^*$$

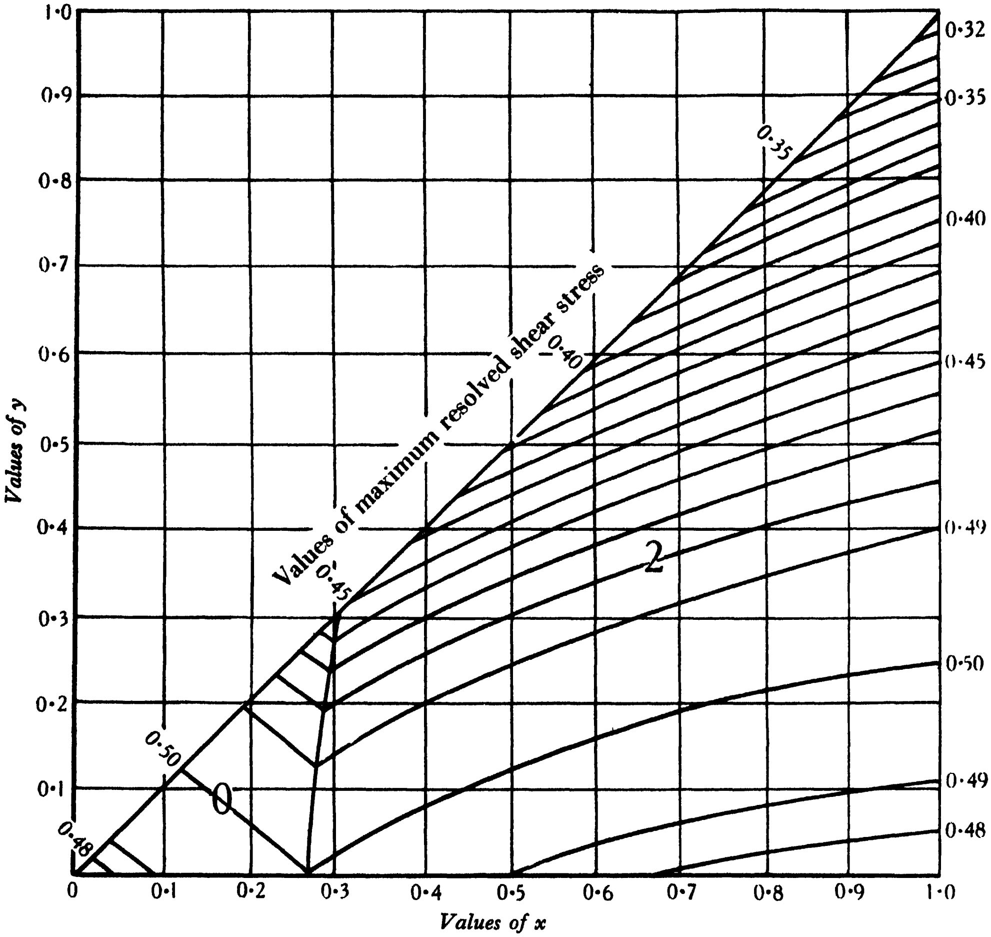

Figure 4

The maximum stress factor for different positions of the axis of the specimen within the elementary triangle, figure 1, may be found by comparison of expressions such as

$$\cos\theta_0 = (a+b+c)/\sqrt{3} \quad \text{and} \quad \cos 2\theta_0 = \tfrac{2}{3}(bc+ca+ab) - \tfrac{1}{3}$$

if we take the greatest numerical value and remember that $c > a > b > 0$, and that

---

* The positive sense of each slip direction is that which makes an acute angle with the positive sense of the axis of the specimen; thus $\theta_0 < \pi/2$.

$a^2+b^2+c^2=1$. Thus it may be shown that within the elementary triangle, figure 1, $\cos^2\theta_0$ is greater than $\cos^2\theta_1$, $\cos^2\theta_2$, $\cos^2\theta_3$ and $\cos^2 2\theta_0$, whilst $\cos^2 2\theta_3$ is greater than $\cos^2 2\theta_1$ and $\cos^2 2\theta_2$. The two coefficients to be considered are therefore $\cos^2\theta_0$ and $\cos^2 2\theta_3$. The contours of constant maximum resolved shear stress for the case of torsion are shown in figure 5. It may be noticed that these contours are lines of constant θ_0 or θ_3. All these contours are conics having their centres on the line $x=y$. The contours of constant θ_0 in the upper part of the triangle are ellipses and in the lower part hyperbolas, whilst the contours of constant θ_3 are hyperbolas including the limiting case of two coincident straight lines $(x+y-1)^2=0$. The lines of intersection, where $\cos^2\theta_0=\cos^2 2\theta_3$, are quartic curves; but these also cut the line $x=y$ orthogonally.

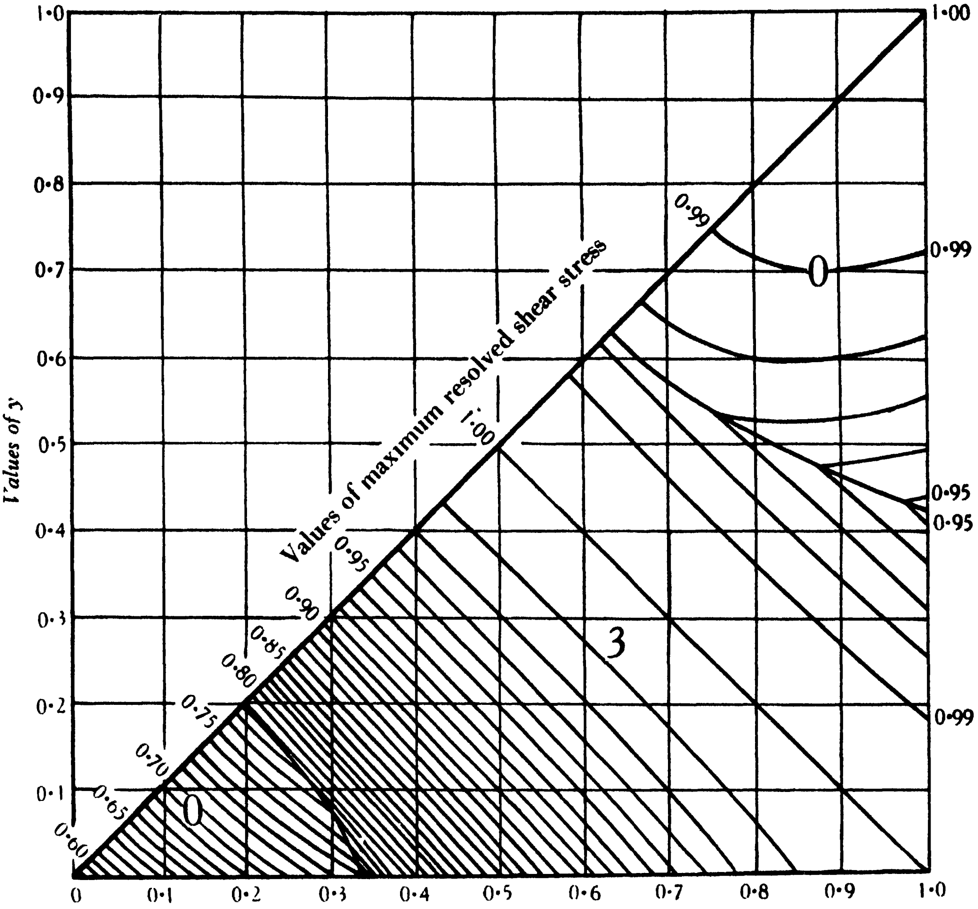

Figure 5

§ 6. ORIENTATION EFFECTS IN POLYCRYSTALLINE SPECIMENS

If a polycrystalline specimen is subjected to any stress system, the behaviour of the specimen as a whole must presumably be determined by the behaviour of the constituent crystals. Apart from any effect due to the intercrystalline boundaries, whether in altering the stress-distribution or in strengthening the individual crystals, the behaviour of the polycrystalline aggregate must depend upon the orientation of the individual crystals. Thus, if the occurrence of some phenomenon in the single crystal (e.g. slip or fatigue failure) is determined entirely by the value of the resolved shear stress, the occurrence of a similar phenomenon in the polycrystalline aggregate should presumably occur at a stress-value intermediate between the two values that give the value of the critical resolved shear stress in the most favourably and most unfavourably oriented crystals.

For the purpose of obtaining an estimate of the effect of varying orientation, it will be assumed that the maximum resolved shear stress in each individual crystal must reach the critical value, but that no increase above this critical value can occur. If fA_m is the value of the maximum resolved shear stress in any crystal due to a tension f in the direction (θ, ϕ), the tension required to give the critical shear stress s is s/A_m, A_m being the maximum resolved shear stress coefficient corresponding to the orientation (θ, ϕ). The total load required to cause complete yield* of all the crystals in a cross-section σ of a specimen will therefore be $\Sigma s\delta\sigma/A_m$, where $\delta\sigma$ is the area of one crystal. If the orientation of the crystals is perfectly random, it may be assumed that each orientation, and therefore each value of A_m, is represented by a crystal of the same area, so that the mean stress on the cross-section is the mean of s/A_m or s times the mean of $1/A_m$, since s is constant. The ratio of the mean stress f_0 required to cause complete yield to the stress f_m which would be required if yield occurred when the maximum shear stress, irrespective of slip-plane-directions, reached the value s is therefore the mean of $1/A_m$. The mean must be found by summation for all possible orientations within the elementary triangle, figure 1, assuming all orientations to be equally probable. We have therefore

$$f_0/f_m = \text{mean of } 1/A_m = \frac{\iint 1/A_m \sin\theta\, d\theta\, d\phi}{\iint \sin\theta\, d\theta\, d\phi} \qquad \text{......(10).}$$

where the denominator is the area of the spherical triangle within which the axis of the specimen lies.

The value of $1/A_m$ as a function of θ and ϕ for the case of the face-centred lattice can be found from equation (8), but it is more convenient to convert the expression (10) from the co-ordinates (θ, ϕ) to the co-ordinates (x, y). It may thus be shown that

$$f_0/f_m = \frac{6\sqrt{6}}{\pi}\int_0^1 dx \int_0^x \frac{dy}{(1+x-y)(1+y)\sqrt{(1+x^2+y^2)}} \qquad \text{......(10a).}$$

This double integral has been evaluated numerically and gives the result

$$f_0/f_m = 1{\cdot}116 \qquad \text{......(10b)}$$

with a possible error of $\pm 0{\cdot}001$.

---

* The sense in which the term "yield" is used will be obvious.

In the case of the body-centred lattice, assuming that slip can occur on any plane through any of the four slip directions, the value of $1/A_m$ cannot conveniently be expressed as a function of θ and ϕ (or x and y), because both the directions 0 and 2 are involved. The mean value of $1/A_m$ over the triangle, figure 4, has therefore been calculated by a process of numerical integration from the plotted contours, the areal distortion of the diagram being of course taken into account. The value thus obtained is

$$f_0/f_m = 1\cdot068 \qquad \ldots\ldots(11).$$

with a possible error of ±0·002, where f_0 and f_m have the same meanings as in the previous case.

In the case of torsion, the effect of varying crystal-orientation is rather more difficult to assess. At radius r and angle λ, let the crystal-orientation be (θ, ϕ). Then the value of the maximum stress coefficient A_e depends not only upon θ and ϕ but also upon λ.* If T_0 is the torque required to cause complete yield, assuming that the maximum resolved shear stress must everywhere reach the value s, and if T_m is the torque which would be required to cause yield if it were necessary only for the actual maximum shear stress everywhere to reach this same value, the ratio T_0/T_m may be expressed in the form

$$T_0/T_m = \frac{\iiiint s/A_e \sin\theta\, d\theta\, d\phi\,.(r d\lambda\,.dr)\,.r}{\iiiint s \sin\theta\, d\theta\, d\phi\,.(r d\lambda\,.dr)\,.r} \qquad \ldots\ldots(12),$$

or since $1/A_e$ is independent of r

$$T_0/T_m = \frac{\iiint 1/A_e \sin\theta\, d\theta\, d\phi\, d\lambda}{2\pi \iint \sin\theta\, d\theta\, d\phi} \qquad \ldots\ldots(12a).$$

To evaluate the right-hand side of this equation it is necessary to determine the value of $\frac{1}{2}\pi^{-1}\int 1/A_e d\lambda$ for a series of different pairs of values of θ and ϕ, and then to find the average value for all possible orientations.

The value of $\frac{1}{2}\pi^{-1}\int 1/A_e d\lambda$ is the mean of the reciprocals of the ordinates of the upper envelope of the usual resolved shear-stress diagram. In the case of the face-centred lattice the evaluation of this mean of the reciprocal of the ordinate involves evaluation of a number of integrals of the form

$$\int_{\beta_1}^{\beta_2} \frac{d\lambda}{A\cos(\lambda-\alpha)},$$

the values of A, α, β_1 and β_2 being first determined. In the case of directed-only slip in the body-centred lattice, the determination of the mean of the reciprocal of the ordinate involves a similar process, but in this case the integrals are elliptic.

The mean value of $1/A_e$ for a number of different orientations has been determined both for the case of the face-centred cubic lattice (aluminium) and for the case of the body-centred lattice (iron, the type of slip plane not being specified). For convenience, the product of the reciprocal of $\frac{1}{2}\pi^{-1}\int 1/A_e d\lambda$ and the nominal maximum shear stress has been termed the *harmonic mean stress*. Contours of constant harmonic mean stress for both cases are shown in figures 6 (face-centred lattice) and 7 (body-centred lattice). The value of T_0/T_m has been calculated both for the face-centred and for the body-centred cubic lattices with the following results:

---

* A_e is taken as the ratio of the maximum resolved shear stress to the actual maximum shear stress *at the same radius*. Thus A_e is independent of r.

for a face-centred cubic lattice, $T_0/T_m = 1{\cdot}281 \pm 0{\cdot}003$;

for a body-centred cubic lattice, $T_0/T_m = 1{\cdot}232 \pm 0{\cdot}003$.

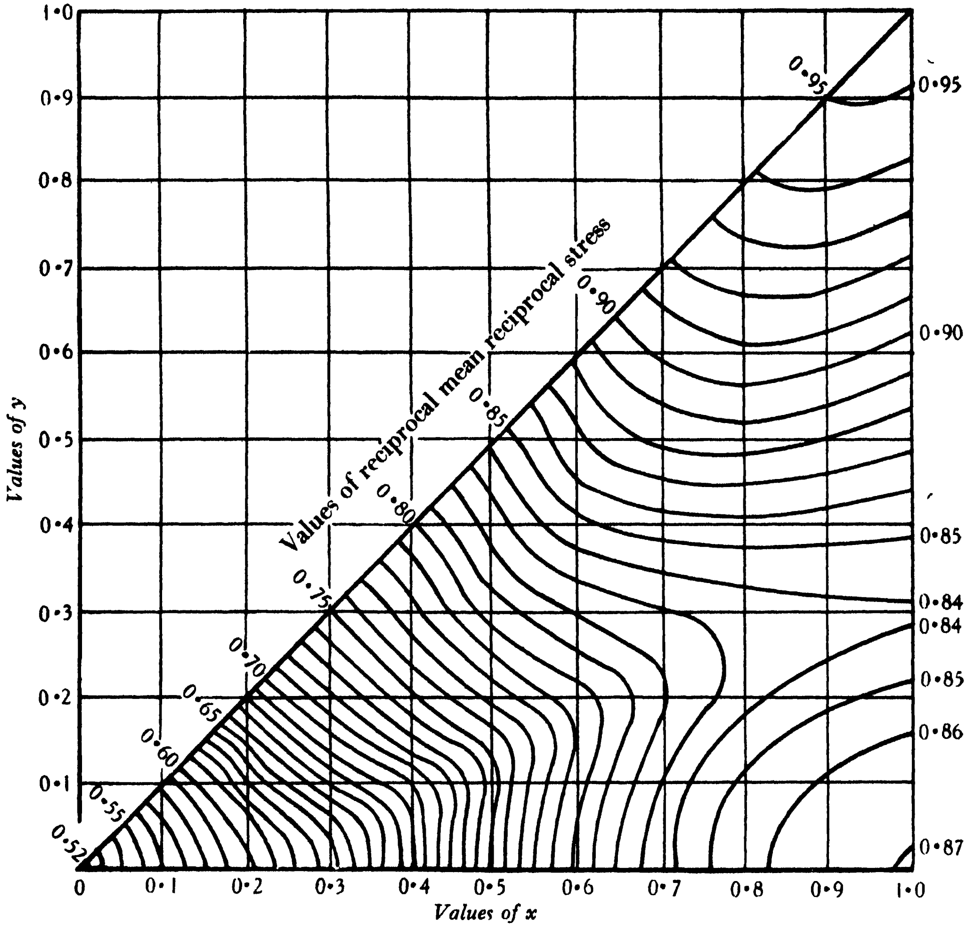

Figure 6

The method developed above for determining the yield in tension or torsion of a polycrystalline specimen is based upon the assumption that each individual crystal in the cross-section of the specimen yields; clearly this condition is a limiting one in the sense that no higher ratios of f_0 to f_m or of T_0 to T_m should be anticipated. On the other hand, if yield of the polycrystalline specimen depends upon yield only of a small number of crystals, lower values of these ratios may be expected. In particular if yield of the specimen is determined by yield of any one individual crystal, the value of both ratios is unity. All possible values of the ratios f_0/f_m and

T_0/T_m lie therefore between unity and 1·116 and 1·281 respectively for the face-centred lattice and between unity and 1·068 and 1·232 respectively for the body-centred lattice.

It is necessary finally to consider whether any intermediate values can be justified by any reasonable assumption that yield of the specimen should depend upon a limited number of crystals intermediate between one and the total number in the cross-section.

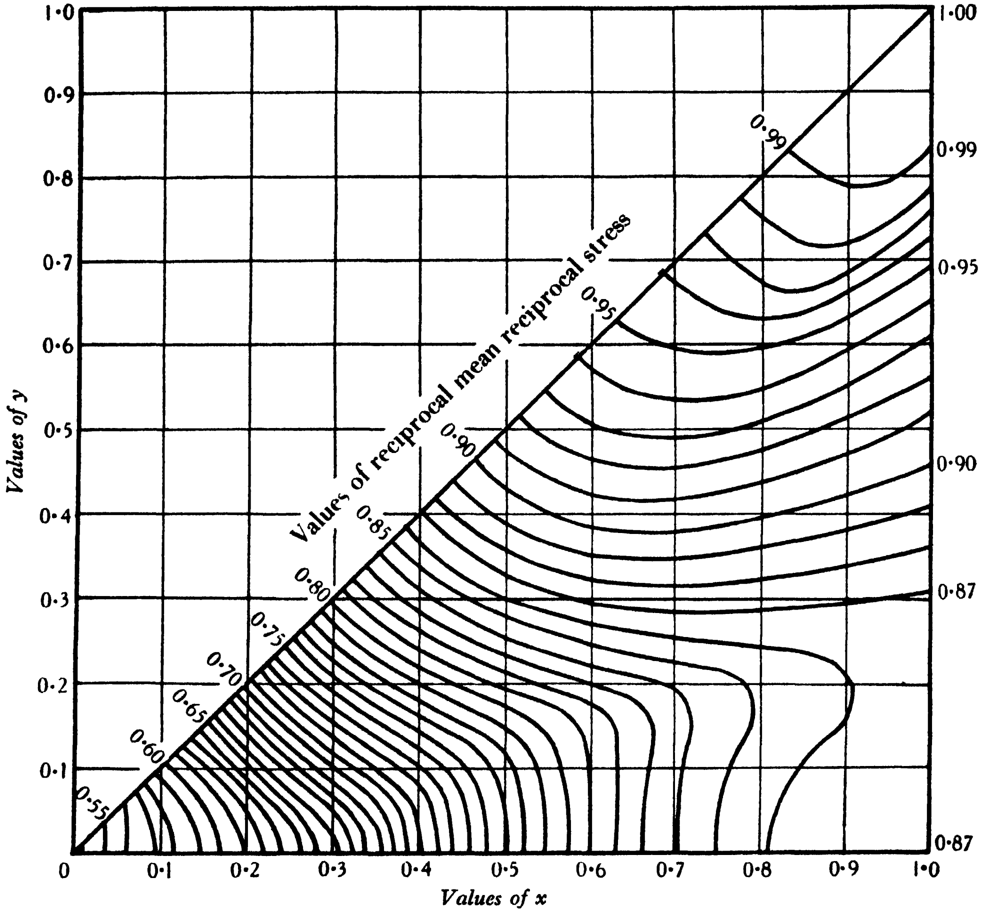

Figure 7

In the case of tension, no other criterion based upon stress conditions alone appears to be justifiable; all the crystals in the cross-section are subjected to the same nominal stress, and there are no logical grounds for dividing the total number into two or more sets. In the case of torsion, on the other hand, the nominal stress (under elastic conditions) is proportional to the radius, so that the stress conditions themselves in some sense differentiate between the surface and the core of the specimen. It is reasonable therefore to consider how the yield of the specimen as a whole would occur if it were determined by yield of all the crystals in the surface at one cross-section. Unfortunately it seems quite impossible to express this criterion in exact terms. Since completely random orientation would give the same (maximum) value of T_0/T_m that was previously obtained, it is clear that the criterion must be based upon some special distribution of orientations of the crystals in the surface; but the sense in which the distribution should be peculiar cannot be defined clearly. There is, however, one possible assumption that may approach reasonably near to the condition required and which has the important advantage that, by its use, the corresponding value of T_0/T_m may be calculated without much difficulty; that is, to assume that, whilst all possible orientations occur at random in the surface, at one cross-section each orientation occurs at the λ-value appropriate to the actual maximum resolved shear stress for that orientation. Under this condition, the corresponding values of T_0/T_m are given merely by the mean reciprocal value of the actual maximum resolved shear stresses, which are shown in figures 2 and 5. These values have been calculated by a process of numerical integration with the following results:

$$\text{for a face-centred cubic lattice } T_0/T_m = 1{\cdot}133 \pm 0{\cdot}002;$$

$$\text{for a body-centred cubic lattice } T_0/T_m = 1{\cdot}100 \pm 0{\cdot}002.$$

The ratios of f_0/f_m and T_0/T_m corresponding to the different criteria are summarized in tables 2 and 3 below.

Table 2. Values of f_0/f_m and T_0/T_m for a face-centred cubic lattice

	Local yield	Surface yield	Complete yield
f_0/f_m	1	—	1·116
T_0/T_m	1	1·133	1·281
Ratio $\dfrac{\text{yield in torsion}}{\text{yield in tension}}$	0·500	0·567 ± 0·001 0·508 ± 0·002	0·574 ± 0·002

Table 3. Values of f_0/f_m and T_0/T_m for a body-centred cubic lattice

	Local yield	Surface yield	Complete yield
f_0/f_m	1	—	1·068
T_0/T_m	1	1·100	1·232
Ratio $\dfrac{\text{yield in torsion}}{\text{yield in tension}}$	0·500	0·550 ± 0·001 0·515 ± 0·002	0·577 ± 0·002

In tables 2 and 3 the values of the ratios of yield in torsion to yield in tension given in the bottom row are obtained merely by dividing T_0/T_m by $2f_0/f_m$. Since the value of f_0/f_m corresponding to the surface-yield value of T_0/T_m cannot be easily decided, in this case the ratio of T_0/T_m to both limiting values of $2f_0/f_m$ has been given.

It is interesting to note that the criterion of local failure gives the ratio 0·500, whereas the criterion of general failure gives the ratio 0·574 in one case and 0·577 in the other. Both these latter values are extremely close to the value $1/\sqrt{3}$ which has been justified mathematically on a different set of assumptions completely independent of the crystalline structure. It is, however, extremely unlikely that the values of these ratios on the assumptions made in this paper should be exactly $1/\sqrt{3}$, although, in view of the approximate nature of the calculations by which the values have been obtained, this possibility cannot be entirely excluded.

If yield or failure of a polycrystalline specimen were determined simply by the maximum stress developed locally in one crystal, the material would certainly be classed as brittle; whereas if yield or failure depended upon yield or failure of each individual crystal, the material would be regarded as ductile. It may therefore be claimed that the effect of variation of orientation of the crystals in a polycrystalline specimen does in itself indicate that the ratio of the yield in torsion to the yield in tension should be 0·500 for brittle materials and about 0·577 for ductile materials.

§ 7. ACKNOWLEDGEMENTS

The work described has been carried out for the Department of Scientific and Industrial Research under the supervision of the Executive Committee of the National Physical Laboratory. The authors wish to express their thanks to Miss W. B. Burns and Mr S. E. Mitchell for considerable assistance in connexion with the calculations, and particularly to Dr H. J. Gough, F.R.S., for the interest he has taken in the work.

REFERENCES

(1) Mark, Polanyi and Schmid. *Z. Phys.* **12**, 58 (1922).
(2) Taylor. Bakerian Lecture, *Proc. roy. Soc.* A, **102**, 643 (1923).
(3) Gough, Hanson and Wright. *Rep. Memor. aero. Res. Comm.*, Lond., No. 995 (1924).
(4) Gough and Cox. *J. Inst. Met.* **45**, No. 1 (1931).
(5) Gough, Wright and Hanson. *J. Inst. Met.* **36**, No. 2 (1926).
(6) Cox and Clenshaw. *Proc. roy. Soc.* A, **149**, 312 (1935).
(7) Gough, Cox and Sopwith. *J. Inst. Met.* **54**, No. 1 (1934).
(8) Wright. *Rep. Memor. aero. Res. Comm.*, Lond., No. 1031 (1926).
(9) Taylor and Elam. *Proc. roy. Soc.* A, **112**, 337 (1926).
(10) Pfeil. *J. Iron Steel Inst.* **15** (1926).
(11) Gough. *Proc. roy. Soc.* A, **118**, 498, 510 (1928).

GLIDE IN METAL SINGLE CRYSTALS

By E. N. da C. ANDRADE, F.R.S.,
Quain Professor of Physics in the University of London
and R. ROSCOE, Ph.D.

Received 7 *November* 1936. *Read* 22 *January* 1937

ABSTRACT. A method is described for producing single crystals of cadmium and of lead which are not affected by annealing, and, in general, show great regularity of mechanical behaviour. A simple recording extensometer also is described. With the cadmium crystals very consistent results have been obtained, and the effects of rate of glide and of impurities on the measured critical shear stress have been investigated. Experiments have been carried out on hardening and recovery of the cadmium crystals, and on the spacing of glide planes in lead crystals, which has been shown to be independent of a range of factors, and so to have a physical significance. It is shown that the results relating to hardening can be explained by a hardening on individual glide lamellae which is proportional to the glide, and it is suggested that the mechanism of the permanent hardening is mainly a rotation of crystallites in the lamellae.

§ 1. INTRODUCTION

The following experiments were carried out in the hope of obtaining information as to the mechanism of the plastic deformation of metal single crystals, and of the significance of the visible slip bands which appear when metal single crystals are deformed. The metals used have been mainly cadmium and lead: cadmium as typical of hexagonal metals, in which, on account of the unique system of glide planes, the phenomena are comparatively simple; and lead on account of the great regularity of behaviour shown by that metal. The work was begun as long ago as 1928 by the senior of us, in conjunction with Dr B. Chalmers, but was held up for some time by the difficulty of obtaining results of sufficient regularity. After the work had been in progress a short time, papers by W. Boas and S. Schmid(1) appeared, which gave some of the results we were in process of obtaining, and so led to a modification of our programme.

We came to the conclusion that much of the irregularity found by previous workers with crystals made under slightly different conditions was due to strain produced during the manufacture of the crystals, and have worked out a new method with the object of producing strain-free single crystals, which, judging from both the low value of the critical shear stress and the consistency of the results, appears to be successful. A simple method of recording photographically the stress-strain relationship is also described. With this we have investigated the question as to whether a finite critical shear stress exists, in particular by varying the initial rate of glide within very wide limits.

The general question of flow, recovery and hardening has been investigated with cadmium, and we have considered, among other things, the effect of small traces of impurity both on the critical shear stress and on the hardening. Our experiments on the spacing of the visible slip bands, in particular with lead, have brought us to consider them as an essential feature of the glide mechanism, and we discuss our results in terms of glide and hardening taking place in laminae separated by distances large compared to their widths.

§ 2. PREPARATION OF THE CRYSTALS

Single crystals of typical metals were first deliberately prepared in 1914(2) by the process of slowly cooling wires which had been heated to the melting point. Since then many other methods have been used, e.g. (*a*) recrystallization of a strained specimen(3), (*b*) crystallization from a point, in tubes or other containing vessels filled with the metal, of which a number of versions have been worked out(4), (*c*) withdrawal from a crucible full of the molten metal of a pointed rod; a crystal forms on the point, which serves as a nucleus on which the single crystal rod forms(5), (*d*) the gradual cooling from one end of a rod actually melted on a flat plate, or in a groove.

In the first three methods it is very difficult not to produce strained crystals, which we particularly wished to avoid. Method (*c*) might at first sight seem to avoid this disadvantage, but actually it does not, judging from the results of Boas and Schmid(1), who found that the behaviour of their crystals depended markedly upon the rate of withdrawal of the rod; the slower the growth the smaller being the critical shear stress. As regards (*d*), in one method, used by Kapitza(6) for bismuth, the rod of metal is placed on a copper plate in which a temperature-gradient is produced by heating one end electrically. The rod is melted, and maintains a cylindrical form due to an oxide coating. Crystallization is then produced by slowly diminishing the heating current. In the method used by Goetz(7) the metal, once more bismuth, is actually melted in a rectangular trough of graphite, arranged with one edge lowermost, so that the rod has an approximately triangular cross-section. A flow of hydrogen is maintained to regulate the thickness of the oxide coat, and the graphite trough, enclosed in an evacuated quartz tube, is slowly drawn through a furnace.

A disadvantage of Kapitza's method is the need of a thick oxide coat, while in Goetz's method the rod produced has an awkward cross-section, especially from the point of view of quantitative measurements of the slip bands.

The method which we have used avoids the thick oxide film, the odd (triangular) cross-section and the possible mechanical disturbances of the crystal due to its motion through the furnace. The loose wire is sealed in a vacuum (about 0·01 mm. of mercury) in a baked out glass capillary tube, which is about twice the diameter of the wire itself. An oxide-free wire so supported can be heated above its melting point and still retain its cylindrical form, except at the ends, where it may run into globules. If melted on a plane surface, it runs entirely into such globules, so that the stability is imparted by the curved solid surface on which it rests.

The crystallization is effected by means of a travelling temperature-gradient. This can be obtained either by using a horizontal furnace with several separate windings (seven, in our case) enclosing the whole length of the tube, or by a very small travelling furnace containing only a short section of the wire at a time. The actual scheme of shunts used with the large furnace is shown in figure 1: by a suitable adjustment of the various resistances it is possible to obtain initially a temperature uniform to within a degree or so all along the furnace. The temperature is measured by means of a thermocouple consisting of two wires, arranged so as to lie in a straight line along the middle of the furnace, as shown in figure 1*a*, *J* being the hot junction. The ends *A* and *B* pass to two cold junctions. The wires are held in a frame *PDQ*, with an indicator at *D*, opposite *J*, by means of which the positions of the hot junction can be read off on a scale. The whole furnace having been adjusted to a temperature of about 15° C. above the melting point, the first section of the winding is short-circuited by means of a key *S*, which produces a steep gradient at the end of the furnace. The resistance R_3 is then gradually diminished by moving the contact of the rheostat at a constant rate, through the agency of a slow-motion geared electric motor. By careful adjustment of the rheostat *R* and of the speed of the motor a constant temperature-gradient and velocity of crystallization can be ensured during the solidification of the whole wire.

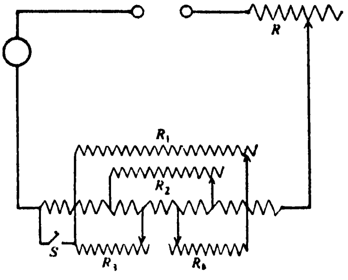

Figure 1.

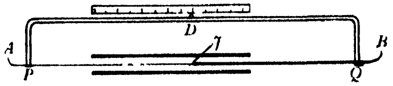

Figure 1*a*.

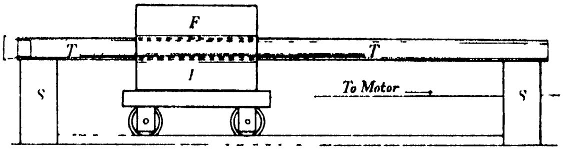

Figure 2.

The method generally adopted, however, is that of the small travelling furnace, which involves the melting of only a short section of the wire at a time (figure 2). Small tubes, each containing a wire, are placed in a hard glass tube of about 1·2 cm. internal diameter which is supported horizontally: the furnace, which fits the tube loosely, is drawn along rails by a slow-motion electric motor.* To ensure steadiness of temperature, the heating current is supplied by accumulators. It is found that, within wide limits, the temperature at a point in the tube depends only on the distance of the furnace from that point, so that a record of the temperature at one point, taken during the whole travel of the furnace, also provides a picture of the distribution of temperature along the tube at any fixed moment. The temperature at one point only was therefore measured with a thermocouple. The temperature-gradient at the point where the wire is melted is controllable; the hotter the furnace the steeper the gradient at the melting point.

---

* This type of instrument, consisting of an ordinary motor provided with heavy reduction gearing, is commercially available, having been designed for slow rotations in shop display.

§3. CONDITIONS GOVERNING THE GROWTH OF SINGLE-CRYSTAL WIRES

In order that the molten wire may solidify as a single crystal it is necessary that the crystallization shall take place over a surface which moves along at the same rate as the furnace. Now the temperature-gradient in the wire near to the surface of crystallization is not uniform or of the same form as that in the surrounding glass tube. It suffers a discontinuity at the surface of solidification, its value being lower in the liquid portion than in the surrounding tube and greater in the solid portion, figure 3. This discontinuity is produced by the liberation of the latent heat of fusion of the metal and the difference between the thermal conductivities of the solid and liquid phases. Since the gradient in the liquid can never assume negative values, there is a minimum value for the gradient in the solid at the melting point. If the gradient in the surrounding tube is too low for this to be attained, solidification has to take place over a finite length of the wire which is at the temperature of the melting point, some of the latent heat being carried away by radiation and conduc-

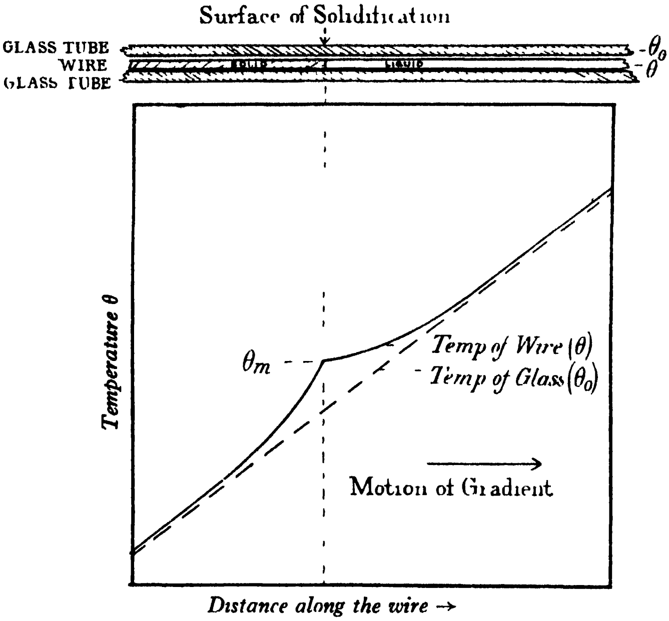

Figure 3.

tion from the surface. In such circumstances crystallization takes place simultaneously at a number of centres, so that growth of single crystals is impossible. By making arbitrary simplifying assumptions, such as uniformity of temperature-gradient in the containing tube, an expression was worked out for the temperature-gradient in the liquid phase. This leads to the condition that, for successful growth,

$$G/V > \frac{1}{1+\sqrt{(K_1/K_2)}}\frac{L}{K_1},$$

where G is the temperature-gradient in the containing tube, V the velocity of travel, K_1, K_2 the thermal conductivities of solid and liquid metal, and L the latent heat per unit volume of the solid. When the numerical values of the constants are inserted we find that G/V must exceed 0·15 deg. hr./cm.^{2} While it has been found experimentally that G/V is the controlling factor for good single-crystal growth, the critical value with our disposition was found experimentally to be about ten or more times as great as that calculated. Since many arbitrary assumptions are made in deriving the formula which, judging from this result, are not justified, the actual deduction is not given here.

The experimental results giving the effect of the ratio G/V on favourable crystal growth are shown in table 1, from which it will be seen that the percentage of good crystals in a batch increases with the ratio G/V, but not with either G or $1/V$, taken separately. In particular, with $G/V = 1{\cdot}1$ no good crystals were grown. It was also found, however, that the temperature-gradient must not be too large, as is shown by the results given in table 2, where the ratio G/V has a favourable value through-

Table 1. Showing the necessity for a high value for the ratio G/V in growing single crystals

Temperature-gradient G (deg./cm.)	Velocity of growth V (cm./hr.)	Ratio G/V	Number of good crystals in a batch of 20
25	5·0	5·0	18
17	4·3	4·0	20
6	2·3	2·6	14
13	5·0	2·6	12
22	11·0	2·0	10
17	11·0	1 6	10
12	11·0	1·1	0

Table 2. Showing the necessity for a low value of the temperature-gradient G in growing single crystals

Temperature-gradient G (deg./cm.)	Velocity of growth V (cm./hr.)	Ratio G/V	Number of good crystals in a batch of 20
35	11·0	3·2	0
30	11·0	2·7	7
28	10·0	2·8	12
26	3·1	8·4	12
25	5·0	5·0	18
17	4·3	4·0	20

out. These two conditions, $G/V \not< 4\cdot0$ deg. hr./cm.², and $G \not> 20$ deg./cm., were found always to give good results. This means in practice that very low velocities of growth are the most favourable.

With our disposition there was a marked tendency for the growth of cadmium crystals for which the angle χ_0, between hexagonal plane and wire axis, was in the neighbourhood of 15°. This is shown in figure 4, which exhibits the results obtained with 105 crystals, the number having a given value of χ_0 being plotted against χ_0. The reason for this has not been worked out, but it may well lie in the difference of thermal conductivity in, and perpendicular to, the hexagonal plane.

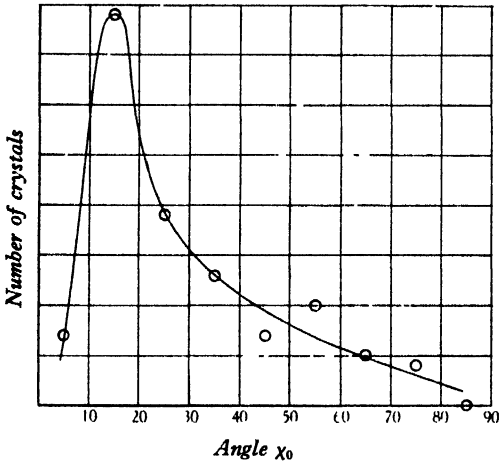

Figure 4.

Very little contamination of the metal occurs in the preparation of crystals by our method. The purest metal used in the course of the work described below was Hilger spectroscopically standardized cadmium, laboratory no. 8961. After a number of rods had been cast and converted into single crystals they were submitted to Messrs Adam Hilger for a second spectroscopic analysis. The estimated amounts of impurity in the original metal and in the finished crystals, as given by the firm, are shown in table 3.

Table 3. Number of parts of impurity present in a million parts of cadmium

Impurity	Hilger cadmium	Crystals
Bismuth	0·25	0·10
Lead	0·15	0·15
Copper	0·50	0·75
Total ...	0·9	1·0

Another quality of cadmium, which is obtainable in the form of wire, was extensively used in this work. On analysis the cadmium was found to contain as much as 0·11 per cent of lead and 0·03 per cent of zinc. This is referred to throughout this paper as the ***standard cadmium***, to distinguish it from the very pure ***Hilger*** *cadmium*. Attempts to produce single crystals having a still higher content of lead (1 per cent) were repeatedly unsuccessful.

§ 4. THE RECORDING EXTENSOMETER

In studying the deformation of single crystals it is desirable to have an instrument which will record the extension and load continuously, the extension ranging up to several centimetres, and the loads being of the order of 100 grams weight. For this purpose the force acting at any moment is measured by the deflection of a metal beam to which the upper end of the wire is attached, a device which makes it unnecessary to measure the actual load applied, which it is often difficult to observe directly. The very small movement of the upper end of the wire makes it easy to control the application of the load. Polanyi and others$^{(8, 9)}$ have already described an extension apparatus which employs the bending of a steel beam to measure the force. Our instrument is simpler in construction, and records automatically.

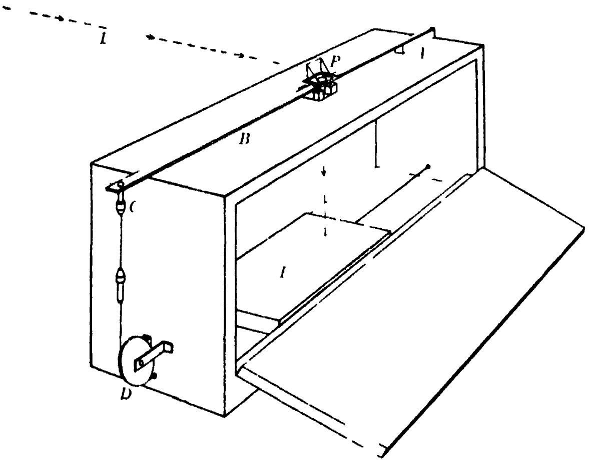

Figure 5.

The beam consists of a brass strip *ABC*, figure 5, measuring 45 × 1·2 × 0·4 cm. and fixed firmly at the end *A* to the top of a stout wooden box. The free end of the beam, which projects about 5 cm. beyond the end of the box, carries a pin-chuck *C*, which holds the upper end of the crystal wire. A second pin-chuck, attached to the lower end of the wire, is pulled down by a fine flexible wire, which passes round the pulley *D*, horizontally through the box by way of two fine holes, and finally over a second pulley, so that tension can be applied by a system of weights. Inside the box the wire is attached to a float *F*, which is carried by a shallow mercury bath. A narrow strip at the bottom retains this mercury, the rest of the opening being closed by a light-tight lid, shown open in figure 5.

The float *F* carries a piece of sensitized paper. On the strip *ABC* at *P* rests one leg of an optical lever, the other two legs of which are rounded at the lower end, one being supported in a groove parallel to the strip, and the other in a triangular depression. Both groove and hole are in brass pieces fixed firmly to the box. The frame of the optical lever carries a right-angle prism. A horizontal beam of light from a pointolite lamp and lens is reflected by this prism through a hole in the top of the box down on to the paper carried by the float, where it is brought to a focus. The angle of the beam of light is always adjusted so that, when the load is increased, for the mean position of the prism the downward beam is truly vertical: this minimizes the deviation from a linear relationship between force and displacement of light-spot. When the end of the wire is loaded, the travel of the float is equal to the extension of the wire, allowance being made for the small elastic yield at the end of the beam, while the displacement of the light-spot measures the applied force. Owing to this yield there is a travel of the float, proportional to the load, even supposing the wire not to stretch at all, and on this account the axes of force and displacement are slightly oblique (see figure 7). For this reason, the single crystal is replaced after the experiment by a practically inextensible polycrystalline wire. A continuously increasing load is then applied, so that the oblique force axis is traced out on the paper. By applying known loads, spots on the paper are then obtained, from which a calibration curve, giving the displacement of the light-spot corresponding to a given load, can be prepared. This turns out to be accurately linear. A displacement of 1 cm. on the paper corresponds to a load of 40 g. wt., and loads up to 300 g. wt. can be used.

The tension is usually applied by a float carried by water in a jar, the level being continuously lowered by a syphon. Although it would be possible, by adjusting the form of the float, to obtain a practically constant rate of extension, this is not worth doing, as it does not ensure that the rate of geometrical glide shall be constant. For more rapid extension it is convenient to let water pass into a light can hanging from the hook: for still more rapid extension, lasting a few seconds, a weight can be applied by withdrawing the hand that holds it. The question of the effect of varying the rate is discussed in § 8, where it is shown that, although gross variations of rate have an important effect, variations of several tens per cent make little difference, so that a precise control is superfluous.

§ 5. DIFFERENT TYPES OF EXTENSION

The general behaviour of hexagonal single crystals under stress has often been described. The glide plane is the hexagonal plane, and the glide direction any one of the digonal axes, the operative one being that lying nearest to the projection of the axis of the wire on the glide plane. Glide takes place when the shear stress per unit area of glide plane, resolved in the direction of glide, attains a critical value. There are, however, various ways in which glide of this kind can manifest itself.

Omitting for the moment the question of double glide and of twinning, we have two main types of extension, due to simple glide. In the one type the wire thins down uniformly along the whole length: in the other type considerable glide takes place locally, over a limited length, before the rest of the wire has extended markedly. In the latter case, as extension proceeds, local thinning, which is accompanied by the usual rotation of the glide planes, ceases, and the adjacent portions of the wire begin to slip. Thus the two discontinuities between the extended and unextended portions of the wire slowly move outwards until they reach the ends, when the wire is uniformly thinned. After this, further extension takes place in a uniform manner. This process has already been described by Boas and Schmid(1). When the glide plane makes a large angle with the direction of pull a still more marked local extension can occur, which consists of a sharply defined glide packet, making a sharp angle with the main wire, like an elbow in a stove pipe, as at (1) in the plate. A picture of this has been given by Boas and Schmid(10), but the phenomenon has not hitherto been systematically discussed.

The cause of the different types of extension lies in the relative importance of the geometrical increase of resolved shear stress and the physical hardening. Owing to the rotation of the planes the resolved shear stress increases during glide. Supposing that the axis of the extended portion coincides with the direction of tension (which, owing to flexual glide, *Biegegleitung*, will be the case when the extended portion is not too short), then

$$d=\frac{l}{l_0}=\frac{\sin\chi_0}{\sin\chi},$$

where l_0 and l are respectively the initial and stretched lengths of the extended portion, to which correspond the angles χ_0 and χ made by the glide planes with the direction of tension. The amount of glide a, defined as the relative displacement of glide planes unit distance apart, is given by

$$a=\frac{1}{\sin\chi_0}\{\sqrt{(d^2-\sin^2\chi_0)}-\cos\chi_0\} \qquad \ldots\ldots(1),$$

if the direction of glide coincides with the projection of the wire axis on the glide plane. (Owing to the three equivalent possible glide directions, this assumption cannot be far from the fact.) Further, with this assumption, the resolved shear stress S is given by

$$S=\frac{W_0\sin\chi_0}{d}\sqrt{(d^2-\sin^2\chi_0)} \qquad \ldots\ldots(2),$$

where W_0 is the load per unit normal cross-section of the unstretched wire. From (1) and (2) a relation between S and a can be worked out for any given value of χ_0. Curves showing this relation for various values of χ_0 are shown in figure 6.

In the same figure is given the experimental hardening curve *AE*, connecting resolved shear stress with glide. This curve depends somewhat on the rate of extension; see figure 9, from which the curve is taken. Figure 6 corresponds to a rate of increase of shear stress of 0·0204 g. wt. per mm.^{2} per sec.

The curves of geometrical increase of stress are given for values of W_0 that correspond to the critical shear stress in each case. It will be seen at once that for small values of χ_0 the slopes of the geometrical hardening curves are less than that of the physical hardening curve, which means that the extension is stable, in the sense that any local slip leads to hardening that will stop the slip until the load is increased. It follows that the wire will extend uniformly. For values of χ_0 greater

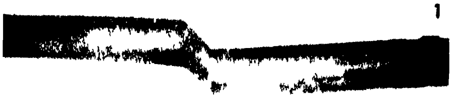
1

× 10

× 25

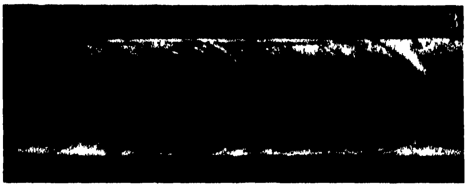
3

× 25

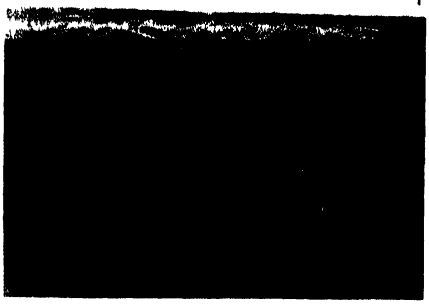
4

× 200

5

× 25

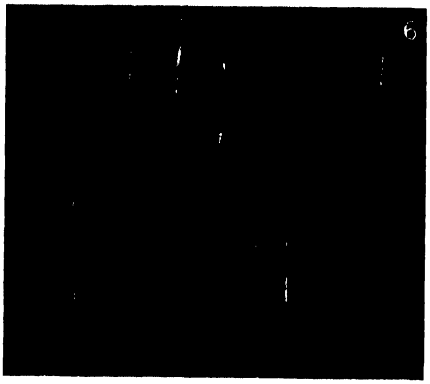
6

× 800

than about 35°, however, the geometrical increase of critical shear stress exceeds the physical hardening: the process is unstable, and any local glide will continue until a point is reached corresponding to the intersection of the two curves (i.e. at a glide about 2·6 for an initial angle of 60°). Owing to the flexure of the planes at the junction at the slipped and the unslipped portions the effect is rounded off if the angle is not very large (e.g. 45° or 50°). If, however, the angle approaches 90° (say 70° or 80°), the geometrical softening and consequent instability is so great that the stove-pipe effect is produced.

The curves of figure 6 assume that the axis of the wire where glide has taken place lies in the direction of tension. This is, of course, not the case with short glide packets. At first sight the wire to either side of the glide packet at (1) in the plate appears to be straight, and the glide to have taken place without rotation. Actually each portion of the wire has bent, so as to bring the axes of the two end portions of the wire, which arc outside the picture, into a straight line, lying along the direction of tension: the bending can be easily verified in the photograph. It is clear that the rotation of the planes in the portion which has experienced glide is far from being sufficient to bring the axis in line with the tension, but there is a small rotation, which is sufficient to produce considerable geometrical softening when, as here, the angle χ_0 is in the neighbourhood of 90°. This is clear from figure 6.

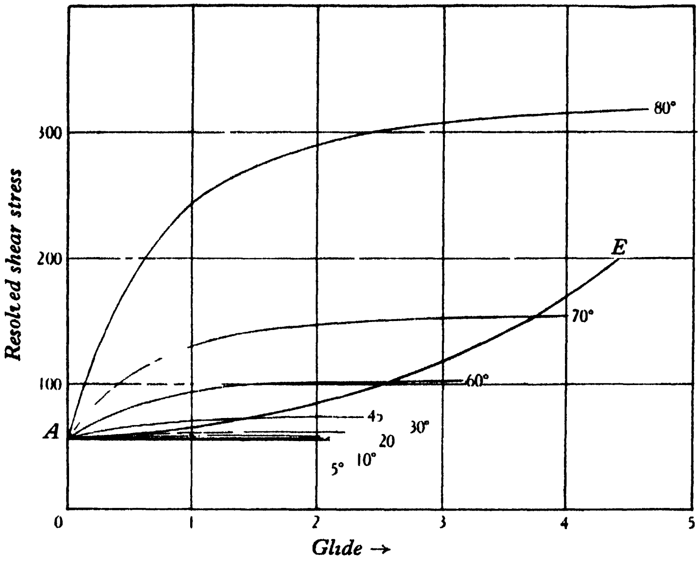

Figure 6.

Curves of the same type have been plotted for a more rapid rate of increase of shear stress, i.e. 8·63 g. wt. per mm.^{2} per sec., but are not shown here, to save space. They show that the stability is here greater, larger angles being required to produce local glide. This is an observed fact: in particular wires rapidly pulled with the fingers generally give a continuous distribution of glide, even with angles that give the discontinuous type at low rates of stretch.

When local glide takes place it invalidates conclusions drawn from the {shear-stress, glide} relation. Figure 7 shows a trace for a wire which initially showed local glide. The linear drop in the force corresponds to the local thinning, the extension under nearly constant stress to the passage of the discontinuities along the wire, and the final phase of hardening to further extension after the wire has become uniform from end to end.

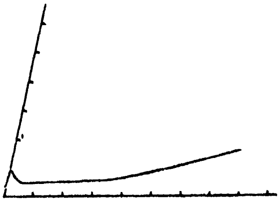

Figure 7.

A particular type of double glide has been observed with cadmium. Although there is only one set of glide planes, there are three equivalent glide directions. In one case two of these were equally favourable, and glide took place in small sections, alternately with one and with the other direction, producing the striking appearance shown at (2) in the plate.

§ 6. THE LAW OF RESOLVED SHEAR STRESS

The crystals prepared by the method described above show a very consistent mechanical behaviour, wires with the same orientation of the crystal axes giving the same mechanical strength. In particular, annealing the wires for either a short or a long period produces no change in mechanical behaviour, which points to a very stable condition. This uniform behaviour seems to offer a favourable opportunity of verifying the law of resolved shear stress to a higher degree of accuracy than has hitherto been possible. According to this law, glide begins in a crystal when

$$\frac{F}{A}\sin\chi_0\cos\lambda_0 = S_0 \qquad \ldots\ldots(3),$$

F being the load, *A* the area of normal cross-section, and λ_0 the initial angle between the glide direction and the wire axis, while S_0 is a constant known as the *critical shear stress*.

The values obtained for the load required to produce glide depend somewhat upon the initial rate of glide which results$^{(11)}$. A particular rate (1 per cent per second) was therefore selected, and automatic records of extension against load were made for rates of increase of load which gave an initial rate of glide of this order. Actually, a short period of stretch occurs before the rate of glide becomes uniform, but since this is very small and the corresponding hardening is negligible, it is permissible to take the load corresponding to the point at which the rate first becomes uniform. The orientation of the glide plane and of the glide direction were determined by an optical method described elsewhere$^{(12)}$, and in this way the angle α between the glide direction and the projection of the axis of the wire upon the glide plane was found.

Since $\cos\lambda_0 = \cos\chi_0\cos\alpha$, equation (3) may be written

$$\frac{F}{A}\cos\alpha = \frac{2S_0}{\sin 2\chi_0} \qquad \ldots\ldots(4).$$

It may be noted that α cannot be greater than 30°, so that $\cos\alpha$ is not far from unity. In figure 8 the experimental points for the standard cadmium, recorded in the following table, are exhibited in a plot of $F\cos\alpha/A$ against χ_0. The curve represents the theoretical equation (4), with the value $S_0 = 55{\cdot}5$ g. wt./mm^2. It will be seen that the agreement is remarkably close. The value of the critical shear stress calculated for each crystal is shown in table 4. Taking the average of the two extreme values at each end of the table, a variation of the normal tension $N = (F/A)\sin^2\chi_0$

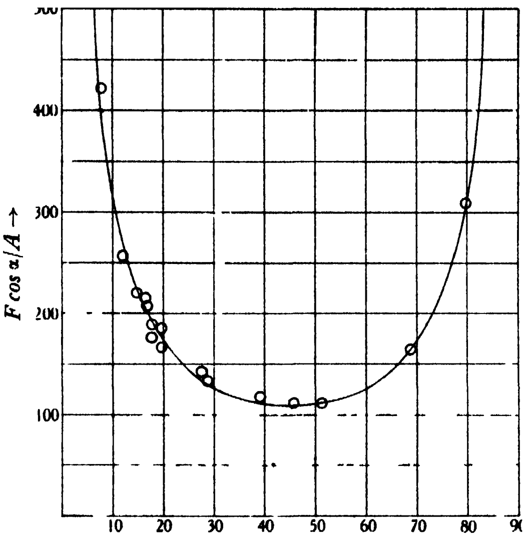

Figure 8.

Table 4. Critical shear stress for standard cadmium (0·11 per cent lead, 0·03 per cent zinc). Rate of glide, 1 per cent per second

Area (mm^2)	Force (g. wt.)	χ_0	α	$\dfrac{F\cos\alpha}{A}$	S_0 (g. wt./mm^2)
0·172	53·2	79·9	6·7	308	52·9
0·170	28·0	68·8	0·0	164	55·8
0·1835	21·8	51·3	20·6	111	54·3
0·1825	22·5	45·7	25·2	112	55·8
0·175	23·8	39·1	30·0	118	57·6
0·181	24·5	28·6	11·0	133	55·9
0·160	24·5	27·5	23·0	141	57·6
0·182	35·9	19·5	19·2	186	58·5
0·185	35·2	19·4	30·0	165	51·7
0·162	30·0	17·8	19·1	175	50·9
0·191	37·2	17·7	15·4	188	54·3
0·171	38·0	16·7	21·4	207	56·8
0·170	39·0	16·4	20·0	215	58·2
0·181	41·0	14·6	14·0	220	56·0
0·179	46·0	11·8	0·0	257	51·5
0·177	75·5	8·2	12·4	422	58·7
				Average value	55·4

from 215 to 10 g. wt./mm.^{2} does not affect the critical shear stress by 2 per cent, which is, of course, well within experimental error. This is probably the most accurate verification of this independence.

It should be mentioned that the critical shear stress for the pure Hilger cadmium is about half this value for the standard cadmium, viz. 26·5 g. wt./mm.^{2} at the same rate of glide.

§7. CRITICAL SHEAR STRESS AND BECKER'S FORMULA

The value for the critical shear stress was obtained by increasing the stress uniformly and noting the value at which plastic yield began, which, as stated in § 6, was found to depend somewhat upon the initial rate of glide. One of us has already published a note on this point(11), and given a curve connecting the critical shear stress with this initial rate: the variation is not great, a tenfold increase of rate changing the critical shear stress by a matter of some 20 per cent only, with the purest cadmium.

The curves suggest some form of logarithmic relation, with log u as a simple function of S_0, the critical shear stress, u being the rate of glide. Such a relation is given by Becker's formula(13, 14),

$$u = Ce^{-V(S_0' - S_0)^2/2GkT} \qquad \ldots\ldots(5),$$

where S_0' is the critical shear stress in the absence of thermal fluctuations, i.e. at absolute zero, S_0 is the actual shear stress, G is the modulus of shear elasticity, k and T have their usual significance, and V is a small volume within which the glide is considered as taking place. Orowan considers that for S_0' and S_0, the macroscopic or experimentally observed values, should be substituted values q times as great, to represent the values in the neighbourhood of the sharp edge of a local crack (*Kerbstelle*), but this clearly contemplates the jump always taking place in a volume V', which is very small compared with the average volume V pertaining to one crack. V is the total volume divided by the number of cracks. To find V, in this latter sense, it seems justifiable to take q equal to 1.

The curve given in Roscoe's paper(11) for Hilger's pure cadmium is well fitted by

$$u = 55e^{-\cdot 00715\,(61\cdot 2 - S_0)^2},$$

u being given as the fractional amount of glide per second; the value 61·2 g./mm.^{2} for S_0' compares well with the 80 g./mm.^{2} obtained by Boas and Schmid(9) at the temperature of liquid hydrogen, considering that we were working with a different specimen of cadmium, and that small impurities have a large effect, as we have established. It may be noted that this formula gives for $S_0 = 17$, 15 and 13 rates of, respectively, 1 per cent glide per 4 minutes, per 13 minutes and per hour. The rate of 1 per cent per hour is a convenient value to adopt as an arbitrary, extremely slow rate, and accordingly we may take $S_0 = 13$ as the critical shear stress.

Since $G = 2 \times 10^{11}$ dynes/cm^2 and $kT = 4 \times 10^{-14}$ erg approximately, we have

$$\frac{q^2 V}{2GkT} = 0{\cdot}00715 \times 10^{-10}\,(\text{dyne/cm}^2)^{-2}$$

or $$q^2 V = 11{\cdot}4 \times 10^{-15}$$

which, taking $q = 1$, gives $V = 11{\cdot}4 \times 10^{-15}$

or $$V^{\frac{1}{3}} = 2{\cdot}3 \times 10^{-5}\ \text{cm}.$$

This is about the value found by Straumanis⁽¹⁵⁾ for the spacing of his layer structure in cadmium crystals, revealed by deposition from the vapour, viz. 8×10^{-5} cm.

§ 8. HARDENING AND RECOVERY

Polanyi and Schmid⁽¹⁶⁾ and Haase and Schmid⁽¹⁷⁾ have carried out experiments on the hardening and recovery of crystals of zinc, tin and bismuth. The former dealt with very small extensions only, of the order of 1 per cent, but the latter extended the considerations to extensions of the order of 200 per cent in the case of zinc. In particular they obtained curves of shear stress against extension at very different rates of extension, the wires being uniformly extended in the Polanyi apparatus. They found that the form of the {shear stress, extension} curve depends upon the rate, the extension corresponding to a given shear stress being greater the slower the rate of extension.

Similar results obtained in the present work on cadmium single crystals are shown in figure 9. The hardening curves I, II and III are the experimental results for the standard cadmium, the curves V and VI for the Hilger cadmium. Each curve represents the mean result for four crystals, and the corresponding rates of application of stress are given beneath the figure, as in these experiments the stress, not the extension, was increased roughly as a linear function of the time. In general the weight was a float sustained in a vessel from which water was withdrawn at a constant rate: strictly speaking this means a uniform increase of load with time, not of resolved shear stress, with the result that the application of stress increases somewhat faster at the end than at the beginning of the extension. As will be seen, however, the curves are not very sensitive to change of rate of application: the differences represented by curves I to III and curves V and VI in figure 9 correspond in each case to changes of rate of the order of a hundred-fold. Hence, changes of rate of increase of stress of tens of per cent produce an altogether negligible effect upon the hardening curves. In the case of the fastest rate the weight had to be applied by hand, with a consequent lack of uniformity, but here again the variations of rate involved are not great enough to affect the curve appreciably.

It has already been remarked that the small amounts of impurities in the standard cadmium produce a marked increase in the critical shear stress necessary to start the deformation. The curves of figure 9 show that this increased shear stress is maintained during the early stages of the deformation, but after a considerable amount of glide (say $a = 4$) has occurred the difference between the curves for the two qualities of cadmium becomes much less pronounced. In order to show this point clearly, curves II*a* and IV have been drawn for the standard cadmium at the same rate of stressing as the curves V and VI for the Hilger cadmium, the ordinates for these rates being calculated by interpolation or extrapolation from the experimental curves. The corresponding curves IV and VI approach one another rapidly as the amount of glide becomes great, while the curves II*a* and V approach one another somewhat less rapidly. It appears, therefore, that when the deformation is very large, impurities (lead and zinc) produce little effect upon the shear stress, particularly when the rate of stressing is high. This would seem to indicate that, when considerable glide has taken place, the resistance to gliding is produced by some factor, such as crystal break-up, which is not important in the early stages of hardening.

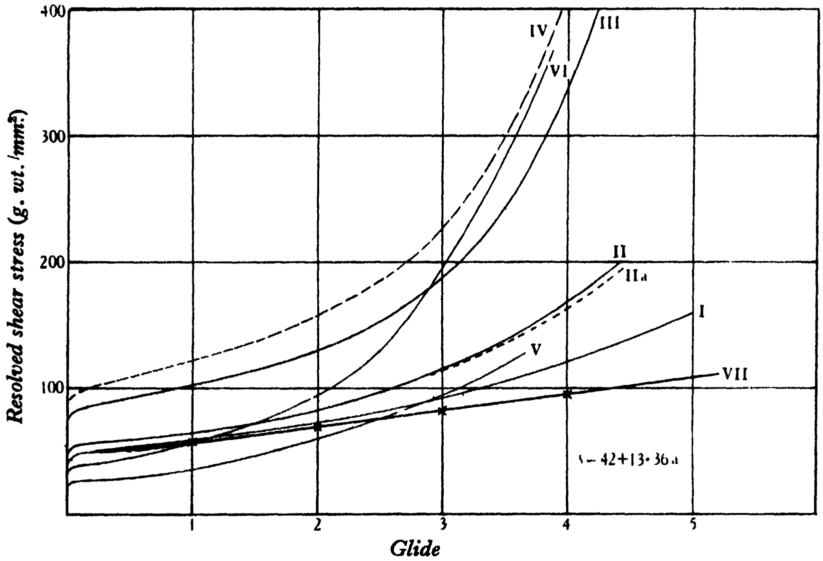

Figure 9. I, II, II*a*, III, IV, our standard cadmium, at rates of increase of shear stress 0·00055, 0·0204, 0·0174, 8·63 and 50·8 g. wt. per mm² per sec. respectively. II*a* and IV are obtained by interpolation, for comparison with Hilger cadmium. V, VI, Hilger's spectroscopically pure cadmium, at rates 0·0174 and 50·8 respectively. VII, standard cadmium, extrapolated to zero rate.

The dependence of the hardening curves upon the rate of glide or rate of stressing may arise in two different ways which have been carefully distinguished by Orowan$^{(18)}$. Thus Haase and Schmid explain their results by supposing that the low values of the hardening at low rates of stretch are due to a recovery which proceeds simultaneously with the deformation—that is to say they assume that the shear stress is a function of the amount of glide and the time. This is called the "static" conception by Orowan, as opposed to the "dynamic" conception, in which the rate of glide is considered as a function both of the stress and of the amount of glide which has taken place, so that flow under constant stress would be possible even in the absence of recovery.

Orowan has put forward the following modification of Becker's formula for the rate of glide in any part of a crystal which is sufficiently large to be considered as homogeneous for glide purposes:

$$u = \frac{da}{dt} = Ce^{-V(R-qS+ba)^2/2GkT},$$

where u is the rate of glide, a the amount of glide, b and C are constants, R represents the theoretical shear stress in the absence of submicroscopic cracks and temperature fluctuations, S is the externally applied shear stress resolved in the direction of glide, G the shear modulus, k Boltzmann's constant, and V a small volume in which there is a probability that the shear stress may be increased locally to the theoretical value by temperature fluctuations. This is effectively Becker's formula for the critical shear stress, equation (5) in § 7, with the addition of the term ba, which represents a hardening assumed to be proportional to the amount of glide.

At constant temperature this equation gives the hardening S against a as a set of parallel straight lines of slope b/q. When the rate of glide da/dt is maintained constant, dS/dt is also constant. If, therefore, Orowan's formula holds, increasing the resolved shear stress at a fixed rate should produce a constant rate of glide, and the hardening curves obtained by increasing the resolved shear stress at different constant rates should be a set of parallel straight lines. Figure 9 shows that this is not the case at high rates of application of stress and large amounts of glide, although the curves for standard cadmium do form a set of approximately straight lines for amounts of glide up to 200 per cent. It should be remarked in this connexion that Orowan's success has been obtained with extensions of a few per cent only. The mechanism of the great and rapid extension of figure 9 must be essentially different from that contemplated by him, for it may be noted that better agreement cannot be obtained by altering the form of the hardening function ba.

If curves be plotted showing S against log (da/dt) for various values of a, we find that S diminishes as da/dt diminishes, the variation becoming exceedingly small at low values of da/dt. S appears to be tending equally to a constant value for large values of a, although constancy is not actually reached. It is possible, however, to extrapolate so as to get the values of S corresponding to different values of a at a rate of, say, 10^{-5} per cent per sec. Such a limiting $\{S, a\}$ curve is shown as VII in figure 9, the crosses representing the extrapolated values, and it will be seen that it is a straight line. It appears, then, that if various stresses be applied, and if in each case sufficient time be allowed for the length to become constant (for a to reach 4, i.e. an extension of 400 per cent, would require over a year at 10^{-5} per cent per sec.), then there is a straight-line relation between S and a. The variation from the straight line at fast rates is in part due to the crystal structure not having time to take up an equilibrium state. As regards the constancy of a at a given S, which appears to be reached after a long time at these slow rates of increase, it will be observed that the highest value of S contemplated in VII, figure 9 (see § 9) is about 100 g. wt. per mm^2, whereas for the lower curve in figure 11 it is 182 g. wt./mm^2

It is remarkable that while the $(S-a)$ curve approaches a limiting form as the rate becomes very small, there is no sign of a limiting form as the rate becomes very large, but rather, as far as our results go, the effect of rate becomes more and more pronounced as the rates are made larger. If the large values of a which correspond to a given S at very low rates of increase of load were due entirely to a time flow, then we should expect smaller and smaller values of a as we increased the rates, but when the rate of load became rapid we should expect to find a limiting value of a corresponding to no flow. It appears, however, that even at high rates an increase of rate still leads to a more rapid rise of the $(S-a)$ curve. This is inexplicable on the static theory.

The reason why, as shown, the Becker-Orowan theory does not apply to these experiments is no doubt to be sought in the rapid rates. The underlying basis of the theory is that within the metal there exists cracks or dislocations in the neighbourhood of which the local stress, produced by the macroscopic load, has nearly the theoretical value. As a result of thermal agitation, the local stress attains from time to time the theoretical value somewhere in the volume V, and glide takes place. The mechanism by which this occurs may be that, put forward by Dehlinger(19), of the propagation of the dislocation. The energy required to raise the stress from S to R is $(R-qS)^2/2G$, if the substance is supposed to be behaving elastically in the neighbourhood of the local irregularity. If, further, each elementary glide yields the same contribution to the macroscopic glide, then there follows at once the formula

$$\log\frac{da}{dt}=\log C-\frac{(R-qS)^2}{2GkT}V \qquad \ldots\ldots(6)$$

$$=\log C-M\,(R/q-S)^2 \text{ if } T \text{ is constant.}$$

The formula appears to hold for certain cases of slow glide, but it clearly cannot hold in extreme cases. If $S=R/q$, for instance, a state which is easily attained, the rate has a maximum value. This is quite contrary to observation and is obviously impossible, so that S must not be taken too large. Another way of reaching the same conclusion is to notice that the theory contemplates static conditions in the neighbourhood of the dislocation, so that elastic strain can be assumed. It is clear that with very rapid glide there is no approach to equilibrium conditions, and the expression for the energy taken in equation (6) is not justified.

To obtain favourable conditions for real recovery we extended a crystal of Hilger cadmium by a very large amount very quickly, the glide being over 300 per cent in 3 sec. When the extension is carried out as rapidly as this, the form of the {stress, glide} curve is insensitive to the exact rate of increase of load, as has already been indicated. After a shear of 334 g. wt./mm.^{2} had been reached the load was taken off for half an hour and the wire was then reloaded to 334 g. wt./mm.^{2} in 3 sec., after which a half-hour period of recovery was again given. This process was repeated, the loading always being carried out in 3 sec. and half an hour allowed for recovery, until the crystal twinned and broke. Figure 10 represents the result. It will be seen that the parts EF, HK, MN, PQ and RS of the {stress, glide} curves are repetitions of the portion BC of the original curve, with the same slope, displaced to the right, so as to correspond to a larger glide in each case. This part, then, represents real recovery, the wire after a period of rest behaving exactly as it did at a lesser glide before rest. The portions *DE*, *GH*, *LM*, *OP*, which represent a spurious recovery due to constant-stress flow in the original curve, become smaller for each successive loading, so that the apparent recovery *QR* tends to be entirely real recovery.

The method of very rapid loading appears to be suitable for the elucidation of the law of hardening and recovery. These experiments serve to establish, then, that while the form of the $(S-a)$ curve is largely influenced by the fact that under the stresses used there is a flow with time, so that the curve depends on the rate, yet there is a large real recovery after even large extension. The separation of the two effects has been clearly effected.

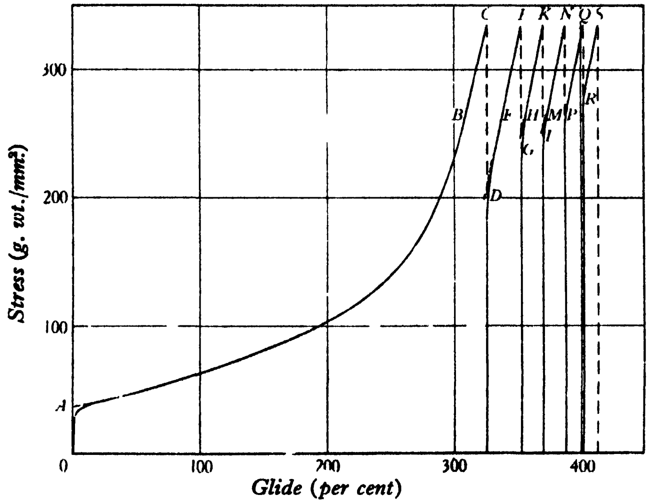

Figure 10. Extension of cadmium single crystal loaded to a stress of 334 g. wt./mm.² in 3 sec. Half-hour recovery intervals.

The position may be summed up as follows. When the rate of glide is very slow, or when the deformation is not very large, the hardening obeys a linear law, and Orowan's theory, considered in conjunction with the idea of recovery, gives an adequate explanation of the dependence of hardening upon rate. With high rates and large extensions another type of hardening appears which is permanent, i.e. has no recovery, although it depends on the rate to a marked extent. This latter type of hardening depends much less upon the presence of small amounts of impurities than does the former type.

§9. FLOW UNDER CONSTANT SHEAR STRESS

When a large load is applied to a single-crystal wire of cadmium, an immediate extension takes place which is followed by a creep continuously decreasing in rapidity, until at last the crystal twins and fractures. With a large load the extension may increase measurably for several weeks, without any sign that a final length is being asymptotically approached.

With a sufficiently large constant load, the glide planes are almost immediately brought so close to the axis of the wire that the resolved shear stress can be treated as constant throughout the flow. The form of the {extension, time} curve is then determined by the rate of flow alone, which is itself a function of the constant stress and the extension. In these experiments a simple method of optical projection, giving a magnification of about 5 times, was used: greater magnification led to no advantage, on account of the jerky nature of the stretch which was then revealed.

The flow curves, figure 11, obtained in this way show a very rapid decrease in the rate of flow u, which, however, exhibits no tendency to become vanishingly small. In fact, when log u is plotted against $1/a$ a straight line results, so that

$$\frac{da}{dt}=u=A.e^{c/a} \qquad \text{......(7).}$$

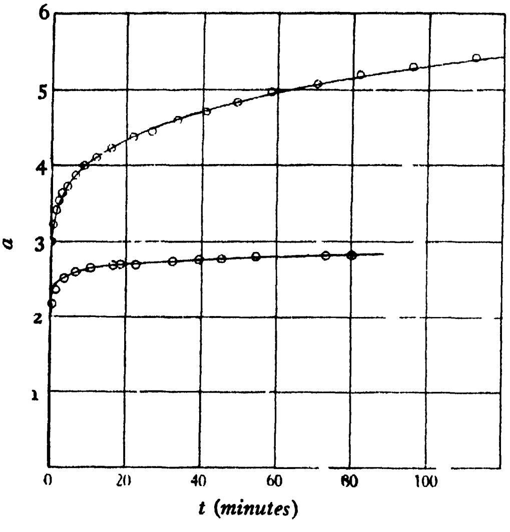

Figure 11.

The points on the curves of figure 11 were obtained with the standard cadmium; Hilger cadmium crystals give the same type of curve. The upper curve corresponds to a shear stress of 282 g. wt./mm.^{2} and the lower to 182 g. wt./mm.^{2} The constants in the above formula come out to be, for the upper curve $A=3{\cdot}27\times10^{-5}$ per min., $c=29{\cdot}0$; and, for the lower curve, $A=4{\cdot}79\times10^{-12}$ per min., $c=64{\cdot}5$.

The following relation is obtained from equation (7):

$$t=\frac{1}{A}\int_0^a e^{-c/a}\,da \qquad \text{......(8).}$$

By using the above constants and calculating the value of this integral for various values of the upper limit, the continuous curves of figure 11 were obtained. The circles, representing the observed values, lie very close to the curves. Other formulae with two constants which were tried gave a very much worse representation.

Equation (7) gives a very different {flow, extension} curve to the Becker-Orowan formula. In particular, when $a=\infty$, u has a finite value, while it should become zero according to the Becker-Orowan formula. It has been shown in § 8 that the latter formula is valid under constant rate of stressing when the rate of stressing is low and the extension small. For large rate and extension, however, there is an abnormal hardening which produces a *lower* value of u than that given by the Becker-Orowan formula. The finite value of u at $a=\infty$ given by equation (7) must therefore be due to a real recovery persisting even at very great extensions. Thus

$$u=\frac{da}{dt}=-\left(\frac{da}{dS}\right)_t\left(\frac{dS}{dt}\right)_a,$$

where $(dS/da)_t$ represents the coefficient of hardening with increasing glide, extrapolated to zero time—corresponding to the b of Orowan's formula, which has been shown in § 8 to be constant—and $-(dS/dt)_a$ represents the true recovery.

§ 10. THE SPACING OF THE SLIP BANDS

The slip bands show irregularity of spacing which has hitherto discouraged measurement$^{(20)}$. With cadmium, slip bands easily visible to the naked eye are seen as soon as a small percentage extension is produced, and become more prominent as extension proceeds. A wire extended by several per cent is shown at (3) on the plate. With a high-power microscope, giving a magnification of 1000, these coarse slip bands resolve themselves into exceedingly close lines, or finer slip bands. This is best seen with the ring type of vertical illumination. With the same methods of observation very close lines have been detected all along the wire, as shown at (4) on the plate. Although a certain regularity in the spacing of the lines is observable at a magnification of 1000, alteration of the illumination brings up a series of still fainter lines between the regularly spaced set. The separation of the planes shown at (4) is about $1{\cdot}5\times10^{-4}$ cm. The separation of the faintest bands detected varies from about 10 to 5×10^{-5} cm., but this limit may be imposed by the resolving-power of the microscope. With great extension the distinction between the different classes of bands becomes more marked: a cadmium wire extended by 400 per cent, with a few very marked bands, is shown at (5). The rest of the wire is covered with fine bands not distinguishable in the photograph.

The most regular results were obtained with lead, where the distinction between prominent and minor bands is very clear. Bands in lead, extended by about 30 per cent are shown at (6); between these are some very much fainter bands not distinguishable in the photograph. This clearly marked nature of the prominent bands encouraged measurement of the separation. Figure 12 shows the distribution of about 120 successive intervals. It will be seen that the form resembles the standard-error curve, with a most probable separation of 17 arbitrary units, which corresponds to a separation (measured normal to the planes) of $4{\cdot}2\mu$.

To see if this spacing had any physical meaning it was measured under a variety of conditions, the diameter of the wire, the temperature at which the extension took place, the rate of extension and the amount of extension being varied. The results are shown in table 5, from which it appears that, within the limits tested, none of the factors has any effect on the spacing. It seems, then, that the spacing is a real property of the metal or, at any rate, of a particular specimen of metal. The effect of impurities in the metal has not been investigated.

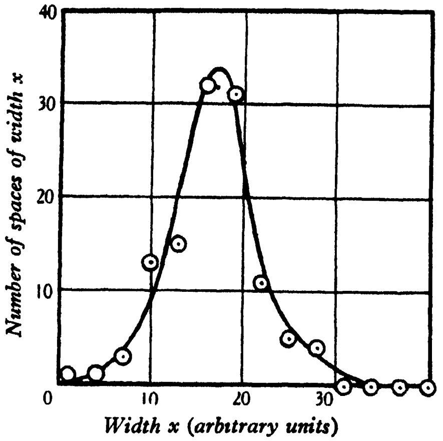

Figure 12.

Table 5. Spacing of glide planes of single crystals of lead

Factor	Magnitude	Mean spacing of glide planes (μ.)
Extension	15 per cent	3·85
	24 ,,	4·27
Rate of deformation	0·001 sec.$^{-1}$	4·31
	0·003 ,,	4·01
	3·0 ,,	4·13
Diameter of wire	0·091 cm.	4·29
	0·045 ,,	4·18
Temperature	15 °C.	4·20
	100 ,,	4·27
		Mean 4·17

In the case of lead an interesting phenomenon was observed which is shown at (6) on the plate. Some of the slip bands did not run completely round the wire, but stopped short opposite one another. This is strongly reminiscent of G. I. Taylor's theory of plastic slip, where he shows that two dislocations of opposite sign will, under stress, move in opposite directions until they come abreast. To make them pass one another the stress has to be increased, and reaches a maximum when the distance by which they overlap equals the separation, measured normally to the path of dislocation. Further increase of stress produces instability, and the dislocations run on indefinitely in opposite directions. Now it is to be observed that in no case were bands overlapping by more than the distance of separation observed, and that, while the ends of the bands are not sufficiently definite for exact measurement, yet the overlap of more widely separated bands is rather more than that of less widely separated bands; see in particular the third, fourth, fifth, sixth and seventh bands from the left in photograph 6 on the plate. This tends to show that the bands are really the paths of dislocations propagated somewhat in the Taylor manner.

§ 11. DISCUSSION OF RESULTS

The results here described do something, it is hoped, to clear up certain obscurities regarding the flow and hardening of single crystals. The preliminary work on the production of strain-free crystals was necessary before a sufficient uniformity of behaviour could be obtained, and the confirmation of the law of resolved shear stress, which is more precise than any previously recorded, seems to show that the crystals were, macroscopically speaking, uniform in structure. It is to be observed that annealing of these crystals, whether for a long or short time, had no effect on their mechanical properties.

As regards the critical shear stress, it has been shown to be dependent on two factors, the initial rate of flow, and the purity of the material. The initial rate can be connected with the critical shear stress by an exponential formula of the Becker type, which gives a finite rate for any shear stress, however small, but nevertheless the form of function is such that the critical shear stress varies extremely slowly with the rate, and an arbitrary small rate of 1 per cent per hour has been selected, which gives $S_0 = 13$ g. wt./mm.^{2} for spectroscopically pure cadmium, which is about one quarter the value given by Schmid⁽²¹⁾ (58 g. wt./cm.^{2}).

In our discussion of hardening we have distinguished the following types: (1) a hardening proportional, with cadmium, to the amount of glide, when the rate of loading tends to zero, although the extension may be considerable. It also holds with high rate, if the extension is very small. This is non-recoverable, and corresponds to a simple case discussed by Orowan⁽²²⁾. (2) With large extensions and high rates of loading we have (*a*) a hardening which increases rapidly with increasing glide and is not subject to recovery, and (*b*) a hardening subject to recovery. The amount of this latter hardening decreases with increasing extension.

We believe that any attempted explanation must take into account the fact that the glide takes place, not uniformly on all equivalent crystallographic planes, but in the limited regions known as glide planes. It has been shown here that in the case of lead, in which definite measurements can be made, the separation of these planes is independent of a wide variation of various physical factors, which points to their having a real significance. The general question is complicated by the different behaviour shown by different metals as regards the appearance of the glide planes. With cadmium, speaking generally, all the planes appear early, and increasing extension takes place by further glide on the planes already developed. With this metal the hardening is, in the simple limiting case where the rate is not involved, proportional to the glide. With aluminium, on the other hand, Yamaguchi⁽²³⁾ has found that new glide planes continually appear between the old as the stretching force is increased, the average distance between the planes being approximately inversely as the force. With this metal a parabolic law of hardening holds, to which G. I. Taylor has directed special attention(24) as a case of particular interest. If, as is here suggested, there is a linear hardening with glide on a single glide plane (which could perhaps be better described as a single glide lamella) in the case where a time flow is not involved, then this law can be readily explained, supposing that the glide planes extend right across the material. For if N is the number of developed glide planes per unit distance, measured normal to the planes, then, according to Yamaguchi

$$N = C(S - S_0),$$

while on our assumption

$$S - S_0 = Bx,$$

where x is the glide in a lamella, B and C being constants.

$$N\,dS = B\Sigma\,dx = B\,da,$$

where a is the total glide, so that

$$C(S - S_0)\,dS = B\,da$$

or

$$S - S_0 = A\sqrt{a},$$

which is Taylor's formula. Whether the different behaviour as regards the appearance of glide planes is governed by the temperature, referred to the melting point, is a question which we hope to investigate later.

As regards the development of glide planes, it seems likely that slip takes place by the propagation of a dislocation from a surface flaw, as illustrated by Orowan(25). That the surface plays a prominent part is illustrated by Roscoe's observations on the large increase of critical shear stress caused by an extremely thin surface film of oxide(11). The propagation of a dislocation, considered as a region of self-strain, has been fully discussed by Taylor, who considers that the travel is stopped by a second series of flaws(24), lying at right angles to the direction of propagation. The exact mechanism of the stoppage is not here considered. It is here assumed, however, that the metal contains, as well as the surface cracks, internal flaws of various degrees of gravity—let us say, for instance, cracks, parallel to the glide planes, of elliptical cross-section and of various radii of greatest curvature—from which dislocations can be propagated. To explain hardening it must be supposed that, with a given force, glide takes place from flaws, which are associated with an enhanced local stress. The regions of high stress are disturbed by the passage of the original dislocation, and, when these are exhausted, flaws where the local stress is not so high can be brought into operation by increasing the force.

This supposes that when a region of dislocation or self-strain approaches flaws of different degrees of severity or local curvatures, the yield tends to take place in the direction of a line joining the region of self-strain to the region of greatest shear stress, that is, towards the most severe flaw, distances being equal. The distribution of stress in such cases has not been worked out, but it may be possible to investigate it by the method of photoelasticity.

Plastic flow can, then, be tentatively explained by considering the visible glide planes as localities of intensive glide, proceeding in the first instance from surface flaws, of the Griffiths type, and involving later less grave local internal flaws. The very marked non-recoverable hardening which takes place under rapid flow may be attributed to the locking action of small fragments of crystal that have rotated. Such localized "crystal break-up", as Gough calls it, has been experimentally proved with aluminium single crystals and with mild steel(26, 27). It has been objected to this view that hard fragments cannot lock soft material, but this objection is based on a misunderstanding. The suggestion is that the general unflawed lattice is strong, but contains flaws which are a source of weakness, from which dislocations are propagated. If the soft regions, which lead to visible glide lamellae, are made hard, the whole crystal becomes hard. When the flow is very slow, so that equilibrium is slowly attained, the exhaustion of first the weak flaws, and then the stronger ones, leads to progressive hardening on the lamellae, but more rapid stressing can lead to actual rotation of fragments, or, in Burgers' terminology(28), local curvatures of glide lamellae. Such rotated crystallites are of unflawed material, and so offer a very effective barrier to the propagation of dislocation. G. I. Taylor(29) has pointed out that, in the case of a face-centred cubic crystal, for instance, however two neighbouring fragments are oriented, the ratio of the values of the components of the maximum resolved shear stress of each crystallite cannot exceed 2 to 1, from which he concludes that rotation cannot lead to much hardening. If, however, the function of the rotated crystallites is to hinder glide proceeding from flaws, then the case considered by Taylor does not apply.

When two of Taylor's dislocations, a positive and a negative, travelling in opposite directions, come opposite to one another there is a turning moment on the substance between them which rises to a maximum: when the normal distance between the paths is very small this moment rises to a high value, and may, it is suggested, lead to the rotation of the crystal fragment.

The recoverable part of the hardening may possibly be connected with the other type of crystal distortion, the existence of which has been proved by Gough and Wood, namely dislocated grains, in which there are changes of direction up to 2°.

The effect of impurity is of some interest. It has been shown that traces of foreign metal increase the critical shear stress considerably, which may be attributed to the impurities segregating to the flaws, and making their edges less sharp. When considerable flow has taken place, however, the behaviour of the contaminated tends to be the same as that of the uncontaminated metal, and this is easily understood if the mechanism of hardening at this stage is mainly that of crystallite rotation.

All these suggestions, some of which have something in common with a theory sketched by Burgers(30), are recognised as being of a tentative nature: further development is postponed in the hope of obtaining more definite experimental evidence.

REFERENCES

(1) Boas, W. and Schmid, E. *Z. Phys.* **54**, 16 (1929); **61**, 767 (1930).
(2) Andrade, E. N. da C. *Phil. Mag.* **27**, 869 (1914).
(3) Carpenter, H. C. H. and Elam, C. F. *Proc. roy. Soc.* A, **100**, 329 (1921).
(4) Tammann, G. *Lehrbuch der Metallographie* (Leipzig, 1923).
Bridgman, P. W. *Proc. Amer. Acad.* **60**, 305 (1925).
Hausser, K. W. and Scholz, P. *Wiss. Veröff. Siemens-Konz.* **5**, 144 (1927).
(5) Czochralski, J. *Z. phys. Chem.* **92**, 219 (1917).
(6) Kapitza. *Proc. roy. Soc.* A, **119**, 358 (1928).
(7) Goetz. *Phys. Rev.* **35**, 193 (1930).
(8) Polanyi. *Z. tech. Phys.* **6**, 121 (1925).
(9) Boas and Schmid. *Z. Phys.* **61**, 767 (1930).
(10) Boas and Schmid. *Z. Phys.* **57**, 575 (1929).
(11) Roscoe, R. *Phil. Mag.* **21**, 399 (1936).
(12) Roscoe, R. and Hutchings, P. J. *Phil. Mag.* **16**, 703 (1933).
(13) Becker, R. *Phys. Z.* **26**, 919 (1925).
(14) Orowan, E. *Z. Phys.* **89**, 605 (1934).
(15) Straumanis, M. *Z. phys. Chem.* B, **13**, 316 (1931).
(16) Polanyi and Schmid. *Z. Phys.* **32**, 684 (1925).
(17) Haase and Schmid. *Z. Phys.* **33**, 413 (1925).
(18) Orowan. *Z. Phys.* **89**, 605, 614 and 634 (1935).
(19) Dehlinger, U. *Ann. Phys., Lpz.*, **2**, 749 (1929).
(20) Schmid and Boas. *Kristallplastizität*, p. 157 (Berlin, 1935).
(21) Schmid. *International Conference on Physics*, **2**, 165 (1934).
(22) Orowan. *Z. Phys.* **89**, 614 (1934).
(23) Yamaguchi. *Inst. Phys. Chem. Res.* Tokio, No. 151, 289 (1928).
(24) Taylor, G. I. *Proc. roy. Soc.* A, **145**, 362 and 388 (1934).
(25) Orowan. *Schweizer Arch.* Heft 7, **5**, figure 7 (1935).
(26) Taylor, G. I. and Gough, H. J. quoted in *Marburg Lecture*, p. 51 (1933).
(27) Gough, H. J. and Wood, W. A. *Proc. roy. Soc.* A, **154**, 510 (1936).
(28) Burgers, W. G. *International Conference on Physics*, **2**, 139 (1934).
(29) Taylor, G. I. *Trans. Faraday Soc.* **24**, 121 (1928).
(30) Burgers, W. G. *Report on Viscosity and Plasticity* (Academy of Sciences, Amsterdam, 1935).

DISCUSSION

Prof. W. **Wilson** asked whether there is an elastic region within which small stresses fail to produce permanent deformation or glide, and what factors determine the thickness of the glide bands.

Prof. A. F. C. **Pollard** asked whether ring illumination, as distinct from critical illumination, had been used for illustration no. 6 in the plate. A photomicrograph with critical illumination might yield an even more beautiful result. Presumably the lines in the illustration were the ill-defined images of the exposed and narrow portions of the slip planes. The two boundaries of such a portion might be resolvable in some places on the crystal surface. The appearance of the two lines in the bottom left-hand corner of the illustration seemed to indicate this.

Dr B. **Chalmers**. It would be interesting to know whether the authors attach any importance to the bend that occurs in the {stress, glide} curves of figures 9 and 10 in the region corresponding to the early stages of glide. It appears that this gradual commencement of glide may be connected with the apparent variation of critical shear stress with rate of application of the stress. The critical shear stress, if defined as the smallest stress that causes glide, cannot depend on the rate of stressing, although its measurement may depend on the sensitivity of the extensometer; if, however, it is defined as the stress that will produce glide at some arbitrary speed, then it will of course depend on this speed.

I should like to know whether the true critical shear stress, as calculated for slow rates, bears any relation to the stress at the first observable point of departure of the {stress, glide} line from the stress axis.

I should like to mention in connexion with the statement on p. 170 of the paper about the jerky nature of the stretch that in experiments on single crystals of tin, in which much higher magnification but slower rates were used, I have detected no jerkiness or irregularity at all.

AUTHORS' reply. In reply to Prof. W. Wilson: There may be an elastic region within which small stresses fail to produce permanent deformation, but our methods were not designed to deal with stresses and strains as minute as those here involved. There is no satisfactory explanation of the observed separation of the regions of intensive glide.

In reply to Prof. A. F. Pollard: The method of critical illumination has been applied to the observation of slip bands, but, in our hands, did not appear to give results sensibly better than those obtained with the ring illumination. In view of some work on slip bands in solid mercury carried out by Dr K. M. Greenland (shortly to be published) in the laboratory at University College it would appear possible that the surface exhibits continuous curvature across the boundary, and that the double line represents reflections from the two curved edges of the band.

In reply to Dr B. Chalmers: Dr Chalmers remarks on the dependence of critical shear stress on rate of glide represent the point of view that we have endeavoured to put forward in the paper. The critical shear stress is defined not as the smallest stress which causes glide, since this is indefinite if our views are correct, but as the stress which causes glide to set in at a given rate. The rate chosen as characteristic is that corresponding to the approximately straight portion of the {stress, glide} curve, which sets in almost immediately after loading (see Figures 9 and 10), and so corresponds to the extrapolated point A in Figure 10. As we have pointed out, the stress is not sensitive to small changes of rate, so that the latter need not be accurately determined. The jerky nature of the deformation which occurred when the crystals were stretched under constant stress may possibly be due to slight vibration, due to chance causes, of the support to which the upper end of the crystals were affixed, which would produce fluctuation in the stress acting upon the crystals.

X-RAY INVESTIGATION OF PURE IRON-NICKEL ALLOYS. PART 2: THERMAL EXPANSION OF SOME FURTHER ALLOYS

By Professor E. A. OWEN, M.A., D.Sc., F.Inst.P.

AND

E. L. YATES, M.Sc., Ph.D., A.Inst.P.

University College of North Wales, Bangor

ABSTRACT. The lattice parameters of three iron-nickel alloys containing respectively 41·1, 32·2 and 24·2 per cent of nickel by weight have been measured at different temperatures. The alloys had to be carefully heat-treated before any spectra could be obtained with them. From the relations between parameter-value and temperature, curves were obtained showing how the coefficient of thermal expansion varied with temperature. The two alloys containing 41·1 and 32·2 per cent of nickel yielded curves which showed that the coefficient of thermal expansion had a somewhat low value at low temperatures. At a particular temperature the value increased suddenly to another value, which on further rise of temperature remained almost constant. These results are in agreement with the results obtained by other observers by other methods of measurement.

The expansion curve of an alloy containing 24·2 per cent of nickel showed the ordinary thermal-hysteresis effect found with the irreversible alloys. The thermal expansion of the components α and γ were measured. The mean atomic volume in the α phase is greater than the mean atomic volume in the γ phase at the same temperature. By the aid of these measurements it was possible to explain the form of the expansion curve obtained with a rod of the material, which shows a contraction when the α phase transforms to the γ phase.

Values are given for the lattice parameters of the pure α and γ phases at different temperatures. The coefficient of thermal expansion of the body-centred α phase is approximately $8{\cdot}2 \times 10^{-6}$ at 0° C. and $14{\cdot}0 \times 10^{-6}$ at 200° C., and that of the face-centred γ and γ' phases is $17{\cdot}5 \times 10^{-6}$ between 0° C. and 630° C.

§ 1. INTRODUCTORY

In a previous paper[1] iron-nickel alloys in the γ' phase containing high percentages of nickel were examined. Two of the alloys dealt with in this paper are also in the γ' phase but contain more iron than those previously considered, being not far removed from the iron-rich boundary of the γ' region. They are of interest because they have compositions on either side of that of invar, which contains about 36 per cent of nickel. The third alloy is in the region which is usually regarded as a mixed phase of α and γ'. It was of particular interest to study the thermal expansion of this alloy by the X-ray method, in view of the somewhat anomalous behaviour of alloys in this region of composition, as observed by Chevenard and others in measurements of their thermal expansions by the ordinary methods.

The alloys were marked 43, 32 and 24 and their compositions are given in table 1.

Table 1. Composition of alloys

Alloy	Nickel content	
	Weight (per cent)	Atoms (per cent)
43	42·7	41·7
32	32·2	31·1
24	24·2	23·3

§ 2. HEAT TREATMENT OF THE ALLOYS

The general experimental procedure was similar to that adopted with the alloys considered in the previous paper, but individual attention had to be given to the heat treatment of the alloys. It was necessary, as with the other alloys, to cool them very slowly after they had been annealed either in lump or in powder form. The heat treatments to which the alloys were submitted are summarized in table 2.

Table 2. Heat treatment of alloys

Alloy no.	Specimen no.	Lump annealing			Powder annealing		
		Temperature (° C.)	Time (days)	Period of cooling (days)	Temperature (° C.)	Time (hours)	Period of cooling (hours)
43	1	800	10	4½	600	14	48
	2	800	10	4½	600	12	129
32	1	800	12	4½	600	14	48
	2	800	12	4½	600	12	129
	3	800	12	4½	600	15	225
24	1	—	—	—	500	1	—
	2	—	—	—	300	24	7
	3	—	—	—	900	1	48
	4	—	—	—	600	15	Quenched
	5	800	12	4½	600	14	48
	6	800	21½	6	600	17	384

§ 3. RESULTS

Alloy 43. Little difficulty was experienced with this alloy in obtaining good reflections Powder cooled from 600° C. in two days gave lines as well defined as those obtained with a specimen of the alloy cooled from the same temperature in five days. Cobalt* radiation was found suitable for use with this alloy as the lines were registered on the film in positions corresponding to the biggest glancing angle possible with the camera and therefore were capable of high accuracy of measurement. This radiation also yielded photographs with clear background, thus greatly facilitating the measurement of the lines. Exposures at temperatures above 500° C.

---

* The wave-lengths taken were Cobalt $K\alpha_1$ (1·78529) and Cobalt $K\alpha_2$ (1·78919).

gave rather weak lines which would have been difficult to measure with high accuracy were it not that the background was comparatively free from fogging.

The alloy possessed a face-centred cubic structure and the lines measured in the photographs were doublets reflected from the (400) planes. The results of the measurements are summarized in table 3; the letters (*c*) and (*h*) which appear in this table have the same significance as they had in our previous paper$^{(1)}$.

Table 3. Lattice parameters of alloy 43 at different temperatures

Film no.	Temperature (° C.)	Lattice parameter (A.)	Film no.	Temperature (° C.)	Lattice parameter (A.)
E 398	10	$3{\cdot}5876_5$	E 404	401	$3{\cdot}5958_2$
E 419 & E 423	12	$3{\cdot}5878_6$	E 415	422	$3{\cdot}5967_1$
E 411 & E 416	13	$3{\cdot}5879_4$	E 421	446 (*h*)	$3{\cdot}5975_6$
E 410, E 429, E 434	14	$3{\cdot}5878_4$	E 435	457	$3{\cdot}5987_0$
E 405 & E 418	15	$3{\cdot}5879_2$	E 417	478	$3{\cdot}5996_4$
E 402 & E 426	16	$3{\cdot}5878_3$	E 425	481 (*h*)	$3{\cdot}5995_9$
E 413	17	$3{\cdot}5878_4$	E 430	489	$3{\cdot}6004_3$
E 400	102 (*c*)	$3{\cdot}5893_8$	E 437	495 (*h*)	$3{\cdot}6005_2$
E 401	200 (*c*)	$3{\cdot}5912_3$	E 440	501	$3{\cdot}6011_0$
E 399	303	$3{\cdot}5928_2$	E 431	511	$3{\cdot}6012_6$
E 414	328	$3{\cdot}5933_2$	E 424	524	$3{\cdot}6019_1$
E 420	346 (*c*)	$3{\cdot}5936_0$	E 432	537 (*c*)	$3{\cdot}6030_0$
E 409	360	$3{\cdot}5943_3$	E 438	572	$3{\cdot}6043_4$
E 412	383	$3{\cdot}5948_9$	E 406	604	$3{\cdot}6069_5$

The parameter increases linearly with temperature up to about 300° C. The lattice then expands rapidly until at about 425° C. the parameter again increases linearly with temperature. The variation of the lattice parameter with temperature is shown in figure 1, from which the values of the coefficients of expansion given in table 4 were obtained.

Table 4. Coefficients of thermal expansion of alloy 43

Temperature (° C.)	Lattice parameter (A.)	True coefficient of expansion ($\times 10^6$)
0	$3{\cdot}5876_5$	4·7
100	$3{\cdot}5893_3$	4·7
200	$3{\cdot}5910_0$	4·7
300	$3{\cdot}5927_2$	5·4
350	$3{\cdot}5939_0$	7·4
400	$3{\cdot}5956_0$	12·1
500	$3{\cdot}6009_2$	15·0
600	$3{\cdot}6067_3$	15·1

Alloy 32. This alloy is just inside the pure γ' phase and the structure should therefore be face-centred cubic. Spectrum photographs of the alloy taken with copper radiation indicated this structure.

Difficulty was experienced in obtaining well-defined spectral lines with this alloy. A powder (specimen 1, table 2) which had been annealed for 14 hours at

600° C., on being cooled from this temperature to room-temperature in two days, gave a broad diffuse band instead of a doublet. The same heat treatment followed by a period of cooling extending over 129 hours yielded a resolved doublet, but the individual lines of the doublet were still too broad. The background was also rather dark and this made measurement of the lines difficult. To reduce the intensity of the background, vanadium radiation was substituted for the copper radiation hitherto used with this alloy. A third specimen was given the same preliminary heat treatment in lump and in powder form as the other two specimens, but was allowed 225 hours to cool from 600° C. to room-temperature. Well defined lines were now obtained in photographs taken with the specimen maintained at temperatures above 200° C., but below this temperature the definition of the lines was still not good. The lines obtained at the lower temperatures were, however, resolved and were situated in positions on the film where they could be fairly accurately measured. It would appear from the broadening of the spectral lines below about 200° C. that the lattice breaks up or becomes distorted when the specimen is cooled to lower temperatures at the rate which was adopted. This matter needs further investigation.

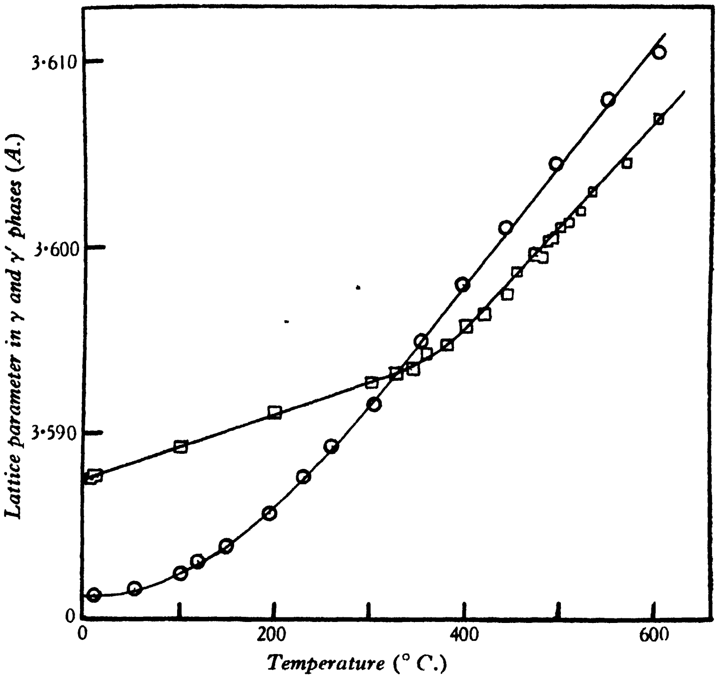

Figure 1. ⊙ 32·2 per cent of nickel; ⊡ 42·7 per cent of nickel.

The lattice parameters recorded in table 5 were measured over the full range of temperatures at which the camera could be used. The powder was changed frequently when the photographs were taken in order to avoid errors due to contamination in the enclosure.

Table 5. Lattice parameters of alloy 32 at different temperatures

Film No.	Temperature (° C.)	Lattice parameter (A.)	Film no.	Temperature (° C.)	Lattice parameter (A.)
E 453 & E 467	12	$3\cdot5814_1$	E 464	305	$3\cdot5915_3$
E 448 & E 451	15	$3\cdot5813_3$	E 469	328	$3\cdot5933_5$
E 454	54	$3\cdot5816_6$	E 452	357	$3\cdot5949_8$
E 455	103 (*c*)	$3\cdot5826_4$	E 461	400 (*c*)	$3\cdot5981_2$
E 456	120 (*c*)	$3\cdot5831_8$	E 465	445 (*h*)	$3\cdot6011_5$
E 450	150 (*c*)	$3\cdot5840_1$	E 462	497 (*c*)	$3\cdot6044_9$
E 457	195 (*h*)	$3\cdot5858_0$	E 468	555 (*h*)	$3\cdot6080_4$
E 466	230 (*c*)	$3\cdot5878_0$	E 460	606 (*h*)	$3\cdot6104_6$
E 449	261 (*h*)	$3\cdot5893_8$			

These results are included in figure 1, from which by drawing tangents to the curve at different temperatures the true coefficients of expansion collected in table 6 were calculated.

Table 6. Coefficients of thermal expansion of alloy 32

Temperature (° C.)	Lattice parameter (A.)	True coefficient of thermal expansion × 10^6
0	$3\cdot5811_0$	2·2
100	$3\cdot5825_7$	5·7
200	$3\cdot5860_7$	14·3
300	$3\cdot5916_8$	16·6
400	$3\cdot5979_0$	17·3
500	$3\cdot6042_0$	17·6
600	$3\cdot6105_6$	17·8

The curves in figure 2 show how the true coefficient of linear expansion varies with the temperature in the alloys examined. The dotted curve was obtained by Chevenard[2] from measurements made on a rod of an alloy containing 35·4 per cent of nickel. This curve closely resembles those now obtained from measurements of the crystal lattices of the alloys. Initially the coefficient of thermal expansion increases very slowly with temperature, but at a certain temperature which increases as the

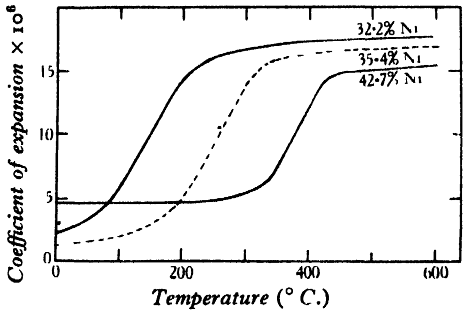

Figure 2.

nickel content of the alloy increases, a sudden rise in the value of the coefficient of expansion takes place, the actual increase in the value being the greater, the lower the nickel content of the alloy. After the sudden rise which is confined to a comparatively narrow range of temperature, the coefficient of expansion on further rise of temperature shows little increase.

The mean temperatures of the ranges in which the coefficient of expansion changes rapidly with temperature for alloys 43 and 32 are respectively about 375° and 150° C., and therefore agree approximately with the temperatures of magnetic transformation, namely 360° and 150° C., for these two alloys. Hence the coefficient of thermal expansion of these two alloys changes from a low to a high value when the temperature passes through that corresponding to the magnetic transformation. This result differs from that obtained with the alloys rich in nickel reported in our previous paper, for which it was found that the coefficient of thermal expansion gradually increased as the temperature was raised. It reached a maximum value at the transformation temperature and suddenly fell to a lower value on passing through this temperature.

The phenomenon now observed with alloys 43 and 32 is similar to that which occurs with β brass when the temperature of the alloy passes through the β-transformation temperature, the thermal coefficient above the β-transformation temperature being greater than that below it. It is to be noted that the coefficient of thermal expansion for both alloys 43 and 32 is abnormally small at 0° C., whereas at temperatures above 400° C. the coefficient is large and greater than that of either nickel or iron.

Alloy 24. Considerable difficulty was experienced in obtaining X-ray reflections which could be measured with this alloy. Six specimens were examined, the heat treatment in each case being different; see table 2.

The annealing given to specimen 1 was considered to be insufficient to remove the distortion produced in the lattice by the cold work done on the material. It was desirable to examine both the phases that were supposed to be present at temperatures not exceeding about 345° C. in this region of composition. The second specimen was consequently annealed at 300° C. for 24 hours and cooled slowly over 7 hours. Very broad faint lines were obtained. A measurement of these lines showed that they were due to the body-centred α phase. No evidence of the face-centred γ phase was obtained with the sample in this condition. The α-phase lines were better defined in a photograph taken with the sample maintained at 306° C., but when the temperature was raised to 632° C. a pair of lines at a smaller arc were recorded on the film. These were due to reflections from the (400) planes of the face-centred γ-phase structure. A photograph taken after the sample had been allowed to cool to room-temperature showed neither α- nor γ-phase lines. When the specimen was heated to 598° C. the γ-phase lines reappeared but they were rather faint.

According to some equilibrium diagrams of this alloy system, the γ phase transforms to $(\alpha+\gamma)$ at 345° C. Three successive exposures were made with specimen 2 at 400° C., the first after 10 min. heating, the second after 1½ hours' heating and the third after heating for a further hour at 400° C. Exposures of 30 min. were given to each photograph so that the powder had received nearly 3½ hours' annealing at 400° C. when the final exposure was made. This annealing was not sufficient to transform the α phase, for the very poor lines in the first photograph remained as a faint band in the last photograph.

On taking a fresh sample of powder and exposing at 603° C. the γ-phase lines again appeared. This same specimen was then heated at 405° C. for 10 hours before being exposed at that temperature and again the γ-phase lines appeared. When it was cooled, however, to room-temperature the α phase did not return.

In order to improve the definition of the lines, some filings were annealed at 900° C. and slowly cooled over 48 hours (specimen 3). An exposure at room-temperature yielded a very faint trace of lines, the arcs corresponding to which were somewhat smaller than those obtained with specimens 1 and 2. These lines gave a lattice parameter of 2·860 A.

As slow cooling appeared to have an adverse effect on the intensity of the lines, quenching from 600° C. was tried (specimen 4) but no lines resulted.

The best results were obtained with specimen 2, which had been annealed at 300° C. for 24 hours and cooled from this temperature to room-temperature in 7 hours. This heat treatment was adopted before the exposures at different temperatures were made. Cobalt radiation was used. Although 26 exposures were made, only 10 of them could be measured with sufficient accuracy to yield reliable results. These are collected in table 7; they are not as accurate as those obtained with the other alloys because the lines were not so well defined. The variation of the lattice parameter of the body-centred α phase with temperature is shown in the top curve of figure 3.

Table 7. Lattice parameters of α phase at different temperatures

Film no.	Temperature (° C.)	Lattice parameter (A.)	Atomic volume (A³)
E 274	15	2·8627	11·730
E 249	16	2·8634	11·739
E 272	98	2·8657	11·767
E 273	198	2·8685	11·801
E 271	293	2·8714	11·837
E 250	306	2·8724	11·850
E 260	340	2·8738	11·867
E 266	405	3·5999	11·663
E 254	598	3·6118	11·779
E 251	632	3·6141	11·802

About 18 months after these preliminary experiments had been made with alloy 24, powder was prepared from an ingot which had been lump-annealed at 800° C. for 21½ days and allowed to cool for 6 days to room-temperature. The powder was annealed at 600° C. for 17 hours and cooled to room-temperature over a period of 384 hours (specimen 6). Photographs taken with specimens of this powder at different temperatures exhibited the lines of the face-centred γ phase. Reflections were obtained from the (310) planes when manganese radiation was used. The lines at room-temperature were broad, and only an approximate value of the lattice parameter could be calculated from them. When heated to 600° C., however, the alloy yielded a pair of resolved lines which could be accurately measured. It was noticed that the lattice parameter of the γ phase at these high temperatures was in close agreement with the values previously obtained for the γ phase when cobalt radiation was employed. There is no structural change in crossing the boundary between the γ' and γ phases, and the lattice expands uniformly from the one phase into the other in alloys in this region of composition.

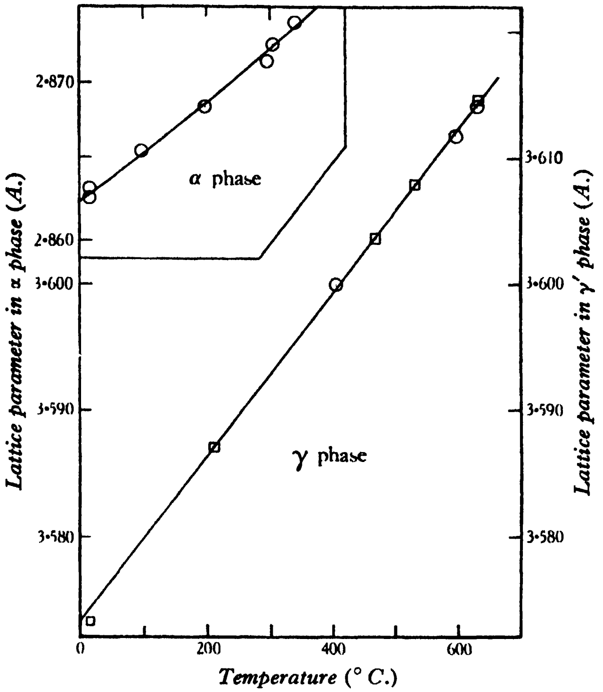

Figure 3.

The results obtained with manganese radiation are recorded in table 8 and are shown in the lower curve of figure 3. In this figure, the parameters of the body-centred α phase and the face-centred γ phase have been plotted on different scales

Table 8. Lattice parameters of γ phase at different temperatures

Film no.	Temperature (° C.)	Lattice parameter (A.)	Atomic volume (A³)
E 649 & E 651	15	3·5757	11·426
E 650	210	3·5874	11·542
E 646	404	3·6000	11·664
E 649	466	3·6036	11·699
E 645	532	3·6079	11·741
E 647	633	3·6146	11·807

so as to show the relation between the atomic volumes in the two structures. The coefficient of expansion of the body-centred α phase is approximately $10{\cdot}1 \times 10^{-6}$ at 0° C., $10{\cdot}3 \times 10^{-6}$ at 100° C., $11{\cdot}1_5 \times 10^{-6}$ at 200° C. and $13{\cdot}2 \times 10^{-6}$ at 300° C., while that of the face-centred γ (or γ') phase has a constant value of $18{\cdot}2 \times 10^{-6}$ between 0° C. and 630° C.

Without a knowledge of the exact proportions of the α and γ phases in the alloy it is impossible to calculate what its mean expansion should be. Hanson and Hanson(3) give the boundaries of the $(\alpha + \gamma')$ region at 9 and 32 per cent of nickel. Assuming that alloy 24, which contains 24·2 per cent of nickel by weight, is made up of 33 per cent of α and 66 per cent of γ, we have calculated with the figures given in tables 7 and 8 how the mean atomic volume should vary with temperature. The mean atomic volume on this basis is 11·52 A.³ at room-temperature, 11·70 A.³ at 340° C., 11·66 A.³ at 400° C., and 11·78 A.³ at 600° C. Thus on the disappearance of the α phase the mean atomic volume of the alloy decreases, and hence a rod of the material would show a contraction at or near this temperature. The results based on the above assumption as to the relative amounts of the α and γ phases in alloy 24 are shown graphically in figure 4, and inset is a curve obtained by Chevenard with an iron-nickel alloy containing 25·9 per cent nickel by weight. The latter shows a contraction between 425° C. and 475° C. and is a curve similar to that now obtained from parameter measurements of the constituent phases. On being cooled to room-temperature the material used by Chevenard contracted uniformly until its dimensions were about 7 per cent smaller than they had originally been at this temperature. This behaviour is characteristic of the irreversible iron-nickel alloys. A bar of an irreversible alloy on being heated, expands up to a certain temperature and then contracts over a range of temperature before expanding again on being further

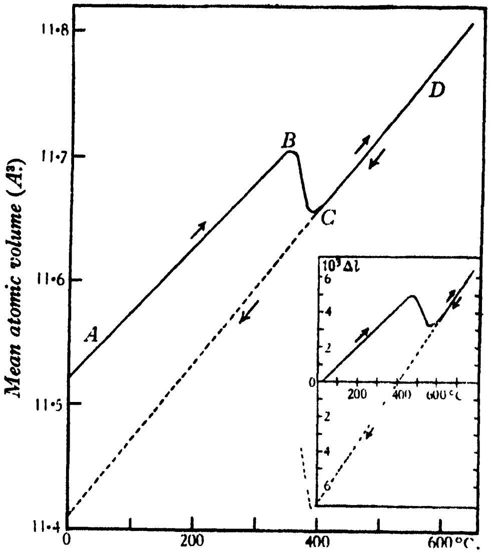

Figure 4. Curve of mean atomic volume for an alloy containing 24·2 per cent nickel by weight, computed on the basis of one-third α phase and two-thirds γ phase.

heated. When cooled from this temperature it contracts uniformly through the temperature at which anomalous contraction took place on heating.

The ordinary methods of measuring thermal expansions do not allow of the same analysis as is possible with the X-ray method of measurement. In the latter it is possible, in the manner described in this paper, to follow the changes in the lattices of the two constituents of the alloy with change in temperature. It is clear from this investigation that the anomalous contraction which occurs at certain temperatures when the irreversible iron-nickel alloys are heated is due to the disappearance of the body-centred or α constituent, the mean atomic volume in which is greater than that in the γ phase at the same temperature. When the alloy is cooled the α phase does not make its appearance at the temperature at which it disappeared on heating, with the result that the alloy now contracts along the pure γ-phase curve to a lower temperature before the α phase appears, thus showing a thermal-hysteresis effect. The temperature at which the α phase appears when the alloy is cooled depends upon the rate of cooling of the alloy.

The difference in the slopes of the portions *AB* and *CD* of the curve shown in figure 4 is due to the fact that the coefficient of thermal expansion of the α phase is smaller than that of the γ phase.

§ 4. CONCLUSIONS

The curves obtained by the X-ray method of measurement described in this paper are similar in form to those obtained with these alloys by previous workers who used different methods of measurement; in fact there is very close agreement between the results obtained by the different methods employed.

It is found that alloys in the region of the γ' phase behave differently according to whether they are in the iron or in the nickel end of the region. In the one case the coefficient of thermal expansion increases suddenly from a low, approximately constant, value to a higher value which shows slight increase on further rise of temperature; in the other case it gradually increases as the temperature is raised, and after reaching a maximum value it suddenly drops on further rise of temperature to a value which remains approximately constant at higher temperatures. The mean temperatures of the sudden rise or the sudden fall in the value of the coefficient correspond to the temperatures of magnetic transformation of the alloys.

The crystal structure on both sides of the magnetic transformation remains the same, but the difference in the behaviour of the alloys as they pass through the temperature of magnetic transformation would seem to point to a radical difference between them.

The boundary of magnetic transformation, that is the boundary of the γ' phase, is usually shown in equilibrium diagrams of this alloy series. Since the crystal structure of the alloys is the same on both sides of the boundary it might be argued that there is no need to include the boundary in the diagram, but the changes that take place in the values of the coefficient of thermal expansion when the temperature passes through the transformation temperature seem to afford sufficient ground for including the boundary in the diagram were there no other reasons for keeping it. The structure of β brass remains the same when the alloy passes through the transformation temperature, but its coefficient of thermal expansion changes in the same manner as do those of alloys 41 and 32 when they pass through the temperature of magnetic transformation. The alloy in the copper-zinc diagram is shown as passing from the β' to the β phase. Similar instances could be cited, all of which indicate that the boundary of magnetic transformation should be shown in the equilibrium diagram.

The results described in this paper point rather to the need for differentiation between the two limbs of the boundary, since it is found that the alloys in passing through the transformation temperature behave differently according as they are of composition near the nickel or near the iron end of the γ' phase.

Alloy 24 is interesting because, unlike the other alloys so far investigated, it is in the mixed $(\alpha+\gamma')$ region at room-temperature. The results described in the paper provide an explanation for the shape of the expansion curves obtained with alloys in this region of composition. They are the irreversible alloys which show thermal hysteresis. This phenomenon is observed because the alloy, which is usually in rod form when its expansion is measured, is not allowed sufficient time to reach the true equilibrium state corresponding to the temperatures at which the observations are made. When an irreversible alloy is heated, the α phase disappears at a comparatively low temperature and the γ phase exists alone at temperatures above this. On cooling the γ phase persists alone at temperatures much below that at which the α phase disappeared on heating. Owing to these facts, a composite bar of the material behaves in an abnormal manner. It shows a contraction in the neighbourhood of the temperature at which the α phase disappears.

By the X-ray method the various phases present can be independently examined, and the results throw light on the shape of the curves obtained from measurements on a composite bar of the alloy in a manner which the ordinary methods of measurement would not render possible.

§ 5. ACKNOWLEDGEMENT

The authors wish to record their indebtedness to Dr L. B. Pfeil of the Mond Nickel Company for his advice and for kindly preparing the alloys and supplying their compositions.

REFERENCES

(1) Owen and Yates. *Proc. phys. Soc.* **49**, 17 (1937).
(2) Chevenard. *Comptes Rendus*, **159**, 177 (1914).
(3) Hanson and Hanson. *J. Iron and Steel Inst.* **102**, 39 (1920).

A PHOTOELECTRIC SPECTROPHOTOMETER OF HIGH ACCURACY*

By J. S. PRESTON, M.A., A.M.I.E.E., F.Inst.P. and
F. W. CUCKOW, B.Sc.
National Physical Laboratory

NOTE ADDED 12 DECEMBER 1936

Our attention has been drawn to a note on the valve bridge published by Dr J. C. M. Brentano in *Nature*, Lond., **108**, 532 (1921). We were unaware of this note at the time of writing the above paper, but of course acknowledge its priority to other publications there referred to.

However, we had in mind strictly only the practical aspects of operating such a valve bridge, and there is nothing in Dr Brentano's note, or in his further papers on the subject,† which affects in any degree the conclusions at which we arrived in regard to the actual circuit which we used. Although Dr Brentano stresses the importance of anode-circuit compensation, we agree with Wynn-Williams that filament-circuit compensation is much more important in securing stability of operation. In fact the theoretical treatment would indicate that with high enough values of anode resistance, and correspondingly high h.t. voltage, the bridge is almost unaffected by small variations in h.t. voltage, even when the anode circuits are not compensated. This was certainly the case with the set-up which we used.

We also regard the setting of the grid of the amplifying valve at the zero grid-current point as of great importance in securing the optimum stability with the type of valves which we used. Since the grid of the other valve can be set at any desired potential to balance the bridge, compensation can still be carried out as desired.

We would finally point out that the references given in our paper are not intended to be in any sense exhaustive, and that we make a definite disclaimer as to novelty.

---

* *Proc. phys. Soc.* **48**, 869 (1936).

† *Phil. Mag.* **7**, 685 (1929); *Z. Phys.* **54**, 571 (1929); *Z. Phys.* **70**, 74 (1931).

THE RESPONSE OF THE MAMMALIAN COCHLEA TO PHASE-REVERSAL IN A CONTINUOUS MUSICAL TONE

By C. S. HALLPIKE, H. HARTRIDGE and
A. F. RAWDON-SMITH,

The Ferens Institute of Otology, Middlesex Hospital, London, W. 1.,
and Physiology Department, St Bartholomew's Hospital
Medical College, London, E.C. 1.

Report given with demonstration, 27 *November* 1936

ABSTRACT. By means of a photocell, light source and interrupter, it has been found possible to produce phase-reversals in a musical tone of approximately sinusoidal waveform. When this tone is caused to fall on the human ear, phase-change beats are heard as has previously been described. When this tone is caused to fall on the ear of a decerebrate cat, and its auditory-tract responses are recorded by means of a cathode-ray oscillograph, a temporary and marked decrease in amplitude of the response occurs, corresponding to each phase-change. This decrease in amplitude corresponds to the phase-change beat which is heard by the human subject and is postulated on the resonance theory of hearing. When the cochlear (Wever-Bray) response of the cat is similarly recorded, the response exhibits no such fall in amplitude in correspondence with the phase-change, which is moreover reproduced with marked fidelity. The cochlear response must therefore originate in some non-resonant structure.

In previous papers by Hartridge(1) evidence has been advanced that a beat, which has been described as a temporary fall in response, is heard by the human subject on changing the phase of a musical tone by π (180°). This evidence has been contested by Békésy(2), who used a method employing current-reversal in telephones; it has also been disputed by L. Hartshorn(3), who used a similar method. It appeared to us to be desirable to obtain, if possible, objective evidence of the existence of such a temporary arrest in the response. The method we have used was to cause a musical tone, which was changed in phase when required, to fall on the cochlea of a decerebrate cat. The changes in potential which are thus set up in the cochlea were amplified and recorded photographically by means of a moving film camera and a cathode-ray tube. The changes in potential which were set up in the auditory tract, as a result of the passage of nervous impulses, were also similarly recorded during the application of the tone.

The method employed by Hartridge for generating the tone which was changed in phase was to blow a jet of air against uniformly placed slots cut in a rotating brass siren disc; the change of phase was produced by reducing the spacing at one point in the disc to half the distance used elsewhere. This method has the advantage of simplicity, but also the disadvantage of generating marked high-frequency components. These components are in part due to the rush of air from the jet, and in

PHYSICAL SOCIETY, VOL. 49, PT. 2 (C. S. HALLPIKE, H. HARTRIDGE and A. F. RAWDON-SMITH)

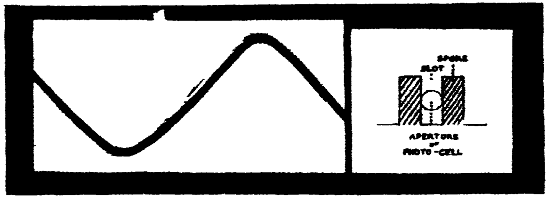

Figure 1.

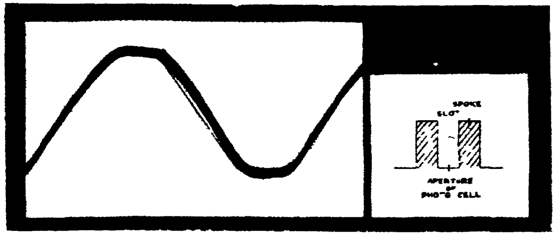

Figure 2

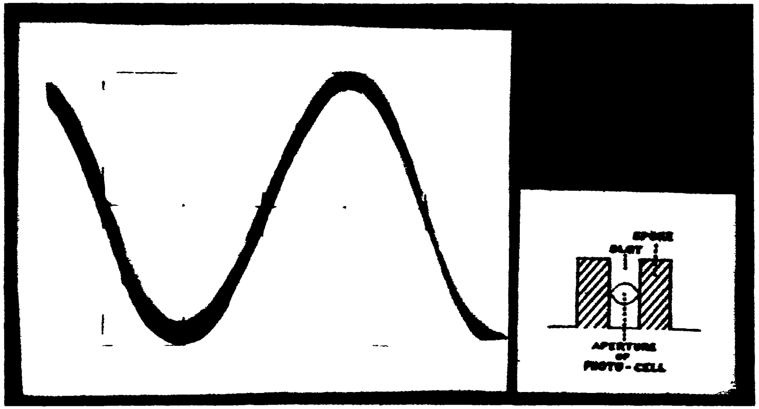

Figure 3.

Figure 5. Microphone and auditory-tract response at 1024 c sec

Figure 6. Microphone and cochlear response at 1024 c. sec.

part to the eddies set up by the passage of air through the siren. A method of generating a tone free from such components was therefore looked for.

It was found that if a beam of light was passed through the slots of the siren, and if this interrupted beam was caused to fall on a photocell, the voltages thus set up, when amplified and fed into a moving-coil loud-speaker, resulted in a tone free from these high-pitched components. A record of this tone taken from a piezo-crystal microphone showed, moreover, that it was of roughly sinusoidal form. By attention to certain details, it was found that the wave-form could be further improved. First, a metal-filament lamp and planoconvex lens were adjusted to produce an approximately parallel beam of light of suitable diameter. A circular disc of cardboard, 12 in. in diameter, was marked with a circle 11½ in. in diameter, and this was divided into 80 equal parts. Radial lines were then drawn through the dividing marks. Using these radial lines as contours, alternate slots and spokes of equal width were now marked out, and the slots were cut out with scissors. This disc was mounted between metal plates on a rotating shaft. The parallel beam was arranged to pass through the slots in the disc on to the photocell. When a restricting aperture equal in diameter to the width of the slot was placed in front of the photocell, the voltage changes were found by experiment to follow the black curve shown in figure 1. Calculation of the area of illumination of the photocell at successive instants gave the curve (fine continuous line) which will be seen superimposed on the black one. The two curves coincide as well as might be expected, and both will be seen to have sharper crests and troughs than a sine wave (dotted line). The observed and calculated curves obtained by using a circular restricting aperture of three-quarters the width of the slots (and spokes), which are shown in figure 2, will be seen to have flat crests and troughs. The observed and calculated curves obtained by using a restricting aperture which was lemon shaped, which are shown in figure 3, will be seen to correspond closely to that of a sine wave.

The output of the photocell was fed into an amplifier and loud-speaker. The change of phase was effected at one point of the disc by replacing the usual spoke-slot alternation by two successive slots, or by two successive spokes. Tones of different pitch were obtained by changing the rate of rotation of the disc by means of a continuously variable gear. With this apparatus, which is shown diagrammatically in figure 4, observations were made on (1) the effect of the phase-reversal of a pure tone on the human ear, (2) the effect of the phase-reversal on the electric responses from the cochlea of a decerebrate cat, and (3) the effect of the phase-reversal on the electric responses from the auditory tract of a decerebrate cat. Each of these observations will now be briefly described.

(1) *The response of the human ear to a phase-reversal.* Hartridge has described the beat produced by a change of phase of an impure musical tone as a sharp fall in intensity followed by a rapid return of the intensity to the normal value. He stated that the temporary depression of intensity is often accompanied by a noise of short duration which produces the effect of a tap or thud. The depression of the intensity of the tone and its partial replacement by a noise has been described as "the phase-change beat". We have repeated Hartridge's observations with pure tones of

different frequencies and intensities. The sound stimulus has been analysed by means of a piezo-microphone, amplifier, and cathode-ray oscillograph. Photographic records show that the phase-reversal was effected without significant disturbance of frequency or amplitude. Nevertheless, the audibility of the phase-change beat was undiminished. It was therefore concluded that the beat must be attributed to the phase-reversal and to this alone.

(2) *The response of the auditory-tract potentials to a phase-reversal.* The musical tone generated by the phase-change siren was led from the loud-speaker by thick-walled rubber tubing simultaneously to a crystal microphone and to the external ear of a decerebrate cat. The output of the microphone, after suitable valve amplification, was recorded by means of a cathode-ray tube and moving-film camera. Electrodes were placed in the auditory tract of the cat and the variations of potential recorded from these were similarly amplified and photographed. The two records were taken side by side on the same film together with a time-marker. A record obtained in this way is shown in figure 5. It will be noticed that the microphone faithfully records the phase-change, but that the auditory-tract potentials do not do so. They show, on the contrary, a temporary fall in amplitude of the response, followed by a rapid recovery to the original value. This finding must be considered to indicate that the vibrating elements of the internal ear in which these auditory-tract potentials originate undergo a period of arrested motion in response to a phase-change. This is in agreement with the hypothesis of Helmholtz according to which these elements are regarded as resonant structures. In addition, the view of Hartridge is confirmed according to which a silent period of this kind has been previously postulated as constituting the physiological basis of the phase-change beat.

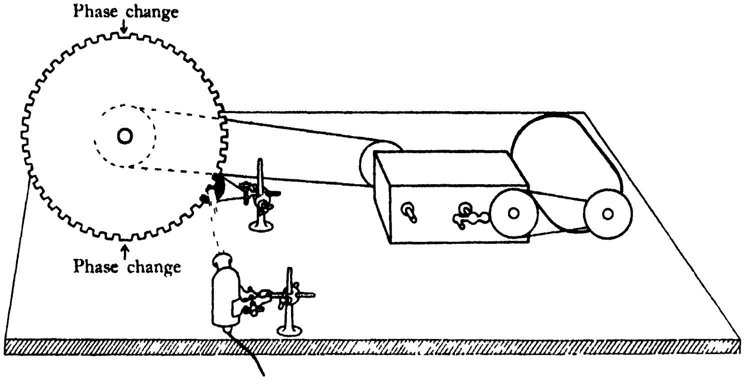

Figure 4.

(3) *The response of the cochlear phenomenon to a phase-reversal.* The cochlear phenomenon was recorded from a platinum electrode placed upon the round window (with an indifferent electrode in the neck muscles) of a decerebrate cat. The output of the cochlea and of the microphone were simultaneously recorded as described above. A comparison of the records, figure 6, shows the marked similarity between

the two, for both follow the phase-change with considerable fidelity. As the microphone consists of carefully chosen parts, light in weight and free from periodic properties, this suggests that the cochlear response originates from structures in the ear with similar properties. If figures 5 and 6 be compared it will be noticed that the tract and cochlear responses are quite unlike one another. Since the tract response originates in nerve endings in the hair cells attached to the basilar membrane, the hypothesis of Davis⁽⁴⁾ that the cochlear response originates in these hair cells is rendered unlikely.

REFERENCES

(1) HARTRIDGE, H. *Brit. J. Psychol.* **12**, 142 (1921); *Proc. phys. Soc.* **48**, 145 (1936).
(2) BÉKÉSY. *Phys. Z.* **29**, 793 (1928).
(3) HARTSHORN, L. (Personal communication).
(4) DAVIS, H., DERBYSHIRE, A. J., LURIE, M. H. and SAUL, L. J. *Amer. J. Physiol.* **107**, 311 (1934).

DEMONSTRATIONS

THE PORTABLE PHOTOELECTRIC DAYLIGHT-FACTOR METER.* *Demonstration given by* GEO. P. BARNARD, B.Sc., A.Inst.P. 11 December 1936.

ADEQUATE natural lighting is, for most buildings, even more important than a satisfactory system of artificial lighting. Insufficient natural lighting has often been an important factor in recent years in the condemnation of dwellings and schools.

In consequence of the great variability of daylight, the structural efficiency of a building in admitting daylight to a given point is expressed by the *daylight factor*, i.e. the ratio (usually given as a percentage) of the illumination at the internal point to the simultaneous illumination at an outside point exposed to a complete hemisphere of sky. The difficulties encountered by public health officers in determining the daylight factor have led to a demand for a simple, portable meter.

The portable photoelectric meter shown is designed to measure daylight factors of from 0·03 to 2·50 per cent. Two rectifier photoelectric cells are used. One is placed on the window sill to receive light from a definite fraction of the whole sky-vault; the other at the point in the room where the daylight factor is required. A Morse key facilitates rapid change-over of a microammeter from one cell to the other. Depression of the key connects the microammeter directly to the terminals of the inside-illumination cell. Release of the key connects the microammeter to the outside-illumination cell, in parallel with a variable resistance acting as a shunt to the microammeter. This resistance is adjusted until depression or release of the key produces no change in the microammeter readings; the value of the resistance at balance gives the daylight factor directly on the curve provided.

Corrections for non-linearity in {current, illumination} relationships and for errors arising from the difference in colour between the illuminations to be measured by the two cells are incorporated in the final curve relating shunting resistance with daylight factor. The inside-illumination cell is compensated for loss of sensitivity with increasing obliquity of the incident light.

In operation it is necessary only to connect the cells in circuit, the remaining instruments being permanently wired and mounted in a portable case which has compartments to hold the photoelectric cells and their holders and the necessary flexible leads.

THE AUDIBLE EFFECT OF A SUDDEN CHANGE OF PHASE IN THE CURRENT SUPPLIED TO A TELEPHONE RECEIVER. *Demonstration given by* L. HARTSHORN, D.Sc. 27 November 1936.

THESE experiments arose directly from a demonstration given to the Physical Society last November by Prof. H. Hartridge, F.R.S., who showed that when a siren is arranged to generate a train of sound waves in which there is a reversal of phase at regular intervals without change of amplitude, a listener observes a kind of beat. This is interpreted as a momentary diminution, consequent upon the change of phase, of the amplitude of those vibrating parts of the ear which are in resonance. The experiment was put forward as evidence of the existence of resonance effects in the ear.

---

* *J. Sci. Instrum.* **13**, 392 (Dec. 1936).

The audible effect of the reversal of phase was most marked and I was very surprised when Dr Beatty stated, in the course of the discussion which followed, that Békésy had performed a similar experiment with electrical technique and had obtained a contrary result. It occurred to me that it ought to be possible to make the electrical experiment at least as convincing as the pneumatic one, and that it would be worth while to compare the two. The experiments now to be shown are the outcome of this idea.

A convenient circuit for the production of a variation of phase with no change of amplitude is that shown in figure 1*a*. The corresponding vector diagram is shown in figure 1*b*. The two resistors *R* are equal and non-inductive, *S* is also a non-inductive resistor and *R* a variable condenser. If V_1 is a constant applied voltage, then the voltage V_2 always has the value $V_1/2$, but varies in phase as *C* is varied. This is immediately seen from the vector diagram. As *C* is varied the point *P* travels round the semicircle having the vector V_1 as diameter, and V_2 is represented by the radius of this semicircle which passes through *P*. Thus any desired change of phase of the voltage V_2 can be produced by a change of capacitance *C*. The actual change produced by any given condenser will of course depend on the values of *C*, *S*, and the frequency, and to produce a change of phase of 180° one must vary *C* instantaneously from zero to infinity. In practice, zero capacitance is an open circuit and infinite capacitance a short circuit. It follows that a complete reversal of phase can be produced by replacing *C* by a tapping key, and simply opening or closing this key. This is the arrangement shown, and the reversal is demonstrated by recording the voltage wave with a cathode-ray oscillograph. On pressing or releasing the key, the voltage wave is seen to be inverted without appreciable change of amplitude. The source of voltage V_1 is a beat-tone oscillator the frequency of which is easily varied from 50 cycles per sec. or less to 10,000 cycles per sec. The arrangement is therefore very convenient for work of this kind, especially as the amount of change of phase is easily controlled.

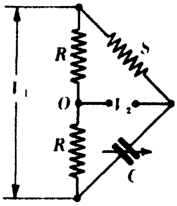

Figure 1 *a*.

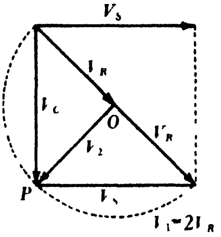

Figure 1 *b*.

The values of *R* and *S* must of course be chosen to suit the work in hand. Those actually used for the demonstration are shown in figure 2. The voltage V_2 is amplified by a resistance-capacity-coupled amplifier. Inductances and transformers were avoided since their behaviour might confuse the issue. The two resistances R each have the value of 100 ohms. The resistance S is one hundred times larger, and a second resistance of 10,000 ohms is placed between the oscillator and the bridge network. In this way the voltage V_1 applied to the bridge network is, to an accuracy of the order of 1 per cent, independent of changes from zero to infinity of the impedance of the variable arm of the network. The input impedance of the amplifier is very high compared with any of the resistances of the network and may therefore be regarded as infinite. The conditions assumed in figure 1 are therefore satisfied.

The output of the amplifier is connected to a cathode-ray oscillograph, in parallel with which we may, by the operation of a selector switch, connect a vibration galvanometer, telephone earpiece, or loud-speaker. Thus the reversal of phase is seen in the cathode-ray oscillograph at the instant when its effect on the ear via the telephone or loud-speaker is heard.

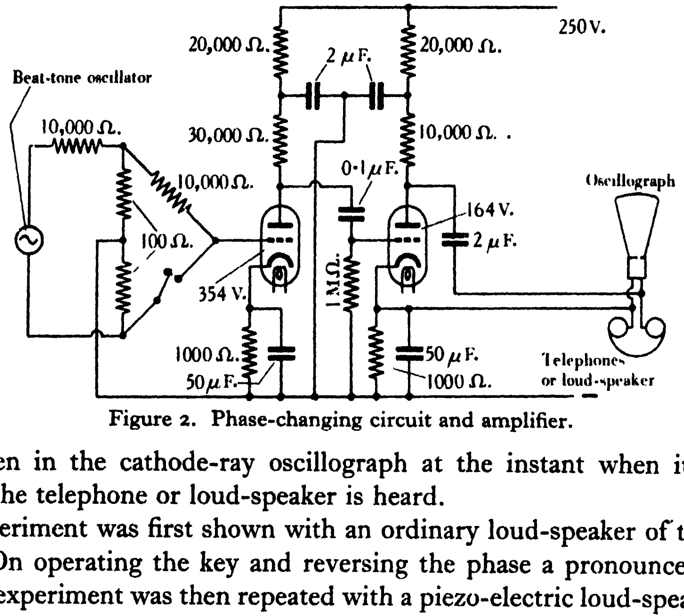

Figure 2. Phase-changing circuit and amplifier.

The experiment was first shown with an ordinary loud-speaker of the moving-coil type. On operating the key and reversing the phase a pronounced click was heard. The experiment was then repeated with a piezo-electric loud-speaker. Again a click was heard, but of a somewhat different character.

The experiments were repeated at various frequencies between 200 and 10,000 cycles per sec. In all cases there is a very pronounced discontinuity in the sound heard, but it is not easy to describe with any precision the nature of this discontinuity. Some observers describe a momentary cessation of the tone heard; others an increase in the loudness of the tone immediately following the change of phase. Others merely a click or a ping such as might be expected to result from a very short impulse applied to the diaphragm of the instrument under observation. Whatever the ultimate explanation may be, there seems to be no reason to suppose that the effect heard is essentially different from that demonstrated by Prof. Hartridge with his original siren and with the photoelectric siren which he has just shown. There can therefore be no question of a contradiction between the results of the experiments made with electrical and with purely acoustic technique. It is only in the interpretation of the result that differences of opinion may arise.

In this connexion the following experiment is interesting. The loud-speaker is replaced by a vibration galvanometer which is tuned to resonance with the applied voltage. On reversing the phase the amplitude of vibration diminishes nearly to zero and then rises to its original value, as is to be expected. If, however, the galvanometer is tuned to be just off resonance, either by increasing or diminishing the frequency, the reversal of phase is seen to cause a temporary *increase* in its amplitude of vibration.

Thus if we suppose the ear to possess a series of resonators graded in frequency, although the amplitude of those which are in tune will be diminished by a reversal of phase, the amplitude of the resonators with frequencies either a little greater or a little less than that of resonance will be increased. It is not therefore surprising that few observers describe a silent period, and it is possible that the temporary increase of intensity sometimes heard is due to this increased response of out-of-tune resonators. Such resonance effects may be due to the loud-speakers as well as to the ear.

Although I do not propose to attempt to discuss the theories of hearing there is one other point which I would emphasize. It is obviously physically impossible to change suddenly the phase of a continuous train of waves without at the same time introducing a transient vibration into the system. Its character may vary according as the change is made at the instant of zero displacement, of zero velocity, or some intermediate point, but it must always be there, and it is possible that when the experiment is made it is this transient vibration which attracts the attention of many observers. It is true that the visual examination of the cathode-ray oscillograph fails to detect the transient with the apparatus now being demonstrated, while the audible effect is most marked. Nevertheless the effect heard frequently suggests a sharp blow on the vibrating system and it is possible that the audible effect of the transient may be more prominent than that of the change of phase.

It is clear from the recent advances made by Prof. Hartridge and his collaborators that much work remains to be done before the theory of hearing will be completely elucidated. The only claim made for the experiments which I have shown is that they might provide a convenient technique for the carrying out of some of the work.

REVIEWS OF BOOKS

Recollections and Reflections, by Sir J. J. THOMSON, O.M., F.R.S. Pp. viii+451. (London: G. Bell and Sons, Ltd.) 18*s*. net.

Here are riches for many types of reader, all of whom will feel and be impressed by the spirit of happiness which runs as *Leit-motiv* through this record of a fruitful life spent in ideal surroundings with hosts of pleasant friendships. "I came up to Trinity College in October 1876 and have kept every term since then, and been in residence for some part of each long vacation." Such long and intimate association with Cambridge enables Sir J. J. Thomson to survey the many changes which he has seen in University life and in the progressive development of teaching and research, and to comment understandingly upon such different topics as the status of women students and the changing popularity of various games. He can and does give us pen pictures of Cambridge men whose names are as household words alike to scientific worker and to general reader. Here also we find appreciative sketches of his predecessors in the Cavendish Chair of Experimental Physics, of Clerk Maxwell (1871–9) with an amusing reminiscence of his first lecture on heat (Sir Joseph's laconic comment on Maxwell's report that the laboratory "now contains all the instruments required by the present state of science" must not fail to bear fruit), and of Lord Rayleigh (1879–84) whom Thomson succeeded at the age of 28. What could be more romantic than his account of Prof. H. L. Callendar, "an intellectual Admirable Crichton whose career at the Laboratory was in some respects the most interesting in all my experience"! In the last hundred pages Sir J. J. Thomson gives some account of the development of that branch of scientific work conveniently classified under the heading of the discharge of electricity through gases.

There is a wealth of good stories, but of set purpose I will quote none, for I am certain that, owing to the interval which must necessarily elapse between the writing of this notice and its date of publication, most if not all of the readers of the *Proceedings* will have read and reread these charming reminiscences of our great physicist.

If I can generalize from my own experience, extending over a period of one week only, I know that the place on our shelves reserved for this fascinating autobiography will rarely house its rightful occupant because we shall have been forced to yield to the loan-requests of our friends in every walk of life.

Gilbert of Colchester has been called the father of the sciences of electricity and magnetism. These sciences have been developed so greatly during the last forty years, largely owing to the work of Thomson at Cambridge, that it would certainly seem more appropriate to put Gilbert one stage further back in the table of consanguinities and to recognize Sir J. J. Thomson as the father of these sciences as we know them to-day. Perhaps we younger members of the world-wide but united family of physicists have unconsciously recognized his paternal standing, for alone amongst scientists with international reputations he stands as a man known by initials which fall trippingly from the tongue, a hero of science respected, admired and held in deep affection, simply as J. J.

J. H. B.

An Introduction to Nuclear Physics, by N. FEATHER, Ph.D. Pp. x+213. (Cambridge University Press, 1936.) 10*s*. 6*d*. net.

To summarize the present position of a subject which is expanding at such a prodigious rate as nuclear physics is no light task, as may be appreciated from the fact that the present volume contains references to some 1200 papers, most of them published within the last three years and not a few within the last twelve months. Dr Feather may be congratulated on his courage in undertaking this much-needed work, and on the ability with which he has carried it out.

In spite of the modesty of its title, the book provides a very adequate critical summary of the present state of knowledge of the nucleus as a structure, and of the transformations produced in it by fast-moving particles and high-energy quanta. No research of importance appears to have escaped notice, and all the important results are exhibited in tabular form. The book is entirely non-mathematical in character, and while the various hypotheses and concepts which are being used at the moment to co-ordinate and interpret the experimental data are adequately described, the author has very wisely eschewed all proofs, and is content simply to quote such formulae as are required for his exposition.

The subject-matter is well arranged and admirably documented; the addition of a subject index would have made easier the task of those who wish to consult the book on special points. The book does not altogether make easy reading, and we can imagine that the average honours student might find it rather beyond his unaided ability. To postgraduate students, and to physicists generally who wish to be *au fait* with this newest branch of their subject, the book can be unreservedly recommended.

J. A. C.

The Electron. (1) *Einführung in die Elektronik*, by O. KLEMPERER. Pp. xi+303. (Berlin: J. Springer, 1933.) RM. 18.60. (2) *Elektronentheorie der Metallen*, by H. FRÖHLICH. Pp. vii+386. (Berlin: J. Springer, 1936.) RM. 27.

These two books are in some ways complementary, that by Klemperer having an experimental outlook and that by Fröhlich a mathematical one, although the distinction is by no means absolute. Each contains some description of experimental work and some account of the theoretical basis of the treatment.

Klemperer deals first with electronic beams and the means of imparting high velocities to them, whereas the first step in the book by Fröhlich is a short treatment of the Schrödinger wave equation. In subject matter, too, they are in some respects complementary, though there is more overlapping than the titles would indicate. Klemperer includes in his range the properties of electrons in metals and has a chapter on electron gas in which velocity-distribution, Fermi statistics, and degeneration are dealt with, even though rather shortly. Moreover, about one third of his book is concerned with electron-emission, and here he is necessarily dealing largely with the indirect evidence as to the properties and behaviour of electrons in metals, as evidenced by the phenomena of the photoelectric, the Richardson and the cold-emission effects. Conversely, Fröhlich, although mainly concerned with electrons in metals, does on occasion refer to the properties of free electrons, generally as illustrations of the mathematical theory. The main part of his book is concerned with quite recent work. His starting point after the classical paper by Pauli (1927) is that by Sommerfeld (1928), in which the Drude-Thomson theory was recast in terms of Fermi statistics. (In passing, one must regret that the charmingly written paper by Sommerfeld, in *Die Naturwissenschaften* for 1927, in which he gave a preliminary account of these results, seems doomed to be forgotten, hidden by the more complete paper of the following year.)

After the introductory and historical matter, Fröhlich takes in turn the problems of conductivity, semiconductors, the chemical bond, and magnetism, following which there is a final chapter discussing the metals as a whole in their relationship to the periodic table.

The treatment is up-to-date (Mott's work of 1936 is included) and accurate, but the book gives an impression of superficiality which is not really justified; this is caused by the rapid transition from subject to subject, with no halts to explain at length the implications of results, though they are there to be dug out by the reader who is prepared to go slowly enough to do the digging himself.

Klemperer's book, which covers a much wider range, can best be exhibited by giving a somewhat breathless list of some subjects included in it. They are all well expounded, though the outlook of 1937 is not that of 1933 on such matters as the numerical value of the electronic charge, or the formulation of electron optics. Here then is the list: the behaviour of electrons in rectifiers, amplifiers, valves, X-ray tubes, photocells and oscillographs; Fermi statistics; refraction, diffraction and polarization of electrons; electron optics, velocity spectra, the cloud chamber, counters, sensitivity of photographic plates to electrons, space-charge effects, plasma; thermionics and cold emission, the photoelectric effect, selective and otherwise, exit work function, ionization potentials, and the grouping of electrons in the atoms of the elements; the Compton effect, secondary electrons (a very thorough and informative chapter of 21 pages); ionization by ions, including positrons and α particles; radioactivity, with no mention of the neutrino; 100 pages on interaction between atoms and free electrons, in which are introduced the wave properties of the electron, and a very interesting discussion of the individual processes by which electrons lose energy in passing through matter; single and multiple scattering. From this it will be seen that the book is very thorough. It is notable for the many numerical tables, and is in every way a useful book to have about the laboratory—even more perhaps than in the study.

J. H. A.

Television Optics, by L. M. Myers. Pp. x+338, 214 figures. (London: Sir Isaac Pitman and Sons, Ltd., 1936.) 30*s*. net.

The appearance of a book on television optics is timely. From different standpoints many members of the general public, students of physics, and workers in one or other of the branches of physics utilized, are interested in learning what is being done in this subject and if possible in understanding the principles employed. To make the widest appeal, and perhaps it may be added to be of the widest scientific service, such a book should be as free as possible from mathematical detail and from mere technicalities. Words used with meanings which are not found in a good dictionary of normal size should be carefully explained. The traveller should not be allowed to wander from the road he has to traverse; his desire, it may be safely assumed, is to understand the special development with which the book deals, not to receive on the way a general education in associated branches of science. Liberal illustration of the text is a valuable feature. In the last respect this book is satisfactory, but in many others it appears to the reviewer to leave much to be desired. It will certainly not be understood, as it might have been, by readers without a special training in science. Readers in general would have been better served by the exclusion of excrescences which are not needed for understanding the ultimate aim of the book. It should not have been difficult to delete a substantial portion of the text without detriment to the rest, and so to lower the price appreciably. In addition the author must be blamed for not taking the trouble to find what are the accepted meanings of some of the technical terms he uses. In the older branches of physics, at any rate, there is no doubt what is to be understood by the more important words, but it would be possible from this volume to illustrate the application of well-known terms to well-known phenomena with which they have nothing to do. For these reasons the reviewer strongly dissents from the advertisement on the jacket, which says "This is an essential book for students and others who need a thorough grasp of the theory underlying this rapidly developing branch of applied science. It is noteworthy for the simplicity of its mathematical analysis and for the elimination of unnecessary practical matter already available from other sources...."

In spite of these defects the book will serve the purpose of indicating what has so far been achieved, on what lines work is being pursued, what are the difficulties encountered, and why development is proceeding in this direction rather than that. This is a proper function for a book dealing with the present state of a subject still in its infancy. For the time being it will rightly be given a place in scientific libraries, but it should be possible before long to replace it by a book free from defects such as have been mentioned.

T. S.

Vibration and Sound, by PHILIP M. MORSE. Pp. xv + 351. (London: McGraw-Hill Publishing Co., Ltd., 1936.) 24*s*.

Prof. Morse is at some pains in the preface of his book to find an excuse for adding yet another to the list of books dealing with the subject of vibrations and sound. He need not be apprehensive, however, for the rapid growth in the importance of the subject would be sufficient justification, if such were necessary, for the book he has now published in the International Series in Physics. This book is different from most of the others; both the style and the manner of treatment are different. It is mainly mathematical, but the physics is not forgotten, in fact, as is stated in the preface, one of the principal aims of the book has been to give to the student examples of the *method* of theoretical physics, "the way a theoretical physicist attacks a problem and how he finds its solution".

The subject matter covered by the book is not comprehensive, but what is done has been done thoroughly—even the section headed "A Little Mathematics" in the introductory chapter is most effective in its appeal and proves of considerable value in the later stages of the book. After the introduction, successive chapters deal with the simple oscillator, the flexible string, the vibration of bars, membranes and plates, plane waves of sound, radiation and scattering of sound, and standing waves. A useful bibliography and tables of functions are given in conclusion. The three-dimensional illustrations of the vibrations of membranes and plates, with the series of high-speed motion pictures of waves on a rubber membrane, are valuable aids to a mental grasp of this difficult subject.

The last chapter in the book serves as an illustration of the original manner of treatment. In this chapter the mathematical methods developed for the study of the radiation of light from an atom are applied to the theory of the acoustic properties of rooms. The reviewer notes with pleasure that the book is dedicated to Prof. Dayton C. Miller.

Prof. Morse's book can be thoroughly recommended both as a textbook and as a work of reference.

A. B. W.

Properties of Matter, by F. C. CHAMPION and N. DAVY (*The Student's Physics*, Vol. III). Pp. xiv + 296. (London and Glasgow: Blackie and Son.) 15*s*. net.

Unless he sets out to write on the lines of a *Handbuch* (i.e. a book apparently so-called because it cannot be moved by hand, without the aid of one of the six mechanical powers), the author of a text on properties of matter is likely to find more difficulty in selecting than in handling his topics. The authors of this text have dealt pretty thoroughly with a number of selected (and on the whole well selected) topics, and jettisoned others more or less completely. From the standpoint of the reader for whom this series is primarily intended—the student reading for honours in physics—this is undoubtedly the best compromise, and it would be unfair to dwell too heavily upon the resulting omissions.

The absence of any reference, in an otherwise rather comprehensive chapter on capillarity, to the dependence of vapour pressure upon curvature of surface, may be excused on the ground that this particular problem is treated in Roberts's companion volume on *Heat and Thermodynamics*. The sketchiness of the chapter on kinetic theory (in which, for instance, transport problems are handled by the simplified six-stream method of Joule) may be partially justified on the same grounds, though in view of recent work on the separation of isotopes we should have liked to see a little more about diffusion in gases.

The chief omissions are however of outmoded methods of measurement—of, for example, determinations of the gravitational constant of which the interest, if any, is purely historical. The space so saved is more profitably devoted to more modern developments. There is a chapter on seismic waves and another on surface films. The chapter on osmotic pressure contains a brief account of the Milner-Debye-Hückel theory of strong electrolytes (nothing about Onsager's additions to the theory), and that on viscosity a brief note on Andrade's theory. The most unusual feature of the book is a summary of methods for the determination of Planck's constant—which, when one thinks of it, is perfectly in place in such a text.

The book is well and clearly written and illustrated; it should have a wide circulation among university students of physics. H. R. R.

Biological Time, by LECOMTE DU NOÜY. Pp. 177. (London: Methuen and Co., Ltd., 1936.) 7*s*. 6*d*. net.

From a study of the rate of cicatrization of wounds, begun during the war, the author has deduced certain general equations which enable a fairly accurate prediction of the date of the completion of healing to be made. Experiments on the behaviour of tissue cultures *in vitro* also have been examined, and from these studies the author produces the idea of a physiological time which bears a certain relation to ordinary time. The conception arrived at is of a "granular, variable, individual time, differing from the continuous, integral, universal time". This physiological time is said to flow more rapidly with increasing age, the rate increasing in proportion to the age of the individual. The book is divided into three parts: the biological problem, and methods; cicatrization of wounds, and tissue-culture; time. The first part serves as a general introduction and the second gives an account of the research methods used and of the experiments on which the author's deductions are based. These two parts are a mixed grill, written partly in a simple and partly in an elaborate style and including both elementary and advanced knowledge, and they touch on many branches of mathematics, physics, chemistry and biology. Some of the interesting work carried out at the Rockefeller Institute and l'Institut Pasteur, with both of which the author has been associated, is recorded. The last part, on time, is on the whole philosophic and contains many sweeping generalizations. The book is occasionally thought-provoking, often fascinating and sometimes abstruse.

H. R. L.

An Elementary Survey of Modern Physics, by G. F. HULL. Pp. xxiv + 457. (London and New York: Macmillan and Co.) 20*s*. net.

This book is remarkable for its completeness, in the sense that practically no topic of interest in modern physics has been completely ignored. It necessarily follows, given the size of the book, that where so many topics have been introduced the majority of them have had to be rather summarily dismissed. As a rule, however, enough has been said to entertain and to stimulate the interest of the average reader.

The treatment is livelier than is customary in English textbooks, and there is a more lavish use of exclamation marks. We quote a few headlines:

"After Seventeen Years a Great Discovery Is Made. X-Rays Are Wavelike."
"The Neutron Enters an Equation for the First Time."
"As a Ghost It Enters Photographs."
"Rush Hour in Twentieth Century Physics."

The treatment is well adapted to the general reader, though in one place "the student" is warned that he "must now be prepared for a headache". The book is (except for a gratuitous and unjustifiable attack on "Rayleigh-Jeans") pleasantly and genially written; it should find favour with a wide circle, even if it does not quite completely equip budding scientific journalists, and if it fails occasionally to enable "students of philosophy" to "confound their opponents". (In the reviewer's experience, a knowledge of physics is not an indispensable passport to journalism, and philosophers are not easily persuaded that they have been confounded.)

The book is well and lavishly illustrated with photographs and line diagrams. Reference has already been made to the width of the field under survey; this may also be illustrated by listing the last six of the many appendices, viz. (1) Schroedinger's equation, (2) A brace of the Cavendish Society's post-prandial dirges, (3) A French mnemonic for π to 30 places, (4) A numerical example on the uncertainty principle, (5) A list of physicists who have been awarded Nobel Prizes (Query: is this to remind us that "Tout soldat français porte dans sa giberne le bâton de maréchal de France"?), and (6) A short list of important physical constants.

The treatment is avowedly elementary, and indeed it is clear that mathematical discussions do not fit comfortably into the general scheme. In spite of this, the book, because it is thoroughly up-to-date both in its information and its viewpoint, will be of value to confirmed physicists as well as to the general reader. This is especially true of such sections as those on spontaneous and induced atomic disintegrations, in which the author has been relatively prodigal of his available space.

On the whole a book which deserves, and will probably obtain, considerable success.

H. R. R.

Mercury Arcs, by Prof. F. J. TEAGO, D.Sc., M.I.E.E. and J. F. GILL, M.Sc. Pp. vii + 104. (London: Methuen and Co., Ltd., 1936). 3*s*. net.

This monograph deals with the mercury arc as a means of converting alternating current to direct current on a large scale. It will be of considerable interest, particularly to electrical engineers, covering concisely as it does the action of this apparatus from the electrical, mechanical and operational standpoints. Since Cooper-Hewitt in 1903 first utilized the rectifying property of mercury vapour, the development of the mercury rectifier has been very rapid, mainly owing to the advent of grid control. Units of capacity up to 2500 kW. at 3300 V. are now in operation, water-cooled containers being employed for sizes above 250 kW.

After an interesting introductory chapter, which includes an exposition of the physical phenomena involved, the authors deal with constructional details, grid control of voltage, grid control of current, {current, voltage} characteristics, and the curious phenomenon of inversion leading to the practicability of interconnexion between alternating current mains of different frequencies through the intermediary of mercury rectifiers. Chapters on wave-form analysis, transformer ratings, and power factor complete a treatment in which mathematical analysis is a prominent feature.

D. O.

THE PROCEEDINGS OF
THE PHYSICAL SOCIETY

VOL. 49, PART 3 *May* 1, 1937 NO. 272

LIBRA

THE VISCOSITY OF AIR

BY W. N. BOND, M.A., D.SC., F.INST.P.,
Lecturer in Physics in the University of Reading

Received 14 *May* 1936. *Read* 13 *November* 1936

ABSTRACT. The viscosity of dry air at atmospheric pressure was measured by a capillary-tube method, at about 15° C. The ends of a wide-limbed U tube containing paraffin oil, of density 0·87, were connected by a pair of capillary tubes in series, so as to form a closed system. The oil was initially displaced, and in proceeding towards its equilibrium position it forced air through the capillaries. Care was taken to avoid constant and systematic errors, and two U tubes, two sets of capillaries and two methods of drying the air were used. Assuming that the viscosity increases by $4{\cdot}93 \times 10^{-7}$ per °C., the value at 23° C. is $(1834{\cdot}7 \pm 0{\cdot}8) \times 10^{-7}$ c.g.s. units. The paper includes a summary of the general theory of the capillary-tube method and the correction terms involved, as well as a detailed theory of the present experiments.

§ 1. GENERAL THEORY

FOR steady stream-line flow of incompressible fluid of constant viscosity η through an infinitely long straight tube of radius r, when there is zero velocity at the walls of the tube, we have Poiseuille's equation

$$V = \frac{\pi r^4}{8\eta}\left(-\frac{dp}{dl}\right),$$

where V is the volume of fluid passing through in unit time and $(-dp/dl)$ is the pressure gradient causing flow, the hydrostatic pressure gradient having been deducted. It will be assumed that all correction terms are so small that they may be treated as if they were independent of one another.

It was shown by Osborne Reynolds that stable stream-line motion only occurs when

$$\frac{vr\rho}{\eta} \leqslant 1000,$$

where ρ is the density of the fluid and v is its mean velocity, defined by $\pi r^2 v = V$.

It may happen that the internal radius r varies as we pass along the tube.

Treating each short part of the tube as if it were part of a circular cone of semi-angle α, we have⁽¹⁾

$$V=\frac{\pi r^4}{3\eta}\frac{\cos\alpha\,(2\cos^3\alpha-3\cos^2\alpha+1)}{\sin^4\alpha\,(3\cos^2\alpha-1)}\left(-\frac{dp}{dl}\right)$$

$$=\frac{\pi}{8\eta}\frac{p_1-p_2}{\int\left(1-\frac{3}{2}\alpha^2+\ldots\right)\frac{dl}{r^4}},$$

where p_1 and p_2 are the pressures at entrance and exit. The hydrostatic difference in pressure must be deducted, as before.

If the cross-section of the tube be elliptic, it can be shown⁽²⁾ that r^4 in the above equation has to be replaced by $2r_1^3r_2^3/(r_1^2+r_2^2)$, where r_1 and r_2 are the semi-axes of the ellipse. If the mass of liquid required to fill the tube is used to deduce the mean radius, the corresponding value of $1/r^4$ requires to be increased by $k^2/200$ per cent, where k is the small percentage difference between r_1 and r_2.

If, instead of measuring the pressure gradient in the tube, we measure the pressure difference between the fluid in the reservoirs to which the tube is joined, then end corrections have to be applied. It has been shown⁽³⁾ that, when $vr\rho/\eta<8$, the total effect of the two ends is to make the effective length of the tube greater than its actual length by an amount $1{\cdot}15r$. For the range of Reynolds' number

$$8<vr\rho/\eta\leqslant 1000,$$

the correction⁽³, ⁴⁾ is chiefly due to the kinetic energy of the fluid, and is made by replacing p_1-p_2 by

$$(p_1-p_2)-1{\cdot}08\,\frac{V^2\rho}{\pi^2r^4},\text{ which equals }(p_1-p_2)-1{\cdot}08\,v^2\rho.$$

For a gas which obeys Boyle's law, Poiseuille's equation is replaced by O. E. Meyer's equation

$$p_1V_1=p_2V_2=\frac{p_1+p_2}{2}\frac{\pi r^4\,(p_1-p_2)}{8\eta l}\qquad\ldots\ldots(1),$$

where V_1, V_2 are the volumes of gas entering and leaving in unit time, provided⁽⁵⁾ that the flow is isothermal and that the forces due to variation in velocity *along* the tube may be neglected. If there is no heat conduction through the walls of the tube, the conditions will not be quite isothermal. We shall have $p/\rho^n=\text{constant}$⁽⁶⁾, where

$$n=1+(\gamma-1)\left(\frac{v}{c}\right)^2,$$

γ denoting the ratio of the principal specific heats of the gas, and c the velocity of sound in the gas. There would also be adiabatic cooling of the gas as it entered the capillary, the fractional decrease in the absolute temperature being equal to

$$\frac{\gamma-1}{2}\left(\frac{v}{c}\right)^2.$$

These two effects are generally quite small, and conduction will usually decrease them considerably.

It has been found that, in the case of a gas, slip occurs at the walls of the tube. The capillary acts as if its radius were greater than r by an amount⁽⁷⁾ $0{\cdot}874\lambda$, where

λ is the mean free path of the gas molecules. Consequently the value deduced for the viscosity requires correction by multiplying by

$$1+4\left(\frac{0{\cdot}874\lambda}{r}\right).$$

For air at normal atmospheric pressure the factor becomes

$$1+\frac{0{\cdot}000{,}033\text{ cm.}}{r}.$$

§ 2. THEORY OF THE PRESENT EXPERIMENTS

In the present experiments two capillary tubes in series were joined to the ends of a wide-limbed U tube containing a paraffin oil, the whole forming a closed system shown diagrammatically in figure 1. The two oil-air surfaces were initially at different levels. In proceeding towards its equilibrium position, the oil forced the air through the capillaries. The rate of flow can be deduced from the rate of movement of the oil surfaces, and their difference in level determines the value of the driving pressure, (p_1-p_2). Thus

$$p_1-p_2=hg\,(\sigma-\rho) \qquad \text{......(2)},$$

where h denotes the difference in level and σ the density of the oil in the manometer. The density ρ of the gas has little effect in decreasing the driving pressure, and need only be known approximately.

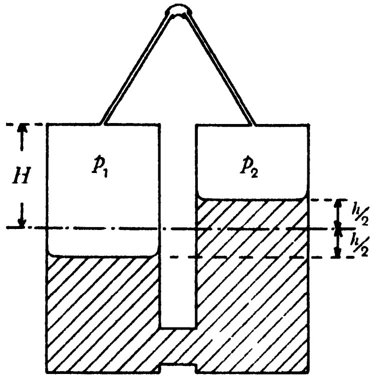

Figure 1.

We require to find expressions for p_1V_1 and p_1+p_2 in order to use equation (1). Let ρ^* be the density of the gas at unit pressure, and let p_0 be the final pressure of the gas when $h=0$. Equating the sum of the masses of the gas in the two sides of the apparatus to the total mass of gas in the final equilibrium condition, we have

$$a\left(H+\frac{h}{2}\right)\rho^*p_1+a\left(H-\frac{h}{2}\right)\rho^*p_2=a\,.\,2H\rho^*p_0 \qquad \text{......(3)},$$

where a and H denote the area of cross-section and final length of each air column, figure 1. From equations (2) and (3) we find

$$p_1 = p_0 + \frac{hg(\sigma-\rho)}{2}\left(1-\frac{h}{2H}\right),$$

and

$$\frac{p_1+p_2}{2} = p_0 - \frac{h^2 g(\sigma-\rho)}{4H} \qquad \text{......(4).}$$

The mass of air passing through the capillary per second is equal to the rate of decrease with time of the mass on the p_1 side. Hence

$$(p_1\rho^*)V_1 = -\frac{d}{dh}\left[a\left(H+\frac{h}{2}\right)\rho^*\left\{p_0+\frac{hg(\sigma-\rho)}{2}\left(1-\frac{h}{2H}\right)\right\}\right]\frac{dh}{dt}.$$

Substituting from this equation and equations (2) and (4) in equation (1), we obtain

$$-\int \frac{1+\frac{Hg(\sigma-\rho)}{p_0}-\frac{3h^2g(\sigma-\rho)}{4Hp_0}}{1-\frac{h^2g(\sigma-\rho)}{4Hp_0}}\frac{dh}{h} = \frac{\pi r^4 g(\sigma-\rho)}{4al\eta}\int dt.$$

The term $h^2g(\sigma-\rho)/4Hp_0$ is to be quite small in comparison with unity, and therefore its square may be neglected. With this approximation, the equation becomes

$$\eta = \frac{\pi g(\sigma-\rho)}{4a\Sigma\left(\frac{l}{r^4}\right)} \times \frac{[t]}{-[\log_e h] + \frac{Hg(\sigma-\rho)}{p_0}\left[\left(\frac{h}{2H}\right)^2 - \log_e\frac{h}{2H}\right]} \qquad \text{......(5),}$$

where quantities in square brackets have to be taken between two limits. The terms involving H are due to the compressibility of the gas (air). The corrections still have to be made for ellipticity and variation in diameter of the capillary, for end effects, and for slip. A small correction may also be necessary for the friction of the oil in the manometer.

In evaluating $\int\left(1-\frac{3}{2}\alpha^2+\ldots\right)\frac{dl}{r^4}$ for a capillary tube, it will usually be found that the term in α^2 can be neglected. The volume of the tube can be obtained accurately by finding the mass of mercury required to fill the tube. A short column of mercury is then inserted in the tube, and its length, q, is measured at a number of points along the tube. A curve can be drawn showing the value of q at different parts of the tube. Denoting the average value of $1/q$ along the tube by $[1/q]$ and the average value of q^2 along the tube by $[q^2]$, we find

$$\int\frac{dl}{r^4} = \frac{\pi^2 l^3}{(\text{volume of tube})^2}\left[\frac{1}{q}\right]^2[q^2] \qquad \text{......(6).}$$

§ 3. EXPERIMENTAL DETAILS

Two U tubes were used in these experiments. The first had thick glass walls and an area of section of $a = 18$ cm.^{2} approximately. The value of a varied along the limbs of the tube, and a complicated method of calculation which need not be described here had to be used. The second U was made of drawn brass and is illustrated in figure 2. Long vertical slots, at the back and front of the limbs of the U, were covered with cellophane and pyrex respectively and used as windows. The oil-air surfaces, about 4½ cm. in diameter, were viewed with a microscope that had vertical and horizontal traverses. The microscope was used with a 1-in. or 2-in. objective, and its position was read by vernier to 1/100 mm. The total vertical travel of the microscope was about 10½ cm. Light from a small lamp was collimated by a lens of focal length 100 cm. and aperture 15 cm., shown on the right in figure 2, and passed in a horizontal beam to illuminate the oil surfaces 3 m. from the lens.

A dense medicinal paraffin oil was used in the U tubes. This oil had a viscosity of about 0·55 at 16° C. and a vapour pressure of not more than 0·15 cm. of mercury column at 15° C. Its density, found by comparison with distilled water by means of three specific-gravity bottles, was $0{\cdot}8716 \pm 0{\cdot}00016$ g./cm³ at 15° C. and $0{\cdot}8649 \pm 0{\cdot}0002$ g./cm³ at 25° C. The density is almost the same as that of Apiezon Oil B at the same temperatures(8).

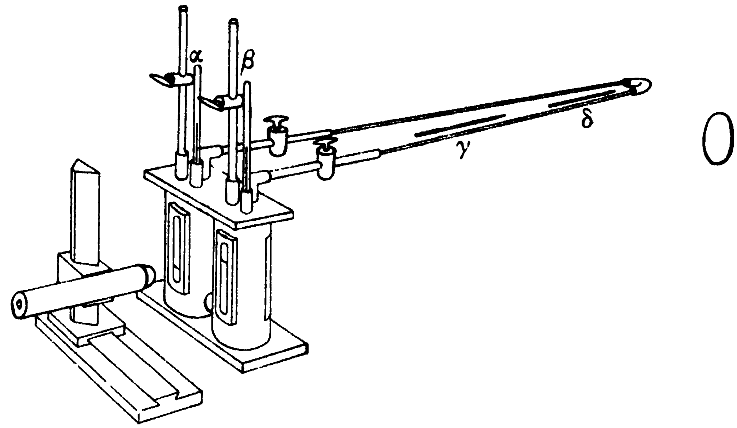

Figure 2.

The value of a for the first U tube was found by measuring the rise in level when known masses of water were inserted. The second tube was calibrated similarly by means of the oil, giving $a = 15{\cdot}526 \pm 0{\cdot}003_5$ cm². Measurements of the diameter of the tube and of the size of the window recesses gave a value $a = 15{\cdot}51_5 \pm 0{\cdot}01$.

Two capillary tubes in series were used in each experiment, and two pairs of such tubes were used. The tubes were of glass, and each had a radius of about 0·036 cm. and a length of about 150 cm. The value of l for each tube was found to an accuracy of about ± 0·005 per cent, and the mass of mercury to fill each tube to an accuracy of about ± 0·01 per cent. The value of q was measured at about 20 places in each tube, all parts of each tube being tested. The maximum value attained by α at any point in the four tubes was 0·0004 radian, and hence the term in α^2 is quite negligible. From each $\{q, l\}$ curve about 30 equally spaced ordinates were read, and the corresponding values of $1/q$ and q^2 were used to calculate the average values $[1/q]$ and $[q^2]$. Four checks on the accuracy of this work were obtained. Firstly, one calculation was repeated by a seven-ordinate method, giving a value of $[1/q]^2 . [q^2]$ that differed from the result obtained by the 30-ordinate method by only 0·01 per cent. Secondly, two of the tubes were calibrated more crudely, and the calculations were carried out by the 7-ordinate method, giving results that only differed from the more precise ones by 0·1 per cent. Thirdly, the mean diameter of each of the four tubes was measured at each end with a travelling microscope, and each result was compared with the value deduced from the mercury weighing together with the $\{q, l\}$ curve. The average of all eight diameters as measured with the microscope was greater than the average of the eight as measured by the mercury column by $(0{\cdot}15 \pm 0{\cdot}13)$ per cent, or $(0{\cdot}000{,}11 \pm 0{\cdot}000{,}09)$ cm.; thus the general accuracy of the measurements was checked. At any one of the eight places the discrepancy between the two methods of measuring the diameter was about $\pm 0{\cdot}3$ per cent or $\pm 0{\cdot}0002$ cm. If all of the discrepancy be attributed to inaccuracy in the $\{q, l\}$ curve, none of the error being attributed to the microscope measurements of the diameter, it would follow that the value of $[1/q]^2 . [q^2]$ of equation (6) had been found to an accuracy of about $\pm 0{\cdot}03$ per cent. Fourthly, the accuracy of the determinations of $\int \frac{dl}{r^4}$ is checked by the close agreement of the viscosity measurements made with the first and second pairs of tubes. The corrections for ellipticity were quite small. The data for the four tubes are given in table 1.

Table 1

Capillary	$\dfrac{\pi^2 l^3}{(\text{volume of tube})^2} \times 10^{-7}$	$\int \frac{dl}{r^4} \times 10^{-7}$	End corrections $\times 10^{-7}$	Ellipticity corrections $\times 10^{-7}$	Corrected $\Sigma \frac{l}{r^4} \times 10^{-7}$
1	8·460	8·507	0·002	0·002	8·511
2	11·767	11·903	0·003	0·007	11·913
1+2	—	—	—	—	20·424 cm.$^{-3}$
3	10·153	10·521	0·003	0·001	10·525
4	5·664	5·692	0·002	0·001	5·695
3+4	—	—	—	—	16·220 cm.$^{-3}$

The maximum Reynolds' number $v r \rho/\eta$ in any of the present experiments was about 10. Consequently, there was no risk of turbulence. Moreover, the end correction was only kinetic for the highest rates of flow used. For the lower rates, at which $v r \rho/\eta < 8$, the end correction was 0·025 per cent. The correction was so small that it could be treated as a constant percentage, even for the highest rates of flow used.

The maximum value of $(v/c)^2$ was about $1{\cdot}7 \times 10^{-6}$, and hence the temperature of the air was not appreciably influenced by expansion and friction. The terms involving H in equation (5), which correct the measurements of rate of flow for the effect of compressibility of the air, had an average value of about 0·3 per cent; the connecting-tubes with taps cause the effective top of each wide air-column to be slightly above the top of the U tube. The maximum possible value of $h/2$ is H. When $h/2$ has the value $H/\sqrt{2}$, the two terms involving H change at equal and opposite rates, and the correction for compressibility is zero. It was not convenient, however, to restrict the experiment to the range in which $h/2$ is nearly equal to $H/\sqrt{2}$. The correction for slip was 0·09 per cent.

In the first apparatus the tube forming the bottom of the U was rather long and narrow: owing to the rather large viscosity of the manometer oil, a correction of −0·35 per cent had to be applied to the apparent viscosity of the air. In the second apparatus the connecting tube was wider and much shorter, and consequently the correction was only −0·03 per cent.

In commencing any experiment, air was drawn into the apparatus through one of the tubes shown at the top of figure 2. The air was always dried before being passed into the apparatus. In some experiments the air had been bubbled through and stored over fairly strong sulphuric acid. In the other experiments the air was drawn from a glass tower packed with soda lime. The pressure of the air in the apparatus was initially atmospheric on one side, and slightly less on the other side. The various parts of the apparatus were tested for air leakage before or after each experiment. This is essential, because changes in atmospheric pressure would cause any leaks to vary in a complicated way

The apparatus was not placed in a thermostat, but in a room in which the temperature only changed very slowly. The temperature was read at various times during each experiment by means of four thermometers α, β, γ and δ, figure 2. The zeros of the thermometers were tested on two occasions, and the thermometers were compared with one another and with a standard. The determinations of temperature cannot have been in error by more than 0·1° C., which corresponds to a change of 0·027 per cent in the viscosity of air.

In a typical experiment the value of h decreased from 10 to 3 cm. in about 15 min. The microscope was adjusted into position, and then the time of passage of the meniscus was recorded with a calibrated stop-watch, fitted with a "split" seconds hand. In this way a series of 8 or 10 timings could be made, by stopping only one part of the hand. Incidentally, the effect of the starting error of the watch is eliminated. Readings were taken on the two oil-air surfaces alternately throughout the experiment. The position occupied by meniscus B at the instant at which meniscus A was being timed can subsequently be deduced from the preceding and succeeding observations of meniscus B by means of logarithmic interpolation. Directly an experiment had been completed a second experiment was performed with the flow in the reverse direction. This procedure avoids any slight error due to the microscope not travelling exactly horizontally.

§ 4. EXPERIMENTAL RESULTS

The results of the experiments are given in table 2. For purposes of comparison with the results of other workers, the value of η at 23° C. has been estimated, on the assumption that the viscosity increases by $4·93 \times 10^{-7}$ per °C. rise in temperature(9).

Tables 3 and 4 show that changes of U tube, capillary, and drying agent had no significant effect.

Table 2

Date	Number of experiments performed	Reference no.		Drying agent	Temperature (°C.)	$\eta \times 10^7$	η at 23° C. $\times 10^7$
		U tube	Capillary				
8 April	2	1	1 + 2	H_2SO_4	$13{\cdot}6_5$	1790·9	1837·0
13 April	4	1	1 + 2	H_2SO_4	$13{\cdot}8_4$	1788·8	1833·9
27 April	2	2	1 + 2	H_2SO_4	$16{\cdot}9_0$	1803·6	1833·6
1 May	2	2	3 + 4	Soda lime	$14{\cdot}2_0$	1792·8	1836·2
4 May	2	2	3 + 4	Soda lime	$15{\cdot}7_2$	1798·5	1834·4
4 May	2	2	3 + 4	H_2SO_4	$15{\cdot}9_0$	1798·8	1833·8

Table 3

U tube	Capillaries	$\eta \times 10^7$ at 23° C.	Number of experiments
1	1 + 2	1834·9	6
2	1 + 2	1833·6	2
2	3 + 4	1834·8	6

Table 4

Drying agent	η 10^7 at 23° C.	Number of experiments
H_2SO_4	1834·4	10
Soda lime	1835·3	4

The probable error of the arithmetic mean of the above results, deduced from the residuals, is ±0·019 per cent. Allowing for uncertainties of ±0·018 per cent in the value of σ, of ±0·023 per cent in the values of a for each U tube, of ±0·03 per cent in the value of $\Sigma\,(l/r^4)$ for each pair of capillaries, and of ±0·027 per cent for an uncertainty of ±0·1° C. in the average of all the temperatures, the final probable error becomes ±0·046 per cent, giving $(1834{\cdot}7 \pm 0{\cdot}8) \times 10^{-7}$ c.g.s. units as the value of η at 23° C.

I was rather surprised to find that my results disagreed with the value adopted by Millikan but agreed well with the result obtained recently by Kellström(10), who used a rotating-cylinder method.

In conclusion, it may be remarked that the amount of vapour that will come from the dense paraffin oil, and diffuse about 8 cm. in 10 min., is almost certain to be very small. Its effect on the viscosity of the air will probably be quite insignificant.

§ 5. ACKNOWLEDGEMENTS

I have much pleasure in thanking Prof. J. A. Crowther, in whose laboratories the work was carried out, for his interest in the experiments. My thanks are also due to the Research Board of this University for making a grant for the purchase of apparatus. Mr J. S. Burgess, the laboratory steward, has helped me considerably by constructing apparatus.

REFERENCES

(1) BOND, W. N. *Proc. phys. Soc.* **34**, 188 (1922).
(2) LAMB, H. *Hydrodynamics*, 3rd ed., p. 545.
(3) BOND, W. N. *Proc. phys. Soc.* **34**, 142 (1922).
(4) SCHILLER, L. *Z. angew. Math. Mech.* **2**, 96 (1922).
(5) POYNTING and THOMSON. *Properties of Matter*, 6th ed.. p. 210.
(6) BOND, W. N. *An Introduction to Fluid Motion*, p. 88.
(7) MILLIKAN, R. A. *The Electron*, 1st ed., p. 113.
(8) BEECK, O. *Rev. sci. Instrum.* **6**, 400 (1935).
(9) MILLIKAN, R. A. *Ann. Phys.*, Lpz., **41**, 759 (1913).
(10) KELLSTRÖM, G. *Nature*, Lond., **136**, 682 (1935).
Note added September 28. Kellström has since confirmed his results (*Phys. Rev.* **50**, 190, 1936).

IONOSPHERIC CONDITIONS DURING THE SOLAR ECLIPSE OF 19 JUNE 1936

By R. NAISMITH, A.M.I.E.E.
Radio Department, National Physical Laboratory

Communicated by Dr R. L. Smith-Rose 13 *January* 1937. *Read* 12 *February* 1937.

ABSTRACT. The radio observations made in south-eastern England during the five days centred on the eclipse of 19 June 1936 are described. The eclipse was sufficient to increase the minimum equivalent height of the F region from 300 to over 600 kilometres and to decrease the ionization of the same region by about 50 per cent although only 56 per cent of the sun's disk was obscured at the maximum phase. The effect on these two elements reached a maximum at the same time and occurred 30 min. after the eclipse reached its maximum. A large magnetic disturbance occurred during the period of observation. The radio observations are therefore discussed in relation also to the changes which occurred in the magnetic elements during the effect of the eclipse on the ionosphere. The results of a number of field-strength measurements made on signals traversing the path of the eclipse are given and interpreted in relation to the ionospheric measurements made at vertical incidence. The coincidence of the eclipse with sunrise over south-eastern England suggests that the minimum of ionization thereby created made this the control region so far as the long-distance transmissions are concerned. This explains the close correlations which have been found to occur. It is shown that a reduction in field-strength was associated with the time during which the eclipse effect occurred in the path of the signals.

§ 1. INTRODUCTION

A SERIES of ionospheric measurements were made at the Radio Research Station of the National Physical Laboratory at Slough, in latitude 51° 29½′ N. and longitude 0° 34′ W., in connexion with the solar eclipse of 19 June 1936. They were carried out in accordance with a programme arranged by a subcommission of the Union Radio Scientifique Internationale, under the Presidency of Prof. E. V. Appleton, and form a part of an extended series of observations carried out on an international scale. This programme was supplemented by a number of field-strength measurements made by the Radio Branch of the British Post Office. The Slough series were confined to measurements of the ionization-density and the equivalent height of the different ionospheric regions returning radio energy at normal incidence. The measurements made by the Post Office supplied data over a more extended area concerning the variation in the amount of radio energy arriving from different directions.

It should be mentioned at the outset that extremely unfavourable conditions existed over south-eastern England on the morning of the eclipse. In the first place, the optical eclipse reached a total magnitude of only 0·56 and began before sunrise.

The difference between a total and a partial solar eclipse is, of course, less important in relation to radio observations than in relation to the corresponding astronomical ones. (In all that follows the term "eclipse" means the "optical eclipse".) In addition, one of the most intense thunderstorms of the year passed overhead during the observations. The system of recording(1) adopted at Slough, however, permitted good observations to be made in spite of the very high atmospheric noise-level thereby created. Whilst the measurements were being made it was obvious that an important magnetic disturbance was in progress; this was later found to be one of the largest for many months. The magnetic character figure for the day, derived according to the formula $(HR_H + VR_V)/10{,}000$, where R_H and R_V are the absolute range in gauss of H and V respectively during the day, was 1224, while the average for the month was only 392·5.

In spite of these unfavourable conditions it has been possible to interpret the results obtained in terms of established theories, although some modification of these interpretations may be necessary when all the results become available under the complete international programme.

A solar eclipse has, in recent years, been regarded as an opportunity for establishing the nature of the agency producing the normal ionization in the upper atmosphere. This normal ionizing agency for regions E and F_1 has been found to travel with a velocity closely approximating to that of light and has therefore been identified with the ultraviolet light from the sun. Similarly for region F_2 it has been concluded that ultraviolet light is responsible for at least part of the ionization, though it is suggested that corpuscles may also contribute(2). A study of the ionosphere during the solar eclipse of 1935 suggested(3) that the electron-dissipative process in region F_2 was by attachment to neutral gas particles and in region E by a process of recombination of the positive and negative charges.

It had been suggested that the two outstanding problems for study during an eclipse were (*a*) the causes of ionization in the F_2 region and (*b*) abnormal region-E echoes.

The observations described in this paper were therefore directed towards a study of these two problems.

§ 2. IONOSPHERIC MEASUREMENTS

Observations on the height and density of the different regions of the ionosphere returning energy at vertical incidence were made half-hourly from 17 to 21 June 1936. During the period of the eclipse they were repeated as rapidly as possible. One complete observation was made on all the frequencies on which echoes were observed in less than 9 mins., so that twelve complete $\{P', f\}$ curves are available for inspection for the $1\frac{3}{4}$ hours during which conditions in the ionosphere were rapidly changing. From this whole series of observations, two series of curves were drawn. One series shows the average values for the 2 days before and the 2 days after the morning of the eclipse, while the other illustrates the different conditions existing on the morning of the eclipse.

(*a*) *Minimum equivalent height of the F region.* The first two curves, plotted in figure 1, show the minimum equivalent heights at which reflection took place from the *F* region. It should be noted that at the times in the morning to which these curves refer, it is not normally possible to distinguish between the F_1 and F_2 regions, owing to the low angle of the sun's rays at this hour. This normal condition prevailed during the observations described in this paper. The relatively small difference between the effective heights shown by the two curves throughout the first 4¼ hours presents a striking contrast to the conditions during the succeeding 2 hours.

The results shown in this graph are therefore interpreted as a clear indication of an eclipse effect which resulted in an increase of the minimum equivalent height of region *F* to almost double the value appropriate at that hour. The time relation suggests that the agency producing this great change in the equivalent height of the region travels with a velocity approaching that of light. The greatest height was recorded at 0445 G.M.T. or approximately 30 min. after the time at which the eclipse reached its maximum phase on the ground. Since the time of maximum phase at a height of approximately 300 km. would not be greatly different from that on the ground, this difference in time cannot be explained in this way.

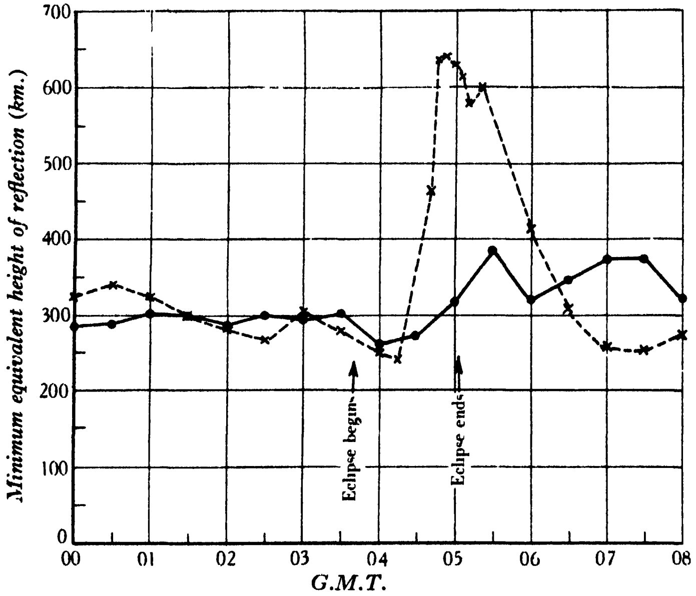

Figure 1. Minimum equivalent height of the F_2 region. ●—● mean for 17, 18, 20, 21 June; ×---× values for 19 June.

(*b*) *Critical frequency of the F region.* It will be seen from figure 3 that considerable magnetic activity was present throughout the whole period. Now, one of the great difficulties associated with the interpretation of the results obtained during the present eclipse will be to separate any effect due to the eclipse from that which can be associated with the magnetic variations which continued throughout the morning of the eclipse.

The changes which occurred in the ionization-density of region F_2 are plotted in figure 2. The quantity measured is the lowest frequency for the ordinary-wave component which just succeeds in penetrating the region. Now it has been shown by Appleton$^{(4,5)}$ that this critical frequency is proportional to the square root of the ionization in the region in question. In order to show how the ionization varies, the measured values of the critical frequency have been squared. One curve shows the average conditions on the control days and the other curve shows the conditions existing on the morning of the eclipse. It is clear from this graph that the time of minimum ionization on the morning of the eclipse was 0445 G.M.T. The delay may have been due to the combination of sunrise and eclipse effects or it may have been due in part to a very reduced recombination or attachment coefficient. It is probable that both effects are present. A similar discrepancy was observed at Washington$^{(3)}$ during the solar eclipse of 3 February 1935, although the delay was only $9\frac{1}{2}$ min. in the case of region F_2 and 20 min. in the case of region F_1. These values were, however, calculated for a height of 250 km., so that the delay times are not strictly comparable.

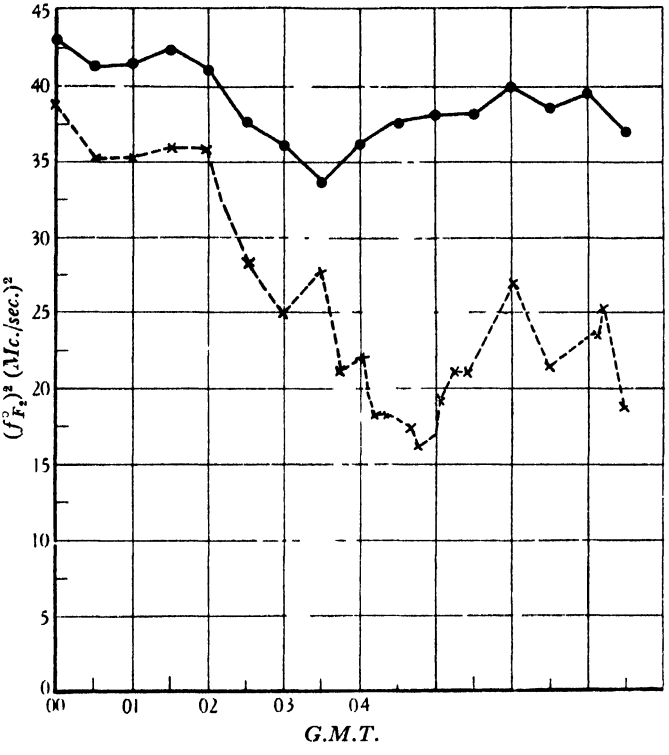

Figure 2 Critical frequencies for the ordinary ray in region F_2 ●—● mean curve for 17, 18, 20–25 June, ×---× values for 19 June

In figure 2 the reduction of ionization on the morning of the eclipse is clearly shown and it is observed to begin about 45 min. before the height begins to alter.

At the minimum the ionization was actually 56 per cent below the normal value, although it must be recorded that the general level of the ionization was about 15 per cent below the normal values on the morning of the eclipse. In this connexion it should be noted that the percentage of the sun's disk which was obscured at the maximum phase of the eclipse was also 56 per cent.

§ 3. COMPARISON WITH MAGNETIC CONDITIONS

To demonstrate the effect of the eclipse on the ionization more clearly, the departures from the normal curve for region F_2 are plotted in figure 3(*a*). On the same graph the values of the horizontal component of the magnetic force are plotted. Here it can be seen that a close correspondence between the curves exists over the eclipse period. The marked minimum at 0445 G.M.T. in both curves is repeated in the vertical-intensity and declination traces shown in figure 3(*b*). Indeed, the marked correspondence, even in detail, between these two elements, one a force and the other an angle, during the period of the eclipse contrasts with their otherwise generally opposite trends.

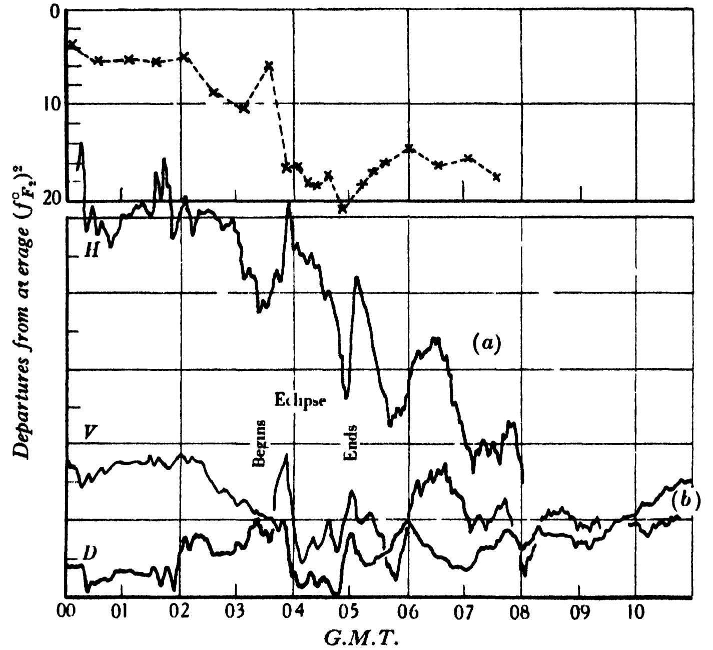

Figure 3. Departures of $(f^0_{F_2})^2$ from the mean values compared with (*a*) variations in the horizontal magnetic force and (*b*) the vertical magnetic force and the declination plotted for the morning of the eclipse. ×---× departures of $(f^0_{F_2})^2$ from average value; *H*, horizontal value of magnetic force; *V*, vertical component of magnetic force; *D*, declination; Scale intervals—26·1γ for *H*, 24·5γ for *V* and 6′·1 for *D*.

Now, it has been shown above that, superimposed on the general effect on the F_2 region of a magnetic disturbance which was in progress throughout the day of the eclipse, there was a marked effect due to the eclipse itself. This eclipse effect resulted in a marked increase in the minimum equivalent height accompanied by a marked decrease in the maximum ionization-content of region F_2. Appleton and Ingram have shown that this same two-element change in this region accompanies a magnetic disturbance(6, 7). It seems reasonable therefore to investigate the changes in the magnetic elements over the period occupied by the eclipse effect on the ionosphere, to see if any special perturbation can be attributed to the eclipse.

From this investigation it is concluded that there is an indication that the effect of the eclipse of the sun can be observed in the magnetic elements.

Now, Prof. Chapman(8) has discussed the effect of a solar eclipse on the earth's magnetic field in relation to data provided by radio observations. In addition, variations in the magnetic elements themselves have been studied (9) during a number of solar eclipses, but there is still no general agreement on the existence of an eclipse effect upon the earth's magnetic field.

In contrast it should be remarked that Dr L. A. Bauer(9) was firmly convinced that a small eclipse effect had been demonstrated in several instances, while Dr C. Nordmann(10) concluded that "during the eclipse of 30 August 1905 there was superposed upon the general magnetic disturbance which took place at that time a special perturbation attributable to the eclipse".

The words of Chree(11) written on this subject nearly a quarter of a century ago are still applicable and are quoted to justify the publication of these comments: "At the present stage of our knowledge, the best course seems to be to describe the phenomena with an unprejudiced mind, in the hope that when sufficient eclipse data have accumulated some common feature or features may become apparent."

If we now consider the *E* region, we find that at the hour of the eclipse the critical frequency for this region was already so low that it was impossible to measure any reduction in its value. This region has already been closely studied during previous eclipses so that attention was concentrated on the abnormalities only in this region. First among these was a notable absence during the early hours of the morning of the type of echo which has been previously designated "*E* persistence".* These echoes appeared on the mornings of the control days, and the mean curve for these is shown in figure 4. It should be observed that on the morning of the eclipse these echoes began to appear at 0100 G.M.T. From 0130 to 0400 G.M.T. no sign of them could be seen. After that period the frequency on which they could be observed increased steadily and afterwards decreased as shown in the graph. The absence of this type of echo at a time when the corpuscular eclipse might be expected to occur must be recorded, although from experience of these echoes from region *E*, particularly in relation to their sudden appearance and disappearance, it is impossible to be certain of any conclusion. The observations which are shown in the dotted curve in figure 4 refer to the lowest frequency on which reflection from the *F* region of the ionosphere was obtained. During the night these values correspond very closely with f_E^0, but in the morning they increase more rapidly than f_E°. The maximum in this curve of abnormal region-E echoes occurred at the same time as the minimum of ionization in region F_2 and the minimum in the magnetic elements, already referred to.

---

* This term has been used to denote the persistence of region *E* echoes at frequencies beyond those corresponding to the normal penetrating value for the appropriate time of the day.

Now there is no clear indication of the amount of ionization existing when these echoes are observed, but it is known that this must be high(12). It is clear from figure 4 that during the period of the eclipse there was certainly no diminution of ionization in this region, but there is rather strong evidence that it actually increased. There is here a clear indication that these abnormal region-E echoes are not caused by increased ultraviolet light from the sun.

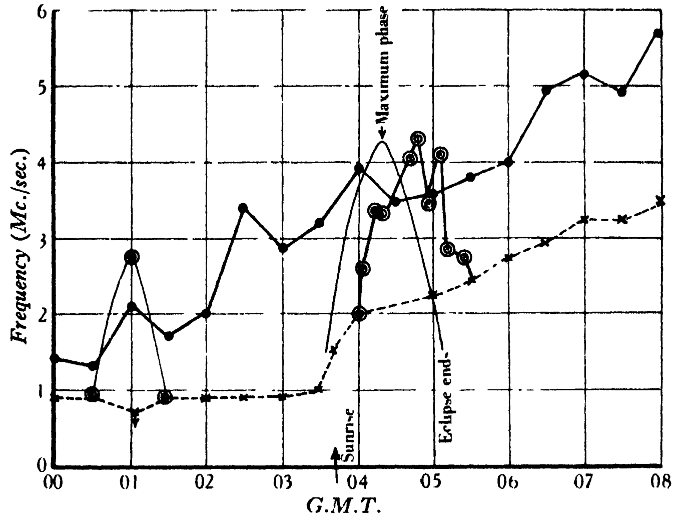

Figure 4. Measurements of the highest frequency on which echoes were obtained from the E region and of the lowest frequency on which echoes were obtained from the F region on the morning of the eclipse. ●—● highest frequency on which region E echoes were observed, mean of 17, 18, 20 and 21 June; ◎---◎ ditto for 19 June; × --- × lowest frequency on which echoes from region F were observed on 19 June.

§4. OBLIQUE-INCIDENCE MEASUREMENTS OF FIELD-STRENGTH

These measurements were made from 17 to 21 June. The four mornings, excluding the morning of the eclipse, have been averaged to form a basis of comparison from which departures on the morning of the eclipse could be assessed.

The observations were made on the following transmissions: (*a*) Rocky Point 5130 metres, 72° 56′ W., 40° 56′ N.; (*b*) Lawrenceville 30·4 metres, 74° W., 40° N.; (*c*) Nagoya 33·41 and 19·08 metres, 137° E., 35° N.; (*d*) Fiskville 28·73 metres, 143° E., 37° S.

In figure 5 are shown the two curves for the low-frequency signal traversing the transatlantic path from Rocky Point to Cupar, lat. 56° 19′ N., long. 2° 57′ W. It is almost certain that this frequency of 60 kc./sec. travelled via the lowest part of the normal E region. It is far removed from the critical penetration value, so that changes in ionization would not be observed. It is evident that approximately the same energy was received on the night of the eclipse as on the other nights.

Next consider a high-frequency transmission on 9·87 Mc./sec., figure 6, from Lawrenceville to Baldock, lat. 51° 57′ N., long. 0° 11′ W., which follows roughly the same path. In this case it is almost certain that the energy travelled via the F_2 region of the ionosphere. There is a marked fade-out of energy shortly after 0400 G.M.T. At vertical incidence at this time the critical frequency for region F_2

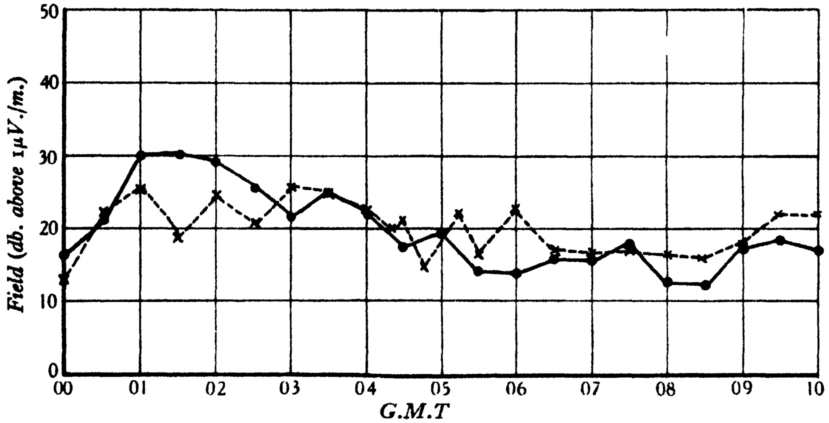

Figure 5. Field-strength measurements made at Cupar, lat. 56° 19′ N., long. 2° 57′ W., on transmissions from Rocky Point, lat. 40° 56′ N., long. 72° 56′ W., on a wave-length of 5130 metres (58·5 kc./sec.). ●—● mean curve for 17, 18, 20 and 21 June; ×---× values for 19 June.

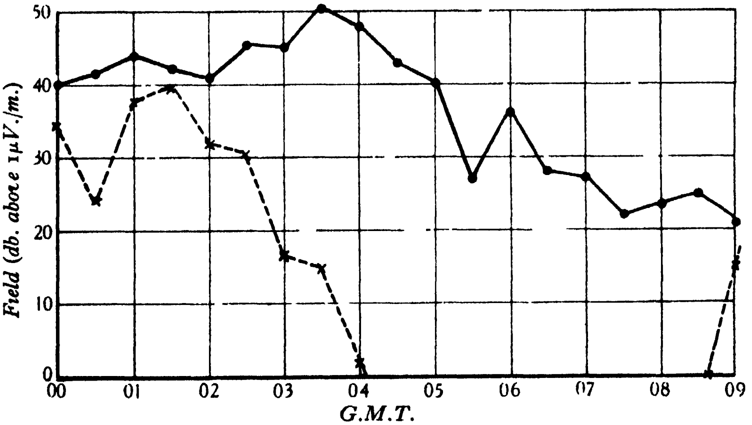

Figure 6. Field-strength measurements made at Baldock, lat 51° 57′ N., long 0° 11′ W., on transmissions from Lawrenceville, lat. 40 N., long 74 W., on a wave-length of 30·4 metres (9·87 Mc./sec.). ●—● mean curve for 17, 18, 20 and 21 June; ×---× values for 19 June.

was 4·25 Mc./sec. If we assume a simple cosine law to hold in relating the highest frequency on which echoes can be observed with $f^{\circ}_{F_2}$ we have

$$\theta_0 = 64\tfrac{1}{2}^{\circ},$$

where θ_0 is the angle of incidence at the layer.

The minimum equivalent height of reflection measured at vertical incidence at 0400 was 300 km. and the distance from the transmitter to the receiver was roughly 5,500 km. Now if we consider that the energy travels by three successive reflections between the earth and the F_2 region, we can calculate the angle of incidence at the layer, and in this way we find that $\theta_0 = 66°$.

This close agreement between the values of the angles of incidence at the layer as calculated from two different measurements, namely the critical frequency and the equivalent height of reflection, is strong evidence that the fade-out observed on the transmission from Lawrenceville was a genuine case of electron-limitation. This linking of vertical-incidence measurement with oblique-incidence measurement is also extremely convincing and shows that, as one would expect from the path of the signals, the conditions at the receiving site control the situation. On this occasion we had the unique situation of the eclipse effect superimposed on a mimimum of ionization or, as it may otherwise be regarded, a delayed sunrise.

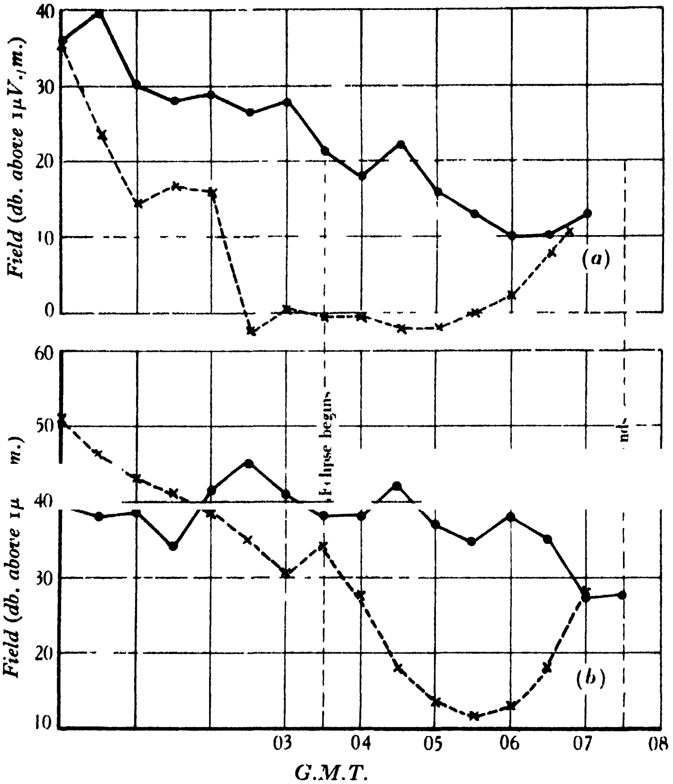

Figure 7. (*a*) Field-strength measurements made at Baldock on transmissions from Nagoya, lat. 35 N., long. 137 E., on a wave-length of 19·1 metres (15·72 Mc./sec.). ●—● mean curve 17, 18, 20 and 21 June; ×---× values for 19 June. (*b*) As figure 7(*a*) but on a wave-length of 33·4 metres (8·98 Mc./sec.). ●—● mean curve 17, 18, 20 and 21 June; ×---× values for 19 June.

This agreement can be tested further if we consider the measurements made at Baldock on the transmissions from Japan and shown in figure 7. The higher frequency of 15·72 Mc./sec. appears to be critical about 0200 G.M.T. when $f^0_{F_2}$ was 6·0 Mc./sec. After performing the same calculations as before we obtain a value of

67½° for the angle of incidence at the layer, and if we determine this quantity from the measurement of equivalent height which was also 300 km. we obtain a value of 68° which is again a very satisfactory agreement. In this case five reflections have been assumed.

The lower frequency of 8·98 Mc./sec. from the same station shows a marked reduction of energy received over the period 0330 G.M.T. till the end of the observation at 0700 G.M.T. In figure 7(*b*) this is shown in relation to the time of the eclipse over the path of the transmission, and the comparison shows that these periods coincide. This reduction in energy may be attributed to the removal, as a result of the decreased ultraviolet light from the sun, of certain of the multiply reflected rays of higher order traversing the path. It should be noted that the return of the energy to normal occurs on both frequencies at about 0700 G.M.T.

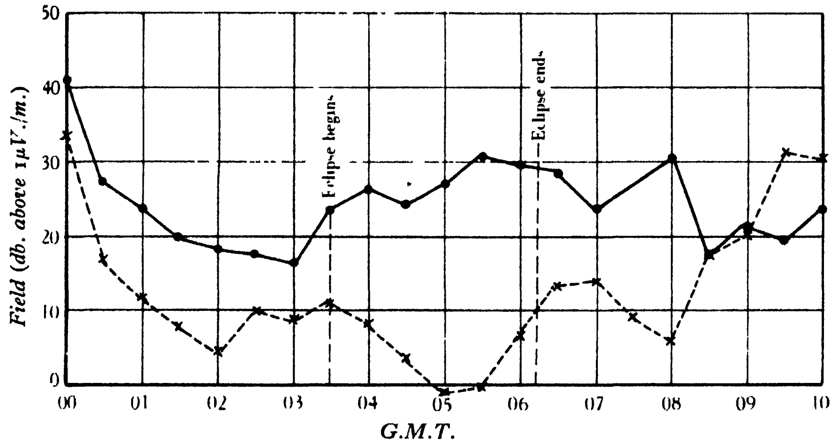

Figure 8. Field-strength measurements made at Baldock on transmissions from Fiskville, lat. 37 S., long. 143' E., on a wave-length of 28·7 metres (10·45 Mc./sec.). ●—● mean curve 17, 18, 20 and 21 June; × --- × values for 19 June.

The energy from the Fiskville transmitting station in Australia on a frequency of 10·45 Mc./sec. is plotted in figure 8, where it is shown that on the morning of the eclipse the energy showed a marked departure from the usual trend over the period 0330 to 0630 G.M.T. This is very similar to figure 7(*b*) except that it reaches its normal value half an hour earlier. If we consider the path of the Australian transmission in relation to the eclipse belt we find that the eclipse was actually over half an hour earlier on this route.

From these five graphs we conclude that the energy-level on the morning of the eclipse was about 10 db. lower than normal and that energy traversing the path of the eclipse was definitely reduced during the period of the eclipse. This can be interpreted in terms of accepted theory. In one case electron-limitation caused the energy to disappear before the beginning of the eclipse. This interpretation of electron-limitation was doubly checked and found to be in agreement with measurements made at vertical incidence. It should be noted that the sunrise and eclipse condition at the receiving site probably represents the minimum ionization in the path the energy travels in the various cases considered. Also, the time and magnitude of the eclipse have been considered only in relation to the surface of the earth. For the regions concerned a small correction would be necessary if high accuracy were required.

§ 5. ACKNOWLEDGEMENTS

In conclusion, the author wishes to thank Prof. E. V. Appleton for helpful discussion during the writing of this paper. He is indebted to Colonel A. G. Lee for arranging for the measurements of field-strength to be made by the British Post Office and to Dr H. Spencer Jones for the Abinger magnetic data discussed in the paper.

The work was undertaken as part of the programme of the Radio Research Board and is published by permission of the Department of Scientific and Industrial Research.

REFERENCES

(1) [Polar Year paper. *Proc. roy. Soc.*]
(2) Appleton, E. V. and Chapman, S. *Proc. Inst. Radio Engrs*, N.Y., **23**, 649 (1935).
(3) Kirby, S. S., Gilliland, T. R. and Judson, E. B. *Bur. Stand. J. Res.*, Wash., **16**, 213 (1936).
(4) Appleton, E. V. *Nature*, Lond., **127**, 197 (1931).
(5) Appleton, E. V. and Naismith, R. *Proc. roy. Soc.* **137**, 36 (1932).
(6) Appleton, E. V. and Ingram, L. J. *Nature*, Lond., **136**, 548 (1935).
(7) International Union of Geodesy and Geophysics, Dept. 1936 Report.
(8) Chapman, S. *Terr. Mag. atmos. Elect.* **38** 175 (1933).
(9) Bauer, L. A. *Terr. Mag. atmos. Elect.* **25**, 81 (1920).
(10) Nordmann, C. *Terr. Mag. atmos. Elect.* **12**, 25 (1907).
(11) Chree, C. *Quart. J. R. met. Soc.* **39**, 232 (1913).
(12) Appleton, E. V. and Naismith, R. *Proc. roy. Soc.* A, **150**, 707 (1935).

NOTE ON THE RADIATION BETWEEN TWO COAXIAL RADIATING CYLINDERS

By H. BUCKLEY, M.Sc., F.Inst.P.,
National Physical Laboratory

Received 12 *August* 1936. *Read in title* 12 *February* 1937

ABSTRACT. The paper discusses the problem of the radiation transfer from an electrically heated inner cylinder to a surrounding coaxial cylinder. Expressions are derived for the total radiation, emitted and reflected, from unit area of each of the cylindrical surfaces between which multiple reflection of radiation occurs. It is then shown how, from these expressions, the relation of the true temperatures to the apparent temperatures of the surfaces (obtained by means of a total-radiation pyrometer or by means of a disappearing-filament optical pyrometer) can be determined.

§ 1. INTRODUCTION

The problem of the determination of the effect of multiple reflections is of practical importance in radiometric measurement of the temperatures of bodies heated by radiation from surrounding or partly surrounding bodies. A particular case mentioned to the author by Dr Ezer Griffiths concerned two coaxial cylinders, of which the outer one was of material whose thermal conductivity was to be deduced from temperature-measurements of its inner and outer surfaces when it was in a steady state under the influence of radiation from the electrically heated inner cylinder.

The problem of the heat-transfer from the inner cylinder in this case has been considered by Merkel(1), Gröber(2), ten Bosch(3), Clausing(4) and Saunders(5).

Clausing's work was in connexion with the anodes and cathodes of thermionic valves and with indirectly heated filaments. Saunders also discussed the effect of displacement of the inner cylinder on the amount of the heat-transfer, when the reflecting power of the outer cylinder was small.

All the above-mentioned authors dealt with the amount of the heat-transfer alone. None of them dealt with the quantity of radiation emitted per unit area from each of the surfaces in the steady state, nor did they deal with the possibility of deducing the true temperatures of the surfaces from radiometric observation of the surfaces between which the heat-transfer occurs. If the inner and outer cylinders are absolutely black bodies, observation by means of a total radiation pyrometer or an optical pyrometer through a small hole in the outer cylinder will determine their temperatures directly. If, however, the two cylinders are not black bodies, the apparent temperatures derived in this way may differ very considerably from the true temperatures, and in consequence may lead, unless corrected, to very serious errors in the determination of the thermal conductivity of the outer cylinder.

It is the purpose of this note to determine the total radiation from each of the two surfaces in this case and to show how their true temperatures may be obtained.

§2. RADIATION BETWEEN INFINITE COAXIAL CYLINDERS

Consider an infinitely long solid cylinder of radius a, coaxial with an infinitely long hollow cylinder of internal radius b and external radius c. This system is further assumed to be surrounded by a non-radiating enclosure at an infinite distance. The inner cylinder A is heated by means of an electric current, and the various surfaces finally attain a steady state. Let the steady temperatures corresponding to this steady state be T_a, T_b and T_c respectively. Let it be further assumed that the surfaces of the cylinders are completely diffusing and have total emissivities of ϵ_a, ϵ_b and ϵ_c respectively which are all independent of wave-length, so that the surfaces are grey radiators. Their reflection factors will therefore be $(1-\epsilon_a)$, $(1-\epsilon_b)$ and $(1-\epsilon_c)$.

The surfaces A and B of the cylinders will emit radiation in virtue of their temperature alone equal to $\epsilon_a\sigma T_a^4$ and $\epsilon_b\sigma T_b^4$ per unit area and will reflect and absorb portions of the radiations falling on them from other parts of themselves or from other bodies. In the case of the outer surface of the outer cylinder no other radiation falls on the surface, so that the total radiation from it is $\epsilon_c\sigma T_c^4$ per unit area.

Thus the total radiation from any point on surface A will consist of the radiation emitted by A in virtue of its temperature, namely $\epsilon_a\sigma T_a^4$, together with the reflected fraction $(1-\epsilon_a)$ of the radiation received from the surrounding surface B. If the total radiation per unit area from surface A is denoted by ϕ_a, we have

$$\phi_a=\epsilon_a\sigma T_a^4+(1-\epsilon_a)\,\phi_b \qquad \ldots\ldots(1),$$

where ϕ_b is the total radiation per unit area from surface B. Similarly, the total radiation per unit area from surface B will consist of its temperature radiation $\epsilon_b\sigma T_b^4$ together with the fraction $(1-\epsilon_b)$ of the radiation received from the rest of the surface B and from the surface A.

Now the radiation received at any point P on surface B from the surface A is equal to the radiation from the projected area of A on surface B, the projected area on surface B being assumed to emit the same amount of radiation per unit area as the surface A. The projected area can be regarded as a series of elementary strips parallel to the common axis of the two cylinders. Now the radiation per unit area received at point P on surface B from an infinitely long elementary strip of width $b\,d\theta$ can be shown to be

$$\frac{\phi}{4}\sin\frac{\theta}{2}\,d\theta,$$

where θ is the angle which the normal to the elementary strip makes with the normal at the point P.

Thus the radiation per unit area received at point P from the projection of surface A on surface B is given by

$$2\int_{2\cos^{-1}(a/b)}^{\pi}\frac{\phi}{4}\sin\frac{\theta}{2}\,d\theta=\frac{a}{b}\phi.$$

Similarly, the radiation per unit area received at point P from the portion of surface B not in the projection of surface A, is given by

$$2\int_0^{2\cos^{-1}(a/b)} \frac{\phi}{4}\sin\frac{\theta}{2}\,d\theta = \frac{b-a}{b}\,\phi.$$

Hence the total radiation per unit area from any point on surface B is given by

$$\phi_b = \epsilon_b\sigma T_b^4 + (1-\epsilon_b)\left\{\frac{b-a}{b}\,\phi_b + \frac{a}{b}\,\phi_a\right\} \qquad \ldots\ldots(2).$$

Equations (1) and (2) are two simultaneous equations in ϕ_a and ϕ_b. The solutions are

$$\phi_a = \sigma T_a^4 - \frac{\epsilon_b b\,(1-\epsilon_a)\,(\sigma T_a^4 - \sigma T_b^4)}{\epsilon_a a + \epsilon_b b - \epsilon_a\epsilon_b a},$$

$$\phi_b = \sigma T_b^4 + \frac{\epsilon_a a\,(1-\epsilon_b)\,(\sigma T_a^4 - \sigma T_b^4)}{\epsilon_a a + \epsilon_b b - \epsilon_a\epsilon_b a}.$$

Thus the total radiation from surface A is less than the full radiation corresponding to its temperature, and that from surface B is greater than the corresponding quantity. In each case the total radiation is a mixture of radiations of two qualities, corresponding to colour temperatures T_a and T_b respectively.

As we have assumed that the system of cylinders is situated at an infinite distance from non-radiating surroundings, the radiation from surface C of the outer cylinder will be unaffected by the surroundings and will be $\epsilon_c\sigma T_c^4$ per unit area, where ϵ_c will equal ϵ_b if emissivity is independent of temperature. This radiation will of course represent the heat transferred from the inner cylinder, which also equals the electrical energy required to maintain the inner cylinder at the steady temperature T_a.

Since radiation-emission involves loss of heat, radiation-absorption involves gain of heat, and reflection of radiation involves neither loss nor gain, the loss of heat per unit area from surface A is given by

$$H_a = \epsilon_a\sigma T_a^1 - \epsilon_a\phi_b.$$

The total heat-loss per unit length from surface A is therefore

$$Q = 2\pi H_a = 2\pi a\,(\epsilon_a\sigma T_a^4 - \epsilon_a\phi_b).$$

On substitution of the value of ϕ_b given above this reduces to

$$Q = \frac{2\pi\epsilon_a\epsilon_b ab\,(\sigma T_a^4 - \sigma T_b^4)}{\epsilon_a a + \epsilon_b b - \epsilon_a\epsilon_b a}$$

$$= \frac{\epsilon_b S_a\epsilon_a\sigma T_a^4 - \alpha\epsilon_a S_b\epsilon_b\sigma T_b^4}{\epsilon_b + \alpha\epsilon_a R_b},$$

where S_a and S_b are the areas of unit lengths of the surfaces A and B, $\alpha = a/b$, the fraction of the radiation from B received by A, and R_b is the reflection factor of surface B. This expression for the total heat-transfer between the two cylinders is the same as that which has been obtained by previous workers on the subject. It might be noted that these previous derivations of the result were rather complicated as they involved the summation of an infinite number of successive reflections or the introduction of fictitious surfaces.

§ 3. DETERMINATION OF THE TRUE TEMPERATURES OF THE SURFACES A AND B OF THE CYLINDERS

Now ϕ_a and ϕ_b can be measured, for example, by observation with a pyrometer through a small hole in the outer cylinder. If the observations are made with a total-radiation pyrometer, the apparent temperatures $\mathcal{T}_a$ and $\mathcal{T}_b$ determined are those for which $\sigma\mathcal{T}_a^4=\phi_a$ and $\sigma\mathcal{T}_b^4=\phi_b$.

From equation (1) $$\epsilon_a\sigma T_a^4=(\phi_a-\phi_b)+\epsilon_a\phi_b,$$

so that $$T_a^4=\frac{\mathcal{T}_a^4-\mathcal{T}_b^4}{\epsilon_a}+\mathcal{T}_b^4.$$

Similarly from equation (2)

$$T_b^4=\mathcal{T}_b^4-\frac{a(1-\epsilon_b)}{b\epsilon_b}(\mathcal{T}_a^4-\mathcal{T}_b^4).$$

These equations enable T_a and T_b to be deduced from observations of $\mathcal{T}_a$ and $\mathcal{T}_b$.

If the observations are made by means of an optical pyrometer with a monochromatic screen, the calculations given above become more general and the restriction that the emissivities be independent of wave-length need no longer apply. Equations (1) and (2) still hold for each wave-length interval in the steady state, so that they become

$$\phi_{a\lambda}=\epsilon_{a\lambda}C_1\lambda^{-5}\exp(-C_2/\lambda T_a)+(1-\epsilon_{a\lambda})\,\phi_{b\lambda} \qquad \ldots\ldots(3),$$

$$\phi_{b\lambda}=\epsilon_{b\lambda}C_1\lambda^{-5}\exp(-C_2/\lambda T_b)+(1-\epsilon_{b\lambda})\left\{\frac{b-a}{b}\phi_{b\lambda}+\frac{a}{b}\phi_{a\lambda}\right\} \qquad \ldots\ldots(4).$$

The apparent temperatures $\mathcal{T}_a$ and $\mathcal{T}_b$ observed with the optical pyrometer are such that

$$\phi_{a\lambda}=C_1\lambda^{-5}\exp(-C_2/\lambda\mathcal{T}_a),$$

$$\phi_{b\lambda}=C_1\lambda^{-5}\exp(-C_2/\lambda\mathcal{T}_b).$$

From equation (3) it can be shown that

$$\exp(-C_2/\lambda T_a)=\frac{\exp(-C_2/\lambda\mathcal{T}_a)-\exp(-C_2/\lambda\mathcal{T}_b)}{\epsilon_{a\lambda}}+\exp(-C_2/\lambda\mathcal{T}_b),$$

and from equation (4) that

$$\exp(-C_2/\lambda T_b)=\exp(-C_2/\lambda\mathcal{T}_b)-\frac{a(1-\epsilon_{b\lambda})}{b\epsilon_{b\lambda}}\{\exp(-C_2/\lambda\mathcal{T}_a)-\exp(-C_2/\lambda\mathcal{T}_b)\}.$$

The table gives the observed temperature corresponding to a true temperature T_b of 1400° K. for different values of ϵ_b when $\epsilon_a=1$, $T_a=\mathcal{T}_b=1600^\circ$ and $a/b=1/2$.

$T_a=\mathcal{T}_b=1600^\circ$ K. $T_b=1400^\circ$ K.			ϵ_a or $\epsilon_{a\lambda}=1$ $\lambda=0{\cdot}62$	
ϵ_b or $\epsilon_{b\lambda}$	$\mathcal{T}_b$ by radiation pyrometer (° K.)	Correction to $\mathcal{T}_b$ (° K.)	$\mathcal{T}_b$ by optical pyrometer (° K.)	Correction to $\mathcal{T}_b$ (° K.)
0·1	1569	−169	1581	−181
0·25	1529	−129	1553	−153
0·50	1476	−176	1508	−108
0·75	1434	−34	1460	−60
0·90	1413	−13	1427	−27
1·00	1400	0	1400	0

REFERENCES

(1) Merkel. *Die Grundlagen der Wärmeübertragung*, p. 168 (1927). Dresden and Leipzig: Th. Steinkopff.
(2) Gröber. *Einführung in die Lehre von der Wärmeübertragung*, p. 131 (1926). Berlin: J. Springer.
(3) ten Bosch. *Die Wärmeübertragung*, p. 26 (1927). Berlin: J. Springer.
(4) Clausing. *Rev. Opt.* **10**, 353 (1931).
(5) Saunders. *Proc. phys. Soc.* **41**, 569 (1928–9).

THE MAGNETIC PROPERTIES OF MANGANESE AMALGAMS

By L. F. BATES, D.Sc., Professor of Physics,
University College, Nottingham,
AND
L. C. TAI, B.Sc. (Nanking), Ph.D. (London).

Received 27 *October* 1936. *Read in title* 12 *February* 1937

ABSTRACT. The variation with temperature of the magnetic susceptibilities of a series of manganese amalgams of known concentration has been determined over a range from 15° to 350° C. The amalgams show pronounced temperature hysteresis of their magnetic properties, and it is found that the manganese becomes more paramagnetic as the temperature rises, until, in the case of the more concentrated amalgams, a steady state is reached. The phenomena are briefly discussed in the light of the recent theories of alloys.

§ 1. INTRODUCTION

In an account of some measurements of the magnetic susceptibilities of mercury amalgams(1) the writers recently described the behaviour of amalgams containing small quantities of manganese. It was pointed out that in very dilute solution manganese possesses an atomic susceptibility of $13{,}700 \times 10^{-6}$ e.m.u./g., a high value which was in accord with the experimental values for manganese dissolved in copper, silver and gold. The atomic susceptibility so found depended on the concentration of the manganese, and the value quoted above refers to solutions containing less than 1 part of manganese in 1000 parts of mercury, where it is thought that manganese does not form complex molecular groups, like Mn_2Hg_5, which are considered to exist in higher concentrations(2). Now, in order to determine the atomic moment of the manganese atom in dilute solution we must know whether the values of the atomic susceptibility for a series of temperatures obey a Curie-Weiss law, and the measurements described below were primarily undertaken with this end in view.

§ 2. EXPERIMENTAL PROCEDURE

The amalgams in the previous investigation were prepared by electrolysis, washed and dried, without being heated. It was now necessary to ensure that all traces of water were completely removed, since in order to prevent oxidation at higher temperatures the amalgams had to be placed in evacuated sealed tubes. Freshly prepared amalgam was placed as quickly as possible in the bulb *A*, figure 1, which was evacuated through *B*. The amalgam was then heated to about 100° C. and finally poured into the tube C which was then sealed at D. A glass hook was provided at D and the tube and its contents suspended together with an evacuated compensating tube from one arm of a sensitive balance, and the susceptibility was measured by the Gouy method as previously described. If the tube containing the amalgam is of uniform cross-section α, and the lower end of the amalgam is in a uniform field H while the upper end is in a field H_0, the additional magnetic force $m_T.g$ on the column is given by

$$m_T.g=\tfrac{1}{2}.(k_{\mathrm{Am}})_T.\alpha.(H^2-H_0^2),$$

where $(k_{\mathrm{Am}})_T$ is the volume susceptibility of the amalgam at the temperature T. In deriving this expression it is assumed that effects due to the magnetic properties of the air are entirely eliminated by the use of the compensating tube. If the tube is now opened and the amalgam replaced by pure mercury of susceptibility $(k_{\mathrm{Hg}})_R$ at room temperature R, the additional force $m_R'.g$ is given by

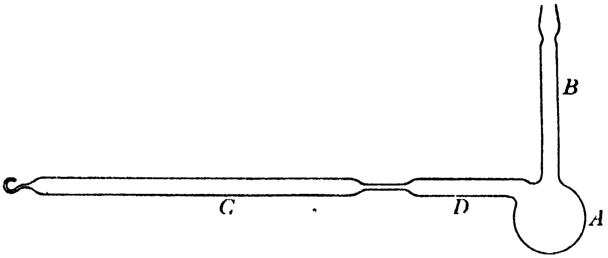

Figure 1. Apparatus for preparation of dry amalgam

$$m_R'.g=\tfrac{1}{2}.(k_{\mathrm{Hg}})_R.\alpha.(H^2-H_0^2),$$

whence
$$(k_{\mathrm{Am}})\,T=\frac{m_T}{m_R'}\,(k_{\mathrm{Hg}})_R=m_T.Q,$$

and, assuming that at any given temperature the density of the amalgam is identical with that of pure mercury at the same temperature,

$$(\chi_{\mathrm{Am}})_T=\frac{m_T.Q}{\rho_T},$$

where χ_{Am} refers to the mass susceptibility of the amalgam and ρ_T is the density of the mercury at that temperature.

The results may possibly be made a little more precise by comparing the magnetic pull m_T with the magnetic pull m_T' for pure mercury at the temperature T, and some experiments on these lines were actually made. A set of results showing how the mass susceptibility of pure mercury varies with temperature is given in table 1, where the values merely rise from $-0{\cdot}168$ at 15° C. to $-0{\cdot}167\times10^{-6}$ at 350° C.

Table 1

T(° K.)	290·3	364·2	448·3	521·2	570·5	618·0
$-\chi\times10^6$	0·1680	0·1684	0·1677	0·1670	0·1668	0·1670

In all, three such sets of results were obtained with different samples of mercury; they agree very well from room temperature up to about 250° C., but at higher temperatures two of the sets show increases to $-0{\cdot}164\times10^{-6}$ at 350° C.; the differences may have been due to the formation of small cavities of vapour between the liquid mercury and the walls of the containers, or to the presence of very small amounts of impurity. However, even if the higher value of the susceptibility at 350° C. is taken as correct, it has very little influence on the amalgam results described here; we prefer to take the lower value in view of the following results.

§ 3. RESULTS

The main experiments were made with amalgams I, II and III respectively containing 0·0016, 0·016 and 0·03 g. of manganese in 100 g. of mercury. In all cases very definite hysteresis phenomena were recorded. The variation with temperature of the mass susceptibility of amalgam I is shown at I in figure 2. Starting at room temperature the mass susceptibility rose regularly from $-0{\cdot}1645\times10^{-6}$ to about $-0{\cdot}155\times10^{-6}$ at about 200° C. after which there was a more definite increase, and eventually a steady state was reached at about 350° C. Each of the experimental points was obtained after the amalgam had been maintained at a chosen temperature for about 45 min.; the arrows indicate the course of the observations and the points marked with open circles were obtained on the same day. The following day the point marked with a cross was obtained before the temperature was raised, and the points marked with filled circles were obtained after the specimen had been raised to 350° C., the value at the highest temperature being recorded after the amalgam had been maintained at 350° for about 1 hour The filled circles clearly lie below the open circles and this feature is attributed to the difference in the times taken in heating and cooling the amalgam on the different days. The point marked with

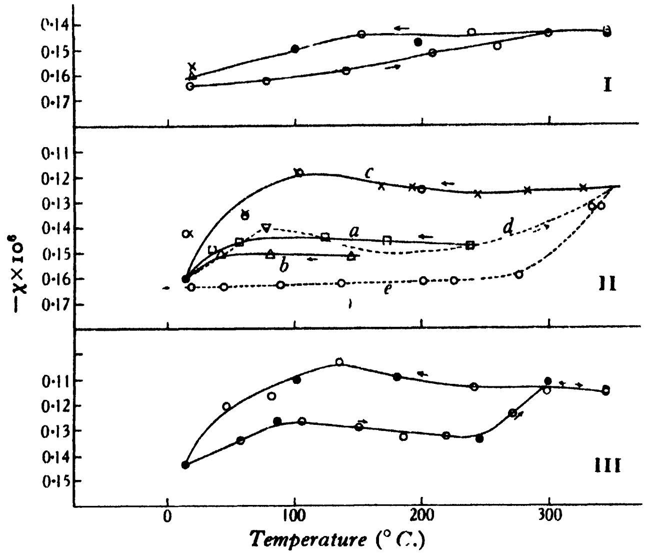

Figure 2. Graphs showing susceptibility of manganese amalgams as a function of temperature. I, 0·0016 g. manganese in 100 g. mercury; II, 0·016 g. manganese in 100 g. mercury; III, 0·030 g. manganese in 100 g. mercury.

an upright triangle was obtained a day later. It is clear that the initial and final values of the susceptibility at room temperature do not coincide and it is considered that this too may be occasioned by the rate at which the cooling was carried out. Further support for this view was obtained from some experiments made on an amalgam IV, containing 0·008 g. of manganese in 100 g. mercury. This was kept at 350° C. for 1 hour and then quenched to room temperature; values of the mass susceptibility found at various mean intervals of time after the quenching are given in table 2.

Table 2. Variation of mass susceptibility of amalgam IV with time after quenching

t (min.)	32	75	123	195
$-\chi_{\mathrm{Am}} \times 10^6$	0·1427	0·1480	0·1501	0·1550

A series of curves obtained with amalgam II are shown at II in figure 2. Curve *a* was obtained by first raising the temperature to 250° C. and maintaining it at 239·4° C. for 1 hour and then observing the susceptibility at chosen temperatures at each of which it was maintained for 45 min. Curve *b* was similarly obtained after the amalgam had been heated to 155° C. and maintained at 146° C. Curve *c* through the points marked with a cross was likewise obtained when the amalgam was initially raised to 345° C. It is seen that whereas the starting and final values at room temperature taken on successive days were the same for curves *a* and *b*, this was not the case in *c*, when the amalgam had been heated to 350°. There appears to be some instability, or at any rate uncertainty, about successive values obtained at room temperature after high-temperature treatment, and it may be that the amalgam near the pole pieces is no longer homogeneous, but it is difficult to see how this state can arise. The broken curve *d* shows approximately the variation of susceptibility as the specimen is heated from room temperature to 350° C. The specimen was now cooled for a short time in carbon dioxide snow and the series of values shown by curve *e* was obtained while the temperature was raised to 345° C. and then lowered to room temperature. The hysteresis in this case is very striking.

The behaviour of the most concentrated amalgam, III, is shown at III in figure 2, where the arrows indicate the direction in which the temperature was changed during the course of the observations, the filled-circle values being obtained on the day following that on which the open-circle values were found. In the case of this amalgam the initial increase in susceptibility is followed by a steady decrease until a rapid rise in susceptibility occurs at about 250° C., as with the other amalgams described above, and a final steady value is reached. Temperature hysteresis is again strongly marked, and the time factor is still involved but to a lesser extent;

Table 3. Variation of mass susceptibility of amalgam III with time after quenching

t (min.)	43	94	150	245	345	$\to\infty$
$-\chi_{\mathrm{Am}} \times 10^6$	0·1344	0·1389	0·1408	0·1432	0·1435	0·1435

in table 3 are given the values of the susceptibility at room temperature observed at various mean times *t* following the quenching of the amalgam from 350° C. to room temperature.

§ 4. DISCUSSION OF RESULTS

The present measurements provide a fresh example of the temperature hysteresis associated with the magnetic properties of manganese. It is well known that manganese forms ferro-magnetic compounds with antimony, arsenic, bismuth, nitrogen and phosphorus and that in many cases, particularly with the arsenide, the ferromagnetic Curie point found when the temperature of the compound is gradually raised is some 15 or 20° C. higher than that found when the paramagnetic substance is slowly cooled(3).

The curves of figure 2 suggest that in these weak amalgams the manganese atom becomes increasingly paramagnetic as the temperature is raised, until when the kinetic energy of the mercury atoms becomes sufficiently great a maximum value is attained. This suggests that the manganese atom or ion becomes increasingly free of its neighbouring mercury atoms as the temperature is raised, attaining a maximum freedom at temperatures above 300° C. On the cooling of a hot amalgam the manganese remains free, and accordingly the paramagnetic susceptibility increases with fall in temperature as it normally does in paramagnetic substances. Finally, a stage is reached when the manganese becomes less free and there is a decrease in the paramagnetism. It is interesting that cooling to low temperatures produces such a marked and persistent diminution in the freedom of the manganese as that shown at II in figure 2.

At first sight it might appear that the behaviour of manganese in amalgams invites discussion on the lines of the theoretical studies of Bragg and Williams(4) and of Bethe(5). Bragg and Williams discuss atomic arrangements in alloys on the supposition that each sort of atoms form on their own a kind of superlattice which repeats itself throughout the specimen, the two lattices existing meshed with each other. This arrangement they call "superlattice order"; Bethe terms it "long-distance order". In Bethe's work it is assumed that the energy associated with the atomic arrangement in the alloy is uniquely fixed by the order of neighbouring atoms, by "local order", and not by a superlattice order. Clearly, in the case of these dilute fluid amalgams the possibility of the existence of long-distance order must be remote, although the general behaviour of amalgams with increasing concentrations shows that there is a tendency to solidify which may possibly be interpreted as due to the establishment of such long-distance order. As the mass susceptibility of manganese in the more concentrated amalgams falls with increase in concentration, it would then follow that long-distance order leads to the suppression of the pronounced paramagnetism of manganese; on this basis the loss of paramagnetism by freezing the amalgam could be explained. Now, the picture of local order given by Bethe was worked out in detail for alloys containing equal numbers of two kinds of atoms, while in the case of these amalgams there is an overwhelming preponderance of atoms of one kind.

The idea of local order is, however, implied in the explanation of the magnetic behaviour which we have given above. For it would appear that each manganese atom or possibly pair of atoms in an amalgam is surrounded by a group of mercury atoms forming a kind of complex molecule. The formation of such complex arrangements must, of course, depend upon the manganese concentration and the temperature. Once a particular set of complex arrangements have been broken down by increase in the kinetic energy of their constituents, they will only be re-formed with some difficulty as the temperature is lowered; in other words, temperature hysteresis will be observed and time will be required for their re-formation at any given temperature. The peculiar shape of the curve III of figure 2 is no doubt due to the successive breaking-down of two different sets of complex arrangements.

Since the completion of the work described in this communication the publication of Hume-Rothery's report on the structure of metals and alloys(6) has directed our attention to the important study of intermetallic compounds formed in mercury, carried out by Russell and his collaborators(7). Using purely chemical methods of examination which did not involve the removal of the compounds from the mercury, they showed that compounds such as Zn_7Mn, Zn_4Mn, Zn_3Mn, Sn_3Mn, Sn_2Mn, SnMn and $SnMn_2$, into which mercury does not enter as a constituent, can be formed. We feel that the magnetic method of examination which we have so far used only for the examination of the single metal manganese dissolved in mercury might also provide useful information in the case of the more complicated binary and ternary compounds studied by Russell, particularly from the examination of compounds containing manganese at temperatures above 100° C.

§ 5. ACKNOWLEDGEMENTS

The above work was in the main carried out at University College, London, and we tender our best thanks to Prof. E. N. da C. Andrade for the many facilities afforded us, to the Government Grants Committee of the Royal Society for the magnet used in the measurements, and to Prof. Lovatt-Evans for the loan of a Bosch and Lomb colorimeter.

Note added 12 *February* 1937

Recent work in Nottingham with iron amalgams suggested that a small quantity of a highly paramagnetic compound, or possibly metallic manganese, might be found at the surface of a manganese amalgam; this has been verified. It has been found that when a manganese amalgam is violently shaken and then allowed to stand, the intensely magnetic constituent very quickly rushes to the surface. In the experiments described in the present paper this constituent would remain outside the magnetic field and play no part in the measurements. The composition of the amalgam was always found as described in an earlier paper(1) by analysing a sample from that portion near the pole pieces where $H . dH/dx$ was at a maximum during the magnetic measurements; the portion mainly responsible for the experimental value of the susceptibility. It is difficult to see how the existence of the highly magnetic constituent outside the field can account for the hysteresis phenomena described, unless it is broken up at high temperatures and dispersed throughout the body of the amalgam; this would not, however, explain why the high value of the susceptibility observed at high temperatures persists on cooling.

REFERENCES

(1) Bates, L. F. and Tai, L. C. *Proc. phys. Soc.* **48**, 795 (1936).
(2) Royce. H. D. and Kahlenberg, L. *Trans. Amer. Electrochem. Soc.* **59**, 791 (1931).
(3) Bates, L. F. *Phil. Mag.* **16**, 657 (1933); *Proc. roy. Soc.* A, **117**, 680 (1928).
(4) Bragg, W. H. and Williams, E. J. *Proc. roy. Soc.* A, **145**, 699 (1934); **151**, 540 (1935); **152**, 231 (1935).
(5) Bethe, H. *Proc. roy. Soc.* A, **150**, 552 (1935).
(6) Hume-Rothery, W. "The Structure of Metals and Alloys," *Rep. Inst. Metals*, No. 1 (1936).
(7) Russell, A. S. *J. chem. Soc.* pp. 841, 852, 857, 2340 (1932); p. 1750 (1934); *Nature*, Lond., **133**, 217 (1934); **138**, 161 (1936).

WOOD-WATER RELATIONSHIPS, PART III. MOLECULAR SORPTION OF WATER BY SITKA SPRUCE WOOD

By WILFRED W. BARKAS, M.Sc., Forest Products Research
Laboratory, Princes Risborough, Aylesbury, Bucks.

Received 15 *December* 1936. *Read in title* 26 *February* 1937

ABSTRACT. The apparent molecular sorption of water by Sitka spruce flour is shown to remain constant at about 23 per cent of the dry weight of the wood over a period of 83 days when a sucrose solution is used as the indicator, but with sodium chloride solutions a gradual fall in the apparent sorption occurs which reaches a value of about 5 per cent after 14 days. This fall is here put down to the slow sorption of the salt and not to a low value of the true molecular sorption. It is also suggested that the low value of the molecular sorption derived by Stamm and Loughborough from considerations of the heat of wetting of wood is due to their assumption that molecular sorption is complete at about 30 per cent relative vapour pressure, when the capillary sorption commences.

In the first paper on this subject(1), which will be referred to in what follows as *paper* 1, the molecular sorption w_a was determined from the change in concentration of an evacuated sucrose solution on being mixed with dry evacuated flour of Sitka spruce wood. The value of the molecular sorption measured in this way would be an apparent and not an absolute one if sorption of sucrose also occurred, because the change in concentration of the solution would be smaller than that represented by the simple extraction of water. Further, the sorption must be in vapour-pressure equilibrium with the solution used, so that each different concentration provides a point on a {moisture-content, vapour pressure} isothermal in w_a which on extrapolation to saturated vapour pressure gives an approximate saturation value w_s equal to 23 per cent of the dry weight of the wood flour. This is considerably higher than the values given by other workers, e.g. Pidgeon and Maass(2) or Stamm and Loughborough(3).

In a recent publication Stamm(4) has offered some criticisms of the method which are based on the author's original note to *Nature*(5). Some of these had already been dealt with in paper 1, which was then in the press, but one point remained which, it was thought, required further consideration. Stamm kindly communicated these criticisms informally, and thus made it possible to consider them before his work appeared.

Stamm had found in similar experiments with sodium chloride solutions that the initial change in concentration was not an equilibrium value but decreased slowly until after several days it corresponded to a value of w_a of approximately

6 per cent, which he considered to be the correct one. He thought that the high initial value might be due to the more rapid diffusion of the water as compared with that of the larger salt molecules, and suggested that the same effect would be found in sucrose solutions, though the fall in apparent sorption might be slower since the sucrose molecules are larger still.

Although in paper 1 evidence was given that the sucrose molecules were small enough to enter the capillaries and that therefore the change in concentration was not due to filtration, Stamm's findings on the still smaller molecules of sodium chloride are obviously important, and I am grateful to him for drawing my attention to them. The present paper describes experiments to test whether for sucrose the apparent value of the sorption is an equilibrium value or not.

First of all Stamm's findings for sodium chloride solution were confirmed by experiments carried out exactly as described in paper 1, the change of refractive index of salt solutions with concentration being obtained from the *International Critical Tables*. A 7 per cent concentration* of sodium chloride was used, as this exerts approximately the same relative vapour pressure as an 18 per cent solution of sucrose, and should therefore give the same initial value of 0·20 for w_a. The changes in refractive index were not so great as for sucrose, so that the accuracy was somewhat less. The sorption bottles were kept in a thermostat at 23° C. and only opened when a sample was removed to measure the concentration. Successive samples could be taken later from the same bottles in order to calculate any further sorption changes, provided allowance was made for the smaller amount of solution present. This calculation is cumbersome but quite straightforward, and need not be given here. Table I gives the results obtained. If these values of w_a are plotted against time they show, except for one reading, a regular decrease from the assumed initial value of 0·20 to an apparently constant value between 0·04 and 0·05 after long periods, thus supporting Stamm's results.

Table I. Change in w_a with time for sodium chloride solutions

Initial concentration, 6·91 per cent; relative vapour pressure 0·981

Reference	$\frac{\text{Weight of solution}}{\text{weight of wood}}$	Time (days)	w_a
120/9A			
1st sample	17·4	7	0·134
2nd sample	—	14	0·087(?)
120/11			
1st sample	16·0	9	0·130
2nd sample	—	13	0·058
120/12			
1st sample	16·7	13·5	0·041
2nd sample	—	19	0·041

Measurements were next made on 18 per cent sucrose solutions. In the original experiments the sorption times had purposely been limited to one or two days, owing to the tendency for mould to grow in the solutions. Since the sorption times were now to be increased, the whole experiment had to be performed under sterile conditions, which was achieved through the co-operation of the Mycology Section of the Laboratory. The wood flour and the solution were autoclaved and the whole apparatus assembled and evacuated as quickly as possible after being sterilized with a 0·1 per cent solution of mercuric chloride and rinsed with sterile water. The flour was dried *in vacuo* for several weeks and then flooded with the solution as before.

---

* Gram of solute per 100 grams of solution.

As it was found impossible to keep the reference solution sterile in the double cell of the interferometer, the refractive index was measured against that of distilled water. For this purpose the interferometer had to be modified to allow of large angles of tilt of the compensating glass which somewhat reduced the sensitivity of the instrument, but it remained sufficiently accurate for the purpose in hand.

After the wood flour had been flooded with solution, the stock solution was measured in the interferometer, first against water and then against a sample of solution taken from the first sorption bottle. This sample was then itself measured against water. On calibrating the interferometer for both ranges of tilt, it was found that values of the change in concentration measured in these two ways were in good agreement. The remainder of the stock solution was held *in vacuo* till the end of the experiment, when a repetition of this cycle of measurements showed that it had in fact remained sterile. This would have been in doubt if the measurements against water had not been made.

Successive samples were also taken from these sorption bottles, but the results were irregular and were discarded, as it seemed that the solutions had become contaminated after being once opened. Table 2 gives the results for first samples only, measured both against water and against the stock solution.

Table 2. Change in w_a with time for sucrose solutions

Initial concentration 0·183; relative vapour pressure 0·984

Reference	$\frac{\text{Weight of solution}}{\text{weight of wood}}$	Time (days)	w_a by comparison with water	w_a by comparison with stock solution
136/1	12·40	4	0·182	0·206
136/12	11·55	83	0·191	0·205

The values obtained by comparison with the stock solution are in agreement with that obtained previously at this concentration, which suggests that the heat treatment in the autoclave does not affect the molecular sorption. The less accurate values obtained against water, though rather low, are also consistent. Both readings show no change in sorption over a period of 83 days, which is about six times as long as was required by the sorption from sodium chloride solutions to reach its minimum value.

If the fall in apparent sorption in the case of the sodium chloride solutions is in fact due to slow *diffusion* of the salt molecules, then the diffusion of sucrose should take place in a longer time proportional to the diffusion rates of the two solutes. The diffusion coefficients of salt and sucrose are in a ratio of approximately 2·4 to 1, and the higher concentration of sucrose would tend to make the ratio of the diffusion-rates smaller than this, so evidently diffusion alone will not account for the apparent stability of w_a in sucrose solutions. Since paper 1 showed that the sucrose molecule is not large enough to be filtered out at the orifices of the colloidal capillaries, the explanation would appear to be that the salt is slowly sorbed on to the wood (possibly by partially displacing water molecules) whereas the sucrose is not. This is in agreement with the polar nature of the salt molecule.

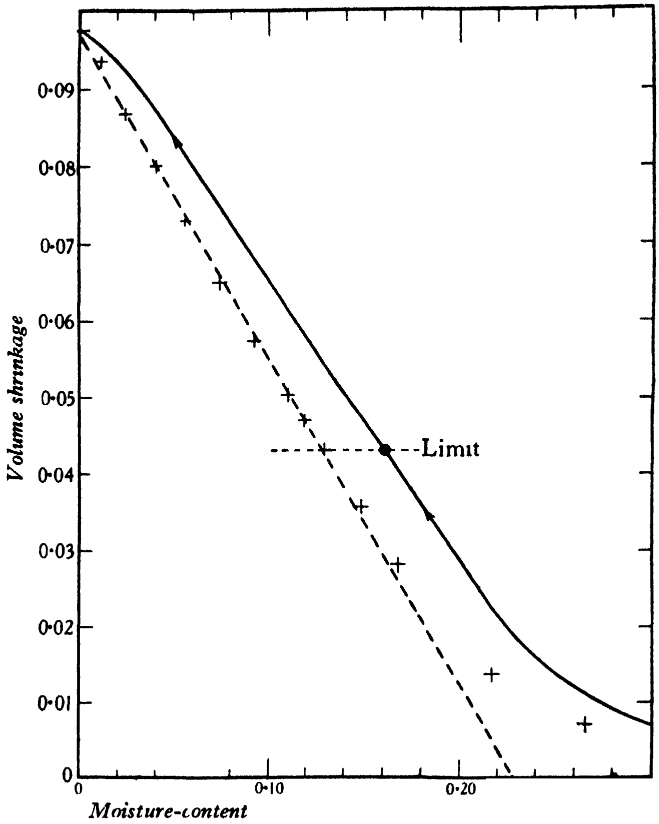

Figure 1. --- $(m-c)$

Independent evidence is now available from consideration of the shrinkage of wood[(6)] to prove that the values of w_a obtained in paper 1 are substantially correct. At the lower moisture-contents where the water is held entirely by molecular forces, the volume of the wood-water aggregate is that of the components less the sorption-compression c which they suffer. If, therefore, the shrinkage is plotted against $(m-c)$, where m is the moisture content, a straight line results as long as m is principally molecular and equal to w_a, but as soon as the capillary sorption becomes apparent, m becomes greater than w_a and the points diverge towards the higher moisture-contents. In the figure it is seen that the straight line holds from dryness to points corresponding to about 16 per cent moisture content. If this line is extrapolated to zero shrinkage (i.e. to saturated vapour pressure) its intersection corresponds to a moisture content of 26 per cent, which compares favourably with the approximate value of 23 per cent obtained from the sorption measurements. As has been pointed out⁽⁶⁾ the values of *c* are obtained under conditions which would measure compression due to both molecular and capillary forces and that the points corresponding to moisture contents below 6 per cent (where by common consent the sorption is entirely molecular), considered alone, tend to lie on a slightly steeper line, giving a value of approximately 0·25 for w_s. This is admittedly straining the limits of accuracy to be expected from the data, and undoubtedly the sorption-compression due to capillary forces is very small; but it does support the opinion of Stamm and Loughborough⁽³⁾ that capillary sorption begins to be apparent at a moisture content of about 6 per cent. The author does not agree, however, that molecular sorption is complete at this moisture-content.

Stamm and Loughborough reach their conclusions from their observation that for a moisture-content below 6 per cent the change with moisture-content of the heat of wetting and the entropy are unaffected by temperature. They state (p. 129) that "According to these conceptions the inflection point in the moisture-content, relative-vapour-pressure curves corresponds approximately to the transition point between the surface-bound water and the water held by van der Waals forces...this point occurs at a relative vapour pressure of about 0·30 for all temperatures...and should represent the limiting capillary (radius) in which capillary condensation can take place." Elsewhere (p. 128) they admit the possibility of "a slight overlap" between these two types of sorption. It seems to the author that the molecular sorption is unlikely to be saturated when the vapour pressure is only 30 per cent saturated, and that it would be expected on the other hand to continue on the external surfaces—and on the interior walls of those larger capillaries which had not yet been filled with water—until the saturated vapour pressure was reached.

If this view is correct, there is no discrepancy between the various values for w_a which have been proposed, since they refer only to particular vapour pressures. In this connexion, by taking the isothermal for white spruce published by Filby and Maass⁽⁷⁾ it will be found possible to construct a plausible isothermal for the molecular sorption which follows their curve up to the point of inflection, runs very close to it as far as 65 per cent relative vapour pressure (corresponding to the desorption moisture-content of 15 per cent) and, after including the author's experimental values of w_a near saturation⁽¹⁾, reaches a saturation value at a moisture-content between 23 per cent and 25 per cent. A hypothetical curve of this type suggests that the hysteresis loop in w_a is of approximately constant width except where it begins to close near zero and at saturated vapour pressure.

The capillary sorption at any vapour pressure is the difference between the total and molecular sorptions, and at the higher vapour pressures is composed of water partly in the colloidal and partly in the anatomical capillaries. The greater width of the hysteresis loop for total sorption, which increases up to vapour pressures indistinguishable from saturation, is to be accounted for in terms of capillary sorption in the anatomical structure$^{(8)}$.

I wish to thank the Mycology section of the Laboratory for their suggestions and assistance in evolving a technique for performing these experiments under sterile conditions. Without their help this paper could not have been written. I am also indebted to the Director of this Laboratory, Mr W. A. Robertson, for permission to publish the paper.

REFERENCES

(1) Barkas, W. W. *Proc. phys. Soc.* **48**, 1 (1936).
(2) Pidgeon, L. M. and Maass, O. *J. Amer. chem. Soc.* **52**, 1053 (1930).
(3) Stamm, A. J. and Loughborough, W. K. *J. phys. Chem.* **39**, 121 (1935).
(4) Stamm, A. J. "Colloid Chemistry of Cellulosic Materials." *Misc. Publ. U.S. Dep. Agric.* No. 240 (1936).
(5) Barkas, W. W. *Nature*, Lond., **130**, 699 (1932).
(6) Barkas, W. W. *Forest Products Research Laboratory*. Project 8, *Progress Report*, No. 1 (1936).
(7) Filby, E. and Maass, O. *Canad. J. Res.* **7**, 1 (1935).
(8) Barkas, W. W. *Proc. phys. Soc.* **48**, 576 (1936).

THE PHASE BOUNDARIES IN BINARY ALLOYS, PART 1: THE EQUILIBRIUM BETWEEN LIQUID AND SOLID PHASES

By H. JONES, H. H. Wills Physical Laboratory, University of Bristol

Communicated by Prof. A. M. Tyndall, F.R.S., 16 December 1936.
Read in title 12 March 1937

ABSTRACT. The thermodynamic theory of the melting-point and freezing-point curves, in the α solid-solution region, of binary alloys is briefly considered. It is shown that the van 't Hoff relation should be applicable to these alloys, and its validity, for sufficiently dilute solutions is verified by comparison with experiment. It is shown from experiment that the change in the latent heat when small quantities of nickel, zinc, gallium or germanium are dissolved in copper is proportional to the electron: atom ratio. Similar results are obtained for cadmium, indium or tin dissolved in silver. A qualitative theory is proposed to account for these effects.

§ 1. INTRODUCTION

It has long been known that in binary alloys in which the atoms are of approximately the same size, the phase boundaries in the solid state are determined by the ratio(1) of the number of valency electrons to that of atoms, and an outline of a theory to account for this has already been given(2, 3, 4, 5). The recent work of Hume-Rothery and his collaborators(6) suggests that the electron : atom ratio is also of importance in determining the melting and freezing-point curves of simple alloys.

In part I of this paper the thermodynamic theory of the liquidus and solidus lines of alloys is considered afresh, and an attempt is made to separate the role played by the electron : atom ratio from the effect of the atomic concentration of solute atoms. We shall deduce from the experiments that, in solutions in copper of elements belonging to the same row of the periodic table, the change in the energy-difference between the liquid and the solid phases at the same composition is proportional to the electron : atom ratio. In § 4 a simple explanation of this result is suggest d.

§ 2. THE GENERAL CONDITIONS OF EQUILIBRIUM BETWEEN TWO PHASES

Let F_1 and F_2 be the free energies per atom of two alloy phases which are in equilibrium with each other. Let x_1 denote the composition of one phase (i.e. the atomic fraction of one element in the alloy) and x_2 that of the other. F_1 is a function of the specific volume of the phase V_1, the common temperature T, and x_1; F_2 is a function of V_2, T and x_2. The condition for equilibrium is expressed by the two equations[(3)]

$$\frac{\partial F_1}{\partial x_1}=\frac{\partial F_2}{dx_2}=\frac{F_1(x_1)-F_2(x_2)}{x_1-x_2} \qquad \ldots\ldots(1).$$

If we regard the volumes as constant, these two equations will determine for given T the values of x_1 and x_2. Thus the solution of equations (1) determines the boundaries in the phase diagram of the mixed-crystal region between the two pure phases 1 and 2. Thus if 1 stands for a solid solution and 2 for the liquid phase, equations (1) determine the liquidus and solidus curves. It has been shown that the free energy per atom may be written[(3)]

$$F_1(x_1)=kT\{x_1\log x_1+(1-x_1)\log(1-x_1)\}$$
$$+U_1(x_1)-T\int_0^T\frac{C_v^{(1)}}{T}\,dT+\int_0^T C_v^{(1)}\,dT \qquad \ldots\ldots(2),$$

where $C_v^{(1)}$ denotes the specific heat at constant volume of phase 1 assuming the alloy to be totally disordered. $U_1(x_1)$ denotes the internal energy of the alloy as a function of its composition at the absolute zero of temperature measured with respect to the energy of the individual atoms. If for convenience we write

$$f_1(x_1, T)=U_1(x_1)-T\int_0^T\frac{C_v^{(1)}}{T}\,dT+\int_0^T C_v^{(1)}\,dT \qquad \ldots\ldots(3),$$

then f is the whole of the free energy except for the disorder term. We obtain from equations (1)

$$\log\frac{x_2(1-x_1)}{x_1(1-x_2)}=\frac{1}{kT}\left(\frac{\partial f_1}{\partial x_1}-\frac{\partial f_2}{\partial x_2}\right)$$
$$\log\left(\frac{1-x_1}{1-x_2}\right)=\frac{1}{kT}\left(f_1(x_1 T)-f_2(x_2 T)-x_1\frac{\partial f_1}{\partial x_1}+x_2\frac{\partial f_2}{\partial x_2}\right) \qquad \ldots\ldots(4).$$

§ 3. EQUILIBRIUM BETWEEN LIQUID AND SOLID PHASES

We consider the equilibrium between a solid solution and the liquid phase. Let T_0 be the melting point of the pure solvent metal. We have the condition

$$f_l(0, T_0)=f_s(0, T_0) \qquad \ldots\ldots(5),$$

where the subscripts l and s refer to the liquid and solid phases. From equation (3) we obtain easily for any temperature T

$$f_l(0, T)-f_s(0, T)=(T_0-T)\frac{\lambda}{T_0}+\int_{T_0}^T(C_v^{(l)}-C_v^{(s)})\,dT-T\int_{T_0}^T\frac{C_v^{(l)}-C_v^{(s)}}{T}\,dT \qquad \ldots\ldots(6),$$

where λ is the latent heat of fusion of the pure solvent. The second and third terms on the right together yield a term of the order of magnitude

$$\tfrac{1}{2}(C_v^{(l)}-C_v^{(s)})(T-T_0)^2/T_0,$$

which for temperatures near to T_0 is negligible in comparison with the first term. We make the following approximation:

$$f_l(x_l, T)-f_s(x_s, T)-f_l(0, T)+f_s(0, T)$$
$$=U_l(x_l)-U_s(x_s)-U_l(0)+U_s(0),$$

and hence obtain from equations (4) and (6) the two equations which determine the liquidus and solidus lines in the region of solid solution, viz.

$$\frac{\lambda}{T_0}(T-T_0)+kT\log\frac{1-x_s}{1-x_l}=\left\{U_l(x_l)-U_s(x_s)-U_l(0)+U_s(0)-x_l\frac{dU_l}{dx_l}+x_s\frac{dU_s}{dx_s}\right\} \quad \text{......(7·1)},$$

$$kT\log\frac{x_s(1-x_l)}{x_l(1-x_s)}=\frac{dU_l}{dx_l}-\frac{dU_s}{dx_s} \quad \text{......(7·2)}.$$

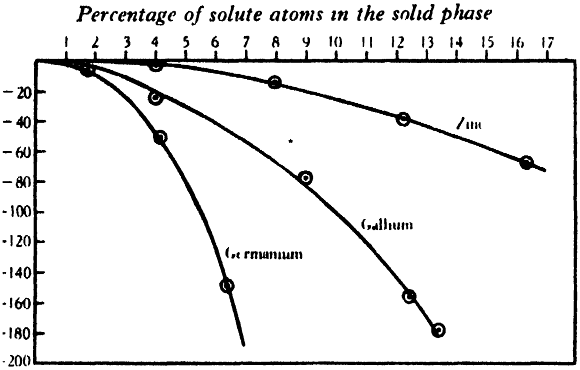

Figure 1.

If $U_l(x_l)$ and $U_s(x_s)$ are developed as power series in x_l and x_s we see that for small concentrations the right-hand side of equation (7·1) is quadratic in x_l and x_s. For small concentrations, x_l, x_s, therefore, the well-known formula of van t' Hoff is obtained from equation (7·1), viz.

$$x_l-x_s=\frac{\lambda}{k}\left(\frac{1}{T}-\frac{1}{T_0}\right) \quad \text{......(8)}.$$

In certain metallic alloys this law is found to agree well with experiment$^{(7)}$. On the other hand for solutions of a number of metals in copper and silver Hume-Rothery and his collaborators do not find good agreement$^{(6)}$. In figure 1 we have plotted the values of the left-hand side of equation (7·1) against x_s for solutions of zinc, gallium and germanium in copper, using the data given in table 1. The value of the latent heat of copper assumed is 3·18 kcal. per gram-atom, which is also the best value obtained by direct observation$^{(8)}$. We see that, as the theory predicts, the curves for small concentrations are approximately parabolas. It appears therefore that the breakdown of the van t' Hoff law for the alloys examined by Hume-Rothery is only apparent; the concentrations used when equation (8) was applied were not small enough.

§ 3·1. From the observed liquidus and solidus curves it is possible to calculate the difference in internal energy between the liquid and the solid phase at the same concentration and at zero temperature. This may be done as follows. Let x_l and x_s be the concentrations at temperature T which are in equilibrium, and let

$$\bar{x}=\tfrac{1}{2}(x_s+x_l).$$

Expanding $U_l(x_l)$ and $U_s(x_s)$ as Taylor's series about the value of the concentration $\bar{x}$ we obtain for the right-hand side of equation (7·1), which we shall denote by P for brevity,

$$P=(U_l-U_s)_{\bar{x}}-(U_l-U_s)_0-\bar{x}\frac{d}{d\bar{x}}(U_l-U_s)$$
$$-\tfrac{1}{2}(x_l^2-\bar{x}^2)\frac{d^2U_l}{d\bar{x}^2}+\tfrac{1}{2}(x_s^2-\bar{x}^2)\frac{d^2U_s}{d\bar{x}^2}+\text{etc.}$$

For the right-hand side of equation (7·2), which we denote by Q, we obtain

$$Q=\frac{d}{d\bar{x}}(U_l-U_s)+(x_l-\bar{x})\frac{d^2U_l}{d\bar{x}^2}-(x_s-\bar{x})\frac{d^2U_s}{d\bar{x}^2}+\text{etc.}$$

and therefore we find that

$$P+\bar{x}Q=(U_l-U_s)_{\bar{x}}-(U_l-U_s)_0-\tfrac{1}{8}(x_l-x_s)^2\frac{d^2}{dx^2}(U_l-U_s)+\text{etc.}$$

We may safely neglect the second and higher powers of (x_l-x_s), especially in view of the fact that they are multiplied by high derivatives of (U_l-U_s). It has been verified *a posteriori* that the error introduced in this way is quite negligible for small values of the concentrations. We obtain therefore finally

$$(U_l-U_s)_{\bar{x}}=\frac{\lambda T}{T_0}+kT\left\{\log\frac{1-x_s}{1-x_l}+\tfrac{1}{2}(x_s+x_l)\log\frac{x_s(1-x_l)}{x_l(1-x_s)}\right\}\quad\ldots\ldots(9).$$

From equation (9), using experimental values of x_s, x_l, λ, we can calculate (U_l-U_s) for small concentrations of nickel, zinc, gallium and germanium individually dissolved in copper. To do this we require the concentrations of the liquid and solid phases which are in equilibrium at a given temperature. These were obtained by plotting the liquidus and solidus curves from experimental data and reading off the values of x_l and x_s for a number of temperatures. The results are summarized in the table. Instead of $(U_l-U_s)_{\bar{x}}$ we give $\Delta U=(U_s-U_l)_{\bar{x}}-(U_s-U_l)_0$, so that in all cases ΔU tends to zero as x becomes zero. ΔU may be regarded as the decrease in the latent heat of fusion due to the addition of a fraction $\bar{x}$ of some other element in solution.

The data for copper-zinc are taken from the work of Ruer and Kremers$^{(9)}$, those for copper-gallium are from the work of F. Weibke$^{(10)}$, those for copper-germanium from the work of Hume-Rothery, Mabbott and Channel-Evans$^{(6)}$, and those for copper-nickel from the work of N. S. Kurnakow$^{(11)}$. The melting point of pure copper is 1356° K. We note that in the case of nickel dissolved in copper the latent heat is increased; this is to be expected since the latent heat of pure nickel is greater than that of pure copper.

Table 1

T (° K.)	x_s	x_l	$\bar{x}$	ΔU (cal./g.-atom)
		Zinc dissolved in copper		
1333	0·041	0·060	0·050	55
1313	0·081	0·111	0·096	101
1293	0·122	0·158	0·140	147
1273	0·163	0·204	0·183	192
		Gallium dissolved in copper		
1323	0·040	0·058	0·049	76
1273	0·090	0·130	0·110	191
1223	0·124	0·176	0·150	305
1203	0·134	0·194	0·164	352
		Germanium dissolved in copper		
1323	0·017	0·044	0·0305	84
1273	0·042	0·094	0·068	199
1223	0·0645	0·124	0·094	310
		Nickel dissolved in copper		
1423	0·205	0·126	0·165	−155
1453	0·330	0·190	0·260	−229
1503	0·495	0·300	0·397	−342

Figure 2 shows ΔU plotted against $\bar{x}$. We see from figure 2 that ΔU is very closely proportional to the valency-electron concentration, i.e. if v denotes the valency of the solute atoms, $\Delta U \propto (v-1)\, x$. Using the data given by Hume-Rothery for solutions of cadmium, indium and tin in silver we find according to

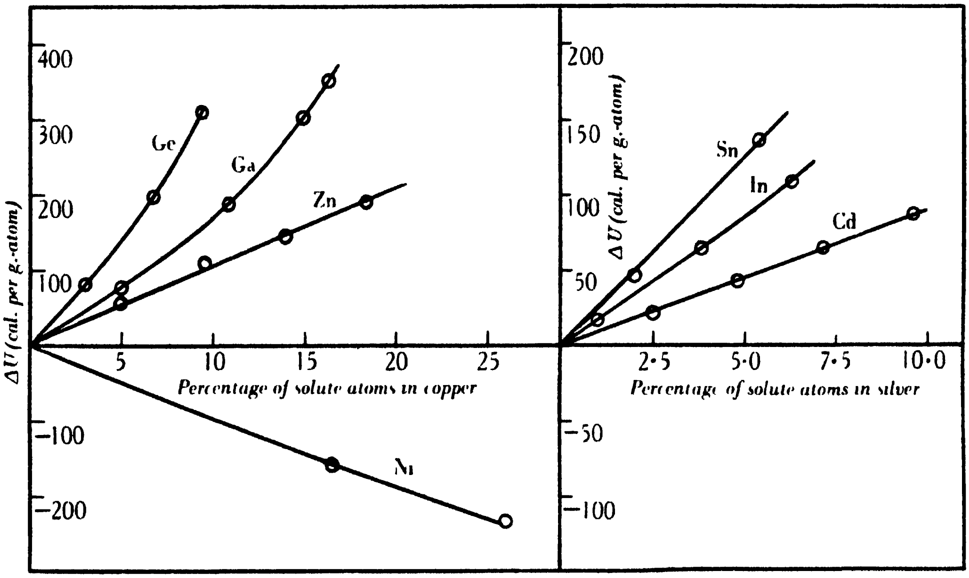

(*a*) (*b*)

Figure 2. The change in the latent heat ΔU as a function of the concentration of solute atoms. (*a*) For nickel, zinc, gallium and germanium dissolved in copper. (*b*) For cadmium, indium and tin dissolved in silver.

equation (9) that $\Delta U = 0{\cdot}9\,(v-1)\,\bar{x}$ kcal. per gram-atom; see figure 2 (*b*). For palladium dissolved in silver, just as for nickel in copper, ΔU is negative. A precise calculation for this alloy cannot be made, for the liquidus and solidus lines are not known with sufficient accuracy.

§4. THE VARIATION OF THE INTERNAL ENERGY OF A PHASE WITH COMPOSITION

We have seen in the previous sections that the first requirement of a theory of the phase boundaries in binary alloys is a knowledge of the internal energy of the various phases as a function of the composition. The modern theory of metals provides a means by which the change of internal energy with composition can be calculated. It is now well established that the energy spectrum of the valency electrons in a metal is a band having a width equal to a few electron-volts. The calculation of the internal energy of a metal compared with the energy of the widely separated individual atoms which compose it is made in two steps. Firstly the energy of the lowest level of the valency electrons should be found by some method such as that of Wigner and Seitz; secondly the whole energy of the band of electrons referred to this lowest level must be calculated. This latter part of the energy we call the Fermi energy. The energy of the lowest level is sensitive to changes in atomic volume, but is not so sensitive to changes in crystal structure for a given atomic volume.* On the other hand the Fermi energy is sensitive to changes in structure even when the atomic volume remains unchanged. It is for this reason that the Fermi energy is of primary importance in determining the phase boundaries in many types of alloys and that the electron-concentration rather than the atom-concentration of solute atoms is of such importance in fixing phase boundaries.

The latent heat of melting may be regarded, therefore, as arising from (*a*) the change in the energy of the lowest state, which depends upon the distortion and volume change of the lattice on melting and (*b*) the change in the Fermi energy which depends on the volume change and also, largely, on the change of structure. Our results can be interpreted if we assume that the first term is largely independent of composition, so that the variation of the latent heat when small quantities of other elements are dissolved in copper will arise mainly from the variation of the change of the Fermi energy on melting. In that case the change in the latent heat would be determined by the electron : atom ratio as found by experiment for solute atoms of approximately the same size as those of the solvent metal. An exact calculation is not at present possible because we do not know how to calculate the Fermi energy in the liquid state.

The proportionality of ΔU with the electron concentration would not be expected to hold for solutions of metals whose atoms are of different size from those of the solvent metals, for instance tin in copper. The reason is that in the solid state there must in such cases be an additional energy which arises directly from the internal strain produced in the lattice. Formula (9) shows that ΔU for tin in copper is considerably greater than for germanium in copper, and this is in agreement with the above consideration.

---

* Fuchs has shown(12) that the difference in energy of the lowest level between the body-centred and face-centred cubic structures having the atomic volume of copper is 4×10^{-4} electron-volts per atom.

REFERENCES

(1) HUME-ROTHERY. *The Metallic State* (Oxford, 1931).
(2) JONES. *Proc. roy. Soc.* A, **144**, 225 (1934).
(3) MOTT and JONES. *The Theory of the Properties of Metals and Alloys* (Clarendon Press, 1936).
(4) DEHLINGER. *Z. Phys.* **94**, 231 (1935).
(5) KONOBEJEWSKI. *Ann. Phys.*, Lpz., **26**, 97 (1936).
(6) HUME-ROTHERY, MABBOTT and CHANNEL-EVANS. *Philos. Trans.* **233**, 44 (1934).
(7) JEFFERY. *Trans. Faraday Soc.* **36**, 86 (1930).
(8) UMINO. *Sci. Rep. Tôhoku Univ.* **15**, 597 (1915).
(9) RUER and KREMERS. *Z. anorg. Chem.* **184**, 196 (1929).
(10) WEIBKE. *Z. anorg. Chem.* **220**, 293 (1934).
(11) KURNAKOW. *Z. anorg. Chem.* **54**, 153 (1907).
(12) FUCHS. *Proc. roy. Soc.* A, **151**, 585 (1935).

THE PHASE BOUNDARIES IN BINARY ALLOYS, PART 2: THE THEORY OF THE α, β PHASE BOUNDARIES

By H. JONES, H. H. Wills Physical Laboratory, University of Bristol

Communicated by Prof. A. M. Tyndall, 16 *December* 1936. *Read* 12 *March* 1937

ABSTRACT. A quantitative theory of the phase boundaries in alloys between the face-centred and the body-centred cubic structures is given. The theory is applied in detail to alloys in which copper is the major constituent. The width of the $(\alpha+\beta)$ mixed-crystal region is obtained with fair approximation; it is found that the width of this region decreases with increasing valency of the solute element, a result which is in accordance with experiment. The variation with temperature of the limits of the α and β regions is obtained also, and again agreement with observations is fairly satisfactory.

§ 1. INTRODUCTION

OUR aim in this part of the paper is to determine theoretically the boundaries limiting the α (face-centred) and the β (body-centred) phases for solutions of such metals as zinc, gallium, germanium, etc., in copper. The method is general and could equally well be applied to any alloys which form these two phases. It is a more quantitative development of the theory previously given by the author to account for the Hume-Rothery rule.

As we have seen in part 1 it is essential for this purpose to know the energies of the two phases as functions of the concentration of the solute atoms. In § 4 of part 1 we have already discussed the factors which contribute to the internal energy of a phase, and have seen that for the present purpose the Fermi energy of the valency electrons is of particular importance. The only other factor contributing to the internal energy which is likely to affect the phase formation in alloys is the energy arising from the repulsive forces between the ions of the lattice. These forces, according to Fuchs(1), are responsible for the fact that copper forms a face-centred lattice, and, as he has shown, they have an important effect on the elastic properties of the noble metals.

If we assume that the energy associated with the repulsive forces between two ions may be written in the form $w=ae^{-r/b}$, where r is the distance between the ions, the constants a and b can be determined from the observed elastic constants(2). The difference in energy between the face-centred and body-centred structures with the same atomic volume, due to ion repulsion, could then be estimated. However, calculation shows that a and b depend somewhat sensitively upon the elastic constants (the difference between two nearly equal quantities is involved) and it was not found possible to obtain in this way reliable comparisons between the contributions to the energy in the different phases.

In the following sections the phase boundaries are determined on the assumption that they arise entirely through the difference in the Fermi energy of the two phases. The good agreement with experiment may be interpreted as confirming the conclusion, which follows from the mere existence of the Hume-Rothery electronic rules, that the repulsive forces between the ions is not of major importance in this connexion for copper alloys.

§ 2. THE CALCULATION OF THE FERMI ENERGY FOR THE FACE-CENTRED AND BODY-CENTRED CUBIC STRUCTURES

According to a well-known theorem of Bloch the wave function of an electron in a metal crystal has the form of a modulated plane wave, $ue^{2\pi i(k,r)}$, where the amplitude u is a function with the same periodicity as the lattice potential. The wave vector k is a measure of the electron's momentum and is used to specify its state of motion. A point in the space of the vector k corresponds to a particular state of the electron and is associated with a certain energy. Our first problem is to find the energy of an electron as a function of position in this k space. Brillouin zones are closed regions in this space, across the boundaries of which the energy changes discontinuously.

We shall consider the energy of the states which lie along a line from the origin of k space perpendicular to some plane across which the energy changes discontinuously by an amount ΔE. We choose axes so that the perpendicular from the origin coincides with the k_z axis, and denote the point where this line cuts the plane of energy-discontinuity by $(00k_0)$. It has been shown⁽²⁾ that in the neighbourhood of $(00k_0)$ for $k_z \leqslant k_0$ the energy E is given by

$$E = \frac{h^2}{2m}\{k_x{}^2 + k_y{}^2 + \alpha\,(k_z - k_0)^2\} - \tfrac{1}{2}\Delta E \qquad \ldots\ldots(1),$$

where α is the oscillator strength of zero frequency of the state at $(00k_0)$ and is connected to the energy gap by the approximate formula

$$\alpha = 1 - 4E_0/\Delta E \qquad \ldots\ldots(1{\cdot}1),$$

E_0 being the energy of a free electron at the point $(00k_0)$; thus $E_0 = h^2 k_0{}^2/2m$. Near the origin the energy must depend upon k in approximately the same way as for free electrons. We are interested, of course, only in those metals for which the valency electrons in the individual atoms are in s states. We shall assume therefore that for all points along the line from the origin to $(00k_0)$, and in the neighbourhood of this line, the energy is given by

$$E = \frac{h^2}{2m}\left[k_x{}^2 + k_y{}^2 + k_0{}^2 + (k_0 - k_z)^2 - 2k_0\sqrt{\left\{(k_0 - k_z)^2 + \frac{k_0{}^2}{(\alpha - 1)^2}\right\}}\right] \qquad \ldots(2).$$

For points near k_0 this reduces to equation (1), and near the origin it gives the form for free electrons.

Our next step in the calculation of the Fermi energy is to consider the Brillouin zone to be divided into prisms, the faces of the zone forming the bases and the origin the vertex. Within each prism, except in the neighbourhood of the corners, formula (2) may be applied, the axes being suitably chosen for each prism. The energies obtained in this way should be satisfactory for occupied states when there are not more than about 1·5 electrons per atom.

The number of states per unit energy range $N(E)$ is given by the formula

$$N(E)=2\int\frac{dS}{|\operatorname{grad} E|} \qquad \text{......(3)},$$

where the integration is over the surface in k space for which the energy has the value E. $N(E)\,dE$ gives per cm.^{3} of metal the number of states, including the factor 2 which occurs on account of electron spin, which lie in the energy-range E to $(E+dE)$. Since the energy, according to equation (2), as a function of k has axial symmetry about the k_z axis we may write equation (2)

$$E=\frac{h^2}{2m}\{k_r^2+f(k_z)\},$$

where $f(k_z)$ is given at once by comparison with (2), and $k_r=\sqrt{(k_x^2+k_y^2)}$. If θ denotes the angle between the normal to a surface of constant energy and the k_z axis, then we may write $\sin\theta\, dS=2\pi k_r\, dk_z$ and

$$\sin\theta\,|\operatorname{grad} E|=\frac{\partial E}{\partial k_r}=\frac{h^2}{m}k_r.$$

Thus in a region in which the energy has axial symmetry about the k_z axis we obtain

$$N(E)=\frac{4\pi m}{h^2}\left(k_{z(\max)}-k_{z(\min)}\right) \qquad \text{......(4)}.$$

This formula gives the contribution to $N(E)$ from that part of the whole energy surface E which may, with sufficient approximation, be regarded as having axial symmetry about some axis which we take to be the k_z axis. $k_{z(\max)}$ is then the maximum value of k_z on this part of the surface and $k_{z(\min)}$ the minimum value. We can apply formulae (2) and (4) to calculate the number of states per unit energy-range in the interior of the first Brillouin zone if we make the approximation of replacing the prisms, into which the zone is divided, by cones having the same solid angle as the prisms. This approximation should not introduce an appreciable error in most cases. From (2) we have

$$\frac{k_{z(\max)}}{k_0}=1-\left\{\frac{2mE}{h^2k_0^2}+1-2\left(\frac{2mE}{h^2k_0^2}+\frac{1}{(\alpha-1)^2}\right)^{\frac{1}{2}}\right\}^{\frac{1}{2}} \qquad \text{......(5)}.$$

In a cone of solid angle ω the height k_z measured from the vertex is related to the radius of the base as follows:

$$k_x^2+k_y^2=k_z^2\{(1-\omega/2\pi)^{-2}-1\}.$$

Thus according to equation (2) the value of $k_{z(\min)}$ is given by the equation

$$E=\frac{h^2}{2m}\left[k_{z\,(\min)}^2\left(1-\frac{\omega}{2\pi}\right)^{-2}+2k_0\left\{(k_0-k_{z(\min)})-\sqrt{\left((k_0-k_{z(\min)})^2+\frac{k_0^2}{(\alpha-1)^2}\right)}\right\}\right]$$

$$\text{......(6)}.$$

We use these equations to calculate $N(E)$ for the body-centred and face-centred cubic structures. For the body-centred structure the first Brillouin zone has 12 faces, therefore $\omega = \frac{1}{3}\pi$ and $k_0 = 1/2^{5/6}\Omega^{1/3}$, where Ω cm^3 is the atomic volume. Thus taking a value less than k_0 for $k_{z(\mathrm{min})}$ we can find the corresponding value of E from equation (6) and therefore $k_{z(\mathrm{max})}$ from equation (5) and therefore finally $N(E)$ by equation (4). To obtain the whole value of $N(E)$ the expression given by equation (4) needs to be multiplied by $4\pi/\omega$, i.e. in this case by 12. Curve (*b*) in figure 1 has been obtained in this way. When the surface of the Fermi distribution has touched the boundary of the zone, $k_{z(\mathrm{max})}$ always remains equal to k_0 and the density of states is given by

$$N(E) = \frac{4\pi}{\omega} \cdot \frac{4\pi m}{h^2} (k_0 - k_{z(\mathrm{min})}) \qquad \text{......(7)}.$$

The peak in the $\{N(E), E\}$ curve corresponds to the energy surface which just touches the zone boundary.

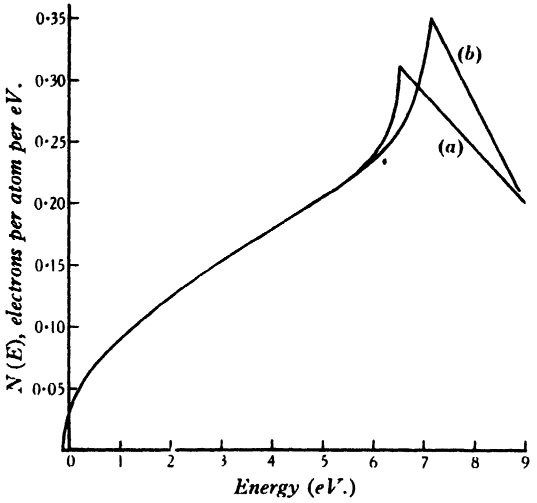

Figure 1 (*a*) and (*b*). Curves showing the number of states per unit energy range as a function of the energy. (*a*) For the face-centred cubic structure, (*b*) for the body-centred cubic structure.

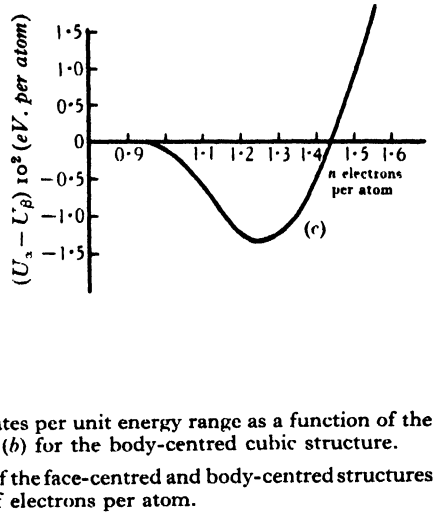

Figure 1 (*c*). The difference between the Fermi energies of the face-centred and body-centred structures as a function of the number of electrons per atom.

Since we are, at present, interested only in the states within the first Brillouin zone which are occupied when the zone is about half filled with electrons, for the face-centred cubic structure, we shall consider only the effect of the octahedral planes of the zone on the density of states. We take therefore $\omega = \frac{1}{2}\pi$, and $k_0 = 3^{1/2}/4^{5/6}\Omega^{1/3}$, where Ω is the atomic volume as before. Curve (*a*), figure 1, shows $N(E)$ for the face-centred cubic structure having the same atomic volume as the body-centred structure (*b*) and having the same value of the energy-discontinuity.

We obtain the value of α for copper from the magnitude of the energy gap as determined by the optical properties. This value $\Delta E = 4{\cdot}1$ electron-volts$^{(2)}$. Since the atomic volume is $11\cdot76 . 10^{-24}$ cm.^{3} we find, for the face-centred cubic structure, that the free electron energy E_0 corresponding to the point k_0 is 8·64 electron-volts and therefore, according to equation (1.1), $\alpha = -7\cdot41$. For the body-centred cubic structure, assuming the same energy gap, we find $E_0 = 9\cdot14$ electron-volts and $\alpha = -7\cdot89$.

When the number of states per unit energy range $N(E)$ is known, we can obtain the Fermi energy $U(n)$ immediately as a function of the number of electrons per atom. We have

$$\left.\begin{aligned} n &= \int_0^{\zeta} N(E)\,dE \\ U &= \int_0^{\zeta} EN(E)\,dE \end{aligned}\right\} \qquad \ldots\ldots(8),$$

where ζ is the energy of the surface bounding the occupied states. Eliminating ζ between these equations gives $U(n)$. Figure 1 (*c*) shows the difference between the Fermi energies of the face-centred and body-centred cubic structures, which have atomic volumes that are the same and are equal to that of copper, as a function of n, the number of valency electrons per atom. The curve has been obtained by numerical integration, according to equation (8), of the data given in curves (*a*) and (*b*), figure 1. For pure copper, for which $n = 1$, we find that the limiting surface of the Fermi distribution of electrons occurs almost exactly at the energy for which $N(E)$ is a maximum. This gives the result $\zeta = 6\cdot6$ volts.

§ 3. THE DETERMINATION OF THE α, β PHASE BOUNDARIES

For the determination of the α, β phase boundaries we only need the variation of the Fermi energy with n for values of n somewhat greater than unity. For this range it is possible, as we shall now show, to obtain simple approximate formulae for the Fermi energies in the α and β phases.

According to equations (6) and (7) for an electron : atom ratio n greater than 1·25, the density of states for either phase may be written

$$N(E) = \frac{4\pi}{\omega} \cdot \frac{4\pi m}{h^2} \left\{ k_0 - \left(1 - \frac{\omega}{2\pi}\right) \sqrt{\frac{2mE}{h^2}} \right\} \qquad \ldots\ldots(9),$$

where ω and k_0 are given their values appropriate to either phase. This formula is only approximate since the term in curly brackets of formula (6) has been neglected. The error introduced, however, is so small as to be of no consequence for our purpose; see figures 1 (*a*) and 1 (*b*).

It can be seen from figure 1 that for a certain energy E_1 the number of states enclosed by this energy surface will be the same in both the α and the β phases. Let the number of states per atom bounded by the surface E_1 be n_0. Numerical integration shows that in the case considered $E_1 = 7\cdot23$ electron-volts and $n_0 = 1\cdot23$ electrons per atom. Formula (9) may still further be simplified if we write $E = E_1 + \epsilon$

and expand the square root for small values of ϵ. We may then write

$$\left.\begin{aligned} N_\alpha(E) &= N_1 - a\epsilon \\ N_\beta(E) &= N_2 - b\epsilon \end{aligned}\right\} \qquad \text{.....} (10),$$

where

$$a = 3\frac{4\pi m}{h^2}\sqrt{\frac{2m}{h^2 E_1}},$$

$$b = 5\frac{4\pi m}{h^2}\sqrt{\frac{2m}{h^2 E_1}},$$

and N_1 and N_2 are the values of $N(E)$ when the energy is E_1 in the α and β phases respectively. The numerical values of these quantities are as follows:

$N_1 = 0{\cdot}280$, $N_2 = 0{\cdot}346$ electrons per atom per volt; $a = 0{\cdot}0454$, $b = 0{\cdot}0757$ electrons per atom per (volt)^2.

Equations (8) and (10) determine the Fermi energies of the two phases as functions of the number of electrons per atom. We find

$$\left.\begin{aligned} U_\alpha(n) &= U_\alpha + E_1(n-n_0) - \frac{N_1^3}{3a^2} + \frac{N_1(n-n_0)}{a} + \frac{N_1^3}{3a^2}\left\{1 - \frac{2a(n-n_0)}{N_1^2}\right\}^{\frac{3}{2}} \\ U_\beta(n) &= U_\beta + E_1(n-n_0) - \frac{N_2^3}{3b^2} + \frac{N_2}{b}(n-n_0) + \frac{N_2^3}{3b^2}\left\{1 - \frac{2b(n-n_0)}{N_2^2}\right\}^{\frac{3}{2}} \end{aligned}\right\} \text{......} (11).$$

U_α and U_β are the energies of the α and β phases when there are n_0 electrons per atom in each. If v denotes the valency of the solute atoms and x denotes their concentration in the phase, the number of electrons per atom n is given by

$$n = (v-1)x + 1.$$

We introduce a variable ξ such that

$$\xi = (n - n_0) = (v-1)x + 1 - n_0 \qquad \text{......} (12).$$

The equations which determine the limits of the α and β phase boundaries at the absolute zero may be written

$$\left.\begin{aligned} \frac{dU_\alpha(\xi_\alpha)}{d\xi_\alpha} &= \frac{dU_\beta(\xi_\beta)}{d\xi_\beta} \\ U_\alpha(\xi_\alpha) - \xi_\alpha\frac{dU_\alpha(\xi_\alpha)}{d\xi_\alpha} &= U_\beta(\xi_\beta) - \xi_\beta\frac{dU_\beta(\xi_\beta)}{d\xi_\beta} \end{aligned}\right\} \qquad \text{......} (13);$$

compare equation (4) of part 1. From equations (11) and (12) we obtain easily, by substituting in (13), the following values for ξ_α and ξ_β:

$$\xi_\alpha = N_1 z - \tfrac{1}{2}az^2,$$

$$\xi_\beta = N_2 z - \tfrac{1}{2}bz^2,$$

where z is the root of the equation

$$z^3 - 3\left(\frac{N_2 - N_1}{b-a}\right)z^2 + \frac{6(U_\beta - U_\alpha)}{b-a} = 0 \qquad \text{......} (14).$$

From figure 1 (*c*) we find that for $n = n_0 \doteqdot 1{\cdot}23$, $U_\beta - U_\alpha = 0{\cdot}0135$ electron-volt, and with the numerical values already given we find, for the solution of equation (14),

$z=0{\cdot}675$ and therefore $\xi_\alpha=0{\cdot}179$ and $\xi_\beta=0{\cdot}217$. Thus since $\xi_\alpha=(n_\alpha-n_0)$ and $\xi_\beta=(n_\beta-n_0)$ we find, for the corresponding values of the electron concentrations, $n_\alpha=1{\cdot}409$ and $n_\beta=1{\cdot}447$.

§4 THE VARIATION OF THE α, β PHASE BOUNDARIES WITH TEMPERATURE

To determine ξ_α and ξ_β when $T>0$ we first expand the energies $U_\alpha(\xi_\alpha)$ and $U_\beta(\xi_\beta)$ about the values $\xi_\alpha(0)$ and $\xi_\beta(0)$ which correspond to $T=0$. We write

$$\xi_\alpha(T)=\xi_\alpha(0)+p,$$

$$\xi_\beta(T)=\xi_\beta(0)+q,$$

and treating p and q as small quantities we obtain

$$\frac{dU_\alpha}{dx_\alpha}-\frac{dU_\beta}{dx_\beta}=(v-1)\left\{\frac{q}{N_2-bz_0}-\frac{p}{N_1-az_0}\right\},$$

$$U_\alpha-x_\alpha\frac{dU_\alpha}{dx_\alpha}-U_\beta+x_\beta\frac{dU_\beta}{dx_\beta}=(v-1)\left\{\frac{x_\alpha^{(0)}p}{N_1-az_0}-\frac{x_\beta^{(0)}q}{N_2-bz_0}\right\},$$

where $x_\alpha^{(0)}$ and $x_\beta^{(0)}$ are the values of the concentrations x_α and x_β at $T=0$. Similarly we have

$$\log\frac{x_\alpha(1-x_\beta)}{x_\beta(1-x_\alpha)}=\log\frac{x_\alpha^{(0)}(1-x_\beta^{(0)})}{x_\beta^{(0)}(1-x_\alpha^{(0)})}+\frac{1}{(v-1)}\left\{\frac{p}{x_\alpha^{(0)}(1-x_\alpha^{(0)})}-\frac{q}{x_\beta^{(0)}(1-x_\beta^{(0)})}\right\},$$

$$\log\frac{1-x_\beta}{1-x_\alpha}=\log\frac{1-x_\beta^{(0)}}{1-x_\alpha^{(0)}}+\frac{1}{(v-1)}\left\{\frac{p}{1-x_\alpha^{(0)}}-\frac{q}{1-x_\beta^{(0)}}\right\}.$$

We have already said that when applying equations (4) of part 1 we assume that the specific heat within a single phase does not change appreciably with composition (cf. § 3). For the present purpose of finding the variation of the α, β limits with temperature we shall assume also that $f_\alpha(x_\alpha T)-f_\beta(x_\beta T)$ may be replaced with sufficient approximation in equation (4) by $U_\alpha(x_\alpha)-U_\beta(x_\beta)$. This approximation will of course be better for low than for high temperatures. The equations for p and q as functions of T are therefore as follows:

$$\left\{\frac{1}{(v-1)(1-x_\alpha^{(0)})}+\frac{(v-1)x_\alpha^{(0)}}{kT(N_1-az_0)}\right\}p-\left\{\frac{1}{(v-1)(1-x_\beta^{(0)})}-\frac{(v-1)x_\beta^{(0)}}{kT(N_2-bz_0)}\right\}q$$
$$=\log\left(\frac{1-x_\alpha^{(0)}}{1-x_\beta^{(0)}}\right),$$

$$\left\{\frac{1}{(v-1)(1-x_\alpha^{(0)})x_\alpha^{(0)}}-\frac{(v-1)}{kT(N_1-az_0)}\right\}p-\left\{\frac{1}{(v-1)(1-x_\beta^{(0)})x_\beta^{(0)}}-\frac{(v-1)}{kT(N_2-bz_0)}\right\}q$$
$$=\log\frac{x_\beta^{(0)}(1-x_\alpha^{(0)})}{x_\alpha^{(0)}(1-x_\beta^{(0)})}.$$

The values of the coefficients in these equations have all been given, and therefore p and q can be found as functions of T. Figure 2 shows the results obtained in this way.

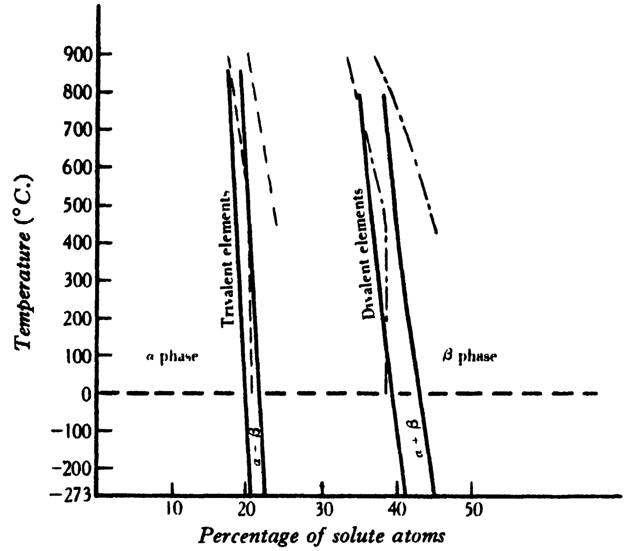

Fig. 2. Phase diagram showing the α, β boundaries. — Theoretical curve for copper. --- Observed lines for aluminium in copper. -·- Observed lines for zinc in copper.

REFERENCES

(1) Fuchs. *Proc. roy. Soc.* **151**, 585 (1935).

(2) Mott and Jones. *The Theory of the Properties of Metals and Alloys*, pp. 83, 118, 147. Clarendon Press (1936).

THE ENERGY OF THE SUPERLATTICE IN β BRASS

BY N. F. MOTT, M.A., F.R.S., H. H. Wills Physical Laboratory,
University of Bristol

Communicated by Prof. A. M. Tyndall, 16 December 1936. Read 12 March 1937

ABSTRACT. An estimate, based on the electron theory of metals, is made of the energy of the superlattice in β brass. The results obtained agree, as regards their order of magnitude, with those for the energy absorbed in the transition from the ordered to the disordered state.

§ 1. ELECTROSTATIC ENERGY OF THE SUPERLATTICE

THE body-centred alloy having the composition CuZn (β brass) forms a superlattice below about 460° C. When the superlattice is complete, the atoms at the centres of the cubes are, say, copper and those at the corners zinc, and the alloy is said to be ordered. The purpose of this note is to deduce from the theory of metals an estimate of the energy required to destroy the superlattice, and hence of the heat absorbed in the transition from the ordered to the disordered state.

The copper ion is larger than the zinc ion;* in the ordered state no two copper ions are in contact, but in the disordered state there will be N pairs of copper ions in a crystal containing N atoms (i.e. $\frac{1}{2}N$ copper and $\frac{1}{2}N$ zinc atoms). The repulsive exchange interaction between the ions will therefore hinder the formation of the disordered state. Since, however, Jones(10) has shown that the phase diagram of these alloys is not appreciably influenced by the exchange repulsion between the ions, we should not expect the ion-ion interaction to be very important. An estimate of it will be made in § 2.

We believe the most important force favouring the formation of the superlattice to be polar in origin. Each copper atom contributes one electron and each zinc atom two electrons to the number of conduction electrons in the alloy. If the charge-density due to the conduction electrons in the alloy were uniform, then the atomic polyhedron† surrounding each zinc ion would contain a positive charge $+\frac{1}{2}e$, and that surrounding each copper ion a charge $-\frac{1}{2}e$. The energy attending the formation of the superlattice would then be about twenty times greater than that observed. We must deduce that the conduction electrons tend to cluster about the zinc ions; the charge-density is greater in their neighbourhood than in that of the copper ions.

This clustering has already been estimated for *dilute* solutions of zinc in copper by the present author in a paper(2) on the electric resistance of dilute solid solutions. It was assumed that when a zinc atom is added to copper the field round the copper is altered in such a way that the electrostatic potential near the zinc atom is greater than that near a copper atom by an amount

---

* The radii given by Grimm and Wolff(1) are, 0·96 A. for Cu^+ and 0·74 A. for Zn^{++}.
† This is defined below.

$$\Phi = \frac{e}{r} \exp(-qr) \qquad \text{......(1)},$$

Φ is then the difference between the potential in the actual lattice and that in a lattice of pure copper. The increase in the resistivity of copper due to the addition of zinc is then due to the perturbing potential Φ. That due to 1 atomic per cent of zinc was shown to be

$$\Delta\rho = \frac{1}{100} \frac{2\pi e^2}{mv^3} \left\{ \log\left(1 + \frac{1}{y}\right) - \frac{1}{1+y} \right\} \qquad \text{......(2)},$$

where $y = q^2\hbar^2/4m^2v^2$.

In these equations v is the maximum velocity of the electrons in metallic copper; this may be calculated(3) to be $1{\cdot}57 \times 10^8$ cm./sec. From the observed(4) value of $\Delta\rho$, viz. $0{\cdot}335\,\mu\Omega$ /cm., we may calculate the screening-constant q and obtain

$$1/q = 0{\cdot}37 \text{ A.}$$

Formula (2) depends on the assumption that the effective number of free electrons in metallic copper is one per atom; this may introduce some error into our estimate of q.

In the paper quoted, the Thomas-Fermi method was applied to the electrons in a metal and it was shown that the extra potential Φ satisfied the equation

$$\nabla^2\Phi = q^2\Phi \qquad \text{......(3)},$$

and a theoretical expression(3) of the right order of magnitude was found for q. Since, however, the electron-density in metals is not great enough for the Thomas-Fermi method to be very accurate, in this paper we shall use the experimental value of q given above.

We now consider the CuZn alloy in either the ordered or the disordered state. Following Wigner and Seitz(1) we divide up the lattice into polyhedra all of the same size, one surrounding each atom. These we call the atomic polyhedra. Then the polyhedron surrounding a zinc atom will be positively charged and that surrounding a copper atom negatively charged. We denote by $\pm\ \Delta Q$ the charge on either polyhedron.

As Wigner and Seitz have shown, the polyhedra are very symmetrical, and to estimate the field outside them we may replace them by spheres of the same volume. It follows that the total energy of these charges in the disordered state is zero, but in the ordered state it is, per *atom*

$$-\frac{1}{2}\frac{\alpha}{a}(\Delta Q)^2 \qquad \text{......(4)},$$

where a is the lattice constant(5) (2·949 A.)* for CuZn, and α is the Madelung number for the body-centred structure, so that

$$\alpha = 2{\cdot}0354\ldots.$$

* For an alloy containing 50·1 per cent Cu.

We have now to obtain ΔQ. We may consider the copper-zinc lattice as a periodic lattice of which each ion has a charge $\frac{3}{2}e$, together with an additional charge $\pm\frac{1}{2}e$ on each copper or zinc ion. The potential due to these additional charges and to the clustering of the conduction electrons that they produce is the extra potential Φ which satisfies equation (3). In the ordered lattice Φ satisfies the boundary conditions

$$\begin{aligned} \Phi &\doteqdot \pm\tfrac{1}{2}e/r \qquad (r\rightarrow 0) \\ &= 0 \text{ at the boundary of each polyhedron.} \end{aligned}$$

As before we replace each polyhedron by a sphere of radius r_0 such that $(4\pi/3)\,r_0^3$ is the atomic volume. The solution of equation (3) is then

$$\Phi = \pm\tfrac{1}{2}e\left[\frac{\exp\{-q(r-r_0)\}-\exp\{q(r-r_0)\}}{\exp(qr_0)-\exp(-qr_0)}\right].$$

We obtain the extra charge on each polyhedron from Gauss's theorem

$$\begin{aligned} \Delta Q &= \frac{1}{4\pi}\int \frac{\partial\Phi}{\partial n}\,dS \\ &= \pm e\,\frac{qr_0}{\exp(qr_0)-\exp(-qr_0)}. \end{aligned}$$

With r_0 equal to 1·46 A., and the above value of q, this gives us

$$\Delta Q = \pm 0{\cdot}075\,e,$$

and for the binding energy of the ordered state

$$W = -0{\cdot}027 \text{ eV. per atom.}$$

In view of our assumption that the screening constant q is the same for CuZn as for copper no significance can be attached to the exact value obtained, but the order of magnitude should be correct.

§ 2. EXCHANGE INTERACTION BETWEEN THE IONS

We assume that the energy per ion pair in copper is given by

$$w(r) = \lambda e^{-r/\sigma},$$

where r is the interatomic distance.

We then deduce λ and σ from the observed elastic constants of copper at low temperatures, namely*

$$\begin{aligned} c_{11}-c_{12} &= 5{\cdot}21\times 10^{11}\text{ dyne/cm}^2 \\ c_{44} &= 8{\cdot}14\times 10^{11}\text{ dyne/cm}^2 \end{aligned}$$

From these we subtract estimates of the terms due to the interaction between the ions and the valence electrons as calculated by Fuchs(6), namely 0·57 for $c_{11}-c_{12}$ and 1·89 for c_{44}. The value assumed for c_{44} differs slightly from that assumed by Fuchs because we have taken the ratio between the two quantities equal to that observed by

---

* For the definitions of these quantities, see for instance reference (3), p. 148.

Bender(7) for sodium. We thus have for that part of the interaction which is due to the exchange repulsion between the ions

$$c_{11} - c_{12} = 4{\cdot}64 \times 10^{11} \text{ dyne/cm}^2$$

$$c_{44} = 6{\cdot}25 \times 10^{11} \text{ dyne/cm}^2$$

λ and σ were then deduced from formulae due to Fuchs.* We obtained

$$w(r) = 3{\cdot}22 \times 10^{-2} \exp\left\{-\frac{r}{0{\cdot}138 \times 10^{-8}} + 18{\cdot}53\right\} \text{ eV.}$$

Taking for r the observed interatomic distance (2·09 A) for CuZn, this gives

$$w(r) = 0{\cdot}0127 \text{ eV.}$$

As we have seen, this is equal to the energy of the superlattice per atom.

Finally, therefore, for the energy per atom of the superlattice we have

$$\left.\begin{array}{ll} \text{Electrostatic energy} & 0{\cdot}027 \text{ eV.} \\ \text{Energy due to exchange repulsion between ions} & 0{\cdot}013 \text{ eV.} \\ \text{Total energy (calculated)} & 0{\cdot}040 \text{ eV.} \end{array}\right\}$$

It is difficult to obtain an accurate estimate of the observed energy absorbed during the order-disorder change. According to the theory of Bragg and Williams(8) the entropy change per atom is

$$\int dQ/T = k \log_e 2.$$

Assuming that the entropy change above the critical temperature T_c can be neglected, the left-hand side is somewhat greater than

$$\frac{1}{T_c}\int dQ.$$

Thus the heat evolved per atom is less than

$$kT_c \log_e 2.$$

If $T_c = 730°$ K., this gives

$$\text{Total energy (observed)} < 0{\cdot}043 \text{ eV. per atom.}$$

§ 3. VARIATION OF DEGREE OF ORDER WITH TEMPERATURE

Finally we must enquire whether the assumptions made by Bethe(9) in calculating the degree of order at any given temperature are correct. Bethe assumes that the work done when a copper atom and a zinc atom change places depends only on the atoms in the lattice which are nearest neighbours to this pair.

For an ionic lattice such as NaCl Bethe's assumption would not be correct; if a kation and an anion were interchanged a dipole would be formed, and the extra potential due to it would fall off only as r^{-2}. These long-range forces cannot however exist in a conductor; in β brass, if a pair of copper and zinc atoms change places the conduction electrons will rearrange themselves round the dipole so formed in such a way as to screen it.

---

* Cf. reference (3), chapter IV, equation (22).

According to equation (3) the potential round a dipole of strength μ will be

$$\frac{\mu \cos\theta}{r^2} e^{-qr}.$$

The term e^{-qr} falls off so rapidly that it is probably correct to assume that the interaction between all but nearest neighbours can be neglected.

On the other hand it is probably not true that the interaction energy between a copper atom and a zinc atom is independent of the degree of order of their neighbours. We have derived the excess charge ΔQ on each atomic polyhedron on the assumption that a copper atom is completely surrounded by zinc atoms and *vice versa*. If, on the other hand, a copper atom is completely surrounded by copper atoms, the charge on its atomic polyhedron will not differ appreciably from zero, because the field due to the copper-zinc boundary falls off as e^{-qr}, so that the atom will not know that it is not in a block of metallic copper. In the intermediate case of a copper or zinc atom in the disordered lattice, with nearest neighbours of both kinds, we should expect the excess charge to be numerically smaller than in the ordered state.

The interaction between neighbouring atoms will therefore decrease as the disorder increases.

In the transition from order to disorder the energy absorbed in the later stages, compared with that absorbed in the earlier stages, is thus less than Bethe's theory indicates. It follows that if the degree of order S is plotted against temperature, S will drop to zero more sharply than in Bethe's theory. This may well be the explanation of the observed fact that the specific-heat bump associated with the transition in β brass is much sharper* than the theory leads one to expect.

---

* Cf. reference (3), figures 14 and 15.

REFERENCES

(1) Grimm and Wolff. *Handb. Phys.* **24** (2), 933 (1933).
(2) Mott. *Proc. Camb. phil. Soc.* **32**, 282 (1936).
(3) Mott and Jones. *The Theory of the Properties of Metals and Alloys* (1936).
(4) Linde. *Ann. Phys.*, Lpz., **10**, 52 (1931).
(5) Owen and Pickup. *Proc. roy. Soc.* A, **140**, 179 (1933).
(6) Fuchs. *Proc. roy. Soc.* A, **153**, 622 (1936).
(7) Bender. *Naturwissenschaften* (in the Press).
(8) Bragg and Williams. *Proc. roy. Soc.* A, **145**, 699 (1934).
(9) Bethe, *Proc. roy. Soc.* A, **150**, 552 (1935).
(10) Jones, page 243 of this volume.

DISCUSSION

Mr Bucknall. Although the constitution of a very large number of alloy systems has been determined* and metallurgists generally realize the significance of equilibrium diagrams, no one yet understands them in the sense of being able to predict the constitution of unexplored systems of alloys. At present the metallurgist who conducts an argument regarding alloy-constitution must constantly refer to original papers, or perform prodigious feats of memory, and therefore he looks forward eagerly to the time when a sound generalized theory of alloys will have been developed by the application of wave-mechanical considerations to alloys. It is recognized that simplifications are essential in the development of such a theory, but there is a real danger that over-simplification may lead to an unfavorable reception of the generalizations advanced. The sentence with which part 1 of Mr Jones's paper† opens would be regarded by many as a dangerous half-truth, as it is only in the alloys of silver and copper that the electron-concentration principle of solid solubility is clearly apparent; as I have pointed out‡, the solutions of the other metals in aluminium, magnesium, nickel, cobalt and iron do not accord with this rule. Again, elements of the same valency and not greatly differing atomic volume, such as silver and copper, do not always show complete solid miscibility, so that some factor other than electron-concentration is clearly important.

With regard to deviations from the ordinary laws of solution, it is interesting to note that while copper alloys generally exhibit these effects according to Hume-Rothery,§ recent German work on the solid solubility of tin in copper has shown the normal relation between concentration and temperature. The interstitial type of solid solution, for instance that of carbon in γ iron, warrants immediate attention by workers in this field.

---

* See M. Hansen, *Der Aufbau der Zweistofflegierungen.*

† Page 243 of this volume.

‡ *Metal Industry*, **48**, 305 (1936).

§ Haase and Pawlek, *Z. Metallkunde*, **18**, 73 (1936).

THE DIVISION OF PRIMARY ELECTRON CURRENT BETWEEN GRID AND ANODE OF A TRIODE

BY D. M. MYERS

Communicated by I. O. Griffith, 24 *July* 1936. *Read in title* 26 *February* 1937

ABSTRACT. The paper describes a method of determining the distribution, between the grid and anode, of the current emitted by the cathode of a cylindrical triode. Measurements of the temperature of the anode are used to verify that this distribution depends on the ratio of the potentials applied to the anode and grid, and not on their absolute values. A direct method is then described in which the grid and anode currents are measured in conditions such that there is no flow of secondary current; by this means, the distribution of primary current from the cathode, and the value of any secondary current flowing between the anode and grid, can be deduced in any conditions of operation. Curves are obtained by the former method, showing the variation with impact energy of the secondary-emission ratio for both nickel and molybdenum anodes.

The effect of the anode-potential : grid-potential ratio on the distribution of primary current is determined for a particular triode, and an empirical relation is shown to hold for a considerable range of potential-ratios. This relation is of the same form for any cylindrical triode, but no general relation, applicable to any cylindrical triode, has yet been found.

§ 1. INTRODUCTION

If a thermionic tube has two collecting electrodes, the current emitted from the cathode will be shared between them in some manner depending on their potentials. Direct measurement of the current stream to each does not necessarily give the distribution of the electrons emitted by the cathode, because in general a secondary stream emitted by the electrode of lower potential will be collected by the other cold electrode.

The problem of calculating the partition of the stream is too complex to solve analytically, although it has been stated(1) that it can be shown theoretically that the stream divides in a ratio which depends on the ratio of the potentials of the two electrodes and not on the absolute magnitude of these potentials. The object of the present work is to test this conclusion and to determine experimentally the manner in which the partition of the stream depends on the ratio of the two potentials.

The distribution of current can be examined by direct measurement if no appreciable secondary current flows between the electrodes, or alternatively by some method where the magnitude of the secondary current can be determined. The former condition obtains when the potential applied to at least one of the collecting electrodes is small, or when both collecting electrodes have the same potential.

In the case where a secondary current exists, two methods for determining its magnitude are described here. One of these depends on direct measurement of the currents but relies on extrapolation of a curve, so that it gives only an approximation. The other method requires direct measurement of the currents, combined with measurement of the temperature of one of the collecting electrodes. This method was used to verify that the partition of the current emitted by the cathode is a function only of the ratio of the applied potentials; moreover, this function was obtained experimentally over a limited range of the said ratio. The experiments using this method will be described first.

The temperature-rise of the anode was measured in terms of the e.m.f. produced by a thermocouple attached to it: the magnitude of this e.m.f. is termed the *temperature reading*. When the anode is subject to electronic bombardment its temperature is thereby raised above the temperature produced by radiation from the cathode. The additional thermocouple e.m.f. resulting from electronic bombardment is termed the *deflection*.

So far as the writer has been able to discover, the temperature-rise of the anode has not previously been used for inferring the magnitude of the primary electron stream incident on it. This part of the work is thus believed to be new, and the results give new information about the partition of the primary electron stream in a triode—a problem about which very little seems to be known.

§ 2. EXPERIMENTAL METHOD

A special triode valve was made, having a pure tungsten filament of V form, a thermojunction attached to the anode, and a grid furnished with a large radiating fin. The electromotive force of the thermocouple and the potential drop across the filament were measured by a potentiometer.

The temperature-rise of the anode is due to radiation from the filament, radiation from the grid and direct electronic bombardment. Since only the temperature-rise from bombardment is of interest, it is necessary to measure the other two components separately.

Thus a curve must be obtained relating the temperature-rise of the anode to the power dissipated in it. This calibration curve having been obtained, the total power received by the anode in any given circumstance of operation can be found from the observed temperature-rise. If the power received by heat-radiation, deduced from other calibrations, is subtracted from the total, the residuum is due to electronic bombardment. The primary stream to the anode can be deduced from this when the anode-potential is known. The main difficulty of the method is to obtain an accurate knowledge of the power received from heat-radiation: the calibration for this has to be built up from many steps, which will now be described in succession.

§ 3. POWER RECEIVED BY THE ANODE FROM HEAT RADIATED FROM THE CATHODE

A considerable fraction of the power received by the anode is due to radiation of heat from the cathode. In all measurements the tube is operated with a constant potential-difference across the filament, and hence to the first order the heat received from the cathode by the anode is independent of the current evaporated from the cathode and its distribution between the two electrodes. Figure 1 shows the observed relation between the e.m.f. of the thermocouple on the anode and the power input to the cathode in the condition when $V_a = V_g = 0$, and thus when the cathode is not evaporating a current. The graph in figure 1 is curved: partly because the radiation from the cathode is approximately proportional to the fourth power of its temperature and partly because the e.m.f. is not strictly proportional to temperature. Since the balance reading of the potentiometer used to indicate the thermocouple e.m.f. is a measure of the anode temperature, this reading will in future be called *the temperature reading*. If the cathode temperature were uniquely determined by the filament p.d., which is kept constant, then the relevant temperature reading when $V_a = V_g = 0$ could be taken as the effective zero temperature reading in all operating conditions. In practice this is substantially the case but not quite accurately so, because the evaporation of current by the cathode ipso facto causes the latter's temperature to fall. But this effect is partly counteracted, since a fall of temperature causes a corresponding decrease in resistance and hence an increase of power input at a constant filament p.d. Hence the effective zero temperature reading has to be corrected slightly, according to the value of the total current evaporated from the cathode. The method of making this small correction is as follows. Let χ_f be the work function of the cathode and J the current emitted by it at temperature T_f, and let R be its resistance, where $R = R_0(1 + \alpha T_f) \div \alpha R_0 T_f$. If the filament p.d. is V_f, then

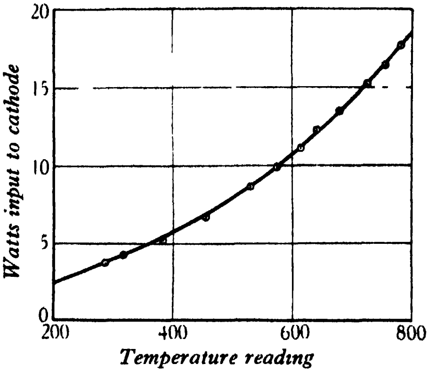

Figure 1. Calibration curve with zero heating of anode by electronic bombardment and by radiation from the grid zero.

$$W_f = \frac{V_f^2}{\alpha R_0 T_f} = kT_f^4 + \chi_f J,$$

where k is some constant, and W_f is the power input to the filament.

In operation W_f is approximately 20 W.: J does not exceed 30 mA., and hence if $\chi_f = 4{\cdot}5$ volts, $\chi_f J / W_f$ is never greater than 0·67 per cent.

The anode temperature T_A is a function of T_f, and hence the quantity which governs T_A is not W_f but kT_f^4, while

$$kT_f^4 \equiv W_1 = W_f - \chi_f J$$

$$= \frac{V_f^2}{\alpha R_0 T_f} - \chi_f J.$$

Now

$$\frac{dW_1}{dT_f} = 4kT_f^3$$

and

$$\frac{dW_1}{dJ} = -\frac{V_f^2}{\alpha R_0 T_f^2}\frac{dT_f}{dJ} - \chi_f,$$

and
$$\frac{dW_1}{dJ}=\frac{dW_1}{dT_f}\cdot\frac{dT_f}{dJ}=-4kT_f^3\left(\frac{dW_1}{dJ}+\chi_f\right)\frac{R_0\alpha T_f^2}{V_f^2}$$
$$=-4\left(\frac{dW_1}{dJ}+\chi_f\right),\text{ since } kT_f^4\gg\chi_f J.$$
$$\therefore\quad \frac{dW_1}{dJ}=-\frac{4}{5}\chi_f.$$

Let R_a stand for the temperature reading of the anode. Then
$$\frac{dR_a}{dJ}=\frac{dR_a}{dW_1}\cdot\frac{dW_1}{dJ}=-\frac{4}{5}\frac{\chi_f}{g}.$$

Hence
$$\Delta R_a=-\frac{4}{5}\frac{\chi_f}{g}J \qquad \text{......(1)},$$
where g is the gradient of the calibration curve, typified by figure 1.

To make clear the use of this correction, consider the following numerical example. Suppose that for some assigned value of V_f, the temperature reading is 700 when $V_a=V_g=0$ and that it is 720 when $J=10$ mA. Then the heating due to bombardment by 10 mA. is not determined by the quantity (720 − 700) but by
$$720-\left(700-\frac{4}{5}\frac{\chi_f}{g}J\right)=720-(700-0{\cdot}94)$$
$$\doteq 21,$$
if we assume that $\chi_f=4{\cdot}5$ and $g=38{\cdot}4$ mW./div., which is the relevant value of g in figure 1, when $R_a=700$.

§4. METHOD OF CORRECTING FOR VOLTAGE DROP ALONG THE FILAMENT

Since the filamentary cathode is not an equipotential surface, the p.d. between anode and filament depends on the point of the filament considered. If i is the current evaporated from some specified short length dx of filament, where the p.d. is v, then the work W done on the anode is given by
$$W=\int_0^l ivdx,$$
where the integration is along the length l of the filament. If J is the total anode current,
$$I=\int_0^l idx.$$

W cannot be evaluated until i, equal to $f(x)$, and v, equal to $\phi(x)$ are known. If the emission is temperature limited, i is independent of x and then $W=I\,(V_a-\frac{1}{2}V_f)$. If the current is space-charge-limited and if the anode is long, then $i=kv^{\frac{3}{2}}$ and
$$v=V_a-\frac{x}{l}V_f.\text{*}$$

---

* Since the total current emitted was of the order of 30 mA. and the filament current 2 A., the voltage drop along the filament remains substantially linear and independent of emission.

Hence it can readily be shown, and is well known, that

$$I=\frac{2kl}{5V_f}\{V_a^{\frac{5}{2}}-(V_a-V_f)^{\frac{5}{2}}\}$$

and
$$W=k\int_0^l v^{\frac{5}{2}}\,dx=\frac{5}{7}IV_a\frac{1-(1-V_f/V_a)^{\frac{7}{2}}}{1-(1-V_f/V_a)^{\frac{5}{2}}}.$$

Hence V_a', the effective anode-potential, is given by

$$V_a'=\frac{5V_a}{7}\frac{1-(1-V_f/V_a)^{\frac{7}{2}}}{1-(1-V_f/V_a)^{\frac{5}{2}}}. \qquad \text{......(2).}$$

In these measurements V_f was 9 V.: hence it may be calculated, for example, that $V_a'=7{\cdot}1$ when $V_a=10$, and $V_a'=21$ when $V_a=25$. If and when temperature saturation occurs, $V_a'=V_a-4{\cdot}5$.

It should be understood that in future any numerical values quoted for anode potential are values of V_a' and not of V_a.

§ 5. EFFECT OF THE WORK FUNCTION OF THE RECEIVING ELECTRODES

If an electrode at effective potential V' receives an electron current I, then the work done on it is $W=J\,(V'+\chi)$, where χ is the work function of the surface. Similarly, if the same electrode emits a current I_s by secondary emission, the net work W will be given by

$$W=I\,(V'+\chi)-I_s\chi.$$

§ 6. THE RELATION BETWEEN THE TEMPERATURE OF AND THE TOTAL POWER INPUT TO THE ANODE

It is now necessary to obtain the calibration curve relating temperature reading with a known input power to the anode. This can be obtained by bombarding the anode, in the condition when $V_g=0$: for then there is no secondary emission from the anode and no additional heat radiated from the grid as a result of grid bombardment. Figure 2 is an experimental curve relating additional temperature reading, corrected for filament cooling, as described in § 3, with power received by the anode from bombardment. The input power is deduced from the relation

$$W=I\,(V'+\chi_a),$$

where I is the measured anode current, χ_a is the work function of the anode surface (taken as 4·5 volts), and V_a' has been defined previously. Hereinafter the additional temperature reading, as defined above, will be termed the *deflection*.

It must now be understood that figure 2 relates the deflection to the power received by the anode, otherwise than by radiation from the filament, whether this power is received solely by bombardment (the condition under which the curve is obtained) or partly by heat radiated from the grid (the condition that must occur in the operating condition where positive potentials are applied to both the anode and the grid so that the grid is being heated by primary bombardment from the cathode and possibly by secondary bombardment from the anode).

§7. THE RELATION BETWEEN DEFLECTION AND THE HEAT RADIATED FROM THE GRID

It is now necessary to obtain a calibration curve relating deflection with the power given to the grid by bombardment* in the condition when $V_a = 0$, and hence when there is no anode-bombardment. Such a calibration curve is shown in figure 3. It will now be assumed that when the grid receives a certain power W_g from any source, then a constant fraction pW_g is radiated to the anode; this is equivalent to assuming that all radiation from the grid occurs at substantially the same temperature, namely the temperature of the grid wires. It must be understood that the ordinates in figure 3 have been adjusted for work function and effective grid voltage, in the manner previously described for the anode. Moreover, the deflection has been corrected for filament cooling.

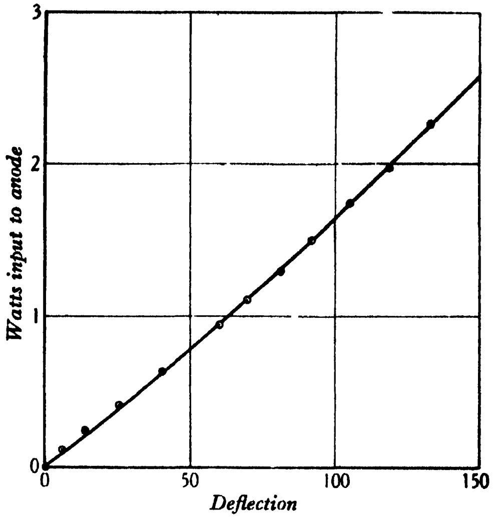

Figure 2. Calibration curve relating additional temperature-rise of anode, due to electronic bombardment, with watts input to anode. The heat-radiation from the grid is zero.

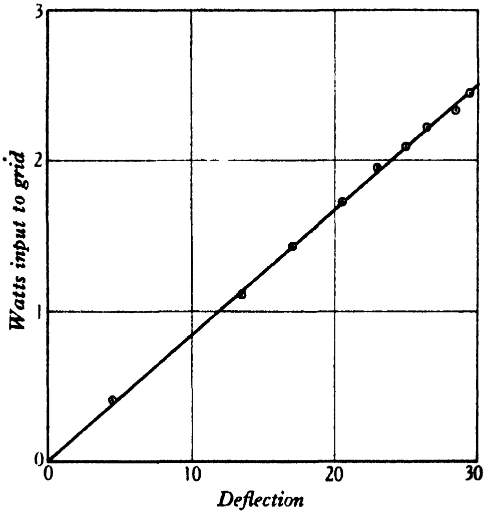

Figure 3. Calibration curve relating additional temperature-rise of anode, due to radiation from grid, with watts input to grid. The anode-bombardment is zero.

The factor p is derived from figures 2 and 3 as follows. When the grid input is W_g' the anode receives energy at the rate pW_g' and there results a deflection D_a' such that $D_a' = f(pW_g')$. Let the same deflection be obtained when the anode receives power W_a' from bombardment alone, so that $V_g = 0$, as in figure 2. Then $D_a' = f(W_a')$.

Hence
$$p = \frac{W_a'}{W_g'}.$$

Since both figures 2 and 3 are substantially linear over the range covered by figure 3, it follows that p is equal to the ratio of the initial gradients of these two curves.

---

* Provision was made for leads to be taken from each of the two support wires of the grid, in order to supply heat to the grid directly instead of by bombardment. This method was not actually used, as it was found that there was considerable risk of damage to the pinch of the triode.

§8. THE METHOD OF DEDUCING THE PRIMARY ANODE CURRENT ${}_pI_a$

The previous sections have explained how the power input due to bombardment of the anode can be deduced when the power input to the grid is known. But if neither V_g nor V_a is zero and if V_g is not equal to V_a, the grid input cannot be deduced from the measured value of grid current because the grid is either receiving or emitting an unknown number of secondary electrons. Nevertheless, it is possible to obtain an expression, from which the primary anode current ${}_pI_a$ can be deduced from the measured temperature deflection and currents and the known correcting factors. The derivation of this expression will now be given. The conditions where V_g is greater than V_a and where V_g is less than V_a will be considered separately.

(*a*) *Grid-potential greater than anode-potential.* Let W_a be the power received by the anode as the result of bombardment: then the total power W it receives is expressed by the equation

$$W = W_a + pW_g \qquad \text{......(3).}$$

But

$$\begin{aligned} W_a &= (V_a' + \chi_a)\,{}_pI_a - \chi_a I_s \\ &= V_a'\,{}_pI_a + \chi_a I_a \qquad \text{......(4),} \end{aligned}$$

where I_s is the secondary current, I_a is the measured anode current, and the subscript p denotes primary currents,

and

$$\begin{aligned} W_g &= (V_g' + \chi_g)\,{}_pI_g + (V_g' - V_a' + \chi_g) I_s \\ &\equiv (nV_a' + \chi_g)\,{}_pI_g + \{(n-1)\,V_a' + \chi_g\} I_s, \quad \text{where} \quad V_g' = nV_a', \\ &= (nV_a' + \chi_g)\,J - \{(n-1)\,V_a' + \chi_g\}\,I_a - V_a'\,{}_pI_a \qquad \text{......(5),} \end{aligned}$$

where $J = I_a + I_g$.

From equations (3) and (4) it follows that

$${}_pI_a = \frac{W_a - \chi_a I_a}{V_a'} = \frac{W - pW_g - \chi_a I_a}{V_a'},$$

whence, in combination with (5), it follows that

$${}_pI_a = \frac{W - p\,(nV_a' + \chi_g)\,J + \{p\,(n-1)\,V_a' - (\chi_a - p\chi_g)\}\,I_a}{(1-p)\,V_a'} \qquad \text{......(6).}$$

Since W is known, by means of figure 2, from the measured temperature deflection, ${}_pI_a$ can now be deduced.

(*b*) *Grid-potential less than anode-potential.*

$$\begin{aligned} W_g &= (V_g' + \chi_g)\,{}_pI_g - \chi_g I_s \\ &= V_g'\,{}_pI_g + \chi_g I_g \qquad \text{......(7),} \end{aligned}$$

and

$$W_a = (V_a' + \chi_a)\,{}_pI_a + (V_a' - V_g' + \chi_a)\,I_s \qquad \text{......(8).}$$

Whence, proceeding as in section (*a*), we deduce that

$${}_pI_a = \frac{W - p\,(nV_a' + \chi_g)\,J + \{(n-1)\,V_a' - (\chi_a - p\chi_g)\}\,I_a}{n\,(1-p)\,V_a'} \qquad \text{......(9).}$$

§ 9. THE EFFECT OF THE RATIO V_g/V_a

When the two potentials are approximately equal, only a certain proportion of the secondary electrons emitted by the electrode of lower potential will be collected by the other. This is partly due to discontinuity of the grid, and probably partly due to space charge at the surface of the emitting electrode. In order to measure total emitted secondary current from one electrode it is necessary that the whole of this current should be collected by the other.

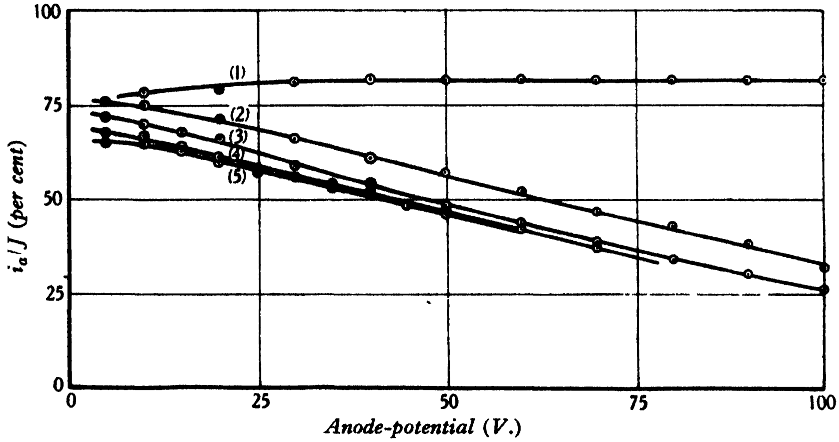

Figure 4. Curves relating I_a/J with V_a when V_g/V_a is maintained constant at five stated values. Curve (1), $V_g/V_a=1\cdot0$; (2), $V_g/V_a=1\cdot5$; (3), $V_g/V_a=2\cdot0$; (4), $V_g/V_a=3\cdot0$; (5), $V_g/V_a=4\cdot0$.

The family of curves in figure 4 shows the observed relation between I_a/J and V_a, in the triode constructed for these measurements, for the values of n, defined as V_g/V_a, specified in the figure. When $n=1$ there is no secondary electron flow and I_a/J is independent of V_a. If n is greater than 1 the anode emits a secondary current, and then I_a/J is a function of V_a. The figure shows that if n exceeds about 2·5, then the members of the family differ only slightly from one another: thus, provided n exceeds about 2·5, the grid collects all the secondary electrons which can be emitted from the anode. Considerations of grid heating have in fact made it desirable to make n equal to 2 in measurements of secondary emission from the anode: the appropriate choice of n must depend on the particular triode in use.

§ 10. EXPERIMENTAL RESULTS

The first series of results was obtained from two special triodes made to the following specification by the British Thomson-Houston Co. Ltd.

Filament. Plain tungsten wire 0·005 in. in diameter, disposed in V-form and of total length 3·25 in.

Grid. Helix of molybdenum wire, 0·008 in. in diameter, wound with 10 turns per inch on a mandrel 0·25 in. in diameter: length of helix, 1·75 in.; 2 nickel support wires, 0·030 in. in diameter. The grid was also furnished with a blackened metal radiator, fixed to it at the end remote from the pinch.

Anode: *Triode A*. Nickel anode, $\frac{5}{8}$ in. in diameter, $1\frac{3}{4}$ in. long. *Triode B*. Molybdenum anode, $\frac{7}{8}$ in. in diameter, $1\frac{3}{4}$ in. long. The anode of either valve had a substantial metal strip welded along a generator of the cylinder; to the middle of this strip was attached a thermojunction.

Thermojunction. Copper, 0·004 in. in diameter, eureka, 0·0032 in. in diameter.

The procedure was to record the temperature reading and the relevant currents when the anode- and grid-potentials were varied and adjusted in such a manner as to keep V_g'/V_a' equal to 2. In figure 5 are shown typical results for valve *A*. In this, curve 1 relates the total emission J to V_a: curve 2 relates the measured anode current I_a to V_a: curve 3 relates V_a to the values of ${}_pI_a$ deduced from the temperature readings. Figures 1, 2, 3 and 4 pertain to triode A, operated with the same filament-potential as that used in the tests graphed in figure 5.

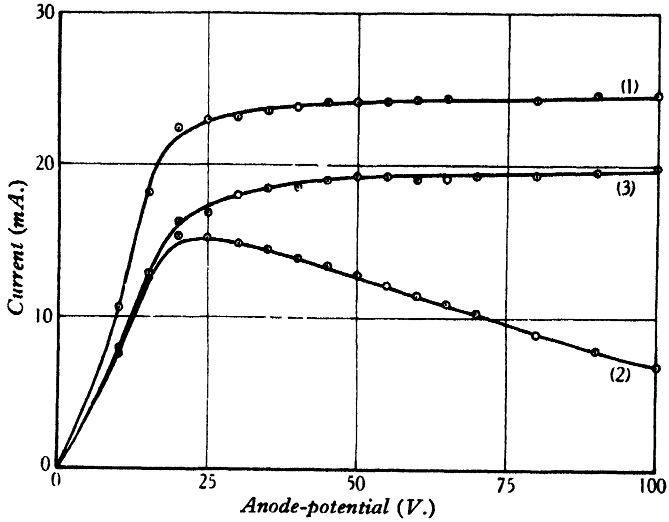

Figure 5. Curves for valve *A* relating emission current (1), anode current (2) and primary anode current (3)*, with V_a when V_g/V_a is maintained constant and equal to 2.

Figure 6 shows the corresponding curves for triode B. In figure 7 is plotted the emission ratio $I_s/{}_pI_a$ as a function of V_a' for both triodes. Considerable difficulty was encountered in taking the necessary temperature readings in the case of triode B, owing to a slight fault in the arrangement of the thermojunction leads. As a result the readings had to be taken very quickly and it was impossible to maintain a constant total emission. Some more triodes, in which this fault will be remedied, are being constructed.

Results obtained by Barber⁽²⁾ show that the secondary-emission ratio is affected by temperature, an increase in temperature of the emitting surface causing a decrease in the emission ratio. In the foregoing experiments, where comparatively

* See the appendix, page 278.

low voltages and currents were used, the rise in temperature of the anode during a set of readings was small, being less than 25 per cent of that due to radiation from the cathode. For this reason the effect of temperature on secondary emission has been ignored.

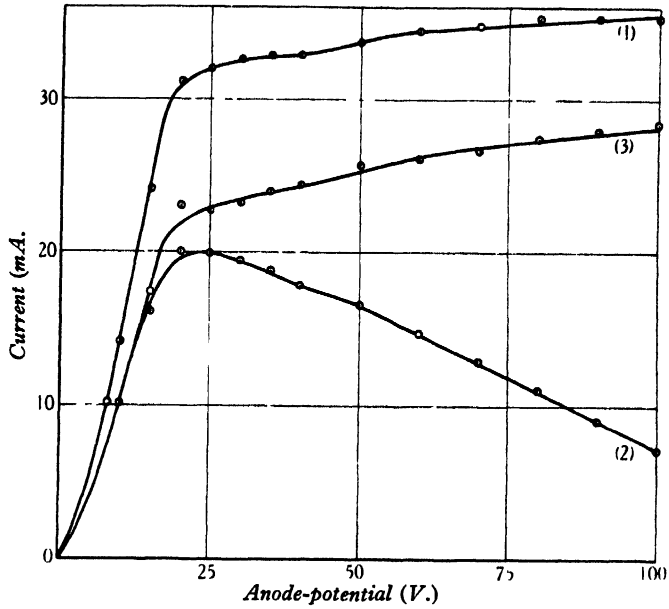

Figure 6. Curves for valve *B* corresponding to figure 5.

§ 11. THE ACCURACY OF THE MEASUREMENTS

As an experimental check on the accuracy of the procedure a similar set of readings was taken, triode A being used under the condition that $V_g = V_a$. In this case there is no appreciable flow of secondary electrons between the anode and grid, and so the total power input to the anode may be evaluated from a knowledge of the measured currents. The table gives comparative results as calculated from the current readings and from the temperature readings.

V_a (and V_g)	I_a	I_g	D	Anode power, from current readings (W.)	Anode power, from temperature readings (W.)
20	12·35	3·25	22	0·33	0·32
40	22·3	5·15	67	1·06	1·04
60	23·2	5·15	96·5	1·58	1·55
80	23·6	5·2	123	2·07	2·07
90	23·9	5·2	136·5	2·32	2·34
100	23·9	5·2	148	2·55	2·59
110	24·1	5·25	162	2·85	2·86

These results indicate that the maximum error is of the order of 2 per cent except when small deflections are to be measured.

§ 12. THE CHARACTERISTIC OF THE DYNATRON

A set of readings was also obtained in the condition pertaining to a dynatron characteristic, i.e. but V_g' is constant. In this case triode A was used, with V_g' equal to 100 V. The results of this test are plotted in figure 8. Curves (1), (2) and (3) represent respectively, as a function of V_a', the measured anode current, the primary anode current deduced from temperature readings, and the corresponding primary grid current.

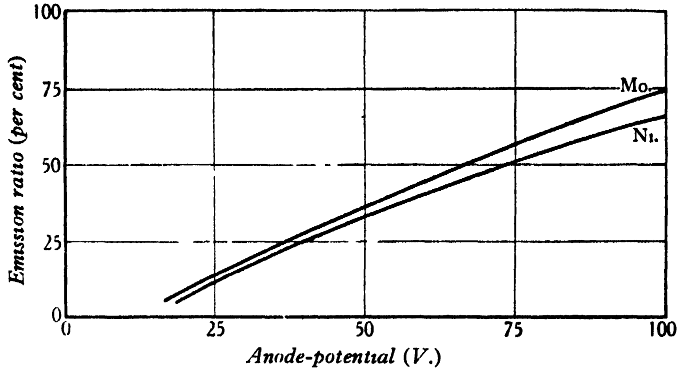

Figure 7. Secondary-emission ratio as a function of anode-potential for valves A and B with nicke and molybdenum anodes respectively

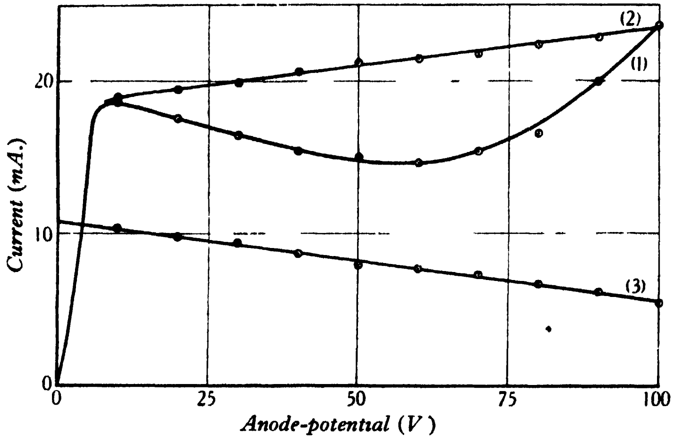

Figure 8. Dynatron characteristic of valve A when $V_g = 100$ V. (1) measured anode current; (2) deduced primary anode current, (3) primary grid current.

The difference between curves (1) and (2) gives the secondary current passing to the grid. In figure 9 the secondary current is plotted as a function of V_a', and in the same figure is a curve, deduced from figure 7 and curve (2) of figure 8, showing the secondary current emitted from the anode. It can be seen that when V_a' exceeds 50 V. some of the secondary electrons are returned to the anode, an effect which had been anticipated (see § 9).

§ 13. SECONDARY EMISSION FROM THE GRID

The theory can be extended to the case where the anode collects secondary electrons emitted by the grid. In this case much greater accuracy of measurement and stability of conditions are required, and no satisfactory readings have yet been taken. In order to obtain results of reasonable accuracy it will be necessary to use a more efficient system for cooling the grid, and so to reduce the factor p without diminishing the ratio of primary grid current to primary anode current.

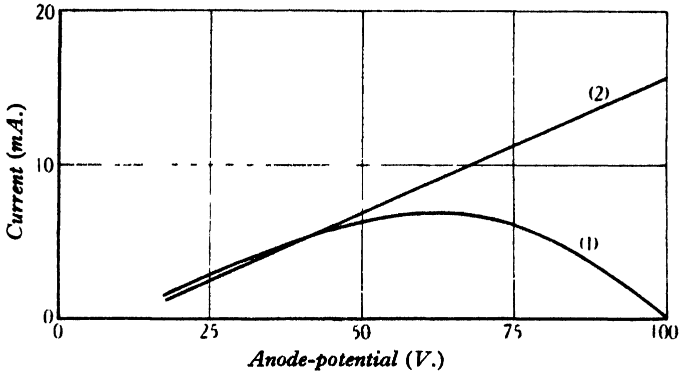

Figure 9. Secondary anode current (1) and secondary anode emission (2) as a function of V_a when $V_g = 100$ V.

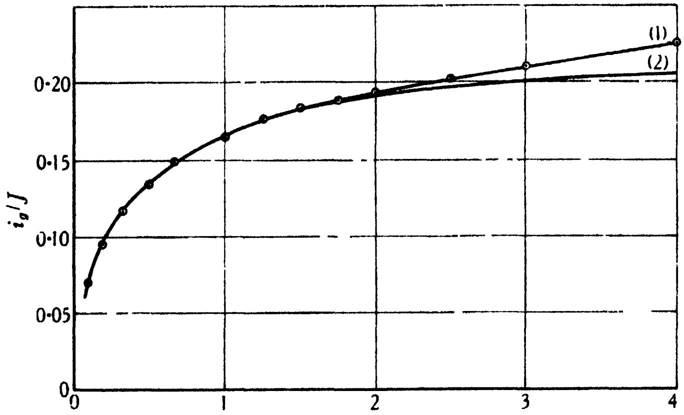

Figure 10. Curve obtained when the anode-potential is insufficient to permit secondary emission: $V_a = 4$ V.

§ 14. MEASUREMENTS IN THE ABSENCE OF SECONDARY CURRENT

A method has been described in the previous sections for examining the distribution of primary current between the anode and grid of a temperature-saturated triode, by making certain assumptions whose validity has been checked experimentally. The problem can be examined by a more direct method if it is assumed that the distribution of primary electrons depends only on the ratio of the potentials applied to the grid and the anode, and not on their absolute values. The results shown in figures 5, 6 etc. justify this assumption.(1) It is also necessary to assume that the emission of secondary electrons from the anode and grid will not affect the distribution of primary electrons.

It is known that, except from specially treated surfaces, secondary emission due to bombardment by electrons having an energy of less than 4 or 5 V. is negligible. If, therefore, the potential of either the grid or the anode is less than 4 or 5 V. there can be no flow of secondary current whatever the value of the other potential. Hence direct measurement of the currents in the grid and anode circuits is sufficient to indicate the distribution of primary current between those electrodes for a given ratio V_g/V_a of applied potentials. If the above assumptions are correct, the primary distribution will be unchanged even though the applied potentials are sufficient to cause the flow of secondary current, provided that they remain in the same ratio.

Hence, for a given triode, curves may be obtained from direct measurements to show the relation between the distribution of primary electrons and the ratio of the applied potentials. The primary distribution may conveniently be expressed as the ratio of primary grid current to total emitted current, i.e. ${}_pI_g/J$. When there is no flow of secondary current, this ratio

$$\frac{{}_pI_g}{J}=\frac{I_g}{J}.$$

Such an investigation must be carried out using very low emission from the cathode, this is necessary in order that temperature saturation may be obtained when the grid- and anode-potentials are both small.

If the cathode is not an equipotential surface a considerable error is introduced, since the potential applied to one of the other electrodes is always small. It was found impracticable to obtain temperature saturation from an indirectly heated oxide-coated cathode when the grid- and anode-potentials were both small. The same effect was observed, to a less degree, with a thoriated tungsten filament. Finally, a plain tungsten filament was used, the mid-point being taken as the zero of potential. In view of the possible error arising from this arrangement, a method, to be described later, was devised for checking experimentally the accuracy of the results. The same means was used to show that no appreciable error is introduced by ignoring the initial velocity of electrons emitted by the cathode.

In the following experimental results the anode-potential was maintained at a constant value of the order of 4 V., while the grid and anode currents were measured for various values of grid-potential. A similar procedure was then followed at a constant grid-potential.

A typical curve obtained in this way is shown in figure 10, curve (1), which relates to the triode A used in the temperature measurements.

In all the triodes examined, the curve was found to follow a relationship of the form

$$\frac{{}_pI_g}{J}=K\sqrt{\frac{V_g}{V_g+aV_a}},$$

within the range

$$0<\frac{V_g}{V_a}<1{\cdot}5 \text{ or } 2.$$

Such an empirical curve is shown at (2) in figure 10. When V_g/V_a exceeds 2 V.

the empirical curve falls below the experimental, since it becomes asymptotic to the line ${}_pI_g/J = K$.

So far it has not been possible to relate the constants K and a with the various dimensions of the triode. However, it has been found that with a given form of grid the ratio ${}_pI_g/J$ is independent of anode-radius when $V_a = V_g$. Thus it appears that $K^2/(1+a)$ is independent of the anode-radius.

No modification has yet been found for the above equation to make it applicable over the complete range $0 < V_g/V_a < \infty$. An approximate theoretical treatment has been attempted, but the differential equations deduced have proved insoluble except by means of tedious numerical approximations.

§ 15. EXPERIMENTAL CHECK

The error due to potential-drop in the cathode and initial energy of emission from it will be negligible if the potentials applied to the anode and grid are much greater than these quantities. The above experiment was therefore repeated with much higher potentials. The resulting curves clearly indicate the existence of a secondary current. Figure 11 shows the results of a test on a certain triode over the range where $V_a > V_g$; for curve (1) the grid-potential was 4 V. and for curves (2) and (3) it was 30 V. and 60 V. respectively. The curves differ according to the existence and magnitude of the secondary current, but all pass through the same point when $V_g/V_a = 1$.

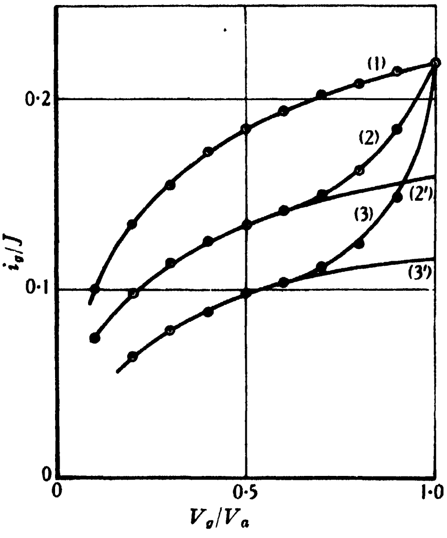

Figure 11. Secondary emission from grid: (1) $V_g=4$ V., (2) $V_g=30$ V., (3) $V_g=6$ V.

As V_g/V_a varies from 0 to 1, a point is reached in curves (2) and (3), where the anode fails to collect all secondary electrons emitted by the grid. This point is indicated approximately by a change in the direction of curvature. If each curve is extrapolated from this point, as shown in the figure, the new curves (2′) and (3′) indicate what the ratio I_g/J would be if all secondary electrons emitted by the grid were collected by the anode. Denote the ordinates of the extrapolated curve, in any particular case, by I_g'/J. Then clearly,

$$\frac{I_g'}{J}=\frac{{}_pI_g}{J}-\frac{I_s'}{J},$$

where I_s' is the maximum secondary current which can possibly be collected from the grid at the relevant potential. At a given potential, I_s'/I_g is a constant whatever the value of I_g, and is equal to the secondary emission ratio q of the surface. Hence

$$\frac{{}_pI_g}{J}=\frac{I_g}{J}\cdot\frac{1}{1-q}.$$

Thus the primary distribution curve can be obtained from the extrapolated curve by increasing the ordinates of the latter in the constant ratio 1 : $(1-q)$. One point on the primary distribution curve is known, namely the point where $V_g/V_a=1$; the corresponding point on the extrapolated curve is also known, and hence the required dividing factor $(1-q)$ can be determined.

If curves (2′) and (3′) are multiplied by their respective factors determined in this way, the resultant curves are sensibly coincident with curve (1). This has been found to apply for a wide range both of applied potentials and of emitted current. This agreement in the results verifies the validity of the assumptions in the previous method.

§ 16. ACKNOWLEDGEMENTS

The work described in this paper was carried out in the Engineering Laboratory, Oxford, and the thanks of the author are due to Mr E. B. Moullin, M.A., for his criticism and advice on many occasions. The author also wishes to express his indebtedness to Messrs Metropolitan-Vickers Electrical Co., Ltd., for the supply of the high-vacuum pumping equipment on which the preliminary experiments were performed, and to Messrs British Thomson-Houston Co., Ltd., who supplied the triodes on which the final measurements were made. The gratitude of the author is also due to Prof. E. V. Appleton, F.R.S., for his advice from time to time.

APPENDIX

Examples showing the relative importance of the corrections for points on curve (3) of figure 5. The correction factor $R_a - 0{\cdot}086$ (for filament-cooling), while $p - 0{\cdot}175$ (for radiation from the grid).

V_a	V_a'	V_g	V_g'	I_a	I_g	J	R_a	R_0*	R_a-R_0	Filament-cooling correction	D	${}_pI_a$	I_s	W_a	${}_pW_g$
13·5	10	24·0	20	7·7	2·9	10·6	752	744·5	7·5	1	8·5	7·9	0·2	0·114	0·016
29·5	25	54·5	50	15·2	7·7	22·9	778	744	34	2	36	16·8	1·6	0·489	0·061
49·5	45	94·5	90	13·4	10·8	24·2	805	741	64	2	66	19·0	5·6	0·917	0·13
69·5	65	134·5	130	10·9	13·5	24·4	829·5	739	90·5	2	92·5	19·1	8·2	1·29	0·22
104·5	100	204·5	200	6·75	18·0	24·75	877	736	141	2	143	19·9	13·15	2·02	0·42

* The change in the zero temperature reading (i.e. when $V_a=V_g=0$) is due to a slight fault in construction of the valve, whereby the connexions between the thermocouple wires and the respective leading-in wires are not quite at the same temperature when power is absorbed by the grid.

REFERENCES

(1) Appleton, E. V. *Thermionic Vacuum Tubes*, p. 50 (Methuen, 1931).
(2) Barber, I. G. *Phys. Rev.*, March 1921, p. 335.

STRUCTURAL CHANGES DURING THE GROWTH OF METAL FILMS

By A. G. QUARRELL, Applied Physical Chemistry Laboratories, Imperial College of Science and Technology

Received 22 *January* 1937. *Read* 26 *February* 1937

ABSTRACT. Electron-diffraction patterns afforded by thin films of face-centred cubic metals prepared by evaporation, electrodeposition, chemical deposition and chemical displacement often show extra rings and bands which may be regarded as typical of the face-centred cubic structure rather than of the metal itself. It is shown that the extra rings are due to the fact that the first deposited layers crystallize in close-packed hexagonal crystals having an axial ratio c/a equal to 1·63, the effective atomic radius being the same as in the normal face-centred cubic form. Further, a gradual transition from close-packed hexagonal to face-centred cubic is postulated, and the prominent band is attributed to the progressive contraction of the (100) hexagonal spacing to the (200) cubic spacing during this transition. Certain very thin evaporated films yield structures intermediate between the hexagonal and cubic modifications, and from this it is inferred that the transition occurs gradually as deposition proceeds, and is not due to an atomic rearrangement occurring when a certain critical film-thickness is reached. These views are supported by the discovery of (i) an electrodeposited silver film consisting solely of close-packed hexagonal crystals, (ii) a similar gold specimen yielding a pattern in which the hexagonal and cubic diffractions are equally pronounced, and (iii) evaporated cobalt films consisting mainly of the hexagonal modification, together with a certain amount of the face-centred cubic form.

§ 1. INTRODUCTION

From time to time electron-diffraction effects have been observed which have not been explicable in terms of normal diffraction by the structure under examination, and the development of electron-diffraction as an established method for the investigation of thin films and surfaces has rendered imperative the elucidation of such diffraction effects.

Finch, Quarrell and Wilman(1) observed extra rings and bands in the transmission patterns afforded by metal films which had been heated in contact with oxygen. It was found that in all cases the spacings were dependent upon the structure of the metal, and that the extra diffractions could be removed by heating the specimen *in vacuo*, or more rapidly by heating in hydrogen. It was therefore suggested that they were caused by an interstitial solution of the gas in the metal lattice; the bands, in particular, being regarded as evidence of a gradual change in lattice-dimensions.

Further, Mark, Motz and Trillat(2) found that traces of grease could yield sharp extra rings whose corresponding spacings were independent of the nature of the metal substrate, but were characteristic of the types of greases likely to be found as adventitious impurities in the laboratory. Such grease-ring systems are therefore easily recognized, as the pattern rings can be divided into those due to the metal and those characteristic of the grease.

More recently it was shown(3, 4) that amalgamation could give rise to extra-ring systems which, unlike the grease rings, had spacings dependent upon the metal and were therefore more easily confused with those due to gas-absorption. Aylmer, Finch and Fordham(5) examined a comprehensive series of amalgamated metal films, but whilst they were able to analyse three of the resulting structures they found that in general the amalgam ring systems were of such complexity as to render their identification uncertain; they therefore emphasized the importance of preparing and examining specimens prone to amalgamation in mercury-free apparatus.

Finally, Finch and Wilman(6, 7) observed extra rings, and also diffractions which were forbidden by normal structure-factor considerations, from thin single crystals and polycrystalline specimens of graphite and molybdenite. They showed that these new.extra diffractions were not due to impurities, but were connected with the thinness of the specimens. They concluded that these extra and forbidden diffractions were due to the fact that whilst the crystals were virtually infinite in the cleavage-plane directions, the number of atom rows in the third dimension was so small that consecutive planes of a parallel group did not contain the same number of lattice points.

During the past two years further search has been made in this laboratory for possible sources of anomalous diffractions other than those outlined above. In addition to these, certain metal films have been found to give rise to sharply defined bands which are characterized by the fact that one head of each band coincides with a ring of the normal metal pattern, whilst the other consists of an extra ring. Such bands and their extra-ring heads cannot be explained on any of the views already discussed. Thus, since the spacings vary from metal to metal, these extra diffractions cannot be due to grease, whilst the possibility of gas-absorption or amalgamation being their true origin is ruled out because bands have been observed in the patterns obtained from specimens which were prepared and examined in the mercury-free high vacuum of a diffraction camera evacuated by oil-diffusion pumps. Nor can these bands be explained in terms of the limited-space-lattice theory put forward for graphite and other layer lattices by Finch and Wilman(6, 7), and we are forced to look for some other explanation. The object of this work was to elucidate this new source of extra diffractions.

§ 2. EXPERIMENTAL DETAILS

The diffraction camera employed was similar in its main design to those previously described(8, 9, 10). In view of the importance of eliminating the possibility of amalgamation of the specimens in the camera, the pumping-equipment consisted in the main of an oil-vapour diffusion pump backed by a two-stage mercury-vapour pump. Prolonged tests with gold-leaf specimens showed that the diffraction chamber was free from mercury.

The filament-heating attachment for preparing metal films by flashing in the evacuated electron-diffraction camera consisted of two long-reach gunmetal sparking-plugs soldered into a brass disc with a standard ground surface, figure 1, the necessary high-vacuum joints being ensured by sealing in the electrodes with picein. Terminals connected to the central electrodes of the plugs received the filament, which was therefore easily replaceable.

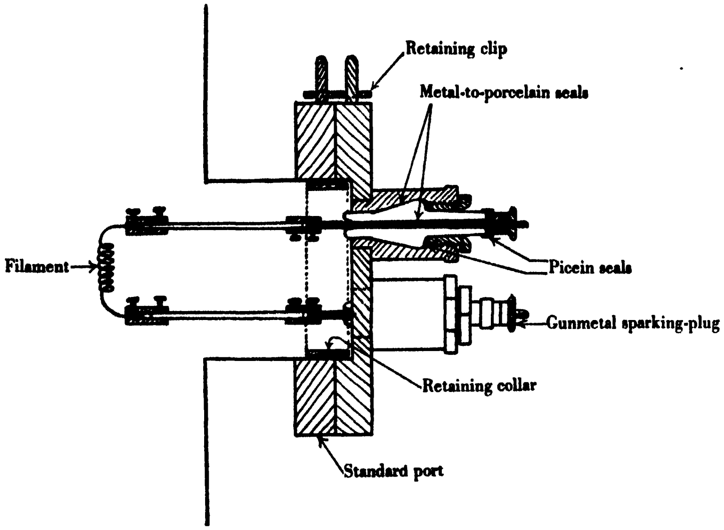

Figure 1. Evaporating assembly.

In view of the importance of avoiding amalgamation, gas-absorption and alloy-formation, specimens were initially prepared by evaporation in the evacuated electron-diffraction camera and the investigation was then extended to films prepared by electrodeposition, chemical displacement and chemical deposition. All transmission specimens were mounted on nickel gauze used as such or thickly electroplated with a deposit of the specimen metal, whilst the filaments used in preparing evaporated films either consisted of the pure metal to be deposited, or else of a tungsten wire so thickly electroplated with the metal that it was still completely coated after flashing. Owing to the slow rate of evaporation employed, the growth of the metal film and the corresponding changes in structure could be followed on the screen. Furthermore, the evaporation could be stopped at any desired stage, and a photographic record made of the diffraction pattern.

§3. RESULTS

Evaporated specimens. Specimens of cobalt, nickel, copper, platinum, palladium, gold and silver evaporated on to cellulosic substrates were examined, and in every case a well-defined band was observed extending from the 200 ring of the normal face-centred cubic structure of the metal to an extra ring just within the 111† diffraction. With nickel, copper, platinum, palladium, gold and silver the effect of gradual deposition of metal atoms by slow evaporation, as observed on the fluorescent screen, was as follows. The cellulose haloes gradually weakened and, just as they were becoming indistinguishable from the general background, a single very broad diffuse ring appeared in approximately the position of the normal 111 and 200 face-centred cubic diffractions. With further deposition this ring appeared to develop into a band on which were superimposed the 111 and 200 rings. Gradually the full face-centred cubic pattern, together with certain extra rings and the band, was built up and the rings became sharper and the background relatively less intense. Patterns recorded at suitable stages during deposition confirmed the visual observations, except that even in the early stages the first broad ring to appear was resolved into two very diffuse and almost overlapping rings. This apparent discrepancy is quite understandable in view of the poor resolving-power of the relatively coarse-grained fluorescent screen compared with that of the photographic plate. Not only was the typical band afforded by specimens which were so thin that they could only be seen in reflected light, but also it was obtained when evaporation had been carried on so long that the electrons could hardly penetrate the resulting thick film.

Cobalt. Whilst behaving in essentially the same manner as the rest of the metals examined, cobalt was peculiar in that the fully developed pattern included diffractions due to both the close-packed hexagonal and face-centred cubic modifications. Kersten(11) has shown by means of X-rays that electrodeposition at low *p*H values gives a deposit consisting of a mixture of the hexagonal and cubic forms, whilst at high *p*H values only the hexagonal β cobalt is deposited. It is our general experience with thin electrodeposited films of cobalt, prepared in a manner already described,(12) that the face-centred cubic structure most frequently occurs. Cobalt is interesting because in the hexagonal form, which is regarded as the stable form at low temperatures, the effective atomic radius is the same as in the face-centred cubic variety. Hence many spacings are common to both hexagonal and cubic structures as is shown in table 1, columns I, II and III, in which the spacings are expressed in terms of a, the side of unit cube of the face-centred cubic modification. The average ratios, d_{hkl}/a, obtained from four patterns, figure 2, of different cobalt specimens, the observed intensities, and the number of plates which afforded each diffraction are given in columns IV, V and VI respectively. It will be seen that the (100) hexagonal spacing coincides exactly with the observed inner band-head. Three rings of spacings 0·707a (M. diff.),* 0·524a (V.F.)* and 0·340a (V.V.F.)* are yet to be explained, but it will be convenient to defer their discussion until later.

The observed intensities would suggest that the orientations are (110) and (001) for the cubic and hexagonal crystals respectively, i.e. the cube-face diagonals and hexagonal major axes fall within a cone of small angle about the normal to the

---

† *Notation.* In accordance with the convention explained by W. H. and W. L. Bragg on page 20 of *The Crystalline State* (Bell, 1933), indices (*hkl*) enclosed in brackets are Millerian indices denoting a plane, while indices *hkl* without brackets are Laue indices defining a diffraction. Thus if $h=nH$, $k=nK$, $l=nL$, *hkl* defines the diffraction of order n from the crystal plane (*HKL*).

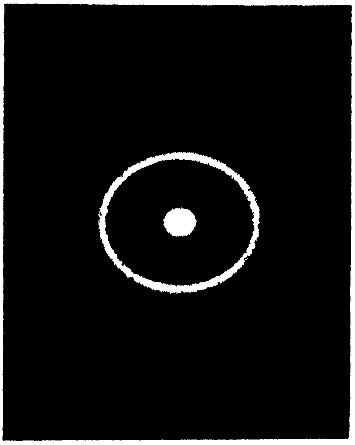

Figure 2. Cobalt evaporated in vacuo.

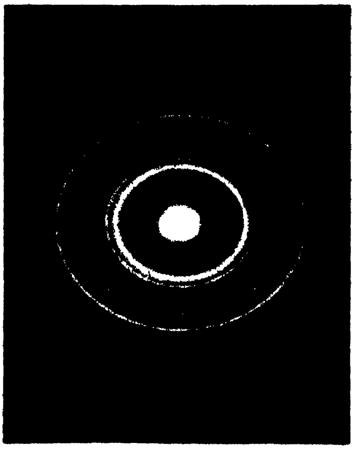

Figure 3. Silver evaporated in vacuo.

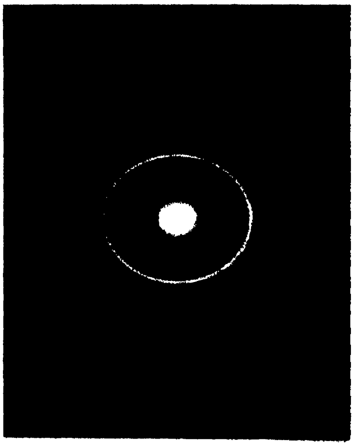

Figure 4. Evaporated copper (Rhombohedral).

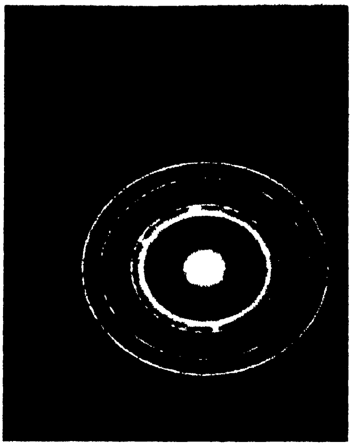

Figure 5. Electrodeposited silver.

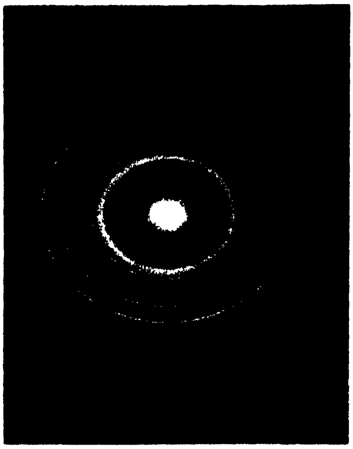

Figure 6. Electrodeposited gold.

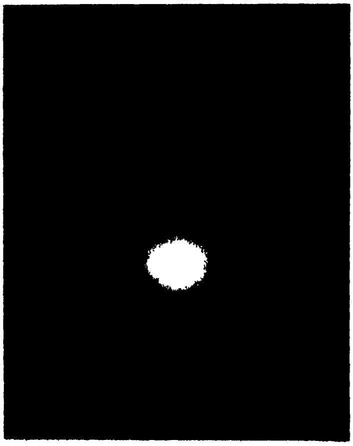

Figure 7. Electrodeposited silver (close-packed hexagonal).

specimen plane. Owing to the superposition of the two patterns it is not possible to arrive at an estimate of the degree of imperfection of these orientations.

Other face-centred cubic metals. The average spacings and intensities for the diffractions observed in typical patterns, figure 3, yielded by three nickel, one copper, one platinum, one palladium, one gold and two silver specimens are given in columns VII and VIII of table 1. For convenience in comparing the results for metals of differing lattice constants, the spacings are expressed as before in terms of the side of unit cube. It will be seen that the patterns consisted of the normal face-centred cubic diffractions together with an extra ring coinciding with the inner band-head, and another between the 200 and 220 face-centred cubic diffractions. The spacings corresponding to these extra rings agree exactly with those of the 100 and 102 diffractions to be expected from a close-packed hexagonal structure of axial ratio c/a equal to 1·63, in which the effective atomic radius is the same as for the normal face-centred cubic metal. The orientation of the face-centred cubic crystals was strongly pronounced (110). With the thinnest films the crystal size was very small, and increased with increasing film-thickness.

Table 1

Diffractions *hkl*		Theoretical d_{hkl}/a	Cobalt			Average values for other face-centred cubic metals	
Close-packed hexagonal $c/a = 1·63$	Face-centred cubic		Mean d_{hkl}/a*	Observed intensity‡	Number of observations	Mean d_{hkl}/a*	Observed intensity‡
—	—	—	0·707	M.	2	—	—
100	—	0·613	[0·613	[M.S. †	4	[0·613	[M. †
002	111	0·577	0·575	V.S.	4	0·577	V.V.S.
101	—	0·541	0·539	S.	4	—	—
—	—	—	0·524	V.F.	1	—	—
—	200	0·500	0·500]	M.]	1	0·500]	M.S.]
102	—	0·420	0·422	F.M.Diff.	4	0·421	M.
110	220	0·353	0·354	S.	4	0·353	S.
—	—	—	0·340	V.V.F.	3	—	—
103	—	0·326	0·322	F.M.Diff.	4	—	—
200	—	0·306	—	—	—	—	—
112	311	0·301	0·302	V.S.	4	0·302	M.S.
201	—	0·296	0·296	V.V.F.	2	—	—
004	222	0·289	0·289	V.V.F.Diff.	1	0·288	M.
202	—	0·270	0·270	V.V.F.Diff.	3	—	—
104	—	0·261	—	—	—	—	—
—	400	0·250	—	—	—	0·249	F.M.
203	—	0·239	0·242	V.V.F.Diff.	4	—	—
120	—	0·231	—	—	—	—	—
—	331	0·229	0·229	M.	1	0·228	M.S.
121	—	0·227	0·226	M.S.	4	—	—
114	420	0·223	0·223	M.	1	0·223	F.M.
105	—	0·216	—	—	—	—	—

* The spacings for cobalt were referred to the most prominent face-centred cubic diffraction, and those for the other metals to the 200 face-centred cubic ring. The maximum divergence of individual values of spacing-ratios from the averages given in this and following tables was ±0·002.

† Square brackets denote the existence of a band.

‡ Throughout this paper the observed intensities are expressed in order of decreasing intensity as follows: V.V.S., V.S., S., M.S., M., F.M., F., V.F., and V.V.F., whilst "Diff." indicates that the diffraction was diffuse.

Whilst the majority of the patterns yielded by evaporated films of face-centred cubic metals afforded the spacing-ratios tabulated in column VII, the patterns from two platinum, one copper, one lead and two nickel specimens were found to correspond to a rhombohedral structure with interaxial angle rather larger than that of the fundamental unit cell of the face-centred cubic lattice. Thus the spacings obtained from the copper pattern, figure 4, differ considerably from those for a face-centred cubic structure, but agree closely with those to be expected from a rhombohedral structure with α equal to 62° 24′, as is shown in table 2. Since the pattern is not face-centred cubic, the spacings are not expressed in terms of the side of unit cube, but as fractions of the spacing corresponding to the first ring. It will be seen that the pattern, figure 4, bears a very marked resemblance to the normal pattern, figure 3, obtained from evaporated films, and includes the characteristic band between what at first sight would appear to be the 200 face-centred cubic ring and an extra ring at a spacing ratio of 1·069. If it be assumed that this inner band-head is due to the 100 hexagonal diffraction as before, then the lattice constants of the rhombohedral structure are $a_r = 2{\cdot}458$ A., $\alpha = 62^\circ\ 24'$, whilst those for the rhombohedral unit cell corresponding to the copper face-centred cubic lattice are $a_r = 2{\cdot}545$ A., $\alpha = 60^\circ$. Referred to hexagonal axes, the corresponding constants are $a_h = 2{\cdot}547$ A., $c/a = 2{\cdot}32$ and $a_h = 2{\cdot}545$ A., $c/a = 2{\cdot}45$, respectively, as compared with $a_h = 2{\cdot}545$ A., $c/a = 1{\cdot}63$ for a truly close-packed hexagonal arrangement of copper atoms. Similar agreement was found with the other rhombohedral structures, the axial ratios being $c/a = 2{\cdot}24$, $2{\cdot}30$ and $2{\cdot}42$, equivalent to interaxial angles $\alpha = 64^\circ$, $62^\circ\ 48'$ and $60^\circ\ 34'$ respectively.

Table 2

Face-centred cubic indices	Theoretical spacing-ratios for face-centred cube	Observed spacing-ratios	Spacing-ratios for rhombohedral structure, $\alpha = 62^\circ\ 24'$	Rhombohedral indices
111	1·000	1·000	1·000	100
200	0·866	0·855	0·855	110
220	0·612	0·590	0·594	213
311	0·522	0·499	0·500	200
222	0·500	0·476	0·476	222

Atmospheric oxidation of evaporated films. The specimens discussed above were exposed to air at normal temperature for about two minutes whilst the photographic plate was being changed, and examined once more immediately afterwards. In general, even with very thin films, no oxide rings were observed in the resulting diffraction patterns. Lead and copper, however, gave two or three very faint oxide rings which were too diffuse to be accurately identified.

Reflection specimens of evaporated silver. Silver was evaporated on to a freshly cleaved rocksalt face which was maintained at room-temperature. The reflection patterns obtained from such specimens invariably consisted of diffuse continuous face-centred cubic rings, and no bands were observed. When the rocksalt was dissolved in water and the silver film mounted as a transmission specimen on thickly silver-plated nickel gauze, however, the resulting pattern consisted of a well-defined face-centred cubic pattern together with the typical band and inner band-head. Although every precaution was taken to prevent contamination of the silver films by mercury whilst they were being removed from the rocksalt, one or two afforded patterns which included typical silver amalgam diffractions as described by Aylmer, Finch and Fordham.(5)

Electrodeposited specimens. Transmission specimens of cobalt, silver, nickel, gold and platinum were prepared by the method described by Finch and Sun.(12)

The patterns afforded by electrodeposited specimens were, in general, similar to those observed with evaporated films except that the electrodeposited cobalt films consisted mainly of the face-centred cubic form. In all cases the patterns exhibited the normal face-centred cubic diffractions of the metal together with the characteristic band and certain other rings which could be attributed as before to a hexagonal modification. The spacing-ratios referred to the side of unit cube agreed well, and were independent of the nature of the metal. The average results obtained from twenty electrodeposited specimens of the above metals are given in table 3.

Table 3

hkl hexagonal	*hkl* face-centred cubic	Theoretical d_{hkl}/a	Observed d_{hkl}/a	Percentage of patterns giving diffraction
100	—	0·613	0·612	100
002	111	0·577	0·576	100
101	—	0·541	0·544	45
—	200	0·500	0·500	100
102	—	0·420	0·421	20
110	220	0·353	0·352	100
103	—	0·326	0·326	10
200	—	0·306	—	—
112	311	0·301	0·301	95
201	—	0·296	0·295	10
004	222	0·289	0·288	100

As will be seen from column V, table 3, not all of the electrodeposited specimens gave rise to all the extra diffractions. Furthermore, in general the extra diffractions were weaker than the true face-centred cubic rings. The orientation of the face-centred cubic crystals was always (110). Occasionally the specimens gave extra rings due to contamination by grease or mercury before insertion in the camera. The available data on such extra diffractions were sufficient to enable them to be identified easily, and they are accordingly omitted from table 3. With most electrodeposited specimens the crystal size was considerably larger than in the corresponding evaporated film; in some cases so much so that the diffraction rings were broken up into spots more or less evenly distributed round the circumference. Whenever the face-centred cubic rings were broken up in this manner, the extra rings included in table 3 also consisted of a series of spots, whilst any extra rings due to grease or mercury were continuous and of uniform circumferential intensity, figure 5. The same type of pattern was observed whether the specimen was mounted on nickel gauze or on nickel gauze thickly plated with the specimen metal.

An abnormal rhombohedral structure could not be assigned to any of the electrodeposited specimens, but two patterns are worthy of special mention in that they did not conform to the general description given above. Thus, in the pattern, figure 6, afforded by an electrolytic gold specimen, all the spacings corresponding to the hexagonal diffractions were present, and were much more intense than usual. Further, one silver specimen yielded a close-packed hexagonal pattern, figure 7, of axial ratio $c/a = 1{\cdot}63$, without face-centred cubic diffractions or band. The analysis of this pattern is given in table 4, and, since the actual spacings are liable to the 2 per cent experimental error involved in the voltage-measurement, the spacing-ratios are also given, referred to the 100 diffraction as 0·613.

Table 4

Diffraction *hkl*	Theoretical spacings for close-packed hexagonal structure $a_h = 2{\cdot}92$ A., $c/a = 1{\cdot}63$	Observed spacings d_{hkl} (A.)	Observed intensity	Observed d_{hkl}/d_{100} ($d_{100} = 0{\cdot}613$)	Theoretical d_{hkl}/d_{100} ($d_{100} = 0{\cdot}613$)
100	2·532	2·557	M.S.	0·613	0·613
002	2·383	2·373	M.S.	0·569	0·577
101	2·235	2·249	M.S.	0·539	0·541
102	1·735	1·751	M.	0·420	0·420
110	1·458	1·482	M.	0·355	0·353
103	1·347	1·355	M.	0·325	0·326
112	1·244	1·254	M.Diff.	0·301	0·301
201	1·223	1·236	M.Diff.	0·296	0·296
202	1·119	1·125	V.V.F.	0·269	0·271
104	1·077	1·080	V.V.F.	0·259	0·261
203	0·987	0·996	V.F.	0·238	0·239
121	0·938	0·948	F.	0·227	0·227
114	0·927	0·928	F.	0·223	0·223
105	0·892	0·894	V.F.	0·214	0·216

Thinned electrolytic specimens. A number of electrodeposited silver specimens, of thickness approaching the penetrating power of the electrons employed, were examined and shown to give the usual face-centred cubic pattern together with the band and extra rings. The specimens were then gradually thinned on a dilute potassium cyanide solution, and examined at various stages. With progressive thinning the band became more and more faint, until finally it could only be detected when viewed against a suitable background. Furthermore, the extra rings, including the inner band-head, virtually disappeared, although the face-centred cubic diffractions were of undiminished intensity.

Chemically deposited silver. A standard silvering solution for the preparation of mirrors(14) was mixed in a porcelain dish. After about 15 min. the surface of the solution became covered with a film of silver sufficiently thick to be picked up on gauze. Three silver specimens prepared in this manner were washed and examined. In each case the pattern consisted of the face-centred cubic diffractions together with a band between the 200 face-centred cubic ring and an extra ring of spacing 0·611*a*, but no other extra diffractions were observed. As with the evaporated and electrodeposited specimens, the orientation of the face-centred cubic crystals was (110), whilst the crystal-size was midway between that observed in evaporated and electrolytic films. The average spacing ratios for the chemically deposited films are given in table 5.

Table 5

hkl hexagonal	*hkl* face-centred cubic	Theoretical d_{hkl}/a	Observed d_{hkl}/a	Observed intensity
100	—	0·613	0·611	M.
002	111	0·577	0·576	V.S.
—	200	0·500	0·500	M.S.
110	220	0·353	0·353	S.
112	311	0·301	0·301	S.
004	222	0·289	0·288	F.

Chemically-displaced silver. A stainless-steel disc was electroplated with cadmium and, after careful washing, immersed in a solution of silver cyanide (36 g./litre). After about one minute the disc was withdrawn from the solution and washed and the composite cadmium-silver film was removed. The cadmium was then dissolved in saturated ammonium-nitrate solution, and the resulting film of chemically displaced silver was mounted as a transmission specimen and examined.

The patterns obtained from the nine specimens prepared in this manner were similar to those afforded by chemically deposited silver films. No extra rings other than the inner band-head were observed, and the normal-pattern rings were true face-centred cubic diffractions, as will be seen from table 6.

Table 6

hkl hexagonal	*hkl* face-centred cubic	Theoretical d_{hkl}/a	Observed d_{hkl}/a	Observed intensity
100	—	0·613	0·610	M
002	111	0·577	0·577	V.S.
—	200	0·500	0·500	S.
110	220	0·353	0·353	S.
112	311	0·301	0·301	V.S.
004	222	0·289	0·289	F.M.

The face-centred cubic crystals were in (110) orientation, and the crystal-size was comparable with that observed in electrodeposited specimens.

§4. DISCUSSION

From the results set forth above it will be seen that the patterns afforded by evaporated, electrodeposited, chemically deposited and chemically displaced face-centred cubic metal films invariably include a typical band extending from the 200 ring to an extra ring just within the 111 diffraction. Further, the spacing corresponding to the inner band-head is always a constant fraction of the side of unit cube, and this fraction is the same for all the face-centred cubic metals examined and independent of specimen thickness and crystal size. Other extra rings have been observed and these, like the inner band-head, may be regarded as characteristic of the face-centred cubic structure, since the spacing-ratios referred to the side of unit cube were the same for all the metals examined. The band and extra rings under discussion were never observed with specimens prepared by thinning beaten leaf, and the effect of thinning electrodeposited specimens was to decrease the intensity of the extra rings and bands. Specimens prepared by evaporation from a filament of the pure metal on to a cellulosic film in the evacuated electron diffraction camera afforded the characteristic band and extra rings. Under such conditions the possibility of contamination by grease or mercury, gas-absorption or alloy formation, is completely eliminated; nor can these extra diffractions be explained in terms of the Finch-Wilman limited-lattice theory because, unlike with graphite and molybdenite, they did not disappear with increasing film-thickness, but could, on the contrary, be eliminated by etching. Again, the results obtained with silver films evaporated on to rocksalt cleavage faces show that with sufficient film thickness the ultimate structure is face-centred cubic yielding no extra rings or bands. Finally, whenever the face-centred cubic rings consisted of a series of spots, the extra rings were broken up in a similar manner. It seems reasonable to suppose, therefore, that these extra diffractions have their origin in some structural abnormalities occurring in the first few atom-layers when a film of a face-centred cubic metal is built up gradually by atomic deposition.

In the case of the evaporated cobalt films, the patterns did not conform to the general description given above, but consisted of a mixture of the diffractions due to the face-centred cubic and close-packed hexagonal modifications(11) of the metal, in which the face-centred cubic rings might justifiably be regarded as extra diffractions. The effective atomic radius is the same in both forms of cobalt, and since a band was observed extending from the 200 face-centred cubic ring to the 100 hexagonal diffraction, the possibility of the other face-centred cubic metals possessing a truly close-packed hexagonal modification was considered.

As will be seen from the tables, all the extra diffractions observed with metals other than cobalt could be quantitatively explained on the supposition that some part of the metal was in the form of close-packed hexagonal crystals in which the atoms retained their normal effective radius. The hypothesis is further strengthened by the discovery of an electrolytic silver specimen which consisted solely of the close-packed hexagonal modification, and an electrodeposited gold specimen which afforded all the hexagonal diffractions in addition to the face-centred cubic rings.

It has already been pointed out by Finch, Quarrell and Wilman(1) that a band may be regarded as evidence of a gradual expansion or contraction of the crystal lattice, and the possibility that the band observed in this work may be due to the transition from a close-packed hexagonal to the face-centred cubic modification immediately suggests itself.

In all cases the face-centred cubic crystals were in approximate (110) orientation, whilst the hexagonal crystals showed a tendency towards (001) orientation. Owing to the fact that many of the hexagonal and cubic rings were superimposed, the degree of imperfection of these orientations could not be estimated, but it will suffice for our purpose if we assume that the orientations were accurately (110) and (001) respectively, and attempt to find some mechanism by which a gradual transition from (001) hexagonal to (110) face-centred cubic can be explained.

Theoretically the normal lattice forces which result in metal atoms taking up positions on a specific crystal lattice only exist between those atoms which are so completely surrounded by other similar atoms, i.e. so remote from the crystal boundaries, as to be unaffected by edge effects. Indeed, in X-ray crystallographic work, which has been so largely responsible for our conception of the crystal lattice, it is usually tacitly assumed that the crystals examined consist of infinite space lattices; the possibility of edge effects being thus precluded. In electron-diffraction, on the other hand, it has long been recognized that the crystals must be limited in the direction of penetration of the electron beam and can no longer be considered as consisting of infinite lattices. In general it is permissible to assume that the lattice has infinite dimensions in directions at right-angles to the beam, and, owing to the cross-grating nature of the observed diffractions, this results in the method affording the same lattice constants as X-rays for a given substance. Recently, however, Finch and Wilman(6, 7) have shown that the effect of lattice-limitation in the direction of the beam sometimes not only is such as to cause the relaxation of the third Laue condition which results in cross-grating diffraction, but may even give rise to new and forbidden diffractions. Whilst they had no reason for believing that the atoms near the crystal boundaries were taking up abnormal positions, nevertheless their results showed that the possibility of edge effects cannot be ignored in electron-diffraction.

When a metal is deposited atom by atom, as in the experiments described above, it is hardly likely that the normal lattice forces will at once come into play. Thus it is to be expected that in the first place, at least locally, a single layer of atoms will be formed, and the interatomic forces will cause the atoms in this first layer to take up relative positions of maximum stability. In a two-dimensional lattice this will clearly result in the atoms being placed at the corners of equilateral triangles whose sides are equal to the atomic diameter. Similarly one might expect the next layer of atoms to be formed in such a manner that each atom is resting in the hollow between three adjacent atoms in the first layer. If now the third layer of atoms is deposited so that each atom is touching three atoms in the second layer and is immediately above an atom in the first layer, figure 8*a*, then the film will consist of a number of coplanar unit cells of a close-packed hexagonal lattice. If, however, the atoms of the third layer take up positions in which they are immediately above a gap between three atoms in the first layer, whilst still touching three atoms in the second layer, figure 8*b*, then the structure will be rhombohedral with interaxial angle α equal to 60°, i.e. face-centred cubic. Thus the structure is close-packed hexagonal in (001) orientation, or face-centred cubic in (111) orientation, according to the positions adopted by every third layer of atoms, and it may well be that in a very thin film the resultant forces between the atoms favour the formation of a hexagonal structure.

The intensities of the hexagonal pattern varied considerably from specimen to specimen. Thus the chemically deposited silver specimens afforded only the 100 hexagonal ring in addition to the normal face-centred cubic pattern, whilst one electrodeposited silver specimen yielded the full hexagonal pattern without face-centred cubic rings. Hence it would seem that the thickness of the hexagonal layer is determined to some extent by the conditions of preparation of the specimen. The results do not enable the thickness for which the hexagonal structure persists in any specimen to be deduced, but it is clear that as the film-thickness increases, and conditions more nearly resemble those in the infinite space lattice, the structure tends towards the normal face-centred cubic in (110) orientation. In an attempt to explain the transition from the hexagonal to face-centred cubic modifications, it will be assumed that the atoms behave as solid spheres of definite radius. This assumption would appear to be justified by the fact that the experimental spacings of the extra rings can be quantitatively explained if the metal atoms in the first layers of an atomically deposited film crystallize in a close-packed hexagonal form in which the normal effective atomic radius observed in the face-centred cubic crystals is preserved.

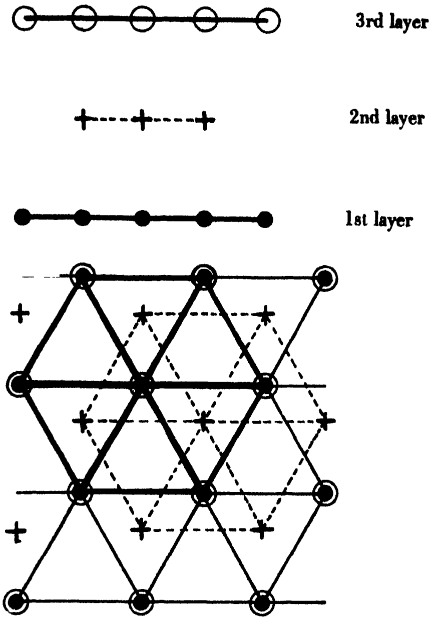

Figure 8*a*. (001) close-packed hexagonal.

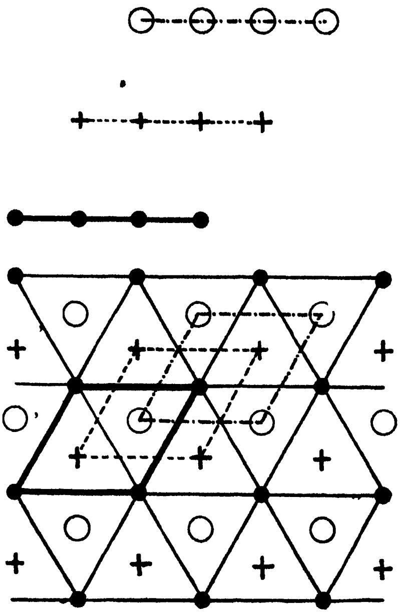

Figure 8*b*. (111) face-centred cubic.

The atomic arrangements in (001) hexagonal and (110) face-centred cubic crystals are shown in figures 9*a* and 9*b*, respectively. Consider the rectangles *ABCDEF* of figure 9*a* and *RSTUVW* of figure 9*b*. It will be seen that whilst

$AC=RV$, $AF>RS$, and furthermore the atoms G and H are coplanar with the atoms $ABCDEF$, whereas in the face-centred cubic form the atoms Y and Z are above the plane $RSTUVW$ by an amount $0{\cdot}353a$. Suppose, therefore, that as the specimen becomes thicker, the hexagonal network puckers in such a manner that, whilst A, B, C, D, E and F remain in the same plane, the atoms of type G and H are lifted out of that plane, thus allowing the atom-row ABC to approach FED. When $AF=RS=a$, the atoms G and H will be in relatively the same positions as Y and Z of figure 9*b*, and the atomic arrangement will be face-centred cubic in (110) orientation. Further, the effective spacing for the planes parallel to ABC was initially such that $AF/2=0{\cdot}613a$, i.e. it was the hexagonal (100) spacing, and this changed during the transition to an effective spacing $a/2$, corresponding to the 200 face-centred cubic diffraction. Thus, if the transition be assumed to take place gradually, extending over a number of atomic layers, a band will be swept out containing all possible spacings within the range $0{\cdot}613a$ to $0{\cdot}500a$.

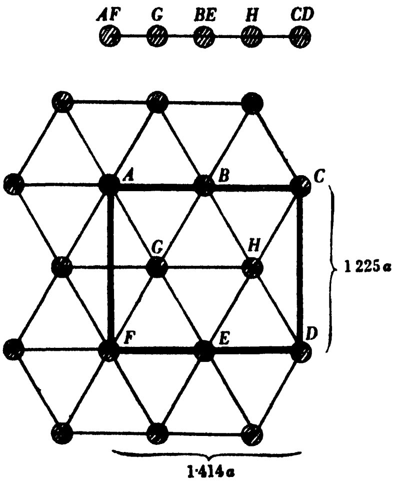

Figure 9*a*. Basal plane of hexagonal lattice.

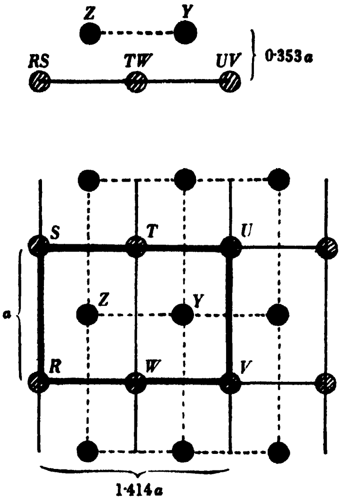

Figure 9*b*. (110) plane of face-centred cubic lattice.

At first sight it might be supposed that if this were the true mechanism entailed in the transition from the hexagonal to the face-centred cubic form, more bands would be observed extending from face-centred cubic rings to the corresponding hexagonal diffraction. Reference to figure 9*a*, however, will show that the (100) hexagonal planes are the only ones which become planes of the face-centred cubic lattice merely by moving closer together, and these are the only conditions under which a band is to be expected. In addition to the very prominent band which is satisfactorily explained by the above theory, a very much weaker band approximately situated between the 400 and 311 cubic rings was observed. The intensity of this band was such that accurate measurements of its limits were not possible, and accordingly its presence has not been noted in the tables. It seems probable, however, that this band is the second order of the one discussed above.

The fundamental unit cell of the face-centred cubic lattice is a rhombohedron with interaxial angle α equal to 60°, and any rhombohedral lattice may be conveniently referred to hexagonal axes. Thus the transition from close-packed hexagonal to face-centred cubic may be regarded, as far as spacing ratios are concerned, as a change in the axial ratio c/a from 1·63 to 2·45, the value of a_h remaining unchanged. A number of specimens were found to give spacings which were definitely not those of a face-centred cubic lattice, but could be fitted to the Hull and Davey(13) chart for a rhombohedral lattice, referred to hexagonal axes, at axial ratios between 2·24 and 2·42. These specimens were exceedingly thin films of the metal evaporated on to the cellulosic substrates in the evacuated electron diffraction camera, and in each case the plate was exposed as soon as the pattern observed on the fluorescent screen appeared to be of the normal face-centred cubic type.

Now, when an electron beam falls upon a crystal sufficiently thin to transmit electrons without giving rise to Kikuchi lines, the first cross-grating encountered by the beam is most effective in causing diffraction. Hence if a transition from one lattice to another occurs within the crystal, those diffractions will be most prominent which correspond to the structure in the layers nearest the electron source, and the stronger rhombohedral patterns observed must therefore be regarded as due to the layers last deposited. In effect, therefore, the rhombohedral structures show the stage in the transition which had been reached when the evaporation ceased. It is rather surprising at first sight that the intermediate structures should be at all stable, yet the rhombohedral copper specimen analysed in table 2 still gave a rhombohedral pattern of axial ratio c/a equal to 2·32, when it had been exposed to air and slightly oxidized as shown by the presence of an additional diffuse ring in approximately the position of the 111 Cu_2O diffraction.

The rhombohedral structures observed enable the conclusion to be drawn that the transition from hexagonal to cubic structure occurs gradually as deposition proceeds, and that the band is not the result of an atomic rearrangement after the metal film has reached a certain critical thickness.

Such intermediate structures were not observed with specimens prepared by any method other than evaporation, but this is easily understood, since the evaporated films were so thin that they could not have been handled had they not been supported on cellulose.

The source of those rings observed in the patterns afforded by certain cobalt specimens, which could not be explained in terms of the hexagonal and cubic diffractions, has not yet been satisfactorily determined. The fact that the strongest of these rings corresponded exactly to the 110 face-centred cubic spacing, however, suggests that perhaps the Finch-Wilman effect is coming into play in those layers which are approximating to the face-centred cubic structure, and allowing forbidden and other extra diffractions to occur.

§5. CONCLUSION

The application of electron-diffraction to the study of surfaces has made it clear that the structure of a thin film may be different from that of the material in bulk. Thus, in the phenomenon of basal-plane pseudomorphism(15), it was found, for example, that the first few layers of aluminium evaporated in vacuo on to a platinum substrate had face-centred tetragonal lattice, whilst thicker films adopted the normal face-centred cubic structure. Similarly, Aylmer, Finch and Fordham(5) found that the structure of amalgam films depends upon film-thickness. In the present work it has been shown that an abnormal structure exists in the first deposited layers of all the face-centred cubic metals examined, and for each of the methods of atomic deposition employed. Even with cobalt, the tendency to change from hexagonal to cubic structure with increasing film thickness was marked, although one would hardly expect it since the hexagonal modification is usually regarded as the stable form at low temperatures. It seems likely, therefore, that abnormal structures will be found in sufficiently thin films of all face-centred cubic metals prepared by atomic deposition.

In view of these facts, the assumption that thin films possess the structure of the bulk metal can no longer be made, and it may well be that many of the properties peculiar to thin films have their origin in the abnormal structures occurring in the first few deposited layers.

§6. ACKNOWLEDGMENTS

I wish to thank Prof. G. I. Finch for his unfailing help and interest in this work, and for the valuable advice he has given me. I also wish to thank the Department of Scientific and Industrial Research for a grant which enabled me to devote my whole time to this research.

REFERENCES

(1) Finch, Quarrell and Wilman, *Trans. Faraday Soc.* **31**, 1085 (1935).
(2) Mark, Motz and Trillat. *Naturwissenschaften*, **20**, 319 (1935).
(3) Finch and Quarrell. *Nature*, Lond., **136**, 720 (1935).
(4) Preston and Bircumshaw. *Phil. Mag.* **21**, 713 (1936).
(5) Aylmer, Finch and Fordham. *Trans. Faraday Soc.* **32**, 864 (1936).
(6) Finch and Wilman. *Proc. roy. Soc.* A, **155**, 345 (1936).
(7) Finch and Wilman. *Trans. Faraday Soc.* **32**, 1539 (1936).
(8) Finch and Quarrell. *Proc. phys. Soc.* **46**, 148 (1934).
(9) Finch, Quarrell and Wilman. *Trans. Faraday Soc.* **31**, 1065 (1935).
(10) Finch and Fordham. *Proc. phys. Soc.* **48**, 85 (1936).
(11) Kersten. *Physics*, **2**, 274 (1932).
(12) Finch and Sun. *Trans. Faraday Soc.* **32**, 852 (1936).
(13) Hull and Davey. *Phys. Rev.* **17**, 549 (1921).
(14) Watson. *A Text-book of Practical Physics*, p. 598 (Longmans, Green and Co., Ltd., 1926).
(15) Finch and Quarrell. *Proc. roy. Soc.* A, **141**, 398 (1933).

INTENSITIES OF X-RAY REFLECTIONS FROM SINGLE CRYSTALS OF SODIUM BETWEEN 120 AND 370° K.

BY RALPH H. V. M. DAWTON, B.SC., Davy Faraday Laboratory of The Royal Institution, London

Received 23 *December* 1936. *Read* 26 *February* 1937

ABSTRACT. Single crystals of sodium are examined by X rays in a temperature range of 120—370° K. Strong hysteresis in the reflecting-power is observed, but this vanishes when the crystals are chilled with liquid air. The normal temperature effect is measured with the chilled crystals and the characteristic temperature is calculated from the Debye-Waller formula.

§ 1. INTRODUCTION

THE object of this paper is the study, with the aid of X rays, of the changes in structure of single crystals of sodium subjected to heating and cooling over a wide range of temperatures, including a close approach to the melting point. The work was suggested by Dr A. Müller.

§ 2. EXPERIMENTAL DETAILS

The X-ray plant and the recording apparatus are described in a previous paper.(1) The characteristic radiation of molybdenum filtered by zirconium is used. The electric heater required for the heating of the crystal above room-temperature is shown in figure 1. It consists of a copper tube with apertures to let the incident and reflected beams pass through. The heating-coil is wound on the outside of this tube. 10 ft. of $\frac{3}{32}$-in. copper pipe are soldered to the inside wall and air is passed through this spiral to ensure thermal equilibrium. The liquid-air cooler is shown in figure 2. *A* is a solid copper rod, which has a $\frac{1}{4}$-in. hole bored longitudinally as shown. The incident and reflected beams pass through *B* and *C* respectively. Thermocouples *D* and *E* can be kept steady to within 3°. The temperature variations are within $\frac{1}{2}$° during an X-ray measurement. At the lowest temperature *D* is 115° K., *E* is 121° K., and the crystal is taken to be at 117° K.

Two methods of mounting the crystals are used: (1) A glass tube is mounted as shown in figure 3*a*. Soda glass is used because it does not react with the sodium. A test tube, figure 3*b*, contains sodium under oil, and is fitted with an exhausting-tube and a sliding rod *A*, to which the glass tube is attached. The procedure is to evacuate the test tube and melt the sodium. Rod *A* is lowered until the open end of the small tube is in the sodium, and air is admitted into the test tube until sufficient

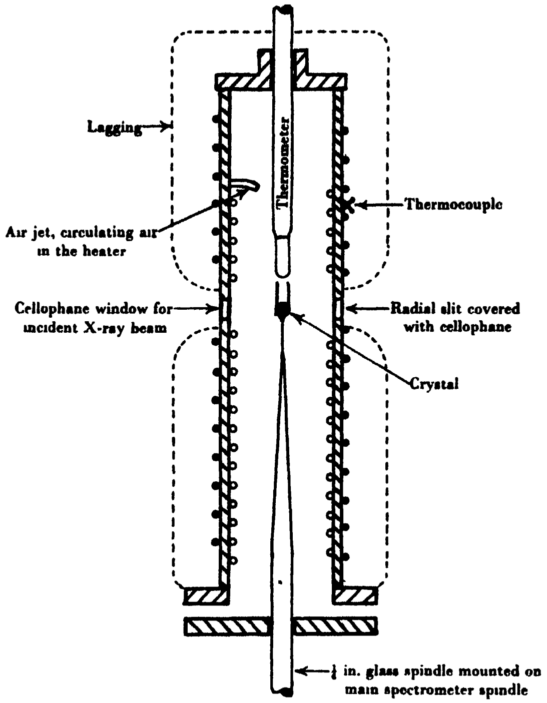
Lagging
Thermometer
Air jet, circulating air in the heater
Thermocouple
Cellophane window for incident X-ray beam
Radial slit covered with cellophane
Crystal
¼ in. glass spindle mounted on main spectrometer spindle

Figure 1.

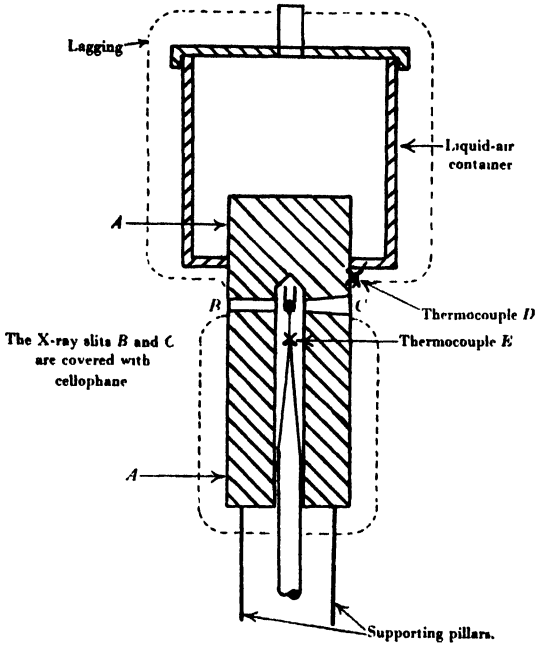

Figure 2.

sodium has entered the small tube. The tube is then lifted until its open end is in the oil, tap T is opened and the apparatus is cooled. With rare exceptions the sodium solidifies in form of a single crystal. (2) Molten sodium in an evacuated flask is broken, by shaking, into small spheres which give single crystals. The crystals are mounted by being placed in one of the small tubes.

By trial and error the axes of the crystal are found on the X-ray spectrometer, the platinum wire being bent for adjustment, figure 3*c*. For liquid-air work the lower end of the platinum wire is spot-welded to the thermocouple E, figure 2.

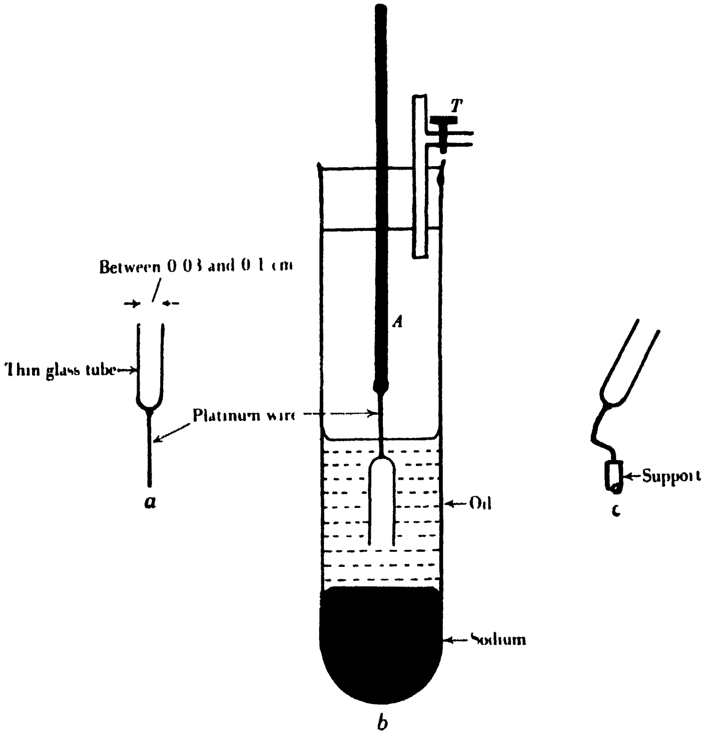

Figure 3.

When the crystal is formed from the molten sodium the rate of cooling affects the intensities of the low-order planes and the magnitude of the non-reversible effect. If the cooling to room-temperature extends over 30 hours it is found that the intensities of the 110 and 310 reflections are only $\frac{1}{6}$ and $\frac{3}{4}$ of the values observed after rapid cooling. If the crystal is chilled with liquid air and the X rays are measured again at room temperature a further increase is found, table 1. The increase in the intensity of a plane is accompanied by an equally marked decrease in the magnitude of the non-reversible effect. No amount of heating and cooling of the crystal can now make it return to its original state. The increases of intensity seem to be permanent.

Reflections of lower order than the 400 show a strong hysteresis which makes a determination of the reversible temperature effect impossible unless a crystal is chilled with liquid air. The high-order reflections, having little or no hysteresis enable a reversible temperature effect for the 330, 400 and 440 reflections to be found without liquid-air treatment. The results are not altered if the crystal is treated.

Table 1

Indices	Intensity at room-temperature before chilling. Crystal formed and cooled during 2 hours to 20° C.	Intensity at room-temperature after chilling with an air blast 80° below crystal-temperature	Intensity at room-temperature after liquid-air chilling
110	500	3600	4100
200	270	1200	1450
220	140	260	300
310	90	144	150
400	23	23	23

Measurements on the 330 reflection are difficult, because overlapping of 110 and 220 reflections due to wave-lengths other than that of the characteristic target radiation occurs. In general this reflection is not measured. Its temperature effect is about 2 per cent greater than that of the 400.

The general accuracy for work above room-temperature may be judged from table 2, where

$$\frac{\text{Change of intensity over the range } 292\text{–}370^\circ\text{ K.}}{\text{Intensity at } 292^\circ\text{ K.}}$$

is given for various crystals. The variations are caused by variations between individual crystals; the errors of observation are smaller. With crystals of moderate size the 440 reflection is so feeble that it can only be measured below 150° K.

Table 2

Reflection 110		Reflection 200	Reflection 220	Reflection 310	Reflection 400
0·168	0·104	0·294	0·432	0·545	0·712
0·130	0·130	0·287	0·431	0·570	0·707
0·128	0·100	0·266	0·485	0·597	0·738
0·155	0·122	—	0·474	0·510	0·743
0·110	0·143	—	0·415	—	0·723
0·130	—	—	—	—	—
Mean 0·129		—	—	—	—

The discrepancies of the reversible temperature effect below room-temperature, as observed with individual crystals, are much less than those above room-temperature. The 440 reflections give values agreeing within the experimental error of 7 per cent. The 400, 310 and 220 reflections gave values agreeing within the experimental error of 4, 4, 5 per cent respectively. If the 200 and 110 reflections disagree by more than 10 per cent a hysteresis loop is present.

Ordinary commercial sodium and a special supply from Kahlbaum give the same result.

§ 3. RESULTS

Hysteresis. Hysteresis occurs above and below room-temperature, but detailed measurements have been made only above room-temperature. When the temperature is raised to 370° K., the 110 intensity sometimes decreases 60 per cent or increases 20 per cent according to the crystal. Increases of intensity are rare. Big changes of the 110 require $\frac{3}{4}$ hour before being within 10 per cent of the apparent steady value obtained after 3 hours heating, figure 4. Higher-order planes have less hysteresis even though the intensity changes are greater. The hysteresis observed with the 310 reflection is about $\frac{1}{5}$ of that observed with the 110 reflection. The intensity when the crystal is cooled to room-temperature depends on the rate of cooling, figure 5.

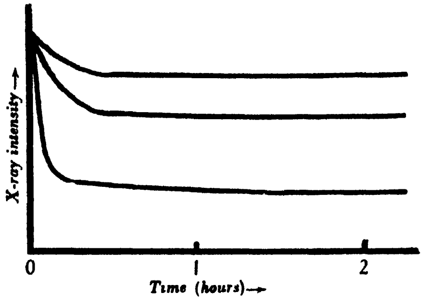

Figure 4. Curves showing 110 intensity for 3 crystals maintained at 370° K. for 2½ hours.

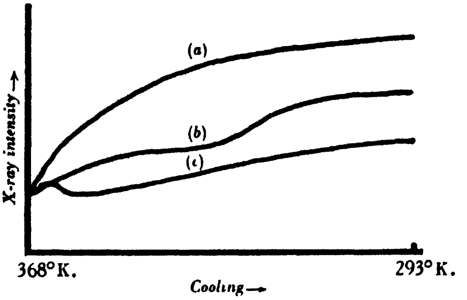

Figure 5. Curves showing, for the same crystal, 110 reflection-intensities during cooling from 368° K. The crystal was cooled (*a*) in 8 minutes; (*b*) in 20 minutes; (*c*) in 50 minutes.

Vibrations seem to change the microstructure of the crystals, particularly at high temperatures. If for instance a crystal is set in vibration by tapping the spectrometer spindle, the intensity measurements before and after the tapping may differ by 30 or even 50 per cent. The effect may be an increase or a decrease, and is sometimes found even at room-temperature. These changes are not in any way connected with accidental mis-settings of the crystal on its support. The intensities are also sensitive to sudden changes of temperature, the effect being larger as the melting point is approached, although no great increase in the effect occurs over the last 10° C. Within this range about one half of the crystals will give a sudden 30 per cent change (almost a jerk on the galvanometer) in the 110 intensity if the temperature, as measured by the thermocouple, changes by 1° C. in a few seconds.

Figures 6α and 6β give the 110 and 310 X-ray intensities as the temperature is increased uniformly and then decreased at the same uniform rate. The pairs β, *b* and γ, *c* give the same for two exceptional crystals. None of these crystals are treated with liquid air. It is found that (1) the size of the loop does not seem to depend on the rate of performing the cycle, which varied between 4 and $\frac{4}{9}$° C./min.; (2) generally the curves cross; (3) the dimensions of the crystal do not seem important; (4) crystals mounted by method (1) are not free in the containing tube, but crystals mounted by method (2) are free; in each case hysteresis is present and hence any restriction which the containing tube has on the crystal does not affect the X-ray intensities.

The reversible temperature effect. Except for occasional observations on the 400 and 440 reflections of untreated specimens, the measurements are made on crystals which have been chilled with liquid air. If the crystals are examined, before and

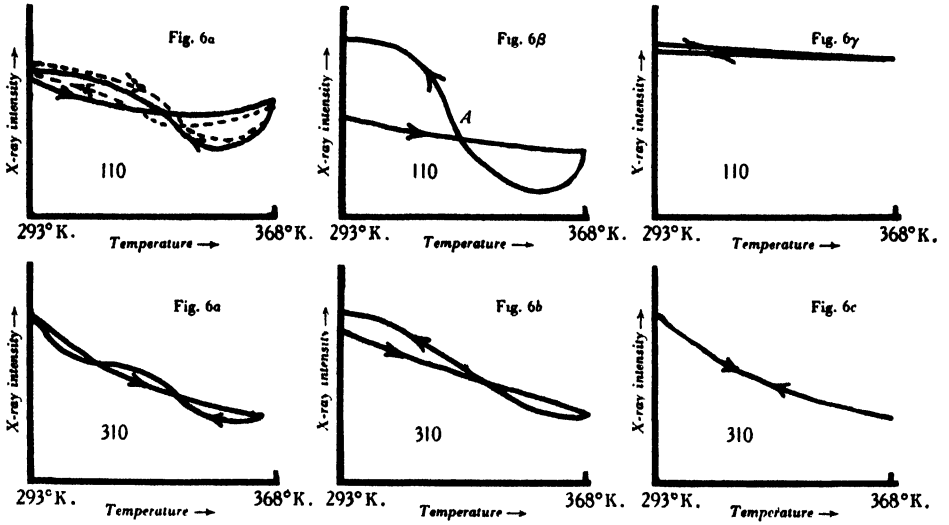

Figure 6. Hysteresis cycles for 3 crystals. The dotted curve of figure 6α is what might be expected if the cycle is repeated. The hysteresis after a large number of repeats is of the same magnitude.

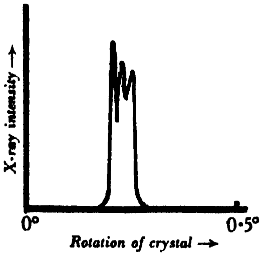

Figure 7*a*. Before chilling.

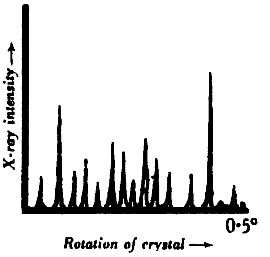

Figure 7*b*. After chilling.

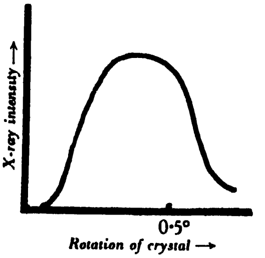

Figure 8.

after this treatment, in monochromatic radiation of divergence less than $\frac{1}{60}°$, it appears, figures 7*a* and 7*b*, that the crystal splits into small units. Figure 8 shows the crystal of figure 7*b* taken in the more divergent molybdenum characteristic radiation direct from the target. The intensities measured are representable by

$$I_T \propto e^{-(0{\cdot}04044T+17{\cdot}08\,.\,10^{-6}T^2)\sin^2\theta},$$

where I_T is the observed intensity at temperature T° K. and 2θ is the angle between incident and reflected beams. In the experiments T ranged from 117 to 368° K.

An indication of the accuracy of the formula is given, for three different temperature ranges, by table 3. The changes of intensity do not seem to be caused by changes in (1) linear absorption of the X-ray beam, (2) the sodium lattice spacing, (3) primary extinction, or (4) secondary extinction, because no change in (1) greater than the experimental error of 3 per cent occurred; the value of (2) given by 2θ does not change more than 1·5 per cent, the limit of error for measurements made in the filtered white X-ray radiation; changes in (3) and (4) affect the strong reflections more than the weak reflections, making it improbable that the experimental temperature factor varies as $\sin^2\theta$.

Table 3

Reflection	Temperature range 117 to 180° K.		Temperature range 117 to 291° K.		Temperature range 117 to 368° K.	
	I_{117}/I_{180}		I_{117}/I_{291}		I_{117}/I_{368}	
	Calculated	Observed	Calculated	Observed	Calculated	Observed
440	3·50	3·26	15·1	Too feeble	81·0	Too feeble
400	1·92	1·96	8·9	8·8	34·6	30·4
310	1·48	1·50	3·7	4·0	8·2	8·3
220	1·37	1·34	2·8	2·9	5·3	5·3
220	1·17	1·23	1·7	2·0	2·3	2·5
110	1·08	1·13	1·3	1·7	1·5	1·9

It is assumed that the reversible temperature effect found is given by the thermal motion of the atoms. On this assumption the characteristic temperature is calculated by using the Debye-Waller temperature factor e^{-M}, where $F_T^2=F_0^2e^{-2M}$ and

$$M=\frac{6h^2}{m_a k\Theta}\left\{\frac{\Phi(x)}{x}+\frac{1}{4}\right\}\frac{\sin^2\theta}{\lambda^2},$$

while Θ is the characteristic temperature, 2θ the angle between incident and reflected beams, λ the wave-length of the X rays, h is Planck's constant, k is Boltzmann's constant, m_a is the mean mass of the atom or vibrating systems in the crystal, $x=\Theta/T$ where T is the absolute temperature, and

$$\Phi(x)=\frac{1}{x}\int_0^x\frac{\xi}{e^{\xi}-1}.d\xi.$$

It is shown, at the end of this paper, that the crystals are nearly of the mosaic type, and hence F_T^2 is not far from being proportional to the reflecting-power of the crystal at $T°$. The value of Θ is calculated as a mean over a range of 20° C. The 310, 400 and 440 reflections are used for this calculation since the agreement from crystal to crystal for these reflections is much better than for the reflections of lower order. Figure 9 gives the results together with the values of Θ determined by other methods. The dotted curves give the experimental error.

The f_0 curve, or atomic-scattering curve, is calculated by using the Debye-Waller formula to extrapolate the X-ray intensities measured at 117° K. Some assumptions as to the value of Θ must be made. Throughout the range of extrapolation an average value is used. Since it is not perfectly legitimate to base this average value on the values of Θ determined by methods other than X-ray data, it was decided to use figure 9. This gives an average X-ray value: $\Theta = 130 \rightarrow 141$, in the range $T = 0 \rightarrow 120°$ K. The f_0 curves calculated for each of these extreme limits are compared with the theoretical Hartree curve in figure 10*a*, in which no zero-point energy is assumed and in figure 10*b* in which zero-point energy *is* assumed. The

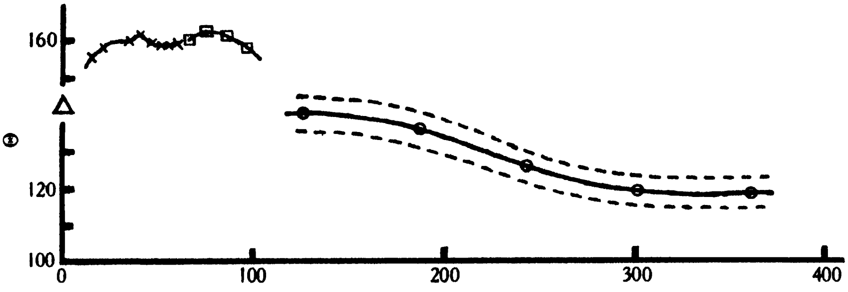

Temperature (° K.)

Figure 9. ○ Author's X-ray points; □ specific-heat points; × results by Fuchs⁽⁴⁾; △ results by Fuchs⁽⁵⁾.

experimental points given by the smaller values of sin θ/λ (i.e. the strong planes) fall below the theoretical curve. This can be caused by (1) primary extinction, (2) secondary extinction, and (3) the crystal not being a perfect mosaic. All three of these affect the strong planes more than the weak planes, and further all three, except possibly (1), which occurs within very small internal blocks of the crystal, are affected by the chilling. Since chilling gives no increase in the 400 intensity, it is believed that the f_0 value of the 400, and consequently the higher-ordered 440 reflection, has no important extinction. (1) and (3) give an extinction error which is independent of the size of the crystal, unless this is extremely small, and can only be eliminated by having the crystal in powder form. The breaking up of the crystal by liquid air is an approach to this state. (2) depends on the size of the crystal, and is investigated by taking some small crystals (about $\frac{1}{5}$ the size of those used for determining the f_0 curves) and disintegrating them as far as possible with liquid air. The average ratios of the intensities given by these crystals are given in table 4, column 1. One crystal gave the values given in column 2. Column 3 gives

Table 4

Reflection	Intensities, proportional to F^2		
	Column 1	Column 2	Column 3
110	204·0	218·0	162·0
200	78·0	81·0	65·0
220	15·7	16·5	14·5
310	7·6	7·8	7·2
400	1·0	1·0	1·0
440	Too feeble	Too feeble	Too feeble

the average values for the crystals used for determining the f_0 curves. It is evident that these crystals show extinction. Figures 11*a* and 11*b* show the curves of figures

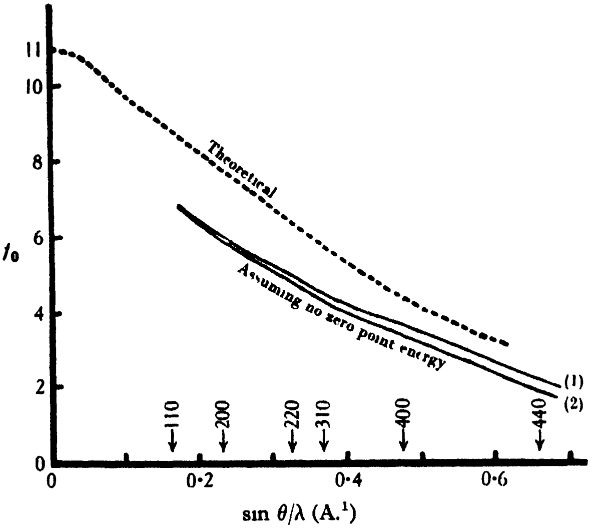

Figure 10*a*. Curve (1), Θ between 0 and 117° K. taken as 130.
Curve (2), Θ between 0 and 117° K. taken as 141.

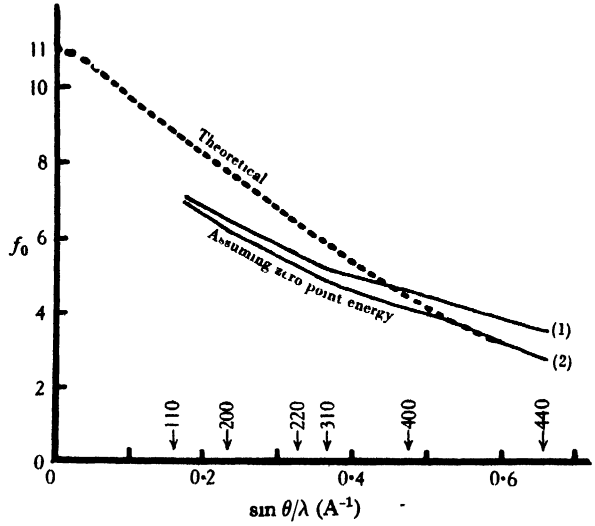

Figure 10*b*. Curve (1), Θ between 0 and 117° K taken as 130.
Curve (2), Θ between 0 and 117° K. taken as 141.

10*a* and 10*b* corrected for the extinction indicated by columns 1 and 3 of table 4. On the assumption that the crystal is mosaic we should correct for extinction by using columns 2 and 3, because the mosaic crystal reflects the maximum possible.

If the results are based on the one crystal giving column 2, the chain curve shown in figures 11*a* and 11*b* results.

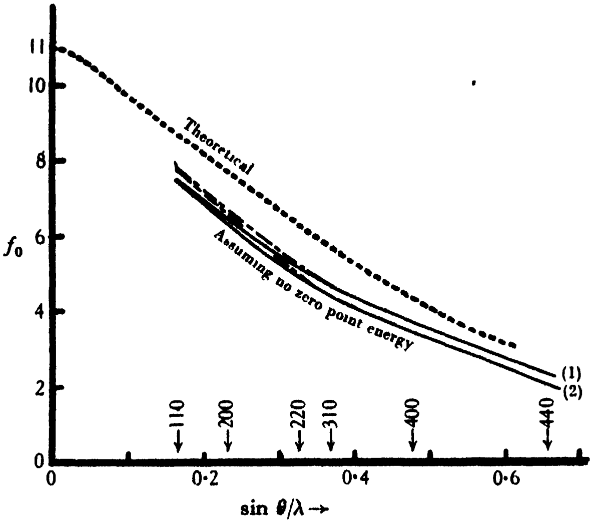

Figure 11*a*. Curve (1), Θ between 0 and 117° K. taken as 130.
Curve (2), Θ between 0 and 117° K. taken as 141.

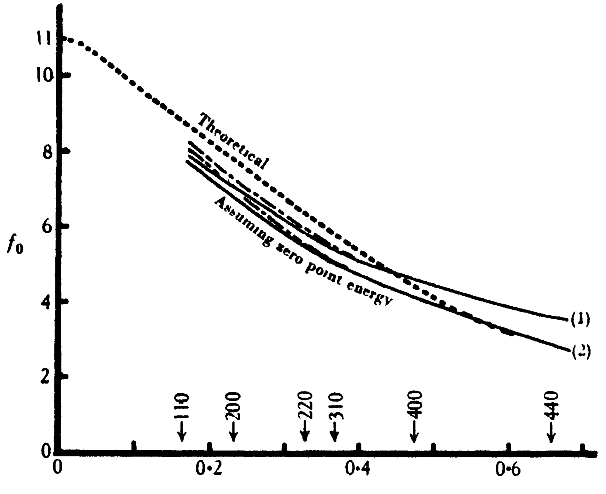

Figure 11*b*. Curve (1), Θ between 0 and 117° K. taken as 130.
Curve (2), Θ between 0 and 117° K. taken as 141.

§ 4. THE ABSOLUTE SCATTERING-POWER OF THE CRYSTALS

The absolute scale of figures 10 and 11 is obtained by determining the scattering-power of the crystal at room-temperature and applying the temperature factor as already explained. Only the more important details of the measurement are given. The error caused by unwanted radiation in the nearly monochromatic

X-ray beam is determined as described in a previous paper.(2) Corrections for the extinctions (*a*) the absorption from photo-electric emission and non-coherent scattering, which is independent of the orientation of the crystal, and (*b*) the shielding of the interior parts of the crystal by the reflection of X rays from the parts lying above them are made. The correction for (*a*) is made to 1·2 per cent by measuring the absorption coefficient and the size of the crystal. (*b*) is lessened by increasing the angular range over which the crystal reflects, as was done for figure 7, and also by measuring a feeble reflection. This latter cannot be realized directly because of lack of intensity in the monochromatic beam. The 110 reflection is therefore measured in monochromatic radiation. With the same crystal the ratio of this plane to the (400) is then measured in the direct filtered radiation from the target. This enables the absolute measurement to be based on the 400 reflection. The maximum experimental error will not affect figures 10 and 11 by more than 6 per cent. The error is probably less than 4 per cent. The crystals are assumed to be near to the mosaic type because the intensities are proportional to the volume of the crystal.

The melting-point of sodium is 97·5° C.(3) The X-ray reflections from sodium behave in a normal manner up to 98·5 ± 0·5° C., when within 0·2° C. the reflections vanish. For comparison *s*-triphenylbenzene may be cited, the melting-point of which is increased by 2° C. if it is enclosed in a small capillary tube. It is therefore possible that a similar effect may occur with sodium. On account of the non-transparency and the softness of sodium this increase could not be observed.

Summary of results. When a small piece of sodium is crystallized from the melt it is, on the average, found to give a lower reflecting-power for X rays than would be expected if it crystallized in the ideally imperfect state. The crystals when subjected to a cycle of heating and cooling show a strong hysteresis effect, as given in figure 6. This applies essentially to the strong planes.

If the crystal is suddenly chilled by liquid air it alters its behaviour. The hysteresis becomes almost negligible and the reflection curves before and after treatment are as shown in figure 7. The intensities increase as shown in table 1. From this it might be assumed that the substance is now an ideally imperfect crystal, but it is found that when the experimental f_0 curve is compared with Hartree's theoretical curve, it still gives too low an intensity for the low-order planes. From this it must be concluded that in spite of the drastic treatment the crystals do not break into blocks small enough to show no extinction.

The characteristic temperature is calculated from the X-ray data by means of the Debye-Waller formula. The result is given in figure 9. The value is based on the weaker planes whose temperature factor is large and whose extinction errors are small. The difference of 20 per cent between the X-ray value and that obtained from specific heats is not excessive, considering the approximate nature of the theory.

§ 5. ACKNOWLEDGMENTS

I wish to express my thanks to the Managers of the Royal Institution and to Sir William Bragg for permission to carry out this work. I am indebted to Dr A. Müller and to Dr R. Eisenschitz for their help in interpreting the experimental results, and also to Dr A. Müller for his interest and advice in the experimental work.

REFERENCES

(1) Robinson, B. W. *Proc. roy. Soc.* A, **142**, 422 (1933).
(2) Robinson, B. W. *Proc. roy. Soc.* A, **147**, 467 (1934).
(3) *International Critical Tables.*
(4) Fuchs, K. *Proc. roy. Soc.* A, **153**, 637 (1936).
(5) Fuchs, K. *Proc. roy. Soc.* A, **157**, 445 (1936).

DISCUSSION

Sir William Bragg. The curious conclusion of these experiments is that the crystal chilled in liquid air arrives at a state which appears to be stable; before the chilling the state is variable. The experiments show that it is stable when the crystal is broken up into a mosaic structure, and the point to be explained is why the material prefers when cold to crystallize as if there were a great number of nuclei, while when prepared from the melt it behaves as if there were a much smaller number of nuclei.

Dr A. Müller. I wish to emphasize one important point in the author's work, namely the fact that the crystal ceases to show hysteresis when it is suddenly chilled and not, as one might expect, when slowly annealed. The results also show that it is very difficult to make certain that a metal shall be in equilibrium.

Mr R. M. Archer. I have made many attempts to produce a gas-free film of sodium on the walls of a soda-glass mercury trap, and was interested to see that the author's method of filling a capsule is almost the same as one which I devised last year. If the author or any other Fellow can help me I shall be grateful, as I have had many difficulties in handling this vicious element. The technique of Hughes and Poindexter is inapplicable to my soda-glass evacuation system because the glass evolves so much water when heated strongly, and hydration follows. My method of filling is the same as the author's, except that all the vessels are of metal, and oil is not used because hydrocarbons would be out of place in valve work. The filled capsule is plugged lightly to exclude air and moisture, and put into a metal test tube wound outside with nichrome strip and insulated with asbestos. This little furnace is mounted concentrically inside the vertical glass tube which forms the trap, the whole being evacuated subsequently. The furnace is purposely made longer than the capsule and its upper end is closed by four or five perforated baffles to prevent the molten sodium from creeping over the rim and severing the nichrome or clinging to the asbestos and puncturing it afterwards. The furnace must be lagged to prevent its overheating or cracking the narrow trap. A difficulty is that the film condenses on a narrow zone of the glass and usually cracks it, presumably because the latent heat is set free in a small area. Moreover the hot glass gives off water and most of the film is spoilt. If the glass tube is very wide the film is better spread and gives little trouble, but a wide trap is probably ineffective. A long perforated delivery tube properly graded might give a longer film, but only a few tests have been made so far. Could an ionic drift of the vapour be effected by applying a suitable field? Another difficulty is that if the furnace is left inside the trap, outgassing of the cold asbestos and metal would be difficult, and further heating of the furnace would disperse the film. Removal after the admission of dry air would involve adsorption of gas by the film, which cannot be safely heated again. Removal in vacuo would be practicable but would involve some complication.

THE AUTHOR said that to his regret he was unable to suggest any solution of Mr Archer's problem.

AN X-RAY INVESTIGATION OF PURE IRON-NICKEL ALLOYS. PART 3: THE THERMAL EXPANSION OF ALLOYS RICH IN IRON

BY E. A. OWEN, M.A., D.SC., F.INST.P., AND E. L. YATES, M.SC., PH.D., A.INST.P., University College of North Wales, Bangor

Received 6 *January* 1937. *Read in title* 12 *February* 1937

ABSTRACT. This part of the paper deals with the measurement of the parameters of pure iron and iron-nickel alloys in the α phase at different temperatures ranging from room-temperature to 600° C. From these measurements the coefficients of thermal expansion of the alloys were determined. The thermal expansion of iron, 99·97-per-cent pure, was obtained at temperatures between 0 and 500° C. The lattice-parameter of iron of this purity at 15° C. was found to be $2{\cdot}8605_0$ A. and the coefficient of thermal expansion at this temperature to be $10{\cdot}7 \times 10^{-6}$ per ° C. At all temperatures the addition of nickel to iron at first lowered and afterwards increased the value of the thermal coefficient.

§ 1. INTRODUCTION

THE iron-nickel alloys rich in iron present more difficulty than the other alloys in the system because they behave irreversibly when alternately heated and cooled. Different workers disagree also as to the extent of the pure α phase and the range of temperature over which irreversibility exists.

The investigations of Hanson and Hanson(1), Hanson and Freeman(2), Honda and Miura(3), Chevenard(4) and others lead to the equilibrium diagram shown in figure 1(5). According to this diagram alloys containing between 0 and about 30 per cent of nickel remain in the α condition until raised up to temperatures exceeding about 450° C.; the temperature at which the transformation to $(\alpha+\gamma)$ takes place rises from about 450° C. for an alloy containing 30 per cent nickel to 900° C. for pure iron. The temperature range over which the $(\alpha+\gamma)$ region exists is limited; the transformation to pure γ for a 30-per-cent-nickel alloy takes place at about 550° C., so that the range for this alloy is about 100° C. This range decreases as the nickel-content diminishes and it vanishes for pure iron at about 900° C. This state of affairs exists if the alloys are in the pure α condition initially. To get them into this state alloys having a nickel-content greater than about 15 per cent have to be specially heat-treated and have to be taken to low temperatures before finally being allowed to return to room-temperature.

If, on the other hand, an alloy in this region is raised initially to a high temperature, say of 1000° C., is allowed to reach a state of equilibrium at that temperature, and is then cooled slowly, the transformation from γ to $(\alpha+\gamma)$ does not take place until a temperature is reached which is much lower than the one at which the transformation ($(\alpha+\gamma)$) to γ took place on heating. The difference between the transformation temperature on heating and that on cooling increases as the nickel-content of the alloys increases.

If, then, the alloys are in the α condition at ordinary temperatures, they can be raised to temperatures between 450 and 900° C., according to their composition, before they enter the $(\alpha+\gamma)$ region. It is advisable therefore to keep the annealing temperatures of the powders, before X-ray photographs are taken with them, below those corresponding with the boundary α, $(\alpha+\gamma)$ on heating. A good deal of work was done on these alloys before this was realized, for the equilibrium table available at the time was that published in the *International Critical Tables*. Our own investigation of the heat treatments of the alloys led us to adopt the course mentioned above before our attention had been drawn to the later diagram. A description of the heat treatments to which the alloys were submitted is given below.

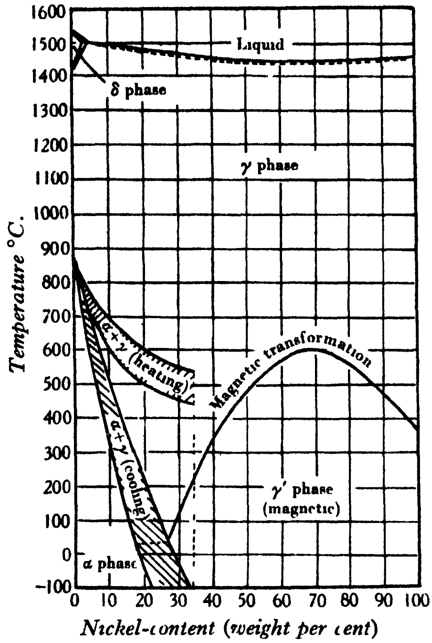

Figure 1. Equilibrium diagram of iron-nickel alloys

In the present part of this paper an account is given of the work done on three alloys of composition ranging between 3 and 16 per cent of nickel. Pure iron also is considered. It is felt that much more work than has already been done is necessary on alloys at this end of the equilibrium diagram. The present contribution is therefore to be regarded as preliminary to a fuller investigation which is now in progress.

§ 2. COMPOSITION OF THE ALLOYS

Three alloys were investigated. They were kindly supplied by the Mond Nickel Company Limited and were prepared from pure materials. Their compositions are given in table 1.

Table 1. Composition of the alloys

Alloy	Nickel-content	
	Weight %	Atoms %
3	3·1	3·1
9	9·0	8·8
16	16·7	16·4

Iron, the purity of which was 99·966 per cent, was available. Its lattice-parameter at 18° C. had already been carefully measured in the laboratory⁽⁶⁾, and it was now decided to investigate its thermal expansion up to 600° C., about the highest temperature attainable with the high-temperature camera which has been employed hitherto for all measurements above room-temperature.

§ 3. HEAT TREATMENT

A good deal of preliminary work had been carried out before this investigation on the heat treatment of these alloys by Mr C. W. Thompson, M.Sc.⁽⁷⁾ of this laboratory. It was found that when a powdered alloy containing 3 per cent nickel was annealed for 3 hours at 600° C. in vacuo and cooled slowly to room-temperature in about 12 hours, well-defined lines were obtained at the greatest glancing angles, and accurate values of the lattice-parameters could be calculated from the measurements of the lines. It should be stated that all the alloys had been lump-annealed at 800 C. for periods ranging between 11 and 21 days and cooled over periods ranging between 6 and 16 days, and it had been found that further lump-annealing did not alter the lattice-parameters.

When powders of alloys containing 9 and 16 per cent of nickel were treated similarly to alloy 3, the lines at great glancing angles were badly defined and could not be measured with the necessary degree of precision. Annealing at 600° C. for 12 hours instead of 3 hours did not improve the definition. After this a detailed investigation of the heat treatment of alloy 16 was carried out, but the annealing temperature in the first instance was never less than 600° C. The powder was annealed at the high temperature for periods ranging from 24 to 192 hours and cooled down to room-temperature over periods ranging from 12 to 144 hours, but in every case the precision lines were unsatisfactory, being broad, faint and ill defined. When the annealing temperature was reduced to 500° C., lines were obtained which could be measured with tolerable accuracy. All the alloys described here were therefore annealed in powder form at 500° C. for 3 hours. In the hope of improving the lines obtained with alloy 16 the powder was further annealed at 300° C. for 24 hours, but little if any improvement was effected by this additional heat treatment. The precision lines in all cases were however measurable, but the accuracy of measurement with alloy 16 was not as great as with the other alloys. Spectrum photographs taken with the alloys at room-temperature showed them to possess body-centred cubic structure only. These results are in conformity with the equilibrium diagram of the alloy system shown in figure 1.

Powder was prepared from the sample of pure iron by two methods, (1) by filing, and (2) by rubbing on coarse glass paper and extracting the iron. By alternately passing the resulting powder through a 250-mesh sieve and extracting the iron with a magnet, iron powder free from contamination was prepared by the second method. Exposures taken with this specimen at 611° C. showed that the lattice-parameter was identical with that of specimens prepared by filing.

When photographs were taken with iron the procedure adopted was to heat the filings in an evacuated glass tube at 500° C. for 50 min. Excellent spectral lines were obtained after this heat treatment.

The usual procedure$^{(8)}$ was adopted in taking the X-ray photographs. The powders were raised to the required temperature in the evacuated chamber enclosing the camera, and the temperature was maintained for at least half an hour before the exposure was started.

Cobalt radiation* was used, reflections being obtained from the (310) planes of the body-centred cubic lattice of the α phase.

The thermocouple used to measure the temperature of the specimen exposed to X rays was carefully calibrated, and a check was frequently made on the calibration by taking exposures with silver raised to different temperatures. With the exception of the exposure made at 640° C. with iron, the accuracy of the temperature-measurement is considered to be within ± 1 per cent.

§ 4 RESULTS

Iron. Two different cameras were employed, one serving as a check on the other. The filings showed a tendency at the highest temperatures to become dark in colour and to lose their metallic lustre. When this occurred new filings were taken, but no change in the lattice-parameter was observed in consequence of the discoloration. The observed values of the lattice parameter at the temperatures stated are collected in table 2. Each value has been corrected for refractivity, as were all other values of lattice-parameters recorded in this paper.

The lattice-parameter values were plotted against the corresponding temperatures and a smooth curve was drawn through the points. The parameter-values given in table 3 were taken from this curve, and the coefficients of thermal expansion were calculated from tangents drawn to it.

The values of the coefficient of expansion are estimated to have an accuracy of ± 5 per cent. The same values of the coefficient of thermal expansion were obtained with a specimen of iron of 99·989-per-cent purity. There is good agreement between the values at the lower temperatures, and the recently published⁽⁹⁾ values of the coefficient of expansion of very pure iron at those temperatures.

---

* The wave-lengths taken were: $\mathrm{CoK}\alpha_1 = 1{\cdot}78529$ A., $\mathrm{CoK}\alpha_2 = 1{\cdot}78919$ A.

Table 2. Lattice-parameter of pure iron at various temperatures

Film number	Temperature (° C.)	Lattice-parameter (A.)	Film number	Temperature (° C.)	Lattice-parameter (A.)
E 632	14	$2\cdot8604_8$	E 631	261	$2\cdot8697_0$
E 641	15	$2\cdot8605_6$	E 179	294	$2\cdot8707_4$
E 177	16	$2\cdot8604_4$	E 636	315	$2\cdot8719_5$
E 176	18	$2\cdot8605_2$	E 627	366	$2\cdot8740_0$
E 185	22	$2\cdot8607_0$	E 182	391	$2\cdot8751_4$
E 181	36	$2\cdot8610_9$	E 634	417	$2\cdot8764_3$
E 178	98	$2\cdot8632_3$	E 630	476	$2\cdot8791_7$
E 633	147	$2\cdot8651_0$	E 180	488	$2\cdot8798_9$
E 183	195	$2\cdot8669_5$	E 642	530	$2\cdot8817_2$
E 635 E 638	208	$2\cdot8674_0$	E 628	576	$2\cdot8842_7$
			E 640	640	$2\ 8883_5$

Table 3. Coefficient of thermal expansion of pure iron

Temperature (° C.)	Lattice-parameter (A.)	True coefficient of expansion $\times 10^6$
0	$2\cdot8600_3$	10·5
15	$2\cdot8605_0$	10·7
100	$2\cdot8633_8$	12·0
200	$2\cdot8671_5$	13·5
300	$2\cdot8711_8$	14·7
400	$2\cdot8755_5$	15·8
500	$2\cdot8803_6$	16·9
600	$2\cdot8854_4$	18·0*

* Extrapolated.

Alloy 3. This alloy according to all the equilibrium diagrams is well within the region of the α phase at all temperatures up to about 600° C. A powder photograph of the sample taken at room-temperature showed that its structure was body-centred cubic, which is the structure of the α-phase alloys.

The crystal lattice was measured over a range of temperature extending from room-temperature to about 600° C. The fact that a smooth curve was obtained when the parameter-values were plotted against temperature indicates that the alloy remained in the α region throughout this range of temperature. It was impracticable to measure the lattice-dimensions at temperatures higher than 600° C. with the camera employed, and so the change taking place at the α, $(\alpha+\gamma)$ boundary for this alloy could not be investigated. Well-defined spectral lines were obtained over the whole range of temperature, those at high temperatures being of weaker intensity owing to the heat motion of the atoms but still quite strong enough for accurate measurement. X-ray exposures of 15 min. were found to be ample.

Table 4. Lattice-parameters of α iron-nickel alloys at various temperatures

Alloy	3			9			16	
Nickel-content (per cent by weight)	3·1			9·0			16·7	
Film number	Temperature (° C.)	Lattice-parameter (A.)	Film number	Temperature (° C.)	Lattice-parameter (A.)	Film number	Temperature (° C.)	Lattice-parameter (A.)
E 186	16	2·8620$_6$	E 224	15	2·8634$_2$	E 243	13	2·8628$_1$
E 190 E 197	17	2·8621$_9$	E 206 E 207	16	2·8634$_1$	E 248	14	2·8629$_3$
E 194	18	2·8622$_7$	E 198	17	2·8634$_9$	E 241	15	2·8630$_9$
E 191	101	2·8650$_1$	E 203 E 217	18	2·8633$_9$	E 225 E 240	16	2·8628$_7$
E 187	199	2·8683$_8$	E 200 E 208	20	2·8635$_2$	E 231 E 232	17	2·8630$_8$
E 193	301	2·8723$_1$	E 202	100	2·8663$_1$	E 227 E 229	18	2·8631$_0$
E 219	360	2·8748$_6$	E 199	203	2·8696$_2$	E 234	100	2·8655$_4$
E 188	393	2·8761$_9$	E 210	294	2·8728$_1$	E 235	200	2·8687$_4$
E 195	444	2·8786$_7$	E 209	295	2·8727$_4$	E 233	304	2·8724$_3$
E 218	457	2·8785$_6$	E 201	296	2·8729$_5$	E 226 E 228 E 230	306	2·8728$_4$
E 192	489	2·8808$_2$	E 220	340	2·8741$_2$	E 246	340	2·8741$_1$
E 196	522	2·8822$_6$	E 200 E 223	394	2·8765$_1$	E 247	345	2·8741$_7$
E 189	575	2·8840$_7$	E 203	416	2·8774$_5$	E 245	350	2·8744$_1$
			F 222	470	2·8793$_4$	E 244	380	2·8757$_4$
			E 204 E 205	502	2·8807$_9$	E 238	418	2·8771$_4$
			E 213	556	2·8827$_7$	E 242	456	2·8787$_6$
			E 212	600	2·8845$_0$	E 239	501	2·8803$_4$
						E 236	598	2·8840$_1$

Table 5. Coefficient of thermal expansion of α iron-nickel alloys at various temperatures.

Temperature	Alloy 3		Alloy 9		Alloy 16	
	Lattice-parameter	Coefficient of expansion × 10^6	Lattice-parameter	Coefficient of expansion × 10^6	Lattice-parameter	Coefficient of expansion × 10^6
0	2·8616$_2$	10·9	2·8629$_0$	10·9	2·8625$_0$	10·3
15	2·8621$_2$	11·0	2·8633$_8$	11·0	2·8629$_6$	10·4
100	2·8649$_4$	11·7	2·8661$_7$	11·5	2·8655$_2$	11·2
200	2·8684$_5$	12·8	2·8695$_2$	12·1	2·8689$_3$	11·9
300	2·8722$_7$	13·7	2·8730$_3$	12·7$_5$	2·8725$_0$	12·7
400	2·8763$_9$	14·8	2·8767$_9$	13·3	2·8763$_8$	13·5
500	2·8809$_2$	16·0	2·8806$_2$	13·7	2·8803$_7$	14·2
600	2·8857$_0$	17·0	2·8845$_4$	14·2	2·8845$_0$	14·9

Alloy 9. According to the equilibrium diagram reproduced in figure 1 this alloy is in the region of the α phase, and when it is heated it remains in the α phase up to a temperature of about 600° C. A spectrum photograph taken with this alloy showed that at room-temperature its structure was body-centred cubic, and in all the photographs taken at higher temperatures no indication of the presence of the γ phase was observed, the lines registered in the photographs being accounted for by the body-centred α phase. Well-defined lines were obtained from the (310) planes with cobalt radiation.

Alloy 16. This alloy also is in the α-phase region. It was observed that the α structure existed at all temperatures up to the highest temperature at which the alloy was examined. This is in agreement with the equilibrium diagram in figure 1 but in disagreement with the phase diagram published in the *International Critical Tables*, according to which the alloy should be in the mixed $(\alpha+\gamma')$ region at ordinary temperatures, transforming to $(\alpha+\gamma)$ at 345° C. and into pure γ at a temperature of about 440° C. No change in phase was detected in the present investigation as the alloy was heated to higher temperatures. It is worthy of note that Chevenard also gives for a 17·2-per-cent iron-nickel alloy a thermal-expansion curve which is smooth up to 550° C.; this shows that the α structure existing at room-temperature probably is not transformed to another phase below this temperature.

It was noted that after the exposure at 598° C. the crystal lattice was much too distorted to yield spectral lines after the material had cooled to room-temperature. This fact suggests that the alloy was already undergoing some structural change at 598° C. and that the change was not complete when the specimen started cooling in the camera enclosure. It should be stated that all the specimens after exposure to X rays at high temperatures were allowed to cool to room-temperature in the camera enclosure in which a vacuum was maintained. When this procedure was adopted the material did not become oxidized and could be used for several exposures.

Poor spectral lines were obtained with alloy 16 at all temperatures, and the measurement of the films was rendered somewhat difficult in consequence. The first seven exposures (E 225 to E 231 inclusive) were made with powder which had been annealed at 500° C. for 3 hours.

The observed lattice-parameters of the alloys at various temperatures are given in table 4, and the coefficients of thermal expansion calculated from them in table 5. It will be observed that the parameter of alloy 16 at room-temperature is less than that of alloy 9, but that the coefficient of thermal expansion increases more rapidly with temperature for alloy 16 than for alloy 9.

These preliminary measurements of the lattice-parameters of the α iron-nickel alloys show that if the material is in the α condition at room-temperature it remains in this condition at all temperatures up to 600° C. in alloys which contain up to about 17 per cent of nickel. This is in accordance with the equilibrium diagram, figure 1. More readings on alloys which have been subjected to varied heat treatments are necessary before it will be possible to make any very definite statements regarding the behaviour of these α alloys and the exact disposition of the phases existing in this part of the equilibrium diagram. The few observations recorded here do, however, confirm, though not as adequately as could be desired, certain features of the equilibrium diagram shown in figure 1. Further work on these alloys is now in progress.

§ 5. ACKNOWLEDGEMENTS

See page 324 of this volume.

REFERENCES

(1) HANSON and HANSON. *J. Iron Steel Inst.* **102**, 39 (1920).
(2) HANSON and FREEMAN. *J. Iron Steel Inst.* **107**, 301 (1923).
(3) HONDA and MIURA. *Trans. Amer. Soc. Steel Treat.* **13**, 270 (1928).
(4) CHEVENARD. *Rev. de Mét.* **11**, 841 (1914); **14**, 618 (1917); *C.R. Acad. Sci.*, Paris, **159**, 53 (1914); **170**, 1499 (1920); **171**, 93 (1920); **172**, 594 (1921); **174**, 109 (1922).
(5) MERICA. *National Metals Handbook*, p. 607 (1930).
(6) OWEN and YATES. *Phil. Mag.* **15**, 472 (1933).
(7) THOMPSON. Thesis submitted for the degree of M.Sc. of the University of Wales.
(8) OWEN and YATES. *Proc. phys. Soc.* **49**, 17 (1937).
(9) ADCOCK and BRISTOW. *Proc. roy. Soc.* A, **153**, 172 (1935).

AN X-RAY INVESTIGATION OF PURE IRON-NICKEL ALLOYS. PART 4: THE VARIATION OF LATTICE-PARAMETER WITH COMPOSITION

By E. A. OWEN, M.A., Sc.D., D.Sc., F.Inst.P., E. L. YATES, M.Sc., Ph.D., A.Inst.P. and A. H. SULLY, M.Sc.

Received 6 *January* 1937. *Read in title* 12 *February* 1937

ABSTRACT. In this part of the paper the variations of lattice-parameter with the composition of the alloys is considered. Twenty alloys in the γ phase ranging in composition from 23 to 97 atomic per cent of nickel, and four alloys in the α phase ranging in composition from 3 to 16 atomic per cent of nickel were studied at different temperatures. At room-temperature, when iron is added to nickel the nickel lattice expands almost linearly with the atomic composition until the lattice-parameter reaches a maximum value of 3·5895 A. for an alloy the composition of which is 39 atomic per cent of nickel. On further addition of iron the lattice contracts. The variation of the parameter of the γ alloys with composition was examined at temperatures ranging up to 600° C. From the values of the lattice parameters the densities of pure iron-nickel alloys over the whole range of composition from pure iron to pure nickel were calculated.

§ 1. VARIATION OF THE LATTICE-PARAMETER WITH COMPOSITION OF γ-PHASE ALLOYS AT ROOM-TEMPERATURE

Twenty alloys ranging in composition from 23 to 97 atomic per cent of nickel were examined with the precision and spectrum cameras at room-temperature. Particular attention was paid to alloys of composition in the neighbourhood of 36 per cent of nickel. The alloys were all given initially a heat treatment in lump form—some were maintained at 1150° C. for 20 hours in a nitrogen atmosphere, others at the same temperature for 8 hours in vacuo, and others at 800° C. for some days in vacuo. The standard treatment adopted with the filings taken from the ingots was to heat them for 14 hours at 600° C. After this heat treatment some of the samples were quenched in iced water and others cooled to room temperature in 120 hours before their parameters were measured. It was found that with all the alloys containing more than about 28 per cent of nickel the same lattice-parameter values were obtained whether the alloys were quenched or slowly cooled. This behaviour is characteristic of unsaturated solid solutions. The γ phase exists alone, therefore, in all alloys containing more nickel than about 28 per cent.

The results of the measurements are collected in table 1. Each parameter-value included in the table is the mean of several determinations obtained with quenched and slowly cooled specimens.

The lattice-parameters are plotted against the compositions of the alloys in figure 1. The lattice-parameter of nickel increases when iron is added. This is in

Table 1. Lattice-parameters of γ-phase iron-nickel alloys at 15° C.

Nickel-content of alloy		Lattice-parameter of γ phase at 15° C.	Nickel-content of alloy		Lattice-parameter of γ phase at 15° C.
Weight per cent	Atoms per cent		Weight per cent	Atoms per cent	
100	100	$3{\cdot}5171_3$	42·71	41·75	$3{\cdot}5882_7$
96·75	96·6	$3{\cdot}5206_6$	40·66	39·7	$3{\cdot}5894_0$
93·95	93·8	3·5241	38·42	37·5	$3{\cdot}5895_4$
91·04	90·8	3·5278	37·17	36·3	$3{\cdot}5884_0$
82·86	82·2	3·5378	35·10	34·3	$3{\cdot}5858_6$
74·00	72·8	3·5494	33·59	32·65	$3{\cdot}5833_4$
63·82	62·6	3·5626	32·20	31·4	$3{\cdot}5807_5$
58·41	57·0	3·5691	31·67	30·9	$3{\cdot}5796_5$
52·15	50·75	3·5779	30·30	29·7	$3{\cdot}5768_9$
48·00	46·7	$3{\cdot}5828_4$	28·12	27·5	$3{\cdot}5743_1$
45·50	44·3	$3{\cdot}5858_6$	24·22	23·4	$3{\cdot}5732_8$

accordance with expectation, as solution takes place by substitution and the atomic volume of iron is greater than that of nickel. The lattice-parameter increases almost linearly with composition for alloys between pure nickel and 40 per cent of nickel. There seems however to be a slight departure from strict linearity, the alloys showing a small contraction the maximum value of which occurs in an alloy containing about 78 atomic per cent of nickel.

The lattice-parameter at 15° C. reaches a maximum value of 3·5895 A. for an alloy containing 39 atomic per cent of nickel. It then diminishes at almost the same rate as that at which it previously increased with increase of iron-content, and reaches a minimum value of 3·5732 A. The composition corresponding to the intersection of the horizontal line through the γ lattice-parameter of the alloy containing 24·2 per cent of nickel, which also contained the α constituent in the specimen as prepared, and the line representing the slope of the left-hand limb of the {parameter, composition} curve is 28 atomic per cent of nickel. It is interesting to note that the boundary $(\alpha+\gamma)$, γ in figure 1 of part 3 (p. 308 of this volume) corresponds to a composition of 28 per cent of nickel at about 20° C. for an alloy which is cooled from above about 550° C. down to room-temperature.

The above results are in approximate agreement with the work of Phragmén(1) on nickel steels of low thermal expansion and ranging in composition from 29 to 50 per cent of nickel. Phragmén finds that the maximum occurs at 38 per cent of nickel by weight, and that the value of the parameter at the maximum is 3·5883 A. at 10° C. Jette and Foote(2) find that the maximum occurs at about 39 atomic per cent nickel and that the value of the parameter at the maximum is 3·5884 at 25° C. These results are all in satisfactory agreement, although the lattice-parameter at the maximum is a little higher according to the present measurements, and whereas Jette and Foote find a strictly linear relation between parameter and composition in atomic per cent of nickel from pure nickel to the maximum, a slight contraction is now observed. The values of the parameters at various compositions are however on the whole in good agreement when reduced to the same temperature.

It is noteworthy that the lattice-parameter of taenite, the γ structure found in meteorites composed of iron and nickel alone, is about 3·59 A.(3), the parameter corresponding to the maximum of the {parameter, composition} curve and an alloy containing 40 per cent of nickel by weight. This would point to the stability of alloy 40, which has an open structure and is able to take into solution either iron or nickel, both metals on solution decreasing the dimensions of the lattice.

The conclusions reached from this part of the investigation carried out on alloys at 15° C. are that: (1) when iron is added to nickel, the nickel lattice which is face-centred cubic expands almost linearly with the atomic composition of the alloy; (2) the lattice-parameter reaches a maximum value of 3·5895 A. for an alloy, the composition of which is 39 atomic per cent of nickel; (3) on further addition of iron, the lattice contracts again almost linearly with composition, reaching a minimum value of 3·5732 A.

§ 2. VARIATION OF LATTICE-PARAMETER OF α-PHASE ALLOYS AT ROOM-TEMPERATURE WITH COMPOSITION

A preliminary study of the variation of the lattice-parameters of the α-phase alloys at room-temperature was made with five alloys ranging in composition from 3 to 24 per cent of nickel. According to the equilibrium diagram in figure 1 of part 3 (p. 308 of this volume) all the alloys except alloy 24 were in the region of the α phase at room-temperature. The behaviour of alloy 24 was considered in part 2, when it was found that both the α and γ phases were present. The expansion of each phase was examined, the α phase disappearing at about 350° C. and leaving only the γ phase. The other alloys remained in the α phase from room-temperature up to 600° C., the lattice-parameters at the higher temperatures are given in part 3, except for alloy 6 which was examined at room-temperature only. Table 2 contains a summary of the lattice-parameters at 15° C. of the α alloys so far examined, and it will be seen that, contrary to expectation, the iron lattice expands when nickel is added, and the increase in parameter does not bear even an approximately linear relation to the composition of the alloys. In addition the parameter reaches a maximum value and then decreases to a steady value for alloys 16 and 24.

Table 2. Lattice-parameters of α-phase iron-nickel alloys at 15° C.

Alloy	Nickel-content of alloy		Lattice-parameter of α phase at 15° C.
	Weight per cent	Atoms per cent	
24	24·2	23·5	2·8630
16	16·7	16·4	$2{\cdot}8629_6$
9	9·0	8·8	$2{\cdot}8633_8$
6	6·0	5·9	2·8629
3	3·1	3·1	$2{\cdot}8621_2$
Fe	0·0	0·0	$2{\cdot}8605_0$

The heat treatment given to the alloys has already been described. It will be necessary, as has already been stated, to vary and extend the heat treatment in order to arrive at more definite information concerning these α alloys.

§ 3. VARIATION OF THE LATTICE-PARAMETER OF γ-PHASE ALLOYS AT VARIOUS TEMPERATURES UP TO 600° C. WITH COMPOSITION

The values of the lattice-parameters of the γ phase in alloys of different compositions at temperatures ranging from 15° to 600° C. are collected in table 3.

Table 3. Parameters of iron-nickel alloys at different temperatures

Alloy	Nickel-content	Parameter (A.)						
	Atoms per cent	15° C.	100° C.	200° C.	300° C.	400° C.	500° C.	600° C.
					γ phase			
Ni	100	$3{\cdot}5171_8$	$3{\cdot}5212_5$	$3{\cdot}5263_7$	$3{\cdot}5317_7$	$3{\cdot}5384_2$	$3{\cdot}5446_2$	$3{\cdot}5508_7$
97	96·6	$3{\cdot}5206_5$	$3{\cdot}5246_1$	$3{\cdot}5294_0$	$3{\cdot}5347_0$	$3{\cdot}5409_2$	$3{\cdot}5467_9$	$3{\cdot}5526_6$
94	93·8	$3{\cdot}5240_5$	$3{\cdot}5280_0$	$3{\cdot}5328_8$	$3{\cdot}5381_8$	$3{\cdot}5443_5$	$3{\cdot}5504_0$	$3{\cdot}5561_8$
91	90·8	$3{\cdot}5277_5$	$3{\cdot}5316_7$	$3{\cdot}5365_3$	$3{\cdot}5418_0$	$3{\cdot}5478_0$	$3{\cdot}5543_8$	$3{\cdot}5601_7$
83	82·2	$3{\cdot}5378_0$	$3{\cdot}5417_0$	$3{\cdot}5466_2$	$3{\cdot}5518_0$	$3{\cdot}5572_0$	$3{\cdot}5630_0$	$3{\cdot}5691_0$
74	72·8	$3{\cdot}5491_6$	$3{\cdot}5529_8$	$3{\cdot}5576_4$	$3{\cdot}5625_6$	$3{\cdot}5676_1$	$3{\cdot}5730_2$	●$3{\cdot}5787_2$
58	57·0	$3{\cdot}5690_8$	3·5728	$3{\cdot}5771_7$	$3{\cdot}5816_0$	$3{\cdot}5861_2$	$3{\cdot}5905_2$	3·5950
45	44·3	$3{\cdot}5855_7$	$3{\cdot}5879_0$	$3{\cdot}5905_7$	$3{\cdot}5928_7$	$3{\cdot}5954_5$	$3{\cdot}5993_0$	$3{\cdot}6061_3$
43	41·75	$3{\cdot}5882_7$	$3{\cdot}5893_3$	$3\ 5910_0$	$3{\cdot}5927_2$	$3{\cdot}5956_0$	$3{\cdot}6009_2$	$3{\cdot}6067_3$
35	34·3	$3{\cdot}5855_6$	$3{\cdot}5863_0$	$3{\cdot}5875_5$	$3{\cdot}5914_8$	$3{\cdot}5974_7$	$3{\cdot}6036_9$	$3{\cdot}6099_9$
32	31·2	$3{\cdot}5812_5$	$3{\cdot}5825_7$	$3{\cdot}5860_7$	$3{\cdot}5916_8$	$3{\cdot}5979_0$	$3{\cdot}6042_0$	$3{\cdot}6105_6$
24	23·4	3·5733	3·5809	3·5872	3·5934	3·5997	$3{\cdot}6059_4$	3·6122
					α phase			
24	23·4	2·8630	2·8655	2·8686	2·8721	—	—	—
16	16·4	$2{\cdot}8629_6$	$2{\cdot}8655_2$	$2{\cdot}8689_3$	$2{\cdot}8725_0$	$2{\cdot}8763_8$	$2{\cdot}8803_7$	$2{\cdot}8844_0$
9	8·8	$2{\cdot}8633_8$	$2{\cdot}8661_7$	$2{\cdot}8695_2$	$2{\cdot}8730_3$	$2{\cdot}8767_9$	$2{\cdot}8806_2$	$2{\cdot}8845_4$
3	3·1	$2{\cdot}8621_2$	$2{\cdot}8649_4$	$2{\cdot}8684_5$	$2{\cdot}8722_7$	$2{\cdot}8763_9$	$2{\cdot}8809_2$	$2{\cdot}8857_0$
Fe	0·0	$2{\cdot}8605_0$	$2{\cdot}8633_9$	$2{\cdot}8671_8$	$2{\cdot}8712_3$	$2{\cdot}8756_0$	$2{\cdot}8803_1$	$2{\cdot}8855_4$

When the results are plotted, figure 1, it is observed that the maximum becomes less pronounced as the temperature is raised, and with increase of temperature it is displaced in the direction of lower nickel-content. At 600° C. the maximum has disappeared, but at this temperature the rate of increase of the lattice-parameter with decrease in nickel-content is much less below about 40 per cent of nickel than it is for higher percentages of nickel. It was impossible with the camera used in the investigation to reach temperatures higher than about 600° C., but it is desirable to extend this work to higher temperatures.

The parameters and the compositions corresponding to the maxima at various temperatures are included in table 4.

Table 4

Temperature (°C.)	Lattice-parameter at maximum	Nickel-content (atoms per cent) at maximum
15	3·5895	39·0
100	3·5898	40·5
200	3·5912	42·0
300	3·5930	43·5
400	3·5952	45·0

The rate at which the lattice-parameter increases with decrease of nickel-content is about the same at all the temperatures investigated up to the maximum, but the rate varies considerably for different temperatures after this.

It is important to note that all the alloys containing more than about 30 atomic per cent of nickel give the same parameter at room-temperature whether they are quenched or slowly cooled. This fact shows that the alloys are unsaturated and are therefore in the pure phase, so that an explanation of the maximum on the supposition that supersaturation occurs is untenable.

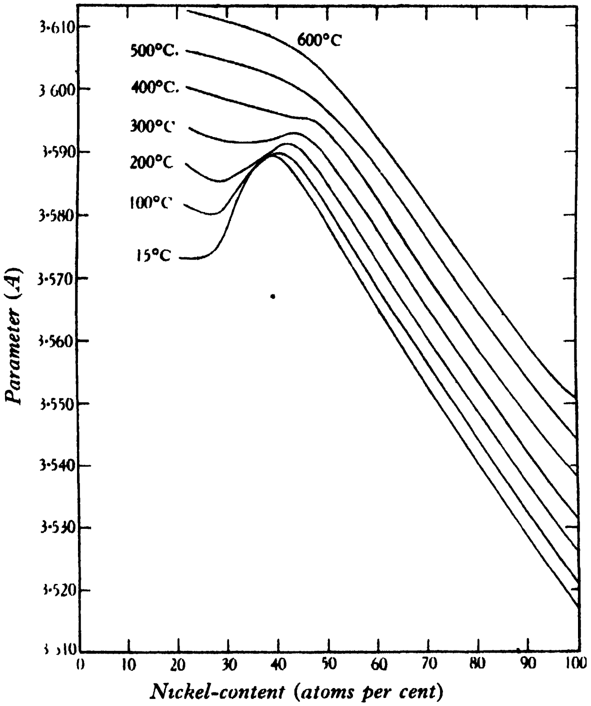

Figure 1. Parameters of γ alloys at different temperatures.

§4. VARIATION OF THE LATTICE-PARAMETER OF α-PHASE ALLOYS AT VARIOUS TEMPERATURES UP TO 600° C. WITH COMPOSITION

The values of the α-phase parameters for the alloys examined are included in table 3. The form of the curves at the higher temperatures is the same as that at room-temperature; a maximum value of the parameter is reached and then there is a drop to a steady value. The position of the maximum moves in the direction of lower nickel-content as the temperature is increased; at 15° C. it occurs for an alloy containing about 11·5 atomic per cent of nickel, while at 500° C. the composition corresponding to the maximum is 5 atomic per cent of nickel. The maximum with the α alloys therefore moves towards higher iron-content and that with the γ alloys towards higher nickel-content as the temperature is increased. The ascending limb of the curve for the α alloys is not a straight line over any portion of its length. The descending part of this curve changes its direction at points corresponding to progressively lower nickel-content as the temperature rises. This point of discontinuity in the curve may prove to be the position of the boundary between α and $(\alpha+\gamma)$ phases, but further observations on more alloys are necessary before any definite statement can be made.

§ 5. DENSITIES OF PURE IRON-NICKEL ALLOYS

The accurate values of lattice-parameters provide data for the calculation of the densities of the alloys. In the density calculations the mass of the hydrogen atom was taken to be $(1{\cdot}662 \pm 0{\cdot}002) \times 10^{-24}$ g. If the atomic weight of hydrogen is taken to be 1·0078 ($O = 16{\cdot}00$), the mass of an atom of unit atomic weight *m* is $(1{\cdot}649_1 \pm 0{\cdot}002) \times 10^{-24}$ g. The atomic weights$^{(4)}$ of iron and nickel are 55·84 and 58·69 respectively. The density was calculated with the aid of the following formula:

$$\rho = \frac{n}{a^3}\{58{\cdot}69x + (100-x)\,55{\cdot}84\}\frac{m}{100},$$

where *a* is the lattice-parameter, *n* is the number of atoms per unit cube and *x* is the nickel-content of the alloy in atoms per cent.

The accuracy of the density-determinations is limited considerably by the accuracy of the determination of the mass of the hydrogen atom. An error of ± 0·0003 A. in the lattice-parameter or an error of ± 0·05 in the atomic weight introduces an error of ± 0·005 g./cm.^{3} in the density. The error of $\pm 0{\cdot}002 \times 10^{-24}$ g. in the mass of the atom with unit atomic weight introduces an error of ± 0·009 g./cm.^{3} in the density of pure iron and ± 0·011 g./cm.^{3} in the density of pure nickel. The values of the densities of all the alloys investigated at room-temperature are included in table 5.

Table 5. Densities of pure iron-nickel alloys at 15° C.

Nickel-content (atoms per cent)	Density at 15° C. (g./cm.^{3})	Nickel-content (atoms per cent)	Density at 15° C. (g./cm.^{3})
γ phase			
100	$8{\cdot}89_8$	41·75	$8{\cdot}14_3$
96·6	$8{\cdot}85_7$	39·7	$8{\cdot}12_7$
93·8	$8{\cdot}81_9$	37·5	$8{\cdot}11_7$
90·8	$8{\cdot}77_8$	36·3	$8{\cdot}12_0$
82·2	$8{\cdot}66_8$	34·3	$8{\cdot}12_9$
72·8	$8{\cdot}54_4$	$32{\cdot}6_5$	$8{\cdot}13_9$
62·6	$8{\cdot}40_7$	31·4	$8{\cdot}15_2$
57·0	$8{\cdot}33_8$	30·9	$8{\cdot}15_7$
50·75	$8{\cdot}25_1$	29·7	$8{\cdot}17_1$
46·7	$8{\cdot}20_0$	27·5	$8{\cdot}18_0$
44·3	$8{\cdot}16_9$	23·4	$8{\cdot}17_0$
α phase			
23·4	$7{\cdot}94_2$	5·9	$7{\cdot}87_8$
16·4	$7{\cdot}91_4$	3·1	$7{\cdot}86_8$
8·8	$7{\cdot}88_2$	α-Iron	$7{\cdot}86_9$

As the nickel-content decreases the density of the γ alloys decreases and reaches a minimum value of about 8·12 g./cm.^{3} when the nickel-content is 37·5 atomic per cent. When the nickel-content is lowered still further, the density increases and reaches a maximum value of 8·18 g./cm.^{3} at a composition of about 27·5 atomic per cent of nickel. The density of the α alloys increases gradually as the nickel-content increases.

The characteristics of the density curve are similar to those of the curve determined by Chevenard$^{(5)}$, but in the present work the curve of the α alloys is not a straight line. The density curve of the γ alloys is however very similar to that determined by Chevenard and by Jette and Foote$^{(2)}$; there is very close agreement between the values of the densities determined by Jette and Foote and the present values for the γ alloys.

In table 6 are included the values of the densities of the iron-nickel alloys at 200, 400 and 600° C. calculated from the parameter-values at these temperatures appearing in table 3. When the results at 600° C. are plotted, the density of the γ alloys shows a continuous fall as the nickel-content decreases; this differs from the curve of densities at 15° C., which shows a minimum value. The α alloys show at 600° C. as at 15° C. a steady increase in density with increase of nickel-content.

Table 6. Densities of pure iron-nickel alloys at various temperatures

Nickel-content (atoms per cent)	Density (g./cm^3)		
	At 200° C.	At 400° C.	At 600° C.
	γ alloys		
100 (Ni)	$8{\cdot}82_9$	$8{\cdot}73_9$	$8{\cdot}64_7$
96·6	$8{\cdot}79_1$	$8{\cdot}70_6$	$8{\cdot}62_0$
93·8	$8{\cdot}75_4$	$8{\cdot}66_9$	$8{\cdot}58_3$
90·8	$8{\cdot}71_4$	$8{\cdot}63_1$	$8{\cdot}54_1$
82·2	$8{\cdot}60_8$	$8{\cdot}52_7$	$8\ 44_2$
72·8	$8{\cdot}48_4$	$8{\cdot}41_8$	$8{\cdot}33_5$
57·0	$8{\cdot}28_1$	$8{\cdot}21_9$	$8{\cdot}15_9$
44·3	$8{\cdot}13_7$	$8{\cdot}10_4$	$8{\cdot}03_2$
$41{\cdot}7_5$	$8{\cdot}12_4$	$8{\cdot}09_3$	$8{\cdot}01_8$
34·3	$8{\cdot}11_7$	$8{\cdot}05_0$	$7{\cdot}96_7$
31·4	$8{\cdot}11_6$	$8{\cdot}03_6$	$7\ 95_1$
23·4	$8{\cdot}07_5$	$7{\cdot}99_1$	$7{\cdot}90_9$
	α alloys		
23·4	$7{\cdot}89_5$	—	—
16·4	$7{\cdot}86_5$	$7{\cdot}80_4$	$7{\cdot}73_9$
8·8	$7{\cdot}83_0$	$7{\cdot}77_1$	$7{\cdot}70_8$
3·1	$7{\cdot}81_5$	$7{\cdot}75_1$	$7{\cdot}67_6$
0·0 (Fe)	$7{\cdot}81_4$	$7{\cdot}74_5$	$7{\cdot}66_6$

§ 6. ACKNOWLEDGEMENTS

See p. 325 of this volume.

REFERENCES

(1) Phragmén. *J. Iron Steel Inst.* **123**, 465 (1931).
(2) Jette and Foote. *Metals Technology,* **3** (1936), Tech. Publ. No. 670.
(3) Young. *Proc. roy. Soc.* A, **112**, 630 (1926).
(4) Guillaume. *Proc. phys. Soc.* **32**, 374 (1920).
(5) Chevenard. *Rev. de Mét.* **11**, 841 (1914); **14**, 618 (1917); *C.R. Acad. Sci.*, Paris, **159**, 53 (1914); **170**, 1499 (1920); **171**, 93 (1920); **172**, 594 (1921); **174**, 109 (1922).

AN X-RAY INVESTIGATION OF PURE IRON-NICKEL ALLOYS. PART 5: THE VARIATION OF THERMAL EXPANSION WITH COMPOSITION

By E. A. OWEN, M.A., D.Sc., F.Inst.P., E. L. YATES, M.Sc., Ph.D., A.Inst.P. and A. H. SULLY, M.Sc.

Received 6 *January* 1937. *Read in title* 12 *February* 1937

ABSTRACT. The variation of the thermal coefficient of expansion with composition of the γ alloys, as deduced from measurements of crystal parameters, agrees in the main with that found by Guillaume and by Chevenard, who made measurements on rods of the materials. Certain divergences, which may be due to differences in the purities of the alloys employed in the different investigations, have been observed.

§ 1. VARIATION OF THE THERMAL COEFFICIENT OF EXPANSION OF IRON-NICKEL ALLOYS AT ROOM-TEMPERATURE WITH COMPOSITION

The measurements already made on the lattice-parameters of the iron-nickel alloys in the course of the present investigation provide sufficient data to follow the variation of the coefficient of expansion of the alloys when the composition is altered. We shall consider first the coefficients of expansion of the various alloys at room-temperature, which are shown in figure 1. The portion *ADBE* of the curve refers to the γ alloys and has been thoroughly investigated by Guillaume(1) and by Chevenard(2). The curve now determined shows the same characteristics as the curves determined by these authors. The coefficient of expansion shows at first a gradual decrease with decrease in nickel content; at about 50 per cent of nickel the value of the coefficient drops rapidly, reaching a minimum value for a composition of about 36 atomic per cent of nickel; it then rises rapidly as the nickel-content is further decreased. In the present instance the curve is shown rising to a value $18{\cdot}2 \times 10^{-6}$ at 28 atomic per cent of nickel. The assumption is made that the boundary γ, $(\gamma+\alpha)$ is situated at 28 atomic per cent of nickel for alloys which have been cooled slowly or quenched from temperatures above 600° C. to room-temperature. Alloy 24 has been found to contain both the α and the γ phases, and the latter if present at room-temperature expands uniformly up to the highest temperature (600° C.) reached in the present investigation. The value of its coefficient of expansion is $18{\cdot}2 \times 10^{-6}$. At 15° C. the region between about 28 and 18·6 atomic per cent of nickel is a duplex region, the latter figure being the composition which contains the saturated α phase. It was found that the coefficient of expansion at 15° C. of the α phase in alloy 24 was $10{\cdot}1 \times 10^{-6}$, which is therefore the coefficient of expansion of the saturated α phase at 15° C. Hence between *C* and *A* in the expansion curve of figure 1 the alloy expands as a mixture of phases, the coefficient of expansion of the saturated pure γ phase being represented by the point *A* and that of the saturated pure α phase by the point *C*. Between *C* and pure iron, the results obtained with alloys reported in part 3 of this paper are shown.

The absolute values of the coefficient of expansion of the γ-phase alloys do not differ greatly from the values given by Guillaume(1). Some difference between the values in the two investigations is to be anticipated because the purities of the materials differ quite appreciably. In Guillaume's work the iron-nickel alloys contained 0·4 per cent of manganese and 0·1 per cent of carbon by weight, whereas in the present work the materials used in making the alloys gave on analysis the following figures:

Nickel. Nickel 99·94, copper 0·008, iron 0·028, carbon 0·011, sulphur 0·004 per cent.

Iron. Iron 99·84, carbon 0·034, sulphur 0·012, manganese 0·10, phosphorus 0·014 per cent, silicon a trace.

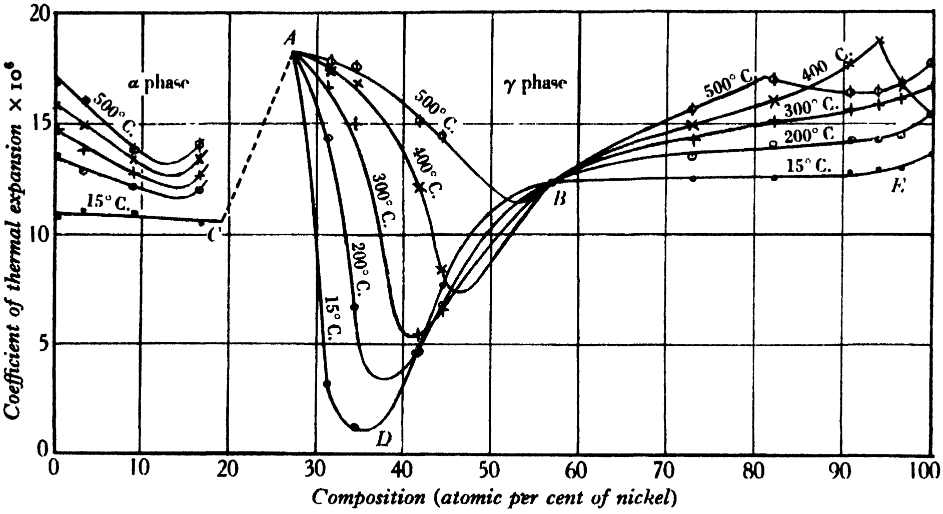

Figure 1. Coefficient of thermal expansion of iron-nickel alloys.

It should be emphasized that the part of the curve representing the coefficient of expansion of the α alloys refers to material which has been brought from high temperature (above about 600° C.) to room-temperature. The shape of the curve might have to be modified, especially in the region *AC*, if the alloys were quenched to temperatures much below atmospheric temperature and then brought up slowly to room-temperature. This point is now being investigated.

§ 2. VARIATION OF THE COEFFICIENT OF THERMAL EXPANSION OF IRON-NICKEL ALLOYS AT VARIOUS TEMPERATURES WITH COMPOSITION

The values of the coefficients of thermal expansion of the alloys examined at various temperatures are plotted against composition in figure 1. The curves are similar in form to those published by Chevenard(2), the differences between the two sets of curves being probably due to the difference between the purities of the alloys used in the two investigations. Since alloy 58 shows a uniform coefficient of expansion over the whole range of temperature investigated, all the curves pass through the point *B*. They all pass also through the point *A*, since the alloy in question expands uniformly over the whole temperature range.

The α alloys also are included in the curves shown in figure 1. These curves might need modification if a different heat treatment were given to the alloys. As the nickel-content increases the coefficient of expansion of the α alloys diminishes, and it reaches a minimum value at a composition which corresponds to a lower percentage of nickel the higher the temperature. When still more nickel is added the value of the coefficient of thermal expansion increases. At 15° C. it increases to $18{\cdot}2 \times 10^{-6}$, the value corresponding to the point *A*. How the other curves converge to this point will be decided when further measurements on alloys in the region *CA* have been carried out. Pure iron-nickel alloys containing respectively 20 and 25 per cent of nickel should have at 15° C. coefficients of thermal expansion of about $11{\cdot}5 \times 10^{-6}$ and 16×10^{-6} when measurements are made on rods of the materials in the usual way. But as has already been stated the material has to be submitted to suitable heat treatment in order that the two phases may be obtained in equilibrium at room-temperature before measurements are made at higher temperatures.

§3. CONCLUSION

The agreement of the results obtained by Guillaume and by Chevenard with those recorded in this paper is closer than had been expected in view of the fact that the alloys used by them contained more manganese and carbon than was contained in the alloys considered in this paper.

§4. ACKNOWLEDGEMENTS

The authors are glad of this opportunity to record their indebtedness to the Research and Development Department of the Mond Nickel Company for their assistance in supplying material to carry out the investigation, and particularly to Dr L. B. Pfeil for his interest throughout the investigation and his readiness at all times to supply information concerning the method of preparation and the heat treatment of the alloys. They also wish to thank the National Physical Laboratory for a sample of pure iron.

REFERENCES

(1) GUILLAUME. *Proc. phys. Soc.* **32**, 374 (1920).
(2) CHEVENARD. See reference (5) on p. 322 of this volume.

REVIEWS OF BOOKS

Radioactivité, by MADAME PIERRE CURIE. Pp. 563, 168 figs. (Paris: Hermann et Cie., 1935.) Price 150 fr.

This voluminous and comprehensive volume on radioactivity was begun by Mme Curie a few years before her death. The book had indeed reached the proof stage, and it has clearly been a labour of love for her distinguished daughter and son-in-law, Irene Joliot-Curie and her husband Frederic Joliot, to complete the work and so pay their tribute to a great woman whom the scientific world had delighted to honour.

That world will be well content too to accept such a book written under such auspices, and we need only mention that there are some 29 chapters dealing authoritatively with, among other matters, ionization, cathode rays, positive rays, X rays, alpha rays, beta rays, gamma rays, artificial radioactivity, and much besides. In accordance with the French custom there is no index, a major omission in a book covering so much ground. There are two excellent portraits of Mme Curie and her husband Prof. Pierre Curie, who predeceased her by many years as the result of a lamentable traffic accident in Paris.

Elements of Nuclear Physics, by F. RASETTI. Pp. xiv+327. (London: Blackie and Son, Ltd., 1937.) Price 18*s*. 6*d*.

Prof. Rasetti is a master of his subject and an able expositor of it. His introductory chapters on radioactivity and on the physics of the various radiations emitted are models of conciseness and clarity. His chapters on the general properties of nuclei and on the artificial disintegration of the elements are almost equally good. The more theoretical portions of the book, though good in their own way, seem, at any rate to a physicist, to be aimed at a different class of reader. Thus, while the author is at pains to explain the distinction between alpha, beta and gamma rays, references to Bose and Fermi statistics, to Schroedinger waves, and to Dirac's relativistic theory are assumed to need little or no explanation. Though, in general, mathematical results are quoted without proof, in some cases the full analysis is included. The book is thus very uneven in the demands which it makes upon the previous knowledge of the reader.

In spite of this it can be recommended. The author has a clear and interesting style, and marshals his extensive material well. The value of the work is increased by numerous tables and diagrams which together afford an excellent summary of the present state of knowledge in the subject. Readers who find the more mathematical portions of the book beyond their scope, or outside their interest, can exercise the reader's prerogative and skip them.

J. A. C.

A Complete Physics written for London Medical Students and General Use, by W. H. WHITE. Pp. viii+850. (London: Richard Clay and Sons, Ltd.) Price 15*s*. net.

Firstly, congratulations to Mr White, as publisher, on the production of a 900-page text-book, of excellent format and fount of type, at a very reasonable price.

This book was published rather over a year ago and now, after some considerable experience of its use by medical students and of its help to one of their teachers, the latter can wholeheartedly express his appreciation of the merits of a handbook on Physics in which emphasis is so clearly and definitely laid on the broad and liberal outlook to be gained by those who study Natural philosophy for its own sake. The book amply covers the purposely restricted syllabus laid down for preliminary medical examinations, and not only the medical student (Mr White's first love) but all other students will find great help from the study of the numerous answers to examination questions. However, in a review that will not be read by many students of medicine it is evidently more appropriate to refer to, and to emphasize, the completeness of the treatment of the subject matter for the use of the general reader. For this nought but the highest encomiums can be offered to the author.

Here we have all the rudiments of physics and Mr White asks—"Can these bones live?" The reply must surely be that the spirit of natural philosophy has imbued the author so plenteously that what might have remained mere osseous relics are here made to stand upon their own feet, to live and to be an exceedingly great army- the whole house of physics. The felicitous treatment of such diverse subjects as meteorology and the thick lens, the inclusion of accounts of the Shortt clock and the copper-oxide rectifier, the many novel illustrations, from that of the tiddlers and the bread (Brownian motion) to propeller troubles (electrolytic corrosion) and many more features might be instanced in order to commend a book which should be in the possession of all.

Mr White's valedictory remarks should be read by all who have to take part in examinations, either as examiners or as examinees.

I end this review in which I have tried to express my own personal gratitude to "good fellow" White by adding that, after using this book for some months, one of my older students told me that for the first time in his life he was *enjoying* a textbook of physics which had a real cultural value.

J. H. B.

Magnetochemie, by W. KLEMM. Pp. xv + 262. (Leipzig: Akademische Verlagsgesellschaft, 1936.) Price M. 18.

The importance of magnetic measurements in deciding points of chemical structure has been increasingly realized in recent years, and the appearance of a book dealing with the subject is very opportune. The volume deals with the classical magnetic theory and methods of measurement in the first part. The second part contains an account of the relations between magnetic moment and atomic theory, in which the deductions of the old and new quantum theories are clearly explained. In this section such matters as quantum numbers and term symbols for atoms and ions receive attention. A thorough discussion of various types of chemical compounds follows, in which numerical results are given in preference to mere symbols, a method of treatment which will commend itself to chemists. The third part of the book illustrates the utility of magnetic measurements in chemistry by the consideration of a large number of typical examples, again from the point of view of arithmetic. Short accounts of Pauling's bond theory and metals and alloys are included in this section. The book is an excellent and intelligible survey of the subject, and can be strongly recommended.

J. R. P.

Instrument Transformers, by B. HAGUE. Pp. xxiv + 656. (London: Pitman and Sons, Ltd.) 35*s*. net.

Comparatively few physicists will require to know more about instrument transformers than that they may provide a more convenient and accurate means of extending the ranges of alternating-current ammeters, voltmeters, and the like, than do shunts and series resistors such as must be used with direct-current instruments. Nevertheless there is a vast amount of published literature concerned with the properties of these instruments and the methods of testing them.

This book presents a digest of all the available information on the subject. To those specially interested it is a work of considerable value, for the author has carried out his laborious task with great thoroughness. The book is quite up-to-date and well arranged, and the subject matter is presented with the skill of an experienced teacher. It may be recommended as a work of reference to all who are interested in precision measurements of current, voltage and power.

L. H.

THE PROCEEDINGS OF THE PHYSICAL SOCIETY

VOL. 49, PART 4 JULY 1, 1937 No. 273

THE SATURATION-DISCRIMINATION OF TWO TRICHROMATS

IMP. AGRI. RES. INST.
31-7-
LIBRARY

BY W. D. WRIGHT, D.Sc., A.R.C.S., D.I.C.

AND

F. H. G. PITT, PH.D., A.R.C.S., D.I.C.

Imperial College of Science and Technology

Received 21 *October* 1936. *Read* 28 *May* 1937

ABSTRACT. Measurements have been made by the authors to determine the values for their own eyes of log $\{(L_W+L_S)/L_S\}$ for the just-noticeable first step from white for a range of spectral colours.

THIS short paper is supplementary to one⁽¹⁾ published in 1935, in which the detailed characteristics of the authors' colour-vision were tabulated. We expressed some dissatisfaction with the data on saturation-discrimination, not because we doubted the accuracy of the measurements but because, when the first step from the spectral locus was measured, each observation was necessarily made in a different part of the colour field, so that the sensitivity of the eye to colour-differences was itself variable. The results thus represented two variables, namely the sensitivity of the eye and the colour valency of the spectral colours, whereas the latter alone should have been measured. It can be effectively isolated if the first step from white is measured rather than the first step from the spectral locus, since the observations will all be made in practically the same part of the colour triangle.

No very simple way of making the measurements with the Wright colorimeter was available at the time, and the less satisfactory step from the spectral locus was measured instead. A straightforward adaptation of the colorimeter has since been devised and the modification and method of observation have been described by Nelson⁽²⁾. The new data obtained in this way for the authors' eyes are shown in figures 1 and 2. The saturation-discrimination has been represented in the conventional manner as log $\{(L_W+L_S)/L_S\}$, where L_S is the luminosity of the spectral colour that has been mixed with white of luminosity L_W to produce the just-noticeable step. A radiation with a small colour valency will thus give a small value of

$\log\{(L_W+L_S)/L_S\}$, and *vice versa.* The steps were measured relative to the white given by the C.I.E. 1931 S_B source, which has a colour temperature of 4800° K.

The general agreement between the authors' curves and the mean curve given

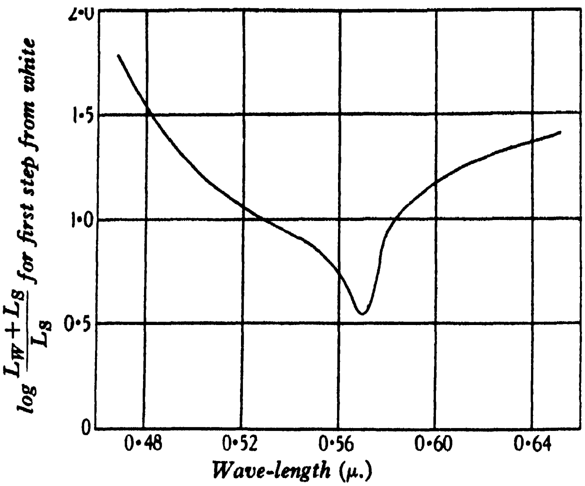

Figure 1. Saturation-discrimination cuive for F. H. G. P.

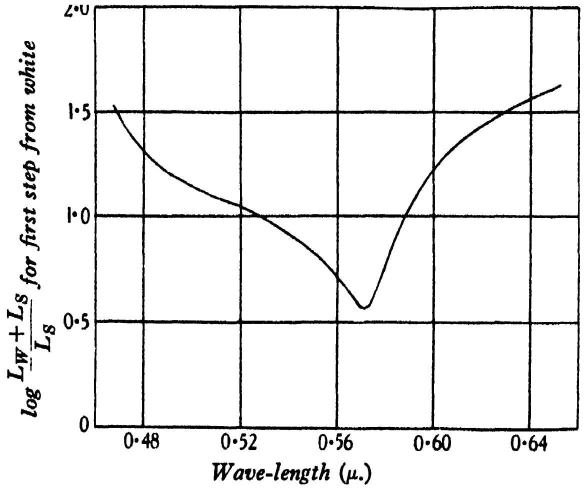

Figure 2. Saturation-discrimination curve for W. D. W.

by Martin, Warburton and Morgan(3) is very good. Undoubtedly the most striking feature is the pronounced minimum shown in all the curves; the very close agreement between one observer and another in the wave-length, about 0·57 μ., at which the minimum occurs, is specially noteworthy.

Saturation-discrimination for F. H. G. P. and W. D. W.

Wave-length λ (μ.)	Saturation-discrimination, $\log \frac{L_W+L_S}{L_S}$		Wave-length λ (μ.)	Saturation-discrimination, $\log \frac{L_W+L_S}{L_S}$	
	F. H. G. P.	W. D. W.		F. H. G. P.	W. D. W.
0·47	1·77	1·48	0·57	0·55	0·58
0·48	1·55	1·32	0·58	0·92	0·75
0·49	1·40	1·22	0·59	1·09	1·02
0·50	1·26	1·15	0·60	1·18	1·21
0·51	1·14	1·09	0·61	1·25	1·35
0·52	1·05	1·04	0·62	1·29	1·43
0·53	0·98	0·98	0·63	1·34	1·51
0·54	0·93	0·92	0·64	1·36	1·57
0·55	0·86	0·83	0·65	1·40	1·62
0·56	0·73	0·72			

REFERENCES

(1) Wright, W. D. and Pitt, F. H. G. *Proc. phys. Soc.* **47**, 205 (1935).

(2) Nelson, J. H., page 332 of this volume.

(3) Martin, L. C., Warburton, F. L. and Morgan, W. J. *Spec. Rep. Ser. Med. Res. Coun.*, Lond., No. 188 (1933).

THE COLOUR-VISION CHARACTERISTICS OF A TRICHROMAT, PART 2

BY J. H. NELSON, A.R.C.S., D.I.C., B.Sc.

Received 21 *October* 1936. *Read* 28 *May* 1937

ABSTRACT. The author's luminosity curve, trichromatic coefficients, mixture curves, complementary wave-lengths and their mixture in terms of luminosity, and the hue- and saturation-discrimination curves have been obtained and the results tabulated.

IN a recent paper by Wright and Pitt(1) the importance of having the complete characteristics of individual observers was pointed out, and they gave the data for their own eyes. In this paper the characteristics of the present author, also a trichromat, are given. The apparatus used for the measurements was the Wright colorimeter, which has been fully described elsewhere(2).

The methods of expressing the results have been dealt with previously, and it is only necessary to repeat them very briefly. The trichromatic coefficients are expressed on the W. D. W. system, in which the primaries are red 0·65 μ., green 0·53 μ. and blue 0·46 μ., and the units are based on two monochromatic matches at 0·5825 μ. and 0·4940 μ. The luminosity is referred to an equal-energy spectrum, the maximum being taken as unity.

The position of the maximum of the luminosity curve for the observer J. H. N. is 0·552 μ., which compares with 0·558 μ. for W. D. W., 0·562 μ. for F. H. G. P., and 0·555 μ. for the standard observer. The position of the standard illuminant B in the colour triangle for the observer J. H. N. lies farther towards the yellow than the normal; this is the reverse of what holds for the observers W. D. W. and F. H. G. P. This indicates a slightly more dense macular pigment than the normal, a conclusion which is further supported by the luminosity curve, which shows a lower luminosity in the blue than those of either W. D. W., F. H. G. P. or the normal.

The complementary wave-lengths have been calculated from the colour triangle, together with the proportions, in luminosity, in which they should be mixed to give the standard illuminant B.

The hue-discrimination for the observer J. H. N. is similar to that for the previous two observers, showing a secondary minimum in the violet, and not in the red.

As has been pointed out by Wright and Pitt, since the saturation-discrimination does not vary very much when measured from the spectral locus, it would be instructive to know the variation of the saturation-discrimination when measured from the white point; the requisite data were therefore obtained by adding a small

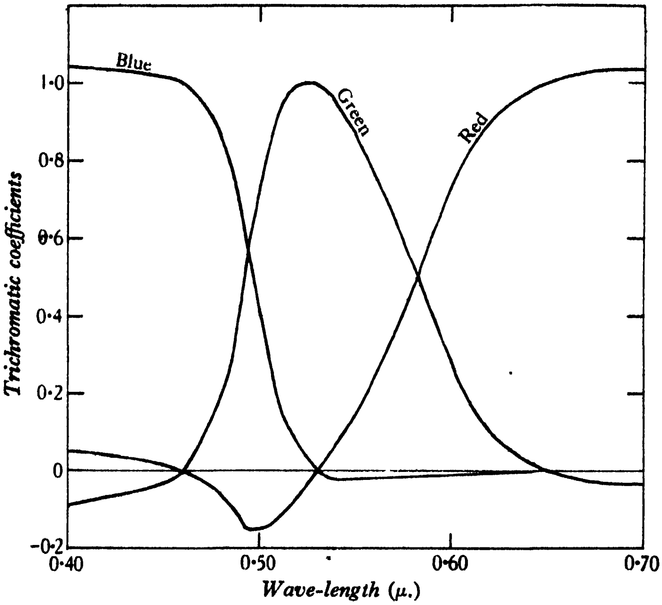

Figure 1. Spectral coefficients.

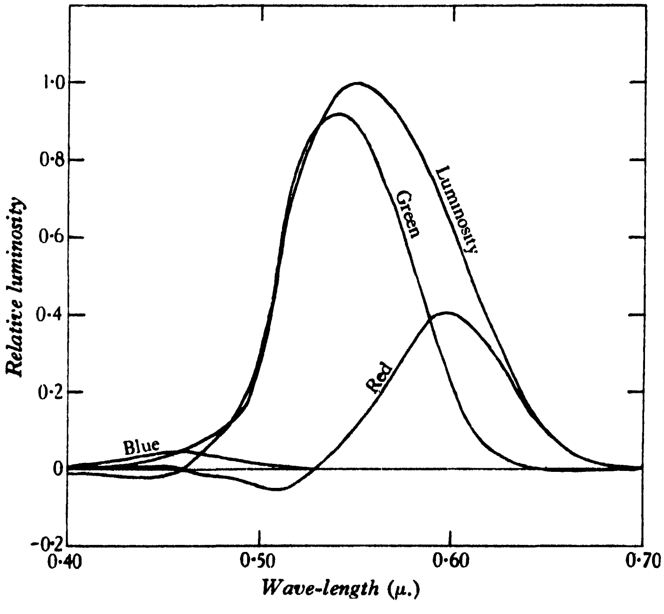

Figure 2. Equal-energy luminosity and spectral mixture curves.

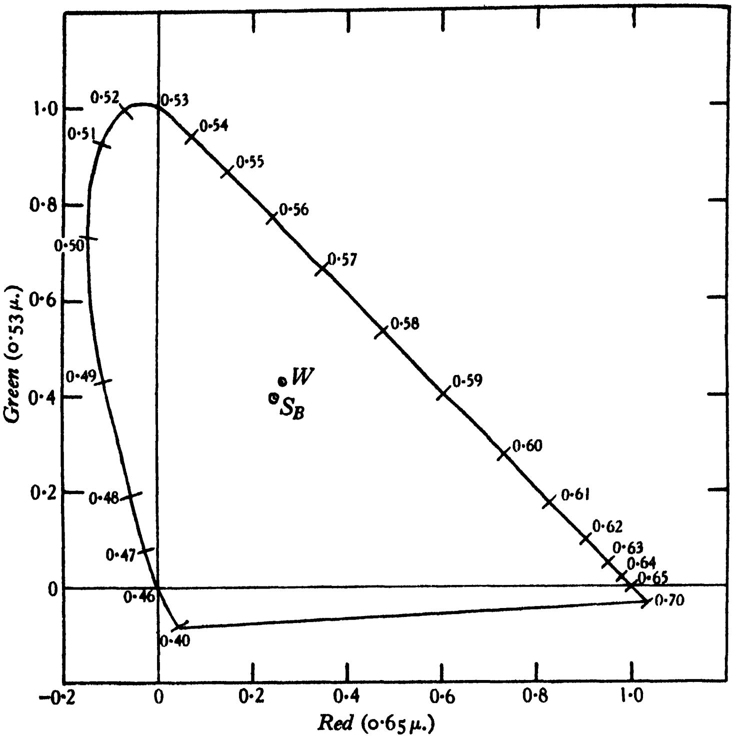

Figure 3. Spectral locus in colour triangle plotted on W. D. W. system. *W*, white point for J. H. N. S_B, white point for standard observer.

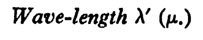

Figure 4. Complementary wave-lengths.

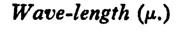

Figure 5. Hue-discrimination.

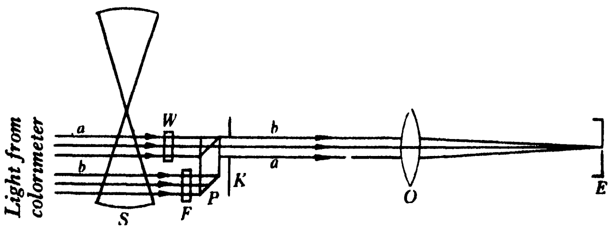

Figure 6. Diagram of optical system for saturation-discrimination.

Colour characteristics for J. H. N.

Wave-length λ (μ.)	Relative luminosity of equal-energy spectrum	Trichromatic coefficients			Mixture curves for equal-energy spectrum			Complementary wave-lengths (μ.)		Luminosity of λ to be mixed with unit luminosity of λ'	Hue-discrimination; just-noticeable wave-length differences (μ.)	Saturation-discrimination, $\log\frac{L_W+L_S}{L_S}$	Wave-length λ (μ.)
		B (0·46μ.)	G (0·53μ.)	R (0·65μ.)	L_B	L_G	L_R	λ	λ'				
0·40	0·0007	1·043	−0·093	0·050	0·0052	−0·0095	0·0038	—	—	—	—	—	0·40
0·41	0·0028	1·038	−0·081	0·043	0·0098	−0·0113	0·0043	0·41	0·5710	0·01006	—	—	0·41
0·42	0·0070	1·033	−0·069	0·036	0·0165	−0·156	0·0061	0·42	0·5712	0·0132	—	—	0·42
0·43	0·0125	1·028	−0·057	0·029	0·025	−0·020	0·0075	0·43	0·5715	0·0164	0·0080	—	0·43
0·44	0·0196	1·023	−0·046	0·023	0·0325	−0·0202	0·0073	0·44	0·5718	0·0195	0·0054	—	0·44
0·45	0·0270	1·018	−0·035	0·017	0·0404	−0·0204	0·007	0·45	0·5722	0·0227	0·0048	—	0·45
0·46	0·0468	1·000	0·000	0·000	0·0468	0·000	0·000	0·46	0·5729	0·0345	0·0054	—	0·46
0·47	0·075	0·951	0·076	−0·027	0·039	0·051	−0·015	0·47	0·5750	0·0676	0·0032	—	0·47
0·48	0·109	0·862	0·194	−0·056	0·030	0·099	−0·020	0·48	0·5780	0·137	0·0018	1·125	0·48
0·49	0·150	0·683	0·430	−0·113	0·018	0·162	−0·031	0·49	0·5894	0·386	0·0016	1·08	0·49
0·50	0·274	0·412	0·736	−0·148	0·012	0·306	−0·044	—	—	—	0·0021	1·04	0·50
0·51	0·528	0·190	0·930	−0·121	0·008	0·575	−0·055	—	—	—	0·0027	0·995	0·51
0·52	0·763	0·070	0·998	−0·068	0·004	0·797	−0·038	—	—	—	0·0031	0·96	0·52
0·53	0·890	0·000	1·000	0·000	0·000	0·890	0·000	—	—	—	0·00315	0·916	0·53
0·54	0·973	−0·020	0·945	0·075	0·000	0·921	0·052	—	—	—	0·0029	0·85	0·54
0·55	0·998	−0·019	0·868	0·151	0·000	0·888	0·110	—	—	—	0·0024	0·78	0·55
0·56	0·978	−0·018	0·776	0·242	0·000	0·801	0·177	—	—	—	0·0018	0·65	0·56
0·57	0·928	−0·014	0·664	0·350	0·000	0·677	0·249	—	—	—	0·00135	0·475	0·57
0·58	0·850	−0·008	0·534	0·474	0·000	0·515	0·335	0·4838	0·58	0·204	0·00105	0·76	0·58
0·59	0·753	−0·007	0·404	0·603	0·000	0·356	0·397	0·4909	0·59	0·428	0·0009	0·93	0·59
0·60	0·625	−0·007	0·277	0·730	0·000	0·221	0·404	0·4940	0·60	0·707	0·0008	1·03	0·60
0·61	0·491	−0·006	0·178	0·828	0·000	0·114	0·377	0·4958	0·61	0·983	0·0009	1·150	0·61
0·62	0·371	−0·006	0·101	0·905	0·000	0·051	0·320	0·4967	0·62	1·18	0·0012	1·245	0·62
0·63	0·261	−0·004	0·052	0·952	0·000	0·019	0·242	0·4973	0·63	1·33	0·0018	1·33	0·63
0·64	0·173	−0·002	0·022	0·980	0·000	0·005	0·168	0·4975	0·64	1·42	0·0028	1·435	0·64
0·65	0·094	0·000	0·000	1·000	0·000	0·000	0·094	0·4976	0·65	1·51	0·0044	1·485	0·65
0·66	0·048	0·000	−0·022	1·022	0·000	−0·001	0·049	—	—	—	—	1·54	0·66
0·67	0·023	0·000	−0·030	1·030	0·000	−0·0009	0·0239	—	—	—	—	1·62	0·67
0·68	0·013	0·000	−0·031	1·031	0·000	−0·0008	0·0138	—	—	—	—	1·66	0·68
0·69	0·0085	0·000	−0·032	1·032	0·000	−0·0005	0·0090	—	—	—	—	1·72	0·69
0·70	0·0059	0·000	−0·033	1·033	0·000	−0·00028	0·00618	0·4979	0·70	1·62	—	1·75	0·70
1931 C.I.E. source S_B		0·307	0·431	0·262	Relative luminosities of trichromatic units of primaries								
λ=0·4940μ.		0·572	0·572	−0·144	0·46μ.	0·53μ.	0·65μ.						
λ=0·5825μ.		−0·008	0·504	0·504	0·068	1·000	0·711						

quantity of spectral colour to white (standard illuminant B). For this purpose it was necessary to make some additions to the apparatus, the optical system necessary in addition to the colorimeter being shown in figure 6. A brass sector *S*, coated with magnesium oxide, is illuminated by the light from a lamp as specified by the C.I.E. (1931) for standard illuminant B(3). The sector is arranged so that both halves of the photometric field in the prism *P* are filled with white light during one half of the revolution, and that during the other half of the revolution a monochromatic radiation of known wave-length is admitted to the top half of the field, forming beam *b*. This monochromatic radiation is obtained from the spectrum supplying the instrument primaries, and the intensity is controlled by a calibrated photometer wedge. The intensity of the white in the top half of the field (beam *b*) may be controlled by neutral filters *F*, but it is advisable to use only the lightest filters as the darker ones may deviate somewhat from neutrality. In the lower half of the field the intensity of the white forming beam *a* is controlled by a very shallow photometer wedge. The sector is arranged to run at two speeds. The fast speed is fast enough to remove flicker and thus provide two uniform fields, a white *a* and a white-plus-monochromatic *b*, between which a saturation step may be made. At the slow speed the intensities of the white and the monochromatic radiation can be compared by means of flicker.

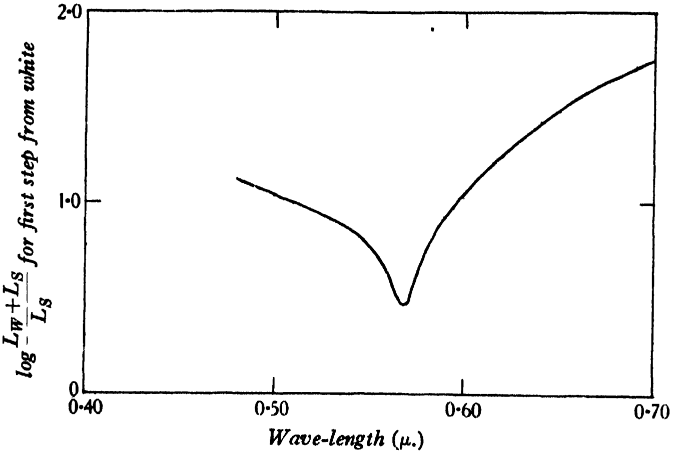

Figure 7. Saturation-discrimination.

When the observations are being taken the sector is first run slowly, and the observer is asked to equate the intensities of the white and the monochromatic radiation by adjusting the intensity of the latter so that flicker may be removed. The sector is then run fast, and the observer is asked to adjust the intensity of the monochromatic radiation until he can just notice a difference in colour between the top and bottom halves of the field, the intensities of both halves being kept the same by adjusting the intensity of the white of the bottom half of the field. In this way the intensity of monochromatic radiation to be added to the white to make one step can be found. If L_W is the intensity of the white and L_S that of the added monochromatic radiation, then the saturation step can be expressed as the logarithm of the ratio $(L_W+L_S)/L_S$. When this fraction is large, only a small quantity of monochromatic radiation is needed to cause a just noticeable change in colour.

The measurements of saturation-discrimination taken by this method may be compared with the results obtained by Martin, Warburton and Morgan⁽⁴⁾. The curve given in the present paper falls below that given by them in the blue-green region, but its general shape is the same.

The author wishes to thank Dr W. D. Wright for his help, and the Medical Research Council for their financial assistance.

REFERENCES

(1) Wright, W. D. and Pitt, F. H. G. *Proc. phys. Soc.* **47**, 205 (1935).
(2) Wright, W. D. *Trans. opt. Soc.*, Lond., **29**, 225 (1927–8).
(3) Smith, T. and Guild, J. *Trans. opt. Soc.*, Lond., **33**, 73 (1931–2).
(4) Martin, L. C., Warburton, F. L. and Morgan, W. J. *Spec. Rep. Ser. Med. Res. Coun.*, Lond., No. 188 (1933).

DISCUSSION

Mr J. Guild. Papers of this kind, giving full details of the colour-vision of individual observers, are of great value. One of the main difficulties in correlating the data on colour-vision accumulated in the past has been due to the fact that the various functions—visibility, colour-matching, hue-discrimination, etc.—have usually been determined by different people using different apparatus and standards. From the point of view of providing knowledge of the visual processes it is much more important to have comprehensive information about a few people than to have a little information about many people. If the programme followed at the Imperial College provides us with one or two more individual studies of this kind it will be of great value. I note that the evidence of this paper and of the former paper by Wright and Pitt goes to show that the wave-length of maximum visibility is on that side of the value 0·555 μ. of the C.I.E. standard visibility function which corresponds to the departure from normality in macular pigmentation, as is indicated by the position of the white point on Dr Wright's form of the colour diagram. This confirms that the standard value must be fairly nearly correct for normal observers, despite the fact that this view has recently been called in question.

THE EFFECT OF SECONDARY BETA RADIATION ON GAMMA-RAY MEASUREMENTS MADE IN AIR

By C. W. WILSON, M.Sc., Physics Dept., Westminster Hospital Annexe, London

Received 6 *January* 1937. *Read* 12 *March* 1937

ABSTRACT. A sensitive method of measuring small ionization currents is described, and the effect of secondary beta radiation upon ionization measurements of gamma radiation is examined. It is shown that if ionization chambers made of light-atom materials have walls less than 4·0 mm. thick, secondary beta radiation is recorded so that readings are in excess of the true values. The results explain some discrepancies found by other workers.

§ 1. INTRODUCTION

FOR the evaluation of the gamma-ray dosage in experiments on the biological effects of gamma radiation it is often necessary to make ionization measurements in air at small distances from radium sources. The literature shows that measurements made in air in the vicinity of radium sources may give values that differ widely from what might have been expected. Spear and Grimmett(1) for example found that the intensity-values due to a one-gramme radium source were consistently 24 per cent higher than the values obtained by calculation. They measured the intensities in air at distances of from 3 to 8 cm. from the radium with condenser chambers of the Sievert pattern(2) which were constructed of elektron metal and had walls 1·0 mm. thick. Similarly Benner(3) found that for distances of from 3 to 14 mm. from a radium source, the intensity-values measured in air with ionization chambers having walls of elektron metal and brass respectively, of thickness 0·3 mm., were always considerably (14 per cent or more) in excess of those calculated.

The purpose of this paper is to describe some experiments which show that the discrepancies referred to can be ascribed to secondary beta radiation from the metal filters of the radium sources. If the chamber wall is sufficiently thin such radiation can enter the air volume of the chamber and add considerably to the ionization produced by gamma radiation. On the other hand, if the wall be thickened by the necessary amount no secondary beta radiation will be recorded.

§ 2. APPARATUS AND METHODS

The ionization chamber and current-measuring system that formed the main part of the apparatus are shown diagrammatically in figure 1. The ionization chamber was of the thimble type and made of elektron metal with a wall 0·5 mm.

thick. Its air volume was 1·31 cm.^{3} The lead from the graphite inner electrode of the chamber is carried to the Lindemann electrometer on a number of polished amber buttons through an air-tight brass tube that is continuously evacuated to avoid ionization losses. The tube also serves as an earthed screen for the lead.

For measuring ionization currents a null method is used, the potential across the capacity *C* being continuously increased to maintain the needle of the instrument at earth potential. The processes of isolating and earthing the electrometer needle start and stop the stop watch incorporated in the circuit, figure 1, so that the time taken for a measured change of potential is automatically recorded. If ionization currents are to be compared, the potential-change per second is a suitable measure. If the capacity *C* is known an absolute determination of the current can be made. Thus with a graphite ionization chamber the apparatus serves as an X-ray dose-meter. This, in fact, is its routine use. The auxiliary circuit *A*, figure 1, is solely for the purpose of providing an easy control upon the sensitivity and zero setting of the electrometer$^{(4)}$.

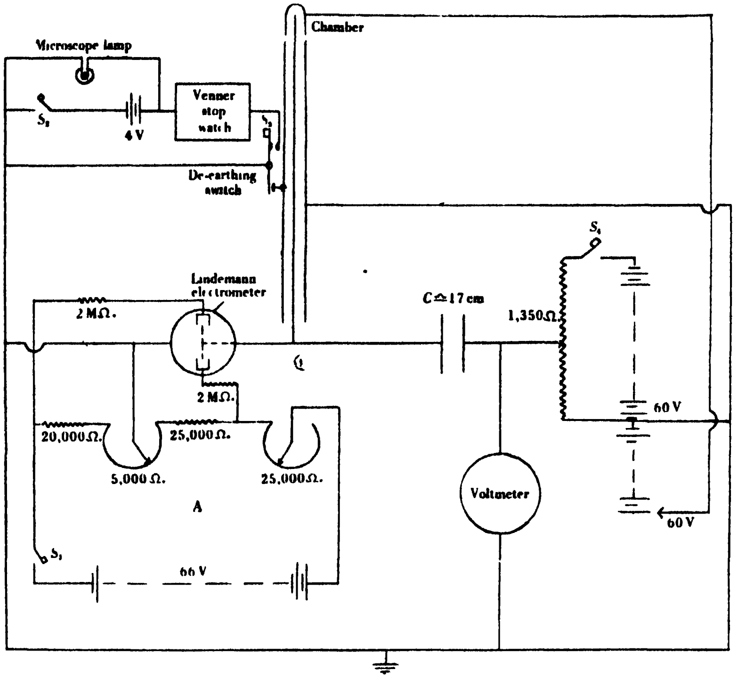

Figure 1. Arrangement for measuring ionization currents.

The construction and mounting of the ionization chamber is shown in figure 2, which also illustrates how the radiation source was set up relative to the chamber. The lead to the electrode is carried through an amber plug which is highly polished and waxed into the brass tube to form an air-tight joint. The thimble fits tightly over the shoulder on the amber plug. The source of gamma rays consists of radon in glass capillaries which are contained in a platinum tube with a wall 0·5 mm. thick.

The latter is sufficient to absorb all primary beta radiation. In all the experiments the source and ionization chamber were arranged parallel to one another and the source was mounted in a holder attached to the evacuated lead. Thus, if any movement of the lead and its chamber occurred, the distance between the source and the chamber did not change.

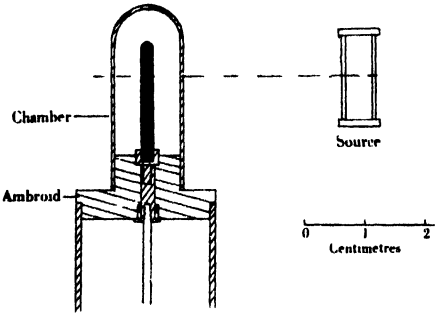

Figure 2. Dispositions of ionization chamber and radon source.

A series of sheaths of various thicknesses were made in elektron metal to fit tightly over the original chamber so that the wall-thickness of the chamber could be increased from 0·5 mm. up to 6·0 mm. as required.

§ 3. EXPERIMENTS

The effect of large metal filters upon the ionization recorded in chambers with walls of various thicknesses. For this experiment two circular metal discs were used as secondary filters. These were of copper and lead respectively. Each was 5·0 cm. in diameter and 0·5 mm. thick. When added to the arrangement shown in figure 2 they were placed between the source and the chamber so that the source was in contact with the centre of the filter. The distance between the centres of the source and chamber was 3·0 cm.

A series of measurements of the ionization current were made under three sets of conditions, (*a*) with no extra filter present, (*b*) with the copper filter added and (*c*) with the lead filter added. For each set of conditions readings were taken for different thicknesses of the wall of the chamber. Alternate records were taken in order to allow for decay of the radon source during the period of the experiment. Figure 3 shows the results expressed in graphical form.

It is seen that when the chamber wall is only 0·5 mm. thick the introduction of the metal filter causes the ionization to increase very markedly in spite of the absorption of gamma radiation that must occur. This increase is about 19 per cent for the copper sheet and as much as 32 per cent for the sheet of lead.

Two distinct types of results are obtained according to whether the large secondary filters are included or not. When no filter is added the ionization in the chamber increases with increase in wall-thickness up to a maximum value when the wall is about 2 mm. thick, after which a slow fall takes place. When either the copper or lead filter is included, the ionization decreases continuously with increasing wall-thickness. Such a result as the latter is to be explained in terms of a strong secondary beta radiation from the filters, which augments the ionization for the smallest wall-thickness and is progressively absorbed as the wall-thickness is increased. Finally the results obtained with the filters present are lower than those with no filter, in consequence of absorption of the primary gamma rays in the filters. The preliminary rise in the curve expressing the results with no filter added is due to extra ionization by recoil electrons liberated from the thickened wall of the chamber. This question has received considerable attention from Mayneord and Roberts⁽⁵⁾.

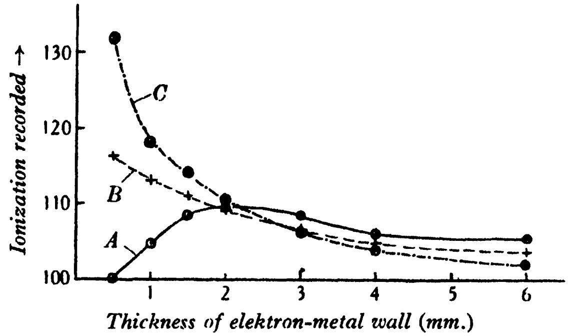

Figure 3. Showing how the current in an ionization chamber is affected by secondary radiation from a metal filter. *A*, no filter included; *B*, copper filter included; *C*, lead filter included.

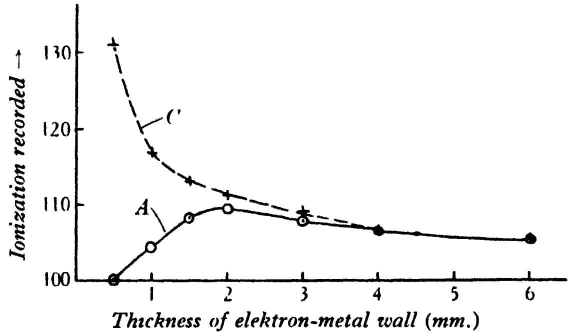

Figure 4. Showing the elimination of the effects of secondary beta radiation by increasing the wall-thickness of the ionization chamber. *A*, no filter included; *C*, lead filter included.

As is to be expected from the work of Stahel⁽⁶⁾, the amount of secondary beta radiation liberated from the lead sheet is very much greater than that from the copper sheet.

The wall-thickness that absorbs all secondary beta radiations from metal filters. In this experiment the same lead filter was used as before but a hole was cut at its centre having exactly the shape and size of the platinum tube that contained the radon source. Thus when the filter was placed in position as in the first experiment no absorption of primary gamma radiation occurred in it. The distance between the source and ionization chamber was 3·0 cm. as before.

Measurements were made of the ionization current within the chamber with and without the filter for the range of wall-thicknesses 0·5 mm. to 6·0 mm.; the results obtained are expressed graphically in figure 4. It is seen that when the chamber wall has a thickness of 4·0 mm. or more, the ionization recorded is not changed by the addition of the filter. Thus all secondary beta radiation is absorbed in the wall of the ionization chamber if its thickness is 4·0 mm. or more. Therefore any ionization chamber of light-atom material that is used for measuring gamma radiation in air is liable to record secondary beta radiation from nearby metal parts if its walls are not at least 4·0 mm. thick.

It seems then that the excess values found by Spear and Grimmett(1) were due to the fact that their ionization chambers had elektron metal walls only 1·0 mm. thick, while a large disc of brass was used as the primary radium filter. To confirm this result a further experiment was carried out.

Comparison of readings made with thin-walled and thick-walled ionization chambers when the large brass disc used by Spear and Grimmett is present. The actual brass filter, 10 cm. in diameter and 2·3 mm. thick, used by Spear and Grimmett was available, and an aperture was cut in it in exactly the same manner as in the case of the lead sheet used in the second experiment. It was therefore possible to add this in the same way to the arrangement already described (figure 2) without absorbing any primary gamma radiation.

Readings were made of the ionization currents with and without the brass disc in position, an elektron-metal ionization chamber with walls (*a*) 1·0 mm. thick and (*b*) 4·0 mm. thick being used. The results are summarized in the table for various distances between the source and chamber, in terms of the ratio of the readings obtained with and without the disc for the two wall-thicknesses.

Table. Comparison between readings obtained with thin-walled and thick-walled ionization chambers

Distance between source and ionization chamber	$\frac{\text{Ionization with brass disc}}{\text{ionization with no brass disc}}$	
	1·0-mm. wall	4·0-mm. wall
2·24 cm.	1·083	1·000
3·00 ,,	1·105	1·012
3·96 ,,	1·130	0·985
5·08 ,,	1·140	1·000
6·03 ,,	1·162	1·008
7·00 ,,	1·144	1·004

These results show that when the wall of the ionization chamber is only 1·0 mm. thick, the brass disc adds from 8 to 16 per cent to the ionization recorded, whereas if the wall is 4·0 mm. thick the presence of the brass does not affect the result within the experimental error. In the experiments of Spear and Grimmett the disc would serve as an even more efficient radiator, since the radium was spaced round a circle 8·0 cm. in diameter so that more of the metal surface was exposed to its action.

§ 4. DISCUSSION OF RESULTS

If satisfactory measurements of gamma radiation are to be made in air with ionization chambers of light-atom materials in the vicinity of radium sources, the walls of the chamber must be at least 4·0 mm. thick in order to avoid excess ionization by secondary beta radiation. It would therefore appear to be impracticable to make reliable measurements of gamma radiation at distances less than 4·0 mm. from a radium source. It is very likely that the calculated values of intensity given by Spear and Grimmett(1) are more nearly correct than those obtained by measurement.

§ 5. ACKNOWLEDGEMENTS

The author wishes to acknowledge his indebtedness to Mr N. H. Pierce for his assistance with the experiments, and to the British Empire Cancer Campaign whose financial support has helped make it possible to carry out the work.

REFERENCES

(1) Spear, F. G. and Grimmett, L. G. *Brit. J. Radiol.* **8**, 231 (1935).
(2) Sievert, R. M. *Acta Radiol.*, Stockh., Supplementum **14** (1932).
(3) Benner, S. *Acta Radiol.*, Stockh., **15**, 85, p. 291 (1934).
(4) Grimmett, L. G. *Proc. phys. Soc.* **45**, 117 (1933).
(5) Mayneord, W. V. and Roberts, J. *Brit. J. Radiol.* **7**, 158 (1934).
(6) Stahel, E. *Strahlentherapie*, **44**, 575 (1932).

DISCUSSION

Mr W. Binks. It is now well known that in order to measure gamma radiation by an ionization method, the walls of the measuring-chamber should be thick enough to prevent extraneous primary and secondary beta radiation from entering the air cavity—that is to say, the thickness of the chamber-wall should not be less than the range of the fastest beta particles in the material of which the wall is composed. In this connexion I would like to draw the author's attention to a number of papers published in recent years by Friedrich, Schulze and Zimmer, Glasser, Mayneord and Roberts and by Kaye and myself. In the case of chambers having walls thinner than the beta-ray range the ionometric conditions are somewhat complex, the measured ionization depending upon the particular experimental arrangement adopted. For example, it seems to depend not only on the material and thickness of the filter but on the latter's position—that is, on whether the filter is near the radium or near the chamber. Further, it depends on the size and shape of the source and chamber and on the distance between them.

The observations of Friedrich and Schulze (1935) on the effects of different filters (0·1 mm. platinum, 0·3 mm. platinum plus 1·5 mm. brass, and 6·6 mm. lead) would appear to contradict those of Mr Wilson, but it should be noted that the sources and chambers and their distances apart were different in the two cases. Thus the ionization measured by means of chambers having too thin walls is dependent upon the distribution of the primary and secondary beta radiation at the location of the chamber, the curves shown by Mr Wilson representing a particular example of this phenomenon.

I agree with the author that it would be impracticable to make reliable measurements of gamma radiation at distances from the source less than the range of the beta particles. But it would seem that when considering the biological effect of the radiations from radium one ought to take into account the beta radiation as well as the gamma radiation received by the tissue. In certain locations, for instance in the case of tissue adjacent to a radium needle or that of the superficial layers of tissue of a patient who is irradiated from an external radium source, the secondary beta radiation has an important bearing on the total energy absorbed by the tissue. It is doubtful, therefore, whether the calculated gamma-ray intensities at distances less than 4 mm. from a radium source give even an approximate idea of the actual energy absorbed. For these distances it would be better to use ionization chambers of appropriate wall-thickness.

AUTHOR'S reply. I was quite aware of the fact that other workers had dealt with the problem of secondary beta radiation, but it was just this particular example of the phenomenon with which I was concerned. The work done by Spear and Grimmett was carried out in this laboratory, and since it dealt with an important biological effect that occurred for a specific gamma-ray intensity, it was essential to know the value of the latter. The experiments I have described seem to show which of the intensity-values published by Spear and Grimmett was correct, and for this reason they appeared to be worth recording.

ON THE OPTICAL CONSTANTS OF ALLOYS OF THE COPPER-ZINC SYSTEM

By H. LOWERY, Ph.D., D.Sc., F.Inst.P., Principal of the North-Western Polytechnic, London; H. WILKINSON, M.Sc.Tech., and D. L. SMARE, M.Sc.Tech., College of Technology, Manchester

Received 13 *February* 1937. *Read* 9 *April* 1937

ABSTRACT. Values of the optical constants (refractive index, reflection coefficient and absorption coefficient) are given for some alloys of the copper-zinc system (α, β and γ brass) over the range λ 4358 to λ 6800, as determined by the method of Drude. Curves showing the variation in the optical constants with composition for particular wave-lengths of light are also shown.

§ 1. INTRODUCTION

In continuation of an experimental investigation on the optical constants of some simple binary alloys (1), the present paper is concerned with dispersion-measurements in the visible region of the spectrum for the copper-zinc system.

This system is interesting from an experimental point of view on account of the extension of the absorption band of copper into the visible, resulting in the very distinct colour-variation in alloys in the α phase. From the red of pure copper the colour changes gradually to the typical yellow of brass at the end of the α phase (39 per cent by weight of zinc). The narrow β phase (46·5 to 49·6 per cent of zinc) again shows the red of copper, and from 60 to 69 per cent of zinc we have the extremely hard, brittle, silvery γ phase.

Measurements of the optical constants of alloys in each of these three phases have been made, though the main part of the work has been concerned with the α phase. An attempt has been made to obtain dispersion curves over the range λ 4358 to λ 6800 for a number of specimens of varying composition, and to obtain curves showing the variation in the optical constants with composition for particular wave-lengths of light.

§ 2. EXPERIMENTAL DETAILS

The general arrangements of the apparatus and method used, essentially that of Drude, have been fully described in previous papers. A parallel beam of light, plane-polarized at an azimuth of 45° to the vertical, is incident at an angle θ on a polished specimen of the alloy mounted vertically. The reflected elliptically polarized light is analysed by a Soleil-Babinet compensator, measuring the phase-difference Δ between the horizontal and vertical components of the beam, and an analysing Nicol prism fitted with a half shade to measure the azimuth ψ of the restored plane-polarized light.

From the measured quantities θ, Δ and ψ the refractive index n and the absorption coefficient K are calculated from the following equations, due to Drude:

$$\begin{aligned}
\tan Q &= \sin\Delta \tan 2\psi,\\
\cos 2P &= \cos\Delta \sin 2\psi,\\
S &= \sin\theta \tan\theta \tan P,\\
A &= S^2 \cos 2Q + \sin^2\theta = n^2 - K^2,\\
B &= S^2 \sin 2Q \qquad\qquad = n^2 + K^2,\\
2n^2 &= \sqrt{(A^2+B^2)} + A,\\
2K^2 &= \sqrt{(A^2+B^2)} - A.^*
\end{aligned}$$

The reflecting-power at normal incidence is given by

$$R = \frac{n^2+K^2+1-2n}{n^2+K^2+1+2n} \times 100 \text{ per cent.}$$

In view of the decay in the measured phase-difference Δ with exposure, corrections have been applied to this constant throughout the work in this paper. The corrections were applied to the compensator scale readings from observations taken at intervals during the experiments. All values of Δ given in the tables were calculated from these corrected compensator readings.

Preparation of the specimens. The copper specimens used were prepared from clean electrolytic copper, melted and allowed to solidify in vacuo. The brasses were prepared in air in an induction furnace. Electrolytic copper was first melted and the zinc, comprising B.D.H. zinc sticks As.T., was dropped into the melt in small pieces, each wrapped in paper to retard volatilization and ignition until the zinc was submerged. By using an excess of zinc to compensate for the loss in melting, alloys of approximately the desired compositions were obtained. The alloys cast cleanly into iron moulds and were quite free from pinholes.

Chemical analysis of the specimens gave the percentages by weight of copper shown in the table.

Composition of specimens

Specimen number Phase	1 α	2 α	3 α	4 α	5 α	6 β	7 γ	Extra specimen, α phase
Weight of copper (per cent)	93·42	91·09	87·60	80·60	74·61	52·85	32·75	86·12
Weight of zinc (per cent) by difference	6·58	8·91	12·40	19·40	25·39	47·15	67·25	13·88
Atomic percentage of zinc	6·42	8·67	11·92	18·98	24·85	46·45	66·63	13·56

---

* The imaginary dielectric constant ϵ occurring in dispersion theory of metals is written $\epsilon=(n-iK)^2$, where n and K are as above. Drude used $\epsilon=n^2(1-ik)^2$ so that his absorption coefficient $k=K/n$.

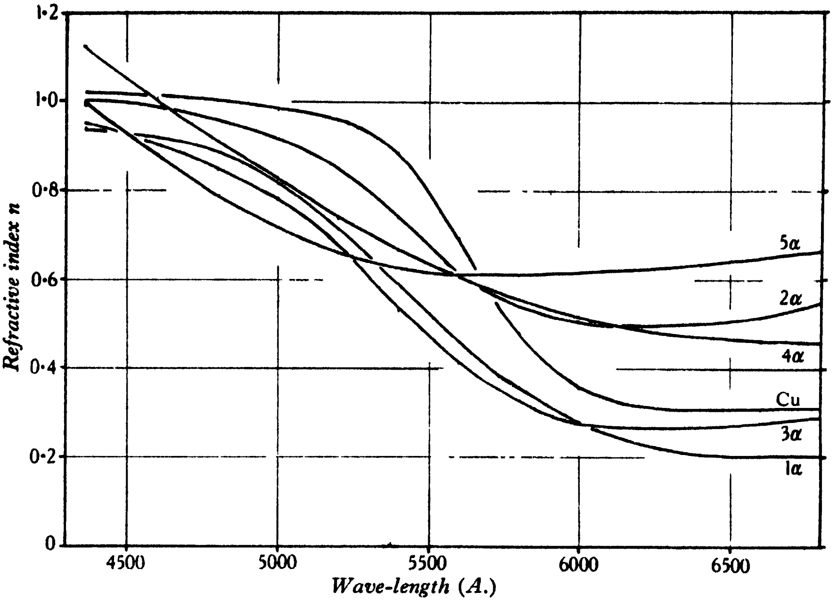

Figure 1.

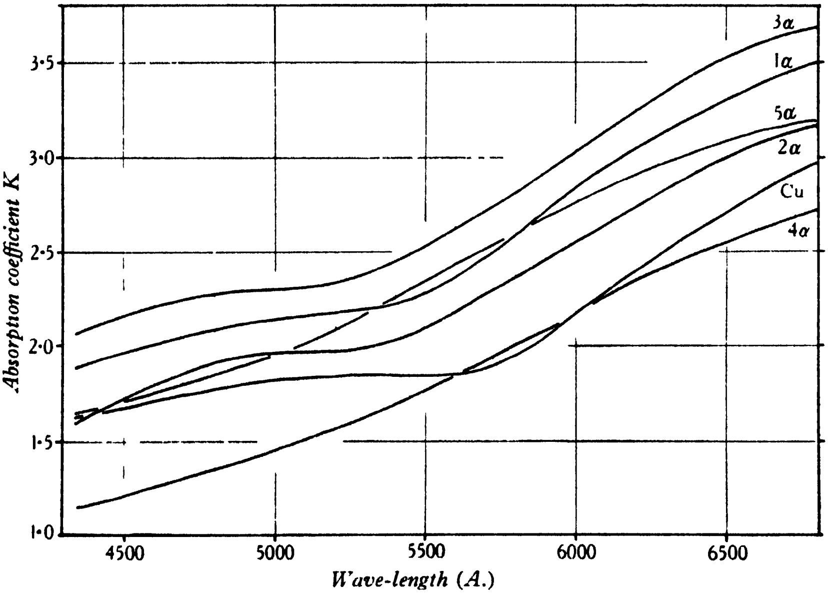

Figure 2.

Micrographic examination of the specimens revealed a cored structure in the α specimens. This was removed by annealing at 580° C. for 40 hours.

The mirror surfaces were prepared, after a preliminary grinding with a 0000 grade of emery paper, by polishing on Selvyt cloth with magnesia. The values of the optical constants for each specimen for a range of wave-lengths in the visible spectrum are plotted against wave-length in figures 1 to 4.

§ 3. DISCUSSION

Though the variation of the constants with wave-length for individual specimens yields smooth curves in every instance, there is no correlation between dispersion curves for specimens of different composition. Attempts to select, for given wave-lengths, series of values of the constants from the dispersion curves, figures 1 and 2, and to plot these against composition result in curves entirely devoid of any distinct form. This lack of coherence is a consequence of differences in the polished surfaces; results of this kind illustrate the difficulties attendant upon the study of the optical properties of an alloy system. If the constants determined for each specimen were truly characteristic of the metal or alloy and were not influenced by the state of the surface, a natural coherence would occur between the results for different specimens. Alternatively, a similar coherence would be obtained if a process of polishing could be devised to produce the same surface condition in each alloy, though the constants would not necessarily represent the optical properties of the undisturbed metallic structure; see figures 5 and 6.

In the case of the copper-nickel alloys(1) some success was attained in producing the same polish with each alloy and, by averaging the results from three separate polishes in order to even out minor irregularities, smooth {constants, composition} curves were obtained. The difficulty as regards repeating this successful procedure in the present instance lies in the fact that whereas the copper-nickel alloys are hard and relatively easy to polish, the brasses are soft and easily scratched; moreover, their colour makes it more difficult to discern a slight tarnish which sometimes appears on the surface during polishing. To polish a piece of copper or soft brass to a clear glass-like state of surface by the usual methods, avoiding excessive cold-working of the surface, is an almost impossible task. Very fine scratches nearly always appear(2) and, as Drude has shown, these are capable of polarizing light, particularly when they are unidirectional. Though the measured phase-difference Δ between the components of the reflected elliptically-polarized light is not influenced by these scratches, the azimuth ψ is increased for scratches parallel to the plane of incidence and decreased for scratches perpendicular to the plane of incidence.

This variation can be observed experimentally. It is of the order of 1°. Discrepancies due to it may be avoided by carrying out the final stages of polishing so as to avoid unidirectional scratches or by taking care always to mount the specimen with the predominating scratch-directions always the same.

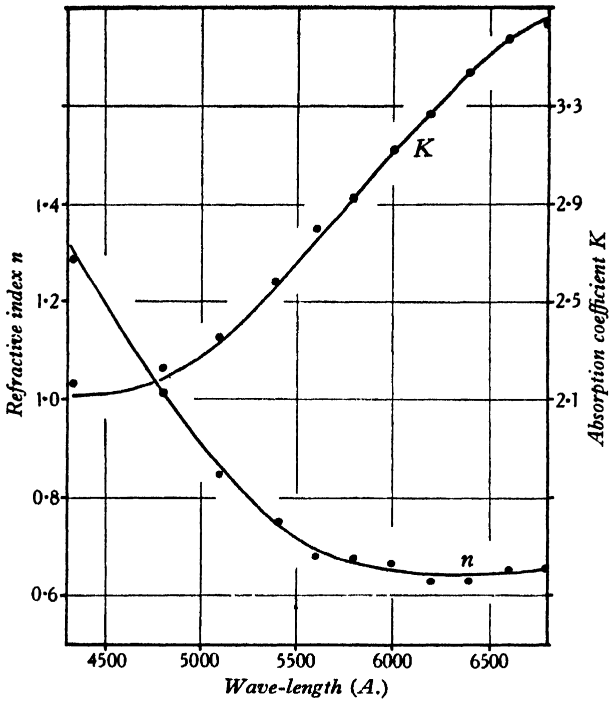

Figure 3. Specimen β brass.

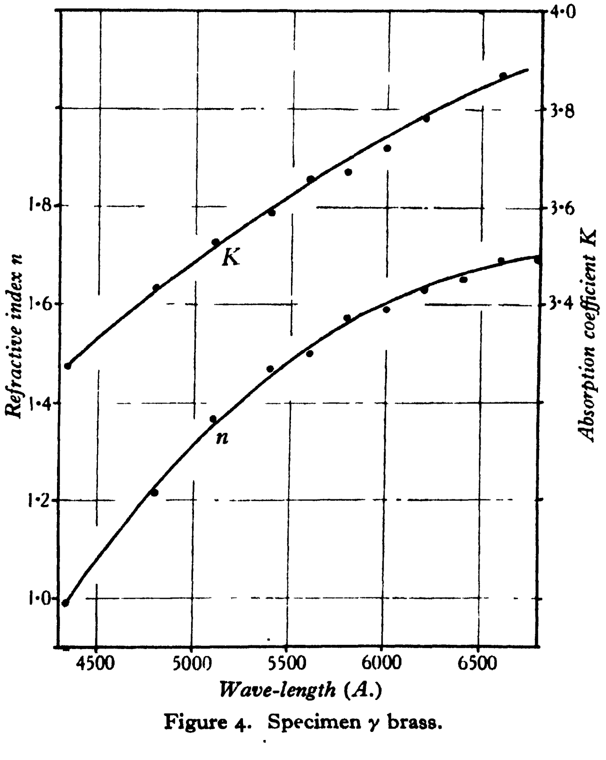

Figure 4. Specimen γ brass.

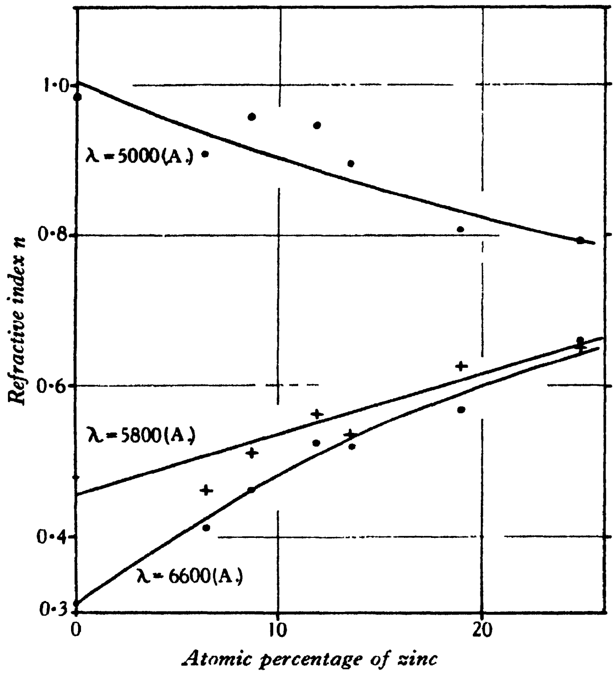

Figure 5.

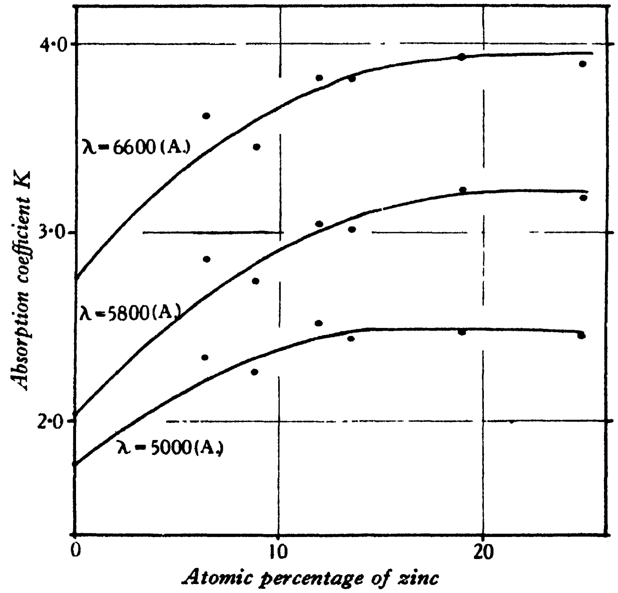

Figure 6.

The possibilities of using the electrolytic polishing process of Jacquet(3), which has proved successful for copper(4), were considered. Here again the position is not satisfactory. Though the method is quite feasible for brasses, it is more tedious in operation since the exact conditions of solution and current and voltage have to be determined separately for each alloy. Again, there is no reason to believe that these conditions, when correctly determined and applied, would effect the removal of the constituents of the alloy (made the anode in the process) in the proportions in which they happened to be present. Finally, the considerable variation found in the measured constants when different depths of the mechanically smooth disturbed surface are removed introduces the disadvantage of having to make an arbitrary choice of the depth of material to be removed, and this in turn entails much laborious work to ensure that the depth shall be the same in every instance.

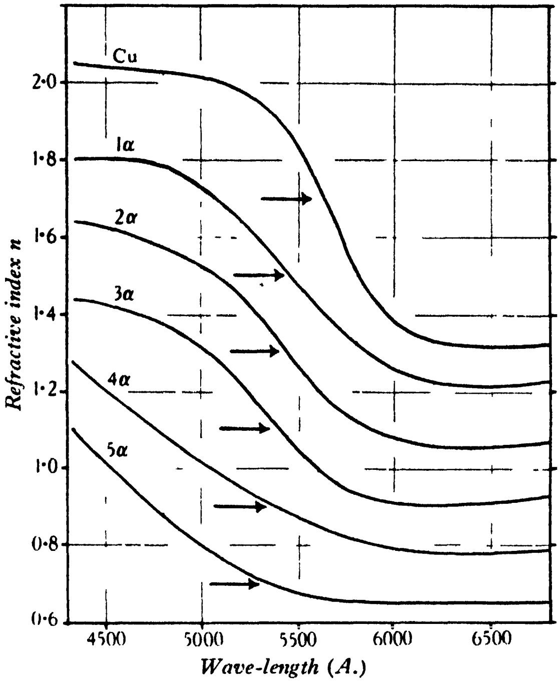

Figure 7. To obtain refractive indices from the graph the following corrections should be subtracted from the ordinates: 1·0 for copper, 0·8 for 1α, 0·6 for 2α, 0·4 for 3α, 0·2 for 4α, 0·0 for 5α. The arrow indicates the value 0·7 of n.

The method employed in the present work is that of embedding all the specimens in a lead block and grinding and polishing them simultaneously. This ensures that each one receives practically the same treatment as regards the amount of cold work sustained. Even so, however, it is hardly probable that alloys with slightly different mechanical properties will receive identical treatment, and the optical constants measured on specimens polished in this way do not give as smooth a curve when plotted against the zinc-content as might be expected for a variation of a physical constant produced by an increasing proportion of zinc in a solid solution. The variation of n and K with composition is shown in figures 5 and 6 for three wave-lengths, λ 6600, λ 5800 and λ 5000 A., for the alloys 1α, 2α, 3α, 4α, 5α, simultaneously polished in the lead block.

It is evident that the dispersion curves, figures 1 and 2, though showing an increasing divergence in form from the curves characteristic of copper as the zinc-content increases, require correction of the constants before any quantitative relationship will appear between them. It was, in fact, principally with the object of suggesting quantitative corrections which could be applied to these dispersion curves in order to locate them in a reasonable relationship that the change in the constants with composition was investigated.

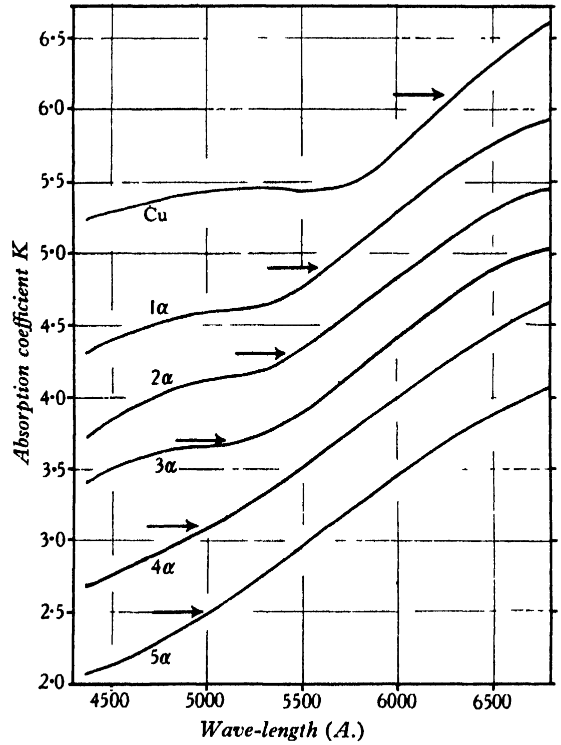

Figure 8. To obtain refractive indices from the graph the following corrections should be subtracted from the ordinates: 3·6 for copper, 2·4 for 1α, 1·8 for 2α, 1·2 for 3α, 0·6 for 4α, 0·0 for 5α. The arrow indicates the value 2·5 of K.

Variations in optical constants due to differences in polish take the form of an approximately parallel shift of the dispersion curves to higher or lower values of the constants. Figures 7 and 8 show the dispersion curves for n and K after the curves for each alloy have been so shifted to such an extent that the values of the constants for the wave-lengths λ 6600, λ 5800 and λ 5000 A. now coincide with the values read off from the smooth curves drawn in figures 5 and 6 for the variation of the constants with composition.

It must be clearly understood that this arrangement of the results is not intended to do more than indicate the interrelationship between the constants of copper and the α brasses shown by our experiments. The values of the constants are correct values only in so far as the constants for the mechanically polished copper specimen may be assumed to be true values. That these may vary considerably upon repetition and with different polishing technique is well established and has been discussed more fully in a previous paper⁽⁴⁾.

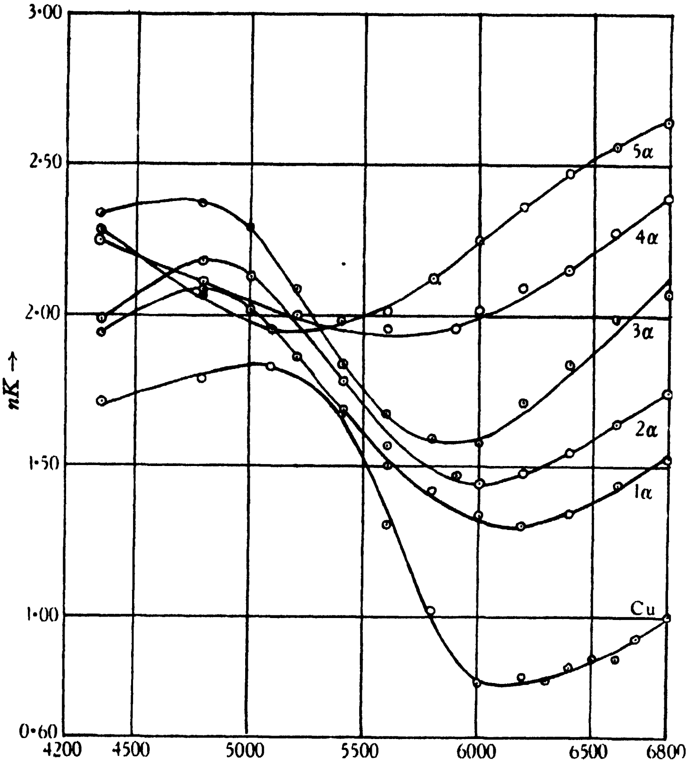

Figure 9.

REFERENCES

(1) Lowery, Bor and Wilkinson. *Phil. Mag.* **20**, 390 (1935).
(2) Drude. *Ann. Phys.*, Lpz., **39**, 481 (1890).
(3) Jacquet. *Trans. electrochem. Soc.* **69**, 629 (1936).
(4) Lowery, Wilkinson and Smare. *Phil. Mag.* **22**, 769 (1936).

THE THEORETICAL INTERPRETATION OF THE OPTICAL CONSTANTS OF COPPER-ZINC ALLOYS

By N. F. MOTT, M.A., F.R.S., H. H. Wills Physical Laboratory,
University of Bristol

Received 13 *February* 1937. *Read* 9 *April* 1937

ABSTRACT. The results of the experiments of Lowery, Wilkinson and Smare on the optical constants of alloys of copper and zinc (α, β and γ brass) are discussed from the point of view of the electric theory of metals.

In this note we discuss the results of the preceding paper(1) from the point of view of the electric theory of metals.

If n, K are the optical constants, then nK is related to the rate of absorption of energy by the metal in the following way. If we consider a volume of metal $d\tau$ in which the electric vector of the light is E, then(2)

$$nK\nu\,d\tau=\frac{\text{rate of loss of energy}}{E^2}.$$

In figure 9 of the preceding paper are shown the values of nK for the copper-zinc alloys. Pure copper is seen to have an absorption band with its long wave-length limit between λ 5500 and λ 6000. It has been suggested(2) that this absorption band is due to the ejection of electrons by the incident light from the 3d level of the copper atom. The type of electronic transition responsible is thus exactly the same as that which gives rise to X-ray absorption edges; as we know from the chemical behaviour of copper, the energy required to remove an electron from the d level is very small, so it is not surprising that the absorption edge lies in the visible. The fact that the absorption edge is not sharp may be ascribed to a broadening of the 3d level of the atom into a narrow band of levels in the crystal.

As zinc is added to copper, three effects may be noticed, as in figure 9 of the previous paper. (*a*) The absorption on the long wave-length side of the edge increases. (*b*) The absorption edge becomes less sharp. (*c*) The absorption edge is displaced in the direction of shorter wave-lengths.

Effect (*a*) can be ascribed simply to the increased resistance of the metal, which damps the induced vibrations of the electrons in the metal and so increases the absorption. We shall not attempt to calculate the absorption to be expected.

Effect (*b*) can be accounted for as follows. In order to find the energy $h\nu$ corresponding to the wave-length of the edge we have to calculate the work required to move an electron from the 3*d* level of one of the copper atoms to the conduction levels of the crystal. This is made up of two parts: (1) The work W_1 required to remove an electron from a *d* level of a copper atom right out of the crystal. (2) The work W_2 (*minus* the work function of the alloy) required to bring the electron back into the crystal. We consider first the term W_1. The picture of a copper-zinc alloy to which one is lead by the electron theory of metals is an array of ions Cu^+ and Zn^{++} embedded in a sea of negative charge. The negative charge tends to cluster round the zinc ions so that each copper atom has only a small excess negative charge and each zinc atom a small excess positive charge. These charges have been estimated from the resistivity(2) and from the energy of the superlattice(3) to be about $\Delta Q = \pm 0{\cdot}075e$, where e is the electronic charge. Now the electrostatic potential at any lattice point due to these charges will on the average be zero, because the copper and zinc atoms are distributed at random in the lattice. But the electrostatic potential at any copper atom which happens to have more zinc atoms as nearest neighbours than the average number will be higher than zero, and at those which have an excess of copper atoms as nearest neighbours it will be lower. The potential of any lattice point will fluctuate by an amount comparable with $\Delta Q/r_0$, r_0 being the interatomic distance. Thus the work required to remove an electron from the lattice will fluctuate by an amount of the order of magnitude $e\Delta Q/r_0$, which is approximately equal to $0{\cdot}075e^2/r_0$ or 0·4 eV. Since a wave-length λ 5500 corresponds to 2·2 eV. this is of the order of magnitude which is observed.

Effect (*c*). According to the electron theory of metals the kinetic energies of the electrons in a metal have values between 0 and a maximum energy E_{max} given by

$$E_{\mathrm{max}} = 36{\cdot}1\ (n_0/\Omega)^{\frac{2}{3}},$$

where Ω is the volume per atom in $\mathrm{cm.}^3 \times 10^{24}$ and n_0 the mean number of free electrons per atom. If an electron is added to the metal, it cannot have kinetic energy less than E_{max}. Thus we may write for the work W_2 required to bring an electron back into the metal

$$W_2 = \text{a negative constant} + E_{\mathrm{max}}.$$

Now in a series of copper-zinc alloys, as the amount of zinc is increased n_0 increases much faster than Ω and so E_{max} increases. The values are as shown in table 1.

Table 1

Composition of alloy (Atoms per cent of zinc)	n_0	E_{max} (eV.)
0	1	6·98
20	1·2	7·70
40	1·4	8·33
50	1·5	8·61

Thus for an alloy containing 20 atoms per cent of zinc, the absorption edge will be shifted towards shorter wave-lengths by

$$7{\cdot}70 - 6{\cdot}98 = 0{\cdot}28 \text{ eV}.$$

Taking the wave-length of the edge for pure copper to be 6000 A., the theoretical values for the alloys shown in figure 9 of the preceding paper are as shown in table 2.

Table 2

Alloy	Composition (Atoms of zinc per cent)	Shift in the edge (eV.)	Absorption edge (calculated)
1α	6·42	0·2	λ 5500
2α	8·67	0·3	5250
3α	11·92	0·4	5000
4α	18·98	0·6	4640
5α	24·85	0·8	4300

The displacements of the edge are rather greater than those observed; the latter are however difficult to estimate, owing to the broadening of the edge discussed above.

REFERENCES

(1) Lowery, Wilkinson and Smare. P. 345 of this volume.
(2) Mott and Jones. *Theory of the Properties of Metals and Alloys*, pp. 107, 119, 294 (Oxford, 1936).
(3) Mott. P. 258 of this volume.

SENSITIVITY VARIATION OF X-RAY PHOTOGRAPHIC FILMS

By WM. H. GEORGE, M.SC., PH.D., F.INST.P., University of Sheffield

Received 14 *November* 1936. *Read in title* 9 *April* 1937

ABSTRACT. An experimental study of the variation of sensitivity from place to place on an X-ray photographic film has been made, so that fluctuations of blackening, due to intensity-variation of the incident radiation, can be distinguished from those due to film sensitivity. Double-film exposures are made with the two sensitive surfaces in contact, and the processing is carried out in a simple mechanical apparatus so that the films move always with accelerated motion relative to the liquids. It is found that if X-ray photographic films are used with the technique described and are blackened until they transmit about half the incident light, then the variations of sensitivity are such as may lead to maximum deviations in the individual measurements of X-ray intensity of the order ± 6 per cent in single-film exposures or of ± 3 per cent in double-film exposures. The mean deviations are of the order ± 2 per cent.

§ 1. INTRODUCTION

The results of the experiments here described relate to the following problem. If a piece of X-ray film exposed in a uniform beam of X rays is then processed (i.e. treated) under prescribed conditions, to what degree of accuracy will adjacent regions of the film be uniformly blackened?

Although the problem arose out of some work on the interaction of polarized X rays and crystals(1), the results are applicable also to X-ray crystallography with tiny single crystals giving small spots in rotation and oscillation photographs, or to fine spectral lines in powder photographs.

§ 2. EXPERIMENTS

Uniform exposure. The object of the work is, in the measurement of a fluctuating X-ray intensity, to differentiate between the X-ray fluctuations and those due to the photographic materials and processes. Since an X-ray beam cannot be directly observed by the coincidence method, the uniformity of the beam cannot be directly judged. In any very sensitive laboratory method of measuring X-ray intensity, the final observations, consisting of deflections of some measuring instrument, may fluctuate about a mean value but are never constant when the ionization chamber or other detecting apparatus is moved across the beam of X rays. It is therefore necessary to define in terms of observable quantities what part of the fluctuations of blackening of a film are to be ascribed to variations of intensity of the incident beam.

Two facts help in formulating the definition Firstly, it is found that the time average of intensity at some distance from an X-ray tube is free from rapid fluctuations in adjacent tiny areas (say 1 × 0·2 mm.). Secondly, the absorption of X rays in photographic film is so slight that the beam transmitted through one film is still sufficiently intense to blacken a second film placed behind and in contact with the first film. Hence if two films are exposed in contact and at some distance from an X-ray tube, any difference between the ratio of blackening of two areas on the first film and the corresponding ratio on the second film will be ascribed to variation in the film-sensitivity. The mean blackening for the two areas will be fixed by using the first fact in the way explained in § 3.

All the experiments were therefore carried out by exposing simultaneously pairs of films in contact. The camera is shown in figure 1. The two films, protected from light by black paper, rest behind two lead screens pierced at front and back by a slit *S* exposing a suitable area of film and allowing the X-ray beam to pass through this part of the camera and its support at the back. The time t of exposure necessary to blacken a film until it transmitted only half of the light incident normally upon it in a microphotometer was first determined. The camera was then loaded with a pair of experimental films and set upon its geometrical supports *A*, *B*, *C*. When the X-ray tube was running steadily, two exposures were made, each for a period of a little more than $\frac{1}{2}t$. During the first period the camera was fixed in the position shown in figure 1, and during the second it was reversed about a vertical axis through *A*. The slit therefore remained in the same position relative to the X-ray tube but during the second period the beam passed through the films in the reverse direction. The exposure for each film was therefore $\frac{1}{2}t$ in the direct beam and $\frac{1}{2}t$ in a beam which had first penetrated the other film. The same region of the beam was used in each period for the same part of each film.

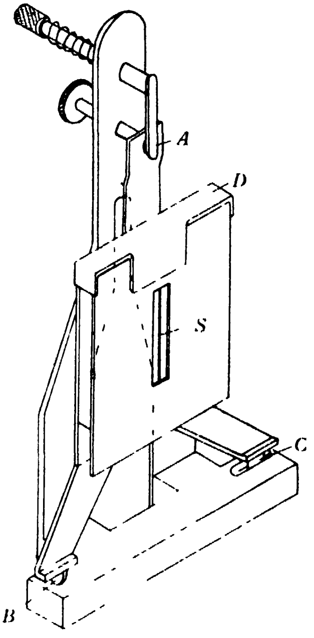

Figure 1. Diagram of camera. *S*, slits; *A*, *B*, *C*, geometrical constraints; *D*, lead cap.

For intensity-calibration the films were then removed from the camera and a rotating-sector exposure was made in another camera upon a part of the unexposed surface.

A filament X-ray tube with copper anticathode and nickel filter was used in all the experiments.

Uniform development. Uniform development as usually defined seems to be inapplicable to experimental work when different parts of a film are exposed in a uniform beam for different times, or when they are exposed in a non-uniform beam for the same time or in fact in any circumstances resulting in non-uniform blackening. Suppose that developer kept at constant temperature and concentration is directed on to such a film in a rapid uniform stream. The developing chemicals will diffuse into the gelatin and react with the affected silver-halide grains, producing various reaction products which diffuse outwards into the stream of fresh developer. Within the film the rate of blackening will depend upon the concentration of developing chemicals, and upon the diffusion rates of their replacement and of the removal of reaction products. These constants are beyond the experimenter's control. In much optical photography, including sound-recording on film, only a thin layer on the upper surface of the emulsion is affected by the radiation, but in the present experiments the absorption of the X rays is so slight that the whole depth of the exposed regions contains developable grains. The chemicals must therefore diffuse through thicker regions than in optical photography. According to common supposition the diffusion must take place also through a layer of liquid adhering to the surface of film in contact with the moving liquid.

Because difficulties arising from the grain and associated with extra background fog, a film which is to be measured on a microphotometer is not developed to gamma infinity. If, therefore, adjacent patches of the film have first been subject to different exposures, it follows that during development they will not be in contact, *within* the film, with the same concentration of developing chemicals for the same time. In this sense then uniform development is impracticable. Since experimental research is concerned with the accessible rather than with the inaccessible it is more helpful here to choose some other definition of uniform development.

Instead of the arbitrarily chosen theoretical definition of uniform development an arbitrarily chosen definition based on the experimenter's actions(2) will be used. Accordingly a film will be said to be subject to uniform development when, at constant temperature, its whole surface has been immersed throughout in rapidly flowing developer of constant composition or in violently stirred developer whose composition is changed only by the progress of the development reactions. A method by which these conditions may be fulfilled for a fairly large film, coated with emulsion on one side and blackened optically, is described elsewhere(3), together with a survey of many other methods. There is considerable difficulty in using the method for X-ray films measuring only 3 × 2 cm. and coated on both sides with emulsion. After trial of a number of different methods the simple apparatus shown in figure 2 was devised; it was found to give self-consistent results.

Processing. The two films are firmly clamped side by side vertically in a detachable framework F made of ebonite and stainless steel. The glass tank T and the block B are removable, but the rest of the apparatus, consisting of reciprocating mechanism, reduction pulleys and electric motor, is screwed to the bench. To avoid delay in making the necessary changes, a separate tank is used for each liquid. When the loaded frame is fixed in position the dry films are quickly plunged into developer by raising the tank, and the reciprocating mechanism is started. This gives 140 complete vibrations per minute, each of total displacement 2 cm.

The films always move with accelerated motion relative to the solutions. This was relied upon to help the interchange of liquids at the film surface. To change the surrounding liquid, a propeller from a toy motor boat was rotated in front of the oscillating films. As the results obtained with and without the use of the propeller appeared to be the same, it was later discarded. The agitation of the liquid was studied by two methods. The first was with coffee grounds, washed and decanted several times to remove all turbidity. These showed the large-scale agitation to be very thorough and free from dead regions. Secondly the regions near the film were examined in close detail by using dye introduced through a fine jet. The removal of liquid introduced as close to the film as possible and the dispersal throughout the bulk of liquid were too rapid to be followed by eye. In all the experiments splashing and the introduction of air bubbles, which accelerate oxidization of the developer, were avoided by adjusting the depth of liquid in the tank.

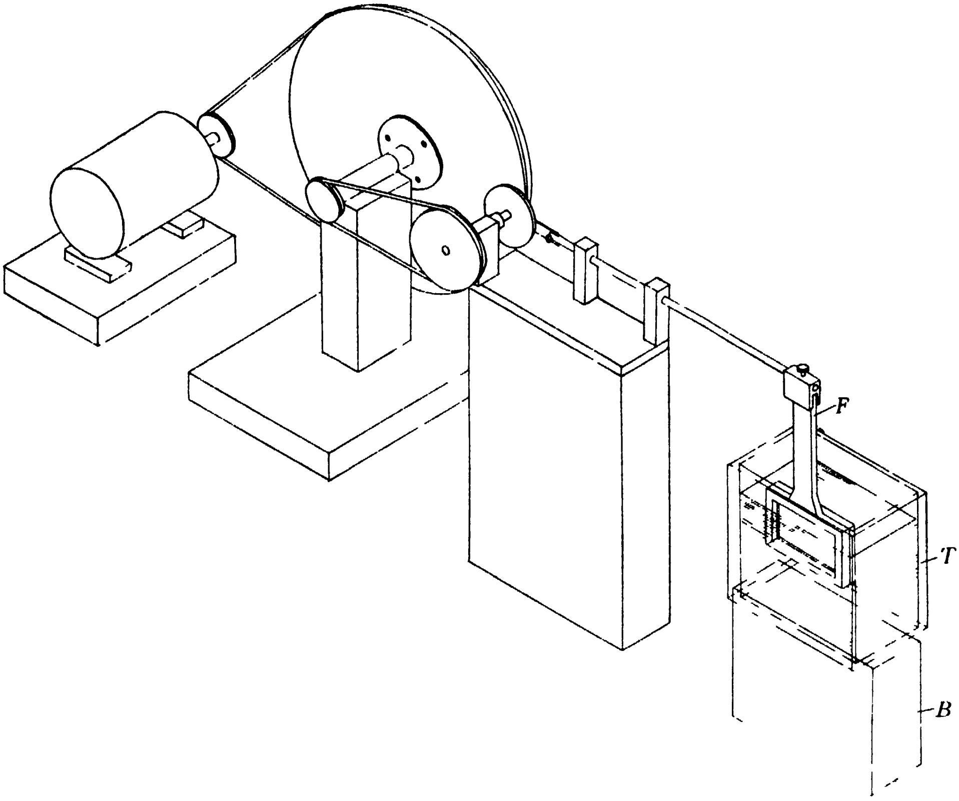

Figure 2.

The routine followed was to develop the film for 5 min. at 18° C. in a solution containing, per litre: Elon 2 g., sodium sulphite (desiccated) 72 g., hydroquinone 8·8 g., sodium carbonate (desiccated) 48 g., potassium bromide 4 g. After being washed for 3 minutes, the film was fixed for 15 minutes in a solution containing, per litre: hypo 240 g., sodium sulphite (desiccated) 10 g., sodium bisulphite 25 g.

The films were then washed for 3 minutes and hardened for 3 minutes in a solution containing, per litre, 10 cm. of formalin (40 per cent formaldehyde solution) and 5 g. of desiccated sodium carbonate. Next, the frame was removed from the oscillator and the films were washed in running water for from 1½ to 2 hours. From time to time the frame was agitated in the water to remove the bubbles which collect on the film surfaces even when rapidly flowing water is used. When the washing was completed, viscose sponge was used to remove as much water as possible from the films which were then dried slowly in a horizontal position at room temperature. Filtered solutions were used throughout to avoid scratching of the film surfaces by particles thrown against them by the rapidly moving liquids.

Microphotometry. The dry films were measured with a Moll microphotometer(4, 5). To ensure that the galvanometer deflections should be, as far as possible, unaffected by deviation of light out of the optic plane containing the thermopile slit, owing to scratches, the viscose sponging of the film was always done in a direction perpendicular to that of its subsequent passage through the microphotometer.

Each instantaneous galvanometer deflection was the result of exploring a region of the film measuring 1 × 0·033 mm.

§ 3. RESULTS

On account of the graininess of the film, the record of galvanometer deflections taken on the microphotometer drum *D* appears as a line subject to many sudden inflections. Each record was therefore divided into strips 5 mm. wide, from which the readings plotted in the two typical pairs of graphs, figure 3, were obtained as follows. The films were exposed in pairs and each half of the figure represents the results got from one pair. Points got from measurements of one film of the pair are joined by solid lines. Broken lines are used to join the points relating to the other film of the pair. A straight line was drawn through each portion of the whole curve contained in each 5-mm. strip of the paper record got from the microphotometer drum, so as to divide its curve into two parts lying equally above and below the straight line. The galvanometer deflection corresponding to the mid-point of this

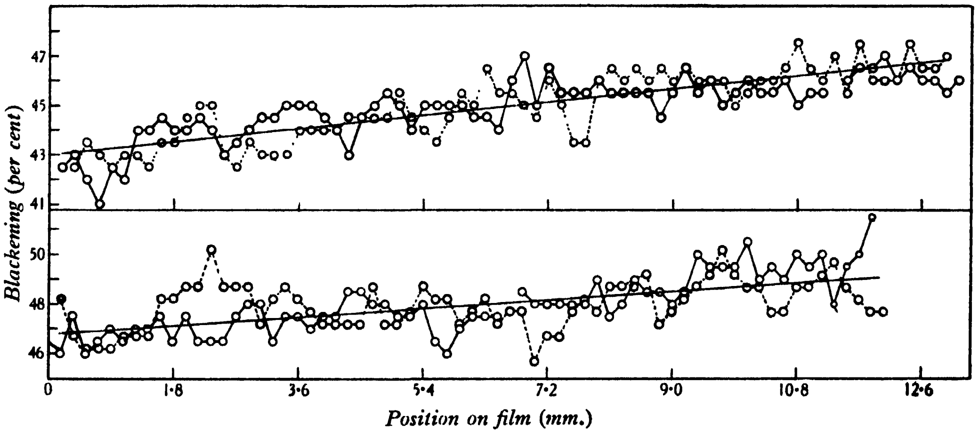

Figure 3.

line was taken as the average of the whole 5-mm. strip. To avoid possible error due to prejudice, strips adjacent to the one studied were hidden from view.

The measurements were expressed in terms of the blackening B defined as follows:

$$B=\frac{\text{galvanometer deflection due to strip of blackened film}}{\text{galvanometer deflection due to clear film}}\times 100;$$

with this definition the blackening of an opaque film would be 100 per cent, of a clear film zero, and of a film transmitting one-half of the light incident normally upon it 50 per cent. Each point on the graphs corresponds to a strip 5 mm. wide on the drum record D or to a region measuring $1 \times 0{\cdot}18$ mm. on the X-ray film. Since the double exposure of each pair of films was made without disturbing the films in their holder, the regions of each in contact could be determined by the distance from a shadow cast by a lead screen behind which part of each film was protected from the X rays. Each unit of displacement on the horizontal axis of figure 3 represents a displacement of 0·18 mm. on the film.

Each of the straight lines, later taken as representing the blackening due to the X-ray intensity to be measured, was got from a mean curve passing through the algebraic mean of each pair of points, one from the solid and one from the dotted curve. For the upper diagram the seventy points of this mean curve were then divided into sets of ten adjacent points and the algebraic mean of each set was used to give one point. The method of least squares was used to draw the straight line through the six points. In the lower diagram the points were grouped into seven sets of eleven each.

An analysis of the deviations of the observations from this derived mean due to sensitivity variation of X-ray film is shown in table 1.

Table 1. Numbers of points representing deviation from mean blackening

	Limits of variation (per cent)					
	± (0 to 0·5)	± (0·5 to 1·0)	± (1·0 to 1·5)	± (1·5 to 2·0)	± (2·0 to 2·5)	± (2·5 to 3·0)
Upper diagram:						
Dotted curve (i)	39	22	6	1	1	—
Solid curve (ii)	36	25	6	3	—	—
Mean of paired points from (i) and (ii)	47	20	2	—	—	—
Lower diagram:						
Dotted curve (i)	35	21	6	2	1	—
Solid curve (ii)	31	17	10	6	1	1
Mean of paired points from (i) and (ii)	41	20	4	—	—	—

The use of simpler methods of processing the films, such as developing in a rocking dish, or stroking with cotton-wool under the liquids or rotating in a flask of liquid, gave fluctuations much greater than those shown in table 1, and the results were too inconsistent to justify their being reported. The results given in figure 3 are typical provided the technique described in this paper is used. When it was found that the method gave self-consistent results, further experiments were discontinued. To establish which parts of the technique may be omitted without affecting the results an elaborate series of control experiments of the cause-and-effect type would be necessary.

The following conditions apply to all the results reported. The exposures were made with general radiation from an X-ray tube with a copper anticathode and a nickel filter. The photographic density of the exposures was about 0·301; the area of blackening was about 1 × 12 mm.; the individual mean measurements relate to tiny strips 1 × 0·18 mm. From rotating sector photographs it was found that under these conditions a variation of blackening of 1 per cent corresponds to a change of X-ray intensity of 2 per cent. The variations of sensitivity are summarized in table 2.

Table 2. Percentage deviation from mean blackening (50 per cent) or density (0·3)

	Single-film exposure	Double-film exposure
Maximum departure by single measurements from mean blackening (per cent)	Blackening 3 X-ray intensity 6	Blackening 1·5 X-ray intensity 3
Percentage of measurements showing this maximum departure	1	4
Percentage of measurements lying between 49·5 per cent and 50·5 per cent	50	65
Percentage of measurements lying between 50·5 per cent and 51 per cent or between 49 per cent and 49·5 per cent	30	30

From this summary it is evident that with the use of the technique described, the variations of sensitivity of X-ray film are such as may lead to maximum deviations in the individual measurements of X-ray intensities of the order ± 6 per cent in single-film exposures or of ± 3 per cent in double-film exposures. The mean deviations are of the order ± 2 per cent.

§ 4. ACKNOWLEDGEMENTS

The work was carried out during my tenure of the Royal Society Sorby Fellowship and I wish to thank Prof. S. R. Milner, F.R.S., for laboratory facilities and the Royal Society and the Department of Scientific and Industrial Research for financial aid. Very generous help in materials, advice and the use of unpublished results was obtained from the Kodak Research Laboratory through the kindness of Mr E. R. Davies.

REFERENCES

(1) George. *Proc. roy. Soc.* A, **156**, 96–107 (1936).
(2) George. *Scientist in Action*, pp. 96–7 and 285 (1936). Williams and Norgate.
(3) Crabtree. *J. Soc. Mot. Pict. Engrs*, **25**, 512–22 (1935)
(4) Moll. *Proc. phys. Soc.* **33**, 207 (1921).
(5) Ornstein, Moll and Burger. *Objektive Spektralphotometrie* (1932). Braunschweig: Vieweg.

RAPID VARIATIONS IN THE MAGNETIC FIELD PRODUCED BY LIGHTNING DISCHARGES

By PROFESSOR HARALD NORINDER, Ph.D.

Communicated from the Institute of High Tension Research of
The University of Uppsala

Received 19 *February* 1937. *Read in title* 9 *April* 1937

ABSTRACT. Measurements of the rapid variations in the magnetic field produced by lightning discharges have been made by means of a frame aerial and a cathode-ray oscillograph. The observations made it possible under certain conditions to calculate the current-variations in lightning discharges, and maximal values up to 100 kA. were derived. These were in good agreement with results obtained by other indirect methods. Conclusions as to the structure of the current-variations in lightning discharges were drawn from the measurements.

§ 1. INTRODUCTION

For several years investigations have been carried out at Husbyborg, near Uppsala, in connexion with the electric properties of thunderstorms, and especially of the discharge characteristics of lightning. In the preliminary stages the work comprised measurements of the slow variation of the electrostatic field in thunderstorms. After some time the main interest turned to investigation of the rapid variations of the electromagnetic field produced by lightning discharges. Experiments in the first place were concentrated on the rapid variations of the electric field. Researches on this subject were especially desirable in regard to an important practical interest—the surges caused on high-tension transmission lines by lightning discharges.

With regard to such a practical application our investigations were in their first stage supported by the Royal Swedish Board of Waterfalls, an enterprise which is responsible for the high-tension transmission lines belonging to the State. A laboratory for surge phenomena and allied high-tension problems was consequently erected at Husbyborg. This laboratory became in 1932 incorporated with a newly erected research institute, which belonged to the University of Uppsala. The new institute had a special scientific purpose, being mainly devoted to the problems of high tensions, electric discharges in the atmosphere, and allied phenomena.

Researches on lightning discharges were thus obviously of special importance to the new institute, and the earlier investigations of the rapid variations in the electric field caused by lightning were continued. The results have been published elsewhere(1). The relations between the variations in the electric field caused by lightning and radio atmospherics were analysed also(2). In addition to these problems we have been occupied with an investigation of the rapid variations in the magnetic field caused by lightning discharges. The main purpose in this undertaking was to analyse the discharge variation of lightning, with special reference to the structure of the currents in the lightning paths. During the season of 1936 the experiments were continued, and improved recording methods, as compared with earlier investigations(3), were used. A considerable amount of new data was collected and it will be the purpose of this paper to give an account of the researches and their main results.

§ 2. THE METHODS OF RECORDING

The measuring instrument. Earlier and preliminary experiments which indicated that the variations within a lightning flash are very rapid enabled us to decide upon the most suitable methods for recording lightning discharges. The total time of discharge in a lightning flash is, on the other hand, rather slow and very often exceeds several hundredths of a second in duration. A lightning discharge was found to be built up of sequences of individual discharges, which sometimes comprised time intervals as small as a few tenths of a microsecond. For instance an individual examination of the slope of the front of the pulse in such partial discharges required an accuracy of measurement of some tenths of a μsec. From this it was evident that the only instrument which could be used with any hope of success must be a cathode-ray oscillograph. Further, it was found that the time variations were so rapid that a cathode-ray tube of the sealed type had not a sufficiently high recording-velocity. Hence it was necessary to use an oscillograph in which the film was placed in a vacuum and directly bombarded by the electron beam from the cathode.

During the experiments a special difficulty arose. When the oscillograph was in operation to record a lightning discharge it was not possible to obtain beforehand any indication of the moment of occurrence of the discharge. Thus a lightning flash with a duration of e.g. 0·001 sec. would require an exposure time of the film up to 10 min. or more. The film in an ordinary oscillograph with such a length of exposure would be much over-exposed, and no rapid transient phenomena could be recorded or recognized on such a film.

A means of avoiding these difficulties would be an electron-tube relay, which would operate by the lightning discharge. The arrangement should operate so that the electron beam of the oscillograph had to be directed into a recording position by means of the relay. The discharge variation of a lightning flash showed, however, such complicated variation forms that the relay would necessarily be very complicated. It was further not very advisable to introduce in the observation circuit a relay with a more or less pronounced time lag. Such an arrangement would, for instance, necessitate propagation of the complicated discharge variation in a delay cable during the time necessary to operate the relay.

It was evident, from the very beginning, that the problem had to be solved in such a manner that the electron beam of the oscillograph itself should be made to function as a relay. By this method a special advantage was gained, which was most useful in the recording of the complicated forms of variation in lightning discharges. With the relay the measuring circuit became very simple and easy to operate.

The principle which throughout has been used in the records of lightning discharges is illustrated in figure 1. The operation of the relay was as follows. When the plates 3, 5 have no voltage, the electron beam will pass from the cathode through the anode-hole between the plates 3 and against the target 4, which has such a position and dimensions that its shadow covers the central hole of the screen 6. A voltage variation derived from the potentiometer 9 and impressed upon the plates 3, 5 will bend the electron beam around the target, and by the cross-coupled system 5 the beam will be bent back and will pass through the hole 6. The plates 7 provide the time base from a circuit with either sinusoidal or linear time variation. The cathode-ray beam will thus fall upon the recording film only during the passage of the impulse, so that the target produces a characteristic zero line or band shadow in the oscillograms. This can be seen in the records here reproduced. In the majority of cases there is no difficulty in interpolating to determine the path of the beam across the zero band.

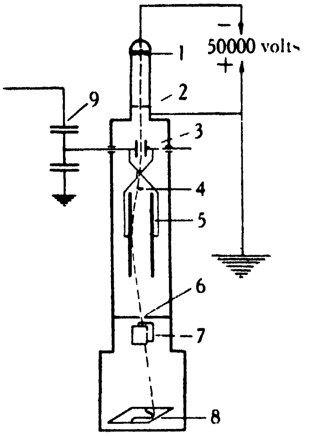

Figure 1. Relay of cathode-ray oscillograph. 1, cathode; 2, anode; 3, 5, deflection plates; 4, target; 6, screen with a central hole; 7, deflection plates for time circuit; 8, record film; 9, potentiometer.

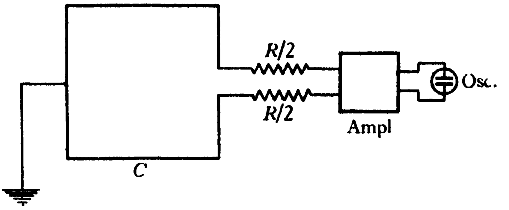

Figure 2. Frame aerial with connexions.

The relay method described by the author[(4)] has been used in various experiments in which the purpose was to record impulses whose time of arrival was not known beforehand. Typical of such unexpected impulses are lightning surges on transmission lines, impulses in radio antenna circuits, and atmospherics arriving from long distances. The method proved also to be very convenient in the recording of the rapid variations in the magnetic field.

The cathode-ray oscillograph constructed by the author and used in these experiments was of the cold-cathode type. The instrument is built of metal with the exception of the glass tube between the cathode and the anode.

The oscillograph contains a film-holder of such construction that the film can be moved to an exposure position from outside. It is possible to make up to 100 exposures without opening the oscillograph. The large number of exposures necessitated loading the film-holder with rolls of film of a length up to 10 metres. Such long films required a very safe and effective system of evacuation. The operation of the oscillographs had to be carried out in movable field stations without any supply of cooling-water. It was thus very inconvenient to use diffusion pumps. A mechanical molecular pump with a conical rotor was therefore constructed for the experiments. The use of a conical rotor had the advantage that the distance between the rotor and the cams between the spiral groove could easily be adjusted to give a very small clearance. The small distance allowed of a very high pump efficiency with as low a rotation speed as 3000 rev./min.

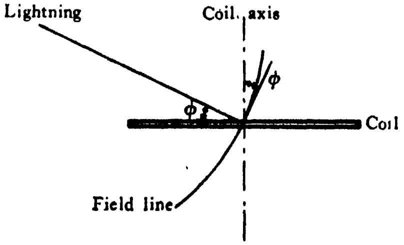

Figure 3. Orientation of coil to lightning path.

During the experiments it often happened that the time between lightning discharges was many minutes. The relay arrangement described did not fully prevent fogging of the film. After an exposure of some minutes it was necessary to shift to a fresh film-surface and thus it was possible that the supply of film in an oscillograph would be totally exposed during thunderstorms of a long duration. In order to avoid such a situation two oscillographs were simultaneously in operation. Both were charged with film and evacuated before the beginning of the observations. During the observation periods one instrument was used for the record and the other for indication by direct observation. The records were shifted over to the oscillograph used for indication when the film-supply of the first recording instrument was consumed, and the instrument with exposed film was subsequently used for indication. This alternation of the instruments was very useful and allowed of very long and undisturbed periods of operation.

§ 3. EXTERNAL EXPERIMENTAL ARRANGEMENTS

Frame aerials of special construction were found to be most suitable for measuring the rapid variation of the magnetic field. Certain precautions were necessary with regard to the winding and the dimensions of the coils; thus it was impossible to use coils with compact turns on account of pronounced disturbances arising in such a case between consecutive turns. It was necessary to separate the wire of each turn by an air distance of at least 2 cm. The coils showed with certain types of discharge-variations a tendency to become the seat of resonant oscillations, which were eliminated by suitable damping resistances.

In our first experiments the ends of the coil were directly connected to the deflection system of the oscillograph. In such a case the dimensions of the coils were to some extent determined by the voltage-sensitivity of the oscillograph. With a distance between the observation station and the lightning path of from 2 to 5 km. we received voltage-variations up to 800 V., which was more than sufficient for a record on the instrument. The coils used in such a case had a turn-surface of $1{\cdot}95 \times 10^7$ turns per cm.² and the wire consisted of copper with a diameter of 1 mm. The connexion of the coil to the oscillograph was symmetrical and the mid-point of the coils was earthed as is illustrated in figure 2. The damping resistance R was 6000 Ω.

Direct control of the oscillograph from the coil was inconvenient as the limited sensitivity only permitted the stronger variations of the magnetic field to be recorded.

Therefore, as has already been mentioned, we introduced during the experiments of the summer 1936 an essential improvement in which the voltage-variations of the frame aerials were amplified by means of a special arrangement. Between the end of the coil and the oscillograph was placed a voltage-amplifier with an amplification up to 800 times. A necessary condition was that this amplifier should work without distortion within the range of variation in the observations. Further, the arrangement had the advantage that smaller amplitude-variations in the field could be recorded, and we received thus more extensive experimental data. The dimensions of the frame aerials were also considerably diminished by the introduction of an amplifier. The coils in the earlier arrangement had a surface of 130 m.², the coils of the new arrangement had a surface of only 12 m.² In the latter case the small dimensions made it possible to use a coil which could easily be turned around a vertical axis. The large coils used in our earlier experiments necessitated, on the other hand, two separate coils mounted in two vertical planes at right angles.

§ 4. THE PRINCIPLE OF THE MEASUREMENTS

The observation of the magnetic-field variations was carried out by using the well-known induced effect of the magnetic fields on frame aerials. We introduce the following symbols: H is the horizontal component of the field in c.g.s. units, A is the surface of the frame in cm.², n is its turn number, V is the induced voltage in volts, and ϕ is in relation to figure 3 the angle between the coil and the direction of the lightning. The relation (1) will be as follows:

$$V = nA\frac{dH}{dt}\,10^{-8}\cos\phi \qquad \text{......(1).}$$

It is obvious that the horizontal component of the field force H can be calculated from equation (1) by integration, and

$$H = \frac{10^8}{nA\cos\phi}\int V\,dt \qquad \text{......(2).}$$

The values of H in what follows have been calculated from this relation.

§ 5. THE CALCULATION OF THE LIGHTNING CURRENTS

Calculation of the current-variation in a lightning flash from the variation of the magnetic field would require a knowledge of the manner in which the magnetic field varied with the distance from the path of the lightning. The ideal solution of this problem would have been to use simultaneous observations from stations situated at suitable distances from the path. Such a method would allow of a determination of the magnetic moment of the lightning discharges; it has not yet been used, however, because we found it to be too expensive since it involved duplication of the experimental arrangements.

Under certain conditions, as has already been shown in my earlier publication on lightning currents, it was possible to use an approximation method in the calculation of the current variations. The calculations were restricted to vertical lightning paths and the following relation was used:

$$I = 10\, V \frac{H\sqrt{(r^2+h^2)}}{h} \qquad \text{......(3)},$$

where I is the current in the lightning path, H the horizontal component of the magnetic field, r the distance of the lightning path from the observation station and h the mean vertical length of the lightning path. For this mean height we have taken a value of 2·5 km. This was a plausible mean value in accordance with other observations which we have carried out on such heights. The amplification of the coil voltages resulted in an increase of several kilometres in the distance between the observation point and the lightning path. The uncertainty of ±0·5 km. in the height of the lightning path will for such longer distances cause an error in the calculated current-values of about ±12 per cent. The errors are smoothed out in the extended series of observations given in this paper.

The displacement currents may influence the determinations of the current-values of the lightning path, especially for the longer distances and to an extent, for the most disadvantageous cases, which has been estimated at 10 per cent. We have further supposed that the magnetic field lines will follow in concentric circles around the lightning path. Topographic conditions can in this respect provoke certain local disturbances. In our case no such disturbances have influenced the results. We estimate the total probable errors in the calculated values of the lightning currents under the most unfavourable conditions to be 20 to 22 per cent. Such errors must on the other hand be smoothed out to a great extent in an extended series of observations. As will be seen from what follows, the individual values of the maximum lightning currents change from a thousand to a hundred thousand amperes, and an error in the individual determinations will thus not be of any appreciable importance when we consider the problem as a whole.

§ 6. OBSERVATIONS

When a thunderstorm passed near the observation station and was suitably located for the production of a record, the frame aerial was directed in accordance with the most probable direction of the lightning paths. One or two observers noted the actual paths of the lightning with reference to their azimuthal positions and to previously determined markings on the horizon. The method provided a sufficiently accurate determination of the direction of the lightning tracks. These were also noted as carefully as possible as regards their angular size and general aspect. The distance to the flash was determined by the time difference between lightning and thunder.

A calculation of the maximum current-variation could be carried out only for vertical lightning flashes. A more limited analysis, however, of discharge characteristics, for instance the time sequences of consecutive partial discharges, and the total duration of lightning discharges were taken also from lightning paths inclined to the vertical or observed to be horizontal.

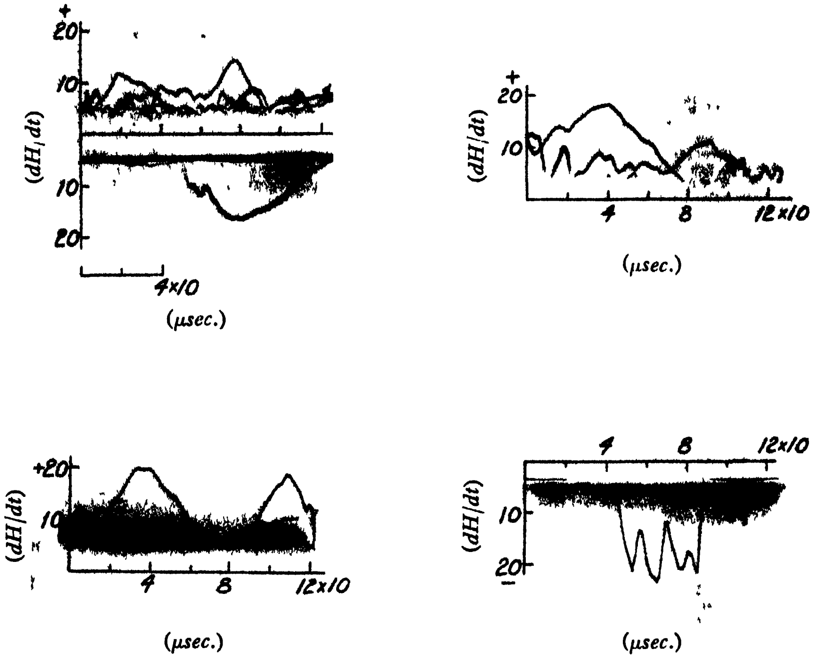

Figure 4. Oscillogram taken with frame aerial, with rapid base time.

Earlier experiments relating to the rapid variations of the electric field caused by lightning proved that, with few exceptions, an ordinary discharge visible as lightning is composed of consecutive partial discharges. The total duration reached values up to a hundredth part of a second. The partial discharges were on the other hand sometimes as short as only 10 μsec. If the oscillograph had its time-base circuit adapted to such short time variations, very complicated oscillograms were obtained from which it was necessary to deduce the individual variations. An example of such complicated oscillograms is reproduced in figure 4. In order to obtain a more general analysis of the variations it was also necessary to operate with a much slower time base. Oscillograms of this kind were better adapted to an analysis of consecutive partial discharges. Such oscillograms are exemplified in figure 5.

§7. DISCUSSION OF THE RESULTS

As has already been mentioned, our first measurements of the variation in the magnetic field were carried out without an amplifier. The advantage of this direct method was that it records where very rapid variations could be obtained without any distortion; its disadvantage was the limitation of sensitivity, and consequent restriction of the observational data which it involved.

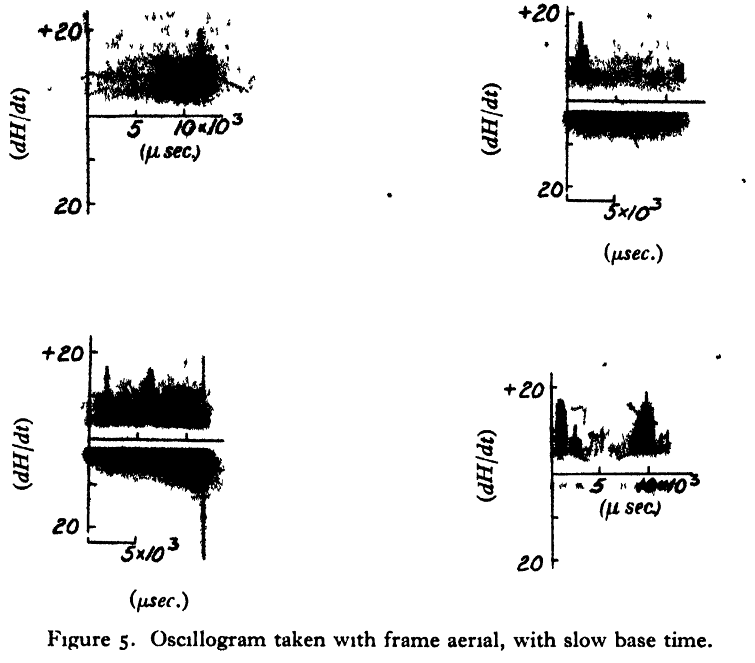

Figure 5. Oscillogram taken with frame aerial, with slow base time.

The advantage of the method now described was that it yielded a substantial increase in the number of observations within a relatively short observation period. On the other hand the improved method was not without inconveniences. With the increase of the distance between the place of observation and the lightning path a transformation in the form of the impulses must ensue. This was especially the case for the variation in the electric field. The influence was not so pronounced for the corresponding variation in the magnetic field and could be completely neglected in the case of the values given in this paper.

The distances between the lightning paths and the point of observation were sometimes so great in the present experiments as to render it possible that a damping effect might be influencing the results. The result of this damping must in the first place have been a slight alteration of the steepness of the front of the impulse in such a way that the time necessary for the current to reach its peak value became longer. A slight indication of such damping effects is visible in some of our records with the longest distances to the lightning path.

§ 8. THE CHARACTERISTIC PROPERTIES OF INDIVIDUAL CURRENT PULSES

The oscillograms provided data for a calculation of the total duration of the current pulses in fifty lightning discharges. The result is reproduced in figure 6, from which it is seen that the majority of the discharges had a duration below 0·005 sec.

The time intervals between successive partial lightning-current pulses for a number of 344 individual cases are reproduced in figure 7. The most usual time interval is characterized by values below 0·001 sec.

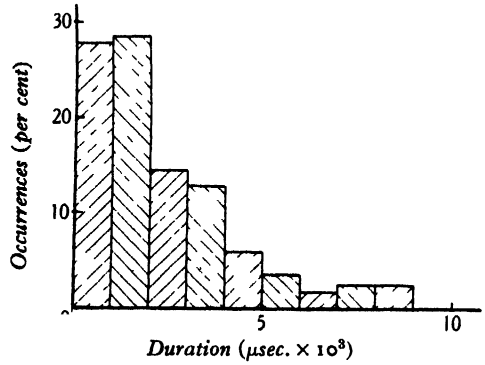

Figure 6. Total duration of current pulses.

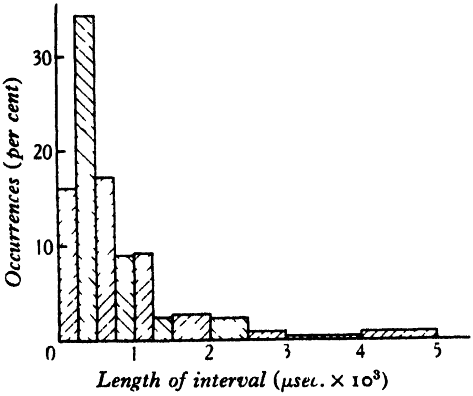

Figure 7. Time intervals between successive partial discharges.

The percentage distribution of the number of current pulses in 127 lightning discharges is reproduced in figure 8, from which it follows that the most usual number consisted of three separate pulses.

It is of interest to analyse the distribution of the maximum current amplitudes in successive individual pulses. In lightning discharges consisting of four or more current pulses the maximum current amplitudes were found in 85 per cent of the cases to occur in the two first pulses, or within the first half of the discharge. In the case of lightning discharges consisting of three pulses the maximum current was found quite as often in the first as in the second of the three discharges.

The percentage distribution of the total duration of individual pulses is reproduced in figure 9. The most usual values reached durations of from 20 to 60 μsec. In our first investigation the corresponding values were from 10 to 30 μsec. This difference in values can be fully explained by the difference in sensitivity during the two periods of observation. In our latest experiments we have used an especially sensitive method, by which impulses with low amplitudes and longer durations also could be recorded.

In 364 discharges we have calculated the time for the current to reach its crest value, and the results are reproduced in figure 10. The most usual values were from 6 to 8 or from 4 to 6 μsec., while earlier observations resulted in corresponding values of from 3 to 6 μsec.

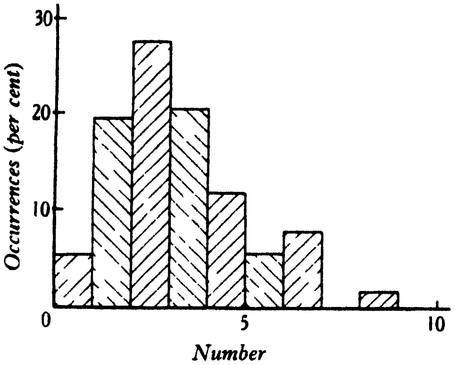

Figure 8. Number of partial discharges.

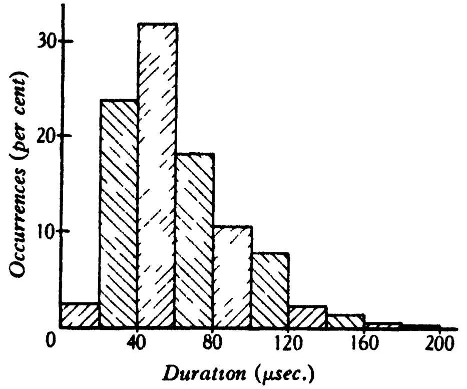

Figure 9. Total duration of individual pulses.

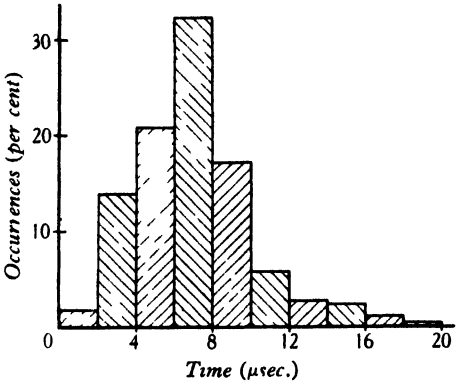

Figure 10 Time intervals for peak values of lightning current

§ 9 CALCULATED HORIZONTAL COMPONENTS OF THE MAGNETIC FIELD

The horizontal components of the magnetic field in c.g.s. units have been calculated from observed vertical lightning discharges and are reproduced in figure 11. The positive sign is used to indicate that a positive charge goes to earth. Of eighty-eight recorded vertical lightning discharges 47 per cent were positive and 53 per cent negative, in full accordance with earlier results.

§ 10. CALCULATION OF THE MAXIMUM CURRENT-VALUES

During the observation period, vertical lightning discharges were in twenty-eight cases so located with regard to the observation station that it was possible to use the relation (3) for calculating the maximum current-values. The observations allowed of calculation for sixty-five partial discharges within the observed lightning paths, and the distribution of the values is shown in figure 12. The data are in full agreement with our earlier results, where the maximum amplitude reached was 120 kA. Figure 12 shows a considerable number of values as low as 1–5 or 6–10 kA. This occurrence of small currents is explained by the improvement in the sensitivity of the experimental methods.

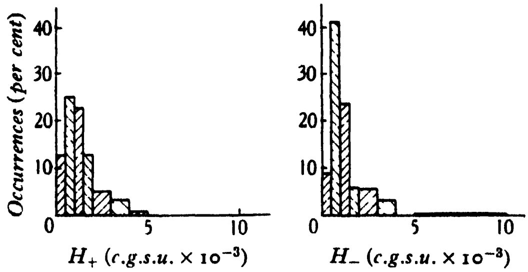

Figure 11. Horizontal components of magnetic field.

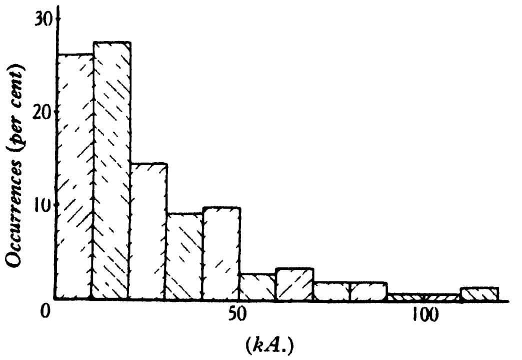

Figure 12. Distribution of peak values of individual current pulses.

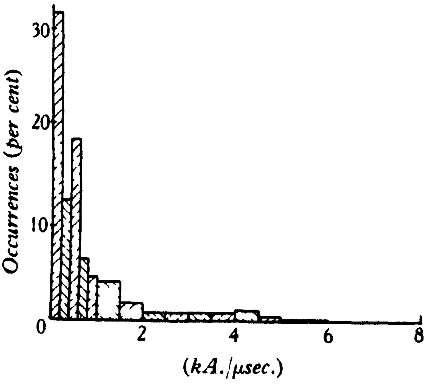

Figure 13. Maximal changes with time in lightning currents.

It is of special interest to compare the calculated maximum current-values with results from an independent and indirect method. On a large number of steel towers supporting high-tension power lines in the United States$^{(5)}$ and Germany$^{(6)}$, small steel links have been used to observe the maximum currents of lightning discharges which strike the towers. The steel of the link consists of a cobalt-nickel-iron alloy or a coal steel with high magnetic retentivity. A lightning stroke to a tower fitted with such a link resulted in magnetization of the link by the current.

The values of the magnetization could be determined subsequently, and from a knowledge of the magnetic constants and the location of the link on the tower it was possible to calculate the current passing through the tower. About 4000 observation stations were used in the United States for this purpose during the years 1932 to 1936.

The maximum observed value was 220·000 A. and there were relatively few values exceeding 100·000 A. The majority of the currents did not attain such high maximum values as 100·000 A. and were in very good agreement with our own values as regards their general distribution. The observational data from Germany were not so extensive as the data from the United States, but they also were in good agreement with our own results. An evident difference existed between our observations and those mentioned above. Both the American and the German observations resulted in a marked preponderance of negative currents, while our measurements indicated only a slight preponderance of this polarity. This smaller preponderance of negative values was quite in agreement with other and earlier observations of the polarity of the rapid variation in the electric field. It must be pointed out that the measurements made by the link method were carried out on very well earthed steel towers. Our measurements on the other hand were carried out in the open field. The marked preponderance of negative current-values for such structures as steel towers must, as we have found, be caused to a considerable extent by a polarity effect. Thus under the same conditions of field-intensity and charge-distribution, lightning discharges over steel structures will be much more easily developed at lower voltages when the cloud-polarity is negative than when it is positive.

From our observations it was possible to calculate the maximum changes of current with time in the lightning currents shown in figure 12. The result is graphed in figure 13. In our earlier investigations we obtained a few values of maximum current-changes amounting to 24–30 kA./μsec. These values were considered to be exceptional and have not recurred in the more recent work. Figure 13 shows also a preponderance of small changes of current with time, and this is to be expected with the improved sensitivity of our experimental methods.

REFERENCES

(1) Norinder, Harald. *J. Franklin Inst.* **218**, No. 6 (December 1934).
(2) Norinder, Harald. *Proc. Inst. Radio Engrs*, N.Y., **24**, No. 2 (February 1936).
(3) Norinder, Harald. *J. Franklin Inst.* **220**, No. 1 (July 1935).
(4) Norinder, Harald. *Z. Phys.* **63**, Heft 9 und 10 (1930).
(5) Lewis, W. W. and Foust, C. M. *Elect. Engng*, N.Y., **54**, No. 9, pp. 934–42 (September 1935).
(6) Zaduk, H. *Elektrotech. Z.* **56**, No. 17, pp. 475–9 (21 April 1935).

THE KNIFE-EDGE TEST FOR SPHERICAL ABERRATION

By R. KINGSLAKE, A.R.C.S., M.Sc., Institute of Applied Optics, University of Rochester, U.S.A.

Received 17 *December* 1936. *Read* 28 *May* 1937

ABSTRACT. A method is given for computing the appearance seen in the knife-edge test, for various positions of the edge in various focal planes, when any specified amount of aberration is present. Series of patterns are given corresponding to (*a*) pure primary spherical aberration, and (*b*) zonal aberration with marginal correction.

---

§1. INTRODUCTION

The knife-edge test as originally described by Foucault(1) was used as a means of ascertaining whether or not a telescope objective was perfect, and also as a guide in the improvement of an objective by local retouching. However, the knife-edge method may also be very usefully applied to lenses having considerable amounts of aberration, as has been shown by Miss Conrady(2).

It was felt desirable to extend this work, particularly in respect of spherical aberration. It will be realized that there is really a double infinitude of possible knife-edge shadows for a given lens, since the knife blade may be situated in any focal plane, and the edge itself may be advanced to any distance into the beam in that plane. In Miss Conrady's paper, only one shadow appearance is given for spherical aberration, namely that for the mid-position of the knife edge in a focal plane about midway between the marginal and paraxial foci.

The aim of the present paper is to explain a method by which the form of the shadow edge for any mixture of aberrations, at any specified position of the knife edge, may be computed.

§2. THEORY OF THE METHOD

It will be clear from elementary considerations that, if a lens possesses a considerable amount of spherical aberration, any zone of the lens will suddenly go dark as the knife edge cuts into its exact focus. Other zones of the lens, of which the foci lie beyond the knife plane, will darken on the side on which the knife is entering, whereas zones whose foci lie closer to the lens than this plane will darken on the opposite side. The result will be an appearance shown diagrammatically in figure 1.

The accurate computation of this and other shadow appearances can be made by differentiating the ordinary expression for spherical aberration as a path difference, namely:

$$P=\frac{A}{2l}r^2+\frac{B}{4l}r^4+\frac{C}{6l}r^6+\ldots \qquad \ldots\ldots(1).$$

Here A represents a change of focus from the paraxial focal plane; B, C, etc. represent successive orders of spherical aberration; r is the radius of the zone; and l represents the distance of the image from the lens.

If we let (x, y) represent the two principal meridians of the lens, respectively perpendicular and parallel to the knife edge, then the path-difference may be written:

$$P=\frac{A}{2l}(x^2+y^2)+\frac{B}{4l}(x^2+y^2)^2+\frac{C}{6l}(x^2+y^2)^3+\ldots \qquad \ldots\ldots(2).$$

By differentiating this, the components of the slope α of the ray from the point (x, y), relative to the ideal path of that ray, are obtained:

$$\left.\begin{aligned}\alpha_x&=\frac{A}{l}\,x+\frac{B}{l}\,x\,(x^2+y^2)+\frac{C}{l}\,x\,(x^2+y^2)^2+\ldots\\ \alpha_y&=\frac{A}{l}\,y+\frac{B}{l}\,y\,(x^2+y^2)+\frac{C}{l}\,y\,(x^2+y^2)^2+\ldots\end{aligned}\right\} \qquad \ldots\ldots(3).$$

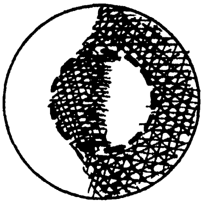

Figure 1. Knife-edge shadow, when knife blade is at focus of dotted zone (schematic).

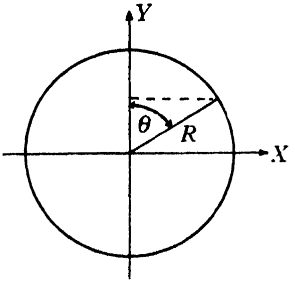

Figure 2. The principal meridians on the lens aperture.

These may be simplified by using polar coordinates on the lens aperture, figure 2, thus

$$\left.\begin{aligned}x&=r\sin\theta\\ y&=r\cos\theta\end{aligned}\right\} \qquad \ldots\ldots(4).$$

We now convert equation (3) to give the linear-displacement components ξ, η of the point at which the ray intersects the chosen focal plane. Since $\xi=-l\alpha_x$, $\eta=-l\alpha_y$, we have:

$$\left.\begin{aligned}\xi&=-\sin\theta\,[Ar+Br^3+Cr^5+\ldots]=-K\sin\theta\\ \eta&=-\cos\theta\,[Ar+Br^3+Cr^5+\ldots]=-K\cos\theta\end{aligned}\right\} \qquad \ldots\ldots(5).$$

The procedure for computing the knife-edge patterns is to calculate the values of K for a series of values of r, say $r=0{\cdot}1$, $0{\cdot}2$, $0{\cdot}3\ldots1{\cdot}0$, and then tabulate the corresponding values of $\sin\theta$, equal to $-\xi/K$, for each of a series of values of ξ. The values of θ itself are then tabulated for all values of $\sin\theta$ less than unity. Now since each value of ξ represents a definite stage in the progress of the knife edge across the beam, the polar graph of (r, θ) for each value of ξ gives the appearance of the shadow edge for that position of the knife blade.

§3. THE PATTERNS FOR PRIMARY SPHERICAL ABERRATION

As an example, suppose it is desired to compute the shadows for pure primary spherical aberration, the knife blade being supposed to lie in the marginal focal plane. Then if $B = 1$ (say), A will be -1, if r is taken as unity at the margin of the lens. Thus $K = r^3 - r$ in this case. The values, with reversed sign, of $\sin\theta$ and θ to the nearest degree, corresponding to a series of values of ξ, are shown in table 1.

Table 1

Values of $-\sin\theta$ and $-\theta$ (degrees) corresponding to given values of r and ξ. The values of θ are printed below those of $\sin\theta$.

r	·05	·1	·15	·2	·3	·4	·5	·6	·7	·8	·9	1·0
$-K$ / $-\xi$	·050	·099	·147	·192	·273	·336	·375	·384	·357	·288	·171	0
·05	1 002 —	·505 30°	·344 20	·265 15	·183 11	·149 9	·133 8	130 7	140 8	·173 10	·292 17	∞ —
·10	2 0 --	1·01 —	·688 43	·521 32	·366 21	·298 17	·267 15	·260 15	280 16	·347 20	·585 36	— —
·15	— —	— —	— —	·786 52	·549 33	·447 26	·400 24	·390 23	·420 25	·520 32	877 61	— —
·20	— —	— —	— —	— —	·732 47	·596 36	·534 32	·520 31	·560 34	·694 44	— —	— —
·30	— —	— —	— —	— —	— —	894 63	·801 54	·780 53	·840 58	— -	-- -	— —
40	—	—	—	—	—	—	—		-	—	—	—

These values are most conveniently plotted on ordinary polar-curve paper, a circle of ten units diameter being taken to represent the rim of the lens aperture. Graph points are marked on this corresponding to all the available pairs of values of r and θ, figure 3. The locus of all points having the same value of ξ represents the

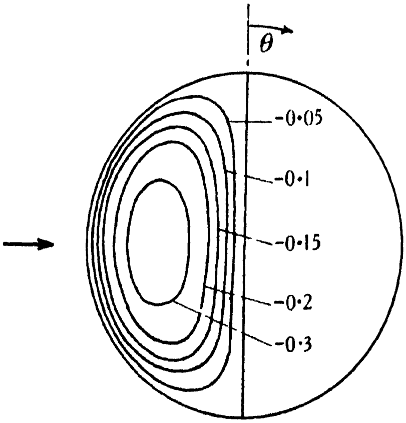

Figure 3. Computed shadow edges for primary spherical aberration, in marginal focal plane.

edge of the shadow corresponding to a knife-position given by ξ; thus by this method the whole family of shadow-boundaries are plotted on the same figure. They can be then traced off in turn and collected as shown in figure 4. For the different focal planes in the diagram, the values of A were respectively $-1{\cdot}5$, $-1{\cdot}0$, $-0{\cdot}5$, 0, and $0{\cdot}5$.

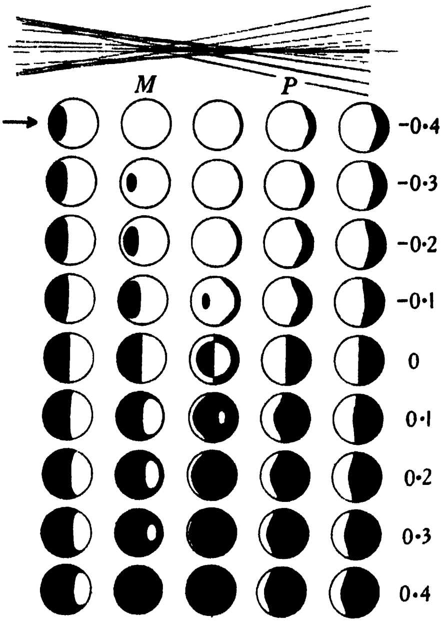

Figure 4. The knife-edge shadows for primary spherical aberration (computed).

In figure 5 is shown a series of actual photographs of knife-edge shadows made on a reversed telescope objective, the position of the knife blade being removed progressively further from the lens from left to right. The knife edge was advanced in each case from above to a point as near to the lens axis as could be secured.

Figure 5. Knife-edge shadow photographs for a reversed telescope objective.

One very characteristic feature of this test is the appearance seen when the knife blade is at the paraxial focus. The central patch of shadow is seen to jump suddenly across the centre of the aperture for an infinitesimal advance of the knife blade. This appears to be the only method of experimentally locating a paraxial image point, since it does not require the stopping down of the lens to a small hole with the consequent great increase in the depth of focus.

§4. THE PATTERNS FOR ZONAL ABERRATION

In the case of zonal aberration, since the marginal aberration is to be zero, the values taken were $B = +1$, $C = -1$, A having the values $-0{\cdot}375$, $-0{\cdot}25$, $-0{\cdot}125$, 0, $+0{\cdot}125$ respectively, and ξ the values $-0{\cdot}15$, $-0{\cdot}10$, $-0{\cdot}05$, $-0{\cdot}01$, and 0.

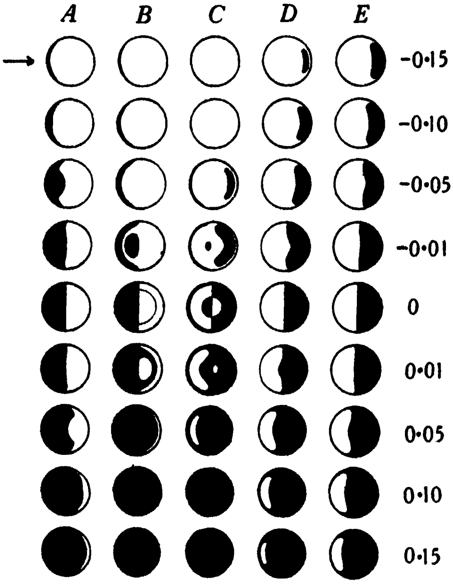

Figure 6. The computed knife-edge shadows for zonal aberration.

The plane for which $A = -0{\cdot}25$ (column B, figure 6) is the plane of the minimum zonal focus, namely the focus of the zone with r equal to $0{\cdot}707$. Column D corresponds to the united marginal and paraxial focus, in which plane the coefficient $A = 0$.

§5. CONCLUSION

In the discussion given above, only the first two orders of spherical aberration have been considered; the same method is of course applicable to the computation of knife-edge shadows for any single aberration or mixture of aberrations which is expressible as a path difference in equation 1. When aberrations such as coma or astigmatism, which do not have rotation symmetry about the lens axis, are present, it is clear that different shadow patterns will be obtained for different directions of entry of the knife blade. Some examples of these are given by Miss Conrady in the paper cited.

REFERENCES

(1) Foucault. *Mon. Not. R. astr. Soc.* **19**, 284 (1859).
(2) Conrady, H. G. *Trans. opt. Soc.*, Lond., **25**, 219 (1924).

THE VELOCITY-DISTRIBUTION IN A LIQUID-INTO-LIQUID JET

By E. N. da C. ANDRADE, F.R.S., Quain Professor of Physics
in the University of London

AND

L. C. TSIEN, B.Sc.

Received 5 *April* 1937. *Read* 7 *May* 1937

ABSTRACT. The distribution of velocity in a liquid-into-liquid jet, issuing from a cylindrical tube with a tapering approach, has been measured by photographing the traces made by suspended particles, with strong illumination and a determined exposure. The results have been compared with the theory for a jet issuing from a point in an infinite plane, and it is shown that, supposing the equivalent point source to be within the orifice, good agreement is found except in the immediate neighbourhood of the orifice. An expression has been derived connecting the distance of the equivalent point source from the orifice with the Reynolds's number. This enables the loss of kinetic energy of the jet to be worked out.

§ 1. INTRODUCTION

For some time experiments have been in progress in the physics laboratory at University College, London, on the instability of a liquid-into-liquid jet. In particular, attention has been devoted to the nature of the motion produced by a periodic disturbance, acting on a fine jet of water flowing through a circular orifice into a shallow tank of water. In this connexion it is of interest to determine the distribution of velocity in the undisturbed jet, especially as comparatively little has been done experimentally on streaming without rigid walls.

The behaviour of a laminar jet of viscous liquid has been recently worked out by Schlichting$^{(1)}$ on certain simplifying assumptions, of which the most serious is that the jet issues from a point aperture, giving, as it does, an infinite velocity. One of the objects of this work was, therefore, to see how far Schlichting's theory could be applied to an actual jet, issuing from a circular aperture of finite size. The theory has proved to be very successful in interpreting the results, and it is shown here how, with slight modification, it can be made to give the velocity everywhere except in the immediate neighbourhood of the orifice. One consequence of this work is that the loss of kinetic energy due to viscosity can be worked out.

§ 2. EXPERIMENTAL METHOD

The experiments, being carried out in a physical laboratory, had to be done on a small scale. The internal profile of the glass jet used is given in figure 2, which shows a photograph obtained by immersing the glass jet, full of air, in a liquid of the same refractive index as the glass, contained in a glass tank with plane sides. The diameter of the orifice was 0·91 mm. The water used contained very fine suspended particles. A horizontal plane through the axis of the jet was strongly illuminated, and photographed with a measured short exposure. The tracks of particles, both in the water constituting the original jet and in the surrounding liquid, appeared as short lines terminating sharply, the lengths giving a measure of the velocity at the mid-point of the line. From these tracks, then, the velocity distribution could be obtained. Subsidiary experiments gave the volume per second passing through the jet at various pressures, measured in the straight approach tube. The pressure in this tube was used to control and determine the mean velocity of efflux.

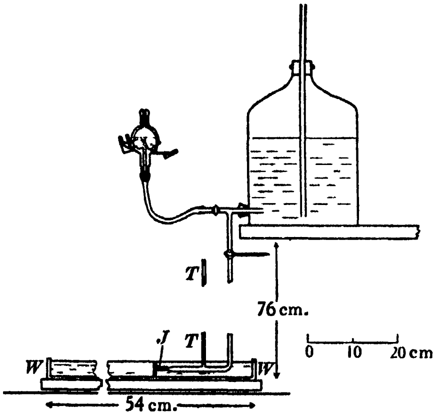

Figure 1

The general arrangement of apparatus is shown in figure 1. Water from a large Mariotte's bottle, containing about 7 litres, was admitted, by a tap capable of accurate adjustment, to a vertical tube, leading to the jet *J*. The vertical tube *TT* allowed the pressure to be read by a cathetometer. The tank *WW* rested on a massive slate slab, supported on folded cloths, to minimize vibration. The level in the Mariotte's bottle was measured on a Casella sensitive pressure gauge, based on the internal reflection of a pointer from the surface of the water, reading to 0·01 mm. This was used to calibrate the outflow against the pressure, the time for the level to fall through 2 mm. being taken on a stop watch, and the corresponding volume being determined independently. The temperature was always maintained at 18° C., so that changes of viscosity had not to be considered.

Various particles were tried, including fish scales (as used for the manufacture of artificial pearls), flue dust and a powdered magnesium-aluminium alloy. Aluminium particles from commercial aluminium powder were finally adopted. The

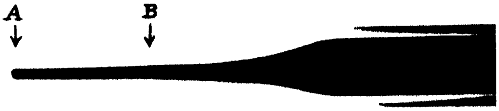

Figure 2. (Magnification × 1·5.)

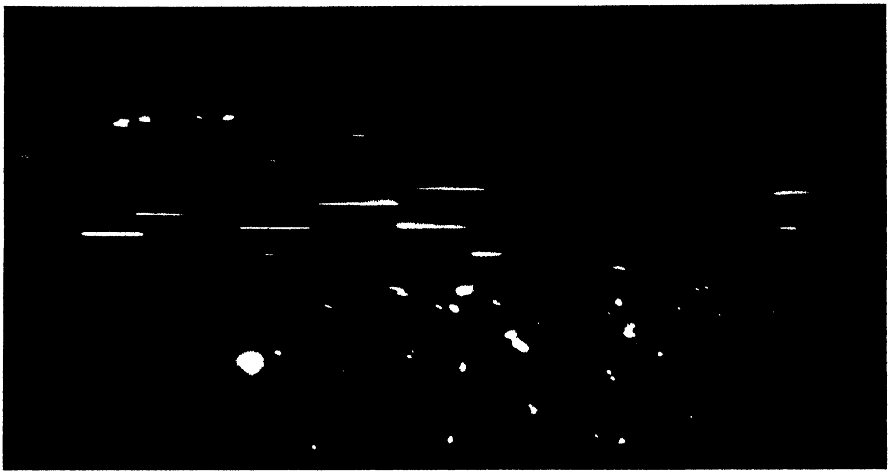

Figure 3*a*. (Magnification × 9·4.)

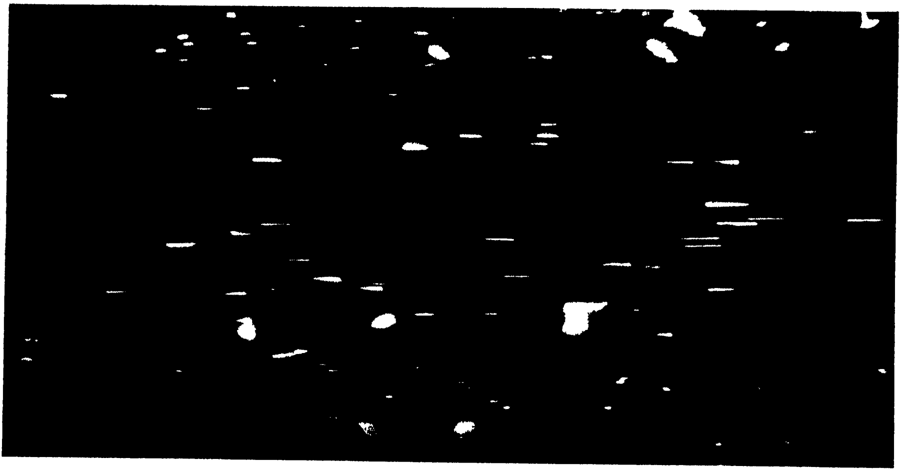

Figure 3*b*. (Magnification × 9·2.)

powder was washed in a separating funnel with alcohol, to remove grease, and the coarser particles run off. The alcohol was then filtered off from the remaining particles, which were dried and then suspended in distilled water, in a vessel about 5 ft. high. The suspension was allowed to stand for about 15 min., and the middle part of the liquid column then drawn off. This liquid, diluted with a large bulk of water, was used for the experiments, being placed both in the tank and in the supply bottle. The particles were from 0·05 to 0·08 mm. in diameter.

For illumination, a 55 A. arc was focused on to a horizontal slit by a wide-angle condensing lens, and an image of the slit formed on the axis of the jet stream by a 1½ in. Mayer lens of aperture *f*/1·5. This image was about 0·1 mm. wide, so that, even allowing for the convergence and divergence of the beam away from the axis, only a central section of the jet was illuminated. To photograph the tracks a similar lens, by Dallmeyer, was used, which gave a magnification of 5 with the distances adopted. The plates were Ilford hypersensitive panchromatic, speed 8000 H. and D. to ½-watt illumination.

A shutter was required which would give exposures of some thousandths of a second with an accuracy of 1 per cent or better. This was provided by a rectangular aperture in a weighted board, falling freely in its own plane under gravity; the horizontal edges of the aperture were accurately straight, and their separation was 2·3 cm., in the normal case, giving an exposure of 0·00782 sec. Another aperture often used gave an exposure of 0·00497 sec. The shutter fell within 2 mm. of the illuminating slit, and was controlled by a magnetic release.

The plates obtained gave sharply terminated lines, as exemplified in figures 3 *a* and 3 *b*, which are selected as showing typical results at two different velocities. To measure up a plate a reference line, drawn parallel to the axis of flow, was taken as a provisional x axis, the y axis being the normal to the axis through the orifice. The length of track was recorded against the coordinates of the mid-point of the track, several photographs being taken for each rate of efflux, so as to provide sufficient material. The exact position of the x axis was then obtained from considerations of symmetry. A standard value of x being selected, the velocity at this distance was obtained, if necessary by interpolation, for different values of y. Three different values of x were used, viz. 0·8, 1·8 and 3·3 cm.

§ 3. TREATMENT OF RESULTS

Schlichting's treatment, which is based on the neglect of the radial accelerations, in the sense of the boundary layer theory, leads to expressions for u and v, the longitudinal and radial velocities, of the following form:

$$u=\frac{3}{8\pi}\frac{K}{\nu x}\frac{1}{(1+\xi^2/4)^2},\qquad v=\frac{1}{4}\sqrt{\frac{3K}{\pi}}.\frac{1}{x}.\frac{\xi-\xi^3/4}{(1+\xi^2/4)^2}\qquad\ldots\ldots(1),$$

where

$$\xi=\sqrt{\frac{3K}{16\pi}}.\frac{1}{\nu}.\frac{y}{x}\ \text{and}\ K=\frac{J}{\rho},$$

J being the momentum crossing a plane normal to the axis of the jet per second, ν the kinematic viscosity and ρ the density of the fluid. The distance x is measured parallel to the axis, from the point origin of the jet. The jet draws the surrounding liquid along, the theoretical stream lines in a particular case being given in figure 9.

We can express u in the following form:

$$u = A\frac{1}{(1+By^2)^2} \qquad \text{......(2),}$$

where $$A=\frac{3K}{8\pi\nu}\frac{1}{x},\quad B=\frac{3K}{64\pi\nu^2}\frac{1}{x^2},$$

so that $$A/B=8\nu x.$$

If then we plot the experimental values of $1/\sqrt{u}$ against y^2 we should obtain a straight line, and this expectation has been realized. The intercept on the vertical axis gives $1/\sqrt{A}$, and the slope of the line gives $B/\sqrt{A}$, from which A and B can be calculated. With the values of A and B so found theoretical curves of u against y have been drawn for comparison with the experimental points.

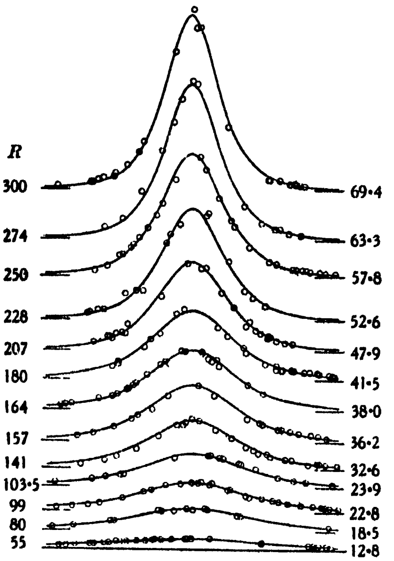

Figure 4

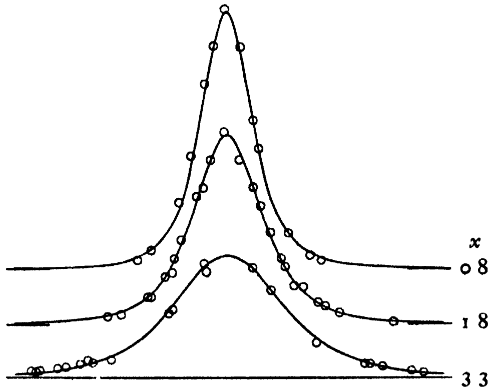

Figure 5

Figure 4 shows the theoretical curves of velocity-distribution across the jet, and the experimental points, at a distance $x=3{\cdot}3$ cm., for various mean velocities of flow in the jet itself, calculated from the volume efflux per second Q and the cross-sectional area of the jet, which was 0·650 mm.^{2} Actually the pressure p was measured in each experiment, and Q found from the experimental curve connecting Q and p. It will be seen that over a wide range (Reynolds's number in the tube, taken as $R=\bar{u}a/\nu$, where a is the radius of the orifice, varies from 55 to 300) the agreement between the theoretical and experimental forms is excellent. The results at three different distances from the jet, viz. $x=0{\cdot}8$, $1{\cdot}8$, $3{\cdot}3$ cm., with a fixed value of $\bar{u}=46{\cdot}7$ cm./sec., are shown in figure 5, where the agreement is equally satisfactory.

§4. THE MOMENTUM OF THE JET

Velocity-distributions were measured at each of the known distances just specified, with various values of $\bar{u}$, and in this way a series of values of A and B were obtained. Now according to theory,

$$A/B = 8\nu x \qquad \ldots\ldots(3),$$

and

$$K = \frac{\pi}{3}\frac{A^2}{B} = 1{\cdot}047\frac{A^2}{B} = \frac{J}{\rho} \qquad \ldots\ldots(4),$$

$$= J \text{ in the case of water.}$$

Equation (4) enables us to find a value for J from each velocity profile measured. These various values are shown in figure 6, plotted against the pressure in centimetres of water, and it will be seen that the measurements made at three different distances are consistent.

The volume issuing from the jet per second has been measured in terms of the pressure, but to find the momentum we must know the velocity-distribution at the orifice, for which we have to consider whether, with the short tube used, the influence of the entry extended to the orifice. At first sight it would seem that we have as a guide the work of Schiller(2), who finds that the Poiseuille regime sets in at a distance l from the entry given by

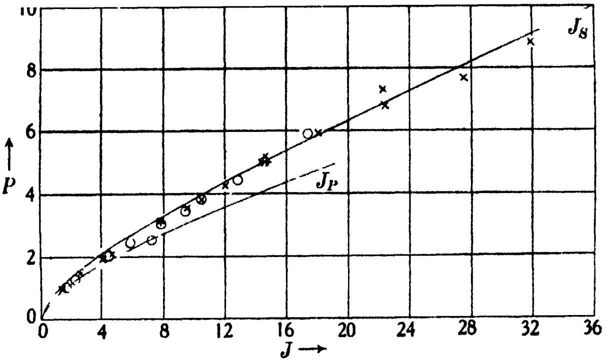

Figure 6. ×, $x = 3{\cdot}3$ cm.; ○, $x = 1{\cdot}8$ cm.; +, $x = 0{\cdot}8$ cm.

$$l/d = 0{\cdot}029\,R.$$

Taking for l, the effective length of our tube, 1·2 cm., which corresponds to the length AB in figure 2, and a mean diameter of 0·103 cm., we find that R must not exceed 400, which would indicate that the parabolic distribution is only beginning to fail at our highest speeds. However, it has been shown that even a slight convergence in a tube (1 mm. in radius on a length of 1 m., while $R = 1000$) causes a marked flattening in the velocity-distribution(3),* while, for the case of convergent parallel walls (two-dimensional streaming) Hamel(4, 5) has shown that U deviates markedly from $U_{\max}$ only at the walls, the velocity being uniform across almost the whole cross-section. We may anticipate, then, that with our convergent nozzle the

* Dr Tietjens informs me that the calculations, on which the figure given in his book(3) is based, were carried out by himself, but that details have never been published.

velocity-distribution across the orifice will be practically square-headed. This anticipation is confirmed when we come to compare the momentum, as deduced from velocity-profile measurements in the jet (where $J=1\cdot047\, A^2/B$) with that calculated from the volume efflux Q per second at the corresponding pressure-head. To find J from Q we must know the velocity-distribution at the orifice; for a parabolic distribution the momentum $J_P=\frac{4}{3}\rho Q^2/\pi a^2$, while for a square-headed distribution the momentum $J_S=\rho Q^2/\pi a^2$. In figure 6 the two curves J_P and J_S, computed from the experimental curve of Q against p, are shown, and it will be seen that, except from the smallest values of R, the points deduced from the velocity-profile agree closely with J_S, indicating a uniform velocity across the jet. It would appear that the parabolic distribution with our particular jet ceases when $R=$ about 80 or less, and the uniform velocity-distribution is certainly in force when $R>$ about 180.

§5. EFFECTIVE ORIGIN OF THE JET

Referring to equation (3), we see that for a given value of x the ratio A/B should be independent of the momentum of the jet. Our experimental results show, however, that A/B increases as the momentum increases, as is shown in figure 7, where the dimensionless quantity $(\nu a)^{-1}\, A/B$ is plotted against R. It is clear that if the jet is to be considered as coming from a point, as the calculation assumes, then that point must be taken not at the mouth of the jet but within it, and the distance x_0 of this imagined point source from the orifice must increase as the momentum increases and the angle of the jet becomes smaller. The simplest assumption, which will be justified by considerations of the kinetic energy, is that x_0 is proportional to Q, or, what is the same thing, to $\bar{u}$, so that

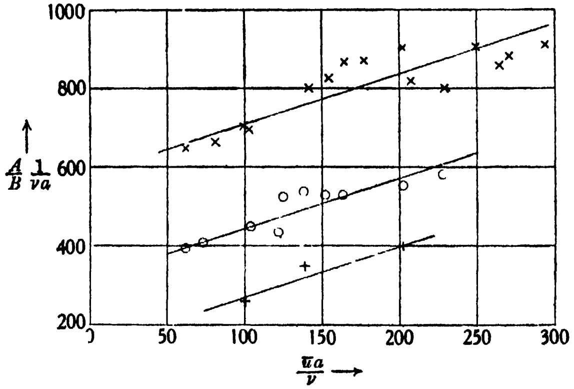

Figure 7. ×, $x=3\cdot3$ cm.; ○, $x=1\cdot8$ cm.; +, $x=0$ 8 cm.

$$A/B=8\nu\,(x+x_0)$$

or

$$\frac{1}{\nu a}\frac{A}{B}=\frac{8}{a}(x+x_0)=8\left(\frac{x}{a}+\frac{x_0}{a}\right).$$

This enables us to find a value of x_0 corresponding to each value of A/B. In figure 8, x_0/a is plotted against $\bar{u}a/\nu$, and it will be seen that the values obtained at the three different values of x are quite consistent. The points show a certain scatter, but it is clear that the method of fixing x_0 makes severe demands on the data, and that discrepancies of a millimetre or two, that is, of 10 to 20 per cent, are to be anticipated. The results can be roughly represented by a straight-line relationship, shown by the full line in the figure, which gives

$$\frac{x_0}{a}=0\cdot160\frac{\bar{u}a}{\nu}=0\cdot160R \qquad \ldots\ldots(5)$$

or

$$\frac{1}{\nu a}\frac{A}{B}=8\left(\frac{x}{a}+0\cdot160\frac{\bar{u}a}{\nu}\right).$$

The three straight lines in figure 7 correspond to this formula, and it will be seen that they represent the experimental results as well as can be expected. In particular one value of x_0, corresponding to a given value of $\bar{u}a/\nu$, represents the results at all three values of x: the separation of the three straight lines, which all have the same slope, is not arbitrary, but given by the formula.

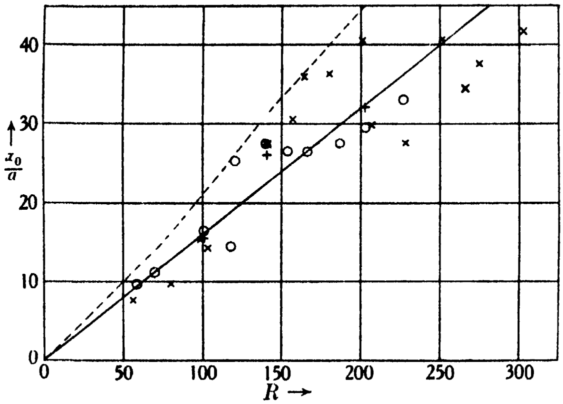

Figure 8. ×, $x=3\cdot3$ cm.; ○, $x=1\cdot8$ cm.; +, $x=0\cdot8$ cm.

In view of the conditions at the orifice, it might at first sight be supposed that the distance of the effective point source within the tube would be such as to make the theoretical lines of flow at the boundary of the orifice continuous with the walls of the tube; that is, that at this boundary $v=0$ and $\partial v/\partial x=0$ for the flow from the point. On reference to the expression for v in equation (1), it is seen that $v=0$ if $\xi=2$, which also gives $\partial v/\partial x=0$. From the expression for ξ we find, remembering that $\rho=1$ and

$$J_s=\frac{\rho Q^2}{\pi a^2}=\pi\nu^2R^2,$$

$$\frac{\sqrt{3}}{4}R\frac{y}{x}=2=\frac{\sqrt{3}}{4}R\frac{a}{x_0}\text{ at the orifice}$$

or

$$\frac{x_0}{a}=\frac{\sqrt{3}}{8}R=0\cdot216\,R.$$

This neglects, however, the fact that the tube and its baffle will interrupt the theoretical lines of flow due to the point source, so that the constant multiple of R cannot be expected to have the value 0·216. It is of interest to note, however, that these considerations give a formula of the same type as equation (5).

To illustrate this point figure 9 has been prepared. It shows the lines of flow from the point *P*, taken at a distance x_0 within the jet given by equation (5), the value of *R* being 200. The lines are shown broken where they lie within the jet and baffle. It is clear that in the liquid half space they cannot have exactly the form shown near the baffle, but it is also clear that only a slight modification is required to make them conform to the actual boundary conditions. The continuity of the tube of flow *FF* with the walls of the jet appears to the eye to be quite good, but actually the point at which $v=0$ is some little distance outside the jet, and is marked with an arrow. The diagram makes it easy to see how it is that the flow from a point source suitably chosen gives a good representation of the actual flow, except in the immediate neighbourhood of the jet. For completeness the velocity-profiles at the three distances *A*, *B* and *C* are given. The scale of x is ten times that of y.

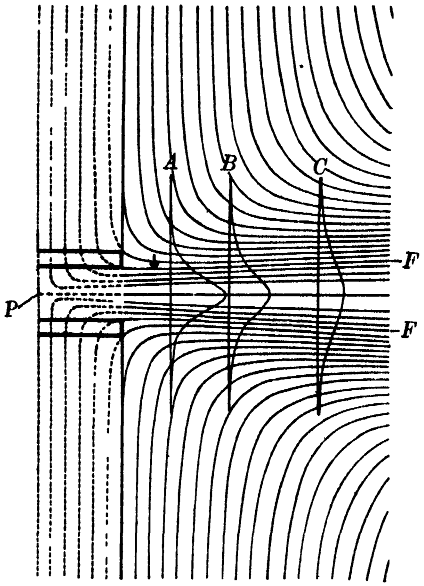

Figure 9.

§6. THE KINETIC ENERGY

If we assume that the velocity at a distance x from the orifice is given by

$$u=\frac{3}{8\pi}\cdot\frac{J}{\eta x'}\cdot\frac{1}{\left(1+C\frac{y^2}{x'^2}\right)^2},$$

where $$C=\frac{3}{64\pi}\cdot\frac{J}{\rho\nu^2} \text{ and } x'=x+x_0,$$

we can derive an expression for the kinetic energy in terms of x_0. Schlichting's calculation with a point source gives, of course, an infinite velocity and energy at the orifice.

The kinetic energy E passing per second through a plane distant x from the end of the tube is given by

$$\begin{aligned} E &= \pi\rho \int_0^\infty u^3 y\, dy \\ &= \frac{27\rho}{512\pi^2}\frac{J^3}{\eta^3 x'^3}\frac{x'^2}{10C} \\ &= \frac{9}{80\pi}\frac{J^2}{\nu\rho x'} = \frac{9}{80\pi}\frac{J^2}{\nu\rho\,(x+x_0)} \qquad \text{......(6),} \end{aligned}$$

or at the orifice

$$E_0 = \frac{9}{80\pi}\frac{J^2}{\nu\rho x_0} \qquad \text{......(7).}$$

A value for x_0 may be obtained by comparing this with the kinetic energy at the orifice as determined by the flow in the tube, which will, however, depend upon the velocity profile assumed. For the parabolic distribution at the orifice

$$J_p = \frac{4}{3}\frac{\rho Q^2}{\pi a^2}$$

and

$$E_0 = \frac{\rho Q^3}{\pi^2 a^4} = \frac{9}{16}\frac{J^2}{\rho Q},$$

while for the rectangular distribution

$$J_S = \frac{\rho Q^2}{\pi a^2} \text{ and } E_0' = \frac{1}{2}\frac{\rho Q^3}{\pi^2 a^4} = \frac{1}{2}\frac{J^2}{\rho Q}.$$

Comparing these values with equation (7) we have for the parabolic profile

$$x_0 = \frac{1}{5\pi\nu} Q \text{ or } \frac{x_0}{a} = 0{\cdot}200\, R \qquad \text{......(8),}$$

and for the rectangular profile

$$x_0 = \frac{9}{40\pi\nu} Q \text{ or } \frac{x_0}{a} = 0{\cdot}225\, R \qquad \text{......(9),}$$

so that the difference between the two cases is not large. As we have seen, when $R < 80$ the value of x_0 should be given by equation (8), while when $R > 180$, or earlier, it should be given by equation (9). The broken line, figure 8, represents the values of x_0 which comply with these conditions. At the higher values of R the values of x_0 derived from the momentum conditions are nearly 30 per cent smaller.

The reason for this discrepancy lies in the nature of the orifice conditions given by the assumption of a point origin within the tube. The actual velocity profile at the orifice varies from parabolic to square, according to R, while the assumption of a point source within the tube must give at the orifice a profile of the form shown in figures 4 and 5. Figure 10 shows, for a particular value of R, the profile from a point source compared with the parabolic and square profiles which give, about the x axis, the same second moment for the enclosed area, i.e. the same momentum at the orifice. The kinetic energy given by the actual profile must clearly, in this case, be less than that given by the assumption of a point source, or, in other words, we must on this assumption increase x_0 to get the right kinetic energy.

The difference between the value of x_0 given by the momentum distribution and by comparison of the kinetic energies at the orifice is, then, due to the fact that the latter method involves the distribution at the orifice itself. When the distance from the orifice exceeds a certain value (which is not greater than 0·8 cm. with our jet of diameter 0·09 cm.) the velocity-distribution, and therefore the kinetic energy, is given to a close approximation by substituting the value of x_0 given by equation (5) in

$$E = \frac{9}{80} \frac{\rho Q^4}{\pi^3 a^4 \nu} \frac{1}{x + x_0}$$

if the distribution at the orifice is rectangular ($R > 180$ with our type of jet). The energy is only $\frac{9}{8}$ times greater if the distribution is parabolic.

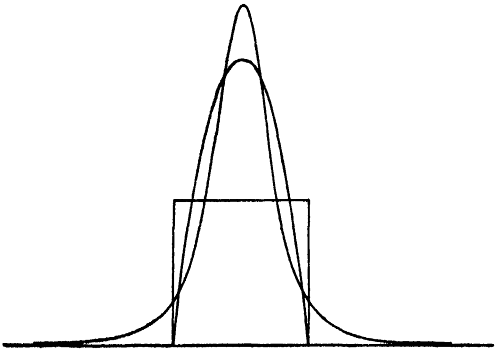

Figure 10.

As regards the loss of kinetic energy which takes place in the jet, for larger values of R we have then

$$\frac{E}{E_0} = \frac{x_0 + x}{x_0} = 1 + \frac{x}{0{\cdot}225 Ra}.$$

§ 7. ACKNOWLEDGEMENTS

We have had the advantage of discussing certain points with Professor L. N. G. Filon, F.R.S., to whom our best thanks are due. The lenses used in the photography were originally purchased from a grant generously made by the Imperial Chemical Industries, Ltd.

REFERENCES

(1) Schlichting. *Z. angew. Math. Mech.* **13**, 260 (1933).
(2) Schiller. *ForschArb. Ver. dtsch. Ing.* No. 248 (1922).
(3) Prandtl-Tietjens. *Applied Hydro- and Aeromechanics*, p. 54 (London, 1934).
(4) Hamel. *Jber. dtsch. MatVer.* p. 34 (1916).
(5) Tollmien. In *Handb. Exp. phys.* **4**, pt. 1, p. 257 (Leipzig, 1931).

DISCUSSION

Mr J. H. Awbery. I wonder whether Prof. Andrade would consider that the formula given for the effective position of the source can be applied generally, even with jets of somewhat different convergence, or whether the coefficient 0·16 is dependent on this factor.

Dr A. B. Wood. A point of great interest is centred at the orifice of the tube, and it would be valuable if the authors could extend their observations (if they have not already done so) to the liquid flow near this point, just inside and just outside the tube.

Dr J. E. R. Constable. With regard to the authors' deduction that, except for low rates of flow, there was an approximately uniform velocity-distribution in the water flowing in the tubes they tested, I should like to ask whether they expect a similar distribution in the gas emerging from a sensitive-flame jet. I understand that the work described in this paper had its inception in a study of the action of sensitive flames.

Miss T. J. Dillon. Could this method be applied to experiments on a blast of air from a jet if suitably light particles were used?

S. R. Bennett. I should like to ask the authors whether the method could be applied to distinguish between the particles originating in the jet itself and those entrained from the surrounding fluid.

Authors' reply. In reply to Mr Awbery and Dr Constable: As long as the velocity is uniform across the orifice the coefficient 0·160 will be appropriate. As is pointed out in the paper, this uniformity of velocity is to be expected so long as the Reynolds's number $\bar{u}a/\nu$ is not very small and so long as the jet does not terminate in a very long uniform tube—that is, so long as it is of anything like the form used in our experiments. In reply to Dr Wood: We tried to measure the velocity in the immediate neighbourhood of the orifice as has been suggested by Dr Wood, but were not successful. We are not clear as to the reason for the unsatisfactory nature of our plates for this region. In reply to Miss Dillon: The method could undoubtedly be applied to a non-turbulent air blast. In reply to Mr Bennett: In order to differentiate between the particles originating in the jet and those entrained, some colouring matter should be introduced into the liquid which issues from the jet. This then distinguishes it from the liquid through which it flows, but does not obscure the particles if a suitable concentration is chosen. We have actually done this in certain experiments.

SECONDARY-ELECTRON EMISSION FROM COMPLEX SURFACES

By L. R. G. TRELOAR, B.Sc., F.Inst.P.

(Communication from the Research Staff of the M.O. Valve Company, Limited, at the G.E.C. Research Laboratories, Wembley, England.)

Received 19 *February* 1937. *Read* 7 *May* 1937

ABSTRACT. The secondary emission from metals on whose surfaces foreign substances (e.g. electropositive metals) have been deposited to various thicknesses up to a few atomic layers has been studied. It is shown experimentally that for sufficiently thin films of the contaminant the secondary emission for a given base metal depends only on the work function of the surface, and not at all on the nature of the contaminant. The form and magnitude of the variation of secondary emission with work function agree with those calculated from the energy-distribution of secondary electrons. From a study of thicker films information is obtained concerning the mean depth of liberation of secondary electrons. The significance of the results in connexion with more complex secondary-emitting materials is discussed.

§ 1. INTRODUCTION

The possibility of making use of secondary-electron emission to obtain an amplification of electronic currents has led to a search for materials having high secondary-emission coefficients. Thus it has been found that certain metallic oxides, after treatment with alkali metal vapours, yield secondary-emission coefficients very much higher than any that have been obtained from clean metals. One of the best of these emitters is caesium on caesium oxide on silver, formed by heating oxidized silver at 200° C. in caesium vapour. This material, which is frequently employed as a photoelectric cathode, has been found by Penning and Kruithof(1) to give a secondary-emission coefficient of between 8 and 10 at 500 volts, and similar values have been reported by other workers.

It is clear that the materials which give these high secondary-emission values have also very low work functions. It is probable, therefore, that the work function must be regarded as one of the fundamental physical factors by which the magnitude of the secondary-emission coefficient is determined. But it is not necessarily the only factor. It is the purpose of the present investigation to determine to what extent changes of work function, unaccompanied (so far as this is possible) by other changes, affect the secondary-emission coefficient.

§ 2. METHOD OF TREATMENT

The work function of a material may be changed by depositing on its surface a thin film of a different material. Thus, for example, the work function of tungsten may be reduced by several electron-volts by the adsorption on its surface of a barium layer less than one atom thick, and the thermionic emission is increased by a large factor as a result of the reduction in the energy which an electron is required to possess in order to pass through the surface.

When a metal is bombarded with electrons the secondary electrons, which originate beneath the surface(2), must lose energy in passing through the surface, in exactly the same way as the thermally emitted electrons. It is to be expected that, in general, there will be some secondary electrons approaching the surface from within which have insufficient energy to escape; these electrons will fall back into the interior of the metal. The relative number of such electrons will clearly depend on the work function, becoming smaller as the work function is reduced. We should therefore expect the relative number escaping, i.e. the secondary-emission coefficient, to increase if the work function of the metal is reduced, for example, by the presence of an adsorbed layer of foreign atoms.

Furthermore, given a knowledge of the energy-distribution of the secondary electrons, it should be possible to calculate how the relative number of electrons escaping will be affected by a given change in the work function.

This calculation is made in the following pages, and the resulting relationship between secondary emission and work function is compared with that found experimentally for a metal contaminated with different substances.

§ 3 THEORETICAL EXAMINATION OF THE RELATION BETWEEN SECONDARY EMISSION AND WORK FUNCTION

The general case. The argument outlined in the preceding paragraph, which will now be developed quantitatively, depends for its validity upon the assumption that the adsorbed film itself neither absorbs primary electrons nor emits secondary electrons. Any effect which it has on the secondary-emission coefficient will be considered to take place solely through the agency of the accompanying changes in work function.

The energy corresponding to the component of velocity normal to the surface will be referred to as the *normal energy* of the secondary electrons. In considering the effect of the work function on the energy of the escaping secondary electrons it is the normal energy only which will be modified, since there are no electrical forces parallel to the surface.

The normal energy distribution of the secondary electrons escaping from a clean metal may be written in the form

$$dn = f(u)\,du \qquad \ldots\ldots(1),$$

where dn is the number of electrons having normal energy between u and $u + du$, measured in electron-volts.

The total number having normal energy greater than any positive value U will be

$$n = \int_U^\infty f(u)\,du \qquad \ldots\ldots(2).$$

If the work function of the metal is now increased by an amount χ eV. by a suitable contamination, only those electrons which formerly escaped from the clean metal with normal energy greater than χ will now be able to escape, and the number n of such electrons will be given by

$$n=\int_{\chi}^{\infty} f(u)\,du \qquad \ldots\ldots(3).$$

If δ_0 and δ are the secondary-emission coefficients for the clean and contaminated metal respectively, it follows that

$$\frac{\delta}{\delta_0}=\frac{\int_{\chi}^{\infty} f(u)\,du}{\int_{0}^{\infty} f(u)\,du} \qquad \ldots\ldots(4).$$

It is therefore possible by means of equation (4) to calculate the effect of an increase of work function on the secondary-emission coefficient, provided that the normal energy distribution of the secondary electrons from the clean metal is known.

The effect of a reduction of work function, with which this paper is mainly concerned, cannot be calculated with the same accuracy, since it is necessary to extrapolate the distribution function represented by equation (1) into the region of smaller values of energy, for which u is negative. (The quantity u in equation (1) represents the energy of the electrons outside the metal. An electron whose energy within the metal is less than the minimum energy which it must possess in order to escape by an amount u may therefore be said to possess an energy $-u$.) If such an extrapolation can be made, the secondary-emission coefficient of the contaminated surface may likewise be deduced from equation (4), but in this case the change of work function χ will be negative.

Application to Maxwellian distribution. If the secondary electrons have an energy-distribution represented by Maxwell's Law, equation (1) becomes

$$du=Ae^{-\alpha u}\,du \qquad \ldots\ldots(5),$$

where A and α are constants. Substitution in (4) gives

$$\frac{\delta}{\delta_0}=\frac{A}{\alpha}\,e^{-\alpha\chi}$$

or

$$\log_{10}\delta=C-b\chi \qquad \ldots\ldots(6),$$

where C and b are constants, δ_0 being fixed. If in this equation χ is taken as the independent variable, it is seen that for a given metal, variously contaminated, the logarithm of the secondary-emission coefficient varies linearly with the work function.

An equation equivalent to equation (6) has been derived theoretically by Sixtus(3) for the special case of a Maxwellian distribution of energy. Sixtus also measured the secondary-emission coefficient and work function for a thoriated tungsten filament in different states of activation. He found the equation to be applicable over a limited range of work functions, but the coefficient b was found to vary greatly with the energy of the primary electrons. These results will be considered in greater detail later.

Derivation of normal energy-distribution. Before considering the applicability of the results deduced in the preceding sections, it is necessary to examine the available data on the energy-distribution of secondary electrons. The first point to be noted is that there are no experimental data for the *normal* energy-distribution. Such measurements as have been made on the energy-distribution fall into the following two classes.

(*a*) The retarding potential method. In this method the secondary electrons from a target are collected by a chamber (usually spherical) surrounding it, to which negative potentials with respect to the target are applied. Provided that the chamber is large compared with the target, this method gives the integral of the *total* energy-distribution curve, i.e. the number of electrons having total energy greater than any given value.

(*b*) The magnetic-spectrum method. In this method a beam of secondary electrons from a target is deviated by a magnetic field, and the total energy-distribution is obtained directly.

The most accurate work on the total energy-distribution is probably that of Haworth, who has obtained curves for molybdenum(4) and columbium(5) by method (*b*). His data for molybdenum will be taken as a basis for the calculations which follow. Curve *a* in figure 1 is taken from Haworth's paper, and shows the total energy-distribution curve up to an energy of 35 eV. This portion of the curve was found to be nearly independent of the primary energy for primary energies greater than 37 eV.

In order to be able to derive the normal energy-distribution from the total energy-distribution, it is necessary to make some assumptions about the distribution in angle of the secondary electrons. On this point the experimental evidence is not conclusive, but it suggests that the number of secondaries emitted per unit solid angle in a direction making an angle θ with the normal is proportional to $\cos\theta$(6). This law will be assumed to be true, and it will be assumed also to apply to any fraction of the emitted electrons having total energies within any given range. The second of these assumptions is equivalent to the statement that the energy-distribution function is the same for beams of electrons emitted in any direction.

If now we suppose the number of electrons emitted, independently of direction, with energy between V and $V+dV$ to be given by

$$dN = F(V)\,dV \qquad \text{......(7)},$$

then, from the cosine law, the number having total energy within this range which are emitted at angles to the normal greater than θ may readily be shown to be $dN\cos^2\theta$. Of the electrons having total energy between V and $V+dV$ these, and these only, have normal energy less than $V\cos^2\theta$. If we now write $V\cos^2\theta = U$, where U is a constant, we obtain for the number having total energy between V and $V+dV$ and normal energy less than U, where $V>U$,

$$dN\cos^2\theta = dN\,.\,U/V = U\,.\,F(V)\,dV/V \qquad \text{......(8)},$$

from equation (7).

The total number having normal energy less than U and any value of total energy greater than U is found by integrating (8) from U to ∞, i.e.

$$U\int_U^\infty \frac{F(V)\,dV}{V} \qquad \text{......(9).}$$

And of course all those electrons for which $V<U$ have normal energy less than U. Adding this quantity to equation (9), we find that the total number having normal energy less than a given value U and any value of total energy is

$$\int_0^U F(V)\,dV + U\int_U^\infty \frac{F(V)\,dV}{V} \qquad \text{......(10).}$$

From this it may readily be deduced that the number N_U having any value of total energy and normal energy greater than U is given by

$$N_U=\int_U^\infty F(V)\,dV - U\int_U^\infty \frac{F(V)\,dV}{V} \qquad \text{......(11).}$$

Since N_U in equation (11) and n in equation (2) both represent the number of electrons having normal energy greater than U, the right-hand sides of these two equations must be equal, and the relation between secondary-emission coefficient and work function is given by an equation analogous to equation (4), namely

$$\delta/\delta_0=N_\chi/N_0 \qquad \text{......(12),}$$

where χ is the increase of work function produced by a contamination.

Starting from Haworth's curve for the total energy-distribution of secondary electrons for a primary energy of 150 eV., and determining the values of the integrals in equation (11) graphically, we obtain the full curve shown in figure 2 when $\log_{10} N_U$ is plotted against U. The portion of the curve shown covers a range of 5 eV., which includes 52 per cent of the secondary electrons.

It will be observed that the curve thus obtained approximates closely to the Maxwellian form given by $\log_{10} N_U=A-bU$. The value of b which best fits the curve over the range shown is found from the slope of the dotted line in figure 2 to be 0·070 (eV.)$^{-1}$. This should therefore also be the value of b in equation (6), representing the relation between secondary-emission coefficient and work function, in the case of contaminated molybdenum. Figure 1 (*b*) shows a Maxwellian distribution of total energy corresponding to this same value of b. It is noteworthy that the integral of the normal energy-distribution curve approaches the Maxwellian form more nearly than does the total energy-distribution.

Deductions from the foregoing theory. The experiments to be described were carried out with the object of testing the applicability of the foregoing theory to the case of a contaminated metal surface. The following four main results are to be expected: (1) A linear relationship should exist between $\log_{10}\delta$ and χ. (2) The constant b, representing the rate of change of $\log_{10}\delta$ with χ, should have the value 0·070 (eV.)$^{-1}$ in the case of molybdenum. (3) For a given metal, the value of b should be independent of the nature of the contaminant. (4) For a given metal, the value of b should be nearly independent of the energy of the primary electrons.

§ 4. EXPERIMENTAL METHOD

In carrying out the experiments, use was made of the method of measuring secondary emission from filaments described by the author in an earlier paper$^{(7)}$. A valuable feature of the method is that it permits of the measurement of changes in the relative contact potential of the filament whose secondary emission is being studied, with respect to a clean tungsten filament. The changes of contact potential give a measure of the changes in work function.

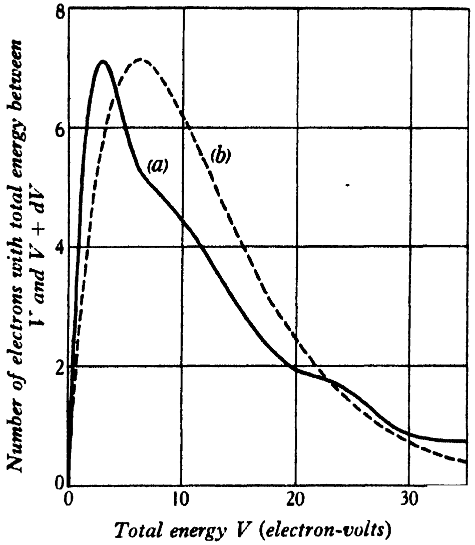

Figure 1. Total energy-distribution curves: (*a*) Secondary electrons (Haworth), (*b*) Maxwellian.

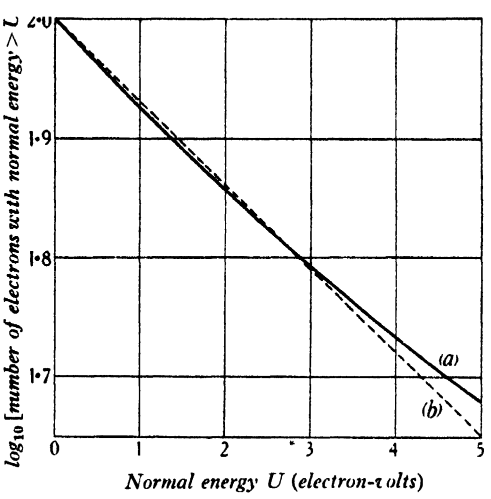

Figure 2. Integrals of normal energy-distribution curves: (*a*) Secondary electrons, (*b*) Maxwellian.

The cross-section of a typical tube is shown in figure 3 (*a*), the main dimensions being the same as those given in the paper previously referred to. The tungsten cathode *C* provides the primary current, *T* is the target (secondary-emitting) filament, and *B* an extra filament to provide the contamination, e.g. an oxide-coated nickel filament. This filament was maintained at cathode potential during the secondary-emission measurements.

The contact-potential measurements. The measurement of the contact potential was carried out in the following way. The cathode was maintained at a temperature such that a saturated thermionic emission current of 5 mA. was drawn to the anode and grid, when these two electrodes were at 100 volts positive potential with respect to the cathode. The target current was then measured, as a function of the target potential, with respect to the cathode, over a range of a few volts above that at which it first assumed a measurable value. The curve obtained under these conditions had a considerable linear portion, which, when extrapolated, cut the zero current axis at a point *x*. The difference between the value of *x* for the uncontaminated target and its value for any state of contamination was taken to be equal to the contact potential-difference between the clean and contaminated surfaces. It is also equal to the difference between their work functions.

It was found that the value of x obtained for any state of the target was not affected by changes of a few volts in the potential applied to the anode and grid. Any changes occurring in the contact potential-difference between these electrodes and the cathode could therefore be neglected.

The value of x obtained in this manner was referred to the potential of the tungsten cathode. In order that changes in x should give a true measure of the changes in contact potential of the target, it was necessary to ensure that the cathode was always in the same condition when the measurement was carried out. Since the cathode, as well as the target, became contaminated during the experiments, it was therefore necessary to remove this contamination by heating the cathode to a high temperature before taking each set of readings.

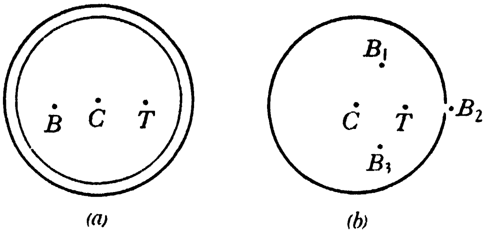

Figure 3. Cross-sections of electrode systems.

§ 5. EXPERIMENTAL RESULTS

The experimental results for films of barium on molybdenum, and of barium, thorium and oxygen on tungsten will now be presented, and a comparison of the results with the theoretical expectations will follow. An examination of some of the effects produced by comparatively thick films will then be made.

Barium (from an oxide-coated filament) on tungsten. Figure 3 (*a*) shows the disposition of the electrodes in this experiment. T was a tungsten filament 0·104 mm. in diameter and 50 mm. long, C was a similar filament 12 mm. long, and B was a nickel wire 0·18 mm. in diameter and 50 mm. long, coated with a mixture of barium and strontium carbonates in equal molecular proportions. During the pumping of the tube the filament B was heated to convert the carbonates to oxides, and eddy-current heating and barium gettering were carried out before sealing off the tube. (A slight modification of the original design, introduced during the course of the work, consisted in making the grid free to slide at one end instead of rigidly fixed. This precaution was taken to prevent distortion of the grid during the eddy-current heating.)

In carrying out the experiment, the target and cathode were first cleaned by heating at 2800° K. for a few minutes, and the contact potential and secondary-emission coefficient for 300 volts bombarding potential were measured. The result of these measurements is indicated by the point *A* in curve *a*, figure 4, which shows the relation between $\log_{10}\delta$ and the change in the work function of the target. The oxide-coated filament was then heated at about 1400° K. for a short time, and after the cathode had been cleaned the measurements were repeated. This second point is shown at *B*. The deposition of barium on the target from the oxide-coated filament had caused a reduction in the work function and an increase in the secondary emission. Successive repetition of these operations gave the points indicated by crosses, the final point being *C*.

On now heating the target at successively higher temperatures so as to re-evaporate the barium, the points marked by circles were obtained. The final condition of the target (point *D*) was nearly the same as its initial condition.

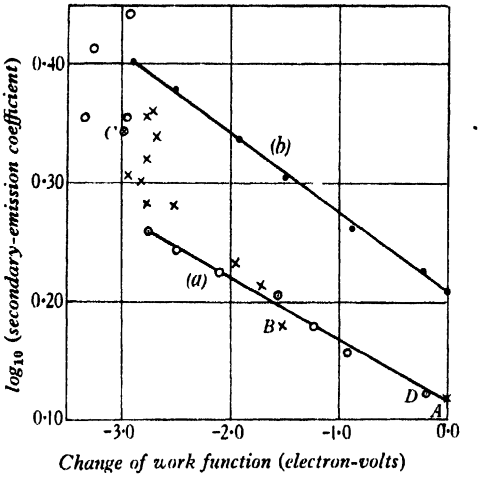

Figure 4. Relation between secondary-emission coefficient and work function: (*a*) Barium (from oxide-coated filament) on tungsten, × deposition, ⊙ evaporation. (*b*) Barium on molybdenum. Primary-electron voltage 300.

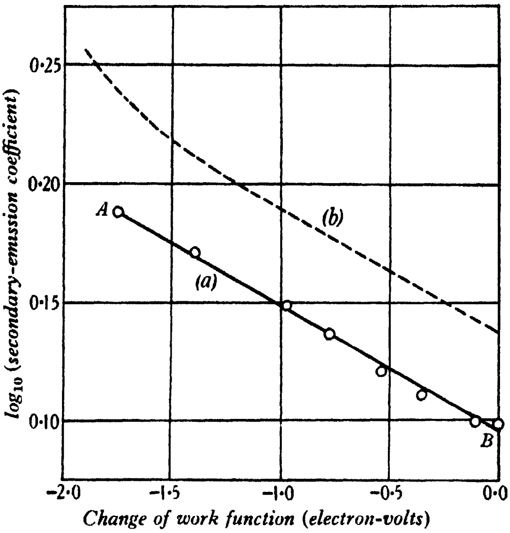

Figure 5. Relation between secondary-emission coefficient and work function for thoriated tungsten: (*a*) Author's results, (*b*) Sixtus's results. Primary-electron voltage 300.

Barium (from an oxide-coated filament) on molybdenum. This experiment was in all respects similar to that described for tungsten, except that points were obtained only during the later stages of evaporation of barium from the target. The results of this experiment, which is shown in curve *b*, figure 4, have already been published in *Nature*(8).

Thorium on tungsten. In this experiment the target was a thoriated tungsten filament of diameter 0·1 mm. The contaminant, thorium, was brought to the surface of the filament by diffusion from within the metal. In curve *a*, figure 5, the point *A* represents the fully activated filament. The remaining points were obtained during deactivation at successively higher temperatures. The final point *B* represents a clean (or very nearly clean) surface of tungsten, and it is noteworthy that the value of δ for this condition is very nearly the same as that found for pure tungsten, point *A*, figure 4 (*a*). A similar experiment has been performed by Sixtus (3), and it is interesting to compare his results, which are reproduced in curve *b*, figure 5, with the author's.*

Oxygen on tungsten. The tube used in this experiment had attached to it a side tube containing a small quantity of potassium permanganate. After measurement of the secondary-emission coefficient at a primary voltage of 300, and of the contact potential of the target, which was of tungsten, the temperature of the target was raised to 1500° K. and oxygen was admitted by heating the permanganate. After the gas had been absorbed by the getter, measurements were made on the oxygenated filament.

The following results were obtained:

For clean tungsten $\delta = 1{\cdot}31$.
For oxygenated tungsten $\delta = 1{\cdot}06$.
Change of work function on oxygenation $= 1{\cdot}78$ eV.

The value for the contact potential difference between clean and oxygenated tungsten is in close agreement with Reimann's value of 1·75 V. (9)

§ 6. DEDUCTIONS FROM THE EXPERIMENTS

The results for barium on tungsten, barium on molybdenum, and thorium on tungsten prove that, provided that the contaminating film is not too thick, there exists a linear relationship between $\log_{10}\delta$ and χ, in accordance with the theoretical expectation. The region representing thicker films in figure 4 (*a*) will be considered later.

The slopes of the curves, giving the values of *b* in equation (6), are given in table 1 for the primary voltages indicated.

Table 1. Values (eV^{-1}) of *b* for various contaminated surfaces

Voltage (V.)	300	150	35
Barium on molybdenum	·067	·057	·050
Barium on tungsten	·052	·060	·043
Thorium on tungsten	·053	—	—
Oxygen on tungsten	·052	—	—

From these figures it is clear that for a given value of the work function and for the different contaminations on tungsten, the secondary emission is independent of the nature of the contamination. The value of *b* is found to change only to a relatively slight extent with variations in the primary voltage. The variations in table 1 are hardly outside the experimental errors.

These variations do not accord with the data given by Sixtus for thoriated tungsten (3). He found the value of *b* to fall considerably as the primary voltage was increased from 200 to 800. Thus at 400 V., for example, its value was 40 per cent lower than at 200 V. No such large variation is to be expected from the theoretical considerations brought forward earlier in this paper.

---

* The author regrets that at the time of reporting his first results to *Nature* he was not aware of the work of Sixtus.

§ 7. COMPARISON OF THEORETICAL AND EXPERIMENTAL VALUES OF *b*

It has been shown that the experimental results are concordant with the main predictions of the theory. The quantitative comparison between the theoretical and experimental values of *b* remains to be made.

The theoretical value was 0·070 (eV.)$^{-1}$ for molybdenum at 150 eV. primary energy.

An examination of the experimental data gives reason to believe that the difference between the 150-V. and 300-V. values for molybdenum shown in table 1 is fortuitous. The mean of these two values will therefore be taken as the most probable experimental value of *b* for 150-V. primaries. The value thus obtained is 0·062 (eV.)$^{-1}$, which is about 12 per cent less than the theoretical value.

It will be remembered that the theoretical value was arrived at from the slope of the line which best fitted the integrated normal-energy-distribution curve over an arbitrary range of positive energies. The experiments are concerned with the region of negative energies (as defined in § 3) covering the approximate range 0 to -3 eV. A more exact comparison of the theoretical and experimental values therefore necessitates finding the mean slope of the extrapolated curve of figure 2 over the range 0 to -3 eV. This extrapolation, though it cannot be made very exactly, yields the value 0·085 (eV.)$^{-1}$ for *b*, a value which should be nearer the truth than 0·070. With this revised value of *b*, the experimental value is 27 per cent low.

The experimental errors involved in the determination of *b* are rather large. The theoretical value involves the errors in the measurement of the energy-distribution and the error introduced by the extrapolation to negative energies. Even when all these errors are considered, however, it is difficult to account for a difference of 27 per cent.

In considering the possible causes of this discrepancy, it must be remembered that the validity of the assumption of a cosine law of distribution in angle of the secondary electrons cannot be regarded as established beyond doubt.

§ 8. EFFECTS WITH THICK FILMS

Our interest thus far has been confined to the thin-film contaminations for which the linear relationship between $\log_{10} \delta$ and χ is applicable. A special experiment was carried out with the object of investigating the thick-film region. The oxide-coated filament, previously used as a source of barium, was replaced by a nickel-barium alloy wire containing about 0·6 per cent of barium. It was hoped that the barium obtained from this source would be purer than that from an oxide-coated filament, since it is known that an oxide-coated filament gives off oxygen as well as barium, the relative amount of oxygen depending upon the amount of ageing to which the filament has been subjected, as well as on its temperature(10).

In order to secure a fairly uniform deposition of barium over the surface of the target, three nickel-barium wires B_1, B_2 and B_3, figure 3 (*b*), were arranged symmetrically round the target *T*. To avoid undue complication the grid was omitted, the primary current calibration (required for the measurement of δ) being taken from the dimensionally similar tubes already described, in which the grid was present.

The relation between $\log_{10} \delta$, at a primary voltage of 300, and χ for this tube is shown in figure 6, which is drawn in a manner comparable with figure 4 (*a*). The portion *AB* of this curve represents the thin-film region, whilst *BC* represents the thick-film region. The thin-film portion of the curve falls along a straight line whose slope is 0·052 $(\text{eV.})^{-1}$. It is interesting to observe that whereas the thin-film portions of the curves of figure 4 (*a*) and figure 6 have exactly the same slope, the thick-film portions are entirely different. The thick-film points lie above the linear portion of the curve for barium derived from an oxide-coated filament, and below for barium derived from a nickel-barium alloy. This difference must be attributed to the presence of oxygen, as well as barium, in the former case. This also accounts for the greater maximum reduction of work function produced when the source of the contamination is an oxide-coated filament. It may be mentioned that these differences are quite typical and have been observed with a number of different tubes.

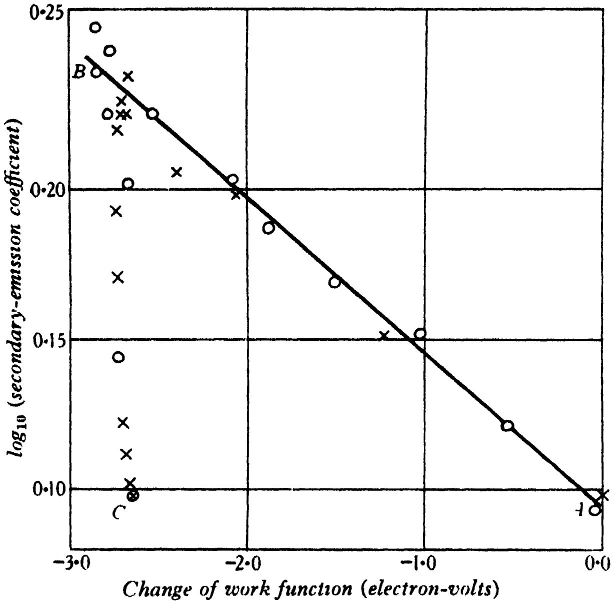

Figure 6. Relation between secondary-emission coefficient and work function Barium (from nickel-barium alloy) on tungsten: × deposition, ⊙ evaporation Primary-electron voltage 300.

In deriving the theoretical expression for the effect of variations of work function on secondary emission, it was assumed that the contaminating film neither absorbed primary electrons nor emitted secondary electrons. It would appear that the region *BC* in figure 6 represents thicknesses of film for which this assumption is no longer true, and that for points in this region the secondary electrons originate at least partly in the barium film itself.

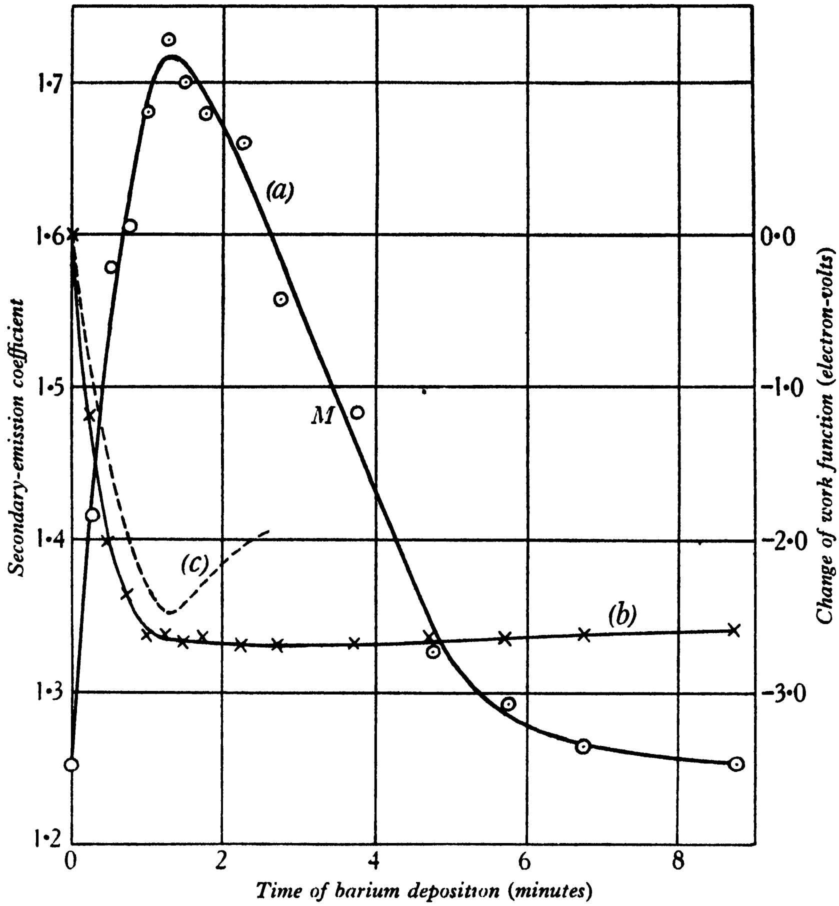

Figure 7. Variation (*a*) of secondary-emission coefficient and (*b*) of work function, with amount of barium on surface of tungsten. (*c*) Becker's work-function curve.

The data from which figure 6 was obtained are represented in a different manner by curve *a*, figure 7. This figure shows the variation of the secondary-emission coefficient with the total time of deposition of barium from the nickel-barium wires. An independent experiment showed that the rate of evaporation of barium was practically constant for the temperature and time used. Hence the time of deposition gives a measure of the relative amount of barium present on the target.

The rising portion of this curve represents the thin-film region, in which the secondary electrons originate almost entirely in the tungsten. The final portion shows a tendency for the secondary emission to approach a constant value and indicates that here the effect of the underlying tungsten is becoming negligible. In the intermediate (falling) portion of the curve the tungsten and the barium both contribute to the secondary emission.

§ 9. THE DEPTH AT WHICH SECONDARY ELECTRONS ORIGINATE

At the point M, figure 7, where the secondary emission is half-way between the thin-film and thick-film values (the work function being approximately constant) the secondaries probably originate in about equal numbers from the tungsten and barium films. The thickness of film corresponding to this point may therefore be taken to be approximately equal to the mean depth at which the secondary electrons originate.

An attempt will now be made to compute this depth. This may be found in terms of the thickness of film which gives the maximum thermionic emission or minimum work function (subsequently referred to as the *optimum thermionic layer*) by reference to the change in work function for different times of barium deposition, curve *b*. This curve may be compared with Becker's(11), which shows how the reduction of work function varies with the relative surface concentration of barium on tungsten. The absence of a clearly defined minimum in the author's work-function curve is probably associated with non-uniformity of the deposit, as a result of which different portions of the target attained the minimum work function at different times. In Becker's experiments such non-uniformities were probably reduced by diffusion of barium over the surface of the tungsten when the filament was heated. However, by considering the rate of fall of work function in the early stages of the deposition, it is possible to obtain a fairly accurate indication of the time at which the optimum thermionic thickness was effectively reached. This time comes out at 1·3 min. The point M therefore corresponds to 2·8 optimum thermionic layers.

If we can now translate depths in terms of optimum thermionic layers into depths in terms of atomic layers, we shall be able to arrive at the mean depth at which the secondary electrons originate. Unfortunately the thickness of film, or surface concentration of barium atoms corresponding to one thermionic layer, has not been experimentally determined. For caesium on tungsten the optimum thermionic layer has been found by Langmuir(12) to be 0·67 of a monatomic layer, but there is no reason to believe that the same value will apply for barium on tungsten. From theoretical considerations de Boer(13) has estimated the optimum covering for barium to be 0·29 of a monatomic layer. Perhaps the best that can be done is to take a value of 0·5 for this quantity. The mean depth at which the secondary electrons originate, according to this assumption, is 1·4 atomic layers.

A correction of this value is necessitated by the fact that the primary electrons strike the target at various angles of incidence. The mean angle of incidence, under the conditions of measurement (i.e. with target potential 300 and anode potential 450), may be taken to be the same as if the electrons remain undeviated from their rectilinear paths by the presence of the target; its value is therefore about 30° to the normal. On the basis of Bruining's work(2) on the effect of angle of incidence on the mean depth at which secondary electrons are liberated, the depth for normal incidence will thus be increased by the factor sec. 30° compared with the depth for 30° incidence. The application of this correction to the value obtained above gives 1·6 atomic layers for the mean depth at which the secondary electrons originate, with a primary voltage of 300 and normal incidence. This figure may be in error by a factor of about 2, on account of the uncertain value of the optimum thermionic layer.

From his experiments Bruining(2) has calculated the product of the absorption coefficient for secondary electrons in nickel and the mean depth at which they originate to be 0·45 for 300-V. primary electrons. He then substitutes Becker's value(14) of $1\cdot5 \times 10^6$ for the absorption coefficient for electrons of energy equal to the mean energy of the emitted secondaries, and obtains the value 30 angstroms for the mean depth at which the secondary electrons originate. This figure, which represents about 14 atom-layers of nickel, is of a different order of magnitude from that found in the present work.

§ 10. OTHER WORK ON COMPLEX SURFACES

It has been shown in § 6 that the effect of a change of work function on the logarithm of the secondary-emission coefficient is nearly independent of the energy of the primary electrons. On this basis it is possible to describe qualitatively how the shape of the curve representing the logarithm of the secondary-emission coefficient as a function of the primary energy will be affected by the deposition on a metal surface of increasing quantities of a contaminant.

So long as the contamination satisfies the thin-film criterion the change of secondary emission will be determined solely by the change in work function, hence the change in log δ will be the same for all values of the primary energy. In this region, therefore, the successive degrees of contamination will be manifested by a displacement of the original curve parallel to the axis of log δ, without alteration of shape. When the thickness of the film becomes sufficient for the effect of the underlying metal to be neglected, a curve will be obtained representing simply the secondary emission of the contaminant in bulk. In the intermediate region, between the thin and very thick films, the shape of the curve will, in general, differ from that for either of the simple materials.

These expectations are substantially verified by the experimental curves of Copeland(15) showing the logarithm of the secondary-emission coefficient, as a function of the primary voltage, for a metal on which were deposited successive amounts of a contaminant. In each of the three cases studied, the first effect of the contamination was to displace the curve parallel to the axis of log δ. Thus, in the case of aluminium contaminated with platinum a reduction of $\log_{10} \delta$ by about 0·15 took place before the shape of the curve became definitely changed. Since the work function of platinum is higher than that of aluminium, a reduction in log δ would be expected as a result of the deposition of the former metal on the latter. An opposite effect was observed when calcium was deposited on gold; this again is to be expected from consideration of the work function.

Since the thickness of film for which the simple work-function effect ceases to apply is related to the depth at which the secondary electrons are liberated, and since this depth increases with the energy of the primary electrons, it would be expected that the shape of the curve typical of the underlying metal would persist to a greater thickness of film at the higher than at the lower primary energies. This expectation also is borne out by Copeland's results.

Whilst Copeland's interpretation of his experiments is concerned chiefly with what has been described in the present work as the "thick-film" region, it seems that his generalization to the effect that the major portion of the observed changes in secondary emission must be ascribed to some other cause than the variation of work function tends rather to underestimate the importance of a factor which has considerable significance in any interpretation of phenomena of this kind.

§ 11. THE SIGNIFICANCE OF THE WORK-FUNCTION EFFECT

The general result of the investigation which has been described may be stated in the following terms: *For any metal whose work function is varied by the deposition on its surface of a thin film of a foreign substance, changes in secondary-emission coefficient are determined solely by the accompanying changes in work function. The magnitude of such changes can be predicted if the energy-distribution of the secondary electrons is known.*

There is no reason to doubt that this law can be generalized to include non-metals as well as metals. On the other hand, it does not account for the changes in secondary emission produced by a thick-film contamination, neither does it give any information about the relative secondary-emission coefficients of different specific materials.

The following discussion, which is admittedly speculative, suggests how the knowledge already gained may be brought to bear on the problems raised by some of the highly complex secondary-emitting materials referred to in § 1.

We may begin by considering what is the maximum secondary emission obtainable from a simply-contaminated metal. The secondary-emission coefficient which would be given by tungsten, for 300-V. primary electrons, if its work function were imagined to be reduced to zero by a thin-film contamination would be 2·3, and that for molybdenum under the same conditions would be 2·9. From the knowledge that the energy-distribution curves for secondary electrons for the dozen or so metals that have been studied in this respect are all quantitatively similar, combined with the fact that the range in the secondary-emission coefficients of the clean metals which have been reliably examined is not very great, it is possible to predict that the highest secondary-emission coefficient obtainable from any metal having a thin-film contamination will not be much more than 3·0 at 300 volts, however much its work function is reduced.

It is known that a number of complex substances yield secondary-emission coefficients much in excess of this value. As a typical case caesium on caesium oxide on silver, referred to in § 1, may be cited. The secondary-emission coefficient for this material at 300 V. may be as high as 8·0. There is nothing in the preceding work which gives any hint of the reason for such a high value.

If, however, we regard the material as a thin-film contamination of caesium on caesium oxide, and if we assume that the uncontaminated caesium oxide would have a very much higher work function than the activated surface, there are two interesting possibilities. It may be (*a*) that the secondary-emission coefficient for the uncontaminated caesium oxide is about the same as that for a metal having the same work function, but the rate of change of secondary-emission coefficient with work function is much greater; or (*b*) that the rate of change of secondary-emission coefficient with work function is about the same as for a metal, but the secondary-emission coefficient for the uncontaminated caesium oxide is very much greater than that for a metal having the same work function. (*b*) is unlikely to be true, since no oxides in the uncontaminated state have been reported as having very much higher secondary-emission coefficients than the pure metals. If, however, (*a*) is true, it follows that the average energy of the secondary electrons from caesium oxide is very much lower than that of the secondary electrons from a metal. This is a matter which could be investigated experimentally.

§ 12. ACKNOWLEDGEMENT

The author desires to tender his acknowledgement to the Marconiphone Company and the General Electric Company on whose behalf the work was done which has led to this publication.

REFERENCES

(1) Penning, F. M. and Kruithof, A. A. *Physica*, 'sGrav., **2**, 793 (1935).
(2) Bruining, H. *Physica*, 'sGrav., **3**, 1046 (1936).
(3) Sixtus, K. *Ann. Phys.*, Lpz., **3**, 1017 (1929).
(4) Haworth, L. J. *Phys. Rev.* **48**, 88 (1935).
(5) Haworth, L. J. *Phys. Rev.* **50**, 216 (1936).
(6) Farnsworth, H. E. *Phys. Rev.* **31**, 414 (1928).
(7) Treloar, L. R. G. *Proc. phys. Soc.* **48**, 488 (1936).
(8) Treloar, L. R. G. *Nature*, Lond., **137**, 579 (1936).
(9) Reimann, A. L. *Phil. Mag.* **20**, 594 (1935).
(10) Reimann, A. L. *Thermionic Emission*, p. 193 (1934).
(11) Becker, J. A. *Trans. Faraday Soc.* **28**, 148 (1932).
(12) Langmuir, I. *J. Amer. chem. Soc.* **54**, 2798 (1932).
(13) de Boer, J. H. *Electron Emission and Adsorption Phenomena*, p. 104 (1935).
(14) Becker, J. A. *Ann. Phys.*, Lpz., **2**, 249 (1929).
(15) Copeland, P. L. *Phys. Rev.* **48**, 98 (1935).

DISCUSSION

Dr J. E. R. CONSTABLE. I should like to ask whether the magnitude of the work function appreciably affects the number of incident electrons which penetrate the target surface and, if so, whether the author has allowed for this effect.

AUTHOR'S reply. If potentials are referred to the cathode, a change in the work function of the target will alter the effective potential outside the metal (i.e. in the vacuum) but not that inside. Owing to the former effect the primary current may be changed by a maximum amount of 0·5 per cent at a primary energy of 300 V., but this has been neglected. Since the potentials within the metal are unaffected, there will be no change in the energy of the primary electrons which penetrate the surface of the target.

THERMIONIC APPROXIMATIONS TO THE GAS-COVERED FRACTION OF AN ADSORBING SURFACE, APPLIED TO THE TEMPERATURE DEPENDENCE OF OXYGENATION AND OXIDATION OF A TUNGSTEN FILAMENT

By M. C. JOHNSON, M.A., D.Sc., Physics Department,
University of Birmingham

AND

F. A. VICK, Ph.D., University of London, University College,
formerly of the University of Birmingham

Received 19 *September* 1936. *Read* 23 *April* 1937

ABSTRACT. A distinction is made between two methods of using thermionic data to estimate for a filament surface the fraction which is covered with oxygen. Conditions are formulated under which either of the two gives approximations to the true fraction defined by concentration of particles in an adsorbed layer. In the method depending upon work functions the necessity for obtaining true instead of apparent thermionic constants for a composite surface is introduced, as these are found to differ widely for oxygenated tungsten. A set of experimental data is analysed by means of the two methods in turn, and empirical graphs are thence obtained representing approximately the temperature variation of the gas content of the surface. The limiting slopes to which these graphs tend in the valid portions of their respective ranges agree with the temperature coefficients of oxidation and oxygen evaporation known from other experiments.

§ 1. INTRODUCTION

In the physics and chemistry of composite surface layers, the fundamental variable is the fraction of surface which is occupied by any given component or which conforms to any given condition. This fraction, written θ in most of the literature, has been estimated in restricted cases only, notably the condensation of alkali vapours upon a refractory metal such as tungsten to which they are electropositive and whose thermionic emission they greatly increase. To determine θ thermionically for the case of an electronegative gas such as oxygen involves considerably greater difficulty, and has mainly been attempted through its intermediate action in cementing more electropositive materials to the underlying metal. In the course of experiments on reactions at a tungsten surface in oxygen at pressures below 10^{-3} mm. of mercury, it was found necessary to reconsider the relation of θ to observable quantities. The results, with their application to the temperature variation of adsorption and oxidation, are presented here. It should be understood that the data are simply saturated thermionic currents obtained with appropriate precautions in the presence of controllable traces of oxygen too small to involve ionization by collision. In addition to the usual pretreatment of all metal surfaces, high-frequency degassing, baking of walls, etc., and the isolation of an isothermal length of filament by means of guard rings, these precautions included technique for maintaining constancy of very small gas pressures over long periods; details may be found in some already published papers(1) on certain other problems for which the experiments were designed.

§ 2. EXPERIMENTAL METHODS FOR OBTAINING AN APPROXIMATION TO THE FRACTIONS OF SURFACE COVERED

In problems in which θ is to be a variable in thermodynamic or chemical equations, its appropriate definition is

$$\theta = N/N_1,$$

where N is the number of gas particles of any one kind per unit area on the surface and N_1 is that number at saturation of the layer. With this definition a plot of $\log_e \{\theta/(1-\theta)\}$ against $1/T$ would express by its slope an energy of adsorption or of surface reaction, in the manner familiar in studies of three-dimensional gas behaviour.

But since no means exists for counting the particles which remain on the surface and so correlating N directly with the accompanying physical changes, an approach must be made to θ through some experimental quantity θ_x to be chosen as follows. (*a*) θ_x must be unambiguously accessible through some observable property of the material. (*b*) Whatever the significance chosen for x, the limits $\theta_x = 0$, $\theta_x = 1$ must denote respectively the state of bare metal and of complete gas covering, satisfactorily related to some chemical or physical criterion of saturation. (*c*) The temperature dependence of θ_x must follow as closely as possible that of N/N_1. For thermionic approaches to θ the chosen indicator must be the simplest function of emission current i consistent with the above conditions, so that

$$\theta_x = f(i)$$

and

$$0 < \theta_x < 1.$$

The requirement (*c*) essentially precludes any one form of θ_x from being used over more than a portion of the range $\theta = 0$ to $\theta = 1$, since any simple function which follows the course of N/N_1 when the adsorbed particles are widely separated will fail to do so when they are so closely packed as to influence each other. Hence any variation of $\log_e \{\theta_x/(1-\theta_x)\}$ which is linear for sparse surface concentrations will become curved before the layer approaches saturation. We proceed to consider two such forms of θ_x, or model approximations to θ.

(A). If the lateral components of the fields of force surrounding adsorbed particles diminish so rapidly with distance that the effects of any local deposit may be considered to cease abruptly at its edge, the whole surface may be regarded as divided into elementary areas of two kinds, whose electron-emitting properties are those of completely bare and completely gas-covered metal respectively. Using the

Richardson equation, with emission constants A_1 for bare and A_2 for covered surface, and work functions ϕ_1 for bare and ϕ_2 for covered surface, we have

$$i_\theta = A_1 T^2 e^{-\phi_1/\kappa T} (1 - \theta_x) + A_2 T^2 e^{-\phi_2/\kappa T} (\theta_x) \qquad \ldots\ldots(1).$$

If, for comparable values of θ_x and $1 - \theta_x$, the first term is large compared with the second term, we have approximately

$$i_\theta = i_0 (1 - \theta_x) \qquad \ldots\ldots(2),$$

whence θ_x can be found directly. We adopt the notation θ_d for this particular instance of a θ_x, determined by current deficiency so that

$$\theta_d = i_0 - i_\theta / i_0 \qquad \ldots\ldots(3).$$

For the highly electronegative deposits with which we deal, the condition $i_0 \gg i_1$ is fulfilled, oxygen reducing the emission from tungsten to about 10^{-4} of its clean value; for a layer of an electropositive element such as caesium, which greatly increases instead of decreasing the emission, a corresponding θ_x would be based on the approximation

$$i_\theta = i_1 \theta_x.$$

(B). If the adsorbed particles modify the field over the whole surface while the layer is still very unsaturated, there is strictly no region behaving as a clean surface, and the whole area may be regarded as altering its properties homogeneously according to the growth of mean surface density of adsorbed material. On this view θ_x is not so much a fraction of area as a measure of partial acquisition of a certain property ascribable to the surface as a whole. The equations of paragraph (A) could not then be used unless an inconveniently large number of terms were introduced, with values of A and ϕ intermediate between those for clean and covered metal.

This second instance of a θ_x accordingly appears as a fractional difference in the work done in emission over the whole surface, and we adopt the notation θ_w, so that

$$\theta_w = (\phi_\theta - \phi_0)/(\phi_1 - \phi_0) \qquad \ldots\ldots(4).$$

The form in which this definition has been used by Langmuir and others may be seen by substituting in the Richardson equation at constant temperature, obtaining

$$\theta_w = (\log i_\theta - \log i_0)/(\log i_1 - \log i_0) \qquad \ldots\ldots(5).$$

Equation (5) is valid only if A is constant or if $\log A$ is proportional to ϕ.

θ_w has been used in studying the deposition of alkali vapours, where i_1 is large and easily determined. The extremely minute and uncertain values of i_1 for electronegative layers has hitherto prevented its application to these. This difficulty is escaped only when (as in one of our previous papers) i_1 can be eliminated by isothermal observation at two different values of θ.

In general θ_w will more nearly approximate to the true θ, or N/N_1, for widely distributed or laterally mobile layers, since they conform more nearly to the physical requirements of paragraph (B), whereas θ_d will follow θ for immobile material sparsely distributed. Adsorbed vapours consisting of strongly dipolar molecules or inert ions will possess the long-range fields assumed for θ_w, while the short-range fields surrounding neutral atoms will allow the assumptions for θ_d to be more nearly correct. These considerations make it clear that neither θ_w nor θ_d bear the same relation to N/N_1 for large as for small values of θ. In particular the contribution made by each additional adsorbed particle to modifying the electronic work function has been shown by several workers to vary with mutual depolarization of neighbours in the surface layer; any such interaction with neighbours will also cause the work of evaporating a neutral particle from the surface to vary with packing of the adsorbed material.

§ 3. θ_w FOR TRUE WORK FUNCTION AND APPARENT WORK FUNCTION

The sensitiveness of θ_w to the value assumed for i_1 in equation (5) shows that this method of approximating to θ requires a reliable estimate of the emission constants of the fully covered metal. For the particular interface with which our experiments deal the term *OW* has been used by most writers, without prejudice to the chemical state of the oxygen covering so long as the latter is regarded as complete, so that $\theta = 1$. Kingdon⁽²⁾ attempted to determine these constants for *OW* by experiments in which gas was admitted to the hot tungsten filament at a rate sufficient to compensate for oxidation, and his values $A_{OW} = 5 \times 10^{11}$ A./cm.^{2} and $\phi_{OW} = 9{\cdot}2$ eV. have been widely quoted. Subsequent work, however, has thrown serious doubt on the possibility either of attaining the condition $\theta = 1$ at any high temperature in the presence of gas, or even of keeping θ at any constant value over a temperature range, during rapid oxidation, while Fowler⁽³⁾ and others have shown the inherent improbability of Kingdon's value of A_{OW} as a genuine thermionic constant. It is generally agreed that A_{OW} is more likely to be equal to or even less than the A_W measured with clean metal, about 10^2 A./cm.^{2}; the form of Richardson's equation then shows that observed values of emission demand a much lower value of ϕ_{OW} than that offered by Kingdon. A more reliable way of estimating ϕ_{OW} is due to Reimann's careful and repeatable measurements of the contact potential-difference between *OW* and *W*, since a contact potential represents, to a first approximation, the difference between the values of ϕ for adjacent surfaces. ϕ_{OW} is thus obtainable by adding Reimann's potential to the ϕ for clean tungsten, the result being $6{\cdot}35$ eV. Reimann has shown⁽⁴⁾ that a quantity of this order can account satisfactorily for the actual small emissions if A is the same for *OW* as for *W*. Since the contact measurements do not involve the above-mentioned temperature control of θ they are free from the objection that applies to Kingdon's experiments, and can replace the latter as the source of ϕ_{OW}.

We have, in the last of the publications referred to, investigated the new interpretation of currents from partially oxygenated tungsten necessitated by the above considerations, and we summarize as follows the portions of our argument relevant to the present need for deducing θ_w.

Consider the Richardson plots typified in figure 1, in which the slope of log i/T^2 against $1/T$ determines ϕ, while the vertical intercept at zero abscissa is measured to obtain log A. The line *bc* for a fully oxygenated surface would, if obtainable, lie below the line *bd* for clean tungsten, and the vertical intercept of *bc* would be either identical with or less than that of *bd* since the adsorbed oxygen cannot increase emission. But if a trace of oxygen, even below 10^{-6} mm., is present while the readings for the Richardson plot are being obtained, the observed currents will distribute themselves over a transition plot typified by the broken curve which intersects in turn the several true Richardson lines, shown dotted, for $\theta_w = 0{\cdot}1$, $0{\cdot}2$, etc., in the area between the lines *bd* ($\theta_w = 0$) and *bc* ($\theta_u = 1$). The course of this transition curve depends upon the rates of adsorption, evaporation, oxidation, etc., which determine the rate of passage from $\theta = n$ to $\theta = m$, where n and m are any fractions. So long as it is impossible to make θ equal to 1 to a higher accuracy than that which, in view of the rapid volatilization of oxide, is available in practice, a nearly linear portion of an observed plot does not yield any true ϕ and A but only apparent constants; these may be considerably in excess of even the true values for the fully oxygenated metal, being merely tangents to some portion of the transition curve. By a series of measurements of pressure and temperature we have proved in detail that the data usually quoted from the work of Kingdon belong to this category of apparent ϕ and A.

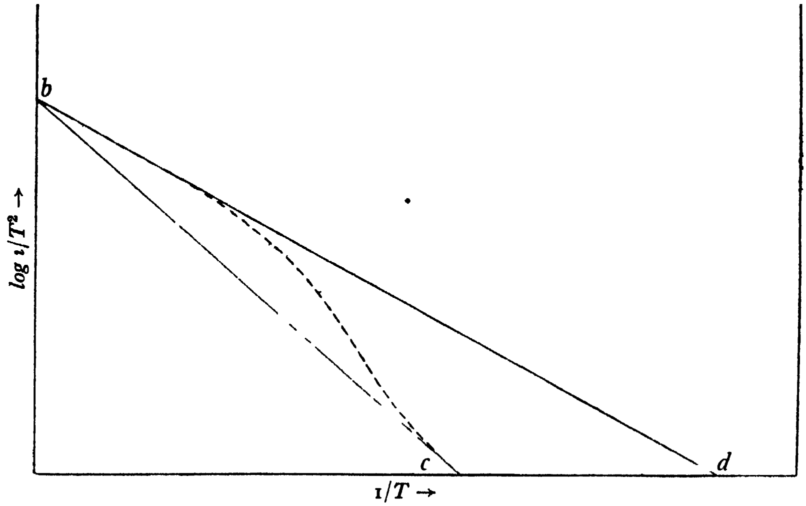

Figure 1. Transition curve between Richardson plots.

To determine a set of values of θ_w, we draw on a large scale a diagram such as that typified in figure 1, inserting all our experimental curves. First the line corresponding to *bd* is obtained from our measurements in the highest vacuum and agrees with the standard determinations of A_W and ϕ_W. Secondly, that corresponding to *bc* is fixed by making a line whose slope gives $\phi_{OW} = 6{\cdot}35$ meet *bd* at $1/T = 0$, thus fulfilling the two consequences of accepting Reimann's contact potentials and the magnitudes of observed emissions.

It is to be noticed that temperature-dependence of any true work function is essentially a second-order correction as compared with the difference between these apparent and true functions, and is neglected throughout, so that all true Richardson plots are taken as straight and only the transition plots as curved.

The diagram fulfils the conditions under which our equation (5) is equivalent to equation (4), so the Richardson plots for various values of θ_w between 0 and 1 will lie between *bc* and *bd*, as dotted in figure 1. These are inserted in the large working graph by geometrical construction, slopes for $\theta_w = 0{\cdot}1$, $0{\cdot}2$, etc. being obtained from the slopes for the work functions $\phi_{OW} = 6{\cdot}35$ and $\phi_W = 4{\cdot}64$ by the relationship of equation (4). For any observed current and temperature, $\log i/T^2$ and $1/T$ then constitute a pair of coordinates determining some particular θ_w as they meet on some particular line intermediate between *bd* and *bc*.

Any other mode of deducing ϕ_{OW} would of course expand or contract the scale of the θ_w thus obtained, but it is clear that no such amendment from thermal measurements is admissible, since the latter only yield a transition plot; in particular, Kingdon's A and ϕ would make *bc* and *bd* intersect at a finite temperature, giving larger emission from gas-covered than from clean metal, which is contrary to the nature of an electronegative layer.

§ 4. THE TEMPERATURE VARIATION OF $\theta/(1-\theta)$ FOR EACH FORM OF θ_x

By the ordinary arguments in the physical chemistry of reactions and the physics of change of state, a plot of $\log_e \{\theta/(1-\theta)\}$ against $1/T$ represents in its slope the energy exchanged in the processes which contribute to growth of θ. Since this is only true in so far as θ measures actual values of N/N_1 or the fractional concentration of deposit, and since we have shown that neither θ_d nor θ_w can follow N/N_1 accurately over their whole range, the energy is only reliably obtained if inferences from each approximation in its own appropriate portion of the range agree with inferences from other experiments. Accordingly we plot in figure 2 this temperature dependence of θ_d determined by inserting the data in equation (3), and also the temperature dependence of θ_w obtained from the same data by the method of evaluating θ_w explained in the preceding section; in each instance three typical sets of measurements are used, curves 15, 19, 17, corresponding to highest, medium, and lowest gas pressures respectively, all at oxygen pressures between 10^{-3} and 10^{-5} mm.

From our physical theory of θ_d and θ_w, it is to be expected that the course of the former will tend more nearly to agree with that of θ itself at the lowest pressures and highest temperatures, i.e. at the smallest values of θ, since a very sparsely separated distribution of adsorbed particles will be unable to affect the large uncovered areas between; but as θ grows the tendency will be for θ_w to represent the molecular state of surface more nearly, as the whole area will become affected by overlapping fields. Hence the portions of these experimental graphs likely to afford the most reliable information as to the temperature dependence of θ or N/N_1 are *AB* and *CD*, where high temperature and low pressure support the approximation θ_d and low temperature and high pressure support the approximation θ_w respectively. Owing to this way in which the temperature and pressure variables combine there is no advantage in attempting to join θ_d and θ_w into a single curve for any given pressure, and we only regard as significant the maximum slope of the one and the minimum slope of the other, since that is where their respective underlying assumptions tend to be fulfilled; numerical comparison between values of θ_d and of any θ_w obtained by any method of estimating i_1 shows that for given pressure and temperature the two approximations to θ may differ widely in absolute magnitude. But since θ is of importance in its temperature coefficient rather than its magnitude at any point, there is no need to do more than compare the slopes at A and D. This will be of interest as comparing the temperature dependence of gas-concentration in very sparse and in very dense adsorbed layers respectively, and can be related as follows to facts previously known concerning the energy needed to remove oxygen in various forms from tungsten.

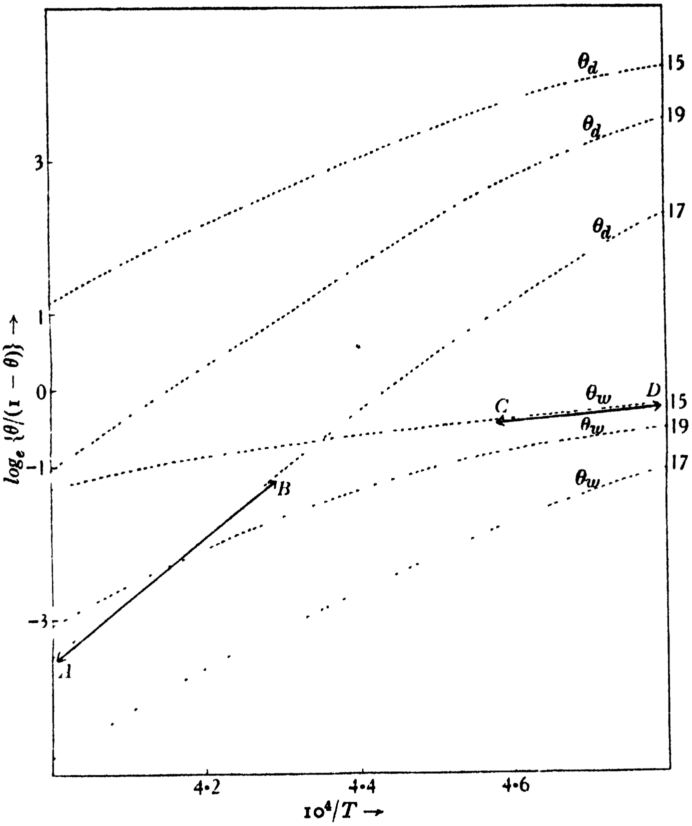

Figure 2. Temperature dependence of surface covering.

§ 5. COMPARISON WITH OTHER EXPERIMENTS

AB and CD are selected not only because each approaches the behaviour of a genuine θ, but also because under the same two extreme sets of conditions the complex action of oxygen on tungsten approaches to the simple states commonly distinguished as "oxygenation" and "oxidation" respectively; the slopes intermediate between AB and CD represent not merely the failure of θ_d and θ_w to follow θ from zero to unity, but also the merging of the temperature dependence of adsorption at small θ into the different temperature dependence of chemical reaction at large θ. For this general reason the graphs would exhibit curvature even if θ were correctly obtainable over the whole range.

Since this chemical reaction at the surface results in slow disappearance of pure metal and pure gas, a tungsten-oxygen interface is not completely described by reversible processes. Hence, although the repeatability of our observations and their independence of the order of sequence indicates that every value of θ and of pressure can be steadied during the time of each experiment, nevertheless no simple balance can represent the complete relation between θ, T and pressure p or number ν of gas impacts per cm.^{2} per sec. Accordingly any isotherm of the Langmuir-Frenkel type suited to any small range of θ will merge into another with a different temperature coefficient in any adjacent range. Let any such restricted equilibrium be expressed by Langmuir's relation

$$\theta = \frac{\alpha\nu}{1+\alpha\nu},$$

$$\frac{\theta}{1-\theta} = \alpha\nu.$$

Let a temperature dependence be added,

$$\alpha = Ce^{E/\kappa T};$$

E calories per mol. represents the energy required for any action resulting in loss of oxygen from the surface. This was first introduced by Frenkel, but the generality of its present definition precludes our identifying C with any particular time interval such as that originally postulated by Frenkel.

This generalization of the well-known grounds for obtaining E from the slope of log $\{\theta/(1-\theta)\}$ against $1/T$ will then refer only to that small region over which the restricted equilibrium holds and there is reason to suppose that a fixed E is applicable; outside each such region E will be modified and possibly also the function of ν as in the different power laws of Fowler and of Roberts.

Two such quantities E, controlling the loss of oxygen from tungsten, are known from measurement, although different authors give different molecular and atomic explanations of them. (*a*) At the lowest gas pressures oxygen is always found to be very strongly attached to the pure metal and slow to evaporate, the E being given by Langmuir and Villars(5) as 162,000 cal., by the present authors(6) as 147,000, and by Roberts(7) as of the order of 130,000. (*b*) At higher pressures a rapid oxidation is always found to set in, WO_3 evaporating readily as fast as it is formed: using some experiments of Langmuir, Rideal and Wansbrough-Jones(8) have estimated the energy required for activation to this more volatile state as 20,000 cal., and on different assumptions we have used the same data to obtain 25,000. Hence the mode of escape of oxygen from tungsten, in opposition to the growth of θ, ranges from the evaporation of an oxygenation layer requiring about 150,000 cal. for its removal, to the instant removal of an oxide layer requiring about 20,000 only for its formation, each of these E's being experimentally defined by an observed temperature coefficient. Hence the slope of our graph of log $\{\theta/(1-\theta)\}$ plotted against $1/T$ should reach approximately 150,000 at $\theta \to 0$ and $\nu \to 0$ and 20,000 when θ and ν become large. These are the two regions AB and CD respectively in figure 2, where θ_d and θ_w each in turn attains some validity as an approximation to the behaviour of θ.

Measurement of figure 2 yields 160,000 and 20,000 as limiting slopes under these two conditions, suggesting that although these thermionic methods may give absolute values of θ much in excess or defect of actual gas concentration, their temperature variation is correct within the accuracy of experiment in those regions where each approximation in turn becomes valid.

§ 6. CONCLUSION

A set of thermionic currents from tungsten, measured in the presence of very small and approximately constant traces of oxygen, can be analysed in two ways for obtaining information as to θ, the fraction of surface covered. Of the current-deficiency approximation θ_d and the work-function approximation θ_w the former is more capable of expressing a correct course of the way surface conditions vary at high temperature and low gas pressure, and the latter at low temperature and high gas pressure. After devising a new method for obtaining the work functions of a partially oxygenated surface, we have plotted a graph of log $\{\theta/(1-\theta)\}$ against $1/T$ for three gas pressures according to each of the two approximations θ_d and θ_w. Measurement of the low-temperature, high-pressure and high-temperature, low-pressure extremes of the graphs yields temperature coefficients corresponding to 160,000 cal. and 20,000 cal. respectively, from the slopes to which they tend where the above conditions for the validity of each approximation in turn is fulfilled. These values agree with the high energy of oxygen evaporation and the low energy of oxidation, previously estimated as from 130,000 to 162,000 and 20,000 or 25,000 respectively.

§ 7. ACKNOWLEDGEMENT

We are very grateful to Prof. S. W. J. Smith, F.R.S. for his kindly provision of all facilities for this work.

NOTE ADDED 15 MARCH 1937

When the concentration of a deposit is such as to justify the common term "film", however dilute, θ_w is the more reliable approximation to N/N_1. But when the adsorbed atoms are so few and widely separated that the regions not contributing to clean emission are isolated, θ_d is the more reliable, as it is not possible to average the work function over such a discontinuous surface.

Since there is no direct evidence as to the concentration at which θ_w supersedes θ_d for the case of OW, our curves are not claimed as independent data for determining E. If θ_w were valid throughout all concentrations, our slope would give the

E of evaporation as 110,000 and the E of oxidation as 20,000, while if θ_d were valid throughout the slope would give 160,000 and 35,000. But as there is independent evidence that these quantities are not far from 150,000 and 20,000 respectively, our results may be taken as indicating that the temperature coefficient of θ_d is a fair approximation under just those conditions that give 160,000, while the temperature coefficient of θ_w is preferable under the conditions that give 20,000.

REFERENCES

(1) JOHNSON and VICK. *Proc. roy. Soc.* A, **151**, 296 and 308 (1935) and **158**, 55 (1937).
(2) KINGDON. *Phys. Rev.* **24**, 510 (1924).
(3) FOWLER. *Proc. roy. Soc.* A, **122**, 44 (1929).
(4) REIMANN. *Phil. Mag.* (7), **20**, 594 (1935).
(5) LANGMUIR and VILLARS. *J. Amer. chem. Soc.* **53**, 486 (1931).
(6) JOHNSON and VICK. *Proc. roy. Soc.* A, **151**, 313 (1935).
(7) ROBERTS. *Proc. roy. Soc.* A, **152**, 467 (1935).
(8) RIDEAL and WANSBROUGH-JONES. *Proc. roy. Soc.* A, **123**, 202 (1929).

DISCUSSION

L. R. G. TRELOAR. The paper gives no information concerning a problem of very considerable physical interest, namely, the way in which the work function varies with the actual number of oxygen atoms present on a tungsten surface, i.e. with the true value of θ. Equation (4) defines a surface covering θ_w such that the relation between ϕ and θ_w is linear. Now in the case of electropositive contaminations, for which the true relation between ϕ and θ is known, it does not even approximate to linearity. For the case of oxygenated tungsten it seems not unlikely that there may be a similarly wide departure from linearity. If this is so, it seems at first sight rather strange that the application of equation (4), even over a small range of θ, should lead to the correct value of the energy associated with the oxidation process.

AUTHORS' reply. The solution of Mr Treloar's problem would constitute a great advance in the subject, but the title of our paper implies correctly that it lies outside our present purpose. We have explained in § 2 that this is because no reliable method yet exists for counting the oxygen particles on the surface as has been done for alkalis: electropositive experiments can be carried out far below the condensation temperature of the alkali vapours involved, but for oxygen the latter is less accessible. Thus even a molecular-ray method cannot decide with precision how many particles have reached the filament and how many remain there. Hence at present the only access to θ with oxygen is through these approximations, for whose validity the correct value of the energy-slope affords some support. Actually, since the departure from linearity of ϕ/θ for alkalis is due to cohesion between the adsorbed particles, this is not to be expected to the same extent with oxygen, which binds more to the tungsten and less to itself. At larger values of θ than we ourselves use, other breakdowns of the relation occur which, however, do not concern the subject-matter of this paper.

THE THERMAL AND ELECTRICAL CONDUCTIVITIES OF A SAMPLE OF ACHESON GRAPHITE FROM 0° C. TO 800° C.

By R. W. POWELL, B.Sc., Physics Department, National Physical Laboratory, Teddington

Received 5 *February* 1937. *Read* 23 *April* 1937

ABSTRACT. Determinations have been made of both the thermal and the electrical conductivities of a sample of Acheson graphite over the temperature-range from 0° C. to 800° C. The thermal conductivity K is found to decrease from a value of 0·40 unit at 0° C. to 0·16 at 800° C., the rate of decrease being greater at lower temperatures. The electrical conductivity σ has at 0° C. a value of 1218 Ω^{-1}-cm^{-1}, which increases to a maximum value of 1518 at 450° C. and decreases to 1444 at 800° C. The corresponding Lorenz function $K\sigma^{-1}T^{-1}$ has a value of 121×10^{-8} at 0° C., which is more than 200 times the value indicated by the electronic theory and possessed by most well-conducting metals. With increase in temperature the value of the Lorenz function decreases rapidly, its value being given by the equation $K\sigma^{-1}T^{-1} = 0{\cdot}0294T^{-1{\cdot}8}$. Thus the Wiedemann-Franz-Lorenz law does not hold for the present sample of graphite, but is replaced by the equation $K\sigma^{-1}T^{0{\cdot}8}$ = a constant. The power to which the absolute temperature is raised is different, as well as the constant value of the expression.

§ 1. INTRODUCTION

In an earlier paper (1) values have been published for both the thermal conductivity K and electrical conductivity σ of several heat-resistant alloys. Some of these values showed considerable departures from the Wiedemann-Franz-Lorenz law, according to which $K\sigma^{-1}T^{-1}$ is constant. The greatest departure occurred at 0° C. where, for two of the metals tested, the value of the Lorenz function was about double that indicated by the electronic theory and possessed by most good conductors. The extent of the deviation decreased with increase in temperature.

Graphite has a thermal conductivity of the same order as that of many metals, yet according to Koenigsberger and Weiss (2), Barratt (3) and Störmer (4), its Lorenz function in the neighbourhood of room-temperature is some 200 to 400 times as great at the normal value. It was considered of interest to ascertain whether the extent of this deviation would also decrease with increase in temperature, and for this purpose determinations of the thermal and electrical conductivities have now been made on a sample of Acheson graphite over a range of temperature similar to that covered by the earlier experiments.

§ 2. EXPERIMENTS

The graphite selected for use in this investigation was a sample of Acheson graphite which was originally in the form of a rod some 9 cm. in diameter and 75 cm. long. From this sample a specimen 7·34 cm. in diameter and 38 cm. long was prepared. This was first tested over the temperature-range from 30° C. to 200° C. by a method similar to that already described for the heat-resistant alloys(1).

The rod was mounted vertically within a coaxial cylindrical guard tube, and the interspace was packed with heat-insulating powder. The lower end of the rod was electrically heated, and the temperature-gradient established in the rod in the final matched steady state was measured by means of thermocouples. The heat flowing along the rod was measured by means of a water-flow calorimeter attached to the upper end, the thermal contact between the graphite and the calorimeter being improved by means of a small mercury bath.

The rod of graphite was later turned down to a smaller diameter of 3·85 cm. and the thermal-conductivity measurements were repeated. For this smaller size of rod a water-flow calorimeter was used which consisted of a coil of tubing soldered to a slightly tapered brass tube about 10 cm. in length and 3·8 cm. in maximum diameter. This unit made good contact with a similar taper on one end of the graphite rod. The values of the thermal conductivity obtained for both sizes of rod are plotted in figure 2, and it will be seen that the two sets of data are in close agreement. The specific resistances also of the two rods agreed. These were measured by the usual method in which the fall in potential along a length of the rod was compared with that across a shunt of known resistance when the same current was passed through each.

To extend the measurements to higher temperatures it was necessary to use an evacuated enclosure to prevent oxidation of the specimen. For these tests the rod 3·85 cm. in diameter was further machined to have a diameter of 1·47 cm. A 20-cm. length of this thin rod was first tested in an apparatus which formed part of an exhibit at the Physical Society's twenty-fifth annual exhibition of scientific instruments and apparatus, and which was subsequently illustrated and described in a published account of the exhibition(5).

The energy input to a platinum heating coil wound on a steatite former and enclosed in an axial hole in the top of the graphite rod was measured. Lateral loss of heat was prevented by the usual matched-guard-tube method, and loss in an upward direction was prevented by mounting a guard heater above the top of the rod and guard tube, and adjusting its energy until a thermocouple located between this heater and the top of the specimen indicated the same temperature as did thermocouples pegged into the upper parts of the rod and guard tube. The current and potential leads and the thermocouple wires were all brought out at the base, vacuum-tight seals being made by water-cooled wax-filled vessels.

In this set-up results were obtained for both thermal and electrical conductivities up to a temperature of about 800° C. It will be seen from figure 2 that over the temperature-range from 200° C. to 300° C., which was common to both the high-temperature and the low-temperature determinations, the values agree to within 2 or 3 per cent. At these temperatures the method employed for the elimination of heat-losses from the small rod would appear to be satisfactory. For tests at higher temperatures it was necessary to verify that the observed energy-input gave a true value for the flow of heat in the specimen. It was found impracticable to do this by measuring the temperature-gradient at the cold end of the rod, and a method resembling that used for the heat-resisting alloys[(1)] was eventually adopted, a short rod of the graphite being screwed into a rod of Armco iron of known conductivity[(6)]. The details of the present set-up in the evacuated enclosure are shown in figure 1.

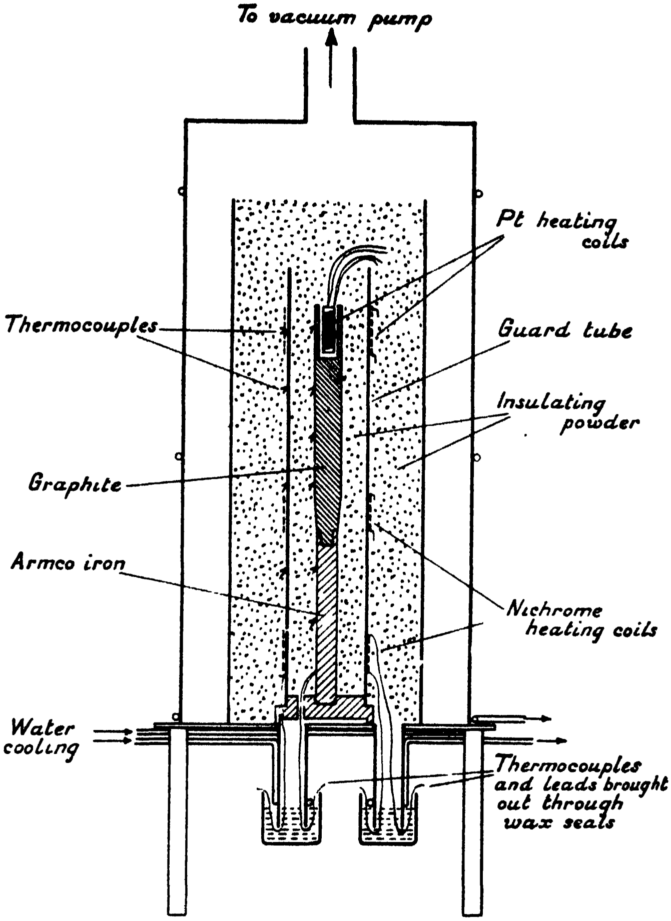

Figure 1. Diagram of apparatus.

The values obtained for the thermal conductivity when this method was used are indicated in figure 2 and are seen to be in general agreement with those obtained in the previous experiment, except that they tend to lie on a somewhat lower curve at the higher temperatures. In drawing the final curve through the experimental points somewhat greater reliance has been placed on these latter values. With neither set-up was it found possible to extend the tests to temperatures much above 800° C., owing to failure of the upper heating coils.

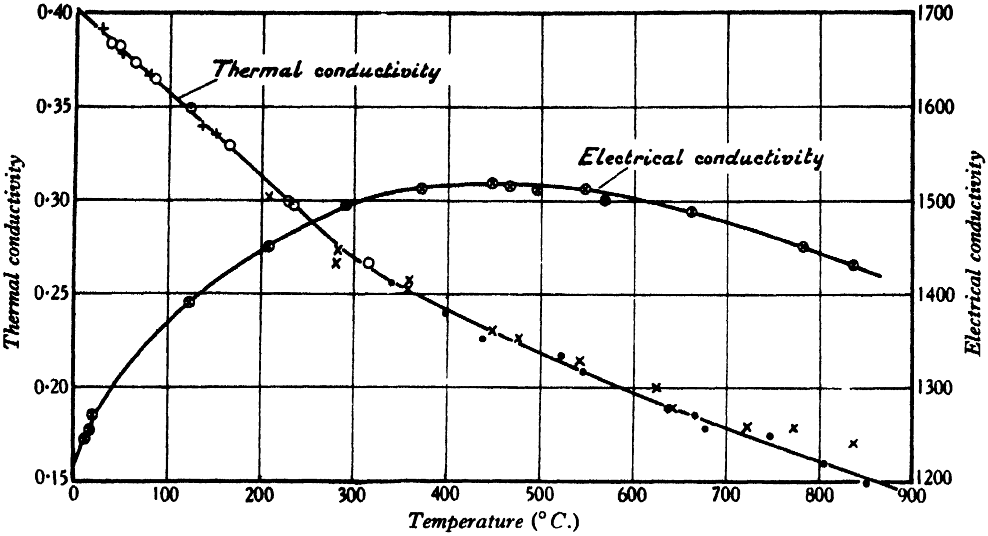

Figure 2. Variation of conductivities of Acheson graphite with temperature. Measured on thick rod, ⊕ ⊕ ⊕ ; on medium rod + + + ; on thin rod by first method × × × ; on thin rod by second method ....

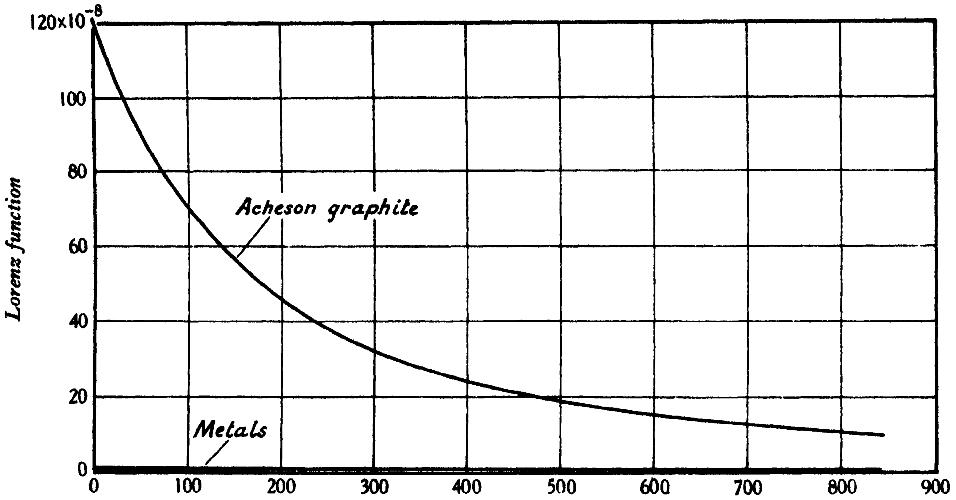

Figure 3. Variation of Lorenz function with temperature.

The curve showing the variation of electrical conductivity with temperature also is plotted in figure 2, whilst that for the Lorenz function, which has been derived from the smoothed values read from the thermal and electrical conductivity curves, is drawn in figure 3. For the purpose of comparison a curve giving the Lorenz function of normal metallic conductors has been included in the same figure.

§ 3. DISCUSSION OF RESULTS

Thermal and electrical conductivities. Graphite is produced when carbon is heated to extremely high temperatures. The physical properties of graphite differ considerably from those of carbon and vary to a lesser extent from sample to sample. The variation presumably depends on the completeness of the transformation, and thus on the temperature of firing, as well as on the purity of the material.

Published values for the thermal conductivity of graphite in the neighbourhood of atmospheric temperature have ranged from 0·037 to 0·85 cal. per cm. per sec. per degree, the corresponding values of the electrical conductivity being 52 and 3000 Ω^{-1}-cm^{-1}. The results for the more poorly conducting graphite were due to Barratt, the others to Koenigsberger and Weiss. Barratt's material, which was a lead extracted from a pencil, would seem to be an unusually poor graphite. Its electrical conductivity was less than that of amorphous carbon, which according to Störmer has an electrical conductivity of 114 Ω^{-1}-cm^{-1} and a thermal conductivity of 0·0048 unit at 13° C.

The present results fall between the above extreme values, and it should be realized that they apply to a particular sample of Acheson graphite. In a future paper the author hopes to deal with the thermal and electrical conductivities of a number of varieties of graphite.

It will be seen from figure 2 that whereas the thermal conductivity of Acheson graphite decreases with increase in temperature throughout the temperature-range covered by the experiments, the electrical conductivity increases to a maximum value at a temperature of about 450° C., and then decreases with further increase in temperature. This maximum value is 1·25 times the value indicated at 0° C. by extrapolation of the curve. The nature of the curve showing the variation of electrical conductivity with temperature agrees with that found for graphite by several other workers, including Noyes(7) and Nishiyama(8) but the temperature at which the maximum value occurs differs from sample to sample. The former used a rod of Acheson graphite for which he found a maximum value of 1·29 times the value at 0° C. to occur at a temperature of about 550° C. Nishiyama studied carbon filaments which had been graphitized to increasingly high amounts by heating to successively higher temperatures. It appears from his results that as the extent of graphitization is increased the maximum occurs at lower temperatures, and at the same time the ratio of its value to that at 0° C. decreases. An X-ray analysis of his specimens was undertaken by Nishiyama, and he considered that the electrical-conductivity results could be explained by the increased grain-size which accompanied increased graphitization.

Three determinations of the thermal conductivity of graphite have been made by other workers over the temperature-range covered by the present experiments. Hansen(9) determined the thermal conductivity of a 1-inch rod of Acheson graphite electrically heated at one end and water-cooled at the other. The rod was lagged, but no guards were used, so that the heat supplied exceeded that collected by the water-flow calorimeter. According to the values derived from the latter measurements, which are probably the more correct, the thermal conductivity decreased from 0·45 at 100° C. to 0·23 at 600° C. and lay from 25 to 15 per cent above that of the present sample of graphite. Hering⁽¹⁰⁾ derived values for the thermal conductivity of graphite from observations on furnace electrodes. Mean values over large temperature-differences are obtained, and these values are probably less exact. They are, however, of the same order of magnitude and show a decrease from 0·34 at 245° C. to 0·29 at 510° C. Crary⁽¹¹⁾ has more recently carried out a determination on Acheson graphite, the source of heat being a flat coil sandwiched between two similar cylinders of graphite 4 in. in diameter. His values for the thermal conductivity range from 0·42 at 0° C. to 0·20 at 730° C. At these extreme temperatures the thermal conductivity is thus only 5 and 15 per cent greater than that of the present experiments. Crary's {conductivity, temperature} curve differs, however, in that it is convex with regard to the axis, and at 400° C. the value of the thermal conductivity is 0·34 compared with the 0·24 obtained in the present investigation. The explanation of this difference is not apparent, but it might be remarked that the method adopted by Crary for the prevention of lateral heat-loss appears to be unsatisfactory in that it assumes the material under test to have a constant thermal conductivity, whereas the conductivity of graphite decreases appreciably with increase in temperature.

The Lorenz function. It will be seen from figure 3 that the Lorenz function of Acheson graphite at 0° C. is some 200 times as great as that of most metals. With increase in temperature its value decreases rapidly, and graphite thus appears to fall in line with such metals as bismuth, nichrome, and F.H. stainless steel in that its Lorenz function approaches the electronic value when the temperature becomes sufficiently high.

A comparison of columns 4 and 5 in table 1 shows that the variation of the Lorenz function with temperature can be represented by the equation

$$L = K\sigma^{-1}T^{-1} = 0\cdot0294T^{-1\cdot8} \qquad \ldots\ldots(1),$$

or

$$K\sigma^{-1}T^{0\cdot8} = 0\cdot0294 \qquad \ldots\ldots(2),$$

where L is the Lorenz function, K the thermal conductivity in cal. per cm. per sec. per degree, σ the electrical conductivity (Ω^{-1}-cm^{-1}), and T the temperature (° K.).

Table 1. Comparison of values of L derived experimentally with those given by equation (1)

T	K	σ	L as $K\sigma^{-1}T^{-1}$	L as $0\cdot0294T^{1\cdot8}$
273	0·402	1218	120·8 × 10⁻⁸	121·1 × 10⁻⁸
373	0·357	1369	70·0	69·1
473	0·312	1445	45·7	45·0
573	0·268	1497	31·3	31·9
673	0·240	1515	23·5	23·9
773	0·217	1517	18·5	18·6
873	0·197	1503	15·0	14·9
973	0·178	1476	12·4	12·3
1073	0·160	1444	10·3	10·3

Extrapolation indicates that at 3800° K., which approximates to the arc-temperature, the Lorenz function of graphite is about 1×10^{-8}, which is still somewhat greater than the theoretical value for metallic conductors.

This investigation has shown that although graphite has a thermal conductivity of the same order as that of many metals, it differs in that the Wiedemann-Franz-Lorenz law is not even approximately true. For the present sample of graphite this law can be replaced by the equation $K\sigma^{-1}T^{0.8}=$ a constant, in which changes have been made in both the power to which the absolute temperature is raised and the constant value of the expression.

§4. ACKNOWLEDGEMENTS

The author desires to thank Dr G. W. C. Kaye, Superintendent of the Physics Department, for his continued interest in this investigation and for the provision of the necessary facilities. He is also indebted to Mr E. E. Smith, B.Sc. for assistance in the preparation of the specimens used in the earlier stages of the investigation and for taking some of the observations, and to Mr M. J. Hickman for rendering similar assistance in the final experiment at high temperatures.

REFERENCES

(1) Powell, R. W. *Proc. phys. Soc.* **48**, 381 (1936).
(2) Koenigsberger, J. and Weiss, J. *Ann. Phys.*, Lpz., **35**, 26 (1911).
(3) Barratt, T. *Proc. phys. Soc.* **26**, 347 (1914).
(4) Störmer, R. *Siemens K. Wiss. Verh.* **13**, 1, 30 (1934).
(5) *The Engineer*, **159**, 68 (1935).
(6) Powell, R. W. *Proc. phys. Soc.* **46**, 659 (1934).
(7) Noyes, B., Jr. *Phys. Rev.* **24**, 190 (1924).
(8) Nishiyama, Z. *Sci. Rep. Tôhoku Univ.* **21**, 171 (1932).
(9) Hansen, C. A. *Trans. Amer. Electrochem. Soc.* **16**, 350 (1909.)
(10) Hering, C. *Amer. Inst. Elect. Engrs*, **29**, 504 (1910).
(11) Crary, A. P. *Physics*, **4**, 332 (1933).

DISCUSSION

Prof. G. I. Finch. Structurally graphite consists of parallel hexagonal-network sheets of carbon atoms. The bindings between the carbon atoms in each sheet are homopolar and very strong but the bindings from sheet to sheet are very loose, of the free electron type, and this is the cause of the colour and good conductivity of graphite. The structure also accounts for the ease with which graphite can be cleaved into thin sheets, and in our laboratory we have succeeded in cleaving off sheets comprising as few as three or four hexagon layers. Such thin sheets are, as one might expect, almost as transparent as glass, and colourless. Owing to the loose binding between the sheets, the graphite structure can be expanded like a concertina by introducing oxygen or alkali metals which do not loosen the homopolar bindings but go in between the sheets. Thus we see that the properties of the graphite crystal in directions parallel and normal to the sheets are quite different, and we should expect to find great differences in the conductivity in a single crystal of graphite according to the direction in which the current flows. It would be of great interest to study the variation of conductivity with direction in a single crystal of graphite. The Natural History Museum possesses some very beautiful specimens containing single crystals measuring as much as 1 cm^3

Miss M. D. WALLER. I should be interested to know how the conductivities of Acheson graphite vary at temperatures below 0° C., as I have found* maximal values of the vibration frequency or Young's modulus of specimens of Acheson graphite and carbon at about -50° C.

Dr O. KANTOROWICZ. A high value of the Lorenz factor for a body like Acheson graphite does not necessarily indicate that the graphite crystals which constitute Acheson graphite show any anomaly at all. Acheson graphite is a kind of ceramic body and contains many pores, and also impurities, which must be suspected of being comparatively bad conductors for electricity and are most likely located on the grain boundaries. Consequently the electric current used to measure the resistance of the sample will flow from grain to grain through those rather restricted passages where one graphite crystal actually touches its neighbouring crystals, and the resistance to electricity of such an agglomerate is rather high. On the other hand the heat-flow is to a far lesser degree affected by the pores and impurities, both of which possess a certain conductivity for heat. The heat therefore flows along a path different from that of the electric current, and partly through other substances. Under these circumstances the quotient of electric and thermal conductivity is probably more a measure for the porosity and impurity of the particular sample than a characteristic of the constituent graphite crystals.

AUTHOR'S reply. I agree with Prof. Finch that it would be interesting to study the conductivities of a single crystal of graphite and appreciate the suggestion as to a possible source from which a suitable crystal might be obtained.

The experiments quoted by Miss Waller are of particular interest, as her observations on the elastic constants presumably indicate some change in the crystalline properties of graphite, and one inference from the high Lorenz function of this material is that a large proportion of the heat is conducted by crystalline rather than electronic processes. So far as I am aware the thermal conductivity of graphite has not been studied at temperatures below 0° C. and I hope to extend my measurements on graphite to lower temperatures.

The factors mentioned by Dr Kantorowicz may also play some part in explaining the high Lorenz function of graphite. X-ray analysis has not revealed any appreciable percentage of crystalline impurity in the specimen used in this work but amorphous carbon is probably present. It is hoped that the tests now in progress on other specimens of graphite will throw further light on the problem.

---

* *Proc. roy. Soc.* A, **157**, 388 (1936).

DEMONSTRATION

A MICROSCOPE FOR USE WITH ULTRAVIOLET LIGHT, EMPLOYING A REFLECTING OPTICAL SYSTEM OF APLANATIC PROPERTIES.

Demonstration given on 28 *May* 1937 *by* B. K. JOHNSON

Experiments have shown that transparent and opaque objects show marked differential absorption and reflection effects when observed with ultraviolet illumination under the microscope. By choosing appropriate wave-lengths, the desired amount of contrast in the image can be obtained; this act suggests a possible means of eliminating staining processes. In order to examine a specimen over a considerable range of ultraviolet wave-lengths it is necessary to have a number of quartz objectives, for it is not yet possible to achromatize the latter. This fact has led the author to design a simplified microscope objective in the form of a lens-mirror and

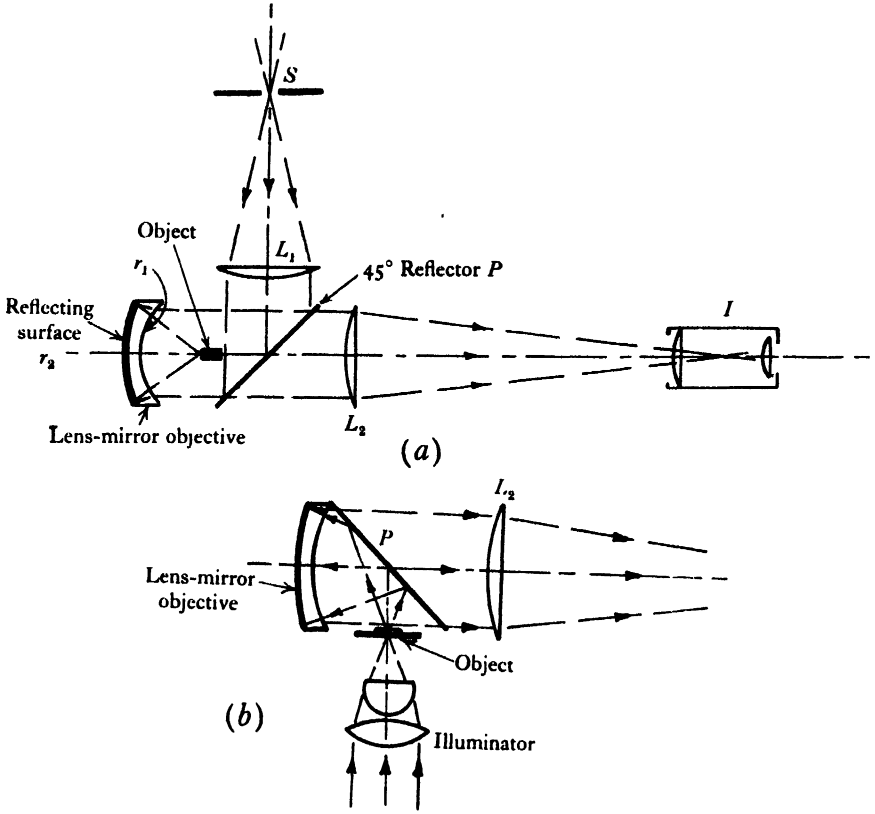

Reproduced by permission of the Journal of Scientific Instruments

The lens-mirror system as applied to the examination of (*a*) opaque objects, and (*b*) transparent objects.

one single lens. Up to numerical apertures of 0·55 such a system can be made free from spherical aberration and coma, whereas all surface-reflecting systems (such as the ellipsoid, the parabola, etc.) suffer from large amounts of coma immediately off the axis. The design of this optical system lends itself for use in the visible region of the spectrum provided that monochromatic light be used, and also in the infra-red. Its chief advantages over the orthodox quartz refracting objectives are (1) simplicity of manufacture and increased accuracy in the making of the surfaces; (2) increased contrast in the image due to reduction of number of air-quartz surfaces; (3) elimination of back-reflections when opaque objects are examined.

A full description of the instrument has been published.*

---

* *J. Sci. Instr.* **11**, 384 (1934).

REVIEWS

The March of Science, 1931–1935. By various Authors. Pp. viii+215. (London: Pitman and Sons, 1937.) 3*s*. 6*d*.

After a long period during which specialization has been increasing, and has indeed been an explicitly announced goal, we seem to be entering on one with somewhat different characteristics. Specialization is of course not losing its importance, but it is now realized that the man who is only a specialist is not thereby superior to another who, in addition to his specialist knowledge, has also a background of wider culture. The changing viewpoint is to be found expressed in the frequent discussions of the examination system and the school curriculum, and is even reflected in popular literature. Wells unifies history, so that specialists in prehistory, archaeology, and the other branches are forced to meet each other and each to see his science against the background of the others. The same tendency is to be recognized in the recent publications of the masters of exposition, such as Andrade, J. A. Thomson and others.

When such a tendency is to be discerned, who better than the British Association should encourage and foster it? That Association was formed for the dissemination of knowledge, and the sections cover between them practically all science. In this book, which is issued under the authority of the Council, eminent practitioners of more than a dozen individual sciences give some account of the main lines of growth in their fields of work during the last five years. Naturally, their methods of treatment vary considerably, and they evidently differ widely as to the standard of knowledge which can be assumed in their readers, as well as in the degree to which they assume these readers desire to pursue the subject. Thus, whereas the physicist deems it desirable to offer an elementary explanation of how a probability wave can represent an electron, and to give us a rapid sketch of the growth of particle physics since 1895, the anthropologist speaks on his first page of the Icenian, Cromerian, Clactonian, Levalloisian, Mousterian, pre-Chellean, Acheulian and Micoquian cultures, and seems to suppose that they represent for us concepts as definite as those which they represent to him. Again, the zoologist gives a bibliography of more than 100 references, in four or five different languages.

On the whole, however, the authors seem to agree in a general way that the man in the street is an intelligent fellow who has some acquaintance with the achievements of science and a real desire to learn more—in short that he is the typical member (or rather, the ideal member) of the British Association.

The existence of this book, with its collection of surveys of recent advances in nearly all the sciences, naturally prompts us to ask the question, "What have been the greatest advances in science in that period?" The answer must depend a good deal on individual bias, but a survey of these chapters certainly seems to make out a good case for psychology as the recipient of the prize for rate of progress. Economics, it is true, may have changed more (and more often) than the others, but the result bears no evident signs of being a better science than its predecessors, whereas all the others do bear the outward signs of an approach to truth.

J. H. A.

Structure of Atomic Nuclei and Nuclear Transformations, by G. GAMOV. Pp. xii+270. (Humphrey Milford, Oxford University Press, 1937.) 17*s*. 6*d*. net.

Though formally a second edition of the author's well-known *Constitution of Atomic Nuclei*, the present volume is to all intents and purposes a new work. The astounding developments which have taken place in the last five years (including on the experimental side the discovery of the neutron and the production of artificial radioactivity, and on the theoretical side the fuller realization of the importance of interaction forces) have both revolutionized nuclear theory and widened its field. Very little of the old book survives in the present pages. It would be interesting, but fruitless, to speculate as to the contents of the next edition. Enough to say that in the present edition the argument moves freely and easily in a region so highly congested that the particles which inhabit it find it impossible to maintain even their identity.

Although the book deals with the theoretical rather than the experimental aspect of the subject, it is not unduly loaded with mathematical calculations, and no reader should be deterred from attempting it through lack of interest in the technique of wave mechanics. The author's main aim has been to discuss, in the clearest possible way, the principles employed in attempting to deduce the laws of physics within the nucleus, and the application of these laws to the problems of nuclear structure and nuclear behaviour. The interdependence of theory and experiment, the nature of the assumptions employed, and the occasional discordance between calculated and experimental results are displayed with clarity and candour. As a result, the book is not only an admirable survey of the present state of the subject, but a fascinating study of new knowledge in the making. The physicist who wishes for an adequate account of the philosophy underlying this new branch of physics will find his requirements well satisfied; and for those who may wish to pursue the mathematical calculations with greater rigour there are numerous references to original papers.

J. A. C.

The Physics of Electron Tubes, second edition, by L. R. KOLLER, Ph.D. Pp. xvii + 234. (International Series in Physics. London: McGraw Hill Publishing Co., Ltd.) 18*s*. 0*d*.

This book gives a very good survey of what takes place inside electronic devices in general. It does not discuss the details of circuits and methods of application of the various electronic tubes. The first four chapters deal with thermionic emission in principle, and cover thoriated tungsten cathodes, caesium on tungsten, caesium on oxygen on tungsten, and oxide-coated cathodes, and also a fair amount of general theory of thermionic emission. Secondary-emission phenomena and their applications are then dealt with, and afterwards special types of electron tubes are described. The omission of any reference to the X-ray tube here is rather surprising, and so is the brief nature of the paragraph on multielectrode tubes. Otherwise the field covered is fairly complete. There is an excellent chapter on the determination of the temperature of the electrodes in electronic devices.

The phenomena of the discharge in gases have been very ably worked into the general scheme of electronic tubes, and there follows a more practical chapter on grid-controlled arcs. There are then chapters on photoelectricity, photoconductivity, and the photovoltaic effect. In the latter two chapters the author has deviated from the title of electron tubes rather considerably, but they are written with the same clarity and conciseness as the rest of the book and therefore form a welcome addition to the text.

This book, which has now reached the second edition, has been brought very fully up to date, and is in touch with all the latest electronic developments. Sections have been added on electron optics, secondary emission multipliers, ignitrons, and positive-ion emission. It is an excellent book for the student of physics and electrical engineering, and will also be useful to the specialist engaged on research in other branches of physics in which these electron tubes find application.

J. A. D.

The Low-Voltage Cathode-Ray Tube, by G. PARR. Pp. x + 177, with 76 figures. (London: Chapman and Hall.) 10*s*. 6*d*. net.

This book should make a strong appeal to a large number of readers. It is sufficiently elementary for the more advanced students of physics and engineering and also sufficiently advanced to be of use to the research worker. The first chapter, entitled "Construction and operation", contains a general introduction to the principle of the cathode-ray tube. The second chapter deals with focusing and performance and is the only chapter in which some weakness makes itself felt. The treatment of electrostatic and electromagnetic focusing in this chapter is rather too scanty, and the distortion effects, as observed on the screen, are not dealt with as fully as one would have expected. The third chapter describes the formation of Lissajou's figures. This is a good feature because it revises a subject about which knowledge is too often taken for granted. The fourth chapter deals very fully with the essentials of the linear time base, and the next chapter goes on to other types of time base. The three remaining chapters deal with the various applications of cathode-ray tubes. In the first place to radio engineering, in the second place to general industrial problems, and finally to television. The chapter dealing with the industrial application is rather speculative, but the sections describing the uses of the cathode-ray tube in radio and television engineering are clear expositions of more well-known methods. The text is concise, but difficult points are explained with considerable care and the book is well illustrated throughout. The general quality of the publication is excellent.

J. A. D.

Atlas der Analysen-Linien der wichtigsten Elements, by Dr F. LÖWE. Pp. iv + 37, with 16 plates. (Dresden and Leipzig: Theodor Steinkopff, 1936.) RM. 10.

This is a second, and much changed, edition of the author's *Atlas der letzten Linien*, the new title being in accordance with Gerlach's nomenclature. To those engaged in spectrographic detection of the small quantities of elements in solutions, ores, alloys and other materials the work can be recommended as a saver of time and trouble. The author is the head of a section of the Zeiss works at Jena. In the first few pages are notes on apparatus and method (condensed spark between carbon electrodes on which a chloride solution has been evaporated) and on other atlases and tables (titles and references are listed). Then follow the 16 plates of selected regions of line spectra of 46 elements, and, printed on opposite pages, brief explanations and lists of wave-lengths. To the latter are added data for 11 elements not included in the plates. The book ends with a ten-page table of analysis lines between λ 1854 and λ 8944. A notable and commendable feature is the fewness of the lines included in this table and in the plates.

W. J.

Ions in Solution, by R. W. GURNEY. Pp. vi + 206. (Cambridge: The University Press, 1936.) 10*s*. 6*d*.

One of the characteristics that distinguish the best conjurers from those of the second rank is the fact that they send their audiences home impressed with the ease of the performance, and filled with the conviction that they have only to snap their own fingers in the air to find pennies in their hands. Dr Gurney shares these powers. Apparently provided only with the common sense necessary to depict qualitatively the form of the potential energy curve of an electron, ion or nucleus as the case may be in the presence of another particle or assemblage of particles, and furnished with a knowledge of what a Boltzmann factor is, he can draw forth the quantitative results of the Debye-Hückel theory so clearly as to persuade the reader that he could have done it himself without the help of these pioneers.

A very big claim is made in the preface, to the effect that the methods employed in the book can be expected to lead to an advance in ionic theory commensurate with that made in atomic theory by Bohr's methods. The reviewer is thus saved the trouble of deciding whether the book is or is not epoch-making—that is already decided for him. It does seem probable, however, that the claim can conscientiously be endorsed. It marks the epoch when attention is transferred from the salt in solution to the ions themselves, just as Bohr's theory completed what Ritz had commenced—the transfer of attention from spectral lines to energy levels.

This alteration in outlook leads (or will lead when the necessary quantitative data are available) to an easy understanding of the relation between ions *in vacuo*, ions in a crystal lattice and ions in solution. It permits of simple deductions relating to solubility, mutual precipitation, and electromotive forces and particularly the electrochemical series. It is very successful in dealing with optical absorption, and therefore with the colours of solutions, and must contain adequate information from which to calculate the electrical conductivity of an arbitrary solution at any degree of concentration. This last matter, however, is one to which little attention is devoted in the book under review.

The outstanding impression which the book leaves, is one of clarity, due to the facts that it is self-contained (there is not one reference in it to any scientific paper) and that the physical principles are kept so well to the fore. There are in it two suggestions that the author contemplates writing a companion volume containing a more detailed treatment, and it is to be hoped that in due course this will in fact appear.

J. H. A.

The Organic Chemistry of Nitrogen, by N. V. SIDGWICK, F.R.S. New edition revised and rewritten by T. W. J. Taylor and W. Baker. Pp. xix + 590. (Oxford: Clarendon Press, and London: Humphrey Milford, 1937.) 25*s*. net.

The first edition of this book, published in 1910, has long been out of print and scarce, and the appearance of a second completely revised edition is welcome. The book deals with selected groups of organic compounds of nitrogen which are in themselves of considerable chemical and biochemical importance, and the treatment is very complete on the chemical side, from the point of view of both the theory and the experimental aspects. What differentiates the book from most treatises on organic chemistry is the unusually full discussion of relevant physical considerations, and at the present time, when so many organic compounds are the subject of study by physicists in various fields, the book is timely and of great interest and value. The eighteen chapters deal with the important groups of simpler organic compounds of nitrogen, and there are full references to the literature. The printing and paper are excellent and the moderate price is worthy of emphatic mention. This is a book of first-rate importance, and the new edition fully maintains the excellent features of the old. All the chemical considerations which must be known in dealing with any compounds from the point of view of physics or physical chemistry are explained, and the book is one which should be included among the works on chemistry in a physical library.

J. R. P.

THE CONDUCTION OF ELECTRICITY IN SOLIDS

Report of the
Conference held in Bristol from 13*th to* 16*th July*, 1937,
under the joint auspices of the Physical Society
and the University of Bristol

CONTENTS

Introduction. By N. F. MOTT . . . .

PART I. CONDUCTION IN NON-METALS

R. W. POHL. Electron conductivity and photochemical processes in alkali-halide crystals 3
R. W. GURNEY and N. F. MOTT. Trapped electrons in polar crystals . 32
Discussion 36
R. HILSCH. Alkali-halide phosphors containing heavy metals . . . 40
J. T. RANDALL. The effects of temperature on the intensity of fluorescence of some impurity solids 46
Discussion 57
J. H. DE BOER and E. J. W. VERWEY. Semi-conductors with partially and with completely filled $3d$-lattice bands 59
Discussion 72

PART II. CONDUCTION IN ALLOYS

G. BORELIUS. Resistance of alloys with disordered and ordered arrangement of atoms 77
W. L. BRAGG, C. SYKES and A. J. BRADLEY. A study of the order-disorder transformation 96
C. H. DESCH. Age-hardening alloys 103
Discussion 108

PART III. CONDUCTION IN THIN METALLIC FILMS

G. I. FINCH. The structure of thin metallic films 113
E. T. S. APPLEYARD. Some factors influencing the resistance of thin metal films 118
A. FÉRY. A study of the electrical properties of thin films of platinum obtained by cathode sputtering in air and other gases (He, N_2, O_2 and H_2) 136
J. BERNAMONT. Fluctuations in the resistance of thin films 138
J. E. LENNARD-JONES. The migration and aggregation of metal atoms on solid surfaces 140
Discussion 151

INTRODUCTION

By N. F. MOTT

Electricity may be carried in solids and liquids either by charged ions (electrolytic conduction) or by electrons. The papers in the present volume are concerned almost entirely with the conduction due to electrons. The first group of papers deals with conduction in insulators and semi-conductors, that is to say in solids in which there are normally at low temperatures no free electrons. They can only conduct if electrons are freed, either by irradiating the solid with light of a frequency which it can absorb, thus releasing electrons by a kind of internal photoelectric effect, or in the case of semi-conductors by keeping the solid at not too low a temperature, so that the thermal agitation of the atoms of the solid is able to free a few electrons.

The first paper is by R. W. Pohl, whose school in Göttingen has been for many years investigating photoconductivity in the alkali halides. These crystals do *not* show photoconductivity if they are illuminated in their own characteristic absorption band; in order to obtain photoconductivity one must first colour the crystal by the addition of some impurity or defect, which gives a new absorption band. The crystals used by Pohl are coloured by heating in the vapour of the alkali metal, which gives the well-known yellow colour of rock salt crystals or blue of KCl. The crystal shows photoconductivity if irradiated in the new absorption band so obtained. This band is known as the *F* band and the absorbing centres as *F* centres; their precise origin is at present uncertain, though hypotheses to explain it are advanced in the papers by Gurney and Mott and in the subsequent discussion.

An electron released from an *F* centre by the absorption of a quantum of radiation travels through the crystal only a certain distance before it is trapped, apparently in a less stable position called an F' centre. Thermal motion may release it, but it does not necessarily form another stable *F* centre until minutes or hours have elapsed. This suggests at once a mechanism for phosphorescence in crystal phosphors, on which we publish papers by R. Hilsch and by J. T. Randall. In the sulphide phosphors made by the addition of a heavy metal, it is possible that an electron is ejected from an impurity atom, forms an F' centre or something of the kind a long way off, and only re-radiates when it finds the parent atom again some time later. This hypothesis is supported by the temperature-dependence discussed by Randall, but cannot be applied to the alkali halides.

In semi-conductors free electrons are released, not by the absorption of light but by thermal agitation. In the theory given by Wilson in 1931 it is suggested that the electrons are released from impurities and defects; according to this theory the conductivity should be given by a law of the type $\sigma = Ae^{-E/kT}$. In the paper on semi-conductors by J. H. de Boer it is shown that experiment is in disagreement with theory in a number of ways. First, the parameter E depends often on the concentration of the impurity; and, secondly, there exists a number of semi-conductors which, according to the theory, ought not to be semi-conductors at all, but metallic conductors. These are ionic crystals with incomplete *d* shells, such as NiO. In the discussion of de Boer's paper, R. Peierls suggests that quite a drastic modification of the present electron theory of metals will be necessary if it is to include these substances.

The second group of papers deals with conduction in metals. Both on the experimental and on the theoretical side the study of conduction in metals is much further advanced than in insulators; so that, whereas in the latter case a host of problems remains to be investigated in connexion with the problem of conduction in the simplest substance, sodium chloride, in the case of metals we deal with problems of a more special nature.

G. Borelius gives an account of the work carried out by his school at the Technical College, Stockholm. This deals mostly with the magnetic and electrical properties of alloys and shows very clearly how the resistance is increased by the addition of any impurity which enters into solid solution, and also how the resistance is intimately related to the magnetism. Of especial interest is his account of alloys in which a superlattice can be formed, and his complete description from the point of view of thermodynamics of the transition between the ordered and disordered states.

W. L. Bragg describes his more recent attempt to obtain an atomic picture of the process, and the work carried out at the University of Manchester and at the laboratories of Metropolitan-Vickers by A. H. Bradley and C. Sykes. In this work again the conductivity and hence the mean free path are always found to be less in the disordered than in the ordered state.

C. H. Desch describes age-hardening alloys with especial reference to their resistance; the mechanism by which atoms in a supersaturated solid solution crystallize out is discussed.

The conduction of electricity in thin metallic films has been the object of a very large number of investigations. In an introductory paper G. I. Finch gives an account of the structure of such films as revealed by electron diffraction. E. T. S. Appleyard describes recent work by Lovell carried out under his direction in which apparently uniform layers of alkali metal are deposited on glass, and which, with a thickness of five or six atomic layers, have a resistance only about ten times greater than that of the bulk metal. The mechanism of conduction in so thin a film is discussed. In other metals (e.g. mercury) islands of metal seem to be formed, and the mechanism by which this can occur is outlined by J. E. Lennard-Jones. The different electrical properties that films of metal can have, according to their past history, is well brought out in the papers by A. Féry and J. Bernamont.

Finally a few words must be said about the account of the discussions published in this volume. This has been prepared by members of the staff of the Physics Department of the University of Bristol, who must take responsibility for the opinions expressed, since in the interests of speed of publication these summaries have not in all cases been submitted to the original speakers. No attempt has been made to include everything that was said; on the other hand, in certain cases remarks made in private discussion after the meetings have been included.

PART I

CONDUCTION IN NON-METALS

ELECTRON CONDUCTIVITY AND PHOTOCHEMICAL PROCESSES IN ALKALI-HALIDE CRYSTALS

BY R. W. POHL, Göttingen

---

§1. INTRODUCTION

THE fact that electrons can move about in the interior of highly insulating crystals was first definitely established in the case of the diamond(87). If a diamond crystal is placed in series with a battery of several hundred volts and a sensitive galvanometer, electron currents of the order of 10^{-9} A. may be observed upon illuminating the crystal with the light of a match. The number of crystals showing similar properties increased rapidly, but the observations continued to be generally of a qualitative nature. To be sure, it soon became evident that this phenomenon was related to photochemical processes, fluorescence and phosphorescence.

Quantitative measurements could be expected as soon as it became possible to work with artificially-produced crystals of well-defined chemical constitution. A series of preliminary experiments showed that this condition could be most simply fulfilled in crystals of the alkali halides. These can be produced with a high degree of chemical purity from fused salts. Single crystals of the size of an apple, or even having a content of a litre are relatively easily obtainable(9, 41). With the help of crystals so produced, the phenomena of electron conductivity and photochemical processes have been quite satisfactorily explained. The following report presents the most important results of the work, not a history of the individual problems. The investigations concerning fluorescence and phosphorescence processes are still in their initial stages, and will therefore not be included in this report, which is divided into the following four parts:

Part 1. The optical properties of the alkali-halide crystals in their pure state as well as when containing a stoichiometric excess of one of the components, i.e. either alkali metal or halogen (§§ 2–6).

Part 2. The motion of electrons released in the interior of these crystals through light, or more briefly: photoelectric currents in the crystals (§ 7).

Part 3. The motion of electrons thermally released, and the connexion between electron conductivity and ionic conductivity (§§ 8–9).

Part 4. Photochemical processes in the crystals (§§ 10–12).

Until 1926 these investigations were made jointly with B. Gudden (Gudden is now Professor of Physics at the University of Erlangen) and in later years with Dr Hilsch (now first assistant in my institute in Göttingen). Among numerous co-workers I should like to mention particularly: Z. Gyulai, E. Mollwo, A. Smakula, O. Stasiw, and recently G. Glaser, W. Lehfeldt, H. Pick and E. Rögener.

PART I. THE OPTICAL PROPERTIES OF THE ALKALI-HALIDE CRYSTALS

§2. THE OPTICAL PROPERTIES OF PURE ALKALIDE CRYSTALS

The alkali-halide crystals, with their cubic lattice composed of positive and negative ions, probably represent the simplest type of solid body. They are perfectly transparent throughout a spectral range of almost six octaves and have a smooth dispersion curve, as illustrated in figure 1 for the case of LiF$^{(16,28,41,79)}$.

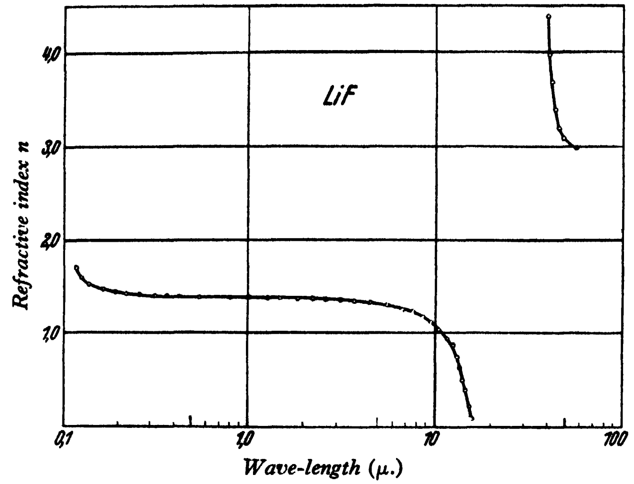

Figure 1.

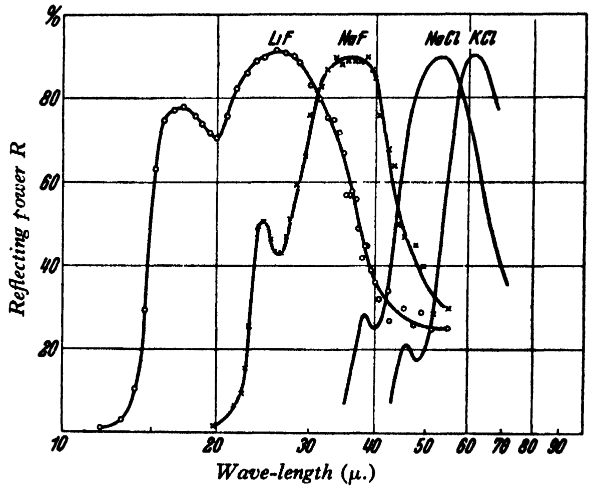

Figure 2. Structure of the Reststrahlen bands.

The rapid decrease of the index of refraction in the infra-red begins as soon as the region of residual rays (*Reststrahlen*), i.e. ionic vibrations, is reached. The structure of the residual ray bands is not as simple as supposed by their discoverer, Heinrich Rubens. Figure 2 gives typical curves for four salts$^{(37,79)}$. The values of the absorption constants in the infra-red have been determined only for a limited range of wave-lengths. The measurements hitherto made do not suffice for a diagram.

In the ultra-violet, the state of affairs is quite different. There the absorption spectra, which cause the rapid increase of the index of refraction in the region of short waves, have been carefully measured(20, 23, 27). Figure 3 shows the absorption spectra of three Na salts and figure 4 of three K salts, which have recently been extended by the measurements of Schneider and O'Bryan(88). The similarity of spectra lying above one another is to be noticed.

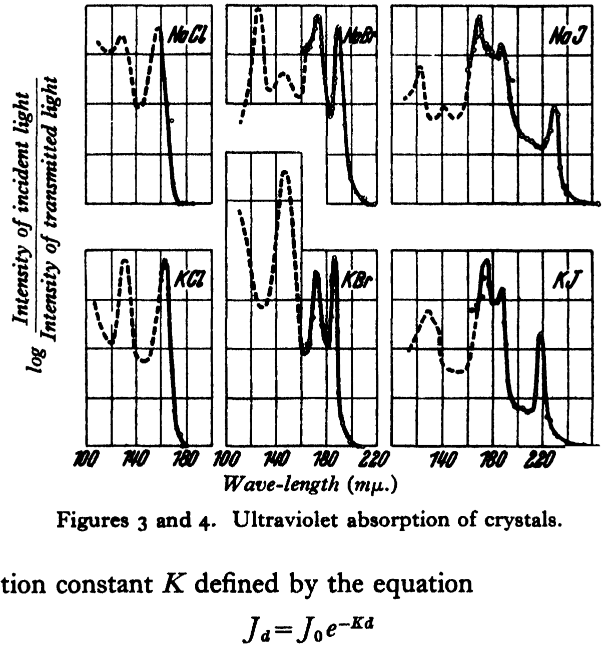

Figures 3 and 4. Ultraviolet absorption of crystals.

The absorption constant K defined by the equation

$$J_d = J_0 e^{-Kd} \qquad \text{......(1)},$$

where J_0 is the intensity of the entering light, J_d the intensity of the transmitted light, and d the thickness of the specimen, has been measured for the first absorption bands of several salts in the form of thin films of thickness(49, 53) 2 to $10 \cdot 10^{-6}$ cm. These are given in table 1. In order to facilitate comparison with the absorption of light in metals, the values of the absorption coefficient $n\kappa$, defined by the equation

$$J_d = J_0\, e^{-4\pi (n\kappa)\, d/\lambda_{\text{air}}} \qquad \text{......(2)},$$

have also been calculated, and are given in col. 4. The fifth column gives the molecular absorption constant β, defined by the equation

$$J_d = J_e . e^{-\beta N/F} \qquad \text{......(3)}.$$

Here N is the number of molecules under the surface F and β represents the absorbing cross-section of the individual molecules for the incident photons.

These data are for crystals of the highest chemical purity obtainable. In experiments dealing with electronic conductivity, photochemical processes and luminescence phenomena, the starting material, if possible, should contain no more *than one foreign molecule in* 10^5 *to* 10^6 halide molecules. Greater concentrations of *foreign molecules cause disturbances and the* appearance of secondary effects(15,45).

Table 1. *Absorption in the first ultra-violet absorption band*

Crystal	Wave-length of the band (mμ.)	Absorption constant K (cm.$^{-1}$ × 10^5)	Absorption coefficient $n\kappa$	Molecular absorption constant β (cm^2 × 10^{-17})
NaBr	192	10·0	1·53	5·5
KBr	189	8·8	1·33	6·3
RbBr	193	7·0	1·07	5·6
KJ	220	7·2	1·26	6·3
RbJ	223	7·0	1·24	6·9

Moreover, for a complete investigation it is necessary to know in addition to the optical properties of the pure crystals the changes which are introduced when small deviations occur in the stoichiometric composition of the crystals. It is possible to produce crystals with a small excess of alkali metal or of halogen.

§3. PRODUCTION OF ALKALI-HALIDE CRYSTALS WITH A STOICHIOMETRIC EXCESS OF ALKALI METAL

If an alkali-halide crystal is heated in the vapour of its cation metal, a stoichiometric excess of alkali metal is produced in the interior of the crystal, which imparts a bright colour to the crystal. In the simplest case this colour is caused by neutral alkali atoms which are loosely bound in the interior of the crystals in some manner or other. These foreign atoms shall be designated by the name *Farbzentren* (colour centres). The absorption spectrum has the form of a simple bell curve such as is shown in figure 5 for the five alkali-chloride crystals(18,60).

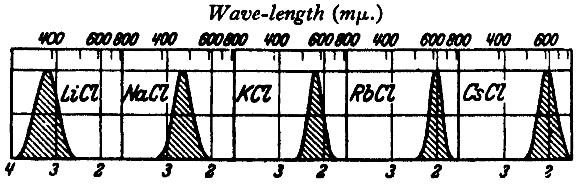

Figure 5. Absorption bands of the Farbzentren at 20° C.

The number of Farbzentren can be determined from the magnitude of the absorption constants and the half-width of the bands. The details of this calculation will be given in § 4.

The number of Farbzentren per cm^3 of the crystal is proportional to the number of metal atoms per cm^3 in the vapour surrounding the crystal(42). Figure 6 shows this fact for the case of KBr(80). In making these measurements, the vapour pressure of the metallic vapour and the temperature of the crystal could be varied independently of one another. The ratio

$$\alpha=\frac{\text{number of Farbzentren per cm}^3}{\text{number of vapour atoms per cm}^3}$$

is always greater than unity. Besides this, α decreases with increasing temperature of the crystal (see figure 7).

The binding of the Farbzentren may be described formally as a solution of alkali metals in the interior of the crystal. The law of mass-action may be applied and the

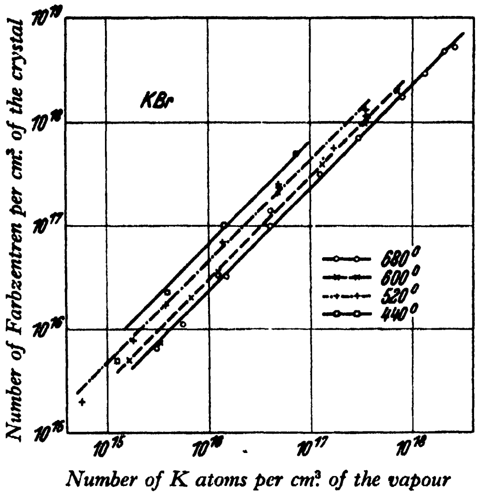

Figure 6. Solubility of K in a KBr crystal.

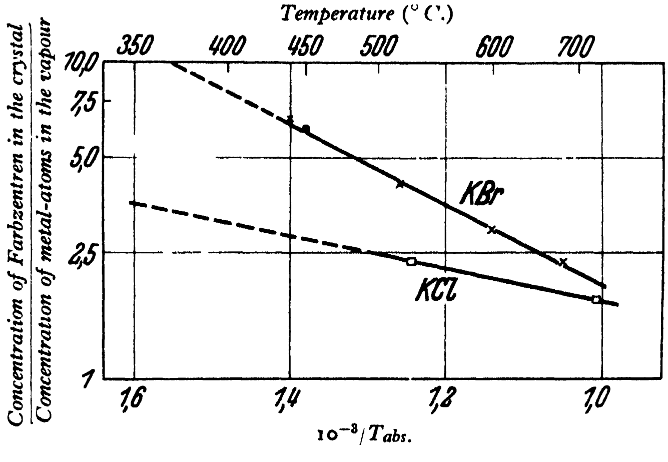

Figure 7.

constancy of the factor α would then mean that the process takes place without any change in the mol-number of molecules. This may be written as

$$K \text{ (in vapour)} \rightleftarrows K \text{ (in crystal)}.$$

According to this conception, the temperature dependence of the proportionality factor α may be considered as consequence of a positive binding energy W_F, according to the equation

$$\frac{d\,(\log \alpha)}{d\,(1/T)} = \frac{W_F}{k} \qquad \ldots\ldots(4).$$

($k = 1{,}37 \cdot 10^{-23}$ watt-sec./° C.)

The binding energy W_F calculated by means of equation (4) from figure 6 gives the value $W_F = 0{\cdot}25$ eV. for the Farbzentren in KBr crystals, and from analogous measurements the value for the Farbzentren in KCl crystals is $W_F = 0{\cdot}10$ eV.(80). Measurements on the other salts are still in progress.

Just how this process of the introduction of extra atoms into the crystal lattice, here formally described as "solution" takes place, remains uncertain. It may be due to inner absorption processes(7, 8, 11). According to the experiments, as the temperature increases, the number of Farbzentren per cm^3 of the crystal approaches that of the atoms per cm^3 in the vapour(80).—As the melting-point of the crystal is passed, a new effect enters: Liquid KBr just above the melting-point is able to take up approximately 15 times as many alkali atoms per cm^3 as are present per cm^3 in the vapour(66).

Extrapolation of figure 7 down to room temperature 20° C., yields $\alpha_{\mathrm{KBr}} = 3{,}6 \cdot 10^4$ and $\alpha_{\mathrm{KCl}} = 9 \cdot 10^1$. Furthermore if the vapour-pressure curve for potassium is extrapolated to this same temperature, the resulting number of atoms per cm^3 is $7{,}5 \cdot 10^8$, and hence the equilibrium-concentration of Farbzentren in the crystal is

$$\left.\begin{aligned} c_{20^\circ} &= 3 \cdot 10^{13}\ \mathrm{cm.}^{-3}\ \text{for KBr} \\ c_{20^\circ} &= 7 \cdot 10^{10}\ \mathrm{cm.}^{-3}\ \text{for KCl} \end{aligned}\right\} \qquad \ldots\ldots(5).$$

These figures are to be considered merely as rough approximations, which indicate simply the order of magnitude. Moreover, an important practical conclusion can be drawn from them: in making experiments upon electron conduction and photochemical processes concentrations of Farbzentren below 10^{15} per cm^3 can rarely be used. Otherwise crystals of great thickness are necessary in order to obtain a measurable light absorption.* Accordingly in order to have enough absorbing centres to work with at room temperature it is practically always necessary to use a quenched crystal previously filled with Farbzentren at a high temperature, whose higher concentration can be preserved in this way. In so doing it is unavoidable that a fraction, albeit a very small fraction in most cases, of the excess of alkali metal atoms combine to form larger colloidal particles, which are precipitated as foreign bodies(11). The absorption spectra of these colloids are very markedly affected by the particle size(32). In individual cases, where these colloids introduce secondary effects, they must be measured and considered. Fortunately, however, in most cases colloid formation can be so far suppressed as to be negligible.

* 10^{15} Farbzentren per cm^3 of KCl, for example, produce (at room temperature) an absorption constant of $0{\cdot}22$ cm.^{1}; i.e. the light traversing the crystal must pass through a thickness of $4{\cdot}5$ cm. in order to be reduced to $1/e$ or 37 per cent of its original intensity.

§4. THE OPTICAL PROPERTIES OF THE FARBZENTREN

The absorption spectrum of the Farbzentren has a simple bell-shaped band, as was shown in figure 5. The form of this band is practically the same for all salts at the same temperature, as indicated in figure 8. In this figure(42) the curves obtained for the four salts have been reduced to the same abscissae by division by the proper frequency $\nu_0 = \nu_{\text{max.}}$. The curve drawn is that calculated on the basis of classical dispersion theory.

The form of the absorption spectra agrees well with the classical dispersion theory. The number N_0 of Farbzentren per unit volume(22), calculated on the basis of this theory, gives the equation

$$N_0 = 1{,}31\cdot 10^{17}\,\frac{n_0}{(n_0^2+2)^2}\cdot K_{\text{max.}}H \qquad \ldots\ldots(6),$$

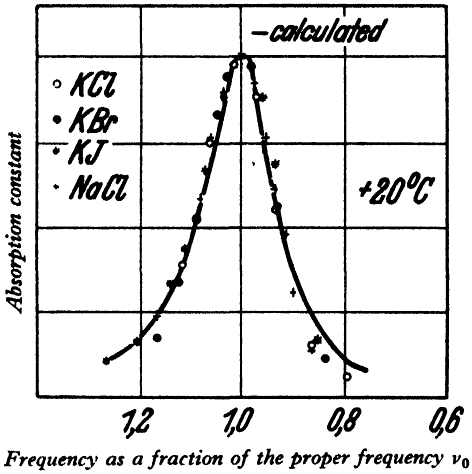

Figure 8.

where n_0 is the index of refraction of the crystal for the same wave-length of the band-maximum, $K_{\text{max.}}$ the absorption constant for the band-maximum in cm^{-1} according to equation (1), and H the half-width of the band in eV. This agrees very well with experiments. This equation may be written more simply

$$N_0 = A\,.\,K_{\text{max.}}\,.\,H \qquad \ldots\ldots(7).$$

The constant A, calculated on the basis of the theory for all halide crystals, has the average value of $10^{16}/\text{eV. cm}^2$. Moreover, for KCl the constant A determined from an analytical chemical measurement(75) has the value $A = 1{,}31\cdot 10^{16}/\text{eV. cm}^2$.*

The position and the form of the absorption spectra change decidedly with temperature(6, 10). As an example figure 9 shows measurements for KBr. A particular wave-length λ_0 is shown by a broken line. For each temperature this marks the point on the violet side of the absorption band at which the absorption-constant K has dropped to half the value of $K_{\max}$.. This wave-length has the same position for all

---

* If all the Farbzentren have been coagulated into small colloid particles, the absorption band changes in both shape and location. In spite of this fact, equation (7) may be used in making estimations, and at least gives values of the right order of magnitude(40).

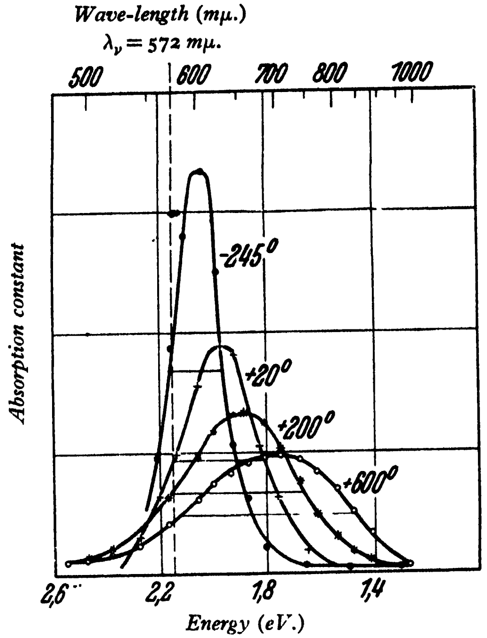

Figure 9. Absorption band of Farbzentren in KBr.

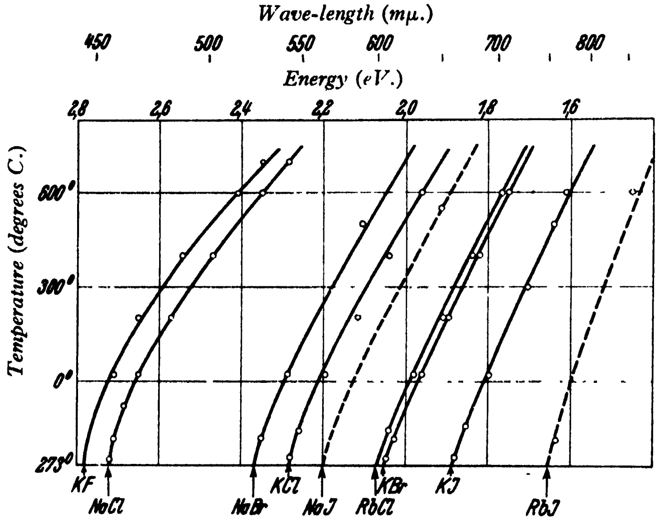

Figure 10. Absorption-band maxima of the Farbzentren.

temperatures(42). This may possibly be ascribed to a transition between two undisturbed energy levels of the crystal. Further, figure 10 shows the position of the band-maximum for nine different crystals as a function of the temperature. For any particular temperature there is a close connexion between the frequency ν_0 of the band-maximum and the lattice-constant d of the crystal under observation(30). At room temperature, the following relation is found to hold with close approximation

$$\nu_0 d^2 = 5\cdot10^{-5}\ \text{sec.}^{-1}\ \text{m.}^2 \qquad \ldots\ldots(8).$$

§5. THE OPTICAL EXCITATION OF FARBZENTREN

By the process of light absorption the Farbzentren disappear and in their place there appear new centres, somewhat more loosely bound, which will be called F' centres. Their absorption spectrum extends further into the region of long wavelengths, and the maximum also is shifted in this direction(4, 29). In favourable cases, the two maxima can be distinctly observed, as in figure 11. Curve A shows the absorption spectrum of the F centres before and curve B after excitation, i.e. after irradiation by light which was absorbed by the F centres. The excitation took place at −100° C. On the contrary, both spectra, A as well as B, were made at −235° C., in order to make the band as narrow as possible and thus to separate them distinctly. As a result of the excitation, the F band has been reduced by about two-thirds and in its place the shaded absorption band of the F' centres appears(86). These F' centres are stable only at low temperatures; they have only a limited life at higher temperatures(14), being changed back into F centres by thermal motion. At 250° these F' centres could not exist longer than one second in any crystal.

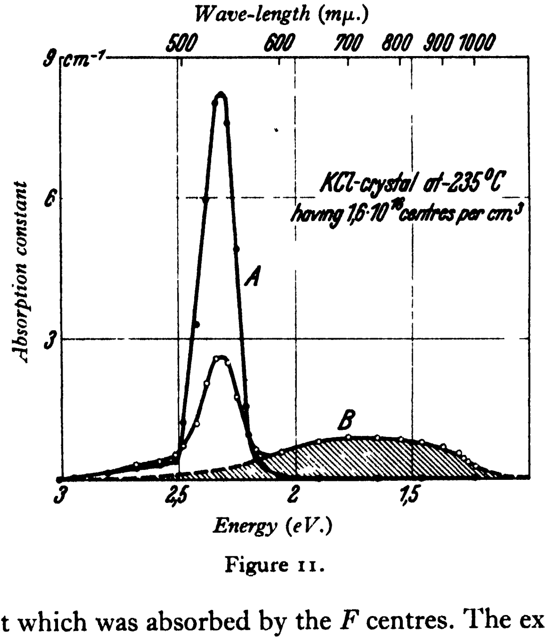

Figure 11.

Light absorption by F' centres, i.e. that of wave-length longer than 700 mμ. (as shown in figure 11) has the same effect as thermal motion. The transition $F \rightarrow F'$ is thus reversible(1). The quantum yield of the transformation $F \rightarrow F'$ has been measured repeatedly(3, 22, 86) but the investigations are not as yet completed. The ratio

$$\eta^* = \frac{\text{number of disappearing Farbzentren}}{\text{number of absorbed light quanta}}$$

is easily measured. More difficult, however, is the measurement of the ratio

$$\eta = \frac{\text{number of } F' \text{ centres formed}}{\text{number of absorbed light quanta}} \qquad \ldots\ldots(9).$$

For temperatures down to − 130° C., $\eta = \eta^*$, but at still lower temperatures it has been possible to measure only η^*, and this has been found to have a value of approximately unity down to − 200° C. (Individual values between 0·4 and 1·6: the reason for this variation is still unknown.) Measurements of η at temperatures below − 150° C. have not as yet been successful. This is connected with another fact, also as yet unexplained: the number of disappearing Farbzentren is only initially proportional to the number of absorbed light quanta, but later approaches a saturation value. Only a fraction of the Farbzentren can be made to disappear by light absorption and this fraction is strongly dependent upon the temperature Figure 12 shows an example of this, for the case of KCl. Principally noteworthy is the decrease in the direction of lower temperatures. The decrease towards higher temperatures is due simply to the experimental conditions. Here F' centres are produced by the disappearing Farbzentren, and the life of the F' centres is very short. By the time that the optical measurement of the number of centres has begun, a part of these F' centres has again disappeared. Further questions connected with figure 12 still need to be thoroughly investigated.

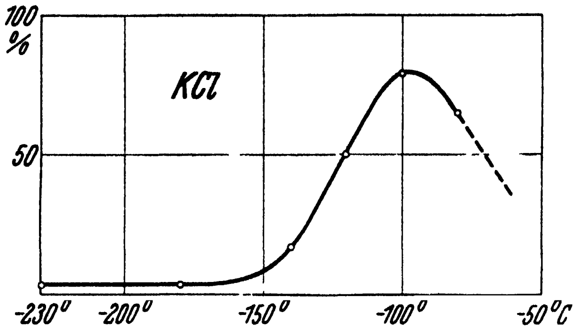

Figure 12. Ratio of decrease in number of Farbzentren due to excitation to number before excitation

Note added in proof. Some new results are shown in figure 12 (*a*). The quantum yield for the $F \rightarrow F'$ transition begins at higher temperatures with the limiting value 2 and, as the temperature is lowered, falls much below 1; the dependence on temperature is much the same as for photochemical transitions (§ 12).

One light quantum can move only *one* electron; the latter can in the limiting case cause two Farbzentren to disappear and produce in their stead two F' centres.

The Farbzentren thus serve not only as sources of electrons, but their presence in the lattice also limits the range of the free electrons. An electron is ejected by a light quantum from a Farbzentrum and leaves in its place a positive alkali ion. The electron then diffuses in the electric field, and at the end of a finite range w is captured by a positive ion in the neighbourhood of another Farbzentrum. Thus it forms a new alkali atom. Both the neighbouring alkali atoms (which are in a region of superfluous negative charge) have an absorption spectrum somewhat different from that of two single Farbzentren, and appear optically in the form of two F' centres.

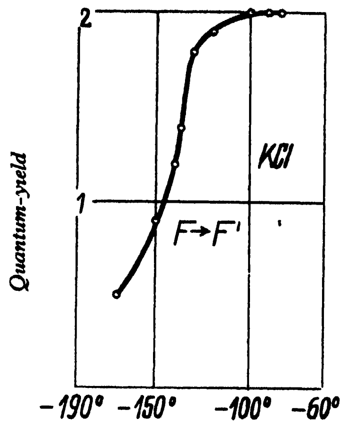

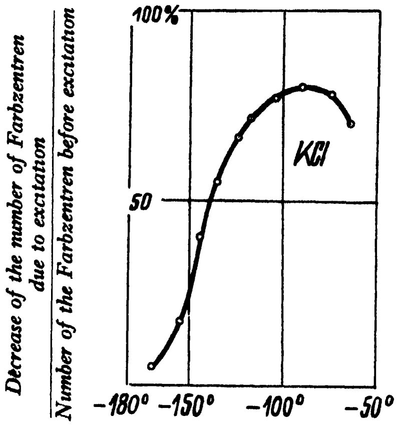

Temperature (° *C.*)

Figure 12 (*a*). Figure 12 (*b*).

Figure 12 (*b*) shows newer measurements of the effect shown in figure 12.

The fact mentioned at the end of § 5 can be explained as follows: The quantum yield of the transition $F \rightarrow F'$ decreases with decreasing temperature, whilst the quantum yield of the transition $F' \rightarrow F$ retains its initial value. The equilibrium is thus displaced to the disadvantage of the F' centres.

§6. PRODUCTION AND OPTICAL PROPERTIES OF CRYSTALS WITH AN EXCESS OF HALOGEN

If an alkali-halide crystal is heated in the vapour of its halogen, a stoichiometric excess of halogen is formed in the interior of the crystal. This imparts a yellowish colour to the iodide and bromide crystals. Two absorption spectra(61, 83) for this case are shown in figure 13. The number of halogen atoms which have penetrated into the crystal can be determined from the maxima I and II* (the third maximum is due to a secondary effect, see below).

* Equation (8) is applied to both maxima, and the constant A is determined by an electrical method to be described later on. For iodine equation (6) may also be used.

The number of halogen atoms per cm^3 of the crystal is proportional to the number of halogen molecules per cm^3 in the surrounding vapour(83). Figure 14 shows this for KBr as an example. In these experiments the temperature of the crystal and the vapour pressure could again be varied independently of one another. The relation

$$\gamma = \frac{\text{number of halogen atoms per cm}^3\text{ of the crystal}}{\text{number of halogen atoms per cm}^3\text{ of the vapour}}$$

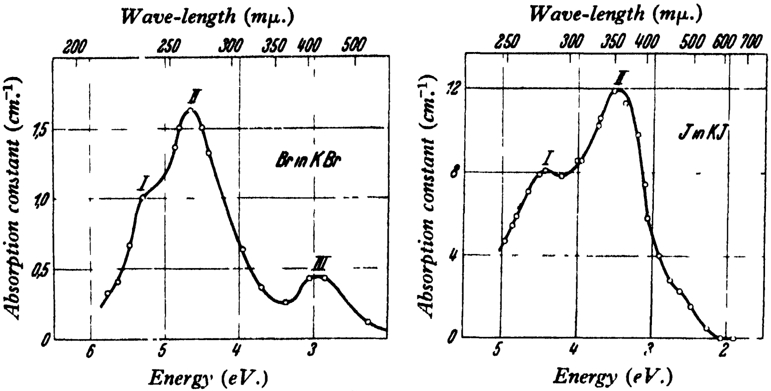

Figure 13.

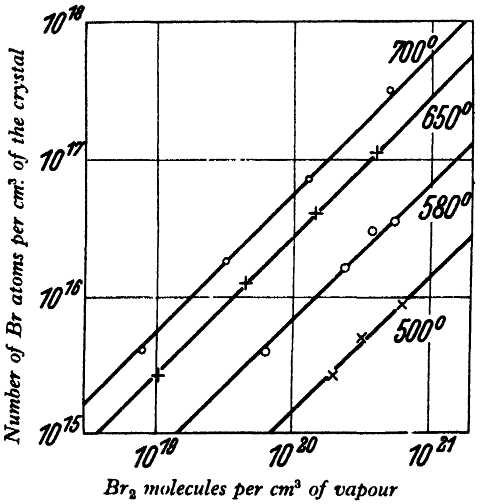

Figure 14. Solubility of Br in a KBr crystal.

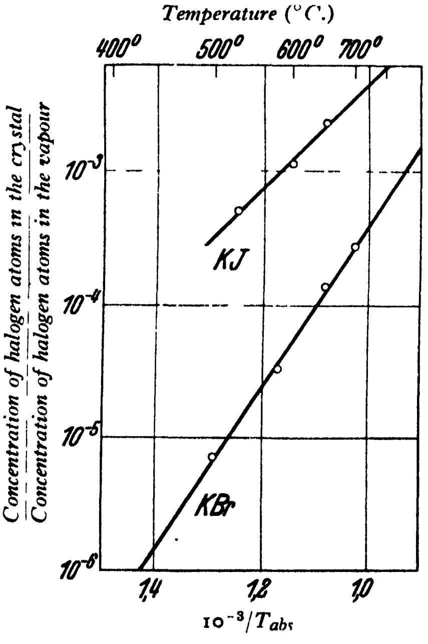

Figure 15.

never reaches unity. Furthermore, it decreases with decreasing temperature of the crystal (see figure 15). The process may here again be treated formally as a solution and a binding-energy of the halogen calculated, just as was done in the case of the excess alkali. This time the binding-energy is negative, being

$$w_{Br} = 1{\cdot}2 \text{ eV. for KBr}$$

$$w_{J} = 0{\cdot}8 \text{ eV. for KJ.}$$

This amount of energy must be given to the crystal in order to introduce an excess halogen atom(83), forming a molecule (see below).

The crystals, coloured at high temperatures, must be quickly quenched to room-temperature. Otherwise the excess halogen separates in individual clots as foreign bodies similar to the formation of colloidal metal particles. The maximum in the absorption spectrum of KBr, designated as III in figure 13, is due to such a precipitation, a slight amount of which is practically unavoidable.

The absorption spectra, i.e. the double bands I and II in figure 13, can thus by no means be ascribed to free halogen atoms. Rather similarly to the spectra of the Farbzentren, they are due to an adsorption compound of the type of KJ_3. The similarity between the absorption spectra of figure 13 and those obtained by de Boer and Custers(89) for the adsorption of halogen on vacuum-sublimated CaF_2 films speaks convincingly for this interpretation.

The mechanism of diffusion, by which the halogen penetrates into the crystal, is quite interesting. The discussion of this, as well as diffusion in the case of the formation of the Farbzentren will be dealt with in connexion with that of conduction (§§ 8 and 9).

PART 2. PHOTOELECTRIC CURRENTS IN THE CRYSTALS

§7. PHOTOELECTRIC PRIMARY CURRENTS IN CRYSTALS WITH EXCESS METAL ATOMS (FARBZENTREN)

The migration of the electrons ejected by the light and their replacement are designated as primary* photoelectric current. This replacement is necessary in order to neutralize the excess positive charge left on the atoms after the migration of electrons, and this can take place in two ways. In the first place, electrons which are later on ejected between the positively charged atoms and the cathode by thermal motion or by light ("electron-replacement-conductivity") may move in. Secondly, the neutralization may result due to electrolytic conductivity of the basic material(47). Unneutralized charges give rise to a polarization and decrease the electric field, often reducing the stationary photoelectric currents to values far below their initial values. This error can always be avoided by going over to the limiting case of sufficiently small light intensities. The fulfilment of this experimental condition is imperative.

---

* In contrast to photoelectric secondary current. This is lacking in the alkali-halide crystals, but in former years caused difficulties in the investigation of photoelectric properties in other crystals. The secondary currents are released in relay-fashion by the light, whereby an electron conductivity (already present without the presence of light) is increased for a long time by the action of the light. The numbers of electrons constituting the secondary current may exceed by a large factor those released by the light by a large factor. Compare the work of W. Lehfeldt(90).

The course of the primary photoelectric current as a function of time is strongly dependent upon the temperature(1,70). Figure 16 shows this for the case of a NaCl crystal containing Farbzentren(72).

The total time of observation is divided into three intervals A, B and C. During the interval A, light is absorbed in the Farbzentren; B is an interval of darkness; and during the interval C the crystal is irradiated by light of long wave-length, which is absorbed practically solely by the F' centres.

At low temperatures, during the light-absorption in the Farbzentren there appears a practically constant current i_e, without any time lag(5). This is interpreted as follows(1,48): the electrons ejected from the Farbzentren move towards the anode, and after traversing a mean range (*Schubweg*) w are brought to rest. This range is composed of many mean free paths and is usually much smaller than the distance d between the electrodes. Furthermore, exhaustive measurements have shown that it is proportional to the electric field strength E. The range is that component of the paths of the electrons in the direction of the anode in which their number is decreased to $1/e$ of the initial number, i.e. to 37 per cent. At the end of their range the electrons by combination with positive ions in the lattice form new centres with looser binding, which are F' centres.

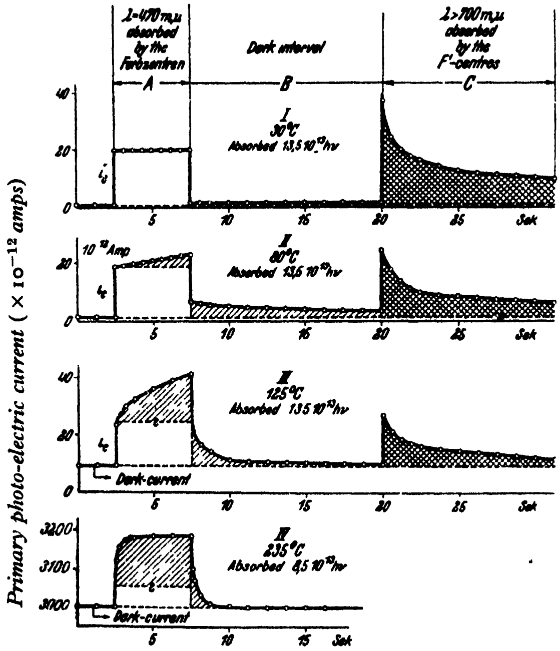

Figure 16. NaCl crystal with $8 \cdot 10^{15}$ Farbzentren per cm.³ Distance of electrodes = 4,2 mm.; $E = 1{,}07 \cdot 10^{5}$ V./m.

At higher temperatures there appears during the period of illumination and after it during the dark period a decaying current whose course is shown by the shaded portion of the current-time curve. The interpretation of this is as follows:

The distance between the electron and the positively charged atoms is increased by thermal motion in the electric field. The electrons loosely bound in F' centres are dissociated thermally, proceed in the electric field, and are then again recaptured. This process can occur repeatedly, until the electron is again captured in an F' binding. Finally at low temperatures the thermal action can be either replaced (section I) or augmented (sections II and III) by a light-absorption in the F' centres as shown by the cross-hatched current-time areas of figure 16[1,12].

In making quantitative observations, either the initial lagless primary photoelectric current i_e is measured, or, at higher temperatures, the total current-time area, including the non-shaded parts in figure 16. The relations which hold for this case are:

$$\eta\frac{w}{E}=\frac{i_e}{J_{\mathrm{abs.}}}\frac{d}{E}P \qquad \text{......(10),}$$

and

$$\eta\frac{w}{E}=\frac{idt}{E_{\mathrm{abs.}}}\frac{d}{E}P \qquad \text{......(11).}$$

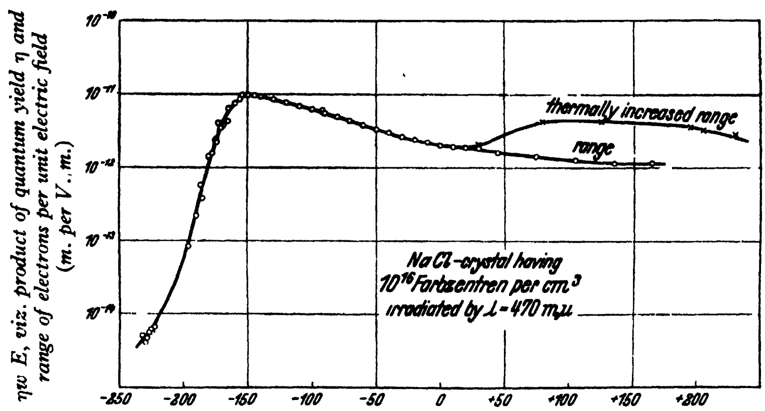

Figure 17.

In these equations, η is the as yet unknown quantum-yield (i.e. ratio of electrons set free to number of quanta absorbed), E the field-strength in Volt/m., d is the distance between electrodes, in m., $J_{\mathrm{abs.}}$ the energy per sec. of the absorbed light, measured in watts, $E_{\mathrm{abs.}}$ the energy of the absorbed light, measured in watt. sec., $P=h\nu/e$, measured in volts ($e=1{,}6\cdot10^{-19}$ amp. sec.), and h is Planck's constant $6{,}55\cdot10^{-34}$ watt. sec^2.

The measurements were carried out at different temperatures, but without the introduction of long-wave-length light such as would be absorbed by the F' centres. This corresponds to the time intervals A and B in figure 16. Figure 17 shows the results for NaCl. For temperatures below 30° C. the course of the photoelectric current as a function of time corresponds to I of figure 16; for temperatures above 30° C., however, it corresponds to II–IV. Below 30° C. the electron ranges are calculated according to equation (10), and above 30° C. according to both equations (10) and (11) wherever possible, and at the highest temperatures by means of equation (11) alone. In this way one finds, for temperatures above 30° C., both the initial range (circles) and the additional thermally increased range (crosses). Both have been reduced to unit field-strength (1 V./m.) and multiplied with the as yet undetermined quantum-yield η.

Corresponding measurements have been made for NaBr, KCl, KBr, KJ, RbCl, RbBr and RbJ. In all cases essentially the same relations are found to hold. As a second example, figure 18 shows the measurements for KCl(85). The types of currents appearing at different temperatures have been schematically represented in the first row. Figure 18 shows a secondary effect not present in figure 17, namely a further increase in the range at the lowest temperatures.

A discussion of figures 17 and 18 should for the time being be limited to the first rise of the curve labelled "range", i.e. down to −150° C. for NaCl and to −130° C. for KCl. If a light quantum is absorbed in this temperature interval, not only a Farbzentrum disappears, but there is also produced an F' centre (§ 5). Therefore it is allowable to put $\eta = 1$ in equation (10) and (11), i.e. to assume an electron is liberated from a Farbzentrum for each light quantum absorbed, and is again fixed in an F' binding. In this case the curves through the circled observed points may be taken directly as the ratio

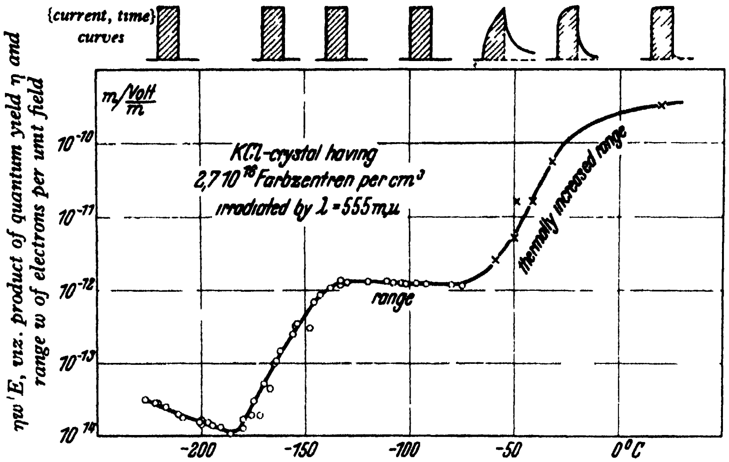

Figure 18.

$$\frac{w}{E} = \frac{\text{range of electrons}}{\text{field-strength}} .$$

The ratio w/E is proportional to a specific electric conductivity(77, 81). This increases initially with decreasing temperature not only for metals but also for isolating crystals as well. The absolute value of the temperature-coefficient is also of the same order of magnitude as for metals. Below the temperature designated, the value of η is as yet unknown. It is not known whether the sharp decrease of the measured value of $\eta\, w/E$ is due to a decrease of η or of w/E. A decrease of the mean range w would occur if some of the electrons liberated by light drop back into the metastable F' level of the same atom, instead of forming a new atom with a *distant* cation and taking a place in its F' level.

The new rise of $\eta\, w/E$ below −180° C. in KCl is certainly due to electrons which are liberated not from Farbzentren but from traces of colloids. Their small effect is not noticeable at high temperatures.

A further fact is important for the interpretation of this electron movement. The range of the electrons per unit field strength w/E is inversely proportional to the concentration of Farbzentren throughout a wide range of concentrations (figure 19). The measurements are for KCl at −100° C. and these have been made upon five different crystals, in order to show the magnitude of the individual variations(85).

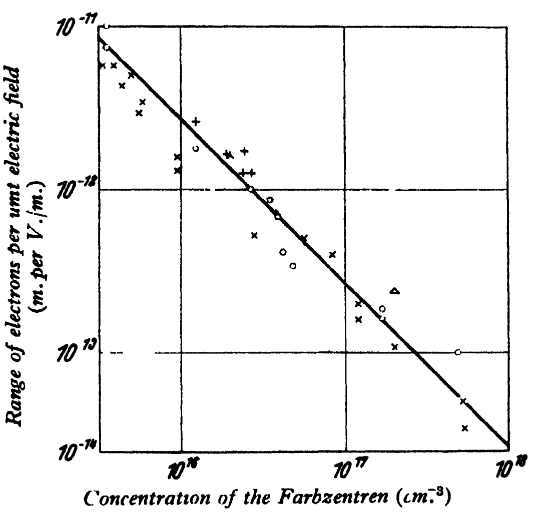

Figure 19. KCl at −100° C.

$1/w$ has the significance of an absorption-constant K_e as in equation (1), if J_e denotes the initial number of electrons and J_a their number after having moved a distance d towards the anode (this presupposes that the zig-zag path of the free electrons is large compared with the mean distance between Farbzentren). $K_e = 1/w$ is proportional to the concentration of Farbzentren, according to figure 19. Accordingly, the absorbing cross-section due to *one* Farbzentrum in the crystal may be calculated by means of equation (3) and at $E = 1$ V./m. this turns out to be $\beta_e = 4\cdot10^{-11}$ m.^{2} for KCl, with numbers at the same order of magnitude for NaCl, KBr, RbCl, and RbBr.

Up to this point only the curves designated as "ranges" (circles in figures 17 and 18) have been considered. At higher temperatures the thermally increased ranges (denoted by crosses) have also been drawn. These are produced by a thermal diffusion of the F' centres. This diffusion is concluded only when all the electrons have returned to the stable Farbzentren binding. The paths traversed by the electrons up to this point in the case of KCl exceed the original range by up to 500-fold. At +20° the value of w/E is $5 \cdot 10^{-10}$ V./m. At a field-strength of 10^6 V./m. the total path traversed by the electrons is thus 0·5 mm. In this case the electrons released by light in a crystal plate a few tenths of a mm. thick can be entirely withdrawn by the electric field and the primary photoelectric current then becomes saturated(17, 31).

Note added in proof. In favour of the hypotheses that the fall in $\eta w/E$ at low temperatures shown in figures 17 and 18 is due to a fall in η, we must add the fact that the quantum yield of the optical transition also decreases, and thus, apparently more than in proportion, the number of electrons which can move through the lattice decreases too. The drop in temperature inhibits the source of electrons, not the mechanism of conduction.

In favour of this explanation we may mention the observations made with KCl at low temperatures (figure 18) of a current due to electrons liberated from colloids by the ordinary surface photoelectric effect, which is known to be practically independent of temperature.

PART 3. MOTION OF ELECTRONS THERMALLY RELEASED

§ 8. THERMALLY RELEASED ELECTRON CURRENTS IN CRYSTALS HAVING AN EXCESS OF ALKALI METAL

The measurements shown in figures 17 and 18 cannot be carried out at temperatures above approximately 200°, because at higher temperatures not only the F' centres, but the Farbzentren as well are dissociated thermally. Consequently great numbers of free electrons are present even without illumination, in comparison with which the number that can be ejected by light is negligible.* For this reason Farbzentren cannot be used at high temperatures for the releasing of electrons by optical means. The thermal dissociation affects not only the Farbzentren, but also the lattice of the crystal, and thus the electrolytic conductivity of the basic material reaches a considerable value. At this stage, this electrolytic conductivity is able to neutralize the positive residual charges caused by the migration of great numbers of electrons.

At high temperatures these two facts cause the Farbzentren to migrate towards the anode as a swarm(33) (figure 20). This migration takes place with a definite rear wall. While the eye follows this, a current-measuring instrument shows the current-time curve(13) shown in figure 21.

Figure 20 corresponds formally to a series arrangement of two crystals having different electrical conductivities. In the part which is already clear, only ions migrate, whereas both ions and electrons migrate in the part still filled with Farbzentren. The number N of Farbzentren originally present in the crystal, which have migrated out of it due to the electric field can be calculated from the shaded current-time area, $\int i dt$ of figure 21. Here

---

* Using monochromatic light, more than some 10^{14} quanta per sec. per cm.^{2} can hardly be introduced.

$$N = 2\frac{\int i dt}{e} \qquad \ldots\ldots(12)$$

where $e = 1{,}6\cdot 10^{-19}$ amp.sec. assuming that the electrolytic conductivity in the coloured part is no greater than in the clear part, in spite of the presence of the Farbzentren. Otherwise the factor 2 in equation (12) must be replaced by a smaller value, between 2 and 1 (51).

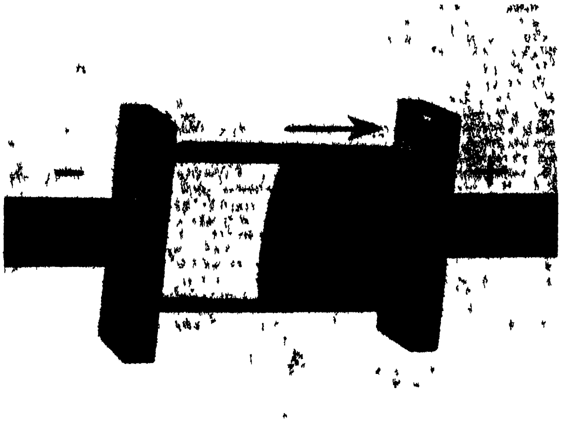

Figure 20.

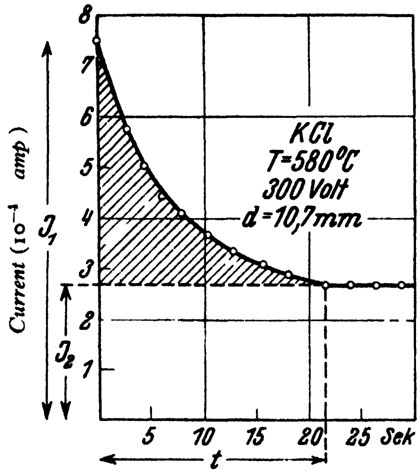

Figure 21. Electric current during the migration of Farbzentren

The experiment represented in figure 20 can be varied. For example, electrons may be made to enter the crystal from a pointed cathode(36). A flat and previously anodically polarized cathode can also be used. In this way the whole crystal can be homogeneously filled with a Farbzentren swarm and an electron current i, constant with time, is obtained. The ionic current i_t due to the non-coloured crystal is superposed upon this. The relevant equation is

$$i = N_0 F e v_f \frac{P}{d}$$

where N_0 is the number of Farbzentren per cm.^{3}, F the cross-section of the crystal, $e = 1{,}6 \cdot 10^{-19}$ amp.sec., d is the distance between electrodes in m, P the applied voltage and v_f the mobility of Farbzentren in m.-sec.$^{-1}$/V.-m.$^{-1}$

The visible migration of the electron swarm is easily interpreted. The thermal dissociation of the Farbzentren produces invisible alkali-metal ions and electrons. The electrons are able to diffuse very quickly in the crystal lattice in traversing their free paths between the atoms of the lattice. If an electric field is applied to the crystal, the diffusion receives a preferential direction towards the anode. In this free condition each electron has only a limited life. This ends when the electron is captured by a positive ion and becomes fixed in the formation of a Farbzentrum. The electron then remains in this condition for some time, until it is again ejected by thermal motion, and the whole process starts over again. Only during these rest periods during which the electron is bound in the Farbzentrum, is the location of the electron rendered visible and in this way the path of the electrons towards the anode can be followed. Apparently, visible Farbzentren, i.e. neutral metal atoms, migrate; in reality, however, the migration is that of invisible electrons (67, 71).

The mobility of the Farbzentren, i.e. their speed of migration in unit electric field, can be measured in different ways. The simplest way is to observe a small, definitely bounded Farbzentren swarm in an otherwise clear crystal and to measure the velocity directly with a scale and stop-watch (44). Equation (12) may also be used (50) or measurements such as those represented in figure 20 may be applied The equation here applicable is (51)

$$v_f = \frac{1 + \frac{1}{2}(J_1 - J_2)/J_2}{TP} d^2 \qquad \ldots\ldots(13)$$

(compare figure 10). Here T is the absolute temperature, P the applied voltage and d the distance between the electrodes.

The mobility measured in this way increases with the temperature of the crystal. Figure 22 shows this for nine salts. In all cases the mobility increases exponentially with temperature (44), according to the empirical formula

$$v_T = v_0 \, e^{-w/kT} \qquad \ldots\ldots(14)$$

where $e = 1{,}37 \cdot 10^{-23}$ watt-sec./degree and w is a work-function.

Interpretation: with increasing temperature the thermal dissociation of the Farbzentren into ions and electrons increases, or, expressed in another way, the rest-periods of the electrons during their binding in the Farbzentren become shorter. In the limiting case of high temperatures these rest-periods disappear entirely and the mobility of the Farbzentren reaches its limiting value v_0. Several values (50) of v_0 will be found in table 2. These values are taken from the measurements represented in figure 22 and are not claimed to be exact. The limiting mobilities v_0 are of the same order of magnitude as that of the electrons in copper and in other metals of high conductivity.

Table 2.

	NaCl	NaBr	NaJ	KCl	KBr	KJ	RbCl	RbBr	RbJ
Limiting mobility v_0 m.-sec.$^{-1}$/V.-m.$^{-1}$	0·002	0·066	0·074	0·014	0·017	0·020	0·011	0·013	0·014
Thermal work function (eV.)	0·94	0·80	(0·76)	1·00	0·84	0·83	0·84	0·68	0·63

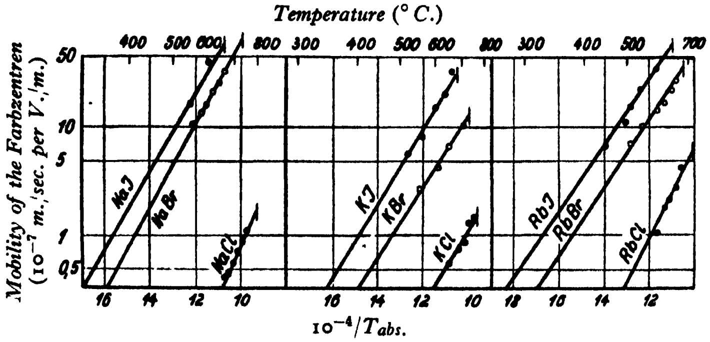

Figure 22. Mobility of Farbzentren.

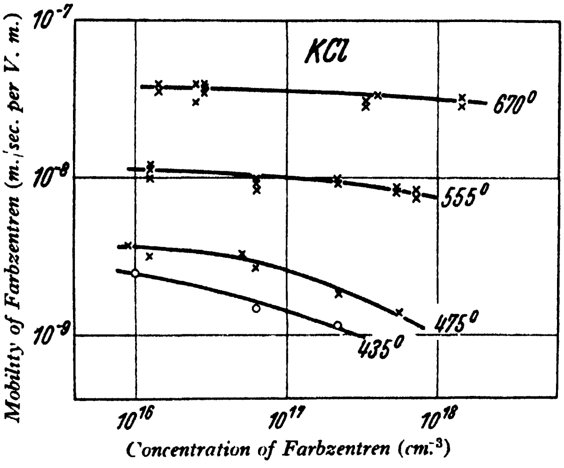

Figure 23.

In the experiments thus far discussed, small concentrations of Farbzentren have to be used. Otherwise the case might occur in which the electrolytic conductivity is not sufficient to neutralize the positive residual charges and thus the measured mobility is too small. Actually the concentration affects the true mobility, but its influence is very small, as figure 23 shows. It is only noticeable at low temperatures, the mobility of Farbzentren being practically constant at high temperatures⁽⁸⁰⁾ up to concentrations of $10^{18}/\text{cm}^3$.

By a proper choice of temperature-scales the curves of figure 23 for salts having the same cation may be made to coincide. In figure 24 the abscissae give the absolute temperature divided by a characteristic temperature for each salt, similar to that which may be derived from the specific heat as a function of the temperature, or in other ways. The ordinates, i.e. the mobilities of the Farbzentren, in contrast to figure 23, are plotted linearly, not logarithmically. From this it seems clear that the degree of dissociation of the Farbzentren, i.e. the exponential factor in equation (14), is determined practically by the thermal motion of the lattice.

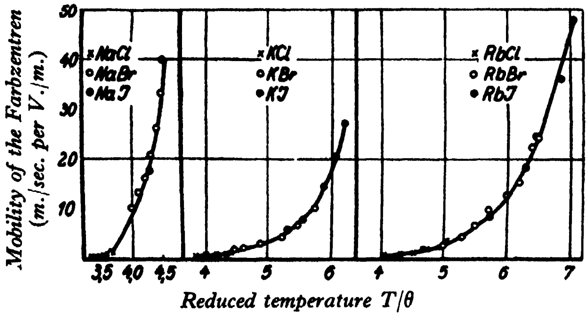

Figure 24.

If no electric field is applied to the crystal, the electrons which are thermally ejected diffuse in all directions⁽⁶⁵⁾. The diffusion-constant D can be measured and the same connexion between it and the mobility exists here as for these quantities in the case of ions in solutions⁽⁷⁴⁾. In the limiting case of high temperature or of very small concentrations the following simple relation is found to hold:

$$v_F = D\frac{e}{kT} \qquad \ldots\ldots(15),$$

where v is in m.-sec.$^{-1}/V$.-m.$^{-1}$ and D in m.^{2}/sec., $k = 1{,}37\cdot 10^{-23}$ watt-sec./degree, and T and e are as in equation (14).

Beyond these limiting cases, the electrolytic conductivity of the basic material and the mechanism of ionic conduction must be considered⁽⁶⁵, ⁵⁶, ⁵⁷⁾.

The thermal diffusion of electrons also explains the phenomenon described in § 3, namely the production of Farbzentren by heating the crystal in the presence of the cation metal.*

§ 9. THERMALLY RELEASED ELECTRON CURRENTS IN CRYSTALS WITH EXCESS HALOGEN

The process discussed in § 8 may be concisely described as electron-excess conductivity. Neutral alkali atoms (Farbzentren) are changed over into positive ions, i.e. normal lattice elements, by giving off excess electrons. The counterpart of this, an electron-deficiency conductivity, can be observed in crystals having a stoichiometric excess of halogen atoms.* Here the visible neutral halogen is changed back into a negative ion, i.e. a normal lattice element, by taking up a lacking electron. This may take place in an electric field, according to the mechanism of electron-replacement (§ 7), if the thermal motion makes a thermal diffusion of electrons possible. Then a neutral halogen atom abstracts an electron from one of its neighbours between it and the cathode, and thereby itself becomes an invisible ion. At the same time it transforms its neighbour into a visible halogen atom. In this way the visible swarm of excess halogen wanders towards the cathode(61). The process is exactly the same as that illustrated in figure 20, with changed sign of the electrodes. Here again apparently a neutral halogen migrates in the electric field. Actually, however, electrons migrate according to the scheme of a replacement current.

---

* J. Eggert and W. Noddack⁽⁹¹⁾ first introduced the idea of tracing back metallic diffusion to the diffusion of electrons, in order to explain the flocking together of silver atoms in AgBr crystals.

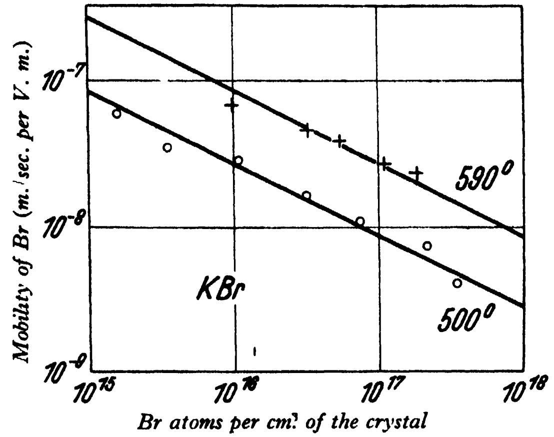

Figure 25.

Everything explained in § 8 may accordingly be applied to the electric measurements on crystals with excess halogen. Thus, for example, the current-time relation for the migration of a halogen swarm has the same form as in figure 21. The number of halogen atoms can be determined by equation (12). Furthermore the mobility of the halogen can be measured in exactly the same way as in the case of Farbzentren. In contrast with the Farbzentren, however, the halogen-mobility is greatly affected by the concentration(83), as shown by figure 25. Here also, however, the mobility increases with increasing temperature of the crystal, as figure 26 shows(83). The relation between the mobility v_T and the temperature may again be represented by the empirical equation (14). Table 3 contains several values for the limiting mobility v_0 and the work function w.

Thus there is an extensive analogy between electron-excess conductivity and electron-deficiency conductivity. However, there are noticeable quantitative differences. These pertain particularly to the thermal diffusion of halogen without application of an electric field. This difference was utilized in § 6 in the production of a stoichiometric halogen excess. This process takes place only partially by electron-diffusion. In the case of KBr under a halogen pressure of one atmosphere, for example, about 50 per cent of the diffusing molecules do so as uncharged bromine molecules (83).

---

* The meaning of a stoichiometric excess of electron-negative lattice-element for thermally released electron currents was, to my knowledge, first recognized by B. Gudden(92). From this C. Wagner and W. Schottky have made deductions which are important in the problem of semiconductors.

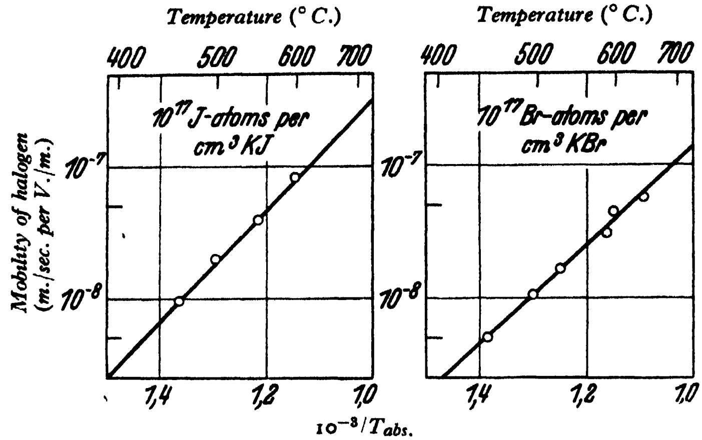

Figure 26.

Table 3.

	KBr	KJ
Limiting mobility v_0 (m.-sec.$^{-1}$/V.-m.$^{-1}$)	0,0007	0,005
Thermal work function (eV.)	0,7	0,8

PART 4. PHOTOCHEMICAL PROCESSES

§ 10. INTRODUCTION

The investigations of photochemical processes in solid bodies are carried out almost solely upon the silver salts, especially AgBr. This emphasis upon the silver salts is due to the extraordinary importance of photography. The majority of the investigations employ the conditions of exposure usual in photographic practice. Approximately 10^{14} light quanta per cm³ are absorbed, and the number of molecules transformed, or the number of individual nuclei produced from them, is of the same order of magnitude. Under these conditions the action of the light is latent, since the silver-salt film of the photographic plates, etc. has a thickness of only a few μ. and consequently there are but 10^{10} transformed molecules under each cm² of surface (24, 38). In thicknesses as small as this, new molecules can first be optically observed when their concentration reaches 10^{18}/cm³, or when there are at least 10^{14} transformed molecules under each cm.^{2} of surface. For this reason, the aid of chemical development is necessary for investigations of such thin photographic films. A number of atoms of silver many thousands of times larger than the number of molecules originally transformed by the light must be deposited upon the primary reaction-products (or the nuclei resulting from them). If one wants to work without development, for example, with printing-out paper, at least 10^{18} quanta per cm.^{3} must be absorbed, a number far different from the normal-exposure condition.

Chemical development, although its practical use is very great, introduces serious difficulties into the investigations of photochemical questions. For this reason it seemed very interesting to be able to avoid the use of chemical development in the investigations of photochemical processes in solid bodies, and to make the elementary or latent action of the light directly observable. This problem was solved in a very simple manner for alkali-halide salts. The primary photochemical reaction-products in these are the Farbzentren. It is easy to work with clear crystals of 1 cm. thickness or more. It is sufficient, as in normal photographic exposure, to absorb approximately 10^{14} light quanta per cm.^{3}. This results in 10^{14} Farbzentren under each cm.^{2} of surface, whereas in the thin photographic films the corresponding number was but 10^{10}. These 10^{14} Farbzentren are capable of investigation both optically and electrically. In this way it is possible to perform experiments upon the latent action of light, whose results may accordingly be applied to the technically important silver salts(26).

§ 11. PHOTOCHEMICALLY ACTIVE LIGHT-ABSORPTION

For the silver salts used in photography, the active spectral range coincides with the absorption band of AgBr extending into the visible. For many years the elementary process in photography has been interpreted as a removal of an electron from a halogen ion to a metal cation. The primary reaction-products were thought to be neutral silver atoms, and these were to be the preliminary step in the formation of the development-nuclei. In line with these photographic investigations, we at first used light, which was absorbed in the region of the first ultra-violet band of the crystal (figures 4 and 5) also in the case of alkali salts(25). This choice was favoured by the fact that the frequencies of the first band of all the salts can be satisfactorily calculated by assuming an electron transition from the anion to the cation and utilizing an empirical formula containing, aside from the lattice constants, only the ionizing potential of the metal and the two electron-affinities of the halogen(23, 35). For experimental reasons, only the long-wave end of the first absorption band could be used, for it was necessary to achieve a homogeneous penetration of photochemically active light through a crystal approximately 1 cm. thick. For the wavelength of the maximum of the first bands a thickness of only 0·01 μ. can be penetrated, because the absorption-constant here has a value of approximately 10^{-6} cm.$^{-1}$ (table 1). We may use only 10^{14} quanta per cm.^{3} in a volume 10^{-6} cm.^{3}, giving 10^8 centres below an area of 1 cm.^{2}, a much less favourable case than the 10^{10} per cm.^{2} in photographic plate.

This choice of photochemically active wave-length was, however, exceedingly unfavourable in another respect. The light-absorption in the long wave-length end of the first absorption band can, as stated above, be due to molecules of the lattice, which are thermally or otherwise disturbed and hence will respond to low frequencies. No less probable, however, is the absorption of light by foreign molecules(46), which can cause absorptions of the amount here utilized even when present only as impurities in a ratio of 1 : 10^6. For this reason it was necessary to find a photochemically active light-absorption whose centres were definitely known. This has been possible.

The most favourable conditions exist in alkali-halide crystals containing small amounts of alkali hydride(78). Such mixed crystals may be produced in a number of ways. The best method is that of heating a crystal containing Farbzentren in an atmosphere of H_2. The H_2 diffuses rapidly into the crystal and changes the visible Farbzentren into invisible hydride molecules. At a pressure of 100 atmospheres this diffusion takes place with surprising speed, at a rate of approximately 1 mm./sec. (This is a diffusion of molecules, not protons(84)!) The alkali hydride, colourless in visible light, has a bell-shaped absorption band in the ultra-violet. Figure 27 shows the measurements for KH in KBr. These absorption bands were formerly designated as *U* bands of the salt, their origin then being unknown(39).

In a similar way crystals containing K_2O crystals can be produced, and their well-defined light-absorption utilized for photochemical purposes(55, 62). Certainly the number of usable additions is much greater(69, 76), but systematic investigations are still lacking.

§ 12. MEASUREMENTS OF THE PHOTOCHEMICAL YIELD BY OPTICAL AND ELECTRICAL MEANS

In gases, the photochemical dissociation of molecules is dependent not only upon the absorption of a light-quantum but also upon the thermal vibrational energy of the molecules as well. The same is true for the photochemical processes in the alkali salts, and also the optical dissociation of KH into invisible hydrogen and visible Farbzentren for example(52). If light is absorbed in the KH band (figure 27), this band disappears, and in its place the band of the Farbzentren appears. Figure 28 shows the yield of this photochemical reaction as a function of the temperature. This may be represented by the equation:

$$\eta_T = 1 - (1 - e^{-\epsilon/kT})^A \qquad \ldots\ldots(16),$$

where $\epsilon = 0{\cdot}85$ eV. and *A* has a value between 7 and 8(59, 82).

The number of Farbzentren formed was determined optically up to approximately 150° C. At higher temperatures this method fails, because the life of the Farbzentren becomes too short, due to their thermal transformation back into KH molecules(64). At higher temperatures, accordingly, an electrical method was applied for the measurement of the Farbzentren. The crystal is illuminated by light of known intensity, generally some 10^{-6} watt, amounting to some 10^{12} quanta per second, and the stationary photoelectric current is measured. If this is considerably smaller than the electrolytic dark current of the crystal, the current voltage curve shows a definite saturation (figure 29). The number of electrons migrating to the anode, and hence the number of Farbzentren formed, can be calculated from the saturation current(59). At the conclusion of the photochemical irradiation, the remainder of the Farbzentren can be observed as they move out of the crystal(46, 63, 73), just as is illustrated in figure 20.

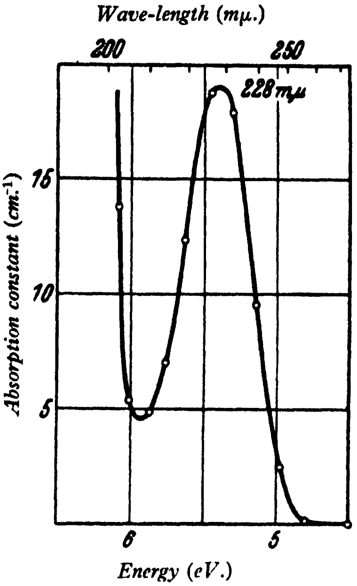

Figure 27. KH in KBr.

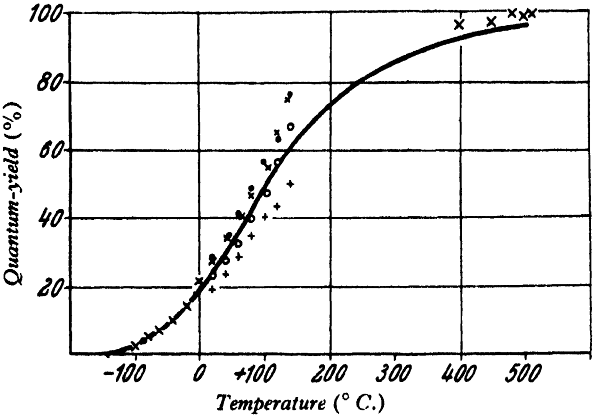

Figure 28.

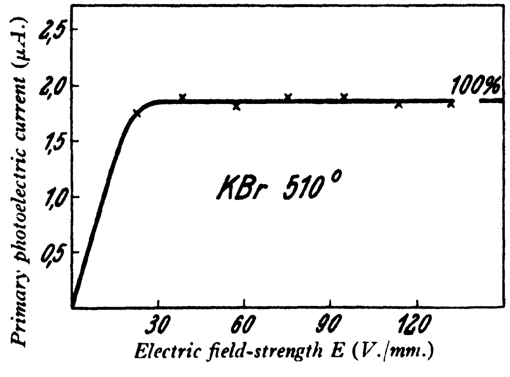

Figure 29.

Here the photoelectric current is solely an aid for the measurement of the number of Farbzentren formed, and thus of the quantum-yield. By utilizing electrical and optical measurements simultaneously, further questions, relating to the mechanism of the elementary process, can be investigated. For example, it turns out that the optical dissociation of the KH molecules and the formation of Farbzentren is not accompanied by a measurable current. The electron-transfer takes place only in molecular dimensions(76).

Electrical methods for the investigation of the photochemical elementary process may still be used even at low temperatures. If the number of Farbzentren formed in the available thickness of crystal does not suffice for the optical detection of these Farbzentren, the following method may be employed. Light is absorbed in the Farbzentren band, and the electrons can there be made as mobile as in the case discussed in § 7(29).

The investigation of photochemical processes in solid bodies is still in a very early stage. But a few of the facts found have been mentioned here. Still, the above illustrations will have served to show that these processes can be successfully investigated with physical means, i.e. optical and electrical observations, alone.

REFERENCES

The following list is that of publications of researches on *alkali-halide* crystals carried out in the Institute in Göttingen, which form the basis of this report.

(1) Gudden, B. and Pohl, R. W. *Z. Phys.* **31**, 651 (1925).
(2) Gyulai, Z. *Z. Phys.* **31**, 296 (1925).
(3) Gyulai, Z. *Z. Phys.* **32**, 103 (1925).
(4) Gyulai, Z. *Z. Phys.* **33**, 251 (1925).
(5) Flechsig, W. *Z. Phys.* **33**, 372 (1925).
(6) Gudden, B. and Pohl, R. W. *Z. Phys.* **34**, 249 (1925).
(7) Gyulai, Z. *Z. Phys.* **35**, 411 (1926).
(8) Pohl, R. W. *Naturwissenschaften*, **14**, 214 (1926).
(9) Kyropoulos, S. *Z. anorg. Chem.* **154**, 308 (Tammann-Festschr.) (1926).
(10) Flechsig, W. *Z. Phys.* **36**, 605 (1926).
(11) Gyulai, Z. *Z. Phys.* **37**, 889 (1926).
(12) Gudden, B. and Pohl, R. W. *Z. Phys.* **37**, 881 (1926).
(13) Hilsch, R. and Ottmer, R. *Z. Phys.* **39**, 644 (1926).
(14) Gyulai, Z. *Z. Phys.* **39**, 636 (1926).
(15) Hilsch, R. *Z. Phys.* **44**, 421 (1927).
(16) Gyulai, Z. *Z. Phys.* **46**, 80 (1927).
(17) Flechsig, W. *Z. Phys.* **46**, 788 (1928).
(18) Ottmer, R. *Z. Phys.* **46**, 798 (1928).
(19) Hilsch, R. and Pohl, R. W. *Z. Phys.* **57**, 145 (1929).
(20) Hilsch, R. and Pohl, R. W. *Z. Phys.* **57**, 145 (1929).
(21) Smakula, A. *Nachr. Ges. Wiss. Göttingen*, p. 110 (1929).
(22) Smakula, A. *Z. Phys.* **59**, 603 (1930).
(23) Hilsch, R. and Pohl, R. W. *Z. Phys.* **59**, 812 (1930).
(24) Hilsch, R. and Pohl, R. W. *Nachr. Ges. Wiss. Göttingen*, p. 176 (1930).
(25) Smakula, A. *Z. Phys.* **63**, 762 (1930).
(26) Hilsch, R. and Pohl, R. W. *Z. Phys.* **64**, 606 (1930).
(27) Fesefeldt, H. *Z. Phys.* **64**, 623 (1930).
(28) Gundelach, E. *Z. Phys.* **66**, 775 (1930).
(29) Hilsch, R. and Pohl, R. W. *Z. Phys.* **68**, 721 (1931).
(30) Mollwo, E. *Nachr. Ges. Wiss. Göttingen*, p. 97 (1931).
(31) Flechsig, W. *Phys. Z.* **32**, 843 (1931).
(32) Mollwo, E. *Nachr. Ges. Wiss. Göttingen*, p. 1 (1932).
(33) Stasiw, O. *Nachr. Ges. Wiss. Göttingen*, p. 261 (1932).
(34) Hecht, K. *Z. Phys.* **77**, 235 (1932).
(35) Hilsch, R. and Pohl, R. W. *Z. Phys.* **77**, 421 (1932).
(36) Pohl, R. W. *Naturwissenschaften*, **20**, 932 (1932).

(37) Korth, K. *Nachr. Ges. Wiss. Göttingen*, p. 576 (1932).
(38) Pohl, R. W. *Naturwissenschaften*, **21**, 261 (1933).
(39) Hilsch, R. and Pohl, R. W. *Nachr. Ges. Wiss. Göttingen*, p. 322 (1933).
(40) Miescher, E. *Nachr. Ges. Wiss. Göttingen*, p. 329 (1933).
(41) Korth, K. *Z. Phys.* **84**, 677 (1933).
(42) Mollwo, E. *Z. Phys.* **85**, 56 (1933).
(43) Lehfeldt, W. *Z. Phys.* **85**, 717 (1933).
(44) Stasiw, O. *Nachr. Ges. Wiss. Göttingen*, p. 387 (1933).
(45) Blau, M. *Nachr. Ges. Wiss. Göttingen*, p. 401 (1933).
(46) Hilsch, R. and Pohl, R. W. *Nachr. Ges. Wiss. Göttingen*, p. 406 (1933).
(47) Hilsch, R. and Pohl, R. W. *Z. Phys.* **82**, 78 (1933).
(48) Pohl, R. W. *Phys. Z.* **35**, 107 (1934).
(49) Bauer, G. *Ann. Phys.* Lpz., (5), **19**, 434 (1934).
(50) Smakula, A. *Nachr. Ges. Wiss. Göttingen*, N.F. **1**, 55 (1934).
(51) Mollwo, E. and Roos, W. *Nachr. Ges. Wiss. Göttingen*, N.F. **1**, 107 (1934).
(52) Hilsch, R. and Pohl, R. W. *Nachr. Ges. Wiss. Göttingen*, N.F. **1**, 115 (1934).
(53) Kublitzky, A. *Ann. Phys.*, Lpz., (5), **20**, 794 (1934).
(54) Pohl, R. W. *Z. Metallk.* **26**, 217 (1934).
(55) von Lüpke, A. D. *Ann. Phys.*, Lpz., (5), **21**, 1 (1934).
(56) Stasiw, O. *Nachr. Ges. Wiss. Göttingen*, N.F. **1**, 147 (1934).
(57) Stasiw, O. *Nachr. Ges. Wiss. Göttingen*, N.F. **1**, 199 (1934).
(58) Mollwo, E. *Nachr. Ges. Wiss. Göttingen*, N.F. **1**, 203 (1934).
(59) Hilsch, R. and Pohl, R. W. *Nachr. Ges. Wiss. Göttingen*, N.F. **1**, 209 (1934).
(60) Pohl, R. W. *Kolloidzschr.* **71**, 257 (1934).
(61) Mollwo, E. *Nachr. Ges. Wiss. Göttingen*, N.F. **1**, 215 (1934).
(62) Korth, K. *Nachr. Ges. Wiss. Göttingen*, N.F. **1**, 221 (1934).
(63) Pohl, R. W. *Z. tech. Phys.* **16**, 338 (1934).
(64) Hilsch, R. *Z. tech. Phys.* **16**, 341 (1934).
(65) Stasiw, O. *Z. tech. Phys.* **16**, 343 (1935).
(66) Mollwo, E. *Z. tech. Phys.* **16**, 346 (1935).
(67) Hilsch, R. *Z. angew. Chem.* **49**, 69 (1936).
(68) Pohl, R. W. *Umschau*, Heft 5 (1936).
(69) Stasiw, O. *Nachr. Ges. Wiss. Göttingen*, N.F. **2**, 1 (1936).
(70) Thiele, W. *Ann. Phys.*, Lpz., (5), **25**, 561 (1936).
(71) Pohl, R. W. *Elektrotech. Zs.* **57**, 321 (1936).
(72) Glaser, G. and Lehfeldt, W. *Nachr. Ges. Wiss. Göttingen*, N.F. **2**, 91 (1936).
(73) Glaser, G. *Nachr. Ges. Wiss. Göttingen*, N.F. **2**, 109 (1936).
(74) Stasiw, O. *Nachr. Ges. Wiss. Göttingen*, N.F. **2**, 131 (1936).
(75) Kleinschrod, F. G. *Ann. Phys.*, Lpz., (5), **27**, 97 (1936).
(76) Glaser, G. *Ann. Phys.*, Lpz., (5), **27**, 217 (1936).
(77) Naumann, A. *Ann. Phys.*, Lpz., (5), **27**, 233 (1936).
(78) Hilsch, R. and Pohl, R. W. *Nachr. Ges. Wiss. Göttingen*, N.F. **2**, 139 (1936).
(79) Hohls, H. W. *Ann. Phys.*, Lpz., (5), **29**, 433 (1937).
(80) Rögener, H. *Ann. Phys.*, Lpz., (5), **29**, 386 (1937).
(81) Pohl, R. W. *Ann. Phys.*, Lpz., (5), **29**, 239 (1937).
(82) Schaitberger, G. *Nachr. Ges. Wiss. Göttingen*, N.F. **2**, 181 (1937).
(83) Mollwo, E. *Ann. Phys.*, Lpz., (5), **29**, 394 (1937).
(84) Hilsch, R. *Ann. Phys.*, Lpz., (5), **29**, 407 (1937).
(85) Glaser, G. *Nachr. Ges. Wiss. Göttingen*, N.F. **2**, in the press (1937).
(86) Pick, H. *Ann. Phys.*, Lpz., (5), in the press (1937).
(87) Gudden, B. and Pohl, R. W. *Z. Phys.* **3**, 123 (1920).
(88) Schneider, E. G. and O'Bryan, H. M. *Phys Rev.* **51**, 293 (1937).
(89) de Boer, I. H. and Custers, I. F. H. *Z. f. phys. Chem.* B, **21**, 208, 1933.
(90) Lehfeldt, W. *Nachr. Ges. Wiss. Göttingen*, N.F., **1**, 199, 1935.
(91) Eggert, J. and Noddack, W. *Z. Elektrochem.* **32**, 496 (1926).
(92) Gudden, B. *Erlanger Berichte*, **62**, 289 (1930).

TRAPPED ELECTRONS IN POLAR CRYSTALS

By R. W. GURNEY and N. F. MOTT

Recently several attempts have been made to explain the nature and account for the properties of the F centres in terms of the atomic theory of polar lattices$^{(1,2,3,4)}$, and it is a matter of dispute to what extent crystal imperfections and faults are essential for the understanding of this phenomenon. In this paper we shall attempt to show how an extra electron may be expected to behave in a crystal *without* crystal imperfections, if we accept the current theory of polar lattices, and shall then make some tentative suggestions about the connexion between our findings and the experimental material. The paper is based on an idea due originally to Landau$^{(5)}$ and developed further by Frenkel$^{(6)}$ and by ourselves. A very similar idea has been used by von Hippel$^{(2)}$.

If we imagine an extra electron brought from outside and placed on one of the metal ions of an alkali-halide crystal, then we should expect that electron to be free to move from one metal ion to the next through the crystal. Such an electron cannot be spoken of as belonging to any particular metal ion, and we speak of it as being in the conduction level of the crystal as a whole. In a crystal which shows photoconductivity the action of the light is to raise electrons from lower, bound, levels into the conduction level.

Now the dielectric constant of a polar crystal is due partly, as in non-polar materials, to the polarizability of the atoms or ions of which it is built up, and partly to the actual displacement of the positive and negative ions in opposite directions by the applied electric field. Owing to the large mass of the ions, they can only be displaced by alternating fields with frequency less than about 10^{12} sec.$^{-1}$ (the Reststrahlfrequenz).

We have used the methods of wave mechanics to investigate the motion of an electron in the conduction band and find that, as in a metal, an electron will not in general stay in the neighbourhood of any one ion for more than about 10^{-15} sec. The field of the electron itself, therefore, changes too rapidly to be effective in polarizing the medium. But suppose that "by accident" an electron remains on one positive ion for about 10^{-12} sec. Then the medium round about will have time to become polarized, the positive ions being displaced towards and the negative away from the electron as shown in figure 1 *a*. The electrostatic field vector E at a distance r from the electron will decrease (numerically) from $e/\kappa_0 r^2$ to $e/\kappa r^2$, where κ_0 ($\sim 2{\cdot}5$) denotes the dielectric constant due to the polarization of the ions only, and κ (~ 5) is the dielectric constant for static fields due to the polarization *and* to the displacement of the ions. The field due to the polarized medium is thus

$$\left(\frac{1}{\kappa}-\frac{1}{\kappa_0}\right)\frac{e}{r^2} \qquad \ldots\ldots(1).$$

This field will now push the electron back if it tries to escape; the potential energy of an electron in this field is

$$V(r) = -\left(\frac{1}{\kappa_0} - \frac{1}{\kappa}\right)\frac{e^2}{r} \qquad \text{......(2).}$$

A "potential hole" is thus formed by the displaced medium, and in this potential hole the electron will have a series of stationary states, just like the stationary states in the field of a proton, for which $V(r) = -e^2/r$. We shall speak of an electron in the lowest of these states as a "trapped electron".

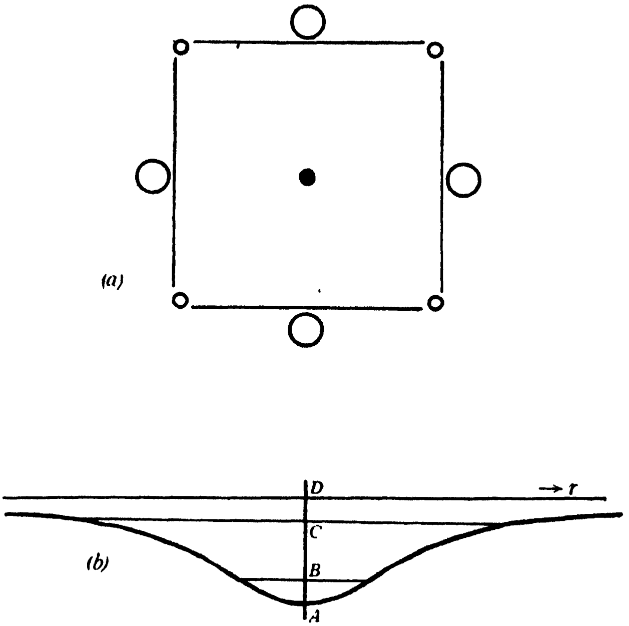

Figure 1. (*a*) Displaced ions round a trapped electron. (*b*) Potential energy of an electron in polarized crystal; the horizontal lines at *B* and *C* represent the energies of the normal and excited states. ● positive ion with electron; ○ positive ion; ◯ negative ion.

An electron trapped in this way can only move from one ion (*a*) to a neighbouring ion (*b*), if *at the same time* the surrounding ions move into new displaced positions about the ion (*b*). The frequency with which such a process takes place may be shown to be very small at room temperature(6), so that we may assume that our trapped electrons are immobile. At high temperatures, however, thermal vibrations may occasionally raise an electron from its trapped position into the conduction band.

Formulae (1) and (2) are valid only at large distances from the electron such that $r \gg a$, where a is the nearest distance between unlike ions. This is for two reasons: first, these formulae neglect the atomic structure of the crystal, and will be entirely incorrect when $r < a$; and secondly, an electron trapped in our "potential box" will have an orbit (wave function) of finite radius comparable with a, and some of the nearest ions will be acted on by a field due to *less* than one electronic charge. The potential energy of an electron in the field due to the displaced ions may be expected to appear as in figure 1 *b*. In this figure B and C represent normal and excited states.

We have estimated the depth of the potential hole AD in figure 1 *b* in a way which will be clearest if we neglect for the moment the polarizability of the ions and so set $\kappa_0 = 1$. Then at large distances the polarization of the medium is

$$P = \frac{1}{4\pi}\left(1 - \frac{1}{\kappa}\right)\frac{e}{r^2},$$

and thus the displacements of the ions are

$$x = \pm\frac{1}{4\pi}\left(1 - \frac{1}{\kappa}\right)\frac{a^3}{r^2} \qquad \text{......(3).}$$

If we were to assume formula (3) to be valid for *all* the ions of the lattice, we should obtain for the potential at the centre

$$-\frac{e^2}{4\pi}\left(1 - \frac{1}{\kappa}\right)\Sigma\frac{a^3}{r^4} = 1{\cdot}31\left(1 - \frac{1}{\kappa}\right)e^2,$$

where the summation Σ over the distances from a given ion to all the other ions of a simple cubic lattice was carried out using formulae due to Lennard-Jones and Ingham (7).

What we actually did was to assume equation (3) to be valid except for the six negative ions which are nearest neighbours to the positive ion on which the electron considered is located. We then determined the displacements x of these ions in the field of the electron and the induced dipoles of all the other ions, the latter being summed numerically. A few calculations for the ions distant $\sqrt{2}a$, $\sqrt{3}a$ and $2a$ showed this to be quite a good approximation.

By these methods we found the depth of the potential hole to be from 6 to 4 eV. for the fluorides and from 2·5 to 1·5 eV. for the other alkali halides. The displacement x of the ions which are nearest neighbours is of the order $\frac{1}{10}a$.

In a potential hole of the form shown in figure 1 *b*, an electron will have an infinite series of stationary states just as in a hydrogen atom. We therefore expect a strong-line absorption corresponding to a transition to the first p state, and possibly other weak lines. All lines will be broadened by the vibration of the ions. There will be also a weak continuous spectrum for higher frequencies.

The question now arises, can these trapped electrons be identified with the F centres? Both Smekal (3) and de Boer (1) have given quite different explanations. We see that the absorption to be expected is in the same part of the spectrum as the F band. We have, moreover, estimated the broadening to be expected as the temperature is raised and find it also in satisfactory agreement with experiment. The photoconductivity observed can be pictured in the following way: the electron is raised by the light to an excited state (C in figure 1 *b*), and the thermal vibrations are then sufficient to raise the electron into the conduction band. This will account for the very marked diminution in the current per absorbed quantum observed by Gläser and Lehfeldt[(8)] below −150° C.*; the thermal vibrations are *not* then sufficient to remove the electron.

Before, however, we can say with any confidence whether our trapped electrons are *F* centres, it will be necessary to discuss in the light of the model the various processes by which *F* centres may be formed, and what happens to the corresponding positive charge. We feel, however, that the theoretical grounds for believing in the existence of trapped electrons are strong, and that it will be surprising if they do not correspond to something in the observed phenomena.

REFERENCES

(1) DE BOER, J. H. *Rec. Trav. chim. Pays-Bas*, **56**, 301 (1937).
(2) VON HIPPEL, A. *Z. Phys.* **101**, 680 (1936).
(3) SMEKAL, A. *Z. Phys.* **101**, 661 (1936).
(4) TARKAKOVSKY. *Z. Phys.* **97**, 765 (1935).
(5) LANDAU. *Phys. Z. Sowjet.* **3**, 664 (1933).
(6) FRENKEL. *Phys. Z. Sowjet.* **9**, 158 (1936).
(7) LENNARD-JONES and INGHAM. *Proc. roy. Soc.* A, **107**, 636 (1925).
(8) GLÄSER and LEHFELDT. *Nachr, Ges. Wiss. Göttingen*, **2**, 91 (1936).

---

* Cf. the paper in this volume by R. W. Pohl, figures 17 and 18, pp. 17, 18.

DISCUSSION OF THE PAPERS BY POHL, AND BY GURNEY AND MOTT

Reported by N. F. MOTT

THE discussion was opened by Dr de Boer, who remarked that although Prof. Pohl refused at this stage to advance any hypotheses as to the nature of the F centres (*Farbzentren*) until the experimental evidence should be sufficient to decide unequivocally between them, it was necessary for other people to do so, because of the great importance of this work of the Göttingen school for the understanding of other phenomena. He then proposed a number of alternative models for the F centres, which have already been published (reference 1 of the preceding paper). The following account describes the hypothesis, which, at the end of an afternoon's discussion, appeared the most probable.

It must first be stated that Landau's trapped electrons, described by Gurney and Mott, certainly do *not* correspond to the observed F centres. This follows from the fact (cf. Pohl's article, figure 6) that when a halide crystal is heated in the vapour of the alkali metal, the number of F centres formed is proportional to the pressure of the alkali vapour. If the alkali atom dissociated into a trapped electron and a positive ion (adsorbed perhaps at an internal crack), the number of F centres would be proportional to the square root of the temperature. Whether Landau's trapped electrons correspond to anything in the observed phenomena must remain an open question.

Any explanation based on cracks or defects of an *irregular* nature was ruled out, since Prof. Pohl stated that the spectrum of the F centres was always the same. This was not however definitely established to be the case for the F' centres.

The most probable hypothesis seems to be the following: in an alkali-halide crystal *in thermal equilibrium* at a temperature T one may suppose that at a certain number of positive lattice points, and at an equal number of negative lattice points, an ion is missing (cf. figure 1). The number of such vacant places will be proportional to a factor $e^{-\frac{1}{2}E/kT}$, where

$$E = E_1 + E_2 - E_3,$$

E_1, E_2 being the work required to remove a positive and negative ion respectively and E_3 the lattice energy per ion pair.*

It is now suggested that an F centre is an electron trapped in the neighbourhood of a point where a negative ion is missing. An F centre is thus as a whole electrically neutral.

---

* A preliminary calculation carried out in Bristol on the basis of the Born lattice theory with polarizable ions gives 1·4 eV. for $\frac{1}{2}E$ in NaCl.

If we neglect the finite radius of the orbit (wave function) of an electron, the energy of an electron located on a positive ion far from any hole will be

$$\frac{\alpha e^2}{r_0} - I \simeq +3 \text{ eV}.$$

where α is the Madelung constant (1·74), r_0 the interatomic distance, and I the ionization potential of the alkali atom. On one of the ions Q next to the missing negative ion the potential is

$$\frac{(\alpha - 1)\, e^2}{r_0} - I,$$

which is about 5 eV. lower, and at the lattice point of the missing ion the energy is $-\alpha e^2/r_0$, which is much lower still, so there is no doubt that an electron could be trapped in such a neighbourhood.*

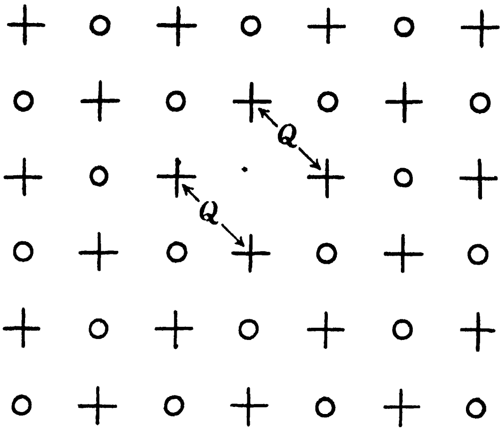

Figure 1. Alkali-halide crystal with one negative ion missing; the crosses represent positive and the circles negative ions. It is suggested that if an electron is trapped in the place left by the negative ion, an F centre is formed.

Dr Verwey suggested that the electron would be trapped on a particular one of the 6 ions Q, and described some recent experiments of his own on the dielectric loss for frequencies of about 200 metres in halide crystals with and without F centres. In the crystal with F centres the dielectric loss was some 50 times greater, although both crystals were insulators for steady fields. Dr Verwey suggested that this loss of energy was due to the electron jumping from one atom Q to another. In subsequent discussion with the present writer, however, it was agreed that the position of lowest energy is the central point, and that in any case an electron trapped in such a potential hole would have a non-degenerate wave function extending over the whole neighbourhood of the six points Q; so the explanation of Dr Verwey's experiments must be found in some other way.

The model given above of the F centres obviously accounts for the dependence of the concentration on the pressure of alkali vapour. Also, when F centres are introduced from a cathode into a hot crystal, halogen is ejected which, according to Prof. Pohl, can be detected by its smell. Further, the explanation of the drop in photoconductive current at low temperatures (Pohl, figure 17) given by Gurney and Mott can be applied to this model also. It also enables one to form a picture of the photochemical transformation of *U* centres into *F* centres. Assuming that a *U* centre is an H^- ion replacing a halogen negative ion in the lattice, the absorption of a quantum in the *U* band (Pohl, figure 27) will remove an electron on to a neighbouring positive ion, leaving behind a hydrogen atom. At sufficiently high temperatures the hydrogen atom will have time to diffuse away before the electron drops back to its normal state, so that an *F* centre is left behind. The necessity for the H atom to diffuse away will account for the fact that the quantum-yield drops low values at low temperatures (Pohl, figure 28).

---

* These energies, being calculated neglecting the polarizability of the ions, are probably much too large, but their relative magnitudes are correct.

Prof. Pohl mentioned the fact, not stated in his report, that in the optical production of *F′* centres from *F* centres, the absorption of *one* quantum destroys *two F* centres and forms *two F′* centres. He suggested that the electron released from an *F* centre is recaptured *most easily* in the neighbourhood of another *F* centre, and that the two *F* centres so formed influence one another in such a way that they give the *F′* absorption spectrum. This hypothesis accounts for the fact (Pohl, figure 19) that the mean range of the liberated electrons is proportional to the number of *F* centres already present.

On the hypothesis given above we may assume that, in the potential hole caused by the removal of a negative ion, *two* electrons may be trapped, just as two electrons may exist in the potential hole of the proton to form a negative ion H^-. What the absorption spectra reveal as a pair of *F′* centres are thus two electrons trapped in the same potential hole. On the other hand this would suggest that all *F′* centres should have just the same absorption band.

In conclusion, it must be emphasized that the correctness of the model given above is by no means proved. Prof. Pohl stated that he liked it the best of the various models suggested, but that further experimental work was required before it could definitely be accepted.

Dr W. F. Berg gave an account of experiments by himself and K. Mendelssohn on photographic sensitivity at low temperatures. According to present-day conceptions the photographic latent image consists of a small speck of silver, which has been formed by a primary photoelectric process and secondary processes which mainly consist of flocking together of silver particles and of getting rid of the bromine. Without going into the mechanism of these processes one can say that they imply the transport of matter through the crystal lattice. This transport should not be possible at sufficiently low temperatures, since the mobility drops with temperature as an exponential function. This was the reason for undertaking a preliminary determination of the photographic sensitivity down to 20° K. (liquid hydrogen). Measurements have already been done at 90° K., e.g. by F. Luft (*Phot. Korr.* **69**, 161–5 (1933)) and S. E. Sheppard, E. P. Wightman, and R. F. Quirk (*J. phys. Chem.* **38**, 817–31 (1934)). Defining sensitivity as the exposure necessary to give a density of 0·1 above fog it was found that (1) for a blue sensitive emulsion the sensitivity at 90° is 7 per cent, at 20° K. is 4 per cent of that at room temperature; (2) for a panchromatic emulsion at 20° the sensitivity is 0·4 per cent of the room temperature sensitivity for unfiltered tungsten light, 0·02 per cent for light filtered through a red No. 22 Wratten filter.

These results are in general agreement with the earlier papers as far as sensitivity at 90° is concerned. They have interest outside photography, which is possibly only a very sensitive means of studying the ionic conductivity in crystals. The sensitivity is surprisingly high in every case and can hardly be understood, if our conceptions are correct.

Prof. Pohl suggested that the actual transport of matter took place only after warming up.

Dr Berg also reported experiments on the print-out effect at 90° K. Solio paper gave a visible effect while still under liquid air, the sensitivity being reduced to about 10^{-5}. Slow Kodaline film gave no effect, the sensitivity being reduced to less than 10^{-6}.

ALKALI-HALIDE PHOSPHORS CONTAINING HEAVY METALS

By R. HILSCH, Göttingen

§ 1. INTRODUCTION

This paper is an account of some of the work on the alkali-halide phosphors carried out in the Göttingen laboratory. The phenomena are simplest in phosphors activated by heavy metal halides(1, 2), and the discussion of these will form the main feature of this paper.

These phosphors can easily be prepared by adding to the molten alkali halides small concentrations of the heavy metal halides; the crystal phosphors can then be produced as single crystals and then the light absorption caused by the heavy metals can be measured easily. In most cases the absorption lies in the range of wave-lengths for which the pure crystal is transparent.

In contradistinction to most of the known phosphors, we are here dealing with the simplest lattices, only one kind of foreign atom being embedded within the body of the crystal.

§ 2. THE ABSORPTION SPECTRA OF THE ALKALI-HALIDE PHOSPHORS

It is often held that in these phosphors a real mixed crystal is formed, the heavy metal ions replacing the alkali ions in the lattice. The following discussion shows that this hypothesis must be accepted with reserve.

Figure 1 shows an example of a silver phosphor, the absorption spectrum of KI with 0·05 per cent AgI(3). A double band at 260 mμ. (at 20° C.) is observed to appear in the neighbourhood of the absorption edge of pure KI. At a temperature of 205° C., the band of longer wave-length alone is found. The behaviour with temperature of this transformation has been carefully investigated. With increasing temperature the intensity of the band at $\lambda = 265$ mμ. increases continuously. The transformation is complete at 148° C. This is a remarkable fact, for at the same temperature AgI possesses a point of transformation(4). In spite of the small concentration, the AgI structure is in some way still conserved within the KI crystal. The assumption that in the mixed crystals one silver ion replaces one alkali atom of the body crystal is thus ruled out.

The absorption bands of the phosphors so far produced, which contain the thallo-halides, are shown in figure 2(5). As well as the sharpness of the bands (in contrast to the diffuse bands of pure thallo-halides), it is striking that the halogen ions of the body crystal determine the situation of both the bands. This behaviour also does not agree with the assumption of a simple mixed crystal. It

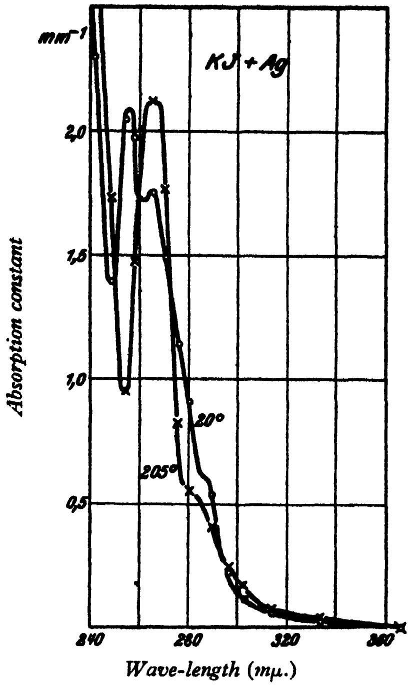

Figure 1. Absorption spectra of a KI phosphor activated by Ag above and below the transition point.

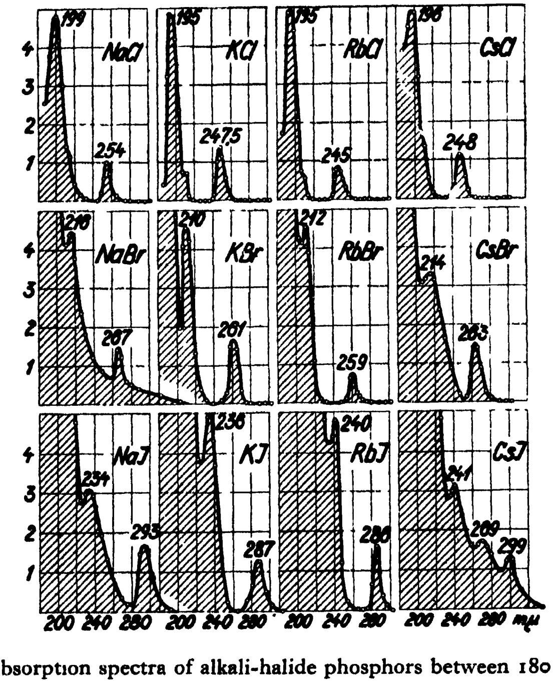

Figure 2. Absorption spectra of alkali-halide phosphors between 180 and 320mμ.

may also be mentioned that the small band in chloride phosphors lying at the foot of the short-wave band increases rapidly at high temperatures (over 500° C.) at the expense of the main band.(6) This also suggests a transformation of the lattice type of the centres responsible for the absorption. The distance between the two bands amounts in every case to about 1 eV. (In the case of chloride phosphors we take the band existing at high temperature.) This reminds one of the excitation energy of the thallium atom which is of the same value.

Similarly, measurements have been made of the absorption of alkali-halide phosphors with the addition of lead halides. The bands are found to be of the same sharpness. These will not be reproduced here. We must, however, stress the unimportant influence of the halogen ions and the determining influence of the alkali ions.

The phosphors activated by the copper halides do not show especially sharp regions of absorption. Moreover, in spite of a large addition of copper halides, only small amounts of copper can be actually dissolved in the atomic form. Several months later the absorption and with it the phosphorescent properties of the crystal are found to have disappeared almost completely, but they can be reproduced by a short period of heating(7, 8).

Thus, the formation of phosphorescent centres is only possible through the application of force, and then only to a small extent.

§ 3. THE MECHANISM OF THE ABSORPTION BANDS

After having noted these facts, the mechanism of absorption still remains to be explained.

Some experimental researches of Fromherz, Menschick and Kun-Hou-Lih are of great importance(9, 10, 11). Starting out from the already known absorption spectrum of alkali-halide phosphors, they investigated the absorption of the heavy metal halides in aqueous solutions. Besides the dissociated metal ions and the halogen ions, uncharged and positively charged molecules of the metal halides will be found in the solution, according to its concentration. The absorption bands of the aforesaid molecules have no similarity with those of the phosphors. When, however, we simultaneously add large quantities of the corresponding alkali halides (for example $H_2O + PbCl_2 + KCl$), we also find negatively charged complex ions (e.g. $PbCl_4$). The addition of alkali halides thus produces new absorption bands which may be ascribed to negatively charged complexes (MeX_n). The maxima of the bands of complex solutions, compared with those of crystal phosphors, are shown in table 1.

Table 1. Wave-lengths of absorption bands (mμ.)

	Crystal	Solution
$NaCl + AgCl$	210	216
$KCl + CuCl$	267	272
$KCl + PbCl_2$	273, 196	272, 195
$KCl + TlCl$	247, 196	242, —

The situation of the bands in solution as well as in the crystals is observed to be practically independent of the nature of the alkali chlorides. The bromides and iodides show the same behaviour.

From this Fromherz concluded that the active centres of the phosphors must have a structure similar to that of the saturated complexes. It must be supposed that within the crystal also there exists a rather isolated complex. This is easy to understand, when the great deformation produced by the heavy metal ion is taken into account. Thus we again approach the ideas put forward by Lenard and Schleede about the *Phosphoreszenzzentrum*.

§4. EMISSION BY ALKALI-HALIDE PHOSPHORS

We discuss only emission by thallium phosphors, which have been investigated thoroughly.

The emission consists of broad characteristic regions of emission with no remarkable structure. When illuminated with light of frequencies lying in the two absorption bands, the phosphors show fluorescence. On employing the radiation which is absorbed within the band at short wave-lengths, we also get phosphorescence up to 5 per cent. Fluorescence and phosphorescence give radiation with the same spectral distribution. One band, in particular, appears in the ultra-violet. The quantum yield, the decay of the after-glow and the spectral distribution of extinction have been closely investigated(12, 13, 14, 15). The results are not simpler than those drawn from sulphide phosphors. The interpretation of the mechanism of emission has not yet been given. It is only in the case of the rare earth phosphors that Tomaschek and his collaborators have succeeded in ascribing the emission to the various states of foreign atoms.

The question of energy transition seems to be the most important one. As has been pointed out in the investigations of Gudden and Pohl(16), a photoelectric conduction appears parallel to the excitation and the emission of the phosphorescence of sulphide phosphors. The electrons ejected by the irradiation are free to move. In contrast to this, the alkali-halide phosphors never show photoelectric conduction, when irradiated with any wave-length(17). We must conclude that in this case the electronic paths are very small and must be compared with the lattice distances. It is moreover certain that F centres will be produced by the accumulation of light-energy. We should suppose them to exist only in the vicinity of the *Zentrenkomplexe*.

In contrast to the absorption bands, the position of the emission bands depends upon the nature of the alkali ions of the body crystal. This is shown in table 2 for the thallium chloride phosphors.

Table 2. Maximum of the emission bands at 20° C. (mμ.)

NaCl	KCl	RbCl
288	300	315

Moreover, we find a considerable dependence upon temperature. The (TlX_n) complex must be considered if we are to interpret the emission bands. The excited states of these complex molecules, broadened by the energy of the lattice vibrations, are supposed to result in the unresolvable bands of the emission spectra. It is quite possible that these bands may be connected with the molecular spectra of thallo-halides investigated by Butkow(18). (Here spectra in the same region of wave-length appear as those emitted by thallium phosphors.) Hence the light absorption in the thallium complexes should cause excited states of thallium-halide complexes, which are similar to those of molecules in the gaseous state. (As has already been pointed out, the distance between the thallium absorption bands in all crystals amounts to about 1 eV., equal to the excitation energy of thallium atom.)

If the TlX_n complex is responsible not only for absorption but also for emission, the complex in solution in water should also show fluorescence. A short time ago I found that this was in fact the case. A strong bluish-violet emission can be excited in an aqueous solution of LiCl+TlCl by illuminating it with light of wave-length 242 mμ., the wave-length of the first absorption band of the complex (TlX_n). The bands of bromides and iodides move still farther towards longer wave-lengths in the visible region. These results seem quite reasonable, for the surroundings of the complex also in the crystal influence the emission spectra, as we see from table 2.

§ 5. PHOSPHORS WITH NO ADDITION OF HEAVY METAL

It has lately been found that at high temperatures gases are able to diffuse in the form of molecules within the pure alkali halide(19, 20). During these researches two further phosphors were produced(21). They were not activated by heavy metals, but by gaseous molecules, CO and O_2. Also in this case the absorption and emission must be ascribed to a complex. In the case of a crystal subject to a high pressure of O_2, ClO_4 might perhaps be the complex in question. The emission spectra are very remarkable. They consist of very sharp equidistant double bands. Their frequencies only depend to a small extent upon the body crystal used.

Until now it has not been possible to give a full explanation of these phenomena.

§ 6. SUMMARY

It is a remarkable fact that very complicated formations of molecules can be observed within the alkali halides in the form of single crystals. The luminescence processes which result from the construction of these complexes cannot as yet be interpreted. The exact process of absorption of light by the complex has also not been determined. Owing to their similarity with phenomena in aqueous solutions, however, the alkali halides have at least one advantage. Very definite complexes (MeX_n) may be shown to be responsible for the whole range of phenomena of light absorption and emission.

REFERENCES

(1) Hilsch, R. *Z. Phys.* **44**, 860 (1927).
(2) Smakula, A. *Z. Phys.* **45**, 1 (1927).
(3) Forró, M. *Z. Phys.* **58**, 613 (1929).
(4) Strock, L. W. *Z. phys. Chem.* B, **25**, 441 (1934).
(5) Hilsch, R. and Pohl, R. W. *Z. Phys.* **48**, 384 (1928).
(6) Forró, M. *Z. Phys.* **56**, 534 (1929).
(7) MacMahon, A. M. *Z. Phys.* **52**, 336 (1928).
(8) Forró, M. *Z. Phys.* **56**, 235 (1929).
(9) Fromherz, H. and Menschick, W. *Z. phys. Chem.* B, **3**, 1 (1929).
(10) Fromherz, H. and Kun-Hou-Lih. *Z. phys. Chem.* A, **153**, 321 (1929).
(11) Fromherz, H. *Z. Phys.* **68**, 233 (1931).
(12) Meyeren, von W. *Z. Phys.* **61**, 321 (1930).
(13) Bünger, W. *Z. Phys.* **66**, 311 (1930).
(14) Bünger, W. and Flechsig, W. *Z. Phys.* **67**, 42 (1931).
(15) Bünger, W. and Flechsig, W. *Z. Phys.* **69**, 637 (1931).
(16) Pohl, R. W. *Naturw.* **16**, 477 (1928).
(17) Hecht, K. Diss. Göttingen (1930).
(18) Butkow, K. *Z. Phys.* **58**, 232 (1929).
(19) Mollwo, E. *Ann. Phys.* **29**, 394 (1937).
(20) Hilsch, R. *Ann. Phys.* **29**, 407 (1937).
(21) Honrath, W. *Ann. Phys.* **29**, 421 (1937).

THE EFFECTS OF TEMPERATURE ON THE INTENSITY OF FLUORESCENCE OF SOME IMPURITY SOLIDS

By J. T. RANDALL

Communication from the Staff of the Research Laboratories of The General Electric Company Limited, Wembley, England

§ 1. INTRODUCTION

The present paper is largely an account of some preliminary measurements on the effects of temperature on the intensity of fluorescence of a number of impurity solids under photoexcitation.

During the last few years it has become clear that the properties of fluorescent solids requiring the presence of impurities are closely linked with those of semi-conductors. The zone theory of electronic energy bands in crystals has been successful in explaining, not only many features of the properties of metals, but, in principle at any rate, some of the features of semi-conductors.

It is not unreasonable to suppose that the same theory, or some modification, will ultimately be of great value in the study of fluorescence. At the present time, however, the difficulties of determining the energy zones in crystals with quantitative accuracy are extremely great, as may be seen from the recent work of Shockley(1) and Ewing and Seitz(2) on the alkali halides. Nevertheless, it remains true that no model of a fluorescent impurity solid other than that which depends on the division of the electronic energies into zones has been seriously proposed. It will be remembered that in the application of this model to certain types of semi-conductor by Wilson and Fowler, a notable feature was the temperature-dependence of the conductivity.

Very little work has as yet been carried out on the temperature-dependence of the intensity of fluorescence. In starting this work it was felt that the results might in due course help to throw some light on the mechanism of fluorescence in impurity solids, and possibly on the interchange of energy between "free" electrons and the lattice atoms. It is clear from the complex nature of the results that a great deal remains to be done.

As will be seen in more detail below, the greater number of powders examined consisted of zinc sulphides, or zinc-cadmium sulphides in solid-solution, each with various activating impurities. In addition, alumina and cadmium iodide were examined. ,It is necessary here to say a little about the zinc sulphide type of fluorescent material.

It is of course well known that the fluorescence effects observed with sulphides are a result of the presence within the solid of minute traces of impurity.* In this they differ from the uranyl salts, for example, where the seat of luminescence is in the co-ordination group of the uranyl ion, and the luminescence spectra are essentially molecular in type(6). It should also be noted that the sulphides, as distinct from the alkali halides considered by Hilsch(3), are photoconducting. The intensity of fluorescence of the sulphides is dependent, not only on the nature and amount of deliberate impurity, but on the complete exclusion of any other foreign material. In these compounds impurities to the extent of one or two parts in a million are frequently of vital importance whenever the details of the fluorescence spectrum have to be repeated with accuracy from specimen to specimen. In the silicates and phosphates, on the other hand, the optimum amount of impurity is frequently in the neighbourhood of from 0·1 to 1·0 per cent. From the point of view of the present experiments this means that one cannot assume that the only impurities present are those deliberately added at the outset of preparation; it is necessary to examine the final product spectroscopically in order to be reasonably sure of the total number of impurities. It was hoped at the start of this work to examine a number of zinc-cadmium sulphide solid-solutions, and also to compare the hexagonal and cubic varieties of zinc sulphide, all with the one impurity. The extreme ease with which sulphides of this group take up any extraneous impurity have made it impossible to carry out such an ideal programme, but the complexity of the results clearly suggests that further attempts in this direction will be worth while fundamentally.

Copious details for the preparation of fluorescent materials have been given from time to time(4), and it is only necessary to emphasize here one or two points of interest in connexion with the results which follow. The initial complex of pure matrix plus activating impurity has always to undergo a heat treatment in order that sensible fluorescence may subsequently be produced. It is also generally assumed that the activator during this treatment enters into solid-solution with the matrix. The work of Hilsch appears, however, to throw some doubt on this in the case of the alkali halides. The activating impurity is frequently added to the pure sulphide matrix in the form of a dilute solution to ensure adequate dispersion, and, theoretically, it should then only be necessary to heat the combination of the two to an appropriate temperature. While this procedure is successful with certain combinations of matrix and activator, others require the further addition of "fluxes". The avowed object of these is to promote crystal growth of the matrix and solid-solution of the main activator. Experiments show, however, that fluxes are frequently real impurities. Spectroscopic examination reveals their presence in the final material, and it is apparently impossible to remove them completely by means of washing processes.

---

* The work of Schleede(7) appears to show that strong blue fluorescence may be obtained from *pure* zinc sulphide, and the necessary condition for this is the presence of mixed crystals of wurtzite and blende. It is not improbable that the juxtaposition of the two types of crystal structure may be regarded theoretically as introducing at boundaries new levels which are effectively of the impurity type.

Before passing on to the experimental work a little must be said about the fluorescence spectra of impurity solids. Such spectra, where excited by ultraviolet, are characterized at room temperature by the presence of broad structureless bands, which may under certain special conditions be accompanied by very narrow bands with definite structure. The lowering of the temperature to that of liquid air, for example, results in a narrowing of the broad bands, but there appears to be no certain evidence that this is accompanied by development of structure within the bands.

The occurrence of very narrow bands, or even line systems, in the fluorescence spectra of impurity solids is usually due to the use of either chromium or one of the rare earths as activating impurity. The fluorescence spectra in cases of this kind are apparently partly made up of rather distorted line spectra of the ions of the activating impurities themselves. Presumably in this case the impurity levels lie just above the bottom of the conduction band. This aspect of the subject bears close resemblances to the work of Spedding(5) on the absorption spectra of rare-earth salts.

In the more normal cases of fluorescence with structureless bands, the impurity levels will lie within the forbidden zone. On this view it is easy to see why different solids require different exciting wave-lengths. In order to excite electrons into the conduction band the exciting wave-length must have an $h\nu$ value at least equal to that of the lowest energy values possible at the bottom of the conduction band. On this view the matrix lattice determines the exciting wave-length, and the impurity the fluorescence colour. In the well-known case of the ZnS/CdS sulphides with constant impurity the average wave-length of fluorescence increases as the cadmium content increases; it appears probable that this is due to the gradual lowering of the conduction band. Such ideas cannot at this stage be regarded as substantiated quantally; they merely serve to give a working picture of the process.

§ 2. SUBSTANCES EXAMINED AND EXPERIMENTAL PROCEDURE

The substances examined, together with the crystal lattices concerned and the impurities detected, are conveniently summarized in the following tables:

Table 1. Series of zinc sulphides

Powder and lattice details	Main impurities	Minor impurities*
(1) Cubic	Ag, Mg	Ba
(2) Hexagonal	Ag, Mg	Cd, Ba
(3) 75 % hexagonal 25 % cubic	Ag, Mg	Cu, Ba, Ni
(4) Cubic	Cu, Mg	Cd, Ba
(5) Hexagonal—slightly contracted lattice	Mn	Ba, Si

* Detected spectroscopically as traces.

Table 2. Series of zinc-cadmium sulphides

Powder and lattice details*	Main impurities	Minor impurities
13 % CdS, 87 % ZnS	Cu, Mg	Ag
16 % CdS, 84 % ZnS	Cu, Mg	Ba
24 % CdS, 76 % ZnS	Cu, Mg	Ag, Ba
29 % CdS, 71 % ZnS	Cu, Mg, Al	Ag, Ba
33 % CdS, 67 % ZnS	Cu, Mg	Ag, Ba

* The percentages refer to molecular proportions.

Table 3. Cadmium iodide and alumina

Powder and lattice details	Main impurities	Minor impurities
Cadmium iodide	Pb	Ag, Cu
Alumina—corundum type	Cr	—

The first column of each table describes the lattice and the constitution of the material, with the exception of table 2 where all the lattices are of the hexagonal type; the term "cadmium iodide" is by now sufficient both to describe the material and the lattice type. In the second column are given the main impurities, and it should be said that these have been identified not only as those which were deliberately added, but also spectroscopically by arcing the powders on graphite electrodes. In all cases where magnesium occurs it was added as flux material, and this also applies to the traces of barium. Any other impurities recorded in the case of the sulphides are accidental, and such as are likely to be picked up in any chemical laboratory by sulphides. It should be added that the compositions of the zinc-cadmium sulphides were determined by means of their X-ray patterns after the final heating process. This is an important point, as cadmium sulphide very readily evaporates from the solid-solution, and it appears that this is the only accurate means of determining the nature of the final product.

Although from general experimental acquaintance with this type of material one would consider it unlikely that variations of crystal size and lack of homogeneity in the powders are of greater importance than the impurities themselves, the X-ray apparatus revealed the following further information.

Table 4. Further details of the zinc-cadmium sulphide series of table 2

Percentage of cadmium sulphide	Details of homogeneity, crystal-size, etc. obtained from X-ray photographs
33	Crystal size about average for Zn/Cd sulphides. Outer diffraction lines fuzzy, indicating distortion or lack of homogeneity
29	Similar to 33 % sample
24	Crystal size probably lower than above. Two distinct phases differing slightly in CdS content revealed by resolution of high angle diffraction line
16	Crystal size similar to 24 %. Uniform composition
13	Crystal size similar to 24 and 16 %. Two distinct phases, but very close together. Less difference than in 24 %, and one phase weaker than the other

Where two distinct phases occur, the difference in CdS content is of the order of 1 per cent.

The fluorescence of the materials examined was excited by means of a high pressure mercury-vapour discharge lamp in conjunction with a Woods Glass filter. The excitation was therefore essentially that of the 3650 A. triplet. The fluorescence intensity was measured by means of a rectifier type of photoelectric cell in series with a galvanometer. The sensitivity of the cell varies a good deal according to the particular spectrum irradiating it, and no attempt has been made in this preliminary work to correct for this. The object of the experiments was mainly to obtain the general shape of the fluorescence-intensity temperature curves. The results are not therefore on an energy basis, and the fact that two powders may give rise to a particular deflection on the galvanometer at a given temperature has no special significance. As will be seen below, the room temperature deflection was usually chosen arbitrarily. At the present stage, also, the small colour changes which occur in the fluorescence spectra as the temperature is changed have been neglected.

With regard to the heating and cooling of the specimens, two pieces of apparatus were used, one for temperatures between 90° and 400° K., and the other from room temperatures to any high temperature desired. The measurements do not in fact extend much beyond 600° K. It was usually arranged for the two sets of readings on a particular specimen to overlap in temperature, in order to be sure of the continuity of the curves. For the higher temperatures the powders were dusted on to a miniature hot-plate fitted with thermocouple. The temperature of the surface of the powder was not exactly the same as that registered by the thermocouple, and the readings taken on a rising temperature scale differed slightly from those taken when the plate was cooling. In the curves reproduced later the means of these two sets of readings are plotted in each case. For the lower temperatures, down to that of liquid oxygen, a small thin quartz tube was used. The tube was fitted with a ground joint, and the cooling liquid poured into the tube, the powder being on the lower part of the outer surface. To insulate the powder from the atmosphere, and also to avoid condensation of moisture on the cooled powder surface, the cooling vessel is surrounded by an outer jacket, which is provided with means for evacuation. In this way it was found that uniform temperature over the whole of the powder surface could be maintained. In front of the photocell were placed a water filter and a Wratten 2*a* gelatin filter to absorb any stray infra-red and ultra-violet. A set of readings was usually started by taking a "room temperature" deflection on the galvanometer with the ultra-violet source in a steady state. The distance of the source from the fluorescent specimen was then adjusted until the deflection was in a convenient region covered by the calibration curve of the photoelectric cell for different intensities of illumination. In the neighbourhood of room temperature water was normally used to aid the equalization of temperature over the surface of the inner tube. After removing the water, liquid air was poured into the inner tube and the equilibrium reading taken. The liquid air was then allowed to evaporate, and, just before this was achieved, a quantity of acetone at approximately the freezing point was poured in. This enabled another "fixed" point on the curve to be obtained, and provided a means of obtaining a comprehensive set of readings between approximately 180° K. and room temperature as the cooling liquid warmed up. The series was then completed by a few readings overlapping with the hot-plate temperature range, and for this either hot water or paraffin was employed.

§ 3. EXPERIMENTAL RESULTS

The general results may be summarized very briefly, although some of the details of the various curves will require further discussion. It appears, for all the substances examined, that there is a critical temperature above which the fluorescence intensity always falls fairly rapidly and uniformly. At still higher temperatures the rate of decrease of intensity with temperature decreases. Below what has been called the critical temperature for convenience, a variety of things may happen. In certain cases the intensity may remain sensibly constant as the temperature is reduced; in others there may be a continuous fall; in the zinc-cadmium sulphides there are usually two maxima, and it is the higher temperature maximum that has been associated with a "critical" value of the temperature.

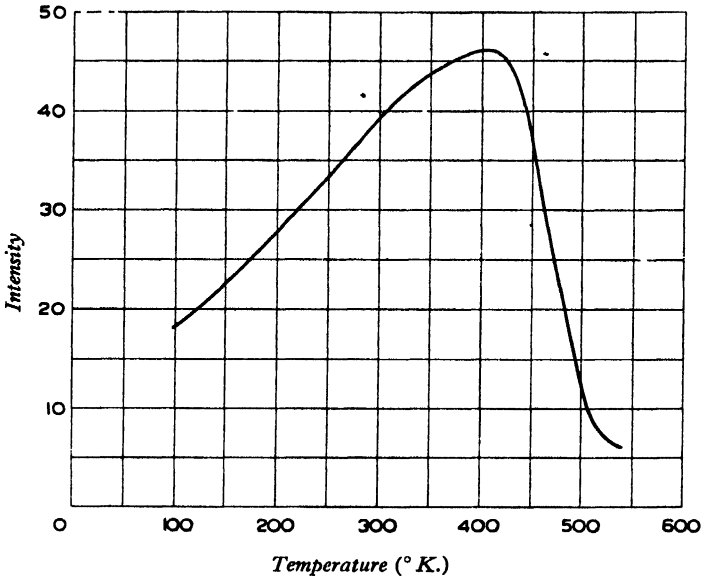

Figure 1. Zinc sulphide hexagonal. Impurities Mn, Mg, (Ba), (Si)

It is convenient to consider first of all the case of hexagonal zinc sulphide with manganese as the main impurity; this is the substance numbered (5) in table 1. For this the intensity variation with temperature appears to be of a fairly simple nature (figure 1). Starting at 100° K. the intensity rises almost linearly with temperature to a maximum value at about 400° K., followed by a sharper linear drop in intensity. Finally at about 500° K. the curve flattens out. It should be noted that this particular powder has a slightly contracted lattice, due no doubt to the presence of manganese sulphide in solid-solution.

Turning now to the curves of figure 2, where the results for the remainder of the "pure" zinc sulphides are recorded, we see that they differ a good deal from those for the manganese-activated powder of figure 1. With the exception possibly of (3) the slopes of the high temperature portion of the curves is rather less, and the low temperature behaviour is considerably different. In three cases, those of powders (3), (4) and (2), there is a distinct small hump at low temperatures, while powder 1 has a minimum at about 180° K. It must be admitted that the complication of the multiple impurities makes it a difficult matter to be certain of the interpretation to be given, but one or two points may be made. First of all comparing powders (2) and (4), it is noticed that in spite of the difference in structure, and the difference in one of the main impurities, these curves are very similar in shape. We are led to assume that in such similar crystal structures, the differences are not of importance, or, if they are, they have been conveniently smudged out by the difference in impurity. If the differences in structure are unimportant, then copper and silver appear to give very similar results. Assuming this, and turning to (1) on the same figure, the minimum in the low temperature part of the curve appears to be associated with the absence of cadmium.

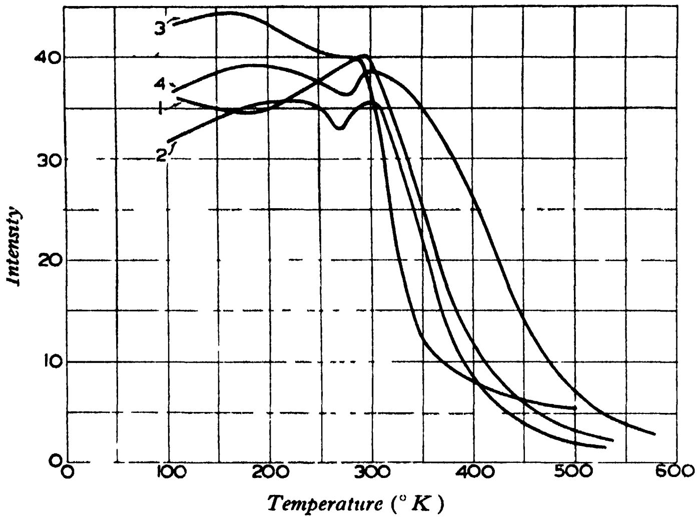

Figure 2. Effect of temperature on fluorescence of cubic and hexagonal ZnS with various impurities (1) cubic ZnS, Ag, Mg, (Ba); (2) hexagonal ZnS, Ag, Mg, (Cd), (Ba); (3) hexagonal + cubic ZnS, Ag, Mg, (Cu), (Ba), (Ni); (4) cubic ZnS, Cu, Mg, (Cd), (Ba).

In figure 3 are reproduced the curves for the solid-solutions of zinc and cadmium sulphides, and with the exception of curve (*e*), representing the 29 per cent cadmium solid-solution, the curves show strong similarities to curves (2), (4) and (3) of figure 2. It is to be noticed that Cu is a common impurity for all the specimens of this series. Although silver is absent only from (*c*) with 16 per cent CdS, its absence makes no general difference to the shape of the curve, which is essentially similar to curve (*a*), which is curve (4) of figure 2 reproduced here for comparison. A further point of interest is that the low temperature peak becomes more pronounced as the proportion of cadmium is increased. In curve (*e*) this peak quite

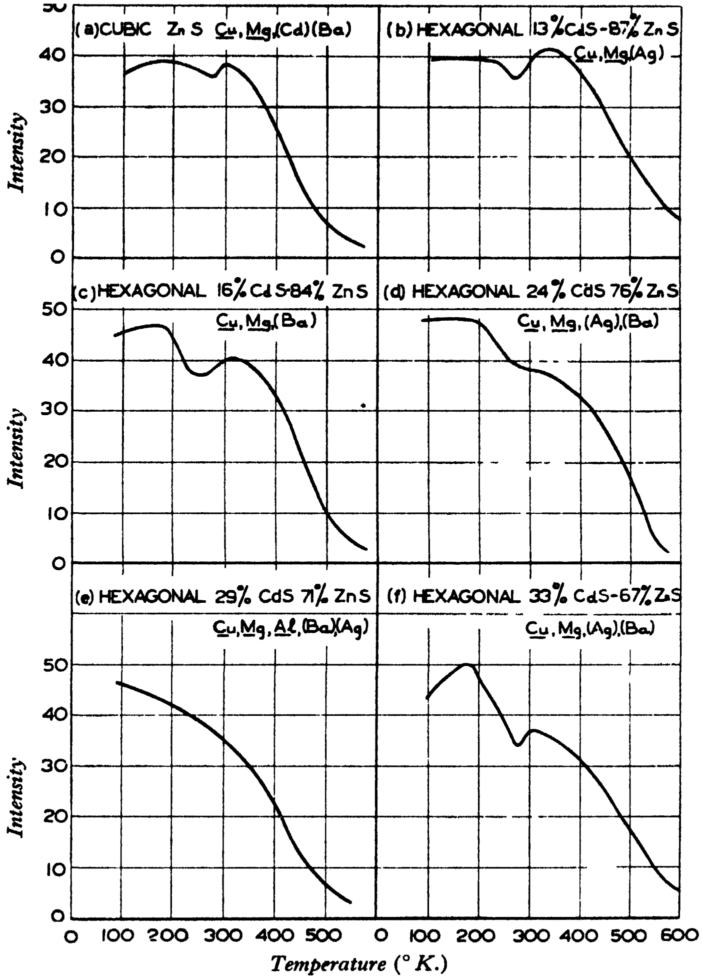

Figure 3.

dwarfs the room temperature peak. In the case of the 29 per cent CdS of (*e*) it is interesting to note that the single curve obtained has no obvious peak and appears to be associated with the presence of a certain amount of aluminium; it is possible that a new peak has been inserted between 250° and 300° K. which has had the effect of smoothing out the curve in this way. The more general significance of these results will be considered later.

Meanwhile it remains to indicate the results on two rather different types of luminescent material; for it was felt advisable even at this stage that experiments on as many different types as possible would be of help in the general interpretation. Figure 4 shows the effect of temperature on the fluorescence of cadmium iodide activated by lead, with minor traces of Ag and Cu present. The intensity is fairly

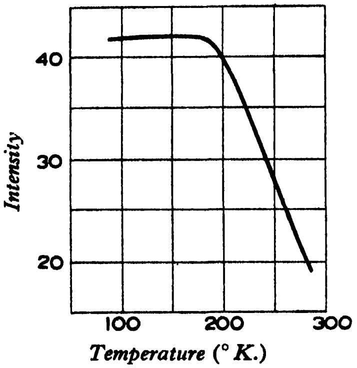

Figure 4. Cadmium iodide, CdI_2; impurities Pb, (Ag), (Cu); yellow fluorescence.

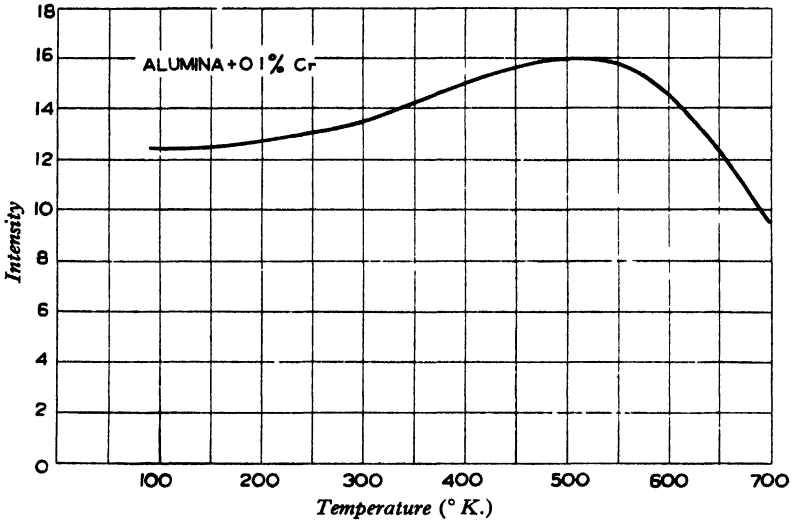

Figure 5. Alumina activated by chromium.

constant at low temperatures but this is followed by a steep and linear fall at about 200° K.

So far, luminescent materials with the broad structureless type of band spectrum only have been considered. In figure 5 is given the curve for alumina activated by chromium. The luminescence spectrum of this material taken at room temperatures consists of a number of rather broad lines together with a rather weak intensity general background. The lines have been attributed by Tomaschek and

Deutschbein to triply ionized chromium. The intensity curve is somewhat similar to that of the hexagonal zinc sulphide of figure 1, except for the rather flat portion at low temperatures. It should also be noted that the maximum in the curve occurs at a much higher temperature, viz. 500° K., than for any others so far examined.

§ 4. DISCUSSION OF RESULTS

While it must be stressed that the present results are only the preliminaries of a rather wider investigation and that minor details may be altered by further work, it is felt that some points of rather general significance may already be deduced from them.

In the first place there is no strong evidence that the change from cubic to hexagonal zinc sulphide produces any marked changes in the intensity curves. It has already been pointed out that the intensity of the low temperature peak of the zinc-cadmium sulphides relative to that of the "high" temperature peak depends to a marked extent on the proportion of cadmium present. This could clearly be ascribed to the gradually changing lattice constant as the amount of cadmium increases, were it not for the fact that in the zinc sulphides the same low temperature peak, present on a rather diminished scale, appears also to depend on the presence of cadmium not as a bulk constituent, as in the solid-solution, but as a minor impurity. This low temperature peak must therefore be associated with the cadmium, and the suggestion is, that even in those powders where the cadmium is already present in bulk, the cadmium, possibly in some other form, is also acting as an important impurity from the point of view of fluorescence. There is nothing particularly objectionable in this idea, as it has been used to explain the behaviour of certain semi-conductors. It is however new as far as the subject of luminescence is concerned, and it remains to be seen what is the exact significance physically of the association of the cadmium as an impurity with the so-called principle activators such as copper and silver. This point is particularly interesting in view of the fact that the X-ray results for the solid-solutions record the definite presence of inhomogeneities.

The curves of figures 2 and 3 were obtained prior to those of figure 1, and their strangely varying slopes at low temperatures were somewhat puzzling at first sight.

The results shown in figure 1, however, together with those on alumina and the known nature of the spectra of the materials, give the general clue.

The susceptibility of all luminescent sulphides to traces of extraneous impurity leads to the presence, in general, of more than one broad band in the fluorescence spectrum. In figures 2 and 3 we appear to be witnessing the superposition of the temperature curves for more than one band. Occasionally, when it is possible to produce a powder with one chief activating impurity, a decidedly simple type of temperature curve results, and this simplicity is shown in figures 1 and 5 in spite of the rather different types of spectra.

It is interesting that all the substances examined show on the high temperature side a rather steep slope, and this rather confirms our view. From the theoretical standpoint there is presumably no difficulty in accounting for the presence of a number of fluorescence bands. One of the problems will be to account for the dependence of the band intensity on temperature, the chief characteristics being a positive slope at low temperatures, followed by a negative slope at higher values of T. At the present time it appears rather easier to understand the high temperature part of the curve. As the temperature increases a decreasing fraction of the total number of excited electrons becomes available for radiative transitions to lower levels. There is at present no evidence to show whether these electrons remain in the upper band, or whether their energy is increasingly lost by collision with lattice atoms as the temperature rises. From the experimental standpoint it is important to determine to what extent the absorption of ultra-violet remains constant over the temperature range considered. I am indebted to Dr Peierls for pointing out the two aspects of this problem: the possible variation of average absorption with temperature, and the dependence of absorption on the nature of the exciting spectrum. Until answers concerning these points have been obtained, no further certain conclusions may be reached from the present experiments.

REFERENCES

(1) Shockley, W. *Phys. Rev.* **50**, 754 (1936).
(2) Ewing, D. H. and Seitz, F. *Phys. Rev.* **50**, 760 (1936).
(3) Hilsch, R. Page 40 of this volume.
(4) See, for example, *Handbuch der Experimental Physik*, **23**, (1927).
(5) Spedding, F. H. *Phys. Rev.* **50**, 574 (1936), **46**, 975 (1934).
(6) Randall, J. T. *J. Roy. Soc. Arts*, **85**, 354 (1937).
(7) Schleede, A. *Angewandte Chemie*, **48**, no. 19, 277 (1935).

DISCUSSION OF THE PAPERS BY HILSCH AND RANDALL

Reported by N. F. Mott

In reply to questions, Dr Hilsch emphasized that photoconductivity was observed in sulphide phosphors, but not in the alkali halides. But in the latter case photoconductivity did not seem to be intimately connected with phosphorescence; the electrons are not removed to any very large distances. Prof. Pohl suggested that *if* there exists a phosphorescence with a long decay period, *then* we may suppose that the electron responsible for the radiation is removed by the absorbed quantum a long way from its original position, i.e. a distance of many atomic diameters. But in the other type of phosphor, in which the electron is not removed, the light absorption causes the transformation of one type of molecule into another; the initial and final states being distinguished for instance by a difference of crystal form—i.e. by the atomic nuclei taking up new positions. Prof. Pohl also emphasized the importance of making large crystals of the sulphide phosphors in order to understand their properties.

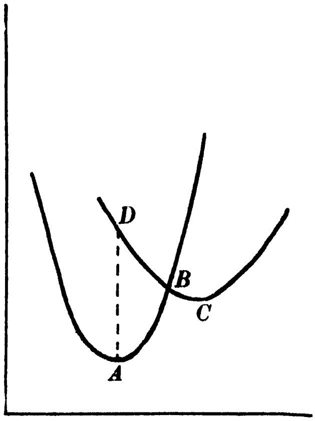

Figure 1.

Prof. Mott and Dr de Boer discussed the mechanism by means of which a molecule in a crystal could re-emit light after a period of minutes or hours. Figure 1 shows the energy of the normal and excited states of the molecule plotted against some parameter *d* representing the configuration of the atoms of the molecule; for example, the distance between two of the atoms. A molecule originally in the state *A* absorbs, by the Franck-Condon principle, light having the quantum energy *AD*. The molecule then moves into the more stable state *C*, in which it cannot radiate.

Thermal agitation might cause the molecule to come into the state A, whence it could descend to A giving up its excess energy as heat, or, owing to the finite velocity of motion of the ions, it might ascend towards D and thus have a chance to radiate. The resulting band would however have its maximum at very large wave-lengths.

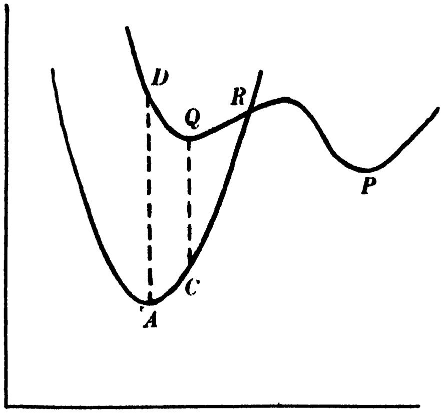

Figure 2.

The more complicated mechanism shown in figure 2 seems necessary in order to account for an emission band in the visible, the upper curve having two minima. After absorption the large amount of energy released takes the molecule to P, where it cannot radiate. If then thermal energy raises it to R, it will drop down to Q, where it will remain until it radiates a quantum of energy QC.

Mr J. Ewles gave an account of experiments on phosphorescence carried out at Leeds. These will be published in the *Proc. roy. Soc.**

---

* See also Ewles, *Proc. roy. Soc.* A, **129**, 509 (1931), *Proc. Leeds Phil. Soc.* **3**, 277 (1936).

SEMI-CONDUCTORS WITH PARTIALLY AND WITH COMPLETELY FILLED 3*d*-LATTICE BANDS

By J. H. DE BOER and E. J. W. VERWEY,
Natuurkundig Laboratorium der N. V. Philips' Gloeilampenfabrieken,
Eindhoven, Holland

ABSTRACT. Attention is drawn to a class of semi-conductors or insulators with incompletely filled 3*d* bands. Their lack of conductivity, if the number of electrons per atom is an integer, is explained by the circumstance that a moving electron will have a large probability of being withdrawn to the initial atom, if only the potential barriers to be penetrated are sufficiently high to reduce the frequency of transition below a certain limit. This inhibiting factor disappears, if for ions of equal electronic levels the number of electrons per atom differs from an integer. In the case of NiO this condition is fulfilled if an electron is brought by thermal excitation from the lattice 3*d* band into the somewhat raised and less occupied levels *a*, *a'* (figure 1); these levels belong to Ni ions adjacent to a vacant Ni lattice point introduced by the deviations from stoichiometry, and two of these Ni ions are at the absolute zero Ni^{3+} ions. An analogous conduction mechanism holds for non-stoichiometric Cu_2O, with a completely filled 3*d* band (figure 2).

Photoconductivity is generally observed with substances with completely filled zones and never with substances of the NiO type. A tentative explanation is given for this fact on the basis of the model of figure 1 and figure 2.

In non-stoechiometric ZnO vacant oxygen lattice points are assumed (figure 3); in that case the calculation of the lattice levels shows that at the lattice holes one Zn^{2+} is converted into Zn, whereas in the lattice the additional electrons form Zn^{+} ions, as will be the case after thermal transitions of the electrons belonging to these Zn atoms into the lattice 4*s* band.

§1. CLASSIFICATION OF SEMI-CONDUCTORS

According to the quantum theory of electronic states in solids, as developed by Sommerfeld, Bloch, Brillouin, Bethe and others(1, 2, 3), with the special aim of understanding the electrical properties of the metals, those substances will be electrical insulators for which the number of electrons is just sufficient to fill up a number of Brillouin zones completely, and the lowest unoccupied Brillouin zone is separated from the occupied zone with the highest energy by a sufficiently broad energy gap (forbidden region). For instance the following ionic compounds NaCl, MgO, AgCl, ZnO, TlCl all contain only ions with closed electronic groups or sub groups and thus only completely filled Brillouin zones, and they are known to be very poor conductors if they are pure and of stoichiometric composition. Though, according to quantum mechanics, all the electrons of a perfect lattice are more or less free to move through the lattice, the electronic states of a completely filled energy zone cannot give rise to electronic conduction, and unidirectional transport of electrons is only possible if a zone is incompletely filled, either because the number of electrons is incapable of filling up the zones completely, or because several zones overlap in the lattice, the electrons of one atomic level being thus distributed over more than one band or zone of lattice levels. On the basis of these conceptions Wilson(4) and Fowler(5) have developed a theory of semi-conductors. Wilson considers the case of two energy zones, one exactly full of electrons at absolute zero and a higher one entirely empty, separated by a narrow forbidden region. Accordingly at a higher temperature there will be a few electrons of the lower zone in the higher one, and necessarily a number of empty states in the lower zone. Both will give rise to electronic conduction, but predominantly the electrons in the higher zone, where the potential barriers are lower with respect to the electronic levels. Such semi-conductors, which owe their conductivity to thermal excitation of electrons from one energy zone into another higher one, were called *intrinsic* semi-conductors.

A substance belonging to the class of semi-conductors in which electronic conduction occurs predominantly according to the model of Wilson is probably Cu_2O of stoichiometric composition. In this compound the cuprous ion Cu^+ contains a closed $3d$ shell and an empty $4s$ shell.

Sometimes insulators of the type considered above can be converted into semi-conductors in two ways, either by small deviations from stoichiometric composition or by foreign impurities. Of these *extrinsic* semi-conductors only the first mentioned will be considered in the present discussion.

(*a*) There exists, however, a large class of semi-conductors of a quite different type, for which it has only been recognized incidentally that they must be treated in a way deviating fundamentally from the Wilson theory. Several substances contain atoms or ions with an odd number of electrons; then, in many cases, at any rate for substances with a simple lattice type (such as simple translation lattices, or lattices with a face centred or body centred unit cell), the amount of electrons is incapable of filling up a number of Brillouin zones completely and we have to deal with a partially occupied Brillouin zone. Nevertheless several substances, especially ionic compounds, of this type do not show a metallic conductivity, but belong to the class of semi-conductors or even insulators.

In the present paper we will restrict ourselves to compounds containing ions of the first long series of the periodic system. As examples may be mentioned MnO ($\log \rho = 8$), CoO ($\log \rho = 8$), Mn_3O_4 ($\log \rho = 7$), Fe_2O_3 ($\log \rho = 10$), CuO ($\log \rho = 7$), etc.* The electronic configurations of the cations involved can be read from table 1. This table, comprising elements which have the argon configuration $(1s)^2; (2s)^2 (2p)^6; (3s)^2 (3p)^6$ in common, shows the distribution of electrons between the $3d$ and $4s$ shells for a number of important atoms and ions from the part of the periodic system considered. These distributions can be derived in some cases from the spectroscopical data(6) concerning the ground state of the free atoms or ions (shown in bold-faced type) and the remainder can then be derived by interpolation or (and) by taking into account the paramagnetism of the ions in the corresponding salts(7). From table 1 it results that all ions present in stable chemical compounds in the transition region of the periodic system considered contain $3d$ electrons and no $4s$ electrons. As a consequence of this circumstance we infer that there is no great difference between substances like those mentioned above, containing odd

---

* The $\log_{10} \rho$ values (ρ = specific resistance in ohm-cm.) are only given as integers because of the inevitable uncertainty in these data; for our considerations only the order of magnitude is significant.

Table 1

Atomic number of atoms / Number of electrons in ion	18 $3d$ $4s$	19 $3d$ $4s$	20 $3d$ $4s$	21 $3d$ $4s$	22 $3d$ $4s$	23 $3d$ $4s$	24 $3d$ $4s$	25 $3d$ $4s$	26 $3d$ $4s$	27 $3d$ $4s$	28 $3d$ $4s$
18	Ar 0 0	K^+ 0 0	Ca^{2+} 0 0	Sc^{3+} 0 0	Ti^{4+} 0 0	V^{5+} 0 0					
19		K 0 1			Ti^{3+} 1 0	V^{4+} 1 0					
20			Ca 0 2		Ti^{2+} 2 0	V^{3+} 2 0					
21				Sc 1 2	Ti^+ (2) (1)	V^{2+} 3 0	Cr^{3+} 3 0	Mn^{4+} 3 0			
22					Ti 2 2	V^+ 4 0	Cr^{2+} 4 0	Mn^{3+} 4 0			
23						V 3 2	Cr^+ 5 0	Mn^{2+} 5 0	Fe^{3+} 5 0	Co^{4+} 5 0	
24							Cr 5 1	Mn^+ 5 1	Fe^{2+} 6 0	Co^{3+} 6 0	Ni^{4+} 6 0
25								Mn 5 2	Fe^+ 6 1	Co^{2+} 7 0	Ni^{3+} 7 0
26									Fe 6 2	Co^+ 8 0	Ni^{2+} 8 0
27										Co 7 2	Ni^+ 9 0
28											Ni 8 2

numbers of electrons, and for instance NiO, with even numbers of electrons, since the band of $3d$ levels contains five $3d$ zones and these $3d$ levels, coinciding in the free ions, presumably are not split up wholly into separate zones in the lattice, and all ions with an incompletely filled $3d$ group will therefore give rise to partially occupied energy bands in the lattice. Actually there is no great difference in the behaviour of CoO and NiO; for the latter also $\log \rho = 8$.

(*b*) Not all substances of the type considered are poor conductors. It is a well-known fact that both the conductivities of Cu_2O, CuJ, ZnO (with cations having a complete $3d$ shell, $3d^{10}$) and of CoO, NiO etc. (incomplete $3d$ shell) can be raised several powers of ten by small deviations from the stoichiometric composition(8, 9, 10, 11) and it has already been suggested by Wagner that this increased conductivity is connected with quasi-free electrons or electron holes owing to the presence of ions of higher or lower valency. A very interesting case is represented by Fe_3O_4 ($\log \rho = -2$), which has a conductivity of about ten powers of ten as high as Mn_3O_4, Co_3O_4, $\gamma\ Mn_2O_3$, $\gamma\ Fe_2O_3$.

In a previous publication we have shown that the cation arrangement in the lattice of Fe_3O_4 shows an "averaged structure" of a special type, viz. a statistical distribution of equal amounts of Fe^{2+} and Fe^{3+} ions about crystallographically identical lattice points(12, 13); in this respect it differs from Co_3O_4, $\gamma\ Fe_2O_3$, etc. with otherwise identical or closely related crystal structures (spinel type). From this we infer that favourable conditions for electronic conduction exist, if for a band of electronic states the number of electrons per atom (ion) differs from an integer, and this is also important in relation to the conductivity of non-stoichiometric compounds.

(*c*) A third point, which seems to be of some importance for a comprehension of the behaviour of the substances considered, is that only those substances (stoichiometric and non-stoichiometric) show photo-conductivity, which are derived from compounds with cations containing a complete 3*d* shell, viz. CuJ, Cu_2O, ZnO. This seems to be a general rule throughout the whole periodic system, since all substances reported to be photoconductors (halides of the alkali- and alkaline earth metals and of Ag^+, Cu^+, Tl^+, Hg^{2+}, Pb^{2+}; very many sulphides, e.g. Ag_2S, Sb_2S_3, HgS, Bi_2S_3, PbS, Ag_3SbS_3; oxides like BaO, Cu_2O, Ag_2O, CdO, Sb_2O_3) contain cations (and anions) with closed electronic groups or sub-groups. No photoconductivity has been observed, as far as we know, for substances like MnO, CoO, NiO, Co_3O_4, Mn_3O_4, Fe_2O_3 etc.; in this laboratory Mr H. H. Kraak has investigated certain of these compounds* by irradiation with a high pressure mercury discharge lamp and has been unable to establish any effect upon their conductivity.

From this discussion, then, a number of interesting points result, which can be summarized in the following three problems:

(1) Why are several of the oxides considered here semi-conductors or almost insulators, although they contain an incompletely occupied 3*d* band?

(2) Why do exceptionally favourable conditions for electronic conduction arise if the number of electrons per atom in this band is different from an integer?

(3) What is the reason why all these substances do not show photoconductivity, whereas those substances containing a completely filled 3*d* band are all photoconductors?

In the following sections we shall consider these substances from the point of view of their electronic bands and the relations between them.

§2. LATTICE DEFECTS

The nature of the lattice deviations involved in deviations from the stoechiometric composition and their significance for electronic conduction have been discussed in detail by Wagner(10). Also in our case we must consider beforehand what changes occur in the lattices of the substances investigated, if the composition is made different from stoichiometry. For our present purpose, we need not consider the small deviations from the perfect lattice, which are present in every real lattice owing to the thermal equilibrium corresponding to the previous thermal history(14).

---

* Namely NiO, NiO containing some oxygen in excess, Co_3O_4 and Mn_3O_4 as pressed bars.

Greenish NiO can be transformed by oxidation into black "NiO" and then contains a small amount of oxygen (e.g. 0·5 per cent) in excess. The extra oxygen may be located between the normal lattice ions (interlattice points), but owing to the small polarizability of the oxygen it is much more likely that the lattice contains vacant nickel lattice points, whereas the additional oxygen is located at normal lattice points. This view is substantiated by the work of Jette and Foote(15), who investigated the crystal structure of Wüstite ("FeO"). A phase of pure FeO is not stable under any conditions; for the Wüstite phase, if prepared at 1050°, they found solid solutions containing 76·7–76·1 per cent Fe, i.e. from $Fe_{0\cdot 94}O$ to $Fe_{0\cdot 91}O$. These phases contain vacant positions in their cation lattice; the latter phase for example contains therefore an averaged distribution of $\frac{8}{11}$ Fe^{2+}, $\frac{2}{11}$ Fe^{3+} and $\frac{1}{11}$ vacant lattice points per oxygen ion about the normal cation position.* Also pure NiO seems to be unstable(16), and identical relations may be expected here, though the deviations from stoichiometry are less than in the case of FeO.

For NiO with an oxygen excess we must therefore assume vacant points in the cation lattice. Such an assumption can also safely be made for the case of CuJ with a small excess of iodine, in view of the large radius of the J^- ion. For Cu_2O the same view has been advocated by Dünwald and Wagner(17). It has generally been assumed in these substances containing a metal deficit that the excess of negative charge originating from the excess of anions is neutralized at the cations, i.e. by the formation of cations of higher valency (Fe^{3+}, Ni^{3+}, Cu^{2+}); in the present cases this conception seems quite reasonable on the basis of chemical arguments, but the possibility that anions of a lower charge (eventually neutral atoms) are formed cannot be excluded *a priori*. Indeed, in KJ containing a small excess of iodine, no K^{2+} ions but J atoms are formed. This can easily be ascertained, however, for every case, by considering to what extent the various electronic levels are shifted in the lattices: the electrons will be removed from the *highest occupied* level. The results of such calculations are summarized in table 2. These calculations yield, of course, the positions that the levels would have, if they were not broadened by the lattice (in the following we denote these positions as "centres" of the bands). We also include the calculations of the electronic levels of ions adjacent to a vacant lattice point, for electrons must be removed as a consequence of the disappearance of a number of cations from the lattice and it is generally more favourable to remove these electrons from a cation that is adjacent to such a lattice hole. For the case of Cu_2O Schottky and Waibel(18) assumed therefore that Cu^{2+} ions are located directly adjacent to a vacant Cu^+ lattice position. For instance, for NiO (NaCl lattice type), where each vacant Ni point is surrounded by 12 nickel ions, we wish to consider the case that two of these nickel ions yield an electron and become Ni^{3+} ions, in order to counterbalance the absent Ni^{2+}. Neglecting polarization energies we see that such a Ni^{3+} is surrounded by a normal lattice minus one Ni^{2+} at a distance $r\sqrt{2}$ (r = shortest Ni-O distance) and plus one positive charge at $2r\sqrt{2}$ (in the most favourable state), hence the *Madelung* energy for one electron at the lattice point considered (Ni^{3+} ion

---

* Another possibility is that the Fe^{3+} seek different interstices, but presumably it can be excluded by the fact that no complete series of solid solutions with Fe_3O_4 exists.

Table 2

NiO			
Lattice type: NaCl,	$a = 4{\cdot}17$ A.	*Lattice:*	
Shortest distance Ni to O	$= 2{\cdot}09$ A.	*Madelung* energy (M)	= 24·2 V.
Distance Ni^{3+} to lattice hole	$= 2{\cdot}98$ A.	Level Ni^{2+} $3d = M - I_3$	= − 6 V.
Distance Ni^{3+} to Ni^{3+}	$= 5{\cdot}96$ A.	Level O^{2-} $2p = -M - E_2$	= − 14 V.
Madelung constant	= 1·748	*At lattice hole:*	
Third ionization energy Ni (I_3)	= *ca.* 30 V.	*Madelung* energy Ni^{2+} (M'_{Ni})	= 31·6 V.
Second electron affinity O (E_2)	= − 10 V.	*Madelung* energy O^{2-} (M'_O)*	= 13·8 V.
		Level Ni^{2+} $3d = M_{Ni}' - I_3$	= + 1 V.
		Level O^{2-} $2p = -M_O' - E_2$	= − 3·8 V.
CuJ			
Lattice type: cubic ZnS,	$a = 6{\cdot}05$ A.	*Lattice:*	
Shortest distance Cu^+ to J^-	$= \frac{1}{4}a\sqrt{3} = 2{\cdot}62$ A.	*Madelung* energy (M)	= 9·0 V.
Distance Cu^+ to lattice hole	$= \frac{1}{2}a\sqrt{2} = 4{\cdot}27$ A.	Level Cu $4s = M - I_1$	= + 1·2 V.
Madelung constant	= 1·639	Level Cu^+ $3d = M - I_2$	= − 11·2 V.
First ionization energy Cu (I_1)	= 7·8 V.	Level J^- $5p = -M - E$	= − 12·1 V.
Second ionization energy Cu (I_2)	= 20·2 V.	*At lattice hole:*	
Electron affinity J (E)	− 3·1 V.	*Madelung* energy Cu^+ (M'_{Cu})	= 12·4 V.
		Madelung energy J^- (M'_J)	= 3·5 V.
		Level Cu^+ $3d = M'_{Cu} - I_2$	= − 7·8 V.
		Level J^- $5p = -M'_J - E$	= − 6·6 V.
ZnO			
Lattice type: hexagonal ZnS,	$a = 3{\cdot}25$ A. $c = 5{\cdot}23$ A.	*Lattice:*	
Shortest distance Zn to O	$= 1{\cdot}98$ A.	*Madelung* energy (M)	= 23·9 V.
Distance Zn to Zn	$= 3{\cdot}25$ A.	Level Zn^+ $4s = M - I_2$	= 6·0 V.
Madelung constant	= 1·639	Level Zn $4s = 2M - I_1 - I_2$†	= 20·5 V.
First ionization energy Zn (I_1)	= 9·4 V.	Level $O^{2-} = -M - E$	= − 13·9 V.
Second ionization energy Zn (I_2)	= 17·9 V.	Lowest member	
		$O^{3-} > -13{\cdot}9 + \frac{2\epsilon^2\ddagger}{r_{O^{2-}}}$	= > 8 V.
		At lattice hole:	
		Madelung energy Zn^+ (M')§	= + 13·7 V.
		Madelung energy Zn (M'')	= + 9·3 V.
		Level Zn^+ $4s = M' - I_2$	= − 4·2 V.
		Level Zn $4s = 2M'' - I_1 - I_2$	= − 8·7 V.
KJ			
Lattice type: cubic NaCl,	$a = 7{\cdot}05$ A.	*Lattice:*	
Madelung constant	= 1·748	*Madelung* energy (M)	= 7·2 V.
Distance K to J	$= 3{\cdot}53$ A.	Level K^+: $M - I_2$	= − 24·5 V.
Distance K to K $= \frac{1}{2}a\sqrt{2}$	$= 4{\cdot}99$ A.	Level J^-: $-M - E$	= − 10·3 V.
Second ionization energy K (I_2)	= 31·7 V.	*Adjacent to failing* K^+	
		Madelung energy K^+ (M')	= 10·1 V.
		Level K^+ : $M' - I_2$	= − 21·6 V.
		Madelung energy J^- (M'')	= 3·1 V.
		Level J^- : $M'' - E$	= − 6·2 V.

* For two O ions adjacent to a vacant Ni^{2+} lattice point.

† For two electrons at one Zn^{2+} lattice ion.

‡ If an electron is added to O^{2-} there are no discrete levels; the lowest member of the continuum will be at least $2\epsilon^2/r_{O^{2-}} = 22$ V. higher ($r_{O^{2-}} = 1{\cdot}3$ A. − radius of O^{2}).

§ For two Zn^+ ions adjacent to a vacant oxygen lattice point.

adjacent to a vacant Ni^{3+} point) amounts to (*A* = *Madelung* constant):

$$\frac{2A\epsilon^2}{r}+\frac{2\epsilon^2}{r\sqrt{2}}-\frac{\epsilon^2}{2r\sqrt{2}}=24{\cdot}2+9{\cdot}8-2{\cdot}4=31{\cdot}6 \text{ volts}$$

The electronic level of these ions is therefore raised 7·4 volts with respect to normal lattice ions, or rather considerably less owing to several polarization effects. The other data are calculated in a similar way.

In the case of ZnO the deviation from stoichiometry causing electronic conductivity is an excess of Zn. In the analogous case of BaO it has been shown that the red BaO containing an excess of about 1 per cent Ba has a density of about 0·5 per cent less than that of normal BaO(19). We will therefore assume in BaO and similar substances that the excess of metal is present at normal lattice points, whereas a number of oxygen lattice points is vacant, though, for the case of ZnO, the possibility cannot wholly be excluded that Zn takes interlattice points, since Zn is more polarizable than Ba, and ZnO has a different lattice type. In the case of ZnO extra electrons must be introduced and we must therefore consider the *lowest unoccupied* level in the lattice and at lattice holes. From table 2 we make the following inferences.

For NiO with oxygen excess: both in the normal lattices as well as at lattice holes the removal of electrons leads to Ni^{3+} ions and never to O^{-} ions.

For CuJ with iodine excess: in the normal lattice Cu^{2+} are formed; adjacent to vacant Cu^{+} lattice points the highest occupied level seems to be J^{-} and therefore J atoms are formed; the latter conclusion is somewhat uncertain owing to the high polarizabilities of the ions involved.

For ZnO with metal excess, assuming vacant oxygen lattice points: adjacent to an absent O^{2-} ion the lowest unoccupied level is that for a Zn atom. In the regular lattice, however, an excess of electrons yields a more uniform distribution of the electrons and leads to Zn^{+} ions. The formation of O^{3-} can be excluded.

For KJ with iodine excess: the electrons are always removed from J^{-} ions.

§3. MECHANISM OF CONDUCTION

We now proceed to a consideration of the mechanism of electronic conduction. The theory of electronic states in metals has been developed on the basis of the assumption that the interaction of the electrons and ions of the lattice can be approached by treating each electron as moving in the field of the ions and the average field of all other electrons. This method of approach implies that all atoms (ions) of a definite kind contain an equal number of electrons, or, since electron movement must necessarily alter the number of electrons of an atom temporarily, that local charge differences are neutralized by other electrons within a short time; in other words that the electrons are free to such an extent that they can still be considered as *not* belonging to definite atoms. If the potential barrier between the atoms (ions) of one kind is increased the probability of interchange of electrons decreases rapidly and the time lag mentioned above increases. Thus, for somewhat higher potential barriers the state of affairs is finally fundamentally different in metallic conduction. There is a certain probability that an electron leaks through a potential barrier to a neighbouring atom, say from one Ni^{2+} to another Ni^{2+} in pure NiO. The immediate result is that in a row of Ni^{2+} ions two adjacent Ni^{2+} ions are changed into Ni^{+} and Ni^{3+}. If the excess of positive charge at the Ni^{3+} ions is not sufficiently rapidly neutralized by other electrons the probability is high that the electron at the Ni^{+} ions does not travel further into the lattice, but moves back, even against the force resulting from the applied electrical field, to the original atom. The theoretical treatment of the electronic movement will obviously be quite different from that in the theory of metals and must consist of a discussion of the probability of the existence and prevalence of such charge disturbances and the chance of propagating the electrons from them to other similar disturbances. In default of such a treatment we may provisionally infer that the nature of such an electronic conduction mechanism probably implies that in a certain region the conductivity will be highly sensitive to the height of the potential barriers. Substances with partially filled energy zones will therefore, according to this qualitative picture, generally be either metals or poor conductors, whereas intermediate cases will probably be rare. Substances of the latter intermediate type, i.e. semi-conductors with appreciable conductivity, will, however, be rather interesting, since one might expect their conductivities to be very sensitive to changes in the lattice spacings and thus to the situation of the bands with respect to the potential barriers, and therefore, not only to temperature, but also to external pressure, formation of solid solutions etc.

The existence of semi-conductors or insulators with partially filled energy zones, could not, indeed, be properly understood from the viewpoint of the present theory of electronic states for metals(20, 21). A peculiar difficulty was also offered by a substance like Fe_3O_4, for according to these views one could not immediately explain why a substance with a partially filled $3d$ band containing $5\frac{1}{2}$ electrons per Fe atom should conduct 10^{11} times as well as a substance of the same lattice type and practically identical lattice dimensions with a partially filled $3d$ band containing 5 electrons per Fe atom (γ Fe_2O_3). Similar arguments hold for the non-stoichiometric compounds. For these substances the Wilson model for extrinsic semi-conductors(4), eventually the modified model of de Boer and van Geel(22), cannot be applied. According to this theory, semiconduction has been explained by discrete impurity levels; if energy is taken up from the thermal movement, electron transitions are assumed to occur from these levels to a normally completely empty band, or from a completely filled band to empty impurity levels. In the cases under consideration, however, this mechanism cannot help us, since the energy band ($3d$) is partially filled with electrons in the stoichiometric compounds as well as in the non-stoichiometric ones; and it cannot explain the considerable increase in the conductivity if the substance no longer contains a whole number of electrons per ion.

Our consideration given above showing that substances with partially filled energy bands must actually be expected to be poor conductors, if only the potential barriers are sufficiently high to reduce the frequency of interchange below a certain limit, which, for instance, can be of the order of the inverse of the duration of an "excited lattice state" (in our example $Ni^+ - Ni^{3+}$), explains immediately the effect of a non-integral number of electrons per atom in a band, or, in other words, of an average structure of a cation lattice with unequally charged ions (or in part atoms) of the same element. If, for instance, in Fe_3O_4 an electron moves from a Fe^{2+} ion to a Fe^{3+} ion at an equivalent lattice point, the initial ion is transformed into Fe^{3+} and the accepting ion into Fe^{2+}. As a consequence of this reaction (indicated according to Wagner by $Fe^{2+} + Fe^{3+} \rightarrow Fe^{3+} + Fe^{2+}$), if only it occurs simultaneously at severa points in the lattice, no fundamental change in the statistical distribution of Fe^{2+} and Fe^{3+} has occurred. The essential difference from the foregoing case is that the electronic movement does not automatically imply the appearance of a charge disturbance inhibiting further electronic transport. In a perfect Fe_3O_4 crystal the chain of electronic interchanges is only broken down at the surface of the crystals. Since after each electronic transition the energy state of the lattice is not altered (except for minor effects), the amount of energy necessary for each electron transition is very small. Such a lattice with a statistical distribution of unequally charged homonymous ions shows therefore a high conductivity and a low temperature coefficient.

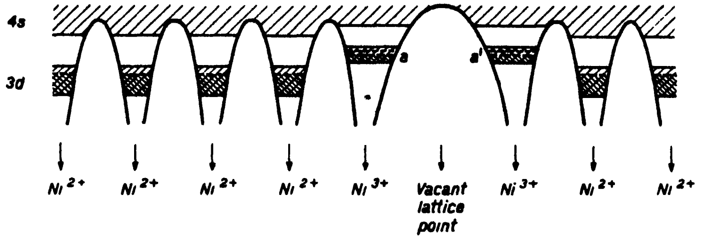

Figure 1. Schematic representation of the 3*d* and 4*s* band in a substance like NiO, containing a small amount of oxygen in excess. Section through a row of Ni^{2+} ions (110 direction) with one absent cation.

Let us now consider the periodic potential field along a row of cations (in a face-centred lattice, therefore a (110) direction) in a substance with a partially filled 3*d* band like NiO, disturbed at one point by the absence of one cation (figure 1).* At absolute zero two of the only slightly broadened levels of the Ni ions adjacent to the lattice hole (in the three-dimensional lattice there are 12 such ions), *a* and *a'*, contain one electron less than the normal lattice ions. The partially filled 3*d* band of the normal lattice ions does not give rise to any appreciable conduction owing to the effect of the potential barriers, as considered above. Electronic interchange takes place easily only between the 12 cations adjacent to the lattice hole sharing 10 electrons, but this does not lead to any transport of electricity in an electric field. The 4*s* band especially is strongly broadened by the lattice, but the bands are still separated by a considerable forbidden energy region. Actually pure NiO does not absorb strongly in the region of visible light; its colour is a light yellowish green.

---

* Strictly speaking also the second nearest neighbours, etc. of a lattice hole have slightly raised levels, and also the potential barriers are slightly changed. The schematic picture of figures 1–3, however, is sufficient for our purpose.

The forbidden region can therefore be estimated to be somewhat less than 3 volts, Upon introduction of a small excess of oxygen, however, the colour turns into black, which is probably connected with transitions from the raised levels *a*, *a′* into the empty 4*s* zone of the lattice. The introduction of an excess of oxygen, i.e. of a number of levels *a*, *a′* (being partially Ni^{3+} ions, namely $\frac{1}{6}$ of them), simultaneously increases the conductivity, of which the mechanism can now be understood in the following way. If the temperature is above absolute zero there is a certain probability that a normal lattice Ni^{2+} ion gives off its electron to one of the Ni^{3+} ions adjacent to the lattice hole, for which transition an amount of energy must be supplied from the thermal movements in order to bring the electron into the higher levels *a*, *a′*. The result is that a row of normal lattice ions contains a Ni^{3+} ion of the same energy level as the Ni^{2+} ions, and conditions as considered for the case of Fe_3O_4 are created. Hence a chain of transitions $Ni^{2+} + Ni^{3+} \rightarrow Ni^{3+} + Ni^{2+}$ sets in, which, in the presence of an electric field, leads to electronic conduction. If during such a chain of transitions the electronic deficit propagated through the lattice meets a lattice hole, i.e. when a Ni^{2+} ion in the neighbourhood of such a hole is converted into a Ni^{3+}, there is a large probability that an electron of a level *a* (*a′*) falls back to this ion, and the chain of transitions is broken down; every new chain must start again with a jump of an electron to a non-occupied level of a Ni^{3+} ion adjacent to a lattice hole. In this way an equilibrium is established, and the total number of Ni^{3+} ions at normal lattice points, and therefore the conductivity, depends on the temperature according to a Boltzmann partition law.

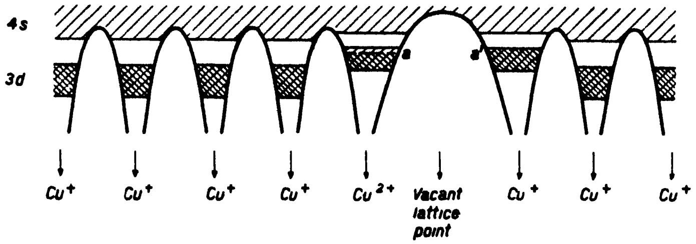

Figure 2. Schematic representation of the 3*d* and 4*s* band in a substance like Cu_2O, containing a small amount of oxygen in excess. Section through a row of Cu^{+} ions with one absent cation.

In the case of Cu_2O or CuJ the picture is somewhat different owing to the fact that here the band of 3*d* electrons is completely occupied. Figure 2 shows again the case of a row of Cu^{+} ions and one absent cation. In this case one of the cations directly surrounding the lattice hole (in figure 2 there are only two, again represented by somewhat raised levels *a* and *a′*) contains one electron less (Cu^{2+} ion). The red colour of Cu_2O indicates that the Cu^{+} 3*s* and the Cu 4*s* zone are separated by a forbidden zone of about 2 volts (the spectral photoelectric region, according to this transition, lies at about 630 mμ. corresponding to about 2 volts); the "centre" of the latter lies 12·4 volts higher than that of the former (§ 2, table 2). At absolute zero no conduction is possible, since the 3*d* band is completely occupied and the 4*s* zone is entirely empty. At higher temperature three conductivity mechanisms are possible:

(1) Electron transitions from $3d$ into $4s$.

(2) Electron transitions from levels a, a' etc. into the $4s$ zone.

(3) Electron transitions from the $3d$ band into the level a.

(1) leads to electronic movement of an electron in $4s$ and of an electron hole in $3d$, the former predominating; (2) leads only to the former, whereas electron transitions (3) imply defect conductivity in $3d$. According to measurements(18) of the Hall constant and measurements of the thermo-e.m.f.(17) of Cu_2O containing a small excess of oxygen this substance shows defect conductivity and therefore obviously the third mechanism prevails. If, however, the Cu_2O is heated in a high vacuum, the substance thus obtained, which will be now close to the stoichiometric composition, is still an electron hole conductor at lower temperatures, but above 500° it shows a negative Hall constant. Obviously the number of Cu^{2+} ions at levels a etc. is so small now that at higher temperatures mechanisms (1) and (2), owing to their larger temperature coefficient, will finally predominate over (3), whereas at lower temperatures the activation energy of (1) and (2) are too high to yield an important conductivity. It should be pointed out that the number of lattice holes of the type of figure 2 will be larger than the number of Cu^{2+} ions at such lattice holes, owing to thermal lattice deviations at the temperature at which the crystal was formed (Schottky-Fehlstellen); all such levels at lattice holes can contribute to mechanism (2), whereas only an unoccupied level a can contribute to mechanism (3). In pure Cu_2O all copper ions are Cu^+ ions and therefore only (1) and (2) should be possible.

With increasing amount of excess oxygen ions the mutual influence of the various lattice holes and of the ions with higher charge lowers the levels a, a' etc. Owing to the statistical distribution of these lattice holes and higher charged ions the levels do not have the same height throughout, but as a whole they are all lowered more or less, since with increasing number of such vacant lattice points the direct environment of ions adjacent to the hole becomes increasingly more symmetrical and their average height above the $3d$ band is therefore lowered continually. The lowest levels give the largest contributions to mechanism (3). Actually we find that the activation energy as derived from the temperature coefficient of the conductivity of Cu_2O decreases from 0·72 volts to 0·13 volts with increasing oxygen content(23). In the case of CuJ(24) a sufficient excess of iodine (corresponding to $Cu_{0\cdot995}J$) leads to a negative temperature coefficient, indicating that in that case the lowest levels a, a' etc. do not rise any more above the highest members of the lattice $3d$ band.

Photoconductivity occurs with Cu_2O and CuJ, not with NiO (independently of deviations from stoichiometry). With the aid of the models given above we may make the tentative hypothesis that photoconductivity, for equal relative positions of the bands with respect to the potential barriers, will be much greater in the case of figure 2 than of figure 1. This can be seen in the following way. Transitions from the lattice $3d$ band into the levels a, a' etc. need not be considered, since as optical transitions they are not allowed. Transitions (1) and (2) are permitted; both transitions can be deduced from the spectral distribution of photoconductivity in the case of Cu_2O with an excess of oxygen, a normal band with a maximum of 630 mμ. and a band connected with the oxygen excess at about 1700 mμ.(25). In the case of a substance with a completely filled $3d$ band a photoelectrically released electron, moving through the lattice under the influence of an applied field, for instance from a Cu^+ ion adjacent to a vacant lattice point, can only fall back to a lower level when it encounters an electronic hole. In the case of NiO, however, the wandering electron can fall back at any time to the $3d$ band, since sufficient empty electronic states are available. Also in this $3d$ band the additional electron can travel further through the lattice, until it reaches an electronic hole (Ni^{3+} ion), but in this band its mobility is considerably smaller than in the $4s$ band, owing to the higher potential barriers to be penetrated; hence only the electrons in the $4s$ band should make a practical contribution to the photoconduction. As a consequence of the much smaller average path length the photoconductivity in NiO will then be correspondingly smaller for otherwise equal conditions.

Another possibility, explaining the photoconductivity of these substances with completely filled bands, which cannot wholly be excluded, is suggested by our remark in § 2 that in CuJ the electron deficit at the lattice holes is perhaps not present at the copper ions (producing Cu^{2+}), but at the J^- ions (thus converted into J atoms). If the latter corresponds to the actual state of affairs for CuJ, the transition of an electron from the Cu^+ $3d$ band into the $5p$ level of those J atoms takes the place of transition (3), and this is permitted as an optical transition. In that case photoconduction can be explained as conduction in the Cu^+ $3d$ band as a consequence of optically released electrons according to the (modified) transition (3). This might be the mechanism for all these substances, if it could be proved to be a general rule that with cations with a complete electronic group or subgroup the electron deficit at the lattice holes is preferably located at the anions. For this a more careful calculation of the electronic levels, which must be reserved to the future, would be necessary.

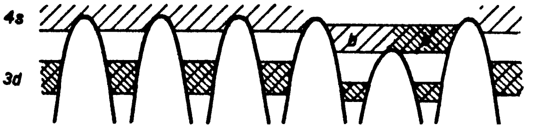

Figure 3. Schematic representation of the $3d$ and $4s$ band in a substance like ZnO, containing a small amount of Zn in excess. Section through a row of Zn^{2+} ions touching a lattice hole due to an absent oxygen ion.

For sake of completeness we also give, figure 3, the situation of the levels for ZnO containing a small amount of metal in excess, on the assumption of vacant oxygen lattice points. Electronic conduction occurs after thermal excitation of an electron from the occupied $4s$ level b' (Zn atom adjacent to a vacant oxygen lattice point) into the $4s$ band, converting a normal lattice ion into Zn^+. Photoconductivity can occur by excitation from $3d$ either into a level b, b' etc. or into the normal $4s$ band.

Finally it should be pointed out that several features of these semiconductors could be understood with the aid of a model using Smekal's structure-sensitive lattice flaws(26). The above picture, however, enables a more complete description of the phenomena and seems preferable in the light of recent results on lattices with vacant lattice points(27, 28) and on the nature of thermal lattice deviations by Wagner and Schottky.*

REFERENCES

(1) Sommerfeld, A. and Bethe, H. *Handbuch der Physik*, **24** (2), 2. Auflage, 368 (1933).
(2) Brillouin, L. Die Quantenstatistik (1931). Berlin: Julius Springer Verlag.
(3) Mott, N. F. and Jones, H. *Theory of the Properties of Metals and Alloys* (1936). Oxford: Clarendon Press.
(4) Wilson, A. H. *Proc. roy. Soc.* A, **133**, 458 (1931); **134**, 277 (1931).
(5) Fowler, R. H. *Proc. roy. Soc.* A, **140**, 505 (1933); **141**, 56 (1933).
(6) Bacher, R. F. and Goudsmit, S. *Atomic Energy States* (1932). McGraw Hill.
(7) Gorter, C. J. Paramagnetische Salze (Diss.). *Arch. Mus. Teyler*, **7**, 183 (1932).
(8) Le Blanc, M. and Sachse, H. *Phys. Z.* **32**, 887 (1931).
(9) Gudden, B. *Ergebn. exakt. Naturw.* **13**, 223 (1934).
(10) Wagner, C. *Z. phys. Chem.* B, **22**, 181 (1933).
(11) Wagner, C. *Phys. Z.* **36**, 721 (1935).
(12) Verwey, E. J. W. and de Boer, J. H. *Rec. Trav. chim. Pays-Bas*, **55**, 531 (1936).
(13) Wagner, C. and Koch, E. *Z. phys. Chem.* B, **32**, 439 (1936).
(14) Schottky, W. *Z. phys. Chem.* B, **29**, 335 (1935).
(15) Jette, E. R. and Foote, F. *J. Chem. Phys.* **1**, 29 (1933).
(16) Klemm, W. and Hass, K. *Z. anorg. Chem.* **219**, 82 (1934).
(17) Dünwald, H. and Wagner, C. *Z. phys. Chem.* B, **22**, 212 (1933).
(18) Schottky, W. and Waibel, F. *Phys. Z.* **36**, 912 (1935).
(19) Schriel, M. *Z. anorg. Chem.* **231**, 313 (1937).
(20) v. Baumbach, H. H., Dünwald, H. and Wagner, C. *Z. phys. Chem.* B, **22**, 226 (1935).
(21) Hund, F. *Phys. Z.* **36**, 728 (1935).
(22) de Boer, J. H. and van Geel, W. Ch. *Physica*, 's Grav., **2**, 286 (1935).
(23) Jusé, W. P. and Kurtschatow, B. W. *Phys. Z. Sowjet*, **2**, 453 (1932).
(24) Bädeker, K. *Ann. Phys.*, Lpz., **29**, 566 (1909).
(25) de Boer, J. H. *Electron Emission and Adsorption Phenomena*, p. 317 (1935). Camb. Univ. Press.
(26) de Boer, J. H. *Chem. Weekbl.* **32**, 106 (1935).
(27) Hägg, G. *Z. Krystallogr.* **91**, 114 (1935).
(28) Verwey, E. J. W. *J. chem. Phys.* **3**, 592 (1935).
(29) de Boer, J. H. *Rec. Trav. chim. Pays-Bas*, **56**, 301 (1937).

---

* A similar treatment of the colour centres in the alkali halides has been given by de Boer(29).

DISCUSSION OF THE PAPER BY DE BOER AND VERWEY

Reported by N. F. MOTT

with the help of some notes from

R. PEIERLS

Considerable surprise was expressed by several speakers that in crystals such as NiO in which the *d*-bands of the metal atoms were incomplete, the potential barriers between the atoms should be high enough to reduce the conductivity by such an enormous factor as 10^{10}. Mr Wilson pointed out that in that case it would hardly be correct to speak of bands at all, but one should think of sharp energy levels, as in the 4*f* shells of salts of the rare earths. This did not seem likely in view of the relatively small distance between nickel lattice points (2·9 A. compared with 2·5 A. for metallic Ni). Prof. Mott stated that in metallic nickel it is known, from experimental data on the specific heat at low temperatures, that the breadth of the *d*-band is quite large, of the order 1 eV.

Prof. Peierls agreed with Dr de Boer that the existence of semi-conductors with incomplete *d*-bands could not be understood merely by considering the low transparency of the potential barrier. This transparency could be perhaps 10^{-2} or 10^{-3} less than for ordinary metal but not 10^{-10}. He suggested that a rather drastic modification of the present electron theory of metals would be necessary in order to take these facts into account. The solution of the problem would probably be as follows: if the transparency of the potential barriers is low, it is quite possible that the electrostatic interaction between the electrons prevents them from moving at all. At low temperatures the majority of the electrons are in their proper places in the ions. The minority which have happened to cross the potential barrier find therefore all the other atoms occupied, and in order to get through the lattice have to spend a long time in ions already occupied by other electrons. This needs a considerable addition of energy and so is extremely improbable at low temperatures.

It appears, therefore, that if the transparency is at all small, the electrostatic interaction would reduce the conductivity still further and thus that at low temperatures the conductivity is proportional to a high power of the initial transparency. No mathematical development of these ideas has however yet been given.

Prof. Peierls made some further remarks about semi-conductors containing impurities. Suppose the impurity is capable of giving off an electron; it is then not sufficient to remove the electron into one of the adjoining lattice ions, in order to make it free for electronic conduction. This is because the impurity is then left in an ionized state and will attract the electron, which therefore moves in the periodic field of the lattice with a Coulomb field superimposed. It is known that in such a field the electron is capable of discrete bound states of negative energy (as in the field of a positive ion). Only if the energy of the electron is still further increased so that it can overcome this attraction and move right away from the impurity centre will it become a conduction electron in the proper sense. This suggests that, even if, as might conceivably happen, an electron would *gain* energy in moving from the impurity atom to an adjacent lattice ion, nevertheless the lowest state of the electron would *always* be a bound state in the neighbourhood of the impurity centre, in which it, so to speak, revolves round the centre, even though it is not definitely attached. Hence a finite activation energy should always be necessary to produce conduction electrons. This conclusion no longer holds when the number of impurity centres becomes large* because then the electron need not overcome the attraction of its "home" centre completely; already at a small distance from it, it will come under the simultaneous attraction of other centres and will thus be released.

From these arguments one may draw the conclusion that one should never find a substance in which a *small* concentration of impurity can produce a conductivity *without* activation energy.

It may be possible to explain on these lines the dependence of activation energy on concentration shown by most semi-conductors.

Similarly it should be true that pure substances of stoichiometric composition should never show a very small number of conduction electrons with zero activation energy. In this connexion it is perhaps significant that one metal with a very small number of conduction electrons, bismuth, shows a correspondingly small effective electron mass. A small mass means a large radius of the orbit and hence the minimum distance at which the centres will interact is correspondingly increased.

Prof. Pohl called the attention of the conference to the behaviour of AgBr, which at room temperature shows electrolytic conductivity, but which is normally an insulator at low temperatures. If it is irradiated with 10^{12} quanta per $cm.^3$ it shows electronic conductivity like a semi-conductor. The state is destroyed by high temperatures and high fields.

---

* I.e. comparable with number of atoms in the lattice.

PART II

CONDUCTION IN ALLOYS

RESISTANCE OF ALLOYS WITH DISORDERED AND ORDERED ARRANGEMENT OF ATOMS

By G. BORELIUS (Stockholm)

§ 1. RESISTANCE CONCENTRATION DIAGRAMS

The general features of the resistance of alloys in the simplest cases is illustrated by the behaviour of the series of binary alloys of gold with silver, copper and platinum shown in figure 1. The simple bent curves in the {resistance, concentration} diagrams, as we now know, belong to homogeneous alloys with a disordered arrangement of the atoms at the lattice points. In the systems Au-Ag this type of curve is obtained whatever the rate of cooling. In the systems Au-Cu and Au-Pt the homogeneous disordered state is stable only at high temperatures and can be preserved at room temperature only by quenching. With slow cooling, ordered states appear in the Au-Cu system with maxima of order and sharp minima of resistance at simple values of the concentration (Cu_3Au and CuAu). In the Au-Pt system the solubility is limited at temperatures below 1150° C., and the resistance curves obtained after quenching from different temperatures are approximately straight lines in the region where two phases co-exist.

Ordered arrangement of atoms (superlattices), and the presence of more than one phase, are thus often very well marked in resistance diagrams. In earlier days most metallographers had very little confidence in resistance measurements as a method in metallography. As the laws of resistance of alloys are now better known, and particularly owing to the increased significance of superlattice formation and segregation processes, the resistance measurements have nowadays an importance in metallography comparable with investigations by microscopes, X rays and thermal analysis. Whereas resistance measurements in recent years have been used by Grube$^{(4)}$ and others for extensive investigations of various complicated systems of alloys, our measurements have been mainly directed to the study of the resistance and the phenomena influencing the resistance from a physical point of view, and we have in the first place sought out the simplest systems showing the various phenomena.

In the following, §§ 2 and 3 will deal with measurements of disordered homogeneous alloys, §§ 4 to 9 with superlattices, and § 10 with the segregation process.

§ 2. RESISTANCE OF DILUTE SOLID SOLUTIONS OF *b* METALS IN COPPER, SILVER AND GOLD

The shape of the {resistance, concentration} curves of homogeneous alloys without superlattices is above all influenced by the slopes at the sides near the pure metals. It is usual to characterize this slope by the increase ζ in the resistance caused by the addition of one atomic per cent to the pure metal.

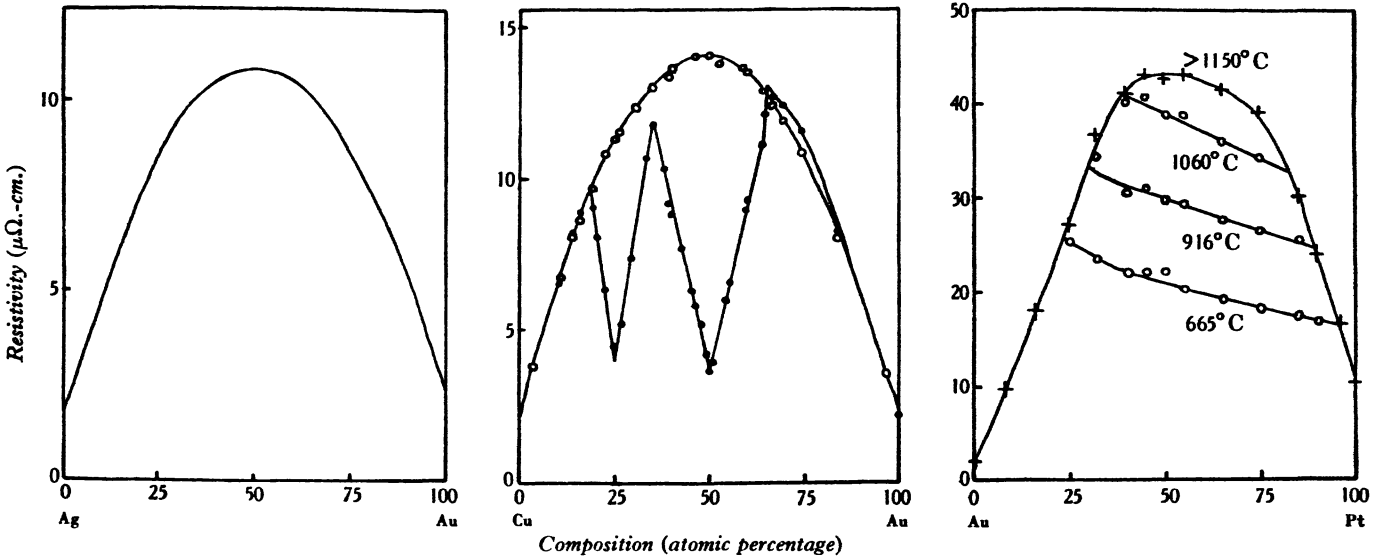

(a) (b) (c)

Figure 1. {Resistance, concentration} diagrams for room-temperature. (*a*) Silver-gold alloys according to measurements of Matthiessen(1). (*b*) Copper-gold alloys according to Johansson and Linde(2). (*c*) Gold-platinum alloys according to Johansson and Linde(3).

It was first pointed out by Benedicks(5) in a paper published in the Swedish language that the additional resistance often increases with the distance in the periodic system between the dissolved metal and the solvent. Better known is the work of Norbury(6), who found the horizontal distance in the long-periodic system to be of decisive importance.

Linde(7) has made a very extensive investigation of the increase in resistance of the metals Cu, Ag and Au of the 11th group of the periodic system due to the addition of various metals. The results are especially simple in the case of addition of *b* metals, that is metals from the groups 12 to 15. Figure 2 shows his results from published and unpublished measurements. The square of the difference of group numbers of dissolved metal and solvent is taken as abscissa in these diagrams. The metals of each period give nearly a straight line.

Linde(7) has also pointed out another interesting feature of these additional resistances. They are nearly the same if a certain *b* metal is added to Au or Ag; but on an average only 80 per cent of these values if the same metal is added to Cu. He relates this observation to the fact that the atomic volumes of Au and Ag are 10·3 and 10·2 respectively, whereas the atomic volume of Cu is only 7·1. From this he became interested in the influence of compression on the additional resistance ζ, and he has during recent years obtained a great number of measurements on this subject which are not yet published. The change of resistance of the dilute alloys, measured at pressures up to 3000 kgf./cm.^{2}, is first corrected for the change of volume so as to give the change of specific resistance ρ. Figure 3 shows these changes reduced to 1 kgf./cm.^{2} for some systems as a function of concentration. The effect of pressure $d\rho/dp$ always gets more negative by addition of *b* metals. This decrease of $d\rho/dp$ for one atomic per cent, divided by the additional resistance ζ per cent, i.e. the quantity $\zeta^{-1}\,d\zeta/dp$, may be looked upon as a pressure coefficient of the additional resistance. As appears from table 1, this quantity is of the same magnitude as the compressibility $V^{-1}\,dV/dp$, as would be expected if the additional resistance contained the atomic volume V as a power not too far from the first as a factor.

Table 1. Pressure coefficients of additional resistance ζ for one atomic per cent of *b* metals in Cu, Ag and Au compared with the coefficient of compressibility of the pure metals. Unpublished measurements by Linde

	Added metals	Copper	Silver	Gold
$\frac{1}{V}\frac{dV}{dp}\cdot 10^6$	—	−0·72	−0·99	−0·58
$\frac{1}{\zeta}\frac{d\zeta}{dp}\cdot 10^6$	Al	−0·4	—	—
	Ga	—	−1·18	−0·68
	Ge	−0·60	—	—
	Sn	−0·66	—	—
	As	−0·45	−0·33	—
	Sb	−0·60	—	—

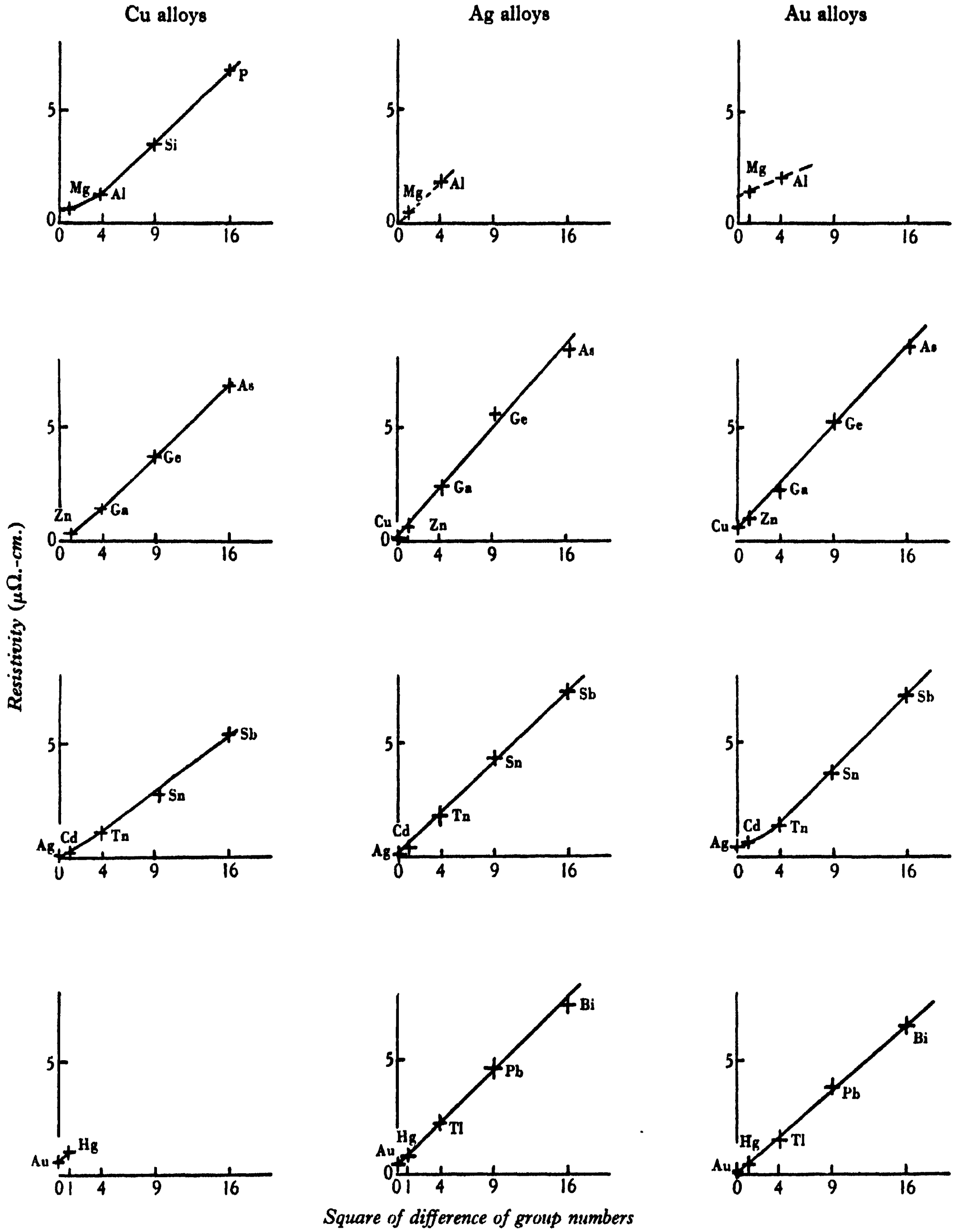

Figure 2. Increase in resistance for 1 atomic per cent of various *b* metals added to copper, silver and gold. (Measurements by Linde.)

For this group of alloys the rule of Matthiessen is also approximately valid. This rule predicts that if the specific resistance ρ of an alloy is written

$$\rho = \rho_0 + \rho_T \qquad \text{......(1),}$$

where ρ_0 is the resistance at the absolute zero and ρ_T thus the thermal electric resistance, the addition of foreign atoms to a pure metal increases ρ_0 but has very little influence on ρ_T. In fact Linde has found $d\rho/dT$ to increase slowly with increasing ρ for the dilute alloys of copper, silver and gold with the *b* metals.

The disordered homogeneous alloys of Cu, Ag and Au with each other and with the other *b* metals thus are especially simple in their electric behaviour and have been the first object for theoretical treatment. In the classical electron theory, insuperable difficulties arose already in connexion with the Matthiessen rule. In the general expression for the specific resistance

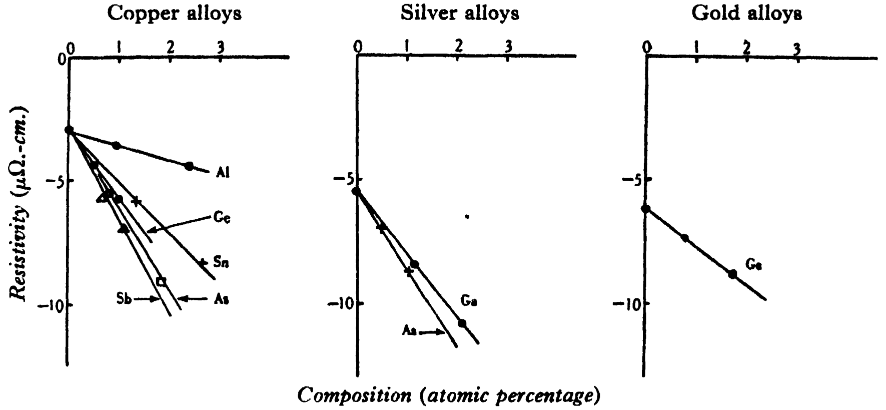

Figure 3. Change of specific resistance for 1 kgf./cm² due to the addition of *b* metals to copper, silver and gold. (Unpublished measurements by Linde.)

$$\rho = \frac{2m}{e^2}\frac{v}{nl} \qquad \text{......(2),}$$

where *m* and *e* denote mass and charge of an electron, the mean velocity *v* was found to be proportional to the square root of the absolute temperature *T*, and the variation of the number *n* of electrons per cm³ and their mean free path *l* could not possibly be accounted for in such a way as to give the Matthiessen formula. The modern theory assumes *v* to be large and, to a first approximation, independent of temperature; and the variations of ρ with temperature are mainly due to the variations of *l*. Now $1/l$ is a measure of the scattering of the conducting electrons, and this scattering is a sum of one part, due to thermal agitation, and one due to the disordered arrangement of the foreign atoms.* The scattering of the conducting electrons was first

* It might be worth mentioning that this general description of the Matthiessen rule was already given by Hojendahl⁽⁸⁾ some years before the appearance of the Sommerfeld theory on the basis of ideas put forward long ago by Wien⁽⁹⁾. Though the theory of Hojendahl is now superceded, it should be remembered for its good services in those years when the problems concerning superlattices were first approached. When the Sommerfeld theory appeared⁽¹⁰⁾ it was at once evident and pointed out⁽¹¹⁾ that this theory was of the general type which could explain the main features of conduction in alloys.

discussed by Bloch(12), who showed that there should be no scattering in a perfect periodic lattice, and the scattering in alloys has been discussed from the standpoint of wave mechanics especially by Nordheim(13) and Mott(14, 15). Mott has managed to give an explanation of the variations of the additional resistance with the group number of the dissolved metal by taking into account the scattering power of the extra field due to the charges of the foreign atoms, those charges being proportional to the differences of the group numbers of the dissolved metal and the solvent.

The pressure dependence of the resistance of dilute alloys has been treated theoretically by Lenssen and Michels(16) and Mott(17). Their results, however, do not seem to be in direct agreement with the experimental results of Linde. A re-examination of the assumptions underlying the calculations, with the guidance of the empirical results, might therefore be of interest.

§ 3. RESISTANCE OF SOLID SOLUTIONS OF TRANSITION METALS IN COPPER, SILVER AND GOLD

As shown definitely by the measurements of Linde, the simple rules valid for the alloys of the monovalent metals Cu, Ag and Au with the *b* metals cannot be extended to their alloys with the *a* metals (or transition elements). As an illustration of Linde's results, figure 4 gives the specific resistance ρ at 0° C., the dependence on temperature $d\rho/dT$, and the pressure dependence $d\rho/dp$ for alloys of Au with the transition metals of the first long period plotted against the atomic concentration. We see from figure 4*a* that the increase in resistance for one atomic per cent does not follow the order of the atomic numbers (Ni, Co, Fe, Mn, Cr, Ti); from figure 4*b* we see that the Matthiessen rule which predicts that $d\rho/dT$ should increase slowly with concentration does not hold for these alloys; and from figure 4*c* that the pressure coefficient is of variable size and in most cases positive (it was negative for the alloys with the *b* elements). For Co, Mn and Cr, $(d\zeta/dp)/\zeta$ has the values $-0{\cdot}2$, $+1{\cdot}3$ and $+1{\cdot}1 \times 10^{-6}$ respectively.

In fact, the transition metals influence the resistance of the monovalent metals in a rather individual and varying way, and these variations are of great practical importance in discovering alloys suitable for resistance materials and for pressure measurements. Linde's results have given rise to various new ideas in these directions.

The peculiar influence of the transition metals on the resistance is obviously connected with their strong paramagnetic or ferromagnetic properties. For information about the electric behaviour of these alloys, it is therefore also a matter of importance to study their magnetic properties. In our laboratory Gustafsson(18) is now investigating the paramagnetism of alloys of Cu, Ag and Au with transition metals at temperatures ranging from room temperature to 450° C. The measurements at present include dilute alloys of Cu, Ag and Au with Mn and the systems CuNi and AgPd. His results suggest that a considerable amount of experimental work will be necessary before the paramagnetic alloys are sufficiently classified even from a purely phenomenological point of view. Nevertheless the theory regarding

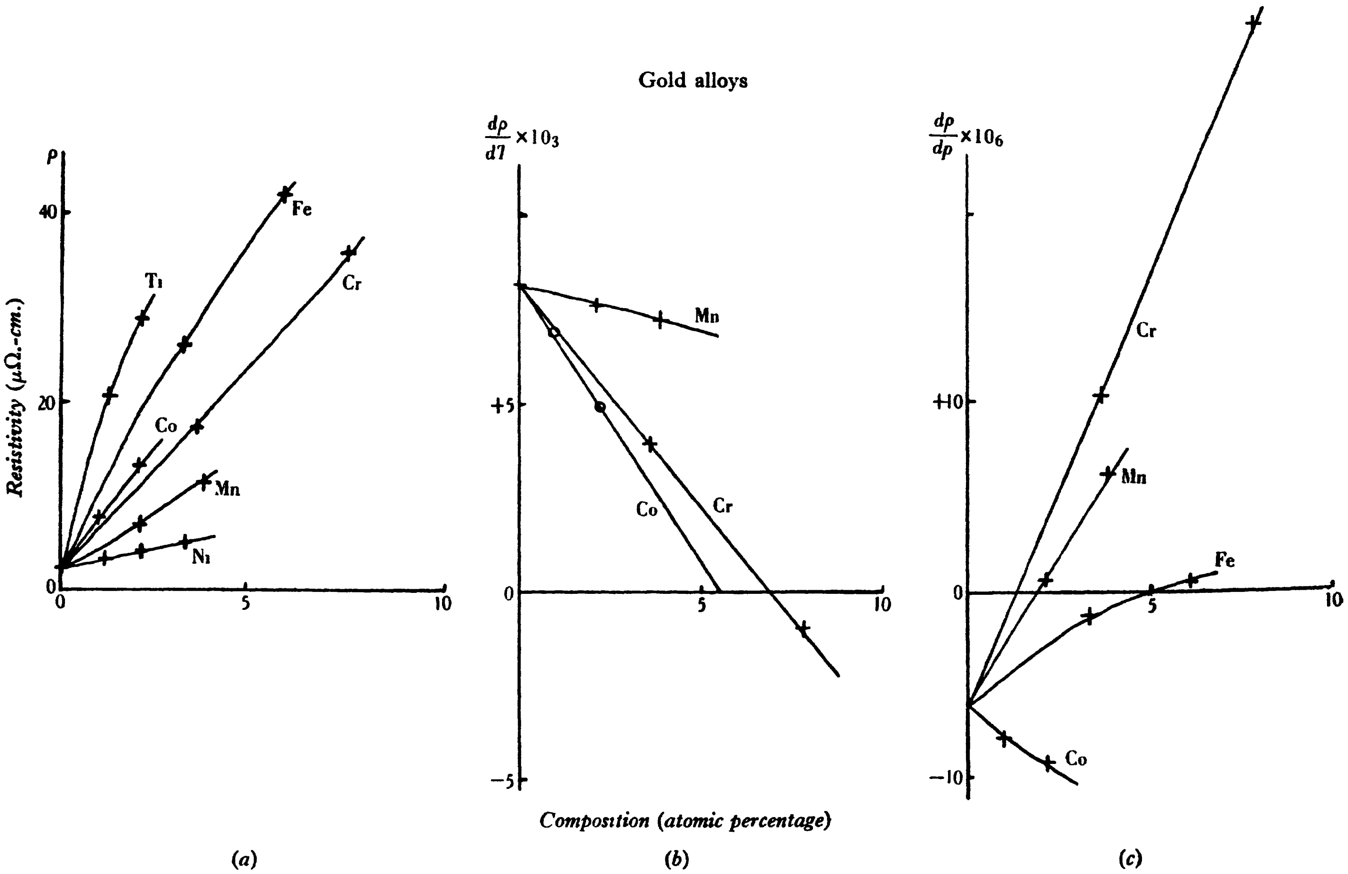

(a) (b) (c)

Figure 4. Specific resistance and its dependence on temperature and pressure for dilute alloys of Au with *a* metals. (Measurements by Linde.)

the exchange of electrons between the unfilled electron bands of the transition metals has proceeded through the works of Stoner(19), Slater(20), Mott(21) and others to a qualitative understanding of various types of paramagnetic phenomena. Indeed, it seems as if the theory is in advance of the experiments and highly in need of the guidance of further experimental work for its definite stabilization.

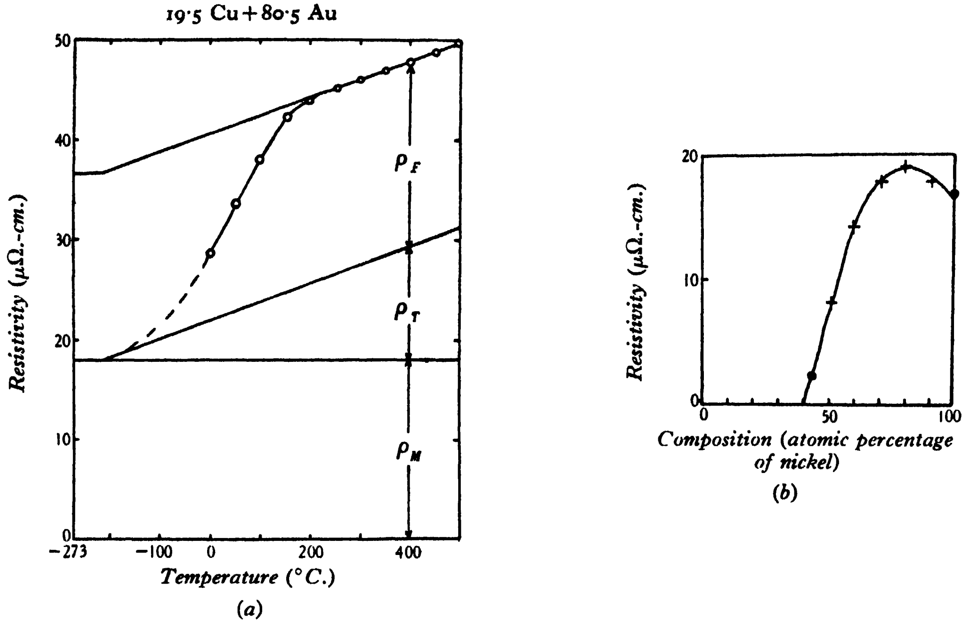

Figure 5. (a) Resistance of a ferromagnetic CuNi alloy. (b) Ferromagnetic part of resistance of CuNi alloys. (Measurements by Svensson(24).)

Experimentally better known are the relations between resistance and ferromagnetic properties, which both have been extensively studied in the system CuNi. The resistance of these alloys has been measured by Chevenard(22), Krupkowski and de Haas(23) and Svensson(24). As is shown in figure 5*a* taken from the paper of Svensson, the resistance of a ferromagnetic alloy can be described phenomenologically as a sum of one part ρ_M due to the mixed arrangement of the Cu and Ni atoms, one normal thermal part ρ_T due to the thermal agitation of atoms, and one magnetic part ρ_F increasing from 0 to its maximal value with increasing demagnetization. The dependence on concentration of the maximum values of ρ_F is shown in figure 5*b*.

§ 4. DEVELOPMENT OF TRANSFORMATIONS FROM DISORDERED TO ORDERED ATOMIC ARRANGEMENTS

The question of the ordered or disordered arrangement of the two kinds of atoms at the lattice points of a binary alloy was first discussed in detail by Tammann(25), his starting point being results from chemical investigations. He found that there existed certain concentration limits for the resistivity to the chemical action of agencies which attack only one of the components of the alloy. Thus, for example, there were limits at 50 per cent Au for the action of nitric acid on CuAu and AgAu alloys. To explain these limits Tammann found it necessary to assume an ordered arrangement of the atoms and predicted these arrangements from a principle of "best possible mixing" (*bestmögliche Durchmischung*).

This hypothesis led to several X-ray investigations of alloys. Vegard(26) and von Laue(27) had pointed out that an ordered arrangement should give rise to certain extra lines. On the one hand the search for such extra lines in several systems, among them also systems such as AgAu, where Tammann had found sharp chemical resistivity limits, gave negative results; on the other hand, Bain(28) on Cu_3Au and Phragmén(29) on Fe_3Si found extra lines, which were looked upon as support for the hypothesis of Tammann. As at that time there was some uncertainty as to the evidence of X-ray results in the case of incomplete order, it was somewhat difficult to draw the right conclusions from these investigations; also the conclusions drawn from the chemical work were found to be very uncertain(30, 31).

My collaborators and I approached the problem from thermoelectric and conductivity measurements carried out especially by Sedström(32) for a number of alloy systems. We found it most likely that the smooth resistance-concentration curves obtained for these properties in most systems of solid solution indicated a disordered arrangement of atoms, whereas the sharp minima in the cases of compounds were due to ordered structures. With this hypothesis X-ray examinations were started with the results of the resistance measurements as a guide. The examination of the systems PdCu and PdAu by Holgersson and Sedström(33) gave some support to this hypothesis and later full evidence was obtained from the examination of the systems CuAu, CuPd and CuPt by Johansson and Linde(34). In the CuAu system the compounds Cu_3Au and CuAu formed by slow cooling of the solid solutions somewhat below 400° C. were known to exist from an investigation by Kurnakow, Zemczuzny and Zasedatelev(35). Johansson and Linde(34) found that alloys of this system quenched from above 400° C., giving high resistance values on the smooth curve in figure 1*b* first observed by Matthiessen, only gave the ordinary X-ray interferences due to the face-centred cubic lattice, whereas the alloys with concentrations in the neighbourhood of 25 and 50 per cent Au, which were tempered below 400° C. to get small resistance values, showed extra interferences indicating ordered arrangement of the two kinds of atoms on the lattice points. These extra interferences appeared not only at exactly 25 and 50 per cent, but on both sides of these concentration points in wide ranges, at the boundary of which the degree of order could only be a very moderate one. Similar results were obtained for the systems CuPd and CuPt.

These investigations thus showed that the X-ray methods were capable of detecting even a very incomplete order, that a highly disordered arrangement of atoms was, especially at high temperatures, a very frequent case in solid solutions, and that the ordered arrangement appeared only at certain limited ranges of concentration and temperature.

These results have been confirmed and extended by a great many investigations in subsequent years. Theoretical discussions have been especially stimulated by the investigations of the CuAu alloys, for which a recent list of references(2) embraces more than 50 papers, and by the investigations of Bradley and Jay(36) of the FeAl alloys.

§ 5. CONTINUOUS VARIATIONS OF DEGREE OF ORDER

The transformations of alloys from disordered to ordered states differed from the well-known transformations of pure metals and salts into new modifications in so far as it was, for the ordering process, possible to imagine a continuous row of intermediate states between full disorder and full order. It was thus possible that the transformations might proceed wholly or in part homogeneously.

To prove this we followed the transformations by resistance measurements(37) and concluded from the results that the transformation was at least in part continuous. The {resistivity, temperature} diagrams obtained for a highly ordered alloy by increasing the temperature had the general appearance shown in figure 6. The straight lines from *a* to *b* and from *e* to *f* apply to the ordered and the disordered states respectively. In both cases the slope $d\rho/dT$ is approximately that calculated from the Matthiessen rule written in the form

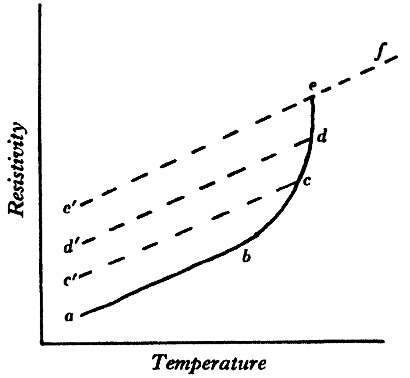

Figure 6. Schematic {resistivity, temperature} diagram of an alloy with superlattice transitions.

$$\frac{d\rho}{dT}=p\left(\frac{d\rho}{dT}\right)_1+q\left(\frac{d\rho}{dT}\right)_2 \qquad \text{......(3)},$$

where $(d\rho/dT)_1$ and $(d\rho/dT)_2$ are the slopes for the pure metals and p and q their fractional parts in the alloy. The curved part of the diagram from *b* to *d* with unusually large values of $d\rho/dT$, represents the continuous variation of structure. That changes of state really occur from *b* to *c* and from *c* to *d* may be proved by quenching the alloy from *b*, *c* and *d* respectively to room temperature. The remaining resistance differences *ac′* and *c′d′* show that a change of state has really taken place. In fact, so far as our present knowledge reaches, values of $d\rho/dT$ much greater than those calculated from the Matthiessen rule always indicate some change either of the magnetic or the structural state. Gorsky(38) at the same time by an X-ray examination of the tetragonality of the AuCu alloy also made the existence of a continuous transformation probable, and, independently of ours, resistivity measurements were carried out by Grube and Weber(38a).

§ 6. DEFINITIONS OF DEGREE OF DISORDER

A homogeneous solid solution with completely disordered arrangement of the atoms, or a compound with complete order is thermodynamically wholly described by its concentration q, its temperature T, and its pressure p. For the thermodynamical treatment of homogeneous solutions with incomplete order we also need a measure, ξ say, of the degree of disorder. As long as only the thermodynamically stable states are considered, ξ is determined by the values of q, T and p. However, the experimental study of the superlattices shows that frozen and unstable states are easily obtainable as well as the stable ones, and that they are often of the same practical and theoretical importance as the latter. These frozen or unstable states and their measurable physical properties such as energy, entropy, free energy, lattice constants, and resistance, are functions not only of q, T and p but also of ξ as a new independent variable.

Here, in fact, a very great difficulty arises in finding a measure of the degree of disorder that may be both theoretically defined without uncertain assumptions and also put in relation to the various physical properties used for the experimental study of the transition phenomena. The attempts made hitherto to define a suitable degree of disorder (or of order) group themselves along three different theoretical lines.

The first line starts from a discussion of the arrangement of the neighbouring atoms, the discussion having hitherto been limited to the consideration of pairs of atoms. To give an example of the theoretical treatment we may take an alloy of the composition A_3B with a superlattice of the sort found in Cu_3Pd and Cu_3Au. Then in the ordered state a fraction $f_0 = 1/2$ of all pairs of nearest neighbours are of the type AB, and by the disordering process this fraction is decreased to $f_d = 3/8$. A state of incomplete order may therefore be described by the fraction f or better by a degree of disorder

$$\delta = \frac{f_0 - f}{f_0 - f_d} \qquad \text{......(4)},$$

ranging from 0 to 1, or by a degree of order $\sigma = 1 - \delta$. My collaborators and I(37) discussed already in 1928 this way of finding a formal description of the transition phenomena though, for reasons mentioned below, we did not find it very suitable. In recent years, however, Bethe(39) and Peierls(40) have made an extended use of an "order of neighbours" σ, which may be identified with the σ above. Their use of this σ is based on the assumption that the energy of transformation should be proportional to it. I cannot find, however, that there is very much physical support for this assumption; the results of specific heat measurements by Sykes and Jones(41) do not support it. Furthermore the simple use of measures of disorder based on the arrangement of pairs of neighbouring atoms seems to be limited to transitions where the number of nearest neighbours is not altered by the transition process. The 50-per-cent alloys CuPd, CuAu and CuPt in the disordered state are all face-centred with 12 nearest neighbours to each atom, whereas in the ordered state CuPd is body-centred with 8 neighbours, CuAu tetragonal with 8 nearest neighbours and 4 at a somewhat greater distance, and CuPt trigonal with 6 atoms nearest and 6 a little more distant from each atom. Here the use of σ is thus already precluded for purely formal reasons.

The second line starts from the state of full order. If we take as example a 50-per-cent alloy AB, this alloy can be described as a combination of two similar lattices, one containing A atoms, the other B atoms. The fraction p of B atoms in the A lattice (or A atoms in the B lattice) varies from 0 to $\frac{1}{2}$ as the alloy goes from the ordered to the disordered state, and $\alpha = 2p$ or $4p\,(1-p)$, etc., are possible measures of the degree of disorder ranging from 0 to 1. To make such measures quite definite, however, it is necessary to assume the distribution of A and B atoms within each lattice to be statistically disordered, and the truth of this assumption is not quite evident as there might for example be a tendency of the atoms to occur in pairs or small groups in the wrong lattice. Further, it is of course unsatisfactory to extend the idea of different A and B lattices also to the case of great disorder.

A measure of degree of disorder of this kind (called *Fehlordnungsgrad*) was first used by Wagner and Schottky(42) and related to the variations of energy, entropy and resistance in small deviations from full order. Ölander(43) later used it for the theoretical discussion of results of measurements of electrode potentials of alloys at high temperatures. The author(44) made an extended use of a measure of this type for a quantitative treatment of the transition in AuCu. Bragg and Williams(45) used a degree of order of this kind for the treatment of transitions in alloys of the type AB or A_3B and the "long-distance order" of Bethe(39) belongs to the same group of parameters.

In a discussion of the general features of the equilibrium diagrams of systems with superlattices, the author(46) has tried a third line, avoiding parameters based on description of atomic arrangements, and using a purely thermodynamical quantity, the zero-point entropy S_0, as a measure of degree of disorder. For this limited purpose, this parameter is a very suitable one. If the zero-point energy is given as a function of S_0 and the concentration q, certain boundary lines of the equilibrium diagram can be constructed in a simple way. It has not, however, yet been shown whether a quantity like S_0 can be useful also for the treatment of physical properties such as the resistance. This will depend upon whether there exists and can be found some direct theoretical connexion, for instance between zero-point resistance and zero-point entropy.

§ 7. ANTIPHASE REGIONS IN PARTLY ORDERED CRYSTALS

The proposed parameters of degree of disorder are of course single-valued only for homogeneous alloy phases and can only be used for the treatment of states of equilibrium of homogeneous frozen states obtained by quenching, and of the homogeneous metastable states which will be discussed in the next paragraph. As soon, however, as the transitions from disordered to ordered states were followed with X-ray and resistance measurements, my collaborators and I(37) found reasons also for the existence of more complicated transitional states neither fully homogeneous nor in the ordinary sense heterogeneous. If the ordering process starts at, and spreads from, a great many points, the nuclei thus formed will as they meet coalesce if they are in phase with each other, or exist side by side as antiphase regions if they are not. This means that a row or plane of *A* atoms in one region will, as is shown in figure 7 taken from our paper of 1928(37), continue as a row or plane of *B* atoms in the next one.

It was pointed out in this paper that such regions, if they were small enough, must have a great influence on the sharpness of the superlattice lines of X-ray photograms and on the resistance.

This hypothesis of antiphase regions also explains the observation later made by Oshima and Sachs(47) and by Dehlinger and Graf(48) by X-ray examination of single crystals of AuCu, that the tetragonality and the intensities of different superstructure lines do not vary in the same way during the ordering transition. The hypothesis put forth by Oshima and Sachs and especially used by Dehlinger(49) to account for these observations, namely that the tetragonality to a certain extent should be independent of the degree of order, is quite incomprehensible and, at least for the present, unnecessary.

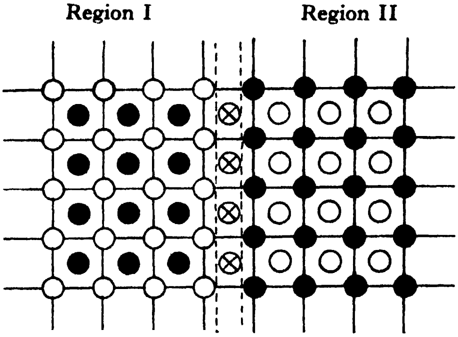

Figure 7. Antiphase regions. ○ *A* atoms, ● *B* atoms, ⊗ *A* or *B* atoms.

In recent years the hypothesis of antiphase regions has indeed obtained very good support in two different ways.

On the one hand Sykes in collaboration with Evans(50) and Jones(41) has made a thorough experimental examination of the transitions in Cu_3Au by measuring lattice constants and intensity of superstructure lines, resistance, and specific heat, and has found it possible to account for a great many details, some even quantitatively, from the assumption of antiphase regions. Figure 8 shows in a schematic way some of their results concerning resistance and energy content, which are interpreted in the following way: As a sample is quenched from above the critical temperature T_0 it remains in the disordered state and resistance and energy varies along the straight lines *a–a*. As the quenched alloy is heated at a rate of about 90° per hour, as shown by the curve *b–b*, the energy begins already at 60° C. to deviate from this line. This decrease in energy content is interpreted as due to the formation of small antiphase regions of an extent of only 6 to 8 atomic diameters. At about 250° C. a new decrease of energy begins owing to an increase of the size of the antiphase regions. At 344° C. this size is about 12 to 14 diameters, being estimated both from the breadth of the superlattice lines and from the energy content. The resistance is not appreciably influenced by the small regions of 6 to 8 diameters but decreases rapidly as the length of the regions exceeds about 10 diameters. This is in qualitative agreement with the fact that the mean free path of the electrons in the ordered alloy is estimated, from modern theory of conduction, at 30 to 40 diameters. The curves *e–e* reached by very slow cooling correspond to regions of about 100 diameters or more and are approximately curves of equilibrium. If an alloy, which is in equilibrium at the point *d'* and thus has large antiphase regions but an incomplete order of atoms, is cooled rapidly enough to preserve the degree of disorder, the resistance follows a straight line *d–d'*. The curve *c–c* finally shows the variation of resistance by slow heating or cooling of a sample with regions of medium size in a temperature

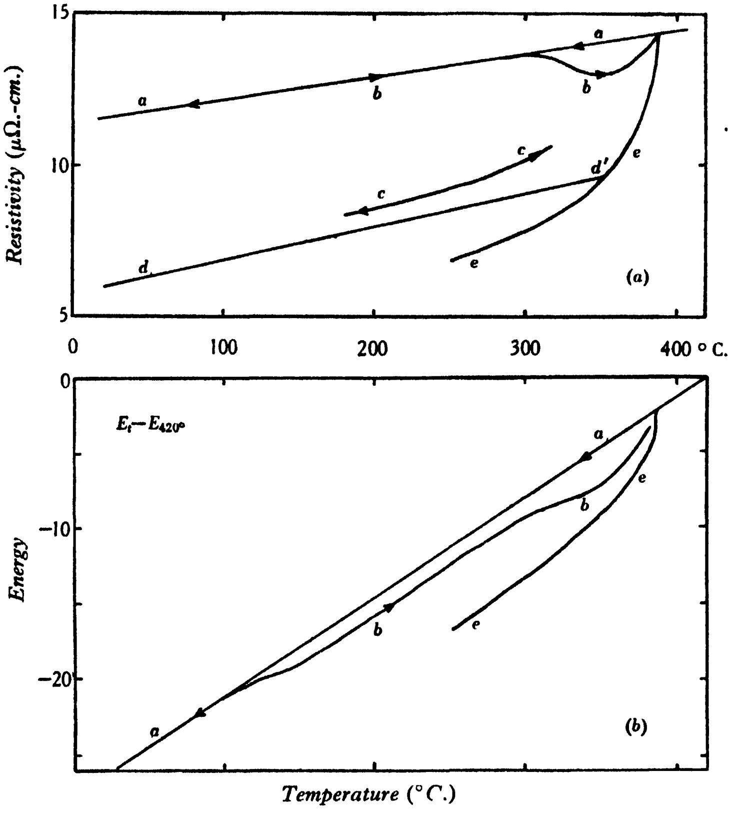

Figure 8. (*a*) Resistivity, (*b*) energy of Cu_3Au. (Measurements by Sykes, Evans and Jones(41, 50).

range where the regions cannot grow. The bend is due to the variation of degree of disorder inside the regions.

On the other hand Johansson and Linde⁽²⁾ have found that alloys with compositions around CuAu after suitable heat treatment occur in an ordered state (CuAu II) that can be described as the well-known ordered tetragonal state (CuAu I) found earlier by the same authors split up in antiphase regions of a fixed length. This structure, being periodic, can be directly established by X-ray examinations. At 50 per cent Au the length of each region is, as shown in figure 9, 10 atomic distances, but it increases at both sides in the concentration diagram. As to the theory of electric resistance, it is interesting to notice that these periodic antiphase displacements do not, like the accidental ones of the same mean distances, increase the resistance. Alloys with the structures CuAu I and CuAu II lie in figure 1*b* on the same resistance curve.

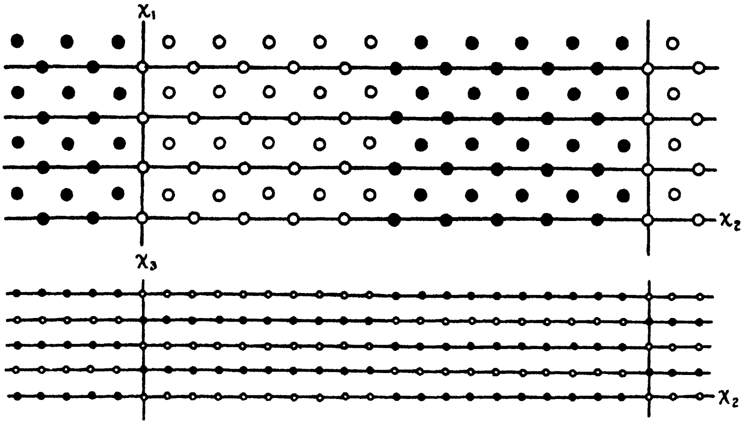

Figure 9. Structure of CuAu II according to Johansson and Linde⁽²⁾.

§ 8. DISORDERING BY MECHANICAL TREATMENT

The superstructure of an alloy can be destroyed not only by heating but also by cold working. This was made probable by X-ray investigations of Dehlinger and Graf⁽⁴⁸⁾ on CuAu and of Schafer⁽⁵¹⁾ on FeAl and is shown very convincingly by Dahl⁽⁵²⁾ by X-ray investigations together with resistance measurements on Cu_3Au. Fig. 10*a* shows the increase in resistance for an annealed Cu_3Au alloy as a function of the decrease of section area by cold workings. Figures 10*b* and 10*c* show corresponding curves for two Cu-Pt alloys obtained by Linde in connexion with an unpublished re-examination of the CuPt system. This effect might be explained by the formation of antiphase regions by the cold working.

§ 9. HYSTERESIS BETWEEN THE ORDERING AND DISORDERING TRANSITIONS

As the transitions between ordered and disordered states were first followed in both directions by resistance measurements, in many cases a well-marked hysteresis loop in the {resistivity, temperature} diagram was found. Figure 11 gives two examples from our first investigation(37), showing the behaviour of quenched alloys during slow heating and subsequent slow cooling. In heating an ordering process is observed to begin at the temperatures marked as T_1 and by further heating full disorder is reached at the temperatures T_3. In the subsequent cooling the alloy remains in the disordered state far below T_3 until about a temperature T_2 when the speed of the ordering process increases rapidly within a range of a few degrees. The disordered alloy could be held for many hours at temperatures between T_3 and T_2 (not too near T_2) without showing any signs of beginning a transition into order. Thus we found a well-established hysteresis in CuAu and CuPd, whereas we estimated the transitions of Cu_3Pd to be without hysteresis. The recent very thorough examinations Cu_3Au by Sykes and Evans(50) have shown that there is also in the case of Cu_3Au a well-marked hysteresis though only extending over a few degrees on the temperature scale.

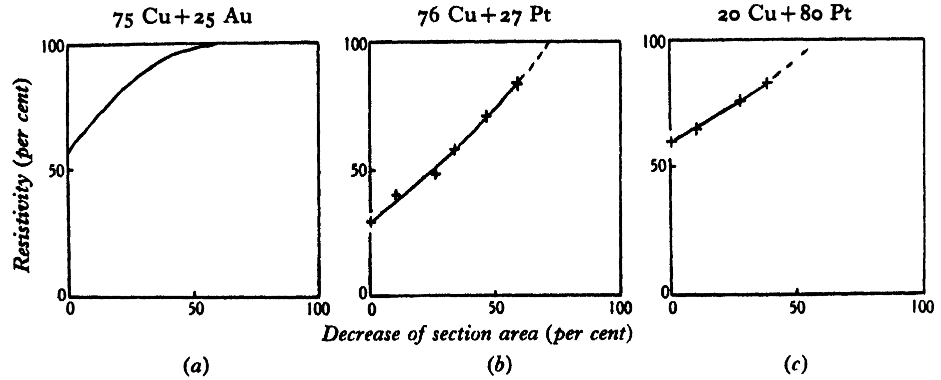

Figure 10. Increase of resistance by cold-working of alloys with super-structures. Resistance as a percentage of the resistance of the disordered state. (Unpublished measurements by Dahl(52) and Linde.)

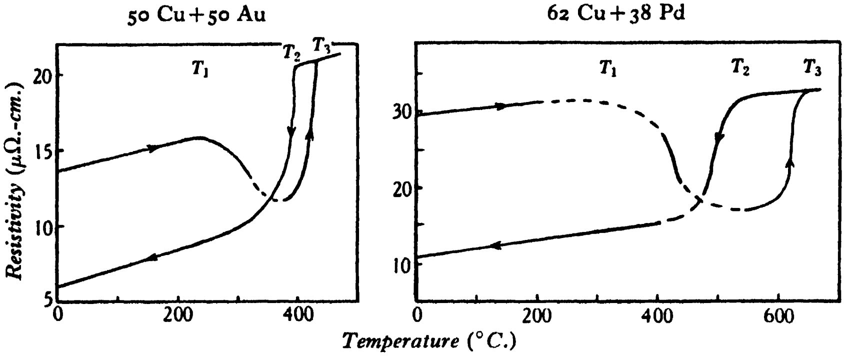

Figure 11. Hysteresis loops measured by Borelius, Johansson and Linde(37).

The transition between ordered and disordered states implies a mutual exchange of places of atoms two by two. It is clear that a slowness of this exchange will, by rapid cooling or heating, cause the state of the alloy to lag behind its stable state and thus gives rise to a hysteresis loop. This type of hysteresis has been mathematically treated by Bragg and Williams$^{(45)}$. It will be expected to be less pronounced the higher the temperature. As, however, the hysteresis found by our measurements was very pronounced also at temperatures at which we must expect a lively exchange of places of the atoms, we found it necessary to ascribe the hysteresis to thermodynamically metastable states and it was shown$^{(44,45)}$ that such metastable states were to be expected for certain types of the free energy F as a function of temperature T and degree of disorder ξ shown in figure 12. Point *a* represents a metastable state in heating, and point *b* in cooling, *c* represents stable states. Even where the free energy is not of this type a certain hysteresis could be expected thermodynamically as a result of internal stresses. There has been some doubt$^{(45)}$ whether such theoretical metastable states could really account for the hysteresis observed but, so far as I can see, no better explanation has as yet been given.

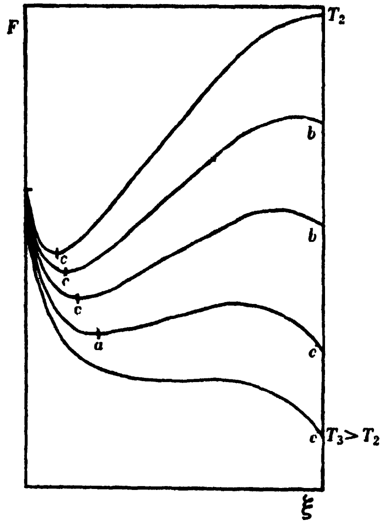

Figure 12 Isothermals of free energy F as a function of degree of disorder ξ according to Borelius$^{(44)}$.

§ 10. HYSTERESIS AT THE SEGREGATION PROCESS

The idea of relative minima of free energy as a cause of hysteresis of the superlattice transitions led to a search for similar phenomena in connexion with the segregation of a homogeneous alloy into two phases, and in fact resistance measurements of the system AuPt have given a very good support for this idea. As was found by Johansson and Linde$^{(3)}$, AuPt alloys of all concentrations can be brought into a homogeneous solid state by heating to sufficiently high temperatures. If these homogeneous alloys are quenched to say 800° C., where there is in the stable state a gap in the solubility from 25 to 90 atomic per cent Pt, the free energy of the homogeneous alloys obtained by quenching will, as was calculated by the author$^{(53)}$ from the equilibrium diagram, depend on the concentration approximately in a way shown in the upper section of figure 13. From *a* to *d* the homogeneous alloys are unstable. From *a* to *b* and from *c* to *d* where the curve is bent upwards the segregation that has to begin as a small increase of the Pt concentration in certain regions and a small decrease in the neighbouring ones will first cause an increase in the free energy and thus to a certain extent be prevented. The resistance measurements of Johansson and Hagsten(54) on an alloy with 30 atomic per cent Pt, and unpublished measurements of Wictorin on alloys from 25 to 50 per cent Pt agree very well with these expectations. The lower section of figure 13 shows the decrease in resistance, here a measure of the segregation, for alloys first quenched in the homogeneous state from high temperatures to 800° C., then held there for τ min. and finally quenched to room temperature. The curves for small values of τ show points of inflexion at a concentration *ii* corresponding to the calculated inflexion in the free-energy diagram. Similar results are obtained at 900° and 700° C. When the free-energy curve is strongly bent upwards, in spite of the high temperatures and the probable high mobility of the atoms, the segregation is still a very slow one. The reverse process, the reconstitution of an homogeneous alloy, presents no such obstacles.

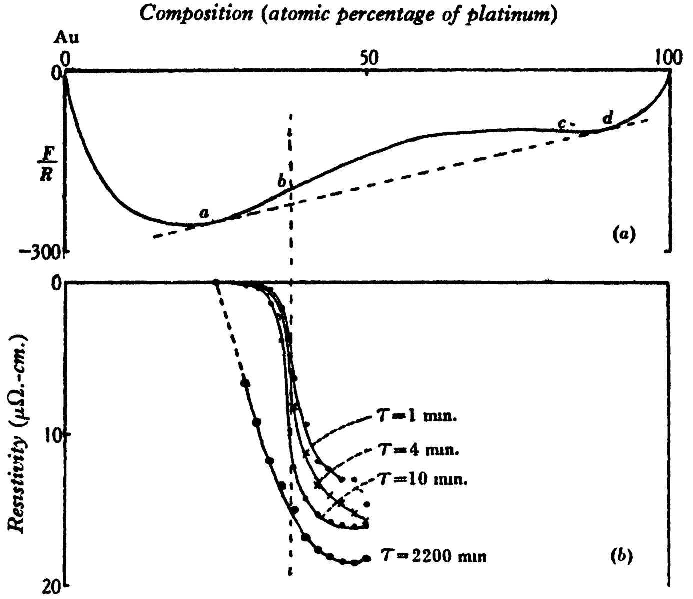

Figure 13. (*a*) Free energy of AuPt alloys at 800° C., calculated from the equilibrium diagram. (*b*) Decrease in resistance by segregation at 800°. (Unpublished measurements by Wictorin.)

REFERENCES

(1) Matthiessen, A. *Ann. Phys.*, Lpz., **110**, 190 (1860).
(2) Johansson, C. H. and Linde, J. O. *Ann. Phys.*, Lpz., **25**, 1 (1936).
(3) Johansson, C. H. and Linde, J. O. *Ann. Phys.*, Lpz., **5**, 762 (1930).
(4) Grube, G. and collaborators. Twenty-two papers mostly in *Z. Elektrochem.* 1929–37.
(5) Benedicks, C. *Jernkontor. Ann.* p. 35 (1916).
(6) Norbury, A. L. *Trans. Faraday Soc.* **16**, 570 (1927).
(7) Linde, J. O. *Ann. Phys.*, Lpz., **10**, 52 (1931); **14**, 353 (1932); **15**, 219 (1932); *Metallwirtschaft.* **12**, 173 (1933).

(8) Höjendahl, K. *Phil. Mag.* **48**, 349 (1924).
(9) Wien, W. *S.B. Akad. Wiss. Wien*, p. 84 (1913).
(10) Sommerfeld, A. *Z. Phys.* **47**, 1 and 43 (1928).
(11) Borelius, G. *Ann. Phys.*, Lpz., **84**, 907 (1927).
(12) Bloch, F. *Z. Phys.* **52**, 555 (1929); **59**, 208 (1930).
(13) Nordheim, L. *Ann. Phys.*, Lpz., **9**, 607 (1931).
(14) Mott, N. F. *Proc. Camb. Phil. Soc.* **32**, 281 (1936).
(15) Mott, N. F. and Jones, H. *Properties of Metals*, p. 286ff. (1936). Oxford.
(16) Lenssen, M. H. and Michels, A. *Physica*, 's Grav., **2**, 1091 (1935).
(17) Mott, N. F. *Proc. phys. Soc.* **46**, 680 (1934).
(18) Gustafsson, G. *Ann. Phys.*, Lpz., **25**, 545 (1936); **28**, 121 (1937).
(19) Stoner, E. C. *Proc. roy. Soc.* **152**, 672 (1935); **154**, 656 (1936).
(20) Slater, J. C. *Phys. Rev.* **49**, 537 and 931 (1936).
(21) Mott, N. F. *Proc. phys. Soc.* **47**, 571 (1935); *Proc. roy. Soc.* **153**, 699 (1936) and **156**, 368 (1936).
(22) Chevenard, P. *J. Inst. Met.* **36**, 39 (1926).
(23) Krupkowski, A. and de Haas, W. J. *Commun. phys. Lab. Univ. Leiden*, **194**, 1 (1928).
(24) Svensson, B. *Ann. Phys.*, Lpz., **25**, 263 (1936).
(25) Tammann, G. *Z. anorg. Chem.* **107**, 1 (1929).
(26) Vegard, L. and Schjelderup, H. *Phys. Z.* **18**, 93 (1917).
(27) v. Laue, M. *Ann. Phys.*, Lpz., **56**, 497 (1918).
(28) Bain, E. *Trans. Amer. Inst. min. (metall.) Met. Engrs*, **68**, 625 (1923).
(29) Phragmén, G. *Stahl. u. Eisen*, no. 9 (1925).
(30) Masing, G. *Z. anorg. Chem.* **118**, 293 (1921).
(31) Borelius, G. *Ann. Phys.*, Lpz., **74**, 216 (1924).
(32) Sedström, E. Dissertation Lund (1924).
(33) Holgersson, S. and Sedström, E. *Ann. Phys.*, Lpz., **75**, 143 (1924)
(34) Johansson, C. H. and Linde, J. O. *Ann. Phys.*, Lpz., **78**, 439 (1925); **82**, 449 (1927).
(35) Kurnakow, N., Zemczuzny, S. and Zasedatelev. *J. Inst. Met.* **155**, 305 (1916).
(36) Bradley, A. J. and Jay, A. H. *Proc. roy. Soc.* **136**, 210 (1932).
(37) Borelius, G., Johansson, C. H. and Linde, J. O. *Ann. Phys.*, Lpz., **86**, 291 (1928).
(38) Gorsky, W. *Z. Phys.* **50**, 64 (1928).
(38*a*) Weber, W. Dissertation Stuttgart (1927).
(39) Bethe, H. *Proc. roy. Soc.* **150**, 552 (1935).
(40) Peierls, R. *Proc. roy. Soc.* **154**, 207 (1936).
(41) Sykes, G. and Jones, F. W. *Proc. roy. Soc.* **157**, 213 (1936).
(42) Wagner, C. and Schottky, W. *Z. phys. Chem.* **11** (B), 163 (1930).
(43) Ölander, A. *Z. phys. Chem.* **165** (A), 65 (1933).
(44) Borelius, G. *Ann. Phys.*, Lpz., **20**, 57 (1934).
(45) Bragg, W. L. and Williams, E. J. *Proc. roy. Soc.* **145**, 699 (1934); **152**, 540 (1935).
(46) Borelius, G. *Ann. Phys.*, Lpz., **24**, 489 (1935).
(47) Oshima, K. and Sachs, G. *Ann. Phys.*, Lpz., **14**, 481 (1932).
(48) Dehlinger, U. and Graf, L. *Z. Phys.* **64**, 359 (1930).
(49) Dehlinger, U. *Z. Phys.* **64**, 359 (1930); **74**, 267 (1932); **83**, 832 (1933).
(50) Sykes, C. and Evans, H. *J. Inst. Met.* **58**, 255 (1936).
(51) Schäfer, K. *Naturwissenschaften*, **10**, 207 (1933).
(52) Dahl, O. *Z. Metallk.* **28**, 133 (1936).
(53) Borelius, G. *Ann. Phys.*, Lpz., **28**, 507 (1937).
(54) Johansson, C. H. and Hagsten, O. *Ann. Phys.*, Lpz., **28**, 520 (1937).

A STUDY OF THE ORDER-DISORDER TRANSFORMATION

By W. L. BRAGG, C. SYKES and A. J. BRADLEY

§1. INTRODUCTION

THE present account is a summary of a series of related researches into the order-disorder transformation, carried out at Manchester University and in the research laboratory of Messrs Metropolitan Vickers. Our researches have been planned to take their places in a concerted scheme, and it is hoped that this general summary and the list of papers at the end of this article will be a useful indication of their scope. Similar researches have been in progress in other laboratories. Though this account is restricted to the researches at Manchester, it is published with full acknowledgement of the work carried out elsewhere, particularly by Borelius, Dehlinger, Johannson and Linde, and others.

The order-disorder transformation has been followed by means of X-rays by Bradley and his coworkers. The theory of the transformation has been developed by Bragg and Williams, by Bethe, and by Peierls. The measurements of the changes in internal energy, in conductivity, and in some cases in magnetic properties, have been made by Sykes. A résumé of the programme of work in hand is given at the end of the article.

§2. THE GENERAL NATURE OF THE ORDER-DISORDER TRANSFORMATION

Examples of the order-disorder transformation and of its effect upon the physical properties of alloys are to be found in Bradley and Jay(1, 2), Bradley and Rodgers(3) and Sykes and Evans(4). All transformations as yet observed in binary alloys occur when the proportions of the constituents are approximately in the ratio 1 : 1 or 1 : 3. In the disordered state observed at high temperatures the atoms *A* and *B* of the two metals are arranged at random amongst the position of a pattern such as the face-centred at body-centred cubic lattice. In the ordered state at low temperatures atoms of each kind segregate into regular positions. For instance, in the classic case of Cu_3Au gold and copper atoms are distributed at random amongst positions of a face-centred cubic lattice when the temperature is high, whereas gold atoms occupy cube corners and copper atoms face centres in a regular way at low temperatures. There are other more complex cases when more than two types of atoms are involved, such as the Heusler alloy Cu_2MnAl or the alloy Fe_2NiAl. In the latter, corners of cubes are occupied by Fe and Ni in a random way, centres by Fe and Al in a random way. The ordering process is thus restricted to a distinction between Ni and Al, but does not extend to a distinction between either of these and iron. We may compare the ordering phenomenon to the passage of the alloy through two successive processes of crystallization on cooling. In the first process the liquid becomes a crystalline solid. Atoms take up positions at regular sites, for instance those of a face-centred lattice, but there is as yet no distinction between atoms of either kind *A* and *B*. As the temperature falls still farther, a second crystallization within the solid crystalline lattice takes place, by the segregation of the atoms into regular positions. In both cases there is an increase of regularity, implying a decrease in the entropy and a decrease in the internal energy. This alteration of internal energy is the latent heat of fusion in the first case, and something analogous to a latent heat in the second case. There is an important difference between the two cases. At the freezing-point the substance passes over completely from the random arrangement of the liquid to the ordered arrangement of the solid. Intermediate states between liquid and solid would have an extremely high internal energy, and therefore the substance does not pass through them. Bernal has illustrated this feature by a striking two-dimensional model⁽¹⁹⁾. If a number of non-overlapping circles are drawn on a sheet of paper, they must either be packed in an orderly way, or there must be numerous gross misfits of contact; a series of slight misfits is geometrically impossible, unless we permit circles to overlap which implies large internal energy of strain. On the other hand, intermediate stages between complete order and disorder involve no excessive values of the internal energy. When crystallization of the second kind sets in, it is at first one of partial order and theoretically does not become one of complete order until the absolute zero is reached. Actually it is nearly complete at 100 or 200° C. below the temperature at which it starts. The ordering goes on over this whole range, and latent energy is evolved in cooling or absorbed on heating. Thus what corresponds to the latent heat of the first crystallization is spread out into an abnormally high specific heat over a wide temperature range in the second crystallization.

Although the completion of ordering is so gradual, it sets in at a sharply marked *critical temperature*. We can see that this must be the case by considering the reverse process of heating the ordered alloy. At first the passage of each atom from an ordered to a disordered position involves a certain amount of work V_0 required to thrust it out of relation to its ordered neighbours. As temperature increases there is an increase in the energy kT which determines the number of atoms in the state of higher energy, and at the same time there is a decrease in the energy V required to move an atom to a position of disorder, because each atom has more neighbours already disordered. These two variations so interact that there is finally a catastrophe, or complete breakdown of general order, at the critical temperature. The critical temperature corresponds to the Curie point of a ferromagnetic. In the general case, there is first a jump from a state of disorder to one of partial order with latent heat at the critical temperature and then a gradual increase of order as temperature falls. In special cases the alloy may pass continuously through all intermediate stages of order; the critical temperature is marked by a peak in the specific heat, but no latent heat is involved or absorbed.

So far it has been assumed that the alloys are in thermodynamical equilibrium at each temperature. Actually at temperatures below 200 or 300° C. the atoms interchange position very sluggishly. The influence of the rate of relaxation upon the degree of order must be studied. It is possible to freeze some alloys in the disordered state by quenching (we may compare them to supercooled liquids). It will be seen below, however, that the slowness with which they devitrify back into an ordered scheme is not so much due to sluggishness of atomic interchange as to the establishment in them of numerous nuclei of order which are out of phase with each other.

§ 3. THE THEORY OF THE DEPENDENCE OF ORDER UPON TEMPERATURE

The order-disorder change provides a very interesting exercise for thermodynamic theory. It may be considered in two ways. At a given temperature there is a partition of the atoms between ordered and disordered positions depending upon the amount of energy V required to move an atom from the ordered to the disordered position. A further assumption as to the dependence of this energy upon the existing degree of order establishes an equation for equilibrium at that temperature, and so leads to the general relation between temperature and degree of order. Alternatively an expression for the free energy F of the alloy in any given state of order may be formed. Since $F = U - TS$, an assumption as to the dependence of the internal energy U upon the degree of order must be made, based on the mutual potential energy of like and unlike neighbours A and B. The entropy S can be calculated from the number of complexions of the given state of order. The condition for equilibrium is then expressed as $\partial S/\partial\sigma = 0$, where σ is a parameter defining the degree of order. The two methods are of course equivalent and lead to the same equation. The latter method has been used by Borelius and by Dehlinger, the former by Bragg and Williams. The particular interest of the order-disorder change is that the entropy S can be calculated by first principles, since it simply depends upon the number of permutations of the atoms A and B. In this respect it is so much simpler than the change between liquid and solid, or between one allotropic modification and another.

Bragg and Williams(5) calculate the degree of order as a function of temperature, for cases where the atoms are in numerical ratios 1 : 1 and 1 : 3. The energy V is supposed to be proportional to the average degree of order of the whole surrounding structure.

Bethe(10) carries out the far more complex calculation of the dependence of order on temperature on the assumption that the mutual potential energy depends upon nearest neighbours alone. When this assumption is made the new and highly interesting feature of local order appears. If it be assumed that the ordering energy V depends on the general scheme of order of the whole structure, then V becomes zero with the vanishing of long-distance order at the critical temperature. If, on the other hand, V depends upon nearest neighbours only as Bethe assumes, we find that, although long-distance order vanishes at the critical temperature, nuclei of local order persist. Schemes of order over restricted volumes are constantly appearing and being broken up, because it is always more likely that the nearest neighbour to an *A* atom will be a *B* atom rather than an *A* atom. Experiment as will be shown below indicates that Bethe's assumption is in closer accord with fact. Local order still has the effect of reducing the entropy and increasing the specific heat even above the critical temperature.

Bragg and Williams(11, 12) contrast the predictions based on their earlier hypothesis and on that of Bethe with the results of Syke's experiment (see below), and the theoretical treatment is amplified. Peierls(13) extends Bethe's treatment to the case of superlattices such as Cu_3Au with a 3 : 1 ratio between the two types of atom. Bethe has confined himself to the case of the ratio 1 : 1. Cu_3Au has been experimentally investigated rather completely, and comparisons between theory and experiment can be made. Neither the assumptions of Bethe nor of Bragg and Williams give a close agreement with the observed energy-temperature curve, but there is sufficient correspondence to prove that theory is on the right lines.

§4. MEASUREMENTS OF ENERGY CHANGES DUE TO THE FORMATION OF THE SUPERLATTICE

The progressive disappearance of superlattice order as temperature is increased is marked by an abnormally high specific heat due to the energy required to transfer atoms into positions of disorder, and by latent heat at the critical temperature where the long-distance order is finally destroyed. In special cases, there is no latent heat because the alloy passes through all stages of order. Above the critical temperature the specific heat should still be slightly above the normal value* due to local order. The measurement of the specific heat for the purpose of testing the theory requires accurate determinations over temperature intervals of a few degrees. Apparatus involving a new principle has been evolved for this purpose by Sykes(7, 16) and has proved to be very successful. The temperature of an outer massive metallic container is raised at a regular rate by a heating coil. The specimen inside the container is also warmed electrically by a measured energy input, which is so controlled that the temperatures of the specimen and container remain closely the same. The apparatus is evacuated. Corrections can be made for the very small heat losses or gains. Difference of temperature between specimen and container can be measured by a thermo-element very exactly indeed since it is so small, and the rate of rise of temperature of the container is accurately known since it can be measured over long time intervals. Hence the data for highly accurate specific heat determinations over short temperature ranges are available.

The features prophesied by theory are all present. The alloys show abnormally high specific heats rising to a maximum just below the critical temperature. The alloy Cu_3Au displays latent heat at the critical temperature, but β brass (CuZn) has none. Above the critical temperature the specific heat is slightly higher than a normal value for pure metals.

---

* There is no direct way of measuring the "normal" specific heat above the critical temperatures, but it can be inferred from the specific heat at low temperatures or the behaviour of alloys of other compositions.

§ 5. TIME OF RELAXATION

An alloy at a given temperature not initially in the state of order characteristic of that temperature will relax towards it at a rate dependent upon the frequency with which atoms interchange their positions. The equation for the time of relaxation τ should have the form

$$\tau = Ae^{W/kT},$$

where A is a constant (of the order 10^{-9} to 10^{-12}) and W measures the energy barrier which has to be surmounted for interchange to take place. The above assumes that we are dealing with a simple case of an alloy in which a general scheme of order is established, but where the number of atoms in ordered positions is not in correspondence with equilibrium. Experiment shows that the actual state of affairs is not so simple (Sykes(14)). It is possible to obtain Cu_3Au at room temperature in a state which is apparently one of disorder as judged by its electrical resistance, by quenching it from above the critical temperature. Measurements made on the relaxation of the alloy back to the equilibrium state cannot be explained by a simple law of the type $\tau = Ae^{W/kT}$. Further, it is known that copper and gold diffuse into each other quite rapidly at 200–250° C., whereas the critical temperature is 391° C. If diffusion takes place at 250° C., atomic interchange at 391° C. should be so extremely rapid that no quenching could be fast enough to preserve the disordered state. Sykes has explained the discrepancy as being due to the formation of antiphase nuclei. Ordering in Cu_3Au takes place by a segregation of the gold atoms at points of one of the four interpenetrating simple cubic lattices which build up its face-centred lattice. All four simple lattices are equivalent, and nuclei of order may start according to any one of four schemes. If numerous nuclei start and grow till they meet the interfaces of nuclei with different schemes (antiphase nuclei), there must be disordered regions, since the atoms at and near the interfaces cannot conform to both schemes. This appears to be the state of affairs in an alloy "frozen" in disorder. The conglomerate of antiphase regions is very stable. Sykes has proved their existence and measured their size by means of X rays. Their effect on internal energy and on electrical resistance has been measured(15). The quenched alloy with its numerous antiphase nuclei has an electrical resistance at room temperature which fits upon an extrapolation of the resistance curve of the disordered alloy above the critical temperature. It behaves electrically, in other words, as if it were completely disordered. On the other hand, the internal energy is lower than would be expected for complete disorder, showing that some approach to ordering has taken place.

Sykes has further shown that if the alloy is soaked for 48 hours at a temperature only a degree or so below the critical temperature, the antiphase nuclei coalesce into large regions over which the scheme of order is consistent. Once the alloy has been brought into this state it remains in equilibrium as its temperature is raised or lowered (even at fast rates), always provided the critical temperature is not exceeded. At low temperatures the alloy in this state has an electrical resistance like that of a pure metal tending towards zero as the absolute temperature is approached.

It is easy to quench Cu_3Au with its four schemes of order into a state resembling one of complete disorder. On the other hand, it is impossible to quench CuZn in the disordered state. This is probably due to the fact that the latter alloy has only two alternative schemes of order (cube corners or centres for Cu or Zn). Four types of antiphase nuclei can form a stable froth (the boundaries behave as if they had surface tension), but two types cannot do so. Hence CuZn always breaks down into large regions which have a consistent ordered scheme.

§ 6. THE INFLUENCE OF ORDER ON MAGNETIC PROPERTIES

The alloy Fe_3Al shows peculiar magnetic effects, having two Curie points. Sykes has shown⁽⁸⁾ that this phenomenon is due to the ordering process. As the alloy in the disordered state cools from a high temperature it reaches a Curie point and becomes ferromagnetic. At a slightly lower temperature order sets in. This critical temperature is below the Curie point for the disordered state but above that for the ordered state, hence the alloy loses its ferromagnetism. On cooling further it reaches the Curie point for the ordered state and becomes ferromagnetic again. Very interesting effects are produced by varying rates of cooling and heating.

Bradley has studied the effect of order on the ferromagnetism of the Heusler Alloys⁽³⁾.

§ 7. WORK AT PRESENT IN PROGRESS OR ABOUT TO BE PUBLISHED

Measurements have been made of the energy of ordering in βCuZn alloys which depart from the equiatomic ratio. These measurements are in satisfactory accord with theory⁽¹⁷⁾. The existence of a superlattice in β brass, hitherto only inferred from its behaviour, has been definitely proved by Sykes and Jones⁽¹⁶⁾. Powder photographs have been taken with ZnK_α radiation. The proximity of this wave-length to the absorption edges of Cu and Zn introduces an enhanced difference of scattering power which causes the lines in the powder photograph for which $(h+k+l)$ is uneven to appear.

Several alloys which show ordering with a 1 : 1 atomic ratio of constituents are being studied thermally, electrically, and by X rays, in order to check theory with more experimental measurements (AgCd, AgZn, MgCd, etc.).

The alloy Cu_3Pd, which it was hoped would behave like Cu_3Au, appears to be tetragonal in the ordered state. The transformation in Cu_3Pd is so sluggish that it may be possible to prove the existence of Bethe's local order by direct methods, quenching and annealing from a temperature above the critical temperature.

The relation between size of antiphase nuclei as measured by X rays and their influence on electrical resistance is being studied.

REFERENCES

(1) Bradley, A. J. and Jay, A. H. *Proc. roy. Soc.* A, **136**, 210 (1932).
(2) Bradley, A. J. and Jay, A. H. *J. Iron Steel Inst.* **1**, 339 (1932).
(3) Bradley, A. J. and Rodgers, J. W. *Proc. roy. Soc.* A, **144**, 340 (1934).
(4) Sykes, C. and Evans, H. *Proc. roy. Soc.* A, **145**, 529 (1934).
(5) Bragg, W. L. and Williams, E. J. *Proc. roy. Soc.* A, **145**, 699 (1934).
(6) Sykes, C. and Bampfylde, J. W. *J. Iron Steel Inst.* **2**, 389 (1934).
(7) Sykes, C. *Proc. roy. Soc.* A, **148**, 422 (1935).
(8) Sykes, C. and Evans, H. *J. Iron Steel Inst.* **1**, 225 (1935).
(9) Bragg, W. L. *J. Inst. Met.* **56**, 275 (1935).
(10) Bethe, H. A. *Proc. roy. Soc.* A, **150**, 552 (1935).
(11) Bragg, W. L. and Williams, E. J. *Proc. roy. Soc.* A, **151**, 540 (1935).
(12) Williams, E. J. *Proc. roy. Soc.* A, **152**, 231 (1935).
(13) Peierls, R. *Proc. roy. Soc.* A, **154**, 207 (1936).
(14) Sykes, C. and Evans, H. *J. Inst. Met.* **58**, 255 (1936).
(15) Sykes, C. and Jones, F. W. *Proc. roy. Soc.* A, **157**, 213 (1936).
(16) Sykes, C. and Jones, F. W. *J. Inst. Met.* **59**, 257 (1936).
(17) Sykes, C. and Wilkinson, H. *J. Inst. Met.* (in the Press).
(18) Sykes, C. and Jones, F. W. *Proc. roy. Soc.* (in the Press).
(19) Bernal, J. *Trans. Far. Soc.* **33**, 27 (1937).

AGE-HARDENING ALLOYS

By C. H. DESCH, National Physical Laboratory

The object of this short note is merely to call the attention of physicists to certain effects observed in alloys, of great technical importance, the explanation of which will have to be sought in the properties of the lattice, and in the changes of energy with temperature in lattices composed of more than one kind of atoms. The literature of the subject is very extensive, and has been reviewed by a number of recent writers.

The effect known as age-hardening, in which an alloy, after being heated and quenched, increases in hardness either spontaneously or on heating to a temperature below that of quenching, depends on the properties of supersaturated solid solutions. In order that an alloy may show this effect, it is essential that a solid solution be formed at a high temperature, from which a second phase can separate on cooling slowly. Quenching retains the solid solution in a supersaturated condition, and reheating causes precipitation, usually in a finely divided form. A marked change in solubility with temperature is essential, but the actual amounts vary widely in different alloy systems. Thus in the iron-nitrogen system the saturated solid solution contains only 0·05 per cent N at 700° C., whilst in the iron-molybdenum alloys the im it is 35 per cent at 1440°. Usually the quantity of the precipitated phase is only a small fraction of the solvent metal, but in the alloy of atomic composition Fe_2NiAl, studied by Bradley, the two phases which separate are in equal quantity.

Prolonged heating at a temperature below that of quenching leads to softening, and when the heating has been continued until particles of the second phase have reached such a size as to be easily visible under the microscope, the maximum hardness has always been passed. The original explanation of age-hardening by Merica, Waltenberg and Scott(9) was based on these facts. It was supposed that precipitation began in the form of very minute particles, and that these agglomerated with continued heating, a certain critical dispersion, below the limits of visibility in the microscope but not otherwise defined, producing the greatest hardness. In broad outline, this view still holds good, at least for those alloys which are hardened by heating, although minor modifications have become necessary. The chief difficulties in its application have arisen in dealing with alloys which harden at atmospheric temperatures, including those light alloys of aluminium in which the effect was first discovered. The nature of the later stages, in which agglomeration and softening take place, is not disputed, but there are differences of opinion regarding the processes which occur before the appearance of detectable particles.

In most age-hardening systems, the phase which can separate on slow cooling is a compound of the two metals, or at least an intermediate phase composed of two kinds of atoms. There is, however, one important exception among alloys which have been studied in detail. This is the system copper-silver, in which hardening occurs by the separation of the pure metals. Copper and silver have identical space lattices, although their atomic diameters differ by 13 per cent, yet appreciable hardening can occur on suitable treatment. Any explanation of age-hardening must account for this simple case as well as for those in which precipitation of a new intermediate phase can occur. The hardening effect is considerable, an alloy with 6·6 per cent of copper, for instance, increasing from 50 to 140 Brinell at 250°(12).

The first objection to the simple hypothesis of hardening by critical dispersion came from determinations of the electrical resistance during the process. The quenched alloy, being a supersaturated solid solution, usually has a higher resistance than the same alloy in the annealed state, when separation into two phases is complete. Any partial separation, as required by the hypothesis of dispersion, might then be expected to cause a fall in resistance. This actually occurs with many alloys, but duralumin was found by Fraenkel(2, 3) to show an initial increase when aged at atmospheric temperature, decreasing normally later. This fact, confirmed for some other alloys, including those of aluminium with small quantities of copper, caused Konno, Fraenkel, Sachs and others to maintain that hardening was caused by the movement of dissolved atoms to new positions in the lattice, favourable to the production of molecules, but causing local strains, thus increasing both hardness and electrical resistance. Rosenhain(10) suggested that, taking the original view, the first production of ultra-microscopic particles would produce such local strains in the lattice as to account for the increase in resistance, thus to some extent reconciling the two views, as the critical dispersion might even be on a molecular scale.

The increase of resistance in the early stages of hardening is not confined to those alloys which "age" at atmospheric temperatures. It is well marked in the alloys of copper with beryllium(8), in austenite containing titanium(13) and in several systems, mentioned below, which are not usually classed as age-hardening, but in which an increase of hardness accompanies precipitation.

The maximum resistivity, when it occurs, is reached before the maximum hardness, and, as shown by Masing, Köster, and others, when various properties which change during ageing are plotted against the time, the maxima do not coincide. It has also been shown by Gayler(5) and by Cohen(14) that two maxima may sometimes be found in the hardness-time curve.

Gayler and Preston(4) regarded the process as taking place in two stages: (1) the rejection of atoms of the dissolved metal from the lattice of the solid solution, with the formation of chemical molecules in certain instances, and (2) the coagulation of these atoms or molecules to form discrete particles. A more elaborate view of the process has since been given by Gayler(5). Tammann(11) considered that the rejected atoms must collect on certain planes of the parent lattice, and that only when many neighbouring planes are so occupied can precipitation occur. This view has been confirmed by much later work by Mehl, Masing, Fink and others, which shows that the particles tend to group themselves to form minute plates or needles parallel with certain crystalline planes or directions in the parent lattice.

The main process is clearly one of diffusion. In accordance with this, when the logarithm of the time taken to reach a maximum value of a property, such as hardness, is plotted against the reciprocal of the absolute temperature, a straight line is frequently obtained(7). The initial stage of the process is, however, the reverse of diffusion (which always tends towards greater homogeneity) since it involves the segregation of certain atoms from a lattice on which they are distributed with statistical regularity. This process is not confined to age-hardening alloys, but must occur whenever one solid phase separates from another. The metallurgist, then, seeks an answer from the physicist to this question: what are the forces which lead to the expulsion of certain atoms from the lattice of a solid solution when the temperature falls to a certain point or when, the solid solution having been preserved in a supersaturated condition by quenching, the temperature is raised? (Alloys which harden at atmospheric temperature fall under this condition, as they are quenched at a lower temperature and do not harden if kept sufficiently cold, as, for instance, when quenched duralumin rivets are preserved in the soft state in solid carbon dioxide.)

The conditions are different from those of a solid crystallising from a liquid. The formation of nuclei of the solid phase by chance collisions is easily understood, but the movement of metallic atoms over a distance of many lattice spacings, making the structure less homogeneous, is more difficult to picture. It must occur very locally, since in the early stages no change in the lattice parameter can be detected by means of X rays.

In the discussion on Dr Gayler's paper(5), Prof. Mott remarked that groupings of, say, five atoms each would have a marked effect in increasing the electrical resistance of the lattice, so that the maximum resistance found in many, but by no means all, age-hardening alloys, must correspond with a very early stage in the formation of nuclei. Such nuclei once formed and the statistical uniformity of the lattice having been destroyed, local concentration gradients exist, and the rest of the process may be looked on as one of diffusion, the growth of the ultramicroscopic particles and their union to form larger masses being one which is very familiar in metallographic studies. The next question is, at what stage in the process will the greatest elastic strains be set up in the lattice, tending to increase the hardness and, to a lesser degree, the electrical resistance?

When the phase which is ultimately precipitated is composed of two kinds of atoms, as in hardening caused by $CuAl_2$, Mg_2Si, or Cu_3Be, what the chemist has been accustomed to call chemical affinity may be supposed to encourage the formation of groups approaching simple atomic ratios, but the separation of nuclei of copper from silver, or of silver from copper, cannot be accounted for in this way, yet the mechanism seems to be the same in each case. (That in the silver-copper alloys no increase in electrical resistance occurs during ageing, is probably due to the close similarity of the silver and copper atoms.) Both in the simple and in the complex examples, the separation occurs along the most closely packed planes in the lattice, and, in those alloys which have been examined in detail, in such a way that the new phase, when formed, is produced with a minimum rearrangement on those planes, so producing *Widmanstätten* structures on a small scale.

There is reason to believe that nuclei of appreciable size exist long before a change in the parameter can be detected by X rays. It must be emphasised that the segregations are very local, leaving the greater part of the lattice unchanged. Such changes in the quantity of background scattering as have been recorded are consistent with such a picture of the process. It is remarkable that chemical methods seem to be capable of detecting an earlier stage. It was first noticed that in the hardening of the beryllium-copper alloys the etching properties were altered at a very early stage, so that, although no separate particles could be seen under the microscope, lines parallel with (111) planes darkened on etching, producing a fine network, indicating a precipitation of ultra-microscopic particles. The same thing is seen in silver-copper alloys, and it is probably responsible for the characteristic etching properties of martensite in steels. That it could not be seen in the light alloys of aluminium was used as an argument for the special character of the hardening process in them, but the writer has always attributed its absence to the lack of delicacy of the methods in use for etching aluminium. Fink and Smith(1) found that in a light alloy containing 5 per cent of copper, precipitation could be seen after heating for an hour at 100°, whilst 34 hours at that temperature were required to produce a measurable change in the lattice parameter. Even at atmospheric temperature precipitation could be seen after three months, which is of course much longer than is needed to produce hardening, but indicates that the process is of the same kind as at higher temperatures. Aluminium containing magnesium gave similar results.

This hurried survey of the age-hardening problem leaves out many complications—the effects of heating to a higher temperature after partly ageing at a lower, and so on—but it is suggested that the mechanism of age-hardening may not be very complex. The original theory was probably too simple, in that it considered only changes in the sizes of the dispersed particles, and did not take account of how those particles came into existence, but in the writer's view it remains essentially true, although the critical dispersion must now imply a stage earlier than that at which it is proper to speak of a distinct phase. The work on order-disorder changes has made us familiar with systems in which local rearrangements can occur without producing a second phase in the ordinary sense.

The complex changes in age-hardening may then be due only to the progressive growth of nuclei formed by the rejection of certain atoms from the lattice. The electrical resistance seems to be most affected by the formation of groups of only a few atoms, the hardness by groupings of a rather larger size, and so on. (The subsequent fall of resistance and later of hardness as the groups grow larger presents no difficulty.) Effects on the magnetic properties are not produced until still later(15, 16). It is the initiation of the process, as mentioned above, that is difficult to picture, on which the advice of physicists is sought. The next problem is that of applying to age-hardening systems the same quantitative treatment that has proved successful in dealing with order-disorder transformations (Bragg and Williams, Borelius, Peierls, Sykes, etc.), so that it may be possible to predict the behaviour of a given system under given conditions of supersaturation.

A new phase separating from a solid solution does not always assume a dispersed form. The α phase in brass, for instance, separates on cooling the supersaturated β solid solution in large crystals. Nevertheless, it must pass through the preliminary stage of forming minute nuclei, and in its behaviour it then closely resembles an age-hardening system(6) although its supersaturated solid solution has a lower, and not a higher, electrical resistance than the two-phase system which is ultimately formed. It would seem that in these alloys the growth of nuclei to form distinct crystals is very rapid. Differences in what may be called the crystal habit of the precipitated particles account for many differences between alloys, and the reasons for such differences must be sought in the mechanism of the separation of the original particles and their subsequent growth.

REFERENCES

(1) Fink, W. L. and Smith, D. W. *Metals Technology*, **3**, (4) (1936); *Tech. Publ. Amer. Inst. Min. Engrs*, No. 706.
(2) Fraenkel, W. and Scheuer, E. *Z. Metallk.* **12**, 427 (1920).
(3) Fraenkel, W. and Seng, R. *Z. Metallk*, **12**, 225 (1920).
(4) Gayler, M. L. V. and Preston, G. D. *J. Inst. Met.* **41**, 191 (1929).
(5) Gayler, M. L. V. *J. Inst. Met.* **60**, 55 (1937).
(6) Hansen, M. *Z. Phys.* **59**, 466 (1930).
(7) Jenkins, C. H. M. and Bucknall, E. H. *J. Inst. Met.* **57**, 141 (1935).
(8) Masing, G. *Arch. Eisenhüttenw.* **2**, 185 (1928–9).
(9) Merica, P. D., Waltenburg, R. G. and Scott, H. *Sci. Pap. U.S. Bur. Stand.* No. 347 (1919).
(10) Rosenhain, W. *Chem. metall. Engng*, **28**, 899 (1923).
(11) Tammann, G. *Z. Metallk.* **22**, 365 (1930).
(12) Ageew, Hansen and Sachs. *Z. Phys.* **66**, 350 (1930).
(13) Hensel, *Trans. Amer. Inst. Min. Engrs.* **95**, 255 (1931).
(14) Cohen, M. *Metals Technology*, 1936, **3** (7); *Tech. Publ. Amer. Inst. Min. Engrs*, No. 751.
(15) Koster, *Arch. Eisenhüttenw.* **2**, 503 (1928–9).
(16) Eilender, Fry de Gottwald. *Stahl u. Eisen*, **54**, 554 (1934).

DISCUSSION OF THE PAPERS BY BORELIUS, BRAGG, DESCH

Reported by N. F. MOTT

In the discussion Prof. Bragg emphasized the contrast between the order-disorder change, which extends over a finite range of temperatures, and the change from liquid to solid, which is sharp. He drew the attention of the conference to some speculations by Bernal* which attempt to show that intermediate states between liquid disorder and crystalline order would have very high energy and therefore do not occur.

Prof. Simon did not agree with Bernal's conclusion that no intermediate phase between solid and liquid can exist.

Both Prof. Fowler and Prof. Bragg were critical of Prof. Borelius' use of the free energy diagram in his discussion of hysteresis in the segregation process (Borelius, § 10). A rough calculation by Prof. Bragg of the life-time of the metastable states envisaged by Borelius suggested that it should be considerably less than 1 sec.

An extension of Bethe's theory of the order-disorder transition by Fowler and Chang to include interaction between next nearest neighbours was announced (to be published). Dr Sykes reported some new measurements of the heat content of CuZn up to the critical temperature, which agreed better with the new calculations than with the old; the new theory contains however an arbitrary parameter. A theory by Mott† of the nature of the ordering force also gives some indication of the shape of the specific heat-temperature curve.

Dr Sykes also reported measurements of the heat content of MgCd, which shows a latent heat at the critical temperature, in disagreement with the theoretical expectations, and also for Cu_3Pd, which does *not* show the latent heat to be expected for an alloy where the two constituents are present in unequal amounts. This may be connected with the change of structure which takes place for this alloy at the critical temperature.

In connexion with Prof. Borelius' measurements of the resistance of nickel, Dr Potter mentioned some recent measurements of his own (to be published shortly in *Proc. phys. Soc.*)

Dr Bradley gave an account of his investigations on the ternary alloys of the system FeNiAl. For certain compositions, alloys of this system would, if cooled slowly, crystallize out as a two-phase system, *both* phases having the same body-centred cubic lattice structure but with very slightly different lattice spacing, so small that it is very difficult to detect by X-ray methods. One of the two phases is magnetic, the other is non-magnetic and shows a superstructure.

---

* *Trans. Faraday Soc.* **33**, 27 (1937).

† *Proc. phys. Soc.* **49**, 258 (1937).

If the alloy is cooled quickly (quenched) a single phase only is obtained. But if the alloy is cooled at a moderate rate, regions of undetermined size (say a hundred to a thousand atoms in length) form in the crystal, having the composition of one or other of the two phases that will eventually crystallize out, but arranged in a *single* body-centred lattice; they have not yet broken away and formed separate crystals with their individual lattice parameters. These regions must thus be highly strained; for their lattice parameters must necessarily be those of the parent lattice (i.e. the quenched alloy), whereas they would be in equilibrium only with different values of the parameters. Dr Bradley ascribed the properties which these alloys have as permanent magnets to this state of strain.

Prof. Bragg stated that the dispersion responsible for age hardening mentioned by Dr Desch must be understood in this way: groups of atoms having the compositions of the phases that eventually crystallize out would form, while still keeping to the old lattice. This would set up strains, and so produce hardening. The second process would be when these groups broke away from the parent lattice; this would decrease the internal strain, and thus the hardness.

Dr Peierls asked why the phase which is precipitated forms crystals with a plate-shaped structure parallel to a definite set of crystallographic planes. Two explanations seemed possible. The crystals might tend to form at internal surfaces of misfit, or cracks; this was favoured by Dr Desch. Prof. Bragg, on the other hand, considered that a given volume of a new phase could crystallize out with less strain to the surrounding medium if it took a plate-like structure than if it were, for example, round. He cited the case of felspar, which, if cooled, breaks up into bands containing alternately an excess of Na and of K. In this way the least strain is produced.

PART III

CONDUCTION IN THIN METALLIC FILMS

THE STRUCTURE OF THIN METALLIC FILMS

By G. I. FINCH

The object of this paper is to draw attention to those structural features which are likely to give rise, at least in part, to the abnormally low conductance associated with thin metallic films(1). The more usual methods for preparing such films in reasonably uniform thickness are (i) cathodic sputtering, (ii) condensation from the vapour *in vacuo*, (iii) chemical deposition and (iv) evaporation of a colloidal solution. Beaten leaf is generally too thick and irregular to be of use in conductivity measurements, and although electrodeposits can usually be freed from the basis metal their further transfer without injury to a non-conducting substrate is difficult.

Electron diffraction has become the most searching method for the study of the structure of thin metallic films. In addition to revealing crystal structure and orientation, electron diffraction will generally afford some indication of other features which are often of too fine a detail to be seen under the microscope, such as crystal size and shape and the nature of the film surface texture.

Consider, for example, the pattern (figure 1) obtained with the electron beam at grazing incidence from a bismuth film electrodeposited on to a polished copper surface. We see that (i) the film is polycrystalline; (ii) the crystals are unorientated; (iii) the pattern dimensions agree with the known structure of bismuth; (iv) the absence of ring-broadening due to refraction towards the central spot shows that the diffraction rings are formed by transmission; thus the diffracting portions of the crystals must project above the surface; (v) the ring definition suggests a size of effectively diffracting crystal projections exceeding 100 A. in directions normal to the beam but, in view of the clearness of the pattern and absence of general background, not exceeding about 200 A. in the beam direction; (vi) the granulated appearance of the rings shows that a relatively small number of crystal projections are diffracting, which suggests that the crystals are large enough to be seen in the microscope. Thus we can picture the general structure of the bismuth film as consisting of disordered array of fairly large crystals terminating in spikes projecting above the mean level of the surface, an impression which would be confirmed if a sharp and strongly granulated ring pattern were obtained by transmission through the film after its being detached from the substrate. It will readily be seen that if the average thickness of the film were only 10 A., the actual crystals could not cover more than one-tenth of the surface, and the film would be discontinuous apart from small areas of contact between neighbouring crystals. Electron diffraction shows that the structure of very thin metallic films with an average thickness of the order of 50 A. and less is in general of this type.

Again, from figure 2, yielded by a platinum fibre sputtered in argon on to a polished glass disk, we see that the platinum crystals are strongly orientated with a cube face parallel to the substrate. The increase in width of the arcs which occurs as the pattern centre is approached is evidence of a refractive effect and shows that the pattern has been formed partly by reflection, i.e. entry and exit of the beam through the same flat crystal faces, in this case (001) faces; since the individual diffractions are not wholly displaced but are spread out between the normal and refracted positions, it is clear that diffraction through projecting crystalline spikes of a wide range of acuteness also occurs. The same film by transmission with the beam normal to the surface gives a complete ring pattern in which the *hk0* diffractions are abnormally strong. The rings show no signs of granulation and their width is such as to suggest a mean crystal size of the order of 50 A.

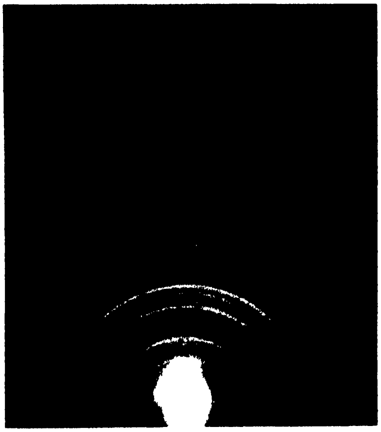

Figure 1.

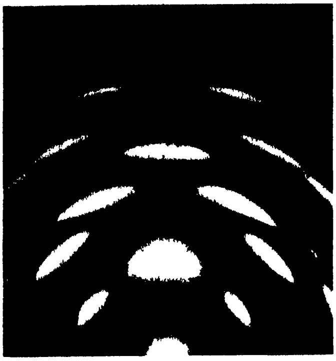

Figure 2.

Caution is necessary in the estimation of crystal size from ring-breadth, especially in the case of reflection patterns. Thus, suppose a metal film of uniform thickness be deposited on a plane surface, the diffraction rings will be very broad, even though the crystals may be large, provided the deposit crystals form such obtuse-angled projections that only a small extent of each projection is thin enough to contribute to the diffraction of the beam. In such a case, if the film is sufficiently thin, a transmission pattern will give a better idea of the crystal size, and will confirm whether the diffuseness of the rings of the reflection pattern is due to the obtuseness of the crystal projections or to small crystals. On the other hand, a reflection pattern is likely to give a better impression of the particle size if the substrate surface be spiky and is more or less uniformly covered by the deposit.

Several workers(2) have ascribed the anomalous conductivity of thin films, prepared as a rule by cathodic sputtering or evaporation, to their supposed amorphous nature. Electron diffraction results negative this view; thus it has been found generally that cathodically sputtered and evaporated metallic films are invariably crystalline, even when deposited at liquid-air temperatures(3). There is, however, a pronounced tendency for the crystal size to increase with the temperature of the substrate during deposition. Sputtered films often contain occluded gas, or the metal may even combine with gas in the process of deposition, though by sputtering in carefully purified argon this effect can be reduced(4). The presence of gas in sputtered films no doubt explains the disappearance of the reflection diffraction pattern from sputtered platinum films during heating *in vacuo*, a result which was first attributed by Finch and Ikin to a reduction in crystal size. More recent experiments in which such heated platinum films were floated off the glass or quartz substrate by a weak solution of hydrofluoric acid revealed, however, a well-developed crystal structure, in that the films yielded sharp ring patterns on transmission. Hence it seems clear that the fading of the initial reflection pattern with heating must have been due to a collapse of the projecting diffracting crystal spikes as a result of the evolution of gas occluded during sputtering, a view which is confirmed by the fact that we have found that platinum films formed by evaporation *in vacuo* give reflection patterns which are virtually unaffected by heating. In view of the uncertainties introduced by the presence of occluded, and often also by combined, gas, sputtered films can hardly be regarded as suitable for critical conductivity determinations.

The structure of films condensed *in vacuo* may be profoundly affected by the nature of the substrate. A pseudomorphic lattice change has only been observed in the case of metals of similar lattice constants and crystal structure in contact as substrate and deposit, and this complication from the point of view of conductivity measurements is therefore easily avoided. Crystalline substrates consisting of natural or cleavage faces of ionic single crystals are rarely, if ever, sufficiently smooth, and in addition they often exert very strong orientating effects. For example, most metals deposited on a suitably heated rock-salt cleavage surface are strongly orientated and may even form single crystal sheets with an orientation governed by the substrate(5). In view of the difference between the metal and rock-salt lattice dimensions it is most unlikely that such sheets are true single crystals; more probably they consist of a mosaic of small crystals of like orientation. Further, in the case of rock-salt and similar cleavage surfaces, it is a moot point as to how far the substrate mosaic structure, cleavage striations and cracks may affect the continuity of the deposit film. On the other hand, extremely smooth non-conducting substrate surfaces, free in all probability from surface flaws and cracks, can be obtained by polishing; for example, the diffraction patterns obtained from polished diamond, quartz, sapphire and many other surfaces are such as to suggest that they are exceedingly smooth and crystalline, whilst polished fused quartz, glass, spinel and other surfaces give patterns which are characteristic of a liquid or vitreous surface(6).

While the orientation which occurs in a deposit formed on a single crystal surface may easily be complete in the sense that both directions of orientation of the deposit are controlled by the structure of the substrate, a twofold orientation has apparently never been observed on a vitreous surface, although an alignment of the deposit crystals with one plane parallel to the substrate surface is so often noticed as to be the rule rather than the exception, particularly if the substrate was suitably heated during deposition.

It frequently happens that the useful life of a thin metallic film ends with the appearance of a fine network of cracks which in some cases may be due to a differential expansion as between deposit and substrate, and in others to contamination of the deposit by traces of organic materials(7). Recent electron diffraction work has shown how easily contamination can occur with greases and mercury vapour(8); hence in the preparation of thin metallic films for conductivity purposes the greatest possible care should be taken to eliminate such impurities. Lovell's(1) recent experiments have shown the great gain in reproducibility of results which follows when proper precautions are taken to eliminate such impurities and gas adsorption. Some workers have observed deviations from the normal lattice constants in thin films. Thus Riedmiller and Cosslett(9) found such an effect with indium and attributed it to gas occlusion: and Quarrell(10) has found similar deviations of lattice dimensions to be general in the initial layers of a deposit and, in the case of face-centred-cubic metals, attributed this to a gradual transition from a hexagonal close-packing of the atoms first deposited to the normal face-centred-cubic packing.

Ample evidence has been obtained for the rapid oxidation of evaporated metal films on exposure to air. Thus Finch and Quarrell(11) found such oxidation with zinc and magnesium, Beeching(12) with aluminium and copper, Riedmiller(9) with nickel, and Nelson(13) with iron. Thin metal films, especially when prepared by evaporation, are much more prone to oxidation than the surface of the metal in bulk. Beeching considers that oxygen may be taken up from the surface of the substrate, where it is present as an absorbed layer; this points to the importance of careful cleaning and degreasing of the substrates employed.

To sum up: For conductivity experiments it would seem advisable to use suitable highly-polished non-conducting substrates. Deposition should be carried out in a high vacuum, the necessary precautions being taken to prevent contamination by either grease, mercury or gas. Wide temperature fluctuations of the substrate should also be avoided both during preparation and use. It should not be difficult to determine the resistance of a film *in vacuo* and thus eliminate errors and uncertainties arising from gas adsorption or compound formation.

REFERENCES

(1) FÉRY, A. *J. Phys. Radium*, **4**, 301 (1933); *Ann. Phys.*, Paris, **19**, 421 (1933).
JAGERSBERGER, A. *Z. Phys.* **87**, 513 (1934).
DEUBNER, A. *Ann. Phys.*, Lpz., **20**, 449 (1934).
BOSWORTH, R. C. L. *Trans. Faraday Soc.* **30**, 549 (1934).
TOWNES, E. and ROLLER, D. *Phys. Rev.* **47**, 197 (1935).
MURMAN, H. *Z. Phys.* **89**, 426 (1934).
KRAMER, J. *Ann. Phys.*, Lpz., **19**, 37 (1934).
JOHNSON, M. C. and STARKEY, T. V. *Proc. roy. Soc.* A, **140**, 126 (1933).
LOVELL, A. C. B. *Proc. roy. Soc.* A, **157**, 311 (1936); *Proc. phys. Soc.* **49**, 89 (1937).
APPLEYARD, E. T. S. and LOVELL, A. C. B. *Proc. roy. Soc.* A, **158**, 718 (1937).
SUHRMANN, R. and BERNDT, W. *Phys. Z.* **37**, 146 (1936).

McLennan, J. C., Burton, A. C., Pitt, A. and Wilhelm, J. O. *Proc. roy. Soc.* A, **138**, 245 (1932).
Misener, A. D. and Wilhelm, J. O. *Trans. Roy. Soc. Canada*, **29**, 5 (1935).
Misener, A. D., Wilhelm, J. O. and Smith, H. G. *Trans. Roy. Soc. Canada*, **29**, 13 (1935).
Cosslett, V. E. *Proc. phys. Soc.* **49**, 121 (1937).
(2) Zahn, H. and Kramer, J. *Z. Phys.* **86**, 413 (1933).
Suhrmann, R. and Berndt, W. *Phys. Z.* **37**, 146 (1936).
(3) Hass, G. *Naturwissenschaften*, **25**, 232 (1937).
(4) Finch, G. I., Murison, C. A., Stuart, N. and Thomson, G. P. *Proc. roy. Soc.* A, **141**, 414 (1933).
Finch, G. I. and Ikin, A. W. *Proc. roy. Soc.* A, **145**, 551 (1934).
(5) Lassen, H. *Phys. Z.* **35**, 172 (1934).
Kirchner, F. and Lassen, H. *Ann. Phys.*, Lpz., **24**, 113 (1935).
Bruck, L. *Ann. Phys.*, Lpz., **26**, 233 (1936).
Cochrane, W. *Proc. phys. Soc.* **48**, 723 (1936).
(6) Finch, G. I. *Nature*, Lond., **138**, 1010 (1936).
(7) Tanaka, S. *Rep. Aero. Res. Inst. Tokyo*, **11**, 369 (1936).
(8) Mark, H., Motz, H. and Trillat, J. J. *Naturwissenschaften*, **20**, 319 (1935).
Aylmer, A. E., Finch, G. I. and Fordham, S. *Trans. Faraday Soc.* **32**, 864 (1936).
(9) Riedmiller. *Z. Phys.* **102**, 408 (1936).
Cosslett, V. E. *Proc. phys. Soc.* **49**, 121 (1937).
(10) Quarrell, A. G. *Proc. phys. Soc.* **49**, 279 (1937).
(11) Finch, G. I. and Quarrell, A. G. *Proc. roy. Soc.* A, **141**, 398 (1933).
(12) Beeching, R. *Phil. Mag.* **22**, 938 (1936).
(13) Nelson, H. R. *J. chem. Phys.* **5**, 252 (1937).

SOME FACTORS INFLUENCING THE RESISTANCE OF THIN METAL FILMS

By E. T. S. APPLEYARD

§ 1. INTRODUCTION

A CONVENIENT summary of the early work on thin metallic films, performed prior to 1928, is provided by Bartlett(1). The observations varied profoundly not only from one worker to another but also in the experiments of the same investigator performed under similar experimental conditions. As a result of these discrepancies, which arose partly from primitive technique and partly from uncontrolled factors whose importance was not then understood (condition and temperature of the substrate, adsorbed gas, etc.), various *ad hoc* hypotheses were produced to explain particular experiments and little advance was made towards obtaining experimental conditions which would give consistent and reproducible results. It would be useless to add to the already copious literature of speculation upon these early observations. This review is, therefore, confined to enunciating briefly and attempting to explain some of the chief experimental observations on the resistance of thin metal films prepared by evaporative deposition in a good vacuum. This method of preparation curtails considerably the number of arbitrary factors which can influence the resistance of the films; and in particular it gives some hope of minimising, if not eliminating, the effects due to adsorbed gas.*

§ 2. TYPICAL EXPERIMENTAL RESULTS

A usual and important type of experiment consists in allowing a calibrated beam of metal atoms to fall upon a cooled surface. Suitable electrical contacts allow the resistance of the film to be measured at frequent intervals as the deposition proceeds, and in this way the relationship between the nominal resistivity† and the nominal thickness† of the film can be obtained experimentally.

Typical of the results obtained by evaporation are those of Reinders and Hamburger(2). These workers paid attention to the temperature of the depositing surface and they worked in a tolerable vacuum probably of the order of 10^{-6} mm. of mercury. (Nevertheless the apparatus could not be properly baked out since it contained greased joints.) The thickness of the deposits was obtained by chemical estimation of the evaporated silver, thus avoiding recourse to speculative formulae which have been used in certain cases.

---

* Nevertheless, even in the best available vacuum, say 3×10^{-8} mm. of mercury, 10^{13} atoms per second strike every square cm. of the internal surface of the apparatus if the residual gas is oxygen. This rate is quite comparable with the rate of condensation of metal atoms in most experiments.

† The nominal thickness of a film is the thickness calculated from the expression $t = m/\rho$ where m = mass of metal per unit area. It only coincides with the geometrical thickness when the film is uniform and has the same density as the bulk metal. The nominal resistivity is calculated by assuming that the nominal thickness is in fact the true thickness. Where we refer to "thickness" and "resistivity" without qualification they are assumed to be derived in this way.

Figure 1, copied from the paper of Reinders and Hamburger, shows the results obtained for silver. Ordinates are logarithms of nominal resistivity in ohm-cm., abcissae are logarithms of the thickness in multiples of 10^{-7} cm. Curve a_3b_3 is the resistivity of silver deposited at room temperatures (300° K.), a_1b_1 deposition at 88° K., a_2b_2 the {resistivity, thickness} relation of films deposited at 88° K. and afterwards raised to room temperatures. For comparison the results of earlier workers are also sketched in; Vincent⁽³⁾ (chemical deposition, 1901); Pogany⁽⁴⁾ (sputtered films, 1916); Weber and Oesterhuis⁽⁵⁾ (evaporation, 1916).

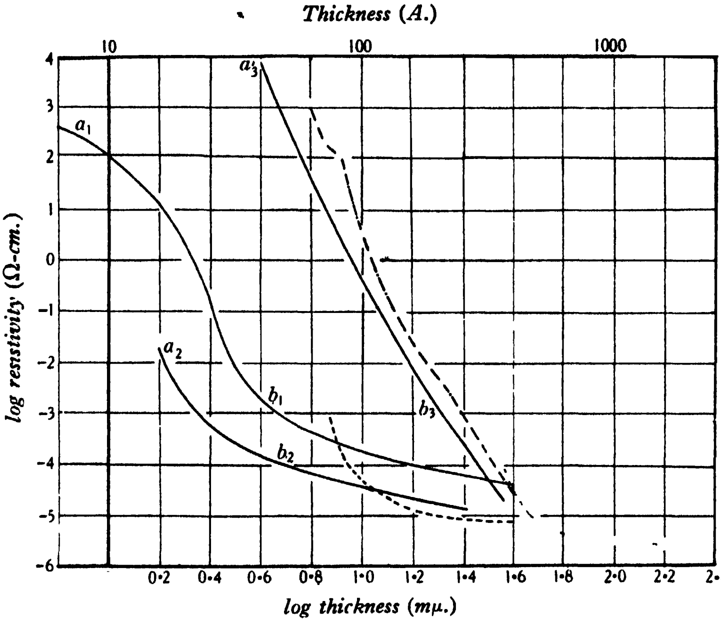

Figure 1. •—•—•—Weber-Oesterhuis; ———— Pogany; •••••• Vincent.

It will be seen that Reinders and Hamburger were successful in obtaining detectable conductivity at only 6 A. thickness, or about two atomic layers. Nevertheless two important features stand out characteristic of all previous work on thin films.

The first is that the resistivity of films less than 100 A. in thickness is from 10^7 to 10^3 times that of the metal in bulk. The second is that the resistivity of the films alters irreversibly on heat treatment by a factor of about ten. Also deposition at 300 K. gives conductivity only at nominal thicknesses greater than 40 A. Reinders and Hamburger suppose that granulation of the film at the higher temperature accounts for this delayed conductivity, but they assume other causes to account for the high resistance of films deposited at 88° K. Before discussing the evidence for their interpretation we propose to describe in brief the results of certain experiments recently carried out in this laboratory on thin films of the alkali metals. These results we believe to be interesting from two points of view: Firstly, because we believe that they are the only metal films ever prepared which can be obtained completely coherent in layers less than 50 A. thick; secondly, because by suitably varying the experimental conditions we have been able to prepare films of any resistivity desired from the extremely low value shown by the coherent films to values 10^5 times greater. We advance reasons for believing that these high resistivities are due to granulation or agglomeration of the film, and that agglomeration may account for both the delayed conductivity and the high resistivity of films prepared by many other workers, though further experiments are needed to decide definitely upon this point.

§ 3. LOW-RESISTANCE FILMS OF THE ALKALI METALS

The experimental methods of preparing these films are fully described in the papers of Lovell(6) and Appleyard and Lovell(7), so it will be sufficient to summarize the chief features of the apparatus and the experimental results.

The apparatus consisted of a molecular gun constructed of pyrex. The stream of atoms from the gun, suitably defined by cooled slits, struck a surface of pyrex glass which could be held at any temperature between 64° K. and 90° K. Here they formed a square patch overlapping end contacts of colloidal graphite spread upon a layer of platinum paint which had previously been burnt into the glass. Prior to any experiment the whole apparatus was baked out at 500° C. for several hours and carefully outgassed alkali metal was then distilled into the oven. The residual pressure varied between 5×10^{-7} mm. of mercury and 5×10^{-8} mm. of mercury and was usually near the lower limit. The results described below were not apparently at all sensitive to variations of this residual pressure.

A continuous series of resistance measurements carried out during and after the deposition showed always the same general character in the case of all the alkali metals. The resistance and the resistivity of the film fell steadily as the thickness of the layer increased. On stopping the deposition the resistance did not remain constant as was to be expected, but rose smoothly so as to increase by a factor of ten or more when the condensing surface was kept at 90° K.

But in the early experiments with rubidium, a consistent value could be obtained at first neither for the value of the resistance nor for the subsequent increase of resistance after deposition was stopped, and a series of experiments carried out under apparently the same conditions gave extravagantly different results, varying by factors of many hundred. The residual pressure and small variations of beam intensity proved to have no critical effect, and it was not until a casual observation forced upon our attention the important role of the surface conditions of the substrate that we were able to obtain consistent results. In Lovell's paper the technique of prolonged local baking necessary to produce a standard surface, upon which results consistent to 3 per cent could be obtained, is fully described.

The general character of the anomalies observed is best illustrated by showing the effect of deliberate contamination upon a surface previously baked to the standard state. Figure 2*a* reproduced from the *Proceedings of the Royal Society*(6) shows the effect of CO_2 contamination upon a standard surface. The pressure in the apparatus was raised to 10^{-6} mm. of CO_2. The pressure was held at this value for some minutes, evolution of CO_2 was stopped, and as soon as the vacuum had reached its original value a distillation was commenced. Throughout the process the surface and defining slits were held at 90° K. The first distillation after this treatment gave no conductivity after 30 min. distillation of rubidium at the rate of $3{\cdot}18 \times 10^{12}$ atoms per cm^2 per sec.

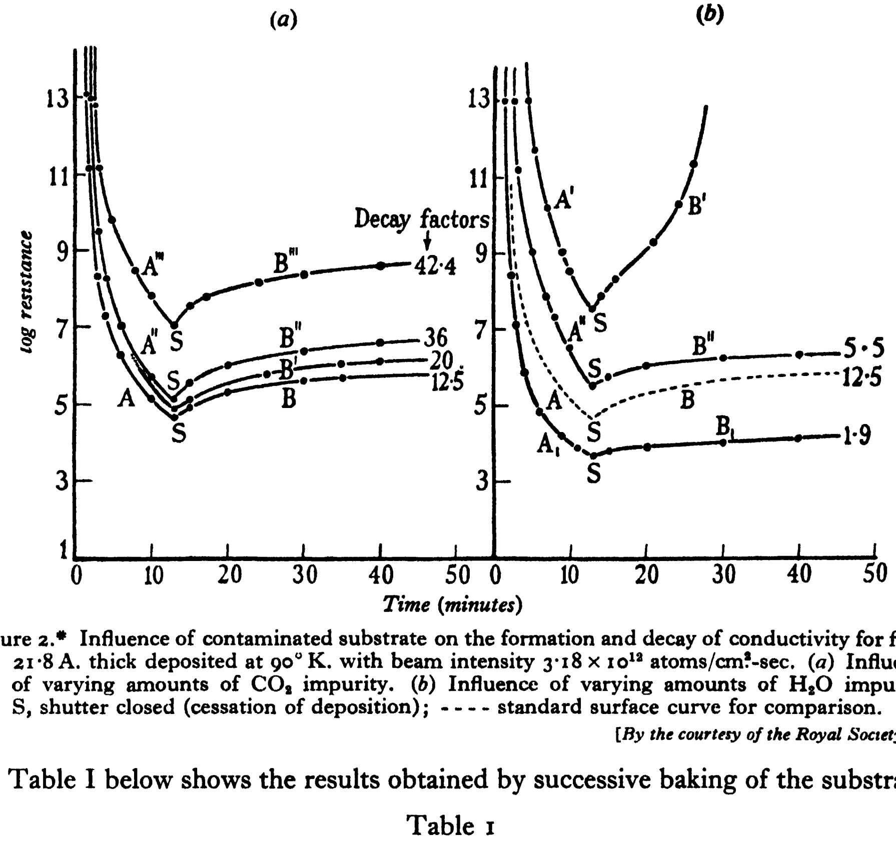

Figure 2.* Influence of contaminated substrate on the formation and decay of conductivity for films 21·8 A. thick deposited at 90° K. with beam intensity $3{\cdot}18 \times 10^{12}$ atoms/cm^2-sec. (a) Influence of varying amounts of CO_2 impurity. (b) Influence of varying amounts of H_2O impurity. S, shutter closed (cessation of deposition); ---- standard surface curve for comparison.

[By the courtesy of the Royal Society

Table I below shows the results obtained by successive baking of the substrate.

Table 1

Experimental curve	Total baking time before distillation (hours)	Remarks
A''' B'''	1	
A'' B''	20	
A' B'	40	
AB	80	Identical with results obtained on standard surface

The numbers to the right of the curves are the so-called decay factors, an arbitrary measure of the instability of the films. The factor is defined as $\Delta R/R$ where ΔR is the change in resistance during the half hour after stopping distillation, and R

---

* The decay factors are inserted at the right-hand side of all decay curves.

is the resistance when the deposition is stopped. The most important feature of the curves is their steady alteration as the heat treatment is continued, and the fact that they converge finally to the value characteristic of the standard surface after prolonged heat treatment of the surface.

Figure 2*b* represents the results of a series of experiments when water vapour and not CO_2 was the contaminating agent. $A'B'$, $A''B''$ represent successive curves obtained at different stages of the baking. The final steady state of the surface gave the curve A_1B_1 after prolonged baking, i.e. a lower resistance and a smaller decay factor than the standard surface which gave the dashed curve AB. Evidently the surface was permanently altered by its previous treatment and no subsequent baking ever restored it to the standard state. Probably rubidium hydrate was produced which gradually soaked into the glass.

These experiments forcibly draw attention to the manner in which the whole history and properties of an alkali metal film are determined by the surface condition of the substrate upon which the metal is distilled. We may now turn from these contaminated surfaces to discuss the results of investigations upon the clean standard surface prepared by prolonged baking.

§4. PRODUCTION OF STABLE AND COHERENT FILMS

A series of experiments carried out with rubidium deposited upon the standard pyrex surface cooled to various temperatures led to the following general conclusions:

(1) For metal films of the same nominal thickness deposited at the same rate, the decay factor diminished as the temperature was reduced, and parallel with this diminution of the decay factor the resistance also fell.

(2) The decay factor diminished as the nominal thickness of the film increased for deposition at a given temperature.

(3) By deposition at 64° K. (the lowest temperature available in the experiments) it was found possible to prepare completely stable films provided the nominal thickness exceeded 40 A. These films remained stable when afterwards raised to 90° K. though a film of this nominal thickness deposited at the higher temperature had the large decay factor of 3·5.

Figure 3 summarizes the results for rubidium.

Potassium and caesium give results of the same general character, except that potassium films were less stable and caesium films more stable than those of rubidium. The case of caesium is particularly interesting, for in this case by deposition at 64° K. stable films of nominal thickness only 5·7 A. were obtained. It was, however, not possible to determine the temperature coefficients of films as thin as this since they began to decay slowly when raised to 90° K. Another curious anomaly exhibited by the caesium films, in which they differ completely from those of potassium and rubidium, is that when deposited at any definite temperature the stability appears to be greater for films of 5·7 A. than it is for those of 24 A. After this thickness the films become more stable again as the thickness increases.

§ 5. RESISTIVITIES OF THE STABLE FILMS

The most obvious peculiarity of these films as compared with those prepared by all previous workers is their low resistivity at thicknesses below 100 A. For example, reference to figure 1 of this account shows that the silver films prepared by Reinders and Hamburger[(2)] had resistivities more than 1000 times those of the bulk metal at a thickness of 40 A. Caesium films of this thickness deposited at 64° K. had only 5 times the resistivity of the bulk metal. Figure 4 below is a graph showing experimental resistivities plotted against nominal thickness for caesium deposited at 64° K. (full curve). Conductivity was first detectable at a nominal thickness of only 0·35 A. or 0·06 atomic layers. These facts lead us to believe that perhaps the films could be regarded to a first approximation as coherent slices of a crystalline, or polycrystalline, metal and that their resistivities (which were still higher than those

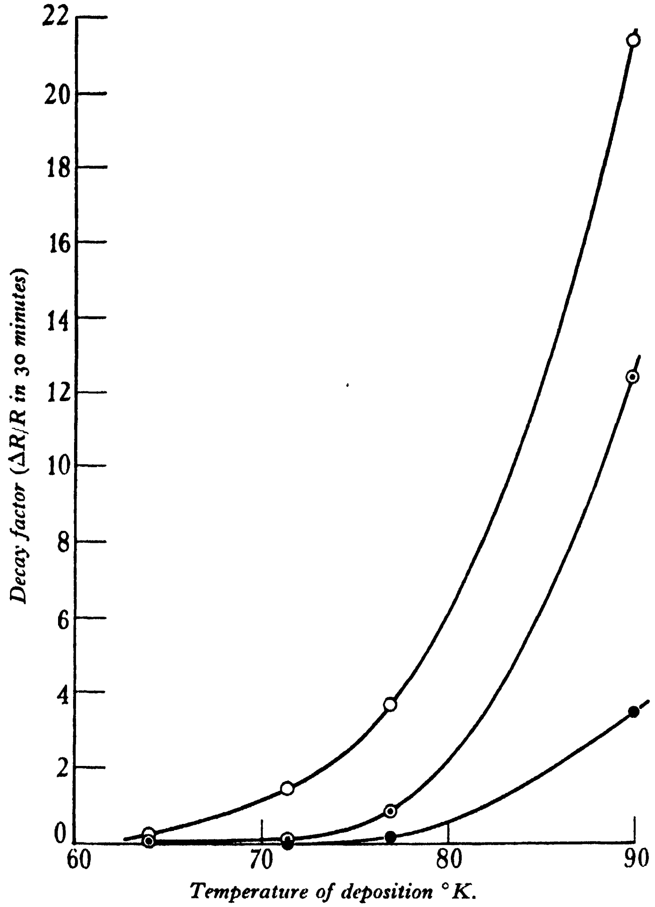

Figure 3. Decay factors as a function of the temperature of deposition for films of a given thickness deposited with beam intensity 3·18 × 10^{12} atoms/cm²/sec. ○ 4·4 A.; ⊙ 21·8 A.; ● 43·6 A.

[*By the courtesy of the Royal Society*

of the bulk metal) could be accounted for by assuming that the mean free path of the conduction electrons was effectively shortened by collision with the boundaries; an idea originally due to J. J. Thomson⁽⁸⁾, who gave a formula for the resistivity to be expected.

Hamburger⁽⁹⁾ had already applied Thomson's formula to much thicker films than this. His calculations contain so many qualifications that they cannot be said to show more than a sudden rise of resistivity when the thickness of the film became comparable with the mean free path calculated on his assumptions. In any case, Thomson's formula was not applicable to our films, for in all cases the thickness here is very much less than the mean free path in the bulk metal, and Thomson took no account of the fact that, under these circumstances, most of the collisions will take place at the boundaries.

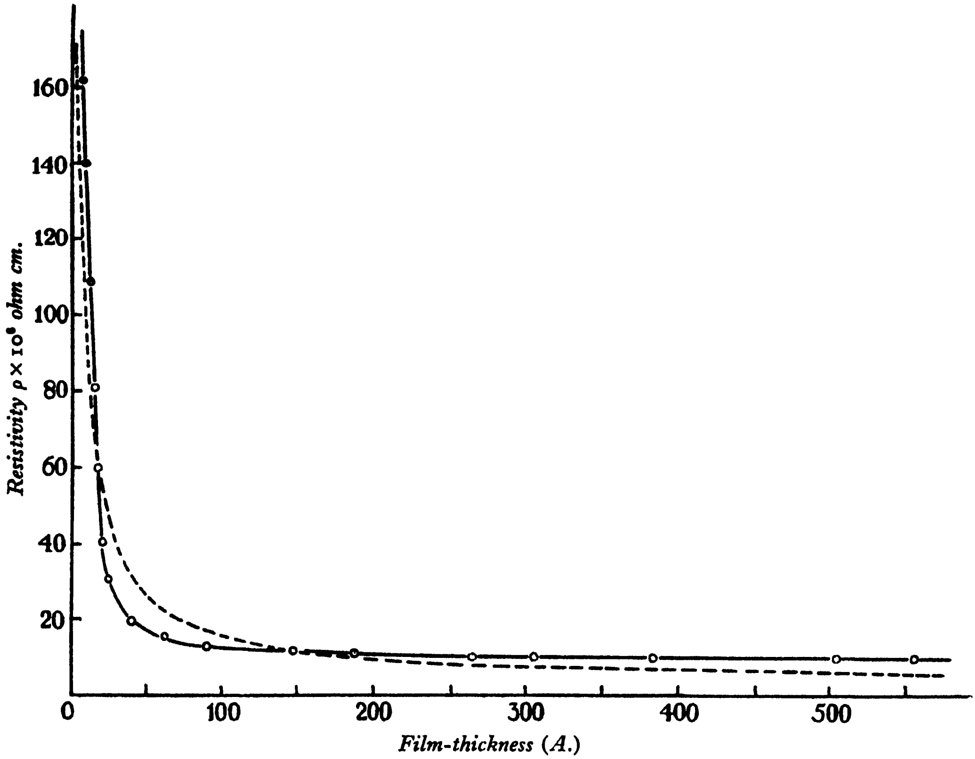

Figure 4. Theoretical - - -, and experimental ⊙. Resistivity/thickness curves up to 550 A. for a caesium film deposited at 64° K.

[*By the courtesy of the Royal Society*

A modified formula⁽⁶⁾ with which we have compared our results is

$$\frac{\sigma_t}{\sigma_\theta} = \frac{t}{\lambda_\theta}\left(1 + \log\frac{\lambda_\theta}{t}\right) \qquad \text{......(1)},$$

where σ_t is the resistivity of the film and σ_θ that of the bulk metal at the same temperature θ. λ_θ is the mean free path in the bulk metal, and may be deduced from the observed resistivity by the formula$^{(10, 11, 12)}$

$$\frac{1}{\sigma}=\frac{Ne^2}{m}\frac{2\lambda_\theta}{v},$$

where N is the number of electrons (atoms) per unit volume and v the velocity of the electrons, given by

$$v=\frac{h}{2m}\left(\frac{3N}{\pi}\right)^{\frac{1}{3}}.$$

The formula is derived making two assumptions: firstly that $t \ll \lambda_\theta$, and secondly that all collisions of the electron with the sides of the film are inelastic. The values of λ_θ are, using accepted values for the resistivity of the bulk metal, 1980 A. at 90° K. in rubidium, 1450 A. at 64° in caesium. All the films described here are less than 500 A. thick, though work with caesium films up to 12,000 A. is in progress (Lovell).

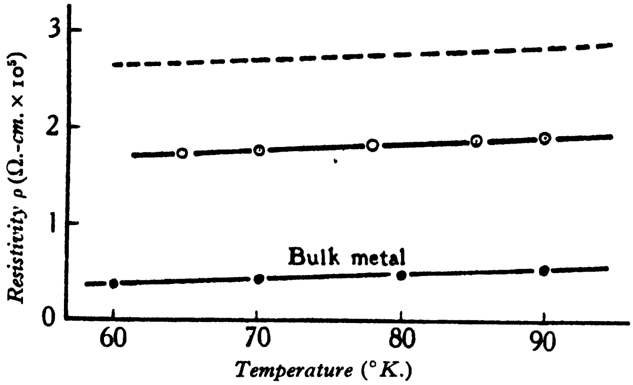

Figure 5. Theoretical - - -, and experimental ⊙. Resistivity/temperature graphs for a film 49·5 A. thick deposited at 64° K. ● bulk metal.

[*By the courtesy of the Royal Society*

The broken curve in figure 4 is obtained by substitution in formula (1), and it will be seen that there is good agreement between the theoretical and the experimental curves. This is all the more satisfactory since formula (1) contains no adjustable constants, but yields at once absolute values of the resistivity. The worst disagreement occurs precisely where we might expect; where the film is so thin that it cannot be expected to show the properties of a regular lattice, that is, at less than 10 A., or two crystalline layers, and at large thicknesses where t becomes comparable with λ_θ.

Rubidium and potassium also show good agreement at thicknesses greater than 30 A., though here it must be remembered that the decay process previously mentioned tends to raise the resistance above the theoretical value since even at 64° K. the first layers put down are disintegrating appreciably.

The temperature dependence of resistivity of the stable films may also be calculated from formula (1), and figure 5 shows a comparison of the results for caesium films 49·5 A. thick deposited at 64° K. It will be seen that they show a positive temperature coefficient.*

There seems little doubt that the explanation put forward above is correct in its broad features, but it is unlikely that the extremely simple assumptions put forward above are entirely correct. Calculations of a formula to replace equation (1) under more general conditions are at present being carried out by Fuchs.

§ 6. DISINTEGRATION OF THE FILMS. THE PHENOMENON OF DECAY

In references (6) and (7) a hypothesis is suggested which explains qualitatively all the phenomena of decay. The view put forward there was that the film was slowly tearing itself up under the influence of surface tension forces which in the thinner films may reach very high values; in a rubidium drop of radius 10 A. the pressure is of the order of 30 tons per square inch,† which is of the same order of magnitude as the ultimate tensile strength of carbon steel. Thus if a slice of an alkali metal could by some means be prepared about 10 A. thick it would immediately disintegrate if any cracks or imperfections existed at any point, because of the low elastic yield point of the alkali metals combined with the high stresses around any hole or crack. When the film is deposited upon a substrate the forces will however be profoundly modified by the magnitude of the surface energy at the metal-substrate interface and the film may become more stable.

Let us take a crude and concrete picture of the disintegrating film as a homogeneous metallic phase riddled with cracks and imperfections which are gradually widening under the influence of the surface forces. We regard these cracks as insulating barriers, the current being carried by bridges of unbroken film which become fewer and narrower as the disintegration proceeds. Assume that the continuous parts of the film are still thin compared with their linear dimensions measured along the surface. Then if E_1 is the surface energy of a free metal surface (necessarily positive) and E_2 is the (negative) surface energy at the metal-glass interface, it is clear that, fixing attention upon a definite geometrical configuration of the disintegrating film, the forces tending to disintegrate it further will be proportional to E_1+E_2. If E_1+E_2 is positive, as appears to be the case in these experiments, the film will continue to shrink away from the cracks, and to thicken up in the parts which remain intact until the curvatures at the free edges have enlarged so much that the surface tension forces can no longer cause flow in the metal. It is conceivable that this flow also produces a violent cold working of the crystals which hardens them and also gives rise to a *Restwiderstand.*

---

* The negative temperature coefficient observed in many early thin films is not explicable upon any simple theory of metallic conduction. It is indeed clear that no form of mere geometrical disintegration of the film (sponginess, porosity, etc.) can give a negative coefficient to a film if the bulk metal has the normal positive coefficient. The most that can happen is that the part of the resistivity due to strain in the lattice, and collision of the conduction electrons with the boundary, may swamp the temperature-dependent part to give a zero coefficient. Hence one may incline to the belief that perhaps septa of occluded gas between the crystals may account both for the negative temperature coefficient and the high specific resistance of such films. Even those prepared in vacuo classed as good by ordinary standards (tungsten(2), molybdenum(13)) cannot be guaranteed free from gas. Septa of gas have been suggested by Johnson and Starkey(14) to account for the high resistivity of certain mercury films.

† Drops as small as this contain relatively few atoms, so that the calculation is only correct as regards order of magnitude.

The above simple view of the decay process accounts satisfactorily for most of the experimental facts in the case of the alkali metals investigated. It describes satisfactorily the diminished decay factor for films deposited at the lower temperatures. At the lower temperatures the mechanical rigidity of the metal is increased, and so the flow will not take place so quickly; also during the deposition when alkali metal atoms are being deposited on the bare glass the lower temperature will diminish the mobility of the atoms over the glass surface, and on this account too the formation of cracks will be hindered. It explains the fact that, all other things being equal, the decay factor diminishes as the thickness of the film increases in the case of rubidium and potassium. And what is perhaps most important it satisfactorily explains why a film which is stable when deposited at a low temperature remains stable when raised subsequently to a higher temperature. For, once a continuous film has been formed, surface tension forces can only act so as to diminish any surface irregularities which do exist. The effect upon the stability of the films of minute traces upon surface impurities on the substrate also is perfectly comprehensible, for it is well known that the surface forces of the type of E_2 are particularly sensitive to contamination of the surface. There is only one observation which is in serious disagreement with the suggested picture: the fact that in caesium there is a certain range of nominal thickness over which the decay *increases* with the thickness. This suggests that the conception of the metal as a homogeneous phase may need reconsideration, as is mentioned later.

Lovell's results (unpublished) for potassium, rubidium and caesium show that only in the case of caesium does the resistivity of thick films converge to the value given for the ordinary bulk metal. Both potassium and rubidium give values about double the bulk resistivity but unfortunately the results so far obtained for rubidium are not very reliable. In the case of potassium, however, the excess resistivity can be accounted for as a *Restwiderstand* due to strain. Some of this strain can be relieved by annealing at 90° K., and a similar, though much smaller strain seems to exist in the thick layers of caesium.

Fuchs has compared the results now available for caesium, which extend from 0 to 12,000 A. with a more general theoretical expression than that previously used. The comparison seems to show that the assumption of inelastic scattering of the conduction electrons at the boundaries holds for the thinner films ($t/\lambda<1/100$) but that at greater thicknesses a considerable proportion of elastic scattering occurs.

Details of these calculations and of the comparison will be published elsewhere in the near future.

§ 7. AGGREGATION IN OTHER METAL FILMS

The idea that agglomeration of the metal might be responsible for the unusually high, or even infinite resistance of thin layers is not new; and its existence has received definite experimental proof in a large number of cases. We may quote, among others, the observations of Estermann(15) (ultra-microscopic examination of thin silver films), Fukuroi(16) (mercury, cadmium and zinc films deposited at 90° K. Optical evidence for agglomeration), Reinders and Hamburger(2) (silver deposited at room temperatures), Cosslett(17) (indium at liquid air temperatures), Andrade and Martindale(18) (sputtered silver films heated subsequently to about 600° K.). But in all previous work, except the last mentioned, the agglomeration has either been rapid and complete so that its intermediate stages could not be observed, or where resistance measurements were also attempted the structure of the films may have been marred by so many other extraneous factors that the primary role of the agglomeration process was obscured. The interest of these experiments on the alkali metals is that the process can apparently be followed in slow motion and under complete control. Moreover, the observation that mere alteration of the surface condition of the substrate without any other change in the experimental conditions can alter the specific resistance of the films by factors of 10^5 or more certainly suggests that the differing results of previous workers may be explicable in terms of a greater or less degree of agglomeration of their films. In fact, we may make the reasonable hypothesis that in all those cases where no electrical conductivity occurs until several atomic layers have been deposited a grained structure is responsible, the agglomeration in these cases being so rapid that with ordinary rates of evaporation no continuous film can be formed in the early stages of the process.

Various other hypotheses have been made to explain the experimental facts. Perucca(19), for example, suggests that all normal metals show anomalously high resistivity in the neighbourhood of a free surface. Thin films would thus show an abnormally high resistance owing to their large surface compared with their volume. There is no theoretical warrant for this belief, and no other experimental evidence to support it.

Zahn and Kramer(20, 21) similarly have proposed upon the basis of certain experimental results that an amorphous non-conducting layer of metal may be put down under certain circumstances. Their experimental results are certainly striking; but again, there is no experimental reason to suppose that thin metallic films are ever amorphous except in the case of antimony, and even if the films were amorphous, they would presumably show no higher resistivity than that of a melted metal.

It seems preferable on this account to exhaust the possibilities of the agglomeration hypothesis before looking elsewhere; and the following remarks tend to show that it may play an important role even at very low temperatures of deposition.

When we attempt to apply to other metals the simple picture already advanced to explain the alkalis, the immediate objection arises that nothing is known of the nature and hence the magnitude of the surface energy E_2, and that therefore the onus of explaining any experimental result can always be thrown upon E_2. We can overcome this objection to some extent, and incidentally get a somewhat clearer picture of the process of formation of evaporated films, by examining in closer detail the processes which take place in putting down the early atomic layers upon the substrate.

Let us first examine from a purely energetic point of view whether or not a layer of atoms approximately monomolecular would be inherently stable. Imagine two possible configurations of the metal upon the substrate. In the first (I) the atoms are supposed to be uniformly dispersed on the substrate; in the second (II) they are gathered up into a globule or agglomerate of small surface. Let L be the latent heat of evaporation of a metal atom from the surface, in electron volts, and L_{metal} the latent heat of evaporation from the metal. Then if $L < L_{\text{metal}}$ the state II or agglomerated form is the one with the lower energy. If $L > L_{\text{metal}}$ state I or the dispersed form has the lower energy. Thus a monolayer will be inherently stable if $L > L_{\text{metal}}$ and inherently unstable if $L < L_{\text{metal}}$.*

Now values for the latent heat of evaporation of metals from glass surfaces have been obtained in a few cases. Examples are given in the table below:

Table 2

Experimenter	Metal and surface	L (k.cal./ g. atom)	L (eV.)	L_{metal} (k.cal./ g. atom)	L_{metal} (eV.)
Estermann(23)	Cd on glass	3·5	0·152	28	1·21
,,	Cd on Cu	3·0	0·130	28	1·21
,,	Cd on Ag	5·0	0·217	28	1·21
,,	Hg on Ag	2·5	0·109	18·5	0·80
Cockcroft(24)	Cd on Cu Cd on Ag	5·7	0·247	28	1·21

The values of L given above represent the heat of evaporation of an atom from a dilute layer plus the heat of dissociation of a doublet upon the surface. L is therefore an upper limit for the latent heat of evaporation from a dilute layer. In all the above cases L_{metal} is about seven times larger than L and the agglomeration of a dilute layer is energetically possible. Now we were considering the general case of a layer which may approach monomolecular thickness. Although it is true that L will vary with the concentration of the layer it is unlikely that it can increase much† with θ (the fraction covered) and it is practically impossible that it should increase by a factor of seven. So a layer of any concentration will be energetically unstable.

The alkalis on clean glass have not yet been systematically investigated from this point of view. But the observation of Ives(27) and the experiments of Lovell(28) show that a clean glass surface placed in an evacuated enclosure filled with the saturated vapour of the alkali metals rapidly becomes coated with an invisible conducting layer of alkali metal which persists even though the glass is raised in temperature above its surroundings. The layer must be nearly monomolecular to conduct at all; and it follows that either the latent heat of evaporation of an atom of the alkali from the glass is greater than its heat of evaporation from the metal surface, in which case the glass will be completely covered, or, if less, L cannot differ from L_{metal} by more than a few kT., that is to say, by more than a few hundredths of an electron volt.

---

* De Boer(22) has previously pointed out that a high latent heat of evaporation for the adsorbed substance in bulk will favour agglomeration.

† Langmuir and Taylor(25) find that the latent heat of evaporation of neutral atoms from the surface actually falls from 2·83 volts at $\theta = 0$ to 1·77 volts at $\theta = 1$. J. K. Roberts(26) (H on W) shows that in this case the latent heat may somewhat more than double from $\theta = 0$ to $\theta = 1$.

It follows that the excess of energy of a dispersed layer over its agglomerated form is either small or is actually negative, and for this reason alone single layers of alkali metal atoms on glass should be more stable than those of cadmium or mercury on the surfaces investigated by Estermann and Cockcroft.

So far we have only discussed whether the agglomeration is energetically possible. Whether it will also in fact take place depends upon the mobility of the atoms over the surface of the glass. Lennard-Jones(29) has given a simple picture of the chief factors which influence this mobility, and we may apply it to the present case.

According to his model an atom on a surface may be regarded as held there by a field of force which has a certain potential. The equipotentials are not however a series of planes parallel to the surface, as we have tacitly assumed till now; a crystal surface, for example, has a periodic structure. On this account regular pockets of low potential will exist upon the surface, and at low temperatures any deposited atoms will vibrate about the minima of these pockets. The latent heat of evaporation of the atom from the surface will then be the energy required to remove an atom from its lowest vibrational level to infinity. But in order to move freely over the surface an atom needs much less kinetic energy than L. In fact, if the atom is given sufficient kinetic energy A for it to surmount the potential barrier between one pocket and the next, it may (so long as it retains the energy) move freely over the surface. Thus, since A is less than L, free motion of the atoms on the surface occurs at temperatures far below those needed to evaporate the atoms from the surface: a well-known experimental fact.

Now A, like L, is dependent both on the nature of the surface and upon the atom concerned. It has been found for metal atoms in a limited number of cases only, and it depends to some extent upon the surface population of the atoms. But we may say in general that L and A increase together. Lennard-Jones(29) estimates that for the particular case of the inert gases upon a surface of alkaline halide A is about $\frac{1}{3}L$. Dilute layers of caesium on tungsten give an activation energy of 0·61 volt and a latent heat of 2·83 volts(25, 30). Bosworth(31) obtains values between 0·14 and 0·57 volt for sodium on tungsten, Frank(32) between 0·2 and 0·6 volt for caesium on tungstic oxide. The latent heats of evaporation of neutral atoms are not known in the latter case but they are certainly greater than 1 electron-volt. We might guess then that the activation energy of an atom on a surface is generally less than a third of the latent heat of evaporation from the surface and may be about a quarter.

On this basis the activation energy of caesium on glass must be at least 0·25 volt, whereas cadmium on glass, using Estermann's value for the latent heat, would have an activation energy of only 0·04 volt. This difference will be reflected in a great difference of mobility in the two cases. Assuming a time of activation of about 10^{-13} second (Lennard-Jones$^{(29)}$) and a surface temperature of 90° K. in both cases we find that a caesium atom would be activated only once every ten seconds, when it would move a distance of 0·6 A., whereas a cadmium atom would be activated nearly 10^{11} times in one second, would move a total distance of about 200 cm., and would migrate about $\frac{1}{100}$ mm. from its original position in this time.

This estimate is purely illustrative and it is of course very sensitive to the actual values of the activation energy assumed. Nevertheless it does enable us to understand how it may be possible in the case of the alkalis to lay down a second layer of atoms before the atoms in the first layer have moved much from their original positions, whereas in the case of cadmium at the same temperatures rates of deposition quite impracticably rapid would have to be used to do this.

We might therefore classify metallic films into three broad classes depending upon the stability of their first layers. For type I, $L > L_{\text{metal}}$ and the first layer is inherently stable. The classical example of this is caesium atoms on clean tungsten for all values of θ. Perhaps caesium on clean glass also belongs to this group; for this would account for the great stability of the early layers in the experiments we have already described using this particular metal. For type II, $L < L_{\text{metal}}$ but $L \sim 1$ electron volt or more. The activation energy is a few tenths of a volt, agglomeration takes a period of minutes at 90° K. and fairly coherent films can be readily prepared at somewhat lower temperatures of deposition, using deposition rates of the order of a molecular layer in a few minutes. For type III $L < L_{\text{metal}}$, $L \sim 0{\cdot}1$ eV. and the activation energy is only a few hundredths of an electron volt.* Films of type III will show rapid agglomeration even at very low temperatures of deposition and in fact approximate to the two-dimensional gas of Frenkel$^{(33)}$ and Cockcroft$^{(24)}$. These metals even when deposited at very low temperatures will show very different resistivity-thickness relations from the alkalis. We may imagine the successive stages in the development of a film of this type somewhat as follows, starting from the bare substrate: As deposition proceeds doublets are first formed which gradually accrete more atoms round them, and island patches of metal are formed. During this stage of the process there can be no electrical conductivity since the film consists of flat isolated aggregates joined only by a very dilute phase of two-dimensional gas. As the deposition proceeds the island patches thicken both from condensation at their free surfaces and by shrinking under their very high surface-tension forces. The next stage in the process occurs when the aggregates have become so thick and the curvatures of their free surfaces have been so diminished that the surface forces can produce no further flow in the metal. The aggregates now thicken only slowly from deposition at their upper faces, and continue to grow edgewise by condensation from the two-dimensional gas. At a certain stage they will touch, and conductivity will abruptly begin. After this the film-resistivity should quickly approximate to that of the bulk metal.

Some preliminary results obtained in this laboratory with thin films of mercury-on-pyrex certainly suggest that these films are an extreme form of type III even when the deposition takes place at temperatures as low as 20° K. Figure 6 shows a family of {resistivity, thickness} curves, each curve characteristic of a different temperature of the condensing surface. (Deposition rate about 9 A./min. in all cases, but this is subject to correction on calibrating the beam, a difficult matter in the case of mercury). The short vertical marks above each curve show the onset of conductivity. This was remarkably sudden, the resistance falling from an unmeasurably high value greater than 10^{10} ohms to a few thousand ohms within about 15 sec., which corresponded to an increase in nominal thickness of less than a monolayer. At this point in the deposition, when the aggregates first touched, the film rapidly disintegrated if currents greater than a few microamps passed through it.

---

* Semenoff, Chariton, and Schalnikoff$^{(38)}$ have discussed films of type III from a similar point of view to the above, without reference however to the effect on the electrical conductivity.

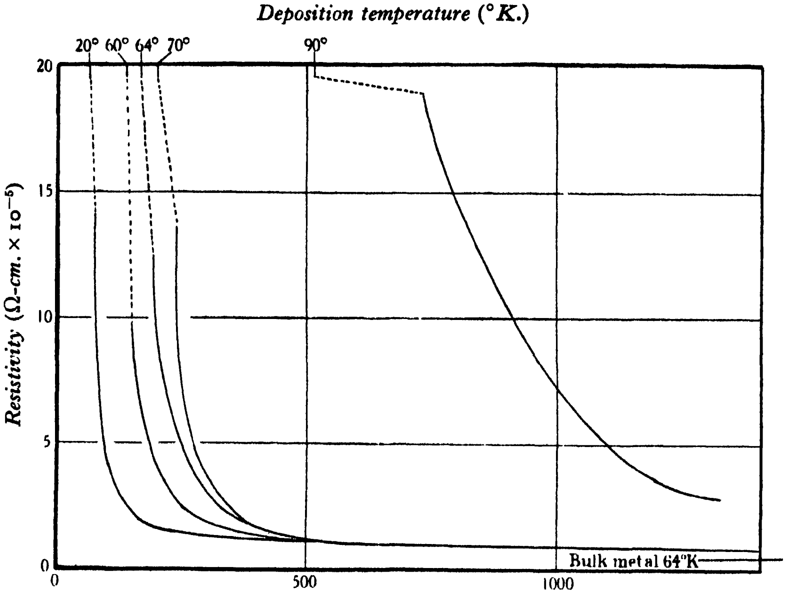

Figure 6.

Figure 7 shows critical thickness plotted against deposition temperature. It will be noticed that there appear to be no signs that by lowering the temperature below 20° K. the critical thickness will much diminish. Thus there appears the surprising suggestion that apparently the atoms of mercury retain their mobility down to very low temperatures. Mercury atoms on pyrex therefore may be similar to helium atoms on lithium fluoride which, according to the theoretical calculations of Lennard-Jones(34), have a finite mobility at all temperatures above absolute zero.

On our picture of the process we should estimate that the critical thickness of the film is about the thickness of an aggregate whose curvatures have so diminished that the surface forces can no longer produce any plastic deformation. Now roughly speaking the stresses due to surface forces in an aggregate are inversely proportional to its thickness. The critical thickness should therefore give us a measure of the weakness of the metal at that temperature. Although no experiments appear to have been done on single crystals of mercury at these low temperatures, a rough comparison with the results for magnesium(35) single crystals suggests that mercury, which has a low melting point, might begin to alter its mechanical properties rapidly in the region of 80° K., where the rapid rise of critical thickness with temperature does set in. But until further evidence accumulates we must regard this as a speculative guess, particularly since all experiments on the mechanical properties of metal crystals have been carried out with large specimens and not with the microscopic or submicroscope aggregates we have postulated in thin films.

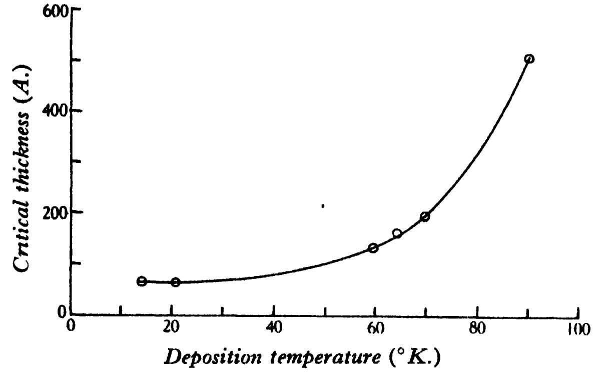

Figure 7.

To summarize the above conclusions: The foregoing discussion suggests that the degree of agglomeration in evaporated films is determined on the one hand by the activation energy of the atom upon its substrate, on the other by the resistance of the metal to plastic deformation, not simply by the melting point of the metal as certain writers have suggested.

§ 8. RECRYSTALLIZATION OF THIN METAL FILMS

Films which agglomerate in their early stages must have a very finely polycrystalline structure which may persist to great thicknesses. The resultant large surface of misfit between the microcrystals may have two effects. First they may increase the resistance of even thick films appreciably above that of the bulk metal; secondly, they introduce a new type of surface energy which may become important when their area becomes large compared with that of the boundaries of the film.

The effect on the resistivity of the film would be to add a *restwiderstand* to the normal resistivity, and on this account even very thick evaporated films deposited at temperatures below that at which recrystallization would occur might show a considerable excess of resistivity over that of the normal metal. It seems possible that in most of the cases where this resistivity excess does not exceed the increase of resistivity on melting for the pure metal, it may be due to this cause. Annealing should then diminish the resistivity of the films by allowing the surfaces of misfit to relax (recrystallization).

The experiments of Suhrmann and Barth(36) on thick films of copper deposited at 20° K. are consistent with this hypothesis. Annealing at successively higher temperatures lowered their resistivity by diminishing the *restwiderstand* without altering the resistivity change between two definite (lower) temperatures. The highest resistivities observed were nevertheless somewhat in excess of the resistivity change of copper on melting, and it seems on this account possible that occluded gas may have introduced a disorder in the lattice exceeding that produced by melting. Wand(37) has worked out a theory of the relaxation of strain in the lattice which is consistent with his own experimental results, and further experimental work on this point would be valuable.

The effect of this new type of surface energy may account too for the observations of Andrade and Martindale(18) (silver films) as also some recent unpublished observations of Lovell on caesium films. In both cases it was found that thick films could disintegrate so as apparently to increase their free surface and hence their ordinary surface energy. These observations therefore apparently contradict the ideas put forward here that the surface forces control the shape of the film. It is in fact true that in the case of films so thin that the number of atoms in the surfaces is comparable with the total number in the film (say up to 20 atomic layers) ordinary surface forces must predominate. But when thicker films recrystallize it is not at all unlikely that the free-surface energy may increase at the expense of the energy gained from recrystallization and relaxation of the surfaces of misfit.

§9. ACKNOWLEDGEMENTS

I wish to express my thanks to Dr Lovell and Dr Fuchs for permission to publish the preliminary account of their results.

I am also indebted to the Royal Society for permission to reproduce figures 2, 3, 4, and 5 of the present paper (which were originally published in their *Proceedings*) and for the loan of the blocks.

REFERENCES

(1) Bartlett. *Phil. Mag.* **5**, 848 (1928).
(2) Reinders and Hamburger. *Rec. Trav. chim. Pays-Bas*, **50**, 441 (1931).
(3) Vincent. *Ann. Chim. (Phys.)*, (8), **9**, 433 (1900).
(4) Pogany. *Ann. Phys.*, Lpz., **49**, 531 (1916).
(5) Weber and Oesterhuis. *Proc. Acad.*, Amsterdam, **25**, 606 (1916).
(6) Lovell. *Proc. roy. Soc.* A, **157**, 311 (1936).
(7) Appleyard and Lovell. *Proc. roy. Soc.* A, **158**, 718 (1937).
(8) Thomson. *Proc. Camb. Phil. Soc.* **11**, 119 (1901).
(9) Hamburger. *Ann. Phys.*, Lpz., **10**, 796 (1931).
(10) Wood. *Phys. Rev.* **44**, 353 (1933).
(11) Zener. *Nature*, Lond., **132**, 968 (1933).

(12) Mott and Zener. *Proc. Camb. Phil. Soc.* **30**, 249 (1934).
(13) de Boer and Kraak. *Rec. Trav. chim. Pays-Bas*, **55**, 941 (1936).
(14) Johnson and Starkey. *Proc. roy. Soc.* A, **140**, 126 (1933).
(15) Estermann. *Z. phys. Chem.* **106**, 403 (1923).
(16) Fukuroi. *Honda Anniversary Volume*, p. 80 (1936).
(17) Cosslett. *Proc. phys. Soc.* **49**, 121 (1937).
(18) Andrade and Martindale. *Philos. Trans.* **235**, 69 (1935).
(19) Perucca. *Ann. Phys.*, Lpz., **4**, 252 (1930).
(20) Zahn and Kramer. *Z. Phys.* **86**, 413 (1933).
(21) Kramer. *Ann. Phys.*, Lpz., **19**, 37 (1934).
(22) de Boer. *Electron Emission and Adsorption Phenomena*, p. 48 (1935).
(23) Estermann. *Z. Phys.* **33**, 320 (1925).
(24) Cockcroft. *Proc. roy. Soc.* A, **119**, 293 (1928).
(25) Langmuir and Taylor. *Phys. Rev.* **44**, 423 (1933).
(26) Roberts. *Proc. roy. Soc.* A, **152**, 445 (1935).
(27) Ives and Johnsrud. *Astr. J.* **62**, 309 (1925).
(28) Lovell. *Proc. phys. Soc.* **49**, 89 (1937).
(29) Lennard-Jones. *Trans. Faraday Soc.* **38**, 333 (1932).
(30) Langmuir and Taylor. *Phys. Rev.* **40**, 463 (1932).
(31) Bosworth. *Proc. roy. Soc.* A, **150**, 58 (1935).
(32) Frank. *Trans. Faraday Soc.* **32**, 1403 (1936).
(33) Frenkel. *Z. Phys.* **26**, 117 (1924).
(34) Lennard-Jones and Devonshire. *Proc. roy. Soc.* A, **158**, 242 (1937).
(35) Schmid and Boas. *Krystallplastizität*, p. 160 (1935).
(36) Suhrmann and Barth. *Z. Phys.* **103**, 133 (1936).
(37) Wand. *Z. Phys.* **104**, 1 (1937).
(38) Semenoff, Chariton and Schalnikoff. *Trans. Faraday Soc.* **28**, 169 (1932).

A STUDY OF THE ELECTRICAL PROPERTIES OF THIN FILMS OF PLATINUM OBTAINED BY CATHODE SPUTTERING IN AIR AND OTHER GASES (He, N_2, O_2 AND H_2)

By A. FÉRY, Collège de France, Paris

For a considerable time attempts have been made to use cathode sputtering in order to obtain thin metallic films so as to study, in particular, the variation of resistivity of these films as a function of their thickness.

All investigators agreed that up to a certain so-called critical thickness the resistivity of the films is a diminishing function of the thickness. Beyond the critical thickness the metal has quite definite physical properties which are those of the *bulk* metal. But for platinum, for example, there are notable discrepancies between the values obtained by different investigators, both for the resistivity of these films at one and the same thickness, and also for the values of the critical thickness. Moreover the resistances obtained in this way were in no way permanent; the adsorption of gas atoms seems to be important. The same uncertainty existed for the temperature coefficients.

I therefore thought that it would be interesting to take up once again the study of the electrical resistance of thin platinum films, with the primary object of getting stable resistances, using first a discharge in air. By taking the same precautions employed in the manufacture of radio valves and, in particular, by getting rid of all traces of water vapour from the apparatus before sputtering (by baking-out in a high vacuum) I was successful in achieving this. The deposits were kept in the apparatus throughout their life. But the platinum so obtained is not ordinary platinum as we shall see in what follows. We shall call it *black platinum.*

I was thus enabled to determine the experimental relationship between the resistivity ρ and the thickness l of these black platinum films. This relationship, which holds between 10 mμ. and 1320 mμ. may be divided into the two curves

$$2 \log (\rho/\rho_0) = 11{\cdot}48 - 0{\cdot}0315\, l$$

and

$$2 \log (\rho/\rho_0) = 3{\cdot}245,$$

where $\rho_0 = 10^{-5}$ ohm-cm. which is the average resistivity of ordinary platinum. These curves are joined up between 237 and 285 mμ. by a very short curved line.

Beyond 285 mμ. the metal may therefore be taken to be compact. But it is nevertheless not ordinary platinum: its resistivity ($4{\cdot}19 \times 10^{-4}$ ohm-cm.) is 42 times higher than the average resistance of bulk platinum. Moreover it appears black. This kind of platinum is adsorbent, has a high resistance, and is catalytic.

Throughout these experiments the temperature of the plate upon which the deposit was received did not increase during the passage of the discharge, for the voltage was low. But if the deposits are heated *in vacuo* their resistance changes. It first increases *reversibly* as the temperature rises, then as soon as the temperature reaches a certain threshold the resistance alters very rapidly and irreversibly, at constant temperature. It diminishes continuously, tending towards a certain limit depending on the temperature of the threshold. By again raising the temperature the same phenomena are reproduced. One thus obtains a series of reproducible transition points 53°, 83°, 97°, 114°, 241° and 340° C. Only at 340° C. do the films have a resistivity between the limits of the tabulated values for normal platinum.

Between any two successive transition temperatures the deposit has quite clearly defined properties. The temperature-coefficient in particular which was $2{\cdot}87 \times 10^{-4}$ for black platinum increases as one approaches the normal bulk metal and finally takes the value $29{\cdot}9 \times 10^{-4}$ very close to that given for the normal metal.

If sputtering is carried out without taking these precautions to avoid heating of the substrate, the form of deposit stable at the temperature reached by the substrate is obtained. This explains the great divergence of the previous results.

The transitions are accompanied by very slight evolution of gas at the first three transition points (the least noteworthy ones). But this evolution of gas is due only to a small adsorption by the deposits (oxygen, nitrogen and oxides of nitrogen) during or after their formation; an adsorption so slight that it can only play a very secondary role in the development of their physical properties.

After transformation into white platinum a new curve is obtained relative to normal platinum. The critical thickness is considerably diminished. It occurs in the neighbourhood of 50 mμ. The "compact" metal has then the resistivity of ordinary platinum. But at very small thicknesses (between 3 and 6 mμ.) this curve is observed to appear to join up again with that of black platinum. The two forms then become indistinguishable.

The properties of the deposits obtained in the simple gases (helium, nitrogen, oxygen, hydrogen) are not clearly defined. During their formation these deposits absorb the gas of the discharge.

At ordinary temperatures after their preparation their resistances fall and tend towards a limit. On heating and holding the temperature at an arbitrarily chosen value, their resistance diminishes again at constant temperature, approaching a new limiting value which is a function of the constant temperature. Parallel with this process the occluded gases are released at a rate which increases the more the temperature is raised. At 500° C. we have still not been able to obtain normal platinum, and the films so obtained are torn up by the evolution of the absorbed gas.

FLUCTUATIONS IN THE RESISTANCE OF THIN FILMS

J. BERNAMONT, Collège de France, Paris

THE study of fluctuations of resistance, begun in 1934(1), has been pursued up to the present time with deposits of graphite(2), with microphone(3) and with metallic deposits(4). The general results obtained are the following: the mean square of electromotive force averaged over a complete period, which we denote by $\overline{e_\nu^2}$, is approximately proportional to the square of the intensity of the current carried by the conductor, at least in the range of frequencies studied. This range is at present too restricted to allow general conclusions to be drawn; in the experiments with metallic deposits it extends from 96 to 162,000 hertz, while other authors have limited themselves to frequencies from 50 to 10,000. The mathematical investigation of the fluctuations(4) makes it possible to predict that for sufficiently low frequencies $\overline{e_\nu^2}$ ought to be independent of the frequency, and for high frequencies $\overline{e_\nu^2}$ ought to diminish at least as fast as $1/\nu^2$. The curve showing $\log \overline{e_\nu^2}$ as a function of $\log \nu$ ought then to be made up of at least three branches of very different slope, viz. (*a*) a horizontal part for low frequencies; (*b*) for intermediate frequencies a part about which nothing can at present be said from the theoretical point of view, but for which experiment gives a slope of 1; (*c*) for high frequencies a branch with a strong negative slope (at least -2).

The branch (*c*) has been observed with a tungsten deposit;(4) the slope was exactly -2 from 72,000 to 162,000 hertz(4). Experiments on graphite and microphone(2) show some indications of (*a*).

Since my first observations I have held the opinion that this fluctuation was due to fluctuations in the number of free electrons in the conductor which would give rise to fluctuations in the resistance. A variable electromotive force ought then to appear in the circuit, whose mean square is given by the formula

$$\overline{e^2} = I^2\overline{\Delta R^2},$$

where ΔR is the instantaneous deviation of the resistance from the mean value.

On the classical theory one can deduce for a cylindrical conductor

$$\overline{e^2} = (I^2R^2/n_0a)\,\overline{\Delta N^2}/N.$$

M. L. Brillouin(5) has shown that this formula follows also from quantum statistics; but the factor $\overline{\Delta N^2}/N$ which is independent of the volume is equal to 1 according to the classical theory but can have another value according to the quantum theory.

To obtain the dependence of $\overline{e^2}$ on ν, one must make a more detailed hypothesis about the mechanism. I have assumed that a free electron has a mean life-time

$\theta = 1/\alpha$. Its collisions with atoms will only alter the direction of its velocity v; and it is only after a very large number of collisions that the electron is captured by an atom and ceases to be free. A group of n free electrons may thus be reduced in number to $ne^{-\alpha t}$ at the end of a time t. Naturally other electrons will be liberated at random during the same interval; this hypothesis leads to the formula

$$\overline{e_\nu^2} = I^2R^2\frac{\overline{\Delta N^2}}{N}\frac{4\alpha}{\alpha^2+4\pi^2\nu^2}.$$

This equation is not in agreement with experiment; but we need not assume that electrons of different velocities have the same life time. If dn is the number of electrons for which the constant α lies in the range $d\alpha$, and if we write

$$\overline{\Delta dn^2}/dn = g$$

then we obtain finally

$$\bar{e}_\nu^2 = \frac{I^2R^2}{n_0^2\,\alpha}\int_{\alpha_1}^{\alpha_2}\frac{4\alpha g\,dn}{\alpha^2+4\pi^2\nu^2},$$

where α_1 and α_2 are the limiting values of α. This formula reproduces the branches (*a*) and (*c*) very well.

Comparison with the experimental branch (*b*) gives us αg as a function of v (for dn is a function of v). But definite conclusions on this subject would be premature.

Actually all experiments of this type have been carried out on conductors of rather badly defined nature. The platinum films have been obtained by M. Féry's method and were very thin. Their thickness was about 40 A., and in M. Féry's experiments conduction only began at 31 A. As one does not know the reason for the absence of conductivity for thinner films the results are rather hard to interpret. It would be desirable to repeat the experiments with films obtained by the method of Appleyard and Lovell and also perhaps with semi-conductors, in such a way as to avoid perturbations which can occur at the contacts where the current enters the film.

REFERENCES

(1) Bernamont, J. *C.R. Acad. Sci., Paris,* **198**, 1755, 2144 (1934).
(2) Meyer, E. and Chiede, H. *Elekt. Nachr.-Tech.* **12**, 237 (1935).
(3) Christensen, C. J. and Pearson, G. L. *Bell Syst. tech. J.* **15**, 197 (1936).
(4) Bernamont, J. Thèse de doctorat, Paris, and *Ann. Phys., Lpz.*, **7**, 71 (1937).
(5) Brillouin, L. *Helv. phys. Acta,* **7**, 47 (1934).

THE MIGRATION AND AGGREGATION OF ATOMS ON SOLID SURFACES

By J. E. LENNARD-JONES, University Chemical Laboratory, Cambridge

§ 1. INTRODUCTION

THE interesting experiments of Appleyard and Lovell(1) on the electrical properties of thin films of the alkali metals on pyrex glass direct attention to a number of important theoretical problems concerning the properties of atoms deposited on surfaces. Appleyard* has suggested that when in his experiments a clean surface is bombarded uniformly by metallic atoms, their subsequent behaviour will be conditioned by the surface field of the substratum and by the relative magnitudes of the heat of evaporation from the surface and the heat of sublimation of the metallic atoms from the bulk phase. If the forces of the substratum are strong enough, the metallic atoms may be held in a continuous (more or less uniform) two-dimensional film and its electrical resistance is then of the same order of magnitude as that of the bulk metal. If, however, the cohesive forces between the metal atoms themselves are stronger than those of the substratum, the metallic atoms may tend to aggregate into "islands", which may be many atoms thick. This tendency to aggregation will be opposed by the periodic nature of the surface field and the time taken for the film to reach its most stable configuration will be governed by the rate at which the atoms can migrate over the surface.

This qualitative picture suggests a theoretical investigation of the behaviour of an atom, deposited on a surface, in terms of the interatomic forces between the atoms themselves and between each atom and the surface. The first problem is to determine what is the most stable configuration of the atoms thus deposited. It may be that of a uniform two-dimensional film, or a number of two-dimensional aggregates. On the other hand small three-dimensional crystallites may be more stable than either. This problem is a thermodynamic or statistical one and the answer to it will give the configuration which will eventually be reached after the lapse of a sufficiently long time. In the actual experiments the atoms are deposited uniformly and may or may not be in the configuration which is most stable. The next problem is therefore a dynamic one and is concerned with the length of time it will take the assembly to change from its initial configuration to the most stable one. This will depend on the rate at which atoms can surmount the energy barriers of the periodic field at the surface(2). In this paper we shall consider some aspects of these two problems.

---

* The author is greatly indebted to Dr Appleyard for an advance copy of his paper to this conference, with its valuable review of the experimental facts.

§ 2. CRITICAL PHENOMENA IN ADSORBED FILMS

The experiments of Cockcroft(3) and others have shown that when metals are deposited on a surface, they form condensed films if the temperature of the surface is less than a certain critical value. The behaviour of atoms adsorbed on a surface is, in fact, somewhat similar to that of gases and vapours, all of which exhibit critical properties below a certain temperature.

The existence of these critical conditions was discussed by Frenkel(4) who considered the formation of doublets on a surface, held together by an energy greater than that binding them to the surface. He showed that under these conditions a dispersed layer of single atoms would become unstable below certain critical conditions and condensation would occur.

Fowler(5) has recently made a new approach to the problem, basing his work on the treatment of order-disorder phenomena in alloys by Bragg and Williams(6) and Bethe(7). The energy of an adsorbed atom is assumed to depend not only on the attraction of the surface but also on the number of nearest neighbouring sites occupied by other adsorbed atoms. The assumption was made that the energy of adsorption was a linear function of the number of nearest neighbours. Peierls(8) has shown the relation of Fowler's treatment to Bethe's method and has obtained the critical conditions for atoms adsorbed on a surface when the number of nearest neighbours has any value, Fowler's results being a special case of his.

It may be of interest to give another method of arriving at similar results. We suppose a number of atoms deposited on a perfectly plane surface. At high temperatures and low concentrations these will behave like a two-dimensional gas and binary encounters will alone be of importance. The potential energy of any one atom, referred to an atom at rest in the gas phase as zero, will then be given by

$$\chi = \chi_0 + \nu \int_0 \chi_1 e^{-\chi_1/kT}\, 2\pi r\, dr \qquad \text{......(1)},$$

where χ_0 is the heat of adsorption of an isolated atom, and χ_1 is the potential energy between any two atoms; ν is the concentration of atoms and is related to θ, the fraction covered by $\theta = \nu S$, where S is the area of each cell into which the surface may be regarded as divided. We see that the equation (1) is similar to the form assumed by Fowler, except that the factor of θ is a function of temperature.

When the concentration becomes high (θ approaches unity), it will not be sufficient to take into account the interaction of pairs only. It will be necessary to calculate the potential of aggregates of atoms. Moreover it will be necessary to work out not only the critical conditions for a two-dimensional phase, but also for the case when the adsorbed atoms can condense together into three-dimensional groups. It is not yet known how the critical conditions for a two-dimensional assembly compare with those of a three-dimensional one. If the critical temperature for two dimensions is higher than that for three, two-dimensional groups may form before three-dimensional ones; but if the critical temperature for two dimensions is lower than that for three, the presumption is that two-dimensional groups will never form, or if they do, they will very quickly change to the more stable configuration.

An approximate answer to this problem may be obtained by means of a model. We consider a two-dimensional assembly on a perfectly smooth surface. At large densities each atom will always be the immediate neighbour of several others, each of which will exert forces on it and contribute to its potential energy. Although the atom may move from one part of the surface to another, it will always appear to be imprisoned by its environment and will make rapid vibrations about its average path. We may represent this state of affairs by supposing the atom confined to an area, constant in amount and equal to the average area available for each atom, and that within this area there is a region of constant potential energy. The average potential of an atom will, however, depend on the density of the assembly. It will be small for low densities and will gradually fall (to negative values) as the density increases, until a density is reached corresponding to that of a two-dimensional liquid or solid. After this the potential will rise if it is further compressed. So we suppose the potential within a cell to be a suitable function of the area so as to reproduce these features.

The partition function of an atom will then be

$$f = A \frac{2\pi m kT}{h^2} e^{-\chi(A)/kT} v_z(T) \qquad \text{......(2),}$$

where A is the area and $\chi(A)$ the potential in the cell, while $v_z(T)$ represents the contribution of the vibration perpendicular to the surface. We assume* that the partition function of the whole assembly can be written as f^N, where N is the number of atoms. Then the free energy of the assembly is

$$F = -NkT \log f \qquad \text{......(3),}$$

and the two-dimensional pressure P is given by

$$\begin{aligned} P &= NkT \left\{ \frac{\partial}{\partial A} \log f \right\}_T \\ &= NkT \left\{ \frac{1}{A} - \frac{\chi'(A)}{kT} \right\} \qquad \text{......(4).} \end{aligned}$$

The potential $\chi(A)$ has the required properties, if it be assumed that

$$\chi(A) = \frac{\lambda}{A^n} - \frac{\mu}{A^m} \qquad \text{......(5)}$$

with $n > m$.

The critical volume and temperature are given by

$$\left(\frac{\partial p}{\partial A}\right)_T = \left(\frac{\partial^2 p}{\partial A^2}\right)_T = 0 \qquad \text{......(6).}$$

These lead to the result that

$$kT_c = \alpha \mid \chi(A) \mid_{\max.} \qquad \text{......(7),}$$

where α is a pure number, given by

$$\alpha = m(m+1)\,[m(m+1)/n(n+1)]^{m/(n-m)} \qquad \text{......(8).}$$

---

* This step is discussed in a forthcoming paper by the author and A. F. Devonshire on critical phenomena in gases.

A similar result could clearly be obtained for a three-dimensional assembly, using similar methods, viz.

$$kT_c^* = \alpha^* \mid \chi^* (v) \mid_{\max.} \qquad \ldots\ldots(9),$$

where α^* is a similar function of numbers m' and n'. A more detailed and accurate calculation by the author and A. F. Devonshire⁽⁹⁾ taking into account the variation of the field within a cell, so that χ is a function not only of v but also of the space coordinates, leads to a similar result for the three-dimensional case and it is found that for the inert gases

$$kT_c = (4/3) \mid \phi \mid_{\max.} \qquad \ldots\ldots(10),$$

where $\mid \phi \mid_{\max.}$ is the energy of dissociation of two atoms. Similar calculations are being made for two dimensions but, in the meantime, it may be said that the indication is that the critical temperature for two-dimensional condensation is lower than that for three dimensions.

The free energy for two dimensions is given by

$$F = -NkT \left\{ \log A + \log (2\pi mkT/h^2) - \frac{\chi(A)}{kT} + \log v_z (T) \right\} \qquad \ldots\ldots(11),$$

and that of a three-dimensional assembly is

$$F^* = -NkT \left\{ \log v + \tfrac{3}{2} \log (2\pi mkT/h^2) - \frac{\chi(v)}{kT} \right\} \qquad \ldots\ldots(12).$$

The difference of the free energies in the two phases is thus (for this model)

$$F^* - F = NkT \left\{ \log \frac{Av_z (T)}{v\,(2\pi mkT/h^2)^{\frac{1}{2}}} + \frac{\chi(v) - \chi(A)}{kT} \right\} \qquad \ldots\ldots(13).$$

If the potential energy of the adsorbed atom as a function of its distance from the adsorbing surface be represented by a region of constant potential χ_0 for a length z_0, when it changes discontinuously to zero, we get for v_z,

$$v_z = (2\pi mkT/h^2)^{\frac{1}{2}}\, z_0 e^{-\chi_0/kT} \qquad \ldots\ldots(14),$$

and then

$$F^* - F = NkT \left\{ \log \frac{Az_0}{v} + \frac{\chi(z) - \chi(A) - \chi_0}{kT} \right\} \qquad \ldots\ldots(15).$$

When the volume of an atom in the adsorbed phase Az_0 is comparable with the volume of an atom in the three-dimensional phase v, we see that F^* is less in absolute magnitude than F when

$$\chi(v) < \chi(A) + \chi_0.$$

Now each of the χ's is the potential energy of a "hole" and is negative, so that we have $\chi = - \mid \chi \mid$ and the condition can be written

$$\mid \chi(v) \mid > \mid \chi(A) \mid + \mid \chi_0 \mid \qquad \ldots\ldots(16).$$

The left hand side may be taken to be the heat of sublimation of the three-dimensional phase and $\mid \chi(A) \mid + \mid \chi_0 \mid$ the heat of adsorption from a condensed two-dimensional phase. This condition is the same as that discussed by Appleyard in his contribution to this discussion, but it is clear that it is only true when the contribution of the vibrational motion to the free energy takes the special form given to it in the above treatment.

The heat of sublimation of a metal is usually much greater than the heat of adsorption of the same metal on to another surface and three-dimensional aggregates are more likely than two-dimensional ones, but the experiments of Appleyard on alkali metals, deposited on pyrex glass, show that in some cases the two energies are comparable in value. For caesium deposited on tungsten special ionic forces are probably brought into play for the first layer owing to the transfer of an electron from an adsorbed atom to the underlying metal and then the two-dimensional phase is unusually stable. These same ionic forces will, however, reduce the value of $|\chi(A)|$ as the film becomes more condensed owing to the mutual repulsion of the dipoles created between caesium and tungsten and eventually $|\chi(v)|$ may be greater than $|\chi(A)|+|\chi_0|$.

§ 3. THE MIGRATION OF ATOMS ALONG SOLID SURFACES

The migration of atoms along solid surfaces has now been investigated by many workers. A summary of work up to 1932 was given by Volmer(10) and since then the technique of measuring the rate of migration has been developed by Langmuir(11), Becker(12), Bosworth(13), and others(14). In all cases the rate of diffusion is found to vary with temperature according to an exponential law, at any rate approximately, but sometimes, as in the case of caesium on tungsten, the rate of diffusion is also a function of the concentration of atoms in the surface phase.

A theory of surface migration was given by the author(2) in 1932. It was there pointed out that the field in which an atom moves near an adsorbing surface is not two-dimensional in character, as had often been assumed, but was undulatory with a double periodicity similar to that of the lattice. A section of a typical field is shown in figure 1. The continuous lines are sections of the surfaces of equal potential energy. In the immediate neighbourhood of the position of minimum energy the surfaces are closed but eventually they open out and consist of two branches, one above and one below the equilibrium positions.

At low temperatures an adsorbed atom will vibrate about one of the points where the potential energy is a minimum, but, as the temperature of the adsorbing solid is raised, the probability increases that the atom will receive sufficient energy to surmount the potential barrier separating one potential minimum from the next. In order that an adsorbed atom may migrate it must be activated sufficiently to pass over the col between two potential pockets. It was shown that if γ is the number of times per second that an atom is activated to this mobile state and l is the average distance travelled before it is deactivated, the coefficient of diffusion D, defined as usual by the equation

$$\frac{\partial n}{\partial t}=D\frac{\partial^2 n}{\partial x^2},$$

is given by

$$D=\alpha\gamma l^2 \qquad \text{......(17)},$$

where α is a certain numerical constant of the order of $\frac{1}{2}$ or $\frac{1}{4}$. If the average lateral velocity of an atom during activation is $\bar{v}$ and the average time it remains activated is τ, while τ^* is the average interval of time between successive activations of the same atom we may write alternatively

$$D=\alpha\bar{v}^2\tau^2/(\tau+\tau^*) \qquad \text{......(18}a\text{)},$$

and if, as in many cases, τ^* is very long compared with τ, we may write

$$D=\alpha\bar{v}^2\tau^2/\tau^* \qquad \text{......(18}b\text{)}.$$

Once D is known from theory or experiment, the bulk diffusion can be calculated by the usual methods(2).

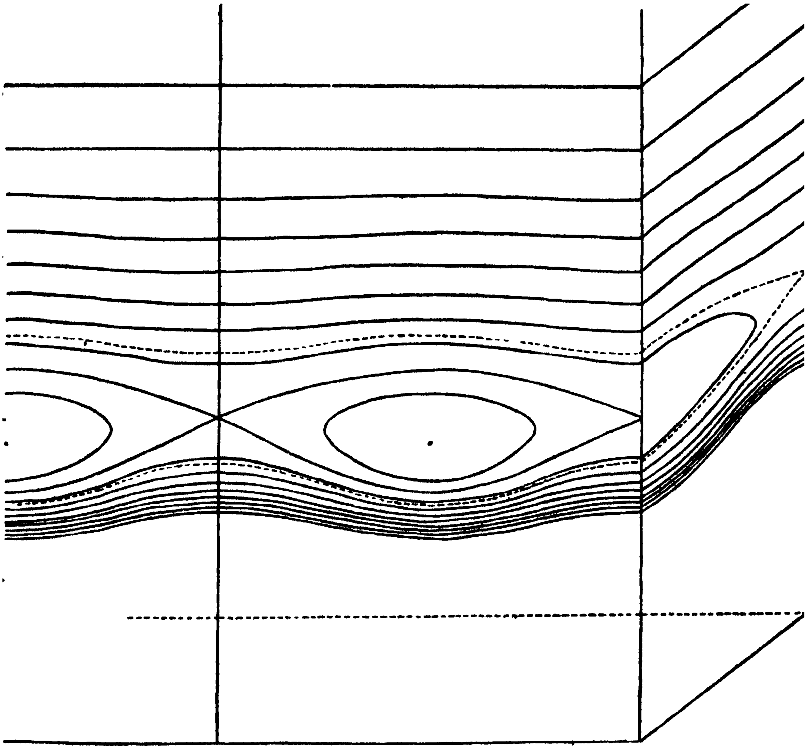

Figure 1. Two cross-sections of the potential field near an adsorbing surface. Continuous lines are sections of equipotential surfaces.

Langmuir in a later paper(11b) gave a special case of (18b), based on the assumption that an adsorbed atom is surrounded by four neighbouring sites and that an activated atom hops only to one of them. This leads to the formula

$$D=a^2/4\tau^* \qquad \text{......(19)},$$

where a is the distance between two neighbouring elementary spaces.

Langmuir also showed that if the time of transit between adjoining sites ($a/\bar{v}$) is not negligible compared with τ^*, then the formula must be modified to

$$D = a^2/4\,(\tau^* + a/v) \qquad \text{......(20)},$$

where $\bar{v}$ is the average velocity parallel to the surface during migration. If τ^* is negligible compared with $a/\bar{v}$, then Langmuir gives

$$D = av/4 \qquad \text{......(21)},$$

which is similar to the formula for a two-dimensional gas when the free path is equal to a, but it is almost certain that for a dilute film the free path would be longer than a, and the formula (21) would have to be modified accordingly.

There remain now the important theoretical problems of calculating the times τ and τ^*. Lennard-Jones and Strachan(15) have obtained theoretical formulae for these quantities for the case when an adsorbed atom is activated from one vibrational state to another for motion perpendicular to the surface and the forces binding the atom to the surface are weak. Since there are forces coupling the adsorbed atom to the underlying solid, the problem is somewhat similar to that of the interaction of coupled oscillators, and energy may be expected to surge to and fro from one to the other. The problem is a little more complicated than that because a solid must be regarded as similar to an assembly of oscillators as in Debye's theory of specific heats. It appears that when an adsorbed atom has been excited to a higher vibrational level, and the temperature is low or (kT) small compared with the energy of excitation, it remains excited for a time of the order of one period of vibration; in a particular example this time was found to about 10^{-12} sec. The important result, however, is that for the range of temperature for which the formula is applicable, the time of excitation is nearly independent of the temperature. For high temperatures the theory indicates a shorter time of excitation inversely proportional to the temperature but the theory is hardly applicable under these conditions.

The formula for the time between successive excitations contains a Boltzmann (exponential) factor corresponding to the energy of activation.

Another mechanism of activation has been considered by Lennard-Jones and Goodwin(16). When the adsorbing solid is a metal, there will in general be an interaction between the free conduction electrons and the link between solid and adsorbed atom. A simple calculation by classical methods indicates that in a typical case a surface atom may suffer as many as 10^{15} collisions per sec. by the conduction electrons of a metal and since, according to modern views, these are moving with an energy of several volts, they provide an ample reservoir of energy from which adsorbed atoms may absorb energy. The general indication is that an atom will remain excited about 10^{-12} sec. before it falls to the next vibrational level and that this time is nearly independent of the temperature. The advantage of this mechanism is that larger quanta of energy can be communicated to the adsorbed link by a single process and atoms held by chemical bonds (such as hydrogen to a metal) can be thus activated. Several thermal quanta of energy would be required to be communicated to the link *simultaneously* to produce excitation. The corresponding formula for τ^* again contains a Boltzmann term appropriate to the energy of activation.

The author has calculated the dispersal of energy from an activated link also by classical methods, considering a linear array of similar atoms infinite in extent and supposing one of them displaced from its equilibrium position and then allowed to oscillate. It is found that after one complete period the potential energy of each of the links, which was disturbed initially, has fallen to a quarter of its initial value. The dispersal of energy along the chain is thus extremely rapid.

Apart from these mechanisms of deactivation a mobile atom may lose energy also by collision with another mobile atom or by collision with an adsorbed atom in a vibrating state. If the energy of activation for migration is small compared with kT, then most of the atoms will be in the migrating phase and collisions will be numerous. If, however, the energy of activation is large compared with kT, collisions between migrating atoms will be rare, and, if the concentration is not too large so that migration is not prevented by other adsorbed atoms, we may conclude that theory indicates at present that the duration of activation will be nearly independent of temperature.

A relation between the average values of τ and τ^* may be obtained by statistical methods. Let E_s denote an energy level of an adsorbed atom in a vibrating state and E_σ a level in the migrating state (each assumed for the moment to be discrete), and let $b_{s\sigma}$ be the probability per unit time of an activation from E_s to E_σ by the underlying solid. The function $b_{s\sigma}$ includes not only the matrix element of the coupling energy but also the probability that the solid is in a state suitable for the emission of the appropriate amount of energy. Let $b_{\sigma s}$ be the probability of the reverse process. Then in general for statistical equilibrium we must have

$$b_{\sigma s} = b_{s\sigma}\, e^{(E_\sigma - E_s)/kT} \qquad \text{......(22).}$$

The average value of τ^* is given by

$$\tau^* = \frac{\sum\limits_{s} \exp(-E_s/kT)}{\sum\limits_{s}\sum\limits_{\sigma} b_{s\sigma} \exp(-E_s/kT)} \qquad \text{......(23),}$$

where the summation in the denominator is over all pairs of states such that one is in the vibrating phase and one in the migrating phase. Similarly

$$\tau = \frac{\sum\limits_{\sigma} \exp(-E_\sigma/kT)}{\sum\limits_{s}\sum\limits_{\sigma} b_{\sigma s} \exp(-E_\sigma/kT)} \qquad \text{......(24).}$$

Using equation (22), we find that the two denominators are equal and so

$$\frac{\tau^*}{\tau} = \frac{\sum\limits_{s} \exp(-E_s/kT)}{\sum\limits_{\sigma} \exp(-E_\sigma/kT)} = \frac{f^*}{f} \qquad \text{......(25),}$$

where f and f^* are the partition functions relating to the migrating and vibrating phases respectively. This result is quite general whether the levels are quantized or not. Hence the formula for the diffusion coefficient D given in (18*a*) can be written

$$D = \alpha \bar{v}^2 \tau f/(f + f^*) \qquad \text{......(26).}$$

In this formula v and τ are by definition *average* values, averaged over all migrating states; in fact, v is averaged twice, once over each migrating state and then over all such states. If the average lateral velocity in a state σ of energy E_σ during migration is v_σ, and τ_σ the duration of time spent in this state in each elementary process, the general formula for D is

$$D = \frac{\alpha \sum\limits_{\sigma} v_\sigma^2 \tau_\sigma \exp(-E_\sigma/kT)}{(f+f^*)} \qquad \text{......(27).}$$

where the numerator is a sum over all migrating states. Equations (26) and (27) are equivalent, when $v^2\tau$ in (26) is an average value, as just explained.

As an example of the application of the formula (26) we may consider the case when the periodic nature of the surface field is represented by a series of circular potential holes arranged regularly like a lattice. Let the height of the barrier separating these holes be V_0 and let the holes occupy a fraction r of the total surface area A. Then

$$f = A\,(2\pi mkT/h^2)\,e^{-V_0/kT} \qquad \text{......(28),}$$

and

$$f^* = rA\,(2\pi mkT/h^2)\,(1 - e^{-V_0/kT}) \qquad \text{......(29),}$$

so that for this model

$$D = \alpha v^2\tau / \{(1-r) + r\exp(V_0/kT)\} \qquad \text{......(30).}$$

When V_0 is large compared with kT, this may be written

$$D = (\alpha v^2\tau/r)\,e^{-V_0/kT} \qquad \text{......(31}a\text{),}$$

and when V_0 is small compared with kT, we have

$$D = \alpha v^2\tau \Big/ \left\{1 + r\frac{V_0}{kT}\right\} \qquad \text{......(31}b\text{).}$$

In the limiting case when V_0 becomes zero, the formula for D is

$$D = \alpha v^2\tau = \alpha v l \qquad \text{......(31}c\text{),}$$

where τ is now the time between successive collisions in a two-dimensional gas and l is the mean free path. This is the usual form for the diffusion coefficient for a two-dimensional gas, and simple theories give for α the value of $\frac{1}{2}$.

As an example of the application of formula (31a), we may examine the experimental results obtained by Bosworth(13) for the migration of sodium atoms along a tungsten surface. Bosworth shows that his observations can be represented by the formula

$$D = aT^{\frac{1}{2}}\,e^{-b/T}$$

and from his figures it may be deduced that $b = 2750$, which is equivalent to an energy of activation V_0 of 5500 cal./gram-atom or 0·24 eV. He does not give the value of a but it appears to be (5·64) 10^{-3}, and comparison with the theoretical formula gives

$$\alpha\bar{v}^2\tau/r = (5{\cdot}64)\,10^{-3}\,T^{\frac{1}{2}}.$$

Taking τ to be 10^{-13} sec. and α/r to be unity, we then get $\bar{v} = (2{\cdot}4)\,T^{\frac{1}{4}}\,10^5$ cm./sec. and the free path ($l = v\tau$) at room temperature is 10^{-7} cm. or about three or four times the length of a unit cell. A rough calculation gives the frequency of vibration of sodium about its position of equilibrium on the surface to be about 2.10^{-13} sec., so that τ may be longer than 10^{-13} sec. Taking it to be 10^{-12} sec., which is likely to be an extreme value, the free path comes out at about $3 \cdot 10^{-7}$ cm., the equivalent of about nine unit cells. In any event the results of Bosworth, interpreted in terms of (31*a*) indicate that the free path is only slightly dependent on temperature. The factor which governs the rate of migration is the rate of activation to the migrating state.

Finally it may be mentioned that migration may occur when atoms collide with the surface from the vapour phase. It has been shown(18) that under certain conditions atoms may be diffracted at a surface without loss of energy in such a way that the atom afterwards runs along the surface. It is caught in one of the vibratory levels perpendicular to the surface, but the energy lost in the normal direction is taken up by the lateral motion and it speeds along in a migratory level. This mechanism satisfactorily explains the observations of Frisch and Stern(19) on the anomalous diffraction of helium by certain crystals and the calculations lead to the conclusion that the mean path of these atoms along the surface before being again diffracted into the vapour phase would be as long as 10^{-5} cm. As they are not so diffracted but are lost from the beam (thus producing the observed anomalies), the inference is that these migrating atoms lose energy either as a result of an encounter with an imperfection in the crystal or with an adsorbed atom or by their interaction with the solid and do not travel so far as 10^{-5} cm. This calculation therefore gives us an upper limit to a free path during migration and, as helium is a light atom and likely to migrate further than heavier atoms under similar conditions, we may infer that free paths are much shorter than 10^{-5} cm.

Migration at very low temperatures will not normally occur except at rates which are so slow as to be unobservable, but helium on certain solids appears to be an exception(20). Owing to the low energy barrier between neighbouring equilibrium positions and the small mass of the helium atom, penetration of the barrier may occur and calculations by quantum methods show that helium atoms may migrate almost like a two-dimensional gas however low the temperature.

REFERENCES

(1) APPLEYARD and LOVELL. *Proc. phys. Soc.* above (1937).
(2) LENNARD-JONES. *Trans. Faraday Soc.* **28**, 333 (1932).
(3) COCKCROFT. *Proc. roy. Soc.* A, **119**, 293 (1928).
(4) FRENKEL. *Z. Phys.* **26**, 117 (1924).
(5) FOWLER. *Proc. Camb. phil. Soc.* **32**, 144 (1936).
(6) BRAGG and WILLIAMS. *Proc. roy. Soc.* A, **145**, 699 (1934); **151**, 540 (1935).
(7) BETHE. *Proc. roy. Soc.* A, **150**, 552 (1935).
(8) PEIERLS. *Proc. Camb. phil. Soc.* **32**, 471 (1936).
(9) LENNARD-JONES and DEVONSHIRE. (To be published shortly.)
(10) VOLMER. *Trans. Faraday Soc.* **28**, 359 (1932).

(11) (*a*) Langmuir and Taylor. *Phys. Rev.* **40**, 463 (1932).

(*b*) Taylor and Langmuir. *Phys. Rev.* **44**, 423 (1933).

(12) Brittain and Becker. *Phys. Rev.* **43**, 428 (1933).

(13) Bosworth. *Proc. roy. Soc.* A, **150**, 58 (1935), **154**, 112 (1936).

(14) (*a*) Gehrts. *Z. tech. Phys.* **15**, 456 (1934).

(*b*) Bresler, Talmud and Talmud. *Phys. Z. Sowjet,* **4**, 864 (1934).

(*c*) Schwarz. *Z. phys. Chem.* **168**, 241 (1934).

(*d*) Alty and Clark. *Trans. Faraday Soc.* **31**, 648 (1935).

(15) Lennard-Jones and Strachan. *Proc. roy. Soc.* A, **150**, 442 (1935).

(16) Lennard-Jones and Goodwin. (To be published shortly.)

(17) Lennard-Jones and Devonshire. *Proc. roy. Soc.* A, **156**, 14, equation (29), (1936).

(18) Lennard-Jones and Devonshire. *Proc. roy. Soc.* A, **158**, 253 (1937).

(19) Frisch and Stern. *Z. Phys.* **84**, 430 (1933).

(20) Lennard-Jones and Devonshire. *Proc. roy. Soc.* A, **158**, 242 (1937).

DISCUSSION OF THE PAPERS BY FINCH, APPLEYARD AND LENNARD-JONES

Reported by E. T. S. APPLEYARD

One of the important questions discussed was the cause of the negative temperature coefficient of resistance observed in so many thin films but not in the case of the alkali metals.

Dr Lovell gave an account of some preliminary results which he had obtained with thin films of thallium deposited under the same high vacuum conditions already used by him for the alkali metals. In the region of thickness between 20 and 30 A., the resistivity of the films was about 10^4 times that of the bulk metal, and they showed a negative temperature coefficient. But both their resistivity and their temperature coefficients were much below those obtained previously by Cosslett using the similar metal indium in a vacuum of about 10^{-5} mm. of mercury. On this account Dr Lovell believed that the idea of Cosslett that the negative temperature coefficient was in some way due to gas adsorbed or occluded in the film was strongly supported, more especially since he himself had been able to alter both the resistivity and the temperature coefficient of his thallium films by altering their rate of deposition.

Dr de Boer was unable to accept the general explanation of negative temperature coefficients given above. On the experimental side he pointed out that the results he had obtained with molybdenum were quite reproducible in successive experiments. Moreover, certain unpublished results obtained recently in his laboratory with evaporated tungsten films exactly reproduced the results obtained many years ago by Reinders and Hamburger. It seemed to him almost inconceivable that this agreement could be obtained if the residual gas played any important part. Moreover, he had found that the influence of gas upon the resistivity of the films once formed was unimportant except in the case of oxygen, and that even here the influence was not appreciable provided that the films were kept at liquid air temperatures. He adhered to the view that the thin films of molybdenum and tungsten showed a different atomic spacing from those of the bulk metal, at any rate in the early layers, and that as a consequence of this larger spacing (for which, as yet, there was admittedly no other experimental evidence) the thin films behaved like a semi-conductor. The lower conductivity could arise either as a result of the raising of the potential barriers between successive metallic ions, or from a diminished overlapping of the electronic bands; both would be favoured by an increased interatomic spacing. He suggested that a direct experimental measurement of the distribution of the electrons in the bands (as compared with the distribution in the bulk metal) might be obtained if Skinner's* method of investigating the X-ray emission spectrum were applied to very thin metallic films.

Dr Fuchs remarked that for monovalent metals a very considerable increase in atomic spacing would be necessary to produce the transition from the metallic to the semi-conducting state, for the potential barrier between successive lattice points was not at all sensitive to small increases of spacing.

Dr Klatzow said that some experiments of his own on the electrical resistance of composite caesium films such as are employed in commercial photoelectric practice had led him to believe that (in agreement with the view of Lovell and Appleyard) their high resistivity and negative temperature coefficients were both to be explained in terms of a disintegrated structure. He suggested that in this case the current was carried across the gaps in the film by cold emission of electrons, i.e. by the movement of electrons across the gaps under the action of the applied electric field (cf. Frenkel, *Phys. Rev.* **36**, 1613 (1930), Ehrenberg and Hönl, *Z. Phys.* **68**, 289 (1931)). On such a theory an increase in the work function would decrease the current. This notion was made more reasonable because on evaporating a thin layer of silver over the composite layer its resistance actually increased. Silver deposition in this way was known quite independently to raise the work function and to diminish the cold-emission of such composite surfaces.

The above discussion clarified the points of difference between the possible hypotheses used to explain the negative temperature coefficient, but no definite conclusions could be drawn as to which one was correct.

Another point discussed was the role of agglomeration in thin films.

Prof. Fowler criticized Dr Appleyard's criterion for agglomeration. He remarked that although it led to the right results when applied at these low temperatures, the general condition for any isothermal process to be possible was of course that the free energy (and not the potential energy) should diminish.

Dr Cockcroft remarked that the values given in table 2 of Dr Appleyard's review should be accepted with reserve since they were obtained in the days before vacuum technique had approached its present level and the surfaces must have been very dirty judged by present standards. This was proved by the fact that the latent heat of evaporation was the same for surfaces of copper, silver and glass. He asked whether the mercury films described in the report were affected by previous heat treatment of the substrate. Dr Appleyard replied that prolonged heat treatment of the type given by Lovell seemed to make no difference whatsoever to the critical thickness or the shape of the resistivity curve, and that this was consistent with the view that mercury-on-pyrex was an extreme case of type-III films.

Dr Skinner observed that zinc, cadmium and mercury seemed to stick with great difficulty to celluloid surfaces. In these cases he had been successful in obtaining films only by saturating the substrate with dirt from the backing vacuum.

Dr de Boer drew attention to the results of some experiments carried out in his laboratory on the electrical resistance of evaporated layers of alkali halides coated with adsorbed films of caesium. The halides have a lamellar and labyrinthine structure; the adsorbed layers of caesium on the surfaces of the lamellae are superposed upon each other and so absorb enough light to be visible. It was found that the electrical resistance of such a composite layer changed only very slowly as the adsorption of caesium continued which suggested that agglomeration might be taking place on top of a stable monolayer. Dr Appleyard said that this effect was perhaps somewhat similar to that observed with caesium-on-pyrex. In this case the early layers appeared to be more stable than thicker layers, which suggested that agglomeration here also took place most rapidly with the second, third ... etc. layers, the first layer agglomerating only slowly.

---

* O'Bryan and Skinner, *Phys. Rev.* **45**, 370 (1934). Skinner and Johnson, *Proc. roy. Soc.* A (in Press).

The discussion on agglomeration continued after the paper of Prof. Lennard-Jones. In reply to questions Prof. Lennard-Jones said that he was quite unable to understand how mercury-on-pyrex could possibly show the high mobility at low temperatures suggested by the experimental results. There was no analogy (as Dr Appleyard had implied) between this case and that of helium-on-lithium fluoride previously discussed by him, for the finite mobility at all temperatures above absolute zero obtained with helium depended entirely upon the small mass of the helium atom. It was, of course, possible in principle to calculate the interaction of a mercury atom with a silica surface, and in this way to obtain values for the latent heat and the activation energy, but he would be surprised if the values obtained were low enough to account for the experimental results. A brief discussion then took place on the proper assumptions to be used in calculating the forces in this case.

The general conclusion seemed to be that the role of agglomeration was extremely important in accounting for the high resistance of metal films, and that the criteria for agglomeration put forward by Prof. Lennard-Jones and Dr Appleyard provided a starting point for understanding the process. In spite of this, the paucity of data on the latent heats of evaporation of metals from insulating surfaces prevented anything but the most general qualitative conclusions being drawn in particular cases.

The sputtered films obtained by Dr Féry were also discussed with interest. Prof. Finch mentioned that certain experiments he had performed some time ago were in agreement with the extended investigations of Dr Féry. He too had been able to obtain a catalytic deposit by suitable sputtering methods, and he had found like Dr Féry that the presence of H_2 or H_2 and O_2 in the discharge inhibited the formation of catalytic platinum. He drew attention also to the experimental fact that metal foils heated in air showed a great tendency to form a single crystal, but metallic deposits on an insulating substrate did not.

On Dr Féry's paper Dr Appleyard remarked that it was extremely valuable in enabling us to understand how the black-white transition in platinum could account for the extravagantly different results of previous workers on sputtered films. He remarked that although the temperature coefficient as ordinarily defined diminished greatly on annealing, nevertheless the resistivity change per degree shown in Dr

Féry's work remained fairly constant and approximately the same as for the bulk metal. This could perhaps be accounted for by assuming a diminishing "restwiderstand".

Dr de Boer then showed another case of an unstable film, in this instance silver evaporated on a liquid air cooled surface. This film on heating suffered an almost explosive disintegration accompanied by a flash of light.

CAMBRIDGE: PRINTED BY WALTER LEWIS, M.A., AT THE UNIVERSITY PRESS

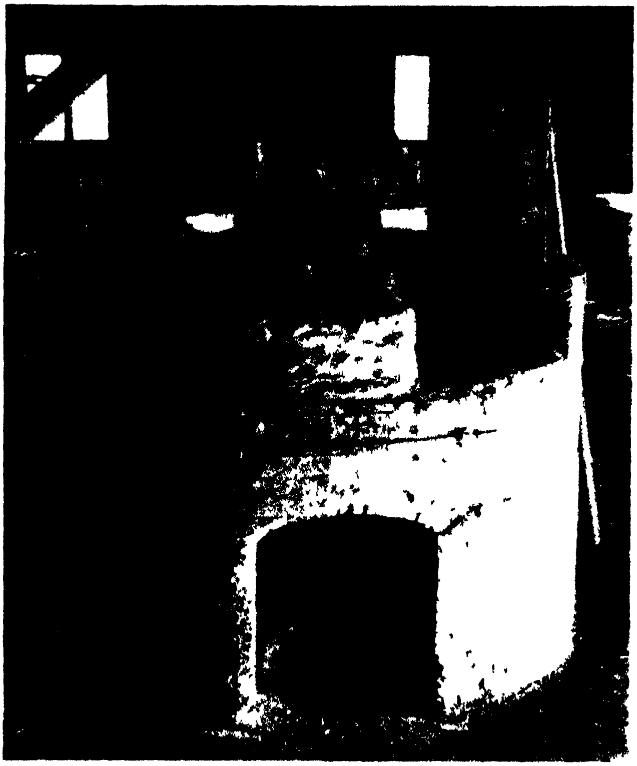

Frontispiece

THE PROCEEDINGS OF
THE PHYSICAL SOCIETY

VOL. 49, PART 5 *September* 1, 1937 NO. 275

THE OPTICAL GLASSWORKS AT BENEDIKTBEUERN

BY W. H. S. CHANCE, M.A. (Cantab.)

Address given before the Physical Society at Burlington House,
3 December 1936

THE history of the manufacture of glass produced specifically for optical use covers the short span of just over 130 years. Although the discovery of the achromatic lens, by Chester Moor Hall between 1729 and 1733 and its development by Dolland from 1758 onwards, was the first radical improvement in optics since the discovery of spectacles about the year 1300, progress was limited owing to the difficulty of obtaining suitable glass, and particularly flint glass, of adequate homogeneity.

Prof. von Rohr has rendered great service to the cause of historical research by his investigations on optics, and it was through a study of his writings that I learnt of Fraunhofer's work at Benediktbeuern. During a visit paid last summer to the Deutsches Museum at Munich, I noticed a photograph of the old works, and determined later to visit this historic spot; but this is getting ahead of our story, and we must revert to Munich in the year 1801, when the French Government were requiring a military map of Bavaria, but were encountering difficulties owing to the lack of suitable surveying instruments. About this time, an artillery officer, Georg Reichenbach, had journeyed to England to study machine construction and foundry work, and had seen some of the important businesses producing mathematical instruments. He determined to set up such a works in Bavaria, so as to make his country independent of foreign supply, and to train a body of highly skilled artisans. In 1802, Reichenbach joined the clever mechanic and watchmaker, Liebherr, who already possessed a small workshop, and two years later they formed a partnership with Geheimreferendar Joseph Utzschneider, a man of affairs no longer active in the service of the State, and possessing interests in cloth and leather works.

It was on 20 August 1804, that the "Mathematical Mechanical Institute Reichenbach, Utzschneider and Liebherr" came into being, and the manufacture of instruments commenced. The concern very soon found itself in difficulties owing to lack of suitable lenses, so Joseph Niggl, a skilful but empirically trained optician, was engaged. However, lenses could not be made without suitable glass, and in particular flint glass, which was almost unprocurable in France and Germany, and could only be obtained with difficulty in England. The success of the new undertaking was at stake, and the energetic Utzschneider set himself to solve the problem. He visited various well-known South German opticians, but it was not until he got in touch through the Swiss J. S. Gruner with another Swiss, by name Guinand, that any prospects of success appeared likely. Pierre Louis Guinand, born on 20 April 1748, was brought up as a skilled cabinet maker and specialized in the production of clock cases. Later he became acquainted with the work of casting metals, and as a hobby interested himself in making spectacles and telescopes. Deciding to make his own instruments, he was faced with the necessity of procuring suitable lenses, and decided to experiment with the production of glass. An account of his experiences is contained in a memorandum prepared by him for Utzschneider in 1804. We learn that after studying books on chemistry and consulting the encyclopaedia, he started in 1774 to make small trial melts using some 3-4 lb. of materials, trying variations in composition and temperature, and recording systematically the results. After 13 years' experimenting, he decided that the scale of his operations was not big enough to achieve results, and in 1787 constructed a furnace in which he could make melts weighing up to 200 lb. He had moved his residence to les Brenets (West Switzerland) in 1781, and purchased a mill with the object of using the water power to drive his glass saws and polishing machines. Owing to lack of means, progress was slow, but it seems that in 1798 he started to improve the homogeneity of his glass by means of stirring, though at first without much success. However, he must have made progress, as he felt sufficiently confident to send samples to French opticians, and later to approach the Elector Palatine of Bavaria with proposals to deliver flint glass free from striae. In 1805, Utzschneider and Guinand came into direct contact and met in Aarau. An agreement was made by which Guinand should carry out some trial melts at Utzschneider's expense, and this was done between April and July 1805. Guinand prepared a memorandum on his results—*Memorandum on Making Glass, especially of High Refraction for the Manufacture of Achromatic Telescopes*—which gives us a mass of detail concerning his early trials and those paid for by Utzschneider. It appears that in July of that year, he used for the first time a stirrer consisting of a hollow fireclay tube, moved through the glass by means of an iron hook-ended rod. This was undoubtedly the secret of his success, and to this day forms the essential feature of the process of optical glass manufacture. Samples were sent to Munich for testing, and must have given satisfaction, as Utzschneider visited Guinand at les Brenets in the autumn, entered into an arrangement with him to come to Bavaria, and gave him a handsome sum towards the cost of his journey.

Utzschneider about this time purchased the Benedictine Monastery at Benediktbeuern, with its farm and lands. It lies about 30 miles from Munich, close to the foothills of the Benediktenwand, and is situated in charming country. Founded in the eighth century, supposedly in connection with the activity of Holy Bonifacius in Bavaria, it had been destroyed by the Hungarians in 985, but rebuilt by the Benedictines of Tegernsee in 1031. It became a great centre of art and learning, but fell on evil times in the Thirty Years' War and in 1632 was plundered by the Swedes. In 1803, it was dissolved and for 130 years put to secular use. It covers a large area of ground and embodies the original cloister adjoining the church, another large cloister built at a later date forming the convent buildings, together with extensive farm and other buildings. At the present time, it is occupied partly by the Salesian order as a theological college and partly by a contingent of the Labour Corps.

Doubtless one of the attractions in Utzschneider's mind was the abundant supply of wood for his furnace and he selected the washhouse to serve as his factory, as being suitable for housing Guinand and as having a mill stream running past which could easily be employed to drive the polishing machinery. Later I shall describe the present state of the house and its wooden extension which houses the furnaces.

Guinand brought with him his young second wife, Rosalie, and set to work to build a furnace and to get together the necessary equipment. Some melts were made, though not altogether with success, but Utzschneider seems to have been satisfied with the glass, which was probably tested by Niggl. At any rate, an agreement was drawn up in May 1806, of which the following is a summary of the terms:

(1) Guinand was to work the furnaces himself with the help of his wife and, with a view to maintaining strict secrecy, was only to employ outside labour for non-essential work.

(2) With a view to making use of the whole of the convent buildings, there should be set up a manufactory for achromatic lenses, but crown and flint glass should not be sold in the raw state except in limited quantity to the partnership in Munich, and all the rest should be used for making lenses under Guinand's control at Benediktbeuern.

(3) In addition to the optical glass, a glassworks was to be started for the manufacture of white glass.

(4) Guinand was to receive 500 florins per annum with lodging and fuel, and one-fifth of the profits of the establishment.

(5) As recompense for his discovery, and to bind him to secrecy, Guinand was to receive 500 florins per year for 10 years.

(6) Guinand's wife, Rosalie, was to assist her husband and after his death to receive 200 florins yearly for life; and Guinand was to instruct one of his sons so as to be able to succeed him in the event of his death.

(7) The management of the concern, the engagement of workers and all financial matters were to be continued by Utzschneider, and, in the event of the venture prospering, a furnace was to be erected for the manufacture of cast glass.

The first agreement did not work out altogether as expected, and in February 1807 a second agreement was signed. Whereas the first was entered into by Utzschneider alone on the one part, the partnership at Munich were the contracting parties on the second. Guinand was engaged for 10 years to concern himself only with optics and principally the mounting of objectives. He was to go to Benediktbeuern several times a year to make glass for the partnership, to instruct a person, nominated by Utzschneider, in his methods, and to receive 1600 florins yearly, with furnished house and fuel. The house at Benediktbeuern was to be put at his disposition as and when required, and his travelling expenses paid. At the end of his contract, he was to receive a yearly pension of 800 florins, together with house and fuel (unless he returned to his native country), and in the event of his death, his wife was to receive a pension of 250 florins yearly, provided she did not disclose his secrets.

In point of fact, Guinand did not go to Munich, presumably because it was decided to transfer the manufacture of lenses to Benediktbeuern, and it was thought vital to the Munich partnership that Guinand should make a real success with his glass.

We must now leave glass for the moment and turn to the optical side, of which Niggl was in charge. Utzschneider decided to provide him with an assistant, and after making enquiries, engaged one, Joseph Fraunhofer, then twenty years old. Fraunhofer was born on 16 January 1787, the son of a master glazier at Straubing, and lost both his parents when only 11 years old. Guardians were appointed, and Fraunhofer was apprenticed to a wood turner. The work did not suit him, and it was decided to make him a glass cutter and mirror polisher, to which end he was apprenticed to one, Weichselberger, who seems to have been a stern taskmaster and disciplinarian. In the second year of his apprenticeship, a fortunate accident—the collapse of the house in which he was working and under the ruins of which he was buried—brought him to the notice of the Elector of Bavaria, who gave him a substantial present, part of which he spent in buying himself out of his contract. After trying to make himself independent, he was forced to return to his master. His education, until now, had been very scanty, but a fortunate meeting with Utzschneider at the time of the accident enabled him to begin to study the best books on optics, and he seems to have made full use of his opportunities, for on Niggl's departure from the Munich establishment towards the end of 1807, Fraunhofer was put in charge in his place, and shortly after moved to Benediktbeuern, where Utzschneider had installed a special optical workshop. I cannot say whether this occupied part of the convent washhouse, or whether it was placed elsewhere, but it would seem possible that the former was the case, as the washhouse is a spacious building and bordered on one side by the mill stream, which could easily have been used for driving Guinand's grinding and polishing machinery, as in the case of the water-driven crusher for raw materials.

Fraunhofer set to work with amazing energy for one so young. He had already shown signs of his inventive genius in undertaking the task of converting a grinding machine for spherical into one for aspherical surfaces. Apprentices were engaged and instructed, new methods of manufacture introduced and the business organized to speed up delivery. From the first there was a clash of temperaments between Guinand and Fraunhofer; the former sanguine and optimistic, the latter cold and patient. Fraunhofer expressed dissatisfaction at the quality of Guinand's glass, while Guinand was piqued that a much younger man should criticize his work.

At last Utzschneider had to intervene, and, in spite of Guinand's objections, it was arranged in accordance with the agreement that Fraunhofer should be instructed in Guinand's methods of glass-making (August 1809).

Although we have little information about what was actually done, great strides must have been made in improving the manufacture, as is shown by the price lists of 1811 and 1812, in which are listed hand telescopes with objectives up to 83 mm. in diameter. There is little doubt that the progress was mainly due to Fraunhofer, and it is probable that, apart from increasing the size of the pot from 2 to 4 cwt. content, improvements in technique rather than improvements in principle were the secret of success.

By 1811, Fraunhofer was put in charge of all the work at Benediktbeuern. He had been taken in as junior partner in 1809, and the firm was known as the "Optical Institute of Messrs Utzschneider, Reichenbach and Fraunhofer at Benediktbeuern".

Ever since Fraunhofer's arrival at Benediktbeuern, Guinand had been unsettled, and a letter to his son, Aimé, shows that he had thoughts of returning home. We know that he had a secret arrangement with a young Strahl, who came to Benediktbeuern in 1809, and whom he instructed in his glass-making methods with a view to using his services later on his own account. In 1813 matters came to a head, and in December of that year it was agreed that Guinand should return home the following May, that his pension of 800 florins annually should commence, the payment for 1814 and 1815 being made in advance, that his wife should receive her pension in the event of his death, and that he and his wife should not interest themselves in optics or make or assist others to make glass, failing which their pensions were to cease.

The design of the original furnace built by Guinand and his young wife can only be surmised by reference to the memorandum in which he describes his early efforts, and by an examination of the two furnaces now standing as they were left when the works closed down in the 90's of last century.

Guinand's first large furnace was heated at the side (by wood) and the waste gases could be passed either through a chimney or used partially to warm a subsidiary chamber in which the blocks of glass were flowed out in moulds into discs or prisms. Another chamber adjoining the melting furnace was used for "fritting" (preheating) the raw materials, and on top of the flowing-out chamber was a large box for drying wood. The stirrer was introduced through a hole arranged vertically above the pot and could be rotated by a rope-driven mechanism.

This furnace seems to have given inadequate heat to free the glass from bubbles, particularly in the case of crown glass melts, and a new design had its fire below the pot and was arranged to tilt, so as to allow the glass after stirring to be poured into a suitable mould. The pot was supported on bearers, and was about 18 in. internal diameter and 1 ft. high. As he had trouble with pots breaking, he fixed the melting pot inside an outer pot which was supported at a number of points against the walls of the furnace; the space between the inner and outer pots being filled with sand. Means for stirring were similar to the first furnace and the stirrer could also be moved up and down, so as to increase the mixing effect.

The Benediktbeuern furnaces are circular and have a tunnel running through the bottom which contains the fire grate. The pot was placed in a chamber in the centre of the furnace and rested upon a hearth through which penetrated the flames from the fire grate. At the top of the furnace two sections, resembling slices from a circular cheese, are cut out and were used for filling the pot and viewing the progress of operations. The walls of the hearth are vertical, thus forming a circular chamber, which is closed at the top by means of a circular fire-clay stopper. Each furnace has its own crane for lifting the pots in and out. The stirring mechanism consists of an iron rod affixed to the roof of the building and hanging vertically over the centre of the pot. It is forked at its bottom end and provision made to attach the fire-clay stirrer. Rotation is effected by means of a long arm attached at one end to a crank, which can be rotated, and at the other to the iron rod. To seal the mouth of the furnace, a second circular fire-clay stopper is attached by three adjustable arms to the stirring rod, such that the disc swings just clear of the circular cover slab, in which is a central hole of size appropriate to allow the stirring rod to move. The movement of the stirrer through the glass does not appear to have been capable of any great regulation, and must have depended to some extent upon the speed of rotation of the driving crank.

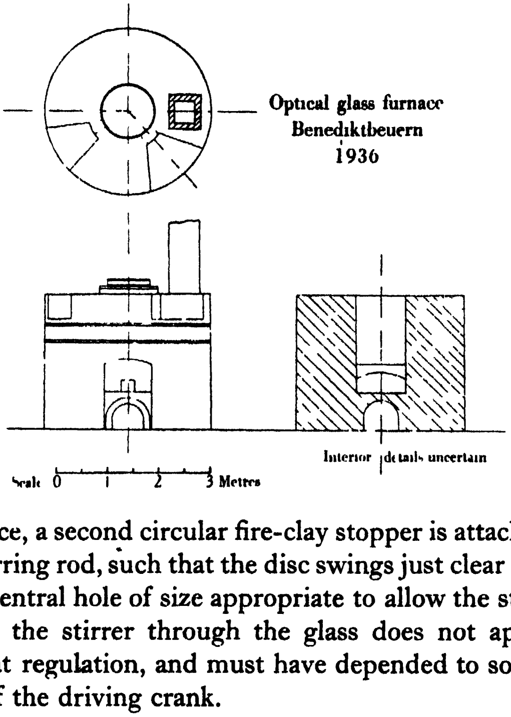

Although the two existing furnaces must have been erected subsequent to Guinand's original furnace, it seems probable that they were built after Fraunhofer's death. They differ little in principle from Guinand's last furnace, except that the means for tilting to effect pouring of the glass into moulds is not incorporated. We know that Fraunhofer made a practice of making one or two small experimental pots of glass with each full scale melt, and the dimensions of the existing furnaces would not seem adequate for this purpose. It is interesting to note that other successors to Guinand's secret altered the method of stirring in that the stirrer was introduced through the side of the furnace, possibly as making a more convenient arrangement and probably also as it was found desirable to use covered pots for the manufacture of flint glass. The dimensions of the pot used would not appear to have been increased beyond the 4 cwt. size, as the furnace chamber is not big enough to take a larger pot.

The two furnaces described are installed in a wooden building 62 ft. long by 18 ft. wide, adjoining the one-time washhouse. In one corner is a kiln used for "flowing out" lumps of glass recovered after the melting pots had cooled down and their contents broken into suitable sized pieces. A short while ago, the property was purchased by Prof. Walther Küchler, late of Vienna and other universities, and has been converted into a charming residence. The main building is spacious and has three floors and an attic which communicates by stairs with the glasshouse. It seems possible that this was used for building and storing pots. In the basement were stored raw materials and the remains of a crusher driven by a water wheel can still be seen. Realizing the historic interest of the place, Prof. Küchler has been wise enough to have the furnace building left intact, and it is to his services, in preserving what might easily have been scrapped as of no practical value, that I am indebted for my information.

Fraunhofer kept careful records of his melts, and on his deathbed dictated to his friend the Mintdirektor von Leprieur a memorandum describing the manufacture of crown glass. Among his papers is an account of a flint glass melt made in 1814. From these sources we know something of his methods and can compare them with the recollections of one of the workmen employed later under Merz (of whom more anon). Fraunhofer's description runs as follows:

> The following were the methods employed with Flint glass No. 16: On 20 January (1814) the pot was brought to the furnace. The bottom of the outer pot was covered with clean crushed quartz to a depth of about 1″, the inner pot placed inside, and the space between the two filled with similar quartz. The pots were then hung by three irons, which could be adjusted with screws, to the rope of the large crane, such that the inner walls of the pot were set vertically. The siege of the furnace was covered with 1½″ of clay and the pots lowered onto the siege. As the inner wall of the pot hung vertically, it must remain vertical in the furnace when it sank onto the clay bed. The inner wall of the small pot was painted with powdered glass before placing it into the furnace. The furnace was not closed, a cover being placed over the pots. The large and small stoppers were bedded in lime and only one of the inspection holes left open, through which on the 21st a fire of undried wood was lighted. At night the inspection hole was closed by a stopper and in the morning fire was again made; until the morning of the 26th this procedure continued, when a fire was made in the fireholes with undried wood. At night dried wood was charged, so that by the morning of the 27th the furnace was hot enough. On this morning the Potash was prepared and added to the batch. Several days previously the Saltpetre had been mixed with the red lead, to which the Quartz had already been added; and last of all the Potash, in proportions shown in the records, and still so wet as not to be quite fluid. Before the furnace had reached its top temperature, it was glazed with flint glass cullet and this was then removed. At 9.30 in the morning filling of the batch commenced. Only two shovelfulls were filled on at a time, so as not to chill the pot excessively and risk losing it; 8–10 minutes pause took place between fillings. At 7 in the evening the filling was finished and the pot quite full, so that 100 lbs. of glass had to be ladled out. From 11 midday to 9 in the evening the glass was stirred with the cylinder every 8–10 minutes. At 9.30 in the morning of the 28th the glass was skimmed and then stirred till 12 noon, at which hour

the furnace required stoking. At 1 o'clock the cover of the furnace was removed and the glass carefully skimmed, and at 1.45 the fire was again stoked, at first lightly and then more heavily. About 3.30 in the afternoon stirring was again started and continued till 5; it took place every ½ hour and at first more often; during this period birch wood was used for firing. At 8.30 in the evening preparations were made for the last stages and at 10 stirring began again. The stirrer moved about 1½" from the pot wall, and was turned evenly backwards and forwards. The glass was fairly fluid. Before the last stirring the glass was again carefully skimmed. At 1.30 a.m. on 29th stirring ceased. The furnace remained open for an hour and the openings were then closed and 5 hours later bushed up with lime and the inner stopper covered with earth so as to slow up the rate of cooling of the furnace.

Fraunhofer's instructions (1826) for making crown glass give some further information about his methods. He stated that a larger furnace was required than when making flint glass. The batch was similar to that used for ordinary white glass, but gave a yellowish green colour and after "flowing out" often devitrified. By raising the chimney flue and thus altering the direction of the flames matters were improved, but the colour was still unsatisfactory and attention was turned to the raw materials. He noted that potash was the most important, and tested its purity by calcining and observing its colour. The selected material was again calcined, dissolved in water and allowed to stand until impurities had settled out. The solution was then poured into a boiler and heated until the neutral salts began to crystallize; the solution was then poured into glazed bottles and allowed to cool and crystallize, the resultant potassium oxide being heated on the day when it was used. The silica was introduced in the form of quartz obtained from the Zillertal (Tirol). It was calcined, cracked in water and the coloured impurities removed; then crushed in the stamp mill and sieved to the desired fineness. The lime needed careful selection and its choice required experience.

The proportioning of the raw materials was considered important, as an excess of lime and potash, though giving a glass free from bubbles, increased the tendency of the resultant glass to weather. It is interesting to note that Fraunhofer discovered that an addition of alumina, though giving rise to poor colour, improved the durability. Crown glass is hard to free from bubbles and small fillings are advised. It is also considered very important to pay particular attention to the firing and not to fill away unless the furnace is at its proper temperature.

Plank, the workman previously referred to, throws some light on the developments since Fraunhofer's time, though procedure seems to have undergone little alteration. It was considered important to dry the wood before firing and this was done in a separate building adjoining the furnace house. Beech wood was considered essential for the furnace and was cut into small pieces to give even firing. Instead of quartz, sand was obtained from Nantesbuch, a small village near Wolfratshausen, and was crushed, washed and sieved. Lead oxide came from abroad and the potash seems to have been obtained locally and purified as before. The pots were made of a mixture of Kassel clay and clay from Kehlheim. Possibly this was a better material than that used by Fraunhofer and obviated the necessity for an outer pot. To the clay was added suitable proportions of broken pots and "flowing-out" moulds.

The furnace nearest the house was used for flints, only one furnace being used at a time. A crew of four men with several boys to assist seems to have been the normal complement. Melts were made at a rate depending upon the demand, but generally one per month; the flints taking 5 days and the crown 8 days, not including the period of about a fortnight during which the furnace was cooling down.

The "flowing-out" furnace was fired with pine wood and heated until the lumps of glass "flowed out" into moulds, whereupon it was sealed and allowed to cool for some 14 days. Unsuitable glass was sent to Munich, where bubbles were ground out, and returned to Benediktbeuern for "flowing-out", the scrap glass being crushed and mixed with the batch.

During the period 1811–14, Fraunhofer not only supervised the glass-making, but was engaged upon a work of fundamental importance—the accurate measurement of the refractive index and dispersion of the meltings made. He hit upon the idea of using the dark lines of the spectrum previously noticed by Wollaston in 1802, and used for his purpose a theodolite. In 1817, he read an important paper before the Munich Academy in which he accounted for 574 of these lines and later was able to determine the length of the corresponding light waves for seven of the most important lines. He was led to this work by the necessity to reduce the secondary chromatism of his lenses and could not tackle the problem satisfactorily until he could measure accurately the optical properties of his glasses. By means of small trial pots which accompanied the full-scale meltings he experimented with different proportions of raw materials and in his paper of 1817 he could describe a pair of flint and crown glasses (Flint 13 and Crown M) which showed considerable improvement in that they possessed a more or less proportionate increase in partial dispersions. Owing to the glass being of poor durability, it was not in fact used commercially.

In 1811, forty-eight people were employed in the works, including five turners, twenty glass polishers, two tube drawers and so on. About this time, the manufacture of spectacle lenses was introduced and continued to persist as a cottage industry after the optical section of the works was transferred to Munich in 1819.

Reichenbach left the partnership in 1814 to found his own workshop for precision instruments, but continued to procure his glass from Benediktbeuern, and in the same year, Guinand left as had been arranged. We hear of him two years later when he endeavoured to persuade Utzschneider to take him back, though without success, as Utzschneider had heard of his attempts to restart his own glass works contrary to the terms of the agreement and refused to reply.

The undertaking was now solely in the hands of Utzschneider and Fraunhofer, and a new partnership was formed, in which Fraunhofer was given a substantial interest. Progress continued to be made in improving the quality of the instruments manufactured, and in increasing the size of the lenses employed. The glass making remained Fraunhofer's sole responsibility, and no one else was allowed to learn its secrets. He looked after the purchases of chemicals and other materials, and was responsible for the whole organization. In 1819, Utzschneider decided to move the optical section of the business to Munich, and sold the convent to the State, retaining only the glasshouse. No doubt it was found inconvenient for visitors to travel the 30 miles from Munich, and possibly the supply of skilled labour presented a difficulty.

Among other problems tackled by Fraunhofer was the question of glass durability, which he tested by using sulphuric and nitric acids. Polished glass surfaces were preferably treated with sulphuric acid and the reduction of surface reflection observed. A price list of optical instruments dated 1820 gives information regarding the instruments then manufactured, which included a heliometer, telescopes up to 6 in. aperture and one of 8½ in. in construction, microscopes, achromatic objectives and so on. In 1824 was completed the great Dorpat refractor of 9½ in. aperture, which Fraunhofer considered his masterpiece, and which won for him the freedom of Munich and the civil order of the Bavarian Crown.

In 1824, Fraunhofer became Professor and Conservator of the Physical Section of The Royal Academy, with a yearly stipend of 800 florins. He was then spending most of his time in Munich, only going to Benediktbeuern periodically to supervise the glass manufacture. He seems to have had little time for relaxation, though he was fond of taking walks in the neighbourhood, and his constitution which was never strong, began to show signs of the strain of his efforts. In 1824, signs of tuberculosis appeared and were aggravated by his catching a chill after bathing when overheated. No one appears to have considered the possibility of his early demise, and it was not until almost too late that he chose one, F. A. Pauli, to be instructed in his knowledge and methods. He continued to conduct his affairs from a sick bed, but in June 1826, he could hold out no longer, and passed away at the early age of 39. He was given a State funeral, and buried in Munich. Prior to his death, negotiations were in hand for the taking over of the Optical Institute by the State, but his death put an end to the proposal.

The remaining partner, already an elderly man of 63, was hard put to it to know how to carry on. He had invested large sums in the business and was determined to continue his policy of monopoly. In the meanwhile, however, Guinand's secret was becoming known to others, and opticians were obtaining glass from Guinand himself, and elsewhere. In 1827, the French glassmaker Bontemps purchased the secret from Guinand's son, Henri, and was soon able to master the process and supply the French opticians.

At first Utzschneider undertook the production of glass himself, and the services of Pauli were not made use of for some reason unknown. The conduct of the optical section of the business was entrusted to Georg Merz, who had worked under Fraunhofer since 1808. He was a local man and came as a boy of 15 to help with the furnace work, experience which came in useful later on. Utzschneider started a school for apprentices, which was attended by five boys of whom Merz was one, and instruction was given by an ex-monk, by name Rauch, in mathematics, geometry and chemistry. During the day the apprentices worked at glass polishing, and it is perhaps hardly to be wondered at that Merz was the only one to survive the rigorous training. Utzschneider seems to have been content to continue to make the usual types of glass, and to have made no effort to follow up Fraunhofer's ideas for reducing the secondary spectrum. Towards the end of 1832, the conduct of the glassworks was handed over to Merz, and in 1839 he purchased the business, including the optical section at Munich. Sigmund Merz, Georg's second son, followed his father from 1867 up till 1883, when he gave up in favour of his cousin Jakob Merz, and the glassworks seem to have been abandoned in 1883 or 1884, probably owing to the fact that wood for firing had become increasingly expensive, and owing to competition from other opticians, who were able to obtain glass of better quality than Merz's from France and England.

It may be of interest here to mention Georges Bontemps's call on the firm in 1850 on behalf of Chance Brothers by whom he was then employed. He reported that the Merz firm continued to make glass for their own use only.

Little, if any, technical progress was made, though Georg and his son made attempts to produce pairs of glasses with more equal partial dispersions, but seemingly without success. Jakob Merz continued for some years as head of the optical firm, which specialized in astronomical telescopes, and sold his businesses to Paul Zschokke in 1903. Some two years ago, the old works were sold by the heirs of the Merz family to Prof. Küchler, before mentioned.

I cannot close this account of these works of historic importance without referring once more to the help I have received from the works of Prof. von Rohr and Dr A. Seitz, the author of *Joseph Fraunhofer and his Optical Institute.* Nearly all my facts are due to their researches.

Fraunhofer's early demise can only be described as a tragic loss to science. The advancement of optics would certainly have been more rapid had he survived, and we cannot but regret that his successors had not the ability to pursue the lines of research upon which he was engaged

THE ESTIMATION OF AMETROPIA BY THE COINCIDENCE OPTOMETER

By

ALLAN H. BRIGGS, M.Sc., M.B., Ch.B., D.O.M.S.,
Senior Resident Officer, Moorfields Eye Hospital

Received 9 *May* 1937. *Read* 3 *June* 1937

ABSTRACT. 110 cases of refractive error* were examined by means of the Fincham coincidence optometer, and seven had to be rejected as unsuitable. The results in the remaining 103 cases were checked by refraction and subjective testing. The patients were unselected, and a wide range of refractive errors was involved. No cycloplegic was employed on any case. On the assumption that the result obtained by retinoscopy and subjective testing to be correct, the margin of error has been determined and is given. The results compare very favourably, as regards accuracy, with the results of retinoscopy by an expert (the patients' pupils being undilated). Possible sources of error are discussed. Special types of case are discussed: aphakia, amblyopia, and irregular astigmatism. The optometer provides a means of analysing cases of irregular astigmatism accurately. Cases unsuitable for examination by the optometer are, with certain exceptions, found to be cases unsuitable for refraction by retinoscopy without the use of a cycloplegic. The estimation of the corneal astigmatism by keratometry is found not to give an accurate measure of the total astigmatism of the eye as a whole.

§ 1. INTRODUCTION

The coincidence optometer affords a novel method of estimating errors of refraction. The purpose of the present paper is to describe the results of an investigation made to assess the clinical and research value of the instrument from three points of view. First, its accuracy; second, to compare it, in practice, with the standard method of estimation of refractive errors by retinoscopy and subjective testing; and third, to appraise the value, for research purposes, of the additional facilities it affords in cases of spherical ametropia and astigmatism.

The results discussed here were drawn from the examination of 110 eyes. The patients were hospital patients, chosen more or less at random from the wards; the only criteria employed in their selection being that the eyes chosen should be free from gross disease, and that the ocular media should be reasonably transparent. The ages of the individual patients ranged from 12 to 74 years, and the refractive errors from about + 12 to − 12 dioptres. Some of the eyes were aphakic, and some were amblyopic; the results of these special cases will be discussed separately under appropriate headings. No mydriatic or cycloplegic was used in any of these cases. Taking into consideration the smallness of the pupils, the irregularity of the refraction, and the lack of co-operation in many of the cases, especially the young or aged patients, it is fair to say that such a series provides a severe clinical test of any method of refraction; and that when examined for control purposes by the routine method of retinoscopy and subjective testing, they presented special difficulties in many cases.

---

* A short definition of certain technical terms which appear in this paper may be of use to some readers. *Amblyopia*: a condition in which the sight of an eye is defective although no organic or structural cause sufficient to account for the defect can be identified. A squinting eye is often found to be amblyopic. The causation of amblyopia is uncertain, and is the subject of controversy; in cases of squint the cause probably lies not in the eye itself, but in the cerebral connexions responsible for the interpretation of the visual pictures; these may never have developed properly, or may have become defective from disuse, or there may be an active process of suppression or inhibition. *Mydriatic*: a term applied to drugs which cause dilatation of the pupil. *Cycloplegic*: a term applied to drugs which paralyse the power of accommodation. *Aphakia*: a term employed to denote an eye from which the crystalline lens is absent.

For purpose of comparison, the cases were all examined by the routine method, and as is customary, the strongest plus or weakest minus sphere, and the weakest cylindrical correction was chosen, which would yield the best visual acuity obtainable for the individual eye under examination. The result so obtained was taken as the standard, to represent the static refraction of the eye examined. Certain theoretical objections can be raised against the use of such a standard, but as the purpose of the investigation was to assess the clinical value and accuracy of the coincidence optometer, this seemed to be the most useful and convenient standard to employ.

The cases were also examined by means of the optometer, and the results obtained in this way were then compared with the standard, and classified according to the amount by which they departed from it. It should be understood that in the preparation of the standard result both objective means (retinoscopy) and subjective checking (subjective testing) had been employed; the optometer figures were used directly, without subjective testing. This should be remembered in considering the results, which are tabulated below.

§ 2. ANALYSIS OF RESULTS

Of the 110 eyes examined, seven were found to be unsuitable for various reasons; the ocular media were cloudy, or central fixation was defective, or the pupils were too large or too small to permit accurate readings. For the remaining 103 cases, the results were recorded in duplicate—the values for the upper and lower halves of the pupil. Then selecting the best or mean of these two halves (for reasons to be discussed later), the agreement with the standard values was as follows:

Within 0·25 D. sphere and 0·25 D. cylinder, and 10° axis, 60 cases agreed, and 43 did not.

Within 0·50 D. sphere and 0·50 D. cylinder, and 10° axis, 85 agreed, and 18 did not.

Spherical error

Considering the spherical correction alone:

Within 0·25 D. sphere	67 cases
Within 0·50 D. sphere	89 cases

Cylindrical error

Within 0·12 D. cylinder and 10°	... ...	59 cases
Within 0·25 D. cylinder and 10°	... ...	88 cases
Within 0·50 D. cylinder and 10°	... ...	94 cases

Cylinder axis error

Omitting 13 cases where a cylinder was shown by the standard, and not by the optometer, or vice versa, the agreement was as follows:

Complete agreement	... ...	65 cases (70 %)
Within 0–5°	... ...	14 cases (16 %)
Within 5–10°	... ...	5 cases (5·5 %)
Over 10°	... ...	6 cases (6·5 %)

Thus in 86 per cent of the cases the agreement was within 5°, and in 91 per cent within 10°.

Considering that no cycloplegic was used in these examinations, it is fair to say that the accuracy obtained in these results compares favourably with the standard of accuracy obtained from retinoscopy by an expert. In 90 per cent of the cases the result was correct within 0·50 D. sphere and 0·25 D. cylinder and 10° of axis. The spherical measurement results are not quite so accurate as the cylindrical, because more sources of error are introduced.

The length of time required to make the observation is about the same as would be required for a retinoscopy of a similar degree of accuracy; and it must be remembered that such quickness and accuracy by retinoscopy requires months of practice, whereas the technique of the optometer can be learnt after a few sittings. Except for expert retinoscopists, the result can be obtained more quickly and accurately by the optometer.

§ 3. SPECIAL CASES

(1) *Aphakia.* Aphakic cases present special difficulties. The maximum hypermetropic error which can be recorded by the optometer is + 12 dioptres. This is frequently exceeded in aphakic eyes, especially in the vertical meridian. In order that very high hypermetropic errors can be recorded, a special auxiliary convex lens may be fitted to the optometer, or worn by the patient in a spectacle frame during the examination; the dioptric value of this lens is then added to the result given by the optometer. The distance of the patient from the optometer must be accurately adjusted, or an appreciable error may be introduced, when high errors are being measured. Apart from these technical difficulties, it is often found that the retinal images are poor and indistinct. This may be the result of cloudiness of the ocular media, but more frequently seems to arise from the presence of opaque strands of the posterior lens capsule in the pupil. The patients examined had all been subjected to the extracapsular cataract operation; in this operation the posterior lens capsule

remains intact, and a hole is subsequently cut in it at a further operation, in order to permit the patient to see through it. It is desirable, for various surgical reasons, that this hole should be small; a small hole will permit of good vision with a correcting glass, but when such an eye is examined by the optometer, the small gap in the opaque capsule acts like a small pupil, and the retinal images are indistinct. The results of six cases are appended. It is hoped that at some later date it may be possible to obtain readings from patients where the intracapsular operation has been performed, when the posterior lens capsule would no longer interfere. In aphakia, of course, accommodation, one potential source of error, is abolished.

(2) *Amblyopia.* Amblyopic eyes present special difficulties in that central fixation is often poor or not well maintained, especially where the visual acuity is poor. Nystagmus may be present. The best subjective correcting glass is often a poor guide to the basic refraction of the eye; if the visual acuity is poor, the discriminative power of the patient tends to be poor also. A number of cases were however examined, and certain interesting points arise from consideration of them.

An amblyopic eye usually has a large error of refraction, and some degree of irregular astigmatism is often found to be present in such eyes. Optically, the amblyopic eye is usually the poorer of the two. Some interesting cases were however encountered in which the refraction of the amblyopic eye was quite regular, and the error of refraction small; in some of these cases there seems to be no substantial difference in refraction between the two eyes, and in some rather rare cases, the amblyopic eye seems optically to be the better of the two. This opens up an interesting field for speculation as to why the patient should have elected to employ the eye more optically defective, and allowed the eye which forms the better optical images to become amblyopic.

(3) *Irregular astigmatism.* The optometer provides a ready means of estimating the total refractive error of the eye in any desired meridian, and therefore allows cases of irregular astigmatism to be analysed and studied in detail. Readings can be taken at 10° intervals over the whole circle of the pupil, and the results plotted on a chart. It is surprising how good the visual acuity of an eye may be, in spite of the presence of a considerable degree of irregular astigmatism.

A simple type of irregular astigmatism is found in such a case as No. 17, where there was a corneal nebula occupying a small area of the pupil. The area covered by the nebula presented quite a different refraction from the rest of the pupillary area, and was appreciably more myopic.

In another type of case, a substantial difference in refraction is found, between two halves of the pupillary area; say, upper and lower. In such cases the difference seems to lie in the spherical and cylindrical powers; the axis of the astigmatism is usually the same, unless the whole cornea is grossly irregular.

The best subjective findings in such cases suggest that in some of them the optical image formed by the one half of the pupillary area is utilized (usually that of the better half), and the image of the other half is disregarded. Sometimes the best subjective correction is the mean of the two.

In these investigations one great merit of the coincidence optometer is clearly shown; by no other means is it possible accurately to estimate the astigmatism of an eye in any desired meridian.

(4) *Unsuitable cases.* Certain cases are found to be unsuitable for examination by the optometer. Some of the difficulties are common to other methods of estimation of errors of refraction, such as poor co-operation, low intelligence, poor fixation, nystagmus, opacities on the cornea (mucus, discharge), opacities in the cornea, lens or vitreous. A pupil less than 2½ mm. in diameter is too small to permit the ingress and egress of the beam of light from the optometer, and the optical images are faint and uncertain. A pupil larger than 6 mm. in diameter may be an advantage for retinoscopy, but is a disadvantage in the use of the optometer, since the boundaries of the pupil are no longer visible, and accurate centration is impossible.

Accommodation provides difficulties common to all methods for the estimation of refraction without the use of cycloplegics.

The type of patient in which the greatest difficulty is encountered in securing full relaxation of the accommodation, is the young adult (often of a rather neurotic tendency), and often the low myope, rather than the hypermetrope. This is perhaps rather surprising. Accommodation in itself provides no insuperable obstacle. Provided that the amount of accommodation remains constant during the examination, the amount of the astigmatic error, and the axis of the astigmatism can be accurately determined, and the final result is incorrect only in that it gives too myopic a spherical correction. This is easily discovered and adjusted by subjective testing afterwards.

Fluctuation of the accommodation during the examination, as with retinoscopy, renders the findings wholly unreliable. Fortunately such cases can be identified at an early stage of the examination by the fluctuating positions of the retinal images, which is highly characteristic; and the refraction must be estimated under a cycloplegic.

§ 4. COMPARISON WITH KERATOMETRY

A number of cases were also examined by means of a keratometer, and the corneal astigmatism was measured and recorded.

The keratometer is the only optical instrument commonly used in refraction work, and while it cannot be denied that it is an instrument of precision, in that it measures the corneal astigmatism with a high degree of accuracy, these investigations tend to show that it is fallacious to assume that the corneal astigmatism is the same as the astigmatism of the whole dioptric apparatus of the eye, or even that the two values bear any constant relationship to each other. It is hardly to be anticipated that such a relation would exist.

Nevertheless correction factors have been devised, by means of which it is said to be possible, given the corneal astigmatism, to deduce the astigmatism of the whole eye.

Javal's rule, the best known of these correction systems, was employed for this investigation. Several keratometers were tried, and the most accurate one was eventually employed. Thirty-five eyes were examined in the present series, and the values for the corneal astigmatism corrected by Javal's rule.

In only ten cases (27 per cent) did the corrected values agree with the standard refraction within an experimental error of 0·50 dioptre, and 10° of axis setting. The corresponding figure for estimations by the optometer was over 90 per cent.

§ 5. SOME THEORETICAL CONSIDERATIONS

For practical purposes it was assumed that the standard value employed represented the nearest readily obtainable approach to the true static refraction of the eye. Although perhaps this may be justifiable for experimental purposes, certain theoretical considerations show that an appreciable error may be introduced in assuming that the best correcting glass obtained in this way represents the static refraction of the eye; in fact the very existence of a definite fixed value for the static refraction of a specific eye can hardly be justified on theoretical grounds. The numerous optical defects to which it is known that the dioptric apparatus of the eye is subject, and indeed the very nature of light itself, entail imperfect resolution in the images they form; spherical aberration, diffraction, and the other optical defects produce imperfect resolution of the image, which is itself formed on a receptive layer of finite depth; and if the accommodation has not been paralysed by a cycloplegic, physiological fluctuations in its tone no doubt provide a further source of possible variation. The concept of a static refraction is thus to some extent a contradiction in terms.

Depth of focus provides another possible source of error, and will permit good vision to be obtained even though a hypermetrope is slightly overcorrected, or a myope slightly undercorrected. Again, conventional subjective testing at 6 m. introduces a possible error of one sixth of a dioptre. Finally, as in all methods depending on subjective testing, the accuracy of the standard depends in the last resort upon the discriminate powers of the patient, thus introducing a variable and incalculable personal element. This factor again will introduce a possible source of error in estimating the astigmatism of the eye, where the other factors are less significant.

The clinical findings are found to agree with the theoretical considerations outlined above. To summarise, it may be said that the results obtained from the optometer, without subjective testing, agree very closely with the results obtained by retinoscopy and subjective testing, the agreement being closer for the astigmatic than for the spherical component of the error of refraction; if subjective testing be omitted, the optometer results agree with the basic refraction of the eye more closely than mere retinoscopy, unchecked, unless the retinoscopy is done very expertly indeed.

For practical purposes, it is very much more important to be able to estimate the astigmatism, and its axis, accurately, than to be able to estimate the spherical error accurately; the latter can be checked subjectively so much more easily.

It must therefore be supposed that the basic refraction of the eye is itself probably variable within small physiological limits, and that the subjective standard chosen for our present purpose may again depart from it within a small range of error.

The possible sources in the observations made with the coincidence optometer have been outlined; the main probable sources of error are two:

(*a*) Spherical aberration; the observations may not have been made upon a zone of the pupil which is a fair mean; the optical and visual axes may not coincide.

(*b*) Accommodation: the adjustment of the fixation target may not have succeeded in producing complete relaxation of the accommodation.

It is therefore apparent that as far as the spherical part of the error of refraction is concerned, the basic value is itself liable to an appreciable error; estimation by the optometer is also liable to certain errors; whereas as far as the astigmatic correction is concerned, the basic values are more rigid, and can be more nearly approached. The main source of astigmatic error in the standard is probably the discriminative powers of the patient, and, with the optometer, fluctuation of the accommodation during the examination. It would thus be anticipated that the agreement between the optometer and the standard would be closer as regards cylindrical, than as regards spherical correction; and this is found to be the case. The margin of error is greater when the eye concerned is amblyopic, and subjective testing is therefore more or less unreliable; or where one eye only is accessible for examination, the other being covered; a circumstance which may affect the state of accommodation of the uncovered eye.

§ 6 ACKNOWLEDGMENTS

The author wishes most gladly to acknowledge his indebtedness to the Honorary Staff at Moorfields Eye Hospital for permission to use their patients in making these investigations, and for their unfailing encouragement and kindness at all times; and to Mr E. F. Fincham, for his advice and co-operation, without which this paper could not have been compiled; also to Mr Victor Purvis, for most helpful criticism and suggestions.

Acknowledgment is also due to the instrument maker for the loan of the instruments employed.

Table 1. Tabulated results of the 103 eyes examined

The first column shows the reference number of the case; the second column gives the side to which the eye belonged; the next section shows the standard result for the refraction of the eye, obtained by retinoscopy and subjective testing, and the best visual acuity obtainable with that correction; the final two sections show the corresponding results for the upper and lower halves of the pupil respectively, obtained by the optometer.

No.	Eye	Age	Standard				Optometer					
							Upper half			Lower half		
			Sphere	Cyl.	Axis	Visual acuity	Sphere	Cyl.	Axis	Sphere	Cyl.	Axis
1	L.	14	+4·50	+0·50	45°	6/5 pt	+2·25	+1·75	82°	+3·50	+1·50	85°
2	L.	16	+0·50	—	—	6/5	+1·00	—	—	+1·00	—	—
3	L.	12	−0·50	+0·25	30°	6/9	−0·25	—	—	−0·25	—	—
4	R.	24	−1·25	—	—	6/5	−1·25	—	—	−1·25	—	—
5	R.	32	+4·00	+1·25	75°	6/5	+4·00	+1·00	75°	+4·12	+1·12	75°
6	R.	24	+1·75	—	—	6/5 pt	+1·25	—	—	+1·25	—	—
7	R.	19	+1·50	+1·75	90°	6/5 pt	+1·50	+2·00	95°	+1·50	+2·25	95°
8	R.	15	+3·50	+0·50	145°	6/5	+3·25	+0·75	145°	+3·25	+0·75	145°
9	R.	17	+2·75	+0·25	90°	6/5	+3·25	+0·25	90°	+3·00	+0·25	90°
10	L.	17	+2·50	+0·75	90°	6/5	+3·25	+0·50	100°	+2·75	+1·00	100°
11	R.	31	+2·25	+1·50	20°	6/5	+2·25	+1·50	30°	+2·50	+1·25	30°
12	L.	31	+1·00	+0·25	90°	6/5	+1·00	—	—	+1·00	+0·25	120°
13	R.	39	+0·75	—	—	6/5	+0·50	—	—	+0·50	—	—
14	L.	39	+1·00	+0·25	180°	6/5	+0·50	+0·25	180°	+0·50	+0·50	180°
15	L.	13	+2·00	—	—	6/5	+2·00	—	—	+2·00	—	—
16	R.	25	—	+0·25	90°	6/5	—	+0·25	90°	—	+0·25	90°
17	R.	25	−1·00	+2·25	145°	6/5	−1·50	+2·25	145°	−1·50	+2·25	145°
18	R.	29	+0·50	+0·25	90°	6/6	+0·25	+0·25	90°	+0·25	+0·50	90°
19	R.	25	−2·25	+2·50	95°	6/9	−2·75	+2·75	100°	−2·75	+2·50	100°
20	L.	25	−1·25	+2·25	80°	6/9	−1·25	+2·75	80°	−1·00	+2·50	80°
21	R.	32	+0·50	+0·25	30°	6/6	+0·50	+0·25	30°	−1·25	+2·25	30°
22	L.	32	—	+2·00	60°	6/6 pt	+0·25	+2·75	60°	+0·75	+2·00	60°
23	R.	23	+2·00	+1·00	40°	6/5 pt	+2·75	+0·75	30°	+2·50	+1·25	30°
24	R.	35	+0·25	—	—	6/5	+0·50	—	—	+0·50	—	—
25	R.	15	−1·00	+3·00	170°	6/6	−1·00	+2·25	170°	−0·75	+2·75	170°
26	L.	15	+2·50	+1·50	150°	6/6	+1·25	+2·50	135°	+2·50	+1·00	150°
27	L.	19	+4·00	—	—	6/6	+4·00	—	—	+4·00	—	—
28	L.	19	+2·25	+0·50	160°	6/5	+2·25	+0·50	160°	+2·25	+0·50	160°
29	L.	25	—	+1·50	90°	6/5	—	+1·00	110°	−0·50	+1·50	120°
30	R.	23	+1·50	−4·00	25°	6/6 pt	+1·50	−4·25	25°	+1·75	−5·00	25°
31	R.	14	+1·00	—	—	6/5	+1·25	—	—	+1·25	—	—
32	L.	19	+1·25	+1·00	110°	6/6	+2·00	+1·25	110°	+1·50	+1·00	110°
33	L.	23	+6·00	+0·50	180°	6/6	+5·50	+0·50	165°	+5·50	+0·50	165°
34	R.	24	—	+2·25	155°	6/9	—	+2·25	155°	—	+2·25	155°
35	L.	24	—	+2·00	40°	6/9	—	+1·75	40°	—	+2·25	40°
36	L.	19	−0·50	+1·50	80°	6/9	−0·75	+2·25	70°	−0·50	+2·00	70°
37	L.	25	+0·25	+0·25	90°	6/5	+0·25	+0·25	100°	+0·25	+0·25	95°
38	R.	53	−1·50	−1·00	90°	6/6	−2·00	−1·00	115°	−1·00	−2·00	105°
39	R.	27	+0·50	+1·00	160°	6/5	+0·25	+1·25	105°	+0·25	+1·00	105°
40	L.	27	+0·50	+1·00	100°	6/5	+0·25	+1·25	105°	+0·25	+1·00	105°
41	R.	19	+0·25	—	—	6/5	—	—	—	—	—	—
42	L.	48	+0·25	+0·25	10°	6/5	+0·25	+0·25	10°	+0·25	+0·25	10°
43	R.	16	—	+3·50	100°	6/6 p	+0·25	+3·00	105°	−0·25	+3·25	105°
44	L.	16	−0·50	+1·50	80°	6/5 p	+0·25	+1·25	80°	−0·50	+2·00	80°
45	L.	50	+0·25	+0·25	90°	6/5	+0·25	+0·25	100°	+0·25	+0·25	95°
46	R.	16	+1·75	+0·25	105°	6/5	+1·00	+0·50	105°	+1·00	+0·75	105°
47	L.	16	+1·50	—	—	6/5	+1·75	—	—	+1·75	—	—
48	L.	27	−11·0	−0·75	170°	6/5	−11·75	−1·25	170°	−11·75	−0·75	170°
49	R.	38	—	—	—	6/6	−0·50	—	—	+0·25	−1·25	120°
50	L.	11	+1·75	—	—	6/5	+1·50	—	—	+1·50	—	—
51	R.	24	—	+2·25	155°	6/6 p	−1·25	+2·50	150°	−1·00	+2·50	150°
52	L.	24	—	+2·00	40°	6/6 p	−1·50	+3·00	45°	−1·25	+2·75	45°

Table 1 (*continued*)

No.	Eye	Age	Standard				Optometer					
							Upper half			Lower half		
			Sphere	Cyl.	Axis	Visual acuity	Sphere	Cyl.	Axis	Sphere	Cyl.	Axis
53	R.	62	—	−1·50	110°	6/6	—	−1·50	110°	−0·50	−1·50	110°
54	L.	19	+0·75	—	—	6/5	+0·50	—	—	+0·50	—	—
55	R.	16	+1·00	+3·00	90°	6/9	+1·00	+3·00	90°	+1·00	+2·75	90°
56	L.	16	+4·00	+1·00	100°	6/6	+3·50	+1·25	105°	+3·50	+1·25	105°
57	R.	16	+2·00	+1·75	70°	6/5	+1·50	+1·75	80°	+1·50	+1·50	80°
58	L.	16	+1·25	+3·00	95°	6/5	+1·25	+2·75	95°	+1·25	+3·00	95°
59	R.	27	−1·25	—	—	6/5	−0·25	−0·75	170°	−0·50	—	—
60	L.	27	−1·00	—	—	6/5	+0·25	−0·25	25°	−0·25	—	—
61	R.	34	+0·25	−0·50	180°	6/5	−0·25	−1·25	180°	—	−1·50	180°
62	L.	28	−0·75	+1·00	10°	6/5	−0·75	+1·00	10°	−0·75	+1·00	10°
63	R.	43	—	—	—	6/5	—	+0·25	80°	—	+0·50	80°
64	R.	62	−0·75	—	—	6/5	−0·75	—	—	−0·75	—	—
65	L.	62	−1·25	—	—	6/5	−1·75	—	—	−1·75	—	—
66	R.	54	+0·25	—	—	6/5	+0·75	—	—	+0·75	—	—
67	L.	41	—	+1·00	140°	6/9	−0·50	+1·75	135°	+0·25	+1·00	150°
68	R.	21	+1·25	+4·00	80°	6/5	−0·25	+4·75	75°	+0·25	+4·50	75°
69	L.	43	+0·25	+0·50	120°	6/5	+0·25	—	—	+0·25	—	—
70	R.	9	+0·25	+0·75	90°	6/5	+0·25	+0·25	85°	−0·25	+0·25	85°
71	L.	9	+0·25	+0·25	90°	6/5	−0·25	—	—	−0·25	—	—
72	R.	57	+1·50	+0·50	50°	6/5	+1·25	+1·00	50°	+1·50	+0·50	50°
73	L.	14	+3·00	—	—	6/5	+0·50	—	—	+0·50	—	—
74	R.	21	+0·25	—	—	6/5	—	—	—	—	—	—
75	R.	67	+2·00	—	—	6/6 pt	+2·00	+0·75	80°	+2·00	+0·75	80°
76	L.	43	+0·75	+0·50	180°	6/5	+1·00	—	—	+1·00	—	—
77	R.	49	−0·25	+0·25	180°	6/5	—	—	—	—	—	—
78	L.	24	+0·25	−0·75	175°	6/5	+0·25	−0·75	175°	+0·25	−1·00	175°
79	R.	44	—	—	—	6/6	−0·50	—	—	−0·50	—	—
80	L.	44	−0·50	—	—	6/6	−1·00	—	—	−1·00	—	—
81	L.	20	—	+0·25	180°	6/5	−1·50	−0·50	105°	−1·75	−0·50	105°
82	R.	30	+0·75	—	—	6/5	+0·50	+0·25	155°	+0·50	+0·25	155°
83	L.	33	−0·25	—	—	6/5	—	—	—	—	—	—
84	R.	57	+0·25	+0·25	180°	6/5	+0·50	—	—	+0·50	—	—
85	R.	27	+0·25	−1·25	20°	6/5	+0·25	−1·50	20°	+0·25	−1·00	20°
86	L.	52	—	−0·25	180°	6/5	−0·25	—	—	+0·25	—	—
87	R.	28	−0·25	+0·75	40°	6/5	−0·25	+0·75	40°	—	+0·50	40°
88	L.	45	+1·00	−0·25	180°	6/5	+1·50	—	—	+1·25	+0·25	180°
89	R.	20	+0·25	—	—	6/5	−0·25	−0·25	90°	−1·00	−0·50	100°
90	L.	17	+3·00	+0·25	95°	6/5	+3·75	+0·75	95°	+4·00	+0·25	95°
91	L.	36	+1·00	+1·75	5°	6/6 pt	—	+1·50	5°	—	+1·50	5°
92	R.	41	−1·25	—	—	6/6	−2·25	—	—	−2·25	—	—
93	L.	41	−1·75	—	—	6/9	−2·75	—	—	−2·75	—	—
94	R.	36	−0·25	−0·75	110°	6/6	−0·50	−0·50	110°	−0·50	−0·25	110°
95	L.	44	−2·00	−0·50	175°	6/5	−2·00	−1·00	175°	−2·50	−0·25	175°
96	R.	42	−0·75	+1·50	85°	6/6	−1·00	+2·00	90°	−0·50	+1·75	85°
97	L.	42	−0·25	+1·50	75°	6/6	−0·75	+2·50	75°	—	+1·50	75°
98	L.	52	−0·50	+0·25	120°	6/5	−0·50	—	—	+0·50	−0·50	35°
99	L.	50	+0·50	+0·50	150°	6/5	+0·25	+0·75	150°	+0·50	+0·75	150°
100	L.	42	+0·50	+0·25	55°	6/5	+0·25	+0·50	55°	+0·75	+0·75	145°
101	R.	26	+2·50	+1·75	45°	6/9 pt	+2·50	+2·00	55°	+2·50	+2·00	50°
102	R.	49	−2·25	—	—	6/5	−2·25	—	—	−2·25	—	—
103	L.	49	−2·00	−0·25	180°	6/5	−2·25	—	—	−2·25	—	—

Table 2. Aphakic cases

This table is an appendix to table 1, dealing with six aphakic cases. The arrangement is the same as in table 1.

No.	Eye	Age	Standard				Optometer					
							Upper half			Lower half		
			Sphere	Cyl.	Axis	Visual acuity	Sphere	Cyl.	Axis	Sphere	Cyl.	Axis
1	R.	50	−3·00	+9·00	160°	6/12	−2·75	+11·00	160°	—	—	—
2	R.	44	+0·50	+4·50	5°	6/5	+0·75	+4·25	5°	+0·75	+4·25	5°
3	L.	74	+12·00	+1·50	180°	6/9	+11·75	+1·00	175°	+11·25	+1·50	180°
4	R.	45	+9·00	+3·50	180°	6/18	+8·25	+3·50	170°	—	—	—
5	L.	45	+7·00	+2·50	180°	6/9	+6·25	+2·75	25°	+6·75	+2·75	180°
6	R.	60	+12·00	+2·00	20°	6/9	+11·25	+0·75	25°	+10·75	+1·00	30°

Table 3. Amblyopic cases

This table deals with eighteen amblyopic cases; the arrangement is as in tables 1 and 2.

No.	Eye	Age	Standard				Optometer					
							Upper half			Lower half		
			Sphere	Cyl.	Axis	Visual acuity	Sphere	Cyl.	Axis	Sphere	Cyl.	Axis
1	R.	14	+5·00	—	—	6/24	+5·00	—	—	+4·50	+1·00	115°
2	R.	16	+0·50	—	—	6/24	+0·75	+0·25	75°	+0·75	+0·50	80°
3	R.	12	−6·50	−1·25	150°	c.f.	−6·00	−2·75	160°	−6·00	−2·00	70°
4	L.	32	+5·00	+1·50	80°	6/18	+5·25	+1·25	90°	+5·00	+1·25	90°
5	L.	24	+2·75	+1·75	75°	6/24	+2·00	+2·00	75°	+2·75	+0·75	75°
6	L.	19	+1·75	+2·75	100°	6/18	+1·75	+3·00	90°	+2·00	+2·75	90°
7	L.	15	+0·75	+1·75	135°	c.f.	+0·75	+2·25	135°	+1·00	+1·50	130°
8	R.	13	+2·00	—	—	3/60	+2·25	—	—	+2·25	—	—
9	L.	29	+0·25	+1·25	60°	6/12	−0·50	+1·25	50°	−0·50	+1·25	55°
10	L.	23	+2·50	+1·50	160°	6/50	+4·50	+1·25	150°	+4·75	+1·25	150°
11	L.	35	—	+3·00	90°	6/24	—	+3·37	90°	—	+3·25	90°
12	R.	19	+5·25	—	—	6/12	+5·25	—	—	+5·25	—	—
13	R.	19	+2·25	+1·00	60°	6/9	+2·25	+1·00	60°	+2·00	+1·25	60°
14	L.	14	—	−1·50	165°	6/9	+0·25	−0·75	165°	+0·50	−1·25	170°
15	R.	19	+0·25	+5·00	110°	6/24	+0·50	+5·00	110°	+0·50	+4·50	110°
16	R.	23	+6·00	+0·75	120°	6/12	+6·25	+0·75	110°	+6·00	+0·75	105°
17	R.	17	+3·00	+1·25	45°	6/9	+4·00	+1·25	45°	+4·25	+0·50	45°
18	L.	26	+4·00	—	—	6/18	+4·25	—	—	+4·25	—	—

Table 4. Comparison of the keratometer and the optometer

This table shows the compared results in 33 cases examined with the optometer and the keratometer. Cylinder values alone are given.

The first column shows the number of the case; the second column gives the cross reference number (see table 1); the next section gives the standard cylinder value; the next two sections give the cylinder values as given by the optometer for the upper and lower halves of the pupil; and the last section gives the corrected keratometer reading, using Javal's rule.

No.	Ref.	Standard		Optometer				Corrected keratometer readings	
				Upper half		Lower half			
		Cyl.	Axis	Cyl.	Axis	Cyl.	Axis	Cyl.	Axis
1	41	—	—	—	—	—	—	+0·50	180°
2	42	+0·25	10°	+0·25	10°	+0·25	10°	+0·50	180°
3	43	+3·50	100°	+3·00	105°	+3·25	105°	+4·25	100°
4	44	+1·50	80°	+1·25	80°	+2·00	80°	+2·75	80°
5	46	+0·25	105°	+0·50	105°	+0·75	105°	+1·75	180°
6	47	—	—	—	—	—	—	+1·00	180°
7	48	−0·75	170°	−1·25	170°	−0·75	170°	+0·50	80°
8	50	—	—	—	—	—	—	—	—
9	51	+2·25	155°	+2·50	150°	+2·50	150°	+0·75	40°
10	52	+2·00	40°	+3·00	45°	+2·75	45°	+2·50	140°
11	53	−1·50	110°	−1·50	110°	−1·50	110°	+1·25	5°
12	54	—	—	—	—	—	—	+1·75	115°
13	59	—	—	+0·75	170°	—	—	+0·50	90°
14	60	—	—	−0·25	25°	—	—	+0·75	60°
15	61	−0·50	180°	−1·25	180°	−1·50	180°	+1·00	105°
16	62	+1·00	10°	+1·00	10°	+1·00	10°	+1·00	145°
17	63	—	—	+0·25	80°	−0·50	80°	+0·75	100°
18	64	—	—	—	—	—	—	+0·75	90°
19	65	—	—	—	—	—	—	+2·25	95°
20	66	—	—	—	—	—	—	+0·25	105°
21	67	+1·00	140°	+1·75	135°	+1·00	150°	+1·50	45°
22	69	+0·50	120°	—	—	—	—	+1·00	90°
23	70	+0·75	90°	+0·25	85°	+0·25	85°	+1·75	95°
24	71	+0·25	90°	—	—	—	—	+0·50	100°
25	72	+0·50	50°	+1·00	50°	+0·50	50°	+1·50	80°
26	74	—	—	—	—	—	—	+0·50	180°
27	75	—	—	+0·75	80°	+0·75	80°	+0·75	85°
28	76	+0·50	180°	—	—	—	—	+1·00	120°
29	77	+0·25	180°	—	—	—	—	+1·00	125°
30	78	−0·75	175°	−0·75	175°	−1·00	175°	+0·75	85°
31	98	+0·25	120°	—	—	+0·50	125°	+1·25	95°
32	99	+0·50	150°	+0·75	150°	+0·75	150°	+0·25	90°
33	100	+0·25	55°	+0·50	55°	+0·75	145°	+0·50	5°

Table 5. Comparison of the keratometer and the optometer. Aphakic cases

This table is an appendix to table 4, dealing with aphakic cases. The arrangement is the same as in table 4.

No.	Standard		Optometer				Corrected keratometer readings	
			Upper half		Lower half			
	Cyl.	Axis	Cyl.	Axis	Cyl.	Axis	Cyl.	Axis
1	+9·00	160°	+11·00	160°	No readings		+12·00	160°
2	+4·50	5°	+4·25	5°	+4·25	5°	+4·50	5°
3	+1·50	180°	+1·00	175°	+1·50	180°	+2·00	170°
4	+2·50	180°	+2·75	25°	+2·75	25°	+2·50	160°
5	+2·00	70°	+0·75	25°	+1·00	30°	+2·75	25°

DISCUSSION

Mr J. Adamson. In dealing with amblyopic cases in connexion with squint treatment I have found that the use of the coincidence optometer has in all cases led me to obtain the best refractive correction. Very satisfactory results have been obtained in cases with irregular astigmatism. Further, I should like to say that in quite a number of cases the optometer result showed a higher cylinder power than the retinoscopy result. In all such cases the optometer finding gave the subject a higher acuity than the retinoscopy finding. This has happened sufficiently frequently to make me wonder whether the cylinder determination by retinoscopy is as reliable as we have always assumed and it seems to me that it is a point which could well be investigated over a larger number of cases.

Author's reply. I am glad Mr Adamson has raised this question. I quite agree that a large proportion of amblyopic eyes show a high degree of astigmatism, not infrequently irregular; and that an examination by the optometer often leads, I think, to a more accurate correction of the refractive error, and an apparent increase in the visual acuity. With regard to the suggestion that the optometer reveals a higher degree of astigmatism, in many cases, than retinoscopy does, I can only say that with the limited data I have tabulated in table 3, this has not been my experience; but I have not sufficient material to justify me in expressing any definite opinion. I am glad the point has been raised however, because this same lack of evidence prevented me from laying any stress on the amblyopic cases in my paper; yet I do feel that it is in the examination of these very cases that the optometer shows itself at the greatest advantage, when compared with retinoscopy. Without the use of a cycloplegic, retinoscopy on an amblyopic eye is difficult; central fixation is poor, and the eye tends to rove about, producing conflicting results; central vision is defective, and in the effort to maintain fixation, the accommodation is apt to fluctuate. I am sure that retinoscopy on an amblyopic eye is not as a rule so accurate as on a normal eye, other things being equal. The optometer is at an advantage. Centration can be frequently and accurately checked; fluctuation of the accommodation can readily be detected by wavering of the images; and I am sure the optometer never shows to better advantage than with such a case. In my paper I have laid no emphasis on this point, which appears to me a very important one, because I had so little evidence, and because I feel that there may be a fallacy in the apparent increase in visual acuity usually obtained. Any prolonged examination and testing of an amblyopic eye tends to show a progressive increase in visual acuity, up to a point, due I believe, to the persevering attention of the patient; but I doubt if much significance can be attached to it, or if it is maintained. Often such a patient will volunteer the information that "the sight comes and goes"; and it is nearly always possible to persuade him slowly to read another line of the test type. Hence I am loath to place much reliance on the increase in visual acuity alone. With these reservations, my experience has been in agreement with that of Mr Adamson, and I agree with him that the investigation of these amblyopic cases is most interesting and, I think, likely to be most profitable.

THE COINCIDENCE OPTOMETER

By E. F. FINCHAM, F.Inst.P.

Received 2 *May* 1937. *Read* 3 *June* 1937

ABSTRACT. The power of the required spectacle lens may be determined objectively by the ophthalmoscopic observation of the retinal image of a target, the position of which can be adjusted relative to an optometer lens to bring it to the conjugate of the retina. In the past the method has depended upon the observer's estimation of focus, or of parallax between the retinal image and the target which is in the field of the observing system, or of coincidence between the retinal image and an index line in the observing system. This paper describes the principle of an instrument in which the adjustments for both refraction measurement and meridian location of an astigmatic eye are made by a coincidence setting between two parts of the retinal image. By this means the sensitivity of the method is increased by more than 100 per cent.

§ 1. INTRODUCTION

The measurement of errors of refraction of the eye may be made either by a subjective test, in which the co-operation of the patient is required in describing the effects of the trial lenses, or by an objective method in which the examiner treats the eye purely as an optical system and endeavours to find the power of the lens required to bring the conjugate of the retina to infinity. Undoubtedly in all cases where the visual acuity is good enough the correction found by objective methods must be confirmed subjectively before the prescription is given; the complexity of the visual mechanism may make the true optical correction undesirable. On the other hand, this complexity may introduce difficulties if reliance is placed upon a subjective test alone. Although defects of the optical part of the visual mechanism can be corrected by lenses, the subjective response to the lenses may be influenced by the physiological and mental parts of the mechanism to such an extent that the true optical condition is obscured. It frequently happens that cases with low astigmatic errors are unable to appreciate the effect of the weak cylindrical lenses which would correct the error, although they may be suffering some strain as a result of the defect. Similarly, it is often impossible by subjective tests to find the true correction of an eye with a high refractive error owing to the low visual acuity in one who has never had a sharply focused retinal image. The correction of an amblyopic eye must also call for the employment of an objective test.

The obvious desirability of a method by which the basic refraction of the eye could be determined independently of the subjective interpretation of the retinal and mental image led to the development of objective methods. Retinoscopy has proved the most valuable of these methods, but owing to the variability of the appearances which it gives in different eyes, its employment calls for a considerable degree of experience and skill on the part of the examiner. For this reason some attention has been given in the past to the design of instruments in which the aim has been to measure refraction by the adjustment required to observe objectively a sharply focused retinal image.

§ 2. HISTORY

The objective optometer in its simplest form consists of the combination of the far-point rule with the direct ophthalmoscope. In such an instrument a suitably illuminated target is movable along the rule with regard to the optometer lens; the light after passing the lens is brought into the patient's eye by means of a perforated or transparent mirror, and the examiner looking through the mirror sees the image of the target upon the patient's retina. The refraction is measured by determining the distance from the lens at which the target has to be placed to produce a sharply focused retinal image. In order that the light from the retinal image emerging from the ametropic eye shall focus upon the retina of the observer's eye correcting lenses must be placed in the sight-hole of the mirror.

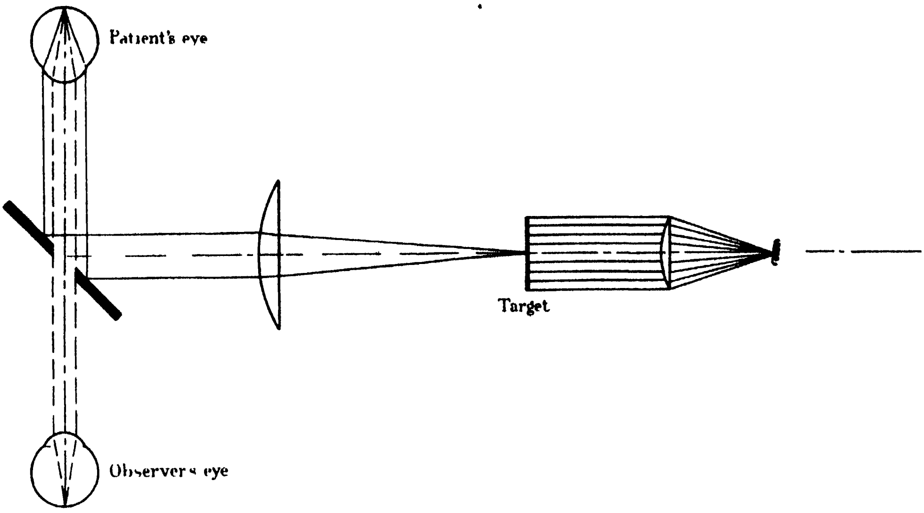

Figure 1. The stigmatometer (Hardy).

The earliest form of this instrument was probably the Hardy Stigmatometer (figure 1). In this the target was caused to move along the rule by a rack mechanism which caused the appropriate correcting lens to be brought before the observer's eye. The principal meridians of an astigmatic eye were determined by the use of targets consisting of radial lines or blocks of lines which could be rotated into different meridians. A separate small target attached to the plate carrying the main target was provided for the patient's fixation. This was set farther away from the optometer lens than the main target in order to induce the eye to relax accommodation, but as it moved with the main target it probably did not achieve its object, especially in astigmatism when the target distance had to be changed in the measurement of the different meridians of the eye.

Later instruments on a similar principle were produced under the name of the Astron Refractometer and the Rodenstock Refractometer. In the last of these a telescopic viewing system was provided to assist the observation of the retinal image.

A difficulty in this type of instrument which employs the direct method of observation is the elimination of the corneal reflexion, as the separation between the illuminating and observing beams which is necessary for the reflex-free condition cannot be achieved. If the usual indirect method for the elimination of reflexions is used, in which the beams are separated by the production of an image of the source of light and of the observing pupil in separate regions of the patient's pupil, a great depth of focus of the target image upon the retina results; thus the required sensitivity is lost.

In an instrument designed by Thorner and manufactured by Busch, the reflex-free condition has been achieved, and by employing almost the full diameter of the pupil for both illuminating and observing systems the maximum sensitivity of the focusing method has been retained.

§ 3. THE DISADVANTAGES OF THE FOCUSING METHOD

Owing partly to the nature of the fundus of the eye the judgement of the exact focus of the retinal image by an observer looking into the eye is somewhat uncertain. The image of a light and dark object is not rendered upon the retina as white and black, but as light red and dark red, and usually some diffusion exists. These effects are probably caused by the colour and translucency of the retina and choroid; they are more marked in fair subjects. The adjustment for focus is rendered more difficult by the necessity of approaching the correct setting from one side only; the effective object must be brought up from beyond the subject's far point and must not be allowed to pass that position in order that the accommodation shall not be stimulated by allowing the subject to see the object within his far point.

In any event the sensitivity of the method is dependent upon the examiner's ability to estimate accurate focus, and it may be argued that in those cases where the visual acuity of the subject is good he may be better able to make the judgement than the examiner viewing his retinal image.

§ 4. THE PARALLAX REFRACTIONOMETER (HENKER)

In this instrument, which is based upon the simplified Gullstrand ophthalmoscope, a new principle which avoids the necessity for the estimation of the sharpness of the retinal image has been introduced in an instrument made by Zeiss.

In the parallax refractionometer the fundamental condition for reflex-free ophthalmoscopy by the indirect method is used. In figure 2 it will be seen that the source of light S which is displaced from the axis of the instrument is imaged by the ophthalmoscope lens in a decentred part of the subject's pupil at S', while the pupil of the observing system P is imaged in the subject's pupil at P'. Thus, whereas the light enters the eye through the area S', only that which leaves through P' can enter the observing system. Reflexions from the surfaces of the eye are thus avoided.

A transparent target T bearing a vertical index line perpendicular to the plane containing the centres of the areas P' and S' is placed upon the axis at the principal focus of the lens, and thus its image will be formed upon the retina of an emmetropic eye again upon the axis at $T'e$. If the eye is hypermetropic the light will not reach the axis, and a somewhat out-of-focus retinal image will be formed displaced from the axis; if the eye were myopic the light would have crossed the axis before reaching the retina. By moving the target along the axis of the instrument, away from the lens for hypermetropia and towards it for myopia, the retinal image will be sharply focused and will fall upon the axis when the target is brought to a position which is conjugate with the subject's retina.

In figure 2 the displacement of the retinal image in an emmetropic eye caused by the movement of the target is shown at $T'm$ and $T'h$.

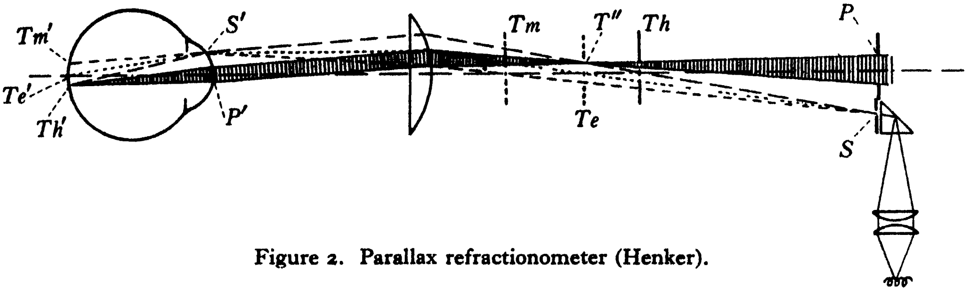

Figure 2. Parallax refractionometer (Henker).

The light of the retinal image emerging again from the eye is reimaged by the eye system and the lens; when the target is conjugate with the retina the emergent image will lie upon the axis and coincide with the target, otherwise it will be displaced to one side or other of the target according to the refractive condition of the eye relative to the position of the target.

In figure 2 it is presumed that the eye is emmetropic and that the target is positioned for a hypermetropic eye at Th. The light emerging from the retinal image is reimaged at T'' displaced from the axis.

The target consists essentially of a glass plate bearing four windows, upon each of which a fine line is ruled. For the measurement of refraction the line of the target is perpendicular to the plane containing the centres of the two areas S' and P'. This target will be seen by the examiner through the observing system; the line will appear black upon the red background of the fundus which is visible through the window. When the target is not conjugate to the retina the displaced retinal image of the line will appear as a dull red line to one side or other of the black target line. When the target is correctly positioned for the refraction of the eye under test the retinal image will coincide with the target line and will be invisible. The slide along which the target travels is scaled to read the refraction of the eye in dioptres.

For the determination of the principal meridians of an astigmatic eye, target lines are provided which lie in the same plane as the centres of the areas S' and P'. In errors of refraction, the images of these lines will be displaced only in the direction of their length. When the lines do not lie in one of the principal meridians of an astigmatic eye the retinal image will suffer an oblique displacement, which will cause a lack of coincidence to appear between the "meridian lines" of the target and the images of them upon the retina. The principal meridians of the eye are located by rotating the instrument about the axis of the system until coincidence of these lines and their images is obtained.

In principle this instrument appears to have advantages over the focusing types. The smallness of the area through which the light enters the eye ensures considerable depth of focus in the retinal image, and its displacement relative to the target should be easily seen. The sensitivity of the method will depend upon the separation between the centre of the area through which the light enters the eye and the centre of the image of the aperture of the observing system at the subject's pupil, i.e. the distance $S'P'$ (figure 2). In practice the sensitivity depends also upon the operator's ability to judge when the retinal image line coincides with the target line; as the target is moved along its slide the red retinal image line is seen to disappear behind the target line. Its complete masking by the latter signifies the correct setting. This could be achieved with more certainty if it were permissible to let the image appear successively on each side of the target and take a mean position, but as the subject is allowed to view the target it must not be brought within his far-point so that accommodation may be kept relaxed; the target must therefore be brought up to the correct setting from the hypermetropic side only.

§ 5. THE COINCIDENCE OPTOMETER

In the type of instrument that we are considering the chief requirement is sensitivity; the correction of refractive errors is now required to an accuracy of 0·25 dioptre, and the meridians of an astigmatic eye must be known to within a few degrees. In the optometer of the focusing type an error of 0·25 dioptre will cause little apparent difference in the definition of the retinal image; in the parallax type of instrument, the shift of the image across the retina, the effect by which the instrument operates, must depend upon the displacement of the area of the pupil through which the light enters the eye from the centre of the area through which observation is made. If we assume that when working centrally upon an eye with a 3 mm. pupil, this distance can be 1·5 mm., the shift of the retinal image for an error of refraction of 0·25 dioptre will be about 0·007 mm.

If we adopt the general principle of this instrument it is obvious that as the displacement of the retinal image cannot be increased for a given separation between the illuminating and observing beams, and as this is governed by the diameter of the pupil, enhancement in the sensitivity of the method can be produced only by an improvement in the method of observing the displacement of the image. In the parallax method the image becomes hidden by the target at the moment of making the setting; if the position of the image could be observed relative to an index mark which did not hide it, so that a coincidence setting could be made the adjustment would be facilitated. To produce this condition the actual target must not appear in the field of the observing system. Its place may be taken by an aerial image of the target, the light forming it being brought on to the axis of the optometer lens by means of an excentrically placed or transparent mirror which does not interfere with observation.

Another method, the one which was used in the original model of the coincidence optometer, is to separate the image-forming and observing systems, providing an optometer lens for each, and to bring the light into the eye through a decentred area of the pupil by reflexions, so that the virtual position of the target is again upon the axis of the observing system. This method is shown in the diagram (figure 3). The comparison of the position of the image with an index mark is, however, not an ideal method, as the impossibility of matching the appearance of a graticle with the retinal image must reduce the accuracy with which a coincidence alignment can be made.

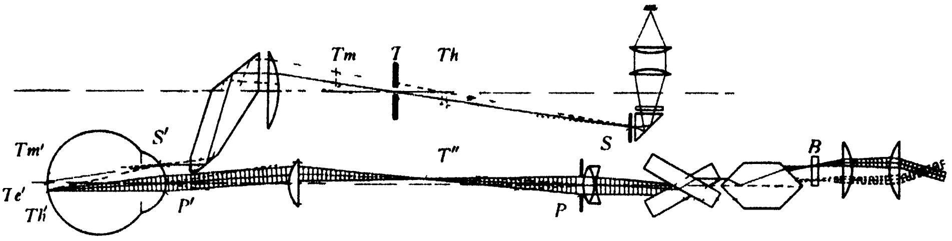

Figure 3. Coincidence optometer.

But provided we obtain an uninterrupted view of the retinal image by using for its "object" an image of the target, we have available a more sensitive method of detecting its displacement than by comparing it with an index mark. Let us suppose that the image whose displacement we wish to detect consists of a single vertical line which lies across the axis of the system when the target is conjugate with the retina, and becomes displaced in a direction perpendicular to its length to the right or left according as the eye is myopic or hypermetropic relative to the position of the target. If now we bisect the field of observation into upper and lower halves and reverse one-half right for left, the effect of displacement of the line will be doubled, the two parts of the line will move at equal rates in opposite directions as the adjustment is made and the setting will consist of bringing the two parts together into coincidence when the image of the target is brought on to the axis of the system.

This is the basic principle of the coincidence optometer. By its adoption we obtain a geometrical increase in the sensitivity of the method of 100 per cent for a given separation between the illuminating and observing beams, i.e. for a given diameter of pupil, in addition to the increased facility of alignment provided by two exactly matched parts of the line. A diagram of the original arrangement of the system is given in figure 3. In this the illuminating system is parallel to the observing system, the light is brought into the eye by means of the rhomboid prism and enters through the decentred area S' the image of the effective source S. The aperture of the observing system P is imaged in the patient's pupil at P'. The target T consists of a single line, perpendicular to the plane of the drawing, across an aperture; it is movable along the axis of the lens, towards the lens for myopia and away from it for hypermetropia. The target shown in full line is in its normal position, i.e. at the principal focus of the optometer lens; light from it will enter the eye through the area S' as a narrow beam parallel to the axis of the observing system, and the target will be imaged upon the axis at Te' if the eye be emmetropic.

In the case which is shown we shall consider the target to be placed beyond the principal focus of the lens at Th, a position which it would have to occupy to bring the retinal image on to the axis in the case of a certain amount of hypermetropia. In the emmetropic eye which is shown the somewhat out-of-focus retinal image of the target in this position will be displaced from the axis at Th'. The light from this image emerging again from the pupil is brought to a focus by the lens of the observing system again off the axis at T'' and is observed by means of a low-powered microscope which contains the image-dividing system.

The means for reversing one-half of the image relative to the other consists in its simplest form of a 90° reflecting prism placed across the upper or lower half of the field before the eyepiece, so that the beam forming half of the image passes through the prism while the other half does not. In the original model of the instrument the beam was divided into upper and lower halves by tilted parallel plates. The upper part passed through a 90° reflecting prism, and the lower part passed through what is in effect a tilted parallel-sided block, produced by cementing on to the hypotenuse of the reflecting prism another 90° prism of half its height. It was arranged that the two parts of the image were formed upon a thin biprism B, the purpose of which was to eliminate the somewhat diffused central part of the image and produce a clean division of the field. The biprism was in the focal plane of the eyepiece. The slide upon which the target moved was scaled to read the refraction of the eye in dioptres.

§ 6. THE DETERMINATION OF THE PRINCIPAL MERIDIANS OF AN ASTIGMATIC EYE

The principal meridians of an astigmatic eye could be located by rotating the apparatus which has been described about the axis of the eye, and by making consecutive measurements the meridians of greatest and least power could be found. Such a method is rather tedious and is not very sensitive; in low amounts of astigmatism the power changes slowly and precise settings are not possible. The method which has been adopted depends upon the displacement of the image in a direction oblique to the plane containing the centres of the illuminating and observing beams when that plane does not coincide with one of the principal meridians of the eye.

We have seen that errors of refraction will cause the retinal image to be displaced in the plane of the illuminating and observing beams, and that such a displacement becomes obvious if the image consists of a line perpendicular to this plane, particularly if the coincidence method of determining its position is used. A line parallel to this plane, however, will be displaced in the direction of its length when an error of refraction is present, and in an oblique direction when the plane of the illuminating and observing beams is not in one of the principal meridians of the eye. In order to detect this displacement due to the obliquity of the principal meridians relative to the plane of the instrument, it is necessary to provide a line in the target perpendicular to the refraction-measuring line, or to rotate the refraction-measuring line through 90°, and also to rotate the image-dividing device in the observing system through 90° so that it will operate upon the line image in its new position.

With the instrument so adjusted errors of refraction will cause no lack of coincidence in the parts of the image because the image will suffer no displacement in the direction in which reversal occurs, but if the eye be astigmatic and the plane of the instrument does not lie in one of the principal meridians, the oblique displacement of the retinal image will become apparent as a lack of coincidence in the two parts of the image seen in the observing system. By rotating the whole system about the axis of the eye the principal meridians can thus be located as the positions in which coincidence occurs, and then by changing back to the refraction-measuring position of the target and image-dividing system, the refraction in each of these meridians may be measured.

In the instrument which has been developed by Messrs Taylor, Taylor and Hobson, and which is described in the paper by Mr Reason, the determination of principal meridians is greatly facilitated by two important improvements in the design. The meridian-location condition is arrived at from the refraction-measuring condition by rotating the effective source of light through 90° about the observing axis; thus, while the target line and the image-dividing system are kept in their original positions the plane of the centres of the illuminating and observing areas is rotated into the direction of the target line. In addition, instead of rotating the whole instrument in order to locate and measure the principal meridians, which is usual with instruments of this type and in keratometers, in the new instrument the image of the pupil formed within the instrument is caused to rotate by the rotation of a reflecting prism. The result of these modifications is that for both refraction measurement and meridian location the observer sees a vertical line image which remains vertical throughout the test whatever meridians of the eye are being tested. The effect of rotating the reflecting prism is to rotate the image of the pupil through twice the angle, and thus the instrument will conveniently operate over the whole 360° of the pupil. This is a valuable asset, as although in a symmetrical eye it is necessary to measure only one-half of the pupil, the detection and measurement of irregular refraction can be made only by a study of all parts of the pupil area.

§ 7. THE SENSITIVITY OF THE METHOD

For an objective method of the determination of refraction to be successful it should be sensitive to differences at least as small as those which can be detected subjectively by a patient with good visual acuity. The sensitivity of the coincidence optometer operating upon an eye can be appreciated from figure 4. This is a photograph of the retinal image in a human eye taken through the optometer. It is reproduced to show the size as it appears to the observer using the instrument and shows the lack of coincidence which occurs between the two parts of the line in an error of 0·5 dioptre. Allowing for some loss of definition in the photography and reproduction it will be seen that a quarter of this error could be detected.

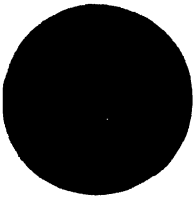
Figure 4. The image on the human retina, photographed through the coincidence optometer. Error of refraction 0·50 dioptre.

Theoretically the sensitivity of the method depends upon the separation between the centres of the illuminating beam and the observing beam in the plane of the pupil (pupil radius), the magnification of the observing system and finally the coincidence acuity of the observer. Assuming a coincidence acuity of 10 sec. (the apparent displacement of the image before it is divided will be half this) and taking the magnification of the system as 1·17, for a pupil radius of only 1 mm. the smallest detectable change in refraction will be about 1/50 dioptre.

An exact test of the sensitivity cannot be made on a living eye owing to small irregularities of refraction which are always present and the possibility of small changes in power due to movement of the patient and to accommodation. I have, therefore, used a model eye constructed of a well-corrected 2-in. microscope objective and a flat metal plate to represent the retina; in the test the optometer adjustment was not altered, settings were made by adjusting the distance of the retina from the lens by means of a divided micrometer screw, until apparent coincidence was obtained in the optometer image. In each test twenty settings were made by an observer with good coincidence acuity. With the minimum pupil radius allowed by the instrument of 1·1 mm., the greatest difference from the mean was 0·016 dioptre. With a pupil radius of 1·5 mm. the greatest difference from the mean was 0·012 dioptre.

The sensitivity of the instrument in the location of a principal meridian of an astigmatic system was also tested. In this case the same model eye was used, its length was kept fixed and a cylindrical trial case lens was mounted in the spectacle plane in a rotating holder. Attached to the lens was a long pointer reading upon a protractor. The optometer, set for meridian location, was kept fixed; settings were made by rotating the cylinder lens until apparent coincidence of the image in the optometer was obtained. Tests were made with a pupil radius of 1·5 mm. The greatest difference from the mean of twenty settings on a 1 dioptre cylinder was 20 min. The greatest difference from the mean of twenty settings on a 0·25 dioptre was 1½°.

This high sensitivity provided by the instrument as it is commercially produced can never be fully reached in working on a human eye, although it will probably be above the differences that can be detected subjectively. The quality of the human retinal image is not so good as that produced by the model eye. This appears to be due to the low optical quality of the eye and to a certain diffusion of light in the substance of the retina or in those tissues which constitute the receiving screen. However, our ability to make an accurate setting by the coincidence method is less affected by diffusion of the image than it is when other methods such as focusing are used.

§ 8. THE CONTROL OF ACCOMMODATION

The measurement of astigmatism of the eye is impossible by any method unless the accommodation is fixed; the measurement of the far-point refraction calls for the complete relaxation of accommodation. In order to achieve relaxation or even fixation of the accommodation, the patient must not be allowed to look at the target of the optometer, because as this is moved towards and away from the eye in the measurement of the various meridians it will cause a variation in the state of accommodation, if it is followed by the patient.

In the coincidence optometer a separate fixation target is provided. It consists of a small aperture in a disk situated in an auxiliary illuminating system. The light from this target is brought on to the axis of the optometer lens by reflexion and thus enters the eye with the light from the main target. The fixation target is separately adjustable and in the usual test is placed as far away from the optometer lens as will permit the patient to see it clearly, i.e. at the equivalent of his far point. The necessary displacement of the measuring target from the fixation target means that the refraction will not be measured at the fovea; the displacement is found to be well within the range over which the refraction is constant.

Another device has been employed to assist in relaxing the accommodation. It is well known that there is a tendency for the eyes to accommodate when looking into a monocular instrument when the eye not in use is occluded. If the optometer is used in a darkened room the effect will be the same as occluding the eye which is not being tested. On the other hand, if the room is not dark there will be a tendency for that eye to look at near parts of the instrument. To overcome these difficulties we present a field of uniform low illumination to the eye by placing before it an opal glass disk which receives light from the lamp of the instrument. The use of this luminous field has another advantage; to the patient it appears to surround the bright image of the target and thus reduces its apparent brightness.

§ 9. SPHERICAL ABERRATION AND IRREGULAR REFRACTION OF THE EYE

The method employed in the coincidence optometer gives the measure of the refraction of the small area of the system through which the light enters the eye relative to the axis of the emerging beam. In the case of an eye which is free from spherical aberration such a measurement would represent the refraction of that meridian, and by rotation of the apparatus about any axis which would allow both entering and emerging beams to remain within the pupil the refraction in the various meridians could be determined. But if the eye has zonal aberration a rotation of the apparatus about the axis of the pupil will allow us to measure the refraction of a single zone of the system; on the other hand, if the apparatus is rotated about some other axis in such a case, the result would show differences in the refraction of different meridians giving a false appearance of astigmatism. It will therefore be seen that some means must be provided by which the instrument can be accurately centred upon the pupil and which will also allow the operator to select the zone of the pupil to be tested.

In the instrument that has been developed by Messrs Taylor, Taylor and Hobson, these means have been provided. The optical details are given in Mr Reason's paper, and it is sufficient here to say that the rapid introduction of an auxiliary lens system into the viewing system permits the observation of the image of the patient's pupil which is formed within the instrument. In the plane of this image are situated the mirrors from which the light is reflected into the patient's eye, and a small area of light upon one or other of the mirrors is the effective source of light which is imaged again by the optometer lens in the plane of the patient's pupil. When the pupil-sighting system is in use the observer sees the image of the patient's pupil with the mirrors projecting into it. The image is divided and one-half is reversed by the viewing system. Mechanical adjustments in the base of the instrument allow the image of the pupil to be brought to the central position. A small patch of light upon the edge of one of the mirrors shows the position at which the light is entering the patient's pupil, and thus the zone of the pupil which is being tested. By means of a simply operated screw adjustment the position of this light relative to the axis of observation can be controlled, and thus various zones of the pupil may be selected.

In the usual routine test a measurement of the spherical aberration of the eye is not advocated, although in a case with a very large pupil the author has found a difference of refraction of 2 dioptres between the central and peripheral zones. In order to minimize the time required for the test it is usual to select an intermediate zone and to ensure that the instrument is centred upon the pupil at the moment of measuring the refraction in each meridian. It will be seen, however, that the spherical aberration of the eye may affect the spherical element of the result and prevent its agreement with the subjective measurement in some cases. The significance of this is discussed in the paper by Mr Briggs dealing with the clinical use of the instrument. The presence of spherical aberration will not affect the measurement of astigmatism, and it is this element of the refractive error which is the most difficult to determine by other methods. It is probable that the exact amount of the spherical correction must always be a matter for final adjustment.

Owing to the selective nature of the method, irregularities of the refraction of the eye become apparent. In some objective optometers provision is made for the measurement of the refraction in only one-half of the pupil; it is presumed that the eye must be either a spherical or sphero-cylindrical system and that the refraction in the two halves of the pupil will be equal. In the final development of the coincidence optometer provision is made for carrying out the test over the complete circle of the pupil so that irregular differences of refraction can be detected and measured. It is probable that no other method of measuring refraction provides a means for the detailed study of irregularities.

It is obvious that as lenses for the correction of vision must have either spherical or sphero-cylindrical powers irregular errors of refraction cannot be corrected, and for this reason they are the frequent cause of difficulties and loss of time in subjective testing. The rapid detection of irregular refraction which is possible with the coincidence optometer will avoid the loss of time occasioned by the apparently inconsistent answers given by the subject, but it is particularly important to be able to apply the results given by the instrument to obtain the best sphero-cylindrical correction of the irregular eye.

A further study of the subject is required, but as far as our clinical experience with the instrument goes it appears that the cases of irregular refraction can be placed in three groups. The commonest type is one in which the principal meridians of astigmatism are found to be symmetrical and the same in upper and lower halves of the pupil, i.e. when the instrument is set for meridian location and is rotated through 360° a meridian is found at every 90°. In spite of this symmetry the refraction, particularly the astigmatism, is found to be different in the upper and lower halves of the pupil, thus two possible corrections are found. In the majority of these cases either the weaker or the mean of the two corrections is preferred subjectively. Another type of irregular case is one in which only a small area of the pupil differs from the remainder, as would result from the presence of a small nebula of the cornea. In such a case the refraction of the small irregular area can be neglected in the prescription. The third type of case is the most difficult to measure and to prescribe for; it is one in which the refractions of various parts of the pupil have no relation to one another, the refraction being completely irregular. In such a case the visual acuity is subnormal and the irregularity becomes manifest when an attempt is made to locate the principal meridians with the optometer; many apparent meridians may occur at various angles bearing no apparent relation to one another. When this effect is found the best method of making the test is to measure the refraction at intervals of 10 or 20° round the complete circle of the pupil. From the results obtained a fairly satisfactory prescription can sometimes be deduced. If an area approaching half the pupil approximates to a sphere or sphero-cylindrical result this will usually prove to be the best correction, but if on the other hand there is no regular portion at all the best correction must be sought for subjectively.

In conclusion, it may be said that this instrument appears to provide a means of making some new investigations in connexion with the optical functions of the eye, in addition to its clinical use in the measurement of refraction. The provision of a duplicate fixation device for the other eye with a means for adjusting the convergence of the visual axis enables accurate objective measurements to be made of the amplitude of accommodation relative to convergence and also the study of changes in astigmatism with accommodation. Some preliminary tests with an experimental apparatus on these lines have given promising results, and it is hoped soon to make a full investigation of these problems.

§ 10. ACKNOWLEDGMENTS

Finally, I wish to acknowledge the helpful advice I have received from Mr H. H. Emsley, and the other members of the staff of the Applied Optics Department of the Northampton Polytechnic where the first model of this instrument was constructed. Also I wish to express my thanks to Mr R. E. Reason of Messrs Taylor, Taylor and Hobson, Ltd., for the admirable work he has done in the design and development of the final instrument, and to Messrs Clement Clarke, Ltd., who have supported the development and commercial production.

THE DEVELOPMENT OF THE FINCHAM COINCIDENCE OPTOMETER

By R. E. REASON, A.R.C.S., Messrs Taylor, Taylor and Hobson, Ltd., Leicester

Received 30 *April* 1937. *Read* 3 *June* 1937

ABSTRACT. The optical and mechanical features of a commercial development of the Fincham Optometer are described. The instrument permits direct measurement of the cylinder axis and of the refraction in different zones of the pupil and through 360°; it incorporates means for transferring the focus from the retina to the pupil to facilitate alignment, and a fixation system for arresting the subject's accommodation.

§ 1. INTRODUCTION

THE instrument about to be described is a commercial development of the Coincidence Optometer designed by Mr E. F. Fincham and described in the previous paper.

The aim has been to produce an instrument which incorporates the basic features of the Fincham Optometer and is suitable for manufacture, which is convenient to manipulate, and is robust and not dependent for its accuracy upon the perfection of its slides and bearings.

The considerations underlying the design of the instrument have been discussed in the previous paper, and the details of the present instrument will therefore be described without further introduction.

§ 2. OPTICAL CONSTRUCTION

The optical system, which is shown in figures 1 to 5, can be subdivided into four sections. The first is the target system, comprising the elements *G* to *L* and *OPQST*, whose function is to produce on the retina a rotatable image of the target, and to form within the instrument an image of the retina. The second section includes the elements *U* to *Z*, which form the reversing microscope through which this image of the retina is seen divided into two parts, one reversed with respect to the other. In the third section come the pupil lenses *M* and *N* (figure 5) which, when they are inserted into the system, transfer the focus from the retina to the pupil to facilitate alignment. The fourth section comprises the fixation elements *B* to *F*, whose function is to form on the retina, quite independently of the target used for measurement, an image of an auxiliary object for fixing the subject's accommodation and direction of sight.

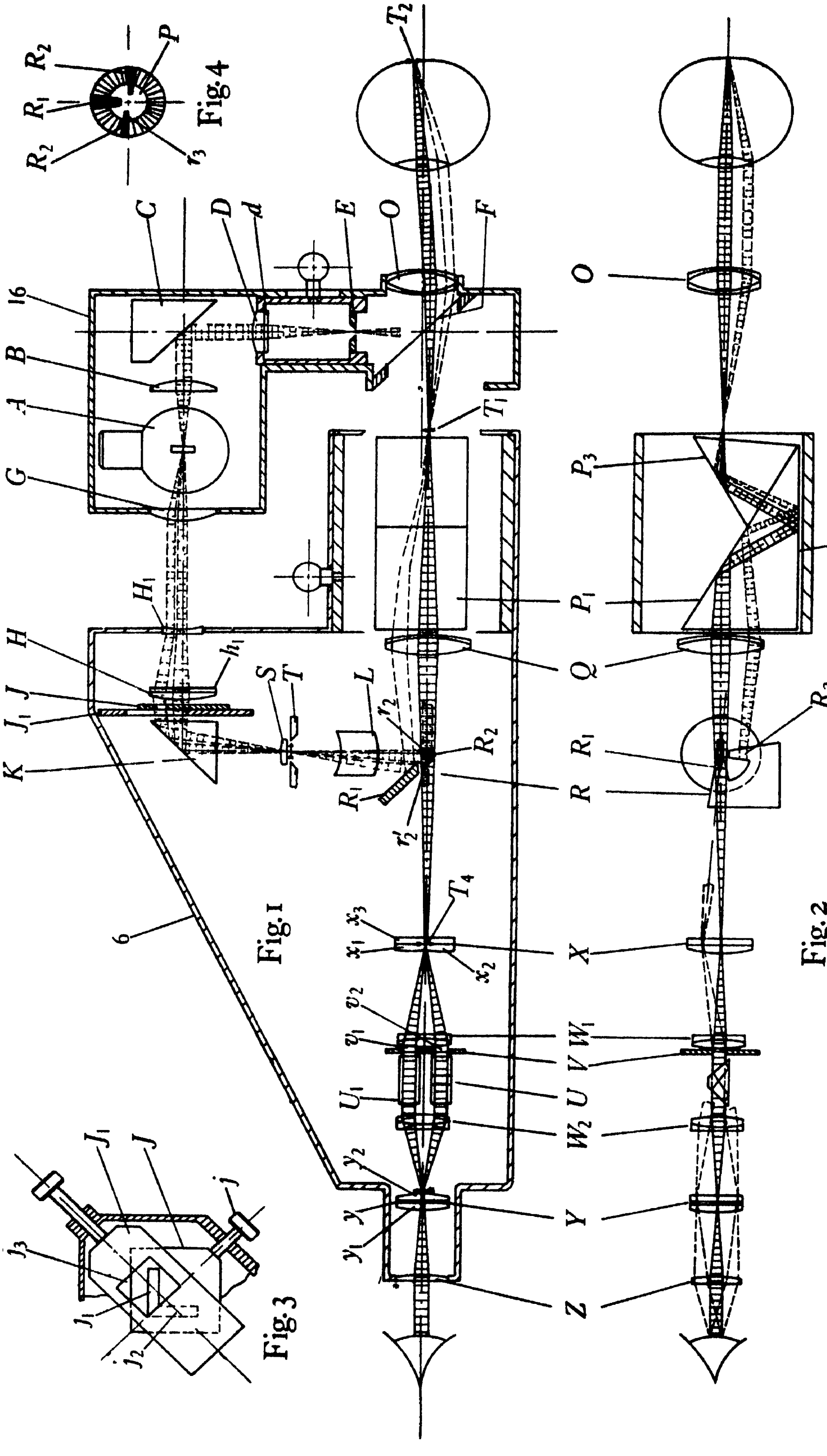

Figures 1 to 4.

§ 3. THE TARGET SYSTEM

The target system is one in which the illuminating and observing beams pass through the same ophthalmoscope lens and is similar in principle to some that have been used before. The usual lens system, however, has been extensively modified to permit more varied measurements and to avoid some ghost reflections that were found very troublesome. The image to be observed is not very bright, and even the third-order ghosts have to be substantially eliminated.

Figure 1 and 2 show the system in side elevation and plan, the elements in the casing 16 being positioned at a fixed distance from the subject's eye, and the elements in the casing 6 being axially movable for measuring the refraction.

Light from the lamp A is collimated by the condenser G, and is then focused on the target T by the condensers H and H_1. These two lenses form an inverted telephoto lens, this construction being used merely to provide an image of the filament of suitable size in the required place. A real image of the target T reflected by the mirrors R_1 and R_2 is formed on the axis of the observing system at T_1 by the lenses L and Q, and an image of T_1 is then formed on the retina through the ophthalmoscope-lens O, which is mounted in the casing 16 with the pupil of the eye at its front principal focus. The target-image is focused on the retina by moving the casing 6 and hence the image T_1 along the axis. When the image is focused the lenses O and Q form an image of the retina suitable for observation at the virtual image of the target T_4 formed by the mirrors.

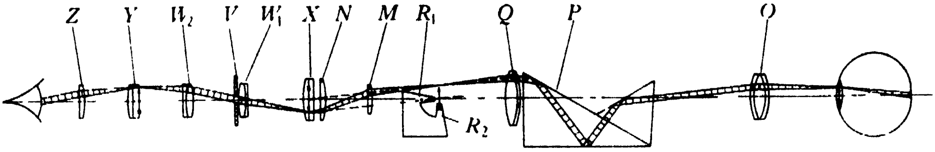

Figure 5.

The marginal area of the pupil through which the retina is illuminated is delimited radially by one or the other of two slits j_1 and j_2 in a mask J (figure 3) which is imaged on the mirrors R_1 and R_2 by the field lens S, and thence on the pupil by the lenses Q and O. The mirrors are mounted in the rear focal plane of the lens Q and are thus imaged on the pupil, together with the mask, independently of the separation of O and Q. A shutter, shown diagrammatically as a plate J_1, admits light to one slit or the other. The slits are tangential to and equidistant from the axis, and the mask J in which they are cut can be moved along their bisector by a screw j so that their distances from the axis, and hence the radius of the zone of the pupil being measured, can be varied. The areas at the pupil are delimited circumferentially by the width of the mirrors. The tips of the mirrors do not actually touch the axis, but leave a small central area through which the retina can be observed. This central area is actually defined by a stop in the reversing system, to be described later.

The images formed on the pupil and on the retina are rotated simultaneously by means of three rotatable reversing reflectors P_1, P_2 and P_3 which may be regarded as a Dove prism in which the refracting faces have been replaced by reflectors in order to avoid unsymmetrical aberrations. These reflectors have been made in the form of an internally reflecting prism with its faces normal to the axis; but it was found that a third order ghost, receiving two reflections off the same prism face, could only be eliminated when the face was exactly normal to the axis, and this led to such fine tolerances on the prism angles that the prism has now been replaced by a system of three first-surface reflectors.

It happens that the only ghosts off the lenses P and Q that are troublesome are the first order ghosts off the surfaces convex towards the incident light. For the reason that the aberrations of both lenses enter into the measurements, removal of the ghosts either by appreciable tilting or by extreme bending of the lenses is impracticable. The lenses work at $f/3$, and have to be allowed their most favourable form. Calculation and trial show that the ghost off the ophthalmoscope lens can be eliminated only when the target image is formed wholly to one side of the axis of the lens, but that the ghost off the second lens can be avoided only when the target crosses the axis. A further requirement is that wherever the target image is formed the images of the mirrors formed by the two lenses must be centred in the pupil of the eye. These conditions are satisfied by mounting the ophthalmoscope-lens on the axis of the eye, and the second lens, together with the rest of the system in the casing 6, on an axis parallel to but sufficiently displaced from the axis of the ophthalmoscope-lens to avoid the ghost which is then reflected away from the axis by the convex lens surface. This separation displaces the target image without displacing the pupil image, as the light imaging the pupil is collimated between the lenses. The prism rotates about the axis of the ophthalmoscope lens; the illuminating and observing beams are therefore rotated round the centre of this lens and no periodic errors due to traces of zonal aberration can arise despite the decentred lens system. When the eye is centred on the axis of the ophthalmoscope-lens, the beams also rotate round the centre of the pupil, and the retinal image of the target is rotated symmetrically round the axis of the eye. The target slit is radial to the axis of the eye and its centre is 3° off the axis. This arrangement permits the fixation object (to be described later) to be imaged centrally on the retina; it causes no error in the determination of the cylinder axis, and it has been found by experiment that even at twice this radius possible errors in the measurement of the refraction are of negligible magnitude.

The target is at a finite distance from the second lens which forms a half-size image of the target, and this arrangement has the advantage that the general direction of the light reaching the convex lens surface, by which the light is outwardly reflected, is already divergent from the axis; so that although the first order ghost inevitably enters the viewing system when the target beam sufficiently approaches the axis, a minimum radius of 1 mm. at the pupil can be attained.

§ 4. THE REVERSING MICROSCOPE

The elements in the reversing system have (1) to divide the field into two parts with a fine dividing line; (2) to hand the light passing through one half of the field; (3) to define the area of the subject's and the observer's pupils through which observation is made. The light passing through the two parts of the field must pass through the same area of each pupil.

The first element is a combined field lens and concave biprism X, mounted at the image of the retina with the roof of the biprism normal to the target line. The element comprises two convex lens segments x_1, x_2, whose centres of curvature are positioned one on each side of the lens-axis. They divide the light into two separated beams, and form two images of the pupil on a two-holed mask whose holes are correspondingly separated and define the single entrance and the single exit pupil of the observing system. The reversing prism U is mounted in one beam and a parallel-ended compensating block U_1 in the other beam. An objective W_1 collimates the light before it passes through the prism and block, and a second objective W_2 forms a further image of the retina and of the field-lens X on a second field-lens and convex biprism Y in the focal plane of the eyepiece. The second biprism is made in one piece to which the field-lens is cemented, and its functions are to superimpose the images of the two holes in the mask on the observer's pupil and to provide a clean dividing line for observation through the eyepiece.

The first biprism is mounted slightly nearer to the observer than the image of the retina; its dividing line, which has nominally to be superimposed on that of the second biprism, is therefore slightly out of focus and the useful result is that a narrow and sharply defined strip of the field at X, about 0·007″ wide, is suppressed. Small chips on the dividing line of X are therefore not seen and there is a reasonable tolerance on the alignment of the system.

This system, although it may seem elaborate, satisfactorily fulfils its functions, and since it is convenient to have a second image of the pupil at which to mount the mask V the system is not really wasteful of elements.

§ 5 THE PUPIL SYSTEM

The third group of elements comprises the two lenses M and N which are used for sighting on the pupil to ensure accurate alignment of the instrument with the eye. When these lenses are inserted into the system the images of the pupil and of the retina are transposed; and the images of the target form the pupils of the system, while the subject's pupil is focused in the eyepiece, as shown in figure 5. The image of the pupil is then seen through the eyepiece as a dull red disc illuminated by light diffused from the retinal image of the target (figure 4).

The insertion of the pupil-sighting lenses makes no difference to the image seen by the subject, and the same small retinal image of the target suffices for the whole process of adjustment and measurement.

In addition to the pupil image the arms of the mirrors R_1 and R_2 are seen projecting into it, because these mirrors are at an image of the pupil. Use is made of the presence of these mirrors to provide an indication of the radius of the pupil at which the illuminating beam enters it. For this purpose the upper edge of the horizontal mirror R_2, intercepting the shaft of light from the parallel slits T and j_2, is made roof-shaped; the polished face r_2 reflects light from the sharply focused image of the slit j_2 forwards towards the subject; the other face r'_2 is diffusive and scatters light from the same image backwards towards the observer. Through the eyepiece a slit of light r_3 is seen crossing the mirror R_2, as shown in figure 4, which indicates the area of the pupil P through which the light is entering it.

Further use is made of the pupil image to indicate when the instrument is at the right distance from the eye. This is of some importance in cases of considerable myopia or hypermetropia as the power-scale can only be calibrated for one distance. The method depends on the separation of the axes of the lenses O and Q, by virtue of which a movement of the instrument along the axis is accompanied by a movement of the image across the field in a direction which is vertical independently of the orientation of the rotating prism. The instrument is so made that if, after it has been aligned so that the pupil image remains stationary while the prism is rotated, the distance is adjusted until the pupil image is bisected by the dividing line of the field, the pupil will be correctly positioned at the focus of the ophthalmoscope-lens. In this way it is not difficult to set the distance within 1 mm. The correct distance also corresponds with the best definition of the pupil image, but owing to the exceedingly small numerical aperture of the system adjustment by focusing is generally not accurate enough.

The technique of adjusting the instrument in such a way that errors of distance and centering are not confused, although a little troublesome to describe, is easily mastered and is quite effective in practice.

§ 6. THE FIXATION SYSTEM

The last section of the optical system includes the elements B to F, which are used for fixing the accommodation and direction of sight. For this purpose a virtual image of an illuminated pin-hole E is formed on the axis of the ophthalmoscope-lens by a pellicle-mirror F which is so thin that it has no measurable effect on the transmitted target image. The pin-hole is provided with focusing adjustment independently of the target used for measurement. The brilliant ghosts inevitably formed off the ophthalmoscope lens and off the eye are eliminated by means of complementary colour filters. It happens that the retina is reddish in colour and reflects very little light of shorter wave-length than 5000 A. A yellow filter having a sharp cut at about this wave-length is therefore mounted in the viewing system at y, and a complementary blue filter in the fixation system at d. The ghosts are thus blue and are completely absorbed by the yellow filter, which, however, reduces the brightness of the observed image by a negligible amount. Since blue light is absorbed by the retina and cannot be used for measurement, a further yellow filter is mounted in the illuminating system at h, so that the blue wave-lengths are eliminated from the target image before the light reaches the eye, with consequent reduction in fatigue for the subject.

§ 7. GENERAL CONSIDERATIONS

The optical system has the useful property that the accuracy of measurement does not depend on precise alignment of the movable elements. The measured quantity is the separation of the two casings 6 and 16, and since the movement in the middle of the scale is 0·05 in. per dioptre there is no difficulty in providing a durable and accurate coupling.

Analysis shows that the stability of the system depends only on the relative positions of the target-slit, the mirrors R_1, R_2, the lens W_1, the reversing prism U, and to a much less extent on the lens L. For making measurements these elements are moved as a whole; they can therefore be securely mounted on a single frame and moved without fear of relative disturbance due to wear. But for this the mounting would have been both costly and liable to error, as a displacement of the slit of 0·0001″ is readily detected. All the other elements of the measuring system are common to both the illuminating and the observing beams, and lateral displacements of these elements therefore deflect both beams equally and introduce no errors. Thus accuracy in the slide and in the mounting of the rotating reversing reflector is not of fundamental importance, and ordinary manufacturing limits are more than good enough.

The change from axis to refraction measurements is effected not by displacement of an optical element but by displacement of an aperture relatively to fixed optical elements, and here again there is no need for great accuracy.

The design of the condensers permits both objects to be properly illuminated from the same lamp independently of their motion; and the inverted telephoto construction happens to be a considerably lesser evil than the mechanical difficulties that would have resulted from the use of a single condenser of suitable focal length.

The numerical aperture of the beams is generally exceedingly small, and in most positions a single plano-convex lens is perfectly satisfactory. The design has further been proportioned so that many of these plano-convex lenses have the same focal length and nearly all have the same diameter. For example, such diverse elements as the two lamp condensers, the slit field-lens, and the two pupil-sighting lenses, are alike. The manufacture of both glasses and cells is thereby greatly simplified.

§ 8. MECHANICAL CONSTRUCTION

The upper part of the instrument housing the optics is carried on a vertical shaft 1 (figure 6) supported in a sleeve 2 mounted on the base. The shaft can be moved vertically for height adjustment by a knob in the base and can be rotated for turning the instrument from one eye to the other by another knob also situated in the base. The shaft thus economically serves two purposes. The working distance of the instrument from the eye is adjusted by the knob 5, and the part of the system axially movable for measurement, which is housed in the box 6, is moved by the graduated wheel 7. The rotatable reversing prism is turned by the graduated wheel 8.

The internal construction of the optical section is shown by the drawings (figure 6), which show a plan and two elevations of the instrument, with a detail of the construction inset. The side elevation is sectioned in the axial plane of the lens system but the end elevation is sectioned in several planes for economy of space.

The upper end of the vertical shaft is forked to form two bearings 9 and 10 for a horizontal shaft 11, and to carry a bar 12. A bracket 13, clamped to the horizontal shaft 11, slidably engages the bar and keys the shaft against rotation. The shaft forms the main slide of the instrument and is movable longitudinally by the rack and pinion 14 and 15.

A casting 16, clamped to the extreme end of the shaft, carries the ophthalmoscope-lens *O* and pellicle-mirror *F*, the lamp house 17 which is heat-insulated from the casting by a bakelite spacing ring 18, and the fixation system 19. The fixation cell slides in a vertical hole 20, and is driven by the rack and pinion 21 and 22. A spring plunger 23 in the end of the pinion-shaft bears against a flat on the cell and, urging it anticlockwise, forces the involute rack teeth into the pinion to eliminate backlash. The mounting of the knob 24, which is graduated, permits adjustment of the zero.

The body 6 in which the axially movable elements are mounted, slides on the same horizontal shaft that forms the main slide and is keyed against rotation by an arm 25 projecting from the lamp house to engage a slot cut on the top of the body. The power wheel 7, by which the body is moved, is pivoted to the body on ball bearings; and a spiral cam slot 26 cut on the underside of the wheel engages a ball bearing roller 27, pivoted to the bracket 13. Backlash between cam and roller is taken out by two further rollers, 29 and 30, mounted on a spring loaded sliding plate 28. The directions of the resulting forces are so balanced that in spite of several pounds loading and a cam angle averaging 1 in 10 there is no appreciable force tending to drive the wheel, which turns equally freely in both directions. No provision is made for taking up shake in the pivot of the cam. The maximum shake permitted by the tolerances is equivalent to an error of 1/50th of a dioptre, and since no wear is to be expected in either of the hardened ball races the shake may be neglected.

To ensure easy motion of the body, the front slide bearing 31, which carries the greatest load, is a ball bearing slide. The balls are kinematically spaced by a cage 32.

The vital elements determining the zero adjustment are fixed to a frame 33. The frame has two surfaces at right angles forming a V machined along its under side in which the pupil mirrors R_1, R_2, the first biprism X, the collimating objective W_1 and mask V, the reversing prism U, and the compensating block U_1, are fixed. No ambiguity in the position of the reversing prism is permissible, and therefore in the plane of reflection the location of the prism is strictly kinematic.

The biprisms and the mask have to be accurately adjusted rotationally and then clamped in position; and the method of clamping is shown inset. The cell screws some distance into a tube, which is slit near the end rather more than half way across. The springy tongue thus formed is pulled down by the clamping screw 54.

The thread in the tube is relieved in the plane of the slit to avoid burring the thread. Very little clamping pressure is required and the cells do not tend to rotate while the screw is being tightened.

The frame is kinematically suspended in the body by the engagement, at 34 and 35, of the ends of the V with the tubes supporting the lens *Q* and the eyepiece unit, and is keyed against rotation by means of a stud and clamping screw, not shown on the drawing, at the top of the body.

The target slit *T* is formed on the upper end of the tube 36, which is spring urged against four adjusting screws 37, 38, 39 and 40. The lower adjusting screw 40 is provided with a hexagon head and is accessible through a hole in the cover in case the need for zero adjustment should arise. It is worth mentioning that in spite of some rough handling, and the apparently crude constraints, the need for an external zero adjustment has not yet been felt.

The field lens *S* and the prism *K* are provided with adjustments for imaging the pupil apertures in the mask *J* correctly on the pupil mirrors, and the lamp filament correctly on the slit. The plate *J* slides along the bisector of the slits and is moved by a screw 43, with which it is held in contact by a spring. Light is admitted to the required slit through a gash in the shutter J_1 which is pivoted to the frame at 45 and moved by the lever 46.

The condensers *H* and H_1 are eccentrically mounted to permit lateral adjustment of the filament image in case the filament distorts after the lamp has been used for some time, although since new lamps are pre-focused this adjustment is not often required.

The pupil-sighting lenses are mounted one at each end of a tube 47, adjustably carried in a bracket 48. The bracket is mounted on a shaft 49, rotatable in V's 50 and 51 formed in the frame, and is moved by the lever 52. When the lenses are in their inoperative positions the field of view is stopped down by a mask 53, carried on the end of the tube, to exclude some ghosts.

The rotatable reversing reflectors are carried in a cylindrical mount 55, which is rotated by means of the key 54 and the wheel 8. The reversing reflector P_2 is fixed in the side of the mount and the remaining two reflectors P_1, P_3 are formed in one piece and are adjustably supported on two screws 56, 57, at one end and on one screw 58 at the other end. The reflectors are pressed in contact with these and with the adjustable end-stop 59 by a U-shaped plunger 60, pressed down by a spring. The reflectors have to be adjusted so that the axes of the cylinder bearings on each side of the reflectors P_1, P_3 are virtual images of each other. The reflectors are made of glass and are aluminized.

The scales are illuminated by a scale lamp 61 on the side of the case, the power scale being seen and illuminated by reflection in a mirror 62. The lamp also illuminates the observer's note pad. Both lamps are wired internally, and the leads 63 up the pillar are aluminium-sheathed to prevent chafing.

The relaxation discs 67 and 68 are mounted one on each side of the lamp bracket and are illuminated through windows in the bottom of the lamp house. A shutter 69 obscures light from one window or the other, or both.

§ 9. MATERIALS

The materials from which the instrument is made are determined by their function and cost. The base and the sleeve mounted on it are of ordinary cast iron for cheapness. The vertical shaft 1 has a ground surface exposed just above the sleeve, and to minimize the possibility of rust the piece is cast in a nickel-silicon cast iron. The same material is used for the headrest on account of its malleability. Since the greater part of the optical system moves for taking measurements, the lightest possible materials have been used to avoid sluggishness due to inertia. The body is cast in a magnesium alloy, and the remaining castings are in aluminium with the exception of the sleeve containing the rotating reflector-mount, which is cast in gun metal. The power-wheel, in which is formed the cam-slot 26 engaging the rollers with line contact, must be light but hard, and is cast in a Rolls-Royce aluminium alloy having about one and a half times the Brinell hardness of *Y* alloy. The horizontal shaft is made of steel, case hardened and ground, and its exposed portion is chromium plated.

§ 10. ACKNOWLEDGMENTS

In conclusion, I would like to thank Mr Fincham, Mr Lee, and Mr Warmisham for their help and advice, and the Directors of Messrs Clement Clarke and Co. and of Messrs Taylor, Taylor and Hobson, Ltd., for their patience during the development, and for permission to publish this paper.

AN EXPERIMENTAL STUDY OF TURBULENCE DIFFUSION

By E. G. RICHARDSON, B.A., Ph.D., D.Sc., Armstrong College, Newcastle-on-Tyne

Received 28 *April* 1937. *Read* 25 *June* 1937

ABSTRACT. This paper describes a method involving study of the rate of diffusion, due to the turbulence prevailing in a stream, of a dye let into the stream. The concentration of the dye is measured with a beam of light and photoelectric cell, and the stream-velocity with a hot-wire anemometer, at various places in the stream. As a test of the method the latter is first applied to molecular diffusion and shown to give results in accordance with those obtained by other methods. Next, turbulence induced in a water channel by gratings of various mesh-widths is traced. By using a pair of sources and light-beams with associated photoelectric cells, the degree of correlation between the motions at two points in the turbulent stream, both along and across it, can be studied.

Finally the diffusion due to turbulence of the dye-source at the head of a plate edge-on to the stream is studied. Smooth plates and those having a sinusoidal roughness are used. It is found that both the velocity-distributions and the rates of diffusion can be expressed in terms of a Blasius parameter and a factor dependent on the wave-length of the roughness.

§ 1. INTRODUCTION. METHODS OF MEASUREMENT

The treatment of turbulence, and especially atmospheric turbulence, as a problem in diffusion is due in the main to G. I. Taylor(1), L. F. Richardson(2) and W. Schmidt(3). Whether the thing transported be called mass, energy or vorticity to suit a particular problem, the form of the resulting equations is the same. The first-named of these physicists has considered the turbulence produced in a channel by disturbing agencies such as honeycombs, and has shown that turbulence as a type of diffusion is intimately related to two other concepts which have proved fruitful in hydrodynamics in recent years, viz. the idea of a correlation coefficient between the conditions at two points in a stream, and that of the mixing-length or mean free path of a disturbance nascent in a stream before it mingles with the circumambient fluid.

The theoretical work of L. F. Richardson was supported by observations of the width of smoke trails from tall chimneys, and Sutton(4) has carried out more extensive measurements of diffusion in the atmosphere. The general principle of diffusion-measurements necessitates the introduction into the fluid of some material or energy whose subsequent distribution can be determined by the analysis of instrumental records. If energy be introduced it may take the form of (A) an inexorable oscillation of fixed frequency and amplitude, or (B) a constant supply of heat. If mass-transport is to be studied the source may take the form of (C) colour or (D) a solid such as smoke, dust or silt.

Method (A) has been used by the writer and E. Tyler⁽⁵⁾. Part of the boundary of a small wind channel run at subcritical speed was oscillated in simple harmonic motion, and the spread of the disturbance was traced downstream with a hot-wire detector. The difficulty in such experiments is that the disturbance in the boundary layer tends to change the character of the flow in the main stream, so that something more than a mere diffusion of the oscillation may result.

Experiments of class (B), in which heat was introduced along a line-source transverse to the channel, have been described by Schubauer⁽⁶⁾, and some others made by Simmons are cited by Taylor⁽⁷⁾. The temperature across various downstream sections may be measured with a thermocouple and hence the rate of diffusion of heat can be calculated, although Schubauer determined three points only on each traverse, viz. that of maximum temperature and those where the temperature was half the maximum. The diffusion so observed is, of course, the combined effect of turbulence-transport and heat-conduction, as in most cases of forced convection. In the same category belong the experiments of Townend⁽⁸⁾ who traces the diffusion of isolated masses of heated air ("hot spots") by the methods of *schlieren* photography.

It may be opportune at this point to compare the advantages and limitations of the four methods. The hot-wire apparatus (A) for tracing fluctuations of velocity possesses the advantage of compactness. It gives the nearest approach to a point-to-point delineation of conditions in the stream, whereas the optical methods involve a beam covering a certain area, of which the minimum workable size is probably 10 mm.^{2} On the other hand, the indications of the hot-wire detector are a function not merely of the amplitude of the velocity-fluctuations but also in a marked degree of the *average velocity* about which those fluctuations take place, so that near a solid boundary a considerable correction is necessary for the change in mean velocity from point to point—a correction which may amount to several hundred per cent of the reading.*

With regard to (B) and (D), the colour method possesses the advantage of producing no appreciable local change of density or viscosity in the fluid. The specific gravity of the solution corresponding to the maximum coloration recorded in the turbulence measurements described later in this paper is 1·005.

In the heat-diffusion method, the source must be at a high temperature and this causes a distortion of the flow by gravity, unless the channel has a vertical axis. Further, the coefficient of thermal diffusivity for air (0·2 c.g.s. unit at 50° C.) is a greater fraction of the turbulent diffusion than is that of molecular diffusion of a dye such as potassium permanganate ($1{\cdot}3 \times 10^{-5}$ c.g.s. unit); hence a larger correction, amounting to 10–15 per cent in Schubauer's experiments, is necessary in the observed temperature-distribution due to this molecular conduction.

§ 2. TECHNIQUE OF PRESENT METHOD (C)

In the present method a dye such as potassium permanganate is let into a water channel along a horizontal line perpendicular to the direction of flow. The dye dissolves and is diffused downstream by the intermingling with neighbouring strata of the fluid passing the source, and the time average of the colour-density at any level (x, y) is measured by a horizontal beam of light traversing the channel and falling upon a photoelectric cell. At first the dye was introduced by siphoning a concentrated solution through a narrow tube, mounted transversely to the stream and pierced at the after edge with a number of small holes. It was found that the tube tended to induce turbulence in its wake. Further, any velocity relative to the main stream which the jets might have on emergence was also a disturbing factor. Latterly a thin phosphor-bronze strip, 2 mm. by 0·3 mm., was stretched tightly across the stream and this, painted with a soluble gum and the finely powdered solid dye, acted as the line source. Several seconds elapsed before the gum was dissolved off and the dye began to colour the stream, so that the fitting of the source in position was not accompanied by a vivid overall coloration of the stream such as resulted when the powder was directly applied to the strip.

---

* Cf. reference (5), figure 2.

The channel was constructed with plate-glass sides and extending between two reservoirs with a capacity of 10 cubic feet. The upstream reservoir was fed by a pipe from the city main at a head of 90 ft., while on reaching the downstream reservoir the water ran over a weir of adjustable height to the waste pipe. Level-gauges could be adjusted to touch the water-surface at intervals along the channel. The channel was 6 ft. long and 10 in. wide, and the maximum depth of water was 1 ft.

It was of course necessary to establish a relation between the colour-density of the diffusing dye and the photoelectric current in the cell, which was illuminated by a horizontal beam of light interrupted by the colour. The voltage at which the photoelectric cell gave a linear response to intensity of illumination was first found by trial, and then a small portion of the channel was sealed off to form a tank into which solutions of known concentration of the dye were introduced in turn, and the response of the cell to light passing through the solution was measured. It was found that over the range of colour-density likely to be used in the experiments a linear relation existed between the concentration and the current-defect, i.e. the difference between the reading of the galvanometer with clear water and that with the dye in solution.* The clear-water reading was maintained constant during the experiments by adjusting the width of the beam whenever necessary. The latter was normally 1·5 cm. wide and 2·5 cm. deep. The velocity was measured with a calibrated hot wire of nickel, 0·002 in. in diameter, which was held on a fork. Both hot wire and photoelectric cell with its associated beam of light could be traversed in the x, y plane through the water.

§ 3. THEORY OF THE METHOD: MOLECULAR DIFFUSION

When the laws of probability are applied to diffusion in fluid motion,† the probability considered is that of finding a given concentration c at any position

---

* This relation does not correspond exactly with the well-known law of Beer, but it must be remembered that that law applies to monochromatic light. In the present experiments, the author was concerned only to get the most sensitive and convenient response of the apparatus to changes of colour-density, and the relation quoted was found to give the best fit.

† H. Gebelein has recently written a general account on this problem(9).

(x, y, z) in the field over a given small interval of time δt. This probability-distribution will be a function whose dimensions are the reciprocal of a time. The first moment of this will be another function which may be called the *expectation*; it has the dimensions of a velocity U, and is in fact that of the fluid conveying the dye. We then have

$$\frac{\partial c}{\partial t}+c.\nabla U+U.\nabla c=k.\Delta c \qquad \text{......(1)},$$

where k is a diffusion constant having the dimensions $[L^2 T^{-1}]$. If u_1 is the observed mean velocity with which the dye spreads, we must have also if there is no loss of dye

$$\frac{\partial c}{\partial t}+c.\nabla u_1+u_1.\nabla c=0 \qquad \text{......(2)}.$$

If $U=0$, we shall then have the case of molecular diffusion at a rate u_0, when (1) becomes

$$\frac{\partial c}{\partial t}=k.\Delta c \qquad \text{......(3)};$$

otherwise we may expect that $u=U+u_0$, so that (2) becomes

$$\frac{\partial c}{\partial t}+c.\nabla\,(U+u_0)+(U+u_0).\nabla c=0 \qquad \text{......(4)}.$$

In most practical cases of fluid motion, the velocity u_0 of pure diffusion is negligible in comparison with that of the fluid U.

In order to test the new method against an experiment for which the results by other methods were available, the molecular diffusion of potassium permanganate in water was followed in a narrow cell measuring 3·5 × 0·7 × 20 cm. through which the beam of light passed parallel to the narrow edge. This cell was mounted in the large channel, filled with slowly running water to act in some measure as a thermostat. The cell was nearly filled with water, and some saturated solution containing excess powder was carefully run to a depth of about 1 cm.; finally a film of oil was added on the top to prevent evaporation. Measurements of the vertical gradient of concentration as indicated by the photoelectric cell were made from day to day for a week, figure 1*a*. There was sufficient saturated solution at the bottom of the cell for this to be considered a level of maintained saturation, although it is true that the exact level at which the concentration began to fall as a result of diffusion may have become lower during the week. The appropriate solution of equations (1) and (2) for diffusion along the y-axis alone is

$$\frac{\partial c}{\partial y}=\frac{c_0}{2\sqrt{(\pi k t)}}\exp\left(-y^2/4kt\right) \qquad \text{......(5)}.$$

Thus the slope of a $\{y^2, \log_e(\partial c/\partial y)\}$ line is equal to $4kt$. Such curves for various values of t in days are shown on figure 1*b*, and the mean slopes are plotted against time in figure 1*c*. One notes the departure from straightness which these lines exhibit at large concentrations, a result to which three causes may contribute: (1) the coefficient of diffusion is known to be relatively greater at large concentrations, (2) the point of departure ($y=0$) from maximum concentration is known to shift somewhat, and (3) the method is uncertain at high concentrations of the dye.

The last point requires elaboration. When the dye is highly concentrated the cell is working close to its dark condition, so that the current is small and difficult to measure. There is, however, another difficulty. The last equation shows that the

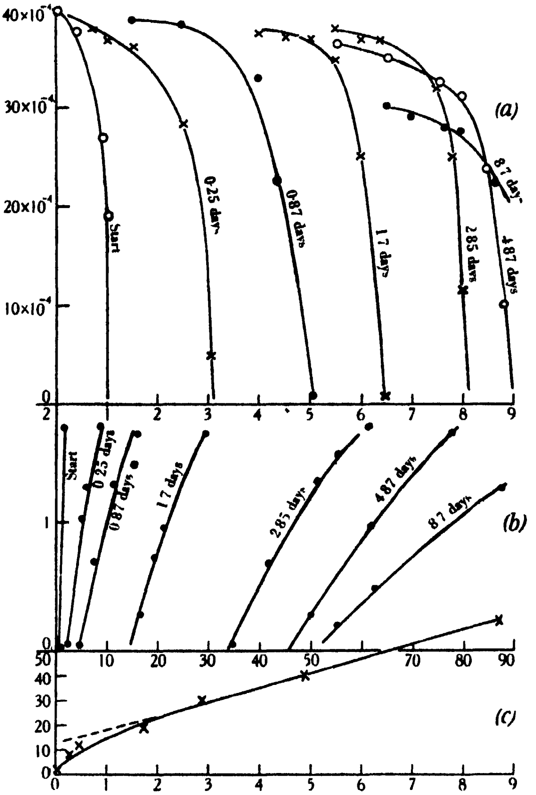

Figure 1. Molecular diffusion.

	Ordinates	Abscissae
(*a*)	*Concentration* (*g./cm*.³)	y (*cm*.)
(*b*)	$log_{10}(\partial c/\partial y)$	y^2 (*cm*.²)
(*c*)	$log_{10}\{y^2/(\partial c/\partial y)\}$	*Time* (*days*).

gradient of concentration is large where the concentration itself is large, and this causes a marked diffraction of the light-beam depending on the width of the cell that lies in the path of the beam. (This diffraction is, in fact, the basis of diffusion measurements in Wiener's method.) Examination of the light passed by the cell as a whole on to a screen shows that the dispersion is small with such a narrow cell, but it is a disturbing factor to be reckoned with in wide tanks and large gradients of concentration. Fortunately turbulence diffuses a dye so rapidly that such gradients are scarcely to be encountered in work other than that dealing with molecular diffusion. The refractive index of the solution at the concentrations used in the subsequent experiments varied between 1 and 1·005, so that dispersion was a negligible factor. If the straight part of the curve of figure 1 *c* is extrapolated to an arbitrary time origin, the mean coefficient of diffusion works out at $1{\cdot}3 \times 10^{-5}$ cm.^{2}/sec., agreeing well with values given by other methods.

§4. DIFFUSION OF TURBULENCE BY A GRATING

The theoretical work of Taylor(7) and the experimental work of Schubauer(6) indicate that the turbulence engendered in a stream by a regular series of slots is a function of the spacing. In the present instance a number of gratings were constructed of horizontal circular rods fixed in a vertical frame with equal spacing.* A grating was introduced about half way down the channel, and the space between it and the end of the channel was traversed in vertical planes with the optical detector. At first a mean channel speed of 4 cm./sec. was used, the water supply being from the mains and the coloured water run to waste. Later, a 2-h.p. circulating pump was installed, allowing of speeds of 20 cm./sec., which correspond to a Reynolds number of 60,000. The difficulty now was that the water returning to the channel was contaminated by the dye and coloured before it reached the grating. This difficulty was overcome by making the water slightly acid and bubbling sulphur dioxide into the pump intake. An attempt was made as follows to reduce the permanganate at the correct rate so that the water returned colourless to the channel. When the sulphur dioxide was in excess it decolorized the fresh dye coming from the source; the reduction was therefore made somewhat incomplete so that the water remained slightly pink in colour on re-emergence. An auxiliary fixed beam of light was sent athwart the channel to another photoelectric cell upstream of the model, and the out-of-balance current between the two photoelectric cells was read on a Wheatstone bridge in which the cells formed one pair of ratio arms. With this compensating device it did not matter if the reduction of the permanganate was incomplete on the return of the water to the channel. It should be added that the channel was given sufficient slope to produce uniform flow as estimated by traversing a hot-wire anemometer across the experimental section.

In turbulent motion, diffusion from the source occurs at rates governed by the velocity-fluctuations, to which we may assign the components u', v', w'. Of these u', parallel to the axis of the channel, is disguised by the much greater general velocity of the stream U, while w' across the channel cannot register impressions in the beam of light which runs in the same direction and therefore averages out any variations of concentration in this dimension. There remains only the vertical component of the turbulent diffusion, so that the equation reduces to

$$\frac{\partial c}{\partial t} = k\frac{\partial^2 c}{\partial y^2} \qquad \text{......(6).}$$

The solution is formally similar to equation (5), but instead of $2kt$, which had the dimensions of the square of a length, we may, following Taylor$^{(7)}$, write $\overline{Y}^2$, where $\overline{Y}$ is the mean vertical distance diffused in the time t that corresponds to a general drift of the whole field through a distance x, so that $t = x/\overline{U}$, $\overline{U}$ being the mean velocity of drift. The gradient of concentration on the left of equation (5) is replaced by the concentration itself, since the dye is only supplied at $x = 0$, and not all along the axis of the channel. When $\overline{U}$ is constant, the distribution of the dye in any vertical plane will be given by

---

* Schubauer actually used honeycombs. Gratings were preferred by the writer for greater ease in construction, and not because it was thought that two-dimensional flow would be induced thereby.

$$c = \frac{c_0}{2\sqrt{(2\pi)}\,\overline{Y}} \exp\left(-y^2/2\overline{Y}^2\right) \qquad \text{......(7)},$$

c_0 being the (maintained) concentration at $(x, 0)$. $\overline{Y}^2$ will be given by the negative slope of the graph of y^2 against $\log c$. Such graphs are given on figures 2 and 3 for two different speeds, with the source 10 cm. downstream from the grid. A slight curvature at regions near the source was attributed to local variations in $\overline{U}$. Figures 4 and 5 show how $\overline{Y}^2$ varies with x, that is with time, as the stream flows away from the source. The initial slopes of these curves are, for a given value of $\overline{U}$, measures of the turbulence induced by the grid. It is this slope that is proportional to the mesh-size of the grid. This statement holds for the present results provided the grids are geometrically similar, but there is also an effect due to the bars of the grid

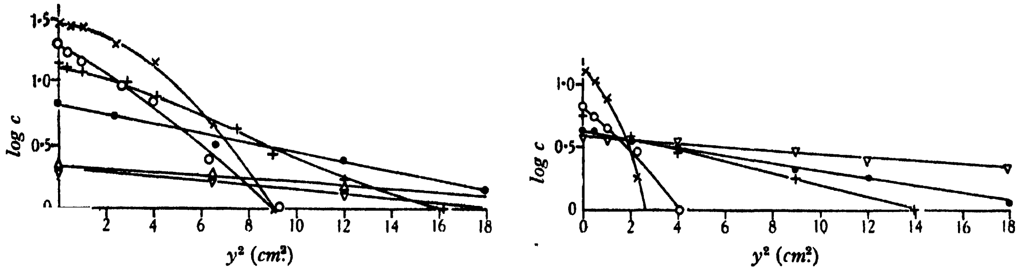

Diffusion due to turbulence induced by a grating.

Figure 2. $U = 1 \cdot 5$ cm./sec.

	×	○	+	●	▽	△
x	4	8	12	23	33	43
Mean Y^2	1·25	1·8	3·3	7·7	11	13

Figure 3. $U = 2 \cdot 5$ cm./sec.

	×	○	+	●	▽
x	4	8	13	23	43
Mean Y^2	0·5	1	2·8	7·5	11·5

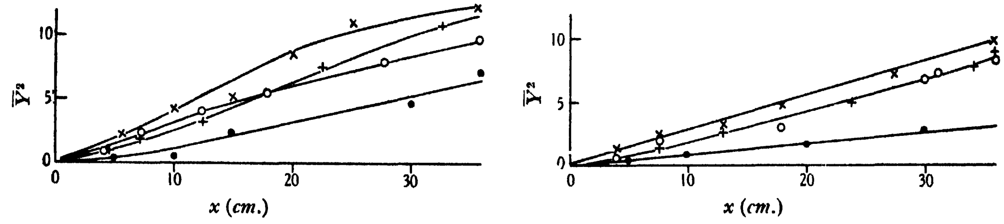

Decay of turbulence downstream from grating.

Figure 4. $U = 1 \cdot 5$ cm./sec.

Figure 5. $U = 2 \cdot 5$ cm./sec.

	×	+	○	●
Mesh of grating (in.)	$\frac{3}{8}$	$\frac{3}{8}$	$\frac{3}{16}$	$\frac{3}{16}$
Bar of grating (in.)	$\frac{3}{8}$	$\frac{3}{16}$	$\frac{3}{8}$	$\frac{3}{16}$

as well as the mesh. Thus the grid with $\frac{3}{8}$-in. bars and spaces does not induce the same turbulence as that with $\frac{3}{16}$-in. bars and $\frac{3}{8}$-in. spaces. Further, if the turbulence is isotropic, as seems to be the case in most channels, we may write for the slopes of these curves

$$\sqrt{\overline{Y^2}}/x = \sqrt{\overline{v}'^2}/\overline{U} = \sqrt{\overline{u}'^2}/\overline{U},$$

where $\overline{u}'$ and $\overline{v}'$ are the amplitudes of velocity-fluctuation in the component directions. Dissipation of turbulence after the stream leaves the grid will result in a reduction of u' and $\overline{v}'$, with decrease of slope of the $\overline{Y^2}:x$ curves, as it were a reduction of diffusion constant with concentration of vorticity. This decay is slow in the writer's channel, possibly owing to accretion of turbulence from the floor, but the commencement of decay may be observed as a diminution in slope on the extreme right of figures 4 and 5.

§ 5. CORRELATION OF FLUCTUATIONS

Closely bound up with this diffusion of turbulence is the decrease in correlation between the fluctuations in magnitude and direction of the mean velocity at two different points in the stream at corresponding epochs, to which Taylor(7) has drawn attention. Thus, to measure the correlation between fluctuations at two points *A* and *B* on a line perpendicular to the axis of the channel at identical instants, two hot wires may be mounted and the magnitude and relative phase of the respective potential-differences induced in them by the turbulence compared. Prandtl and Reichardt(10) do this by bringing each potential-difference to one pair of plates in the cathode-ray oscillograph. The figure traced by the electron spot then depends on the correlation coefficient between the fluctuations in potential-difference, being a circle when the coefficient of correlation is 1, and a straight line when it is 0.*

In adapting the optical method to the measurement of correlations one proceeds as follows. A thin glass tube lets in dye from an orifice pointing downstream at the point *A*, and at the same point a pencil of light restricted by diaphragms to a diameter of $\frac{1}{2}$ cm. crosses the channel horizontally to one of a pair of matched photoelectric cells. A similar arrangement suffices for the point *B* with a second photocell, except that the whole of this duplicate device can be racked up and down without alteration of the relative orientation of lamp, orifice and photocell. Thus while *A* is fixed in the channel, *B* can be at any desired height in the vertical plane through *A*. The two photocells were connected with two variable 10,000-ohm resistances, a rectifier connected to a galvanometer, and a battery of 200 volts to form a Wheatstone bridge, the idea being that as long as the *déroulement* at *A* and at *B* remained the same no current would pass through the rectifier, but as the correlation between *A* and *B* became less, an increasing but, of course, alternating current would pass through the rectifier, and in consequence the mean deflection of the galvanometer would increase. To indicate the relation between this deflection and the correlation, and in some measure to act as a calibration of the apparatus, the sources of the water and the dye were removed from the channel and a disc driven by a motor was mounted in the channel. The circumference of the disc was cut in the shape of an epicycloid with two cusps. When the two cells were mounted at opposite ends of a diameter and the disc was rotated, the light on each cell varied in simple harmonic fashion but in the same phase, so that no deflection was recorded on the galvanometer. One cell being kept fixed, the other with its associated beam was moved round the circumference of the disc, the deflection increasing as the light fluctuations got out of step, until at a phase-difference of π (corresponding to an angular separation of the cells of $\pi/2$) the deflection reached a maximum, to fall again as the cells approached the diametrically opposed positions. In this way, a calibration curve, figure 6, of deflection plotted against phase-difference was obtained.

---

* Actually it is the correlation in *resultant* fluctuations which is measured, though theory discriminates between u' and v' in this respect. Neither the optical nor the double-hot-wire method discriminates between directions of fluctuation, but in isotropic turbulence this does not matter.

The correlation coefficient as usually defined between a fluctuation u_1' at station A and that u_2' at station B is

$$R = \frac{u_1' . u_2'}{\sqrt{(\bar{u}_1'^2 . \bar{u}_2'^2)}}.$$

When u_1' and u_2' are simple harmonic motions of equal frequency and amplitude, but having a phase-difference of δ, this expression reduces to $\cos \delta$. Approximate proportionality between galvanometer deflection and the cosine of the phase-difference is indicated by figure 6. Accordingly it was assumed that when the procedure was applied to the stream in the channel the deflection of the rectifier-galvanometer would measure the correlation coefficient directly, with the help of this calibration curve.

The pair of cells and associated light-beams were then arranged in a vertical plane across the channel, and the dye was let in from two jets just upstream of the light-beams. While one was kept still, the other was moved to various heights and the galvanometer deflection was noted when the cells were connected in the circuit described above.

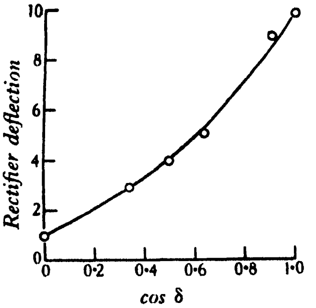

Figure 6. Calibration curve for correlations.

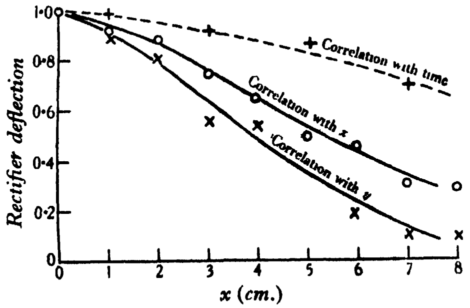

Figure 7. Correlation in turbulence due to a grating.

The two correlations, across the stream and down the stream, with one beam at a fixed point 20 cm. behind the $\frac{3}{8}$-in. grating are shown by continuous lines in figure 7. As Taylor indicates from theoretical considerations, the correlation with x is much closer than that with y, although the type of correlation here measured is not quite the same as that considered by Taylor, since the present measurements are concerned with the relative phase as well as the magnitude of the fluctuations.

Another type of correlation can be measured by comparing the oscillation at station A with that at B downstream, after allowing sufficient time to elapse for the general current to pass from A to B. A length of photographic film must then intervene between the records of the respective fluctuations. The two beams of light after passing perpendicularly across the stream were inclined by small-angled prisms until focused side by side on the film in continuous movement through a camera at known speed,* figure 8. The dye caused fluctuations in the intensity of the light, revealed as variations in blackness of the film on development. The film was then passed again through the two light-beams and cells, one for each half of the film, with the cells connected in circuit, but the pick-up for B was proportionately lower down the film than for A—somewhat after the fashion in which light and sound are picked up from a talking film—so that the galvanometer deflection measured the correlation between A and B after the proper time interval had elapsed. This correlation with time is shown by a dotted line in figure 7. In the absence of dissipation, a disturbance would be conveyed with unchanged amplitude down the stream, but in fact the correlation gradually departs from unity as the time increases. This type of correlation is analogous to that obtained by Townend(8) from the observation of the passage of hot spots downstream.

§ 6. TURBULENCE DIFFUSING FROM A BOUNDARY

The complete theory for the diffusion of turbulence from a solid boundary has yet to come and there are few experiments on the subject other than those on the heat-losses from hot plates, in which the matter is complicated by a temperature-gradient. It was thought that it would be of interest to apply the present apparatus to the securing of related data on diffusion and velocity-gradients near a plate edge-on to the stream, plates both smooth and of determined roughness being used.

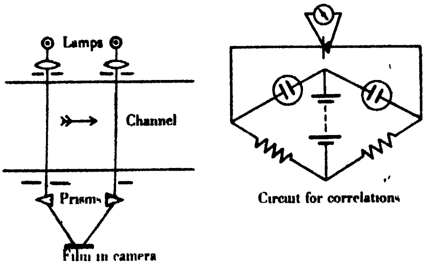

Circuit for correlations

Figure 8. Correlation apparatus and circuit.

Smooth plates of varnished wood and brass having a width equal to the full width of the channel and either 30 or 60 cm. long were used. The wooden plates were bevelled at the leading edge, and for the slower speeds the linear dye source was let in as a fillet to the front edge. The brass plate used at the higher speeds has a circular tube of the same outer diameter as the thickness (2 mm.) of the plate soldered along the front edge and pierced with a few small holes. The dye was fed to this source through vertical tubes coming down the sides of the channel. The only new experimental difficulty was that in the passage of the beam of light just above the surface of the plate some light was reflected into the photoelectric cell, so that the clear-water reading of the cell differed in this region from the more distant ones and made a measurement of the darkening produced by the dye less certain than at places remote from the plate. This influence extended to about 3 mm. from the surface of the plate. The hot-wire measurements of velocity in this region were corrected for proximity to the plate by the method devised by Piercy and the writer(11).

---

* A single wide beam was used when x was less than 2 cm.

For the rough plates it was decided to idealize the roughness into a sinusoidal boundary having an amplitude equal to half the wave-length λ. These were constructed of a series of equally spaced wires set transversely to the stream and soldered on a plate. Wax was then run on to the plate, and when it had hardened it was gouged out of the interspaces to the set template. The three constructed had $\lambda = 0{\cdot}5$, $\lambda = 1$, and $\lambda = 1{\cdot}6$ cm. respectively, and troughs of depth $\frac{1}{2}\lambda$. The plates were mounted in mid-stream, in a region of (originally) uniform velocity. The velocities in the neighbourhood of the smooth and the two roughest plates are shown on figures 9, 10 and 11. To conform with the Blasius theory of skin friction(12), the velocities are plotted against the parameter ξ, equal to $\sqrt{(Uy^2/kx)}$ where k now represents the dynamical coefficient of viscosity. In fact, the broken line drawn in figure 9 represents the Blasius distribution, for comparison with the experimental points. In figures 10 and 11, y is measured from the tops of the undulations, which admittedly afford an uncertain zero, but at this level the distribution of velocity does show a steeper gradient than the smooth plate, which does in some measure serve as a criterion of the roughness. The gradients for the three rough plates were

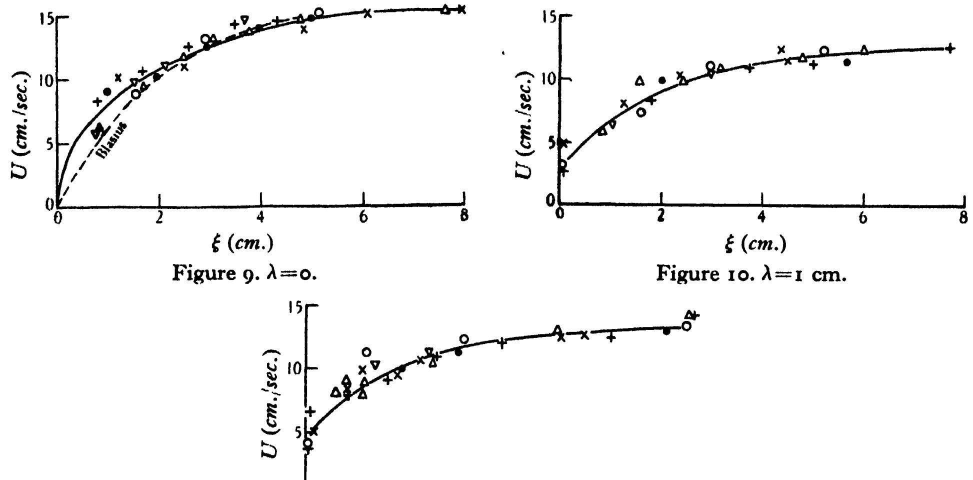

Figure 9. $\lambda = 0$.

Figure 10. $\lambda = 1$ cm.

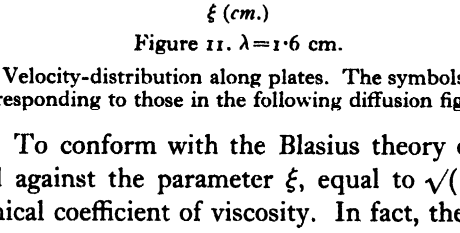

Figure 11. $\lambda = 1{\cdot}6$ cm.

Figures 9, 10, 11. Velocity-distribution along plates. The symbols refer to values of x corresponding to those in the following diffusion figures.

in the ratio 4 : 5 : 6, as nearly as could be estimated. The observed distributions satisfy, except very close to the boundary, that postulated by Prandtl (13), i.e.

$$U + a \log (\xi + b)$$

where a and b are constants dependent on the roughness so that the gradient

$$\frac{\partial U}{\partial \xi} = \frac{a}{\xi + b}.$$

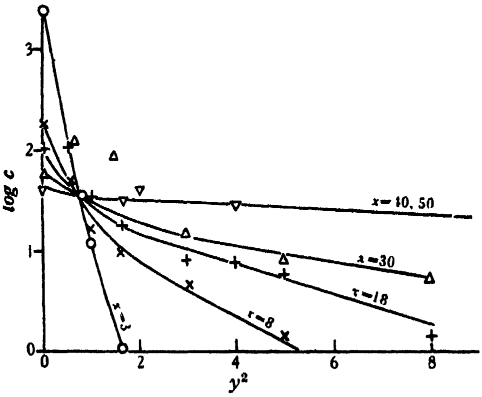

Figure 12. λ=0.

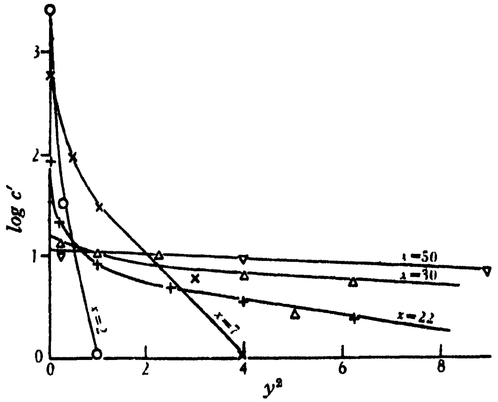

Figure 13. λ=1 cm.

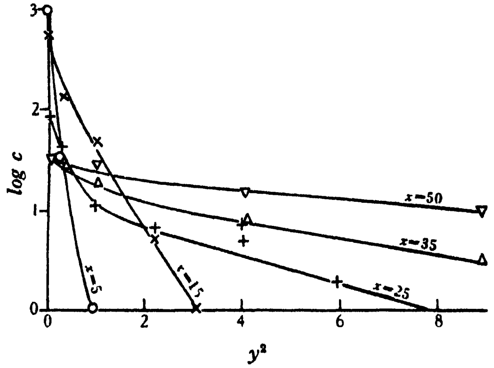

Figure 14. λ=1·6 cm.

Figures 12, 13, 14. Diffusion of turbulence along plates.

Measurements of the concentration of the dye in various planes perpendicular to the plate, at distances x from the leading edge, were made, but before $\{\log c, y^2\}$ curves could be plotted a correction had to be made for the gradient of U near the surface of the plate. In consequence of this velocity-gradient the diffusion appears more rapid at first as the dye leaves the plate. In actual fact the concentrations recorded for small values of y represent a proportionately higher value of t than those for larger values of y and the same value of x. It will appear that the velocity v of scattering in the direction perpendicular to the plate is nearly constant, whereas the drift velocity parallel to the plate increases outwards, and the average velocity $\bar{U}$ where

$$\bar{U}=\frac{1}{\xi}\int_0^{\xi} U\,d\xi$$

had to be determined for each value of x, y. Hence the time taken for particles of dye to reach a given co-ordinate (x, y) was calculated by using the curves of figures 8, 9, 10 and integrating the necessary areas under the curves. The equation corresponding to equation (7) is then

$$(\log c_0-\log c).\,\bar{U}=\xi^2/Y^2 \qquad \ldots\ldots(8),$$

U (contained in ξ) being the drift velocity of the whole stream in the absence of the plate. With the introduction of this correction factor the $\{\log c, y^2\}$ lines become nearly straight, figures 12, 13, 14, although there is still a tendency for the velocity of diffusion to increase over the first few millimetres from the plate as well as with time. The former increase may be accounted for by an hypothesis that the vortices originate from a level slightly above the level of the plate or of the crests on it. The latter increase is brought out by the $\{\overline{Y^2}, x\}$ curves, figure 15, which indicate that vorticity is added to the stream by its passage over the plate, and particularly over the rough plates for which a rapid increase of slope of the $\{\overline{Y^2}, x\}$ line occurs as the stern is approached. This rate is roughly proportional to λ. The short smooth plate shows a less rapid growth, with the usual dissipation occurring beyond the stern (with decreasing slope). The importance of the parameter ξ can be shown in respect of these diffusion measurements, as well as in relation to velocity-gradients, for it is possible to reduce all the measurements for a given plate to a single curve by plotting them against $1/\xi^2$. In figure 16 this has been done for the smooth plate. The slopes of the lines in figure 12, *uncorrected* for variation in drift velocity, are plotted against y^2/x.

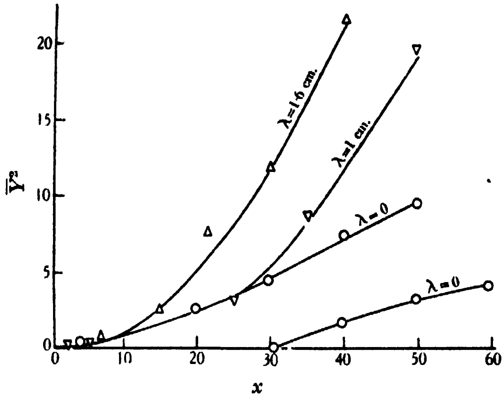

Figure 15. Growth and decay of turbulence along plates.

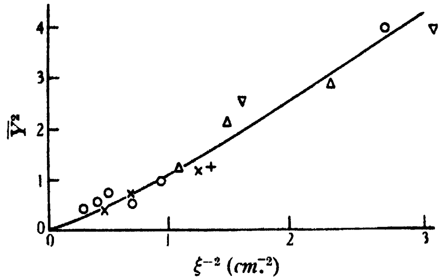

Figure 16. Growth of turbulence along smooth plate in relation to Blasius parameter.

§ 7. ACKNOWLEDGMENTS

The author wishes to express his indebtedness to Prof. W. E. Curtis and the Research Grants Committee of Armstrong College for the facilities to carry out this work, and to Prof. G. I. Taylor for much helpful criticism and advice during the course of its execution.

REFERENCES

(1) Taylor, G. I. *Philos. Trans.* **215**, 1 (1915).
(2) Richardson, L. F. *Proc. roy. Soc.* **97**, 357 (1920).
(3) Schmidt, W. *Der Massenaustausch in freier Luft* (1925).
(4) Sutton, O. G. *Proc. roy. Soc.* **135**, 143 (1932).
(5) Richardson, E. G. and Tyler, E. *Phys. Z.* **32**, 509 (1931).
(6) Schubauer, G. B. *Rep. nat. adv. Comm. Aero.*, Wash., No. 524 (1935).
(7) Taylor, G. I. *Proc. roy. Soc.* **151**, 421 (1935).
(8) Townend, H. C. H. *Proc. roy. Soc.* **145**, 180 (1934).
(9) Gebelein, H. *Turbulenz* (1935).
(10) Prandtl, L. and Reichardt, H. *Dtsch. Forsch.* **14**, 111 (1934).
(11) Piercy, N. A. V. and Richardson, E. G. *Rep. Mem. aero. Res. Comm.*, Lond., No. 1224 (1929).
(12) Blasius. *Z. Math. Phys.* **56**, 1 (1908).
(13) Prandtl, L. *Z. Ver. dtsch. Ing.* **77**, 105 (1933).

THE VORTEX MOTION CAUSING EDGE TONES

By G. BURNISTON BROWN, M.Sc., Ph.D., Lecturer in Physics,
University of London, University College

Received 10 *April* 1937. *Read* 25 *June* 1937

ABSTRACT. A detailed investigation has been made of the tones produced when a jet of air strikes an edge, with velocities extending from the lowest possible to those in the neighbourhood of the Reynolds critical velocity in the orifice. Four different stages of stable vortex-formation occurred and the whole phenomenon was found to lie within the sound-sensitive range of the jet. Throughout this range the dependence of the frequency n on the distance h of the edge and the mean velocity U can be closely represented for a 1-mm. slit-width and a wedge of angle 20° by the formula

$$n = 0{\cdot}466\,j\,(U-40)\,(1/h - 0{\cdot}07),$$

where $j = 1$, 2·3, 3·8 and 5·4 for the four stages respectively.

The stage represented by $j = 1$ may occur simultaneously with the other stages and thus two notes of different pitch may be produced. Comparison with the vortex motion in sensitive jets shows marked similarity, but it cannot be assumed that the vortex motion in edge tones has its origin at the orifice, as it always has in sensitive jets.

§ 1. INTRODUCTION

It was first noted by Sondhaus(1) in 1854 that tones can be produced by blowing a jet of air against an edge, and that a resonating column, such as is always found in musical wind instruments is not essential. In the eighty years following, the subject has received the attention of many investigators and it has been realized that vortex motion plays a large part in the production of sound. It was reasonable to expect, therefore, that the information gained by the detailed examination of the vortex motion in jets subjected to sound and the author's theory of the mechanism of sensitivity(2) would be of use in attempting a more comprehensive explanation of the phenomena of edge tones than has hitherto been possible.

It has, however, unfortunately been found necessary to repeat much of the work of former investigators. The reasons for this were: (1) arguments have been made from analogies with water jets which have led to conflicting conclusions(3, 4); (2) in most cases only the pressure has been measured from which the velocity of the jet cannot be obtained with certainty; (3) some writers maintain that as many as six jumps in tone may occur(5) while others have denied that any occur at all if sufficient care is taken in the experimental arrangements(6); (4) the jumps in frequency have been commonly stated to be in simple numerical relation (e.g. in octaves), and this in the absence of resonators is *a priori* unlikely; (5) the experimental methods adopted in obtaining some of the material leave the interpretation of the results open to considerable doubt$^{(4,6,8)}$; (6) no systematic and thorough examination has been made which would enable a formula for the frequency to be deduced. The formulae given involve assumptions with regard to Kármán vortex-sheets which are quite inadmissible and yield results which are only approximately correct$^{(3,9)}$.

§ 2. EXPERIMENTAL METHOD

The apparatus used was that described in detail in former papers$^{(2,10)}$.

A brass wedge of angle 20° and width 5 cm., and having a height of 7·5 cm., was suspended from a mounting by which it could be raised and lowered and also moved across the orifice by a delicate screw motion. It could also be set accurately parallel to the orifice in the vertical plane. The mounting was attached to an iron bar which was screwed on to the outside of the wooden box containing the slit. This formed a very rigid system and was carefully adjusted so that when the wedge was raised its edge remained always in a plane passing through the centre of the slit and parallel to its sides. The under side of the movable slit was slightly modified so as to be accurately symmetrical and this made the stream of air flow in such a manner that it was accurately bisected by the wedge at all heights.*

The stroboscopic disc was, when necessary, covered with insulation tape so that only three slits were uncovered and this allowed of photography at frequencies as low as 20 c./sec., although the intensity of the illumination was thereby reduced fourfold. In addition a separate stroboscopic disc was used for observation and the visual determination of frequencies. It was found convenient to have two rows of viewing-holes in the disc, one with 12 holes and a subsidiary one with 24. Any danger of running the disc too slowly at a fraction of the correct speed when the former row is being used can be obviated by observing through the latter, when the well-known doubled appearance should be seen.

All the films and nearly all the observations refer as in the former paper to a jet width of 1 mm., depth 1 cm. and length 2·3 cm.

§ 3. VARIATION OF FREQUENCY WITH EDGE-DISTANCE WHEN THE VELOCITY IS CONSTANT

The variation of the frequency n of the sound with the distance h of the slit from the edge when the mean velocity U of the stream is constant has never been thoroughly investigated, although for limited regions it has been observed that the product nh is approximately constant$^{(11,9,12,8)}$.

The procedure adopted in this present research was as follows. The velocity was adjusted to a given value and the apparatus was left for half an hour to attain a steady state, the pump working against a leak in the manner formerly described.† Then the time for 50 to 100 litres to pass the gas-meter was observed and these readings were taken throughout the whole period during which measurements of h

---

* Cf. reference (2), p. 714.

† Reference (2), p. 704.

and *n* were being made. Thus a series of times were recorded from which the mean velocity could be obtained and which showed that the velocity had been constant. All frequencies under 300 c./sec. were observed visually through the stroboscopic disc to which a counter working over a period of 15 sec. was attached. The mean of several observations was taken. The visual method was essential since no clearly audible sound occurs below 500 c./sec. Above 500 c./sec. the frequency was found by the method of beats with the calibrated heterodyne oscillator. It was found to be of the greatest value in obtaining beats to be able to decrease the output of the loudspeaker until the intensities of the two beating sounds were approximately equal. The height *h* was measured with calipers. The results obtained by visual means are shown in figure 1 and those obtained aurally in figure 2. In both cases the frequency is plotted against the reciprocal of the height of the wedge. The width *d* of the slit was 1 mm.

In every case it is clear that each curve consists of four distinct portions each of which is very nearly a straight line. The curve for $U = 984$ cm./sec., shown in figure 2, is typical and can be considered in detail.

Starting with the wedge close to the orifice ($1/h = \infty$) no tone is heard, as is well known, until a certain minimum height is reached. This is represented by the point *N*. A clear bright tone then commences and the frequency decreases with increase in *h* until a point such as *L* is reached. The tone then jumps suddenly to *J*, but in certain cases, viz. those in which the velocity is above about 600 cm./sec., it is possible for the original tone to persist as well, and this gives the dotted portion *LZ*. At *Z* the lower note becomes inaudible. The upper note decreases in frequency with increase in *h* but at a more rapid rate than in the first case. On arrival at *H* a second jump takes place to *F* and the note again falls to *D*, and then a third jump to *B* occurs, when a weak tone drops to a confused irregular noise at *A*. From the point *F* onwards the original tone is again heard as well and gives the portion *YX*. There are therefore four clearly defined stages which will be referred to as stage I (*NL*), stage II (*KH*), stage III (*GD*) and stage IV (*CA*).

If now the curve is retraced in the opposite direction, i.e. if the wedge is lowered downwards towards the orifice, the sequence of events is not exactly the reverse of those occurring when the wedge is raised. Starting again at *A* the frequency rises now to *C* and then drops suddenly to *E* in stage III, from which point the frequency rises to *G* before falling suddenly to *I* in stage II. It increases then to *K*, from whence it drops to *M* and rises to *N*, at which point it ceases abruptly. In this case stage I is audible throughout the whole range, and persists in addition to the higher notes, where these occur. This is brought about by the fact that in certain circumstances stages I and III may be possible while I and II are not, a condition which occurs in the region *FGIH*. If stage II is in progress between *I* and *H*, stage I is not possible. But if stage III is in progress, stage I is possible as well and the region *YZ* occurs with *FG*. Thus the stage I is complete from *X* to *N* when we pass from left to right across figure 2, i.e. with the wedge approaching the orifice.

This fact accounts for a very confusing observation which can be made at the value of *h* corresponding to the points *Z*, *I* and *G*. At this height a jump in tone is

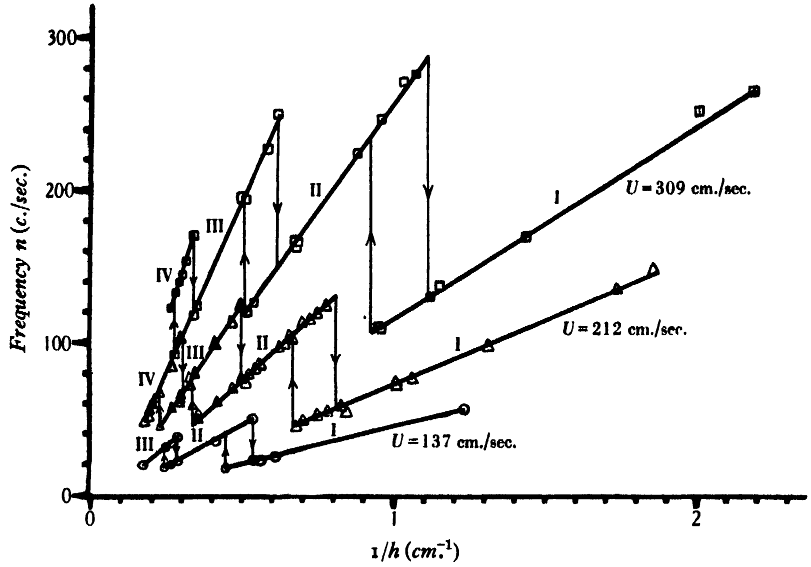

Figure 1. Variation of frequency with reciprocal of wedge-distance for low velocities.

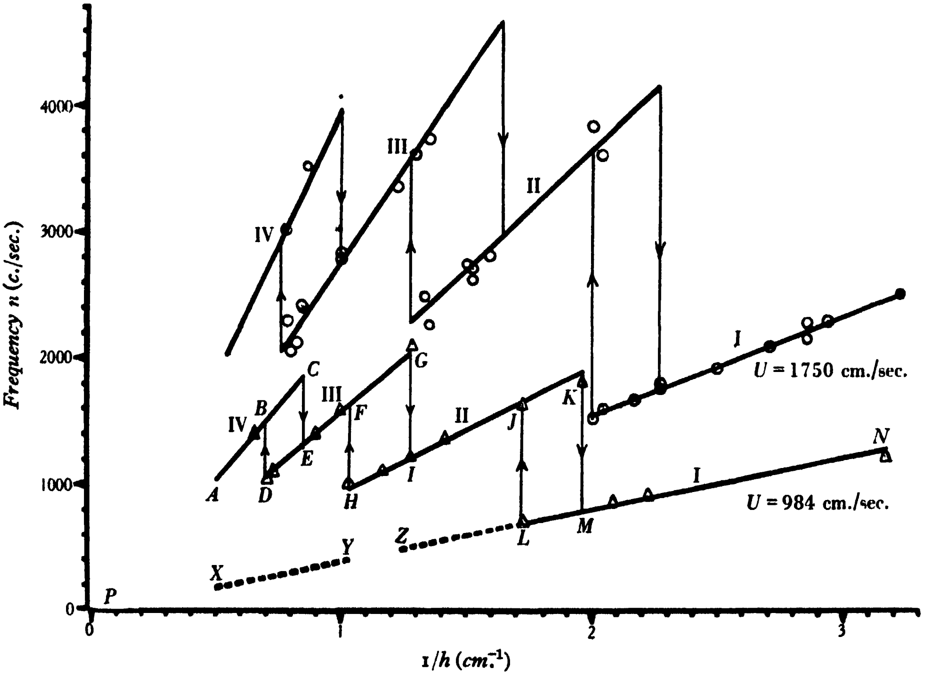

Figure 2. Variation of frequency with reciprocal of wedge-distance for high velocities.

heard which can be recorded as a jump up or a jump down according to whether the investigator is concentrating attention on the lower or upper note, i.e. he may hear the sequence of tones represented by *XYZIJK* or *EFGIJK*. This confusion is made possible by the fact that the intensity of stage I changes suddenly at *Z*. When stage I occurs with III it is easily audible but when combined with II in the neighbourhood of *Z* it is nearly inaudible. The intensity of stage I does not change appreciably in the region corresponding to the jump *DBCE*, and the possibility of confusion does not arise so readily.

The phenomenon mentioned above is probably the explanation of some otherwise curious results obtained by Richardson* which give a graph of n against $1/h$ consisting of a line sloping upwards and then a jump *upwards* to another line of increasing frequency. It seems possible that Richardson has recorded only the lower note and has therefore plotted the curve *XYZIJK*.

Again, the occurrence of stage I simultaneously with the other stages when the velocity is high, which was noted long ago by Wachsmuth(7), is probably the cause of Benton's assertion that if sufficient care is taken no jumps in tone occur at all(6).

A detailed study of his description indicates that the jumps took place in his experiments but that changes in intensity of the various components led him to infer that only the quality of stage I gradually altered.

In the graph under discussion ($U=984$ cm./sec.) the intensity of the sounds produced in stages II and III appears to the ear to be about the same, and much greater than in stage I. For high velocities (2000 cm./sec.) the intensities in stages I, II and III are nearly equal. Stage IV is very weak and unstable, and in the case of the lowest velocity, 137 cm./sec., it could not be observed at all.

It was discovered by inspection that all the points lie very nearly on straight lines radiating from a point P on the $1/h$ axis at a distance of 0·07 from the origin, and in figures 1 and 2 the straight lines are drawn so as to pass through this point.

§ 4. THE FOUR VORTEX STAGES

The four possible vortex stages are illustrated in figure 3, plate 1. For this purpose the stroboscope was set rotating so as to produce 126 interruptions of the illumination per second. The velocity was kept constant at a convenient value, 272 cm./sec., and the wedge was slowly raised until first of all a stationary view of stage I appeared. Photographs were taken and then the wedge was raised again until a second stationary appearance, showing stage II, was obtained. In a similar manner stages III and IV also were photographed, the frequency and velocity in each being constant. The distances of the wedge were $h=0{\cdot}81$, $1{\cdot}73$, $2{\cdot}65$ and $3{\cdot}5$ cm. The photographs show the four different ways in which one and the same frequency can be produced with a given fixed mean velocity of the stream.

In the former paper on sensitive jets(2) it was found that

$$\omega=\pi n,$$

---

* Reference (8), figures 6 and 10.

where ω is the angular velocity of the leading filament of the vortex in radians per second, and this result was also found in the present research.

Since ω depends only on n, and n is constant in figure 3, the angular velocity is the same in each case and equal to 63 rev./sec. If the filament, on its first appearance, is taken to subtend an angle θ equal to 0 at the centre of the vortex then the values of θ at the edge are approximately as follows: In stage I $\theta=0$, in stage II θ lies between $\pi/2$ and π, in stage III θ lies between $3\pi/2$ and 2π, and in stage IV $\theta=5\pi/2$. Examination of the vortices formed in sensitive jets by sound showed that the vortex ceases to entrain air, revolution of the filament slows down and ceases, and the boundary of the jet is closed, at a certain distance from the orifice.* This is a distance corresponding to θ between 2π and 3π and so it seems that once the boundary of the stream is closed and the rotation ceases, the disturbance which maintains the periodicity in stages I to IV no longer occurs, since stage V is unstable.

The vortex-formation after the edge has been passed depends on the stage. In stage I the vortices complete a revolution and start a fresh series caused by friction with the wedge-face rotating in the opposite direction, and a vortex-street is thus formed. This is shown by the first photograph in figure 3 in the plate†, and in its most striking form in figure 4. In stages II to IV the vortices continue upwards, apparently little affected by the presence of the wedge. No sign of a secondary series forming a vortex street occurs.

The heights of the wedge which produce the same frequency with a constant velocity are examined in detail in table I. It will be seen that if the heights are called h_1, h_2, h_3 and h_4 for the stages I to IV, then the distances between them (h_4-h_3), etc., are, for the higher velocities, nearly but not quite constant. This agrees with some results for $U=562$ cm./sec. and $d=1{\cdot}02$ mm. found by Rieth(12), but Schmidtke(3) inferred from them that the distances were constant and hence that a Kármán vortex street must be present, an inference which is not supported by the present research.

Table I

n (c./sec.)	h_4 (cm.)	h_3 (cm.)	h_2 (cm.)	h_1 (cm.)	h_2-h_1 (cm.)	h_3-h_2 (cm.)	h_4-h_3 (cm.)	U (cm./sec.)
20	—	5·68	3·92	2·02	1·90	1·76	—	137
100	3·48	2·41	1·57	0·75	0·82	0·84	1·07	212
150	3·33	2·50	1·64	0·79	0·85	0·86	0·83	309
1200	1·74	1·28	0·79	0·34	0·45	0·49	0·46	984
2400	1·58	1·15	0·75	0·33	0·42	0·40	0·43	1750

§ 5. THE VARIATION OF FREQUENCY WITH VELOCITY

A careful investigation of the variation of n with U when h is constant was made with values of h from 3·5 cm. downwards, with jets of width 4, 3, 2, 1, 0·5 and 0·25 mm. There is a close resemblance between the forms of the graphs of n against U obtained for all jet-widths, and it was found that as the jet-width decreased, the

---

* Reference (2), p. 708. † The photographs on the plate have been reduced in the ratio 6 : 5.

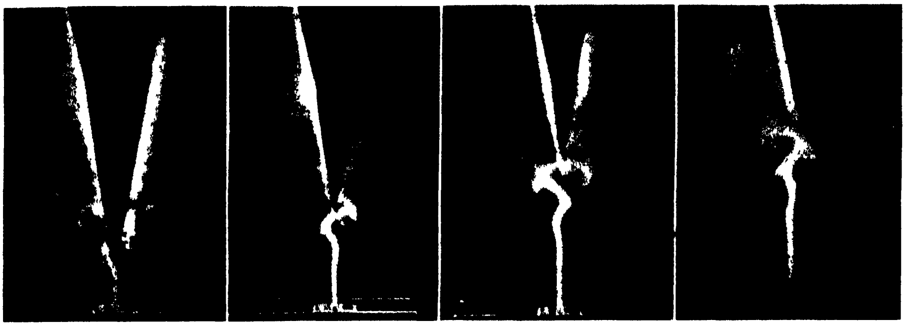

Stage I $h=0{\cdot}81$ cm. Stage II $h=1{\cdot}73$ cm. Stage III $h=2{\cdot}65$ cm. Stage IV $h=3{\cdot}5$ cm.
$n=126$ c./sec. $U=$const.$=272$ cm./sec.

Figure 3. The four stages in vortex formation producing the same frequency.

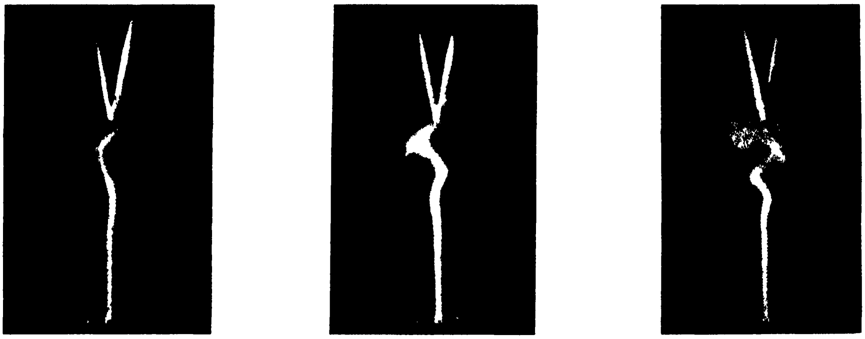

Stage II $n=25$ $U=162$ cm./sec. Stage III $n=75$ $U=254$ cm./sec. Stage IV $n=126$ $U=272$ cm./sec.

Figure 6. Three vortex formations produced with a constant wedge-distance $h=3{\cdot}5$ cm.

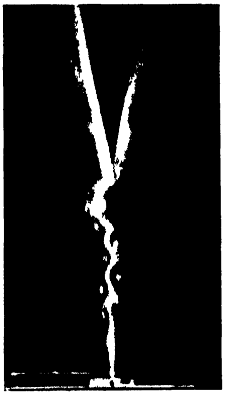

Figure 9. Sound $n=102$ c./sec. superimposed on edge tone $n=20{\cdot}5$ c./sec. $h=3{\cdot}5$ cm. $U=127$ cm./sec.

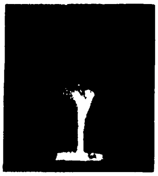

Figure 7.

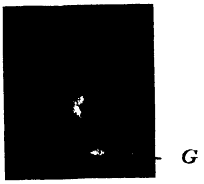

Figure 8.

Simultaneous production of two sounds of different pitch.

Fig. 7 $\begin{cases} n_1=210 \text{ c./sec. stage I} \\ n_3=800 \text{ c./sec. stage III} \end{cases}$

Figure 8. $n_1=210$ c./sec. suppressed by beard G.

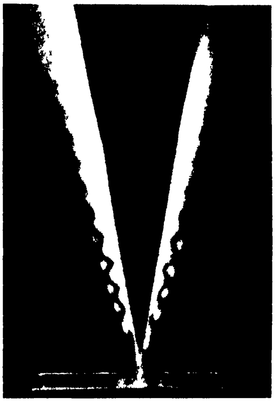

Figure 4. Vortex streets in stage I $n=126$ c./sec. $h=0{\cdot}6$ cm. $U=210$ cm./sec.

The photographs on this plate have been reduced in the ratio 6 : 5.

frequency of a given stage became lower for the same velocity and height. This is in agreement with some results obtained by Carrière⁽⁴⁾. The present discussion will be confined to a jet of 1 mm. In this case, when $h=3{\cdot}5$ stage I is not obtained; the first sign of oscillation is found when $U=120$ cm./sec. and $n=17$ c./sec. (stage II). As the velocity is increased the amplitude of the vortex motion becomes greater, and when U equals about 230 cm./sec. and $n=38$ c./sec. stage II suddenly ceases and stage III appears, the frequency jumping to 66 c./sec. With further increase in the velocity, the amplitude of stage III grows, and when $U=310$ cm./sec. and $n=99$ c./sec. the frequency jumps to 146 c./sec. (stage IV), and this continues till $U=330$ cm./sec. and $n=160$ c./sec. After this point no periodic motion is observed and the jet resembles a turbulent jet without a wedge. If now the velocity is reduced slowly, stage IV lasts until $U=200$ cm./sec. and $n=95$ c./sec., and then the motion jumps to stage III which lasts until $U=150$ cm./sec. and $n=38$ c./sec. The motion then jumps to stage II and continues down to the initial point where $U=120$ cm./sec. and $n=17$ c./sec. In each case the amplitude decreases. The three curves are slightly convex to the axis of U, approaching a straight line as the higher values of U and n are reached.

An attempt was made with U and h constant, to get different amplitudes and therefore possibly different frequencies, but this was not successful and it was concluded that U and h determine the vortex motion and therefore the frequency completely. It may be noted that U must be greater than about 500 cm./sec. for sound to occur. As h is decreased the range of the vortex motion increases: figure 5 shows n plotted against U, for h having the values 1·5, 1·0, 0·75, and 0·5 cm. The stages are indicated and it will be seen that each stage is linear, and when produced backwards towards the origin, cuts the axis of U in the neighbourhood of the point $U=40$ cm./sec.* On the same graph are also plotted the limits above and below which the jet exhibits no sound-sensitivity. These are taken from the former research,† together with extra observations made specially. The graph indicates clearly that, by means of the jumps, the edge tones remain within the central region of the sound-sensitive area.

An illustration of stages II to IV in the case where $h=3{\cdot}5$ cm. is given in figure 6, plate 1.

§ 6. MEASUREMENT OF THE WAVE-LENGTH

As in the former research on sensitive jets⁽²⁾, a series of films were taken in order to determine the wave-length λ, i.e. the distance between two successive vortices on the same side of the stream. A different convention with regard to the definition of λ was, however, found necessary. As was stated in the paper referred to, the estimation of the distance between the centres of two successive vortices is easy when the vortex-development is not great (and this applies to most of the results in that paper) but becomes increasingly difficult with greater development. In the case of edge tones the vortex development is always very marked, and therefore, in view of the fact that the central portion of the stream, which does not form into rotating filaments, presents a wave-like appearance, λ was defined to be the distance between successive troughs. When comparison with the films of sensitive jets was made, therefore, these films were re-measured with the new convention. This results in an increase of about 28 per cent in λ.*

---

* To avoid confusion only a few of the observed values are plotted on the graph.

† Reference (2), figure 7.

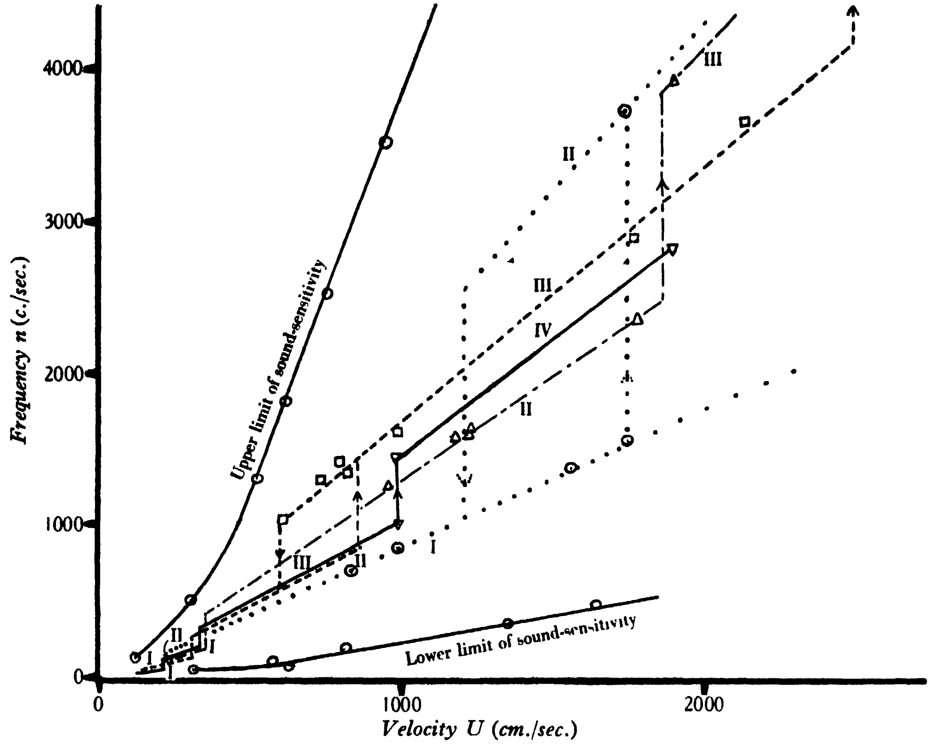

Figure 5. Range of edge-tone production: —▽— $h=1\cdot5$ cm.; ---□--- $h=1\cdot0$ cm.; —-△-- $h=0\cdot75$ cm.; ···⊙·· $h=0\cdot50$ cm.

Table 2 shows the results obtained for various values of h, U and n. The final column gives the value of $2hn/JU$, which according to König should be approximately unity. The comparisons with the results found for sensitive jets (where the vortex motion was produced by a loudspeaker in the absence of any wedge) show that there is no appreciable difference in the vortex motion in the two cases, and the steadiness of the relative vortex velocity u/U at all heights of the wedge confirms this conclusion.

Only one result for stage I is included, since the definition of λ is not clear in this case: it is assumed here that $\lambda=h$.

---

* In table 2 of reference (2) this convention would only alter some 1-mm. jet values viz. 8B, 8C, 17C and the right hand column.

It should be noted that if cases are chosen in which the velocity is approximately the same, then the wave-length for a given stage increases with the distance of the wedge; compare, for example, stage II 28 B with 27 F, and 28 C with 27 G.

Table 2.

Height h of wedge (cm.)	Reference number of film	n (c./sec.)	λ (cm.)	U (cm./sec.)	u/U	Stage J	h/λ	$\frac{2hn}{JU}$ $J=1$, 2, 3 or 4
3·5	25 A, B and C	97	0·85	215	0·38	IV	4·1	0·79
3·0	*8 C comparison*	*97*	*0·90*	*237*	*0·37*			
	26 A and B	97	0·93	248	0·36	III	3·2	0·78
	C	194	0·68	321	0·41	IV	4·4	0·91
	8 D comparison	*194*	*0·51*	*253*	*0·39*			
2·5	*8 B comparison*	*97*	*0·75*	*185*	*0·39*			
	26 D	97	0·81	210	0·37	III	3·1	0·77
	E	194	0·77	380	0·39	III	3·2	0·85
	F	291	0·56	391	0·42	IV	4·5	0·93
	G	388	0·57	508	0·43	IV	4·4	0·95
2·0	27 A and D	97	0·89	227	0·38	II	2·2	0·85
	B	291	0·57	422	0·39	III	3·5	0·91
	C	388	0·59	550	0·42	III	3·4	0·94
1·5	27 E	97	0·78	200	0·38	II	1·9	0·73
	F	194	0·64	345	0·36	II	2·3	0·84
	G	291	0·64	502	0·37	II	2·3	0·87
1·0	28 A	97	1·00+	268	0·36+	I	1·0	0·72
	B	291	0·45	342	0·38	II	2·2	0·85
	C	485	0·43	517	0·40	II	2·3	0·94
1·17	40 A	800	0·36	616	0·47	III	3·2	1·01

It is also clear that h/λ is not a whole number, as it has often been assumed to be$^{(5, 9, 26)}$. Table 3 records the results obtained when the height of the wedge was kept constant at $h = 3{\cdot}5$ cm. and the velocity was varied almost throughout its whole possible range. A striking feature is the constancy of the wave-length throughout each stage. In stage III, for instance, the velocity can be doubled without alteration of λ.

§ 7. FORMULA FOR EDGE TONES

The fact that in figures 1 and 2 all the lines when produced backwards cut the $1/h$ axis near $1/h = 0{\cdot}07$, and in figure 5 the U axis in $U = 40$, allows a simple formula for the frequency in terms of the velocity of the stream and height of the wedge to be derived. The gradient $n \div 1/h$ for each stage was found to be closely linear with U. The formula obtained for a 1-mm. slit, a wedge of angle 20°, and air at 20° C. was

$$n = 0{\cdot}466\, j\, (U - 40)\, (1/h - 0{\cdot}07),$$

where j has the values 1, 2·3, 3·8, 5·4 for stages I, II, III and IV respectively. This formula gives the frequency correctly within 6 per cent for frequencies from 20 to

5000 c./sec. and with velocities from 120 to 2000 cm./sec. Graphs plotted for jets from 4 mm. to 0·25 mm. indicated that a similar formula would hold in these cases also, but the determination of the constants, a research in itself, was not attempted. The limits of h were found to be 0·31 cm. and 6 cm. The lower limit, however, rises when the velocity exceeds the Reynolds critical velocity for the given slit-width, reaching, for instance, 0·34 cm. at 3000 cm./sec.

Table 3.

Height of wedge = 3·5 cm.

Reference number of film	n (c./sec.)	λ (cm.)	U (cm./sec.)	u/U	Stage J	h/λ
36 A, B, C, G and H	20	1·51	138	0·22	II	2·3
32 A and B	21	1·56	142	0·23	II	2·2
33 B	25	1·51	162	0·23	II	2·3
34 A	29·5	1·50	187	0·24	II	2·3
35 C_1	36	1·55	200	0·28	II	2·3
35 F	36	1·00	140	0·26	III	3·5
33 C	50	1·05	185	0·28	III	3·3
35 C	53	1·02	186	0·29	III	3·4
35 A	58·8	1·04	210	0·29	III	3·4
34 C and D	59	1·07	212	0·30	III	3·3
35 D	71·5	1·08	245	0·31	III	3·2
33 E	75	1·02	254	0·30	III	3·4
32 C	84	1·11	277	0·34	III	3·2
33 A	84	1·00	271	0·31	III	3·5
31 F	89	1·02	283	0·32	III	3·4
31 F	125	0·90	283	0·40	IV	4·0
37 A	126	0·87	272	0·40	IV	4·0
35 G	143	0·88	305	0·41	IV	4·0
34 B	147	0·81	311	0·38	IV	4·3

§ 8. SIMULTANEOUS PRODUCTION OF TWO DIFFERENT FREQUENCIES

Visual observation did not disclose any vortex motion of more than one frequency until a velocity of about 600 cm./sec. was reached, and this, it should be noted, is just above the velocity when sound first becomes audible; see § 3. When this velocity is attained, the vortex system in stage III begins to oscillate from side to side as a whole, resembling the motion of stage I. It is, in fact, stage I superimposed on a stream already disturbed by stage III, and this can clearly be seen in figures 7 and 8, which illustrate the case in which $h = 1·17$ cm., $U = 616$ cm./sec., and $n = 210$ c./sec. in stage I and 800 c./sec. in stage III. In figure 7 both motions occur together. Stage I is shown with a vortex just forming on the left side of the edge; cf. figure 3. The marked widening of the jet before it reaches the edge, however, shows that it is already turbulent, and if a glass plate G is introduced as shown in figure 8, stage I is prevented and stage III then shows up clearly in a similar phase to the illustration above it in figure 6. The vortices are not well defined because the photograph was taken with the stroboscope running at 200 c./sec. while the frequency was 800 c./sec.; consequently about half a period instead of an eighth of a period was illuminated at each instant, with the result that the outlines are blurred. The stroboscope could not be run at higher speeds, and high speed is not desirable in any case since sound which affects the jet is then produced.

The simultaneous production of two different frequencies commences with part of stage III accompanied by stage I. As the velocity increases, stage I accompanies other stages. This is indicated by the experiments recorded in table 4, for which U is constant and h is slowly increased.

Table 4.

U (cm./sec.)	Stages accompanied by stage I	Range through which stage I accompanies	n observed (c./sec.)	n calculated (c./sec.)	Remarks
583 to 725	III				
1200	II	Half way, till $h=0\cdot 74$			
	III	Half way, till $h=1\cdot 20$	600, when $h=0\cdot 81$	645, when $h=0\cdot 81$	
	IV				Stage I difficult to distinguish
1520	II	Half way			
	III	All			
	IV	All			Stage I, not clear
2000	II	All			Intensity of stage I varies throughout the range
	III	All	$n_1=1180$, $n_3=5040$, when $h=0\cdot 70$	$n_1=1240$, $n_3=4730$, when $h=0\cdot 70$	
	IV	All			
2030	II	All	$n_1=1400$, $n_2=3480$, when $h=0\cdot 59$	$n_1=1510$, $n_2=3480$, when $h=0\cdot 59$	
	III	All			
	IV	All			

These results indicate that the frequencies in stage I, when accompanied by other stages, are about 7 per cent lower than anticipated. It must be remembered, however, that the formula may in some cases have an error of 6 per cent: it may be concluded therefore that stage I remains practically unaltered when accompanied by other vortex motion.

In the case illustrated in figure 7 it could easily be proved, by listening through a rubber tube, that the sound from stage I came from a small region extending from the edge upwards, whereas the sound from stage III came from a millimetre or two below the edge where the vortices were entraining air.

§ 9. THE DISCONTINUITIES OF FREQUENCY

In view of the many assertions that have been made that the frequency-changes are octaves or some other simple intervals, it is necessary to examine the results of the present research in detail.

Table 5.

Velocity (cm./sec.)		Stage				Ratio			
		I	II	III	IV	I	II	III	IV
137	Up	17–39	18–29	—	—	2·29	1·61	—	—
	Down	56–	49–22	37–23	—	—	2·23	1·61	—
212	Up	45–105	47–75	45–66	47–	2·33	1·60	1·46	—
	Down	144–	130–57	126–76	104–70	—	2·28	1·66	1·49
309	Up	107–236	120–195	92–130	120–	2·21	1·62	1·41	—
	Down	263–	285–130	246–150	172–120	—	2·19	1·64	1·43
984	Up	700–1660	980–1650	1060–1510	—	2·37	1·68	1·42	—
	Down	1300–	1900–800	2080–1240	1860–1320	—	2·37	1·68	1·41
1750	Up	1560–3680	2300–3650	2060–2940	2000–	2·36	1·59	1·43	—
	Down	2550–	4160–1770	4640–2960	4000–2800	—	2·35	1·57	1·43

Mean value for jump I–II = 2·298 (taken as 2·3 in formula).
Mean value for jump II–III = 1·627
1·627 × 2·298 = 3·74 (taken as 3 8 in formula).
Mean value for jump III–IV = 1·435
1·627 × 2·298 × 1·435 = 5·37 (taken as 5·4 in formula).

It will be seen at once that there is no evidence for jumps in tone which are simply related to one another. And, as has been stated earlier in this paper, in the absence of resonators there is no a priori reason for supposing that there would be a simple numerical relation.

§ 10. EFFECT OF SOUND ON PRODUCTION OF EDGE TONES

As has been mentioned in § 5, the whole edge-tone phenomenon occurs within the sound-sensitive range of the jet. It is of interest therefore to compare the vortex motion due to sound with that produced by edge tones, and to examine the effect of superimposing one on the other.

It has already been seen that the wave-length of the edge tones for a given frequency and velocity is in good agreement with that found for sensitive jets, table III. If now the development is considered, it was found in the former research* that for maximum development (an angular spreading of about 60° and this corresponds approximately with edge-tone formations) the following relation holds:

$$u/Ud^{\frac{1}{2}} = 0{\cdot}29,$$

---

* Reference (2), p. 718.

where d is in mm., which, with the new convention adopted for λ, becomes

$$u/Ud^{\frac{1}{2}} = 0{\cdot}37.$$

A glance at table 3 shows that u/U when $d = 1$ mm. only reaches this value when U is about 300 cm./sec. Consequently, correspondence between edge-tone and sound-produced vortex motion is not to be expected below this velocity. This is well borne out by observations made at random, the first similarity in appearance being found for the following values:

Stage II, $h = 1{\cdot}55$ cm., $n = 164$ c./sec., $U = 300$ cm./sec.
Stage III, $h = 1{\cdot}89$ cm., $n = 204$ c./sec., $U = 329$ cm./sec.
Stage III, $h = 2{\cdot}03$ cm., $n = 189$ c./sec., $U = 300$ cm./sec.

It is to be noted that in the above cases the intensity of the sound from the loudspeaker was such that it was easily audible, whereas when $U = 300$ cm./sec. no edge tone can be heard. This important fact indicates that the vortex motion in edge tones, although only occurring with sound-sensitive jets, is nevertheless not entirely maintained by the sound emitted, a view which the writer favoured when he first took up this research.

The effect of sound upon the edge tones for velocities above 300 cm./sec. was examined in the following manner. The stream was given a fixed velocity, and the frequency of the loudspeaker at full strength was adjusted until the stream was most disturbed. The stroboscope was run at this frequency and then the wedge was slowly lowered into the stream until the frequency changed, i.e. the wedge controlled the frequency of the vortex motion. The results can be summarized as follows:

(*a*) *Stage I*: The loudspeaker never retained control during stage I whatever the values of h and U.

(*b*) *Stage II*: For velocities from 150 cm./sec. to 330 cm./sec. the loudspeaker prevents the formation of any stage except I. From $U = 330$ onwards it ceases to control the whole of stage II. For instance the wedge controls stage II from $h = 1{\cdot}00$ cm. downwards for $U = 339$ cm./sec., from $h = 1{\cdot}31$ cm. downwards for $U = 358$ cm./sec., and from $h = 1{\cdot}56$ cm. downwards for $U = 482$ cm./sec.

(*c*) *Stage III*: The loudspeaker controls stage III up to $U = 725$ cm./sec. Visual observation becomes difficult above this value, but at higher velocities beats are heard showing that the wedge does regain control when $U > 1000$ cm./sec.

(*d*) *Stage IV*: The wedge never controls stage IV.

(*e*) It is possible to observe vortex motion superimposed on the edge-tone vortices, provided that the frequency is from four to five times that of the edge tone. Figure 9 of the plate illustrates this phenomenon for the case where $h = 3{\cdot}5$ cm. and $U = 127$ cm./sec., giving an edge tone for which $n = 20{\cdot}5$ c./sec. (stage II). Superimposed are sound-produced vortices for which $n = 102$ c./sec. It is interesting and important to note that the sound vortices grow in a perfectly normal manner* until they reach the region near the edge, and how, even afterwards, they still retain some of their features whilst forming part of the larger edge-tone vortices. This fact will be used later as evidence against the hypothesis that edge tones are due to disturbances starting from the orifice.

---

* Cf. reference (2), plate 2, figure 5*F*.

(*f*) An interesting case occurs when $h = 4{\cdot}5$ cm. and $U = 182$ cm./sec. (stage III). The range of frequency of the loudspeaker controlling the vortex motion is from 46 to 230 c./sec. When $n = 136$ c./sec., however, the loudspeaker loses control and the vortices are superimposed on the edge-tone motion which is now able to maintain itself. When $n = 134$ c./sec. and $n = 138$ c./sec., and throughout the rest of the range, the loudspeaker controls the motion. Now this frequency was found to produce a marked minimum disturbance of the jet in the former research on sensitive jets.* It appears therefore that it may be the widening-out effect of the sound on the jet that makes its edge-tone formation impossible.

§ 11. EDGE TONES AND BEATS

As has been mentioned in § 10, when the velocity is high the effect of sound on stages II and III is to produce beats; the loudness increases with the amplitude of the impinging sound waves. The following are typical examples: (1) $U = 1200$ cm./sec. $h = 0{\cdot}75$ cm., stages I and III together giving $n_1 = 680$ c./sec. and $n_3 = 2580$. Lowering the loudspeaker frequency from 2580 c./sec. to 2500 c./sec. caused a beat note to rise from zero. Raising the frequency above 2580 did not produce any effect. (2) $U = 1660$ cm./sec. $h = 0{\cdot}57$ cm., stages I and II together giving $n_1 = 1270$ c./sec. and $n_2 = 2910$ c./sec. Raising the loudspeaker frequency from 2910 c./sec. to 5560 c./sec. caused a beat note to rise from zero.

§ 12. EFFECTS PRODUCED BY BEARDS

Obstructions placed in the immediate neighbourhood of the air stream between the orifice and edge are called by organ builders "beards"; they consist usually of pieces of wood, circular or oval in cross-section, held near the mouth of the pipe by being pinned through the "ears".† With a beard consisting of a glass photographic plate of length equal to that of the slit (2·36 cm.) at a height of about 2 mm. above the orifice, the following observations were made: $U = 262$ cm./sec.; $h = 2$ cm.; stage III. With the beard almost touching the stream it was deviated towards the beard and no oscillation was observable, but as it was pulled away first stage I appeared ($n = 45$ c./sec.), then stage II ($n = 105$ c./sec.), and finally stage III. If this was done very carefully the final stage was II, which is just possible (cf. figure 1). As the beard was pulled away the frequency increased slightly. Thus stage I can be brought back, after it has jumped to stage II or III, by interposing the beard, and the action of the latter appears to be simply that it deviates the stream towards itself in such a manner that the stream does not strike the edge centrally. A similar result can be obtained without the beard by moving the edge a little to one side: this has the effect of prolonging the lower stage as has been observed by

---

* Cf. reference (2), table 1, p. 708.

† Cf. reference (13), p. 163.

Wachsmuth(7). The beard is most effective in deviating the stream when it is placed near the orifice and this is in accordance with organ building practice where it is used to bring back the prime from the octave(14).

When stage I occurred with stage III in the case already referred to (§ 8), it was found that the beard had the effect of stopping stage I rather than augmenting it, and this was the way in which stage III was isolated for the photograph, figure 8. It appears that when stage I occurs with a stream that it already disturbed by another vortex motion, it is much more sensitive to slight displacements.

§ 13. ACKNOWLEDGMENTS

The author's best thanks are due to Prof. E. N. da C. Andrade, F.R.S., for the facilities for this research and for his continued interest in it. Thanks are also due to Mr C. Jolliffe of Stowe School for many references especially on the subject of organ pipes.

REFERENCES

For references see page 520 of this volume.

THE MECHANISM OF EDGE-TONE PRODUCTION

By G. BURNISTON BROWN, M.Sc., Ph.D., Lecturer in Physics,
University of London, University College

Received 10 *April* 1937. *Read* 25 *June* 1937

ABSTRACT. Former theories of the production of edge tones are reviewed and a new theory is put forward which accounts in a qualitative manner for the phenomena described in the preceding paper. The effect of the wake of a disturbance on the portion of the jet immediately following it is considered, and it is concluded that the compressibility and structure of the surrounding medium must be taken into account, and that, for low velocities, wake disturbance is the controlling factor, whilst for higher velocities the effect of the sound emitted must be taken into account. An attempt is made also to account for the differential sensitivity to frequency found in sensitive jets in a former research.

§ 1. FORMER THEORIES

Although edge tones had been discovered for some fifteen years, Helmholtz(15) did not discuss them except in connexion with an organ pipe. In this connexion he refers to his earlier paper on "The discontinuous motions of fluids"(16) and states that the bounding surfaces of the stream must be looked upon as vortical surfaces, i.e. surfaces "faced with a continuous stratum of vortical filaments or threadlike eddies. Such surfaces have a very unstable equilibrium." An example of this instability is the phenomenon of sensitive flames, and he makes a reference to Tyndall's experiments on gas jets. He continues: "This revolution into vortices takes place in the blade of air at the mouth of the pipe, where it strikes against the lip. From this place on it is resolved into vortices, and thus mixes with the surrounding oscillating air of the pipe, and accordingly as it streams inwards or outwards, it reinforces its inward or outward velocity, and hence acts as an accelerating force with a periodically alternating direction, which turns from one side to the other with great rapidity. Such a blade of air follows the transversal oscillations of the surrounding mass of air without sensible resistance."*

The view that the vortices form only at the edge is not borne out by experiment(4). Helmholtz also refers to Schneebeli's(17) mechanical explanation, which was that the air stream took the place of a solid reed. This view was also held by Cavaille Coll(18), Sonreck(19) and Hermann Smith(20). It is clear, however, that the tone-production is only explained if a pipe or other resonator is present, the oscillations in which cause the transverse motion of the air stream.

Lord Rayleigh in his *Theory of Sound*, 2nd edition (1896), does not attempt any explanation, but in connexion with the bird-call suggests that "when a symmetrical excrescence reaches the second plate, it is unable to pass the hole with freedom, and the disturbance is thrown back, probably with the velocity of sound, to the first plate, where it gives rise to a further disturbance, to grow in its turn during the progress of the jet" (p. 412).

---

* Reference (15), p. 395.

The first attempt to account for the production of tones in the absence of any resonator was made by Wachsmuth(7). According to him, with a blunt edge no sound occurs until the distance of the edge from the orifice is such that the stream can spread on to both sides: the sharper the edge, the smaller this distance, but he does not explain why a minimum distance exists however sharp the wedge. When the stream spreads over the edge it must pass up one side first, and thus an asymmetry occurs which produces a periodicity in the velocity, through the alternate freeing and checking of the stream, and this must cause a pulsation in the air supply. That the stream starts to bend before the edge is reached is due to its behaving like a flexible bar, which buckles in the middle when it first strikes the edge. The bent portion travels up without returning to the vertical, since it is not a rigid body and the backwash (*Rückstau*) from it maintains the stream in a disturbed condition at a point below the edge. Wachsmuth adds that his researches did not decide whether the actual tone-production was due to the to-and-fro motion of the lower straight portion of the stream or to vibration of the wedge itself: he preferred the latter theory since, when h is large, the tone is heard near the wedge and not near the orifice.

With regard to the latter question, it can easily be shown that vibration of the wedge is not the cause of the tone, by holding the edge with the fingers, which, as Benton* has remarked, provide very efficient damping. No difference in tone-production occurs.

Wachsmuth did not justify his assumption that an air stream can be treated as a flexible rod and that it would break in the middle on striking an obstacle. He gave no physical explanation of the jumps in tone, and there is no evidence for the pulsation in the air supply.

The problem was next examined by König(9), who developed a hypothesis similar to that made by Lord Rayleigh in connexion with bird-calls. He pointed out that the jet could not be treated as a body with periods of its own, so that a simple resonance principle cannot be invoked, and he added that neither considerations of friction along the wedge nor of pendulation of the stream threw much light on the mechanism of tone-production. He assumed that when the edge was struck a sudden stoppage in the stream occurred and a compression wave travelled out in all directions with the velocity of sound. This would produce a disturbance at the orifice which would travel upwards with the velocity of the stream and create a new stoppage. If the velocity of sound in air is c, the period would be $h\,(c+U)/cU$, and with c very much greater than U the frequency n would be given by

$$n=\frac{U}{h}.$$

But this gives double the observed frequency. König therefore was forced to suppose that somehow the first compression produces a rarefaction at the orifice and he then obtained

$$n=\frac{1}{2}\frac{U}{h}.$$

---

* Reference (6), p. 126.

He had to admit, however, that Göller's results(11), which he was using, showed that the factor was not $\frac{1}{2}$ but between 0·4 and 0·5, and that for other intervals it became 1·0 and 1·5, and that his theory gave no account of this, neither did it explain why the tones do not commence with the highest audible note. He concludes by suggesting that since the velocity of sound is $(c-U)$ in the stream and c outside, this may cause pressure differences which might affect the tone.

Schmidtke(3) begins by asserting that the results of Wachsmuth and Göller show that n is proportional to U and inversely proportional to h and that the jumps in tone are octaves. This being so, König's formula can be written

$$\frac{2hn}{JU} \simeq 1,$$

where $J=1$ for the first interval, 2 for the second and so on. (The last column in table 2 on p. 501 of this volume shows the value of $2hn/JU$.) Schmidtke points out that König's derivation of the formula is unsatisfactory, and then attempts to make use of Kármán's vortex street. Such a street, he suggests, is set up along the sides of the wedge in stage I and between the orifice and wedge in later stages. Since he held that the frequency of the tones was equal to the number of vortices set free per second, it followed that in a Kármán street the same frequency could be produced again by moving the wedge a distance of $\lambda/2$; i.e. for the same frequency and velocity the difference between the wedge-distances must be constant. Schmidtke could not prove this with the results he had obtained for water jets since he did not succeed in getting more than one jump. He quotes, therefore, some values from a research by Rieth(12) with air jets, which support this conclusion. A table similar to that drawn up by Schmidtke but covering a much greater range of velocities has been given in table 1 of the preceding paper, and it can be seen that $(h_{m+1}-h_m)$ is approximately a constant, but it should be noted that the constant is not $\lambda/2$ but more nearly λ. A glance at figure 3 of that paper shows that although with respect to the vortex motion the wedge has moved only $\lambda/2$ each time, with respect to the orifice it has moved a distance λ, the vortex motion having moved away from the orifice by a distance $\lambda/2$. Further, on Schmidtke's theory, the product of n by the mean of $(h_{m+1}-h_m)$ ought to be constant and he had to admit that it was not. Schmidtke, however, concluded that a case had been made out for a Kármán street between the orifice and edge, but he did not attempt an explanation of its origin and did not provide any direct evidence of its existence.

Krüger(26) was the first to realize that a disturbance travelling up the jet would have a velocity u different from the stream-velocity U. He made the further suggestion that the jet has a natural wave-length λ_0 corresponding to its own tone ("jet tone") in the absence of the wedge. The oscillation of the stream would therefore be greatest when the edge-tone wave-length and jet-tone wave-length were the same. As h increases, the difference between it and λ_0 becomes greater, and the amplitude of the forced oscillations consequently smaller. When h approaches the value $2\lambda_0$, the wave-length jumps back to λ_0, corresponding to an octave jump in tone, and resonance again occurs. Krüger did not substantiate this hypothesis by comparison with experimental results. If this is done, the present research shows that the heights at which jumps in tone take place are not simple multiples of a fixed length, and further, the suggestion that the oscillations of the stream will become smaller as h approaches $2\lambda_0$ is the reverse of what actually occurs: the oscillations increase in amplitude as h increases in stage I until the jump occurs to stage II, and then the amplitude of stage II increases until the jump to stage III and so on. The use of a resonance principle by Krüger does not, therefore, seem to be justified, and there is no explanation of λ_0.

Benton(6) is another investigator who has claimed to show that a Kármán vortex system exists. He assumed that if the wedge were moved across the stream the point at which the tone disappeared would be a point on the path of the vortex centre. He measured the width b of this tonal boundary at different heights of the wedge and further assumed that h was equal to λ. He found that b/λ fell from 0·5 to 0·28 as the slit-width increased from 0·1 mm. to 1·88 mm. Instead of proceeding with wider slits, he assumed that this was a limiting value independent of the slit-width, and so concluded that for "very wide slits" b/λ approaches the Kármán value of 0·28. It happens that for $d=2$ mm. this ratio has a value close to Kármán's but for other widths it differs widely.* So that, even if Benton's assumptions are admitted as correct, he does not succeed in presenting any evidence for the Kármán vortex street, and, further, he gives no theory of its origin or of the jumps, since he has denied the occurrence of the latter (cf. § 3).

Richardson(8) while favouring the Kármán street theory, although providing no direct evidence for it, describes an experiment which indicates that the theory of a compression wave travelling backwards from the edge to the orifice with the velocity of sound is not correct. A second jet near the first one, but without a wedge, should have been affected by the sound wave, but no disturbance of any kind was observed. This experiment was made with water.

§ 2. THE KÁRMÁN VORTEX STREET

In view of the assumption by many writers that the conception of the Kármán street is applicable to fluid jets, an assumption which has led to the superficial claim that the phenomenon of edge tones and jet tones is thereby explained, and to the neglect of further research, it is important to consider this theory in greater detail.

Von Kármán considered the case of two parallel rows, of indefinite extent, of isolated, equal, point vortices in a fluid which was incompressible and without viscosity. He was then able to show that there was instability for infinitesimal disturbances unless $a/\lambda=0{\cdot}28$, where a is the distance between the rows. He concluded that this configuration was definitely stable, but, as Lamb(21) remarks, he did not prove this, and lately Schmieden(22) has shown that for certain finite disturbances it is certainly unstable.

It is clear that any application of this result to physics would have to be made with caution, and the experimental verification has never been satisfactory, even in the case of vortices at some distance in the wake of an obstacle⁽²³⁾. When gaseous jets are considered, the vortex rows cannot be of indefinite extent nor can the vortices be equal, and further, the fluid is not incompressible or free from viscosity. A priori, therefore, there is no reason for expecting to observe a constant ratio of a/λ and certainly no reason to suppose that this will be 0·28.

---

* Reference (2), table 3.

The lack of evidence for the assumption of the Kármán street in the theory of edge tones has already been commented upon in § 1. In the case of jet tones which are produced in the absence of the wedge, Krüger and Schmidtke⁽²⁴⁾ claimed to have found the exact Kármán ratio using water. Four observations only are given, viz. 0·30, 0·27, 0·28 and 0·29 from which a triumphant mean of 0·285 is obtained. It may be concluded, therefore, that there is no reason for supposing that the constant Kármán ratio would occur in jets and that, in fact, it has never been observed.* Indeed it is remarkable that a mathematical theorem which neglects the compressibility of the medium should ever have been expected to account for the alternate compressions and rarefactions of which edge tones consist.

§ 3. THE PHYSICAL THEORY OF EDGE-TONE PRODUCTION

As was mentioned earlier, the present writer, after giving a theory of the action of sound on fluid jets, favoured the hypothesis that edge tones are maintained by the sounds travelling back to the orifice and producing a vortex formation similar to that in sensitive jets, and that, in some way, the edge stabilizes the motion. The sound has been shown to arise in the region where the vortex first begins to throw out a filament; this filament as it advances from $\theta = 0$ to $\theta = 3\pi$ (cf. § 4 of the preceding paper) entrains air, and it is the sudden pressure changes in this region† that result in the propagation of sound waves. Although this hypothesis is partly correct it fails to account for the following facts: (*a*) In some of the cases where it was found that vortex motion which was apparently identical with that due to the wedge could be produced by the loudspeaker alone, it was observed that the intensity of the sound from the loudspeaker had to be easily audible, whereas no audible edge tone occurred. (Cf. § 10 of the preceding paper.) The wedge therefore must do something more than just stabilize sound-produced vortex motion. (*b*) In a case such as that illustrated in figure 9 of the plate facing p. 498 it is impossible that an edge-tone vortex-formation with the wave-length shown could originate in disturbance at the orifice and not be affected by the superposition of vortices developed to the extent of those in figure 9. The only observable effect is the widening of the stream: the frequency is not altered. (The superimposed frequency was made to be a simple multiple of the edge tone in figure 9 merely to obtain a stationary stroboscopic view.) (*c*) Similarly it is difficult to see how a jet can give out two nearly pure tones simultaneously, if each is produced by vortices developed from a periodic disturbance propagated from the orifice.

In consequence of these facts it is necessary to examine the effect of interposing an obstacle in a jet of fluid. The easiest case to consider first is that in which the angle of the wedge is increased until it is 180°, i.e. the jet impinges normally on a flat plate (see figure 1 *a*). In this case it is evident that if the jet is deviated towards the right side, the surrounding fluid in the neighbourhood of A is displaced. If this displacement takes place sufficiently rapidly a local increase of pressure occurs at A, and this in dissipating itself reacts on the jet, deviating it towards the left; this deviation, in its turn, produces an excess pressure driving the jet back towards the right, and so an oscillatory motion is set up. Such motion is easily observed with a stroboscope: no developed vortex formation is seen, but undulations such as are shown in the illustration[*] are observed.

---

* Cf. reference (2), table 3.

† Reference (2), p. 730.

The nature of this type of disturbance of the surrounding air is a problem which has not yet been considered quantitatively. It is well known that if an obstacle is vibrated with very low frequency, there is a mass motion of the air from the front to the back and vice versa, and that pressure changes are negligible and can only be observed in the vicinity of the obstacle. At higher frequencies the reverse is the case: the mass motion becomes negligible and a pressure wave spreads to great distances with the velocity of sound. It is between these limits that the types of disturbance that are responsible for the oscillations producing edge tones occur.

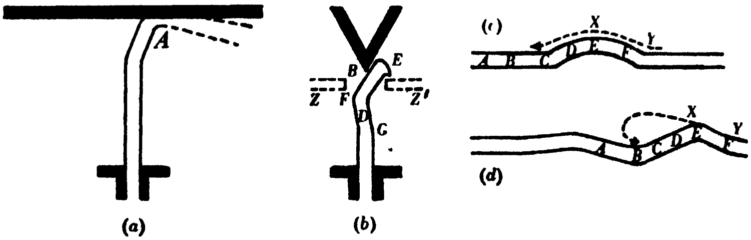

Figure 1.

Turning now to the wedge, it was found that with the velocity far below that at which oscillation commences, e.g. 82 cm./sec., it was possible to produce a vortex motion corresponding to that found in edge tones by moving the wedge slowly from side to side with an amplitude of about 1 mm. and a frequency of 1 or 2 per second. In this case the effect of such a slow motion is to cause the air to pass round the edge, from the side which the wedge is approaching to the opposite side. While this is done the stream is displaced: in figure 1 *b* for instance, if the wedge is moved to the left the air at B flows round the edge and moves the jet to the right; if this movement is large enough the portion of jet lower down at D may move to the left. The first appearance of the vortex filament may now occur at the exposed portion F, instead of at E.

If now the wedge is considered to be stationary, as it is in practice, the air at B can be displaced by the stream instead of the wedge. In the non-disturbed condition

[*] The fact that oscillation can be set up when a jet impinges on a flat plate or on a plate with a hole in it, as in the bird-call, or on other forms of obstacle, makes the effect of introducing an obstruction sideways towards the stream, as was done by Klug(28), very difficult to interpret since it may itself produce oscillation.

the stream bifurcates at the edge and passes half up one side of the wedge and half up the other. Now it has been shown that the whole of the edge-tone phenomena occur within the sound-sensitive range of the jet (see figure 5 of the preceding paper), so that a slight vibration of the apparatus, or a sound of the order of the minimum audibility of the human ear, is sufficient to produce a vortex which will pass up one side or the other.* The passage of the vortex along the side of the wedge displaces air, and it is suggested that in flowing back again in the wake of the vortex this air has sufficient momentum to deviate the stream towards the opposite side of the wedge. The momentum of the jet itself would merely cause it to return to the symmetrical position.

What occurs in the wake of an undulation in the surface of separation of two fluid media is a problem that has not so far been solved mathematically. Rayleigh's original calculations for a non-viscous fluid led to the result that a small sine-wave disturbance in the boundary of a jet should continue to grow in amplitude with time.† This, however, does not occur unless the velocity exceeds a certain value: below this value the crests flow over into the troughs and the boundary becomes straight once more.‡ Rosenhead⁽²⁵⁾ has attempted an extension of Rayleigh's treatment which indicates that the boundary between two non-viscous incompressible fluids would curl up in vortex-like shapes, but suggests that the distance λ between them cannot be derived without considering viscosity and diffusion. Rosenhead begins with a sine-wave disturbance already present in the boundary: his attempt to determine the result of a single undulation was not altogether satisfactory as it seemed to indicate a rupture of the surface; it seems possible that if he had represented the undulation by the displacement of several elementary vortices, a more definite result might have been obtained. This is a question of importance in the discussion of the mechanism of edge-tone production, since it seems clear that the wake of a vortex encountering the edge must exert a pressure on the following stream causing it to be deviated to the opposite side, see *FE*, figure 1 *b*; and further that the motion of this portion may itself cause a reaction in the surrounding fluid which results in the portion *GF* being also displaced. In the absence of mathematical treatment a few qualitative general considerations can be made.

In figure 1 *c*, *ABCDEF* represents a section through a laminar stream travelling towards the right with a small mean velocity *U*. *DEF* is an undulation travelling with velocity *u*. In discussing the reactions of the external air, it is legitimate to consider the undulation as stationary and the air as moving towards the left with velocity *u*. (Actually the relative velocity is less than *u* since the air is dragged along by the stream.) The particles at *Y* on being deflected at *F* exert a pressure on the surface tending to flatten it, and move upwards towards *X*. The excess of particles at *X*, tending to expand, exerts a pressure downwards on *E* and *D* and the flow is parallel to the surface as indicated by the arrow. The reaction on *F*, *E* and *D* is such as to produce a flattening and change of shape⁽²⁵⁾. Particles of the stream on the boundary get carried in the direction *FEDCB* since, owing to viscosity, there is no discontinuity of velocity, and thus the amplitude of the undulation gradually diminishes and the boundary becomes straight again. This is what is in fact observed; the undulations die out in a few wave-lengths.

---

* Since the alternate position is adopted two vortices cannot pass the edge at the same instant. Cf. reference (2), p. 725.

† For references and criticism see reference (10), pp. 189–91.

‡ Reference (2), p. 710. Cf. figure 4A of plate I.

As the velocity is increased, however, a different type of flow must occur. This is represented in figure 1 *d*. The particles at *Y* after deflection at *F* now have sufficient momentum to continue in their path when they reach *E* in spite of the excess pressure at *X* acting towards *E*. They therefore cannot enter the region *BCD* by the former path, but take a course indicated by the arrow, and this is followed by particles torn from the jet-surface; in other words a small filament extends outwards away from the stream and later bends inwards towards it, and thus the amplitude increases. The excess pressure at *X* can only be relieved in a finite time owing to the compressibility of the medium. No attempt appears to have been made to estimate this time quantitatively, but in the limit where the mass-motion is neglected it corresponds with Maxwell's "time of relaxation"⁽²⁹⁾. As the relative velocity increases, the reaction of the sudden formation of pressure at *X* will not affect the stream at the undulation *EDC* but later at *B*. The effect of this is to produce a deviation of the stream *ABC*. It is to be expected, therefore, that if a single-crest undulation is produced in a column of fluid it will be followed by a trough and possibly by further diminishing undulations, if the amplitude of the initial undulation is sufficiently great, since *ABC* may in its turn cause another crest. The amplitude will diminish since the particles condensed at *X* spread outwards in all directions and only a portion reacts on the stream: in this research the diminution of the amplitude was such that a crest was never followed by more than two others on the same side. Measurement of the wave-length is not easy, but the indications in the photographs are that it remains very nearly constant. This wave-length of the undulations following a disturbance travelling up a jet, in the absence of a wedge or other obstruction, may be called the ***natural wave-length*** λ_0 for the given velocity.

It seems physically possible therefore for a vortex-formation to occur in the jet before the edge is reached, although the actual cause of it is disturbance of the surrounding air at the edge. It is not necessary for the vortices to originate at the orifice, and this explains a feature of the cases illustrated in figure 3 of the plate facing p. 498: the velocity and frequency are constant and the vortex-formation is similar in each case except that it develops at a point farther from the orifice in each stage. If the vortices were initiated at the orifice, it would be difficult to account for this, but if the above hypothesis is correct it is clear that distance from the edge, and not distance from the orifice, is the deciding factor. It has already been pointed out in § 1 that this fact invalidates Schmidtke's hypothesis that $(h_{m+1} - h_m)$ would be equal to $\lambda/2$. This vortex formation occurring in the wake of a disturbance will be referred to as the ***wake formation***.

Now although the wake formation is accompanied by pressure-changes in the surrounding medium, these may not at low velocities be sufficiently rapid to produce sound, but it must not be forgotten that when sound is produced there will be vortices formed which develop from the orifice in the manner described in a former paper[(a)], and the resultant formation will be a combination of the two. The velocity at which tones first become audible (and jets are of the same order of sensitivity as the human ear) was found to be about 500 cm./sec., and this was also found to be just below the velocity at which two notes of different frequency could be produced simultaneously. This can be accounted for on the above theory since two more or less distinct methods of vortex-production are now available, wake-production and sound-production. Figure 8 in the plate shows stage III with *n* equal to 800, and figure 7 shows the whole vortex formation moving from side to side in such a way as to produce the effect of stage I with *n* equal to 210. If stage III were entirely wake-produced it is difficult to believe that it would not be greatly modified by the wake of stage I. On the other hand, if stage III is maintained by sound waves affecting the sensitive region near the orifice these waves will be relatively independent of draughts in the wake of stage I. The edge, however, must still retain some wake effect on stage III sufficient to stabilize the tone. Stage I itself, at higher velocities, produces sound, but the wake formation is always the controlling factor (cf. § 10 of the preceding paper), and stage I is the only stage of which this is true, the other stages being due to a combination of a wake formation and a sound formation. It is therefore to be expected that stage I will be the only stage (above $U = 500$ cm./sec.) that can occur simultaneously with one of the others. The sound is produced mainly by the to-and-fro motion of the jet at the edge, which is not modified appreciably by superimposed vortex motion as long as this is not greatly developed; cf. figure 8 of the previous paper.

§ 4. EXPLANATION OF FREQUENCY VARIATION AND DISCONTINUITIES

The physical processes underlying the variation of frequency with height of the wedge when the velocity is constant can be indicated with the help of the considerations given above.

Starting with $h = 0$ there is no possibility of oscillation of the column, and any disturbances would not grow into a vortex producing an effective wake until they reached a point some distance up on the side of the wedge. Thus a minimum value h_0, below which no sound can be produced, must exist for each width of stream. This is well known from experiment and Benton found that $h_0 \propto d^{\frac{1}{2}}$: this is in agreement with another observation that was made, namely that when the velocity exceeded the Reynolds turbulence velocity, and the stream was therefore widened by vortex growth commencing at the orifice, the value of h_0 rose from 0·31 cm. to 0·34 cm. It was possible with h equal to 0·31 cm. and U equal to 3000 cm./sec. to hear no tone and then, on stopping the air pump, to hear the tone suddenly begin as the velocity dropped below the Reynolds value.

As h is increased, the position at which a vortex is formed on the side of the wedge approaches the edge.* This increases the effect of its wake disturbance at the edge, and this coupled with the decrease of velocity of the jet with distance from the orifice causes the amplitude of the oscillation to increase, accompanied by an increase in λ and therefore a decrease in frequency.

---

* Compare figure 4 with figure 3 in the plate facing p. 498. In figure 3 a jump to stage II is imminent.

This increase in amplitude continues until the column is deflected through a very acute angle, as can be seen by examination of the plate. (All the stages in figure 3 are advanced developments, i.e. close to a jump to a higher stage. In figure 6, stage II is very close to a jump to stage III. Figure 8 is an example of vortex-formation at small amplitude, i.e. near a jump *down* to stage II if the velocity is decreased.) This deflection of the stream varies between a minimum of about 25° and a maximum of about 60°. As this deflection increases, it produces a wake disturbance itself, sufficient to deflect the stream to the opposite side, for instance, in figure 10*b* FE to the right is followed by GF to the left. As h is increased, the deflection of GF becomes such that the first vortex filament is thrown out at F instead of at E. The whole vortex formation then changes, since the vortices now reach a development represented by $\theta = \pi/2$ before encountering the edge. The effect of this appears to be to diminish the wave-length, and the frequency consequently jumps up. Further increase in h causes the amplitude and wave-length to increase as before (cf. table 2 on page 498, films 28 B and 27 F, where λ rises from 0·45 to 0·64 cm. on h being increased from 1 to 1·5 cm. while $U = 344$ cm. in stage II). Another point is then reached where the amplitude is such that a filament spreads out at a point still further from the edge and develops to $\theta = 3\pi/2$ before striking the edge. The vortex formation again changes and the frequency jumps once more corresponding to the change from stage II to stage III. The jump from stage III to stage IV is similar but no jump from stage IV is possible since after the vortex development represented approximately by $\theta = 3\pi$, the jet has a straight closed boundary and therefore cannot produce a wake disturbance of the kind considered in § 15.

It is reasonable to suppose that the edge-tone wave-lengths bear some relationship to the natural wave-length λ_0 for a given velocity. If it is supposed that these vary about λ_0 as a mean, this supposition is equivalent to expecting that the jet-tone curve would pass through the centre of the conical area occupied by the edge tones in figure 5, page 498. No values for the jet tones emitted by a 1-mm. jet are available and they are extremely difficult to determine: the maximum jet-width used by Kohlrausch(30) was 0·75 mm. and extrapolation from his graphs indicates that the jet tone is much lower than any edge tone. The author verified many of Kohlrausch's observations but found that two notes are produced, the higher one being the octave of the one measured by Kohlrausch, and for a 0·75-mm. jet-width these tones lie approximately in the centre of the conical area in figure 5 and about half way between the two extreme limits of sound sensitivity. If it is assumed that there is little difference between the jet tones for 0·75-mm. and 1-mm. jets, and that the octave note is the one corresponding to the wave-length λ_0, there is some support for the relationship expected. The author hopes to deal with the problem of jet tones in a further research.

The variation of frequency with the velocity of the stream when the height of the wedge is constant can be considered in a similar manner. Starting with the wedge at some fixed height, the first possibility of oscillation will occur when the velocity is such that any disturbance develops sufficiently to produce a vortex whose wake deviates the oncoming stream. Which of the four stages then sets in depends on the height: i.e. on the distance from the orifice. Once a stage is formed, increasing the velocity causes greater vortex growth and therefore greater wake-disturbance, but it seems that the resultant of this effect and the increased momentum of the jet is such as to keep λ constant although the amplitude increases. This rather remarkable fact, which is demonstrated by table 3 on p. 502, results in the frequency rising linearly with the velocity since $n=u/\lambda$ and varies as U/λ for large values of U. For values of U for which u/U is not constant the relation between n and U is no longer so closely linear.

It is possible, therefore, in a general qualitative way to account for the phenomena exhibited when a wedge is inserted into a jet of fluid. To attain quantitative results a detailed treatment involving the structure of the fluid is required, and so far this has not received attention in hydrodynamics; the difficulty has been avoided by taking either pv or pv^γ as constant; in other words the pressure changes considered are either very slow or very rapid in comparison with the molecular interchange of momentum.

§ 5. FACTS SUPPORTING THE PRESENT THEORY

It is clear that for velocities well below 500 cm./sec., for which the vortex formation is due entirely to wake disturbance, an obstruction such as zz' in figure 1*b*, would interfere with the propagation of any disturbance in the surrounding air in the direction of the orifice. If, however, edge tones are maintained by a compression wave travelling back from the *edge* and causing a disturbance at the orifice, as was supposed by Wachsmuth, Rayleigh, König and others, the presence of zz' should not prevent the initiation of oscillation.

A brass plate containing a slit 2 mm. wide was placed in the position of zz', and the height of the wedge was made to be 3·5 cm. The first sign of oscillation as the velocity was increased from zero did not occur until $U=200$ cm./sec. and then stage III began with a frequency slightly above the normal. Without the plate, oscillation starts when $U=117$ cm./sec., stage II. Stage II, therefore, was prevented, and this was found to be the case even when the width of the slit in the plate was increased to 8 mm.

When $h=0{\cdot}5$ cm. the minimum velocity without the plate is 251 cm./sec.; with the plate this must be increased to 594 cm./sec. This corresponds to the elimination of stage I. The vortices are much smaller in this case (cf. figure 8 of the plate facing p. 498) and sound is also produced, so that in this case stage II is not prevented.

Stages III and IV are almost independent of conditions near the edge. For example it was found that if z and z' approach until they actually touch the wedge and are then moved down towards the edge, stages III and IV are not affected until z and z' approach within about half a millimetre of the edge. The oscillation then adopts the form illustrated in figure 1*a*.

These facts are such as would be expected on the present theory, and the latter receives further support from the following considerations. If the wedge is replaced by a wire in the position of its edge the wire may not deviate the stream sufficiently to produce a large wake-disturbance, and it is possible that stage I, at least, might not be possible. This was confirmed by experiment. A wire of diameter 0·12 cm. was rigidly fixed at heights varying from 3·5 cm. down to 1·8 cm. Neither stage I nor stage II was possible. With the diameter reduced to 0·07 cm., only stage IV could be obtained, and the minimum velocity was approximately 320 cm./sec., which is the velocity at which a free jet becomes turbulent without any obstacle, so as to adopt the well-known wedge-shaped appearance. (Flickering appears at 150 cm./sec.) On the compression-wave theory these facts would again be difficult to account for, since the wire is a blunter object than the sharp edge of the wedge.

Another effect to be expected according to the present theory would be a change in frequency with angle of the wedge. If the wedge in figure 1 *b* is opened out until its angle is 180° as in figure 1 *a* the wake disturbance occurs under different conditions. The dissipation of excess pressure at A in figure 1 *a* in a more confined region would lead to the expectation that λ would increase, and that in consequence a decrease in frequency would occur. This is in agreement with experiment.

With U equal to 239 cm./sec. and h equal to 1·07 cm. in stage I it was found that the frequency fell from 66 c./sec. to 61 c./sec. when the wedge angle changed from 20° to 90°. Richardson also found a decrease when the wedge angle increased from 5° to 30°.*

The important role played by movement of the surrounding air accounts for the ease with which the frequency of edge tones is controlled by any form of resonator near the edge, a fact noticed by Wachsmuth(7) and familiar in musical instruments.

§ 6. APPLICATION OF THE THEORY TO SENSITIVE JETS

The effect produced by the wake of a vortex on the stream which has had to be considered in this research obviously has an important bearing on the problem of explaining why jets exhibit a sensitivity to sound which varies with the frequency. It has been necessary to suppose that a vortex passing up a jet will be followed by an undulation of a definite wave-length owing to the reaction of the surrounding air. If then the impressed sound is of such a frequency as to produce alternate vortices having this wave-length, the undulation and consequent vortex-growth will be greatly enhanced. On the other hand if the frequency is such that the wave-length is just half the natural or wake wave-length, it seems likely that for this frequency the jet would appear almost undisturbed. Examination of the results obtained for illuminated coal gas supports this view,† but there are many subsidiary maxima and minima and the subject requires further investigation. The hypothesis that the reaction of the surrounding air has a controlling influence on the wake wave-length is rendered more acceptable when it is recalled that the frequencies of maximum and minimum disturbance are independent of the shape and size of the jet.

* Reference (8), figure 6.

† Reference (10), figure 9.

§ 7. CONCLUSION

The detailed examination of edge tones described has shown that former theories cannot adequately account for all the phenomena observed, and that the evidence supporting the hypothesis of a Kármán vortex street, and of jumps in tone bearing a simple numerical relationship, is not reliable.

The effect of a disturbance travelling up one side of a jet is considered, and it is concluded that this produces in the surrounding air a sudden local increase of pressure, which in dissipating itself reacts on the jet in the rear of the disturbance, deviating it towards the opposite side. This deviation, if its amplitude is sufficient, may itself be followed by wake disturbance causing the jet to be deflected once more, and thus undulation may occur in portions of the jet which have not yet reached the edge. The fact that all the edge-tone phenomena occur within the sound-sensitive velocity-range of the jet has been made use of to explain the initiation of the original disturbance. Above a certain minimum velocity such disturbances develop into vortices on being deflected by the edge. According to the amplitude of the resulting wake disturbance (and this can be increased by augmenting the velocity or the wedge-distance), vortex motion may begin at the first, second or third crest of the following undulations. This results in four vortex stages, and in jumps in tone. The periodic increases of pressure near the edge produce the edge tones. For high velocities, the effect of sound on the vortex formation in the jet, described in a former paper, must be taken into account as well as the wake disturbance. In general the vortex motion is the resultant of both causes, but in certain cases they can act separately, and then two different vortex formations are produced simultaneously and these result in two tones of different pitch being heard.

In sensitive jets both causes are active and it is suggested that in the resultant complex reaction is to be found the origin of the differential sensitivity to sound of varying frequency.

§ 8. ACKNOWLEDGMENTS

The author's best thanks are due to Prof. E. N. da C. Andrade, F.R.S., for the facilities for this research and for his continued interest in it. The author is also indebted to Dr R. E. Gibbs for help in matching jet-tone frequencies.

REFERENCES

Pertaining to the preceding two papers.

(1) Sondhaus, C. *Ann. Phys.*, Lpz., **91**, 128 and 214 (1854).
(2) Brown, G. Burniston. *Proc. phys. Soc.* **47**, 703 (1935).
(3) Schmidtke, E. *Ann. Phys.*, Lpz., **60**, 715 (1919).
(4) Carrière, Z. *J. Phys. Radium*, **6**, 52 (1925).
(5) Richardson, E. G. *Sound* (1929). London: Arnold.
(6) Benton, W. E. *Proc. phys. Soc.* **38**, 109 (1926).
(7) Wachsmuth, R. *Ann. Phys.*, Lpz., **14**, 469 (1904).
(8) Richardson, E. G. *Proc. phys. Soc.* **43**, 239 (1931).
(9) König, W. *Phys. Z.* **13**, 1053 (1912).

(10) Brown, G. B. *Phil. Mag.* **18**, 161 (1932).
(11) Göller, H. R. Dissertation. Giessen (1912).
(12) Rieth, J. Dissertation. Giessen (1917).
(13) Lewis, W. *Modern Organ Building*, 2nd ed. (1923). London: William Reeves.
(14) Bonavia-Hunt, N. A. *Modern Organ Stops* (1923). London: Musical Opinion.
(15) Helmholtz. *Sensations of Tone*, 2nd English ed. (1885). London: Longmans, Green and Co.
(16) Helmholtz. *Proc. Acad. Sci. Berlin* (23 April 1868).
(17) Schneebeli. *Ann. Phys.*, Lpz., **153**, 301 (1874).
(18) Cavaille Coll. *C.R. Acad. Sci.*, Paris, p. 176 (1860).
(19) Sonreck. *Ann. Phys.*, Lpz., **158**, 129 (1876).
(20) Smith, Hermann. *Nature*, Lond., **10**, 161 (1874).
(21) Lamb, H. *Hydrodynamics*, 6th ed. p. 229.
(22) Schmieden, C. *Ingen.-Arch.* **7**, 215 (August 1936).
(23) Hooker, S. G. *Proc. roy. Soc.* A, **154**, 67 (1935).
(24) Krüger, F. and Schmidtke, E. *Ann. Phys.*, Lpz., **60**, 701 (1919).
(25) Rosenhead, L. *Proc. roy. Soc.* A, **134**, 170 (1931).
(26) Krüger, F. *Ann. Phys.*, Lpz., **62**, 673 (1920).
(27) Krüger, F. and Casper. *Phys. Z.* **22/23**, 842 (Dec. 1936).
(28) Klug, H. *Ann. Phys.*, Lpz., **11**, 53 (1931).
(29) Jeans. *Dynamical Theory of Gases*, 2nd ed. p. 260.
(30) Kohlrausch, W. *Ann. Phys.*, Lpz., **13**, 545 (1881).

THE PRODUCTION OF CHLADNI FIGURES BY MEANS OF SOLID CARBON DIOXIDE. PART 1: BARS AND OTHER METAL BODIES

By MARY D. WALLER, B.Sc., F.Inst.P., Lecturer in Physics,
London (R.F.H.) School of Medicine for Women

Received 31 *March* 1937. *Read, with demonstration,* 11 *June* 1937

ABSTRACT. Chladni figures can be very readily produced by means of solid carbon dioxide: some photographs of results obtained on metal objects of various shapes are shown. The frequencies of the vibrations excited in objects of low fundamental tone usually lie between about 1000 and 4000. The theoretical implications of this fact are considered.

§1. INTRODUCTION

A general theory of the production of pure loud notes from metal bodies by means of solid carbon dioxide has been given previously(1), and the circumstances which led to the discovery have also been recorded(2). The production of Chladni figures, more especially of the nodal lines that may be produced on metal bars, has been undertaken in a further study of the phenomenon. At the same time it has been established that the method of excitation provides a rapid and simple way of obtaining these figures on bodies both of regular and of irregular shape.

By means of these overtones, the limits of frequency within which the carbon-dioxide method of excitation is effective can be estimated with considerable accuracy. It appears that this preferred range depends relatively little upon the size, shape, mass, material or temperature of the excited metal. Conversely, a knowledge of the preferred range enables bodies of suitable dimensions to be chosen on which to produce Chladni figures corresponding to given overtones. The observations that are recorded below serve therefore two purposes. The one concerns the theoretical interpretation of the excitation phenomenon; the other a new method of obtaining Chladni figures that may be useful in the future.

§2. TECHNIQUE

The following points of technique, some of which have been mentioned previously, are important for producing effective vibrations.

(1) The solid carbon dioxide used must be of the high-density "ice" variety. I am indebted to Imperial Chemical Industries Ltd., for kindly supplying the solid carbon dioxide known as "Drikold" which was used in the present investigation.

(2) The area of contact between the metal and solid carbon dioxide must be small, and the pressure of application light. Figure 1 and the inset of figure 8 show pointed pieces of carbon dioxide which are suitable for purposes of excitation. It does not appear to be possible to substitute a mechanical device for the hand, and the skill of the operator in sensing the onset of vibration, the amplitude of which grows with remarkable rapidity, increases with practice. The point of application of the solid carbon dioxide (at or near an anti-node) may be either on the upper or the lower surface of the bar; for producing sand patterns it is often convenient to excite from below.

(3) The atmosphere should be dry. It was originally stated⁽¹⁾ that humidity did not affect the production of vibrations. This conclusion was based on observations made on a brass bar which vibrated so readily in the free-free fundamental mode of 2000 c./sec. that the difficulties subsequently encountered in moist weather with other vibrators were not anticipated. These may be partially overcome by warming the bars before use, and by sprinkling dried sand on to the cleaned surface at the last moment before excitation. Moisture from the air formed on the surface of the solid carbon dioxide cannot however be avoided; and when one is investigating the higher tones of the larger bars, especially if their vibration frequencies lie above or below those which are most easily excited by the solid carbon dioxide, it is well to experiment on a dry day. It is also sometimes desirable to discard a piece of carbon dioxide, if it appears sugary or breaks up easily, in favour of a piece broken by means of hammer and chisel from another part of the solid carbon-dioxide block. This last observation is of theoretical as well as of practical importance.

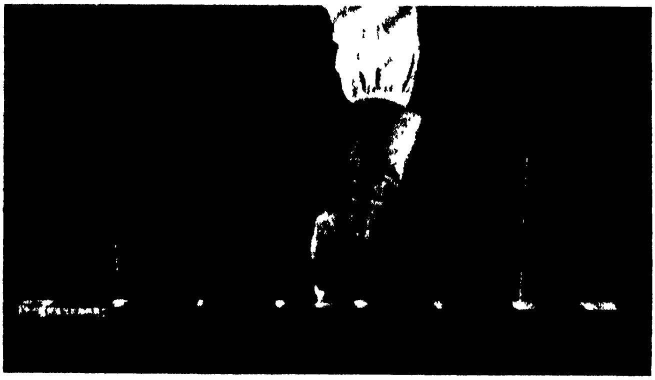

Figure 1. Production of Chladni nodal lines by means of solid carbon dioxide. Frequency, 1317 c./sec.

§ 3. FREQUENCIES OF VIBRATIONS EXCITED BY SOLID CARBON DIOXIDE

Provided that the fundamental of a metal object is high enough, that is to say about 1000 c./sec., this will be excited by means of solid carbon dioxide; it has been found possible to produce the two nodal lines on bars vibrating in the free-free manner up to 7000 c./sec. and to detect notes up to much higher frequencies.* The observations that have been made on objects of low fundamental are described below.

Brass bars of varying length and thickness. Figures 2 and 3, together with the data given in tables 1 and 2, illustrate the fact that the overtones that may be excited by means of solid carbon dioxide become progressively higher as the fundamental becomes lower. This latter varies inversely as the length squared in each of the series of bars of figure 2, and directly as the thicknesses of the brass bars shown in figure 3. It will be noted that all the frequencies lie between 1000 and 4325.

Table 1. Brass bars of varying length

Thickness, 1·27 cm. Thickness, 0·9 cm.

Length (cm.)	Tone*	Frequency		Length (cm.)	Tone*	Frequency	
		Excited	Fundamental (first tone, 2 nodal lines)			Excited	Fundamental
11·5	1†	3358	3358	11·5	1†	2156	2156
15·0	1†	1964	1964	15·0	1†	1263	1263
22·9	2†	2301	836	17·9	2†	2381	860
30·0	2	1298	469	20·2	2	1876	683
	3†	2523	,,		3†	3700	,,
				30·8	3	1588	300
					4†	2638	,,

* Rayleigh notation. † See figure 2.

Table 2. Bars of varying thickness

Length, 60·45 cm.

Thickness (cm.)	Fundamental (to nearest whole number)	Tones excited*	Frequencies†
1·302	121	4–7	1098, **1630**‡, 2266, 2977
0·612	57	6–10	(1011) 1476, **1892**, **2328**‡, 2875
0·325	32	8–15, 17	(1010) 1280, 1560, **1880**‡, **2260**, 2504, 2950, 3400, 4325
0·624§	65	6–10	(1211) 1568, **2080**, **2500**, 3005‡

* Add one to obtain number of nodal lines. † The frequencies most usually obtained are in black type; brackets denote chattering. ‡ See figure 3. § Copper.

Metal objects of varying material, dimensions and temperature. In order to avoid giving lengthy tables, the essential details of a number of observations have been collected in figure 4. The frequencies of each tone excited are plotted on the right. A list of the objects excited, together with notes giving the main purposes of the various observations and the fundamentals are shown in the columns on the left.

Summary of results. A glance at figure 4 is sufficient to show that the range of frequencies that can be excited by means of solid carbon dioxide is remarkably definite, and does not vary very much from object to object. The results for the first

---

* Frequencies were determined by means of a mains-operated calibrated valve oscillator, the property of the Augustus and Alice Waller Memorial Trust.

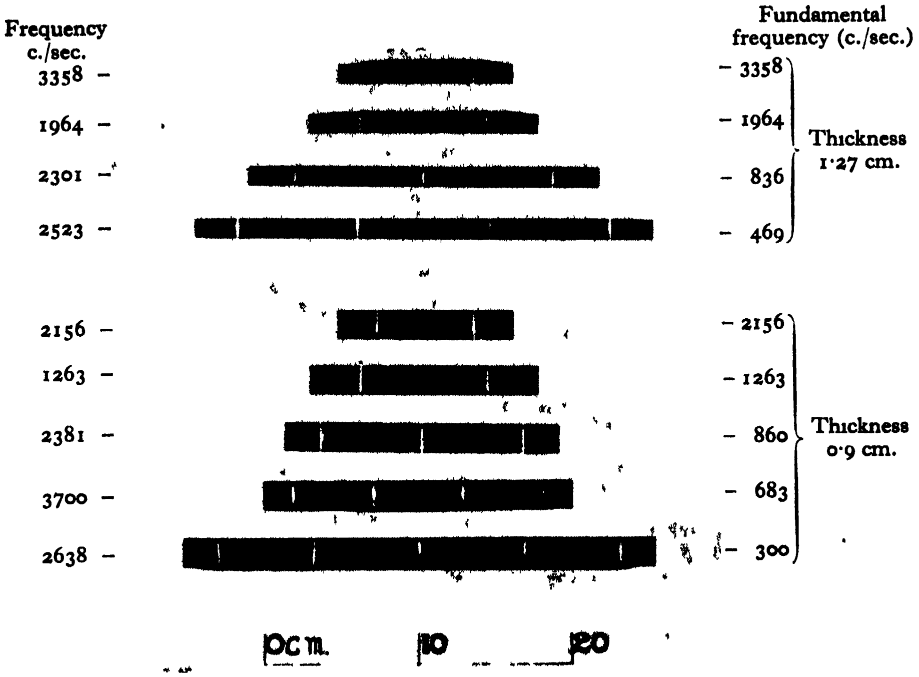

Figure 2. Varying length.

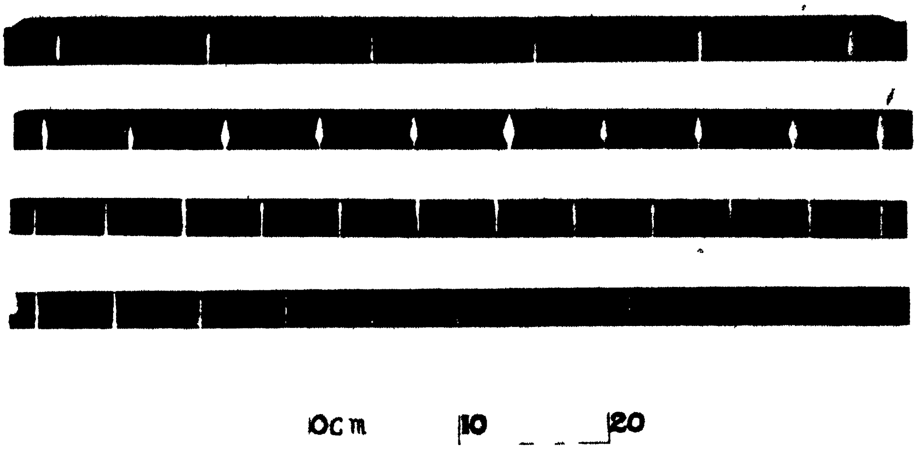

Figure 3. Varying thickness.

	Vibrating object	Notes	Fundamental (first tone)	Tones excited
1	Copper bar	60·7 × 1·27 × 1·27 cm.	130	4–8
2	Mild steel bar	K = 0·9, 0·1	177	3–6
3	Copper bar	44·8 × 1·27 × 1·27	206	3–5
4	German silver bar	K = 0·9, 0·07	198	3–5
5	Brass bar, figure 1	m = 3·29 kg.	71	5–11
6	Aluminium bar	120·8 × 1·27 × 1·27	43	7–12
7	,,	l = 122. Diameter = 1·27	38	7–13
8	Mild steel bar	92·5 × 1·27 × 1·27	78	5–8
9	Brass bar	l = 91·35. Diameter = 1·27	84	5–8
10	,,	42·5 × 1·27 × 1·27	206	3–6
11	,,	20° C.	50	7–12
	,,	150° C.	48·5	7–12
12	,,	20° C.	21	10–20
	,,	150° C.	20	9–19
13	Narrow rods	Diameter = 4 to 6 mm.	—	Misc.
14	Brass plate	Diameter = 13 cm.	—	,,
15	,,	Diameter = 20 cm.	—	,,
16	,,	Diameter = 30 cm.	—	,,

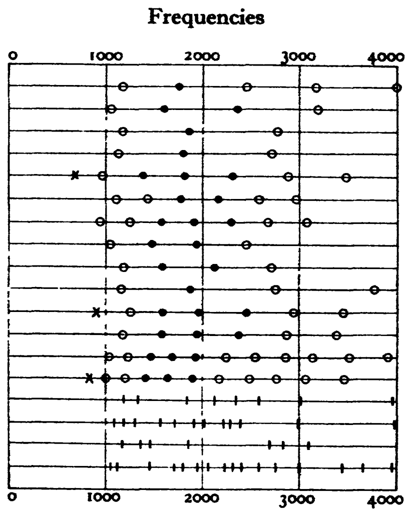

Figure 4. Frequencies of vibrations excited by solid carbon dioxide. K, thermal conductivity; •, most usual frequencies; ×, accompanied by chattering; |, miscellaneous overtones. The frequencies, N_1, given in the fourth column were calculated by means of the relation

$$N_1 = N_n\, 9{\cdot}061/(2n+1)^2.$$

The tones excited in bars of circular cross-section were inferred from the ratios of the experimental frequencies which approximate to the squares of the odd numbers.

four bars show that a change of conductivity from 0·9 to 0·07 makes no detectable change in this range. The range is definitely lower for the massive fifth bar (938–3468), a photograph of which was given in figure 1, than for the small rods (1146–>4000) or brass plates (1070–>4000), 3 mm. thick (see also figure 9). It was difficult to establish any change due to temperature variation, but the final observations undertaken on a brass bar, no. 12, of particularly low fundamental frequency, 21, showed that the range was a little lower when the bar was heated to 150° C.* The intensity of the vibrations is often very great for the heated bars, provided always that the temperature is not sufficient to impair the vibrating properties of the metal. The latter is very important; it is, for example, easier to produce figures with hard brass than with annealed pure copper in spite of its high conductivity. The theoretical significance of these results will be considered in § 5.

§ 4. VIBRATIONS OF METAL OBJECTS OF IRREGULAR SHAPE

Excitation by means of solid carbon dioxide is very intense, and the fact that it can be effected at any point of the metal surface makes it possible to excite single overtones in objects of irregular shape which emit but a jangle of sound when struck with a hammer. A few illustrations of the possibilities of studying resonances by the method are given in figures 5 to 8. Incidentally the frequencies of the vibrations confirm the results of the previous paragraph.

Figure 5 (triangle) gives an idea of how far the ordinary transverse vibrations in the plane of the thickness are affected by breadth, while figure 6 (wedge) shows the manner of vibration when the thickness varies (from approximately zero to 8 mm.). The vibration frequencies of the triangle are from 7 to 10 per cent greater than those of the bar from which it was cut, and the nodal lines are very slightly displaced towards the base. The frequencies of the wedge are very roughly double those of the parent bar, and the adjustment of nodal distances to varying thickness and the large displacements of the nodal lines towards the thin end of the wedge will be noted.

The familiar Trevelyan rocker is shown, as it vibrated with and without its handle, in figure 8; these elastic vibrations are of course much higher than the gravity vibrations of the bar when it is rocking as a whole about its two ridges, and the figure is of interest in connexion with recent discussion concerning this ancient rocker$^{(3)}$.

Figure 7 shows the nodal lines produced on some spanners and a chisel, and suggests the possibility of studying resonances in pieces of machinery. The vibrations of large pieces could be investigated by means of small-scale models.

§ 5. MECHANISM OF PRODUCTION OF VIBRATIONS BY MEANS OF SOLID CARBON DIOXIDE

The production of vibrations by means of solid carbon dioxide, the temperature of which is at about −80° C., depends upon the sublimation which occurs when it touches the metal in the process. A large quantity of gas is produced, as has been

* The slight shift of the frequencies that will be noticed in figure 4 for the heated bars is of course due to the temperature-diminution in Young's modulus.

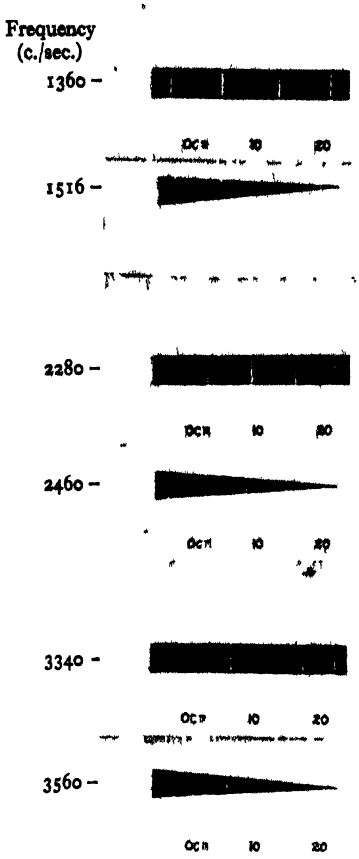

Figure 5. Bar and triangle Thickness 6 84 mm

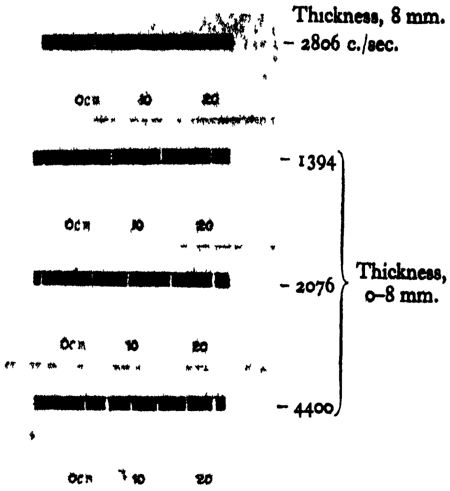

Figure 6. Bar and wedge.

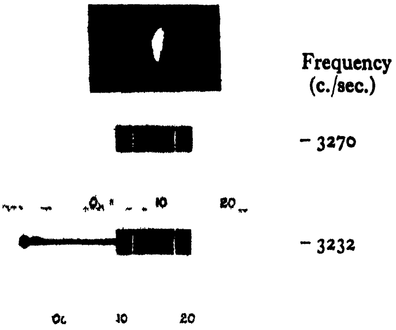

Figure 8 Trevelyan rocker (inset solid carbon dioxide).

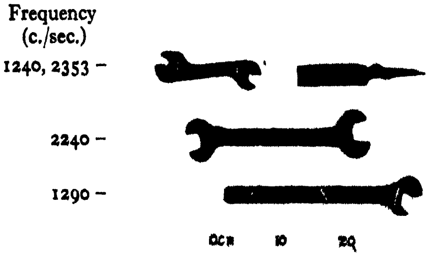

Figure 7 Spanners and chisel.

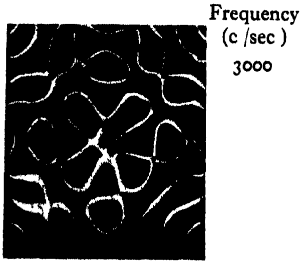

Figure 9 Plate

Figures 5–9. Study of vibrations of metal objects by means of Chladni figures produced by solid carbon dioxide.

shown by means of a Foucault-Toepler or Schlieren photograph$^{(4)}$, the pressure of which is most obvious in the experiments made with mercury$^{(1)}$.

The experimental results that have been summarized in § 4 can be explained by supposing that the main impulse depends upon the irresistible molecular forces of sublimation which are operative at the moment of contact. Each impulse lasts only for a small fraction of the total period and is given except at the beginning, while the vibrating object is at one extreme of its swing. The localized pressure is then very great as compared with that which exists during the rest of the vibration.

It is of interest to consider the relation between the mean free path of the CO_2 molecule, which is about $3{\cdot}9 \times 10^{-6}$ cm. at normal temperature and pressure, and the amplitudes of vibration. Andrade and Smith$^{(5)}$ have investigated the latter in connexion with the production of Chladni figures. Thus the motion at an antinode of the vibrating surface may be represented by $a \sin nt$, the maximum acceleration amounting to an^2. In order that figures may be produced on a bar, an^2 must be greater than g, or a must be greater than $g/4\pi^2N^2 > 25/N^2$, where N is the frequency of vibration. The frequency of vibration corresponding to an amplitude of vibration of $3{\cdot}9 \times 10^{-6}$ cm. just sufficient to produce motion of the sand under favourable conditions would be 2530. The vibrations being intense, at any rate at the higher frequencies, the amplitudes are no doubt considerably greater than these minimum values.

The mean free path cannot of course be estimated accurately. At the first moment of sublimation while the main impulse is occurring, it should be equal to about $p^{-1}.3{\cdot}9.10\ {}^{6}\sqrt{(193/273)}$ cm., where p is possibly many atmospheres; but half a period later, when the vibrating object is at the other extreme of its swing, if the pressure is nearly atmospheric and the temperature not much below that of the room, the mean free path will not differ greatly from $3{\cdot}9 \times 10^{-6}$ cm. It is probable therefore that the upper limit of frequency that can be obtained with the carbon-dioxide method of excitation depends upon the vibration amplitude becoming comparable to the mean free path, and the impulse lasting too long in relation to the period to be effective.* The lower limit of frequencies is imposed by the increase in the chattering which is no doubt connected with the larger amplitudes of vibration.

It is evidently sufficient to have a material of relatively low thermal conductivity in order to produce enough sublimation to separate the two surfaces, and loud notes have been produced in a quartz bar cut from a large crystal, the conductivity of which is 0·06 or 0·03 according to direction$^{(1)}$. At the same time the production of gas is essential and no sound can be produced from insulators. Incidentally this provides a convenient way of distinguishing quartz from glass lenses since the former only, emit a rattle when touched with the carbon dioxide.

In the case of heated metals the impulses are more intense and the mean free path greater, so that the slight decrease of both the upper and lower limits of frequencies is also accounted for by the theory proposed. It might be possible to investigate this matter further with some alloy for which the internal damping remains small at high temperatures⁽⁶⁾. One of the difficulties of producing maintained vibrations at higher temperatures is, however, that the shape of the solid carbon dioxide alters rapidly on account of the increased rate of sublimation.

---

* The theory suggested experimenting with a very narrow, thin, long strip of brass ($1{\cdot}276 \times 0{\cdot}333 \times 86{\cdot}64$ cm.) and exciting it near one end. In such a case the range of frequencies excited should be higher. Clear nodal lines were obtained for all tones from the 15th to the 29th corresponding to frequencies ranging from 1690 to 6000. The fundamental can be calculated with accuracy and is found to be 15·61.

§ 6. CONCLUSION

The production of overtones in metal bodies by means of solid carbon dioxide has enabled the mechanism of the production of vibrations by this method to be studied in considerable detail. At the same time it has become apparent that solid carbon dioxide provides a peculiarly simple and effective method of obtaining Chladni figures. Powerful excitation can be immediately produced and maintained for some seconds at any point of either plane or curved metal surfaces, and it is possible by this means to study the resonances of objects of irregular shape.

REFERENCES

(1) Waller, M. D. *Proc. phys. Soc.* **45**, 101 (1933).
(2) Waller, M. D. *Nature*, Lond., **135**, 475 (1935).
(3) Richardson, E. G. *Phil. Mag.* **45**, 976 (1923).
(4) Waller, M. D. *Proc. phys. Soc.* **46**, 116 (1934).
(5) Andrade, E. N. da C. & Smith, D. H. *Proc. phys. Soc.* **43**, 405 (1931).
(6) Waller, M. D. *Proc. roy. Soc.* A, **156**, 383 (1936).

DISCUSSION

Dr O. Kantorowicz. I should like to ask whether it is possible to control the mode of vibration of a body, if this body has several possible modes in the frequency-range available. Does the author consider the method a suitable one for estimating the damping-capacity of metals, or does damping by sound-radiation mask the effect of internal damping so as to make its observation impossible? Even a rough method would be quite valuable.

Mr J. H. Awbery asked why the author expected to find a simple relation between the mean free path of carbon dioxide and the amplitude of vibration of the metal. He pointed out that in any event air would be mixed with the carbon dioxide. He suggested that local stresses might be set up in the metal as a result of contraction and expansion with changes of temperature.

Mr H. R. Calvert asked whether the author had tried ammonium chloride and other substances which sublimate under attainable conditions.

Author's reply. In reply to Dr Kantorowicz: The desired partials can be obtained by using very hard-pointed pieces of solid carbon dioxide for the higher notes and blunter pieces for the lower notes, the vibrating object being suspended from, or supported at, two nodal positions. The method of measuring the vibration-damping has been described in a previous paper⁽⁶⁾; the air resistance can be neglected to a first approximation. Vibration-damping is probably connected with damping-capacity (as defined by Föppl) though the latter deals with conditions outside the elastic limit.

In reply to Mr Calvert: Vibrations have been produced in heated metals by means of a number of substances which either sublime, or boil, or decompose, with the evolution of gas(2). I did not succeed in detecting the vibrations when using ammonium chloride. The notes produced are feeble and transitory, and the phenomenon, except in the case of solid carbon dioxide, would not be noticed unless looked for.

In reply to Mr Awbery: The experiments just quoted, together with the fact that vibrations cannot be produced in the absence of evolved gas, show that radiation pressure due to the presence of air does not play any detectable part in the production of the vibrations. Nor do I think that local stresses are responsible, since the contact is so slight and the fall in temperature of the metal small. On the other hand the pressure produced by the carbon-dioxide gas is very obvious. The theory developed in connexion with the amplitude of vibration and mean free path of the carbon-dioxide molecule offers some explanation of the fact that the range of frequencies that can be obtained is so definite and varies so little from metal to metal. Longitudinal vibrations also have been produced(1), and further experiments with these might reveal the existence of higher zones of excitable vibrations.

ULTRA-VIOLET BAND-SYSTEMS OF GeCl AND GeBr

By W. JEVONS, L. A. BASHFORD and H. V. A. BRISCOE,
Departments of Physics and Inorganic Chemistry, Imperial
College, London, S.W. 7

Received 26 *May* 1937. *Read in title* 11 *June* 1937

ABSTRACT. Band-systems of GeCl and GeBr are developed in the regions λ3202–λ2847 and λ3260–λ2946 respectively in heavy-current tube-discharges through continuous flows of $GeCl_4$ and $GeBr_4$ vapours. Each consists of two subsystems of bands degraded towards shorter wave-lengths, the heads being represented approximately by

$$\text{GeCl}: \nu=\begin{Bmatrix}33992\cdot2\\33017\cdot2\end{Bmatrix}+(526\cdot6u'-0\cdot3u'^2)-(408\cdot4u''-1\cdot6u''^2),$$

$$\text{GeBr}: \nu=\begin{Bmatrix}33413\cdot4\\32263\cdot4\end{Bmatrix}+(383\cdot7u'-0\cdot7u'^2)-(296\cdot6u''-0\cdot9u''^2),$$

where $u=v+\frac{1}{2}$. The systems are probably $^2\Sigma\rightarrow{}^2\Pi$, the lower states, with electronic intervals 975 and 1150 cm.^{1} respectively, being the ground states of GeCl and GeBr. The electronic intervals $\delta\nu_e$, the upper state energies (system-origins) ν_e, and the vibrational coefficients ω_e and $x_e\omega_e$ for both electronic states are compared with those of band-systems of other monohalides of group-IV (*b*) elements. With increasing atomic number and mass of either atom (group-IV (*b*) or halogen) the expected trend is observed in each case, namely an increase in $\delta\nu_e$, and decreases in ν_e, ω_e and $x_e\omega_e$, except for $\delta\nu_e$ in SiBr and the Pb monohalides; the apparent anomalies are discussed.

§ 1. INTRODUCTION

Although a large number of investigations have been made of the band spectra of diatomic fluorides, chlorides and bromides of the group-IV (*b*) elements silicon, tin and lead, the results for the group as a whole are somewhat fragmentary and give apparently conflicting indications of the nature of the ground states. The ground states of the atoms Si, Ge, Sn and Pb are $ns^2np^2\,{}^3P$ with $n=3$, 4, 5 and 6 respectively, and those of F, Cl and Br are $ns^2np^4\,{}^2P_{\text{inv.}}$ with $n=2$, 3 and 4 respectively, the inner electrons being omitted in each case. From these states a $^2\Pi$ ground state may be expected for the monohalides(1, 2), though $^2\Sigma$ also is possible. It will be well to review briefly the results of observations so far recorded.

For SnCl two ultra-violet band-systems, with 0 → 0 bands near λλ3198, 2973 A. and λλ3761, 3487 A., have been observed in emission(3, 4) and assigned to transitions $^2\Sigma\rightarrow{}^2\Pi$ and $^2\Delta\rightarrow{}^2\Pi$ respectively, the lower state $^2\Pi$ with an electronic separation of 2360 cm.$^{-1}$ being common to the two systems. That this is the ground state of SnCl is suggested by a recent observation of the former system in the fluorescence of $SnCl_2$ vapour with ultra-violet excitation(5).

For SiCl three emission systems B → X, C → X and D → X, having 0 → 0 bands near λλ 2942, 2924 A., λλ 2436, 2424 A. and λλ 2232, 2221 A. respectively, have been analysed(6); they, too, have a common doublet lower state, which has an electronic separation of 207·9 cm.$^{-1}$ and appears, from its analogy to the lower state of SnCl, to be a $^2\Pi$ ground state.

In the case of the SiF emission spectrum the earlier vibrational analysis(7) has recently been revised and extended(2). Three systems, with 0 → 0 bands near λλ4270, 4241 A., λλ2893, 2880 A. and λλ2539, 2529 A., have been attributed to transitions $A\,^2\Pi \rightarrow X\,^2\Pi$, $B\,^2\Sigma \rightarrow X\,^2\Pi$ and $C\,^2\Sigma \rightarrow X\,^2\Pi$ respectively. The common lower $^2\Pi$ state is regarded as the ground state and has an electronic interval of 161 cm.$^{-1}$ A revision of the partial analysis of the rotational structure of the 3 → 3 band λ4368, of the first of these systems, has been reported(8).

The $^2\Pi$ lower states of the above three emitters, then, have electronic intervals which increase, as would be expected, in going from SiF to SiCl and from SiCl to SnCl; they are probably the ground states although there are no absorption observations to put the matter beyond doubt.

The analyses of the known band systems (or subsystems) of PbF, PbCl and PbBr indicate a single electronic level, such as $^2\Sigma$, $^2\Pi_{\frac{1}{2}}$ or $^2\Pi_{1\frac{1}{2}}$ but not a complete $^2\Pi$, in the ground state of each. The PbF system occupies the region λ4110–λ5277 (0 → 0 band at λ4441·1) and has been observed in emission(9) and in absorption(1). The PbCl system in the region λ4108–λ5170 (0 → 0 band at λ4579·6) has been observed in emission(9), in absorption(1, 9) and in fluorescence of $PbCl_2$ vapour with ultra-violet excitation(10). The PbBr system, which extends from λ4482 to λ5320 (0 → 0 band at λ4793·3), has been observed in absorption(1) and in fluorescence of $PbBr_2$ vapour with ultra-violet excitation(11). Only in these three cases is there such abundant proof that the lower state is actually the ground state. The electronic interval in a $^2\Pi$ ground state of each of these molecules would be expected to be much larger than that of SnCl; for example, it has been estimated(1) as 7000 cm.$^{-1}$ for PbCl. This implies that if the observed PbCl bands form the *less* refrangible subsystem of a doublet such as $^2\Sigma \rightleftarrows {}^2\Pi$, the missing subsystem would be very much more intense in absorption and very favourably situated for observation in the near ultra-violet. No bands are observed here, however. On the other hand, if the observed PbCl bands form the *more* refrangible subsystem, the missing subsystem would be very much weaker in absorption, and less favourably placed for observation in the extreme red and near infra-red. A search in this region for PbCl bands in emission from a heavy-current discharge tube might be worth attempting.

For SiBr, the only other emitter for which data are available, a system occurs in the region λ3233–λ2875, and the analysis(12) indicates an apparently single electronic level in the lower state, although comparison with SiF and SiCl (and with the emitters discussed in the present paper) would suggest a $^2\Pi$ state with an interval of 350–450 cm.$^{-1}$ The emission band spectrum of SnBr has also been observed(13) but no data and analysis have been published.

In the absence of any rotational analysis other than that of SiF(8), vibrational analyses of the band-systems of the remaining halides SnF, SnBr, GeF, GeCl and GeBr would seem to be the most promising means of gaining further insight into the nature of the ground states of the subgroup. Investigations of the spectra of the last two of these emitters, the results of which have already been announced in a preliminary note$^{(14)}$, are described in the following pages. In view of the apparently anomalous result (noted above) for SiBr, and the lack of data for SnBr, similar investigations have been made of these two emitters and will be described in a later paper$^{(15)}$; the result for SiBr has already been given in the preliminary note.

During the writing of the present paper it has become possible to include CCl in this discussion. A prominent cluster of band-heads near λ2788 in the uncondensed discharge through carbon tetrachloride vapour has been known for some time$^{(16)}$ but has not been interpreted until quite recently$^{(17)}$; it forms the strong part ($0 \rightarrow 0$ and $1 \rightarrow 1$ bands) of a $^2\Sigma \rightarrow {}^2\Pi$ system of CCl, in which the lower state has an electronic separation of 136 cm.$^{-1}$

§ 2. EXPERIMENTAL

The sources used for the development of the GeCl and GeBr band-systems were heavy-current uncondensed tube-discharges through continuous streams of the vapours of the tetrachloride and tetrabromide. The tetrachloride was prepared by the action of hydrochloric acid on the dioxide$^{(18)}$ and purified by treatment with anhydrous sodium carbonate and subsequent distillation in an all-glass apparatus (B.P. 83° C.). The tetrabromide was prepared by the prolonged action of A.R. bromine on metallic germanium$^{(19)}$ and purified by fractional distillation under the same rigorous conditions (M.P. 26° C., B.P. 184° C.).

The discharge carried a current of about 0·25–0·35 A. from a 2400-V. transformer whose primary was connected through a suitable rheostat to 230-V. mains (50 c./sec.); a bank of tungsten filament lamps (100 V., 40–60 W.) connected in series with the discharge tube served as an additional control and as a rough indicator of the magnitude of the secondary current.

The discharge tube, which is shown in figure 1, is of pyrex. An essential feature is the large area of contact of the cylindrical sheet electrodes with the water-cooled walls of the bulbs. For the electrodes and leads nickel* is used in preference to aluminium in order to avoid the AlCl band-system in the region of λλ2600–2700.

As the germanium compounds have to be used with as little loss as possible, their vapours cannot, of course, be continuously pumped through the discharge into tubes of soda-lime or other absorbent as in the case of cheaper material such as $SiCl_4$ or $SnCl_4$. The inflow and outflow tubes are therefore connected (through picein joints) to glass traps T_1 and T_2 provided with stopcocks A_1, B_1 and A_2, B_2.

---

* The same type of tube, but without the traps T_1 and T_2 shown in figure 1, had previously been used for SiCl$^{(6)}$. Opportunity has now been taken to replace the impure nickel first used (which, on account of its copper content, gave rise to Cu lines and CuCl bands) by pure nickel which later became available.

One trap, say T_1, which initially contains the whole of the tetrahalide, is cooled in liquid air, and the whole apparatus as far as the closed stopcock A_1 is evacuated by an oil-pump connected to A_2. Stopcocks B_1 and A_2 are then closed and the liquid-air bath is transferred from T_1 to T_2. When the substance in T_1 has warmed up to its melting point, B_1 is partly opened so that the vapour may slowly pass through the discharge tube and freeze out in T_2. A suitable vapour pressure (as a rule, not much below the highest at which the discharge will easily pass) is maintained in the tube by adjustment of B_1 and, if necessary, occasional pumping through A_2 for a few seconds. When all the substance has passed into T_2, the liquid-air bath is returned to T_1, the pump connexion transferred to A_1, and the flow of vapour reversed; and so on throughout the time of the exposure. The discharge through either substance results in a black deposit of metallic germanium, especially in the central part D; and there is also a coloured deposit near the

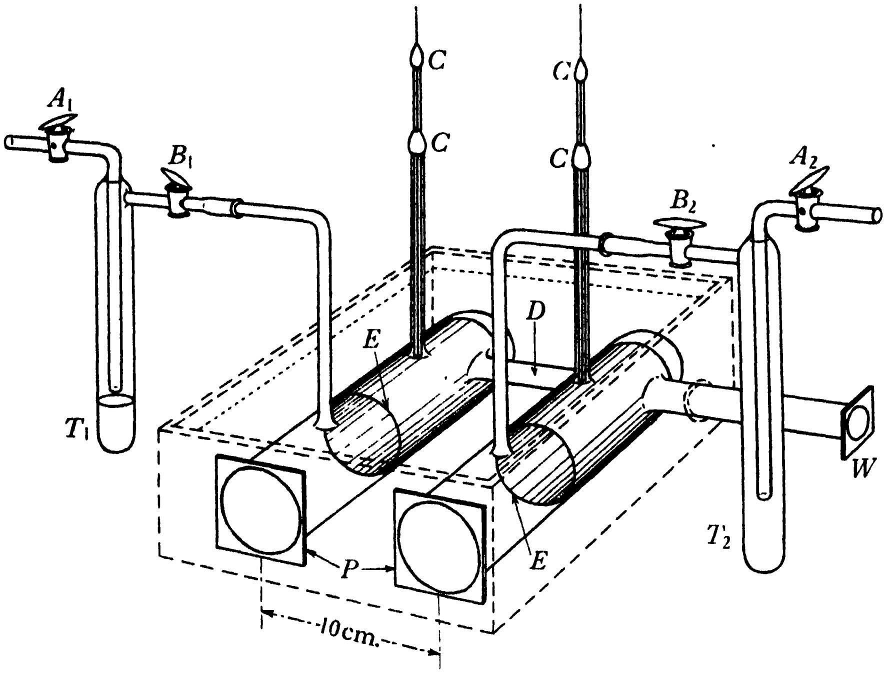

Figure 1. Water-cooled pyrex discharge tube used for continuous streams of $GeCl_4$ and $GeBr_4$ vapours. *E*, sheet nickel cylindrical electrodes. *C*, cement (picein) joints between the nickel leads and soda-glass capillary tubes and between the latter and the vertical pyrex tubes. *P*, glass plates, cemented with picein to the ground open ends of the pyrex bulbs, so that the tube may easily be dismantled for cleaning purposes. T_1 and T_2 soda-glass traps cemented with picein to the inflow and outflow pyrex tubes. The whole discharge tube, except the side tubes, is immersed in running water in an open-top paraffin-waxed wooden box shown in broken lines; the tube is supported in a cradle (not shown), also of paraffin-waxed wood, fixed down in the box. *W*, quartz window through which the column of the discharge *D* is viewed end-on, holes being made in the electrodes for this purpose; the window is cemented with picein to the extension tube which passes through a plasticine joint closing a slotted hole in the side of the box.

electrodes, which is purple in the case of the tetrachloride and light brown in that of the tetrabromide.

The desired band-systems of GeCl and GeBr were first sought in spectrograms obtained with exposures of about 30 and 15 min., respectively, in a small quartz instrument (Hilger's E 6), and the final measurements were made on spectrograms obtained with a quartz Littrow instrument (Hilger's E 1) of much larger dispersion, namely 6·40–4·25 A./mm. between λ3260 and λ2840. The diaphragm used at the slit of each spectrograph is so designed that the exposure of one-half of the total width of the discharge spectrum can be continued after that of the other half has been stopped, and each half has the usual iron-arc comparison spectrum juxtaposed. Thus any band-head can be examined and measured on differently exposed strips with the minimum expenditure of the tetrahalide. With Ilford Ordinary plates in the larger instrument the exposure times were about 1 and 2 hr. for the GeCl system and about ½ and 1 hr. for the GeBr.

§ 3. GeCl BAND-HEAD DATA AND VIBRATIONAL ANALYSIS

In the tetrachloride discharge an ultra-violet band-system occurs in the region λ3202–λ2847, as shown in figure 2(*a*), and a continuum extends from λ2660 to λ2510 with maximum intensity near λ2570. The bands degrade toward shorter wave-lengths as in the case of the SiCl, SiBr and SnCl band-systems in roughly the same region. These facts and the structure of the new system at once pointed to the diatomic emitter GeCl. Measurements of the band-heads, visual estimates of the relative intensities of the bands, and the assigned values of the vibrational quantum numbers are set out in table 1; and a Deslandres arrangement of the wave-numbers and intervals is shown in table 2. The system consists of two overlapping subsystems. The heads of the less refrangible and the more refrangible subbands are designated as (i) and (ii) respectively, in order to avoid an incorrect use of theoretically significant symbols, such as P_1 and P_2 or Q_1 and Q_2, since it is not known whether the measured heads are of P-form or of Q-form. Their wave-numbers are approximately represented by

$$\nu=\begin{Bmatrix}33992{\cdot}2\\33017{\cdot}2\end{Bmatrix}+(526{\cdot}6u'-0{\cdot}3u'^2)-(408{\cdot}4u''-1{\cdot}6u''^2),$$

where $u'=v'+\frac{1}{2}$ and $u''=v''+\frac{1}{2}$; the residuals, $\nu_{\text{obs.}}-\nu_{\text{calc.}}$, are included in table 1. The independent coefficients are fairly close approximations to the subsystem origins, and the electronic separation, 975 cm.$^{-1}$, represented by the difference of these coefficients, is, as would be expected, intermediate between those already quoted for the lowest states of SiCl and SnCl.

The abundance ratios of the chief isotopes(20) of Ge and Cl are

$$^{74}\text{Ge} : {}^{72}\text{Ge} : {}^{70}\text{Ge} = 100 : 73{\cdot}6 : 57{\cdot}2 \text{ and } {}^{35}\text{Cl} : {}^{37}\text{Cl} = 100 : 31{\cdot}4.$$

Hence in the composite GeCl system the intensities of bands of the more important isotopic emitters ^{72}Ge^{35}Cl, ^{70}Ge^{35}Cl, ^{74}Ge^{37}Cl will be about 74, 57 and 31 per cent, respectively, of those of the corresponding bands of the most abundant emitter $^{74}Ge^{35}Cl$. The values of the displacement coefficient $\rho - 1$ for these three isotopic emitters are +0·00445, +0·00913 and −0·01840 respectively. If, then, all emitters less abundant than these be ignored, each prominent band-head of $^{74}Ge^{35}Cl$ should be accompanied by two relatively close and weaker heads due to the Ge isotope effect on the side remote from the system-origin, and by one less close and still weaker head due to the Cl isotope effect on the side towards the system-origin. No band of the system is expected, however, to be favourable for the observation of all three companion heads. Since the bands degrade in the high-ν direction the heads due to the Ge isotope effect are only likely to be detected for a strong band on the low-ν side of ν_e while a strong band on the high-ν side is

Table 1. GeCl band-heads

v', v''	Sub-band	λ_{air}	Int.	ν_{vac}	$\nu_{obs} - \nu_{calc}$
1, 6	(i)	3202·22	1	31219·3	−0·1
0, 4	(i)	3176·40	2*n*	473·1	−1·9
1, 5	(i)	62·80	2*n*	608·4	−0·2
0, 3	(i)	36·77	4	870·7	+0·1
0, 2	(i)	3097·99	5	32269·7	+0·3
0, 1	(i)	59·83	6	672·1	+0·7
0, 3	(ii)	43·40	2*n*	848·5	+2·9
0, 0	(i)	22·43	5	33076·4	−0·2
1, 1	(i)	11·42	2	197·3	−0·1
0, 2	(ii)	07·03	6	245·7	+1·3
1, 0	(i)	2975·09	4	602·6	0·0
0, 1	(ii)	71·25	7*d* ?	646·1	−0·3
0, 0	(ii)	36·04	8*d*	34049·5	−2·1
2, 0	(i)	29·38	4	127·0	−1·0
1, 1	(ii)	25·75	5	169·3	−3·1
1, 0	(ii)	2891·25	8*d*	577·0	−0·6
2, 0	(ii)	47·88	4*d*	35103·5	+0·5

n, nebulous, rather difficult to locate exactly; *d*, double, see text (p. 538).

Table 2. GeCl band-heads

2	(ii)	35103·5											
		976·5											
	(i)	34127·0											
		526·5											
		524·4											
1	(ii)	34577·0	*407·7*	34169·3						—	—		—
		974·4		*972·0*									
	(i)	33602·6	*405·3*	33197·3						*	31608·4	*389·1*	31219·3
		527·5		*523·2*									
		526·2		*525·2*									
0	(ii)	34049·5	*403·4*	33646·1	*400·4*	33245·7	*397·2*	32848·5		—			
		973·1		*974·0*		*976·0*		*977·8*					
	(i)	33076·4	*404·3*	32672·1	*402·4*	32269·7	*399·0*	31870·7	*397·6*	31473·1			
↑ v'	v'' →	0		1		2		3		4	5		6

* Hidden by Ge line λ3124·84, ν 31992·4.

more favourable for the detection of the head due to the Cl isotope effect. In the present system, bands of the former description are much the more numerous. The complex type of the bands (probably $^2\Sigma \rightarrow {}^2\Pi$, as will be seen in a later section) and the presence of incompletely resolved rotational structure of neighbouring bands in the higher-dispersion spectrograms, combine to render the detection of either isotope effect exceedingly difficult and uncertain. Additional possible heads have been observed for several of the subbands. Two of these, which are sufficiently clear of overlying band structure for measurement, have positions and intensities appropriate to heads of $^{70}Ge^{35}Cl$ and $^{74}Ge^{37}Cl$, the main system (tables 1 and 2) being attributed to $^{74}Ge^{35}Cl$. Data for these heads are as follows:

Emitter	Subband	λ^i	ν^i	$(\nu^i - \nu)_{\text{obs.}}$	$(\rho - 1)(\nu - \nu_e)$
$^{70}Ge^{35}Cl$	0 → 1 (ii)	2971·60	33642·1	− 4·0	$(+0{\cdot}00913)(-346) = -\ 3{\cdot}2$
$^{74}Ge^{37}Cl$	1 → 0 (ii)	2892·12	34566·6	− 10·4	$(-0{\cdot}01840)(+585) = -10{\cdot}8$

Further possible heads, which have been measured at $\lambda 2936{\cdot}31$, $\nu 34046{\cdot}4$ for the 0 → 0 (ii) subband and $\lambda 2848{\cdot}59$, $\nu 35094{\cdot}8$ for the 2 → 0 (ii) subband, are certainly not attributable to an isotope effect, and are presumably the heads of other branches of the main $^{74}Ge^{35}Cl$ bands.

§ 4. GeBr BAND-HEAD DATA AND VIBRATIONAL ANALYSIS

The tetrabromide discharge develops a similar doublet system of bands degraded towards shorter wave-lengths in roughly the same region. This system is reproduced in figure 2 (*b*) and is due, no doubt, to the diatomic emitter GeBr. The bands extend from $\lambda 3260$ to $\lambda 2946$, and are followed by a continuum extending from about $\lambda 2930$ to about $\lambda 2850$ and having a maximum intensity near $\lambda 2900$. In tables 3 and 4 the band-head data are presented in the same way as those of GeCl, the low-ν and high-ν subbands being again denoted by (i) and (ii) respectively. The heads are fairly well represented by

$$\nu = \begin{Bmatrix} 33413{\cdot}4 \\ 32263{\cdot}4 \end{Bmatrix} + (383{\cdot}7u' - 0{\cdot}7u'^2) - (296{\cdot}6u'' - 0{\cdot}9u''^2),$$

in which $u = v + \frac{1}{2}$, the residuals being shown in table 3. As was to be expected, the separation of the subsystem origins is greater for GeBr than for GeCl, namely 1150 cm.$^{-1}$ as against 975.

The fuzziness of many of the heads, and the consequent difficulty of locating them exactly, may be due in part to the complexity of the bands (probably $^2\Sigma \rightarrow {}^2\Pi$ as will be seen in the following section) and in part to unresolved isotope effects. On account of the large masses and nearly equal abundances of the Br isotopes, the pattern formed by corresponding band-heads due to isotopic GeBr emitters will be rather close and complicated, even if again only the three chief Ge isotopes are considered$^{(20)}$. Starting with a relatively strong head (ν) due to $^{74}Ge^{81}Br$ and ending with a relatively weak one due to $^{70}Ge^{79}Br$, the pattern will consist of three pairs, in each of which the components will have equal intensities. The first pair, due to ^{74}Ge^{81}Br and ^{74}Ge^{79}Br, will have a separation of about 0·006 $(\nu-\nu_e)$ and relative intensities 100; the second, due to ^{72}Ge^{81}Br and ^{72}Ge^{79}Br, will have nearly the same separation but relative intensities 74; and the third, due to ^{70}Ge^{81}Br and ^{70}Ge^{79}Br, also nearly the same separation, but relative intensities 57. The three pairs will be very close to one another, being nearly equally spaced at about 0·0075 $(\nu-\nu_e)$. Thus, the ^{74}Ge^{79}Br and ^{72}Ge^{81}Br heads will be only about

Table 3. GeBr band-heads

v', v''	Sub-band	λ_{air}	Int.	$\nu_{\text{vac.}}$	$\nu_{\text{obs.}}-\nu_{\text{calc.}}$
1, 7	(i)	3259·69	1*n*	30669·0	+5·5
0, 5	(i)	40·75	2*n*	848·2	−2·8
1, 6	(i)	30·48	2*n*	946·3	−1·2
0, 4	(i)	10·73	3	31136·6	−2·0
1, 5	(i)	00·67	3*n*	234·5	+1·2
0, 3	(i)	3181·04	5*n*	427·2	−0·8
1, 4	(i)	71·65	3*n*	520·2	−0·7
0, 2	(i)	51·65	7	720·3	+1·1
0, 1	(i)	22·81	7	32013·2	+1·0
1, 2	(i)	14·16	5	102·1	+0·6
0, 4	(ii)	3096·44	4*d* ?	285·8	−2·8
0, 0	(i)	94·33	5	307·8	+0·8
1, 1	(i)	86·02	7	394·8	+0·3
0, 3	(ii)	68·83	8	576·3	−1·7
1, 0	(i)	58·48	6*n*	686·5	−2·8
0, 2	(ii)	41·34	10	870·7	+1·5
0, 1	(ii)	14·68	10	33161·4	−0·8
1, 2	(ii)	06·36	8	253·2	+1·7
0, 0	(ii)	2987·99	8	457·6	+0·6
1, 1	(ii)	80·22	10	544·8	+0·3
1, 0	(ii)	54·24	12	839·8	+0·5
2, 1	(ii)	46·76	5	925·7	+0·3

n, nebulous, rather difficult to locate exactly; *d*, double, see text (p. 540).

Table 4. GeBr band-heads

v' ↑		v''→0		1		2		3		4		5		6		7
2	(ii)			33925·7												
	(i)			—												
				380·9												
				—												
1	(ii)	33839·8	*295·0*	33544·8	*291·6*	33253·2				—		†		‡		§
		1153·3		*1150·0*		*1151·1*										
	(i)	32686·5	*291·7*	32394·8	*292·7*	32102·1				31520·2	*285·7*	31234·5	*288·2*	30946·3	*277·3*	30669·0
		382·2		*383·4*		*382·5*				—		—				
		378·7		*381·6*		*381·8*				*383·6*		*386·3*				
0	(ii)	33457·6	*296·2*	33161·4	*290·7*	32870·7	*294·4*	32576·3	*290·5*	32285·8		*				
		1149·8		*1148·2*		*1150·4*		*1149·1*		*1149·2*						
	(i)	32307·8	*294·6*	32013·2	*292·9*	31720·3	*293·1*	31427·2	*290·6*	31136·6	*288·4*	30848·2				

* Hidden by Ge line λ3124·84, ν31992·4. † Hidden by structure of 0→0 subband (i).
‡ Hidden by structure of 0→1 subband (i). § Hidden by structure of 0→2 subband (i).

0·0015 $(\nu-\nu_e)$ apart and will probably be observed as a blend (*a*) with relative intensity approaching 100+74; and similarly the $^{72}Ge^{79}Br$ and $^{70}Ge^{81}Br$ heads will probably be observed as a blend (*b*) with relative intensity approaching 74+57. It seems reasonable to ascribe each of the heads in tables 3 and 4 to the stronger blend (*a*), and then examine each strong and favourably placed subband either for the $^{74}Ge^{81}Br$ head at about $-0{\cdot}0065\,(\nu-\nu_e)$ or for the weaker blend (*b*) and the $^{70}Ge^{79}Br$ head at about $+0{\cdot}007\,(\nu-\nu_e)$ and $+0{\cdot}014\,(\nu-\nu_e)$ respectively. No subband is expected to be favourable for the observation of all of these, and, moreover, the calculated displacements are rather small for all the strong subbands. While this interpretation is probably correct, no bands attributable to an isotope effect have been measured with certainty. In the 0 → 4 (ii) subband a rather doubtful second head is observed which may be blend (*b*); the data are: $\lambda^i=3097{\cdot}21$, $\nu^i=32277{\cdot}8$, $(\nu^i-\nu)_{\text{obs.}}=8{\cdot}0$, $(\nu^i-\nu)_{\text{calc.}}=7{\cdot}9$ cm.$^{-1}$

§ 5. DISCUSSION OF RESULTS

Analogy with SiCl and SnCl suggests that the electronic intervals of 975 and 1150 cm.$^{-1}$ established by the foregoing analyses occur entirely in the lower states of GeCl and GeBr, and that these are $^2\Pi$ ground states.

The observed electronic intervals $\delta\nu_e$ and vibrational coefficients ω_e'' and $x_e''\omega_e''$ for the lowest states of this subgroup of diatomic halides are collected in table 5. In each case, as the atomic number and mass of either the group-IV (*b*) atom or the halogen increase, the expected trend is observed: namely, an increase in $\delta\nu_e$ (apart from the possibly exceptional cases of the Pb halides already discussed on p. 533) and decreases in ω_e'' and $x_e''\omega_e''$. The regularities shown by these latter suggest, as a further step, a comparison of the rough estimates of the dissociation energies D obtained by extrapolation of the vibrational energies for these states by means of the well-known expression

$$D=(\omega_e-x_e\omega_e)^2/(4x_e\omega_e\times 8106)\text{ e.V.}$$

The values of D are also shown in table 5. Although they are subject to large errors on account of inaccuracies in the small coefficients $x_e''\omega_e''$, it is evident that their trend is the same as that of ω_e'' and $x_e''\omega_e''$.

The foregoing assumption that the observed GeCl and GeBr separations occur wholly in the lower states implies, of course, that the upper states have single electronic levels, as in the case of the λ2924 system ($\text{B}\,^2\Sigma(?)\rightarrow\text{X}\,^2\Pi$) of SiCl and the λ2973 system ($^2\Sigma\rightarrow{}^2\Pi$) of SnCl.* If the upper states in these four cases are truly comparable we should expect to find that the electronic energy (as determined by the greater of the two subsystem origins) in GeCl is greater than that in GeBr and intermediate between the electronic energies in SiCl and SnCl. This is, in fact, observed to be the case, as will be seen in table 6, where these electronic energies

---

* The present suggestion that these are comparable systems requires an amendment to figure 2 in the paper on SiCl(6). The broken lines connecting D to $^2\Sigma$ and C to $^2\Delta$ should be replaced by one connecting B to $^2\Sigma$.

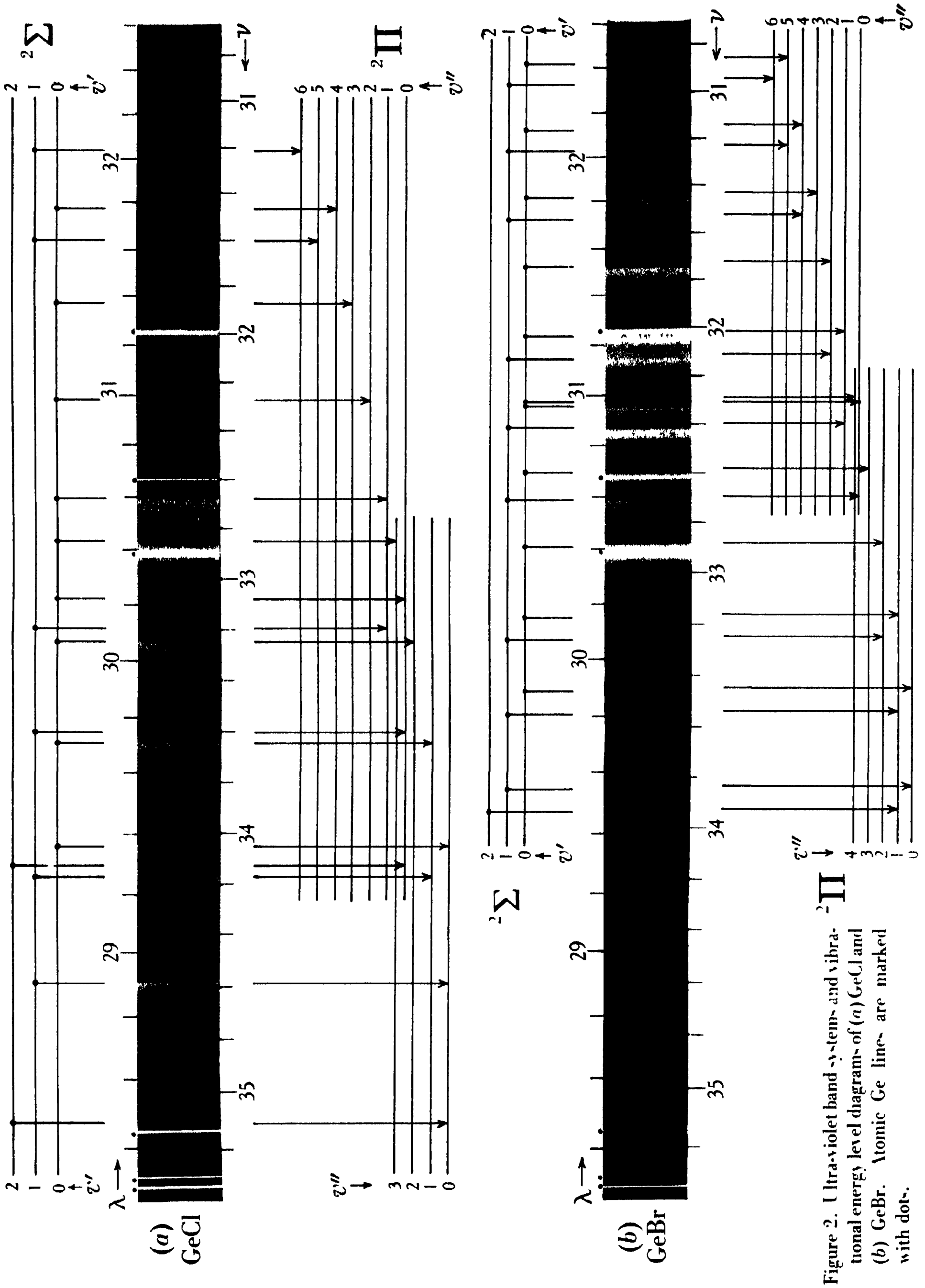

Figure 2. Ultra-violet band-systems and vibrational energy level diagrams of (a) GeCl and (b) GeBr. Atomic Ge lines are marked with dots.

are set out with the corresponding data from the λ2880 system ($B\,^2\Sigma \rightarrow X\,^2\Pi$) of SiF and from the only recorded systems of PbF, PbCl, PbBr, SiBr and CCl. Table 6 also shows the total energies of the $v = 0$ levels (as determined by the wave-number of the more refrangible component of the $0 \rightarrow 0$ band in each system) and the vibrational coefficients ω_e' and $x_e'\omega_e'$. Here again, with increasing atomic number and mass of either atom, the expected trend is observed in each case, namely a slight decrease in ν_e, a corresponding red-shift of the $0 \rightarrow 0$ band, and decreases in ω_e' and $x_e'\omega_e'$, except for $x_e'\omega_e'$ of GeCl where the estimate is rather unreliable as the observed bands with $v' = 1$ and 2 are too few.

Table 5. Data for lower ($^2\Pi$) states

	Electronic separation $\delta\nu_e$ (cm.$^{-1}$)			ω_e'' (cm.$^{-1}$)			$x_e''\omega_e''$ (cm.$^{-1}$)			Dissociation energy, D'' (e.V.)		
	F	Cl	Br	F	Cl	Br	F	Cl	Br	F	Cl	Br
C		136			(843·6)‡							
Si	161	208	418*	856·7	535·4	425·4*	4·7	2·20	1·5*	4·8	4·0	3·7
Ge		975	1150		408·4	296·6		1·6	0·9		3·2	3·0
Sn		2360	2467†		353·5	247·7†		1·2	0·62†		3·2	3·0†
Pb	0?	0?	0?	506·9	304·2	207·5	2·29	0·89	0·50	3·4	3·2	2·6

Table 6. Data for upper ($^2\Sigma$) states

	Electronic energy (system-origin) ν_e (cm.$^{-1}$)			Energy of $v = 0$ level above that of lower state (cm.$^{-1}$)			ω_e' (cm.$^{-1}$)			$x_e'\omega_e'$ (cm.$^{-1}$)		
	F	Cl	Br	F	Cl	Br	F	Cl	Br	F	Cl	Br
C					35975			(863)§				
Si	34639·4	34102·7	33571·0*	34716·6	34185·3	33645·6*	1011·2	(698·7)§	573·6*	4·8		3·1*
Ge		33992·2	33443·4		34049·5	33457·6		526·6	383·7		0·3	0·7
Sn		33582·6			33622·6	33094·5†		432·5			1·2	
Pb	22565·2	21866·9	20884·3	22510·4	21829·8	20856·8	397·8	228·6	152·5	1·77	0·76	0·4

* SiBr data taken from a forthcoming paper(15) in preference to those given in the preliminary note(14).

† SnBr data taken from a forthcoming paper(15).

‡ Value of $\omega_{\frac{1}{2}}''$ inserted for CCl(17) as ω_e'' and $x_e''\omega_e''$ are not known for lack of bands with $v \geqq 2$.

§ Value of $\omega_{\frac{1}{2}}'$ inserted for CCl(17) and SiCl(6) as ω_e' and $x_e'\omega_e'$ are not known for lack of bands with $v \geqq 2$.

In conclusion, then, it would appear that the band systems of GeCl and GeBr, like those cited for SiF, CCl, SiCl and SnCl, are due to transitions $^2\Sigma \rightarrow {}^2\Pi$, the lower states being the ground states. In view of this result, the anomaly mentioned in the introduction, that SiBr appears to have a single level as its lower state, becomes even more striking. New investigations of the spectrum of SiBr and that of SnBr (for which data have hitherto been lacking) are described in a forthcoming paper(15), some data from which are included in tables 5 and 6 for the sake of completeness. In each case it appears that the ground state is a doublet (probably $^2\Pi$) with electronic separations of 424 and 2710 cm.$^{-1}$ respectively. Thus, as the preliminary note(14) indicated, the apparent anomaly in the case of SiBr is removed.

§ 6. ACKNOWLEDGMENTS

The authors have pleasure in recording their indebtedness to Prof. Sir Gilbert Morgan and Dr G. R. Davies for the gift of germanium, germanium dioxide and other germaniferous material from which the tetrachloride and tetrabromide were prepared. They also express their thanks to the Government Grant Committee of the Royal Society for grants for apparatus; to the Fereday Electors of St John's College, Oxford, for the opportunity afforded to one of them (W. J.) of taking part in this work; and to the Governors of Collyer's School, Horsham, and the Education Committee of the West Sussex County Council for personal grants to another (L. A. B.).

REFERENCES

(1) MORGAN, F. *Phys. Rev.* **49**, 47 (1936).
(2) ASUNDI, R. K. and SAMUEL, R. *Proc. Ind. Acad. Sci.* **3**, 346 (1936).
(3) JEVONS, W. *Proc. roy. Soc.* A, **110**, 365 (1926).
(4) FERGUSON, W. F. C. *Phys. Rev.* **32**, 607 (1929).
(5) NEUJMIN, H. *Acta Physicochim. U.S.S.R.* **2**, 595 (1935).
(6) JEVONS, W. *Proc. phys. Soc.* **48**, 563 (1936).
(7) JOHNSON, R. C. and JENKINS, H. G. *Proc. roy. Soc.* A, **116**, 327 (1927).
(8) BADGER, R. M. and BLAIR, C. M. *Phys. Rev.* **47**, 881 (1935).
(9) ROCHESTER, G. D. *Proc. roy. Soc.* A, **153**, 410 (1936).
(10) POPOV, B. and NEUJMIN, H. *Phys. Z. Sowjet.* **2**, 394 (1932).
(11) POPOV, B. *Acta Physicochim. U.S.S.R.* **6**, 159 (1936).
(12) MIESCHER, E. *Helv. Phys. Acta*, **8**, 587 (1935).
(13) HOWELL, H. G. and ROCHESTER, G. D. *Proc. Univ. Durham phil. Soc.* **9**, 126 (1934).
(14) BASHFORD, L. A., BRISCOE, H. V. A. and JEVONS, W. *Nature*, Lond., **138**, 883 (1936).
(15) JEVONS, W. and BASHFORD, L. A. *Proc. phys. Soc.* **49**, 554 (1937).
(16) JEVONS, W. *Proc. roy. Soc.* A, **106**, 174 (1924).
(17) ASUNDI, R. K. and KARIM, S. M. *Curr. Sci.* **9**, 474 (1937).
(18) DEDE, L. and RUSS, W. *Ber. dtsch. chem. Ges.* **61**, 2456 (1928).
(19) MORGAN, G. T. and DREW, H. D. K. *J. chem. Soc.* **125**, 1264 (1924).
(20) International Table of Stable Isotopes, *Rev. sci. Instrum.* **7**, 334 (1936).

THE ULTRA-VIOLET BAND-SYSTEM OF GERMANIUM MONOXIDE

By W. JEVONS, L. A. BASHFORD and H. V. A. BRISCOE

Departments of Physics and Inorganic Chemistry, Imperial College,
London, S.W. 7

Received 21 *April* 1937. *Read in title* 11 *June* 1937

ABSTRACT. The GeO band-system, recently investigated by Shaw between λ2989 and λ2441 in the flame surrounding an arc charged with GeO_2, has been measured over the larger range λ3319–λ2441 in an uncondensed discharge through a mixture of $GeCl_4$ vapour and oxygen flowing continuously through the discharge tube. The number of bands measured is increased from 18 to 32, and the highest observed value of v'' from 5 to 10. The band-heads of the extended system are approximately represented by

$$\nu = 37762{\cdot}4 + (651{\cdot}3u' - 4{\cdot}24u'^2) - (985{\cdot}7u'' - 4{\cdot}30u''^2),$$

where $u = v + \frac{1}{2}$. This system being attributed to ^{74}GeO, a few other observed heads may be due to ^{72}GeO and ^{70}GeO. Rotational analysis being impossible, there is no further evidence for or against the transition $^1\Pi \rightleftarrows {}^1\Sigma$ suggested by Shaw. The data are compared with those for band-systems of other monoxides and monosulphides of group-IV*b* elements, and the observed decreases of ν_e, ω_e and $x_e\omega_e$ with increasing atomic number or mass of either atom are shown graphically.

§ 1. INTRODUCTION

RECENTLY, R. W. Shaw⁽¹⁾ has analysed the vibrational structure of a system of GeO bands, degraded towards the red and extending from λ2989·3 to λ2441·0. The source used was the flame surrounding an 8–10 A. arc in air between graphite rods charged with germanium dioxide. In spectrograms taken with a quartz Littrow instrument (Hilger's E 1, dispersion about 4·7 to 2·5 A./mm. in this region) twenty-one bands were observed, and the *R* heads of eighteen of them were measured and closely represented by the formula

$$\nu = 37763{\cdot}7 + (649{\cdot}4u' - 3{\cdot}81u'^2) - (985{\cdot}0u'' - 4{\cdot}36u''^2),$$

where u' and u'' are written for $v' + \frac{1}{2}$ and $v'' + \frac{1}{2}$; the heads of the other three observed bands were obscured by atomic lines. Estimates of the relative intensities of the bands were not very reliable and any attempt at rotational analysis was inadvisable, on account of overlapping of bands: this is readily understandable in view of the high-temperature distribution of line intensities in each branch of the bands in the source employed.

In order to obtain greater contrast between a band-head and the overlying structure of neighbouring bands a source giving a lower temperature distribution would appear to be necessary. One such source, which had already been used for the ultra-violet systems of the analogous emitters SiO⁽²⁾ and SnO,* was clearly applicable to the GeO system, and was, in fact, being so applied when Shaw's recent paper appeared. An uncondensed discharge is passed through a mixture of oxygen and the chloride vapour ($SiCl_4$, $SnCl_4$ or $GeCl_4$) pumped continuously through the discharge tube. With comparatively little oxygen in the mixture the bands of the monoxide are accompanied by those of the monochloride, but with sufficient oxygen the latter may be entirely quenched, so that the monoxide bands are developed with little but a few strong atomic lines to interfere with good measurement. As this is a very convenient method, which, judging from published observations, has been little used, it would seem desirable to redirect attention to it, especially as its employment is now greatly facilitated by the substitution of a suitable transformer for the induction coil previously used in the cases of SiO and SnO.

Apart from the question of intensity distribution, this discharge-tube method is more economical in material than the arc in air; this is an important advantage in the case of GeO. In this work the band-system has been considerably extended by the measurement of band-heads not previously measured and by the recognition of some heads due to the germanium isotope effect. It seemed, therefore, that there would be no advantage in making observations either with the arc in air as used by Shaw, or with the uncondensed discharge through a flame as used by Connelly(5) for the SnO bands. It might be added that, even had they been desirable, neither of these sources could have been employed with the limited supply of germanium available.

§ 2. EXPERIMENTAL

The germanium tetrachloride used was a part of that already prepared for the investigation of the GeCl band-system(7). As in that work, the discharge carried a current of about 0·3 A. from a 2400-V. transformer connected to the 230-V. supply of A.C. at 50 c./sec. The same water-cooled pyrex discharge tube with large cylindrical electrodes of nickel sheet was used, but for the present purpose the inlet tube leading to one of the electrode bulbs has two branches, one connected to a bulb containing the tetrachloride, and the other to an oxygen cylinder. The exit tube leading from the other electrode bulb is connected, as in the previous work, through a trap to an oil-pump.

With both bulb and trap immersed in liquid air, the apparatus is evacuated and flushed through with oxygen at low pressure, and the discharge is started. The tetrachloride bulb is then immersed in a bath of alcohol cooled with solid carbon dioxide to about −30° C. By careful adjustment of the stopcocks in the two inlet branches it is easy to admit the required amounts of the tetrachloride and oxygen, the appearance of the glow on the electrode near the inflow tube affording a reliable guide to their correct proportioning. The glow on each electrode is blue when oxygen alone is admitted, and pink with tetrachloride alone. With a mixture of the two in certain proportions the glow on the first (inflow) electrode is blue and that on the second (outflow) electrode is pink, and the spectrum of the column of the discharge shows the GeO system almost entirely free from the GeCl system. This is the mixture which it is sought to maintain throughout the spectrographic exposure. With a slight reduction in the flow of oxygen or a slight increase in that of the tetrachloride the glow on the first electrode changes from blue first to a greyish or neutral tint and then to pink, and the GeCl band-system appears in the spectrum of the column; care is taken just to avoid this condition throughout the exposure. Free chlorine and any tetrachloride which has escaped decomposition in its passage through the discharge are condensed in the trap, which remains immersed in liquid air. A white deposit of the dioxide is formed on the walls of the discharge tube.

---

* Unpublished work, put aside for the preparation of this Society's *Report*(3). The SnO bands were afterwards observed and measured by Mahanti, using an arc in air(4), and by Connelly, using an uncondensed discharge through a flame(5). The unpublished measurements and analysis were in close agreement with Connelly's. The present method had previously been used also in observations of the BO bands and the other boron oxide (B_2O_3?) bands(6).

A quartz spectrograph (a forerunner of Hilger's E 2) of medium dispersion (22 to 8 A./mm. from λ 3320 to λ 2441) was used in the first stages. A five minutes' exposure of an Ordinary plate sufficed to record the whole system between these wave-lengths, and further exposures up to an hour were also made in an unfruitful search for a weaker system. The greater part of the system, excluding only a few of Shaw's more refrangible bands, was afterwards photographed on an Ordinary plate exposed for 20 and 50 min. in a large quartz Littrow instrument (dispersion 5·3 to 2·2 A./mm. in the range λ3320 to λ2530). Only 2–3 c.c. of the liquid tetrachloride was used for these spectrograms. In view of an earlier observation(8) that hot germanium monoxide vapour tends to form a glaze on quartz windows which prevents the taking of satisfactory absorption spectrograms, it may be mentioned here that no such action has been detected in the course of the present observations.

§ 3. BAND-HEAD MEASUREMENTS AND VIBRATIONAL ANALYSIS

In the smaller spectrograms, one of which is reproduced in figure 1 *a*, the GeO bands appear with single (*R*) heads; and in spite of the fact that the conditions in the discharge had not secured the complete elimination of the strongest GeCl bands(7), the GeO heads were measurable over the whole range λ 3320–λ2441. No undue difficulty or uncertainty arose except where the system merges into a continuum which extends from about λ2630 to about λ2380 and has its maximum intensity near λ2560. It was evident from the first measurements that all the bands belong to a single system, which thus extends beyond the GeCl system in both directions, and not only in the short-wave direction as had appeared from the arc observations(1). In the larger spectrogram, a part of which is reproduced in figure 1 *b*, some of the bands appear to have two or even three heads; in such cases all the more certain heads were measured, but only the most refrangible (*R*) head of each band is considered at present. In table 1 the data from this spectrogram are given to six significant figures and those from the smaller spectrograms to five. The incom-

Table 1. Deslandres arrangement of data for band-heads of ^{74}GeO. Wave-lengths in air are printed in Italics, rough estimates of intensity in Italics in parentheses, wave-numbers *in vacuo* in large Roman type and differences between wave-numbers in small Roman type.

v' ↑ / v'' →	0		1		2		3		4		5		6		7		8		9		10
7			*2441·9 (2)* 40939																		
			593																		
6			*2477·8 (3)* 40346*																		
			595																		
5	*2454·8 (4)* 40724	973	*2514·88 (4)* 39751·4																		
	611																				
4	*2492·2 (5)* 40113		‡		*2619·5 (4)* 38164*																
	616				614																
3	*2531·10 (5)* 39496·6		‡		*2662·33 (4)* 37549·9*	962	*2732·3 (4)* 36588*										*3131·6 (1)* 31923*	904	*3222·9 (2)* 31019*	902	*3319·4 (2)* 30117*
	625·4				625		624										626		630		
2	*2571·83 (5)* 38871·2	977 4	*2639·17 (2)* 37893·8	969	*2707·4 (3)* 36925*	961	*2779·71 (6)* 35964·4	953 5	*2855·42 (4)* 35010·9						*3103·1 (3)* 32217*	920	*3194·3 (3)* 31297*	908	*3289·7 (2)* 30389*		
	633 4		632·9						634						640						
1	*2614·43 (5)* 38237·8	976 9	*2682·98 (8)* 37260·9		†		†		*2908·1 (8)* 34377	941	*2989·89 (5)* 33436·3	932	*3075·7 (3)* 32504*	927	*3165·9 (2)* 31577*						
	646·8		642·0						637		645 6										
0	*2659·42 (3)* 37591·0	972·1	*2730·02 (8)* 36618·9	968 2	*2804·17 (10)* 35650·7	959 7	*2881·75 (10)* 34691·0	951 7	*2963·04 (7)* 33739·3	948 6	*3048·76 (5)* 32790·7*										

* Band-heads not hitherto recorded

† The 1 → 3 and 1 → 2 band-heads are obscured by the Ge lines λ2829·09, ν35336·7 and λ2754·59, ν36292·3 respectively.

‡ The 3 → 1 and 4 → 1 band-heads are obscured by the strong continuum; they are near λ2595·3, ν38519 and λ2554·6, ν39133 respectively, and clear of the Ge lines λ2592·55 and λ2556·32.

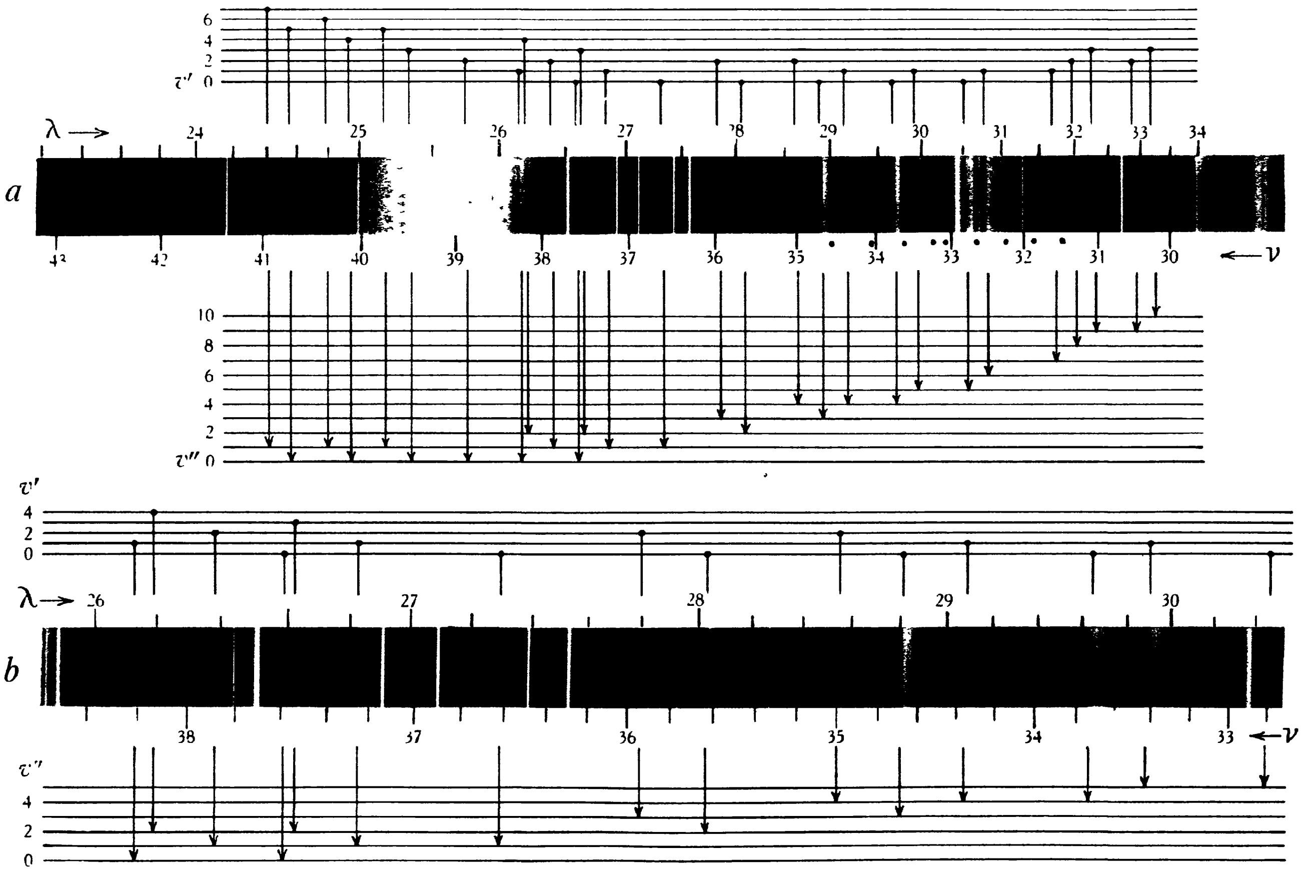

Figure 1. GeO bands in an uncondensed discharge through mixture of O_2 and $GeCl_4$: (*a*) the whole system in medium dispersion (Hilger's E2); (*b*) part of the system in higher dispersion (large Littrow spectrograph). All the strong atomic lines are Ge. The dots mark heads of unquenched GeCl bands, degraded in opposite direction to GeO bands. The black vertical lines in strip (*a*) are due to small holes in the film of the photographic plate and the use of a cylindrical lens in the enlarger.

To face page 546

pleteness of the former data is due to two facts: (i) the length of plate used (12 in.) is not enough to cover the whole system in a single setting, and (ii) the OH bands at λ3064 and λ2811 appeared in the larger spectrogram as a result of an accidental leakage of a trace of water-vapour into the tube. It was decided to rely on the smaller spectrograms for some of the bands rather than use more germanium tetrachloride for another exposure in the larger instrument.

To avoid another table of data, the wave-lengths and rough visual estimates of intensities are inserted above the wave-numbers in the Deslandres scheme (Table I), Shaw's data are omitted, and the band-heads now measured for the first time are denoted by an asterisk. These additions to the former observations pertain chiefly to the higher values of the vibrational quantum number of the lower state ($v''=5$ to 10). The more extensive data are not satisfactorily represented by Shaw's formula, either in its original form as already quoted or with a slight modification of the independent coefficient (ν_e approximately) to allow for the fact that, on the whole, the present wave-numbers are slightly lower than Shaw's. A better representation, especially for the higher values of v' and v'', is afforded by

$$\nu = 37762{\cdot}4 + (651{\cdot}3u' - 4{\cdot}24u'^2) - (985{\cdot}7u'' - 4{\cdot}30u''^2),$$

where, as before, u is written for $v+\frac{1}{2}$. Even this formula leaves residuals ($\nu_{\text{obs.}} - \nu_{\text{calc.}}$) considerably larger than Shaw's, which are surprisingly small. It is the extent of the present data rather than any unusual accuracy that appears to the writers to be the useful feature. An unexplained difficulty arises in the identification of the head of the 0 → 0 band, which, although not expected from the wide-open Condon curve of intensity distribution to be a prominent band of the system, is undoubtedly present and is easily seen near the 3 → 2 band-head in the prints from which figure 1 has been made. Shaw's wave-number, 37596·1, for this head agrees closely with that calculated from any formula, such as his own or the present one, in which the independent coefficient is so chosen that the smallest residuals occur for the best measured heads. The present spectrograms, however, show nothing that can be interpreted as a head in this position, but give either 37591·0 or 37600·8 as the apparent position of the head; the former, which seems the more probable, is about 4 cm^{-1} less, and the latter about 6 cm^{-1} greater, than the calculated wave-number.

We have now to see whether any of the additional band-heads previously mentioned can be attributed to the Ge isotope effect. The relative abundances of the five known isotopes ^{74}Ge, ^{72}Ge, ^{70}Ge, ^{73}Ge, ^{76}Ge are 37·1, 27·3, 21·2, 7·9, 6·5 respectively(9). In the GeO spectrum, therefore, the bands of ^{72}GeO and ^{70}GeO will have about 0·74 and 0·57, respectively, of the intensity of the corresponding bands of the most abundant molecule ^{74}GeO, whilst those of ^{73}GeO and ^{76}GeO, having only about 0·21 and 0·18 of that intensity, may be ignored in the first instance. The vibrational displacements of bands of the lighter molecules ^{72}GeO and ^{70}GeO from those of the heavier molecule ^{74}GeO are in a direction away from the system-origin ν_e throughout the system, and are given by

$$\nu^i - \nu = (\rho - 1)(\nu - \nu_e) \text{ approximately},$$

where the coefficient $\rho - 1$ takes the values $+0{\cdot}00247$ and $+0{\cdot}00507$ respectively, ^{16}O alone being considered with each Ge isotope.

It is reasonable to assign the system in table 1 to ^{74}GeO. As the bands are degraded towards the red, the most favourable bands for the detection of ^{72}GeO and ^{70}GeO heads would normally be those on the high-ν side of the system-origin, 37762·4. In the discharge, however, a continuum extending over a considerable part of this region reduces the chance of detecting these heads, and the only promising bands seem to be the strongest and least confused bands on the low-ν side of ν_e, which are quite clear of the continuum. Additional heads have, in fact, been measured for several such bands and for one band on the high-ν side. The data in table 2, though very fragmentary and of no great accuracy, suggest that some features of the Ge isotope effect have been recognised.

Table 2. Observed band-heads of ^{72}GeO and ^{70}GeO

v', v''	^{72}GeO				^{70}GeO			
	λ^i	ν^i	$\nu^i - \nu$ obs.	calc.	λ^i	ν^i	$\nu^i - \nu$ obs.	calc.
1, 5	2990·64	33427·9	−8·4	−10·6				
0, 4	2963·87	33729·8	−9·5	−9·9	2964·67	33720·7	−18·6	−20·4
0, 2	2804·60	35645·2	−5·5	−5·2	2805·02	35639·9	−10·8	−10·7
0, 1				−2·8	2730·40	36613·9	−5·0	−5·8
1, 1				−1·2	2683·22	37257·6	−3·3	−2·5
2, 0				+2·7	2571·52	38875·9	+4·7	+5·6

§ 4. DISCUSSION

Shaw states that the available evidence favours $^1\Pi \rightarrow {}^1\Sigma$ rather than $^1\Sigma \rightarrow {}^1\Sigma$ as the electronic transition producing the system, the lower state being undoubtedly the ground state since bands of this system occur in absorption$^{(8)}$. In the larger spectrogram of the discharge some of the bands are fairly well resolved over short and isolated ranges remote from band-heads, but the confusion at the heads prevents any attempt at analysis of rotational structure. All that can be stated at present is that the structure appears to be too complex for $^1\Sigma \rightarrow {}^1\Sigma$, and that Shaw's interpretation of the system as the analogue of the CO Fourth Positive system and the corresponding systems, $\mathrm{A}^1\Pi \rightarrow \mathrm{X}^1\Sigma$, of CS and SiO seems the more probable, although the complexity must be due in part to the Ge isotope effect.

Now in the case of what appear to be analogous band-systems of some monohalides of group-IV*b* elements$^{(7)}$, the observed changes of the molecular constants with increase of atomic number and mass of either atom are, as was to be expected, an increase of the electronic separation $\delta\nu_e$ in the $^2\Pi$ ground state, a decrease or "red-shift" of the system-origin ν_e, and a decrease of each of the vibrational coefficients ω_e and $x_e\omega_e$ in both the upper and the lower electronic states. Similar decreases are expected in case of corresponding band-systems of the monoxides and monosulphides of group-IV*b* elements.

In applying the test, we take the data of this GeO system and the above systems of CO$^{(10)}$, CS$^{(11)}$ and SiO$^{(12)}$. For SiS no observations have been recorded, and no system of any of the other molecules has been interpreted as $^1\Pi \rightarrow {}^1\Sigma$. For GeS$^{(3,8)}$ and SnS$^{(13)}$ two and three systems, respectively, have been observed in absorption but the transitions have not been determined; the strong systems, A ← X of GeS and B ← X of SnS, are taken. For SnO the strong system observed in emission and absorption is tentatively ascribed to a transition A$^1\Sigma \rightleftarrows$ X$^1\Sigma$, and the remaining bands have not been satisfactorily interpreted$^{(5)}$. PbO has five emission and absorption systems$^{(14)}$, the strongest of which (B $\rightleftarrows$ X$^1\Sigma$) is taken; for two of the other systems (D $\rightleftarrows$ X and A $\rightleftarrows$ X) rotational analysis has established the transition $^1\Sigma \rightleftarrows {}^1\Sigma$. The PbS absorption bands form five systems$^{(15)}$ the transitions for which are undetermined; either of the two less refrangible systems (A ← X and B ← X) serves the present purpose, and the second is taken as for PbO.

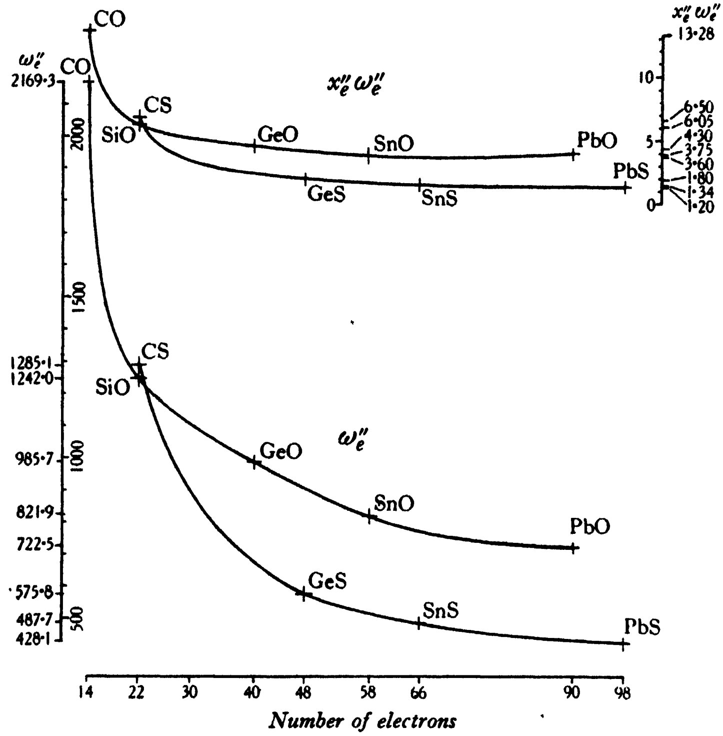

Figure 2. Variations of vibrational coefficients in the ground states of monoxides and monosulphides of group-IV*b* elements.

For the ground states, which are probably all $^1\Sigma$, the results of the test are shown in figure 2, where ω_e'' and $x_e''\omega_e''$ are plotted against the number of electrons in the molecule. The points lie on uninflected curves for the oxides and for the sulphides and the variations are as stated above, with the single exception that $x_e''\omega_e''$ is very slightly smaller, instead of larger, for SnO than for PbO; the difference is so small (0·15 cm^{-1}) that it might well be changed in sign as well as in magnitude as a result of remeasurement of one of the systems concerned. CS and SiO, the only isoelectronic pair of molecules, have very close values of ω_e'' and of $x_e''\omega_e''$, CS having slightly the higher value of each (even on the small scale of reproduction of figure 2, the intersection of the curves can easily be seen, especially for ω_e''). The curves are of the same general form as those given by Shaw$^{(1)}$ for the spectroscopic estimates of the dissociation energies (D_e'') of these ground states. In contrast to the curves

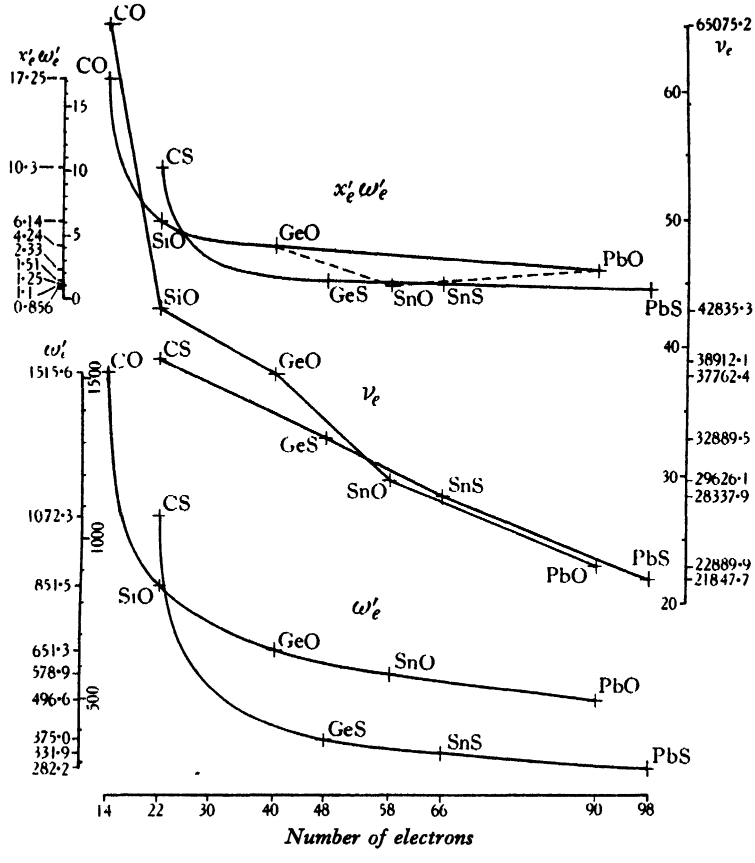

Figure 3. Variations of energies of excitation (ν_e) and vibrational coefficients of the upper states for some band-systems of monoxides and monosulphides of group-IV*b* elements.

for ω_e'' and $x_e''\omega_e''$, however, Shaw's curves for D_e'' show a higher value for PbS than for PbO.

In figure 3, the corresponding curves for the excited states show similar variations in ω_e' and $x_e'\omega_e'$, but with a bigger difference of values for CS and SiO and a much bigger discrepancy in the value of $x_e'\omega_e'$ for SnO. The diagram also includes the graphs of the system-origins, i.e. the energies of excitation of upper electronic states; although no uninflected curves can be drawn through the points the variation is as described above for the monohalides.

To sum up, the observed changes in all the constants (except $x_e'\omega_e'$ of SnO) are of the kind to be expected on the assumption that the band-systems considered correspond to the CO Fourth Positive, $A^1\Pi \rightarrow X^1\Sigma$, but they are not a sufficient proof that such is the case. Although the general decrease of ω_e with increase of molecular mass or electron number is already well known for this group and others, attention has not hitherto been directed, so far as the writers are aware, to the smoothness of the decreases of ω_e and $x_e\omega_e$ shown in figures 2 and 3. From these diagrams it seems safe to predict that SiS (30 electrons) will have a band-system, probably ${}^1\Pi \rightleftarrows {}^1\Sigma$, with bands degraded towards the red and roughly represented by

$$\nu = 37000 + (550u' - 3u'^2) - (850u'' - 3u''^2),$$

the 0 → 0 band being near λ2713. Preparations are being made for a search for this system. Finally it may be mentioned that if the reduced mass (μ)* is used as abscissa instead of the number of electrons, smooth and almost uninflected curves are obtained for all the five constants for the monosulphides, giving about the same predicted values for SiS, but the curves obtained for the monoxides are of a less simple form.

§ 5. ACKNOWLEDGMENTS

The authors are glad to record their indebtedness to Prof. Sir Gilbert Morgan and Dr G. R. Davies for the gift of germanium oxide and other germaniferous material from which the germanium tetrachloride was prepared, and to the Government Grant Committee of the Royal Society for grants for apparatus. They also record their thanks to the Fereday Electors of St John's College, Oxford, for giving one of them (W. J.) the opportunity of taking part in this work, and to the Governors of Collyer's School, Horsham, and the Education Committee of the West Sussex County Council for personal grants to another (L. A. B.).

NOTE ADDED 11 JUNE 1937

Since this paper was communicated, one by Sen Gupta(16) has appeared recording new and extensive observations of this system in the carbon arc with potassium germanifluoride in the lower (+) pole, the arc being found to be steadier with this substance than with the dioxide. Exposures of an hour and a half were made in a quartz Littrow spectrograph (Hilger's E 1) similar to that used by Shaw, of whose recent paper Sen Gupta was evidently unaware since he refers only to the earlier abstract(1). To add a table here for the comparison of the three sets of data now available would involve needless expense, but the following remarks may usefully be made.

Sen Gupta has measured forty-six band-heads extending from λ 3292 to λ 2342 and finds that they are approximately represented by

$$\nu = 37775{\cdot}65 + (651{\cdot}9u' - 4{\cdot}2u'^2) - (981{\cdot}2u'' + 3{\cdot}6u''^2).$$

The present observations include twenty-six of these heads, and for ten of the

* Values of $10^{24}\mu$ (gr.):

CO	11·31	SiO	16·80	GeO	21·62	SnO	23·25	PbO	24·49
CS	14·40	SiS	24·67	GeS	36·67	SnS	41·62	PbS	45·78

twenty-six (including all the strong heads from the 0 → 5 to the 5 → 1) the two sets of measures agree fairly well, the biggest differences ($\nu_{\text{S.G.}} - \nu_{\text{authors}}$) being $-1{\cdot}3$ and $+1{\cdot}1$ cm.$^{-1}$ for the 0 → 1 and 3 → 0 heads. In view of our remark on the 0 → 0 band (*vide supra*, p. 547), it may be noted here that Sen Gupta's result, 37591·6 cm.$^{-1}$, supports our figure rather than Shaw's. For the remaining sixteen heads common to the two investigations the agreement is less satisfactory, particularly large differences ($\nu_{\text{S.G.}} - \nu_{\text{authors}}$) being found for the 2 → 9, 2 → 4, 3 → 3, 2 → 2, 3 → 2 and 4 → 2 heads, namely -23, $+6{\cdot}6$, $+11{\cdot}9$, $+7$, $+9{\cdot}1$ and $+10{\cdot}2$ cm.$^{-1}$ respectively. It seems probable that the identification of these six heads is erroneous in one investigation or the other. Sen Gupta measures the four heads marked † and ‡ in our table 1; and at the high-ν end of the system ($\nu > 39300$ cm.$^{-1}$), where a continuum prevents observation of band-heads in our discharge spectrum, he records eight additional weak heads with $v' = 6, 8, 9, 10$. At the low-ν end ($\nu < 37300$) eight heads (mostly weak) are given only by Sen Gupta, and six (apparently rather stronger) occur only in our table.

Whereas Sen Gupta's wave-lengths, as is to be expected with his dispersion, are given to six significant figures, his wave-numbers are stated to seven, thus implying a precision in the latter which they do not in fact possess. This practice is, of course, to be deprecated.

Sen Gupta observes ^{72}GeO heads of the 2 → 0, 3 → 0 and 4 → 0 bands and ^{70}GeO heads of the 1 → 0, 2 → 0 and 3 → 0 bands. As we have pointed out on p. 548, these bands on the high-ν side of the system-origin are the most favourable for the observation of the Ge isotope effect, but the continuum which occurs here in the discharge obscures them on our spectrograms. It is therefore not surprising that comparison with our table 2 reveals only one such observation common to the two investigations. Sen Gupta erroneously gives ρ as 1·00582 (instead of 1·00507) for ^{70}GeO, and in consequence the agreement between his observed and calculated displacements for this isotope is not, in fact, quite as close as it appears to be in his table 3.

Sen Gupta, like Shaw and ourselves, is inclined to attribute the system to a $^1\Pi \rightarrow {}^1\Sigma$ transition (as in CO and SiO) rather than to a $^1\Sigma \rightarrow {}^1\Sigma$ transition (as in SnO and PbO), and from a consideration of the estimated energies of dissociation he concludes that both upper and lower states of the emitter are derived from the unexcited states of Ge and O, namely $4s^2\,4p^2\,{}^3\mathrm{P}$ and $2s^2\,2p^4\,{}^3\mathrm{P}$.

It is fortunate that, since two different sources have been used and the ways in which the results have been discussed are also different, the two investigations, so far from being a case of needless overlapping, may be regarded as usefully complementary.

REFERENCES

(1) Shaw, R. W. *Phys. Rev.* **43**, 1043, abstract 15 (1933) and **51**, 12 (1937).

(2) Jevons, W. *Proc. roy. Soc.* A, **106**, 174 (1924).

(3) Jevons, W. *Report on Band Spectra of Diatomic Molecules*, Phys. Soc. (1932).

(4) Mahanti, P. C. *Z. Phys.* **68**, 114 (1931).

(5) Connelly, F. C. *Proc. phys. Soc.* **45**, 780 (1933).
(6) Jevons, W. *Nature*, Lond., **113**, 785 (1924).
Mulliken, R. S. *Nature*, Lond., **114**, 349 (1924).
(7) Bashford, L. A., Briscoe, H. V. A. and Jevons, W. *Nature*, Lond., **138**, 883 (1936); *Proc. phys. Soc.* **49**, 532 (1937).
(8) Shapiro, C. V., Gibbs, R. C. and Laubengayer, A. W. *Phys. Rev.* **40**, 354 (1932).
(9) International Table of Stable Isotopes, *Rev. sci. Instrum.* **7**, 334 (1936).
(10) Read, D. N. *Phys. Rev.* **46**, 571 (1934).
(11) Crawford, F. H. and Shurcliff, W. A. *Phys. Rev.* **45**, 860 (1934).
(12) Saper, P. G. *Phys. Rev.* **42**, 498 (1932).
(13) Rochester, G. D. *Proc. roy. Soc.* A, **150**, 668 (1935).
Shawhan, E. N. *Phys. Rev.* **48**, 521 (1935).
(14) Shawhan, E. N. and Morgan, F. *Phys. Rev.* **47**, 377 (1935).
(15) Rochester, G. D. and Howell, H. G. *Proc. roy. Soc.* A, **148**, 157 (1935).
(16) Sen Gupta, A. K. *Z. Phys.* **105**, 487 (1937).

ULTRA-VIOLET BAND SYSTEMS OF SnBr AND SiBr

By W. JEVONS and L. A. BASHFORD,

Departments of Physics and Inorganic Chemistry, Imperial
College, London, S.W. 7

Received 25 June 1937

ABSTRACT. The ultra-violet systems of SnBr and SiBr, as developed in heavy-current tube-discharges through continuous flows of $SnBr_4$ and $SiBr_4$ vapours, are investigated in relation to those of other monohalides of group IV(*b*). For SnBr there are two systems:

(*a*) at λλ3428–3021, of bands degraded towards the further ultra-violet,

$$\nu_{\text{head}}=\left\{\begin{matrix}33094{\cdot}5\\30627{\cdot}5\end{matrix}\right\}-(247{\cdot}1v''-0{\cdot}62v''^2);$$

(*b*) at λλ3709–4255, of bands degraded towards the red,

$$\nu_{\text{head}}=\left\{\begin{matrix}26654{\cdot}3+(162{\cdot}3v'-6{\cdot}8v'^2)\\24557{\cdot}9+163{\cdot}6v'\end{matrix}\right\}-(247{\cdot}1v''-0{\cdot}62v''^2).$$

These appear to be the analogues of the $^2\Sigma\rightarrow{}^2\Pi$ and $^2\Delta\rightarrow{}^2\Pi$ systems, respectively, of SnCl. The electronic separation in the common $^2\Pi$ state is 2467 cm.^{1}, and that in the $^2\Delta$ state is 371 cm.$^{-1}$ Matters of doubt or difficulty in the analysis are discussed.

Miescher's analysis of the SiBr system is modified to include a few hitherto unobserved band-heads and to conform to the doublet transition $^2\Sigma\rightarrow{}^2\Pi$ suggested by analogy to the SiCl and GeBr systems. The more probable of two expressions representing the new measurements is

$$\nu_{\text{head}}=\left\{\begin{matrix}33571{\cdot}0\\33153{\cdot}0\end{matrix}\right\}+(573{\cdot}6u'-3{\cdot}1u'^2)-(425{\cdot}4u''-1{\cdot}5u''^2),$$

where $u=v+\frac{1}{2}$, and the electronic separation in the $^2\Pi$ state is 418 cm.$^{-1}$ The values of the constants for the $^2\Pi$ ground states and $^2\Sigma$ excited states of the monochlorides and monobromides of group IV(*b*) are studied graphically.

§ 1. INTRODUCTION

BAND-SYSTEMS of monohalides of group-IV(*b*) elements have been the subject of several recent investigations, which are summarized in a paper in these *Proceedings*$^{(1)}$ recording the discovery and analysis of ultra-violet emission systems of GeCl and GeBr. These latter resemble the λ2924 system of SiCl$^{(2)}$ and the λ2973 system of SnCl$^{(3, 4)}$ and there seems little doubt that they are due to the same transitions, namely $^2\Sigma\rightarrow{}^2\Pi$, the lower ($^2\Pi$) state being the ground state of each of these four emitters. The same interpretation is indicated by recent analyses of the least refrangible (λ4241) system of SiF$^{(5)}$ and the CCl system near λ2788$^{(6)}$.

In contrast to these six cases of a $^2\Pi$ ground state are four in which the vibrational analysis of the band-system indicated a single electronic level in the ground state but afforded no information as to the nature of the level, which must presumably be $^2\Sigma$, $^2\Pi_{\frac{1}{2}}$ or $^2\Pi_{1\frac{1}{2}}$. Further investigations appear to be necessary to establish the existence or non-existence of a second electronic level which would complete a $^2\Pi$ ground state. In three of the four cases, namely those of PbF, PbCl and PbBr(7, 8) a search for near infra-red subsystems in emission seems desirable, as has previously been pointed out(1). In the remaining case, however, namely that of SiBr, a solution is to be sought, as will be made clear presently (§ 4), in a reinvestigation of the ultra-violet emission system discovered and analysed by Miescher(9).

The band spectra of two other emitters of this subgroup, namely SnBr and SnI, have been sought by Howell and Rochester(10) in high-frequency discharges through externally heated tubes having external electrodes and containing stannic bromide and stannic iodide, respectively. In the case of the bromide the observed spectrum consisted of a very strong continuum beginning at λ6500 and ending abruptly at λ4400, a set of diffuse bands in the region λ4400–λ3750 followed by a continuum with a maximum at λ3600, and another set of diffuse bands whose resemblance to some bands of the λ2973 system of SnCl suggested that they might be due to a chloride impurity. Analysis of the spectrum could not proceed until a comparison with the bromine emission spectrum had been made. No further data were published. In the case of the iodide a similar spectrum was observed, consisting of a visible continuum, diffuse bands from λ4900 onwards with sharp heads at λλ4350 and 4150, and the iodine continuum near λ3460.

In the present paper the SnBr and SiBr band systems are dealt with, and there remain to be investigated those of CF, GeF, SnF, CBr and all five monoiodides.

§ 2. EXPERIMENTAL

A heavy-current tube-discharge through a continuous flow of the tetrabromide vapour was used as the source for each series of observations. Tin tetrabromide was prepared by direct action of bromine on pure metallic tin; the resulting liquid was distilled from the residual tin and the fraction boiling at 200–207° C. was collected (M.P. 30° C.). The preparation of silicon tetrabromide was effected by the passage of a slow current of nitrogen saturated with bromine vapour over purified silicon maintained at a bright red heat; the colourless condensate was purified by distillation in an all-glass apparatus, the fraction of B.P. 153° C. being collected.

The discharge tubes previously used for germanium tetrachloride and tetrabromide, and shown in figure 1 of the earlier paper(1), were again employed. The only modification necessary was that in the case of tin tetrabromide a pyrex bulb containing the substance was sealed directly on to the pyrex inlet of the discharge tube in place of the soda-glass trap T_1, the stopcock B_1 and the adjacent picein joint having to be dispensed with on account of the higher temperatures to which the substance had to be raised in order to maintain the flow into the discharge tube. The transformer and electrical circuit were also the same as in the previous work.

For the investigation of SnBr a quartz spectrograph (Hilger's E 2 size, dispersion 24–17 A./mm. in the range λ3420–λ3020) and the stronger first order of a 2·4 m. concave grating in an Eagle mounting (dispersion 7·4 A./mm.) were used, Ordinary plates being exposed for 15 and 30 min. in the former instrument and for 2, 3½ and 5 hr. in the latter. A quartz Littrow spectrograph (Hilger's E 1, dispersion 6·0–4·3 A./mm. in the range λ3233–λ2875) was employed for the reinvestigation of the ultra-violet system of SiBr, which was well recorded on an Ordinary plate exposed for 25 min. Miescher(9) had used an electrodeless discharge in a tube containing silicon tetrabromide vapour, and a three-prism quartz spectrograph of much smaller dispersion (about 15 A./mm. at λ3000).

§ 3. TWO BAND-SYSTEMS OF SnBr

Predictions. For SnBr we may expect to find a $^2\Sigma \rightarrow {}^2\Pi$ system analogous to the SnCl and GeBr systems which have 0 → 0 bands at λλ3198, 2973 and λλ3094, 2988 respectively, and a $^2\Delta \rightarrow {}^2\Pi$ system analogous to the SnCl system whose 0 → 0 band is at λλ3761, 3487. Useful guidance in the detection and analysis of such systems is to be obtained from a study of the trends of the electronic and vibrational constants for SnCl, GeBr and PbBr as shown in tables 5 and 6 of the previous paper(1) and the additional data for SnCl tabulated in Appendix II of the *Physical Society's Report*(11). The information so derived may briefly be set out as a number of conditions to be satisfied by the coefficients for the three predicted electronic states of SnBr, thus:

$^2\Pi$ ground state:

(*a*) $1150\ (\mathrm{GeBr}) < 2360\ (\mathrm{SnCl}) < \delta\nu_e\ (\mathrm{SnBr})$.

(*b*) $353{\cdot}6\ (\mathrm{SnCl}) > 296{\cdot}6\ (\mathrm{GeBr}) > \omega_e''\ (\mathrm{SnBr}) > 207{\cdot}5\ (\mathrm{PbBr})$.

$^2\Sigma$ excited state:

(*c*) $33582{\cdot}6\ (\mathrm{SnCl}) > 33443{\cdot}4\ (\mathrm{GeBr}) > \nu_e\ (\mathrm{SnBr}) > 20856{\cdot}8\ (\mathrm{PbBr})$.

(*d*) $432{\cdot}5\ (\mathrm{SnCl}) > 383{\cdot}7\ (\mathrm{GeBr}) > \omega_e'\ (\mathrm{SnBr}) > 152{\cdot}5\ (\mathrm{PbBr})$.

$^2\Delta$ excited state:

(*e*) $28665\ (\mathrm{SnCl}) > \nu_e\ (\mathrm{SnBr})$.

(*f*) $274\ (\mathrm{SnCl}) < \delta\nu_e\ (\mathrm{SnBr})$.

(*g*) $301\ (\mathrm{SnCl}) > \omega_e'\ (\mathrm{SnBr})$.

The direction of degradation of the bands in the two expected systems of SnBr is not indicated unambiguously by these numerical conditions, although analogy with SnCl suggests that it will be towards the further ultra-violet in the $^2\Sigma \rightarrow {}^2\Pi$ system and towards the red in the $^2\Delta \rightarrow {}^2\Pi$.

The $^2\Sigma \rightarrow {}^2\Pi$ *system.* In the stannic bromide discharge the simplest, though not the strongest, molecular feature is a pair of progressions of bands degraded towards shorter wave-lengths in the region λ3428–λ3021, as shown in figure 1(*a*). They are presumably the bands which Howell and Rochester[(10)] described as diffuse and regarded as being possibly due to a chloride impurity. These progressions are accompanied by a continuum, not mentioned by Howell and Rochester, extending from about λ2950 to the strong Sn lines λλ2863·32, 2850·61, 2839·99, and having its intensity maximum near the Sn line λ2913·54. Band-head data (to six significant figures) for these progressions from a grating spectrogram are presented in tables 1(*a*) and 2(*a*), which also include data (given to five significant figures) for three heads measured in a quartz prism spectrogram only. It cannot but be of significance that, if regarded as the $v'=0$ progressions of a doublet system, these

Table 1. SnBr band-heads

(*a*) $^2\Sigma \rightarrow {}^2\Pi$ system; bands degraded to further ultra-violet

v', v''	Subband (ii)			Subband (i)		
	λ_{air}	Int.	$\nu_{\text{vac.}}$	λ_{air}	Int.	$\nu_{\text{vac.}}$
0, 0	3021·09	4	33091·0	3263·74	*	30621·5
0, 1	43·58	7	32846·5	90·40	7	30382·7
0, 2	66·42	6	32601·9	3317·22	6	30137·1
0, 3	89·23	5	32361·2	44·56	5	29890·7
0, 4	3112·25	4	32121·8	72·02	4	29647·3
0, 5	35·9	2	31880	98·96	2	29412·4
0, 6	59·0	1 ?	31646	3426·3	1 ?	29178

(*b*) $^2\Delta \rightarrow {}^2\Pi$ system; bands degraded to red

v', v''	Subband (ii)			Subband (i)		
	λ_{air}	Int.	$\nu_{\text{vac.}}$	λ_{air}	Int.	$\nu_{\text{vac.}}$
3, 0	3691·31	0†	27083·0			
2, 0	3709·47	2	26950·4			
3, 1	24·81	1 ?	26839·4			
1, 0	29·37	6	26806·6	4043·95	4	24721·3
2, 1	43·66	5	26704·3			
0, 0	50·84	8	26653·2	70·66	10	24559·1
1, 1		‡		84·70	3	24474·7
0, 1	85·83	7	26406·8	4112·10	10	24311·6
1, 2	98·41	7	26319·5	25·82	5	24230·8
0, 2	3820·78	6*n*	26165·3	53·88	8	24067·1
1, 3	33·74	6	26076·8	67·58	4	23988·0
2, 4	48·89	4	25974·2			
0, 3	57·24	3§	25918·0	96·47	6	23822·8
1, 4	69·56	5	25835·4	4211·10	3	23740·1
2, 5	85·02	4	25732·6			
0, 4				40·37	3	23576·2
1, 5	3906·90	5	25588·4	54·57	1 ?	23497·5
0, 5						
1, 6	44·52	3 ?	25344·6			

Notes:

? Doubtful head.

* Suspected band-head obscured by Sn line λ3262·33, ν30644·1; measure unreliable.

† May be head of SnO band, 0→3.

‡ Subband present but head obscured by atomic line. *n*, nebulous and difficult to locate exactly.

§ Atomic line superposed; measure probably faulty.

progressions give electronic and vibrational separations which satisfy the above requirements, (*a*) and (*b*), of a $^2\Pi$ ground state of SnBr. It will be convenient to refer to the subsystems of lower and higher wave-numbers as (i) and (ii) respectively, as in the case of the GeCl and GeBr systems(1).

With the numeration shown in the tables, the band-heads are represented approximately by

$$\nu = \left\{\begin{matrix}33094{\cdot}5\\30627{\cdot}5\end{matrix}\right\} - (247{\cdot}1v'' - 0{\cdot}62v''^2).$$

Unfortunately the values of v'' cannot be settled beyond doubt, because the strong Sn line λ3262·33, ν30644·1, falls very near the head of a suspected subband which, if real, is the 0 → 0 (i), the first measurable head of this progression being the 0 → 1 (i). The existence of the suspected subband has been assumed;[*] it was suggested by a study of microphotometer traces of a quartz spectrogram, and a rough measure of its head was attempted in a grating spectrogram. Analogy with the case of SnCl suggests that the whole of the difference, 2467 cm.$^{-1}$, of the independent coefficients in this expression represents the electronic interval in the lower ($^2\Pi$) state. This implies an upper state with a single $v' = 0$ level 33094·5 cm.$^{-1}$ above the lower $v'' = 0$ level of the ground state, and it is significant that this satisfies

Table 2. SnBr band-heads (see notes under table 1)

(*a*) $^2\Sigma \rightarrow {}^2\Pi$ system

(ii) $v' = 0$	33091·0	244·5	32846·5	244·6	32601·9	240·7	32361·2	239·4	32121·8	242	31880	232	? 31648
	2469·5		*2463·8*		*2464·8*		*2470·5*		*2474·5*		*2468*		*2470*
(i) $v' = 0$	* 30621·5	238·8	30382·7	245·6	30137·1	246·4	29890·7	243·4	29647·3	236·9	29412·4	234	? 29178

(*b*) $^2\Delta \rightarrow {}^2\Pi$ system

(ii) $v' = 3$	† 27083·0	243·6	? 26839·4										
	132·6		135·1										
$v' = 2$	26950·4	246·1	26704·3						25974·2	241·6	25732·6		
	143·8								138·8		144·2		
$v' = 1$	26806·6		‡		26319·5	242·7	26076·8	241·4	25835·4	246·9	25588·4	243·9	25344·6 ?
	153·4				154·2		158·8						
$v' = 0$	26653·2	246·4	26406·8	241·5	26165 3	247·3	25918·0 §						
	2085·4		—		*2088·7*		*2088·8*		*2095·3*		*2090·9*		
	2094·1		*2095·2*		*2098 2*		*2095·2*		—				
(i) $v' = 1$	24721·3	246·6	24474·7	243·9	24230·8	242·8	23988·0	247·9	23740·1	242·6	23497·5 ?		
	162·2		163·1		163·7		165·2		163·9				
$v' = 0$	24559·1	247·5	24311·6	244·5	24067·1	244·3	23822·8	245·6	23576·2				
$v'' \rightarrow$	0		1		2		3		4		5		6

---

[*] If no such assumption were made, and the first measured head of the progression were taken to be the 0 → 0 (i), the electronic separation would be about 2710 cm.$^{-1}$ instead of 2467, and the values of the vibrational coefficients would be slightly different from those in the above formula.

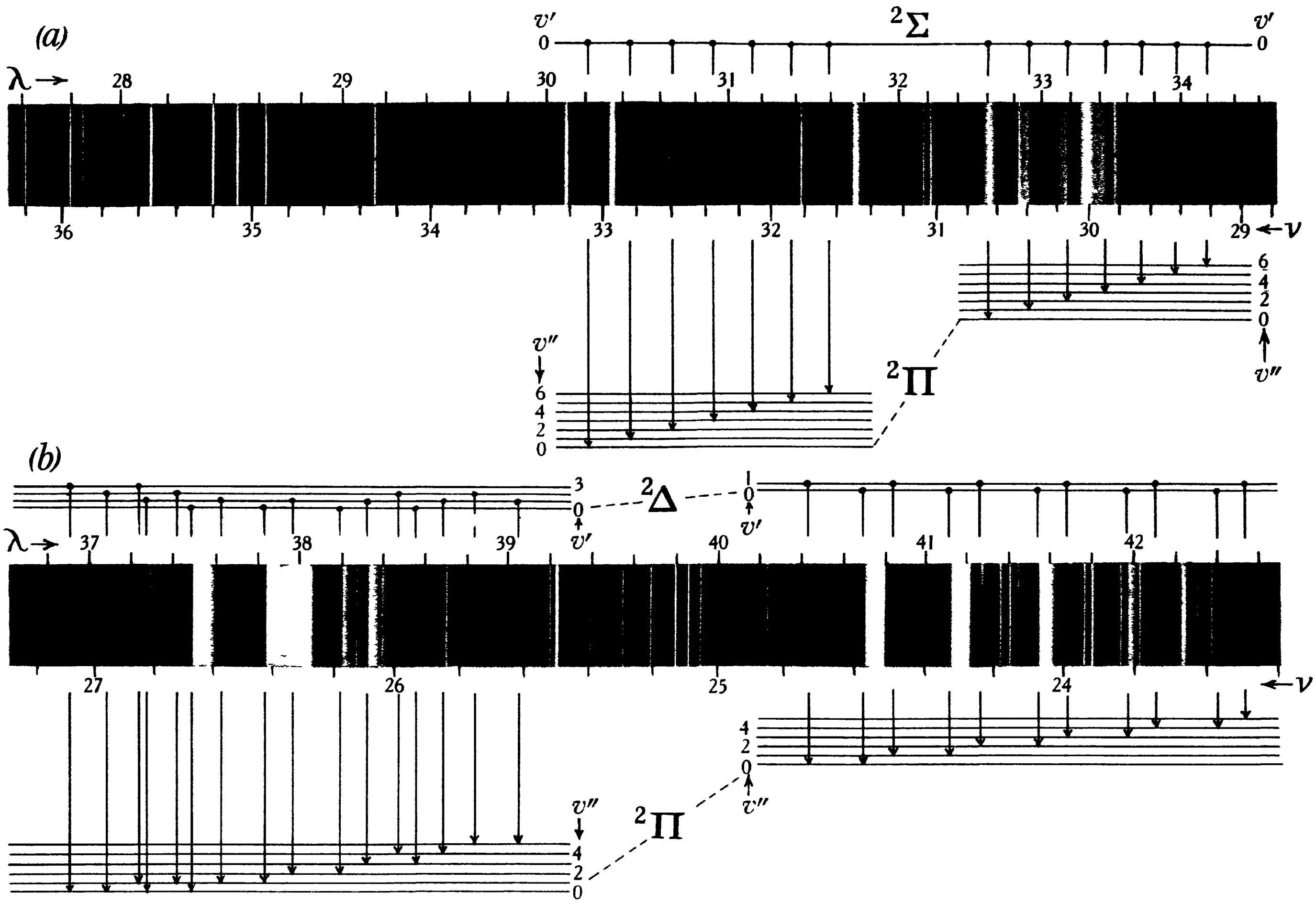

Figure 1. SnBr band systems: (a) λ3021 system, $^2\Sigma \rightarrow {}^2\Pi$ (quartz prism); (b) λ3751 system, $^2\Delta \rightarrow {}^2\Pi$ (grating).

one requirement (*c*) of the $^2\Sigma$ state of SnBr. Although no vibrational levels are observed for the upper state, it is probable that the remaining condition (*d*) is also fulfilled, since the direction of degradation indicates that ω_e' exceeds ω_e'', which is 247·7 cm.$^{-1}$, and in a later section (§ 5) it will be shown that ω_e' would probably be of the order 300 cm.$^{-1}$ It would appear, then, that these two progressions belong to a $^2\Sigma \rightarrow {}^2\Pi$ system.

The $^2\Delta - {}^2\Pi$ *system*. More prominent, but less simple, features of the discharge spectrum are two subsystems of bands degraded towards the red in the region $\lambda 3709$–$\lambda 4255$. Some of these may, perhaps, be identical with some of Howell and Rochester's diffuse bands between $\lambda\lambda 3750$ and 4400, for which no data were published. A grating spectrogram of this region is reproduced in figure 1 (*b*), and the band-head data obtained from it are set out in tables 1 (*b*) and 2 (*b*). It is at once evident that the v'' progressions in each of the subsystems now under consideration have the same vibrational intervals as the two progressions considered above. These subsystems therefore involve the same lower state, $^2\Pi$.

Further, the two prominent v'' progressions with $v' = 0$ are separated from one another by about 2096 cm.$^{-1}$ The difference, 371 cm.$^{-1}$, between this and the electronic interval, 2467, in the $^2\Pi$ state may be interpreted as the electronic interval in the upper state.* As such it will satisfy one of the above requirements (*f*) of a $^2\Delta$ state of SnBr corresponding to the upper state of the $^2\Delta \rightarrow {}^2\Pi$ system of SnCl$^{(4,11)}$. The position of the 0 → 0 (ii) subband, $\nu 26653{\cdot}2$, which gives the energy of one of the $v = 0$ levels of the upper state relative to that of the ground state, satisfies a further requirement (*e*) of the $^2\Delta$ state.

As to the remainder of the analysis shown in table 2 (*b*), while no special difficulty is encountered in the more refrangible subsystem (ii), a little uncertainty remains in the case of the less refrangible (i). The latter consists of a progression of very strong and narrow bands ($v' = 0$) and a progression of relatively weaker bands; and so marked is the difference of appearance in the two progressions, that some hesitation is felt in interpreting the weaker as the $v' = 1$ progression of the same subsystem (i). The doubt is increased by the fact that the resulting mean value, 163·6 cm.$^{-1}$, of the vibrational interval $\omega_{\frac{1}{2}}$ is considerably greater than that in the other subsystem (ii), namely 155·5 cm.$^{-1}$ This inequality is not, of course, a fatal objection, since many cases of a discrepancy between the vibrational coefficients derived from measurements (mostly band-head measurements) in a pair of subsystems have been recorded, as will be seen in Appendix II of this Society's *Report*$^{(11)}$; e.g. in the $^2\Pi$ and $^2\Delta$ states of the analogous emitter SnCl, and in $^2\Pi$ states of ScO, YO, LaO, CaF, SrF, BaF, NO and NS. Only in the last-named case, however, is the discrepancy as great as (it is actually much greater than) the one mentioned here.

The band-heads are approximately represented by

$$\nu = \begin{Bmatrix} 26654{\cdot}3 + (162{\cdot}3v' - 6{\cdot}8v'^2) \\ 24557{\cdot}9 + \;163{\cdot}6v' \end{Bmatrix} - (247{\cdot}1v'' - 0{\cdot}62v''^2).$$

---

* If the electronic interval in the $^2\Pi$ ground state were taken as 2710 cm.$^{-1}$ in accordance with the preceding footnote (p. 558), the interval in this upper state would be $2710 - 2096 = 614$ cm.$^{-1}$, which would also fulfil the condition (*f*) for the predicted $^2\Delta$ state of SnBr.

The function of v'' is identical with that in the expression for the $^2\Sigma \rightarrow {}^2\Pi$ system, since the data for both systems have been used together in the derivation of the coefficients of v'' and v''^2. It should be pointed out that although the value of ω'_e remains rather uncertain the observed vibrational intervals in the upper state satisfy the remaining requirement (g) of a $^2\Delta$ state of SnBr, and there appears to be ample reason for regarding this system as the expected $^2\Delta \rightarrow {}^2\Pi$, in spite of the difficulties to which attention has been drawn.

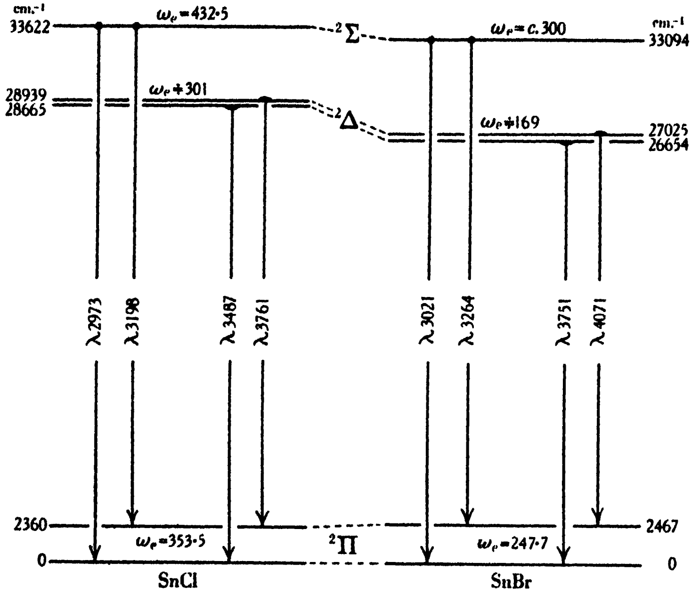

Figure 2. Electronic energy levels and band systems of SnCl and SnBr. The energies given are for the $v = 0$ levels. The rough estimate of ω_e for the $^2\Sigma$ state of SnBr is obtained from figure 4, and not from direct measurement of band heads.

Tables 1 (*b*) and 2 (*b*) exclude a few observed heads (mostly weak or doubtful) for which no place is found in this system. Some of the subbands (ii) appear to have second heads with wave-numbers from 2·5 to 5·0 cm.⁻¹ higher than those of the heads tabulated. Some of the second heads, if real, have displacements of the same order as those in the Br isotope effect, $0{\cdot}0075\,(\nu - \nu_e)$, but others certainly cannot be so interpreted.

The peculiar appearance of the strong narrow subbands (i) referred to above is shown to some extent in the reproduction, figure 1 (*b*), but far more detail is seen in microscopic examination of the grating spectrograms. Thus the strong subband at λ4070·66 extends only as far as an abrupt edge at λ4080·54 and also has between these limits other edges or heads separated by sharp minima at λλ4076·0 and 4078·5. Similarly the neighbouring strong subband whose head is at λ4112·10 ends abruptly at λ4121·45 and has two minima; and the next two extend only from λ4153·88 to λ4155·96 and from λ4196·47 to λ4199·64 respectively. In each case the long-λ edge of the subband simulates a head degraded in the short-λ direction.

In the region (omitted from figure 1) between the two SnBr systems, the spectrograms show the continuum observed by Howell and Rochester (maximum near λ3600). Superposed on this continuum are the unquenched 0 → 1 and 0 → 2 bands of SnO near λ3484 and λ3585(12), and it is possible that the 0 → 3 band near λ3691 is also present (see note † under table 1).

Vibrational energy level diagrams of the two SnBr systems are included in figure 1, and the electronic energy level diagram of SnBr is compared with that of SnCl in figure 2.

§4. A REINVESTIGATION OF THE SiBr BAND-SYSTEM

In view of the fact that seven of the eight analysed band spectra of monohalides of C, Si, Ge and Sn are now known to involve doublet lower states, which are almost certainly $^2\Pi$ ground states, the apparently exceptional case of SiBr needs careful examination. The order of magnitude of the electronic separation to be expected in the ground state of SiBr can roughly be estimated from a consideration of the separations, $\delta\nu_e$, as set out in table 5 of the earlier paper(1). It should be (*a*) larger than that in SiCl (208 cm.$^{-1}$), (*b*) very much smaller than that in GeBr (1150), as is suggested by the ratio of the SiCl and GeCl separations (208: 975), and (*c*) perhaps less than one-half of that in GeCl (975) as is suggested by the ratio of the GeBr and SnCl separations (1150: 2360). It may accordingly be expected to lie between the limits 350 and 450 cm.$^{-1}$

Miescher(9) represented the band-heads in the ultra-violet system of SiBr by

$$\nu = 33570 + (578{\cdot}3u' - 4{\cdot}3u'^2) - (424{\cdot}6u'' - 1{\cdot}3u''^2),$$

where $u = v + \frac{1}{2}$. There seems to be no doubt that this is the system in which some indication of a $^2\Pi$ lower state with an interval of the above order of magnitude should be sought, for in every other respect the values of the constants satisfy the obvious requirement that they should fall between those of the constants for SiCl and GeBr, namely, $\nu_e = 34102{\cdot}7$ and $33443{\cdot}4$ respectively, $\omega_e'' = 535{\cdot}4$ and $296{\cdot}6$, $x_e''\omega_e'' = 2{\cdot}20$ and $0{\cdot}9$, and $\omega_e' = 700$ (approximately) and $383{\cdot}7$.

It will be seen that the intervals between the vibrational levels of the lower state are of the same order of magnitude as the expected electronic separation; and it is possible that this fact might account for the non-detection, with the comparatively small dispersion used by Miescher, of band-heads belonging to the missing subsystem. This might well be the case if the electronic separation happened to be not more than, say, 5 cm.$^{-1}$ greater or less than one of the vibrational intervals $\omega_{\frac{1}{2}}''$, $\omega_{1\frac{1}{2}}''$, $\omega_{2\frac{1}{2}}''$, which the above formula gives as 422·0, 419·4, 416·8 cm.$^{-1}$ respectively.

Dispersion roughly three times that used by Miescher has been employed in obtaining new band-head data, which are shown in tables 3 and 4. The heads detected with certainty are slightly less numerous than those listed by Miescher, but they include a few additions which indicate that his analysis, although the best attainable with the low-dispersion data used, needs a slight but important modification. The 0 → 2, 0 → 1 and 1 → 1 heads in Miescher's analysis are now measured as close doublets, with separations of 4·0, 3·6 and 5·0 cm^{-1}, respectively; and the 0 → 3 head also appears to be a doublet with an even smaller separation. These doublets cannot be satisfactorily interpreted as *P*-form and *Q*-form heads of the bands mentioned, since no corresponding doubling is found in the 0 → 0 band. Nor can they be explained by the Br isotope effect, as the isotopic displacements 0·00325 $(\nu - \nu_e)$ at the positions of these heads are 2·5, 1·1 and 0·7 cm^{-1} respectively, and (except perhaps the first) would be too small for measurement.* Moreover, the

Table 3. SiBr band-heads

Miescher				Authors				
v', v''	λ_{air}	Int.	$\nu_{\text{vac.}}$	v', v''	Sub-band	λ_{air}	Int.	$\nu_{\text{vac.}}$
1, 8	3233·6	2	30916	1, 8	(ii)	3233·34	0*n*	30918·9
2, 9	17·4	2	31072	2, 9	(ii)	17·27	1	31073·3
1, 7	3192·0	4	319	1, 7	(ii)	3192·38	3	315·6
2, 8	76·3	4	474	2, 8	(ii)	75·46	4	482·4
0, 5	67·5	5	562	0, 5	(ii)	67·49	5	561·6
				1, 5	(i)	52·45	6 ?	712·4
1, 6	51·7	6	720	1, 6	(ii)	51·68	6	720·0
2, 7	36·0	4	879	2, 7	(ii)	36·96	6 ?	868·8
0, 4	26·6	7	974	0, 4	(ii)	26·63	8	974·1
1, 5	11·3	7	32132	1, 5	(ii)	11·55	8	32129·0
2, 6	3096·7	4	283	2, 6	(ii)	3096·46	4 ?	285·6
0, 3	86·9	8	386	0, 3	(ii)	86·78	10*d*	386·8
				0, 2	(i)			
1, 4	72·2	7	541	1, 4	(ii)	72·31	9	539·5
2, 5	57·6	3	696	2, 5	(ii)	58·01	4 ?	691·5
0, 2	47·5	9	804	0, 2	(ii)	47·68	20	802·3
				0, 1	(i)	47·31	20	806·3
1, 3	33·4	6	957	1, 3	(ii)	33·65	12	954·0
				0, 1	(ii)	09·17	15	33222·1
0, 1	08·8	10	33226	0, 0	(i)	08·84	25	225·7
1, 2	2995·0	5	379	1, 1	(i)	2995·69	6*n*	371·6
2, 3	82·3	4	521					
0, 0	71·2	6	647	0, 0	(ii)	71·29	8	645·6
				1, 1	(ii)	58·73	10	788·5
1, 1	58·3	7	793	1, 0	(i)	58·29	10	793·5
2, 2	45·7	5	938					
1, 0	21·8	8	215	1, 0	(ii)	21·98	10	34213·3
2, 1	10·3	4	351	2, 1	(ii)	10·25	5 ?	351·3
2, 0	2874·9	4	774	2, 0	(i)	2874·96	2	772·9

? Doubtful head.
n, nebulous and difficult to locate exactly
d, probably double, but not measured as such on account of an atomic line.

---

* No band-heads attributable to the Br or the Si isotope effect have been measured, with the possible exception of a doubtful one at λ2922·25, ν34210·2, which may be the ^{28}Si^{81}Br head of the 1→0 subband (ii) if the head at ν34213·3 in tables 3 and 4 is attributed to the equally abundant emitter ^{28}Si^{79}Br, the observed and calculated displacements being 3·1 and 2·1 cm^{-1} respectively. Observation of the isotope effects is expected to be rendered more difficult and unreliable by the doubling of heads due to the near equality of the electronic and vibrational separations discussed in this section.

additional heads appear to be quite genuine and cannot be ignored as fortuitous blends of rotational structure lines. It therefore seems reasonable to accept them as indications of the missing subsystem; and, as table 4 shows, they can be included in either of two alternative arrangements of this part of a doublet system, both of which are presented since neither appears to be markedly inferior to the other.

Table 4. Two possible arrangements of a part of the SiBr doublet system

(*a*)

2	(ii)	34772·9	421·6	34351·3								32691·5
	(i)	—		—								—
		559·6		557·8								562·5
		—		—								—
1	(ii)	34213·3	419·8	33793·5	421·9	33371·6	417·6	32954·0	414·5	32539·5	410·5	32129·0
		424·8										
	(i)	33788·5		—		—		—		—		—
		567·7		567·8		565·3		567·2		565·4		567·4
		566·4		—		—		—		—		—
0	(ii)	33645·6	419·9	33225·7	419·4	32806·3	419·5	32386·8	412·7	31974·1	412·5	31561·6
		423·5		*423·4*								
↑ v'	(i)	33222·1	419·8	32802·3		—		—		—		—
v'' →		0		1		2		3		4		5

(*b*)

2	(ii)	34772·9	421·6	34351·3								32691·5
	(i)	—		—								—
		559·6		562·8								562·5
		—		—								—
1	(ii)	34213·3	424·8	33788·5				32954·0	414·5	32539·5	410·5	32129·0
		419·8		*416·9*								*416·6*
	(i)	33793·5	421·9	33371·6				—		—		31712·4
		567·7		566·4				567·2		565·4		567·4
		567·8		565·3				—		—		—
0	(ii)	33645·6	423·5	33222·1	419·8	32802·3	415·5	32386·8	412·7	31974·1	412·5	31561·6
		419·9		*415·8*		*415·5*						
↑ v'	(i)	33225·7	419·4	32806·3	419·5	32386·8		—		—		—
v''		0		1		2		3		4		5

In table 4(*a*) the three components of slightly *larger* ν are regarded as the 0 → 2, 0 → 1 and 1 → 1 heads in the more complete subsystem (ii), and those of slightly *smaller* ν as the 0 → 1, 0 → 0 and 1 → 1 heads in the hitherto undetected subsystem (i). With this interpretation the band-heads of the whole system are approximately represented by the expression given in a preliminary note(13), namely

$$\nu = \left\{\begin{matrix}33571{\cdot}2\\33147{\cdot}2\end{matrix}\right\} + (574{\cdot}8u' - 4{\cdot}0u'^2) - (424{\cdot}7u'' - 1{\cdot}4u''^2).$$

This gives 424 cm.$^{-1}$ as the electronic interval in the lower ($^2\Pi$) state, and, apart from the inclusion of the smaller of the two independent coefficients, differs but slightly from Miescher's expression.

In table 4(*b*) the quantum numerations of the components of each of the three observed doublets are interchanged, so that the *smaller-ν* components become the 0 → 2, 0 → 1 and 1 → 1 heads in subsystem (ii), and the *larger-ν* components the 0 → 1, 0 → 0 and 1 → 0 heads in subsystem (i). A single head is transposed from 1 → 2 (ii) to 1 → 1 (i); another head, suspected to be a close doublet but not measured as such, appears not only as 0 → 3 (ii) but also as 0 → 2 (i) (this is quite reasonable but is numerically unsatisfactory in table 4(*a*)); and another probable head, hitherto unallocated, finds a place as 1 → 5 (i). With this arrangement, the band-heads are approximately represented by

$$\nu=\begin{Bmatrix}33571\cdot0\\33153\cdot0\end{Bmatrix}+(573\cdot6u'-3\cdot1u'^2)-(425\cdot4u''-1\cdot5u''^2),$$

and the estimate of the electronic interval in the lower ($^2\Pi$) state is rather lower, namely 418 cm.$^{-1}$

The v', v'' numbering for the latter arrangement, which a study of the vibrational separations seems to indicate as the more satisfactory of the two, is provisionally adopted and also included in table 3. Whichever arrangement is adopted there is no longer any reason to regard SiBr as an exceptional case in which the ground state is single rather than a $^2\Pi$ state with an electronic separation of the expected order of magnitude.

An examination of the intensities of the bands supports this conclusion; for both in the reproduction published by Miescher and also in the new spectrograms Miescher's 0 → 2, 0 → 1 and 1 → 1 bands appear to be abnormally strong in comparison with his 0 → 0 band, the reason being, according to the present interpretation, that another subband is superposed on each of them.

The numerical results of this study were included, for the sake of completeness, in tables 5 and 6 of the earlier paper$^{(1)}$.

§ 5. $^2\Pi$ AND $^2\Sigma$ STATES OF GROUP-IV(*b*) MONOCHLORIDES AND MONOBROMIDES

In another recent paper in these *Proceedings*$^{(14)}$, on the ultra-violet band-system of GeO, the available data for certain band-systems of the monoxides and monosulphides of group-IV(*b*) elements were studied graphically. Both for the ground states and also for the excited states in the selected systems, many of which are known to be $^1\Pi \rightarrow {}^1\Sigma$, the decrease of each of the vibrational coefficients ω_e and $x_e\omega_e$ with the increase of the number of electrons in the molecule follows an uninflected curve, while no such smoothness is shown by the decrease of electronic energy ν_e of the upper state.

Of the spectroscopic investigations of the monohalides of this subgroup only those of the monochlorides and monobromides are sufficiently complete for a similar graphical test to be applied. As $^2\Delta \rightarrow {}^2\Pi$ systems are known for only SnCl and SnBr, the test must be restricted to the $^2\Sigma \rightarrow {}^2\Pi$ systems and the PbCl and PbBr systems, the data for which are collected in tables 5 and 6 of the paper on GeCl and GeBr(1). Further, $x_e\omega_e$ is excluded from the test as in some cases it is either unknown or only roughly estimated.

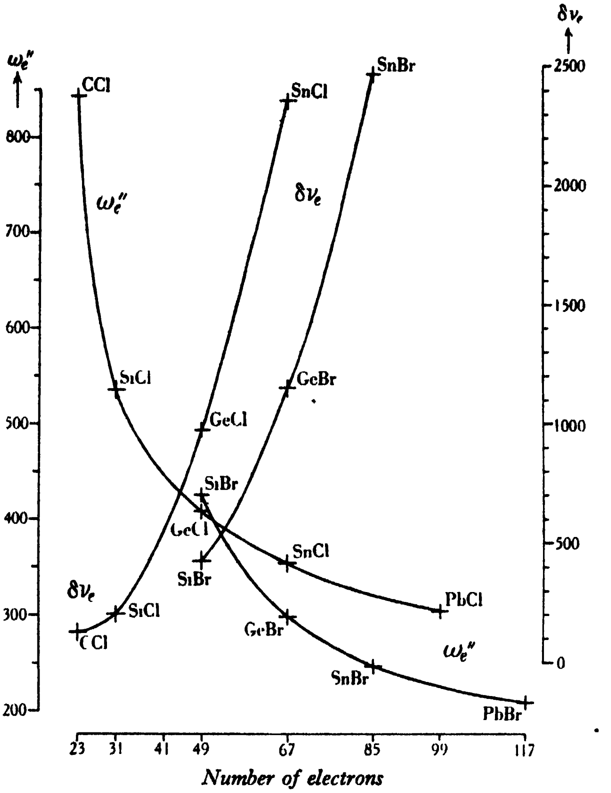

Figure 3. Variations of the electronic separations ($\delta\nu_e$) and vibrational coefficients (ω_e'') in the $^2\Pi$ ground states of monochlorides and monobromides of group-IV(*b*) elements. The numerical values are given in table 5 of a previous paper(1). The tentative results, $\delta\nu_e = 0$, for PbCl and PbBr are omitted.

The results for the lower states are shown in figure 3. For ω_e'' of the chlorides and bromides (including PbCl and PbBr), two uninflected curves are obtained, which are similar in form and disposition to those for ω_e'' of the oxides and sulphides, respectively; the curves intersect between the points for the two isoelectronic pairs of emitters GeCl, SiBr and SnCl, GeBr. A pair of uninflected curves is also obtained for the electronic separation $\delta\nu_e$ in all emitters except PbCl and PbBr, for each of which only a single electronic level has so far been found in the ground state. These regularities seem to support the view that similar states are in fact being compared, and that since some of them are known to be $^2\Pi$ ground states all must be.

Figure 4 shows the results for the upper states, some of which are known to be, and all may be, $^2\Sigma$. In the case of ω_e' the points for all the chlorides except PbCl lie on a curve of the same form as that for the oxides, but in the absence of observational data for CBr and SnBr little can be said of the bromides, except that the intersection of the two ω_e' graphs is similar to that of the two ω_e'' curves in figure 3. The value of ω_e' for SnBr would appear to be of the order 300 cm^{-1} In the case of

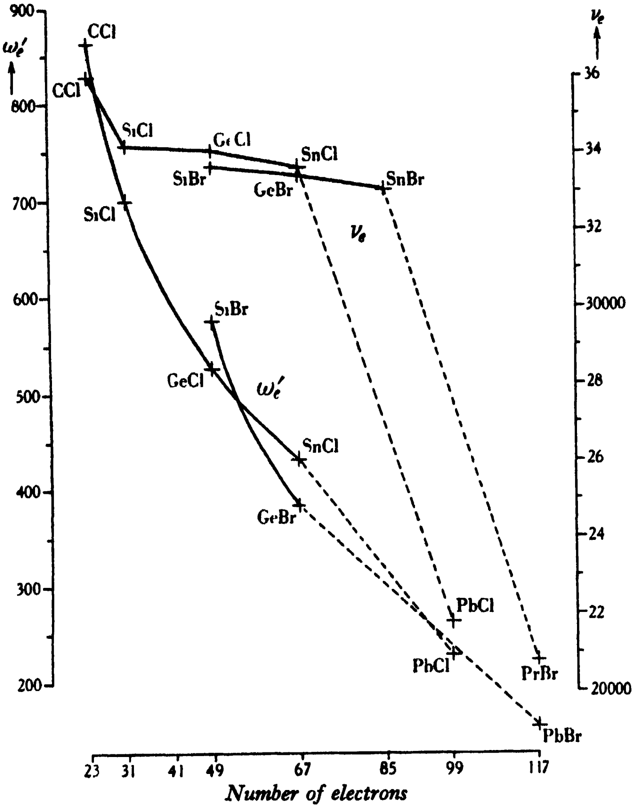

Figure 4. Variations of the electronic energies (subsystem origins ν_e, or wave-numbers of 0→0 subbands) and vibrational coefficients (ω_e') for $^2\Sigma$ excited states of monochlorides and monobromides of group-IV(*b*) elements, probably all analogous states except for PbCl and PbBr. Numerical values are given in table 6 of a previous paper(1).

the electronic energy ν_e the result is the same as for the oxides and sulphides, no simple curves being obtained; and, moreover, the sudden falls to the points for PbCl and PbBr, considered together with the change in the ω_e' curve beyond SnCl, suggest that the upper states of PbCl and PbBr may not be strictly analogous to those of the other emitters.

If, instead of the number of electrons in the molecule, the reduced mass* (μ) is used as abscissa, the graphs obtained are somewhat similar to those in figures 3

* Values of $10^{24}\mu$ (g.):

CCl	14·78	SiCl	25·83	GeCl	39·29	SnCl	45·02	PbCl	49·92
CBr	17·20	SiBr	34·24	GeBr	62·73	SnBr	78·76	PbBr	95·08

and 4, except that for the chlorides both the ω_e' curve and the ω_e'' curve have inflections between the GeCl and SnCl points. This loss of simplicity of the curves is similar to that previously noticed in the case of the monoxides.

§ 6. ACKNOWLEDGMENTS

One of the authors (W. J.) has pleasure in expressing his indebtedness to the Fereday Electors of St John's College, Oxford, for enabling him to take part in the work, to Prof. G. P. Thomson for excellent laboratory facilities, and to the Government Grant Committee of the Royal Society for grants for apparatus. The other (L. A. B.) records his thanks to the Governors of Collyer's School, Horsham, and the Education Committee of the West Sussex County Council for personal grants. The authors also have pleasure in thanking Prof. H. Dingle for helpful discussions of this and other papers of the series.

REFERENCES

(1) Jevons, W., Bashford, L. A. and Briscoe, H. V. A. *Proc. phys. Soc.* **49**, 532 (1937).
(2) Jevons, W. *Proc. phys. Soc.* **48**, 563 (1936).
(3) Jevons, W. *Proc. roy. Soc.* A, **110**, 365 (1926).
(4) Ferguson, W. F. C. *Phys. Rev.* **32**, 607 (1929).
(5) Asundi, R. K. and Samuel, R. *Proc. Ind. Acad. Sci.* **3**, 346 (1936).
(6) Asundi, R. K. and Karim, S. M. *Curr. Sci.* **9**, 474 (1937).
(7) Morgan, F. *Phys. Rev.* **49**, 47 (1936).
(8) Rochester, G. D. *Proc. roy. Soc.* A, **153**, 410 (1936).
(9) Miescher, E. *Helv. Phys. Acta*, **8**, 587 (1935).
(10) Howell, H. G. and Rochester, G. D. *Proc. Univ. Durham phil. Soc.* **9**, 126 (1934).
(11) Jevons, W. *Report on Band Spectra of Diatomic Molecules*, Phys. Soc. (1932).
(12) Connelly, F. C. *Proc. phys. Soc.* **45**, 780 (1933).
(13) Bashford, L. A., Briscoe, H. V. A. and Jevons, W. *Nature*, Lond., **138**, 883 (1936).
(14) Jevons, W., Bashford, L. A. and Briscoe, H. V. A. *Proc. phys. Soc.* **49**, 543 (1937).

ABSORPTION SPECTRA OF SOME CARBON AND TIN HALIDES IN THE VAPOUR STATE*

By Y. P. PARTI and R. SAMUEL

Received 15 *February* 1937

ABSTRACT. The absorption spectra of the vapours of $SnCl_4$, $SnBr_4$ and of molecules of the types CX_4, CHX_3, and CH_2X_2 (X = Cl, Br, I) are investigated. From the number of maxima and their energy differences, and a comparison of the beginnings of the various absorption regions with thermochemical data, it is concluded that the first process of photodissociation corresponds not to the process $MX_4 \rightarrow MX_3 + X$ but to $MX_4 \rightarrow MX_2(^1\Sigma) + 2X$ etc.; the further absorption regions are due to one or two excited halogen atoms.

§ 1. INTRODUCTION

Recently it has been shown(1) that the photodissociation of polyatomic molecules, formed by atoms of groups V and VI of the periodic table, follows different courses according to the state of valency of the central atom. In lower states of valency, i.e. as long as chemical combination is brought about by the p electrons of the central atom, the bond energies D_B are decisive for the photolytic process. In the state of maximal valency involving the activation of the two electrons of the group s^2, the thermochemical difference D_T of the atomic energy of formation of this molecule and the corresponding one of lower valency determines the decomposition by light. According to Heitler and London's(2) conception, the unexcited carbon atom is divalent only from the point of view of a pair-bond theory of valency, and, whichever its partner may be, it becomes tetravalent by excitation to a term of sp^3 or p^4. Accordingly the same ideas should apply to tetrahalides formed by atoms of group IV in their maximal state of valency. We have reinvestigated the absorption spectra of some molecules of this type in the vapour state and present the result in this paper. They lead, as will be seen, to a new interpretation of the photodissociation of simple organic compounds. The products of decomposition by light of a molecule of the type CH_4 are $CH_2 + 2H$, CH_2 being a saturated molecule in a $^1\Sigma$ state which does not possess free valencies as $SnCl_2$, for instance, does. This will lead to a reinterpretation of certain absorption spectra of organic molecules because it shows that the photodissociation sometimes takes place, not through the rupture of a bond according to its adiabatic energy of dissociation, but by the excitation of the molecule to the repulsive excited term involving unexcited radicals and atoms. The energy of such an excitation is generally lower than a true bond energy. The bond energies themselves can then be found from the measured values of D_T. In the present paper, dealing with absorption in the quartz ultra-violet, at first only such bond energies, involving unexcited carbon atoms ($s^2p^2\ {}^3\mathrm{P}$), are investigated.

---

* A preliminary report on this subject has been published in *Current Science*.

§ 2. EXPERIMENTAL

The experimental method has been the same as that described earlier; but for some of the substances we took additional plates on a small Hilger quartz spectrograph of exceptionally good transparency, using the positive crater of the carbon arc as a source of light. By means of plates treated with mineral oil we could photograph the spectrum down to $\lambda 1950$ with a few minutes' exposure. Figures 1–3 show microphotometer records of the spectra of CI_4 and CHI_3 as examples of the ordinary method described earlier and a record of the $CHBr_3$ spectrum as an example of the second method. It will be seen that the instability of the carbon arc and the oiling of the plate, whereby a strong general background is often produced owing to fluorescence on account of scattered light, make this method much less reliable. But while the last absorption limit is rather uncertain and falls just short of the region where the plate becomes entirely blank, the preceding two maxima and limits can be determined quite well. The values finally accepted are the weighted means from several spectrograms.

Some further remarks on the determination of the long-wave limits appear necessary. The first beginning of continuous absorption is never well defined. In $SnCl_4$, for instance, with an absorption cell of length 10 cm. at room-temperature ($\sim 25°$ C.) and a vapour pressure of about 1 mm. of mercury, it is at $\lambda 2450$ A. With 9 mm. of mercury and a cell of length 80 cm., it reaches 2570 A.; and with the temperature increased to 300° C. and the pressure to 18 mm. of mercury, with the same cell, the limit goes up to 2820 A. This difficulty in the determination of the true long-wave limit for the vibrationless molecule has been discussed by Jan Khan and Samuel(1), and it has been shown that this large red shift is simply due to the absorption from higher vibrational levels of the ground state. The higher the level the less it contributes to the selective absorption, and the contribution of higher levels beyond a particular one according to the particular conditions (length of absorbing layer, temperature, and vapour pressure) will fall below the last value indicated by the photographic plate on account of its threshold value. An increase of any of the above three parameters increases the number of molecules in higher levels, either by an increase of the population of the higher ones at the expense of the lowest or simply by an increase in the absolute number of molecules. A red shift of the first long-wave limit results naturally, but this has no physical meaning for the vibrationless molecule, either as to its dissociation energy, or as to the shape of its potential curve, or as to the character of the bond. Since there appears to be some confusion on this point in the literature, attention may be drawn to two simple experimental facts which establish this interpretation. First,

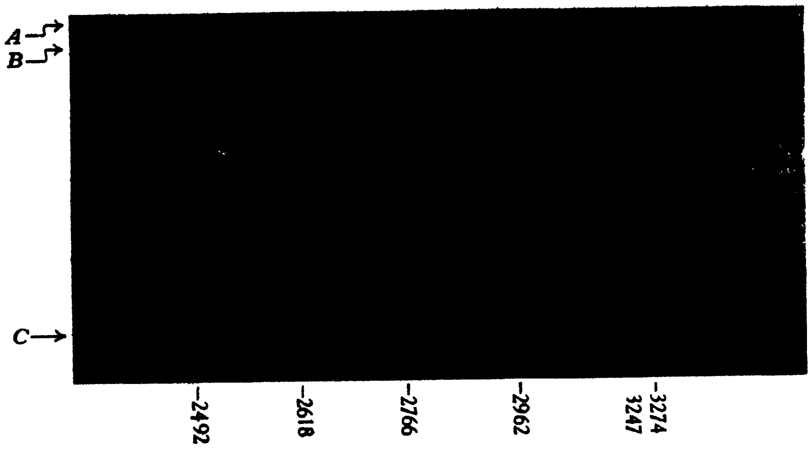

Figure 1. CI_4.

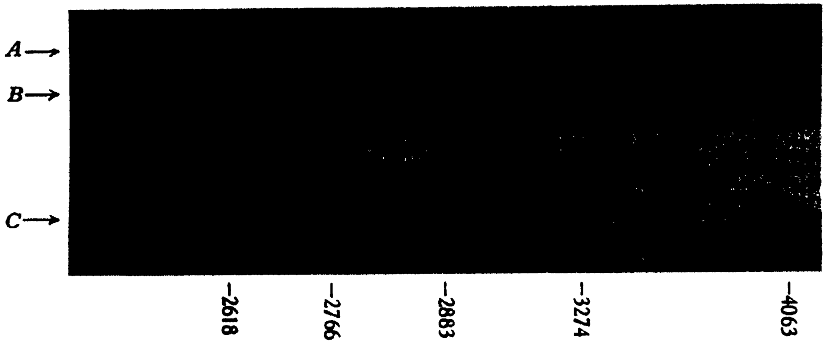

Figure 2. CHI_3.

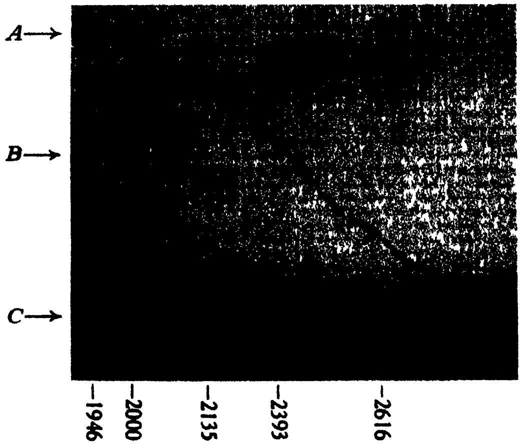

Figure 3. $CHBr_3$.

Microphotometer records of absorption spectra: *A*, absorption spectrum; *B*, source of light; *C*, copper arc.

it can be seen from molecules exhibiting band spectra that the absorption is indeed by no means confined to the vibrationless molecule. For instance, bromine vapour in a layer of 10 cm. and a pressure of about 5–10 cm. exhibits the five lowest vibrational levels of the ground state of Br_2. Again in SO_2 in a 10-cm. cell and pressure of the order of some tenths of a millimeter the first three levels of the symmetric and antisymmetric valence vibration appear. These higher vibrational levels of the ground state are important, not only with regard to the actual energy-difference between the higher and the lowest level, but even more on account of the change of relative position of two potential curves with increase of internuclear distance. Secondly, in certain favourable cases we are able to estimate the beginning of absorption of a continuous spectrum independently of the experimental long-wave limit. If, for instance, a molecule decomposes under the action of light in such a way that in the first region of selective absorption one of the dissociation products is an unexcited Br atom in its ground state $^2P_{\frac{3}{2}}$, and in the second absorption region an excited Br atom ($^2P_{\frac{1}{2}}$), the absorption spectrum will show two maxima whose energy-difference is approximately equal to the term difference $^2P_{\frac{1}{2}}-{}^2P_{\frac{3}{2}}$ of Br, e.g. 3685 $cm.^{-1}$ or about 10·5 kcal./mol. The position of these two maxima will not be influenced very much by the experimental conditions; and the more nearly parallel the two repulsive curves concerned run, the better will the energy difference between the maxima agree with the energy of excitation of the Br atom. The two maxima preserving their wave-lengths, the point of retransmission between them also has a fairly constant wave-length. This latter point is near the beginning of the second absorption region and hence the true long-wave limit of the first absorption region of the vibrationless molecule should be found at a distance towards the red from the point of retransmission which corresponds approximately to the excitation energy of Br($^2P_{\frac{1}{2}}$) or the energy-difference of the two maxima. Obviously, only for one of the many possible values of the first long-wave limit is this necessary condition valid, and empirically this particular value lies rather more often than not in the vicinity of the maximum. As a rule the value of its extinction coefficient is of the order of one-tenth of that of the maximum. Such a value of the first long-wave limit generally appears, e.g., in a 10-cm. absorption tube at room-temperature with a pressure of 1–10 mm. of mercury. Indeed, in recent years wherever a correlation of long-wave limits to photolytic processes has been possible, whether in the case of gases and vapours at room-temperature or even in the experiments of Franck and his collaborators on alkali and silver salts of high melting-points, the first beginning of absorption has, with a number of absorbing molecules generally been found to be roughly equal to that obtaining under the conditions described above, while measurements with absorbing layers of 10 or 30 m. have not led to values related to thermochemically measured energies, and such observations do not concern the vibrationless molecule.

Table 1 displays the wave-lengths of the beginnings and maxima of absorption measured by us under conditions such as those outlined above. They are weighted means from several spectrograms, each measured directly on the microphotometer records.

Table 1

Molecule	First long-wave limit	First maximum	Second long-wave limit	Second maximum	Third long-wave limit	Third maximum
$SnCl_4$	~2500	—	—	—	—	—
$SnBr_4$	3471	3063	2915	2728	2442	—
CI_4	3930	3449	3177	3010	2795	2700
CHI_3	4230	3429	3229	3029	2872	2828
CH_2I_2	3499	2955	2640	2474	2365	2220
CBr_4	2932	2525	2453	—	—	—
$CHBr_3$	2750	2559	2497	2275	2195 (?)	—
CCl_4	~2350	—	—	—	—	—
$CHCl_3$	~2200	—	—	—	—	—

§ 3. SPECTRA OF $SnCl_4$ AND $SnBr_4$

There exists only one molecule of the CH_4 type, i.e. $SnCl_4$, whose energy of formation (Q) is known along with that of the corresponding dihalide $SnCl_2$. Consequently we took this as the starting point. The thermochemical values in kcal./mol. are,* for $SnCl_4$: $Q = 126{\cdot}4$, $S(\text{Sn}) = 69{\cdot}9$, $S(\text{SnCl}_4) = 9{\cdot}6$, and for $SnCl_2$: $Q = 80{\cdot}8$, $S = 26{\cdot}7$. By means of Born's cycle we obtain, with $D(\text{Cl}_2) = 56{\cdot}9$, the values $D(\text{SnCl}_4) = 300{\cdot}5$ and $D(\text{SnCl}_2) = 180{\cdot}9$. The difference D_T of these figures is 120 kcal./mol.

The absorption spectrum of $SnCl_4$ has been investigated independently by Sharma(3) and by Hukumoto(4). While the latter records a long-wave limit of continuous absorption at λ2820 or 99 kcal./mol., the former finds two regions of absorption with beginnings at λ3400 and λ2750. We have ascertained that Sharma's first maximum belongs to free Cl_2 molecules.†

With an absorption tube of length 10 cm. and vapour pressure of 1–10 mm. of mercury the beginning of absorption of $SnCl_4$ lies at about λ2450 to 2500 A., corresponding to 116 to 114 kcal./mol., i.e. values in agreement with that of D_T calculated from thermochemical data, namely 120 kcal./mol.

This close agreement between D_T and the first long-wave limit of molecules of MX_4 type will be further confirmed by the experimental results set out below. At the present stage it is not necessary to attach too much importance to the actual value, which depends on the pressure in the absorption tube, and it is sufficient to conclude that a long-wave limit, measured under reasonable conditions, does indeed fall near about the region indicated by the energy difference $D(\mathrm{SnCl_4}) - D(\mathrm{SnCl_2})$.

---

* All values are taken from Landolt-Boernstein's tables. The procedure and the symbols used are the same as in Jan Khan and Samuel's paper(1).

† It is well known that Cl_2 at low pressures exhibits only the continuous spectrum associated with its band spectrum, on account of the particular position of the potential curve of the excited term; the absorption maximum of this continuous lies at about λ3350. Sharma has not recorded the maximum of his first region of selective absorption, but we also obtained it sometimes after a fresh refilling of the apparatus; it disappeared gradually on evacuating and repeated careful washing of the absorption cell with $SnCl_4$ vapour. It can be reproduced by decomposition of the $SnCl_4$ in the side bulb; the saturation pressure of $SnCl_4$ is about 20 mm. of mercury at room temperature, and this maximum appeared always when the manometer shows a pressure of 3–10 cm.

Definite confirmation as to the products of photodissociation have been obtained from the spectrum of $\mathrm{SnBr_4}$. Its heat of formation from the elements is not known, but $Q(\mathrm{SnBr_2})$ is measured as 61·5 kcal./mol. and by estimating S as 22 kcal./mol., we can calculate $D(\mathrm{SnBr_2})$ by means of Born's cycle to be about 160 kcal./mol.

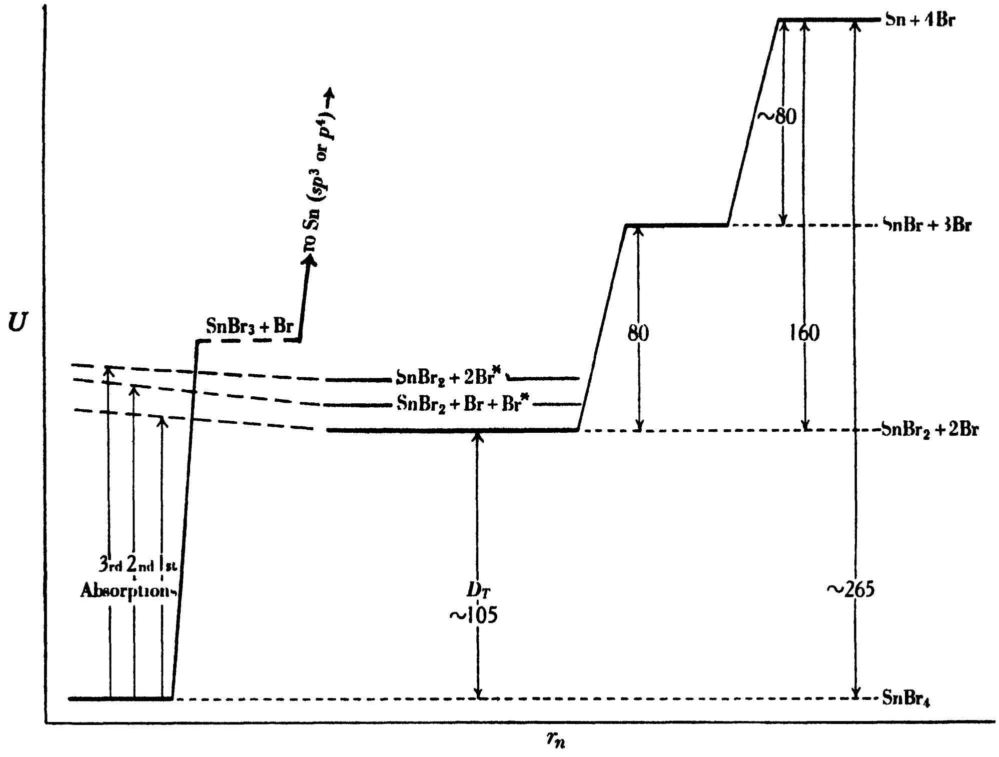

Figure 4 Simplified Franck-Condon diagram of the lower electronic terms of $\mathrm{SnBr_4}$.

The values of $D(\mathrm{SnCl_2})$ and $D(\mathrm{SnCl_4})$ are in the ratio of about 3 : 5, and if such an extrapolation is possible at all, $D(\mathrm{SnBr_4})$ should be 66 per cent greater than $D(\mathrm{SnBr_2})$, i.e. about 265 kcal./mol. Assuming that the photolytic process takes place according to the equation

$$\mathrm{SnBr_4} + h\nu = \mathrm{SnBr_2} + 2\mathrm{Br},$$

we can represent the position of the electronic terms and their dissociation in the simplified Franck-Condon diagram of figure 4, which also will serve as an example for the molecules discussed below. The Sn atom still being in its divalent state, the approach of the two Br atoms towards the $\mathrm{SnBr_2}$ molecule produces a repulsive potential curve without a minimum, the selective absorption of $\mathrm{SnBr_4}$ being the transition from the ground level to this repulsive curve. Provided that the extrapolation of $D(\mathrm{SnBr_4})$ holds and that this repulsive curve is not too steep, the selective absorption should have a long-wave limit corresponding to the energy-difference

$$D_T = D(\text{SnBr}_4) - D(\text{SnBr}_2) = 105 \text{ kcal./mol.}$$

While in the case of $SnCl_4$ only this one absorption can be observed in the quartz ultra-violet, in that of $SnBr_4$ *two more* regions of selective absorption should be observable. The separation of the ^2P term of Br mentioned above is 3685 $cm.^{-1}$ or about 10·5 kcal./mol., while for the Cl atom the same term-difference is 881 $cm.^{-1}$, which is too small to be observed in continuous absorption spectra. Above the level belonging to the system $SnBr_2 + 2Br(^2P_{3/2})$ two more levels will exist corresponding to $SnBr_2 + Br(^2P_{3/2}) + Br(^2P_{1/2})$ and to $SnBr_2 + 2Br(^2P_{1/2})$. The transition to the repulsive curves involving these levels of the separated system should therefore produce two more regions of selective absorption, the products of photodissociation being one excited and one unexcited Br atom in the second region and two excited Br atoms in the third region. Provided all three repulsive curves are rather flat and run more or less parallel to each other, the beginnings of absorption of the second and third regions will correspond to energies of $105 + 10{\cdot}5 = 115{\cdot}5$ and $105 + 21 = 126$ kcal./mol. respectively while the maxima will also show distances of the order of 3685 $cm.^{-1}$

Sharma⁽³⁾ found one long-wave limit in the spectrum of $SnBr_4$ at λ3510 but no structure. Introducing the substance directly into an absorption cell of length 1 cm. and heating it by means of a current of warm air, we have observed all three predicted regions of selective absorption at low vapour pressures. At a pressure at which the points of retransmission are just about to disappear the three long-wave limits are at λλ3471, 2995 and 2442 or 83, 97·5 and 116 kcal./mol. For the first two absorption regions the maxima also could be determined at λλ3063 and 2995, $\nu = 32638$ and 36646 their difference being 4000 $cm.^{-1}$ The difference of the limits is in 14·5 and 18·5 kcal./mol. The fact that the three beginnings of absorption show an absolute difference of about 15 kcal./mol. against the predicted ones is of no consequence. Not only has $D(\text{SnBr}_4)$ been extrapolated from $D(\text{SnCl}_4)$, but the heat of formation of $SnBr_2$ is an old figure by Berthelot, and $S(\text{SnBr}_2)$ has been extrapolated, and both values together may easily be incorrect by 15 kcal./mol. Under these conditions, it is rather surprising that the experimental values approach the predicted ones at all. More important is the fact that the differences both between the three limits and also between the two maxima are all of the order of magnitude of the doublet separation of Br. Above all it is most significant that three different regions of absorption with this energy difference are observed. Since Br possesses only one excited term in this region, the second energy of excitation being 63,430 $cm.^{-1}$ or about 181 kcal./mol., this obviously establishes that two Br atoms are split off in this photolytic process. Without the second atom neither the doubling of the energy differences of the first two long-wave limits nor the very existence of a third region of selective absorption could be understood. Otherwise it would mean that the radical $SnBr_3$ produces the third maximum just at the required wave-length, but since the same phenomenon is found again in, for example, CHI_3 and CI_4, $CHBr_3$ and CBr_4, such an interpretation is obviously impossible.

§ 4. ALKYL HALIDES; THERMOCHEMICAL CALCULATIONS

The absorption spectra of molecules of $\mathrm{Sn}X_4$ type lead to an interpretation of the photodissociation processes similar to that for molecules formed by atoms of the fifth and sixth groups in their state of maximal valency; and there is no reason why organic molecules should behave differently. Molecules $\mathrm{C}X_2$ are not stable compounds in the chemical sense; however, this is not an inherent property of organic molecules, but is mainly due to the large sublimation energy of carbon itself. While the formation of gaseous C and H atoms has to overcome the sublimation energy of carbon (~156·2 kcal./mol.) plus the dissociation energy of H_2 (102·7 kcal./mol.), even with the slightly higher value for the C—H bond in CH_2 deduced below, the formation of CH_2 from gaseous atoms liberates only 228 kcal./mol. Only if the same C atom, whose sublimation energy has been taken account of already, forms two more C—H bonds is an excess of energy liberated, since $D(\mathrm{CH_4}) = 379{\cdot}7$ kcal./mol., while $S(\mathrm{C}) + 2D(\mathrm{H_2}) = 361{\cdot}6$ kcal./mol. For the metallic elements of the fourth group the sublimation energies are lower and molecules of MX_2 type have therefore a greater probability to be stable in the chemical sense. This difference of behaviour is, however, of no importance whatever as to the relative positions of the energy levels of the system C + 4H, on which its photodissociation depends.

The atomic energies of dissociation of organic molecules necessary for comparison with the absorption spectra are obtained in the usual way. From the heat of combustion (*HC*) the heat of formation from the element (*Q*) is calculated, and from the latter *D* is derived by means of Born's cycle. Iodoform ($HC = 162{\cdot}1$) may serve as an example.* From the equation

$$[\mathrm{CHI_3}] + \tfrac{5}{4}(\mathrm{O_2}) = (\mathrm{CO_2}) + \tfrac{1}{2}\mathrm{H_2O} + \tfrac{3}{2}[\mathrm{I_2}] + 162{\cdot}1,$$

it follows that

$$[\mathrm{C}] + \tfrac{1}{2}(\mathrm{H_2}) + \tfrac{3}{2}[\mathrm{I_2}] = [\mathrm{CHI_3}] - 33{\cdot}6$$

and

$$(\mathrm{C}) + (\mathrm{H}) + 3(\mathrm{I}) = [\mathrm{CHI_3}] + 249{\cdot}4$$

or

$$D \text{ of gaseous } (\mathrm{CHI_3}) = 241 \text{ kcal./mol.}$$

The values in kcal./mol. used in these calculations are as follows:

$2(\mathrm{H}) - (\mathrm{H_2}) = 102{\cdot}72,$

$2(\mathrm{O}) - (\mathrm{O_2}) = 116{\cdot}40,$

$(\mathrm{C}) - [\mathrm{C}] = 156{\cdot}2,$

$2(\mathrm{Cl}) - (\mathrm{Cl_2}) = 56{\cdot}9,$

$2(\mathrm{Br}) - (\mathrm{Br_2}) = 45{\cdot}23,$

$(\mathrm{Br_2}) - \mathrm{Br_{2(liq)}} = 7{\cdot}69,$

$2(\mathrm{I}) - (\mathrm{I_2}) = 35{\cdot}39,$

$(\mathrm{I_2}) - [\mathrm{I_2}] = 14{\cdot}88,$

$[\mathrm{C}] + (\mathrm{O_2}) = (\mathrm{CO_2}) + 94{\cdot}27,$

$\tfrac{1}{2}(\mathrm{H_2}) + \tfrac{1}{2}(\mathrm{Cl_2}) = (\mathrm{HCl}) + 21{\cdot}9,$

$(\mathrm{HCl}) - \mathrm{HCl_{aq.}} = 8{\cdot}4,$

$(\mathrm{H_2}) + \tfrac{1}{2}(\mathrm{O_2}) = \mathrm{H_2O_{liq.}} + 68{\cdot}31.$

The value 156·2 for the heat of sublimation of carbon is in agreement with the general trend of thermochemical literature, which inclines more and more to a value slightly higher than 150. It is calculated* from $D(CO) = 10{\cdot}45$ V., which as discussed earlier$^{(5,6)}$ to our mind is still the best available value. If, however, the value 150 kcal./mol. is preferred, all energies of dissociations have to be reduced by 6·2. This would decrease the final D_T values by 2–3 kcal./mol. The results of these calculations are collected in table 2. For CH_2I_2, CHI_3, and $CHBr_3$ the heats of sublimations are not known. The calculation from Forcrand's rule gives slightly too high values for these organic compounds as can be seen by calculating some of the known energies of sublimation in this way. Therefore 2, 8, and 10 kcal./mol. respectively have been finally adopted for these three compounds, the possible error is in any case negligible. It is generally assumed that the products of combustion of halides are $HCl_{aq.}$, $Br_{2\,liq.}$ and $[I_2]_{solid}$, and the values for Q are calculated according to this view. It may be due to an error of measurement or to a different reaction, that some of the values obtained for D obviously are not correct, as can be seen from the differences of the D values in the last column. The replacement of one H atom by a Cl atom decreases the energy of formation by 21–26 kcal./mol., if the values of CH_4, CH_3Cl, $CHCl_3$ and CCl_4 are taken into account. Calculation for CH_2Cl_2 gives 347 with a difference of 12 against $D(CH_3Cl)$ and of 33 against $D(CHCl_3)$, the mean of these two differences being 22·5. Hence the true value of $D(CH_2Cl_2)$ will be about 335 kcal./mol. Again $D(CH_4) - D(CH_3Br)$ indicates a decrease of 35 for the replacement of H by Br, but $D(CHBr_3)$ indicates 25 or 15 when compared with CH_4 or CH_3Br respectively. This value will therefore be too high; and since Thomsen's results have often been shown to be quite reliable, we adopt 30 as the weighted mean for this difference, and $D(CH_4) - 90 = 290$ kcal./mol. as the true energy of formation of $CHBr_3$. In the same way $D(CBr_4)$, for which no thermochemical data are available, is estimated as about 260 kcal./mol. $D(CI_4)$, for which again no thermochemical data are available, is placed at ~176, four times the difference $D(CH_4) - D(CH_3I)$ being deducted from $D(CH_4)$.

---

* All values are taken from Landolt-Boernstein tables. Some of the figures are slightly different from those used in previous publications(1). In particular $S(\mathrm{I_2})$ has been changed from about 3 to 7·4 kcal./g. atom on account of Kelley's critical review of all available data. All other changes are small.

Table 2

	HC	*Q*	*D*	Differences of *D*
1. CH_4	212·79 (R.)	18·1	379·7	
2. CH_3Cl	176·95 (T.)	19·8	358·5	(1–2) : 21·2
3. CH_2Cl_2	106·8 (B.)	31·3	347 (335)	(2–3) : 12
4. $CHCl_3$	107·03 (T.)	21·4	314·4	(3–4) : 33; (2–4) : 44 = 2 × 22; (1–4) : 66 = 3 × 22
5. CCl_4	75·93 (T.)	18·34	288·3	(4–5) : 26; (1–5) : 92 = 4 × 23
6. CH_3Br	184·71 (T.)	8·2	345	(1–6) : 35
7. $CHBr_3$	90·3 (P.S.)	38·2	315 (290)	(6–7) : 30 = 2 × 15
8. CBr_4	—	—	(~260)	
9. CH_3I	196·08 (T.)	−6·8	328·6	(1–9) : 51·1
10. CH_2I_2	178·4 (B.)	−69·2	283 (?)	(9–10) : 46
11. CHI_3	162·1 (B.)	−33·6	223	(10–11) : 61; (9–11) : 106 = 2 × 53
12. CI_4	—	—	(~176)	

(R.) = Rossini, (T.) = Thomsen; (B.) = Berthelot; (P.S.) = Popoff and Schirokich. For references see Landolt-Boernstein tables.

---

* With 5·05 instead of 5·09 V. as in the original paper for $D(O_2)$, according to H. P. Knauss and S. S. Ballard, *Phys. Rev.* **48**, 796 (1935).

To interpret the absorption spectra of the alkyl halides CX_4, CHX_3, CH_2X_2, and CH_3X in a similar manner as those of $SnCl_4$ and $SnBr_4$, the dissociation energies of the molecules CH_2, CHX, and CX_2, should be known, or in other words the bond energies $C^{II}—H$ and $C^{II}—X$ in saturated molecules formed by unexcited divalent C atoms. At present there is no other way but to extrapolate these energies according to the known ratio

$$D(SnCl_4) : D(SnCl_2) = 5 : 3 \sim D(CX_4) : D(CX_2).$$

In other words it is assumed, that the excited electronic levels of a system $C+4X$ have a similar position compared with the known ground level of the system as those of $Sn+4Cl$ against the ground state of unexcited $SnCl_4$. Such an extrapolation cannot be expected to give more than approximate values but as a matter of fact it will be seen that the agreement of the estimated figures with those measured experimentally is much better than was hoped for originally. This extrapolation therefore falls in line with the many empirical laws and rules, known in atomic physics, which, beginning with atomic terms up to the constants of diatomic molecules like ω, r, or D, represent quite well the change of such a constant in a homologous series of related atoms or molecules.

For CH_4 the position of the energy levels is as follows: $D(CH_4)$ being 379·7 kcal./mol., 228 is obtained for $D(CH_2)$ according to the above ratio, and this gives 114 for the mean bond energy $D_B(C^{II}—H)$. According to the theory of Heitler and London, the C atom becomes tetravalent on excitation from s^2p^2 to sp^3 or p^4. While Heitler and Herzberg(7) assumed that the lowest possible term of tetravalent carbon, i.e. $sp^3\ {}^5S$ has an energy of excitation of 1·6 e.V. only, Lessheim and Samuel(5) pointed out that this energy is much higher and estimated 5·2 V. for $sp^3\ {}^5S$ and 17·4 V. for $p^4\ {}^3P$ from the spectrum of C^+. Simultaneously Van Vleck(8) estimated 5–8 V. for the excitation energy of ${}^5S$ and later reduced this value to 4·3 V. on account of new measurements of Edlén for N^+ and O^{++} and a new extrapolation by Bacher and Goudsmit. At the same time he concludes from wave-mechanical calculations, that the term belonging to the configuration sp^3 in which C becomes tetravalent is not the term ${}^5S$ but a higher one at about 7 V. (161 kcal./mol.) on account of a strong repulsive force between the H atoms. If this be true the adiabatic dissociation energy of CH_4 is $370+161=532$ kcal./mol. and the mean bond energy $D_B(C^{IV}—H)=532/4=133$ kcal./mol. With an excitation energy of about 100 kcal./mol. for ${}^5S$, $D_B(C^{IV}—H)$ comes to 120 kcal./mol. Bond energies involving activated s^2 groups are naturally stronger than those involving the p electrons only, as can be seen from the example of CO_2, where the energy of adiabatic dissociation has been calculated(5). Thus both figures show that the value 114 kcal./mol. for $D_B(C^{II}—H)$ is by no means too high. In the radical CH_3 the bond energy will be strengthened on account of decreased repulsion of the H atoms, but weakened by the disturbing electron not taking part in the linkage. The latter influence will probably be the stronger one and therefore the C—H bond will be weaker in CH_3, and stronger in CH_4, than that indicated by the mean ratio calculated above, and the same is true for CH_2 and CH. (The dissociation energy of CH cannot be extrapolated directly from the band spectrum, the anharmonic constant not being known.) The corresponding values for $D(CX_4)$ can be estimated in the same approximate manner to be 172, 156 and 104 kcal./mol. for $X=$ Cl, Br and I respectively. The mean bond energies $D_B(C^{II}—X)$ are in the same order 86, 78, and 53 kcal./mol. With $C(^5S)$ the bond energies $D_B(C^{IV}—X)$ of the molecules formed by tetravalent carbon will be about 97, 90 and 69 kcal./mol. for $X=$ Cl, Br and I respectively.

§ 5. ABSORPTION SPECTRA OF METHYL HALIDES

The first experimental confirmation of the value 222 kcal./mol. for $D(CH_2)$ will be found in the absorption spectra of the methyl halides. The absorption spectra of the monohalides of this series have been measured by Herzberg and Scheibe[(9)], and their results have been confirmed by later work[(10, 4)]. The beginning of absorption (taken at a value of the absorption coefficient of about 1/10 of the selective maximum and about equal to the value of the following point of retransmission) lies at a wave-length corresponding to 151, 123, and 102 kcal./mol. for CH_3Cl, CH_3Br, and CH_3I respectively. On the basis of 92 (or with more recent values 95) kcal./mol., equal to one-quarter of $D(CH_4)$ for the C—H bond (i.e. if the excitation of the C atom for it to become tetravalent is not considered), the values of about 72, 59 and 45 kcal./mol. are conventionally deduced for the energies of the C—Cl, C—Br, and C—I bonds. But compared with these values the experimental long-wave limits are about 100 per cent too high and this discrepancy has never been properly understood. Even if one-quarter of the excitation energy of $C(^5S)$, equal to 25 kcal./mol., are added to the above energies of the C-X bonds, the resulting values of 98, 84 and 70 kcal./mol. are still far too low in the light of the experimental results. The same is true, if the values deduced (as above) from those of $D(CX_4)$ are taken into account; these are 97, 90 and 69 kcal./mol. To account for these high experimental values a high excitation of the dissociation products has been assumed and in addition an extremely steep repulsive curve (whose tangent above the minimum of the unexcited state would form an angle of about 45° with the internuclear axis). Both these assumptions are theoretically possible, but do not in the least agree with our experience as to the photodissociation of other multiatomic covalent molecules.

If, however, the unexcited C atom is divalent only the photodissociation will take place, as in $SnCl_4$, by a transition from the ground level of the molecule CH_3X to the repulsive level of the system CH_2+H+X. The position of this level is $D_T=D(CH_3X)-D(CH_2)$, and for CH_3Cl, CH_3Br, and CH_3I the values 131, 117 and 103 kcal./mol. are obtained deducting 228 from the atomic heat of formation. In table 3 these figures are compared with those of Herzberg and Scheibe, Henrici, and Hukumoto. Hukumoto's values are slightly too low, because, as he states, only the values for the highest pressures are recorded in his paper. Considering the many unavoidable extrapolations and the experimental difficulty of determining the long-wave limit of the vibrationless molecule, it may be said that the gross discrepancy, discussed above, has entirely disappeared and that the new interpretation submitted here is fully supported by experimental evidence.

Table 3

Molecule CH_3X	Dissociation products	$D_T = D(CH_3X) - D(CH_2)$ (kcal./mol.)	Observed long-wave limit (kcal./mol.)		
			Herzberg and Scheibe	Henrici	Hukumoto
CH_3Cl	CH_2+H+Cl	131	151	143	125
CH_3Br	CH_2+H+Br	117	123	117	96
CH_3I	CH_2+H+I	103	102	96	90*
$CH_3.OH$	CH_2+H+OH	140	142	—	—

* In the original paper 70·2 is given for CH_3I, an obvious misprint, since the recorded wave-length $\lambda 3100 = 90{\cdot}2$ kcal./mol.

Since the photodissociation involves the separation of one halogen atom, a second maximum of selective absorption should be expected for CH_3Br and CH_3I at a wave-length representing a value 10·5 and 21·5 kcal./mol. higher, respectively, in accordance with the excitation energy of the Br and I atoms. For CH_3I this maximum has been found by Hukumoto using a thin film of liquid methyl iodide as absorbing layer, with an energy difference of 0·75 e.V. from the first maximum, while the doublet separation of I is 7600 cm.$^{-1}$ = 0·94 e.V. = 21·5 kcal./mol.

Herzberg and Scheibe have also measured the absorption of methyl alcohol and find a condition similar to those of the halides. The beginning of absorption lies at about $\nu 50000 = 142$ kcal./mol. From the heat of combustion (182·58 kcal./mol.), it follows that $Q = 48{\cdot}3$ and D (for gaseous $CH_3.OH$) = 468·1, and when $D(CH_2)$ is deducted, a value 240 kcal./mol. is obtained. On account of the general similarity of the absorption curve with that of the methyl halides Herzberg and Scheibe assume that the dissociation involves an OH radical. The bond energy of this radical is independently known(11) to be 100 kcal./mol. Deducting this figure we obtain 140 kcal./mol. for the dissociation $CH_3.OH \rightarrow CH_2 + H + OH$, again in good agreement with the experimental result.

§ 6. ABSORPTION SPECTRA OF HIGHER ALKYL IODIDES

The iodides are easily the most interesting compounds, because, on account of their smaller bond energies, a greater part of the absorption spectrum lies in the quartz ultra-violet. We shall deal with them first (table 4).

For carbon tetraiodide it follows from the figures of table 2 that

$$D(CI_4) - D(CI_2) = 176 - 106 = 70 \text{ kcal./mol.}$$

The first region of absorption should therefore have a long-wave limit of this value and should correspond to the dissociation process $CI_4 \rightarrow CI_2 + 2I(^2P_{\frac{3}{2}})$. At distances corresponding to 21·5 kcal./mol., two more regions of absorption should follow towards shorter waves, corresponding to the dissociations

$$CI_4 \rightarrow CI_2 + I(^2P_{\frac{3}{2}}) + I(^2P_{\frac{1}{2}}) \quad \text{and} \quad CI_4 \rightarrow CI_2 + 2I(^2P_{\frac{1}{2}}).$$

Table 4

Molecule	Dissociation products	D_T calculated (kcal./mol.)	Observed beginnings of absorption	
			(kcal./mol.)	λ (A.)
CI_4	CI_2+2I	70	72	3930
	CI_2+I+I^*	91·5	89·5	3177
	CI_2+2I^*	113	102	2795
CHI_3	$CHI+2I$	56	67	3780
	$CHI+I+I^*$	77·5	88	3229
	$CHI+2I^*$	99	99	2872
CH_2I_2	CH_2+2I	55	81	3499
	CH_2+I+I^*	76·5	107	2640
	CH_2+2I^*	98	120	2365
CBr_4	CBr_2+2Br	104	97	2932
	$CBr_2+Br+Br^*$	114·5	116	2453
	CBr_2+2Br^*	125	—	—
$CHBr_3$	$CHBr+2Br$	98	103	2750
	$CHBr+Br+Br^*$	108·5	114	2497
	$CHBr+2Br^*$	119	129	2195 (?)

The long-wave limits of these absorption regions therefore should lie at wave-lengths corresponding to about 91·5 and 113 kcal./mol., the maxima having a separation of approximately 7600 cm^{-1}

The absorption spectrum of carbon tetraiodide has not previously been investigated. We observed it by introducing the substance directly into the absorption tube and heating it with a current of warm air up to about 60° C. (cf. figure 1). All the predicted maxima have been observed (cf. table 1). We obtained also the two first maxima at 345 and 305 mμ. in a solution of CI_4 in CCl_4, the third one being overlapped by the self absorption of the solvent. Since iodine has no absorption at these wave-lengths, this observation shows that the substances did not appreciably decompose on heating, even though some of the bands of I_2 at shorter waves could faintly be seen on the plates. The differences of the maxima, 4227 and 4813 cm^{-1} are slightly less than the expected ones, probably on account of the repulsive curves not running entirely parallel. The long-wave limits at λλ3930, 3177 and 2795 A. correspond to 72, 89·5 and 102 kcal./mol., and comparison with the predicted values, 70, 91·5 and 113, leaves little doubt that the above interpretation is essentially correct.

The absorption of iodoform was first measured by Scheibe and collaborators(12) in various solvents; e.g. in hexane it shows maxima at λλ348, 307 and 275 mμ. Although the distance in cm^{-1} between these maxima is about 4800 and 3800 respectively, i.e. again slightly smaller than what could be expected from the excitation energy of iodine, this can easily be accounted for, as in the case of CI_4, by the repulsive curves approaching each other; and, as a matter of fact, the existence of the third maximum appeared to be so significant, that it first led us to undertake the present investigation. Henrici(10) was unable to measure the absorption of iodoform since in his apparatus it was not possible to produce sufficient vapour pressure. Our measurements have been carried out similarly to those of CI_4. All those maxima have been observed for the vapour state, figure 2, the wave-length of the maxima and long-wave limits being listed in tables 1 and 4. Deducting from $D(CHI_3) = 223$ the values $D_B(C^{II}—H) = 114$ and $D_B(C^{II}—I) = 53$, we obtain a value of D_T equal to 56 kcal./mol. Provided the repulsive curves run flat and parallel, three regions of absorption are expected with long-wave limits corresponding to 56, 77·5 and 99 kcal./mol. The wave-lengths observed experimentally correspond to 67, 88 and 99 kcal./mol. Although the differences between the maxima again are slightly smaller than the separation of the ^2P term of I, the existence of these absorption regions with long-wave limits so close to the estimated positions makes it practically certain that the decomposition has taken place according to the equation: $CHI_3 + h\nu = CHI + 2I$. The possibility of a process like $CHI_3 \rightarrow CI_2 + H + I$ would lead to a long-wave limit corresponding to 117 kcal./mol., equivalent to $D(CHI_3) - D(CI_2)$, and since only one I atom is split off, only two maxima would exist. Such a long-wave limit is impossible for a coloured compound.

The spectrum of methylene iodide has been investigated previously by Iredale(13), Henrici(10) and Hukumoto(4). Iredale and Henrici record only one maximum in the quartz ultra-violet, at about λ3000, and Henrici also observes two small regions of selective absorption at λλ1865 and 1970, which being very close together and situated directly at the beginning of the region of band absorption are probably diffuse bands. Hukumoto records three maxima at λλ2860, 2460 and 2210. Our own experimental results agree with those of Hukumoto. For some time we were unable to obtain all three maxima in the vapour state. We therefore measured quantitatively the absorption curve of CH_2I_2 dissolved in ether. The sample used for this purpose was carefully purified, free iodine being removed by washing it with a weak solution of sodium hyposulphite and drying it after separation by means of calcium chloride. The absorption curve shows all three maxima very clearly, but the absorption coefficient of the middle one is lower than of both its neighbours. The absorption coefficients* of the three maxima, counted from longer to shorter waves are $\log K = 3{\cdot}5$, 2·8 and 3·3 respectively. In the vapour state, the middle maximum is easily overlapped by the others and can be obtained only by careful adjustment of the vapour pressure, the probability of transition being considerably smaller for it than for the others. The three beginnings of absorption are at λλ3499, 2640 and 2365, or 81, 107 and 120 kcal./mol. respectively, the maxima at νν34062, 40638 and 45031, with differences of 6576 and 4393 cm^{-1} There are various possibilities for the process of dissociation of the molecule CH_2I_2. Its dissociation products may be $CI_2 + 2H$, $CHI + H + I$, or $CH_2 + 2I$. Deducting $D(CI_2)$ from $D(CH_2I_2)$, we obtain 177 kcal./mol. for the first process, and no maxima due to excited

---

* K represents Bunsen and Roscoe's extinction coefficient defined usually by $I = I_0 \times 10^{-kcd}$.

I atoms are possible. In the second case the energy difference

$$D(CH_2I_2) - D_B(C^{II}—H) - D_B(C^{II}—I)$$

gives a long-wave limit of 116 kcal./mol., and one further region of absorption beginning at 137·5 kcal./mol. is expected. The third possibility indicates a long-wave limit at $D(CH_2I_2) - D(CH_2)$, equal to 55 kcal./mol., and two more maxima with beginnings at 76·5 and 98 kcal./mol. Actually the experimental values do not agree with any of these calculated thermochemically. This may be due partially to the heat of combustion being an older value of Berthelot's, but the discrepancy is more than can probably be accounted for in this way. On the other hand, the very good agreement obtained with other molecules of this kind shows the present view to be essentially correct, and the existence of three maxima indicates the last of the three possible dissociation processes, in which two I atoms are separated simultaneously. It therefore appears as if the repulsive curves, and particularly the lower two of them, have a rather steep slope which increases the energy difference from the ground level at that internuclear distance where the transition occurs.

§ 7. ABSORPTION SPECTRA OF HIGHER ALKYL BROMIDES

The value 260 kcal./mol. of $D(CBr_4)$ has been estimated, no thermochemical measurement being available. From this $D_B(C^{II}—Br) = 78$ has been obtained, which leaves 104 kcal./mol. for $D_T(CBr_4)$. According to the photolytic process $CBr_4 \rightarrow CBr_2 + 2Br$, $CBr_4 \rightarrow CBr_2 + Br + Br^*$ and $CBr_4 \rightarrow CBr_2 + 2Br^*$, three regions of selective absorption with beginnings at 104, 114·5 and 125 kcal./mol. are expected. Carbon tetrabromide is one of the less stable molecules of this series, and decomposes easily when heated to obtain the required vapour pressure. Henrici(10) therefore found only one long-wave limit, corresponding to about 81 kcal./mol. We have been able to determine two regions of selective absorption with long-wave limits at λλ2932 and 2453 (97 and 116 kcal./mol.) and a maximum at λ2525 without succeeding in tracing the second maximum or a further region of absorption. The energy-difference between the long-wave limits agrees almost exactly with the excitation energy of the Br atom, and considering the inaccuracy of the estimated value of $D(CBr_4)$ the agreement between the calculated values 104 and 114·5 and the observed values 97 and 116 kcal./mol. is very good indeed.

For $CHBr_3$ again three regions of absorption are expected. Deducting from $D(CHBr_3) = 290$ the values $D_B(C^{II}—H) = 114$ and $D_B(C^{II}—Br) = 78$, a value 98 kcal./mol. is obtained for the process $CHBr_3 \rightarrow CHBr + 2Br$. The long-wave limits of the two regions corresponding to one or two excited Br atoms as dissociation products would then correspond to 108·5 and 119 kcal./mol. These figures, however, may be incorrect by some kcal./mol. on account of the discrepancy in $HC(CHBr_3)$, discussed above.

While Hukumoto(11) records a long-wave limit at λ2690 only, Henrici(10) finds λ2863 and a maximum at a very large distance away at λ1695. We have found two regions of selective absorption and the beginning of a third one. For the long-wave limits we obtain λλ2750, 2497 and 2195, corresponding to 103, 114 and

129·5 kcal./mol., both differences being about 11 kcal./mol. in very good agreement with the bromine excitation of 10·5 kcal./mol. The two maxima have λλ2559 and 2275, νν39066 and 43942 the difference of 4876 $cm.^{-1}$ is again in fair agreement with the term difference of Br. It can however be seen from figure 3, that the second maximum and the third limit occurring in a region in which the density of the spectrum is already weak, are difficult to locate and therefore less accurate. The above values are means from three spectrograms. All three values of the beginnings agree closely with the predicted ones.

§ 8. HIGHER ALKYL CHLORIDES

The absorption spectra of the higher chlorides exhibit maxima only in the Schumann region, and the maxima due to the excitation energy of one or two $Cl(^2P_{\frac{1}{2}})$ atoms cannot be distinguished from the first maximum, this excitation energy being too small. Without accurate knowledge of the position of the maximum and its absorption coefficient, the determination of the long-wave limit of the vibrationless molecule in the quartz ultra-violet therefore becomes rather inaccurate and the discrepancies between the results of various authors is considerably increased. The energies of dissociation and the value of $D_b(C^{II}—Cl)$ have been calculated above; and in table 5 we compare the values of the beginning of the absorption with the D_T values.

Table 5

	Dissociation products	$D(CX_4) - D(CX_2) = D_T$ (kcal./mol.)	Long-wave limit (kcal./mol.)		
			Henrici	Hukumoto	Present paper
CCl_4	$CCl_2 + 2Cl$	$288 - 172 = 116$	124	117	~121
$CHCl_3$	$CHCl + 2Cl$	$314 - 186 = 128$	134	121	~128
CH_2Cl_2	$CHCl + H + Cl$ (?)	$335 - 186 = 149$	136	123	—

Considering the experimental difficulties the agreement is again quite good.

§ 9. DISCUSSION OF RESULTS

It has been seen that the absorption spectra of molecules of MX_4 type are in good agreement with the interpretation of the photolytic process discussed above. According to this view one of the dissociation products is a saturated molecule $MX_2(^1\Sigma)$ and the absorption of light induces an excitation of the molecule MX_4 from its ground level to the repulsive curve $MX_2(^1\Sigma) + 2X$. The significance of this type of photolytic dissociation is that it does not refer to any bond energy. The possibility of the breaking up of a molecule in this way has been recognized previously; Mecke(14) particularly has discussed it at greater length. A mechanism of photodissociation rather nearly related to this conception has been set up for keten by Norrish(15); and certain results of Terenin(16), which will be discussed below, also support this type of interpretation. Some years ago, on the basis of the meagre experimental results then available, one of us suggested(17) a division of the photodissociation processes of inorganic molecules, according to the two types involving bond energies and radicals or excitation to the repulsive curve produced by saturated molecules of lesser state of valency. This has been justified by many subsequent experimental results(18). This conception which, in fact, involves the rupture of two bonds by an amount of energy less than the bond energy of one of them, is therefore not as extraordinary as it appears at first.

Attention may therefore be directed to the experimental results of Terenin(16) and of Norrish(15) and their collaborators, which strongly support the interpretation presented here. Terenin illuminated SnI_4 vapour of low pressure with ultra-violet light of short wave-length and obtained a bright visible fluorescence of the band spectrum of I_2. From our results on $SnBr_4$ we are now able easily to understand his result. The upper level for the visible I_2 bands is known to dissociate into one excited and one unexcited atom, and the recombination of two such atoms produces an I_2 molecule in this excited electronic level. Illumination with any light of shorter wave-length than the second long-wave limit will result in a decomposition $SnI_4 \rightarrow SnI_2 + I + I^*$ and the recombination of the two atoms produces the band spectrum of I_2 in emission. Terenin's experiments show that, at least for SnI_4, such a recombination occurs frequently and immediately after the decomposition of the original molecule, since the life-time of the two free atoms is increased on account of the low pressure.

The experiments of Norrish and his collaborators concern the photodissociation of ketones. While in heavier ketones the hydrocarbon chain is ruptured by the action of light, simple ketones decompose into hydrocarbon and carbon monoxide. Formaldehyde may be taken as an example. It possesses a band spectrum whose origin, according to the vibrational analysis, lies at slightly longer waves than $\lambda 3530$, equal to 80 kcal./mol. A point of predissociation is observed at $\lambda 2750$, equal to 103 kcal./mol., but, according to new conceptions for polyatomic molecules, decomposition by light will occur at appreciably longer waves than the point of predissociation, and the quenching of fluorescence should be taken as the true threshold value of photodecomposition(15). This happens near $\lambda 3600$, equal to 78 kcal./mol. The photochemical experiment shows indeed that photodecomposition begins at least at about $\lambda 3300$, equal to 86 kcal./mol., and the final products are formed according to the process $H_2CO \rightarrow H_2 + CO$. From comparison with other ketones and aldehydes it is obvious that the band spectrum belongs to the chromophoric group $> CO$, while the absorbed energy is transferred to other parts of the molecule by the coupled modes of vibrations. Since the energy of two C^{IV}—H bonds is at least twice 120, equal to 240 kcal./mol. (with $C^3\ sp^2\ {}^5S$), and the contribution of two such bonds to the atomic energy of formation is $2 \times 95 = 190$ kcal./mol., Norrish assumes that the mechanism of photodissociation involves two steps, i.e.

$$H_2CO + h\nu = H + HCO,$$

$$HCO \rightarrow \quad H + CO(x^1\Sigma).$$

The primary change concerns the splitting of the true bond energy $D_B(C^{IV}—H)$ by the action of light, while the spontaneous decomposition of the remaining radical is due to the excitation energy liberated by the CO molecule on its transition from the excited (carbonyl) term, in which it possesses two free valencies, to the ground state $x^1\Sigma$ formed by O and divalent C (energy of reorganization).

This mechanism is very near to the view presented here, since it makes use of the repulsive curve originating in the level of $CO(x^1\Sigma)$, but, according to the results obtained for the CX_4 molecules, it appears as if it may be further simplified. We submit that the true bond energy* $D_B(C^{IV}—H)$ does not play any role in the photolytic process, but that photodissociation occurs simply by the excitation of the molecule H_2CO to the first repulsive curve, which is the level $2H+CO(x^1\Sigma)$. $Q(H_2CO)$ being 28·5, we obtain by means of Born's cycle $D(H_2CO)=345{\cdot}6$, and deducting $D(CO)=241{\cdot}1$, we obtain the level $2H+CO(x^1\Sigma)$ 104·5 kcal./mol.† above the ground level of H_2CO. The other possible repulsive level, $O+CH_2$, which includes the energy of reorganization of the CH_2 molecule, lies 14 kcal./mol. higher, since $D(H_2CO)-D(CH_2)=118$ kcal./mol., and thereby explains why the decomposition by light liberates CO and not CH_2, whereas the electronic excitation of the band spectrum almost certainly concerns an electron of the carbonyl group. While the value of $D_B(C^{IV}—H)$ no longer agrees with the point of predissociation at 103 kcal./mol., the close agreement of this value with the above 104·5 kcal./mol. is obvious. It is true that the photodissociation begins at longer waves in the region of discrete band absorption, but this discrepancy occurs in both interpretations and even if not $D_B(C^{IV}—H)$ but $Q(C—H)=1/4.380=95$ kcal./mol. could be considered as an explanation. The very existence of a discrete band spectrum suggests that in this region decomposition is due to transition from excited vibrational levels to the same repulsive curve, the more so since a single CO or CH vibration represents the considerable energy of 5 or 8·5 kcal./mol. respectively. The quantum yield in this region, which varies for different molecules of this type, will then depend on the percentage of the bands which, under the particular experimental conditions, are due to excited vibrational levels. The question as to the lowest repulsive curve in more complicated aldehydes and ketones cannot be answered at the present moment, and, moreover, the same view may not be applicable to processes of thermal decomposition. But it appears as if, at least for molecules with short hydrocarbon chains, this view of the simultaneous splitting of two bonds meets best the requirements of the results of photochemical experiments as to the main process of decomposition. Naturally such experiments always include the possibility of secondary reactions which may obscure the issue.‡ It is, however, significant that for keten $H_2C{=}CO$, where on account of the double bond there is no other alternative but to assume that both are fissured simultaneously, the mechanism set up by Norrish (on the basis of the new figures for the excitation of C) practically comes to the same result as that presented here.

---

* The value of 103 kcal./mol. for $D_B(C^{IV}—H)$ used in the earlier papers of Norrish and collaborators is based on the estimate of 1·7 e.V. for $C(^5S)$ and is therefore much too low. The true values are discussed above in the thermochemical section of this paper.

† This value is, of course, independent of the exact absolute value of $D(CO)$, since $S(C)$ is derived from the latter, and is used again for $D(H_2CO)$.

‡ According to Spence and Wild(19) the mechanism of photodecomposition of acetone varies with temperature. This may be due to experimental conditions, which are not described in their preliminary note, or to the fact that the repulsive curve of the system $R+RCO$ is slightly lower than that of $2R+CO(^1\Sigma)$. For $D_B(C^{IV}—C)$ a value of about 115 kcal./mol. only can be deduced from the heat of sublimation of carbon and its energy of excitation to the term ^5S. The curve $2R+CO(^1\Sigma)$ will then be reached from excited vibrational levels of the ground term whose population increases with temperature.

These few remarks do not aim at an exhaustive explanation of the photodissociation of ketones, but they show that the conception of the excited repulsive terms of organic molecules provide an alternative interpretation in many cases. In spite of the fact that they represent a simultaneous rupture of those two bonds which are due to the original *s* electrons of C, N, S, etc., they have a lower position because they involve unexcited radicals without free valencies, and therefore often provide a very simple explanation of the decomposition of the molecule. To our mind their existence is established by the third maximum of the compounds of MX_4 type. On the application of this conception to more complex organic molecules we hope to report shortly.

REFERENCES

(1) Asundi, R. K. and Samuel, R. *Proc. phys. Soc.* **48**, 28 (1936).
Khan, M. Jan and Samuel, R. *Proc. phys. Soc.* **48**, 626 (1936).
Cf. Hussain, S. L. and Samuel, R. *Curr. Sci.* **4**, 734 (1936).
(2) Heitler, W. and London, F. *Z. Phys.* **44**, 455 (1927).
London, F. *Z. Phys.* **46**, 455 (1928).
(3) Sharma, R. S. *Bull. Acad. Sci. Allahabad*, **3**, 87 (1933).
(4) Hukumoto, Y. *J. chem. Phys.* **3**, 164 (1935).
(5) Lessheim, H. and Samuel, R. *Proc. phys. Soc.* **46**, 523 (1934); cf. *Curr. Sci.* **1**, 374 (1933), **2**, 347 (1934).
(6) Asundi, R. K. and Samuel, R. *Proc. Ind. Acad. Sci.* (Bangalore), **3**, 562 (1936).
(7) Heitler, W. and Herzberg, G. *Z. Phys.* **53**, 52 (1929).
(8) Van Vleck, J. H. *J. chem. Phys.* **2**, 20, 297 (1934).
(9) Herzberg, G. and Scheibe, G. *Z. phys. Chem.* B, **7**, 390 (1930); cf. *Trans. Faraday Soc.* **25**, 716 (1929).
(10) Henrici, A. *Z. Phys.* **77**, 35 (1932).
(11) Sponer, H. *Landolt-Boernstein Tables* (1936).
(12) Scheibe, G., Roessler, G. and Backenkoehler, F. *Ber. dtsch. chem. Ges.* **58**, 586 (1925).
(13) Iredale, T. *Z. phys. Chem.* B, **20**, 340 (1933).
(14) Mecke, R. *Z. phys. Chem.* B, **7**, 108 (1930).
(15) Norrish, R. G. W. *Trans. Faraday Soc.* **30**, 103 (1934); *Acta Physicochim.* **3**, 171 (1935) and literature mentioned there.
Norrish, Crone and Saltmarsh. *J. chem. Soc.* p. 1535 (1933).
(16) Terenin, A. N. *Nature*, Lond., **135**, 543 (1935); *C.R. Acad. Sci. U.R.S.S.* **1**, 482 (1935).
(17) Samuel, R. *Absorption Spectra and Chemical Linkage.* Symposium Ind. Acad. Sci. (Bangalore), 1934; cf. also ref. (5).
(18) Cf. ref. (1) and literature mentioned there.
(19) Spence, R. and Wild, W. *Nature*, Lond., **138**, 206 (1936).

THE EFFECT OF PRESSURE AND TEMPERATURE ON THE OCCLUSION OF HYDROGEN BY PALLADIUM

By PROFESSOR E. A. OWEN, M.A., D.Sc.,

AND

JOHN IDWAL JONES, Ph.D.,

University College of North Wales, Bangor

Received 9 *April* 1937. *Read in title* 11 *June* 1937

ABSTRACT. The X-ray method has been employed to investigate the occlusion of hydrogen by palladium when the pressure of the hydrogen surrounding the palladium and the temperature of the palladium are varied. Measurements were made of the parameter of palladium at temperatures of 80, 100, 120, 140 and 160° C. when the palladium was surrounded by an atmosphere of hydrogen, the pressure of which ranged from zero to 76 cm. of mercury. When the temperature was kept constant, a linear relation was found to exist between the lattice parameter and the pressure for both of the two phases in the system. For dilute solutions of hydrogen in palladium over the ranges of temperature and pressure investigated, the change in parameter of palladium due to the occlusion of hydrogen was found to vary directly as the pressure of the hydrogen and inversely as the square of the temperature of the palladium. The entrance of hydrogen atoms into the palladium lattice loosens the bonds between the palladium atoms, thus allowing them to separate more readily under the action of heat. The value of the parameter of pure palladium free of gas was found to be $3{\cdot}8825_6 \pm 0{\cdot}0003$ A. at 20° C., and the mean coefficient of thermal expansion between 0 and 300° C. to be $12{\cdot}7 \times 10^{-6}$ per ° C.

§ 1. INTRODUCTION

The interactions of gases with metals have been extensively studied. Of all the systems examined it is probably the hydrogen-palladium system that has had the most attention, but the results of different investigators who have examined the system by various methods are not all in agreement. A full account of the work done in this field up to 1925 is contained in a paper by Lambert and Gates⁽¹⁾, who themselves made an important contribution to our knowledge concerning the relationships existing between hydrogen and palladium. They found that the relation between the pressure of hydrogen surrounding the palladium at any temperature and the concentration of the gas in the palladium, depended upon whether the pressure of the gas was increased or decreased to its final value. The ascending isothermal differed in shape from the descending isothermal, thus exhibiting a cycle similar to a hysteresis loop. This effect will be considered in detail in a later paper.

The present paper is concerned with the relation which exists between the lattice parameter of charged palladium, the temperature of the specimen and the pressure of the hydrogen surrounding it, attention being paid to the method of charging the specimen in view of the results just mentioned. Unlike the investigation of Lambert and Gates, the present work was carried out by X-ray analysis.

Yamada⁽²⁾ appears to have been the first to use the X-ray method to investigate the effect of the occlusion of hydrogen on the crystal structure of palladium. The investigation was carried out under limited conditions and it is doubtful whether the deductions made were justified, as they were based on too small a number of observations. It was concluded however that the system contained only solid solution of hydrogen in palladium and no compounds of the two elements.

McKeehan⁽³⁾ discovered two crystal lattices, both being face-centred cubic, one having a parameter of 3·900 A. and the other a parameter between 4·000 and 4·039 A. depending upon the degree of saturation. Two structures were suggested which would at the same time satisfy the observed cubic structures and the formula Pd_2H proposed by earlier investigators, but unfortunately these structures could not be checked by intensity-measurements owing to the low atomic number of hydrogen.

Linde and Borelius⁽⁴⁾ also found two face centred cubic lattices, the parameter value 3·978 A. being associated with the compound Pd_2H. The measurements were made under definite conditions of temperature and pressure in an air-tight enclosure with a spectrum camera which yielded results accurate to within ±0·01 A. The variation in parameter with electrolytic charging was also investigated with a focusing camera and two phases found as before, the accuracy of the parameter determination being of the order of ±0·002 A. Measurements of the change in specific resistance of palladium with charging also pointed to the existence of two phases.

Hanawalt⁽⁵⁾, from his measurements, was led to suggest the existence of the compound Pd_2H, and observations made on the *L* absorption limit of charged palladium pointed to the same conclusion.

A considerable amount of work has been done in Greifswald and Stockholm⁽⁶⁾ on the adsorption of palladium and its alloys; the results favour the existence of two solid solutions. Different types of cameras were employed including the Debye type of spectrum camera and the camera described by Sachs and Weerts⁽⁷⁾. The accuracy of the parameter-determinations was about 1 in 4000 and the exposures were made in air at room-temperature. The specimens were charged electrolytically and the hydrogen-content estimated from the current-strength and time as described by Berry⁽⁸⁾. Rosenhall⁽⁹⁾, using a focusing camera, the limits of accuracy being ±0·002 A., also charged the specimens electrolytically, but measured the concentration after each exposure at room-temperature by heating the specimen *in vacuo*.

A comprehensive examination of a series of alloys was made by Hägg⁽¹⁰⁾ who found that solutions of boron, carbon, nitrogen or hydrogen with the transition elements, one of which was palladium, possess a typically metallic character in comparison with solutions of these metalloids with other elements. The metalloid atoms were found to enter the metal lattice interstitially forming simple structures when $(r_x/r_m) < 0{\cdot}59$ and complicated structures when $(r_x/r_m) > 0{\cdot}59$, where r_x is the radius of the metalloid atom and r_m that of the metal atom.

In some of the foregoing investigations the specimen was charged with hydrogen electrolytically; it was then removed from the bath and allowed to dry before the X-ray exposure was made. In others the specimen was charged from the gaseous phase in an electric furnace, and after being charged it was allowed to cool in the gaseous atmosphere before making an exposure at room-temperature. In both of these procedures an element of uncertainty arises as to what may happen in the specimen between its charging with hydrogen and its exposure to X-rays. The investigations of Rosenhall and of Linde and Borelius are free from these sources of uncertainty.

In the present work the procedure is similar to that adopted by Linde and Borelius. The specimen is charged from the gaseous phase and the X-ray exposure is made whilst the specimen is maintained at a definite temperature and the pressure of the gas is kept constant. An attempt is made also to increase the accuracy of measurement. The high accuracy obtainable with the focusing camera renders it most suitable for observing small changes in parameter and the spectrum camera supplies information concerning the change in structure.

For simplicity in making reference, the two phases mentioned above will be referred to as the α and β phases, the α being what may be termed the palladium-rich phase, and the β the hydrogen-rich phase.

§ 2. APPARATUS

Two cameras were used in the investigation, one a focusing camera and the other a spectrum camera, both of which were designed for high-temperature work and could be mounted in enclosures which could be evacuated. An accuracy of at least 1 in 10,000 could be obtained in the values of the parameters as deduced from measurements made on films taken with the focusing camera. A much higher accuracy than this was obtainable under certain conditions. A high order of accuracy may also be obtained with the spectrum camera by adopting the extrapolation method suggested by Bradley and Jay(11). In this investigation the spectrum camera was used mainly to obtain the structure but on occasions it was also employed to obtain accurate values of the parameters although normally the focusing camera was used for this purpose. The cameras were carefully calibrated, and they both yielded consistent results.

§ 3. TEMPERATURE-MEASUREMENT

The measurement of temperature differed with the two cameras. In the focusing camera a thermocouple was inserted into the face of the thick copper sheet on which the specimen was mounted. This thermocouple was calibrated by inserting it in different materials whose melting points were known.

In the spectrum camera a different procedure was adopted; in this case use was made of the thermal expansion of a pure metal like silver, the parameter of the silver at different temperatures being employed to deduce the temperature. For this purpose a curve was drawn connecting the current passing through the heater and the temperature of the furnace. The calibration had to be carried out both *in vacuo* and in hydrogen. (*a*) *In vacuo.* The temperature attained with a given current passing through the heating-coil depends to a large extent on the pressure of the gas. It is therefore essential when taking a calibration *in vacuo* to render the enclosure and its connexions perfectly free from air leaks. The heater was calibrated for the range from room temperature to 300° C. The results are given in table 1.

Table 1. Calibration of heater *in vacuo*. Silver powder. Cobalt radiation

Current through heater (amp.)	Parameter of silver (A.)	Temperature ° C.
$0\cdot20_0$	4·0799	50 ± 5
$0\cdot30_0$	4·0842	105 ± 5
$0\cdot40_0$	4·0890	154 ± 5
$0\cdot50_0$	4·0941	226 ± 5
$0\cdot60_0$	4·1011	308 ± 5

(*b*) *In hydrogen.* Measurements with the precision camera showed that within the temperature range 15–140° C. and a hydrogen pressure-range 0 to 76 cm. of mercury the lattice parameter of silver was not altered by the presence of hydrogen, within the limits of accuracy of measurement. The calibration of the heater could therefore be carried out in exactly the same manner in hydrogen as *in vacuo*.

Two films taken under identical conditions of pressure and current showed that the lattice parameter of silver was the same after heating for 1 hour and for 3 hours, thus indicating that the motion of the governor of the clockwork, which consisted of a rotating vane, and the water-cooling system had produced a uniform steady temperature in 1 hour. Subsequently films were taken after the specimen had been heated for 1 hour. The following measurements show how the calibration curve at 100° C. was determined.

Two films were taken and the currents were chosen to give temperatures near 100° C. For example a current of $0\cdot55_0$ amp. gave a temperature of 88° C. whilst $0\cdot60_0$ amp. gave 120° C. These two points were plotted and the current necessary to give a temperature of 100° C. was deduced by interpolation. In this case the necessary current was $0\cdot57_0$ amp. A film taken with this current gave a parameter of 4·0838 A., corresponding to a temperature of 99° C. Thus, within the accuracy of the temperature measurements, the interpolation is justified.

Films were taken at various pressures from 10 to 76 cm. of mercury and the current i_{100} necessary to give 100° C. found by interpolation. The results are given in table 2 and the graph of i_{100} against the pressure p is given in figure 1. The current corresponding to a pressure of 0 cm. of mercury was read off the calibration curve *in vacuo* already determined. It is seen from the curve in figure 1 that the current is approximately independent of the pressure over the range 10–76 cm. of mercury, a rapid increase occurring over the first 10 cm. of mercury pressure.

Table 2. Calibration of heater in hydrogen

Film number	Pressure cm. Hg.	Current (amp.)	Parameter of silver (A.)	Temperature (° C.)	i_{100} (amp.)
8	75·3	$0{\cdot}55_0$ 1 hr.	4·0828	87	$0{\cdot}57_0$
9	75·3	$0{\cdot}55_0$ 3 hr.	4·0829	88	
15	75·3	$0{\cdot}60_0$ 1 hr.	4·0854	120	
26	75·3	$0{\cdot}57_0$,,	4·0838	99	
18	66·0	$0{\cdot}60_0$,,	4·0855	121	$0{\cdot}56_5$
22	66·0	$0{\cdot}53_0$,,	4·0824	82	
24	50·0	$0{\cdot}57_0$,,	4·0847	111	$0{\cdot}55_8$
28	50·0	$0{\cdot}55_5$,,	4·0836	97	
19	36·0	$0{\cdot}55_5$,,	4·0845	109	$0{\cdot}53_8$
23	36·0	$0{\cdot}51_0$,,	4·0829	88	
25	20·0	$0{\cdot}48_0$,,	4·0824	82	$0{\cdot}53_5$
27	20·0	$0{\cdot}50_0$,,	4·0829	88	
29	10·0	$0{\cdot}48_0$,,	4·0828	87	$0{\cdot}51_3$
32	10·0	$0{\cdot}52_0$,,	4·0842	104	

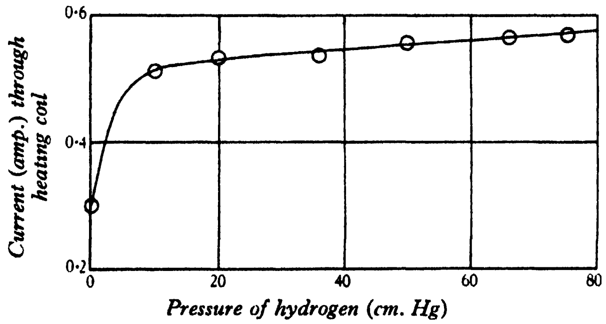

Figure 1.

§4. THE PREPARATION OF HYDROGEN

It is well known that impurities have a marked effect on the occlusive power of palladium for hydrogen. Maxted(12) found that a very small amount of sulphuretted hydrogen was sufficient to inhibit completely the adsorption of hydrogen. On exhausting at a temperature of 100° C. a volume of gas approximately equal to that of the sulphuretted hydrogen absorbed was evolved and was found on analysis to consist almost entirely of hydrogen, the sulphur being retained by the palladium.

The volume of the camera enclosure and the glass reservoir connected to it was of the order of 10 litres. It was therefore not expedient to generate the hydrogen by the electrolysis of barium hydroxide in the manner recommended for obtaining a very pure supply. Electrolysis of dilute acids or salts was not considered advisable, partly because of the slow rate of generation and partly because of the possibility of the formation of sulphur dioxide and sulphuretted hydrogen. It was finally decided to generate the gas in a Kipp apparatus by the action of pure hydrochloric acid on pure zinc, a few drops of a solution of cobalt sulphate being added as a catalyst to increase the velocity of reaction. The gas was bubbled slowly through the following train of purifying agents: (*a*) alkaline potassium permanganate; (*b*) a 5 to 10-per-cent solution of silver nitrate, to remove sulphuretted, arseniuretted and phosphoretted hydrogen, oxides of nitrogen, sulphur dioxide and halogens; (*c*) acid chromous chloride or alkaline pyrogallol, to remove traces of oxygen; (*d*) water to wash the gas free of traces of the other baths. The gas was then passed through calcium-chloride tubes and allowed to stand for some hours over phosphorus pentoxide contained in two large reservoirs, from which it could be passed through taps into either of the two camera enclosures. When measurements were made with a pressure of over 40 cm. of mercury it was necessary to close the taps connecting the enclosures with the glass reservoirs, as the latter were not of sufficient size to fill the whole apparatus to such pressures. A long boat containing phosphorus pentoxide and situated in the tube leading from the reservoirs served to remove the last traces of moisture from the gas. That the gas was rendered free from moisture is shown by the fact that the drying agent in this boat had to be renewed but once during the course of the work, which occupied about three years.

The presence of free sulphur in rubber was a possible source of sulphuretted hydrogen. As far as possible, rubber-glass connexions were not used in the generating apparatus, but for convenience in replacing purifying reagents (this was done about once every four weeks) it was necessary to make use of a few, the seals being made airtight with apiezon wax. Also, a rubber washer was used to render the camera enclosures airtight and ordinary pressure tubing was used in connecting parts of the apparatus. All these rubber parts before being connected up were boiled in a 10-per-cent solution of caustic potash for about eight hours, and then in water for three hours with frequent changing of water. They were then thoroughly dried in a current of warm air. This treatment was considered sufficient to remove any free sulphur from the rubber. Two small beakers containing caustic potash and phosphorus pentoxide were kept in the camera enclosures. The grease used for lubricating glass taps and rubber washers was made from sulphur-free rubber and pure petroleum jelly with a trace of paraffin wax. All parts of the apparatus were rendered gas-tight with apiezon wax.

The pressure in the apparatus was measured with a Bourdon gauge which was calibrated before and during the course of the work. A trap for oil vapour cooled to − 18° C. was inserted between the camera enclosure and the Cenco pump employed to evacuate the chamber.

§ 5. THE DEPENDENCE OF THE CONCENTRATION OF HYDROGEN IN THE SPECIMEN ON THE TEMPERATURE AND PRESSURE

In the X-ray study of alloy systems, it is necessary to know the composition of each alloy investigated. This entails little difficulty in metallic alloys, but in a metal-gas system difficulties arise owing to the number of factors which affect the composition. To determine the concentration of gas in the palladium specimens in this work would have needed an additional research, so that it was necessary to use the results obtained by other workers to translate the conditions of exposure into concentration when this was required. The concentration is usually expressed as the ratio of the number of atoms of hydrogen to the number of atoms of palladium and is denoted in symbolic form by H/Pd.

The most comprehensive set of {pressure, concentration} curves is that given by Hoitsema and Roozeboom(13), who used palladium in the form of powder and sponge. These curves were obtained with increasing pressure of hydrogen, which was the procedure mainly followed in this section of the present investigation. Also the curves cover a very wide range of temperature. In the absence of other data these curves were adopted for estimating the concentration of hydrogen in the charged samples whose X-ray spectra were taken.

§ 6. THE THERMAL EXPANSION OF PURE PALLADIUM

Pure palladium powder was prepared from material the purity of which was not less than 99·9 per cent, and this was annealed *in vacuo* for 3½ hours at 450° C. A number of photographs were taken at various temperatures over the range from 10 to 300° C., when the specimen was mounted on the focusing camera enclosed in an evacuated chamber. These photographs yielded sharp lines which could be measured to a high degree of accuracy. The temperatures were measured by means of copper-constantan and nickel-nichrome thermocouples which had already been calibrated. The K_α radiation of copper was used, and the indices of the reflexions obtained were 422. The values of the parameters at various temperatures are shown in table 3.

Table 3

Film number	Temperature (° C.)	Parameter (A.)
1	10	$3·8820_9$
2	11	$3·8822_5$
3	10	$3·8820_1$
6	10	$3·8820_1$
10	64	$3·8846_0$
29	110	$3·8869_1$
7	132	$3·8879_6$
8	181	$3·8905_3$
28	217	$3·8922_7$
4	231	$3·8928_9$
5	286	$3·8957_0$

These figures yield a value for the mean coefficient of thermal expansion over the range 0–300° C. of $12·7 \times 10^{-6}$. The corresponding value calculated from the figures given in the *International Critical Tables* is $12·33 \times 10^{-6}$. The experimental and calculated coefficients at 20° C. are respectively $11·75 \times 10^{-6}$ and $11·8 \times 10^{-6}$, which are in good agreement.

§7. THE DEGASSING AND ANNEALING OF CHARGED PALLADIUM SPECIMENS

In the course of the investigation each specimen powder was used several times, and in order to ensure that the effect observed should be that corresponding to the conditions obtaining in any particular experiment and not to those obtaining in previous experiments, it was essential to degas the powder and treat it thermally in such a manner as to bring it back to a standard state before the commencement of each experiment.

Previous workers have found that the hydrogen is liberated if a charged specimen is heated at approximately 150° C. in a maintained vacuum. That this is so may be demonstrated by enclosing the specimen in a glass tube and connecting it to the hyvac pump. The hard note of the pump is modified as soon as the flame of a match is applied to the tube. Not only is it important to know that all the gas has been removed, but it is equally important to know that the material has regained its normal state of equilibrium and is free from distortion. The X-ray method of investigating the degassing conditions supplies information on both of these points, and on that account is superior to other methods employed for the purpose.

A thorough investigation was carried out on this point and many photographs were taken of a specimen after various heat treatments. A specimen maintained at 100° C. and charged with hydrogen at a pressure of 76 cm. of mercury for three hours yielded a photograph, taken at room-temperature *in vacuo* with the focusing camera, which showed an unresolved band reflected from the β phase, the parameter being about 4·03 A. The specimen was heated *in vacuo* at 250° C. and photographed every half hour for the first 1½ hours. At the end of the first half hour it showed an unresolved band corresponding to the α phase, the parameter being 3·8819 A. The appearance of the band did not alter after 1½ hours' heating. The temperature was then raised to 290° C. and the specimen heated for various periods. After 4 hours' heating at 290° C. the band showed signs of resolution. After a further 5½ hours' heating the $K_{\alpha 1}$ could be distinguished from the $K_{\alpha 2}$ line, but the resolution was not good. After 6½ hours' further heating at 290° C. the $\alpha 1$ and $\alpha 2$ lines were separated. Satisfactory resolution of the doublet was not obtained until the specimen had been heated *in vacuo* at 290° C. for about 24 hours. The parameter calculated from the measurement of the resolved doublet, namely 3·8820 A., did not differ from the parameter deduced from the unresolved band photographed after half an hour's heating *in vacuo* at 250° C., indicating that all the gas had been removed by this amount of heating but that the distortion brought about by the occlusion of hydrogen in the palladium had not been removed. To remove this distortion a much longer period of heating was required.

The next operation was to charge the palladium powder, maintained at 100° C., with hydrogen at a pressure of 66 cm. of mercury for half an hour. After evacuation of the chamber, the specimen being still maintained at 100° C. as in the previous instance, the unresolved band appearing on the photograph yielded a parameter of 4·07 A. The specimen was then heated for 1 hour at 450° C. *in vacuo* and an exposure was taken at 18° C. *in vacuo*. The doublet was as well resolved after this treatment as after 24 hours at 290° C., and on measurement it yielded a parameter of 3·8825 A. A further treatment of 2½ hours at 450° C. was more than ample to give complete resolution.

In those cases in which the adsorption caused an expansion of the lattice without change of phase, the doublets were in general well resolved, but they showed a certain lack of definition which was probably due to the distortion of the lattice. It was found that annealing for one hour at 450° C. was sufficient again to produce well defined lines. Linde and Borelius⁽⁴⁾ state that in all their exposures the specimen was previously heated at 250° C. in air for 4 hours and that from the photographs taken they concluded that this treatment was sufficient to render the specimens free of hydrogen. The experiments that have just been described show, however, that the specimen was free from gas after being heated *in vacuo* at 250° C. for half an hour, but that heating the specimen for 29 hours at 250° C. *in vacuo* was not sufficient to remove the lattice-distortion caused by the occlusion of the hydrogen in the specimen. The results are important in that they throw some light on the mechanism of absorption and desorption. It appears that the absorbed hydrogen atoms push the palladium atoms farther apart and that in this state the palladium atoms take up positions that are slightly different from those occupied by the atoms in the normal face-centred lattice. Thus, the value of the crystal spacing given by the ordinary Bragg equation no longer has a singular value, and the reflexions of the $K_{\alpha 1}$ and $K_{\alpha 2}$ wave-lengths overlap on the film and give the unresolved band already mentioned. When the specimen is heated at 250° C. *in vacuo* the gas present in the lattice is very easily removed, but though the cause of the displacement of the metallic atoms has been removed the temperature of 250° C. is too low to produce sufficient thermal agitation to cause the palladium atoms to resume their true positions of equilibrium in a reasonable time. The higher temperature of 450° C. however brings the metal to its state of equilibrium in three hours. It is interesting to note in this connexion that palladium powder on which cold work has been done in the filing process, and which gives a band showing lack of resolution comparable to that produced by occluded gas, requires to be annealed at 450° C. for about 3 hours to remove distortion caused in the filing process.

The results of Nähring's⁽¹⁴⁾ investigation of the variation in the width of the X-ray spectral lines of palladium with electrolytic charging and discharging are now readily understood. Nähring obtained an unresolved doublet on charging electrolytically. He observed that if the charged specimen were degassed by making it the anode of an electrolytic cell the increase in line-width produced by the charging was not reduced no matter how long a time for degassing was given. The doublet remained unresolved. He observed also that during anodic degassing the line-width of the second phase remained constant and had the same value as on charging. This was not so for the first phase, for which the line-widths during the discharging were greater than during charging. He found that if the degassing were continued for such a long time that the adsorbed gas was completely removed, as was shown by the return of the lattice-parameter to its original value, the width was still greater than that of uncharged palladium and the doublet remained unresolved. The explanation of these results is that the anodic degassing at room-temperature caused the hydrogen to be removed from the lattice and the mean parameter to assume its original value, but the temperature was not high enough to remove the distortion of the lattice.

§ 8. THE TREATMENT OF THE SPECIMEN BEFORE AND AFTER EXPOSURE TO X RAYS

The method of admitting the hydrogen and of heating the specimen underwent several changes during the course of the work, but in all cases the enclosure was evacuated immediately after exposure and the powder maintained at a temperature of 250° C. for at least 30 min. *in vacuo* to remove the adsorbed gas. During an exposure the temperature was frequently checked and adjusted if necessary. At all temperatures the variation from the required value was not more than 1 per cent as registered on the galvanometer scale.

The greatest difficulty with the apparatus was to render it vacuum-tight. Some exposures had to be made with hydrogen at a pressure of a few millimetres of mercury and a temperature had to be maintained constant for some hours. Under such conditions it was difficult to be free entirely from leakage into the apparatus. To diminish the effect of any slight leakage, a reservoir of about 6 litres capacity was connected to the enclosure and by this expedient the gas pressure could be maintained without appreciable change over long periods.

Three different methods were employed to charge the specimen with hydrogen. In method (1) the hydrogen was admitted into the evacuated enclosure and reservoir to approximately the desired pressure, the temperature being then raised to its proper value and the pressure finally adjusted. The {pressure, concentration} isothermals of Hoitsema and Roozeboom show that, when the gas is admitted at room temperature, the concentration in the specimen almost immediately reaches a value of the order of 0·6 H/Pd, when the β phase is formed. As the temperature is raised to its final value, say 100° C., the concentration gradually adjusts itself to the value corresponding approximately to the final pressure and temperature. If, under these conditions, the α phase existed alone it was found that the doublet could not be resolved, owing to the fact that the β phase had been in existence at room temperature; although the lattice parameter had assumed the value corresponding to the final conditions, distortion was still present. The method was discarded for this reason. In method (2) the temperature of the specimen was adjusted to the desired value *in vacuo* and the gas was admitted in small volumes until the desired pressure was reached. The temperature dropped rapidly over the first few minutes and was adjusted to its proper value after each small addition of gas. On a few occasions, however, at very critical pressures, the temperature was not controlled successfully enough and the α-phase doublet was unresolved. In method (3) the gas was admitted as in method (2), but the temperature in the steady state was approached from the high-temperature side, the temperature of admission being consistently 20° C. higher than the steady-state value. The time taken to cool to this latter value was usually about 15 minutes. In both methods (2) and (3) the concentration of hydrogen in the specimen was being gradually increased, in correspondence with the ascending isothermals of Hoitsema and Roozeboom and of Lambert and Gates. An investigation of the effect of the temperature of admission on the lattice parameter showed that within experimental error the parameter was independent of that temperature.

It may perhaps be desirable to point out here that the term "steady state" is applied to the system when the values of the temperature and pressure during an experiment remained constant. It should not be confused with the term "equilibrium state", which applies to the specimen.

§ 9. THE OCCLUSION OF HYDROGEN BY SILVER

It was important to investigate the occlusion of hydrogen by silver, because this metal was to be used to calibrate the heater of the spectrum camera. The investigation was carried out with a focusing camera, measurements of the parameter of silver being made over a temperature-range from 15° C. to 140° C. and over a pressure-range of 0 to 76 cm. of mercury. The gas was admitted at the temperatures given in column 3 of table 4.

Table 4

Film number	Pressure of hydrogen cm. Hg	Temperature (° C.)	Parameter in hydrogen (A.)	Parameter *in vacuo* (A.)	Occlusion effect (A.)
232	0	16	—	$4{\cdot}0769_2$	0·0001
235	57·5	15	$4{\cdot}0768_1$		
240	76	15	$4{\cdot}0769_7$		
238	76	15	$4{\cdot}0767_0$		
		Mean	$4{\cdot}0768_2$		
234	0	140	—	$4{\cdot}0868_0$	0·00007
236	57·5	140	$4{\cdot}0866_6$		
239	76	140	$4{\cdot}0866_4$		
242	76	140	$4{\cdot}0867_8$		
		Mean	$4{\cdot}0867_3$		
233	0	100	—	$4{\cdot}0836_8$	$0{\cdot}0002_5$
235	57·5	100	$4{\cdot}0835_2$		
237	76	100	$4{\cdot}0832_4$		
241	76	100	$4{\cdot}0835_4$		
		Mean	$4{\cdot}0834_3$		

Copper radiation was used throughout, the reflections from the silver being 333 and 511. The parameter values are probably accurate to within ± 0·0003 A. It will be observed from the last column of the table that the effect of adsorption on the lattice parameter of silver is well within limits of experimental error. Silver could therefore be used for temperature calibration even when surrounded by an atmosphere of hydrogen.

§ 10. PARAMETER-MEASUREMENTS AT VARIOUS TEMPERATURES AND PRESSURES

The first set of parameter-measurements was deduced from spectra taken at a temperature of 100° C. with the focusing camera, the gas being admitted as described under method (2) above. Copper K_α radiation was used for most of the exposures, the reflexions being 422.

To find the length of time necessary to allow the material to reach a state of equilibrium, the lattice parameter of the charged palladium was measured after various intervals of time during which the pressure of the gas in the enclosure and the temperature of the specimen were maintained constant. At a pressure of 16 cm. of mercury, when the times in the steady state were 30 and 60 min. respectively, the parameters had identical values 3·8910. At a pressure of 17 cm. of mercury the parameters were 3·8911, 3·8914 and 3·8912, corresponding to times of 30, 40 and 55 min. respectively in the steady state. The differences between these values were within the limits of experimental error and it was therefore inferred that equilibrium was attained after 30 min. in the steady state. Similar observations at higher pressures, when the β phase was observed, led to the same conclusion, but owing to lack of definition the measurements made on the spectral lines from this phase were not as satisfactory as on those from the α phase. For instance at a pressure of 66 cm. of mercury the parameters found were 4·027, 4·026, 4·024 and 4·027, corresponding to times in the steady state of 30, 60, 60 and 180 min. respectively. These values agree within the limits of accuracy of 0·004 A. which are claimed for these measurements on the β phase.

The results yielded by photographs taken at a pressure of 26 cm. of mercury are of interest. One film showed a strong band from the β phase corresponding to a parameter of 4·019 A. together with a faint line due to 422 reflections of the α phase which gave a parameter value of 3·892 A. Another film which was taken under the same experimental conditions showed only the α phase line, the corresponding parameter being 3·8914 A. Another exposure taken under similar conditions of charging when the specimen was kept for 270 min. in the steady state prior to making the exposure, also showed the lines of the α phase, the parameter being 3·8914 A., and again there was no indication of a reflection from the β phase. The parameters of the α phase however were identical after the pressure and the temperature had been maintained constant for periods of 30 and 270 min. respectively. A satisfactory explanation of the appearance and non-appearance of the β-phase band under apparently the same experimental conditions could not at this stage be given. The matter will be referred to and an explanation will be given in a later paper.

At present it suffices to record that two face-centred lattices of widely differing parameters coexisted at certain temperatures and pressures and no intermediate parameter values were observed. Ubbeholde(15) has pointed out that this absence of intermediate values may be fortuitous and may be due to insufficient precaution against poisoning of the specimen. Every precaution was taken to avoid such poisoning, and the fact that palladium specimens which were newly prepared, and also those which had been used several times over, yielded points falling on the same curve provided evidence that there were no serious errors arising from contamination.

Before proceeding, a detailed investigation was made of the factors governing the values of the lattice parameter. It was found that the parameter was independent of (1) the wave-length of the radiation employed, (2) the atomic planes which were effective in reflecting the incident beam, (3) the temperature of admission of the gas, (4) the rate of cooling from the temperature of admission to the final steady temperature, and (5) the time during which the specimen was kept in the steady state before the exposure was made, provided it exceeded a certain minimum value. The results indicated that the parameter at a given temperature was dependent only on the pressure of the gas surrounding it.

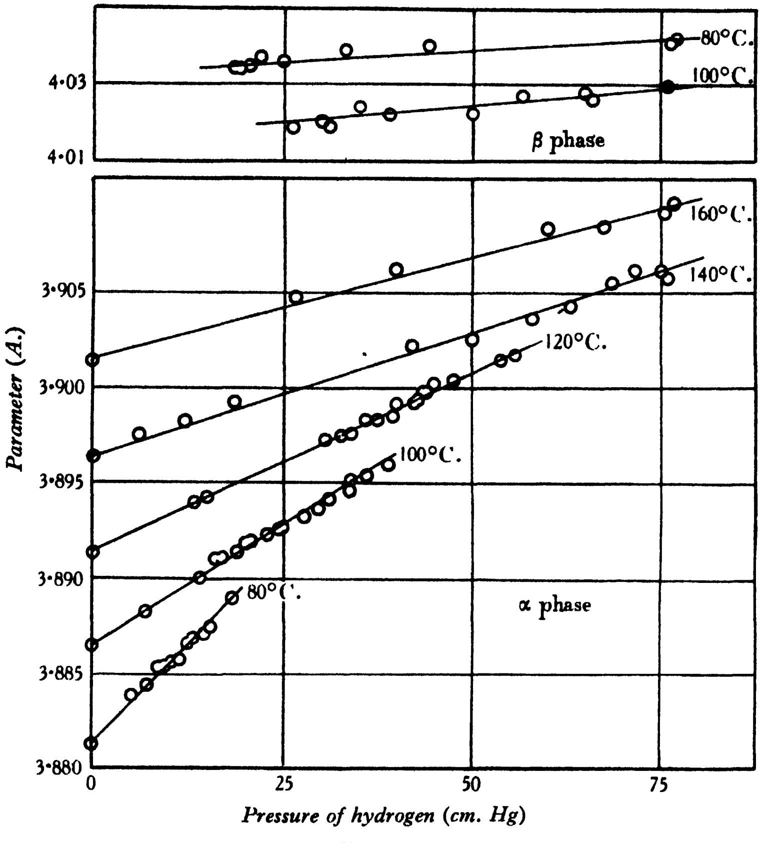

Figure 2.

Attempts were made to find what relation, if any, existed between the parameter of charged palladium and the pressure of the surrounding gas. For this purpose investigations at different temperatures were conducted along the same lines as that carried out at 100° C., the temperatures chosen being 80, 120, 140 and 160° C. When the parameter was plotted against the pressure it was found that the best graphical representation at each temperature was a straight line, both for the α and for the β phase. The results are shown in figure 2, the curves in which have been displaced relative to one another for clearness of presentation. The parameters along the ordinate axis in the diagram refer to the curves at 100° C. At zero pressure the α-phase parameters are 3·8854, 3·8864, 3·8874, 3·8884 and 3·8894 at the temperatures 80, 100, 120, 140 and 160° C. respectively. The parameters of the β phase at a pressure of 25 cm. of mercury are 4·026 and 4·019 at 80 and 100° C. respectively.

The slope of the α-phase lines diminishes with increasing temperature. There does not appear to be much difference between the slopes of the β lines at the two temperatures taken, namely 80 and 100° C., but these lines are not so definitely fixed as the α lines owing to the difficulty of measuring the spectral lines from the β phase. For this reason the α-phase lines only will be considered in detail here.

§ 11. THE RELATION BETWEEN THE PARAMETER OF THE α PHASE, THE TEMPERATURE OF THE SPECIMEN AND THE PRESSURE OF THE GAS

Table 5 gives the values of the slopes of the α curves at the various temperatures.

Table 5

Temperature ° C.	$\frac{da}{dp} \times 10^5$	$\log \frac{da}{dp}$	$\log t$
80	39·0	$\bar{4}$·5911	1·9031
100	24·3	$\bar{4}$·3856	2·000
120	18·4	$\bar{4}$·2648	2·0792
140	12·0	$\bar{4}$·0792	2·1461
160	10·4	$\bar{4}$·0170	2·2041

The linear relations found between p and a in figure 2 and between log da/dp and log t in figure 3 lead to the following equation:

$$a = a_0\,(1 + \alpha t) + 2{\cdot}5\,pt^{-2} \qquad \text{......(1)},$$

where a is expressed in angstroms, p in cm. of mercury and t in degrees Centrigrade.

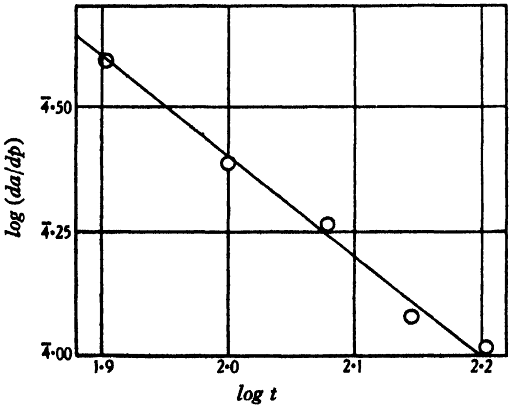

Figure 3.

Hence for the α phase, that is the palladium-rich phase, the change in the parameter of palladium due to the occlusion of hydrogen is directly proportional to the pressure of the hydrogen and inversely proportional to the square of the temperature of the palladium, i.e. $\Delta a = cp/t^2$. This holds for temperatures ranging from 80° C. to 160° C.

Table 6 gives the values of the parameter as calculated from equation (1) and as read off the graph for various arbitrary values of pressure and temperature.

Table 6

t (° C.)	p cm. Hg	$a_0(1+\alpha t)$ A.	$\frac{5}{2}pt^{-2}$ (A.)	a, calculated A.	a, from graph A.
80	15	3·8854	0·0061	3·8915	3·8915
100	30	3·8864	0·0075	3·8939	3·8939
120	30	3·8874	0·0052	3·8926	3·8930
140	50	3·8884	0·0064	3·8949	3·8950
160	50	3·8894	0·0049	3·8943	3·8947

The difference between the calculated and observed values is within the limits of experimental error claimed in the measurement of the parameter, namely ± 0·0004. Equation (1) seems therefore to fit the observations satisfactorily.

The relation also yields information concerning the variation of the rate of change of the parameter of charged palladium with temperature. Differentiating equation (1) we get

$$\frac{1}{a_0}\frac{da}{dt} = \alpha - \frac{5p}{a_0 t^3} \qquad \ldots\ldots(2),$$

where the quantity a_0 is the value of the parameter of pure palladium *in vacuo* at 0° C. The second term on the right-hand side of the equation shows the effect of the occlusion of hydrogen by the palladium on the thermal expansion of the material.

If instead of the pressure of the gas surrounding the palladium the concentration of the gas in the palladium is taken, the relation between parameter and temperature at concentrations not exceeding 10 atomic per cent of hydrogen, and over the range of temperature between 80 and 160° C., is linear as shown in figure 4. Values of the rate of increase of parameter with temperature at the different concentrations are given in table 7.

Table 7

Hydrogen content (atoms per cent)	$\frac{da}{dt}$
0	50×10^{-6}
3·5	78×10^{-6}
5·0	90×10^{-6}
7·5	98×10^{-6}

The absolute values of the slopes of the lines in figure 4 are not accurate, but the curves serve to show that the rate of expansion of the lattice with temperature increases as the hydrogen-content increases. It would appear that the entrance of the hydrogen atoms into the lattice, even though they enter it interstitially, loosens the bonds between the palladium atoms, thus allowing the latter to separate more readily under the action of heat.

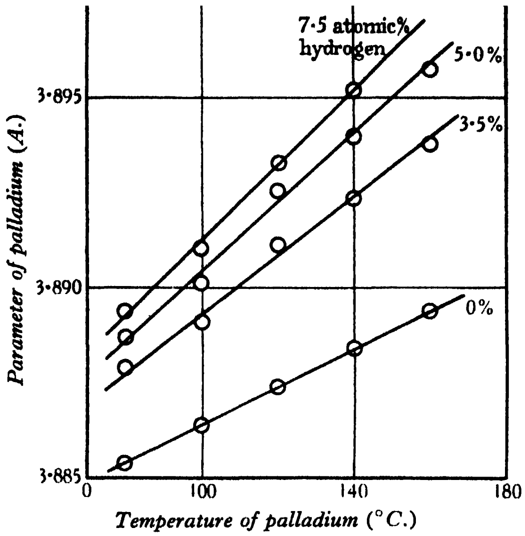

Figure 4.

§ 12. ACKNOWLEDGEMENT

We have pleasure in thanking the Department of Scientific and Industrial Research for a grant which enabled us to carry out the work.

REFERENCES

(1) Lambert and Gates. *Proc. roy. Soc.* A, **108**, 456 (1925).
(2) Yamada. *Phil. Mag.* **45**, 241 (1923).
(3) McKeehan. *Phys. Rev.* **21**, 334 (1923).
(4) Linde and Borelius. *Ann. Phys.*, Lpz., **84**, 747 (1927).
(5) Hanawalt. *Phys. Rev.* **33**, 444 (1929).
(6) Kruger and Sacklowski. *Ann. Phys.*, Lpz., **78**, 72 (1925).
Kruger and Gehm. *Ann. Phys.*, Lpz., **16**, 174 (1933).
Mundt. *Ann. Phys.*, Lpz., **19**, 721 (1934).
Rosenhall. *Ann. Phys.*, Lpz., **18**, 150 (1933).
Nähring. *Ann. Phys.*, Lpz., **21**, 303 (1934).
(7) Sachs and Weerts. *Z. Phys.* **60**, 481 (1930).
(8) Berry. *J. chem. Soc.* **99**, 463 (1911).
(9) Rosenhall. *Ann. Phys.*, Lpz., **18**, 150 (1933).
(10) Hägg. *Z. phys. Chem.* B, **12**, 33 (1931).
(11) Bradley and Jay. *Proc. phys. Soc.* **44**, 563 (1932).
(12) Maxted. *J. chem. Soc.* **2**, 2203 (1931).
(13) Hoitsema and Roozeboom. *Z. phys. Chem.* **17**, 1 (1895).
(14) Nähring. *Ann. Phys.*, Lpz., **21**, 303 (1934).
(15) Ubbeholde. *Trans. Faraday Soc.* **28**, 278 (1932).

THE PALLADIUM-HYDROGEN SYSTEM

By PROFESSOR E. A. OWEN, M.A., D.Sc.,
AND
JOHN IDWAL JONES, Ph.D.,
University College of North Wales, Bangor

Received 4 *June* 1937.

ABSTRACT. The hysteresis effect observed in the palladium-hydrogen system when the pressure of the gas is taken through a cycle of changes has been examined by the X-ray method. Measurements of the parameter of charged palladium at different pressures were made when the temperature was kept constant. When the pressure was increased and the temperature kept at 100° C. the α phase appeared alone up to a pressure of about 20 cm. of mercury, the parameter increasing as the pressure was increased. Between pressures of 20 and 45 cm. of mercury the α and β phases appeared together and on further increase of pressure the β phase appeared alone. With decreasing pressures, starting from an initial pressure of 66 cm. of mercury, the β phase appeared alone until a pressure of about 21 cm. of mercury was reached. Over the range of pressure from 21 to about 17 cm. of mercury the α and β phases appeared together, but at a pressure of 17 cm. of mercury the β phase disappeared, the α phase remaining alone until the pressure was reduced to zero. Those parts of the ascending or descending isothermals in which a single component existed, could be retraced by altering the pressure but this reversibility disappeared when the second component made its appearance.

The concentration of hydrogen in palladium changed rapidly when the β phase appeared or disappeared. The measurements support the view that the palladium-hydrogen system consists of two solid solutions at the two temperatures chosen, namely 100° and 120° C., the hydrogen rich phase being closely associated with the combination Pd_2H, which is capable of taking hydrogen into solution.

The β phase lattice was always found to be distorted; every attempt to obtain this phase free from distortion failed. No such distortion was found with the α phase. The distortion of the β phase lattice remained after the gas had been removed from the metal. It required a temperature well above that necessary to displace the hydrogen from the metal to remove the distortion. It is concluded that the gas is not in its normal state when it leaves the metal.

§ 1. INTRODUCTION

In a previous paper⁽¹⁾ the effect of pressure and temperature on the occlusion of hydrogen by palladium was studied. The change in the parameter of palladium due to occlusion of hydrogen was found to vary directly as the pressure of the hydrogen and inversely as the square of the temperature of the palladium. In the paper reference was made to the work of Lambert and Gates⁽²⁾ who found that the relation between the pressure of hydrogen surrounding the palladium at any temperature and the concentration of the gas in the palladium depended upon whether the pressure of the gas was increased or decreased to its final value. The ascending isothermal differed in shape from the descending isothermal, thus exhibiting a cycle similar to a hysteresis loop. In the present paper this effect is studied in detail by X-ray analysis.

The results of Hoitsema and Roozeboom(3) indicated the existence of two immiscible solutions of hydrogen in palladium. Their curves were of the same general shape as those of the ascending isothermals obtained by Lambert and Gates who, however, found a number of factors which had a profound effect on the equilibrium of the system. The last named authors observed, in addition to the hysteresis effect already noted, that the shape of the ascending isothermal depended upon the method adopted to vary the pressure. Thus the curve obtained when the pressure was increased in a regular manner differed from that obtained by alternately adding and withdrawing from the reaction vessel known quantities of hydrogen, the quantities added being always greater than those withdrawn. Whereas a smooth curve could be drawn through the points connecting equilibrium pressure and concentration in the first case, no such smooth curve could be drawn in the second case. Also it was found that if the controlled temperature of the system was allowed to fall to that of the room and was restored after some hours to its original value, the new equilibrium pressure differed appreciably from the original value and no tendency was noted for this pressure to attain its former value even on long standing. The general conclusion reached by these authors is that the ascending isothermals, even for identical experimental conditions, are not repeatable, whilst the descending isothermals are. These results were considered by the authors to indicate the existence of at least two allotropic forms of metallic palladium which probably differed in their rate of adsorption of hydrogen.

A great change in concentration for a small change in pressure was found in the descending isothermals obtained at 75, 103 and 120° C. This took place at each temperature at a concentration of approximately two atoms of palladium to one of hydrogen. In view of the comparatively wide range of temperature over which this effect occurred, it might be considered evidence of the existence of the compound Pd_2H.

The {pressure, concentration} isothermals of the palladium-hydrogen system obtained by Hoitsema and Roozeboom are reproduced in figure 1 together with the descending isothermal at 100° C. (represented by the dotted line) obtained by Lambert and Gates.

§ 2. APPARATUS AND EXPERIMENTAL PROCEDURE

Two cameras, the focusing camera and the fibre camera, were employed in the investigation as explained in our previous paper.

The method of temperature measurement was different in the two cameras. In the focusing camera the temperature of the specimen at any instant could be estimated from the galvanometer deflection. The variation in temperature during the admission of the gas was no more than ± 1° C. With the fibre camera no visible control of temperature was possible. The current through the heater required to produce a given temperature varies with the gas pressure and in consequence it is difficult to maintain a steady temperature whilst the pressure is being altered. An attempt was made to overcome this difficulty by increasing the pressure very slowly and at the same time increasing the heating-current as required by the calibration curve. A similar method was also used when the pressure was decreased. After some practice, it was possible to maintain a fairly constant temperature during the admission of the gas, but owing to the difficulties involved it was not as constant as that obtained with the focusing camera when the temperature could be controlled by keeping the galvanometer spot steady.

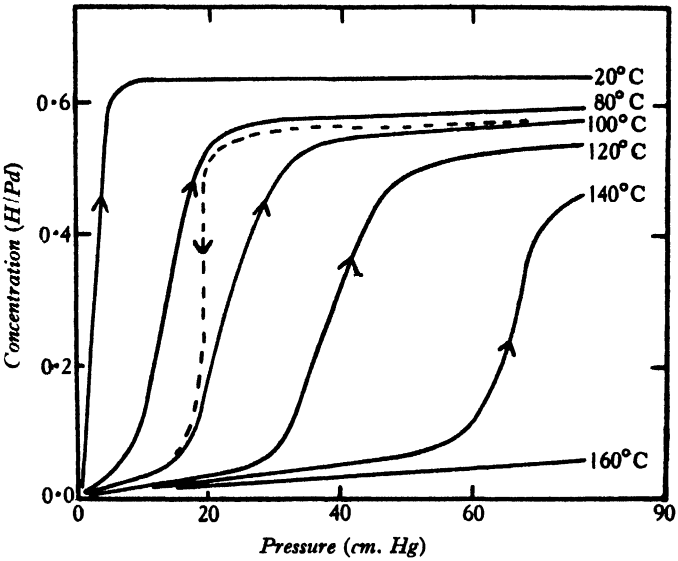

Figure 1.

The first temperature chosen was 100° C., the gas being admitted slowly into the evacuated chamber enclosing the camera until the desired pressure was reached; the temperature of the palladium was maintained at this value throughout the operation. The pressure was kept constant at its final value for 2 hr. before exposing the specimen to the X-ray beam.

The initial part of the investigation was carried out with the focusing camera and it was found that at certain pressures only the α phase was recorded. At higher pressures both the α and the β phases were recorded together and at still higher pressures the β phase was recorded alone. Although the estimated values of the lattice parameter calculated from measurements made on films taken with the focusing camera were more accurate than those calculated from the spectrum photographs obtained with the fibre camera, yet the latter proved more suitable for the work in hand as the structure could continuously be kept under observation. The spectra showed that the structure of the charged palladium remained unchanged as the concentration was varied; they also showed more definitely than the focusing-camera photographs when the β phase made its first appearance. For the latter part of the work, therefore, the fibre camera was almost exclusively used.

§ 3. RESULTS

(i) *The ascending isothermal at* 100° *C*. The first six films reproduced in figure 2 show very clearly what takes place when the pressure of the gas is gradually increased to its final value and kept at this value for 2 hr. before making the exposure. The temperature was maintained at 100° C. throughout these changes of pressure.

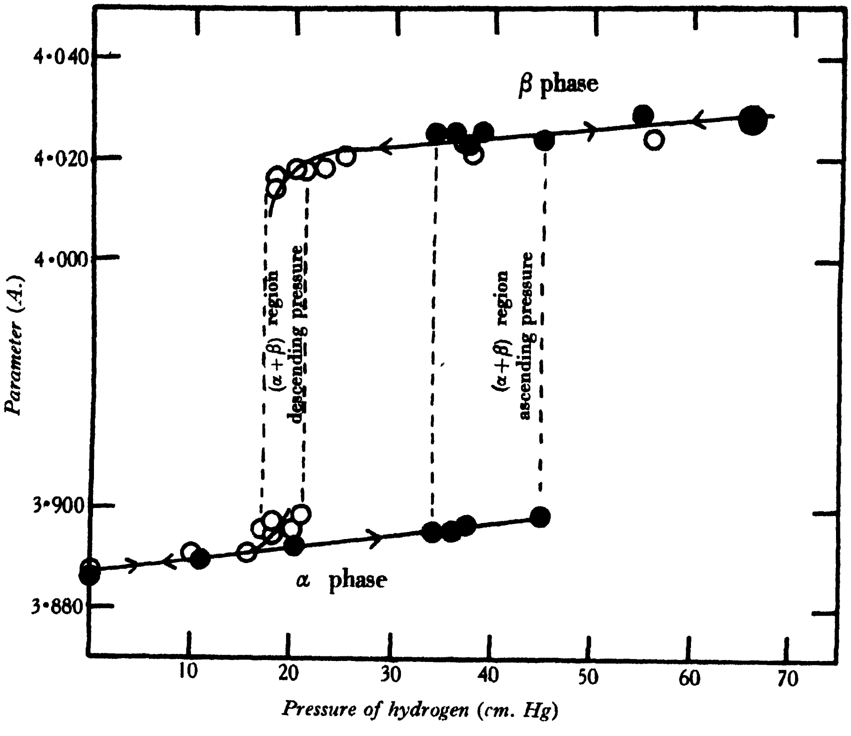

Figure 3. ● ascending pressure; ○ descending pressure.

Up to a pressure of about 20 cm. of mercury only the α phase appears, and if this pressure is not exceeded the curve is retraced on lowering the pressure, that is, the change is reversible. When the pressure is increased to about 34 cm. of mercury, the α and the β phases appear together and they are both present until the pressure is increased to about 45 cm. of mercury. Beyond this pressure only the β phase appears.

(ii) *The descending isothermal at* 100° *C*. To obtain the descending isothermal the pressure of the hydrogen was initially fixed at 66 cm. of mercury and maintained at this value for 2 hr. The pressure was then decreased gradually to a definite value in the range of pressure between 56 cm. and about 0·001 mm. of mercury,

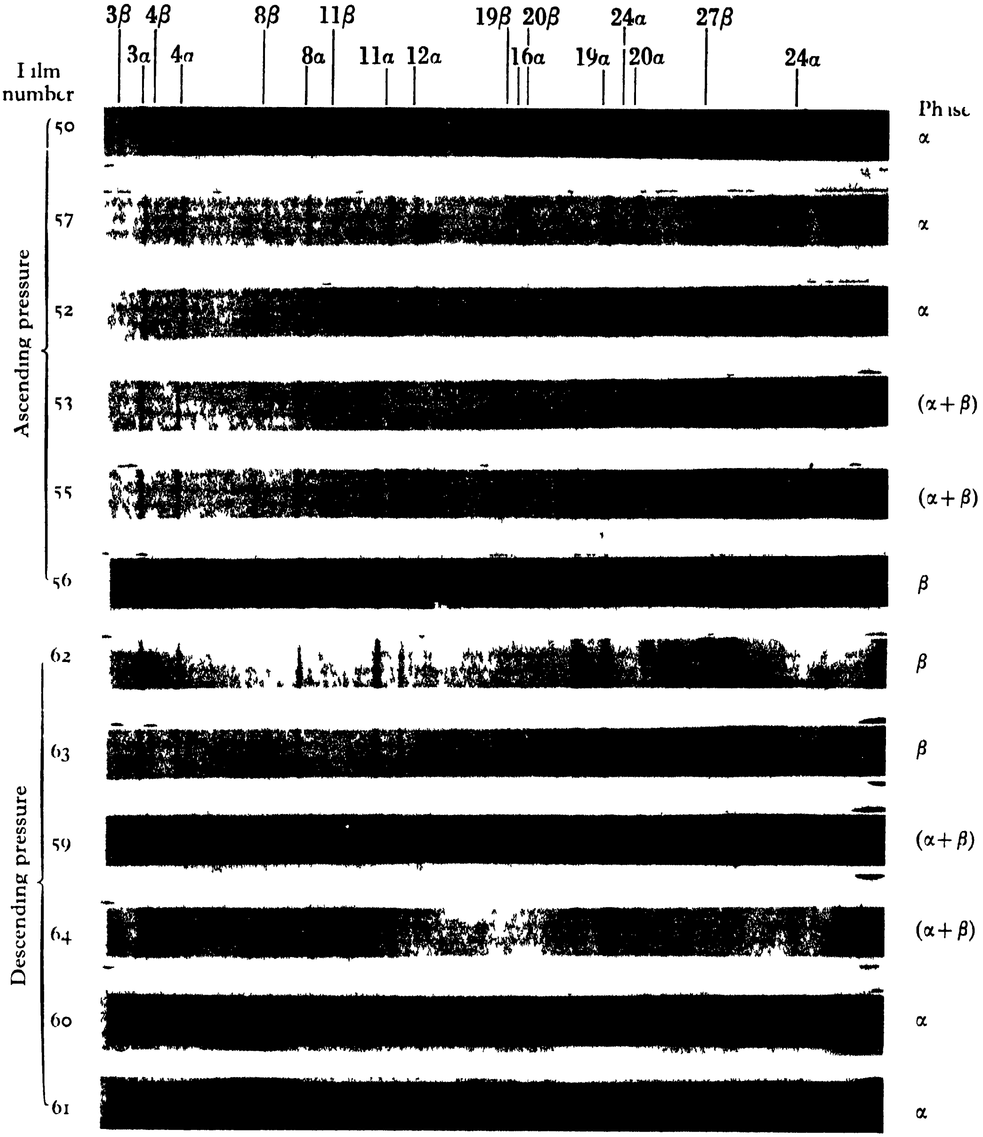
3β
4β
8β
11β
19β
20β
24α
27β
3α
4α
8α
11α
12α
16α
19α
20α
24α
Film number
Phase
Ascending pressure
Descending pressure
50
57
52
53
55
56
62
63
59
64
60
61
α
α
α
(α+β)
(α+β)
β
β
β
(α+β)
(α+β)
α
α

Figure 2

and maintained at this value for 2 hr. before making the exposure. The temperature was kept at 100° C. as near as possible while the pressure was changed.

When the final pressure was reached in the manner just described, it was found that the β phase appeared alone in the range of pressure between 56 cm. and about 21 cm. of mercury. Over the range from 21 cm. to about 17 cm. the two phases appeared together, but at 17 cm. the β phase disappeared, the α phase remaining alone until the pressure was reduced to zero. Here is a definite indication of the hysteresis effect which had already been observed by Lambert and Gates. The results now obtained are shown in figure 3.

It is of interest to note that only those parts of the ascending or descending isothermal, where a single component exists, could be retraced by altering the pressure; this reversibility disappears immediately the second component makes its appearance.

The values of the lattice parameters of charged palladium after various changes in pressure of the surrounding gas when the temperature of the specimen was kept at 100° C., are collected in table 1.

Table 1. Parameters of charged palladium at 100° C.

	Film no.	Charging pressure maintained for 2 hr. (cm. Hg)	Final pressure for descending isothermal (cm. Hg)	Time in steady state for descending isothermal (hr.)	Parameters (A.)	
					α	β
←Ascending pressure→	50	0·0	—	—	3·8863	—
	57	10·8	—	—	3·8900	—
	52	20·2	—	—	3·8930	—
	105	34·0	—	—	3·8952	$4{\cdot}025_6$
	102	36·0	—	—	3·8954	$4{\cdot}025_6$
	53	37·5	—	—	3·897	$4{\cdot}022_9$
	55	38·7	—	—	Faint	$4{\cdot}025_6$
	103	39·0	—	—	3·896	$4{\cdot}025_6$
	104	45·0	—	—	Very faint	$4{\cdot}024_0$
	69	55·0	—	—	—	$4{\cdot}029_1$
	56	66·0	—	—	—	$4{\cdot}028_1$
←Descending pressure→	62	66·0	56·0	2	—	$4{\cdot}024_1$
	63	66·0	37·7	2	—	$4{\cdot}021_0$
	58	66·0	37·0	2	—	$4{\cdot}023_0$
	90	66·0	25·0	4	—	$4{\cdot}020_3$
	319	66·0	20·0	5	3·896	4·018
	320	66·0	20·0	21	3·896	4·018
	321	66·0	20·0	72	3·896	4·018
	70	66·0	21·0	2	3·899	$4{\cdot}018_0$
	59	66·0	18·0	2	$3{\cdot}898_2$	$4{\cdot}014_4$
	91	66·0	18·0	4	$3{\cdot}895_0$	$4{\cdot}016_4$
	92	66·0	17·0	4	$3{\cdot}896_4$	$4{\cdot}016_6$
	64	66·0	16·0	2	$3{\cdot}891_3$	Faint
	60	66·0	10·0	2	$3{\cdot}891_2$	—
	61	66·0	0·0	2	$3{\cdot}888_0$	—

When the intensities of the lines in the spectra were weak, only an approximate value of the parameter could be obtained; in some cases the lines were so faint that no measurement was possible, but the presence of the phase is indicated in the table so that it may be known when the phases appeared together.

There are wide ranges of pressure over which the two phases coexist; the range is wider for the ascending than for the descending pressure curve. The ascending pressure-range is slightly greater than 11 cm. of mercury but the descending pressure-range is less than 9 cm. of mercury. The extent of these ranges might be modified if a different procedure as regards pressure changes and time during which the pressure remains constant, were adopted. Thus, it was found that the system required a longer time to attain an equilibrium state when the final pressure was reached from the low-pressure side than when it was reached from the high-pressure side. Also the relative amounts of the α and β phases when they appeared together depended upon the time of charging or discharging the palladium. For instance, after the specimen had been charged at a pressure of 66 cm. for 2 hr. at 100° C. and the pressure then reduced to 20 cm. and kept at this value for 5, 21 and 72 hr. respectively, the values of the parameters of the α and β phases were the same but the relative intensities of the lines from the phases changed. Whereas at the beginning the lines of the α phase were weaker than those of the β phase, the reverse was the case after the pressure had been maintained constant for a period of 72 hr. These effects are now being investigated in greater detail.

(iii) *The ascending and descending isothermals at* 120° *C.* The results obtained at this temperature were in general agreement with those found at 100° C. but the ranges over which the two phases appeared together both with ascending and descending pressures, were wider at 120° C. than at 100° C. under the same conditions of pressure and time in the steady state. It was again found that the curves obtained when only one constituent appeared were reversible.

§4. DISCUSSION

The curves obtained by Lambert and Gates giving the relation between the pressure of hydrogen and the concentration of hydrogen in palladium at 103° C., when the pressure is increased or diminished as already described, are shown in figure 4. The ascending isothermal takes different forms according to the method of charging the specimen, but the shape of the descending isothermal is practically the same for all conditions of charging and at all temperatures, and a sharp bend occurs in these curves at a concentration of about 0·5, that is, when there are two palladium atoms to each hydrogen atom. After this, the concentration decreases very rapidly as the pressure is lowered; it drops from 0·5 to 0·1 H/Pd whilst the pressure changes from about 18 to 16 cm.

In the ascending isothermal the concentration changes rapidly between pressures of about 36 and 70 cm. of mercury. This may vary according to the method adopted to increase the pressure.

Comparing these curves of change in concentration with pressure with those in figure 3 showing the change in parameter with pressure we find that the region where the concentration changes rapidly with pressure corresponds with the regions where the α and β phases appear together. In other words, the increase or decrease in concentration corresponds with the appearance or disappearance of the β phase. And from the parameter-pressure curves of figure 3, we should expect the slope of the ascending isothermal in the critical region to be less than that of the descending isothermal, as is actually the case in the curves of Lambert and Gates.

If then the sudden rise and fall in the concentration may be associated with the appearance and disappearance of the β phase, the β phase disappears when the concentration is 0·5 H/Pd; this is so at all temperatures according to Lambert and Gates and it is quite definite. The concentration at which the β phase makes its appearance in the ascending isothermals is not so definite; at 100° C. it appears with the α phase over a range of pressure which is greater than that observed in the descending isothermal and the range embraces the concentration 0·5 H/Pd.

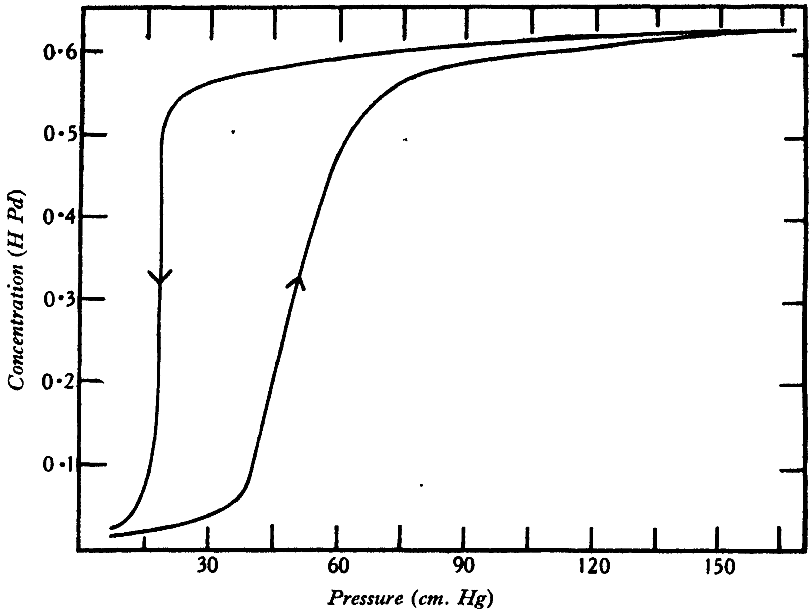

Figure 4.

Since equilibrium is more difficult to attain from the low-pressure than from the high-pressure side, the explanation of the smaller slope of the {pressure, concentration} curve in the critical region of the ascending isothermal may be due to the fact that the state of true equilibrium was not reached. This point needs further investigation. A special apparatus has now been designed to do this.

The disappearance of the β phase at a concentration of two atoms of palladium to one atom of hydrogen would seem to indicate the presence of the compound Pd_2H. The simultaneous existence of both α and β phases would point to duplex regions of solid solutions, which occur at different pressures according as the pressure is increased or decreased to its final value. These facts support the view that the palladium-hydrogen system consists at 100° C. of two solid solutions, the hydrogen-rich phase being closely associated with the combination Pd_2H which is capable of taking more hydrogen into solution.

Another experimental fact to be taken into consideration in arriving at a solution to the problem is the distortion of the β lattice. This was referred to in our previous paper(1). Every attempt to obtain the β phase free of distortion failed. The α phase showed no such distortion up to the highest hydrogen concentrations. Nähring(4) suggested the formation of an orthorhombic lattice, but the results of the present investigation did not confirm this. There is no doubt however, that a distortion of the β lattice takes place, and that the distortion remains after the gas has been removed. The presence of the hydrogen, even though it enters the palladium lattice interstitially, causes a permanent displacement of the palladium atoms which if the concentration is high enough, cannot be removed without subjecting the material to a temperature well above that required to remove the hydrogen from the metal. This would suggest that at certain concentrations the gas may not be in its normal state when it leaves the metal.

§ 5. ACKNOWLEDGEMENT

We have pleasure in thanking the Department of Scientific and Industrial Research for a grant which enabled us to carry out the work.

REFERENCES

(1) Owen, E. A. and Jones, J. I. Page 587 of this volume.
(2) Lambert, B. and Gates, S. E. *Proc. Roy. Soc.* A, **108**, 456 (1925).
(3) Hoitsema and Roozeboom. *Z. Phys. Chem.* **17**, 1 (1895).
(4) Nähring. *Ann. Phys.*, Lpz., **21**, 303 (1934).

THE MAGNETIC PROPERTIES OF IRON AMALGAMS

By L. F. BATES, Professor of Physics, University College, Nottingham
AND
P. F. ILLSLEY, B.Sc.

Received 6 *May* 1937. *Read in title* 25 *June* 1937

ABSTRACT. Amalgams of iron and mercury have been prepared by electrolysis and the magnetic properties of the frozen amalgams investigated by the Gouy method. Only very minute quantities of iron can possibly be absorbed before ferromagnetic properties are evident in the amalgams. The iron behaves as if it possesses a specific magnetization of 130 c.g.s. units instead of the 220 normally exhibited by pure iron in bulk at the temperature of the experiments, −78·5° C. With increasing iron-content the paramagnetism of the amalgam, as distinct from the ferromagnetism of the iron, also increases steadily, for which it is suggested that a combination of iron and mercury is responsible.

§ 1. INTRODUCTION

The magnetic properties of amalgams have not been extensively studied. A few amalgams have recently been examined by Bates and Tai(1), who drew attention to the behaviour of ferromagnetic materials present as impurities in mercury amalgams. Although its effects may be of considerable importance when precision susceptibility measurements are being made, little is known about the magnetic behaviour of iron when it exists in small quantities in a para- or diamagnetic substance. On the evidence obtained from a study of copper amalgams in which iron was present as an impurity, Bates and Tai concluded that the ferromagnetic nature of the iron was only apparent when a certain concentration of iron was exceeded. The present communication gives an account of an examination of the magnetic properties of mercury amalgams containing small known quantities of iron.

Some of the physical properties of iron amalgams have been studied by Rabinowitsch and Zywotinski(2), who emphasized that it is extremely difficult to cause iron to enter into solution in mercury. They considered that the iron behaves as if it were in a colloidal state or, at any rate, as if it were dispersed throughout the mercury in the form of small particles, which ascend to the surface at rates determined by Stokes's law. They found that it is possible to remove practically all the iron from an amalgam by the application of a magnetic field, an observation which was often confirmed in the course of the present work. When a vertical tube containing an iron amalgam is allowed slowly to descend between the poles of an electromagnet the iron is pulled to the surface of the amalgam, and when the tube is lowered until the amalgam surface no longer lies between the pole pieces, a drop of amalgam is detached from the surface. By lowering the tube still further the drop can be moved to any distance from the surface of the amalgam and can be held in the field for an indefinite period, while mercury drips slowly away from it until only a small quantity remains. The residual drop contains nearly all the iron previously put into the amalgam, and it is hoped later to use this method of separation in the preparation of highly concentrated amalgams. The rate at which iron can thus be drawn to the surface of an amalgam is quite remarkable.

§ 2. METHOD AND PREPARATION OF AMALGAMS

In view of the facts outlined above it is clearly impossible to make susceptibility-measurements with liquid amalgams by means of an electromagnet used in the ordinary way. In the present work the amalgams after thorough mixing by agitation were frozen, and the susceptibilities of the solid amalgams were then determined. The mercury used was Analar mercury which, for our purposes, was not considered to need any further purification. The amalgams were all prepared by electrolysis with the complete denudation of a solution of ferrous sulphate of known iron-content, to which a small quantity of pure sulphuric acid had been added. The anode was a platinum foil and the cathode a pool of mercury of known mass, and currents of from 2 to 4 A. were usually employed with a cathode-area of some 12 cm.^{2} On completion of the electrolysis the amalgam was rapidly washed with distilled water, partially dried with filter paper and introduced into the bulb *A* of a pyrex glass apparatus of the form shown in figure 1. This was quickly evacuated through a series of drying-tubes attached to a Hyvac pump, and the amalgam was transferred to the uniform tube *C* which was then sealed off at *B*, where a hook for suspending the tube was later made.

The tube *C* was then inverted and rotated many times while wrapped in solid carbon dioxide until the amalgam had solidified, care being taken to freeze the amalgam so that a rod of uniform cross-section and as homogeneous as possible was formed. The tube was then suspended from one arm of a sensitive chemical balance inside a copper tube mounted within a Dewar flask and surrounded with solid carbon dioxide. The latter was placed between the flat pole pieces of an electromagnet, so that the surface of the amalgam lay approximately on the line of centres of the pole pieces. The arrangement is shown in figure 2, a brass tube to protect the suspension from draughts being omitted from the drawing.

Let us suppose that the magnetic pull on the tube and its contents for the field *H* between the pole faces and zero at the lower end of the tube is $\delta m_{0,H}$ when the tube contains pure mercury, and $\delta m_{c,H}$ when it contains an amalgam of concentration *c*. Then, using the modified Gouy formula given by Vogt(3), we have

$$\delta m_{0,H}\, g = \tfrac{1}{2}(k_{\mathrm{Hg}})\, \alpha H^2 \qquad \ldots\ldots(1),$$

and

$$\delta m_{c,H}\, g = \tfrac{1}{2}(k_c)\, \alpha H^2 + \sigma_c \alpha H \qquad \ldots\ldots(2),$$

whence

$$2\,(\delta m_{c,H} - \delta m_{0,H})\,\frac{g}{\alpha H^2} = (k_c - k_{\mathrm{Hg}}) + \frac{2\sigma_c}{H} \qquad \ldots\ldots(3),$$

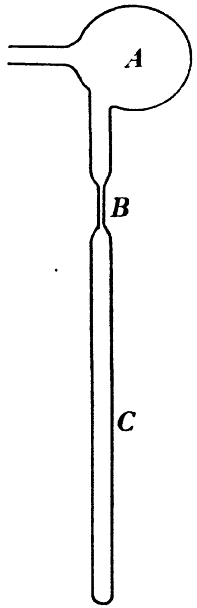

Figure 1. Apparatus for preparation of iron amalgams.

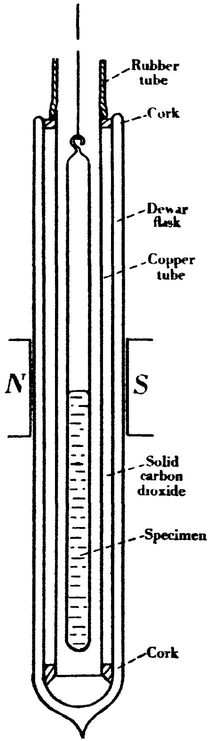

Figure 2. Apparatus for magnetic measurements on frozen amalgams.

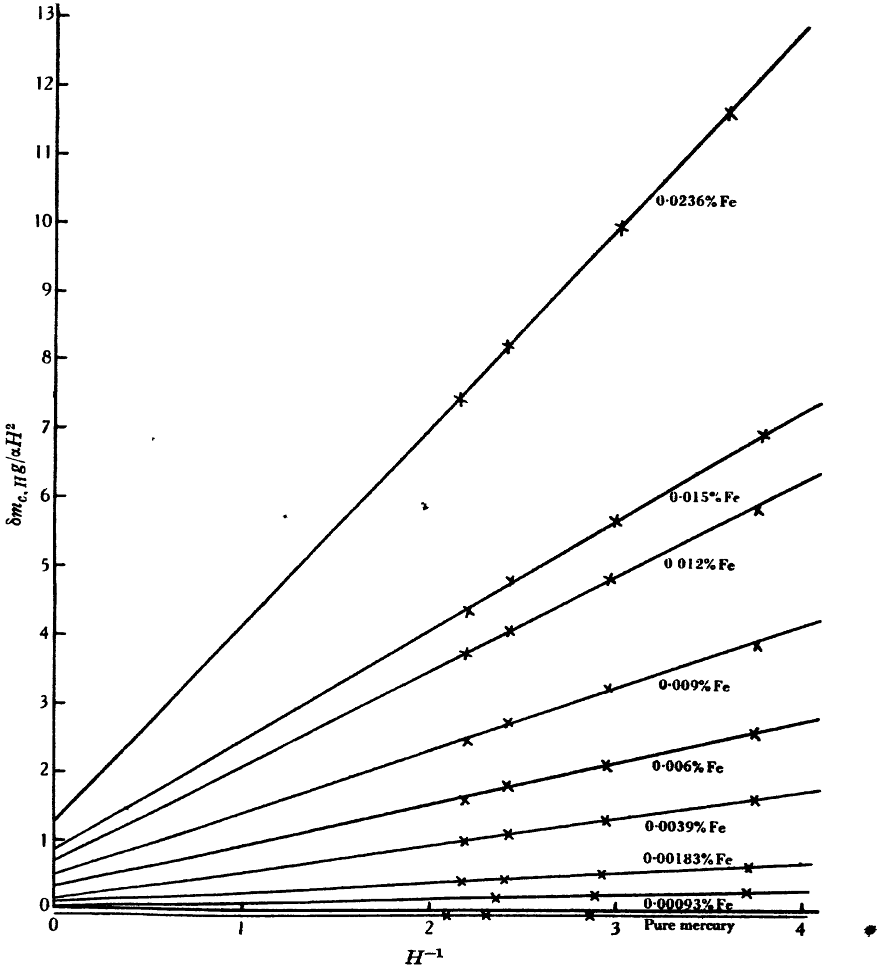

Figure 3. Graphs showing relation between $\delta m_{c,\,H}g/\alpha H^2$ and H^{-1} for a series of iron amalgams of stated concentrations by weight. Ordinates have been multiplied by $9{\cdot}37\times10^4$ and abscissae by 14,800 oersted^{-1}.

where k_{Hg} and k_c respectively represent the volume susceptibilities of pure mercury and of an iron amalgam of concentration c, both at $-78\cdot5°$ C., and σ_c is the saturation intensity of magnetization of the iron per unit volume of amalgam. The above equations contain no terms corresponding to the magnetic forces acting upon glass and air, for these forces should vanish because of the symmetry of the arrangement, and this condition was found to obtain in these experiments. The complete equation given by Vogt contains a further term in H^{-2} which is to be introduced when the iron exhibits marked hysteresis properties. This term is usually negligible, and the results given below show that it need not be introduced in the present work, at any rate for the values of H used. In the above equations k_{Hg} is, of course, negative, while k_c is always positive. The field H was measured with a calibrated fluxmeter. From equation (2) it follows that if $\delta m_{c,H}g/\alpha H^2$ is plotted as a function of H^{-1}, a series of linear graphs should be obtained, each line corresponding to a known concentration of iron, while its slope gives the value of σ_c.

§ 3. EXPERIMENTAL RESULTS

The values of $\delta m_{c,H}g/\alpha H^2$ plotted against H^{-1} for a series of amalgams of known concentrations are shown in figure 3. The concentrations range from 0·00093 to 0·0236 g. of iron in 100 g. of mercury. Although we were primarily interested in the behaviour of iron in small quantities in mercury we wished to extend the results to amalgams of somewhat higher concentrations, but the experimental method suffers from the disadvantage that asymmetry in the distribution of the iron results in the establishment of transverse forces, which may make accurate weighing impossible when the field is on. The maximum field used was 7100 oersteds and the maximum magnetic pull recorded with the most concentrated amalgam in a tube approximately 7 mm. in internal diameter was 1·64 g., so that transverse forces could be large. The scope of the work can only be extended by another method which we hope to arrange later. The line for solid mercury corresponds to a value $-1\cdot95\times10^{-6}$ for k_{Hg} or $0\cdot137\times10^{-6}$ for χ_{Hg}, found by comparing the magnetic pulls on a tube containing pure mercury at $-78\cdot5°$ C. and at room-temperature. The values given by Vogt(4) for single crystals of mercury at liquid-air temperatures are $\chi_{\parallel}=-0\cdot112$ and $\chi_{\perp}=-0\cdot121\times10^{-6}$ c.g.s. units for fields parallel and perpendicular to the crystalline axis respectively.

The main experimental difficulty was the obtaining of a uniform distribution of iron throughout the volume of the amalgam, for on repetition of the magnetic measurements after successive mixing and freezing operations very considerable differences were found between the individual values of the magnetic pull for a fixed value of H. Consequently, to obtain $\delta m_{c,H}$ the average of at least eight observations was taken. It might appear *a priori* that the differences seriously limit the accuracy of the work, but this is not the case. The magnetic pull is determined mainly by the concentration of iron in a limited volume of the amalgam situated in the tube just below the edges of the pole pieces, and the concentration here may not, of course, be equal to the average concentration. Hence by taking the mean of many values of the magnetic pull for a chosen value of H we merely ensure that the final result corresponds to the correct value of the total iron-content, provided that there are no marked discontinuities, in the relation between the magnetic properties and the quantity of iron present. Moreover, it was evident that when the individual determinations from which any one graph shown in figure 3 was found, were plotted as a function of H^{-1}, a series of lines with a common intercept on the axis of ordinates was obtained in all cases except that of the most concentrated of the amalgams.

The lines of figure 3 ought all to meet at $H^{-1}=0$ on the line of $\delta m_{0,H}g/\alpha H^2$ against H^{-1}, the horizontal line for pure solid mercury, which lies below the H^{-1} axis, provided that the iron is present in the mercury in a free state—i.e. if the properties of the mercury are unchanged by the presence of iron. This is clearly not so, and all the lines do not meet in a single point when produced. In figure 4 the slopes of the several lines of figure 3 are plotted against the corresponding concentrations, and within the limits of experimental error the resulting graph is practically a straight line intersecting the concentration axis where c equals about 0·00063 g. of iron in 100 g. mercury. We see, then, that for concentrations over 0·001 g. of iron in 100 g. of mercury the magnetic properties of the iron atoms are constant.

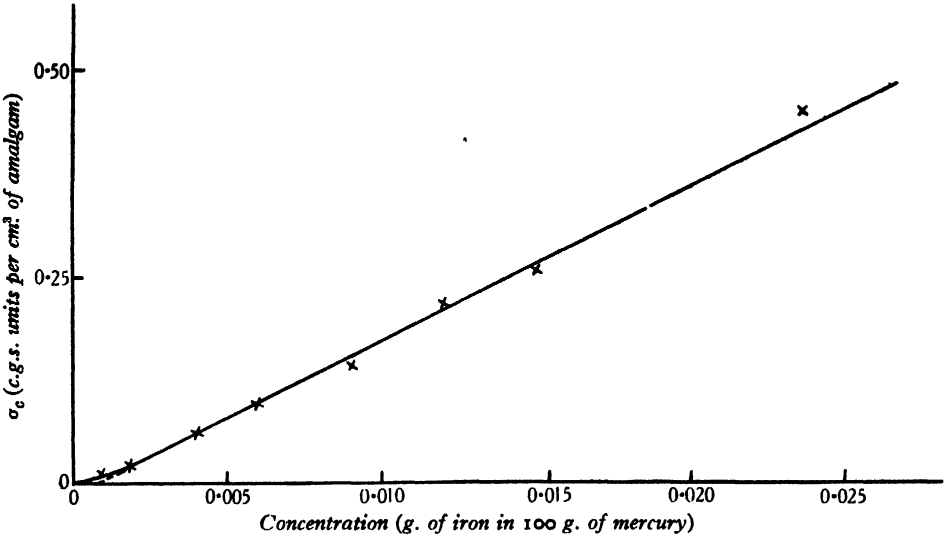

Figure 4. Relation between saturation intensity of magnetization of amalgam and concentration.

Returning to figure 3, we see that k_c, which is measured by the intercept on the axis of ordinates, is also a function of the concentration. In figure 5 the values of these intercepts above the line for pure mercury are plotted against the corresponding values of c. The values are not very accurate, particularly in the cases where c is very low, but we consider the graph, which must pass through the origin, to represent fairly the variation of k_c with c. From it we conclude that the paramagnetism of the amalgam as a whole increases more or less linearly with the iron-content at higher concentrations.

It is of interest to compare the mean value of the specific magnetization of iron in mercury at $-78{\cdot}5^\circ$ C., obtained from the slope of figure 4, with the value found by direct measurements on iron in bulk. From figure 4 it is found that for iron-concentrations of 0·005 and 0·025 g. in 100 g. of mercury, the respective values of the saturation intensity of magnetization per cm.^{3} of amalgam are 0·0806 and 0·4485 c.g.s. units, or 0·0056 and 0·0315 per gram of amalgam, assuming that in these dilute amalgams there is no appreciable change in density with iron-content, and that the density of the solid amalgam is 14·24 g./cm.^{3} Hence, it follows that the magnetization of 1 g. of amalgam is increased by 0·0259 unit by the addition of 0·0002 g. of iron, whence the specific magnetization of iron in mercury at $-78{\cdot}5^\circ$ C. is 130 units. Now, the value found by Weiss and Forrer$^{(5)}$ and amended by Fallot$^{(6)}$ may be taken to be 220 units approximately, so that each atom of iron dissolved in mercury appears to possess only about 0·59 of the ferromagnetic moment of an atom of iron in bulk at the same temperature.

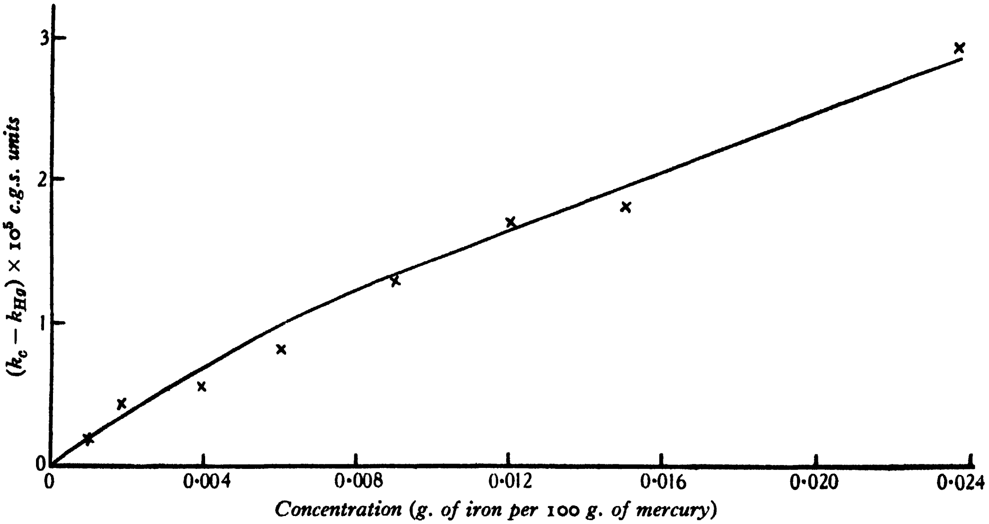

Figure 5. Relation between the paramagnetic susceptibility in infinite field and concentration of iron in amalgam.

§4. DISCUSSION OF RESULTS

The first interesting point which emerges from this work is the minuteness of the quantity of iron which can possibly be absorbed by solid mercury before signs of ferromagnetism occur, for it is known that copper can assimilate small quantities and aluminium quite large quantities before this occurs. It is not generally realized how rapidly the iron in an amalgam is carried to the surface. Indeed, these measurements showed that the Gouy method cannot safely be used with a liquid amalgam, unless either it has first been ascertained that no intensely magnetic constituent is to be found at the surface, or the composition of the amalgam in the immediate neighbourhood of the pole pieces has been specially determined. The latter procedure was adopted by Bates and Tai in the case of manganese amalgams, in which it has recently been found in this laboratory that a strongly magnetic constituent rises to the surface.

A second point is the exactness with which the simple Gouy relation holds, for it means that the iron present was saturated in the technical sense of the term, at any rate in those portions of the field which gave rise to appreciable magnetic pulls. We have already mentioned that when the individual determinations of $\delta m_{c,H} g/\alpha H^2$ for a given amalgam (except in the case of the most concentrated *one* investigated) were plotted against H^{-1}, a series of lines giving the same intercept on the ordinate $H^{-1}=0$ were obtained, although the slopes of the lines varied. This is an important point because it means that the properties of the mercury are changed by the presence of the iron. For it is easy to show that if the paramagnetism represented by the intercept on $H^{-1}=0$ was associated with the ferromagnetic iron alone, then the intercept should vary with each individual determination made on the same amalgam, owing to lack of homogeneity. Moreover, if the paramagnetism were directly proportional to the concentration of the iron, it is also easy to show that the lines of figure 3 should all pass through the same point on the line for solid mercury when produced to the left of $H^{-1}=0$.

We have seen that the intercept for each amalgam has a definite value, and the several lines of figure 3 do not meet in a single point. Therefore we conclude that with increasing iron-content an increasing quantity of iron is combined with the mercury to form a paramagnetic. Hence to some extent the low value of the specific magnetization is explained by the loss of atoms combined with mercury. Now during the electrolysis considerable quantities of hydrogen are evolved, and it is also possible that a combination of iron and hydrogen occurs, or the hydrogen may be occluded in the particles of iron. This too would reduce the value of the specific magnetization. In the case of chromium prepared from chromium amalgams, Bates and Baqi(7) have shown that a ferromagnetic compound of chromium and hydrogen is formed and can only be broken down by heating to about 1200° C. *in vacuo*. The main difficulty in the way of the above explanations is the fact that the percentage of iron atoms which are ferromagnetic in the amalgams is so constant that the explanations virtually amount to the assumption that definite equilibrium compounds of iron and mercury or of iron and hydrogen are formed.

§ 5. ACKNOWLEDGEMENT

The magnetic measurements were made with apparatus purchased in part with a grant to one of us from the Government Grants Committee of the Royal Society.

REFERENCES

(1) Bates, L. F. and Tai, L. C. *Proc. phys. Soc.* **48**, 795 (1936).
(2) Rabinowitsch and Zywotinski. *Kolloidzschr.* **52**, 31 (1930).
(3) Vogt, E. *Ann. Phys.*, Lpz., **14**, 1 (1932).
(4) Vogt, E. *Ann. Phys.*, Lpz., **21**, 798 (1935).
(5) Weiss, P. and Forrer, R. *Ann. Phys.*, Lpz., **12**, 297 (1929).
(6) Fallot, M. Thèse, Strasbourg (1936).
(7) Bates, L. F. and Baqi, A. *Proc. phys. Soc.* **48**, 781 (1936).

THE DIAMAGNETIC SUSCEPTIBILITIES OF DISSOLVED AND HYDRATED SALTS

By F. E. HOARE, Ph.D., University College, Exeter
AND
G. W. BRINDLEY, Ph.D., Physics Laboratories, University of Leeds

Received 28 *April* 1937. *Read in title* 25 *June* 1937

ABSTRACT. From a wide survey of the available experimental data for the diamagnetic susceptibilities of salts in aqueous solution, the effective susceptibilities of the ions in solution are obtained and their additivity is established to within 1 per cent of the observed values. There are shown to be systematic differences between the susceptibilities of ions in solution and in crystals. Small univalent ions and all bivalent ions have effectively smaller susceptibilities in solution than in crystals owing to the effect of the ions on the surrounding water molecules; this effect is correlated with the field at the boundary of the ions. Large univalent ions have effectively larger susceptibilities in solution than in crystals, owing mainly to the change in coordination of these ions when they are dissolved.

New measurements are given of the susceptibilities of a number of hydrated salts. It is shown that the susceptibilities of salts obtained from results for hydrated crystals, by assuming the water of hydration to have the same susceptibility as ordinary water, approximate more closely to the effective susceptibilities of salts in solution than to the true susceptibilities of the anhydrous salts.

§ 1. INTRODUCTION

The effect of solution on the diamagnetic susceptibility of certain salts has been discussed briefly in a previous note(1),* but as the account there given was necessarily very restricted it has been thought worth while to amplify the analysis of the data and also to give the sources from which the values of the susceptibilities were obtained. In addition the discussion has been extended to hydrated salts for which a number of new measurements have been made. Some slight repetition is inevitable in the tabulation of the results if continual reference to the former note is to be avoided, but the method of presentation of the data has been somewhat revised and the significance of the results made clearer by an analytical treatment.

§ 2. SUSCEPTIBILITIES OF DISSOLVED SALTS

The calculation of the susceptibilities of dissolved salts has usually been based on the assumptions that the susceptibility of the solution varies linearly with concentration and that the susceptibility of the solvent is unaffected by the presence of the dissolved salts. The legitimacy of these assumptions must be examined in the light of the experimental data. Weiss(2) has shown that there is probably an appreciable effect due to the action of the dissolved ions on the surrounding water molecules, but he was unable to proceed very far in an attempt to link up this effect with a similar one for refractivities owing to a lack of sufficiently extensive data. Furthermore, there may be mutual effects between ions in solution making the susceptibilities of particular ions dependent upon the other ions present. This may be tested directly by determining whether the susceptibilities are additive within the limits of experimental error, i.e. whether a definite susceptibility can be attributed to an ion in solution independently of the other ions present. The experimental data will be examined with these points in view.

---

* This paper will be referred to in the text as "paper I".

The assumption of a linear variation of solution susceptibility with concentration appears to be justified for many simple salts by the results obtained, but that it may not be universally true, has been shown by the work of a number of investigators(3). In fact it would not be expected to be true unless the substance is completely dissociated over the range of concentrations used.*

To examine the other points it is first necessary to obtain the most probable values of the susceptibilities of salts in solution. As the data for solvents other than water are very meagre the discussion will be restricted to aqueous solutions. The majority of measurements have been made for simple salts of the type AB and AB_2 and for the acids HCl, HBr and HI; recent results for these compounds are summarized in table 1. It will be seen that there is reasonably good agreement between the results obtained by different observers, particularly those shown in columns (3) to (6). The occasional divergences of Kido's(4) results, in column (2), are probably due to the use of only one solution-strength for each salt. It should be mentioned, however, that Kido's results for solutions represent only a fraction of the total number of his measurements, the majority of which were made with crystalline powders. The results obtained by Ikenmeyer(5) and given in column (1) of the table often show considerable divergences from those obtained by other investigators and consequently where his is the only available value for a particular salt it must be regarded with caution. In arriving at the most probable values given in the last column, most reliance has been placed on the measurements made by Hocart(6), Abonnenc(7), Frivold and others(8), and Veiel(9); when other measurements are in substantial agreement with the results obtained by these investigators they have been incorporated in finding a mean value. The results used in finding the mean values are indicated by the numbers in parentheses. Susceptibilities dealt with in this paper are all diamagnetic and are given in units of 10^{-6}; i.e. the values quoted have to be multiplied by 10^{-6} to give the diamagnetic susceptibility per gram-molecule.

---

* The work of Rao on the Raman spectra of solutions indicates that HNO_3, H_2SO_4 and all oxyacids dissociate progressively with increasing dilution. The halogen acids and salts of the alkali and alkaline-earth metals, apart from acid salts, appear to be fully dissociated even in strong solutions. In the case of the acid salts of the alkali metals there is complete dissociation into the metal ion and the acid radical, but further dissociation of the acid radical occurs with increasing dilution(21).

Table 1. Susceptibilities of salts in aqueous solution, per gram-molecule

Salt	(1) Iken-meyer	(2) Kido	(3) Hocart	(4) Abon-nenc	(5) Frivold and others	(6) Veiel	(7) Other values	(8)	Most probable values
LiF	—	—	—	—	—	—	—	—	—
LiCl	26·8	24·9	—	24·6	24·2	25·1	27·0(10)	25·4(10)	24·7 (2, 4, 5, 6)
LiBr	37·3	—	—	—	36·0	35·9	—	—	36·0 (5, 6)
LiI	55·6	55·8	—	—	—	52·7	—	—	54·2 (2, 6)
NaF	—	—	—	—	—	—	—	—	—
NaCl	30·0	—	30·8	30·1	30·4	30·3	—	—	30·3 (1, 3, 4, 5, 6)
NaBr	43·2	42·9	—	—	—	40·7	—	—	42·3 (1, 2, 6)
NaI	60·4	60·6	—	—	—	59·6	59·1(11)	—	59·9 (1, 2, 6, 7)
KF	—	—	—	24·5	24·1	—	—	—	24·3 (4, 5)
KCl	36·2	—	39·6	39·4	39·4	39·2	—	—	39·4 (3, 4, 5, 6)
KBr	52·6	—	—	—	50·3	50·1	—	—	50·2 (5, 6)
KI	67·8	—	—	—	—	68·0	66·6(12)	—	67·9 (1, 6)
RbF	—	—	—	—	—	—	—	—	—
RbCl	—	—	—	48·1	—	—	—	—	48·1 (4)
RbBr	65·5	—	—	—	—	—	—	—	65·5 ? (1)
RbI	—	—	—	—	—	—	—	—	—
CsF	—	—	—	—	—	—	—	—	—
CsCl	—	—	—	61·4	—	—	—	—	61·4 (4)
CsBr	—	—	—	—	—	—	—	—	—
CsI	92·5	—	—	—	—	—	—	—	92·5 (1)
MgF_2	—	—	—	—	—	—	—	—	—
$MgCl_2$	49·7	49·0	—	49·7	—	—	50·5(13)	—	49·7 (1, 2, 4, 7)
$MgBr_2$	72·2	—	—	—	—	—	—	—	72·2 (1)
MgI_2	111·4	—	—	—	—	—	—	—	111·4 ? (1)
CaF_2	—	—	—	—	—	—	—	—	—
$CaCl_2$	51·2	51·1	55·6	56·2	56·7	55·7	—	—	56·0 (3, 4, 5, 6)
$CaBr_2$	—	—	—	—	78·5	77·3	—	—	77·9 (5, 6)
CaI_2	—	—	—	—	—	111·3	—	—	111·3 ? (6)
SrF_2	—	—	—	—	—	—	—	—	—
$SrCl_2$	61·6	61·3	—	65·2	65·3	64·2	—	—	64·9 (4, 5, 6)
$SrBr_2$	85·3	87·4	—	—	87·9	87·9	—	—	87·7 (2, 5, 6)
SrI_2	131·1	—	—	—	—	123·2	—	—	123·2 (6)
BaF_2	—	—	—	—	—	—	—	—	—
$BaCl_2$	74·0	—	—	77·1	76·3	75·8	—	—	76·4 (4, 5, 6)
$BaBr_2$	103·6	—	—	—	—	100·7	—	—	100·7 (6)
BaI_2	—	—	—	—	—	137·8	—	—	137·8 (6)
HCl	—	21·9	22·0	21·9	—	20·9	21·9(14)	22·0(10) 23·0(15)	21 9 (2, 3, 4, 6, 7, 8)
HBr	—	34·6	—	33·0	—	32·5	32·5(14)	31·4(15)	32·8 (2, 4, 6, 7, 8)
HI	—	53·5	—	48·8	—	50·2	50·2(14)	49·3(15)	49·6 (4, 6, 7, 8)

Table 2. Comparison of susceptibilities with observed values. $\Delta\chi = \chi_{\text{calc.}} - \chi_{\text{obs}}$

	Chlorides			Bromides			Iodides		
	χ_{obs}	χ_{calc}	$\Delta\chi$	χ_{obs}	χ_{calc}	$\Delta\chi$	χ_{obs}	χ_{calc}	$\Delta\chi$
H	21·9	21·3	−0·6	32·8	32·6	−0·2	49·6	50·4	0·8
Li	24·7	24·8	0·1	36·0	36·1	0·1	54·2	53·9	−0·3
Na	30·3	30·7	0·4	42·3	42·0	−0·3	60·2	59·8	−0·4
K	39·4	39·1	−0·3	50·2	50·4	0·2	67·9	68·2	0·3
Rb	48·1	48·1	0·0	?	59·4	—	—	77·2	—
Cs	61·4	62·4	1·0	—	73·7	—	92·5	91·5	−1·0
Mg	49·7	49·7	0·0	72·2	72·3	0·1	?	107·9	—
Ca	56·0	55·7	−0·3	77·9	78·3	0·4	?	113·9	—
Sr	64·9	65·0	0·1	87·7	87·6	−0·1	123·2	123·2	0·0
Ba	76·4	78·0	1·6	100·7	100·6	−0·1	137·8	136·2	−1 6

From the most probable values of the susceptibilities shown in table 1, the ionic susceptibilities in terms of an assumed value x for the smallest ion H^+ were obtained by a method previously described (table 1 *a*, paper I). These values were obtained by assigning equal weight to the results for all the salts and acids except RbBr, MgI_2 and CaI_2, for which the results are doubtful and were therefore omitted. The additivity principle may be tested by comparing the sums of appropriate ionic susceptibilities with the experimental values. The results of this comparison are shown in table 2.

It will be seen that the difference between the observed and calculated values is generally less than 1 per cent of the observed value, so that the calculations indicate that within the limits of experimental error the susceptibilities are additive.

From the ionic susceptibilities in terms of x the absolute susceptibilities were obtained in the manner explained in paper I and will be found tabulated in tables 1 *b* and I *c* of that paper and in table 3 of this. Briefly, the method consisted in assuming that the susceptibilities of the large, singly charged ions Cs^+, Rb^+, Cl^-, Br^- and I^- in solution are in the same ratio as in the corresponding crystalline halides.

§ 3. COMPARISON OF SUSCEPTIBILITIES OF IONS IN SOLUTION AND IN CRYSTALS

The effect of solution on the susceptibility of an ion will in general be different from the effect of packing it in a crystal. The type of variation to be expected has already been discussed qualitatively, in paper I, and it has been shown that there is a difference between the apparent ionic susceptibilities in solution and in crystals. The results are given in table 3, the columns headed χ_s' and χ_c giving the apparent susceptibilities in aqueous solution and in the crystalline state(16) respectively. The difference $\chi_s' - \chi_c$ or $\Delta\chi$ is given in column 6. The main point to be noticed in these values is that $\Delta\chi$ is negative for small and doubly charged ions and positive for large singly charged ions.

The significance of this variation in $\Delta\chi$ is brought out by the following analysis. The true susceptibility χ_s of an ion in solution is to be distinguished from the apparent value χ_s' obtained by assuming the solvent to be unaffected by the dissolved ions. Let χ_w be the susceptibility of pure water and χ_w' the susceptibility of water molecules immediately surrounding or attached to dissolved ions. It will be assumed that only water molecules in immediate contact with a dissolved ion are appreciably affected. If we write

$$\chi_w' = \chi_w + \Delta\chi_w \qquad \text{......(1)},$$

then $\Delta\chi_w$ is the change in susceptibility of water per gram-molecule due to the presence of ions. If $\Delta\chi_w$ is positive the numerical value of the susceptibility of water is increased by the dissolved ions and vice versa. If C is the average number of water molecules attached to a dissolved ion then

$$\chi_s' - \chi_s = C\Delta\chi_w \qquad \text{......(2)}.$$

The susceptibility χ_c of an ion in a crystal, or its susceptibility χ_s in a solution differs from that χ_0 of a free ion, owing to the effect of the surrounding atoms or molecules; in general it appears that the susceptibility is numerically greater in the free state than in the crystalline or dissolved state. Hence, if we write

$$\chi_0 - \chi_c = \Delta\chi_0^c \qquad \ldots\ldots(3),$$

and

$$\chi_0 - \chi_s = \Delta\chi_0^s \qquad \ldots\ldots(4),$$

$\Delta\chi_0^c$ and $\Delta\chi_0^s$ will usually be positive quantities. Combining equations (2), (3), and (4) we have

$$\chi_s' - \chi_c = (\Delta\chi_0^c - \Delta\chi_0^s) + C\Delta\chi_w \qquad \ldots\ldots(5).$$

Table 3. Comparison of susceptibilities of ions in solution and in crystals. χ_s', apparent susceptibility in solution; χ_c, susceptibility in crystalline state; R, ionic radius; C, number of water molecules surrounding each ion in solution.

Ion	R (angstrom)	n/R^2	χ_s'	χ_c	$\chi_s' - \chi_c$	C	$(\chi_s' - \chi_c)/C \doteqdot \Delta\chi_w$
H^+	—	—	−3·8	0	−3·8	—	—
Be^{+2}	0·39	13·15	−0·4	0·3	−0·7	4	−0·18
Mg^{+2}	0·71	3·97	−0·5	4·3	−4·8	6	−0·80
Zn^{+2}	0·83	2·90	9 ?	16 ?	−7 ?	6	−1·2 ?
Li^+	0·68	2·16	−0·3	0·7	−1·0	4	−0·25
Ca^{+2}	0·98	2·08	5·5	10·7	−5·2	6	−0·87
Cd^{+2}	1·03	1·88	20·7	24 ?	−3·3 ?	6	−0·55 ?
Sr^{+2}	1·15	1·52	14·8	18·0	−3·2	6	−0·53
Ba^{+2}	1·31	1·16	27·8	29·0	−1·2	6	−0·20
Na^+	0·98	1·04	5·6	6·1	−0·5	4	−0·12
K^+	1·33	0·56	14·0	14·6	−0·6	4	−0·15
F^-	1·33	0·56	10·3	9·4	0·9	4	0·22
Rb^+	1·48	0·46	23·0	22·0	1·0	4	0·25
Cs^+	1·67	0·36	37·3	35·1	2·2	4	0·55
Cl^-	1·81	0·31	25·1	24·2	0·9	4	0·22
Br^-	1·96	0·26	36·4	34·5	1·9	4	0·48
I^-	2·19	0·21	54·2	50·6	3·6	4	0·90
NH_4^+	—	—	16	13·5			
NO_3^-	—	—	20·8	19·6			
ClO_3^-	—	—	32	26			
ClO_4^-	—	—	33	30			
SO_4^{-}	—	—	43	38			

The main difficulty in applying this equation to the data given in table 3 is that no very reliable estimate can be made of the quantities $\Delta\chi_0^c$ and $\Delta\chi_0^s$. It is probable, however, that these quantities will be of the same sign and of comparable magnitude, so their difference will usually be small. In particular this will be true for the smallest ions which under all conditions have small susceptibilities. Moreover, for these ions we should expect $\Delta\chi_w$ to be largest, which is a further justification for neglecting the first term. Consequently to a first approximation for small and multiply charged ions we may write

$$\chi_s' - \chi_c \doteqdot C\Delta\chi_w$$

or

$$\Delta\chi_w \doteqdot (\chi_s' - \chi_c)/C \qquad \ldots\ldots(6).$$

The fact that $(\chi_s' - \chi_c)$ is negative for small ions means that the effect of these ions in solution is to reduce the diamagnetic susceptibility of the water.

Values of C as given by Bernal and Fowler(17) and values of $(\chi_s' - \chi_c)/C$ are given in the last two columns of table 3. It should be noted that the values given for C represent the maximum number of water molecules which will form a quasi-stable system round a dissolved ion. From an examination of the strengths of solutions used in measuring the susceptibilities of dissolved salts it is found that in all cases the ratio of the number of water molecules to the number of dissolved ions is sufficiently large for each ion to be surrounded by a fully coordinated group of water molecules.

If the values of $(\chi_s' - \chi_c)/C$ can be taken as approximating to $\Delta\chi_w$, then the figures in the final column of table 3 are to be compared with the susceptibility 12·96 of pure water. The maximum negative value of $\Delta\chi_w$ is of the order of 0·8 to 0·9 (the slightly larger value 1·2 for Zn^{+2} is not very reliable) which indicates a change of about 6 or 7 per cent in the susceptibility of the water in contact with the dissolved ions.

The effect of the neglected term $(\Delta\chi_0^c - \Delta\chi_0^s)$, which may be important for large and singly charged ions, can now be considered. From the discussion in previous papers (16) it appears that the susceptibility of an ion decreases numerically with an increase in the co-ordination number. For large univalent ions the co-ordination number in solution, according to Bernal and Fowler(17), is 4, and in crystals of the rocksalt type is 6. We therefore expect $\Delta\chi_0^c$ to be numerically greater than $\Delta\chi_0^s$ and the term $(\Delta\chi_0^c - \Delta\chi_0^s)$ to be positive. Writing out the full expression for $\Delta\chi_w$, we have

$$\Delta\chi_w = (\chi_s' - \chi_c)/C - (\Delta\chi_0^c - \Delta\chi_0^s)/C \qquad \text{......(7).}$$

Reference to table 3 shows that for large univalent ions the term $(\chi_s' - \chi_c)/C$ is positive. Hence for these ions $\Delta\chi_w$ will be negative only if the second term in equation (7) is numerically greater than the first, i.e. only if

$$(\Delta\chi_0^c - \Delta\chi_0^s) > (\chi_s' - \chi_c).$$

This cannot be tested very exactly, but there are sufficient data to enable an estimate of the magnitude of $(\Delta\chi_0^c - \Delta\chi_0^s)$ to be made for the ions Cl^-, Br^- and I^-. From a study of these ions in the crystalline state we have obtained* their susceptibilities in crystals where the coordination numbers are 6 and 8; the values are as follows, where in each case the larger of the two values corresponds to a co-ordination number 6: Cl^-, 24·2 and 22·9; Br^-, 34·5 and 33·4; I^-, 50·6 and 48·8. If the change in susceptibility in going from coordination number 6 to coordination number 4, i.e. in solution, is assumed to be comparable with the change in going from coordination number 8 to coordination number 6, then we see that $(\Delta\chi_0^c - \Delta\chi_0^s)$ will be of the order of 1·3 for Cl^-, 1·1 for Br^- and 1·8 for I^-. The corresponding values of $(\chi_s' - \chi_c)$ from table 3 are 0·9 for Cl^-, 1·9 for Br^- and 3·6 for I^-. Hence, in all three cases, $(\Delta\chi_0^c - \Delta\chi_0^s)$ is comparable with $(\chi_s' - \chi_c)$, but only in the case of Cl^- is $(\Delta\chi_0^c - \Delta\chi_0^s)$ greater than $(\chi_s' - \chi_c)$. Too much reliance cannot be placed on these differences of susceptibilities, however, which are only small percentages of the actual susceptibilities. The evidence is sufficient to show that, for large univalent ions, $(\Delta\chi_0^c - \Delta\chi_0^s)$ is comparable with $(\chi_s' - \chi_c)$ and hence that $\Delta\chi_w$ is small for these ions. Alternately we may say that the positive values of $(\chi_s' - \chi_c)$ given in table 3 for the large univalent ions arise more from the change in coordination of the ions when they are dissolved than from the effect which these ions have on the water molecules.

---

* See reference (16*c*), table IX on p. 405.

The magnitude of the effect of the ions on the water molecules will depend on the field produced by the ions. Since diamagnetic susceptibilities depend largely on the electron-distribution at large values of the radius, it is of interest to consider $\Delta\chi_w$ in relation to the field at the boundary of the ions. If R is the packing radius of an ion as obtained from crystal-structure data, and n the charge in electron units, the field at the boundary will be given approximately by n/R^2. In table 3 the ions are arranged in order of the quantity n/R^2; the values of R are mainly those of Zachariasen. On comparison of the values of n/R^2 and $(\chi_s' - \chi_c)/C$ it will be seen that for the most part there is a progressive change of the latter quantity with n/R^2. This is in accordance with the view that the smaller and more highly charged the ions the greater is their effect on the surrounding water molecules. The only two ions which do not fit into this scheme satisfactorily are Be^{+2} and Li^+. The paucity of experimental data for beryllium salts renders the results in table 3 for Be^{+2} uncertain; this however cannot be the explanation in the case of Li^+.

A few results are included in table 3 for polyatomic ions. These are all approximate, and in the case of the solution values χ_s' there is an additional element of uncertainty arising from the possibility that the salts containing these ions may not be completely dissociated in the solutions used for the susceptibility measurements. For all these ions, however, $(\chi_s' - \chi_c)$ is positive, a fact which is consistent with the positive values obtained for the large monatomic ions. Unfortunately the uncertainty in the values renders any further discussion of little use.

§4. THE SUSCEPTIBILITIES OF HYDRATED SALTS

The practice of estimating the susceptibilities of anhydrous salts from the values for hydrated salts has little real justification. In recent years the crystal structures of a number of hydrated salts have been determined in detail, and the results indicate in all the cases yet examined that the water molecules are grouped round the positive ions in a more or less regular manner,* in agreement with the views of Bernal and Fowler. In crystals in which the number of water molecules is sufficient to build up a complete group of coordinated water molecules round the positive ions, the hydrated state resembles a solution more closely than the anhydrous state in so far as the immediate surroundings of each ion are concerned. When the number of water molecules is insufficient to form a complete group, the positive ions in the crystal are only partially separated from the negative ions by intervening water molecules.

In view of these results, it is to be expected that the diamagnetic susceptibilities of hydrated crystals will approximate more closely to the values obtained for solutions than to those for anhydrous crystals. In order to test this expectation a careful search was made through the literature for substances whose susceptibilities have been measured in the three states, anhydrous, hydrated, and dissolved. It is only for relatively few substances that such measurements have been made, but the results available tend to support the above view. New determinations were made for the substances listed in table 4 by the method previously described(16a).

---

* The following are typical examples: Hexahydrates of $MgCl_2$, $MgBr_2$, $CrCl_3$, $AlCl_3$, and of the halides of Ca, Sr and Ba; the alums; $CuCl_2.5H_2O$; $NiSO_4.6H_2O$; $NiSO_4.7H_2O$; $H_3PW_{12}O_{40}.29H_2O$; $3CdSO_4.8H_2O$.

Table 4

Salt	Susceptibility of hydrated salt	Calculated susceptibility of anhydrous salt assuming that $\chi_w = 12{\cdot}96$
$MgCl_2.6H_2O$	128·1	50·3
$CaCl_2.6H_2O$	132·1	54·3
$BaCl_2.2H_2O$	98·5	72·6
$SrBr_2.6H_2O$	160·4	82·6
$BaBr_2.2H_2O$	119·3	93·4

In table 5 are compared the susceptibilities of various salts as obtained by the three different methods, i.e. directly from measurements on anhydrous salts, from measurements on hydrated salts assuming the susceptibility of water to be 12·96 per gram-molecule, and from measurements on solutions again assuming the susceptibility of water to be 12·96. The values obtained from hydrated salts in this table without a reference number are from table 4; values obtained from salts in solution are taken from table 1, while the results for anhydrous salts are those we have recently obtained(16c).

Table 5. Comparison of susceptibilities

Salt	Susceptibility			
	Anhydrous	Hydrated	Degree of hydration	Dissolved
$MgCl_2$	49·2	50·3	6	49·7
$CaCl_2$	54·7	54·3	6	56·0
$SrBr_2$	78·9	82·6	6	87·7
$BaCl_2$	72·3	72·6	2	76·4
$BaBr_2$	88·6	93·4	2	100·7
BaI_2	124·4	137·1(19)	2	137·8
$CdCl_2$	68·7(18)	73·1(18)	1	72·3(20)
$CdBr_2$	87·2(18, 8)	93·0(4)	4	92·1(8)
$Cd(NO_3)_2$	55·1(18)	62·7(18)	4	62·3(4)
$CdSO_4$	59·2(18)	61·4(18)	8/3	—
		64·3(18)	1	—
$Cd(CH_3COO)_2$	83·7(18)	84·3(4)	3	—

For the six halides of Mg, Ca, Sr, and Ba the experimental results for the anhydrous and hydrated salts have been obtained mainly with the same apparatus used under standard conditions, and the results for the dissolved salts are averages of the results obtained by several investigators. As a whole these results are probably more certain than those given in the second part of the table.

A comparison of the values in the different columns of table 5 confirms the anticipated result that hydrated salts give for the susceptibility of the salt itself values approximating more closely to the values for the dissolved salts than to those for the true anhydrous salts. In some cases, such as that of $CdCl_2$, in which the number of water molecules is small, the close agreement between the results for the hydrated and dissolved salts is probably to some extent fortuitous. In every case except that of $CaCl_2$ the value is higher for the hydrated salt than for the anhydrous form; no significance can be attached to exceptional character of $CaCl_2$ because in this case there is little difference between the anhydrous and solution values. On the whole the conclusion may be drawn that susceptibilities estimated from results for hydrated salts fall between the values for dissolved and anhydrous salts, but probably nearer the values for dissolved salts.

§ 5. GENERAL CONCLUSIONS

The analysis of the data given in the foregoing sections leads to the following conclusions:

(i) Diamagnetic susceptibilities of salts in solution are additive within the limits of experimental error.

(ii) The values of the susceptibilities as calculated from measurements upon solutions, assuming the solvent susceptibility to remain unchanged, are different from the values obtained for the same substance in the crystalline form.

(iii) There is a definite effect of the ions upon the susceptibility of the surrounding water molecules. There is a correlation between the magnitude of this effect and the field at the boundary of the ion.

(iv) From the limited data available it appears that susceptibility-values obtained from measurements on hydrated salts are different from the values obtained for anhydrous salts, approximating more closely to the values found from measurements upon solutions.

§ 6. ACKNOWLEDGMENTS

Our thanks are due to Prof. F. H. Newman and Dr E. C. Stoner for their continued interest in this work.

REFERENCES

(1) Brindley and Hoare. *Trans. Faraday Soc.* **33**, 268 (1937).
(2) Weiss. *J. Phys. Radium*, **1**, 185 (1930).
(3) Farquharson. *Phil. Mag.* **12**, 283 (1931).
Rao. *Proc. Ind. Acad. Sci.* A, **3**, 188 (1936).
Ranganadhan and Qureshi. *Z. phys. Chem.* B, **33**, 290 (1936).
(4) Kido. *Sci. Rep. Tôhoku Univ.* **21**, 149, 288, 869 (1932).
(5) Ikenmeyer. *Ann. Phys.*, Lpz., **1**, 169 (1929).

(6) Hocart. *C.R. Acad. Sci.*, Paris, **188**, 1151 (1929).
(7) Abonnenc. *C.R. Acad. Sci.*, Paris, **190**, 1395 (1930) and **198**, 2237 (1934).
(8)(*a*) Frivold and Sogn. *Ann. Phys.*, Lpz., **23**, 413 (1935).
(*b*) Flordal and Frivold. *Ann. Phys.*, Lpz., **23**, 425 (1935).
(9) Veiel. *Ann. Phys.*, Lpz., **24**, 697 (1935).
(10) Scott and Blair. *J. phys. Chem.* **37**, 475 (1933).
(11) Freed and Kasper. *Phys. Rev.* **36**, 1002 (1930).
(12) Cabrera and Fahlenbrach. *Z. Phys.* **89**, 166 (1934).
(13) Cabrera and Duperier. *J. Phys., Radium*, **6**, 121 (1925).
(14) Reicheneder. *Ann. Phys.*, Lpz., **3**, 58 (1929).
(15) Gray and Farquharson. *Phil. Mag.* **10**, 191 (1930).
(16)(*a*) Hoare. *Proc. roy. Soc.* A, **147**, 88 (1934).
(*b*) Brindley and Hoare. *Proc. roy. Soc.* A, **152**, 342 (1935).
(*c*) Hoare and Brindley. *Proc. roy. Soc.* A, **159**, 395 (1937).
(17) Bernal and Fowler. *J. chem. Phys.* **1**, 515 (1933).
(18) Hollins and Spencer. *J. chem. Soc.* p. 495 (1935).
(19) Angus. *Proc. roy. Soc.* A, **136**, 569 (1932).
(20) Farquharson. *Trans. Faraday Soc.* **31**, 1004 (1935).
(21) Rao, R. and Rao, S. *Nature*, Lond., **137**, 580 (1936).

REVIEWS OF BOOKS

The Newer Alchemy, by Lord RUTHERFORD. Pp. viii + 67. (Cambridge: University Press, 1937.) 3*s*. 6*d*.

This is an account (expanded from the Henry Sidgwick Memorial Lecture delivered at Newnham College in November, 1936) of natural and induced radioactive transformations, with a summary of the more important experimental methods used in their investigation. There are also descriptions of some of the high-voltage devices used for obtaining swift charged particles for disintegrating atomic nuclei.

As would be expected, the treatment is lucid and the tone inspiring. The book is meant for the general reader, but the student beginning radioactivity would do well to read it, as a pleasant means of acquiring the necessary background. There are thirteen fine plates, mainly reproductions of Wilson cloud tracks.

Molecular Beams, by R. G. J. FRASER. Pp. ix + 70. (London: Methuen and Co.) (Methuen's Monographs.) 2*s*. 6*d*.

This is a short, readable and up-to-date account by an author who has had the advantage of working in Stern's laboratory, and who is already known as the author of a larger work (*Molecular Rays*) on the same subject, to which he has been an active contributor. There are four chapters, on molecular beams, gas kinetics, magnetic moments and electric moments respectively. The treatment, from the experimental viewpoint, is as full as can be expected within the obvious limitations of space, and the little book should be very useful to students of physics and physical chemistry. H. R. R.

1. *Kernphysik*, by P. AUGER, G. BERNARDINI, W. BOTHE, J. CLAY, J. D. COCKCROFT, J. R. DUNNING, R. FLEISCHMANN, S. FRANCHETTI, H. GEIGER, H. von HALBAN, Jr., L. MEITNER, M. L. E. OLIPHANT, P. PREISWERK and E. J. WILLIAMS; edited by E. BRETSCHER. Pp. iv + 141. (Berlin: Springer, 1936.) RM. 12.
2. *Die Atomkerne*, by C. F. von WEIZSÄCKER. Pp. viii + 214. (Leipzig: Akad. Verlagsgesellschaft m.b.H., 1937.) M. 14.40.

These are two important additions to the literature of nuclear physics. The first is a collection of papers read at the summer meeting of 1936 in the Physical Institute of the Technische Hochschule, Zürich, by a number of specialists. Each paper gives a summary of recent work in a moderately restricted field, and the editor, Dr Bretscher, has added an introductory chapter designed to link these summaries together as closely as is practicable, and to make the book more acceptable to non-specialists. The summaries and the accompanying bibliographies are excellent, and the book can be warmly recommended to students. The contributions of the British and American specialists are in English, Auger's in French, and the remainder in German.

Von Weizsäcker's book is of an entirely different type. It gives a short, but clear and systematic, treatment of the whole range of nuclear physics, with special insistence on the theoretical aspects of the subject. It is a valuable contribution to a theory which is now at a particularly interesting stage of development, and it may be very profitably read by a student who has already some familiarity with, for instance, the books of Feather and Rasetti and the sections on atomic physics in the Physical Society's *Progress Reports*.

There may be sweeping changes in the next edition of von Weizsäcker's book, but as it stands the volume gives an excellent picture of the present state of nuclear physics, and it is far more than a mere compilation. H. R. R.

Hand- und Jahrbuch der chemischen Physik, Band 9. Abschnit v, *Kernspektren*, by K. PHILIPP. Pp. ii + 105. (Leipzig: Akademische Verlagsgesellschaft m.b.H., 1936.) M. 11.20.

This monograph is a recent addition to a series that is now well-known to English physicists and chemists. It forms, in fact, a further section of the volume, *Die Spectren*, which includes the two monographs previously reviewed in the present volume of these *Proceedings* (p. 79), namely *Anregung der Spektren* by Hanle and *Molekülspektren von Lösungen und Flüssigkeiten* by Scheibe and Frömel. The numeration of its pages (185–283 and 17–22) is in continuation of that of the monographs named. Its five chapters deal with the theoretical and experimental investigations of α, β and γ radiations, and nuclear spectra, structures and transformation processes. In the text are thirty-three tables of numerical data, forty-two figures and numerous references to original papers. W. J.

Hand- und Jahrbuch der chemischen Physik, Band 8, Abschnitt II, *Lichtzerstreuung*, by H. A. STUART and H. G. TRIESCHMANN. Pp. ix + 191 + 20. (Leipzig: Akademische Verlagsgesellschaft m.b.H., 1936.) M. 24.

This section of the volume *Licht und Materie* in the same series consists of two monographs of nearly equal lengths. In the first, entitled *Lichtzerstreuung im Gebiete des sichtbaren Spektrums*, Stuart deals with the theories and measurements of light scattering by non-absorbing and absorbing particles, Rayleigh and Raman scatterings by molecules, scattering as a vibration phenomenon in pure liquids and in mixtures, critical opalescence, optical anisotropy, etc. The second monograph, entitled *Kohärente Streuung von Röntgenstrahlen an Atomen und Molekülen*, is by Trieschmann. He first discusses X-ray scattering by a free electron, a single atom, gases (both atomic and molecular), liquids and solids; and then describes the experimental methods and results of investigations of charge distribution in atoms, and of investigations of molecular structure. Appended to this monograph are three tables of (i) internuclear distances of atoms in molecules, (ii) atom factors by James and Brindley and (iii) four-figure values of sin x/x by Sherman. Both monographs contain figures, tables of numerical data and numerous references to original investigations, and are adequately indexed. W. J.

Collisions of the Second Kind, their Rôle in Physics and Chemistry, by E. J. B. WILLEY. Pp. viii + 150. (London: Edward Arnold and Co., 1937.) 10*s*. 6*d*. net.

In this monograph the author describes how Franck's general theory of collisions of the second kind has been invoked in the last ten or twelve years to explain many phenomena the origin of which would otherwise have remained obscure. Following an introductory chapter there are five chapters dealing with excitation of spectra, ionization by electron transfer, collisions of the second kind at gas-solid interfaces, the quenching of resonance radiation, and chemical reactions involving collisions of the second kind. In view of the wide range of topics discussed, from spectroscopy to chain reactions with sections touching on thermionics and biology, the author has adopted a descriptive rather than a critical style, leaving the reader, with the aid of an extensive bibliography, to form his own conclusions where differences of opinion exist. It is regrettable, however, that he has kept so closely to this style, as to leave the reader to transcribe the spectroscopic terminology used in many of the original papers cited into that more recently and widely adopted. This matter, as well as the correction of several misprints, should receive careful attention in a future edition. W. J.

Anleitungen zum Arbeiten im Röhrenlaboratorium, by M. KNOLL. Pp. ii + 67. (Berlin: Springer, 1937.) RM. 3.

This—the third part of a manual of experimental electrotechnics begun some years ago by the late Dr E. Orlich—deals with thermionic tube (including vacuum) technique. The contents are arranged as a set of fourteen laboratory exercises, each of which is intended to keep the student occupied during a 4-hour period. The exercises range from the calibration of vacuum gauges to work with an electron microscope.

The course was developed in the Technische Hochschule, Berlin. In all probability, few English readers will follow out the complete course in this form, but many will find in this little book a very useful collection of practical hints. H. R. R.

Electrical Measurements, by H. L. CURTIS. Pp. xiv + 302. (London: McGraw-Hill Publishing Company, 1937.) £1. 4*s*.

This is not a laboratory manual of the usual type; its aim is sufficiently well indicated by the sub-title "Precise Comparisons of Standards and Absolute Determinations of the Units", and by this significant sentence in the preface: "The discussion of the methods is based on the assumption that an accuracy of one part in a million is desirable in every type of measurement."

Thus warned, the reader will not look for information on "Resistance of a cell; Lodge's modification of Mance's method"—he will not even find the Carey-Foster bridge, though he will find the Kelvin double bridge. What he will find—and what will be of the greatest use to the majority of readers—is an admirable critical, and in part historical, account of methods which have been used, or may be used, to establish the electrical units with the highest attainable precision. Some knowledge of these methods is required by every serious student of physics, even though he himself may never be called upon to measure any electrical quantity with an accuracy better than one part in ten thousand.

In addition to experimental details concerning the realization of the units and the comparison of standards, there are valuable sections on the computations of fields and inductances. As Principal Physicist at the Bureau of Standards, and a former collaborator with the late Dr E. B. Rosa, Dr Curtis is obviously able to write with authority on these topics, and he is to be warmly congratulated on the production of this book, which is a notable addition to that notable Series—The International Series in Physics. H. R. R.

Alternating Current Measurements, by D. OWEN. Pp. vi + 120. (London: Methuen and Co.) 3*s*. 6*d*. net.

This, one of Methuen's Monographs on Physical Subjects, shows a rather more practical bias than some of the recent items which have appeared. It falls roughly into three sections, of which the first deals with bridge methods for the measurement of inductance and capacitance. The various bridges are dealt with, using a consistent method of expressing the theory, and thus making the book easier to study, and rendering comparisons between the different bridges easier to make. An extremely valuable addition to this section forms the fifth chapter, and deals with the conditions of accuracy in bridge measurements. The numerical effects of the residual components in the impedance of a quantity which is intended to function either as a pure resistance, pure inductance or pure capacitance are considered, and the Wagner earthing device is both described and explained.

The second section is devoted mainly to short but satisfactory explanations of both the polar and rectangular co-ordinate types of a.-c. potentiometer, and includes also Robinson's method of measuring frequencies by means of a modification of Wien's bridge.

In the final section, attention is directed chiefly to resonance methods of measuring inductance, capacitance, resistance and frequency at radio-frequencies. A useful and well worded reminder is given that the first three of these quantities are themselves functions of frequency, and must therefore be measured under operating conditions. Moreover, for an impedance which is not purely one of the three, its effective value is what is measured—and may sometimes, though not always, be the quantity required.

Although it is easy to outline the contents of the book (and indeed easy to read it), it can have been no easy task to write it. The difficulty of lucid expression increases within limits with the compression imposed, but in this case, any difficulties which may have been encountered, have been overcome so skilfully that the reader fails to notice where they may have been. J. H. A.

Über einige neuere Fortschritte der Additiven Zahlentheorie, by E. LANDAU. (Cambridge Tracts in Mathematics and Mathematical Physics, No. 35.) Pp. ii + 94. (Cambridge: University Press.) 6*s*. net.

Natürlich kann dieses Buch die ganze Primzahlentheorie nicht enthalten, sondern es ist auf einige der neuesten Entdeckungen beschränkt. Es entsteht aus einer Reihe von vier Vorträgen, die der Schriftsteller in Cambridge gehalten hat, und es besteht folglich aus vier Kapiteln, die die Sätze von Winogradoff, Schnirelmann, Erdös und Romanoff, und Khintschine, Besicovitch und Tchowla behandeln, nebst einem Anhang, welcher einen Satz von Siegel enthält. Am Anfang findet man eine kurze Übersicht, die den Inhalt jedes Kapitels erklärt.

Die Theorie ist ziemlich schwierig, aber der Leser der sich nicht erschrecken lässt, wird sie für höchst interessant halten. Er wird auch einige Probleme zur Forschung entdecken.

Wie die andere "Cambridge Tracts" ist das Buch ausserordentlich gut gedruckt. Es kostet mehr als Nummer 34, aber mit Rücksicht auf der Schwierigkeiten, mathematische Formeln zu drucken, ist es gar nicht teuer. J. H. A.

The Elements of Mathematical Analysis, by J. N. MICHELL and M. H. BELZ. Pp. xxiii + 516 (vol. 1) and xii + 570 (vol. 2). (London: Macmillan and Co.) 42*s*. net each volume.

This is a most interesting essay in a systematic unfolding of the fundamentals of analysis according to modern principles. It could be attacked by a student who has a moderate knowledge of algebra and (geometrical) trigonometry, and would leave him with nothing to unlearn when he came to modern advanced treatises. Volume 1 is devoted to the differential calculus, which is treated, as far as subjects and applications are concerned, in a manner reminiscent of the Williamson of last generation, although the similarity only emphasizes the difference in underlying treatment. The method of sections and the use of nests of intervals to define a number, are not only explained, but actually used. In general, in fact, the volume is a text on the properties of sequences—as it ought to be—and there is only a passing reference to the properties of series and their convergence. The subject of the complex variable is not taken up.

There is a claim that the book is adapted to the particular needs of students of science and engineering, and it is impossible to disprove such a claim until the book has been tried with classes, but one feels that in general the needs of the student of applied science are somewhat different from those catered for here. Thus, the practical man is usually satisfied with the degree of rigour that can be attained by assuming the intuitive properties of curves: if he uses numerical methods to solve equations he would often prefer iterative methods (which are quite ignored), to Newton's method of applying a correction. These methods are useful in practice, and would illustrate well the subject in hand, since the theory is that of the convergent sequence; moreover, unlike Newton's method, the margin of error can be assessed without heavy arithmetic.

The second volume, dealing with integral calculus, has the same general features as the first as regards rigour. The treatment of lengths and areas, particularly the areas of the surfaces of solids, is thus rather more difficult than is usual in books of this standard, though the examples chosen for treatment are of quite normal type. This volume contains an excellent chapter on numerical integration, which might have been even more valuable if it had pointed out that expansion in series is often the best method of all. It is true that such expansions have been dealt with earlier, but the student could hardly be expected to remember them in this connexion, unless his attention is specially directed to the point.

A distinct innovation is a chapter on the methods of moments and of least squares in curve-fitting, but this again (perhaps justifiably) dismisses very briefly the problem where the given function is represented by a table and not by a formula. The opportunity is taken to introduce zonal harmonics in a rather novel way in this chapter. The book concludes with a short course on ordinary differential equations treated in a conventional manner.

The departures from standard nomenclature are rather numerous, and many of them are probably improvements. Among them we may note "barrier" for "bound", "arsin" for "arcsin", "$ex \sin c\,(kx, \alpha)$" for "$e^{kx \cos c} \sin (kx \sin c + \alpha)$" and the introduction of a name and symbol for the function which equals $\cosh \sqrt{h}$ when $h > 0$ and $\cos (x\sqrt{-h})$ when $h < 0$, and for the function equal to $(x\sqrt{h})^{-1} \sinh (x\sqrt{h})$ or to $(x\sqrt{-h})^{-1} \sin (x\sqrt{-h})$, according as h is greater or less than zero.

The book is well printed and bound, and is provided with an excellent index. Even so, four guineas seems rather a high price, and one that will make many a student hope that it will not be selected for his course of lectures. J. H. A.

Elementare Physik, by ARTHUR HAAS. Pp. x + 204, with 85 figures in text. (Vienna: Julius Springer, 1937.) RM. 4.80.

This little book makes no claim to be regarded as a textbook, but is intended to supply a concise survey of the most important problems and results in experimental physics for those who have already done an elementary course and wish to continue their reading. This purpose it should serve admirably. It is divided into four parts dealing, respectively, with mechanics and acoustics (49 pages), heat (23 pages), optics (46 pages) and electricity (72 pages). The variety of the topics included in each part is far too wide for description in this short notice; the treatment of most of them is necessarily very brief, and no higher mathematics is invoked. Two errors have been noticed which the brevity and elementary nature of the treatment in no way explain or excuse: in figure 48 (*b* and *b'*), illustrating long sight and its correction, the incident rays of light are indicated as coming from a far distant, instead of a near, object; and on p. 138 the kilowatt-hour is defined as the work done by a current of 1 watt in 1000 hours, although the watt is correctly defined a few lines before. W. J.

Contributions from the Physical Laboratories of Harvard University for the Year 1935. Series II; Vol. II. (Cambridge, Mass., and London (Humphrey Milford), 1937.) 10*s*. 6*d*.

This handsome volume, containing 57 papers, arranged alphabetically under authors and beginning with five (aggregating 84 pages) by Bridgman, forms a most impressive record of a year's output from the Harvard Physical Laboratories. The range of topics is very wide, and in this age of specialization it must be of immense cultural value to the young physicist at Harvard to see such varied types of research in progress—but again, in this age of specialization, there must be very few readers who are equally interested in (for instance) the high-pressure work of Bridgman and the magnetic work of Van Vleck, important though these both are. Furthermore, with the exception of a short paper by Chaffee from the *New England Journal of Medicine*, all the papers are readily accessible to English readers—nearly half are from the *Physical Review*. There seems therefore to be no particular reason, apart from a special interest in Harvard, why many readers should wish to possess the complete collection in this form. H. R. R.

Zero to Eighty. by AKKAD PSEUDOMAN (E. F. NORTHRUP). Pp. viii + 284. (New York: The Scientific Publishing Co.) $3.50.

Dr Northrup has been experimenting with "electric guns" which are essentially solenoids placed end to end and operated by polyphase a.c. in such a way that a magnetic field travels continuously along the axis at high velocity, and pulls a metal object along, so that it leaves the tube at enormous speed. He believes that with a gun of this nature it would be quite feasible to project a vessel in which men might travel around the moon, and return to earth. In order to convince the world of this, he has chosen to present his case in the form of an autobiography written in the year 2000 A.D. by Akkad Pseudoman, an individual who was born in 1920, and made the flight in middle age. The arguments are plausible, perhaps convincing, even though we may doubt the validity of the method which he outlines for steering. After all, there are others available, of which the simplest is a system of rockets directed outwards along the principal axes of the momental ellipsoid of the vessel.

A book written in this way naturally invites—or demands—comparison with its numerous predecessors in the field of scientific romance, and it emerges pretty well from the ordeal. The characterizations may be weak—Pseudoman's wife, who was such an inspiration and a help to him, is the central figure in one chapter, and yet is a shadowy, unreal figure even to the end of the book. Still, the same fault is shared by better-known writers; Mr Britling and Mr Lewisham are more real persons than he who ate the Food of the Gods or than that other who travelled with the Time Machine: Micah Clarke and Dr Watson have more humanity than the professor who found the Lost World.

On the other hand, the professional writers who have peeped into the future, have usually succeeded in mentioning some changes—in roads, clothes, food, reproduction or what-not—which strike the reader with surprise, because he had not thought of it himself. Admittedly, this book only extends 63 years from to-day, but one might have hoped for more changes. True, the aeroplane is the common mode of travel, with stratospheric flight for inter-continental voyages, and a televisor is attached to the telephone. But the economic system is apparently unaltered, gold has its outstanding place among commodities, gangsters can still be found in the U.S.A., the American language has stood still (save that the irritating growth which occurred in the late 30's, typified by the statement "we have thus proved *rather definitely* that the theory is correct", has disappeared), Russia is still the most progressive nation, and American students still "elect" subjects and collect "credits". (Young Pseudoman's decisions as to his course of study remind the English reader irresistibly of Stephen Leacock's student who, because the time of day suited him, elected Music, Religion, and Turkish, to the bewilderment of one of his acquaintances, who assumed that he must be preparing for a life as organist in a mosque).

The lay reader will presumably judge the book from this aspect of entertainment value, and will find that, though not in the front rank, it is a sound piece of workmanship, better conceived than at least half the detective novels and written in better English. The price, which is probably raised considerably by the many plates, will put it out of reach of many on this side of the Atlantic. J. H. A.

THE PROCEEDINGS OF
THE PHYSICAL SOCIETY

VOL. 49, PART 6 . *November* 1, 1937 NO. 276

20—/
LIBRAR

THE ELECTRICAL RESISTANCE OF MANGANESE AMALGAMS

BY L. F. BATES, D.SC., Professor of Physics, University College, Nottingham

AND

P. G. DAY, B.SC.

Received 25 *June* 1937. *Read* 8 *October* 1937

ABSTRACT. The variation with temperature of the electrical resistance of a series of manganese-mercury amalgams of known composition has been studied over the range −78 to 340° C., and an attempt has been made to correlate the electrical data with previous measurements of the magnetic susceptibility of similar amalgams.

§ 1. INTRODUCTION

In a recent paper Bates and Tai(1) have described experiments on the magnetic properties of dilute amalgams of manganese with mercury. They found that in all cases pronounced changes of the magnetic susceptibility occurred with rise in temperature, and that temperature-hysteresis phenomena were present. With the more concentrated amalgams there was at first a decrease in the value of the diamagnetic susceptibility as the temperature rose from 20° C. to approximately 80° C., followed by an increase continuing to temperatures as high as 250° C., after which there was a rapid decrease in the diamagnetic susceptibility until a steady value was reached at about 300° C. On cooling from temperatures above 300° C. the diamagnetic susceptibility decreased slightly as the temperature fell until 120° C. was reached, after which there was generally a rapid increase until the initial value at room temperature was attained. In some cases the initial value was not always reached upon cooling and the magnetic behaviour was to some extent determined by the rate at which the amalgam was cooled. It seemed desirable to find whether the magnetic changes thus observed were accompanied by peculiarities in the electrical behaviour of the amalgams. A search of the literature showed that in general the electrical properties of amalgams have only been investigated over somewhat more restricted ranges of temperature than had been employed in the above magnetic measurements, and, in particular, no record of resistance measurements with manganese amalgams was found. Presumably this is in part due to the fact that manganese amalgams have hitherto been regarded as difficult to produce and readily oxidized in the presence of air.

Bates and Tai also made preliminary investigations of the variation of the magnetic susceptibility of pure mercury with temperature, using for the purpose three different specimens. Two of these specimens showed that the diamagnetic susceptibility decreased with rise in temperature from 20 to 340° c., but the third showed little change. More recently, Bates and Ireland(3) have specially examined the behaviour of several specimens of pure mercury and found that the numerical value of the diamagnetic susceptibility of all the specimens decreased with rise of temperature from $0{\cdot}168 \times 10^{-6}$ c.g.s. units per gram at 18° c. to $0{\cdot}161 \times 10^{-6}$ at about 340° c. It is known, of course, that the resistance of pure mercury increases in a regular manner over a similar temperature range.

§ 2. EXPERIMENTAL PROCEDURE

It was realized at the outset that, on account of the difficulty of handling the more concentrated amalgams, experiments would have to be confined to specimens containing not more than 0·15 per cent of manganese by weight. The amalgams were produced by electrolysis of a concentrated solution of manganese chloride, the anode being a platinum plate immersed in a solution of manganese sulphate within a porous pot, and the cathode a pool of mercury of known mass which was continually stirred. An amalgam of known concentration was obtained by passing a current of 0·5 amp. for a fixed time. In preliminary experiments, Analar mercury which was not redistilled was used, but in later experiments the mercury was first distilled in vacuo at a high temperature. Air was bubbled through the distilled mercury for 24 hr., and it was then filtered and finally redistilled at a low temperature by the Hulett(2) method. It was magnetically tested for impurity before use. The freshly prepared amalgam was quickly washed with distilled water and poured into the conductivity apparatus described below, a small amount of water being intentionally left with the amalgam to prevent oxidation of the surface. This method of producing a known concentration of manganese is not entirely satisfactory, since some of the manganese may redissolve during electrolysis, but it was considered adequate for the present purposes, and the fact that very little gas was generated at the cathode indicated that the concentrations given below are reasonably accurate.

The pyrex glass conductivity apparatus is shown diagrammatically in figure 1. In the main it consisted of a horizontal capillary U tube provided with the limbs *A* and *B* at the ends. The effective length of the capillary was approximately 160 cm. and its bore about 1·5 mm. Ground glass joints were provided at *G* and *G′* and served to carry the tubes *ab* and *a′b′* through which platinum potential and current leads were taken to the specimen. The potential leads passed along the whole lengths of *ab* and *a′b′* and emerged through the lower ends as shown. The current leads emerged through the small holes *c* and *c′* in the sides of the tubes and were bound to the outsides of the tubes by platinum wire; in this way the relative positions of the electrical contacts were adequately fixed. The leads passed through ebonite plugs, waxed in position, at the upper ends of the tubes. The limbs *A* and *B* could be evacuated through the side tubes *F* and *F′*, connected through drying tubes to a Hyvac pump. A suitable clamp held apart the ends of the capillary tube near the limbs to facilitate handling of the apparatus. The conductivity apparatus could be placed in a special furnace constructed of copper plates ¼ in. thick and 2¾ in. wide, such as are normally used for electrical bus bars, forming a chamber of length 90 cm., width 7 cm., and depth 2 cm. with highly conducting walls. Upon two layers of asbestos paper over the copper a single layer of Glowray tape was wound

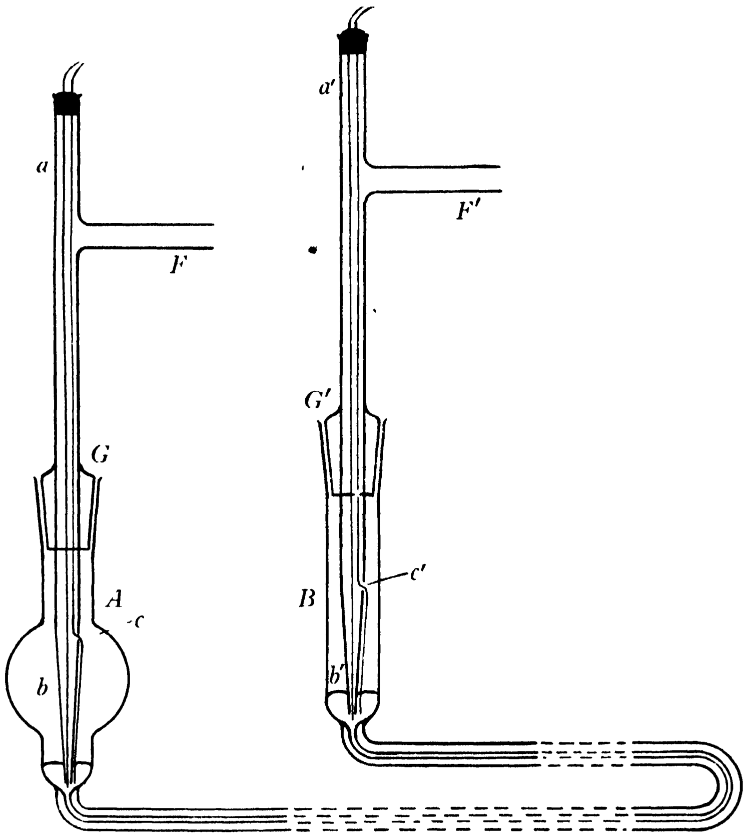

Figure 1. Conductivity apparatus for measurements with amalgams.

and the whole was thoroughly lagged. One end of the furnace was specially extended to hold the two limbs *A* and *B* of the conductivity apparatus and an end plate of the extension could be removed to permit introduction of the capillary tube. When the conductivity apparatus was in position, *A* and *B* were packed around with asbestos wool. The temperature of the capillary was measured by two thermometers inserted longitudinally into the furnace through holes in the ends. The heating filament was centre-tapped and the two halves connected in parallel to the supply mains, one half also being in series with a variable rheostat whose adjustment enabled the temperatures in the two halves of the furnace to be equalized.

Immediately after the introduction of the amalgam into the conductivity apparatus the latter was evacuated, placed in the furnace, and heated to about 360° C. This ensured complete removal of water and occluded gas, while the amalgam boiled vigorously and was thoroughly mixed. The apparatus was then removed from the furnace and tilted so that the whole of the amalgam collected in the bulb *A*, whereupon, by careful manipulation, an unbroken thread of homogeneous amalgam was run into the capillary tube. The apparatus was now connected through a drying tube to a nitrogen cylinder, a simple barometer tube acting as a safety valve in maintaining a pressure of nitrogen above the amalgam slightly greater than atmospheric. The apparatus was then replaced in the furnace and measurements made of the resistance of the amalgam thread. It was found practically impossible to mix the amalgam and repeat the measurements as the surfaces in *A* and *B* showed some permanent changes.

The resistance was measured by a double-potentiometer method. The potential falls across a standard 100,000-Ω. resistance and across an adjustable standard resistance connected in one circuit, were respectively balanced against those across a standard 10-Ω. resistance and across the amalgam thread connected in a second circuit. A shallow trough of mercury formed in a block of paraffin wax provided a particularly fine resistance-adjustment in the latter circuit and the usual precautions were taken to eliminate thermoelectric effects. The resistance of a thread of pure mercury was later found in the same apparatus over the same range of temperature. The resistance at room temperature was of the order of 0·5 Ω. and could easily be measured to an accuracy of 1 part in 50,000 with our apparatus, an accuracy sufficient for the present purposes. Measurements on amalgams and pure mercury at temperatures down to that of solid carbon dioxide were also made, using a special apparatus for the purpose, but as these appear to provide no results of significance they will not be described here.

§ 3. EXPERIMENTAL RESULTS

Final measurements were made with a series of five amalgams whose concentrations varied from 0·01 to 0·15 per cent of manganese by weight. The most concentrated amalgam represents the upper limit with which one can work with the apparatus here described. More concentrated amalgams are lacking in homogeneity and cannot be satisfactorily introduced into the capillary tube; moreover, it is extremely difficult to clean the apparatus when once it has contained a very concentrated amalgam. The results of measurements with the five amalgams are shown graphically in figure 2, in which is plotted the difference ΔR between the resistances of the pure mercury and the amalgam threads, divided by the resistance R of the pure mercury thread, at each of a series of known temperatures. The upper temperature in these experiments is, of course, limited by the boiling point of mercury at the particular nitrogen pressure used in the apparatus. All the curves show the resistance of an amalgam thread to be less than that of a pure-mercury thread, and, with the possible exception of the curve for the weakest amalgam, the curves show the same general form. The value of $\Delta R/R$ remains constant over a small temperature range above that of the room and then shows a sudden change. The higher the concentration of the amalgam, the higher appears to be the temperature at which this change occurs. The initial value of $\Delta R/R$ also appears steadily to increase with increase in manganese content, but while we are confident that the curves of figure 2 accurately represent the nature of the temperature variation, we do not consider these initial values to be entirely reliable.

Following the above sudden change, the value of $\Delta R/R$ appears to increase at a uniform rate over an appreciable range of temperature and eventually becomes fairly constant. The higher the concentration of the amalgam, the higher the temperature at which the constant value is attained and the more restricted its range. It would appear that if the use of more concentrated amalgams had been possible the numerical value of $\Delta R/R$ would have been found steadily to increase from about 100° c. until the boiling-point of mercury was reached. In all cases there was found a marked increase in the numerical value of $\Delta R/R$ as the boiling-point of mercury was approached. This increase is not shown in some of the graphs because the measurements were not recorded at sufficiently high temperatures.

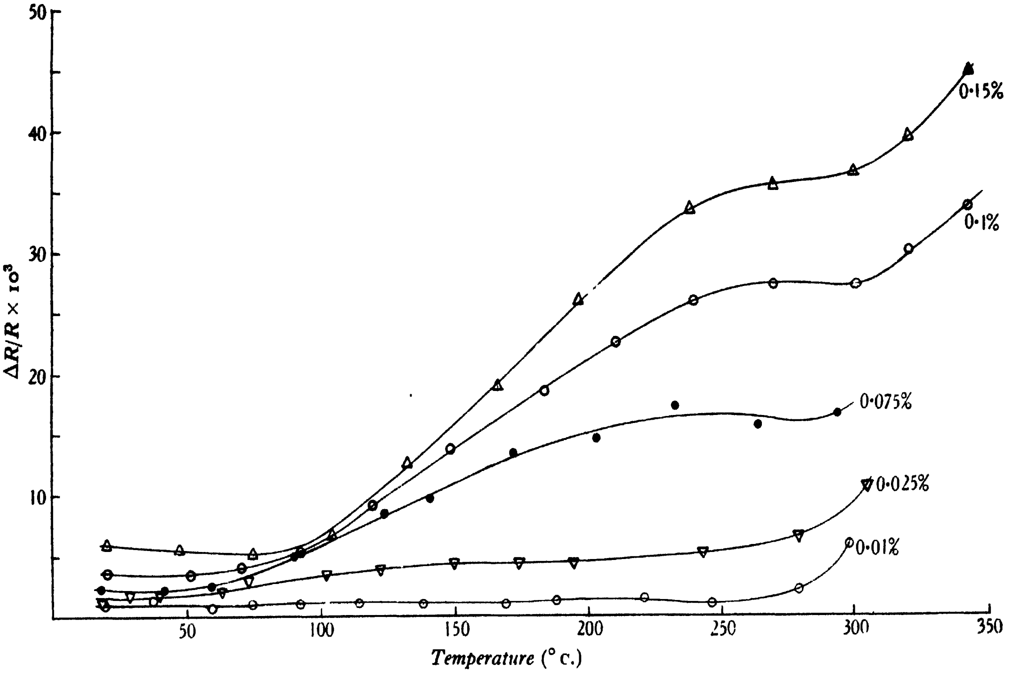

Figure 2. Curves showing how the ratio, $\Delta R/R$, the difference in resistivities of pure mercury and manganese amalgam divided by the resistivity of pure mercury, varies with temperature. Concentrations of manganese stated in per cent by weight. (The resistance of the amalgam is less than that of pure mercury.)

In view of the pronounced temperature-hysteresis phenomena recorded by Bates and Tai, a careful search for allied resistance phenomena was made. In the preliminary experiments with Analar mercury considerable hysteresis changes were found in the case of concentrated amalgams. The resistance of an amalgam thread in process of cooling was always slightly lower than the resistance of the same thread at a given temperature when its temperature was being raised, except in the region of 110° c. where the heating and cooling curves merged. Moreover, when the temperature of the amalgam was being raised there was a sudden drop in the value of $\Delta R/R$ between 60 and 80° c., but during cooling the value of $\Delta R/R$ fell almost to zero at 60° c. and remained very low until room-temperature was reached, when the initial value was again reached after the apparatus had remained at room-temperature for many hours. In the final measurements with specially purified mercury practically no trace of hysteresis phenomena was found, although the final value of ΔR at room-temperature was slightly lower than the initial value in the case of the two most concentrated amalgams of figure 2, but the small differences might easily have been due to effects other than hysteresis, e.g. the formation of minute, invisible bubbles in the thread.

§4. DISCUSSION OF RESULTS

It is difficult to make a precise comparison of these electrical results with the magnetic results obtained by Bates and Tai. In the electrical experiments the amalgams were well mixed, and by their confinement in the capillary tube their homogeneity was preserved. In the magnetic experiments the amalgams were placed in vertical tubes and it was possible for a certain amount of separation to occur; e.g. evidence has been found that a strongly magnetic component moves to the surface of a manganese amalgam. In the electrical experiments the constitution of the amalgams was calculated from electrolysis data, while in the magnetic experiments the constitution of that portion of the amalgam which was most effective in the magnetic field was directly measured by a colorimeter method, and there was no way of proving that mixing of the strongly magnetic constituent at the surface and the main body of the amalgam, although unlikely, did not occur at high temperatures, giving rise to an amalgam of concentration greater than that measured directly.

There are, however, certain points which definitely justify comment. For instance, the initial decrease in magnetic susceptibility with rise in temperature of all the amalgams is not accompanied by a corresponding change in the value of $\Delta R/R$. Again, the steep rise in the value of $\Delta R/R$ with further increase in temperature occurs when the diamagnetic susceptibility is more or less constant or increasing slowly, and there is a considerable increase in $\Delta R/R$ between 300 and 350° c. in the case of the concentrated amalgams while the susceptibility here remains more or less constant. Finally, with pure amalgams, there is practically no temperature hysteresis of the electrical resistance, although the magnetic susceptibility shows the marked temperature hysteresis and quenching phenomena which were discussed by Bates and Tai.

The initial decrease of the diamagnetic susceptibility with rise in temperature above that of the room might be ascribed to the manganese atoms or ions becoming increasingly free of the surrounding mercury atoms so that the pronounced paramagnetic properties of manganese could be exhibited, and as this paramagnetism is due to uncompensated spins in the incomplete electron shell we should expect it to be unaccompanied by marked resistance changes. If this process does not continue indefinitely, then the paramagnetic susceptibility should decrease with further rise in temperature, while that part of the resistance which is partly electrolytic in character should decrease (i.e. $\Delta R/R$ would increase) because of the decrease in the viscosity of mercury. The magnetic changes manifested by the large fall in diamagnetic susceptibility between 250 and 300° C. are presumably due to further changes in the association between manganese and mercury atoms, and when these are completed the value of $\Delta R/R$ again changes rapidly because of the rapid fall in the viscosity of mercury as the boiling point is approached.

§ 5. ACKNOWLEDGEMENTS

We are indebted to the Government Grants Committee of the Royal Society for a grant with which apparatus used in this investigation was purchased.

REFERENCES

(1) Bates, L. F. and Tai, L. C. *Proc. phys. Soc.* **49**, 230 (1937).
(2) Hulett, G. A. *Phys. Rev.* **33**, 307 (1911).
(3) Bates, L. F. and Ireland, A. W. *Proc. phys. Soc.* **49**, 642 (1937).

THE MAGNETIC PROPERTIES OF SILVER AMALGAMS

BY L. F. BATES, D.Sc., Professor of Physics, University College, Nottingham

AND

A. W. IRELAND, B.Sc.

Received 1 *July* 1937. *Read* 8 *October* 1937

ABSTRACT. The Gouy method has been employed in the measurement of the magnetic susceptibilities of silver amalgams containing 0 to 5 per cent of silver by weight; the method was found unsuitable for gold amalgams. Silver enters into solution in mercury as if it possessed a molar susceptibility of about -18×10^{-6} c.g.s. units in very dilute amalgams and -77×10^{-6} in more concentrated ones, instead of the molar susceptibility $-21 \cdot 6 \times 10^{-6}$ usually found for solid silver.

§ 1. INTRODUCTION

In an examination of the magnetic properties of mercury amalgams, Bates and Tai(1) showed that the added metal and mercury in an amalgam did not form a simple mechanical mixture as had previously been suggested. For example, manganese, which in the solid state has a molar susceptibility of 648×10^{-6} c.g.s. units, exhibits a molar susceptibility of $13,700 \times 10^{-6}$ when in dilute solution in mercury. Again, bismuth, which is strongly diamagnetic in the solid state is strongly paramagnetic when in dilute solution in mercury. In the case of copper, there seems to be little change when dissolved in mercury, for Bates and Tai found that in the latter circumstances the molar susceptibility was about $-7 \cdot 3 \times 10^{-6}$ instead of the value $-5 \cdot 4 \times 10^{-6}$ normally associated with solid copper; at the same time it must be recorded that it is extremely difficult to obtain copper entirely free from iron, and the experimental results were subject to a correction for ferromagnetism which was large and somewhat uncertain. It was therefore decided to examine the behaviour of gold and silver amalgams in mercury. Davies and Keeping(2) previously worked with gold amalgams, but as the value they obtained for the susceptibility of pure mercury is in error, we concluded that their results were mainly of qualitative interest.

As the susceptibility of pure mercury at room temperature may now be taken as $0 \cdot 1680 \times 10^{-6}$ e.m.u. per gram to a high degree of accuracy, our measurements have been referred to this value as standard. The pure mercury used in these experiments was first bubbled with air, washed in dilute nitric acid and water, and distilled in a quartz high temperature still. It was then bubbled with air for 24 hours, filtered, and redistilled in a form of apparatus like that described by Hulett[(3)] in a stream of air at a pressure of 1 to 2·5 cm. of mercury to remove any of the more volatile metals. Our amalgams were prepared both by electrolysis and by boiling metal foil with mercury in an evacuated tube, the purest gold and silver available being used. The pure mercury and the amalgams were tested for ferromagnetic impurity, but none was found.

The apparatus used in the susceptibility determinations consisted of a uniform pyrex tube which was approximately half-filled with mercury or amalgam before being evacuated and sealed. The tube was suspended vertically from one arm of a sensitive balance between the pole pieces of an electromagnet so that the line of centres passed through the surface of the liquid. On account of symmetry there was no measurable magnetic pull upon the glass tube itself when the field was excited, a point checked by measurements with an empty tube. As mercury is diamagnetic there was an additional downward force upon the liquid when a field H was excited and the usual Gouy formula could be used, giving

$$\delta m_g g = \tfrac{1}{2}\alpha k_{\mathrm{Hg}} H^2 \qquad \ldots\ldots(1)$$

and

$$\delta m_a g = \tfrac{1}{2}\alpha k_a H^2 \qquad \ldots\ldots(2),$$

where δm_{Hg} and δm_a were the additional weights in the balance pan required to restore equilibrium when the tube of area of cross section α respectively contained pure mercury and amalgam. Hence $k_a = k_{\mathrm{Hg}}\delta m_a/\delta m_{\mathrm{Hg}}$, assuming the field H to be constant. H was of the order of 10,000 oersteds for experiments at room-temperature, and its constancy was systematically checked by a calibrated Grassot fluxmeter, and by the values of δm_{Hg} for a standard tube.

§ 2. EXPERIMENTAL RESULTS

The results for silver amalgams are shown in figure 1 where are plotted the ratios of k_a/k_{Hg} for a series of amalgams of known concentrations. As the density of all amalgams containing up to 2 per cent of silver is very approximately 13·55 g./cm.^{3}, this ratio is the same as that of the corresponding mass susceptibilities. The curve shows an initial portion in which the quantity of dissolved silver has little effect upon the susceptibility. At higher concentrations there is a more or less linear increase in diamagnetic susceptibility with concentration.

The points marked χ on the graph were obtained from measurements with amalgams produced by the complete denudation of a known solution of silver nitrate by electrolysis. In general, we found that silver amalgams so prepared were unsatisfactory, particularly at lower concentrations, where very erratic variations in the susceptibility with concentration were observed. We found also that those impurities which may be removed by high temperature distillation of mercury produced much more pronounced effects with electrolytically prepared amalgams than with those prepared by heating silver foil in mercury in vacuo. On the other hand, it is only possible to prepare homogeneous amalgams of high concentration by electrolysis. If we consider that m g. of silver of mass susceptibility χ_M are amalgamated with $(100-m)$ g. of mercury, giving an amalgam of mass susceptibility χ_a, we have

$$100\chi_a = m\chi_M + (100-m)\,\chi_{\mathrm{Hg}}$$

and, on differentiation, we get

$$\chi_M = 100 d\chi_a/dm + \chi_{\mathrm{Hg}}.$$

In the initial portion of the curve, then, $\chi_M = \chi_{\mathrm{Hg}}$ approximately, whence the molar susceptibility of silver is $-108 \times 0{\cdot}168 \times 10^{-6} = -18{\cdot}1 \times 10^{-6}$ unit. In the region where the linear relation between diamagnetism and concentration exists we find that

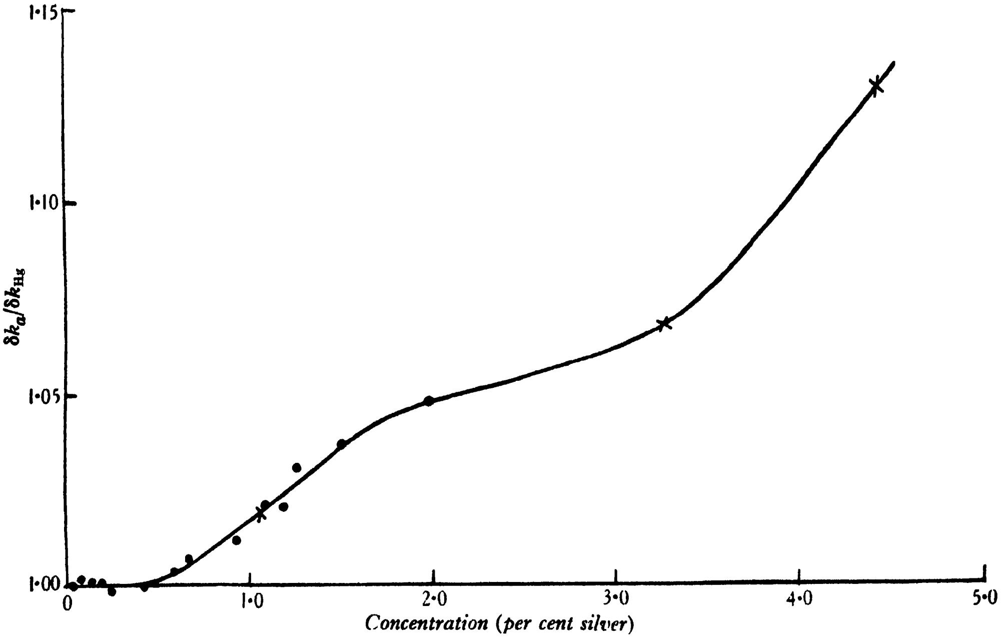

Figure 1. Ratio of susceptibility of silver amalgam to susceptibility of pure mercury at 20° C. as function of silver content by weight.

$$100 d\chi a/dm = -0{\cdot}546 \times 10^{-6},$$

whence $$\chi_M = (-0{\cdot}546 - 0{\cdot}168) \times 10^{-6},$$

or the molar susceptibility of the silver added in this region is $-77{\cdot}1 \times 10^{-6}$ unit. The value usually given for the susceptibility of silver in bulk is $-21{\cdot}6 \times 10^{-6}$.

Our experimental results for gold amalgams were disappointing, for we found that in this case the Gouy method could not be used, as the amalgam rapidly resolved itself into a gold-rich and a gold-free portion, the former lying at the bottom of the tube and outside the field. Such separation also occurred with silver amalgams, but it took place very much more slowly, and, as the amalgams were thoroughly mixed immediately before values of δm_a were recorded, we do not think that our results are in error due to lack of homogeneity. Measurements are therefore being made by a translational method using pole-pieces of the Fereday$^{(4)}$ type.

These measurements will take some time to complete, and as one of us (A. W. I.) is taking up an appointment overseas, it is considered desirable at this stage to publish the results so far obtained. It is particularly important to use this method for an investigation of the temperature dependence of the susceptibility of silver amalgams, as there is an interesting change in physical properties at 80° C.

§ 3. ACKNOWLEDGEMENTS

The experiments were made with an electromagnet and other apparatus purchased from grants made by the Government Grants Committee of the Royal Society, and A. W. I. is indebted to the Department of Scientific and Industrial Research for a maintenance allowance.

REFERENCES

(1) Bates, L. F. and Tai, L. C. *Proc. phys. Soc.* **48**, 795 (1936).
(2) Davies, W. C. and Keeping, E. S. *Phil. Mag.* **7**, 145 (1929).
(3) Hulett, G. A. *Phys. Rev.* **33**, 307 (1911).
(4) Fereday, R. A. *Proc. phys. Soc.* **43**, 383 (1931).

THE LONGITUDINAL PIEZOELECTRIC EFFECT IN ROCHELLE-SALT CRYSTALS

By WALTER G. CADY, Wesleyan University, Middletown, Conn.

Received 9 *July* 1937. *Read* 9 *July* 1937

ABSTRACT. The piezoelectric coefficient d_{11}' relating the compressional stress in any direction to the resulting polarization in the same direction is given from well-known transformation formulae. When the x' axis, with respect to which d_{11}' is defined, makes equal angles with the three crystallographic axes, this longitudinal effect is a maximum. A plate cut with its normal in this direction is designated as "*L*-cut". Experiments made with a number of such plates are described, including their use as microphones and as sound-emitters at acoustic frequencies, as piezoelectric resonators for thickness vibrations, and as sources of ultrasonic waves. By a static method the value of d_{11}' was found to be from 5400×10^{-8} to 6300×10^{-8} electrostatic units.

§ 1. INTRODUCTION

Since the earliest quantitative measurements on the piezoelectricity of Rochelle salt(1), experimenters have made use of the fact that a piezoelectric polarization parallel to any one of the crystallographic axes can be produced by a compressional stress at 45° with the other two axes. In recent years this fact has led to many investigations on Rochelle-salt resonators employing longitudinal vibrations, and to various practical applications. The effect is commonly known as the *transverse piezoelectric effect*, the electric polarization being at right angles to the direction of compression. By proper orientation of the specimen it can be realized with all piezoelectric crystals.

The existence of a *longitudinal* piezoelectric effect in Rochelle salt, characterized by a polarization in the same direction as the mechanical pressure, seems to have been generally overlooked,* in spite of the fact that the Curies(4) may have utilized it in their discovery of piezoelectricity in this substance. Moreover, Voigt(5) subsequently derived general equations from which such an effect necessarily follows.

§ 2. THEORY

Voigt's general equation for the longitudinal effect(5), with slight change in notation, is as follows:

$$\begin{aligned} P = -\Pi\,[&l^3 d_{11} + m^3 d_{22} + n^3 d_{33} + l^2 m\,(d_{21} + d_{16}) + l^2 n\,(d_{31} + d_{15}) + m^2 n\,(d_{32} + d_{24}) \\ &+ m^2 l\,(d_{12} + d_{26}) + n^2 l\,(d_{13} + d_{35}) + n^2 m\,(d_{23} + d_{34}) + lmn\,(d_{14} + d_{25} + d_{36})] \\ = -&d_{kk}'\Pi \qquad \ldots\ldots(1), \end{aligned}$$

where P is the component of polarization parallel to Π caused by pressure Π, and

---

* The author confesses to having shared in this oversight(2). Even very recently R. Hiltscher(3) stated categorically that thickness vibrations cannot be excited in a Rochelle-salt plate.

l, m, and n are the direction cosines of both P and Π, while the ds are the piezoelectric coefficients with respect to the crystallographic axes. Equation (1) holds for all piezoelectric classes, and shows that a longitudinal effect is in general present for *all* directions of pressure so long as the direction cosines are not such as to make the expression vanish.

The present discussion has to do with the digonal holoaxial (or rhombic hemihedral) class, to which Rochelle salt belongs, involving only the piezoelectric coefficients d_{14}, d_{25}, and d_{36}. However, the equations are equally applicable to all piezoelectric classes which do not possess any other than these three coefficients. For such classes, the {polarization, stress} equations reduce simply to

$$-P_x = d_{14} Y_z, \quad -P_y = d_{25} Z_x, \quad -P_z = d_{36} X_y,$$

the polarization parallel to one of the crystallographic axes being in each case given in terms of a shearing stress in a plane normal to the axis in question. For rhombic crystals the x, y, z axes are identical with the crystallographic a, b, c axes(5). All that remains of Equation (1) is then the last term.

Any cut made from a crystal belonging to one of these classes will show a longitudinal effect so long as the direction cosines l, m, and n are all different from zero. The maximum effect occurs when the product lmn is a maximum, so that $l = m = n = 1/\sqrt{3}$ and the normal to the plate makes equal angles with the three crystallographic axes.

It should be stated that in the class to which Rochelle salt belongs either end of any two of the crystallographic axes may be taken as positive. The positive end of the third axis is then determined by the requirement that the x, y, and z axes shall form a right-handed coordinate system. The crystal may be rotated 180° about any one of the three crystallographic axes without any change in magnitude or sign of the piezoelectric coefficients.

§ 3. OBLIQUE CUTS

For an oblique cut in any orientation we adopt a system of orthogonal axes designated as x', y', and z'. The x' direction is taken as that in which the longitudinal effect is to be investigated; a plate cut with its thickness in this direction may be termed an X'-cut plate. So far as the longitudinal effect is concerned the directions of the other axes are arbitrary.

For generality, let it be assumed that the x', y', and z' axes have been chosen with the direction cosines indicated in table I:

Table I

	x'	y'	z'
x	l_1	l_2	l_3
y	m_1	m_2	m_3
z	n_1	n_2	n_3

By the use of the transformation equations given by Voigt(5), and by Davies(6) and Stamford(7) all of the piezoelectric coefficients with respect to the new axes can be expressed. Three such equations are given below. When the pressure and polarization are parallel to x', giving the longitudinal effect, we have from the last term in equation (1):

$$d_{11}' = l_1 m_1 n_1 (d_{14} + d_{25} + d_{36}) \qquad \ldots\ldots(2).$$

When the pressure is parallel to y' and the polarization to x', giving the transverse effect,

$$3d_{12}' = (l_1 m_2 n_2 + m_1 n_2 l_2 + n_1 l_2 m_2)(d_{14} + d_{25} + d_{36}) + l_2 l_3 (d_{25} - d_{36}) + m_2 m_3 (d_{36} - d_{14}) + n_2 n_3 (d_{14} - d_{25}) \qquad \ldots\ldots(3).$$

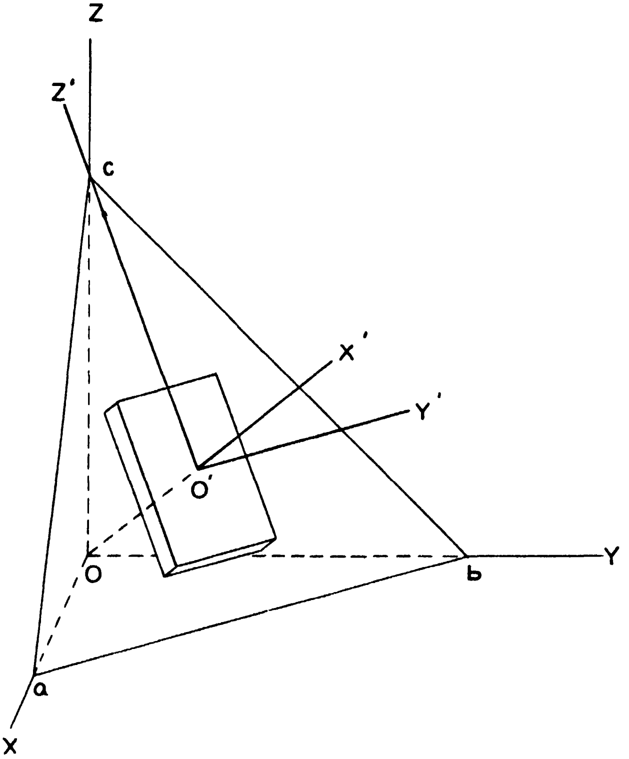

Figure 1. Orientation of axes for the L-cut crystal of Rochelle salt.

When the pressure is parallel to z' and polarization to x', giving the transverse effect,

$$3d_{13}' = (l_1 m_3 n_3 + m_1 n_3 l_3 + n_1 l_3 m_3)(d_{14} + d_{25} + d_{36}) - l_2 l_3 (d_{25} - d_{36}) - m_2 m_3 (d_{36} - d_{14}) - n_2 n_3 (d_{14} - d_{25}) \qquad \ldots\ldots(4).$$

§ 4. THE *L* CUT

The only oblique cut with which the experiments here described are concerned is that X' cut for which the x' axis makes equal angles with the three crystallographic axes, since, as was indicated in § 2, the longitudinal effect is a maximum for this orientation. We shall refer to it as the L cut. The x' axis makes an angle of 54° 44′ with the x, y, and z axes, as shown in figure 1, in which the equilateral triangle *abc* represents the plane of the L cut. The y' axis is taken in the xy plane, at 45° to the x and y axes and hence parallel to *ab* and perpendicular to the z axis. The z' axis is such as to make a right-handed orthogonal system with x' and y'. The edges of the plate are cut parallel to the y' and z' axes.

The direction cosines now have the following values:

$$l_1=m_1=n_1=0{\cdot}5774;\quad -l_2=m_2=0{\cdot}7071;\quad n_2=0;\quad l_3=m_3-\ -0{\cdot}4083;$$
$$n_3=0{\cdot}8165.$$

For the fundamental piezoelectric coefficients we may use the widely quoted values of Pockels:

$$d_{14}=1000\times10^{\ 8}\text{ e.s.u.},\quad d_{25}=-165\times10^{-8}\text{ e.s.u.},\quad d_{36}=35\times10^{-8}\text{ e.s.u.}$$

From them we obtain

$$d_{11}'=168\times10^{-8}\text{ e.s.u.},\quad d_{12}'=-10\times10^{-8}\text{ e.s.u.},\quad d_{13}'=-157\times10^{-8}\text{ e.s.u.}$$

If on the other hand we call $d_{14}=10{,}000$, a value which seems reasonable from the results obtained by more recent investigators, we have $d_{11}'=1900$, $d_{12}'=-10$ (this coefficient depends on d_{36} alone), $d_{13}'=-1890$.

§ 5. OBLIQUELY CUT CRYSTALS AS RESONATORS

When obliquely cut crystals are used as resonators, it is desirable to compare observed values of frequency with those computed from the elastic constants. The best available complete data for the latter are those of Mandell(8), obtained by a statical method. For a bar with its length parallel to x' we find for Young's modulus, derived from equation (4) on p. 627 of Mandell's paper(8), p. 758 of Voigt's book(5),

$$1/s_{11}'=1{\cdot}70\,.\,10^{11}\text{ dyne/cm}^2$$

For a plate with its normal in the x' direction vibrating in thickness(9), we use the coefficient c_{11}', which from the equation on p. 596 in Voigt's book(5) is found to be

$$c_{11}'=2{\cdot}99\ (10^{11})\text{ dyne/cm}^2$$

From these values and the density (1·77), the wave constants, in metres of electromagnetic wave-length per millimetre of crystal in the direction of vibration, are found to be 193 for the bar and 146 for the plate.

§ 6. PLATES USED IN EXPERIMENTS

From a single crystal three L-cut plates designated as A, B, and C were prepared. At various stages they were reduced in size or subdivided in the manner indicated by subscripts. In all cases the edges were approximately parallel to the x', y', and z' axes defined in § 4. Errors in orientation may have amounted to as much as 2°. Table 2 contains the list of plates with their dimensions, their observed fundamental frequencies of compressional vibration in the x' direction (the applied electric field being also in this direction), and their wave constants h in metres per millimetre.

Table 2

Plate no.	x' (mm.)	y' (mm.)	z' (mm.)	f (kc./sec.)	h (m./mm.)
A	—	Irregular: area about 7·5 cm^2			
A_1	3·52	19·9	25·7	605	141
A_1'	3·26	19·5	25·5	—	—
A_3	3·42	9·05	9·05	605	145
A_4	1·93	11·9	11·9	1070	145
B_1	7·78	33	25	267	144
B_2	7·4	27	22	278-284	143–146
B_3	7·2	Irregular: area about 2·5 cm^2			
C	19·0	5·68	6·19	78·8	200

§ 7. STATIC TESTS

The only piezoelectric coefficient measured was d_{11}'. As was to be expected, the anomalies that are so conspicuous in the behaviour of X-cut Rochelle-salt plates are prominent here also, owing to the presence of d_{14} in equation (2). Plates A and A_1' were subjected to varying pressures in the x' (thickness) direction, the resulting charges being measured with a ballistic galvanometer. Thin tinfoil electrodes were cemented to the plates with a very small amount of Canada balsam dissolved in xylol, after the plates had been carefully ground and polished. The results for plate A are shown in figure 2. The maximum value of d_{11}', obtained from the slope of the dotted line, is 6300×10^{-8} e.s.u. The temperature was 21° C. The phenomena are

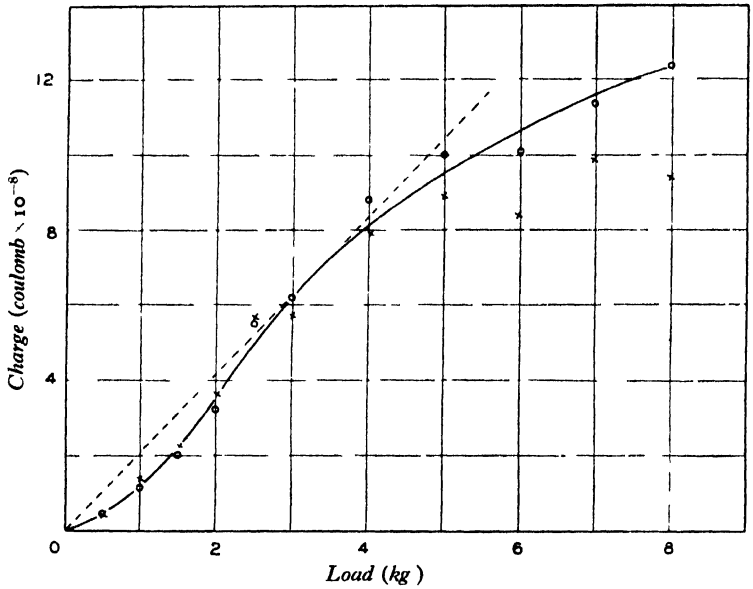

Figure 2. Polarization curve for plate A. Circles represent application of load, and crosses, release.

of essentially the same character as those observed by others with *X*-cut 45° plates for the transverse effect. This is to be expected, since the value of d_{11}' is due almost wholly to the influence of d_{14}. For the same reason it was not surprising to find that the value of d_{11}' at 23° C. was twice as great as at 20°, and that at 28° C. it had sunk to about one-tenth of the value at 20°. Plate *A* showed pronounced fatigue: after the application of 8 kg. for 6 hr. the activity was reduced to $\frac{1}{4}$ of its former value. In one day it recovered to $\frac{1}{2}$ of the latter.

After an interval of three months, plate *A* had become plate A_1' and was again tested, at a temperature of 21° C., giving a curve similar to that shown in figure 1. The maximum value of d_{11}' was found to have been reduced to 5400×10^{-8} e.s.u. By substitution of this quantity in equation (2), d_{14} was found to be $28,000 \times 10^{-8}$ e.s.u.; for plate *A* the value was $32,500 \times 10^{-8}$ e.s.u. These figures are of the same order of magnitude as the large value, $26,000 \times 10^{-8}$ e.s.u., recorded by Schulwas-Sorokin(10). It may be said in general that those sources of error that depend on faulty orientation, treatment, mounting, and electrodes always tend to make the observed piezoelectric coefficient d_{14} too small: the largest observed values are likely to be nearest the truth.

Observations of the dielectric constant k_{11}' were made with plate A_1' also. From 200 V./cm. upward, saturation was approached, and a reversal of field gave slightly different values. At small fields the mean value of k_{11}' was 1400. From this the value of k_{11} parallel to the *x* axis is found to be 4200. This is of the same order of magnitude for this very inconstant constant as that observed in the *x* direction with the same fields by Oplatka(11), Sawyer and Tower(12), and others.

§ 8. ACOUSTIC TESTS

Plates A_1 and B_3 gave comparable results, although B_3 (a portion of B_1, part of which was destroyed by overvoltage) had in static tests shown piezoelectric and dielectric coefficients only about one-tenth as great as those of A_1. The tests were merely for the purpose of demonstrating the longitudinal piezoelectric effect in Rochelle salt at acoustic frequencies. The plate under test, with tinfoil electrodes, lay exposed on a wooden base. It was found to function either as a microphone or as a sound-emitter, being more effective at high than at low frequencies. All natural frequencies of both plates were far above audibility.

In the sound-emission tests, made while the crystal was emitting a note of constant pitch, the sound-field close to the crystal was explored by means of a stethoscope and found to be strongest immediately above the plate, though considerable sound was given off from two opposite corners also. The transverse piezoelectric coefficients were computed from Pockels' data for the two diagonal directions and found to be 112 and -278; and when for d_{14} the value 10^{-4} was assigned instead of 10^{-5}, the computed values became 750 and -2640.

§ 9. RESONATOR TESTS

The plate under test was connected in the grid circuit of a calibrated r.f. oscillator, and its various frequencies of response observed by the "click" method. In many cases nodal regions were mapped by means of dust patterns. Many frequencies were observed with each plate. As is usually the case with thickness vibrations in quartz plates that are not ground with high precision, so also here in the neighbourhood of the computed frequencies for thickness vibrations (plates *A* and *B*) there were many resonance points close together. Nevertheless, the dependence of these response regions upon thickness made identification fairly certain, so that mean values for thickness vibration could be recorded. Such values are listed in table 2 for those plates that were thus examined. Agreement is satisfactory between the observed wave constant h in m./mm. and the computed value 146 (see § 5). Certain other frequencies having a linear dependence on thickness were recorded also; they are probably attributable to shear modes of vibration.

Crystal *C* was in the form of a rod with its length parallel to x'. The electrodes were placed opposite the ends of the rod. The frequency for lengthwise vibration recorded in table 2 has been corrected for cross-section by Rayleigh's formula, the correction amounting to about ½ per cent. The wave constant, 200 m./mm., is somewhat greater than the value 193 computed in § 5. This may be due in part to the fact that the wave-propagation was not strictly parallel to the length of the rod. Powder sprinkled over the vibrating rod (magnesium flashlight powder gave best results) indicated a single nodal plane which was not normal to the length of the rod but roughly at 60° to the length (x' axis) and parallel to the z' axis. This seems to be related to the oblique nodal line(13, 14, 15) observed by Meissner in X-cut quartz plates undergoing lengthwise vibrations parallel to the y axis, which he attributed to the tendency for wave-propagation to take place in the direction of maximum or minimum elasticity. In order to investigate this point, a computation was made of the elastic coefficient s_{11}' for various directions, with the result that the maximum value was found to lie in the *ac* plane, at an angle of about 42° with the *a* axis. This direction is inclined at about 35° to the x' axis, and a plane normal to it agrees fairly well with the observed nodal plane. Before definite conclusions can be drawn, however, it will be necessary to repeat the experiment with other specimens. The discrepancy between the observed and calculated values of the wave constant is in accordance with the above hypothesis.

§ 10. ULTRASONIC TESTS

This portion of the work has been carried only to the point of exploring the possibilities of Rochelle salt as a source of ultrasonic waves. A cylindrical glass tube 6 cm. in diameter with its axis vertical, containing water or toluol, was closed at the bottom by a brass diaphragm 0·14 mm. thick. The optical system was similar to that of Debye and Sears(16). Diffraction bands could be projected on to a screen or observed by the aid of an eyepiece. In the later tests the cylindrical vessel was replaced by a flat-walled projection cell.

In the experiments with water, the crystal was provided with an upper brass electrode about 1·5 mm. thick, soldered to the outside of the diaphragm. It was found that the material and thickness of the lower electrode had but little effect on the results. On the other hand, for maximum amplitude of vibration at which the diffraction bands became visible, the values of frequency were such as to indicate that the upper electrode and the diaphragm played an important part in determining the fundamental and overtone frequencies of the system. Bands including the second order were observed, in water, at about 1330, 2290, and 3370 kc./sec., with a plate 2·65 mm. thick. A quartz plate 2·4 mm. thick cemented to the outside of the diaphragm showed only first-order diffraction with the same voltage (around 200 volts).

Much better results were obtained when the crystal was laid above the diaphragm, immersed in toluol, with tinfoil electrodes. Diffraction spectra up to the fifth order were observed up to 3900 kc./sec., which was as far as the tests extended. They correspond to the fundamental and various overtones of the crystal.

At the same voltage, the number of orders observed and their distinctness were about the same with Rochelle salt as with quartz when the crystal was immersed in the liquid. It is not yet clear why Rochelle salt did not give as good results as quartz at much lower voltages, considering the much larger piezoelectric coefficient. It is possible that at these high frequencies the effective coefficient is very much less than when it is measured statically. It may at least be stated, however, that owing to its low cost the Rochelle-salt *L*-cut plate deserves consideration as a generator of ultrasonic waves of moderate intensity. In the course of these experiments it was found that the plates will stand voltages up to about 1000 v./cm. without breakdown, when immersed in an insulating liquid.

REFERENCES

(1) POCKELS, F. *Abh. Ges. Wiss. Göttingen*, **39**, 183 (1894).
(2) CADY, W. G. *Proc. Inst. Radio Engrs, N.Y.*, **18**, 2141 (1930).
(3) HILTSCHER, R. *Z. Phys.* **104**, 672 (1937).
(4) CURIE, P. and J. *C.R. Acad. Sci., Paris*, **91**, 383 (1880).
(5) VOIGT, W. *Lehrbuch der Kristallphysik* (Leipzig, 1910), pp. 99, 836–42, 849, 872.
(6) DAVIES, R. M. *Phil. Mag.* **16**, 97 (1933).
(7) STAMFORD, N. C. *Proc. Inst. Radio Engrs, N.Y.*, **25**, 465 (1937).
(8) MANDELL, W. *Proc. roy. Soc.* A, **116**, 623 (1927).
(9) CADY, W. G. *Physics*, **7**, 248 (1936).
(10) SCHULWAS-SOROKIN, R. D. *Z. Phys.* **73**, 700 (1932).
(11) OPLATKA, G. *Phys. Z.* **34**, 296 (1933).
(12) SAWYER, C. B. and TOWER, C. H. *Phys. Rev.* **35**, 269 (1930).
(13) MEISSNER, A. *Z. Techn. Phys.* **7**, 585 (1926).
(14) STRAUBEL, H. *Phys. Z.* **32**, 222 and 379 (1931).
(15) STRAUBEL, H. *Hochfrequenztech. u. Elektroakust.* **38**, 14 (1931).
(16) DEBYE, P and SEARS, F. W. *Proc. Nat. Acad. Sci., Wash.*, **18**, 409 (1932).

AN APERIODIC AMPLIFIER FOR INVESTIGATING THE WAVE-FORM OF ATMOSPHERICS

By H. C. WEBSTER, Ph.D., F.Inst.P.

Received 20 *May* 1937. *Read in title* 9 *July* 1937

ABSTRACT. An amplifier is described which produces a voltage amplification of about 120, with a maximum output of about 200 v. r.m.s., the amplification being independent of frequency between 50 c./sec. and 5×10^6 c./sec. This amplifier was designed for use with an aperiodic aerial circuit for investigating the wave-form of atmospherics, suitable means of calibration being provided. Disturbances due to fluctuations in a.-c. supply mains are eliminated by means of a push-pull arrangement.

§ 1. INTRODUCTION

Various investigators(1, 2, 3) have described apparatus for the registration of the wave-form of atmospherics. The amplifier described herein has been designed by the writer for an investigation of the wave-form and energy-content of atmospherics at Melbourne, in which several workers have been associated. It incorporates the new principles of amplifier design developed by von Ardenne(4) and others, and is compact and easy to construct. It has been used successfully in analysis of transients in piezo-electric crystals and in switchgear, as well as with atmospherics(5).

§ 2. DETAILS OF THE AMPLIFIER

The circuit diagram of the amplifier and the values of components used are given in figure 1. In all the diagrams the valves are of standard American types and the resistances are of the carbon type. Although this type of resistance is somewhat crude and has a large temperature coefficient, it has the advantage of being non-capacitative as well as non-inductive, and is capable of carrying relatively large currents. The load resistance of each of the output valves needs to have a rather larger power-dissipating capacity (5 w.) than those normally used in wireless receivers.

The general design is somewhat similar to that of von Ardenne(4), but push-pull amplification is used after the first stage. The valve V_1 is a reversing valve, with zero gain. The remaining valves are connected in pairs, the grid swings of corresponding valves being equal and opposite, and the final output is of push-pull type, suitable for direct application to a pair of deflecting plates of the cathode-ray tube. An important property of this arrangement is that variations in anode voltage due to fluctuations of the mains affect both valves of a pair equally and hence do not, except in extreme cases, produce any deflection of the cathode-ray beam. Thus no

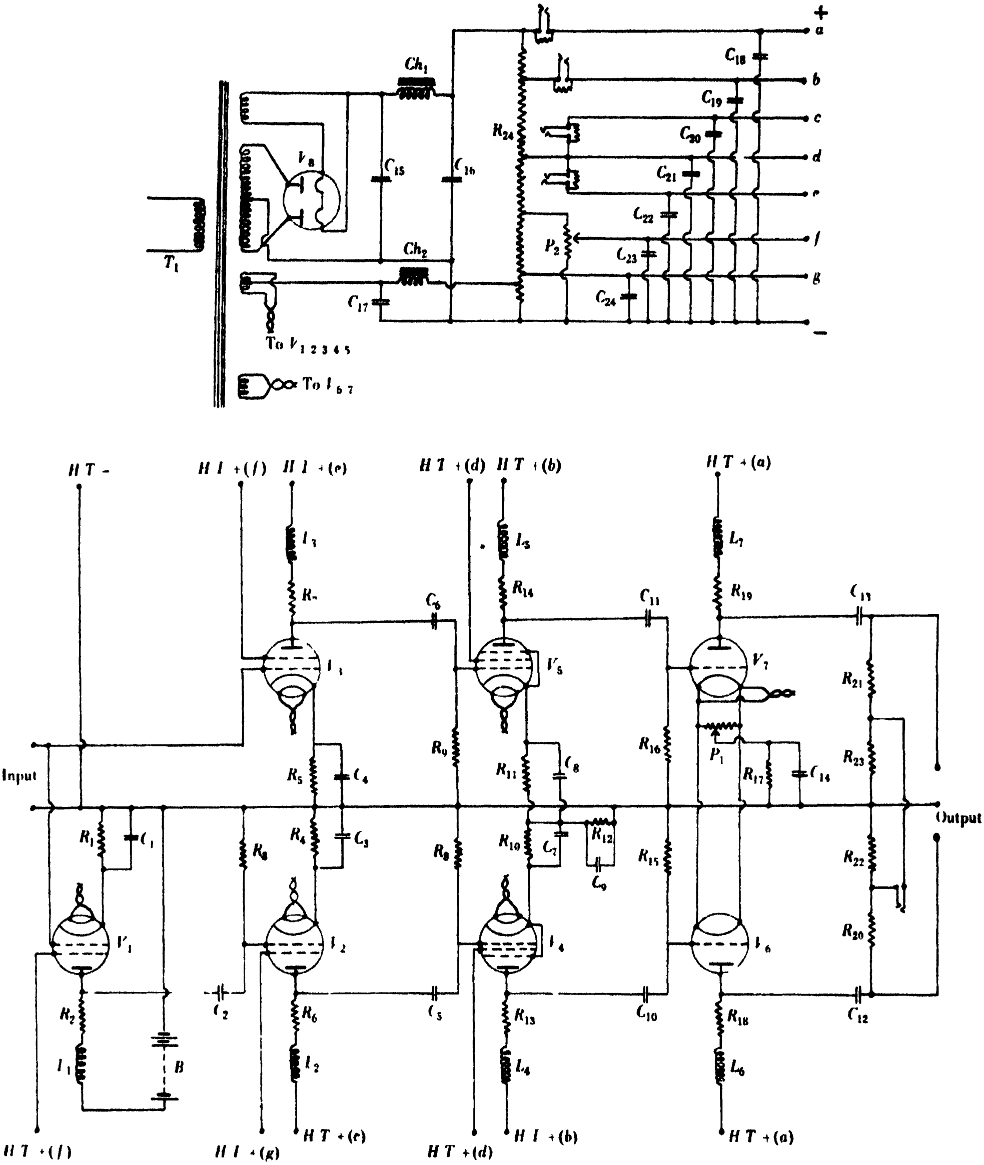

Figure 1. Amplifier circuit, with power pack shown separately for clarity. Particulars of components: Valves V_1 to V_8, Radiotrons 36, 36, 36, 38, 38, 10, 10, and 523 respectively. Resistances R_1 to R_{24}, 10^3, 2×10^3, 10^5, 10^3, 10^3, 10^4, 10^4, 10^5, 10^5, 10^3, 10^3, 5×10^3, 10^4, 10^4, 10^5, 10^5, 10^3, 10^4, 10^4, 2×10^5, 2×10^5, $2\cdot5\times10^4$, $2\cdot5\times10^4$, and 5×10^4 Ω. respectively. Potentiometers P_1, P_2, 10^3 and 10^5 Ω. respectively. Condensers C_1 to C_{24}, $1\cdot5\times10^{-3}$, 0·5, 10^{-3}, 10^{-3}, 0·5, 0·5, 10^{-3}, 10^{-3}, 25, 0·5, 0·5, 0·5, 0·5, 25, 4, 8, 25, 8, 8, 8, 4, 8, 4, and 4 μF. respectively. Inductances L_1 to L_7, 0·5, 1·8, 1·8, 1·8, 1·8, 2·2, and 2·2 mH. respectively. Chokes Ch_1, Ch_2, 60 and 30 H. respectively. Battery, 120 V. Transformer 230 V. to 5 V., 900 V. (centre-tapped), 6·3 V. and 7·5 V.

voltage-regulation device is required. The anode voltage of valve V_1 is supplied from a battery, the current consumption being about 2 mA.

The amplifier has been designed to give a linear output up to about 200 V. r.m.s., which suffices for nearly full-scale deflection on the cathode-ray oscillograph, and to amplify equally all sinusoidal voltages with frequencies between 50 c./sec. and 500 kc./sec., though there is a small phase displacement at frequencies near the upper limit. The lower of these two limits is set by the fact that individual pulses of an atmospheric never appear to have periods much greater than 10^{-3} sec. The upper limit is set by the fact that very rapid movements of the fluorescent spot cannot at present be recorded photographically, as the total light energy then falling on the relevant portions of the photographic film is below the threshold for photographic action. The choke-resistance method and cathode-resistance-condenser method of compensating for the drop of amplification at high frequencies(4) have both been used.

It should be mentioned that the stray capacities of the cathode-ray tube plates and connexions thereto amount to about 20 $\mu\mu$F., and therefore rather larger chokes are needed in the anode circuits of the output pair of valves, since the cathode-resistance bridging method is here inapplicable. Owing to the smallness of the overall amplification, interstage electrostatic screening can be dispensed with.

§ 3. THE ANTENNA CIRCUIT

Included in the same unit as the amplifier and connected permanently thereto is the antenna circuit by means of which voltages proportional to E, the electric field strength of the atmospheric, are produced at the input of the amplifier. A steel box of 16 gauge covers the aperiodic amplifier and the antenna circuit, excepting the antenna itself and the resistance R, and serves as an electrostatic and magnetic screen.

The antenna circuit is shown in figure 2. The selector switch is so arranged that one of the four condensers is always in circuit. The resistance R in series with the aerial renders the circuit aperiodic. Calculations showed that 10 Ω. would suffice for aperiodicity and would give the most uniform frequency response; but on account of the interference due to local broadcast stations it was found desirable to increase R to 10^4 Ω., and thus reduce the response at high frequencies.

This distortion being neglected, the output voltage V of the circuit is, with the values of components indicated under the diagrams, given by

$$V = E\,h_0\,\frac{C_0}{C' + C_0},$$

where C_0 is the capacity of the aerial, h_0 its equivalent height, and C' the capacity of whichever of the condensers $C_1 \ldots C_4$ is in circuit. With the aerial at present in use (L-type, 15 m. high, 60 m. long) C_0 was found to be (270 ± 20) $\mu\mu$F.

The equivalent height h_0 for purposes of the present measurements is defined by

$$h_0 = \frac{\int C(x)\,h(x)\,dx}{\int C(x)\,dx},$$

where $C(x)\,dx$ represents the capacity to earth of an element dx of the aerial distant x from the end, and $h(x)$ is the height of the element in question. With an L-type aerial with a long horizontal portion, it is clear that h_0 is nearly the mean height of the horizontal portion. This has been confirmed experimentally.

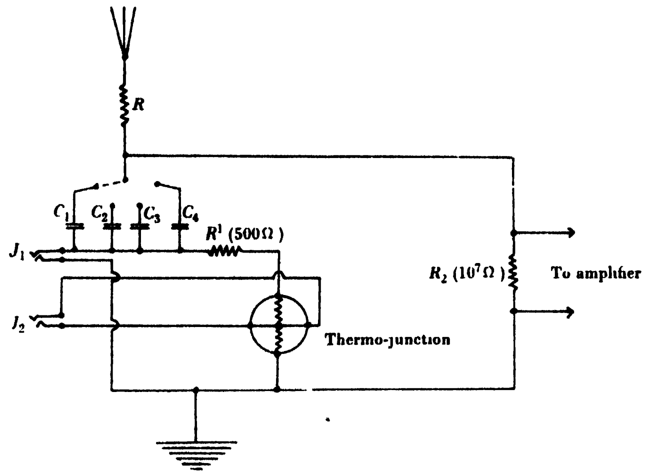

Figure 2. Antenna circuit. Capacities of condensers, 114, 345, 2000, and 4750 μμF. respectively.

The overall amplification of the apparatus (about 120) is checked periodically by injecting an e.m.f. of 2 v. at 1000 c./sec. from a test oscillator across the Ayrton-Perry wound resistance R', figure 2, with a Cambridge 10-mA. thermo-junction in series. The voltage is determined by measuring the thermo-electric e.m.f. with a Tinsley portable galvanometer, the system having been previously calibrated on d.c.

§4. ACKNOWLEDGEMENTS

I wish to thank Prof. T. H. Laby, F.R.S., for suggesting the investigation of wave-form and energy content of atmospherics. This work has been carried out as part of the programme of the Radio Research Board of the Council for Scientific and Industrial Research of the Commonwealth of Australia, and the author wishes to thank the Board for permission to publish the paper.

REFERENCES

(1) Watson Watt, R. A., Herd, J. F. and Bainbridge-Bell, L. H. *The Cathode-ray Oscillograph in Radio Research*, pp. 101–110, also 75–80 (1933). H.M. Stationery Office.
(2) Norinder, H. *Proc. Inst. Radio Engrs, N.Y.*, **24**, 587 (1936).
(3) Appleton, E. V. and Chapman, F. W. *Nature, Lond.*, **134**, 968 (1934); *Proc. roy. Soc.* A, **158**, 1 (1937).
(4) von Ardenne, M. *Wireless Engr*, **13**, 59 (1936).
(5) Laby, T. H., Nicholls, F. G., Nickson, A. F. B. and Webster, H. C. *Nature, Lond.*, **139**, 837 (1937).

APPLICATIONS OF THE MODULATING ELECTRODE OF TELEVISION CATHODE-RAY TUBES IN INVESTIGATIONS OF THE WAVE-FORM OF ATMOSPHERICS

By H. C. WEBSTER, Ph.D., F.Inst.P.

Received 20 *May* 1937. *Read in title* 9 *July* 1937

ABSTRACT. An apparatus is described which, when applied to the modulating electrode of an electron-lens cathode-ray oscillograph tube, prevents the electron-beam current from flowing except when a deflecting voltage in excess of a defined minimum is present between one pair of deflecting plates, and/or for a predetermined time following the occurrence of a specified deflecting voltage. The apparatus has been found useful for visual and photographic observations on the non-recurrent electric transients as produced by atmospherics.

§ 1. INTRODUCTION

During an investigation in Melbourne of the wave-form of atmospherics, in which several workers have been associated, the author has designed an electrical circuit by means of which the brightness of the fluorescent spot of a cathode-ray tube can be related to the deflection of the spot along one of the electrical axes of the tube. The particular relation chosen was: (*a*) zero brightness for deflections less than about 2 mm. (adjustable); (*b*) rapidly increasing brightness for deflections slightly exceeding this amount; (*c*) maximum possible brightness for deflections exceeding the threshold by 50 per cent.

A formidable difficulty in design has been the reduction of time-lag between brightness and deflection, since rapidly changing deflections arise from atmospherics. This time lag has been reduced to less than 10^{-5} sec. The unit may conveniently be known as the *deflection-modulation unit.*

A subsidiary trigger circuit* used in some cases maintains the brightness of the spot for a specified time after any deflection greater than a specified limit has occurred. This unit is somewhat sluggish in action and cannot be used alone. The two units have been used for visual and photographic observations of the wave-form of atmospherics. Examples of the photographs so obtained are shown in figure 1; others are included in a recent communication to *Nature*(1). The chief virtue of the apparatus is that it leads to economy of film; with it no photographic action takes place in the intervals between atmospherics.

---

* The unit was designed by the writer and constructed in collaboration with Mr A. F. B. Nickson, B.Sc.

The units have been used in investigations of transients in piezo-electric crystals and switch-gear, and it is suggested that they would form a useful adjunct to the cathode-ray direction-finder of Watson Watt, Herd and Bainbridge-Bell⁽²⁾, and in other studies of non-recurrent electrical transients.

Figure 1 (*a*). Deflection-modulation unit only.

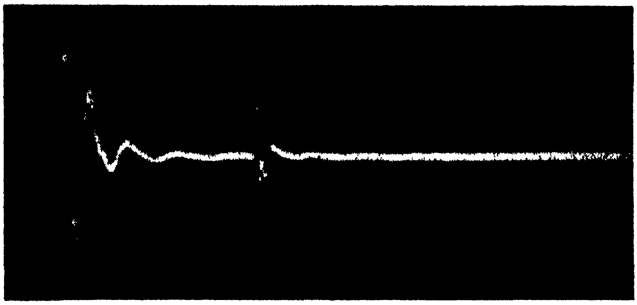

Figure 1 (*b*). Both units.

§ 2. DETAILS OF DEFLECTION-MODULATION UNIT

The circuit of the deflection-modulation unit is shown in figure 2. The power pack has been omitted, being of standard type. The point A of the output is connected to the modulating electrode of a cathode-ray tube of the electron-lens type⁽³⁾. At present a Cossor tube, type 3271 J, is used, in which the cylinder round the cathode acts as a modulating electrode. This electrode controls the current in the cathode-ray beams, the current increasing with a positive swing of the voltage of this electrode. The voltage of the point B is so adjusted that the beam current is normally zero. Since the beam-accelerating voltage used is 4000 v., the two 1-μF. condensers in the output circuit have each to stand a voltage-drop of about 2000 v., the resistances shown serving to divide this equally between the two condensers.

The input jack is connected to the output jack of the aperiodic amplifier described in the preceding paper (see figure 1 of that paper), so that about one-tenth of the amplifier output voltage (i.e. the voltage applied to the deflecting plates of the tube) is applied to the grids of the valves V_1 and V_2. These serve together as a rectifier unit which gives a negative output whenever the output voltage of the aperiodic amplifier exceeds a few volts in either direction. The grids of the valves are biased so that the anode current is normally zero, in fact they are given about 1 v. more negative bias than suffices to attain this condition. When the output voltage of the aperiodic amplifier is finite but less than 10 v. in either direction, the grid of one of the valves becomes positive and the other negative. Since, however, the positive voltage is less than 1 v., still no anode current flows. When the amplifier output exceeds 10 v., anode current flows in one of the valves, and consequently the grid of V_5 acquires a small negative voltage, and hence the anode of V_5 and thus the modulating electrode become more positive. As the output voltage of the amplifier increases these voltage swings increase very rapidly, so that for an output instantaneous e.m.f. of about 15 v. the grid swing of V_5 suffices to prevent any anode

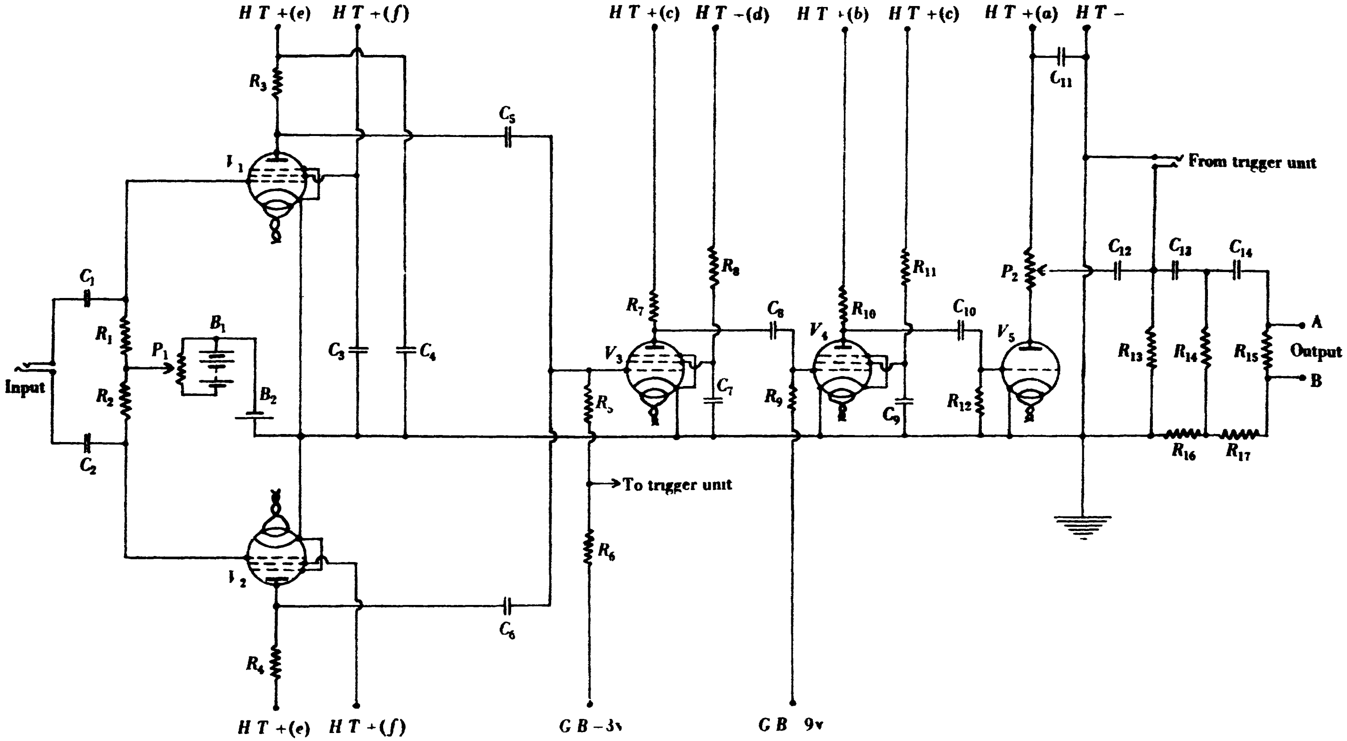

Figure 2. Deflection-modulation unit. Particulars of components: Valves V_1 to V_5, Radiotron 57, 57, 58, 57, and 56 respectively. Resistances R_1 to R_{17}, 10^6, 10^6, 5×10^4, 5×10^4, 10^6, 10^5, 10^4, 10^4, 10^5, 10^4, 10^4, 10^5, 10^6, 2×10^6, 10^6, 3×10^6, and 3×10^6 Ω. respectively. Potentiometers P_1, P_2, $1{\cdot}5 \times 10^4$ and 10^5 Ω respectively. Condensers C_1 to C_{11}, 0·5, 0·5, 8, 4, 0·5, 0·5, 8, 0·5, 8, 0·5, 8, 0·5, 1, and 1 μF respectively.

current from flowing in this valve, and thus there is no further increase in the voltage change of the modulating electrode. By means of the potentiometer P_2 the amount of the limiting voltage swing can be adjusted so that the spot is just brought up to full brightness, excessive positive voltage causing defocusing. This adjustment and the adjustment of the voltage of the point B are, of course, interdependent.

The potentiometer P_1 allows adjustment of the threshold deflection, i.e. the minimum deflection of the spot actually visible. In practice it is found desirable to set this at about 2 or 3 mm. to eliminate very small atmospherics from distant sources, and local man-made static.

The amplifying stages V_3, V_4 are designed to give as small a time-lag as possible in the operation of the unit. Thus stray capacities are reduced to a minimum, and the coupling resistances are kept small. As the amplification is much greater than is really necessary, it is found that with rapid pulses there is considerably greater delay in switching off the spot than in switching on.

§3 TRIGGER UNIT

The circuit of the trigger unit is shown in figure 3. The power pack, being of standard design, is omitted. The input jack A is connected through a key to the appropriate terminal of deflection-modulation unit. The actuating pulse due to the atmospheric, initially negative, is amplified and converted to a positive pulse by the valve V_1. This positive pulse is applied to the grid of the thyratron V_2, and provided it is large enough an arc will occur in V_2. The resultant sudden drop in anode voltage of V_2 gives a large negative bias to the grid of V_4 and hence prevents anode current from flowing in that valve, making its anode, and thus the modulating

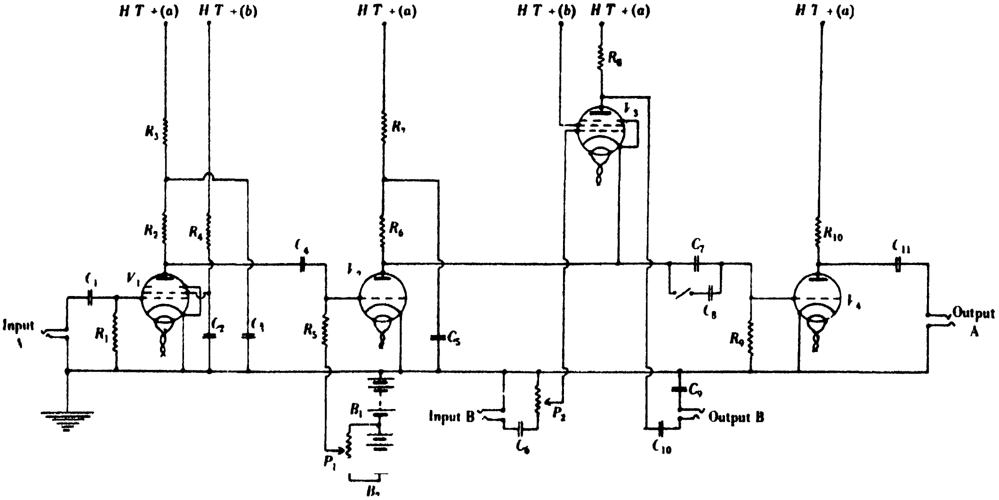

Figure 3. Trigger unit Particulars of components Valves V_1 to V_4, Radiotron 57, 885, 57 and 56 respectively Resistances R_1 to R_{10}, 5×10^5, 10^5, 10^5, $2{\cdot}5 \times 10^5$, 10^5, 10^4, 5×10^5, 10^5, 2×10^5, and 10^5 Ω. respectively Potentiometers P_1, P_2, 10^4 and 10^5 Ω respectively. Condensers C_1 to C_{11}, 0·1, 0·5, 8, 0·1, 4, 0·5, 10^{-2}, 5×10^{-2}, 0·1, 0·1 and 0·5 μF. respectively.

electrode of the cathode-ray tube, more positive. To reduce multiplicity of controls the output resistance is fixed at a value found by trial to give satisfactory results, the necessary fine adjustment being made by altering the voltage of the point B, figure 2. Owing to the relatively short time-constant of the grid coupling circuit, this change in anode voltage persists for only a short time, the spot of the cathode-ray tube actually remaining bright for about 0·05 sec. with the switch open or 0·3 sec. with the switch closed.

The arc in V_2 soon discharges the 4-μF. condenser to below 10 V., when the arc stops. The condenser then recharges through the $5 \times 10^5\,\Omega$. resistance, and as it does so the anode voltage of V_2 rises to its original value, the rise having a time constant of about 2 sec. It should be noted that by altering the grid bias of V_2 it is possible to control the minimum size of atmospheric necessary to operate the unit, and thus to select the larger atmospherics from among the many that operate the deflection-modulation unit.

The valve V_3 is a keying valve, the 1000-c./sec. voltage introduced at the input jack *B* being transmitted to the output jack *B* only during the existence of the arc in V_2 and part of the subsequent recharging of the condenser. For it is only during these periods that the anode and screen grid of V_3 are positive with respect to its cathode and hence that the valve is able to perform its normal functions. The automatic keying is required for various subsidiary purposes in the wave-form investigations.

§4. ACKNOWLEDGEMENTS

This research has been carried out as part of the programme of the Radio Research Board of the Council for Scientific and Industrial Research of the Commonwealth of Australia, and the author wishes to thank the Board for permission to publish the paper.

The author also wishes to thank Prof. T. H. Laby, F.R.S., under whose direction the work has been done, for his advice and encouragement.

REFERENCES

(1) Laby, T. H., Nicholls, F. G., Nickson, A. F. B. and Webster, H. C. *Nature, Lond.*, **139**, 837 (1937).

(2) Watson Watt, R. A., Herd, J. F. and Bainbridge-Bell, L. H. *The Cathode-ray Oscillograph in Radio Research*, pp. 126–86 (1933). H.M. Stationery Office.

(3) Cossor Booklet B 26 A.

ON THE USE OF ROTATING PARALLEL-PLANE GLASS BLOCKS FOR CINEMATOGRAPHY AND FOR PROJECTION WITH CONTINUOUSLY MOVING FILMS

By H. DENNIS TAYLOR, Research Department,
Taylor, Taylor and Hobson, Ltd.

Received 8 *March* 1935. *Read in title* 1 *November* 1935.
Revised 11 *October* 1937

ABSTRACT. A theory is developed of the method of taking cinema pictures of rapidly moving objects by projecting their images on to a continuously moving film with the aid of a moving glass element. The comparative advantages of different forms of rotating element are considered, and the magnitude of the outstanding errors are determined. Suggestions for improving the method are made.

§ 1. INTRODUCTION

Within the last few years a method of photographing rapidly moving objects on a continuously travelling film has been developed, and several different ways of accomplishing this aim by the employment of a revolving slab of glass have been described in French and American patent specifications. It has been claimed(1) that as many as 2500 exposures per second can be made by this method. I propose to consider the theory of the method and to ascertain the most efficient form for the plane-parallel-surfaced slab.

The function of this slab, which is mounted between the lens and the travelling film, is in virtue of its constant angular velocity to convert a stationary image formed directly by the lens into an image as nearly as possible sharply focused on the film and moving with the same velocity.

In its simplest form the slab has a single pair of parallel surfaces, but this clearly implies a great waste of film. For instance if the slab has to rotate through 30° while a point on the film travels from the centre to the edge of the exposure gate, only the first and the last 30° of a half-revolution are effective; two-thirds of the film are not utilized. This result points to the desirability of discarding the glass block having only one pair of opposing parallel surfaces in favour of one having two, three or more pairs of parallel surfaces. Even a ten-sided block may be found necessary for the best results, provided that the focal length of the lens leaves room enough for its use.

§ 2. DISPLACEMENT THEORY

In a previous paper[2] an expression was obtained for the displacement or side-stepping of a ray caused by traversing a glass plate of thickness t and refractive index μ. If χ is the angle the ray in air makes with either surface, formula (2) of that paper, when the first-order term $t(1-1/\mu)\tan\phi$ is included, gives for the displacement d, measured along the second surface of the plate, the value

$$d=t\left\{\frac{\mu-1}{\mu}\tan\chi+\frac{\mu^2-1}{2\mu^3}\tan^3\chi-\frac{3}{}\frac{(\mu^2-1)^2}{8\mu^5}\tan^5\chi+\frac{5}{}\frac{(\mu^2-1)^3}{16\mu^7}\tan^7\chi\ldots\right\} \quad \ldots\ldots(1).$$

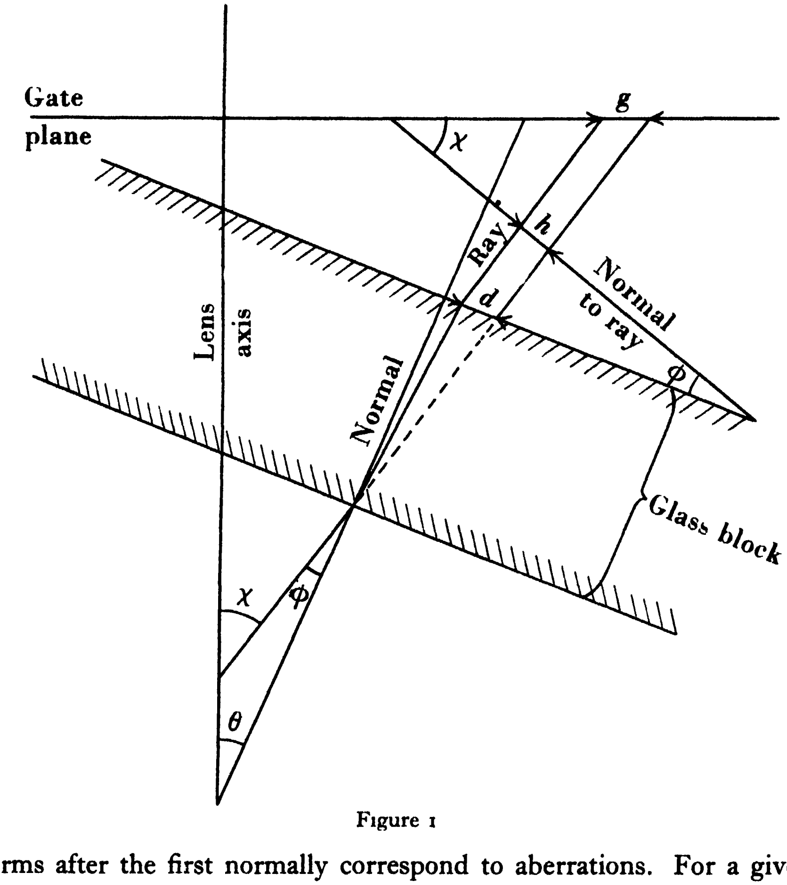

Figure 1

The terms after the first normally correspond to aberrations. For a given value of d the aberrational effects will obviously be diminished by reduction of the value of $\tan\chi$ and increase of t in about the inverse ratio. Clearly then the glass block should be as thick as is practicable.

I convert the linear side-stepping d of oblique rays along the second surface of the parallel slab into its corresponding value g in the plane of the gate as follows.

If the ray makes an angle ϕ with the optical axis, since this axis is normal to the gate the side-stepping measured perpendicular to the ray is $g\cos\phi$. Similarly it is equal to $d \cos \chi$, since χ is the angle between the ray and the normal to the surface of the slab. Therefore

$$g = \frac{d \cos \chi}{\cos \phi} \qquad \ldots\ldots(2).$$

If the angle ϕ is considered positive when the direction of the ray is obtained by a clockwise rotation from the direction of the optical axis, and if the slab is in a position derived by clockwise rotation through an angle θ from its neutral position (with surfaces parallel to the gate plane) the three angles are connected by the relation

$$\chi = \phi - \theta \qquad \ldots\ldots(3).$$

These equations cover every case when the usual sign conventions are observed. The length g represents the distance of the point in which the actual refracted ray meets the gate plane from the point in which that ray would meet the same plane if the slab were simply removed, so that the ray travels unrefracted to the plane occupied by the gate.

§ 3. HEXAGONAL PRISM

The considerations already mentioned seemed to indicate that either hexagonal or octagonal blocks would be required. In the first case considered I assumed the glass block to be six-sided, 1·92 in. thick, and the refracted index was taken to be 1·50. The gate-opening or picture-pitch is 0·74 in. and the projector lens is of 3·52-in. focus, so that the picture subtends an angle of 12° at the principal point of the lens. This case was investigated partly by trigonometrical calculation and partly by careful drawing. Diagrams on a scale three times larger than the actual apparatus were drawn for three stages of rotation such that $\pm\theta = 10°$, 20° and 30°.

For the purpose of graphically illustrating the effects of the rotating parallel slabs upon the image of the exposure gate and the pictures travelling across it, I have assumed the eye to be placed at the first principal point P of the projector lens and to view through each of the three revolving parallel glass slabs in turn an undistorted film picture subtending an angle of 12° at P, and travelling uniformly past the gate, the time for the complete passage being equal to the time the block takes to rotate through 60°. The displacements of the rays which travel from P towards the film along the axis and at 6° on either side of the axis and thus correspond to points at the centre and on the two edges of a picture were determined, these displacements being measured from their ideal positions in the plane of the gate. They were then expressed in terms of the angles they subtend at P. It should be borne in mind that if first-class definition is required in the photographing or screen-projection of pictures, it is desirable that no flicker or blurring which will subtend a visual angle greater than 1 or 2 min. at the eye should be allowed to occur, assuming that the eye is placed at a distance from the picture yielding the original angle of view. Figure 2 is a diagrammatic summary of the results obtained. It shows (compressed vertically to one-third) the various angular distortions or displacements caused by the passage through any one of the three 1·92-in. parallel blocks involved in the hexagonal prism when the angular rotations of the latter are 10°, 20° and 30°.

It will be noticed that for a rotation of 10° a right-hand portion of the following picture appears on the left while a corresponding portion in the right is missing or dark. At 20° two-thirds of the following picture shows on the left, while the corresponding two-thirds of the picture on the right is missing. For a rotation of 30° the picture is distorted by each margin being stretched out by 31 min. of arc, or one-twelfth part of each half picture. In this position the axial ray from the principal point *P* of the lens is virtually split at the sharp intersection of two adjacent surfaces of the block into two symmetrical principal rays. These coincide with a reasonable degree of accuracy (departures − 1·4 min. on the left hand and + 1·4 min. on the right hand) with the centres C_1 and C_2 of two adjacent pictures at once. This implies a duplication of the centre point of the picture with a separation of 2·8 min. The figure also gives the angular displacements for rotations of 40° and 50°: these are clearly the same as those found at 20° and 10° respectively with certain transpositions and changes of sign.

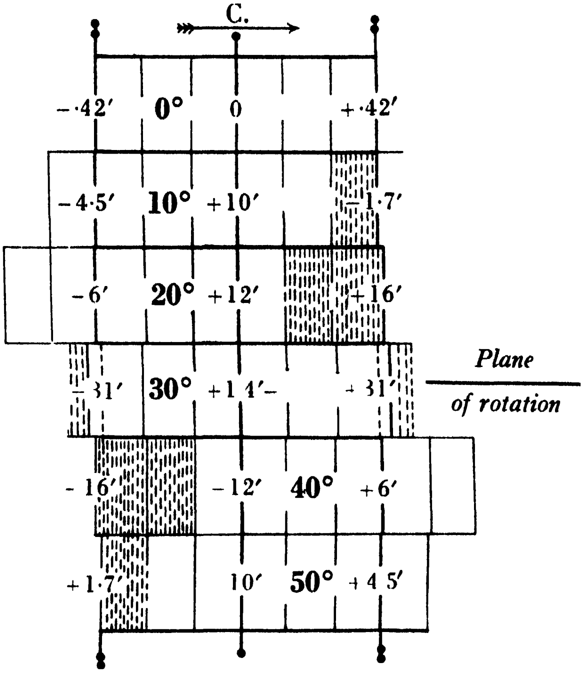

Figure 2.

I have not worked out the displacements corresponding to the lines in figure 2 dividing each picture into three, but their values will be intermediate between those at the centre and the margins. Therefore for a rotation of 10° it will be found that an intermediate or neutral point can be found somewhere in each half of the picture where there is no displacement: a neutral point also exists in the left half for a rotation of 20° and in the right-hand half of each picture for rotations of 40° and 50°.

And now regarding the side rays from the centre of the lens, along which the divisions between pictures should be seen, I must call attention to the arbitrary and indeterminate nature of the apparent displacements produced. First, it is clear that the wider the angle of view the more obliquely do these rays strike the film, so that a very slight movement of the gate to or from the revolving prism, for focusing purposes, will seriously alter their points of incidence on the film picture. Moreover it can be shown that the focal distances from P to the images of points in the picture have undergone a considerable lengthening-out effect owing to their passage through the glass block. The effect of the latter is to apparently throw back the image of the picture to oblique curved focal surfaces, presenting their convexities towards the glass hexagon, and on the opposite side of the gate plane. I mention these matters as they point to a more or less ill-defined image being presented to the projector lens. Any attempt at focusing the picture will have a large influence on the apparent distortion of any points situated near the upper and lower margins of the screen picture.

These facts constitute a very strong objection to the use of any projector lens of focal length less than 4 in., and even then various synchronized shutter devices, such as one for blocking out the central part of the gate when it is occupied by a division between two pictures,* which is subject to a displacement of half a degree, may have to be resorted to.

§ 4. OCTAGONAL PRISM

I now consider the result of increasing the number of flat surfaces of the revolving glass polygon from six to eight, with an increase of its diameter to about 2·70 in. After this, in order to secure working-room for the rotating prism, any further reduction of the flickering can be attained only by substantially reducing the vertical angular diameter of the picture, which I have so far assumed to be 12°. For instance, if the angular vertical height of the picture were reduced to 6° then a glass polygon of a doubled diameter of about 5·4 in. and having 16 flat surfaces might be accommodated. But it would be very difficult to find discs of glass, 5–6 in. in diameter and at least 1½ in. thick, sufficiently homogeneous and well annealed for the forming of such a sixteen-sided prism. Also the practical difficulties attending the correct shaping and polishing of the sixteen faces of such a large glass polygon with sufficient accuracy, in both linear and angular measurements, consistently with well-figured and well-polished plane faces, would be far more than doubled. Moreover, the bulkier the rotating block, the more must its speed of rotation be reduced if its rupture under the great centrifugal forces generated is to be avoided.

For the application of the formulae already derived (which have been utilized alone in this case) I consider seven rays proceeding from the principal point P to the film. Three of these are the axial ray and those proceeding to the middle of the top and the bottom of the picture, inclined at angles of $\pm 6^\circ$ to the axis. The remaining four, which for descriptive purposes may be called the $\pm 4^\circ$ and $\pm 2^\circ$ rays, are chosen to correspond to the partition of each half-picture exactly into thirds in the absence of distortion.

---

* This would of course somewhat darken the upper and lower strips of the projected screen pictures.

The angular distortion in minutes of arc is shown diagrammatically in figure 3, where the film's movement is supposed to be horizontally from left to right, so that the vertical distortions given in the tables can be shown horizontally. Here the usually greater width of the horizontal film picture is represented by a vertical width on $\frac{1}{10}$ of the full vertical scale, in order to save room. The eight narrow parallel strips marked *d*...*d* containing short vertical lines at equal distances apart are lines representing the 6°, 4° and 2° viewing rays on the left of the centre or axial ray, and also the 2°, 4° and 6° viewing rays on the right. These short vertical lines enclosed in the strips *d*...*d*, etc. thus represent distortionless or correct projection. The longer vertical solid lines show graphically for each of the several prism rotations, 0, $7\frac{1}{2}^\circ$, 15°, $22\frac{1}{2}^\circ$, 30°, $37\frac{1}{2}^\circ$ and 45°, the various linear displacements or distortions relative to the seven viewing rays represented by *d*...*d*...*d*, which have radiated from the principal point of the lens, been refracted through the octagon, and then intersected the gate plane. The squares marked *g* down each side of figure 3 indicate darkness owing to the obstruction of the metal plate in which the gate opening is cut out, the plate being supposed fixed.

The squares marked *f.p.* with dotted diagonals are each occupied by a sixth part of the following picture, no. 2, while those marked *p.p.* with dotted diagonals are each occupied by one sixth part of the preceding picture. It will be seen that at $7\frac{1}{2}^\circ$ and at $37\frac{1}{2}^\circ$ of prism rotation only $\frac{4}{6}$ of picture no. 1 is illuminated, together with $\frac{1}{6}$ of the following picture, no. 2, on the left, and $\frac{2}{6}$ eclipsed on the right; at 15° and 30° prism rotation only $\frac{2}{6}$ of the picture is illuminated together with $\frac{2}{6}$ of the following picture, no. 2, on the left, and $\frac{2}{6}$ is eclipsed by the gate plate. In the lowest strip of figure 3, picture no. 2 is shown to have fully taken the place of picture no. 1.

One obvious inference can be drawn from figure 3 and this analysis, namely that a movable gate-opening should be arranged to be central for rotation 0°; to follow the picture, embraced by the refracted 6° viewing rays, up to 15° rotation; then to return to the central position as rotation $22\frac{1}{2}^\circ$ is attained; to continue to the left to frame the following film picture no. 2; and then to come back to the central position as the prism rotation reaches zero again. At rotation 15°, instead of the greatest concentration of light taking place on the central $\frac{2}{6}$ only, the three divisions to the right shown obscured in figure 3 would become illuminated together with the central third. But as regards the central position at rotation $22\frac{1}{2}^\circ$, the policy of obstructing the waist of the gate and thus eclipsing the left and right ends of the picture, which show such very marked distortion, is worth serious consideration, for a displacement amounting to about half a degree for rotation $22\frac{1}{2}^\circ$ does not recommend itself to onlookers with normal eyesight, since only the central $\frac{2}{6}$ of the screen picture at $22\frac{1}{2}^\circ$ rotation can be said to approach the standard of definition expected from ordinary intermittent cinema projection. And here it is worth noting that if the thickness of the glass octagon is reduced to $\frac{77}{78}$ of its present value, the central dark gap shown in figure 2 for $22\frac{1}{2}^\circ$ rotation will be closed up, while the distortion for 6° becomes 22', for 4° becomes 17' and for 2° becomes 6'. But there would be slight increases in some of the distortions at rotations 7½°, 15°, 30° and 37½°.

So far we have not considered what happens in the way of distortion of position to the top, bottom and the two end margins of the film picture 0·74 in. high and 1·0 in. wide; but whatever the linear displacements or distortions may be down the central vertical waist of the picture, they will certainly be much increased at the four corners of the picture, while the usually straight picture-borders will be curved either towards or away from the centre, according to the signs.

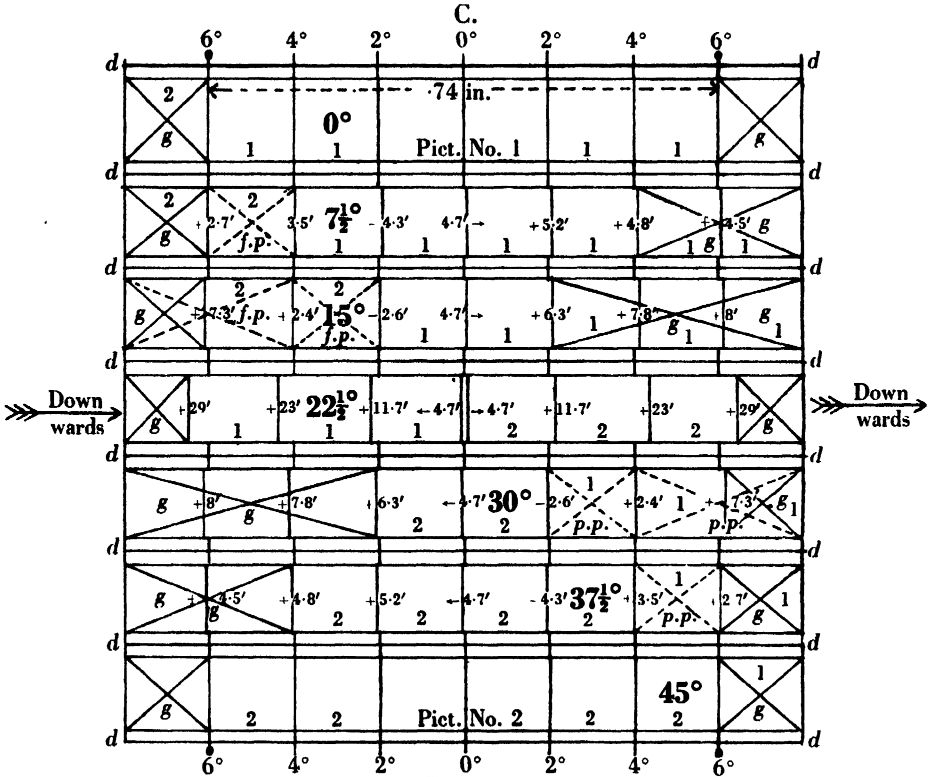

Figure 3.

1 minute = 0·0055 in. and height of gate = ·74 in.

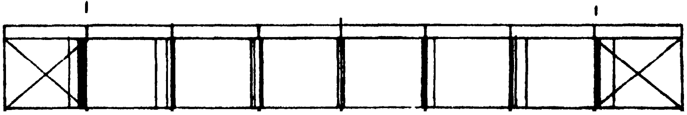

Figure 4.

The distortions of position marked in minutes of arc in figure 3 obviously imply more or less up-and-down oscillation, and some very interesting points may be noted, as for instance the varying amount of distortion or oscillation as the rotation of the glass octagon changes from 0° to 22½° and back to 0° again. A point 6° to the left suffers 2·7′ for 7½° rotation, 7·3′ for 15° rotation and 29′ for 22½° rotation—i.e. an over-all scattering of $29' - 2{\cdot}7'$ or 26·3′.

This, of course, implies oscillation and fuzzy definition, for not only have the displacements of the images for the three successive rotations of 7½°, 15° and 22½° been worked out, as illustrated in figure 3, but we must also allow for the fact that in between 0° and 7½°, 7½° and 15°, and 15° and 22½° rotations, there will occur intermediate displacements, filling in between the images of vertical lines shown in figure 3, so that the complete effect in the developed film negative or positive will be a broad, blurred grey line which will not, as a rule, be of uniform intensity. This means that the images of seven horizontal black lines equally distributed over the vertical white board presented to the camera for projection on to the sensitive film on a much reduced scale will be found registered, after development, as broadened out into nebulous grey bands of uneven greyness, showing on the more or less black background of the negative. Figure 4 gives a rough idea of the broadening-out effects upon lines consequent upon these oscillations of position.

There are two inferences suggested by the facts in the case applicable to both the photographing and the projecting machines. The first is the desirability of reducing the 12° vertical diameter of the field of view to about 8°, and the second is the advisability of keeping the working speed of film feed, together with the rotational speed of the prism, as low as possible. In other words, any moving feature in the instantaneous phenomenon being photographed by this apparatus has the best chance of being distinctly defined on the film when its duration is not more than one sixth of the time required for the transit of the film picture across the gate.

Better definition as the rotation of the octagon exceeds 15° could be secured by cutting down the vertical gate-opening automatically. This would result in the brightness of the top strip (2° high) and the bottom strip (2° high) being reduced to two thirds of the brightness of the middle zone of the picture (8° high). There would be a very substantial gain in definition at the cost of a little light in the upper and lower thirds of the picture, and should the line of demarcation between the upper and lower thirds be at all conspicuous the effect could be softened by arranging the two screening strips somewhat out of the focal plane, as, for instance, $\frac{1}{10}$ in. on the lens side of the gate.

REFERENCES

(1) Tuttle, F. E. *J. Soc. Mot. Pic. Engrs.*, **21**, 474 (1933).
(2) Taylor, H. D. *Proc. phys. Soc.* **46**, 283 (1934).

THE ELECTRICAL RESISTANCE OF FERROMAGNETICS

By H. H. POTTER, H. H. Wills Physical Laboratory,
University of Bristol

Received 17 *June* 1937

ABSTRACT. The resistance of nickel and iron is measured between 20 and 1200° K. From the measurements it is concluded that: (1) the kink in the {resistance, temperature} curve at the Curie point is sharp to within a small fraction of a degree; (2) above the Curie point the {resistance, temperature} curve is concave to the *T* axis as in a paramagnetic metal such as palladium; (3) the small change in spontaneous magnetization which takes place at low temperatures has a comparatively large effect on the resistance.

---

§ 1. INTRODUCTION

In 1930 Gerlach and Schneiderhahn$^{(1)}$ drew attention to the connexion between true magnetization and electrical resistance. In the neighbourhood of the Curie point the application of a magnetic field causes a reduction in the electrical resistance of a nickel wire which is proportional to the change in magnetic energy. Similar results were obtained by the writer for iron and Heusler alloy$^{(2)}$.

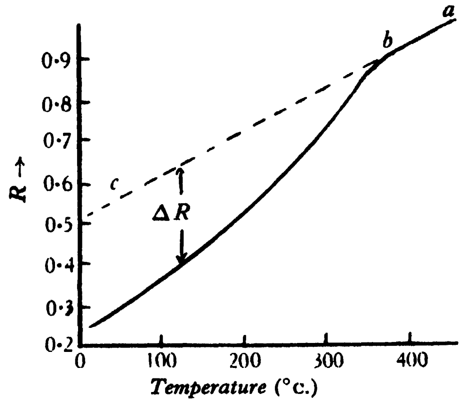

Figure 1.

The {resistance, temperature} curve as given by Gerlach and Schneiderhahn for zero external field is reproduced in figure 1. As the Curie point was approached from the low-temperature side the resistance rose more and more quickly, but the rate of rise of resistance decreased as the metal passed over into the paramagnetic state. On rather incomplete evidence Gerlach concluded that some little distance above the Curie temperature the {resistance, temperature} curve became a straight line *b*, *a*. On extrapolation of this line backwards, the distance ΔR was found to be fairly accurately proportional to the square of the spontaneous magnetization. It was therefore concluded that when the metal entered the ferromagnetic state the resistance fell by an amount which was proportional to the magnetic energy. This leads at once to a very serious difficulty. The extrapolated portion *b*, *c* of the line *a*, *b* cannot represent the course of the {resistance, temperature} curve of a normal, non-ferromagnetic, metal since such a curve must pass through the origin of coordinates.

A further point of interest was raised recently by Svensson(3), who found a discontinuity in the temperature coefficient of resistance of nickel at its Curie temperature. He found this discontinuity to occur in a temperature range as small as $\frac{1}{10}$° C. In view of the growing volume of evidence, from measurements of magnetic energy, that the Curie temperature is not in general a sharply defined point but spreads over some 20 or 30°, this result was very surprising. The difficulties encountered in trying to reconcile the various experiments with one another and with theory seemed to make it desirable to repeat both the Gerlach and the Svensson experiments.

§ 2. METHOD OF MEASUREMENT

Experiments have been carried out both on nickel and on iron. Both metals were obtained from Messrs Adam Hilger, the former having a purity of 99·971 per cent with 0·018 per cent of iron and 0·010 per cent of carbon as the chief impurities. The iron had a purity of 99·96 per cent with silicon and oxygen as the main impurities. In addition a specimen of very pure nickel was obtained from the International Nickel Co.[*] This contained 99·99 per cent of nickel with 0·009 per cent of carbon as the main impurity.

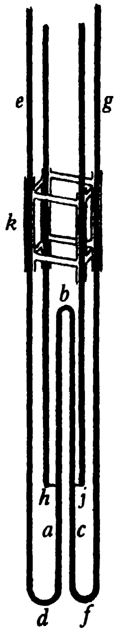

Figure 2.

The resistance was obtained from current-voltage measurements in a specimen in the form of a rod 2 mm. in diameter and 8 cm. long. This was bent into an inverted U as shown at *a*, *b*, *c* and spot-welded at *a* and *c* to long rods of commercially pure nickel *de*, *fg*, figure 2. Two nickel potential leads were mounted parallel to *de* and *fg*, contact with the specimen being made by spot-welding thin platinum wires at *h* and *j*. The whole system was held rigidly together by quartz frames, one of which is shown at *k*. These consisted of four parallel tubes banded together, as shown, by eight quartz rods.

A potentiometer-controlled current of 0·5 amp. was passed through the specimen, and the potential between *h* and *j* was measured on a Tinsley potentiometer. To correct for stray e.m.fs. in the circuit either the potential was remeasured after reversal of the current, or the potential was measured with and without the current. The two methods always gave identical results. An attempt to avoid this correction altogether, by using fine nickel wires to join the potential leads to the specimen, failed. Firstly, the stray e.m.fs. did not disappear completely, and secondly the thin nickel wires were too brittle after spot-welding. The resistance could be measured, except at temperatures below 0° c., to about 1 part in 2000.

---

[*] Our thanks are due to Mr Wise of the International Nickel Co. who kindly presented us with this specimen through the agency of Messrs Metropolitan-Vickers Electrical Co.

A platinum, platinum-rhodium thermocouple spot-welded midway between *h* and *b* served to measure the temperature. The thermocouple was calibrated in boiling water and melting tin, zinc, aluminium, common salt and copper. The calibration was in good agreement with the figures supplied with the couple by Messrs Johnson Matthey. Thermoelectric e.m.fs. at intermediate temperatures were calculated by means of an interpolation formula. The accuracy of absolute temperature measurement was probably not better than $\frac{1}{2}$ up to 500° c., with perhaps even bigger errors at high temperatures, but changes in temperature of $\frac{1}{10}$° c. could easily be measured. In order to allow for the small e.m.f. (of the order of 1 μv.) produced in the thermocouple by the current, the thermal e.m.f. was remeasured after reversal of the current. This method was preferred to measurement with the current off, since the latter produces a slight temperature rise. Consequently the temperature should be measured with the current on, in order that it may correspond with the potential measurement.

§ 3. FURNACE AND TEMPERATURE CONTROL

The furnace consisted of an evacuated quartz tube with two concentric copper tube liners which served to equalize the temperature along the length of the furnace. The tubes were of 4 mm. in wall-thickness and 30 cm. long, and were heat-insulated from one another by an evacuated annular space. The temperature-gradient in the specimen was only a small fraction of a degree except for temperatures above 700° c., when it amounted to about $\frac{1}{2}$° c. In order to investigate in the neighbourhood of the Curie point of nickel in detail, an automatic furnace control was used. This consisted of a modified Cooke-Swallow regulator$^{(4)}$ made for us by Messrs Metropolitan-Vickers Electrical Co. The platinum thermometer which operated the regulator was between the furnace wall and the outer copper tube. Inside the inner copper tube where the specimen was situated, the temperature could be kept constant to within $\frac{1}{10}$° c. for several minutes and to within $\frac{1}{2}$° c. for indefinite periods.

§ 4. RESULTS

The results are shown in figures 3, 4 and 5 and in tables 1 and 2. They all refer to annealed specimens. The existence of a kink in the {resistance, temperature} curve at the Curie point, first detected by Svensson in nickel, has been verified, and a similar kink has been found in iron. Detailed graphs for the Curie-point regions are given in figure 3*a* for nickel and in figure 5 for iron. The curves for the various specimens of nickel were almost identical. The data given are for a Hilger specimen and show a kink at 629·3° k. and a value 4·627 of R/R_0, where R_0 is the resistance at 0° c. A second Hilger specimen gave a kink at 629·8° k., with R/R_0 equal to 4·603.

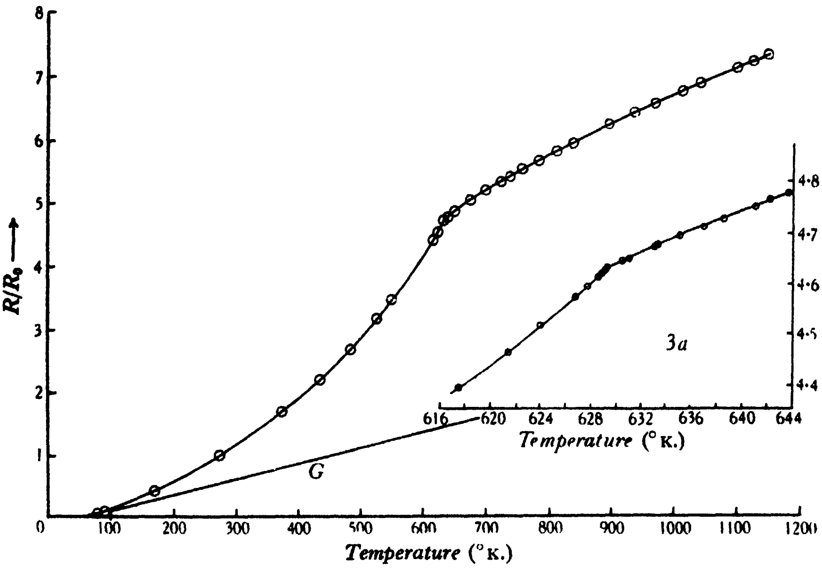

Figure 3. Resistance of nickel as a function of temperature.

Figure 3*a*. The neighbourhood of the Curie point.

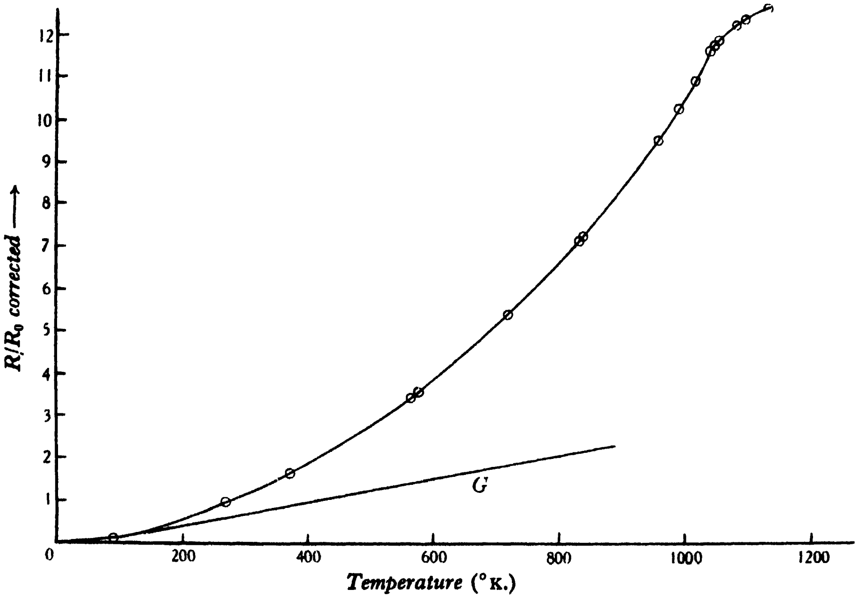

Figure 4. Resistance of iron as a function of temperature.

The specimen of nickel from the International Nickel Co. had corresponding values of 629·6° K. and 4·605. In iron the kink was found at 1039° K. with R/R_0 equal to 11·67.

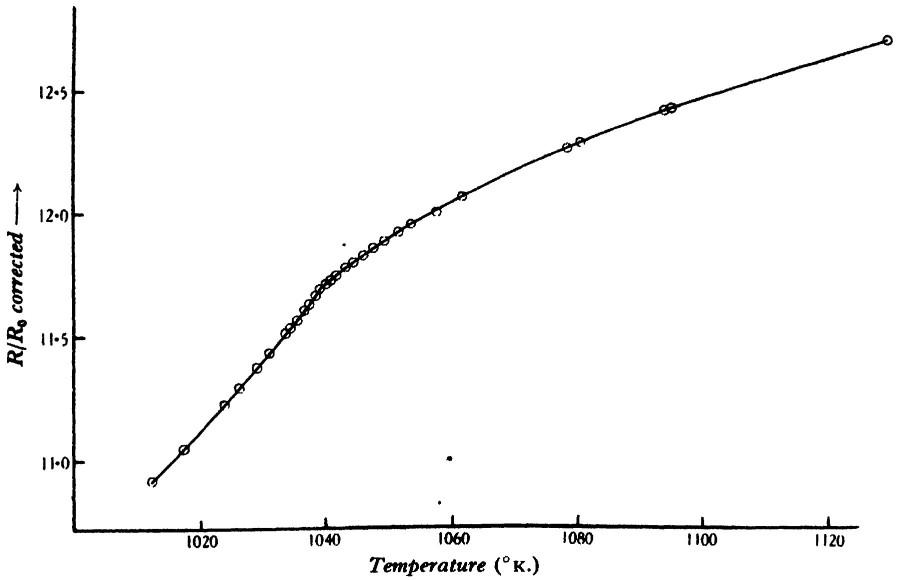

Figure 5. Resistance of iron as a function of temperature.

Table 1. Resistance of nickel as a function of temperature

T (° K.)	R/R_0	T (° K.)	R/R_0	T (° K.)	R/R_0
77	0·090	629·2	4·622	740·1	5·384
90	0·125	629·4	4·627	760·0	5·493
169	0·440	630·5	4·641	785·8	5·626
273	1·000	631·1	4·645	815·3	5·775
373	1·681	633·2	4·669	839·5	5·898
435	2·196	633·4	4·673	898·6	6·178
483·5	2·679	635·2	4·690	939·7	6·366
526	3·149	637·1	4·706	972·6	6·513
551·5	3·450	638·7	4·723	1016·0	6 703
617·5	4·392	641·1	4·746	1044·0	6·825
621·5	4·461	642·3	4·759	1102·0	7·064
624	4·513	643·8	4·774	1128:2	7·171
626·9	4·570	651·8	4·838	1143·1	7·228
627·8	4·590	675·3	5·005	1153·1	7·265
628·6	4·608	701·2	5·166		
628·9	4·615	724·8	5·302		

In table 2 a third column showing R/R_0 corrected has been added. The work of Meissner and Voigt⁽⁵⁾ has indicated that iron of a quite high degree of purity may have a very marked residual resistance. The resistance of the iron specimen was therefore measured in liquid hydrogen, which led to an estimate of 0·020 R_0 for the residual resistance. Assuming then that this amount should be subtracted from the resistance at any other temperature, we have

$$R/R_0 \text{ corrected} = (R/R_0 - 0{\cdot}02)/0{\cdot}98.$$

Table 2. Resistance of iron as a function of temperature

T (°K.)	R/R_0	R/R_0 corrected	T (°K.)	R/R_0	R/R_0 corrected
20	0·021	0·001	1037·1	11·404	11·612
90	0·122	0·104	1038·3	11·439	11·647
273	1·000	1·000	1039·1	11·464	11·673
373	1·638	1·650	1039·9	11·483	11·692
566	3·398	3·446	1040·6	11·499	11·709
578·3	3·531	3·581	1041·6	11·520	11·730
719·5	5·300	5·386	1043·0	11·549	11·760
830·6	7·026	7·146	1044·2	11·570	11·781
837·8	7·144	7·266	1045·9	11·600	11·812
955·9	9·378	9·545	1047·5	11·624	11·836
989·1	10·124	10·306	1049·2	11·657	11·870
1012·2	10·670	10·863	1051·4	11·693	11·906
1017·25	10·821	11·017	1053·6	11·723	11·937
1023·8	11·000	11·200	1057·5	11·770	11·985
1026·1	11·062	11·263	1061·6	11·831	12·047
1028·9	11·145	11·347	1078·4	12·027	12·247
1031·0	11·205	11·409	1080·4	12·050	12·271
1033·4	11·287	11·492	1093·9	12·176	12·399
1034·3	11·307	11·513	1095·2	12·187	12·410
1035·3	11·339	11·545	1129·6	12·449	12·678
1036·6	11·378	11·585			

In our earliest experiments on nickel a second kink was found at 740° K. This kink was much less well defined than the one at the Curie temperature, and was probably due to impurity, as it could not be verified after extremely careful examination of the very pure specimen from the International Nickel Co., or of specimens subsequently obtained from Messrs Hilger.

§ 4. DISCUSSION OF RESULTS

The explanation of the sharp kink at the Curie point has already been discussed elsewhere(6). Further discussion here seems unnecessary. From the Curie point up to the highest temperatures used, the curves for both nickel and iron are markedly concave to the temperature axis. This fact presumably invalidates Gerlach's extrapolation and consequently his formal theory concerning the connexion between resistance and energy of spontaneous magnetization.

An entirely different explanation of the resistance of ferromagnetics and other transition metals has been given by Mott(7, 8, 9). Palladium, a paramagnetic transition metal in the same column of the periodic table as nickel, has 0·6 electron per atom in the 5*s* shell and consequently a similar number of positive holes in the 4*d* shell. The energies of the two bands overlap, but the density of the states at the surface of the Fermi distribution is much greater in the 4*d* band than in the 5*s* band. Consequently during scattering processes $s \rightarrow d$ transitions will be more probable than $s \rightarrow s$ transitions. This gives rise to the abnormally high resistance which is characteristic of the transition metals. The theory has been successful in explaining the concavity of the palladium {resistance, temperature} curve towards the temperature axis and various facts concerning the resistance of palladium-gold alloys(10).

Above its Curie point nickel will be expected to behave like palladium and therefore to give a curve concave to the temperature axis.

If the transition metal happens also to be ferromagnetic, then other considerations will also apply below the Curie point. In the ferromagnetic state the spins of the positive holes will be aligned so that in accordance with the exclusion principle only electrons of the correct spin can undergo the $s \rightarrow d$ transition. Thus one-half of the conduction electrons (i.e. electrons in the s band) have a much larger mean free path, actually four or five times as large, as the other half. With rise of temperature the alignment of the spins of the positive holes becomes less perfect, and scattering of electrons of both spins into the d band becomes possible. Thus as the spontaneous magnetization disappears the resistance rises owing to this additional scattering.

In figures 3 and 4 a line (marked G in both cases) has been drawn representing a rough estimate of what the resistance of nickel and iron would have been if the ferromagnetism had remained unchanged with rise of temperature. These lines have been calculated from the Gruneisen formula, characteristic temperatures of 375 and 420° K. being assumed for the two metals. The absolute values of the ordinates have been obtained by fitting them to the experimental resistance curves at low temperatures where the ferromagnetism has not decreased sufficiently to modify greatly the resistance. The rapid deviation of the experimental curves from the Gruneisen curves is very striking, particularly as the fitting at low temperatures will assign a maximum value to the ordinates of the latter curves. In iron at 0° C., for instance, R/R_G, where R_G is the Gruneisen resistance, is of the order 1·6, whereas the decrease in the spontaneous magnetization from the value at absolute zero is something under 2 per cent. This seems incompatible with any theory which ascribes the resistance-change to a change in the magnetic energy. It is, however, in striking agreement with the Mott theory in which the probability of scattering into the d band is proportional to

$$\left\{1-\frac{\sigma}{\sigma_0}\right\}^{\frac{1}{3}},$$

where σ_0 is the spontaneous magnetization at the absolute zero of temperature and σ is its value at any other temperature.

According to Mott$^{(9)}$ the conductivity of the half of the electrons with spins in the direction of magnetization is proportional to

$$\frac{}{(1-\sigma/\sigma_0)^{\frac{1}{3}}+\frac{1}{4}},$$

so that if $1-\sigma/\sigma_0=0{\cdot}01$, the cube root is 0·21, and the contribution from these electrons to the conductivity is about halved. The effect of change of magnetization on the resistance may thus be quite large at low temperatures.

§ 5. ACKNOWLEDGEMENTS

My best thanks are due to Prof. Mott for much helpful discussion and advice, and to the Colston Research Society of the University of Bristol for a grant towards the expenses of this investigation. I also wish to thank Dr L. C. Jackson for supplying me with liquid hydrogen which he produced in a liquefier erected in this department under his direction.

REFERENCES

(1) Gerlach and Schneiderhahn. *Ann. Phys., Lpz.*, **5**, vi, 772 (1930).
(2) Potter. *Proc. roy. Soc.* A, **132**, 560 (1931); *Phil. Mag.* **13**, 233 (1932).
(3) Svensson. *Ann. Phys., Lpz.*, **5**, xxii, 97 (1935).
(4) Cooke and Swallow. *J. sci. Instrum.* **6**, 287 (1929).
(5) Meissner and Voigt. *Ann. Phys., Lpz.*, **5**, vii, 761 and 892 (1930).
(6) Mott. *Proc. phys. Soc.* **47**, 571 (1935).
(7) Mott. *Proc. roy. Soc.* A, **153**, 699 (1936).
(8) Mott. *Proc. roy. Soc.* A, **156**, 368 (1936).
(9) Mott and Potter. *Nature, Lond.*, **139**, 411 (1937).
(10) Conybeare. *Proc. phys. Soc.* **49**, 29 (1937).

ABSORPTION SPECTRA AND PHOTODISSOCIATION OF HALIDES AND OXYHALIDES OF SULPHUR, SELENIUM AND TELLURIUM

By S. L. HUSSAIN and R. SAMUEL

Received 1 *March* 1937

ABSTRACT. The absorption spectra of $SOBr_2$, $S_2O_5Cl_2$, $SeCl_4$, $SeOCl_2$, Se_2Cl_2, $SeBr_4$, Se_2Br_2, $TeCl_2$, $TeCl_4$, $TeBr_2$ and $TeBr_4$ in the vapour state are investigated, and the photodissociation processes and bond energies are determined. The results confirm those previously obtained for the chlorides and oxychlorides of sulphur.

§ 1. INTRODUCTION

Recently some investigations of the continuous absorption spectra of polyatomic inorganic molecules have been undertaken in order to extend the spectroscopic basis of the theory of valency$^{(1)}$. Such investigations are interesting because the correlation of the beginnings of regions of selective absorption in the vapour state to photodissociation processes permit us to determine the single-bond energies directly, and not as part of a grand total, as in thermochemical observations. In these experiments it has been found that the bond energies are additive in the same inorganic molecule and remain constant in different molecules, so long as the central atom is in a minor and not in its maximal state of valency. In the latter case the energy conditions are entirely changed, and this has been connected with the fact that maximal valency always means the activation of the group of s^2 electrons, whose repulsive character is now well established by new band-spectroscopic evidence concerning diatomic halides of the second and fourth groups and oxides of the second and third groups of the periodic table$^{(2)}$. Particularly striking examples of the additivity and constancy of the bond energies have been found among the chlorides and oxychlorides of sulphur, and the object of the present paper is to extend these investigations to similar molecules. We have measured the absorption spectra and determined the photodissociation processes and bond energies of the following molecules in the vapour state: $SOBr_2$, $S_2O_5Cl_2$, $SeCl_4$, $SeOCl_2$, Se_2Cl_2, $SeBr_4$, Se_2Br_2, $TeCl_2$, $TeCl_4$, $TeBr_2$, $TeBr_4$. The experimental results entirely confirm those obtained earlier, and cannot be understood otherwise than in a pair-bond theory of valency, in which each linkage is produced by a pair of electrons, one from each atom, and localized between the atoms.

§ 2. THERMOCHEMICAL CALCULATIONS

In the previous papers, since the thermochemical data are more or less known, we were able to calculate, for the derivatives of sulphur, the heat of dissociation into the gaseous atoms directly and individually in the usual way by means of Born's cycle. For derivatives of selenium and tellurium, however, the thermochemical data are much less known, the heat of formation from the elements is unknown for some of the compounds, and their heats of sublimation are entirely missing. We shall therefore follow a slightly different course here, and first calculate the most probable values for the various bond energies and then compare them with the experimental results obtained from the absorption spectra.

As the basic values of the energy of dissociation of S_2, Se_2 and Te_2 into unexcited atoms we use the values of 88, 59 and 44 kcal./mol. obtained, as in the earlier papers, from the direct observations of the convergence point(3) of the band spectrum by deducting the excitation energy of the ^1D term of the corresponding atom. This procedure involves the assumption that the ground state of each of the three molecules is $^3\Sigma$, because in the case of a $^1\Sigma$ state the excitation energy of ^1D would have to be deducted twice. For S_2 the triplet character is established by the rotational analysis of Christy and Naudé(4) and the above value from the convergence point appears to be the most accurate one. Olsson's rotational analysis(5) of some bands of the Se_2 spectrum might suggest that those bands are due to transitions between singlet levels, but it is not yet clear whether this interpretation is correct and whether the bands involve the ground state at all. Lessheim and Khanna* have found selenium vapour to be paramagnetic—a result which definitely supports this view. These points will be discussed at greater length in forthcoming papers from this laboratory; here it might be sufficient to point out that the above dissociation energies, as will be seen, agree perfectly well with the values obtained from the photodissociation of the halides and oxyhalides, which, in conjunction with the thermochemical data, are an independent means of obtaining the dissociation energies of the ground states of the diatomic molecules. Furthermore the triplet character of the ground states of Se_2 and Te_2 is corroborated by the fact that the assumption of a $^1\Sigma$ state would lead to dissociation energies of 35 and 14 kcal./mol., respectively, which appear too low as compared with the values obtained by the extrapolation of the vibrational levels, and also as compared with the values which have been estimated by means of the law of mass action from observations of the vapour pressure(6). To the values, 88, 59 and 44 kcal./mol., of the dissociation energy of the molecules S_2, Se_2 and Te_2, respectively, the heat of sublimation (S) has to be added in order to obtain the total energy necessary to transform the solid elements into gaseous atoms. Furthermore, for sulphur and selenium the heat of polymerization (P) has to be added too, while the vapour of tellurium consists of diatomic molecules. The values† used here are (in kcal./g.-atom):

$$S(\mathrm{S})+P(\mathrm{S})=15, \quad S(\mathrm{Se})+P(\mathrm{Se})=17{\cdot}5, \quad S(\mathrm{Te})=31.$$

The energy to convert 1 g.-atom of the solid elements into gaseous atoms comes therefore to 59, 47 and 53 kcal. for sulphur, selenium, and tellurium respectively. The increase for tellurium is remarkable and will be discussed below. For bromine we obtain 25 kcal. in a similar way, while for oxygen and chlorine the dissociation energy of the diatomic molecule is directly known.

---

* Private communication from Dr H. Lessheim.

† These figures are taken mostly from Mellor's *Treatise*, a few from Landolt-Boernstein's *Tables*.

The atomic energy of dissociation (*D*) of a molecule into its constituent atoms is obtained by means of Born's cycle by adding to the above values the thermochemical heat of formation from the elements (*Q*) and deducting the heat of sublimation (*S*) of the compound itself. The latter are not known at all, and are estimated here mostly from the boiling-points by means of Forcrand's formula, as discussed in earlier publications. They represent small amounts of energy as compared with *D* or *Q*, and the error cannot seriously influence the final result.

Table 1

MX_n	Q	S	D	$D(M_2)$	$D_B(M-X)$
S_2Br_2	2	10	162	S—S 88	S—Br = 37
$SeCl_2$	−11	(~5)	88		$\frac{1}{2}D$ = Se—Cl = 44
$SeCl_4$	36	~14	188		$\frac{1}{4}D$ = Se—Cl = 46
Se_2Cl_2	22	~12	162	Se—Se 59	Se—Cl = 51
$TeCl_4$	77	24	226		$\frac{1}{4}D$ = Te—Cl = 56·5
$TeBr_4$	57	~21	193		$\frac{1}{4}D$ = Te—Br = 48

The first four columns of table 1 give the results of the final calculations for those halides of selenium and tellurium where *Q* is known, and for thionyl bromide. If the bond energies (D_B) are rigorously additive, the division of the atomic heats of formation given in columns 5 and 6 obtains. For the Se—Cl bond three figures are available, which are quite close to each other, in spite of the error brought about by the estimated heats of sublimation and in spite of the fact that the additivity of the bond energies holds only approximately on account of the varying repulsive forces between the atoms. For the S—Cl bond the corresponding figures have been calculated in earlier publications, the values obtained from $SOCl_2$, S_2Cl and SCl_2 being 48, 46 and 60 kcal./mol. respectively. Taking, as far as possible, the weighted mean of several values, we obtain the following figures for the bond energies in molecules formed by divalent and tetravalent atoms of the sixth group:

Table 2

	S	Se	Te
Cl	50	47	55
Br	37	(~42)	48

For the Se—Br bond no figures are available at all and the value of 42 kcal./mol. is estimated from the S—Br and Te—Br bond according to the corresponding energy differences in the series of the chlorides. It is remarkable that the energies of the Te—Cl and Te—Br bond are higher than those of the corresponding bonds of S and Se, while generally the bond energies decrease in the same group of the periodic system with increasing atomic number. This exception, however, appears to be quite genuine. It already finds expression in the corresponding values of *S* (Te) and *Q*; and Roth and Becher(7) have observed a similar phenomenon for the trioxides of these elements. The values for the Te—Cl and the Te—Br bond agree approximately with those calculated by Larionov(8). The anomalous course of the bond energies in this group is doubtless connected with the fact that the energies of excitation, and probably also those of ionization, increase again from Se to Te instead of decreasing.

Although the above figures do not claim great accuracy, they are sufficient to make possible a comparison with the photolytic dissociation energies. As remarked above, the photodissociation, as measured by the long-wave limit of a region of continuous absorption, investigates directly the dissociation energy of a single bond, as distinct from thermochemical measurement, where mainly the energy due to the grand total of several bonds is observed. If therefore the long-wave limits agree with the above values and with those of the S=S, Se—Se, S=O, and Se=O bonds known from the band spectra of the diatomic molecules, this will be a confirmation of the earlier experiments, and will show that in these molecules also the bond energies behave approximately additively in the same molecule and are constant in different molecules.

§ 3. REMARKS ON THE EXPERIMENTAL RESULTS

The absorption spectra were taken with the apparatus described earlier(1), and the long-wave limits and the maxima of the various regions of selective absorption were determined by means of a recording microphotometer. Figures 1 to 3 are samples of these photometer records. As discussed elsewhere, the long-wave limits of such maxima are not easy to measure with accuracy, because, if the vapour pressure is too low, only those wave-lengths are absorbed for which the absorption coefficient already has appreciably high values, and consequently the energy-values obtained are too high. If, on the other hand, the vapour pressure is increased too much, the absorption obtained does not belong to the lowest vibrational level of the molecule, because the number of molecules in higher vibrational levels increases with the vapour pressure (and temperature), and the absorption spectrum yields too low values of the energy of dissociation. These difficulties are unavoidable because the continuous absorption measures transitions between stable and unstable states and the energies obtained are, in reality, energies of excitation not of dissociation. They can be minimized to some extent by taking the absorption spectrum over a long range of varying pressures, and a comparison of different spectrograms of the same substance makes it easier to determine that long-wave limit belonging to the molecule in its lowest state of vibration. Because most of the compounds investigated here have rather low saturation pressures, and because most of them are inclined to decompose on heating,* not so many spectra could be obtained as, for instance, in the case of chlorides and oxychlorides of sulphur, and the following figures cannot

---

* The experiments recorded here were carried out in the spring of 1936, and the result was published in a preliminary note(9). To ascertain that the absorption maxima are due to these compounds and that no decomposition occurs on heating, the absorption spectra of those for which a suitable solvent could be found have been measured in solution(10). The same regions of selective absorption have been found in solution as in the vapour state.

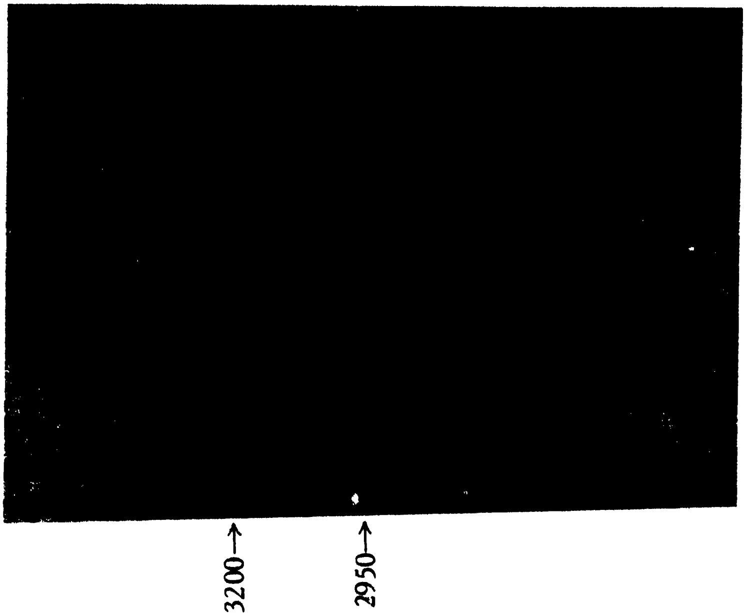

Figure 1. Photometer record of Se_2Cl_2 absorption. Lower curve, source of light; upper curve, Se_2Cl_2 vapour in 5-cm. absorption tube at 1 mm. vapour pressure.

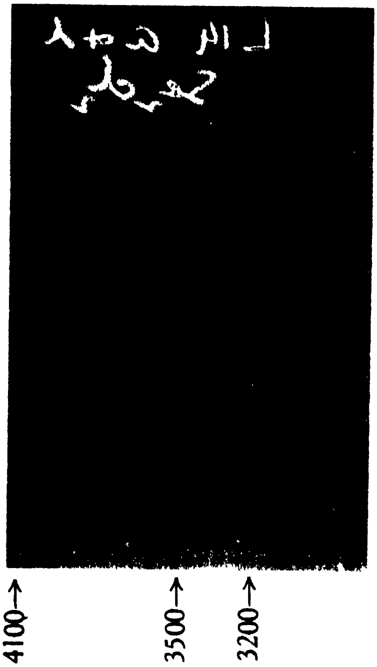

Figure 2.

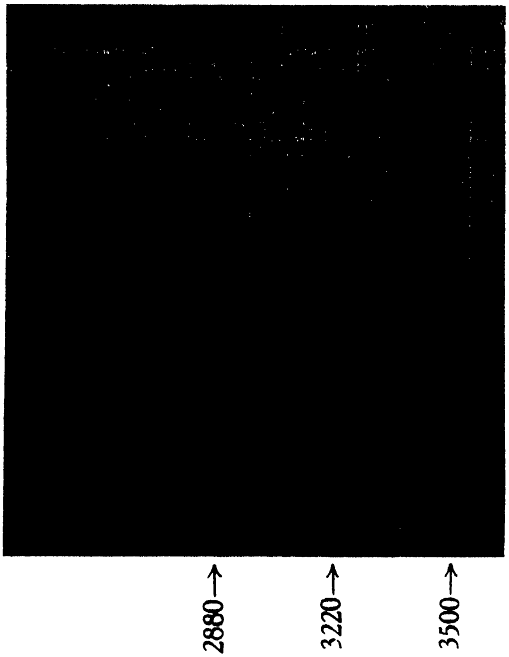

Figure 3.

Figure 2. The same, at longer wave-length. Lowest curve, source of light; second curve, 1 mm. vapour pressure; third curve, 3 mm. vapour pressure. Development of maximum at λ3500 A.

Figure 3. Photometer record of Se_2Br_2 absorption, main maximum at λ3220 A. Lower curve, source of light; upper curve, Se_2Br_2 vapour in 10-cm. absorption tube at 75° C.

Table 3

	First absorption				Second absorption				Third absorption				Fourth absorption			
	Long-wave lim.		Maximum		Long-wave lim.		Maximum		Long-wave lim.		Maximum		Long-wave lim.		Maximum	
	λ (mμ.)	kcal./mol.	λ (mμ.)	Volts	λ (mμ.)	kcal. mol.	λ (mμ.)	Volts	λ (mμ.)	kcal./mol.	λ (mμ.)	Volts	λ (mμ.)	kcal./mol.	λ (mμ.)	Volts
$SOBr_2$					378	75	327	3·7	281	101	265	4·6	245	116		
					$2D_B(S—Br) = 74$				$2D_B(S—Br^*) = 95$				$D(S=O) = 116$			
$SeCl_4$	(415)	(68)	325	3·8					301	94	275	4·5	(250)	(114)	(240)	(5·1)
$SeOCl_2$									315	90	266	4·6	250	114		
Se_2Cl_2					410	69	350	3·5	320	89	295	4·2	249	114	(237)	(5·2)
	$D_B(Se—Cl) = 47$				$D(Se_2) = 59$				$2D_B(Se—Cl) = 94$							
$SeBr_4$	580	47	490	2·5	530	55	427	2·9	350	81	262	4·7	250	114		
Se_2Br_2					465	61	384	3·2	350	81	322	3·8	288	98	257	4·8
	$D_B(Se—Br) \sim 42$				$D_B(Se—Br^*) \sim 53$ $D(Se_2) = 59$				$2D_B(Se—Br) \sim 84$				$2D_B(Se—Br^*) \sim 106$ $D(Se=Se^*) = 87$			
$TeCl_2$	480	59	317	3·9					290	98	251	4·9	246	115		
$TeCl_4$	480	59	324	3·8					272	105	247	5·0				
	$D_B(Te—Cl) = 55$								$2D_B(Te—Cl) = 110$							
$TeBr_2$	535	53	473	2·6	420	67	380	3·2	340	84	314	3·9	293	97	(228)	5·4
$TeBr_4$	525	54	465	2·7			(400?)		296	96	265	4·6	(249)	(114)		
	$D_B(Te—Br) = 48$				$D_B(Te—Br^*) = 59$				$2D_B(Te—Br) = 96$				$2D_B(Te^*—Br) = 124$ $2D_B(Te—Br^*) = 108$			

claim the same degree of accuracy. It is also possible that maxima which would be stronger with increased vapour pressure of the undecomposed compound have not been found. The figures of the absorption maxima and their long-wave limits are collected in table 3, where the energy values of the photodissociation processes also are given for comparison. D_B denotes bond energies obtained from thermochemical data, D denotes dissociation energies taken from band spectra of diatomic molecules, and dissociation processes involving an excited product are marked by an asterisk against the atom which dissociates in an excited state.

§ 4. EXPERIMENTAL RESULTS FOR THIONYL BROMIDE AND PYROSULPHURYL CHLORIDE

Thionyl bromide possesses three regions of selective absorption with long-wave limits at 378, 281 and 245 mμ. respectively. The maxima corresponding to the first and second are at 327 and 265 mμ.; that belonging to the third region could not be found. The first long-wave limit extends more and more towards the visible spectrum with increasing vapour pressure or temperature. The first figure 378 mμ. belongs to a spectrum taken in a 10-cm. cell with 0·5 mm. pressure. With pressures of some millimetres the beginning of absorption can be shifted into the violet region, to about 425 mμ.; this explains why $SOBr_2$ in the liquid state possesses a brownish red colour. The energy difference between long-wave limit and maximum is small and about the same for the two first maxima, i.e. about 4000 and 5000 $cm.^{-1}$ respectively. This indicates that the two repulsive curves are rather flat and run nearly parallel, and that the second maximum represents a dissociation into excited products. Indeed, the obvious correlation of the photodissociation processes agrees very well with this view. Expressed in kcal./mol., the values of the three long-wave limits are $h\nu_1 = 75$, $h\nu_2 = 101$, $h\nu_3 = 116$ respectively. The first figure agrees very well with twice the bond energy of the S—Br bond, i.e. 74, and the third one is exactly equal to the dissociation energy of SO, as known from the band spectrum. The electronic separation of the ground state of the Br atom is 3685 $cm.^{-1}$ or about 10·5 kcal./mol. If twice this amount is added to the value of 74 kcal./mol., we obtain 95 kcal./mol., in fairly good agreement with the value of the second long-wave limit. The three regions of selective absorption therefore represent the following dissociation processes:

$$SOBr_2 + h\nu_1 = SO + 2Br(^2P_{\frac{3}{2}}),$$
$$SOBr_2 + h\nu_2 = SO + 2Br(^2P_{\frac{1}{2}}),$$
$$SOBr_2 + h\nu_3 = SBr_2 + O(^3P).$$

This is exactly the behaviour to be expected from our knowledge of $SOCl_2$. Also, the first photodissociation of thionyl chloride is due to the splitting off of both the chlorine atoms together. The only difference is that the doublet separation of Cl is 881 $cm.^{-1}$ or 2 kcal./mol. only, and maxima due to a dissociation involving two excited chlorine atoms merge with those due to unexcited atoms and cannot be separated from them. The molecules $SOCl_2$ and S_2Cl_2 possess a first maximum of selective absorption at about 250 mμ. with a long-wave limit at about 280 mμ., corresponding to the energy of two S—Cl bonds. A similar maximum appeared in SCl_2 as the second one. The fact that the first maximum of $SOBr_2$ shifts to a longer wave-length by an amount of almost 10000 cm.$^{-1}$, to the position corresponding to the breaking up of two S—Br bonds, makes it perfectly certain that the above correlation and the earlier one for the chlorides and the oxychloride are correct. The energy of the S—Br bond was calculated from sulphur monobromide S_2Br_2 because the heat of formation of $SOBr_2$ is not known. That of the S=O bond was taken directly from the band spectrum of SO. The good agreement of these figures with those of the long-wave limits of the absorption spectrum of $SOBr_2$ thus confirms at once that the bond energies remain nearly unaltered in all the derivatives of divalent and tetravalent sulphur.

Pyrosulphuryl chloride, $S_2O_5Cl_2$, possesses a continuous end-absorption only, whose long-wave limit in a 10-cm. cell at about 2 mm. vapour pressure lies at 246 mμ. at room temperature, and at 251 mμ. (113 kcal./mol.) at slightly increased temperature (40° c.). The absorption appears to be very similar to that of SO_2Cl_2, and it is therefore probable that the same photolytic process, i.e. the separation of an unexcited O atom, takes place here also.

§ 5. EXPERIMENTAL RESULTS FOR HALIDES AND OXYHALIDES OF SELENIUM

Selenium tetrachloride possesses a main maximum of selective absorption at 275 mμ. with a long-wave limit at 301 mμ. (94 kcal./mol.). On the long-wave side there appears a second maximum at about 325 mμ. which develops better at higher temperatures, and whose long-wave limit we followed up to 415 mμ. (68 kcal./mol.); but this energy value is certainly considerably too high. We could not raise the temperature above 80 to 100° c., because dissociation occurs at atmospheric pressure at 200° c. and is complete at about 290° c. (cf. Mellor's *Treatise*). Also, on the short-wave side a further region of selective absorption appears, but here again we could not obtain very accurate determinations on account of the facile decomposition of this substance. It appears, however, to lie somewhere in the neighbourhood of 240 mμ. and to have its long-wave limit near 250 mμ.

Selenium oxychloride possesses two regions of selective absorption. The first maximum lies at 266 mμ., but the second maximum could not be measured; the two long-wave limits are at about 315 mμ. (90 kcal./mol.) and 250 mμ. (114 kcal./mol.) respectively.

Selenium monochloride Se_2Cl_2 exhibits three regions of selective absorption with maxima at 350, 295 and about 237 mμ. respectively, and long-wave limits at 410, 320 and 249 mμ. respectively, the corresponding values in kcal./mol. being 69, 89 and 114 respectively.

From these figures it can be seen that all three compounds possess a similar maximum of selective absorption at about 270 mμ. The energy values of the three long-wave limits, i.e. 94, 90 and 89 kcal./mol., agree very well with the not very accurate value of 94 kcal./mol., obtained from thermochemical data for the splitting of two Se—Cl bonds. The same phenomenon was shown by the corresponding sulphur compounds and it will be seen later that the tellurium chlorides behave in the same way. Always, the most pronounced maximum of absorption of the chlorides and oxychlorides and the bromides and oxybromides of divalent and tetravalent S, Se and Te possesses a long-wave limit in very good agreement with the thermochemical value of the adiabatic dissociation of *two* halogen atoms. We therefore correlate this region of selective absorption to the photodissociation processes $SeCl_4 \rightarrow SeCl_2 + 2Cl$, $SeOCl_2 \rightarrow SeO + 2Cl$ and $Se_2Cl_2 \rightarrow Se_2 + 2Cl$.

While in the corresponding molecules $SOCl_2$, S_2Cl_2 and $SOBr_2$ this maximum was that with the lowest energy value and no photodissociation due to the separation of a single halogen atom occurs with appreciable probability, Se_2Cl_2 exhibits a new maximum at longer wave-length than the above maximum. Se_2Cl_2, however, is also the first molecule in this series which possesses another linkage with a bond energy lower than that of the two halogen bonds together, i.e. the Se=Se bond. Indeed the observed 69 kcal./mol. is in fairly good agreement with the 59 kcal./mol. taken from the convergence point of the band spectrum of Se_2, and since we find a similar maximum in Se_2Br_2, there is little doubt about the correlation of its long-wave limit to the dissociation process $Se_2Cl_2 \rightarrow SeCl_2 + Se$.

The short-wave maxima will belong to photolytic processes involving excited dissociation products, and for $SeOCl_2$ the process $SeOCl_2 \rightarrow SeCl_2 + O$ also has to be considered, the dissociation energy of SeO being about 97 kcal./mol. according to its band spectrum(11). The data are, however, not accurate enough definitely to decide this question.

There remains still the first maximum of $SeCl_4$. Its long-wave limit at 68 kcal./mol. is rather high compared with the energy of 47 kcal./mol. calculated for the Se—Cl bond. But in $SeBr_4$ we find a similar region of selective absorption, which doubtless corresponds to the breaking up of a single Se—Br bond; and, again, the same occurs in $TeCl_4$ and $TeBr_4$. Knowing that the energy value of this maximum must be too high, because it was very weakly developed on the original plates, and the true beginning of absorption of the vibrationless molecule was not reached, we correlate the first absorption region of selenium tetrachloride to the process $SeCl_4 \rightarrow SeCl_3 + Cl$. But it should be clearly understood that this correlation is based mainly on the analogy with the tetrahalides discussed below.

Denoting the energy of the long-wave limits at 415 mμ. (or, probably, longer waves) by $h\nu_1$, at 410 mμ. by $h\nu_2$, and at 301, 315 and 320 mμ. respectively by $h\nu_3$, we obtain the following equations for the photodissociation processes:

$$SeCl_4 + h\nu_1 = SeCl_3 + Cl; \quad Se_2Cl_2 + h\nu_2 = SeCl_2 + Se;$$

$$SeCl_4 + h\nu_3 = SeCl_2 + 2Cl; \quad Se_2Cl_2 + h\nu_3 = Se_2 + 2Cl; \quad SeOCl_2 + h\nu_3 = SeO + 2Cl.$$

Selenium monobromide, Se_2Br_2, and *selenium tetrabromide*, $SeBr_4$, behave exactly similarly. Both possess a very pronounced maximum of selective absorption with a long-wave limit at 350 mμ. (81 kcal./mol.). This is again in very good agreement with 84 kcal./mol. the energy estimated for two Se—Br bonds. It is interesting to note that the maxima themselves are different, namely at 322 mμ. and 262 mμ. respectively, although the long-wave limits are identical. It appears, however, to be premature to discuss such differences concerning the probabilities of transition by means of a poly-dimensional Franck-Condon diagram.

A maximum, which could be correlated to the separation of a single Br atom according to the bond energy of 42 kcal./mol. of the Se—Br linkage, is missing in Se_2Br_2, but is very clearly exhibited in $SeBr_4$ at 490 mμ., with a long-wave limit at 550 mμ. (47 kcal./mol.). This maximum is already well developed at about 70° C., and the reddish brown colour of the substance indicates that it is due to the non-decomposed compound. It is the first clear evidence that the tetrahalides behave differently from the mono- and oxyhalides but similarly to the dihalides in as much as the photolytic process due to the separation of a single halogen atom occurs with them.

Between this and the main maximum, $SeBr_4$ exhibits another one at 427 mμ., whose long-wave limit lies at 530 mμ. (55 kcal./mol.). The energy difference between this maximum and the first one is 0·4 v., in very good agreement with the doublet separation of the ground state of Br, namely 3685 cm.$^{-1}$ or 0·45 v. Also the main maximum is accompanied by one of shorter wave-length, for which the maximum itself could not be determined, but whose long-wave limit lies at 250 mμ. The energy difference from the corresponding value of the main maximum is 0·6 v.; and, because the differences between the long-wave limits are always less reliable than those of the maxima themselves, we believe that it will correspond to the dissociation of two excited Br atoms rather than to a process involving an excited polyatomic radical. Denoting by $h\nu_1$ to $h\nu_4$ the energy values corresponding to the four long-wave limits of $SeBr_4$ at 580, 530, 350 and 250 mμ. respectively, we correlate the photolytic processes to them as follows, that of the last one not being quite certain:

$$\begin{aligned} SeBr_4 + h\nu_1 &= SeBr_3 + Br(^2P_{3/2}), \\ SeBr_4 + h\nu_2 &= SeBr_3 + Br^*(^2P_{1/2}), \\ SeBr_4 + h\nu_3 &= SeBr_2 + 2Br(^2P_{3/2}), \\ SeBr_4 + h\nu_4 &= SeBr_2 + 2Br^*(^2P_{1/2}). \end{aligned}$$

Se_2Br_2 also possesses two more maxima besides the main maximum. That on the long-wave side lies at 384 mμ. with a long-wave limit at 465 mμ. (61 kcal./mol.). This latter value is slightly higher than that of the second maximum of $SeBr_4$ and agrees better with the dissociation energy of Se_2, namely 59 kcal./mol. It also cannot be correlated to an excited Br atom as a dissociation product, because a single Se—Br bond is not fissured at longer wave-lengths, such a region of selective absorption being entirely missing. A third region of selective absorption occurs, which has a long-wave limit at 288 mμ. and a maximum at 257 mμ. The energy difference between the second and third maxima is 1·0 v., in good agreement with the excitation energy of two Br atoms (0·9 v.). If the three long-wave limits in order of increasing energy be again denoted by $h\nu_1$, $h\nu_2$ and $h\nu_3$, their obvious correlation to photodissociation processes is:

$$\begin{aligned} Se_2Br_2 + h\nu_1 &= SeBr_2 + Se(^3P), \\ Se_2Br_2 + h\nu_2 &= Se_2 + 2Br(^2P_{3/2}), \\ Se_2Br_2 + h\nu_3 &= Se_2 + 2Br^*(^2P_{1/2}). \end{aligned}$$

§ 6. EXPERIMENTAL RESULTS FOR CHLORIDES AND BROMIDES OF TELLURIUM

Tellurium tetrachloride and *tellurium dichloride* possess continuous absorption spectra which are surprisingly similar. In the solid state the two substances are quite differently coloured, $TeCl_4$ being white, and $TeCl_2$ black, and green if powdered. At first, therefore, we believed that one of the two absorption spectra would be due to the decomposition of one of these compounds; but from measurements of the vapour pressure (cf. Mellor's *Treatise*) it appears to be certain that both these molecules do not decompose till about 400° c., whereas the spectra are already well developed at temperatures of about 250 and 190° respectively, which are near the melting-points ($TeCl_4$ 224°, $TeCl_2$ 175°). Indeed, both these compounds are known to give yellow vapours in spite of their different colours in the crystalline state, and these are probably due to a deformation (in the Fajana sense) and disappear for the isolated gaseous molecules. Slight differences in the colour of the vapour occur, because the value of the absorption coefficient is different in the visible region. Another reason is that the vapour of $TeCl_2$ exhibits a band spectrum in addition to its continuous absorption, which lies between 5570 and 5010 A. These bands, and also similar ones for $TeBr_2$ and $SeCl_2$, have been recorded in the meantime by other authors and correlated to these triatomic molecules$^{(8)}$. We have observed these systems in $TeCl_2$ and $TeBr_2$, and some preliminary observations of Larionov on some of the maxima of selective absorption of these compounds agree very well with the figures obtained by us. Both molecules, $TeCl_2$ and $TeCl_4$, exhibit again a pronounced maximum of selective absorption in the ultra-violet and a slightly weaker one extending towards the visible spectrum. The former maximum was found at 251 mμ. in $TeCl_2$ and at 247 mμ. in $TeCl_4$, the long-wave limits lying at 290 mμ. (98 kcal./mol.) and 272 mμ. (105 kcal./mol.) respectively. The latter maximum is at 317 mμ. for $TeCl_2$ and 324 mμ. for $TeCl_4$, the long-wave limit has been found at 480 mμ. (59 kcal./mol.) for both. The first long-wave limits of $TeCl_4$ and $TeBr_4$ have been measured by Sharma$^{(12)}$ at slightly different values. The exactly identical position of the beginnings of absorption is of course fortuitous, since the experimental conditions play such a great role just for the first long-wave limits, but there is no doubt that the two molecules possess essentially the same continuous absorption spectrum. For $TeCl_2$ a third absorption region with a limit at 246 mμ. (115 kcal./mol.) was found, indicating a dissociation involving excited radicals, or an excited Te atom in the ^1D state, for which the energy value, however, appears to be somewhat too low.

The energy value of the long-wave limits at 480 mμ. agrees very well with that of the Te—Cl bond calculated thermochemically as 55 kcal./mol.; those of the limits at 290 and 272 mμ. are only slightly smaller than double this figure. Denoting these energy values by $h\nu_1$ and $h\nu_2$ respectively, we obtain the following equations for the photolytic processes:

$$TeCl_2 + h\nu_1 = TeCl + Cl \text{ and } TeCl_4 + h\nu_1 = TeCl_3 + Cl,$$

$$TeCl_2 + h\nu_2 = Te + 2Cl \text{ and } TeCl_4 + h\nu_2 = TeCl_2 + 2Cl.$$

Both are in complete agreement with the results obtained in similar di- and tetrahalides of sulphur and selenium.

Again the continuous absorption spectra of *tellurium dibromide* and *tellurium tetrabromide* are almost exactly identical. They differ from those of the chlorides again in that they show a doubling of certain maxima, because a dissociation involving excited Br atoms is now possible, which cannot be found in chlorides on account of the extremely low excitation energy of the $^2P_{\frac{1}{2}}$ term of Cl.

As in the case of the chlorides, the vapours of these substances appear to be coloured differently from the crystals, slight differences between the colours of $TeBr_2$ and $TeBr_4$ in the gaseous state being due to the value of the absorption coefficient and the band spectrum of $TeBr_2$, observed also by us between about 7000 and 5500 A. The maxima of continuous absorption are developed clearly at temperatures of about 50° above the melting-points, where no decomposition appears to be possible.

Starting from the visible region, the first absorption maximum lies at 473 mμ. in $TeBr_2$ and at 465 mμ. in $TeBr_4$, the corresponding long-wave limits being at 535 mμ. (53 kcal./mol.) and 525 mμ. (54 kcal./mol.), in fair agreement with the 48 kcal./mol. calculated thermochemically for the Te—Br bond. In $TeBr_4$ a second maximum at about 400 mμ. is just indicated but could not be measured accurately; in $TeBr_2$, however, it appears more clearly at 380 mμ. with a probable beginning at 420 mμ. (67 kcal./mol.). The energy difference from the first maximum of $TeBr_2$ is 0·6 v., which agrees fairly well with the 0·45 v. of the doublet separation of Br(^2P). In the ultra-violet again a pronounced main maximum is found at 314 mμ. for $TeBr_2$ and at 265 mμ. for $TeBr_4$; the long-wave limits are at 340 mμ. (84 kcal./mol.) and 296 mμ. (96 kcal./mol.) in good agreement with the thermochemical value of two Te—Br bonds, which comes to 96 kcal./mol. Still farther in the ultra-violet a fourth region of absorption is characterized by two wave limits at 293 mμ. (97 kcal./mol.) in $TeBr_2$ and 249 mμ (114 kcal./mol.) in $TeBr_4$. The corresponding photolytic processes may involve two excited Br atoms, or, in the case of $TeBr_2$, an excited Te atom. Adding the excitation energies to the thermochemical value of 96 kcal./mol. for the splitting of two Te—Br bonds, we obtain 124 kcal./mol. if a Te(^1D) atom is involved and 108 kcal./mol. if two Br($^2P_{\frac{1}{2}}$) atoms are involved. The agreement is not very good, but the dissociation of two excited Br atoms appears to be more probable. If the energy values of the first three maxima are denoted by $h\nu_1$, $h\nu_2$ and $h\nu_3$, the following correlation to photodissociation processes appears well established, which is also in agreement with the correlations for similar molecules formed by S and Se:

$$TeBr_2 + h\nu_1 = TeBr + Br(^2P_{\frac{3}{2}}) \text{ and } TeBr_4 + h\nu_1 = TeBr_3 + Br(^2P_{\frac{3}{2}}),$$

$$TeBr_2 + h\nu_2 = TeBr + Br(^2P_{\frac{1}{2}}),$$

$$TeBr_2 + h\nu_3 = Te + 2Br(^2P_{\frac{3}{2}}) \text{ and } TeBr_4 + h\nu_3 = TeBr_2 + 2Br(^2P_{\frac{3}{2}}).$$

§ 7. CONCLUSIONS

The results of the present investigations can be summarized as follows:

(1) The long-wave limits of the continuous absorption spectra of halides and oxyhalides formed by the atom of the sixth group of the periodic system agree entirely with the energies calculated for the various processes of photodissociation from thermochemical data.

(2) Considering the experimental difficulties in the accurate determination of long-wave limits of continuous absorptions and the uncertainty of the thermochemical figures, the agreement can be said to be satisfactory. This indicates a very flat potential curve of the upper repulsive levels which are the final terms of the absorption spectra. This may be connected with the fact that the diatomic molecules of this group possess two free valencies and exhibit as ground level a $^3\Sigma$ term. It appears plausible to assume that such a term produces strong van der Waals forces, on account of which the unstable terms of the polyatomic molecules will be less repulsive than in similar cases of other groups of the periodic system. The strong van der Waals forces are also shown by the great tendency of the diatomic elements to polymerize.

(3) Particular interest attaches to the fact that the region of selective absorption with lowest energy of the di- and tetrahalides uniformly corresponds to the dissociation of a single halogen atom, while in the mono- and oxyhalides such a photolytic process does not occur. As soon as the molecule possesses a double bond between two atoms of the sixth group, both the halogen atoms always dissociate simultaneously.

(4) The absorption spectra show directly the rupture of a single bond, not the grand total only as in many thermochemical observations. It is therefore established that the *bond energies*, at least in this class of molecules, are in the main *additive*, slightly modified rather than changed by the different forces of repulsion between the atoms of a molecule.

(5) Furthermore, the energy of one and the same bond remains practically constant in all possible combinations so long as the central atom is divalent or tetravalent. Only the transition to the hexavalent state changes the energetic conditions on account of the activation of the group of s^2 electrons, as discussed elsewhere at greater length.

The experimental facts mentioned under (4) and (5), i.e. the additivity of bond energies in the same molecule and their constancy in different molecules, can only be understood on the basis of strong localization of the bonds. The method of molecular orbitals can of course describe such strong localization by deep potential moulds. But it is at a loss to explain why it occurs, since the electrons act as bonding by themselves and the electron pairs are formed rather incidentally. In Heitler and London's pair-bond theory, however, the strong localization in molecules possessing a pronounced central atom is an outcome of the saturation of valencies, each of which is produced by a pair of electrons one from each atom and localized between them. The photodissociations of the halides and oxyhalides of the sixth group therefore indicate that the additional assumption of the method of molecular orbitals, by which it becomes a single-electron-bond theory of valency (i.e. the general identification of non-premoted with bonding electrons and of premoted with antibonding or non-bonding ones), is not correct, and that it is not permissible to neglect the wave-mechanical interaction of electrons being on the same orbital. While there is no doubt about the application of the method of molecular orbitals to the description of the undisturbed molecule, this result as to the dissociation (or formation) of the molecules is again in agreement with a great amount of experimental and theoretical evidence⁽¹³⁾.

REFERENCES

(1) ASUNDI, R. K. and SAMUEL, R. *Proc. phys. Soc.* **48**, 28 (1936).
KHAN, MOHD JAN and SAMUEL, R. *Proc. phys. Soc.* **48**, 626 (1936).
PARTI, Y. P. and SAMUEL, R. *Proc. phys. Soc.* **49**, 568 (1937).
(2) LESSHEIM, H. and SAMUEL, R. *Phil. Mag.* **21**, 41, 1936 and earlier.
ASUNDI, R. K. and SAMUEL, R. *Proc. Indian Acad. Sci.* (*Bangalore*), **3**, 466 (1936), and a later paper in the Press.
(3) ROSEN, B. *Z. Phys.* **43**, 69 (1927).
(4) CHRISTY, A. and NAUDÉ, S. M. *Phys. Rev.* **37**, 490, 903 (1931).
(5) OLSSON, E. *Z. Phys.* **90**, 138 (1934).
(6) WARTENBERG, H. v. *Z. anorg. Chem.* **56**, 332 (1908).
(7) ROTH, W. A. and BECHER, G. *Z. phys. Chem.* (A), **159**, 1 (1932).
(8) WEHRLI, M. *Helv. phys. Acta*, **8**, 487 (1935); **9**, 329, 637 (1936).
LARIONOV, J. *Acta Physico-chimica, U.S.S.R.* **2**, 67; **3**, 11 (1935).
(9) HUSSAIN, S. L. and SAMUEL, R. *Curr. Sci.* **4**, 734 (1936).
(10) SAMUEL, R. and USMAN, M. *Proc. Indian Acad. Sci.* (*Bangalore*) (in the Press).
(11) ASUNDI, R. K., JAN KHAN, M. and SAMUEL, R. *Nature, Lond.*, **136**, 642 (1935); *Proc. roy. Soc.* A, **157**, 28 (1936).
(12) SHARMA, R. S. *Bull. Acad. Sci. Allahabad*, **3**, 87 (1933).
(13) HUNTER, R. F. and SAMUEL, R. *Nature, Lond.*, **138**, 411 (1936) and literature mentioned there.

PRESENTATION OF THE FOURTEENTH DUDDELL MEDAL TO PROFESSOR WALTER G. CADY, 9 JULY 1937

THE PRESIDENT, MR T. SMITH, made the following remarks in presenting the medal:

The Duddell Medal is awarded to "persons who have contributed to the advancement of knowledge by the invention or design of scientific instruments, or by the discovery of materials used in their construction".

The Council of the Physical Society has awarded the fourteenth Duddell Medal to Walter G. Cady, Professor of Physics at the Wesleyan University, Middletown, Connecticut, U.S.A., for his work on piezo-electric resonators and oscillators as standards of frequency.

Prof. Cady's pioneer work on the subject was published in 1922 (*Proc. Inst. Radio Eng.*, **10**, 83) and the value of the device may be judged from the fact that it stimulated research work on the subject in all parts of the world, over a thousand papers having been published on the properties of piezo-electric crystals since the appearance of Cady's first paper. Of course, not all of these are due to Cady's researches, for Langevin had previously used piezo-electric crystals as vibrators for under-water signalling, but Cady's particular contribution—the use of the quartz resonator as a standard of time or frequency—has quite obviously inspired most of the work. The use of these resonators as standard vibrators has made it possible to measure frequency and intervals of time with an accuracy not previously attained. It is scarcely necessary to emphasize the importance to physics of increased accuracy in such fundamental measurements. Among the applications which have already been made the following may be mentioned: (1) The quartz-clock which is now used as standard in some observatories. It is in some respects superior to the pendulum clocks, and in any case is a most valuable supplement to them. (2) The measurement and control of the frequency of alternating currents in connexion with measurements of dielectric constant, absolute electrical measurements, and the like. (3) The measurement of the velocity of ultrasonic sound waves.

Duddell, who was responsible for so much elegant instrumental work, would have been the first to recognize the beauty of Prof. Cady's device, and it will be a source of great satisfaction to all scientific workers to know that the value of Prof. Cady's work has been recognized in such an appropriate manner.

OBITUARY NOTICES

PROFESSOR ALEXANDER ANDERSON

ON 5 September 1936 died the able mathematician, physicist, and administrator who was widely known as "Anderson of Galway". He was an Ulsterman by birth and descent, but during nearly the whole of his life he was connected with the college in Connaught which was originally Queen's College and is now University College, Galway. He entered it in 1877 and graduated as B.A. and M.A. in the old Queen's University of Ireland. In 1881 he took an entrance scholarship at Sidney Sussex College, Cambridge. He came out Sixth Wrangler in the Mathematical Tripos of 1884, and in the following year went back to Galway as Professor of Natural Philosophy. In 1899 he was appointed President of the College, while retaining his Chair, and he continued to discharge the combined duties until his retirement in 1934. He then went to live in Dublin, where he had many friends and where he continued to take an interest in the proceedings at the Royal Dublin Society and the Royal Irish Academy. His death came as a shock to those who knew him, for he was a man over whom the years seemed to pass without making any appreciable diminution of his vigour of mind or body.

During the year which intervened between his Tripos and his return to Galway, Anderson worked in the Cavendish Laboratory, where Sir Joseph Thomson was then at the beginning of his Professorship. He is mentioned as one of the early workers of that time in the published history of the laboratory, but no indication is there given of the subject which occupied him. It seems probable, however, that he was interested in electrical measurements, for his first paper, published from Galway in 1891, was an account of the now well-known Anderson's method for comparison of inductances. In the same year he was elected to a Fellowship at Sidney Sussex College. Under Anderson and his colleagues on the mathematical side—Allman, A. C. Dixon, Bromwich, Houston, Power—Galway became an active centre of scientific teaching and research. His advanced pupils were few, but he gave them of his best and they drew from him inspiration as well as sound knowledge. The late Professor J. A. McClelland, F.R.S., was one of those who owed much to his teaching. Anderson's theoretical papers were the outcome and evidence of his thoroughness of method as a teacher. They are concerned with clearing up or simplifying some difficult matter of which the textbook treatment seemed to him inadequate, illogical or erroneous. He wrote, for example, on the motion of an iron ball in a magnetic field, on the quadrant electrometer, on the theory of moving charges, and on electrical distributions on two charged spheres. In his laboratory he kept experimental work going on questions which lay within the scope of his equipment, such as surface electrification, contact difference of potential, and measurement of surface tension and of the constants of lens systems.

Special reference should perhaps be made to the part taken by Anderson in the discussion of the results of the Sobral Eclipse Expedition in 1919. The observations were taken as affording confirmation of the Einstein deflexion, but he put forward the startling suggestion that the true cause of the observed effects was to be sought in the unequal heating of the earth's atmosphere during the passage of the moon's shadow. The matter was examined by Eddington, Crommelin, Dines, Richardson and Schuster. The outcome of their work was unfavourable to Anderson's theory, but he himself was not completely convinced.

Anderson was a man of very wide general culture. He was a fine linguist and read books on all sorts of subjects in many languages. His talk was full of humour as well as knowledge. He was a staunch and helpful friend, and a teacher who made friends of his pupils and who never forgot them.

W. B. MORTON.

PROFESSOR H. E. ARMSTRONG, F.R.S.

WHEN the Physical Society (of London) began in 1874, Armstrong was 26 years of age, and he was apparently sufficiently sympathetic to the science of physics to become a founder fellow, though his later contacts with that science seem to have been few. There is no record of his having read a paper to this Society, but he attended, and spoke, at the Jubilee celebrations in 1924, and his distinctive figure was not unknown on the occasions of the delivery of the Guthrie lectures. At that date (1874), four years after joining the Chemical Society, he had taken his Ph.D. degree at Leipzig, and was in charge of the chemistry classes for medical students at London. During this period he took an active part in the founding of the Institute of Chemistry, in the same year (1876) as he was elected a Fellow of the Royal Society. He lived to become the senior Fellow of the latter Society.

Later, he occupied the Chair of Chemistry at the London Institution, where the discovery of one of Sir William R. Grove's batteries first roused his interest in the general problem of chemical interchange, an interest which lasted until the end of his life and (in later years) left him as almost the sole opponent of the current theories of electrolysis, and therefore as the one chemist who resented the invasion of his subject by physics.

His next appointment was that of Professor of Chemistry at the City and Guilds Institute, first in temporary quarters at the Cowper Street Schools, Finsbury, and then, in 1883, at the City and Guilds College, South Kensington; this period lasted until 1911, when the College was fused with the Imperial College, and ceased to have its own Chemical department.

Armstrong is probably best known for his ardent advocacy of the view that "ordinary chemical actions...are themselves electrical", with the corollary that chemical reactions are nothing but reversed electrolysis. With this thesis, he never ceased to urge the view that solution is not something passive, but is a definite chemical reaction, and he fought violently against the orthodox treatment in which the ions are imagined as leading an existence almost independent of the solvent; in his opinion, the solvent and solute react, and are equal partners.

Apart from his purely chemical work—an investigation on the naphthalene series and another on the structure of camphor are probably the most important items—Armstrong will be remembered for his development of the heuristic method of teaching chemistry. This was first worked out during his tenure of the Chair at the London Institution, and was designed, in contrast to the didactic method, to train the student "to observe and think and act with clearly defined purpose, the work being carried out with common materials and in relation to common phenomena". In his hands the method worked well, and many of his pupils themselves reached some measure, greater or less, of renown. Nevertheless, the method is less in favour than it was, perhaps because it requires for its success an inner conviction, almost a missionary spirit, such as he had in abundance.

As an individual Armstrong was not well known to the present generation, to whom his love of polemics and his taste in dress clothes were the most familiar traits. The vigorous language of his letters to *Nature* and *The Times* will long be remembered. But his bark was worse than his bite, and does not represent the whole of his character. Actually he had a marked streak of the artistic temperament and was an enthusiastic opera-goer and a discriminating lover of pictures. This being so, we are not surprised to learn that gardening was one of his hobbies, though it may be news to some that another was field geology, to which he had made contributions. It throws light on his character to be told that in later years his favourite holiday centre was Borrowdale, though earlier he had been fond of continental travel (and did he ever rid himself of the idea that Germany was the only place in which chemistry could be really learnt?)

The span of his life was from 6 May 1848 to 13 July 1937, and during this time many honours came to him, among them the LL.D. of St Andrews, the D.Sc. of Melbourne and of Madrid, the Davy Medal from the Royal Society, the presidencies of various societies, including of course the Chemical Society, and medals from the Royal Society of Arts, the Society of Chemical Industry and the Institute of Brewing.

WILFRID NOEL BOND, M.A. (CANTAB), D.SC. (LOND.), F.INST.P.

THE untimely death of Dr W. N. Bond at the age of 39 has come as a great blow to his many friends. Modest, unselfish and entirely free from pretence, he radiated goodwill and endeared himself to all who came in contact with him. He was always ready to give of his best to all who consulted him, whether colleagues or students, and his advice on any problem in physics, however remote from his own particular interest, was always worth having. It would be true to say of him that his interest in other men's discoveries was at least as great as in his own. He will be missed by a much wider circle than he would have deemed possible.

Bond was born on 27 December 1897. Educated first at St Albans School, he received his early academic training at East London College and the Royal College of Science, graduating with first class Honours in the University of London, of which he subsequently became a Doctor of Science. His early academic studies were combined, during the Great War, with nearly two years' experience in industrial physics in the works of Messrs Kent, and his first publication (a joint paper with Mr J. L. Hodgson on the Fan dynamometer in 1916) dates from this period. It is probable that the interest in problems connected with the flow of fluids which inspired so much of Bond's later work was due to these early experiences.

Subsequent experience of research was gained at University College, London, under Professor Porter, and at the Cavendish Laboratory, Cambridge, under Professor Sir J. J. Thomson, where he graduated as B.A. by research. In 1921 he was appointed to the Lectureship in Physics in the University of Reading, which he continued to hold with distinction until his death.

Indefatigable in research, Bond has made numerous contributions to the pages of the *Proceedings of the Physical Society* and the *Philosophical Magazine*, not by any means all confined to one branch of physics. His main interest, however, was in the flow of fluids, and the related problems of viscosity and surface-tension measurements. With an unusual flair for experimental observation, he delighted in extorting from any given apparatus the maximum degree of accuracy of which it was capable, and all his experimental work is marked by an almost classical simplicity and elegance. His experimental insight and power of direction were maturing from year to year, and undoubtedly his latest work on the measurement of surface tension by a moving-sheet method and his recent determination of the viscosity of air represent him at his best.

Bond's interests in physics were by no means confined to his own experimental work, and his constructive analysis of the most probable values of the fundamental constants, undertaken in connexion with the theories of Sir Arthur Eddington, will be fresh in the minds of most readers. A strong, one might almost say mystical, belief in the fundamental unity and simplicity of the universe was a vital part of Bond's philosophy, and Eddington's theory moved him very deeply.

Bond was a kind, thorough and patient teacher, and was particularly successful in instilling into his students in the laboratory something of that love of accuracy and dislike of the slipshod which was such a marked characteristic of his own work.

In addition to his original work, Bond published three books, *Numerical Examples in Physics*, *An Introduction to Fluid Motion* and *Probability and Random Errors*. He leaves a widow and three children.

J. A. C.

JOHN FLEMING

MR JOHN FLEMING died at his home in St John's Wood, London, on 26 March 1937, in his 58th year.

Born in Scotland, on a moorland farm in the hills between Ayrshire and Lanarkshire, he came to London with his brother, Robert, to complete his education. Leaving school, the two brothers entered the optical industry and in 1905 founded the firm of J. and R. Fleming.

His journeyings abroad enabled him to acquire a deep knowledge of optical conditions outside Great Britain and to adopt and adapt many ideas formulated on his business travels, especially in the United States.

Members of his staff held him in true affection and esteem. He showed a paternal interest in their welfare, and there were many manifestations of a kindly and gentle nature in his business relationships.

He became a Fellow of the Optical Society in 1906, and a Fellow of the Institute of Ophthalmic Opticians in 1912.

DR GEORGE FORBES, LL.D., F.R.S.

DR GEORGE FORBES (or, as he was I think more commonly known, Professor Forbes) was born at Edinburgh on 5 April 1849 and thus was nearly 88 at the time of his death. His father was Professor of Natural Philosophy at Edinburgh and an F.R.S. when he was born, and was also one of the founders of the British Association. Later his father became Principal of St Andrews University, and it was here that Forbes was educated until he went to complete his training at Cambridge.

In 1872, that is when he was 23, he was appointed Professor of Natural Philosophy at Anderson's College, Glasgow, and there he remained until 1880. In the meantime, perhaps taking advantage of the long Scottish summer vacation, he was able to engage in several outside activities. For instance in 1874 he joined an expedition to Hawaii to observe the transit of Venus. The following year he crossed Asia from Pekin to St Petersburg by way of Siberia. Two years later during the Russo-Turkish war of 1877 he got himself appointed as a special correspondent of *The Times* and later in February 1930, when he was about 80, *The Times* published two articles by him in which he recounted his personal experiences.

About the end of this period, or about 1879, he was associated with James Young of Kelly in experiments to check previous determinations of the speed of light and to find if there were any differences in the speed for different colours.

In the meantime the telephone had been invented as well as the Gramme armature for dynamos and motors, and much attention was being given to the possibilities of electric lighting and traction. Forbes had already in lectures pointed out the possibilities of electric traction. He visited the Electrical Exhibition in Paris in 1881 and described it for *The Times*. In 1884 at the Philadelphia Electrical Exhibition there was exhibited a form of dynamo designed by him.

It was in connexion with his experiments on dynamos that Forbes, being troubled by sparking at the commutator, hit on the idea which has since revolutionized continuous-current practice both for generators and motors. It is only those who are old enough to remember when copper-wire brushes were used for collecting the current, and later brushes of copper gauze, the trouble and anxiety which these caused from their liability to heavy sparking resulting in cutting of the commutator. Faced with this trouble, Forbes hit on the idea of employing brushes of moulded graphite. These brushes had a double advantage, the higher resistance of the carbon prevented heavy sparking at any one point, and the graphite acted as a lubricator. Forbes for some reason did not patent this invention or discovery, but it soon began to attract adherents and when proper designs had been worked out gradually came into universal use. He always referred to this work with much modesty, but there can be no doubt that almost without acknowledgement he presented to the world an idea of great engineering and commercial value, the importance of which he does not seem to have fully grasped at the time.

Between 1884 and 1900 transformers in parallel, high voltages, and finally two- and three-phase motors were developed and became practicable, and the whole question of the possibilities of power-transmission and distribution over considerable areas began to receive serious attention. Forbes followed this work closely and when in 1900 the International Niagara Commission offered prizes for proposals for power-transmission from their proposed enterprise at Niagara, he put in plans for a scheme using two-phase current. Forbes was awarded a premium for this, though at the time the views of the Commission inclined to a continuous-current installation. The success of the Lauffen transmission at Frankfort in 1891, however, turned attention again to Forbes's proposals, and finally he was appointed one of the Company's consulting engineers on the understanding that the polyphase system would be adopted and that he should consider both the electric generating plant and the transmission to Buffalo. In connexion with this he designed a vertical form of alternator, the armature of which was fixed while the field magnets revolved outside it, thus forming a powerful flywheel. The practical engineering forms of these alternators were manufactured by the Westinghouse Co., and were the alternators used in the first generating station. Forbes later read a paper before the Institution of Electrical Engineers describing the installation, and his work is also referred to several times in the special issue of *Cassier's Magazine* which was devoted to a description of the Niagara installation.

It is worthy of note that even before the above work had been done Forbes had been asked to report on the best method of working the City and South London Railway, the first of the tube railways, and had recommended that it should be driven electrically.

Naturally Forbes's connexion with Niagara led to his being asked to advise as to the possibility of other water-power projects, and in this connexion he visited the Cape in 1895 and New Zealand in 1896, and in 1897–8 at the request of the Egyptian Government he made a study of the cataracts of the Nile with a view to their being utilized for electric power supply.

At this juncture the South African war took place, and this led Forbes to turn his attention to the design of range-finders, and one of his instruments was used in the war. Another gift of great value which Forbes gave to the nation was a very simple formula whereby the range table of a gun can be accurately calculated from that of another gun of a different calibre.

Forbes was now getting into the sixties and as his age increased his old interest in astronomy began to come to the front again; he lived henceforth most of the year at Pitlochry and devoted a good deal of time to writing and lecturing on the subject.

Either during this period or earlier he was the author of ***Lectures on Electricity, Alternating and Interrupted Currents*** and ***Elektrische Wechselsstrome und Unterbrochener Strome.*** He also wrote a number of works on astronomical subjects, including *The Transit of Venus*, *The Theory of the Glaciers of Savoy* and a biography, *Sir David Gill, Man and Astronomer.*

Towards the latter part of his life his eyesight failed very much and he came south and made his headquarters in Worthing. His books and papers he had given to St Andrews University.

Forbes was elected F.R.S. in 1887, he was also a Fellow of the Royal Society of Edinburgh and of the Royal Astronomical Society, and a member of the Institutions of Civil and Electrical Engineers, the Astronomische Gesellschaft, the Franklin Institute and the American Philosophical Society. He was an honorary LL.D. of St Andrews and held the Russian Order of St George and the French Legion of Honour.

G. L. ADDENBROOKE.

PROFESSOR ALBERT GRIFFITHS, A.R.C.S., D.Sc.

1867–1937

ALBERT GRIFFITHS was born at Chester in 1867. He received his scientific training at the Royal College of Science, South Kensington, at Owens College, Manchester, and at the University of Freiburg. He returned to Owens College as Demonstrator in Physics and Research Assistant to Schuster, and in 1893 was elected Berkeley Fellow. In 1898 he became a Lecturer in Physics at University College, Sheffield. From 1900, until his retirement in 1933, he was head of the Department of Physics at Birkbeck College, London, being appointed University Professor in 1922, shortly after the College became an Evening School of the University of London.

He became a Fellow of the Physical Society in 1896, and has served on its Council. His first contribution to the Society's *Proceedings*, a paper entitled "Diffusive convection", was made in 1898, and in it he struck the key-note of his future research. The paper excited the interest of Professor G. F. FitzGerald, whose subsequent letter to *Nature* probably served to confirm Griffiths in his determination to devote himself to the measurement of the coefficients of diffusion of salts in aqueous solutions. His work was characterized by extreme patience and scrupulous care. Some years of preliminary work were spent before in 1915 he was satisfied that his results had attained an accuracy warranting publication. Several methods of determination of the diffusion coefficient were devised, some being carried out by himself, some by his colleagues. A measure of accuracy in these difficult determinations was finally reached far exceeding that approached by previous workers in the subject.

His interest in slow movements in liquids was also manifested by his work on the coefficient of viscosity of water at low rates of shear. Observations were made of the rate of flow through capillary tubes under a pressure head of the order of a tenth of a millimetre of water. The conclusion was that the coefficient is sensibly the same as for normal rates of stream-line flow. These results (by two independent methods), like those on diffusion, were presented before the Physical Society; and on more than one occasion the author's work evoked a meed of praise from the President for its exemplary care and accuracy of execution. Griffiths had a persistent enthusiasm for research, and communicated this enthusiasm to those around him. Many good pieces of experimental work carried out by others in his laboratories were the fruits of his original suggestions. His kindly consideration and readiness to help will be long remembered by colleagues and students.

D. OWEN.

MR A. C. JOLLEY, A.M.I.E.E., F.INST.P.

BY the sudden death of Mr A. C. Jolley on 5 December 1936, a few months after his retirement from the headship of the Electrical Engineering Department of the Northampton Polytechnic Institute, Clerkenwell, technical education has lost one of its most valuable and earnest teachers. In spite of his having had little scientific education, his interest in physics led him to become laboratory assistant first under Prof. Cheshire and later under Dr Clay at Birkbeck College, where the present writer first met him in 1898 and was so impressed with his zeal and earnestness as to invite him to become lecture assistant in the Electrical Engineering and Applied Physics of the Northampton Institute. From this appointment he soon advanced to the position of senior demonstrator and lecturer and took a leading part in planning and equipping the electrical engineering and optical laboratories. Having great mechanical skill, he was of great assistance in developing the new electrical and optical instruments which were constantly being devized for extending the investigations in progress, on which he worked day and night. After the writer's retirement from the Northampton Polytechnic in 1910, Mr Jolley remained under Mr F. Denton, but he assisted the writer again in developing anti-submarine devices at the Admiralty Experimental Station at Parkeston Quay, where his technical skill was invaluable. After the death of Dr Walmsley in 1924 and the appointment of Mr S. C. Laws as Principal of the Northampton Polytechnic, Mr Jolley was appointed Head of the Electrical Engineering Department. The excellence of his general teaching was shown by the great success of his students, but his chief interest centred in electrical instruments, and he collaborated with the writer in a book on *Electrical Measuring Instruments* which involved careful dissection of numerous instruments, determining their properties, and making accurate drawings, all of which he carried out personally. His culminating work was the completion of a new instrument-making workshop in 1935, which stands as a monument to his careful planning. He developed considerable artistic skill, and his work was appreciated by several well-known artists.

Mr Jolley's retiring disposition and devotion to his department prevented him from taking any prominent part in scientific gatherings, but all his students and others with whom he came in contact soon came to appreciate the thoroughness and honesty of his nature. His loss will be severely felt by many instrument-makers who used to consult him on their problems, as well as by all his colleagues and past students, and above all by the present writer, by whom his unfailing help and devotion can never be adequately acknowledged. C. V. DRYSDALE.

PROFESSOR THOMAS MATHER, F.R.S.

PROFESSOR T. MATHER was born at Higher Walton near Preston on 15 December 1856, and died in London on 23 June 1937. His career illustrates the public value of the Whitworth System of Scholarships. After attending a local church school he was apprenticed first to an engineering firm at Higher Walton and afterwards (1875–8) to a firm of engineers and boilermakers at Preston. During these years he attended evening classes at Preston. He started from home at 5 a.m. and did not usually return till after 10 p.m. He gained a Whitworth Scholarship, and at the age of 22 entered Owens College for a full-time engineering course which lasted for three sessions, 1878–81. At the end of the course he was awarded the Ashbury Scholarship in engineering. He continued his studies at the Royal College of Science during the session 1881–2. He became assistant to Professor Ayrton at the Finsbury Technical College in 1882, and in 1884 moved with Professor Ayrton to the City and Guilds Central Institution in South Kensington which is now part of the Imperial College. On Professor Ayrton's death he was appointed, in 1908, acting Professor and, in 1910, permanent Professor of Electrical Engineering. He retired in 1922 with the title of Emeritus Professor. When he died he was close upon 81 years of age.

He was elected Fellow of the Royal Society in 1902 at the age of 46. He was a Life Fellow of the Physical Society, a Member of the Institution of Electrical Engineers, and a Fellow of the City and Guilds of London Institute.

The most important papers which bear his name as part author are three printed by the Royal Society, two in the *Philosophical Transactions*, vol. **207** (1908), and a third in *Proceedings of the Royal Society*, vol. **80** (1908). They are entitled "A new current weigher, and a determination of the electromotive force of the normal Weston cadmium cell"; "The silver voltameter"; and "The comparison of the Board of Trade ampere-standard balance with the Ayrton-Jones current weigher, with an appendix on the electromotive forces of standard cells". The authorship of the first paper was shared with Professor Ayrton and F. E. Smith (now Sir Frank Smith), and that of the other two papers with Sir Frank Smith.

These papers represent part of work of the first importance which resulted in the setting up of the national standards of current and of electromotive force. Such work necessitated not only most accurate experimental measurements but also the investigation of an almost endless number of practical details, proper attention to which was essential for the production of satisfactory standards. From the papers themselves it is not possible to judge the part undertaken by Professor Mather, but there can be no doubt that it was a most important one. His thoroughness, close attention to detail, and powers of initiative were qualities needed in order to carry out such work satisfactorily. The investigation was a continuation of work of the same type carried out by Professor Ayrton for some years in conjunction with Professor Viriamu Jones. Professor Mather was in intimate touch with all the work done in the College laboratories. His election to the Fellowship of the Royal Society in 1902 was an indication of the value of his help in laboratory investigations, and also a recognition of his work in connexion with the improvement of electrical instruments. He was a skilful mechanic, a good designer, and a ready deviser of teaching appliances. His interest in science was more concerned with its industrial application than with its theoretical development. He was not a writer of papers. There does not appear to be a single paper of which he was sole author.

His name in association with that of Professor Ayrton appears on many papers dealing with improvements in the construction of electrical instruments and accessories. Three papers on galvanometers were read before the Physical Society and printed in the *Philosophical Magazine* for July 1890, November 1896, and October 1898. Two others are to be found in vol. **23** of the *Proceedings of the Institution of Electrical Engineers* and are entitled "A universal shunt box for galvanometers" and "An astatic station voltmeter". The Ayrton-Mather shunt was highly appreciated and is in very common use. The electrostatic voltmeter is due to the skilful design of Professor Mather, and the first forms of it were constructed with his own hands. These voltmeters have been extensively used in practice. The precision Wattmeter of Mather and Duddell is another instance of the excellence of Mather's work. First-rate instruments and appliances, suitable for college or industrial testing, are now commonplaces of commerce, but industrial laboratories are quite a recent development and before such excellent results could be reached commercially it was necessary for much previous work to be done in laboratories established for technical teaching. Mather was one of the earliest and ablest pioneers in such work.

When Mather joined Professor Ayrton's staff in 1882 electrical engineering was an entirely new industry. There were no college departments providing a training for it, and trained men did not exist. There was a sudden demand for evening classes to train large numbers of adult students for work in the new industry. The development of suitable courses and training appliances called for much initiative and ability. Professor Ayrton at first directed this work but later on was content to leave it almost entirely in the hands of his capable assistant. The work grew in volume and developed in scope with the transfer from the Finsbury College to that at South Kensington, with the establishment of three-year college courses, and with the rapid development of electrical engineering. The main work of Mather's life consisted in the development of these laboratories and in the constant help given by him to those who worked in them, whether as ordinary students or as exceptional research students.

For many years Mather's speech suffered from an impediment so serious that he could not lecture or take part in public discussions. Had he been able to do so he would have been more fully appreciated outside the college than he was. Fortunately he was at length able to overcome this defect and to lecture in a way highly thought of by his students. In his nature he was most modest and retiring. He was always kindly and willing to help in either simple or advanced work. He was much liked personally and was held in honour by all who knew him.

W. E. SUMPNER.

JOHN ALBERT MORROW

MR JOHN ALBERT MORROW was born at Bedford Park, London, on 28 April 1902. His early education was at St Paul's School, Southdown College and Brighton College, after which, in 1921, he entered the Royal College of Science. In 1924 he was awarded the Associateship of the College in Physics, and in 1925 the Diploma of the Imperial College for advanced study and research in spectroscopy under the supervision of Professor A. Fowler. On leaving South Kensington he took up an appointment at the Shirley Institute of the British Cotton Industry Research Association at Didsbury, Manchester, and continued in that position until his death on 25 May 1936.

Mr Morrow acquired considerable skill in experimental work, and at the Shirley Institute was especially noted among other members of the staff for his ingenuity in the design and construction of working models of testing-apparatus of various kinds which were subsequently turned out in more permanent form in the workshop. Unfortunately he suffered from poor health during a large part of his life, but he nevertheless always maintained a cheerful disposition. He leaves a widow, but no children.

He was elected a Fellow of the Physical Society in 1926 and an Associate of the Institute of Physics in 1933.

A. FOWLER.

JAMES RICE, M.A.

MR JAMES RICE, M.A., who died on Friday, 17 April 1936, at the age of 62, was Associate Professor of Physics and Reader in Theoretical Physics in the University of Liverpool.

After a very distinguished career at Queen's College (now the Queen's University), Belfast and in the Royal University of Ireland, where he obtained the highest honours in mathematics and mathematical physics, he was appointed in 1902 Senior Physics Master at the Liverpool Institute. In 1914 he was appointed to a Senior Lectureship in Physics in the University of Liverpool. His excellent work at this University secured for him the title and status of Associate Professor in 1924, and the additional title and status of Reader in Theoretical Physics in 1935.

Rice's early interests lay chiefly in the fields of thermodynamics, kinetic theory, and statistical mechanics. His mastery of these subjects is shown by his excellent

Introduction to Statistical Mechanics for Students of Physics and Physical Chemistry (Constable and Co., 1930), and by the important articles on "Strained elastic solids" and "Surfaces of discontinuity", which he contributed to vol. 1 (Thermodynamics) of the *Commentary on the Scientific Writings of J. Willard Gibbs* (Yale University Press, 1936).

The newer developments of theoretical physics appealed strongly to Rice's eager and receptive mind. His mastery of the general theory of relativity was demonstrated by the publication of his *Relativity; a Systematic Treatment of Einstein's Theory* (Longmans, Green and Co., 1923). This excellent book dealt with the complete mathematical theory of the subject, and soon became a valuable textbook for advanced University students of theoretical physics. His popular book on *Relativity* in Benn's well known sixpenny series had an extensive sale, and did very much to spread a knowledge of the new concepts in the minds of the general English-reading public.

To vol. 3 of Professor Lewis's well-known *System of Physical Chemistry* (Longmans, Green and Co., 1924) Rice contributed valuable appendices dealing with Maxwell's distribution law and the principle of equipartition of energy, quantum theory, and the correspondence principle.

Rice possessed a clear and logical mind, a sound knowledge of mathematics, and a wonderful gift for lucid exposition of the principles of theoretical physics. His unselfish devotion to teaching and the heavy burden of being almost the sole representative of modern physics in the University of Liverpool during many years left him little time foı original work, so he devoted himself to the task of mastering and expounding to his students the great discoveries and principles of physical science during 33 years (1902–35) of almost miraculous development—a development too overwhelming in its abundance for one man. The success which he achieved in this great work is only very partially revealed in his books, excellent though they be. Like many another good teacher, his success and his reward dwell in the grateful hearts and illuminated minds of those whom he taught, and of the many colleagues and friends who derived knowledge and inspiration from a mind and spirit well informed, generous, and forgetful of everything save the progress of the knowledge and well-being of mankind.

F. G. DONNAN.

JOHN ROSE-INNES, B.A., B.Sc.

JOHN ROSE-INNES was a Fellow of University College, London, a graduate of Cambridge University, and a member of King's College. He served on the staff of the Department of Physics, University College, London, from 1889–90 to 1892–3. He took a keen interest in experimental work, but not being naturally endowed in that direction confined himself to the mathematical treatment of such problems as interested him. His very considerable skill in this is illustrated by two papers, one on the motion of a pendulum through an arc of finite magnitude(1) and the other the integration of the differential equation applicable to a plane progressive wave(2).

The rest of his work is more directly connected with some practical problem. Besides a slight paper$^{(3)}$ on the ratio of the two specific heats of air, there is a paper$^{(4)}$ on the physical interpretation of the Michelson-Morley experiment. In a series of papers$^{(5)}$ the isothermals of ether, pentane, and isopentane are obtained, on the basis of Ramsay and Young's experimental results.

But the work in which Rose-Innes took the most interest was the practical attainment of the thermodynamic scale of temperature. At the time with which we are dealing, only the Joule-Thomson results on the porous plug experiment were available. It will be remembered that Kelvin interpreted these results as indicating that the Joule-Thomson effect was inversely proportional to the square of the absolute temperature. In an early paper$^{(6)}$ Rose-Innes was the first to call this assumption into question, adopting a formula involving a constant term and a term inversely proportional to the temperature. The formula thus involves two constants, but allows an inversion point. With this assumption the constant-volume gas thermometer required, to a first approximation, no correction of its readings; the correction to the constant-pressure thermometer was worked out. Applying these formulae to the known experimental results for hydrogen and nitrogen, Rose-Innes did not obtain, for the value of the melting-point of ice on the thermodynamic scale, the consistency he expected. In a second paper$^{(7)}$ the equations were recast to avoid extrapolation of the Joule-Thomson effect, while the isothermal compressibility of the gas used was assumed as known through the same range as this effect. In a third paper$^{(8)}$ the isothermal compressibility is taken as known at one temperature only, an assumption more in accord with figures at our disposal. The values for the melting-point of ice were in better agreement than before, but still, in his opinion, unsatisfactory. In a further paper$^{(9)}$ with great ingenuity Rose-Innes recast his equations so that the actual numerical values of the Joule-Thomson effect were not assumed, but only their general form. In this paper the values obtained from the hydrogen and nitrogen thermometers were 273·04 and 273·13 respectively. The difference between these two values was even then considered larger than the experimental results would appear to warrant, and was attributed to a possible influence of the material of the containing vessel. In a final paper$^{(10)}$, with the conviction that the discrepancy was to be attributed to the uncertainty of the values for the Joule-Thomson effect, he again recast his equations so that only relative values of this effect were made use of. The values now obtained were 273·131 and 273·136. The Leiden Laboratory's latest (1936) value is 273·14.

Rose-Innes was never a strong man, and the privations of the war considerably weakened his health and undermined his working-power. He published nothing after the war, and passed away at Bournemouth on 9 July 1933, at the age of 68.

N. EUMORFOPOULOS.

REFERENCES

(1) *Phil. Mag.* **6**, xix, 851 (1910).
(2) *Phil. Mag.* **7**, xxvii, 669 (1914).
(3) *Phil. Mag.* **5**, xlviii, 286 (1899).

(4) *Phil. Mag.* **6**, xxvii, 150 (1914).
(5) *Phil. Mag.* **5**, xliv, 76 (1897); xlv, 102 (1898); xlvii, 353 (1899); xlviii, 213 (1899); and **6**, ii, 208 (1901).
(6) *Phil. Mag.* **5**, xlv, 227 (1898).
(7) *Phil. Mag.* **5**, l, 251 (1900).
(8) *Phil. Mag.* **6**, ii, 130 (1901).
(9) *Phil. Mag.* **6**, vi, 353 (1903).
(10) *Phil. Mag.* **6**, xv, 301 (1908).

JOSEPH HERBERT VINCENT, M.A., D.Sc., A.R.C.S.

Dr J. H. Vincent, who died on 27 January 1937, served on the Council of the Society from 1920 to 1924 and was a Vice-President from 1925 to 1927; he also served on the Board of the Institute of Physics from 1925–9. He began his studies in physics at the Mason College, Birmingham, under Professor Poynting, and afterwards proceeded to the Royal College of Science, London, where he studied under Rucker and Boys, gaining the Associateship in 1895. After serving as a Demonstrator at that College for a short period he went to the Cavendish Laboratory, Cambridge, where he was engaged in research work under the direction of J. J. Thomson. After leaving Cambridge he became Head of the Physics Department at the Paddington Technical Institute, a position he retained until his retirement in 1934.

Vincent's published researches always represented work of a high order. His method of photographing ripples, generated on the surface of mercury by a glass style attached to one prong of a vibrating tuning-fork and dipping into the mercury, was published in volume **15** of the *Proceedings*. By attaching a second style to the same prong he was able to generate two sets of waves in the same phase, and to photograph the effects of interference on the ripples produced. These experiments immediately became popular, and associated Vincent's name with this branch of physics. Unfortunately his duties allowed him little time for the prosecution of research, and he was unable to follow out several lines of work which he had planned. In 1918, however, he was freed from his duties at Paddington, and joined Professor Eccles at Finsbury Technical College in what was then the Admiralty's Electrical Laboratory in London. One of the first problems he took up was that of the inconstancy of the frequency of the oscillations generated by triodes in back-coupled circuits of various kinds; and he succeeded in devising methods of keeping the frequency extremely constant, the results being published in a joint paper with Eccles in the *Proceedings of the Royal Society*. Whilst at Finsbury he also investigated certain troubles in heterodyne reception with triodes, and the production and reception of supersonic waves in water. In the latter connexion difficulty in obtaining quartz led Vincent to consider the possibilities of magnetostriction in nickel, but owing to the resumption of his teaching duties he was unable to follow out his ideas in this direction. He took up the work again with great success in 1925, and later read several papers before the Society describing his results.

During his later years Vincent was dogged by ill health, which caused his early retirement and put an end to his investigations. All who had the privilege of working with him found him a most estimable colleague, and will remember him as one who planned his work so thoughtfully that the experimental test of his project was almost always successful at the first trial.

C. R. DARLING.

RICHARD SMITH WILLOWS, M.A., D.Sc.

On 10 January 1937 a life devoted to the interests of physics and physical research came to an end by the death of Richard Smith Willows, M.A., D.Sc., at the age of 61. Born in the village of Foston, near Grantham, Lincolnshire, a member of a farming family, R. S. Willows was educated first at the village school and later at Sedgebrook Grammar School, subsequently proceeding to Nottingham University College, and thence to Cambridge University. At Nottingham he came under the influence of the late Professor E. H. Barton, F.R.S., D.Sc., whom he always held in the highest esteem. From Nottingham, after graduating in the University of London, he proceeded to Trinity College, Cambridge with an 1851 Exhibition, where he did research in the Cavendish Laboratory in association with Sir J. J. Thomson, O.M., F.R.S., whose inspiring influence made a profound impression upon him. Willows was destined to spend a large part of his life as a teacher of physics, for which profession he had ability of a high order. He was for a short time Lecturer in Physics on the Staff of Battersea Polytechnic, and from 1902 until 1918 occupied the post of Head of the Department of Mathematics and Physics at the Sir John Cass Technical Institute, London. During his tenure of the latter post many of his students caught his enthusiasm for the subject of which he was a master, and not a few owe their success in life largely to him. His lectures were always lucid and replete with interest, and the fascinating lecture experiments which he devised and prepared were the admiration of all who were so fortunate as to come under his tuition. But it will perhaps be by his admirable work in the laboratories, and especially in research, that his students will remember him best. He was always ready to help them when in difficulties, however insignificant, and the charm of his personality and his kindly, sympathetic manner made him beloved by all who came into close contact with him. His knowledge of published researches was profound.

The great war provided an opportunity for Willows's skill in and knowledge of physical research to be utilized in the service of the country. Selected specially on account of his excellent work on the conduction of electricity through gases, Willows was enabled to conduct researches which led to the perfecting of the manufacture in this country of X-ray tubes. It was largely as a result of these researches that the supply of X-ray tubes to the Services was maintained at a time when importation was a matter of extreme difficulty. As a result of this work, unobtrusively performed, his ability to deal with research problems in applied science was recognized, and in 1918 he was appointed as Head of the Physics

Department in the newly established research laboratories of Messrs Tootal, Broadhurst, Lee & Co., of Manchester. So successful was he in solving some of the difficult problems of the cotton industry in a much shorter time than was expected, that he was soon promoted to take complete charge of the firm's research laboratories, and in the later years of his life he became a director of the company.

His outstanding achievement was perhaps his successful solution of the problem which had baffled the industry for many years, that of producing a cotton fabric which would not crease. The utility of cotton cloth was widened enormously by this discovery, and thousands of workers benefited at a time of acute trade depression through there being placed upon the market a cotton fabric which could compete with fabrics made of other textile materials. The discovery was a triumph for R. S. Willows and his staff as well as of the application of scientific research to industry. Amongst the other scientific studies in which he excelled was that of colloids. One of the first to organize a course of lectures in this subject in his Department at the Sir John Cass Technical Institute, he was afterwards closely associated with the establishment of a Chair of Colloids in the University of Manchester.

The part which recreation played in Willows's life contributed to no small extent to his success. He knew when to work and when to play. He was keenly interested in reading history, and was an enthusiast at golf. He was twice married, first to Miss Kemp of Sedgebrook, Lincolnshire, and four years before his death to his second wife, who survives him. He leaves also a son and daughter, and many friends to mourn his loss.

F. J. HARLOW.

SYDNEY YOUNG, F.R.S.

1857–1937

SYDNEY YOUNG, the son of a Liverpool merchant, was a Lancastrian, born at Farnworth on 29 December 1857. He was trained in chemistry under Roscoe and Schorlemmer at Owens College, and under Fittig at Strasburg, where he developed that skill in glass-blowing which stood him in such good stead in his later work.

His outlook on his science was distinctly physical, and this bias, it has been suggested, may have arisen from an early demonstration which he gave to the Chemical Society at Owens College of Carnelley's discovery that the application of very considerable heat fails to liquefy ice at very low pressures.

Be this as it may, the physical world owes much to Young's careful investigations of the thermal properties of pure liquids—a long-continued series of researches which culminated in his famous paper of 1910 (published in the *Proceedings of the Royal Dublin Society*) wherein he tabulates the vapour pressures, specific volumes and critical constants of some thirty carefully purified compounds. In this and in earlier papers he discusses the law propounded by Cailletet and Mathias that the mean of the orthobaric densities of the liquid and its saturated vapour is a linear function of the temperature. The only substance for which Young found this to be strictly true was for *n*-pentane. For all other substances the law of rectilinear diameters is no more than a convenient approximation, and the march of the ***mean*** density (ρ) with temperature is better represented by

$$\rho = \alpha + \beta t + \gamma t^2,$$

where γ is small, but appreciable.

Young was much interested in boiling point relations in homologous series and established a useful general formula giving the difference (Δ) between the boiling-point of one homologue and the next in the series in the form

$$\Delta = A/T^{B\sqrt{T}}.$$

His work on the problem of distillation is classical in quality.

Young succeeded Ramsay in the Chair of Chemistry at Bristol in 1887. On the retirement of Emerson Reynolds in 1903, he was appointed to the Chair of Chemistry at Trinity College, Dublin, a position which he held with distinction until his retirement in 1928. He was elected to the Royal Society in 1893.

It was not the fortune of the present writer to know Young personally. Many years ago, however, he wrote to Young for assistance in certain physico-chemical problems and he has very happy memories of a correspondent who was most friendly and helpful, and who spared no pains in elucidating the difficulties of a young research student.

A. F.

The Council have learned with profound regret of the loss which has been inflicted by the death of Lord Rutherford upon physics and upon his many friends in the Physical Society. A biographical notice of Lord Rutherford will be published in the *Proceedings* of the Society at a later date.

REVIEWS OF BOOKS

Principles of Quantum Mechanics, by ALFRED LANDÉ. Pp. xii+117. (Cambridge: University Press, 1937.) 7*s*. 6*d*. net.

In reading this short account of the principles of quantum mechanics one cannot fail to appreciate the fact that the author has thought about the subject in his own particular way and has resolved a number of difficulties which originally presented themselves to him. Having thus thought and learned much about the subject he decided to write a book upon it. This is the proper sequence of events in the development of a book and it cannot fail to produce a work bearing the characteristics of an original thinker.

Professor Landé's object in writing this addition to the literature of the quantum theory has been principally to eliminate some non-physical confusions which have crept into it and to show that it is based wholly on physical ideas.

The book takes as its text the complementarity of waves and corpuscles, and by means of individual examples, treated from both points of view, the quantum theory is presented as a method for translating corpuscular data into wave data and vice versa. The relations necessary for connecting the apparently antagonistic conceptions of the two points of view emerge very simply and clearly in the examples.

The second of the five parts into which the book is divided is devoted to the uncertainty principle. This is examined very thoroughly, and the treatment is based upon the introduction of an amplitude variation in the form of the Gaussian error curve. The more familiar method of introducing the principle by means of the theory of optical instruments is probably more acceptable to many physicists, but the method chosen here is not so widely known and has the advantage of giving greater mathematical precision to the principle, while it fits better into the plan of the book.

The later parts of the book, which include a discussion of the principles of interference and of correspondence, are especially useful as an explanation of the mathematical apparatus of the more advanced parts of the theory, and on account of the precision given to terms often loosely used, such as "interference of probabilities" and "probability packets". The work is certain to appeal to those who have already a good knowledge of the quantum theory and they will find in following the line of thought of the author a clarity and precision in the physical ideas not always to be found in works on this subject. H. T. F.

Atomic Spectra and the Vector Model, by A. C. CANDLER. Volume I: *Series Spectra*. Pp. viii+237. Volume II: *Complex Spectra*. Pp. vi+279. (Cambridge: University Press, 1937.) 15*s*. net each volume.

As is pointed out in the preface to these volumes, the empirical laws forming the basis of present knowledge of atomic spectra were originally stated in notations that now seem cumbrous and even misleading, and no adequate review of the earlier work on series spectra has appeared in this country since the universal adoption, in 1929, of the relatively simple and more convenient modern notation. In Prof. A. Fowler's *Report on Series in Line Spectra*, which was published by our Society in 1922 and is the one English work to which reference must still be made for ground-work and data, we encounter one of the old notations which we now wish to forget.

In the first volume, dealing with series spectra, this omission in regard to notation is repaired, and an account is given of the splitting of atomic lines in magnetic and electric fields, this being essential to a complete understanding of the series laws. The last two chapters of this volume deal with such matters as the periodic table, valency and covalency, X-ray spectra and the doublet laws.

In the second volume, dealing with complex spectra, the theory is developed, the spectral types are described, and recent topics, such as hyperfine structure, quadripole radiation and fluorescent crystals, are taken up one after another. So much research is now concentrated on matters discussed in this volume that some of the statements made will, unfortunately, very soon need revision, notably in regard to the rare earths in view of Albertson's investigations.

The argument is entirely within the easy comprehension of all physicists, physical chemists and spectroscopists with no more than ordinary mathematical equipment, for not only is the vector model used throughout, but also, wherever the predictions of the model have been refined by means of the quantum mechanics, the results are freely quoted and compared with observational data, and the rather heavy mathematical proofs are entirely excluded. The plan adopted is first to present experimental facts and then to introduce the theory as a means of correlating them; this is the order in which the subject has been developed and that in which many spectroscopists still prefer to approach it. These at least will be grateful to the author for his decision to avoid the opposite plan—which has been favoured by several modern writers on both atomic and molecular spectra, and would, doubtless, have been quite easy to the author—of presenting, in outline at least, the principles of the quantum mechanics and the special results of the general theory and afterwards comparing these with experimental facts. The latter plan is more suited to a theoretical treatise such as the excellent one by Condon and Shortley, *The Theory of Atomic Spectra*, which came from the same press two years ago, than to a book for the beginner or one for the experimental physicist. Judging by the opinions which are being expressed by several actively engaged spectroscopists who have examined Candler's volumes during the summer vacation, it seems safe to predict that many readers will prefer them to any other recent introduction to atomic spectra.

Amongst other merits of this scholarly work, mention must be made of the beautifully clear style in which it is written and the care which has been devoted to the bibliographies at the ends of the chapters and in appendix VI. Not content to give a list of bare references, the author adds notes indicating briefly the topic of each paper, the scope of each book, and the conversions from the older notations used in some of the papers into the modern notation. The text contains numerous tables and line diagrams and is illustrated by eight plates of well-chosen spectrograms. Each volume is adequately indexed and, needless to say, excellently produced by the Cambridge University Press.

W. J.

Atomic Spectra and Atomic Structure, by GERHARD HERZBERG. Pp. xiv+257. (London and Glasgow: Blackie and Son, 1937.) 18*s*. 6*d*. net.

This is an English translation, by J. W. T. Spinks with the co-operation of the author, of Herzberg's *Atomspektren und Atmostruktur: eine Einführung für Chemiker, Physiker und Physikochemiker* (Dresden and Leipzig: Steinkopff, 1936), which appeared so recently that it is unlikely to have become well known in this country. It is smaller and less detailed than either of the other two English introductions to this subject that have appeared recently, namely White's *Introduction to Atomic Spectra* (1934) and Candler's *Atomic Spectra and the Vector Model* (1937). In order to meet the requirements of beginners and of those seeking some knowledge of the subject on account of its applications to other branches of knowledge, the author lays stress on fundamental principles and makes no attempt to satisfy the needs of practical spectroscopists by the inclusion of tables of numerical data and discussions of special cases. This omission may be welcomed rather than deplored, since such material is to be found in the two larger works. As in those works, a statement of experimental results relating to a given topic precedes the theoretical treatment, complicated mathematics is avoided, and theoretical results are quoted without rigid proof. This, too, is a good feature, as the full treatment is now at hand in Condon and Shortley's *The Theory of Atomic Spectra* (1935). Nevertheless, a good and comparatively long wave-mechanical section follows the early sections on Bohr's theory of the H spectrum in chapter I, and shorter ones are included in the discussions of the He spectrum in the same chapter, the normal Zeeman effect in chapter II, and Pauli's exclusion principle in chapter III. These theoretical sections and certain other discussions are printed in smaller type than the rest of the text, as an indication that they may well be omitted in a first reading without loss of grip of the argument. In view of the applications, especially to the investigations of molecular spectra and molecular structure, certain topics are dealt with at greater length than others that would appear to be more important to the study of atomic spectra alone; for example in the last chapter (VI) there are sections on ionic (heteropolar) and atomic (homopolar) binding and elementary chemical processes. The book is well illustrated with line diagrams, tables and spectrograms, and is well indexed. The English edition is better printed and produced than the original, and in the course of its preparation the author has improved upon the original presentation in several places. The reproductions of typical photographs of White's electron-cloud models in figure 21, however, are not quite as good as in the German edition and not nearly as good as those in White's book (p. 71).

W. J.

Atomic Structure of Minerals, by W. L. BRAGG. Pp. xiii + 242. (Oxford: University Press.) 18*s*. net.

This book is a review of the investigation of the atomic structure of minerals by means of X rays. Professor W. L. Bragg was the first to analyse the structure of a mineral by such means, since in 1913 he determined the positions of the carbon atoms in diamond, and many of the results described in this book are due to him and to his co-workers. Their well-known work on the silicates may be mentioned as an example.

The greater part of the book consists of a description of structures; a list of headings will give some idea of its scope. The elements are treated, and the halides, the sulphides, arsenides, oxides and oxygen salts, the silicates and alumino-silicates, the pyroxene and amiphole groups and the mica and clay groups, the felspar group, and the zeolites and other framework structures. The book is fully illustrated, and the author shows his usual talent for making the most complicated structure clear. Many physical properties of various minerals, besides their actual structures are discussed and related to the latter; for instance, the twinning of the felspars and the refractive indices and birefringence of calcite and aragonite.

The book contains also three introductory chapters on the geometry of crystal patterns, the analysis of crystals by means of X rays and an especially interesting one on the general principles of mineral structure. This chapter gives a very clear account of Pauling's principles in ionic structures, according to which, in the specially stable structures taken up by all natural minerals, the lines of force starting from any ion must always end on a nearest neighbour. This rule imposes a most rigorous condition upon the geometrical configuration of a structure, and is constantly referred to in the book. The printing of the book, and especially of the figures, is excellent.

N. F. M.

Electricity and Magnetism for Degree Students, by S. G. STARLING. Sixth edition. Pp. 630, with 449 diagrams and illustrations. (London: Longmans, Green and Co.) 12*s*. 6*d*. net.

The appearance of a new edition of this well-known textbook deserves notice. The new format, with its larger type and page, first strikes the eye. The total content of the book is also slightly greater. Some matter is omitted, new matter is introduced, and minor corrections here and there indicate that the whole book has received careful revision. The essential character of the work remains, however, unchanged, and on this the author can be congratulated. The difficulty of writing a textbook to cover a degree course in this branch of physics is quite obvious, in view of the immense rate of advance in so many directions in recent years. It is above all necessary that the student should acquire a firm command of fundamentals in respect of facts, instruments, and principles, before he engages in the exploration of the fascinating but lengthy pathways of the newer knowledge. The author has by no means ignored the later developments, and place has been found for many new sections. To give some instances: Langevin's theory of paramagnetic bodies and Weiss's theory of ferromagnetic bodies, the Stern-Gerlach experiment, electron optics, the neutron, the positron, cosmic rays, artificially induced radio-activity, the ionosphere, the Compton effect. But the author's primary consideration has been to retain intact the adequate treatment of what is customarily designated "classical" physics.

It is, of course, a facile exercise to compile lists of what one would like to see included, and to advise on the omission or reduction of certain sections. Yielding to the impulse, the reviewer would suggest for inclusion in a future edition: Dye's method of determining the vertical component of the earth's magnetic field, the electric dipole and its place in dielectric theory, Professor E. Taylor Jones's work on the induction coil, the ruled grating method of measuring the wave-length of X rays and the refractive index for X rays, the work of Dempster and of Bainbridge on positive rays. The task of making compensatory exclusions should not be insuperable.

This is a textbook, then, which has the merit of laying the stress on the classical ground of electricity and magnetism, on both the theoretical and experimental sides, whilst presenting the later advances, so often involving the quantum idea, in briefer setting. A literature is now available affording sources of information on the various branches constituting the modern side, so that the specialist student may readily supplement his knowledge in any direction.

D. O.

Gases and Metals, by COLIN J. SMITHELLS. Pp. vii + 218. (London: Chapman & Hall.) 18*s*. net.

When a gas atom strikes a metal surface it may, if not reflected again, either stay on the surface, or penetrate into the body of the metal and remain there, or emerge at the other side. The book under review devotes one chapter to each case, i.e. to adsorption, to solution and to diffusion. On reading the book, one is impressed by the rapidity with which events now move in physics, for the outlook in each chapter is one which could not have been conceived twenty-five years ago. In adsorption problems, as in the analogous problem of films on liquids, the work of Langmuir is of fundamental importance, and directs attention to the individual molecule and its relationships with the metal atoms. The question whether a molecule can migrate from place to place would once have seemed impossible of answer, but here it is dealt with as quite an ordinary question. Again, in solution, we are no longer forced to be satisfied with empirical laws true in bulk. Once more, the new knowledge requires us to answer the question as to how the foreign molecules are located relatively to the metal atoms, and once again an answer is forthcoming. Even the diffusion problem raises the question as to the route by which the molecules migrate through metal. Do they pass between the atoms in the lattice, or through the cracks between crystals? These reflections may suggest that the book is devoted to pure or academic physics, but whilst this may be true, it is none the less useful, and much of the information with which it is packed has in fact been obtained for direct industrial application.

The book is printed on very thick paper, and is profusely illustrated, containing more than two diagrams for every three pages of text.

J. H. A.

Tables of Physical and Chemical Constants, by G. W. C. KAYE and T. H. LABY. Eighth edition. Pp. 162. (Longmans Green.) 14*s*. net.

A quarter of a century has elapsed since the first appearance of this book of tables. Many will remember it as a slim volume with flexible covers easily slipped into a pocket. On reaching the eighth edition it has inevitably grown more portly, but the authors are to be congratulated on having succeeded in keeping it still within reasonable limits. The present edition shows evidence of considerable revision and, apart from major changes, examination of almost any page will show alterations where a more recent determination has replaced an older value of a constant. A noteworthy change is on pp. 40 and 41, where the earlier hygrometric tables, which included Glaisher's factors, have been replaced by a set of tables for the wet-and-dry-bulb hygrometer which cover the temperature-range from $-18°$ to $+100°$ C. On turning over the page from this table, another completely recast table is found, viz. that for the boiling point of water at pressures from 680 to 780 mm. This table, to 0·001° C., replaces the older one which was to 0·01° C. only, and is in terms of the international temperature scale, instead of the hydrogen scale. Incidentally, it is interesting to note that room has been found for the vapour pressure of heavy water at two temperatures. The section on temperature-measurement, too, has been largely rewritten, and new values are given for the thermodynamic temperature of the ice point, the corrections to mercury-in-glass thermometers and the e.m.fs. of typical thermoelements. The four pages devoted to magnetic data have been almost completely rewritten, and the fact stated in the preface that Mr C. E. Webb of the National Physical Laboratory has assisted with them is a guarantee that the selection of materials is a useful one.

A completely fresh system has been adopted for the tabulation of the X-ray spectra, including the K and L absorption edges, whilst other constants of modern physics have been added or revised. Thus, the X-ray grating methods for determining e are mentioned, as is Kellström's recalculation of Millikan's data using recent values for the viscosity of air. That ubiquitous element, heavy hydrogen, appears in connexion with the value of e/m for electrons, having been used for a spectroscopic determination. The Abraham electron has disappeared, and in its place is a table of the exit work functions of a few important metals, whilst ionizing and resonance potentials have been introduced for the first time on p. 111.

On the last page of the book, again, is an almost new table, in which the individual isotopes of each element are set out. A reviewer elsewhere has expressed his regret that abundance ratios were not included, but it is difficult to see how the authors could have included these unless they had abandoned the attempt to set out the 92 elements on a single page. The remaining changes in the sections on general physics and heat appear to be restricted to minor improvements in data, due in the main to the publication of new determinations.

The acoustical section, as befits the new outlook on acoustics, has been appreciably altered, and the book now contains an explanation of the bel and the decibel, as well as data for the variation in sensitivity of the normal ear over the frequency range 20 to 20,700 c./sec. In the section on the velocity of sound, an error has crept in, whereby Sherratt and Ezer Griffiths are credited with a value for the velocity of sound in air at 1800° C.; actually, no data are available for air from any source at such temperatures, and the authors of the tables have informed the reviewer that the entry will be deleted in the next edition. It is worthy of note that over a third of the values in the section are new.

In the second half of the book, the efforts to meet the needs of the student of the newer physics are noteworthy. Thus, on p. 73 there is a section, which will frequently be of value for reference, explaining the spectroscopic symbolism such as $3d^6 4S^2$; several such explanatory passages have been added, and the one on p. 99 giving the general formula for inter-plane distances in the general triclinic crystal may be particularly noted.

At this stage of its career the utility of the volume needs no emphasis and one would like to see the price reduced so as to render the book available to the student of limited means who now may be inclined to borrow a library copy instead of securing a copy for his personal use.

E. G.

British Polar Year Expedition, Fort Rae, N.W. Canada, 1932–3. Volume I: *Discussion of Results; Meteorology, Terrestrial Magnetism and Aurora, Atmospheric Electricity*. Pp. xv + 336 + 5 plates and numerous diagrams. Volume II: *Tables; Meteorology, Terrestrial Magnetism, Atmospheric Electricity*. Pp. ix + 228. Published under the direction of the British National Committee for the Polar Year, The Royal Society, Burlington House, London. (London: Percy Lund, Humphries and Co., Ltd., 1937.) Volume I, 21*s*. net; volume II, 15*s*. net.

These two volumes give an admirably full and clear account of the main British contribution to the work of the Second International Polar Year, 1932–3. This great scientific enterprise, successfully accomplished in a time of world economic depression, was a jubilee repetition and extension of the First Polar Year of 1882–3, the main object in each case being to obtain geophysical (mainly geomagnetic and meteorological) observations throughout a complete year simultaneously at a large number of high-latitude, mainly temporary, stations. Each of the cooperating nations maintained one or more stations. In 1882–3 Great Britain and Canada jointly sent an expedition to Fort Rae. In 1932–3 Canada set up its own station at Chesterfield Inlet, and Great Britain, besides reoccupying Fort Rae, sent an important radio expedition to Tromsø, in Norway, whose results have recently been published by the Royal Society in its *Philosophical Transactions*.

The present volumes are, of course, chiefly interesting to the specialist, meteorologist or geomagnetician, and even to him are interesting not so much in themselves as in conjunction with the similar volumes published by other nations for other polar stations. This is because both meteorology and geomagnetism are largely synoptic sciences, requiring the study of great masses of data from a network of stations over the globe. The laboratory physicist, however, would do well, in some leisure hour in the library, to read the charming brief narrative of the expedition given in the introduction, volume I, by the leader of the expedition, Dr J. M. Stagg. Enlivened by occasional humorous touches, it gives an admirable picture of the struggle of the physicist to observe some of Nature's most interesting moods in conditions which Nature herself has made exceptionally difficult. It is in arctic wilds, mostly remote from civilization, that geomagnetic disturbances and aurorae are most intense; there also the meteorological conditions have special interest, the troposphere being far thinner and the stratosphere much warmer than over the equator.

S. C.

Famous American Men of Science, by J. G. CROWTHER. Pp. xvi + 413. (London: Secker and Warburg, Ltd.) Price 15*s*. net.

The investigation of the role of science in modern life is, according to the author, a social duty and this unusual book is his contribution. The American scientists chosen for study are Franklin, Henry, Gibbs and Edison. The theme is that the progress of science is not accidental but is due to the needs of society at the time. Although for the most part the reasoning seems logical, sound and restrained, now and again the author's journalistic and socialistic connexions predominate. For example, he says: "Galileo and Newton discovered their system of mechanics, because the progressive social thought of their time, that of the rising trading classes, already interpreted phenomena quantitatively rather than qualitatively"; or again: "Newton and his discoveries in mathematical astronomy were a product of the urge of the ruling mercantile classes to discover how they could increase their knowledge of the technique of transport, and discover new sources of wealth, and increase their freights and profit."

There are many interesting things in the book concerning the four scientists with whom it is primarily concerned and others. We are told that many persons earned a livelihood by going about and showing Leiden jars, that Franklin predicted aerial warfare, the League of Nations and other modern conceptions and that G. Bernard Shaw was at one time employed by Edison. The book is a useful contribution to the study of the history of science and to sociology.

H. R. L.

Actualités Scientifiques et Industrielles. Under this general heading we have received the monographs listed below. Each is written by an authority on his subject and the treatment is, in general, concise and clear. The publishers are Herman and Co., 6, Rue de la Sorbonne, 6, Paris.

332. M. E. NAHMIAS. *Analyse des Matières Cristallisées au Moyen des Rayons X.* 15 fr.
334. M. RADU TITEICA. *Spectres de Vibration et Structure des Molécules Polyatomiques.* 18 fr.
338. I-V. KOURTSCHATOV. *Le Champ Moléculaire dans les Diélectriques.* 12 fr.
339. J. SOLOMON. *Théorie du Passage des Rayons Cosmiques à Travers la Matière.* 18 fr.
340. *Les Rayons Cosmiques.* (International Conference on Physics, London, 1934.) 10 fr.
341. *Transmutations.* (International Conference on Physics, London, 1934.) 18 fr.
342. *L'État Solide de la Matière.* (International Conference on Physics, London, 1934.) 18 fr.
363. RENÉ FORTRAT. *L'Effet Zeeman dans les Spectres de Bandes.* 12 fr.
365. G. ALLARD. *Polarisation Diélectrique.* 10 fr.
366. GUY EMSCHWILLER. *Les Données Spectrales.* 12 fr.
369. G. GAMOW. *Cinétique des Réactions Nucléaires.* 8 fr.
373. A. FROUMKINE. *Couche Double. Électrocapillarité. Surtension.* 10 fr.
374. P. RUMPF. *La Théorie de l'Ion Amphotère.* 12 fr.
399, 400. R. FREYMANN. *Les Ondes Hertziennes et la Structure Moléculaire.* Part I, 10 fr. Part II, 15 fr.
406. THÉODORE KAHAN. *Théorie de L'Émission des Rayons Alpha à Travers une Double Barrière de Potentiel.* 12 fr.
409. JEAN-LOUIS DESTOUCHES. *La Cinétique Opératorielle.* 18 fr.
411. LOUIS DE BROGLIE. *Nouvelles Recherches sur la Lumière.* 12 fr.
424. F. DUPRÉ LA TOUR. *Le Polymorphisme des Acides Gras.* 14 fr.
457. JACQUES BRILLOUIN. *L'Acoustique et la Construction. Bases de la Technique.* 18 fr.
458. F. LONDON. *Une Conception Nouvelle de la Supra-Conductibilité.* 20 fr.
473. M. P. LACROUTE. *Raies d'Absorption dans les Spectres Stellaires.* 20 fr.
509, 510. MAURICE LETORT. *Les Conceptions Actuelles du Mécanisme des Réactions Chimiques.* Parts I and II, 15 fr. each.

INDEX

Numbers preceded by the letter E *refer to pages in the extra part, bound at the beginning of this volume*

PAGE

Aberration, The knife-edge test for spherical 376
Absorption coefficients, Further experiments on the photographic action of gamma rays and their 1
Absorption spectra and photodissociation of halides and oxyhalides of sulphur, selenium and tellurium 679
Absorption spectra of some carbon and tin halides in the vapour state . . 568
Adsorbing surface, applied to the temperature dependence of oxygenation and oxidation of a tungsten filament, Thermionic approximations to the gas-covered fraction of an 409
Aggregation of metal atoms on solid surfaces, The migration and . . . E 140
Air, The viscosity of 205
Alkali-halide phosphors containing heavy metals . . . . E 40
Alkali metals spontaneously deposited on glass surfaces, The electrical conductivity of thin films of the 89
Alloys, Age-hardening . . . . E 103
Alloys, conduction in . . . . E 75
Alloys of the copper-zinc system, On the optical constants of 345
Alloys. Part 1: The equilibrium between liquid and solid phases, The phase boundaries in binary 243
Alloys. Part 2: The theory of the α, β phase boundaries, The phase boundaries in binary 250
Alloys. Part 1: Thermal expansion of alloys rich in nickel, An X-ray investigation of pure iron-nickel 17
Alloys. Part 2: Thermal expansion of some further alloys, An X-ray investigation of pure iron-nickel 178
Alloys. Part 3: The thermal expansion of alloys rich in iron, An X-ray investigation of pure iron-nickel 307
Alloys. Part 4: The variation of lattice-parameter with composition, An X-ray investigation of pure iron-nickel 315
Alloys. Part 5: The variation of thermal expansion with composition, An X-ray investigation of pure iron-nickel 323
Alloys, The resistance of palladium and palladium-gold 29
Alloys, The theoretical interpretation of the optical constants of copper-zinc . 354
Alloys with disordered and ordered arrangement of atoms. Resistance of . . E 77
Amalgams, The electrical resistance of manganese 635
Amalgams, The magnetic properties of iron 611
Amalgams, The magnetic properties of manganese 230
Amalgams, The magnetic properties of silver 642
Ametropia by the coincidence optometer, The estimation of 444
Amplifier for investigating the wave form of atmospherics, An aperiodic . . 654
Anderson, John S.: The measurement of distortion in a gauge protection lens . 112
Andrade, E. N. da C., and L. C Tsien: The velocity-distribution in a liquid-into-liquid jet 381
Andrade, E. N. da C., and R. Roscoe: Glide in metal single crystals . . . 152
Appleyard, E. T. S.: Some factors influencing the resistance of thin metal films E 118
Atmospherics, An aperiodic amplifier for investigating the wave form of . . 654
Atmospherics, Applications of the modulating electrode of television cathode ray tubes in investigations of the wave form of 658

PAGE
Band-systems of GeCl and GeBr, Ultraviolet . . . 532
Band-system of germanium monoxide, The ultraviolet . . . 543
Band-systems of SnBr and SiBr, Ultraviolet . . . 554
Band, William: Thermomagnetic properties of nickel wire. Part 3 . . . 14
Barkas, Wilfred W.: Wood-water relationships. Part 3: Molecular sorption of water by Sitka spruce wood . . . 237
Bashford, L. A., *see* Jevons
Bates, L. F., and A. W. Ireland: The magnetic properties of silver amalgams . 642
Bates, L. F., and L. C. Tai: The magnetic properties of manganese amalgams . 230
Bates, L. F., and P. F. Illsley: The magnetic properties of iron amalgams . . 611
Bates, L. F., and P. G. Day: The electrical resistance of manganese amalgams . 635
Bernamont, J.: Fluctuations in the resistance of thin films . . . E 138
Beta-radiation on gamma-ray measurements made in air, The effect of secondary 338
Boer, J. H. de, and E. J. W. Verwey: Semi-conductors with partially and with completely filled 3*d*-lattice bands . . . E 59
Bond, W. N.: The viscosity of air . . . 205
Borelius, G.: Resistance of alloys with disordered and ordered arrangement of atoms . . . E 77
Bradley, A. J., *see* Bragg
Bragg, W. L., C. Sykes, and A. J. Bradley: A study of the order-disorder transformation . . . E 96
Brass, The energy of the superlattice in β . . . 258
Brentano, J. C. M.: An X-ray goniometer using beams of large aperture for photographically recording crystal-powder reflections . . . 61
Briggs, Allan H.: The estimation of ametropia by the coincidence optometer . 444
Brindley, G. W., *see* Hoare
Briscoe, H. V. A., *see* Jevons
Brown, G. Burniston: The mechanism of edge-tone production . . . 508
Brown, G. Burniston: The vortex motion causing edge-tones . . . 493
Buckley, H.: Note on the radiation between two coaxial radiating cylinders . 225

Cady, W. G.: Presentation of the fourteenth Duddell Medal to . . . 693
Cady, W. G.: The longitudinal effect in Rochelle salt crystals . . . 646
Campbell, N. R., and R. S. Rivilin: The effect of hydrogen on the time-lag of argon-filled photoelectric cells . . . 12
Carbon and tin halides in the vapour state, Absorption spectra of some . . 568
Cathode ray tubes in investigations of the wave form of atmospherics, Applications of the modulating electrode of television . . . 658
Chance, W. H. S.: The optical glassworks at Benediktbeuern . . . 433
Chladni figures by means of solid carbon dioxide. Part I: Bars and other metal bodies, The production of . . . 522
Cinematography and for projection with continuously moving films, The use of rotating parallel-plane blocks for . . . 663
Cochlea to phase-reversal in a continuous musical tone, The response of the mammalian . . . 190
Cockburn, R.: A determination of the fundamental types of electron oscillations in a triode valve . . . 38
Colour-vision characteristics of a trichromat, Part 2, The . . . 332
Conduction of electricity in solids, Report of conference on the . . . E 1
Conductivity and photochemical processes in alkali-halide crystals, Electron . E 3
Conductivity of a sample of Acheson graphite from 0° to 800° C., The thermal and electrical . . . 419
Conductivity of thin films of indium, The structure and electrical . . . 121
Conductivity of thin films of the alkali metals spontaneously deposited on glass surfaces, The electrical . . . 89

PAGE

Conference on the conduction of electricity in solids, Introduction to the report of E v
Conybeare, J. G. G.: The resistance of palladium and palladium-gold alloys . 29
Copper-zinc alloys, The theoretical interpretation of the optical constants of . 354
Copper-zinc system, On the optical constants of alloys of the 345
Cosslett, V. E.: The structure and electrical conductivity of thin films of indium 121
Counting impulses at high speeds of counting, A circuit for 85
Cox, H. L., and D. G. Sopwith: The effect of orientation on stresses in single crystals and of random orientation on strength of polycrystalline aggregates 134
Crystals and of random orientation on strength of polycrystalline aggregates, The effect of orientation on stresses in single 134
Crystals, Glide in metal single 152
Crystals of sodium between 120° and 370° K., Intensities of X-ray reflections from single 294
Crystals, The longitudinal effect in Rochelle salt 646
Cuckow, F. W., *see* Preston

Dawton, Ralph H. V. M.: Intensities of X-ray reflections from single crystals of sodium between 120 and 370° K. 294
Day, P. G., *see* Bates
Daylight-factor meter, Demonstration of the portable photoelectric . . . 194
Demonstration of a microscope for use with ultraviolet light, employing a reflecting optical system of aplanatic properties 427
Demonstration of the audible effect of a sudden change of phase in the current supplied to a telephone receiver 194
Demonstration of the portable photoelectric daylight-factor meter . . . 194
Desch, C. H.: Age-hardening alloys . . . . E 103
Diamagnetic susceptibilities of dissolved and hydrated salts, The . . . 619
Diffusion, An experimental study of turbulence 479
Distortion in a gauge protection lens, The measurement of 112
Duddell Medal, Presentation to Prof. G. W. Cady of the fourteenth . . . 693

Eclipse of 19 June 1936, Ionospheric conditions during the solar . . . 214
Edge-tone production, The mechanism of 508
Edge-tones, The vortex motion causing 493
Electron conductivity and photochemical processes in alkali-halide crystals . E 3
Electron emission from complex surfaces, Secondary- 392
Electron oscillations in a triode valve, A determination of the fundamental types of 38
Electrons in polar crystals, Trapped . . . . E 32
Expansion of alloys rich in iron, An X-ray investigation of pure iron-nickel alloys. Part 3: The thermal 307
Expansion of some further alloys, An X-ray investigation of pure iron-nickel alloys. Part 2: Thermal 178
Expansion with composition, An X-ray investigation of pure iron-nickel alloys. Part 5: The variation of thermal 323

Ferromagnetics, The electrical resistance of 671
Féry, A.: A study of the electrical properties of thin films of platinum obtained by cathode sputtering in air and other gases (He, N_2, O_2 and H_2) . . E 136
Films, Conduction in thin metallic . . . . E 111
Films, Fluctuations in the resistance of thin . . . . E 138
Films of indium, The structure and electrical conductivity of thin . . . 121
Films of platinum obtained by cathode sputtering in air and other gases (He, N_2, O_2 and H_2), A study of the electrical properties of thin . . . . . E 136
Films of the alkali metals spontaneously deposited on glass surfaces, The electrical conductivity of thin 89

PAGE
Films, Some factors influencing the resistance of thin metal . . . . . E 118
Films, Structural changes during the growth of metal 279
Films, The structure of thin metallic . . . . E 113
Finch, G. I.: The structure of thin metallic films . . . . E 113
Fincham coincidence optometer, The development of the 469
Fincham, E. F.: The coincidence optometer 456
Fluorescence of some impurity solids, The effects of temperature on the intensity of . . . . E 46

Gamma-ray measurements made in air, The effect of secondary beta-radiation on 338
Gamma-rays and on their absorption coefficients, Further experiments on the photographic action of 1
GeCl and GeBr, Ultraviolet band-systems of 532
George, Wm. H.: Sensitivity variation of X-ray photographic films . . . 357
Germanium monoxide, The ultraviolet band-system of 543
Glassworks at Benediktbeuern, The optical 433
Gold alloys, The resistance of palladium and palladium- 29
Goniometer using beams of large aperture for photographically recording crystal-powder reflections, An X-ray 61
Graphite from 0° to 800° C., The thermal and electrical conductivity of a sample of Acheson 419
Griffiths, J. H. E.: A circuit for counting impulses at high speeds of counting . 85
Gurney, R. W., and N. F. Mott: Trapped electrons in polar crystals. . . E 32

Halides and oxyhalides of sulphur, selenium and tellurium, Absorption spectra and photodissociation of 679
Hallpike, C. S., H. Hartridge, and A. F. Rawdon-Smith: The response of the mammalian cochlea to phase-reversal in a continuous musical tone . . 190
Hartridge, H., *see* Hallpike
Hilsch, R.: Alkali-halide phosphors containing heavy metals . . . . . E 40
Hoare, F. E., and G. W. Brindley: The diamagnetic susceptibilities of dissolved and hydrated salts 619
Hussain, S. L., and R. Samuel: Absorption spectra and photodissociation of halides and oxyhalides of sulphur, selenium and tellurium 679
Hydrogen by palladium, The effect of pressure and temperature on the occlusion of 587
Hydrogen system, The palladium- 603

Illsley, P. F., *see* Bates
Indium, The structure and electrical conductivity of thin films of . . . 121
Ionospheric conditions during the solar eclipse of 19 June 1936 214
Ireland, A. W., *see* Bates
Iron amalgams, The magnetic properties of 611
Iron-nickel alloys. Part 1: Thermal expansion of alloys rich in nickel, An X-ray investigation of pure 17
Iron-nickel alloys. Part 2: Thermal expansion of some further alloys, An X-ray investigation of pure 178
Iron-nickel alloys. Part 3: The thermal expansion of alloys rich in iron, An X-ray investigation of pure 307
Iron-nickel alloys. Part 4: The variation of lattice-parameter with composition, An X-ray investigation of pure 315
Iron-nickel alloys. Part 5: The variation of thermal expansion with composition, An X-ray investigation of pure 323

Jet, The velocity-distribution in a liquid-into-liquid 381

PAGE

Jevons, W., L. A. Bashford, and H. V. A. Briscoe: Ultraviolet band-systems of GeCl and GeBr 532
Jevons, W., L. A. Bashford, and H. V. A. Briscoe: The ultraviolet band-system of germanium monoxide 543
Jevons, W., and L. A. Bashford: Ultraviolet band-systems of SnBr and SiBr . 554
Johnson, M. C., and F. A. Vick: Thermionic approximations to the gas-covered fraction of an adsorbing surface, applied to the temperature dependence of oxygenation and oxidation of a tungsten filament 409
Jones, John Idwal, *see* Owen
Jones, H.: The phase boundaries in binary alloys. Part 1: The equilibrium between liquid and solid phases 243
Jones, H.: The phase boundaries in binary alloys. Part 2: The theory of the α, β phase boundaries 250

Kingslake, R.: The knife-edge test for spherical aberration 376

Lennard-Jones, J. E.: The migration and aggregation of metal atoms on solid surfaces . . . . E 140
Lens, The measurement of distortion in a gauge protection 112
Lightning discharges, Rapid variations in the magnetic field produced by . . 364
Lovell, A. C. B.: The electrical conductivity of thin films of the alkali metals spontaneously deposited on glass surfaces 89
Lowery, H., H. Wilkinson, and D. L. Smare: On the optical constants of alloys of the copper-zinc system 345

Magnetic field produced by lightning discharges, Rapid variations in the . . 364
Magnetic properties of iron amalgams, The 611
Magnetic properties of manganese amalgams, The 230
Magnetic properties of silver amalgams, The 642
Manganese amalgams, The electrical resistance of 636
Manganese amalgams, The magnetic properties of 230
Microscope for use with ultraviolet light, employing a reflecting optical system of aplanatic properties, Demonstration of a 427
Migration and aggregation of metal atoms on solid surfaces, The . . . E 140
Mott, N. F.: Introduction to the report of conference on the conduction of electricity in solids . . . . E v
Mott, N. F., *see* Gurney
Mott, N. F.: The energy of the superlattice in β brass 258
Mott, N. F.: The theoretical interpretation of the optical constants of copper-zinc alloys 354
Musical tone, The response of the mammalian cochlea to phase-reversal in a continuous 190
Myers, D. M.: The division of primary electron current between grid and anode of a triode 264

Naismith, R.: Ionospheric conditions during the solar eclipse of 19 June 1936 . 214
Nelson, J. H.: The colour-vision characteristics of a trichromat, Part 2 . . 332
Nickel alloys. Part 3: The thermal expansion of alloys rich in iron, An X-ray investigation of pure iron- 307
Nickel alloys. Part 4: The variation of lattice-parameter with composition, An X-ray investigation of pure iron- 315
Nickel alloys. Part 5: The variation of thermal expansion with composition, An X-ray investigation of pure iron- 323
Nickel wire. Part 3: Thermomagnetic properties of 14
Nickel, An X-ray investigation of pure iron-nickel alloys. Part 1: Thermal expansion of alloys rich in 17

PAGE
Non-metals, conduction in . . . . E 1
Norinder, Harald: Rapid variations in the magnetic field produced by lightning discharges 364

Obituary notices 694
Occlusion of hydrogen by palladium, The effect of pressure and temperature on the 587
Optical constants of alloys of the copper-zinc system, On the 345
Optical constants of copper-zinc alloys, The theoretical interpretation of the . 354
Optometer, The coincidence 456
Optometer, The development of the Fincham coincidence 469
Optometer, The estimation of ametropia by the coincidence 444
Owen, E. A., and E. L. Yates: An X-ray investigation of pure iron-nickel alloys. Part 1: Thermal expansion of alloys rich in nickel 17
Owen, E. A., and E. L. Yates: An X-ray investigation of pure iron-nickel alloys. Part 2: Thermal expansion of some further alloys 178
Owen, E. A., and E. L. Yates: An X-ray investigation of pure iron-nickel alloys. Part 3: The thermal expansion of alloys rich in iron 307
Owen, E. A., E. L. Yates, and A. H. Sully: An X-ray investigation of pure iron-nickel alloys. Part 4: The variation of lattice-parameter with composition . 315
Owen, E. A., E. L. Yates, and A. H. Sully: An X-ray investigation of pure iron-nickel alloys. Part 5: The variation of thermal expansion with composition 323
Owen, E. A., and John Idwal Jones: The effect of pressure and temperature on the occlusion of hydrogen by palladium 587
Owen, E. A., and John Idwal Jones: The palladium-hydrogen system . . 603
Oxygenation and oxidation of a tungsten filament, Thermionic approximations to the gas-covered fraction of an adsorbing surface, applied to the temperature dependence of 409

Palladium and palladium-gold alloys, The resistance of 29
Palladium, The effect of pressure and temperature on the occlusion of hydrogen by 587
Palladium-hydrogen system, The 603
Parker, R. C.: The smoke method of measuring supersonic velocities . . 95
Parti, Y. P., and R. Samuel: Absorption spectra of some carbon and tin halides in the vapour state 568
Phosphors containing heavy metals, Alkali-halide . . . . E 40
Photochemical processes in alkali-halide crystals, Electron conductivity and . E 3
Photodissociation of halides and oxyhalides of sulphur, selenium and tellurium, Absorption spectra and 679
Photoelectric cells, The effect of hydrogen on the time-lag of argon-filled . . 12
Photoelectric daylight-factor meter, Demonstration of the portable . . . 194
Photographic films, Sensitivity variation of X-ray 357
Photometric test plates 105
Pitt, F. H. G., *see* Wright
Platinum obtained by cathode sputtering in air and other gases (He, N_2, O_2 and H_2), A study of the electrical properties of thin films of . . . . . E 136
Pohl, R. W.: Electron conductivity and photochemical processes in alkali-halide crystals . . . . E 3
Potter, H. H.: The electrical resistance of ferromagnetics 671
Powell, R. W.: The thermal and electrical conductivity of a sample of Acheson graphite from 0° to 800° C. 419
Preston, J. S., and F. W. Cuckow: A photoelectric spectrophotometer of high accuracy 189

Quarrell, A. G.: Structural changes during the growth of metal films . . 279

Radiation between two coaxial radiating cylinders, Note on the 225

PAGE
Randall, J. T.: The effects of temperature on the intensity of fluorescence of some impurity solids . . . . E 46
Rawdon-Smith, A. F., *see* Hallpike
Reason, R. E.: The development of the Fincham coincidence optometer . . 469
Resistance of alloys with disordered and ordered arrangement of atoms . . E 77
Resistance of ferromagnetics, The electrical 671
Resistance of manganese amalgams, The electrical 635
Resistance of palladium and palladium-gold alloys, The 29
Resistance of thin films, Fluctuations in the . . . . E 138
Resistance of thin metal films, Some factors influencing the . . . . E 118
Reviews of books 78, 198, 326, 429, 629
Richardson, E. G.: An experimental study of turbulence diffusion . . . 479
Rivlin, R. S., *see* Campbell
Rochelle-salt crystals, The longitudinal effect in 646
Rogers, J. S.: Further experiments on the photographic action of gamma rays and on their absorption coefficients 1
Roscoe, R., *see* Andrade

Samuel, R., *see* Hussain
Samuel, R., *see* Y. P. Parti
Selenium and tellurium, Absorption spectra and photodissociation of halides and oxyhalides of sulphur 679
Semi-conductors with partially and with completely filled $3d$-lattice bands . E 59
SiBr, Ultraviolet band-systems of SnBr and 554
Silver amalgams, The magnetic properties of 642
Smare, D. L., *see* Lowery
SnBr and SiBr, Ultraviolet band-systems of 554
Sopwith, D. G., *see* Cox
Sodium between 120 and 370° K., Intensities of X-ray reflections from single crystals of 294
Sorption of water by Sitka spruce wood, Wood-water relationships. Part 3: Molecular 237
Spectra of some carbon and tin halides in the vapour state, Absorption . . 568
Spectrophotometer of high accuracy, A photoelectric 189
Spherical aberration, The knife-edge test for 376
Sulley, A. H., *see* Owen
Sulphur, selenium and tellurium, Absorption spectra and photodissociation of halides and oxyhalides of 679
Superlattice in β brass, The energy of the 258
Supersonic velocities, The smoke method of measuring 95
Surfaces, The migration and aggregation of metal atoms on solid . . . E 140
Sykes, C., *see* Bragg

Tai, L. C., *see* Bates
Taylor, A. K.: Photometric test plates 105
Taylor, H. Dennis: The use of rotating parallel-plane glass blocks for cinematography and for projection with continuously moving films 663
Telephone receiver, Demonstration of the audible effect of a sudden change of phase in the current supplied to a 194
Tellurium, Absorption spectra and photodissociation of halides and oxyhalides of sulphur, selenium and 679
Thermomagnetic properties of nickel wire. Part 3 14
Tin halides in the vapour state, Absorption spectra of some carbon and . . 568
Tin, *see* Sn
Transformation, A study of the order-disorder . . . . E 96
Treloar, L. R. G.: Secondary-electron emission from complex surfaces . . 392

PAGE
Trichromat. The colour-vision characteristics of a 332
Trichromats, The saturation-discrimination of two 329
Triode, The division of primary electron current between grid and anode of a . 264
Triode valve, A determination of the fundamental types of electron oscillations in a 38
Tsien, L. C., *see* Andrade
Tungsten filament, Thermionic approximations to the gas-covered fraction of an adsorbing surface, applied to the temperature dependence of oxygenation and oxidation of a 409

Ultraviolet band-systems of GeCl and GeBr 532
Ultraviolet band-system of germanium monoxide, The 543
Ultraviolet band-systems of SnBr and SiBr 554
Ultraviolet light, employing a reflecting optical system of aplanatic properties, Demonstration of a microscope for use with 427

Verwey, E. J. W., *see* Boer
Vick, F. A., *see* Johnson
Viscosity of air, The 205
Vortex motion causing edge-tones, The 493

Waller, Mary D.: The production of Chladni figures by means of solid carbon dioxide. Part 1: Bars and other metal bodies 522
Webster, H. C.: An aperiodic amplifier for investigating the wave-form of atmospherics 654
Webster, H. C.: Applications of the modulating electrode of television cathode-ray tubes in investigations of the wave-form of atmospherics . . . 658
Wilkinson, H., *see* Lowery
Wilson, C. W.: The effect of secondary beta-radiation on gamma-ray measurements made in air 338
Wood-water relationships. Part 3: Molecular sorption of water by Sitka spruce wood 237
Wright, W. D., and F. H. G. Pitt: The saturation-discrimination of two trichromats 329

X-ray goniometer using beams of large aperture for photographically recording crystal-powder reflections, An 61
X-ray investigation of pure iron-nickel alloys. Part 1: Thermal expansion of alloys rich in nickel, An 17
X-ray investigation of pure iron-nickel alloys. Part 2: Thermal expansion of some further alloys, An 178
X-ray investigation of pure iron-nickel alloys. Part 3: The thermal expansion of alloys rich in iron, An 307
X-ray investigation of pure iron-nickel alloys. Part 4: The variation of lattice-parameter with composition, An 315
X-ray investigation of pure iron-nickel alloys. Part 5: The variation of thermal expansion with composition, An 323
X-ray reflections from single crystals of sodium between 120° and 370° K., Intensities of 294

Yates, E. L., *see* Owen

Zinc alloys, The theoretical interpretation of the optical constants of copper . 354
Zinc system, On the optical constants of alloys of the copper 345

CAMBRIDGE: PRINTED BY WALTER LEWIS, M.A., AT THE UNIVERSITY PRESS